

LNAI 3684

Rajiv Khosla
Robert J. Howlett
Lakhmi C. Jain (Eds.)

Knowledge-Based Intelligent Information and Engineering Systems

9th International Conference, KES 2005
Melbourne, Australia, September 2005
Proceedings, Part IV

4
Part IV

Lecture Notes in Artificial Intelligence 3684

Edited by J. G. Carbonell and J. Siekmann

Subseries of Lecture Notes in Computer Science

Rajiv Khosla Robert J. Howlett
Lakhmi C. Jain (Eds.)

Knowledge-Based Intelligent Information and Engineering Systems

9th International Conference, KES 2005
Melbourne, Australia, September 14-16, 2005
Proceedings, Part IV

Series Editors

Jaime G. Carbonell, Carnegie Mellon University, Pittsburgh, PA, USA
Jörg Siekmann, University of Saarland, Saarbrücken, Germany

Volume Editors

Rajiv Khosla
La Trobe University
Business Systems and Knowledge Modelling Laboratory, School of Business
Victoria 3086, Australia
E-mail: R.Khosla@latrobe.edu.au

Robert J. Howlett
University of Brighton, School of Engineering, Engineering Research Centre
Moulsecoomb, Brighton, BN2 4GJ, UK
E-mail: r.j.howlett@bton.ac.uk

Lakhmi C. Jain
University of South Australia
School of Electrical and Information Engineering, KES Centre
Mawson Lakes Campus, Adelaide, South Australia SA 5095, Australia
E-mail: Lakhmi.Jain@unisa.edu.au

Library of Congress Control Number: 2005932202

CR Subject Classification (1998): I.2, H.4, H.3, J.1, H.5, K.6, K.4

ISSN 0302-9743
ISBN-10 3-540-28897-X Springer Berlin Heidelberg New York
ISBN-13 978-3-540-28897-8 Springer Berlin Heidelberg New York

This work is subject to copyright. All rights are reserved, whether the whole or part of the material is concerned, specifically the rights of translation, reprinting, re-use of illustrations, recitation, broadcasting, reproduction on microfilms or in any other way, and storage in data banks. Duplication of this publication or parts thereof is permitted only under the provisions of the German Copyright Law of September 9, 1965, in its current version, and permission for use must always be obtained from Springer. Violations are liable to prosecution under the German Copyright Law.

Springer is a part of Springer Science+Business Media
springeronline.com

© Springer-Verlag Berlin Heidelberg 2005
Printed in Germany

Typesetting: Camera-ready by author, data conversion by Olgun Computergrafik
Printed on acid-free paper SPIN: 11554028 06/3142 5 4 3 2 1 0

Preface

Dear delegates, friends and members of the growing KES professional community, welcome to the proceedings of the 9th International Conference on Knowledge-Based and Intelligent Information and Engineering Systems hosted by La Trobe University in Melbourne Australia.

The KES conference series has been established for almost a decade, and it continues each year to attract participants from all geographical areas of the world, including Europe, the Americas, Australasia and the Pacific Rim. The KES conferences cover a wide range of intelligent systems topics. The broad focus of the conference series is the theory and applications of intelligent systems. From a pure research field, intelligent systems have advanced to the point where their abilities have been incorporated into many business and engineering application areas. KES 2005 provided a valuable mechanism for delegates to obtain an extensive view of the latest research into a range of intelligent-systems algorithms, tools and techniques. The conference also gave delegates the chance to come into contact with those applying intelligent systems in diverse commercial areas. The combination of theory and practice represented a unique opportunity to gain an appreciation of the full spectrum of leading-edge intelligent-systems activity.

The papers for KES 2005 were either submitted to invited sessions, chaired and organized by respected experts in their fields, or to a general session, managed by an extensive International Program Committee, or to the Intelligent Information Hiding and Multimedia Signal Processing (IIHMSP) Workshop, managed by an International Workshop Technical Committee. Whichever route they came through, all papers for KES 2005 were thoroughly reviewed. The adoption by KES of the PROSE Publication Review and Organisation System software greatly helped to improve the transparency of the review process and aided quality control.

In total, 1382 papers were submitted for KES 2005, and a total of 688 papers were accepted, giving an acceptance rate of just under 50%. The proceedings, published this year by Springer, run to more than 5000 pages. The invited sessions are a valuable feature of KES conferences, enabling leading researchers to initiate sessions that focus on innovative new areas. A number of sessions in new emerging areas were introduced this year, including Experience Management, Emotional Intelligence, and Smart Systems. The diversity of the papers can be judged from the fact that there were about 100 technical sessions in the conference program. More than 400 universities worldwide participated in the conference making it one of the largest conferences in the area of intelligent systems. As would be expected, there was good local support with the participation of 20 Australian universities. There was a significant business presence, provided by the involvement of a number of industry bodies, for example, CSIRO Australia, DSTO Australia, Daewoo South Korea and NTT Japan.

KES International gratefully acknowledges the support provided by La Trobe University in hosting this conference. We acknowledge the active interest and support from La Trobe University's Vice Chancellor and President, Prof. Michael Osborne, Dean of

the Faculty of Law and Management, Prof. Raymond Harbridge, Dean of the Faculty of Science and Technology, Prof. David Finlay, and Head of the School of Business, Prof. Malcolm Rimmer. KES International also gratefully acknowledges the support provided by Emeritus Prof. Greg O'Brien.

A tremendous amount of time and effort goes into the organization of a conference of the size of KES 2005. The KES community owes a considerable debt of gratitude to the General Chair Prof. Rajiv Khosla and the organizing team at La Trobe University for their huge efforts this year in bringing the conference to a successful conclusion. As the conference increases in size each year the organizational effort needed increases and we would like to thank Prof. Khosla and his colleagues for coping efficiently with the largest KES conference to date.

We would like to thank the Invited Session Chairs, under the leadership and guidance of Prof. Lakhmi Jain and Prof. Rajiv Khosla for producing high-quality sessions on leading-edge topics. We would like to thank the KES 2005 International Program Committee for undertaking the considerable task of reviewing all of the papers submitted for the conference. We express our gratitude to the high-profile keynote speakers for providing talks on leading-edge topics to inform and enthuse our delegates. A conference cannot run without authors to write papers. We thank the authors, presenters and delegates to KES 2005 without whom the conference could not have taken place. Finally we thank the administrators, caterers, hoteliers, and the people of Melbourne for welcoming us and providing for the conference.

We hope you found KES 2005 a worthwhile, informative and enjoyable experience.

July 2005

Bob Howlett
Rajiv Khosla
Lakhmi Jain

KES 2005 Conference Organization

General Chair

Rajiv Khosla
Business Systems and Knowledge Modelling Laboratory
School of Business
La Trobe University
Melbourne, Victoria 3086
Australia

Conference Founder and Honorary Program Committee Chair

Lakhmi C. Jain
Knowledge-Based Intelligent Information and Engineering Systems Centre
University of South Australia, Australia

KES Executive Chair

Bob Howlett
Intelligent Systems and Signal Processing Laboratories/KTP Centre
University of Brighton, UK

KES Journal General Editor

Bogdan Gabrys
University of Bournemouth, UK

Local Organizing Committee

Malcolm Rimmer – Chair, School of Business, La Trobe University
Rajiv Khosla, Selena Lim, Brigitte Carrucan, Monica Hodgkinson, Marie Fenton,
Maggie Van Tonder, and Stephen Muir
La Trobe University, Melbourne, Australia

KES 2005 Web Page Design Team

Joe Hayes, Anil Varkey Samuel, Mehul Bhatt, Rajiv Khosla
La Trobe University, Melbourne, Australia

KES 2005 Liaison and Registration Team

Rajiv Khosla, Selena Lim, Brigitte Carrucan, Jodie Kennedy, Maggie Van Tonder,
Marie Fenton, Colleen Stoate, Diane Kraal, Cary Slater, Petrus Usmanij, Chris Lai,
Rani Thanacoody, Elisabeth Tanusasmita, George Plocinski
La Trobe University, Melbourne, Australia

KES 2005 Proceedings Assembly Team

Rajiv Khosla
Selena Lim
Monica Hodgkinson
George Plocinski
Maggie Van Tonder
Colleen Stoate
Anil Varkey Samuel
Marie Fenton
Mehul Bhatt
Chris Lai
Petrus Usmanij

International Program Committee

Hussein Abbass, University of New South Wales, Australia
Akira Asano, Hiroshima University, Japan
Robert Babuska, Delft University of Technology, The Netherlands
Patrick Bosc, IRISA/ENSSAT, France
Pascal Bouvry, Luxembourg University of Applied Sciences, Luxembourg
Krzysztof Cios, University of Colorado, USA
Carlos A. Coello, LANIA, Mexico
Ernesto Damiani, University of Milan, Italy
Da Deng, University of Otago, New Zealand
Vladan Devedzic, University of Belgrade, Serbia and Montenegro
Vladimir Gorodetski, Russian Academy of Sciences, Russia
Manuel Grana, UPV/EHU, Spain
Lars Kai Hansen, Technical University of Denmark, Denmark
Yuzo Hirai, University of Tsukuba, Japan
Daniel Howard, QinetiQ, UK
Tzung-Pei Hong, National University of Kaohsiung, Taiwan
Hisao Ishibuchi, Osaka Prefecture University, Japan
Naohiro Ishii, Aichi Institute of Technology, Japan
Seong-Joon Yoo, Sejong University, Korea
Nikos Karacapilidis, University of Patras, Greece
Rajiv Khosla, La Trobe University, Australia
Laszlo T. Koczy, Budapest and Szechenyi Istvan University, Hungary
Andrew Kusiak, University of Iowa, USA
W.K. Lai, MIMOS Berhad, Malaysia
Ian C. Parmee, University of the West of England, UK
Dong Hwa Kim, Hanbat National University, Korea
Jingli Cao, La Trobe University, Australia
Da Ruan, Belgian Nuclear Research Centre, Belgium
Ang Yang, University of New South Wales, Australia
Adrian Stoica, NASA Jet Propulsion Laboratory, USA
Janusz Kacprzyk, Polish Academy of Sciences, Poland
Vijayan Asari, Old Dominion University, USA
Raymond Lee, Hong Kong Polytechnic University, Hong Kong, China
Chee-Peng Lim, University of Science, Malaysia
Ignac Lovrek, University of Zagreb, Croatia
Bob McKay, University of NSW, Australia
Dan C. Marinescu, University of Central Florida, USA
Radko Mesiar, Slovak Technical University, Slovakia
Hirofumi Nagashino, University of Tokushima, Japan
Ciprian Daniel Neagu, University of Bradford, UK
Ngoc Thanh Nguyen, Wroclaw University of Technology, Poland

Toyoaki Nishida, University of Tokyo, Japan
Vasile Palade, Oxford University, UK
John A. Rose, University of Tokyo, Japan
Rajkumar Roy, Cranfield University, UK
Udo Seiffert, Leibniz Institute of Plant Genetics and Crop Plant Research, Germany
Flavio Soares Correa da Silva, University of Sao Paulo, Brazil
Von-Wun Soo, National Tsing Hua University, Taiwan
Sarawut Sujitjorn, Suranaree University of Technology, Thailand
Takushi Tanaka, Fukuoka Institute of Technology, Japan
Eiichiro Tazaki, University of Yokohama, Japan
Jon Timmis, University of Kent, UK
Jim Torresen, University of Oslo, Norway
Andy M. Tyrrell, University of York, UK
Eiji Uchino, University of Yamaguchi, Japan
Jose Luis Verdegay, University of Granada, Spain
Dianhui Wang, La Trobe University, Australia
Junzo Watada, Waseda University, Japan
Xin Yao, University of Birmingham, UK
Boris Galitsky, University of London, UK
Bogdan Gabrys, Bournemouth University, UK
Norbert Jesse, Universität Dortmund, Germany
Keiichi Horio, Kyushu Institute of Technology, Japan
Bernd Reusch, University of Dortmund, Germany
Nadia Berthouze, University of Aizu, Japan
Hideyaki Sawada, Kagawa University, Japan
Yasue Mitsukura, University of Okayama, Japan
Dharmendra Sharma, University of Canberra, Australia
Adam Grzech, Wroclaw University of Technology, Poland
Mircea Negoita, Wellington Institute of Technology, New Zealand
Hongen Lu, La Trobe University, Australia
Kosuke Sekiyama, University of Fukui, Japan
Raquel Flórez-López, Campus de Vegazana, Spain
Eugénio Oliveira, University of Porto, Portugal
Roberto Frias, University of Porto, Portugal
Maria Virvou, University of Piraeus, Greece
Daniela Zambarbieri, Università di Pavia, Italy
Andrew Skabar, La Trobe University, Australia
Zhaohao Sun, University of Wollongong, Australia
Koren Ward, University of Wollongong, Australia

Invited Session Chairs Committee

Krzysztof Cios, University of Denver, USA
Toyoaki Nishida, University of Tokyo, Japan
Ngoc Thanh Nguyen, Wroclaw University of Technology, Poland
Tzung-Pei Hong, National University of Kaohsiung, Taiwan
Yoshinori Adachi, Chubu University, Japan
Nobuhiro Inuzuka, Nagoya Institute of Technology, Japan
Naohiro Ishii, Aichi Institute of Technology, Japan
Yuji Iwahori, Chubu University, Japan
Tai-hoon Kim, Security Engineering Research Group (SERG), Korea
Daniel Howard, QinetiQ, UK
Mircea Gh. Negoita, Wellington Institute of Technology, New Zealand
Akira Suyama, University of Tokyo, Japan
Dong Hwa Kim, Hanbat National University, Korea
Hussein A. Abbas, University of New South Wales, Australia
William Grosky, University of Michigan-Dearborn, USA
Elisa Bertino, Purdue University, USA
Maria L. Damiani, University of Milan, Italy
Kosuke Sekiyama, University of Fukui, Japan
Seong-Joon Yoo, Sejong University, Korea
Hirokazu Taki, Wakayama University, Japan
Satoshi Hori, Institute of Technologists, Japan
Hideyuki Sawada, Kagawa University, Japan
Vicenc Torra, Artificial Intelligence Research Institute, Spain
Maria Vamrell, Artificial Intelligence Research Institute, Spain
Manfred Schmitt, Technical University of Munich, Germany
Denis Helic, Graz University of Technology, Austria
Yoshiteru Ishida, Toyohashi University of Technology, Japan
Giuseppina Passiante, University of Lecce, Italy
Ernesto Damiani, University of Milan, Italy
Susumu Kunifugi, Japan Advanced Institute of Science and Technology, Japan
Motoki Miura, Japan Advanced Institute of Science and Technology, Japan
James Liu, Hong Kong Polytechnic University, Hong Kong, China
Honghua Dai, Deakin University, Australia
Pascal Bouvry, Luxembourg University, Luxembourg
Gregoire Danoy, Luxembourg University, Luxembourg
Ojoung Kwon, California State University, USA
Jun Munemori, Wakayama University, Japan
Takashi Yoshino, Wakayama University, Japan
Takaya Yuizono, Shimane University, Japan
Behrouz Homayoun Far, University of Calgary, Canada
Toyohide Watanabe, Nagoya University, Japan
Dharmendra Sharma, University of Canberra, Australia
Dat Tran, University of Canberra, Australia

Kim Le, University of Canberra, Australia
Takumi Ichimura, Hiroshima City University, Japan
K Yoshida, St. Marianna University, Japan
Phill Kyu Rhee, Inha University, Korea
Chong Ho Lee, Inha University, Korea
Mikhail Prokopenko, CSIRO ICT Centre, Australia
Daniel Polani, University of Hertfordshire, UK
Dong Chun Lee, Howon University, Korea
Dawn E. Holmes, University of California, USA
Kok-Leong Ong, Deakin University, Australia
Vincent Lee, Monash University, Australia
Wee-Keong Ng, Nanyang Technological University
Gwi-Tae Park, Korea University, Korea
Giles Oatley, University of Sunderland, UK
Sangkyun Kim, Korea Information Engineering Service, Korea
Hong Joo Lee, Daewoo Electronics Corporation, Korea
Ryohei Nakano, Nagoya Institute of Technology, Japan
Kazumi Saito, NTT Communication Science Laboratories, Japan
Kazuhiro Tsuda, University of Tsukuba, Japan
Torbjørn Nordgård, Norwegian University of Science and Technology, Norway
Øystein Nytrø, Norwegian University of Science and Technology, Norway
Amund Tveit, Norwegian University of Science and Technology, Norway
Thomas Brox Røst, Norwegian University of Science and Technology, Norway
Manuel Graña, Universidad País Vasco, Spain
Richard Duro, Universidad de A Coruña, Spain
Kazumi Nakamatsu, University of Hyogo, Japan
Jair Minoro Abe, University of São Paulo, Brazil
Hiroko Shoji, Chuo University, Japan
Yukio Ohsawa, University of Tsukuba, Japan
Da Deng, University of Otago, New Zealand
Irena Koprinska, University of Sydney, Australia
Eiichiro Tazaki, University of Yokohama, Japan
Kenneth J. Mackin, Tokyo University of Information Sciences, Japan
Lakhmi Jain, University of South Australia, Australia
Tetsuo Fuchino, Tokyo Institute of Technology, Japan
Yoshiyuki Yamashita, Tohoku University, Japan
Martin Purvis, University of Otago, New Zealand
Mariusz Nowostawski, University of Otago, New Zealand
Bastin Tony Roy Savarimuthu, University of Otago, New Zealand
Norio Baba, Osaka Kyoiku University, Japan
Junzo Watada, Waseda University, Japan
Petra Povalej, Laboratory for System Design, Slovenia
Peter Kokol, Laboratory for System Design, Slovenia
Woochun Jun, Seoul National University of Education, Korea
Andrew Kusiak, University of Iowa, USA
Hanh Pham, State University of New York, USA

IIHMSP Workshop Organization Committee

General Co-chairs

Jeng-Shyang Pan

National Kaohsiung University of Applied Sciences, Taiwan

Lakhmi C. Jain

University of South Australia, Australia

Program Committee Co-chairs

Wai-Chi Fang

California Institute of Technology, USA

Eiji Kawaguchi

Keio University, Japan

Finance Chair

Jui-Fang Chang

National Kaohsiung University of Applied Sciences, Taiwan

Publicity Chair

Kang K. Yen

Florida International University, USA

Registration Chair

Yan Shi

Tokai University, Japan

Electronic Media Chair

Bin-Yih Liao

National Kaohsiung University of Applied Sciences, Taiwan

Publication Chair

Hsiang-Cheh Huang

National Chiao Tung University, Taiwan

Local Organizing Chair

R. Khosla
La Trobe University, Australia

Asia Liaison

Yoiti Suzuki
Tohoku University, Japan

North America Liaison

Yun Q. Shi
New Jersey Institute of Technology, USA

Europe Liaison

R.J. Howlett
University of Brighton, UK

IIHMSP Workshop Technical Committee

Prof. Oscar Au, Hong Kong University of Science and Technology, Hong Kong, China
Prof. Chin-Chen Chang, National Chung Cheng University, Taiwan
Prof. Chang Wen Chen, Florida Institute of Technology, USA
Prof. Guanrong Chen, City University of Hong Kong, Hong Kong, China
Prof. Liang-Gee Chen, National Taiwan University, Taiwan
Prof. Tsuhan Chen, Carnegie Mellon University, USA
Prof. Yung-Chang Chen, National Tsing-Hua University, Taiwan
Prof. Yen-Wei Chen, Ritsumeikan University, Japan
Prof. Hsin-Chia Fu, National Chiao Tung University, Taiwan
Prof. Hsueh-Ming Hang, National Chiao Tung University, Taiwan
Prof. Dimitrios Hatzinakos, University of Toronto, Canada
Dr. Ichiro Kuroda, NEC Electronics Corporation, Japan

KES 2005 Reviewers

H. Abbass, University of New South Wales, Australia
J.M. Abe, University of Sao Paulo, Brazil
Y. Adachi, Chubu University, Japan
F. Alpaslan, Middle East Technical University, Turkey
P. Andreae, Victoria University, New Zealand
A. Asano, Hiroshima University, Japan
K.V. Asari, Old Dominion University, USA
N. Baba, Osaka-Kyoiku University, Japan
R. Babuska, Delft University of Technology, The Netherlands
P. Bajaj, G.H. Raisoni College of Engineering, India
A. Bargiela, Nottingham Trent University, UK
M. Bazu, Institute of Microtechnology, Romania
N. Berthouze, University of Aizu, Japan
E. Bertino, Purdue University, USA
Y. Bodyanskiy, Kharkiv National University of Radioelectronics, Ukraine
P. Bosc, IRISA/ENSSAT, France
P. Bouvry, Luxembourg University, Luxembourg
P. Burrell, South Bank University, UK
J. Cao, La Trobe University, Australia
B. Chakraborty, Iwate Prefectural University, Japan
Y.-W. Chen, Ryukyus University, Japan
Y.-H. Chen-Burger, University of Edinburgh, UK
V. Cherkassky, University of Minnesota, USA
K. Cios, University at Denver, USA
C.A. Coello, LANA, Mexico
G. Coghill, University of Auckland, New Zealand
D. Corbett, SAIC, USA
D.W. Corne, University of Exeter, UK
D. Cornforth, Charles Sturt University, Australia
F.S.C. da Silva, University of Sao Paulo, Brazil
H. Dai, Deakin University, Australia
E. Damiani, University of Milan, Italy
M.L. Damiani, University of Milan, Italy
G. Danoy, Luxembourg University, Luxembourg
K. Deep, Indian Institute of Technology Roorkee, India
D. Deng, University of Otago, New Zealand
V. Devedzic, University of Belgrade, Serbia and Montenegro
D. Dubois, Université Paul Sabatier, France
R. Duro, Universidad de A Coruña, Spain
D. Earl, Oak Ridge National Laboratory, USA
B. Far, University of Calgary, Canada

- M. Fathi, National Magnet Laboratory, USA
R. Flórez-López, Campus de Vegazana, Spain
M. Frean, Victoria University of Wellington, New Zealand
R. Frias, University of Porto, Portugal
T. Fuchino, Tokyo Institute of Technology, Japan
P. Funk, Mälardalen University, Sweden
B. Gabrys, University of Bournemouth, UK
B. Galitsky, University of London, UK
T. Gedeon, Murdoch University, Australia
M. Gen, Waseda University, Japan
A. Ghosh, ISICAI, India
V. Gorodetski, Russian Academy of Sciences, Russia
M. Grana, Facultad de Informatica UPV/EHU, Spain
W. Grosky, University of Michigan-Dearborn, USA
A. Grzech, Wroclaw University of Technology, Poland
D. Gwaltney, NASA George C. Marshall Space Flight Center, USA
L.K. Hansen, Technical University of Denmark, Denmark
C.J. Harris, University of Southampton, UK
D. Helic, Graz University of Technology Austria
L. Hildebrand, University of Dortmund, Germany
Y. Hirai, University of Tsukuba, Japan
D.E. Holmes, University of California, USA
B. Homayoun, Far University of Calgary, Canada
T.-P. Hong, National University of Kaohsiung, Taiwan
S. Hori, Institute of Technologists, Japan
K. Horio, Kyushu Institute of Technology, Japan
D. Howard, QinetiQ, UK
B. Howlett, University of Brighton, UK
M.-P. Huget, University of Savoie, France
H. Iba, University of Tokyo, Japan
T. Ichimura, Hiroshima City University, Japan
N. Inuzuka, Nagoya Institute of Technology, Japan
H. Ishibuchi, Osaka Prefecture University, Japan
Y. Ishida, Toyohashi University of Technology, Japan
N. Ishii, Aichi Institute of Technology, Japan
Y. Iwahori, Chubu University, Japan
L. Jain, University of South Australia, Australia
M.M. Jamshidi, University of New Mexico, USA
N. Jesse, Universität Dortmund, Germany
S. Joo, Sejong University, Korea
W. Jun, Seoul National University of Education, Korea
J. Kacprzyk, Polish Academy of Sciences, Poland
N. Karacapilidis, University of Patras, Greece
V. Kecman, Auckland University, New Zealand
R. Khosla, La Trobe University, Australia

XVIII KES 2005 Reviewers

- D.H. Kim, Hanbat National University, Korea
S. Kim, Korea Information Engineering Service, Korea
T.-H. Kim, Security Engineering Research Group (SERG), Korea
L.T. Koczy, Budapest University of Technology and Economics, Hungary
P. Kokol, Laboratory for System Design, Slovenia
A. Konar, Jadavpur University, India
I. Koprinska, University of Sydney, Australia
H. Koshimizu, Chukyo University, Japan
S. Kunifugi, Japan Advanced Institute of Science and Technology, Japan
A. Kusiak, University of Iowa, USA
O. Kwon, California State University, USA
W.K. Lai, MIMOS Berhad, Malaysia
P.L. Lanzi, Polytechnic Institute, Italy
K. Le, University of Canberra, Australia
C.H. Lee, Inha University, Korea
D.C. Lee, Howon University, Korea
H.J. Lee, Daewoo Electronics Corporation, Korea
R. Lee, Hong Kong Polytechnic University, Hong Kong, China
V. Lee, Monash University, Australia
Q. Li, La Trobe University, Australia
C.-P. Lim, University of Science, Malaysia
S. Lim, La Trobe University, Australia
J. Liu, Hong Kong Polytechnic University, Hong Kong, China
I. Lovrek, University of Zagreb, Croatia
H. Lu, La Trobe University, Australia
B. MacDonald, Auckland University, New Zealand
K.J. Mackin, Tokyo University of Information Sciences, Japan
L. Magdalena-Layos, EUSFLAT, Spain
D.C. Marinescu, University of Central Florida, USA
F. Masulli, University of Pisa, Italy
J. Mazumdar, University of South Australia, Australia
B. McKay, University of NSW, Australia
S. McKinlay, Wellington Institute of Technology, New Zealand
R. Mesiar, Slovak Technical University, Slovakia
J. Mira, UNED, Spain
Y. Mitsukura, University of Okayama, Japan
M. Miura, Japan Advanced Institute of Science and Technology, Japan
J. Munemori, Wakayama University, Japan
H. Nagashino, University of Tokushima, Japan
N. Nagata, Chukyo University, Japan
K. Nakajima, Tohoku University, Japan
K. Nakamatsu, University of Hyogo, Japan
R. Nakano, Nagoya Institute, Japan
T. Nakashima, Osaka University, Japan
L. Narasimhan, University of Newcastle, Australia

- V.E. Neagoe, Technical University, Romania
C.D. Neagu, University of Bradford, UK
M.G. Negoita, WelTec, New Zealand
W.-K. Ng, Nanyang Technological University, Singapore
C. Nguyen, Catholic University of America, USA
N.T. Nguyen, Wroclaw University of Technology, Poland
T. Nishida, University of Tokyo, Japan
T. Nordgård, Norwegian University of Science and Technology, Norway
M. Nowostawski, University of Otago, New Zealand
Ø. Nytrø, Norwegian University of Science and Technology, Norway
G. Oatley, University of Sunderland, UK
Y. Ohsawa, University of Tsukuba, Japan
E. Oliveira, University of Porto, Portugal
K.-L. Ong, Deakin University, Australia
N.R. Pal, Indian Statistical Institute, India
V. Palade, Oxford University, UK
G.-T. Park, Korea University, Korea
I.C. Parmee, University of the West of England, UK
G. Passiante, University of Lecce, Italy
C.-A. Peña-Reyes, Swiss Federal Institute of Technology - EPFL, Switzerland
H. Pham, State University of New York, USA
D. Polani, University of Hertfordshire, UK
T. Popescu, National Institute for Research and Development Informatic, Italy
P. Povalej, Laboratory for System Design, Slovenia
M. Prokopenko, CSIRO ICT Centre, Australia
M. Purvis, University of Otago, New Zealand
G. Resconi, Catholic University, Italy
B. Reusch, University of Dortmund, Germany
P.K. Rhee, Inha University, Korea
J.A. Rose, University of Tokyo, Japan
T.B. Røst, Norwegian University of Science and Technology, Norway
E. Roventa, York University, Canada
R. Roy, Cranfield University, UK
D. Ruan, Belgian Nuclear Research Centre, Belgium
A. Saha, NCD, Papua New Guinea
K. Saito, NTT Communication Science Laboratories, Japan
T. Samatsu, Kyushu Tokai University, Japan
E. Sanchez, Université de la Méditerranée, France
B.T.R. Savarimuthu, University of Otago, New Zealand
H. Sawada, Kagawa University, Japan
M. Schmitt, Technical University of Munich, Germany
M. Schoenauer, INRIA, France
U. Seiffert, Leibniz Institute of Plant Genetics
and Crop Plant Research Gatersleben, Germany
K. Sekiyama, University of Fukui, Japan

- D. Sharma, University of Canberra, Australia
H. Shoji, Chuo University, Japan
A. Skabar, La Trobe University, Australia
B. Smyth, University College Dublin, Ireland
V.-W. Soo, National Tsing Hua University, Taiwan
A. Stoica, NASA Propulsion Jet Laboratory, USA
M.R. Stytz, Yamaguchi University, Japan
N. Suetake, Yamaguchi University, Japan
S. Sujitjorn, Suranaree University of Technology, Thailand
Z. Sun, University of Wollongong, Australia
A. Suyama, University of Tokyo, Japan
H. Taki, Wakayama University, Japan
T. Tanaka, Fukuoka Institute of Technology, Japan
M. Tanaka-Yamawaki, Tottori University, Japan
E. Tazaki, University of Yokohama, Japan
S. Thatcher, University of South Australia, Australia
P. Theodor, National Institute for Research and Development Informatics, Romania
J. Timmis, University of Kent at Canterbury, UK
V. Torra, Artificial Intelligence Research Institute, Spain
J. Torresen, University of Oslo, Norway
D. Tran, University of Canberra, Australia
K. Tsuda, University of Tsukuba, Japan
C. Turchetti, Università Politecnica delle Marche, Italy
A. Tveit, Norwegian University of Science and Technology, Norway
J. Tweedale, Defence Science and Technology Organization, Australia
A.M. Tyrrell, University of York, UK
E. Uchino, University of Yamaguchi, Japan
A. Uncini, University of Rome, Italy
P. Urlings, Defence Science and Technology Organization, Australia
M. Vamrell, Artificial Intelligence Research Institute, Spain
J.L. Verdegay, University of Granada, Spain
M. Virvou, University of Piraeus, Greece
S. Walters, University of Brighton, UK
D. Wang, La Trobe University, Australia
L. Wang, Nanyang Technical University, Singapore
P. Wang, Temple University, USA
K. Ward, University of Wollongong, Australia
J. Watada, Waseda University, Japan
K. Watanabe, Saga University, Japan
T. Watanabe, Nagoya University, Japan
T. Yamakawa, Kyushu Institute of Technology, Japan
Y. Yamashita, Tohoku University, Japan
A. Yang, University of New South Wales, Australia
X. Yao, University of Birmingham, UK
S.-J. Yoo, Sejong University, Korea

K. Yoshida, Kyushu Institute of Technology, Japan
T. Yoshino, Wakayama University, Japan
T. Yuizono, Shimane University, Japan
L. Zadeh, Berkeley University of California, USA
D. Zambarbieri, Università di Pavia, Italy
X. Zha, National Institute of Standards and Technology, USA

KES 2005 Keynote Speakers

- 1. Professor Jun Liu**, Harvard University, MA, USA
Topic: From Sequence Information to Gene Expression
- 2. Professor Ron Sun**, Rensselaer Polytechnic Institute, New York, USA
Topic: From Hybrid Systems to Hybrid Cognitive Architectures
- 3. Professor Jiming Liu**, Hong Kong Baptist University, Hong Kong, China
Topic: Towards Autonomy Oriented Computing (AOC):
Formulating Computational Systems with Autonomous Components
- 4. Professor Toyoaki Nishida**, Kyoto University and Tokyo University, Japan
Topic: Acquiring, Accumulating, Transforming, Applying,
and Understanding Conversational Quanta
- 5. Professor Marimuthu Palaniswami**, University of Melbourne, Australia
Topic: Convergence of Smart Sensors and Sensor Networks

Table of Contents, Part IV

Innovations in Intelligent Systems and Their Applications

| | |
|---|----|
| A Method for Optimal Division of Data Sets for Use in Neural Networks | 1 |
| <i>Patricia S. Crowther and Robert J. Cox</i> | |
| Excluding Fitness Helps Improve Robustness of Evolutionary Algorithms | 8 |
| <i>Matej Šprogar</i> | |
| Testing Voice Mimicry with the YOHO Speaker Verification Corpus | 15 |
| <i>Yee W. Lau, Dat Tran, and Michael Wagner</i> | |
| Image Multi-noise Removal via Lévy Process Analysis | 22 |
| <i>Xu Huang and A.C. Madoc</i> | |
| Evaluating the Size of the SOAP for Integration in B2B | 29 |
| <i>Alexander Ridgewell, Xu Huang, and Dharmendra Sharma</i> | |
| Personalised Search on Electronic Information | 35 |
| <i>G.L. Ligon, Balachandran Bala, and Sharma Dharmendra</i> | |

| | |
|---|----|
| Data Mining Coupled Conceptual Spaces for Intelligent Agents in Data-Rich Environments | 42 |
| <i>Ickjai Lee</i> | |

Data Mining and Soft Computing Applications II

| | |
|---|----|
| An Evolutionary Algorithm for Constrained Bi-objective Optimization Using Radial Slots | 49 |
| <i>Tapabrata Ray and Kok Sung Won</i> | |
| An Optimization Approach for Feature Selection in an Electric Billing Database . | 57 |
| <i>Manuel Mejía-Lavalle, Guillermo Rodríguez, and Gustavo Arroyo</i> | |
| Integrating Relation and Keyword Matching in Information Retrieval | 64 |
| <i>Tanveer J. Siddiqui and Uma Shanker Tiwary</i> | |
| Production Testing of Spark Plugs Using a Neural Network | 74 |
| <i>Simon D. Walters, Peter A. Howson, and Bob R.J. Howlett</i> | |
| Variable Neighborhood Search with Permutation Distance for QAP | 81 |
| <i>Chong Zhang, Zhangang Lin, and Zuoquan Lin</i> | |
| Using Rough Set to Induce Comparative Knowledge and Its Use in SARS Data . | 89 |
| <i>Honghai Feng, Cheng Yin, Mingyi Liao, Bingru Yang, and Yumei Chen</i> | |

| | |
|--|----|
| Mining Class Association Rules with Artificial Immune System | 94 |
| <i>Tien Dung Do, Siu Cheung Hui, and Alvis C.M. Fong</i> | |

| | |
|---|-----|
| Discovering Fuzzy Association Rules with Interest and Conviction Measures | 101 |
| <i>K. Sai Krishna, P. Radha Krishna, and Supriya Kumar De</i> | |

Skill Acquisition and Ubiquitous Human Computer Interaction

| | |
|---|-----|
| Automatic Generation of Operation Manuals Through Work Motion Observation . | 108 |
| <i>Satoshi Hori, Kota Hirose, and Hirokazu Taki</i> | |

| | |
|--|-----|
| A Method of Controlling Household Electrical Appliance by Hand Motion in LonWorks | 115 |
| <i>Il-Joo Shim, Kyung-Bae Chang, and Gwi-Tae Park</i> | |

| | |
|---|-----|
| Contribution of Biological Studies to the Understanding and Modeling of Skilled Performance: Some Examples | 124 |
| <i>Atsuko K. Yamazaki and J. Rudi Strickler</i> | |

| | |
|--|-----|
| Measurement of Human Concentration with Multiple Cameras | 129 |
| <i>Kazuhiko Sumi, Koichi Tanaka, and Takashi Matsuyama</i> | |

| | |
|--|-----|
| Constructive Induction-Based Clustering Method for Ubiquitous Computing Environments | 136 |
| <i>Takeshi Yamamoto, Hirokazu Taki, Noriyuki Matsuda, Hirokazu Miura, Satoshi Hori, and Noriyuki Abe</i> | |

| | |
|--|-----|
| Indoor Location Determination Using a Topological Model | 143 |
| <i>Junichi Sakamoto, Hirokazu Miura, Noriyuki Matsuda, Hirokazu Taki, Noriyuki Abe, and Satoshi Hori</i> | |

| | |
|--|-----|
| Lightweight Agent Framework for Camera Array Applications | 150 |
| <i>Lee Middleton, Sylvia C. Wong, Michael O. Jewell, John N. Carter, and Mark S. Nixon</i> | |

Soft Computing and Their Applications – IV

| | |
|--|-----|
| The Location of Optimum Set-Point Using a Fuzzy Controller | 157 |
| <i>Li Yan and Bin Qiu</i> | |

| | |
|--|-----|
| Genetic Modeling: Solution to Channel Assignment Problem | 164 |
| <i>Preeti Bajaj, Avinash G. Keskar, Amol Deshmukh, S. Dorle, and D. Padole</i> | |

| | |
|--|-----|
| On Self-organising Diagnostics in Impact Sensing Networks | 170 |
| <i>Mikhail Prokopenko, Peter Wang, Andrew Scott, Vadim Gerasimov, Nigel Hoschke, and Don Price</i> | |

| | |
|---|-----|
| A Coevolutionary Algorithm with Spieces as Varying Contexts | 179 |
| <i>Myung Won Kim, Joung Woo Ryu, and Eun Ju Kim</i> | |

| | |
|---|-----|
| Hybrid Filter Fusion for Robust Visual Information Processing | 186 |
| <i>Mi Young Nam and Phill Kyu Rhee</i> | |
| Edge Detection in Digital Image Using Variable Template Operator | 195 |
| <i>Young-Hyun Baek, Oh-Sung Byun, Sung-Ryong Moon, and Deok-Soo Baek</i> | |
| Combining Demographic Data with Collaborative Filtering for Automatic Music Recommendation | 201 |
| <i>Billy Yapriady and Alexandra L. Uitdenbogerd</i> | |
| Agent-Based Workflows, Knowledge Sharing and Reuse | |
| Different Perspectives on Modeling Workflows in an Agent Based Workflow Management System | 208 |
| <i>Bastin Tony Roy Savarimuthu, Maryam Purvis, and Martin Purvis</i> | |
| An Agent-Enhanced Workflow Management System | 215 |
| <i>Bastin Tony Roy Savarimuthu, Maryam Purvis, Martin Purvis, and Stephen Cranefield</i> | |
| Knowledge Sharing Between Design and Manufacture | 221 |
| <i>Sean D. Cochrane, Keith Case, Robert I. Young, Jenny A. Harding, and Samir Dani</i> | |
| Toward Improvement-Oriented Reuse of Experience in Engineering Design Processes | 228 |
| <i>Michalis Miatidis and Matthias Jarke</i> | |
| A Hybrid Approach to Determining the Best Combination on Product Form Design | 235 |
| <i>Yang-Cheng Lin, Hsin-Hsi Lai, Chung-Hsing Yeh, and Chen-Hui Hung</i> | |
| Utilizing Active Software to Capture Tacit Knowledge for Strategic Use | 242 |
| <i>Jenny Eriksson Lundström</i> | |
| Multi-media Authentication and Watermarking Applications | |
| A Bandwidth Efficiency of Lempel-Ziv Scheme for Data Authentication | 249 |
| <i>Chin-Chen Chang, Tzu-Chuen Lu, and Jun-Bin Yeh</i> | |
| Research on Confidential Level Extended BLP Model | 257 |
| <i>Xin Liu, Zhen Han, Ke-jun Sheng, and Chang-xiang Shen</i> | |
| Secure Tamper Localization in Binary Document Image Authentication | 263 |
| <i>Niladri B. Puhan and Anthony T.S. Ho</i> | |
| A Seal Imprint Verification with Rotation Invariance | 272 |
| <i>Takenobu Matsuura and Kenta Yamazaki</i> | |

| | |
|--|-----|
| Robust Authenticated Encryption Scheme with Message Linkages | 281 |
| <i>Eun-Jun Yoon and Kee-Young Yoo</i> | |
| BPCS-Steganography – Principle and Applications | 289 |
| <i>Eiji Kawaguchi</i> | |
| Improved Video Watermark Detection | |
| Using Statistically-Adaptive Accumulation | 300 |
| <i>Isao Echizen, Yasuhiro Fujii, Takaaki Yamada, Satoru Tezuka, and Hiroshi Yoshiura</i> | |
| Comparison of Feature Extraction Techniques for Watermark Synchronization | 309 |
| <i>Hae-Yeoun Lee, Heung-Kyu Lee, and Junseok Lee</i> | |
| Reversible Watermarking Based on Improved Patchwork Algorithm and Symmetric Modulo Operation | 317 |
| <i>ShaoWei Weng, Yao Zhao, and Jeng-Shyang Pan</i> | |
| Knowledge and Engineering Techniques for Spatio-temporal Applications | |
| Spatial Knowledge-Based Applications and Technologies: Research Issues | 324 |
| <i>Elisa Bertino and Maria Luisa Damiani</i> | |
| Managing Spatial Knowledge for Mobile Personalized Applications | 329 |
| <i>Joe Weakliam, Daniel Lynch, Julie Doyle, Helen Min Zhou, Eoin Mac Aoidh, Michela Bertolotto, and David Wilson</i> | |
| Geospatial Clustering in Data-Rich Environments: Features and Issues | 336 |
| <i>Ickjai Lee</i> | |
| Spatio-temporal Modeling of Moving Objects for Content- and Semantic-Based Retrieval in Video Data | 343 |
| <i>Choon-Bo Shim and Yong-Won Shin</i> | |
| Calendars and Topologies as Types | 352 |
| <i>François Bry, Bernhard Lorenz, and Stephanie Spranger</i> | |
| Moving Object Detection in Dynamic Environment | 359 |
| <i>M. Julius Hossain, Kiok Ahn, June Hyung Lee, and Oksam Chae</i> | |
| A General Framework Based on Dynamic Constraints for the Enrichment of a Topological Theory of Spatial Simulation | 366 |
| <i>Mehul Bhatt, Wenny Rahayu, and Gerald Sterling</i> | |
| Automatic Geomorphometric Analysis for Digital Elevation Models | 374 |
| <i>Miguel Moreno, Serguei Levachkine, Miguel Torres, Rolando Quintero, and G. Guzman</i> | |

Intelligent Data Analysis and Applications II

| | |
|---|-----|
| The Study of Electromagnetism-Like Mechanism Based Fuzzy Neural Network for Learning Fuzzy If-Then Rules | 382 |
| <i>Peitsang Wu, Kung-Jiuan Yang, and Yung-Yao Hung</i> | |
| Statistical Data Analysis for Software Metrics Validation | 389 |
| <i>Ming-Chang Lee</i> | |
| A Multi-stage Fuzzy-Grey Approach to Analyzing Software Development Cost .. | 396 |
| <i>Tony C.K. Huang, Gwo-Jen Hwang, and Judy C.R. Tseng</i> | |
| A Two-Phased Ontology Selection Approach for Semantic Web | 403 |
| <i>Tzung-Pei Hong, Wen-Chang Chang, and Jiann-Horng Lin</i> | |
| A Method for Acquiring Fingerprint by Linear Sensor | 410 |
| <i>Woong-Sik Kim and Weon-Hee Yoo</i> | |
| Evaluation and NLP | 417 |
| <i>Didier Nakache and Elisabeth Metais</i> | |

Creativity Support Environment and Its Social Applications

| | |
|--|-----|
| A Handwriting Tool to Support Creative Activities | 423 |
| <i>Kazuo Misue and Jiro Tanaka</i> | |
| Natural Storage in Human Body | 430 |
| <i>Shigaku Iwabuchi, Buntarou Shizuki, Kazuo Misue, and Jiro Tanaka</i> | |
| Computerized Support for Idea Generation During Knowledge Creating Process | 437 |
| <i>Xijin Tang, Yijun Liu, and Wen Zhang</i> | |
| Awareness in Group Decision: Communication Channel and GDSS | 444 |
| <i>Hitoshi Koshiba, Naotaka Kato, and Susumu Kunifugi</i> | |
| Aware Group Home: Person-Centered Care as Creative Problem Solving | 451 |
| <i>Ryozo Takatsuka and Tsutomu Fujinami</i> | |
| COLLECT-UML: Supporting Individual and Collaborative Learning of UML Class Diagrams in a Constraint-Based Intelligent Tutoring System | 458 |
| <i>Nilufar Baghaei and Antonija Mitrovic</i> | |
| Using Affective Learner States to Enhance Learning | 465 |
| <i>Amali Weerasinghe and Antonija Mitrovic</i> | |

Collective Intelligence

| | |
|--|-----|
| Three Foraging Models Comprised of Ants with Different Pheromone Sensitivities | 472 |
| <i>Mari Nakamura</i> | |
| Emerging of an Object Shape Information Caused by Signal-Transmission Relay of Multi-robots | 480 |
| <i>Sumiaki Ichikawa, Koji Hatayama, and Fumio Hara</i> | |

| | |
|--|-----|
| Autonomous Synchronization Scheme Access Control for Sensor Network | 487 |
| <i>Kosuke Sekiyama, Katsuhiro Suzuki, Shigeru Fukunaga, and Masaaki Date</i> | |
| Supporting Design for Manufacture Through Neutral Files and Feature Recognition | 496 |
| <i>T.J. Jones, C. Reidsema, and A. Smith</i> | |

| | |
|--|-----|
| A Programmable Pipelined Queue for Approximate String Matching | 503 |
| <i>Mitsuaki Nakasumi</i> | |

| | |
|--|-----|
| A Framework for Mining Association Rules | 509 |
| <i>Jun Luo and Sanguthevar Rajasekaran</i> | |

Computational Methods for Intelligent Neuro-fuzzy Applications

| | |
|--|-----|
| Near-Optimal Fuzzy Systems Using Polar Clustering: Application to Control of Vision-Based Arm-Robot | 518 |
| <i>Young-Joong Kim and Myo-Taeg Lim</i> | |

| | |
|---|-----|
| Door Traversing for a Vision-Based Mobile Robot Using PCA | 525 |
| <i>Min-Wook Seo, Young-Joong Kim, and Myo-Taeg Lim</i> | |

| | |
|--|-----|
| Local Feature Analysis with Class Information | 532 |
| <i>Yongjin Lee, Kyunghee Lee, Dosung Ahn, Sungbum Pan, Jin Lee, and Kiyoung Moon</i> | |

| | |
|---|-----|
| Training of Feature Extractor via New Cluster Validity – Application to Adaptive Facial Expression Recognition | 542 |
| <i>Sang Wan Lee, Dae-Jin Kim, Yong Soo Kim, and Zeungnam Bien</i> | |

| | |
|---|-----|
| Adaptive Fuzzy Output-Feedback Controller for SISO Affine Nonlinear Systems Without State Observer | 549 |
| <i>Jang-Hyun Park, Sam-Jun Seo, Dong-Won Kim, and Gwi-Tae Park</i> | |

| | |
|---|-----|
| High-Speed Extraction Model of Interest Region in the Parcel Image of Large Size | 559 |
| <i>Moon-sung Park, Il-sook Kim, Eun-kyung Cho, Young-hee Kwon, and Jong-heung Park</i> | |

| | |
|---|-----|
| Using Interval Singleton Type 2 Fuzzy Logic System in Corrupted Time Series Modelling | 566 |
| <i>Dong-Won Kim and Gwi-Tae Park</i> | |
| Evolutionary and Self-organizing Sensors, Actuators and Processing Hardware | |
| Defining and Detecting Emergence in Complex Networks | 573 |
| <i>Fabio Boschetti, Mikhail Prokopenko, Ian Macreadie, and Anne-Marie Grisogono</i> | |
| Annealing Sensor Networks | 581 |
| <i>Andrew Jennings and Daud Channa</i> | |
| Measuring Global Behaviour of Multi-agent Systems from Pair-Wise Mutual Information | 587 |
| <i>George Mathews, Hugh Durrant-Whyte, and Mikhail Prokopenko</i> | |
| In Use Parameter Estimation of Inertial Sensors by Detecting Multilevel Quasi-static States | 595 |
| <i>Ashutosh Saxena, Gaurav Gupta, Vadim Gerasimov, and Sébastien Ourselin</i> | |
| Knowledge Based Systems for e-Business and e-Learning I | |
| Self-restructuring Peer-to-Peer Network for e-Learning | 602 |
| <i>Masanori Ohshiro, Kenneth J. Mackin, Eiji Nunohiro, and Kazuko Yamasaki</i> | |
| An Improvement Approach for Word Tendency Using Decision Tree | 606 |
| <i>El-Sayed Atlam, Elmarhomy Ghada, Masao Fuketa, Kazuhiro Morita, and Jun-ichi Aoe</i> | |
| A New Technique of Determining Speaker's Intention for Sentences in Conversation | 612 |
| <i>Masao Fuketa, El-Sayed Atlam, Hiro Hanafusa, Kazuhiro Morita, Shinkaku Kashiji, Rokaya Mahmoud, and Jun-ichi Aoe</i> | |
| New Approach for Speeding-up Technique of the Retrieval Using Dynamic Full-Text Search Algorithm | 619 |
| <i>Kazuhiro Morita, El-Sayed Atlam, Masao Fuketa, Elmarhomy Ghada, Masaki Oono, Toru Sumitomo, and Jun-ichi Aoe</i> | |
| Multi-agent Systems and Evolutionary Computing | |
| Dafo, a Multi-agent Framework for Decomposable Functions Optimization | 626 |
| <i>Grégoire Danoy, Pascal Bouvry, and Olivier Boissier</i> | |
| Parameter Space Exploration of Agent-Based Models | 633 |
| <i>Benoît Calvez and Guillaume Hutzler</i> | |

| | |
|---|-----|
| Efficient Pre-processing for Large Window-Based Modular Exponentiation Using Ant Colony | 640 |
| <i>Nadia Nedjah and Luiza de Macedo Mourelle</i> | |
| COSATS, X-COSATS: | |
| Two Multi-agent Systems Cooperating Simulated Annealing, Tabu Search and X-Over Operator for the K-Graph Partitioning Problem | 647 |
| <i>Moez Hammami and Khaled Ghédira</i> | |
| Building Hyper-heuristics Through Ant Colony Optimization for the 2D Bin Packing Problem | 654 |
| <i>Alberto Cuesta-Cañada, Leonardo Garrido, and Hugo Terashima-Marín</i> | |
| Real-Time Co-composing System Using Multi-aspects | 661 |
| <i>Jens J. Balvig and Taizo Miyachi</i> | |
| Ubiquitous Pattern Recognition | |
| Empirical Study on Usefulness of Algorithm SACwRApper for Reputation Extraction from the WWW | 668 |
| <i>Hiroyuki Hasegawa, Mineichi Kudo, and Atsuyoshi Nakamura</i> | |
| New Logical Classes of Plausibility Functions in Dempster-Shafer Theory of Evidence | 675 |
| <i>Tetsuya Murai and Yasuo Kudo</i> | |
| Person Tracking with Infrared Sensors | 682 |
| <i>Taisuke Hosokawa and Mineichi Kudo</i> | |
| Entropy Criterion for Classifier-Independent Feature Selection | 689 |
| <i>Naoto Abe and Mineichi Kudo</i> | |
| Finding and Auto-labeling of Task Groups on E-Mails and Documents | 696 |
| <i>Hiroshi Tenmoto and Mineichi Kudo</i> | |
| Person Recognition by Pressure Sensors | 703 |
| <i>Masafumi Yamada, Jun Toyama, and Mineichi Kudo</i> | |
| Extraction and Revision of Signboard Images for Recognition of Character Strings | 709 |
| <i>Hirokazu Watabe and Tsukasa Kawaoka</i> | |
| Neural Networks for Data Mining | |
| Model Selection and Weight Sharing of Multi-layer Perceptrons | 716 |
| <i>Yusuke Tanahashi, Kazumi Saito, and Ryohei Nakano</i> | |
| Detecting Search Engine Spam from a Trackback Network in Blogspace | 723 |
| <i>Masahiro Kimura, Kazumi Saito, Kazuhiko Kazama, and Shin-ya Sato</i> | |

| | |
|---|-----|
| Analysis for Adaptability of Policy-Improving System with a Mixture Model of Bayesian Networks to Dynamic Environments | 730 |
| <i>Daisuke Kitakoshi, Hiroyuki Shioya, and Ryohei Nakano</i> | |
| Parallel Stochastic Optimization for Humanoid Locomotion Based on Neural Rhythm Generator | 738 |
| <i>Yoshihiko Itoh, Kenta Taki, Susumu Iwata, Shohei Kato, and Hidenori Itoh</i> | |
| Visualizing Dynamics of the Hot Topics Using Sequence-Based Self-organizing Maps | 745 |
| <i>Ken-ichi Fukui, Kazumi Saito, Masahiro Kimura, and Masayuki Numao</i> | |
| Intelligent Consumer Purchase Intention Prediction System for Green Products .. | 752 |
| <i>Rajiv Khosla, Clare D'Souza, and Mehdi Taghian</i> | |
| Intelligent Systems for e-Business and e-Learning II | |
| Reverse-Query Mechanism for Contents Delivery Management in Distributed Agent Network | 758 |
| <i>Yoshikatsu Fujita, Jun Yoshida, and Kazuhiko Tsuda</i> | |
| A My Page Service Realizing Method by Using Market Expectation Engine | 765 |
| <i>Masayuki Kessoku, Masakazu Takahashi, and Kazuhiko Tsuda</i> | |
| Multi-agent Modeling of Peer to Peer Communication with Scale-Free and Small-World Properties | 772 |
| <i>Shinako Matsuyama, Masaaki Kunigami, and Takao Terano</i> | |
| A Case-Oriented Game for Business Learning | 779 |
| <i>Kenji Nakano and Takao Terano</i> | |
| Learning Value-Added Information of Asset Management from Analyst Reports Through Text Mining | 785 |
| <i>Satoru Takahashi, Masakazu Takahashi, Hiroshi Takahashi, and Kazuhiko Tsuda</i> | |
| HHM-Based Risk Management for Business Gaming | 792 |
| <i>Toshikazu Shimodaira, Hua Xu, and Takao Terano</i> | |
| An Efficient Method for Creating Requirement Specification of Plant Control Software Using Domain Model | 799 |
| <i>Masakazu Takahashi, Kazutoshi Hanzawa, and Takashi Kawasaki</i> | |
| Knowledge-Based Technology in Crime Matching, Modelling and Prediction | |
| The Study and Application of Crime Emergency Ontology Event Model | 806 |
| <i>Wenjun Wang, Wei Guo, Yingwei Luo, Xiaolin Wang, and Zhuoqun Xu</i> | |

| | |
|--|-----|
| From Links to Meaning: A Burglary Data Case Study | 813 |
| <i>Giles Oatley, John Zelezniak, Richard Leary, and Brian Ewart</i> | |
| A Methodology for Constructing Decision Support Systems for Crime Detection | 823 |
| <i>John Zelezniak, Giles Oatley, and Richard Leary</i> | |
| AASLMA: An Automated Argument System Based on Logic of Multiple-Valued Argumentation | 830 |
| <i>Kumiko Matsunaga and Hajime Sawamura</i> | |
| Trust and Information-Taking Behavior in the Web Community | 839 |
| <i>Yumiko Nara</i> | |
| Soft Computing Applications | |
| Robust Intelligent Tuning of PID Controller for Multivariable System Using Clonal Selection and Fuzzy Logic | 848 |
| <i>Dong Hwa Kim</i> | |
| Intelligent Control of AVR System Using GA-BF | 854 |
| <i>Dong Hwa Kim and Jae Hoon Cho</i> | |
| Fault Diagnosis of Induction Motor Using Linear Discriminant Analysis | 860 |
| <i>Dae-Jong Lee, Jang-Hwan Park, Dong Hwa Kim, and Myung-Geun Chun</i> | |
| Classifier Fusion to Predict Breast Cancer Tumors Based on Microarray Gene Expression Data | 866 |
| <i>Mansoor Raza, Iqbal Gondal, David Green, and Ross L. Coppel</i> | |
| An Efficient Face Detection Method in Color Images | 875 |
| <i>Hongtao Yin, Ping Fu, and Shengwei Meng</i> | |
| A Robust and Invisible Watermarking of 3D Triangle Meshes | 881 |
| <i>Wang Liu and Sheng-He Sun</i> | |
| Advances of MPEG Scalable Video Coding Standard | 889 |
| <i>Wen-Hsiao Peng, Chia-Yang Tsai, Thao Chiang, and Hsueh-Ming Hang</i> | |
| Extended Fuzzy Description Logic ALCN | 896 |
| <i>Yanhui Li, Baowen Xu, Jianjiang Lu, Dazhou Kang, and Peng Wang</i> | |
| Automated Operator Selection on Genetic Algorithms | 903 |
| <i>Fredrik G. Hilding and Karen Ward</i> | |
| Weak Key Analysis and Micro-controller Implementation of CA Stream Ciphers | 910 |
| <i>Pascal Bouvry, Gilbert Klein, and Franciszek Seredyński</i> | |
| Author Index | 917 |

Table of Contents, Part I

Soft Computing Techniques in Stock Markets

| | |
|---|----|
| Multi-branch Neural Networks and Its Application to Stock Price Prediction | 1 |
| <i>Takashi Yamashita, Kotaro Hirasawa, and Jinglu Hu</i> | |
| An Intelligent Utilization of Neural Networks for Improving the Traditional Technical Analysis in the Stock Markets | 8 |
| <i>Norio Baba and Toshinori Nomura</i> | |
| Minority Game and the Wealth Distribution in the Artificial Market | 15 |
| <i>Mieko Tanaka-Yamawaki</i> | |
| A R/S Approach to Trends Breaks Detection | 21 |
| <i>Marina Resta</i> | |
| Applying Extending Classifier System to Develop an Option-Operation Suggestion Model of Intraday Trading – An Example of Taiwan Index Option . . . | 27 |
| <i>An-Pin Chen, Yi-Chang Chen, and Wen-Chuan Tseng</i> | |
| Applying Two-Stage XCS Model on Global Overnight Effect for Local Stock Prediction | 34 |
| <i>An-Pin Chen, Yi-Chang Chen, and Yu-Hua Huang</i> | |

Intelligent Network Based Education

| | |
|--|----|
| Automatically Assembled Shape Generation Using Genetic Algorithm in Axiomatic Design | 41 |
| <i>Jinpyoung Jung, Kang-Soo Lee, and Nam P. Suh</i> | |
| Network Based Engineering Design Education | 48 |
| <i>Kang-Soo Lee and Sang Hun Lee</i> | |
| Representative Term Based Feature Selection Method for SVM Based Document Classification | 56 |
| <i>YunHee Kang</i> | |
| The Design and Implementation of an Active Peer Agent Providing Personalized User Interface | 62 |
| <i>Kwangsu Cho, Sung-il Kim, and Sung-Hyun Yun</i> | |
| Using Bayesian Networks for Modeling Students' Learning Bugs and Sub-skills | 69 |
| <i>Shu-Chuan Shih and Bor-Chen Kuo</i> | |

| | |
|---|----|
| A Case-Based Reasoning Approach to Formulating University Timetables Using Genetic Algorithms | 76 |
| <i>Alicia Grech and Julie Main</i> | |
| A Computational Korean Mental Lexicon Model for a Cognitive-Neuro Scientific System | 84 |
| <i>Heui Seok Lim</i> | |
| An Application of Information Retrieval Technique to Automated Code Classification | 90 |
| <i>Heui Seok Lim and Seong Hoon Lee</i> | |

Maintenance and Customization of Business Knowledge

| | |
|---|-----|
| A Framework for Interoperability in an Enterprise | 97 |
| <i>Antonio Caforio, Angelo Corallo, and Danila Marco</i> | |
| Detecting <i>is-a</i> and <i>part-of</i> Relations in Heterogeneous Data Flow | 104 |
| <i>Paolo Ceravolo and Daniel Rocacher</i> | |
| OntoExtractor: A Fuzzy-Based Approach in Clustering Semi-structured Data Sources and Metadata Generation | 112 |
| <i>Zhan Cui, Ernesto Damiani, Marcello Leida, and Marco Viviani</i> | |
| Generate Context Metadata Based on Biometric System | 119 |
| <i>Antonia Azzini, Paolo Ceravolo, Ernesto Damiani, Cristiano Fugazza, Salvatore Reale, and Massimiliano Torregiani</i> | |
| Complex Association Rules for XML Documents | 127 |
| <i>Carlo Combi, Barbara Oliboni, and Rosalba Rossato</i> | |
| A Rule-Based and Computation-Independent Business Modelling Language for Digital Business Ecosystems | 134 |
| <i>Maurizio De Tommasi, Virginia Cisternino, and Angelo Corallo</i> | |

| | |
|--|-----|
| Building Bottom-Up Ontologies for Communities of Practice in High-Tech Firms | 142 |
| <i>Marina Biscozzo, Angelo Corallo, and Gianluca Elia</i> | |

Intelligent Data Processing in Process Systems and Plants

| | |
|--|-----|
| Decision Support System for Atmospheric Corrosion of Carbon Steel Pipes | 149 |
| <i>Kazuhiro Takeda, Yoshifumi Tsuge, Hisayoshi Matsuyama, and Eiji O'shima</i> | |
| Analogical Reasoning Based on Task Ontologies for On-Line Support | 155 |
| <i>Takashi Hamaguchi, Taku Yamazaki, Meng Hu, Masaru Sakamoto, Koji Kawano, Teiji Kitajima, Yukiyasu Shimada, Yoshihiro Hashimoto, and Toshiaki Itoh</i> | |

| | |
|--|-----|
| Development of Engineering Ontology on the Basis of IDEF0 Activity Model | 162 |
| <i>Tetsuo Fuchino, Toshihiro Takamura, and Rafael Batres</i> | |
| A Novel Approach to Retrosynthetic Analysis | |
| Utilizing Knowledge Bases Derived from Reaction Databases | 169 |
| <i>Kimito Funatsu</i> | |
| Reconfigurable Power-Aware Scalable Booth Multiplier | 176 |
| <i>Hanho Lee</i> | |
| Base Reference Analytical Hierarchy Process for Engineering Process Selection . | 184 |
| <i>Elina Hotman</i> | |
| A Multiagent Model for Intelligent Distributed Control Systems | 191 |
| <i>José Aguilar, Mariela Cerrada, Gloria Mousalli, Franklin Rivas, and Francisco Hidrobo</i> | |
| Study on the Development of Design Rationale Management System for Chemical Process Safety | 198 |
| <i>Yukiyasu Shimada, Takashi Hamaguchi, and Tetsuo Fuchino</i> | |
| Intelligent Agent Technology and Applications I | |
| A Multiple Agents Based Intrusion Detection System | 205 |
| <i>Wanli Ma and Dharmendra Sharma</i> | |
| Agent-Based Software Architecture for Simulating Distributed Negotiation . . . | 212 |
| <i>V. Kris Murthy</i> | |
| A Multi-agent Framework for .NET | 219 |
| <i>Naveen Sharma and Dharmendra Sharma</i> | |
| On an IT Security Framework | 226 |
| <i>Dharmendra Sharma, Wanli Ma, and Dat Tran</i> | |
| Investigating the Transport Communicating Rates of Wireless Networks over Fading Channels | 233 |
| <i>Xu Huang and A.C. Madoc</i> | |
| Agent Team Coordination in the Mobile Agent Network | 240 |
| <i>Mario Kusek, Ignac Lovrek, and Vjekoslav Sinkovic</i> | |
| Forming Proactive Team Cooperation by Observations | 247 |
| <i>Yu Zhang and Richard A. Volz</i> | |
| Intelligent Design Support Systems | |
| Microscopic Simulation in Decision Support System for the Incident Induced Traffic Management | 255 |
| <i>Hojung Kim, S. Akhtar Ali Shah, Heyonho Jang, and Byung-Ha Ahn</i> | |

XXXVI Table of Contents, Part I

| | |
|---|-----|
| Development and Implementation on a Fuzzy Multiple Objective Decision Support System | 261 |
| <i>Fengjie Wu, Jie Lu, and Guangquan Zhang</i> | |
| IM3: A System for Matchmaking in Mobile Environments | 268 |
| <i>Andrea Calì</i> | |
| Towards Using First-Person Shooter Computer Games as an Artificial Intelligence Testbed | 276 |
| <i>Mark Dawes and Richard Hall</i> | |
| Structured Reasoning to Support Deliberative Dialogue | 283 |
| <i>Alyx Macfadyen, Andrew Stranieri, and John Yearwood</i> | |
| A New Approach for Conflict Resolution of Authorization | 290 |
| <i>Yun Bai</i> | |
| Knowledge-Based System for Color Maps Recognition | 297 |
| <i>Serguei Levachkine, Efrén González, Miguel Torres, Marco Moreno, and Rolando Quintero</i> | |
| Data Engineering, Knowledge Engineering and Ontologies | |
| Constructing an Ontology Based on Terminology Processing | 304 |
| <i>Soo-Yeon Lim, Seong-Bae Park, and Sang-Jo Lee</i> | |
| A Matrix Representation and Mapping Approach to Knowledge Acquisition for Product Design | 311 |
| <i>Zhiming Rao and Chun-Hsien Chen</i> | |
| A Unifying Ontology Modeling for Knowledge Management | 318 |
| <i>An-Pin Chen and Mu-Yen Chen</i> | |
| A Model Transformation Based Conceptual Framework for Ontology Evolution | 325 |
| <i>Longfei Jin, Lei Liu, and Dong Yang</i> | |
| On Knowledge-Based Editorial Design System | 332 |
| <i>Hyojeong Jin and Ikuro Choh</i> | |
| Knowledge Representation for the Intelligent Legal Case Retrieval | 339 |
| <i>Yiming Zeng, Ruili Wang, John Zelezniak, and Elizabeth Kemp</i> | |
| An OCR Post-processing Approach Based on Multi-knowledge | 346 |
| <i>Li Zhuang and Xiaoyan Zhu</i> | |
| Knowledge Discovery and Data Mining | |
| Data Mining in Parametric Product Catalogs | 353 |
| <i>Lingrui Liao and Tianyuan Xiao</i> | |

| | |
|--|-----|
| Mining Quantitative Data Based on Tolerance Rough Set Model | 359 |
| <i>Hsuan-Shih Lee, Pei-Di Shen, Wen-Li Chyr, and Wei-Kuo Tseng</i> | |
| Incremental Association Mining Based on Maximal Itemsets | 365 |
| <i>Hsuan-Shih Lee</i> | |
| Information-Based Pruning for Interesting Association Rule Mining in the Item Response Dataset | 372 |
| <i>Hyeoncheol Kim and Eun-Young Kwak</i> | |
| On Mining XML Structures Based on Statistics | 379 |
| <i>Hiroshi Ishikawa, Shohei Yokoyama, Manabu Ohta, and Kaoru Katayama</i> | |
| A New Cell-Based Clustering Method for High-Dimensional Data Mining Applications | 391 |
| <i>Jae-Woo Chang</i> | |
| An Application of Apriori Algorithm on a Diabetic Database | 398 |
| <i>Nevcihan Duru</i> | |
| Advanced Network Application | |
| Network Software Platform Design for Wireless Real-World Integration Applications | 405 |
| <i>Toshihiko Yamakami</i> | |
| Development of Ubiquitous Historical Tour Support System | 412 |
| <i>Satoru Fujii, Yusuke Takahashi, Hisao Fukuoka, Teruhisa Ichikawa, Sanshiro Sakai, and Tadanori Mizuno</i> | |
| Capturing Window Attributes for Extending Web Browsing History Records | 418 |
| <i>Motoki Miura, Susumu Kunifugi, Shogo Sato, and Jiro Tanaka</i> | |
| Development of an Intercultural Collaboration System with Semantic Information Share Function | 425 |
| <i>Kunikazu Fujii, Takashi Yoshino, Tomohiro Shigenobu, and Jun Munemori</i> | |
| Position Estimation for Goods Tracking System Using Mobile Detectors | 431 |
| <i>Hiroshi Mineno, Kazuo Hida, Miho Mizutani, Naoto Miyachi, Kazuhiro Kusunoki, Akira Fukuda, and Tadanori Mizuno</i> | |
| Dual Communication System Using Wired and Wireless Correspondence in Home Network | 438 |
| <i>Kunihiro Yamada, Kenichi Kitazawa, Hiroki Takase, Toshihiko Tamura, Yukihsia Naoe, Takashi Furumura, Toru Shimizu, Koji Yoshida, Masanori Kojima, and Tadanori Mizuno</i> | |
| The Architecture to Implement the Home Automation Systems with LabVIEW TM | 445 |
| <i>Kyung-Bae Chang, Jae-Woo Kim, Il-Joo Shim, and Gwi-Tae Park</i> | |

XXXVIII Table of Contents, Part I

| | |
|---|-----|
| Separated Ethernet Algorithm for Intelligent Building Network Integration Using TCP/IP | 452 |
| <i>Kyung-Bae Chang, Il-Joo Shim, and Gwi-Tae Park</i> | |

Approaches and Methods of Security Engineering I

| | |
|---|-----|
| Operational Characteristics of Intelligent Dual-Reactor with Current Controlled Inverter | 459 |
| <i>Su-Won Lee and Sung-Hun Lim</i> | |

| | |
|--|-----|
| Design and Evaluation of an SARHR Scheme for Mobility Management in Ad Hoc Networks | 465 |
| <i>Ihn-Han Bae</i> | |

| | |
|---|-----|
| Reliability and Capacity Enhancement Algorithms for Wireless Personal Area Network Using an Intelligent Coordination Scheme .. | 472 |
| <i>Chang-Heon Oh, Chul-Gyu Kang, and Jae-Young Kim</i> | |

| | |
|--|-----|
| A Study of Power Network Stabilization Using an Artificial Neural Network .. | 479 |
| <i>Phil-Hun Cho, Myong-Chul Shin, Hak-Man Kim, and Jae-Sang Cha</i> | |

| | |
|---|-----|
| An Adaptive Repeater System for OFDM with Frequency Hopping Control to Reduce the Interference | 485 |
| <i>Hui-shin Chae, Kye-san Lee, and Jae-Sang Cha</i> | |

| | |
|---|-----|
| Intelligent and Effective Digital Watermarking Scheme for Mobile Content Service | 492 |
| <i>Hang-Rae Kim, Young Park, Mi-Hee Yoon, and Yoon-Ho Kim</i> | |

| | |
|---|-----|
| Performance Improvement of OFDM System Using an Adaptive Coding Technique in Wireless Home Network | 498 |
| <i>JiWoong Kim and Heau Jo Kang</i> | |

| | |
|---|-----|
| Arbitrated Verifier Signature with Message Recovery for Proof of Ownership .. | 504 |
| <i>Hyung-Woo Lee</i> | |

Chance Discovery I

| | |
|---|-----|
| Human-Based Annotation of Data-Based Scenario Flow on Scenario Map for Understanding Hepatitis Scenarios | 511 |
| <i>Yukio Ohsawa</i> | |

| | |
|--|-----|
| A Scenario Elicitation Method in Cooperation with Requirements Engineering and Chance Discovery | 518 |
| <i>Noriyuki Kushiro and Yukio Ohsawa</i> | |

| | |
|---|-----|
| The Interactive Evolutionary Computation Based on the Social Distance to Extend the KeyGraph | 526 |
| <i>Mu-Hua Lin, Hsiao-Fang Yang, and Chao-Fu Hong</i> | |

| | |
|--|-----|
| Chance Path Discovery: A Context of Creative Design by Using Interactive Genetic Algorithms | 533 |
| <i>Leuo-hong Wang, Chao-Fu Hong, and Meng-yuan Song</i> | |
| Supporting Exploratory Data Analysis by Preserving Contexts | 540 |
| <i>Mitsunori Matsushita</i> | |
| Chance Discovery and the Disembodiment of Mind | 547 |
| <i>Lorenzo Magnani</i> | |
| Modeling the Discovery of Critical Utterances | 554 |
| <i>Calkin A.S. Montero, Yukio Ohsawa, and Kenji Araki</i> | |

Information Hiding and Multimedia Signal Processing

| | |
|---|-----|
| Optimizing Interference Cancellation of Adaptive Linear Array by Phase-Only Perturbations Using Genetic Algorithms | 561 |
| <i>Chao-Hsing Hsu, Wen-Jye Shyr, and Kun-Huang Kuo</i> | |
| Optimizing Linear Adaptive Broadside Array Antenna by Amplitude-Position Perturbations Using Memetic Algorithms | 568 |
| <i>Chao-Hsing Hsu and Wen-Jye Shyr</i> | |
| Stability in Web Server Performance with Heavy-Tailed Distribution | 575 |
| <i>Takuo Nakashima and Mamoru Tsuichihara</i> | |
| Using Normal Vectors for Stereo Correspondence Construction | 582 |
| <i>Jung-Shiong Chang, Arthur Chun-Chieh Shih, Hong-Yuan Mark Liao, and Wen-Hsien Fang</i> | |
| Color Image Restoration Using Explicit Local Segmentation | 589 |
| <i>Mieng Quoc Phu, Peter Tischer, and Hon Ren Wu</i> | |

| | |
|--|-----|
| Weight Training for Performance Optimization in Fuzzy Neural Network | 596 |
| <i>Hui-Chen Chang and Yau-Tarng Juang</i> | |
| Optimal Design Using Clonal Selection Algorithm | 604 |
| <i>Yi-Hui Su, Wen-Jye Shyr, and Te-Jen Su</i> | |

Soft Computing Techniques and Their Applications I

| | |
|---|-----|
| Wrist Motion Pattern Recognition System by EMG Signals | 611 |
| <i>Yuji Matsumura, Minoru Fukumi, and Norio Akamatsu</i> | |
| Analysis of RED with Multiple Class-Based Queues for Supporting Proportional Differentiated Services | 618 |
| <i>Jahwan Koo and Seongjin Ahn</i> | |

| | |
|--|-----|
| Learning Behaviors of the Hierarchical Structure Stochastic Automata. Operating in the Nonstationary Multiteacher Environment | 624 |
| <i>Norio Baba and Yoshio Mogami</i> | |
| Nonlinear State Estimation by Evolution Strategies Based Gaussian Sum Particle Filter | 635 |
| <i>Katsuji Uosaki and Toshiharu Hatanaka</i> | |
| Feature Generation by Simple FLD | 643 |
| <i>Minoru Fukumi and Yasue Mitsukura</i> | |
| Computational Intelligence for Cyclic Gestures Recognition of a Partner Robot | 650 |
| <i>Naoyuki Kubota and Minoru Abe</i> | |
| Influence of Music Listening on the Cerebral Activity by Analyzing EEG | 657 |
| <i>Takahiro Ogawa, Satomi Ota, Shin-ichi Ito, Yasue Mitsukura, Minoru Fukumi, and Norio Akamatsu</i> | |
| Intelligent Agent Technology and Applications II | |
| A Goal Oriented e-Learning Agent System | 664 |
| <i>Dongtao Li, Zhiqi Shen, Yuan Miao, Chunyan Miao, and Robert Gay</i> | |
| iJADE Tourist Guide – A Mobile Location-Awareness Agent-Based System for Tourist Guiding | 671 |
| <i>Tony W.H. Ao Leong, Toby H.W. Lam, Alex C.M. Lee, and Raymond S.T. Lee</i> | |
| The Design and Implementation of an Intelligent Agent-Based Adaptive Bargaining Model (ABM) | 678 |
| <i>Raymond Y.W. Mak and Raymond S.T. Lee</i> | |
| Behavior-Based Blind Goal-Oriented Robot Navigation by Fuzzy Logic | 686 |
| <i>Meng Wang and James N.K. Liu</i> | |
| iJADE Reporter – An Intelligent Multi-agent Based Context – Aware News Reporting System | 693 |
| <i>Eddie C.L. Chan and Raymond S.T. Lee</i> | |
| Architecture of a Web Operating System Based on Multiagent Systems | 700 |
| <i>José Aguilar, Niriaska Perozo, Edgar Ferrer, and Juan Vizcarondo</i> | |
| A Study of Train Group Operation Multi-agent Model Oriented to RITS | 707 |
| <i>Yangdong Ye, Zundong Zhang, Honghua Dai, and Limin Jia</i> | |
| Representation of Procedural Knowledge of an Intelligent Agent Using a Novel Cognitive Memory Model | 714 |
| <i>Kumari Wickramasinghe and Damminda Alahakoon</i> | |

Smart Systems

| | |
|--|-----|
| A Knowledge-Based Interaction Model Between Users and an Adaptive Information System | 722 |
| <i>Angelo Corallo, Gianluca Elia, Gianluca Lorenzo, and Gianluca Solazzo</i> | |
| Smart Clients and Small Business Model | 730 |
| <i>Phu-Nhan Nguyen, Dharmendra Sharma, and Dat Tran</i> | |
| Synthetic Character with Bayesian Network and Behavior Network for Intelligent Smartphone | 737 |
| <i>Sang-Jun Han and Sung-Bae Cho</i> | |
| The Virtual Technician: An Automatic Software Enhancer for Audio Recording in Lecture Halls | 744 |
| <i>Gerald Friedland, Kristian Jantz, Lars Knipping, and Raúl Rojas</i> | |
| Intelligent Environments for Next-Generation e-Markets | 751 |
| <i>John Debenham and Simeon Simoff</i> | |
| Autonomous and Continuous Evolution of Information Systems | 758 |
| <i>Jingde Cheng</i> | |
| Dynamic Location Management for On-Demand Car Sharing System | 768 |
| <i>Naoto Mukai and Toyohide Watanabe</i> | |

Knowledge – Based Interface Systems

| | |
|--|-----|
| Writer Recognition by Using New Searching Algorithm in New Local Arc Method | 775 |
| <i>Masahiro Ozaki, Yoshinori Adachi, and Naohiro Ishii</i> | |
| Development of Judging Method of Understanding Level in Web Learning | 781 |
| <i>Yoshinori Adachi, Koichi Takahashi, Masahiro Ozaki, and Yuji Iwahori</i> | |
| Organising Documents Based on Standard-Example Split Test | 787 |
| <i>Kenta Fukuoka, Tomofumi Nakano, and Nobuhiro Inuzuka</i> | |
| e-Learning Materials Development Based on Abstract Analysis Using Web Tools | 794 |
| <i>Tomofumi Nakano and Yukie Koyama</i> | |
| Effect of Insulating Coating on Lightning Flashover Characteristics of Electric Power Line with Insulated Covered Conductor | 801 |
| <i>Kenji Yamamoto, Yosihiko Kunieda, Masashi Kawaguchi, Zen-ichiro Kawasaki, and Naohiro Ishii</i> | |
| Study on the Velocity of Saccadic Eye Movements | 808 |
| <i>Hiroshi Sasaki and Naohiro Ishii</i> | |

| | |
|---|-----|
| Relative Magnitude of Gaussian Curvature from Shading Images Using Neural Network | 813 |
| <i>Yuji Iwashiori, Shinji Fukui, Chie Fujitani, Yoshinori Adachi, and Robert J. Woodham</i> | |

| | |
|---|-----|
| Parallelism Improvements of Software Pipelining by Combining Spilling with Rematerialization | 820 |
| <i>Naohiro Ishii, Hiroaki Ogi, Tsubasa Mochizuki, and Kazunori Iwata</i> | |

Intelligent Information Processing for Remote Sensing

| | |
|---|-----|
| Content Based Retrieval of Hyperspectral Images Using AMM Induced Endmembers | 827 |
| <i>Orlando Maldonado, David Vicente, Manuel Graña, and Alicia d’Anjou</i> | |

| | |
|---|-----|
| Hyperspectral Image Watermarking with an Evolutionary Algorithm | 833 |
| <i>D. Sal and Manuel Graña</i> | |

| | |
|---|-----|
| A Profiling Based Intelligent Resource Allocation System | 840 |
| <i>J. Monroy, Jose A. Becerra, Francisco Bellas, Richard J. Duro, and Fernando López-Peña</i> | |

| | |
|---|-----|
| Blind Signal Separation Through Cooperating ANNs | 847 |
| <i>Francisco Bellas, Richard J. Duro, and Fernando López-Peña</i> | |

| | |
|---|-----|
| Tropical Cyclone Eye Fix Using Genetic Algorithm with Temporal Information .. | 854 |
| <i>Ka Yan Wong and Chi Lap Yip</i> | |

| | |
|---|-----|
| Meteorological Phenomena Measurement System Using the Wireless Network .. | 861 |
| <i>Kyung-Bae Chang, Il-Joo Shim, Seung-Woo Shin, and Gwi-Tae Park</i> | |

| | |
|---|-----|
| An Optimal Nonparametric Weighted System for Hyperspectral Data Classification | 866 |
| <i>Li-Wei Ko, Bor-Chen Kuo, and Ching-Teng Lin</i> | |

| | |
|--|-----|
| Regularized Feature Extractions and Support Vector Machines for Hyperspectral Image Data Classification | 873 |
| <i>Bor-Chen Kuo and Kuang-Yu Chang</i> | |

Intelligent Human Computer Interaction Systems

| | |
|---|-----|
| An Error Measure for Japanese Morphological Analysis Using Similarity Measures | 880 |
| <i>Yoshiaki Kurosawa, Yuji Sakamoto, Takumi Ichimura, and Teruaki Aizawa</i> | |

| | |
|--|-----|
| Distributed Visual Interfaces for Collaborative Exploration of Data Spaces | 887 |
| <i>Sung Baik, Jerzy Bala, and Yung Jo</i> | |

| | |
|---|-----|
| Attribute Intensity Calculating Method from Evaluative Sentences by Fuzzy Inference | 893 |
| <i>Kazuya Mera, Hiromi Yano, and Takumi Ichimura</i> | |
| Proposal of Impression Mining from News Articles | 901 |
| <i>Tadahiko Kumamoto and Katsumi Tanaka</i> | |
| An Experimental Study on Computer Programming with Linguistic Expressions | 911 |
| <i>Nozomu Kaneko and Takehisa Onisawa</i> | |
| Enhancing Computer Chat: Toward a Smooth User-Computer Interaction | 918 |
| <i>Calkin A.S. Montero and Kenji Araki</i> | |
| Effect of Direct Communication in Ant System | 925 |
| <i>Akira Hara, Takumi Ichimura, Tetsuyuki Takahama, Yoshinori Isomichi, and Motoki Shigemi</i> | |
| Multi-agent Cluster System for Optimal Performance in Heterogeneous Computer Environments | 932 |
| <i>Toshihiro Ikeda, Akira Hara, Takumi Ichimura, Tetsuyuki Takahama, Yuko Taniguchi, Hiroshige Yamada, Ryota Hakozaki, and Haruo Sakuda</i> | |
| Experience Management and Knowledge Management | |
| Exploring the Interplay Between Domain-Independent and Domain-Specific Concepts in Computer-Supported Collaboration | 938 |
| <i>Christina E. Evangelou and Nikos Karacapilidis</i> | |
| Using XML for Implementing Set of Experience Knowledge Structure | 946 |
| <i>Cesar Sanin and Edward Szczerbicki</i> | |
| A Framework of Checking Subsumption Relations Between Composite Concepts in Different Ontologies | 953 |
| <i>Dazhou Kang, Jianjiang Lu, Baowen Xu, Peng Wang, and Yanhui Li</i> | |
| A Knowledge Acquisition System for the French Textile and Apparel Institute ... | 960 |
| <i>Oswaldo Castillo Navetty and Nada Matta</i> | |
| Two-Phase Path Retrieval Method for Similar XML Document Retrieval | 967 |
| <i>Jae-Min Lee and Byung-Yeon Hwang</i> | |
| MEBRS: A Multiagent Architecture for an Experience Based Reasoning System . | 972 |
| <i>Zhaohao Sun and Gavin Finnie</i> | |
| Experience Management in Knowledge Management | 979 |
| <i>Zhaohao Sun and Gavin Finnie</i> | |

Network (Security) Real-Time and Fault Tolerant Systems

| | |
|---|------|
| Rule Based Congestion Management – | |
| Monitoring Self-similar IP Traffic in Diffserv Networks | 987 |
| <i>S. Suresh and Özdemir Göl</i> | |
| A Parallel Array Architecture of MIMO Feedback Network | |
| and Real Time Implementation | 996 |
| <i>Yong Kim and Hong Jeong</i> | |
| Wavelength Converter Assignment Problem in All Optical WDM Networks | 1004 |
| <i>Jungman Hong, Seungkil Lim, and Wookey Lee</i> | |
| Real-Time System-on-a-Chip Architecture | |
| for Rule-Based Context-Aware Computing | 1014 |
| <i>Seung Wook Lee, Jong Tae Kim, Bong Ki Sohn, Keon Myung Lee, Jee Hyung Lee, Jae Wook Jeon, and Sukhan Lee</i> | |
| Mobile Agent System | |
| for Jini Networks Employing Remote Method Invocation Technology | 1021 |
| <i>Sang Tae Kim, Byoung-Ju Yun, and Hyun Deok Kim</i> | |
| Incorporating Privacy Policy | |
| into an Anonymity-Based Privacy-Preserving ID-Based Service Platform | 1028 |
| <i>Keon Myung Lee, Jee-Hyong Lee, and Myung-Geun Chun</i> | |
| A Quantitative Trust Model Based on Multiple Evaluation Criteria | 1036 |
| <i>Hak Joon Kim and Keon Myung Lee</i> | |

Advanced Network Application and Real-Time Systems

| | |
|---|------|
| Groupware for a New Idea Generation | |
| with the Semantic Chat Conversation Data | 1044 |
| <i>Takaya Yuizono, Akifumi Kayano, Tomohiro Shigenobu, Takashi Yoshino, and Jun Munemori</i> | |
| Dual Communication System Using Wired and Wireless | |
| with the Routing Consideration | 1051 |
| <i>Kunihiro Yamada, Takashi Furumura, Yoshio Inoue, Kenichi Kitazawa, Hiroki Takase, Yukihisa Naoe, Toru Shimizu, Yoshihiko Hirata, Hiroshi Mineno, and Tadanori Mizuno</i> | |
| Development and Evaluation of an Emotional Chat System | |
| Using Sense of Touch | 1057 |
| <i>Hajime Yoshida, Tomohiro Shigenobu, Takaya Yuizono, Takashi Yoshino, and Jun Munemori</i> | |

| | |
|---|------|
| Theory and Application of Artificial Neural Networks for the Real Time Prediction of Ship Motion | 1064 |
| <i>Ameer Khan, Cees Bil, and Kaye E. Marion</i> | |
| Soft Computing Based Real-Time Traffic Sign Recognition: A Design Approach | 1070 |
| <i>Preeti Bajaj, A. Dalavi, Sushant Dubey, Mrinal Mouza, Shalabh Batra, and Sarika Bhojwani</i> | |
| A Soft Real-Time Guaranteed Java M:N Thread Mapping Method | 1075 |
| <i>Seung-Hyun Min, Kwang-Ho Chun, Young-Rok Yang, and Myoung-Jun Kim</i> | |

| | |
|---|------|
| A Genetic Information Based Load Redistribution Approach Including High-Response Time in Distributed Computing System | 1081 |
| <i>Seong Hoon Lee, Dongwoo Lee, Wankwon Lee, and Hyunjoon Cho</i> | |
| An Architecture of a Wavelet Based Approach for the Approximate Querying of Huge Sets of Data in the Telecommunication Environment | 1088 |
| <i>Ernesto Damiani, Stefania Marrara, Salvatore Reale, and Massimiliano Torregiani</i> | |

Approaches and Methods of Security Engineering II

| | |
|--|------|
| Performance Comparison of M-ary PPM Ultra-wideband Multiple Access System Using an Intelligent Pulse Shaping Techniques | 1094 |
| <i>SungEon Cho and JaeMin Kwak</i> | |
| Implementation of a Network-Based Distributed System Using the CAN Protocol | 1104 |
| <i>Joonhong Jung, Kiheon Park, and Jae-Sang Cha</i> | |
| Implementation of Adaptive Reed-Solomon Decoder for Context-Aware Mobile Computing Device | 1111 |
| <i>Seung Wook Lee, Jong Tae Kim, and Jae-Sang Cha</i> | |
| Authenticated IPv6 Packet Traceback Against Reflector Based Packet Flooding Attack | 1118 |
| <i>Hyung-Woo Lee and Sung-Hyun Yun</i> | |
| A Relationship Between Products Evaluation and IT Systems Assurance | 1125 |
| <i>Tai-hoon Kim and Seung-youn Lee</i> | |
| Knowledge Acquisition for Mobile Embedded Software Development Based on Product Line | 1131 |
| <i>Haeng-Kon Kim</i> | |
| Gesture Recognition by Attention Control Method for Intelligent Humanoid Robot | 1139 |
| <i>Jae Yong Oh, Chil Woo Lee, and Bum Jae You</i> | |

| | |
|---|------|
| Intelligent Multimedia Service System Based on Context Awareness in Smart Home | 1146 |
| <i>Jong-Hyuk Park, Heung-Soo Park, Sang-Jin Lee, Jun Choi, and Deok-Gyu Lee</i> | |
| Chance Discovery II | |
| Analysis of Opinion Leader in On-Line Communities | 1153 |
| <i>Gao Junbo, Zhang Min, Jiang Fan, and Wang Xufa</i> | |
| Optimum Pricing Strategy for Maximization of Profits and Chance Discovery | 1160 |
| <i>Kohei Yamamoto and Katsutoshi Yada</i> | |
| Risk Management by Focusing on Critical Words in Nurses' Conversations | 1167 |
| <i>Akinori Abe, Futoshi Naya, Hiromi Itoh Ozaku, Kaoru Sagara, Noriaki Kuwahara, and Kiyoshi Kogure</i> | |
| Extracting High Quality Scenario for Consensus on Specifications of New Products | 1174 |
| <i>Kenichi Horie and Yukio Ohsawa</i> | |
| How Can You Discover Yourselves During Job-Hunting? | 1181 |
| <i>Hiroko Shoji</i> | |
| An Extended Two-Phase Architecture for Mining Time Series Data | 1186 |
| <i>An-Pin Chen, Yi-Chang Chen, and Nai-Wen Hsu</i> | |
| Intelligent Watermarking Algorithms | |
| A Performance Comparison of High Capacity Digital Watermarking Systems | 1193 |
| <i>Yuk Ying Chung, Penghao Wang, Xiaoming Chen, Changseok Bae, ahmed Fawzi Otoom, and Tich Phuoc Tran</i> | |
| Tolerance on Geometrical Operation as an Attack to Watermarked JPEG Image . | 1199 |
| <i>Cong-Kha Pham and Hiroshi Yamashita</i> | |
| A High Robust Blind Watermarking Algorithm in DCT Domain | 1205 |
| <i>Ching-Tang Hsieh and Min-Yen Hsieh</i> | |
| Improved Quantization Watermarking with an Adaptive Quantization Step Size and HVS | 1212 |
| <i>Zhao Yuanyuan and Zhao Yao</i> | |
| Energy-Efficient Watermark Algorithm Based on Pairing Mechanism | 1219 |
| <i>Yu-Ting Pai, Shanq-Jang Ruan, and Jürgen Götze</i> | |
| Implementation of Image Steganographic System Using Wavelet Zerotree | 1226 |
| <i>Yuk Ying Chung, Yong Sun, Penghao Wang, Xiaoming Chen, and Changseok Bae</i> | |

| | |
|--|------|
| A RST-Invariant Robust DWT-HMM Watermarking Algorithm Incorporating Zernike Moments and Template | 1233 |
| <i>Jiangqun Ni, Chuntao Wang, Jiwu Huang, and Rongyue Zhang</i> | |
| Security Evaluation of Generalized Patchwork Algorithm from Cryptanalytic Viewpoint | 1240 |
| <i>Tanmoy Kanti Das, Hyoung Joong Kim, and Subhamoy Maitra</i> | |
| Soft Computing Techniques and Their Applications II | |
| Reinforcement Learning by Chaotic Exploration Generator in Target Capturing Task | 1248 |
| <i>Koichiro Morihiro, Teijiyo Isokawa, Nobuyuki Matsui, and Haruhiko Nishimura</i> | |
| Prediction of Foul Ball Falling Spot in a Base Ball Game | 1255 |
| <i>Hideyuki Takajo, Minoru Fukumi, and Norio Akamatsu</i> | |
| Automatic Extraction System of a Kidney Region Based on the Q-Learning | 1261 |
| <i>Yoshiki Kubota, Yasue Mitsukura, Minoru Fukumi, Norio Akamatsu, and Motokatsu Yasutomo</i> | |
| Drift Ice Detection Using a Self-organizing Neural Network | 1268 |
| <i>Minoru Fukumi, Taketsugu Nagao, Yasue Mitsukura, and Rajiv Khosla</i> | |
| Word Sense Disambiguation of Thai Language with Unsupervised Learning | 1275 |
| <i>Sunee Pongpinigpinyo and Wanchai Rivepiboon</i> | |
| Differential Evolution with Self-adaptive Populations | 1284 |
| <i>Jason Teo</i> | |
| Binary Neural Networks – A CMOS Design Approach | 1291 |
| <i>Amol Deshmukh, Jayant Morghade, Akashdeep Khera, and Preeti Bajaj</i> | |
| Video Rate Control Using an Adaptive Quantization Based on a Combined Activity Measure | 1297 |
| <i>Si-Woong Lee, Sung-Hoon Hong, Jae Gark Choi, Yun-Ho Ko, and Byoung-Ju Yun</i> | |
| Author Index | 1303 |

Table of Contents, Part II

Machine Learning

| | |
|--|----|
| POISE – Achieving Content-Based Picture Organisation for Image Search Engines | 1 |
| <i>Da Deng and Heiko Wolf</i> | |
| Estimation of the Hierarchical Structure of a Video Sequence Using MPEG-7 Descriptors and GCS | 8 |
| <i>Masoumeh D. Saberi, Sergio Carrato, Irena Koprinska, and James Clark</i> | |
| Using Relevance Feedback to Learn Both the Distance Measure and the Query in Multimedia Databases | 16 |
| <i>Chotirat Ann Ratanamahatana and Eamonn Keogh</i> | |
| Multi-level Semantic Analysis for Sports Video | 24 |
| <i>Dian W. Tjondronegoro and Yi-Ping Phoebe Chen</i> | |
| Aerial Photograph Image Retrieval Using the MPEG-7 Texture Descriptors | 31 |
| <i>Sang Kim, Sung Baik, Yung Jo, Seungbin Moon, and Daewoong Rhee</i> | |
| Yet Another Induction Algorithm | 37 |
| <i>Jiyuan An and Yi-Ping Phoebe Chen</i> | |
| An Implementation of Learning Classifier Systems for Rule-Based Machine Learning | 45 |
| <i>An-Pin Chen and Mu-Yen Chen</i> | |
| Learning-by-Doing Through Metaphorical Simulation | 55 |
| <i>Pedro Pablo Gómez-Martín, Marco Antonio Gómez-Martín, and Pedro A. González-Calero</i> | |

Immunity-Based Systems

| | |
|---|----|
| Emergence of Immune Memory and Tolerance in an Asymmetric Idiotype Network | 65 |
| <i>Kouji Harada</i> | |
| Mutual Repairing System Using Immunity-Based Diagnostic Mobile Agent | 72 |
| <i>Yuji Watanabe, Shigeyuki Sato, and Yoshiteru Ishida</i> | |
| A Network Self-repair by Spatial Strategies in Spatial Prisoner's Dilemma | 79 |
| <i>Yoshiteru Ishida and Toshikatsu Mori</i> | |

| | |
|--|----|
| A Critical Phenomenon in a Self-repair Network by Mutual Copying | 86 |
| <i>Yoshiteru Ishida</i> | |

| | |
|--|----|
| A Worm Filter Based on the Number of Unacknowledged Requests | 93 |
| <i>Takeshi Okamoto</i> | |

| | |
|---|-----|
| Comparison of Wavenet and Neuralnet for System Modeling | 100 |
| <i>Seda Postalcioğlu, Kadir Erkan, and Emine Doğru Bolat</i> | |

| | |
|---|-----|
| Neurone Editor: Modelling of Neuronal Growth with Synapse Formation for Use in 3D Neurone Networks | 108 |
| <i>Johan Iskandar and John Zakis</i> | |

Medical Diagnosis

| | |
|---|-----|
| A Hybrid Decision Tree – Artificial Neural Networks Ensemble Approach for Kidney Transplantation Outcomes Prediction | 116 |
| <i>Fariba Shadabi, Robert J. Cox, Dharmendra Sharma, and Nikolai Petrovsky</i> | |

| | |
|--|-----|
| Performance Comparison for MLP Networks Using Various Back Propagation Algorithms for Breast Cancer Diagnosis | 123 |
| <i>S. Sugasini, Mohd Yusoff Mashor, Nor Ashidi Mat Isa, and Nor Hayati Othman</i> | |

| | |
|---|-----|
| Combining Machine Learned and Heuristic Rules Using GRDR for Detection of Honeycombing in HRCT Lung Images | 131 |
| <i>Pramod K. Singh and Paul Compton</i> | |

| | |
|--|-----|
| Automatic Detection of Breast Tumours from Ultrasound Images Using the Modified Seed Based Region Growing Technique | 138 |
| <i>Nor Ashidi Mat Isa, Shahrill Sabarudin, Umi Kalthum Ngah, and Kamal Zuhairi Zamli</i> | |

| | |
|--|-----|
| An Automatic Body ROI Determination for 3D Visualization of a Fetal Ultrasound Volume | 145 |
| <i>Tien Dung Nguyen, Sang Hyun Kim, and Nam Chul Kim</i> | |

| | |
|---|-----|
| Swarm Intelligence and the Holonic Paradigm: A Promising Symbiosis for a Medical Diagnostic System | 154 |
| <i>Rainer Unland and Mihaela Ulieru</i> | |

| | |
|---|-----|
| Analysis Between Lifestyle, Family Medical History and Medical Abnormalities Using Data Mining Method – Association Rule Analysis | 161 |
| <i>Mitsuhiko Ogasawara, Hiroki Sugimori, Yukiyasu Iida, and Katsumi Yoshida</i> | |

Intelligent Hybrid Systems and Control

| | |
|--|-----|
| A Moving-Mass Control System for Spinning Vehicle Based on Neural Networks and Genetic Algorithm | 172 |
| <i>Song-yan Wang, Ming Yang, and Zi-cai Wang</i> | |
| Two-Dimensional Fitting of Brightness Profiles in Galaxy Images with a Hybrid Algorithm | 179 |
| <i>Juan Carlos Gomez, Olac Fuentes, and Ivanio Puerari</i> | |
| A Hybrid Tabu Search Based Clustering Algorithm | 186 |
| <i>Yongguo Liu, Yan Liu, Libin Wang, and Kefei Chen</i> | |
| Neural Network Based Feedback Scheduling of Multitasking Control Systems | 193 |
| <i>Feng Xia and Youxian Sun</i> | |
| An HILS and RCP Based Inter-working Scheme for Computational Evaluation of Manipulators and Trajectory Controller | 200 |
| <i>Yeon-Mo Yang, N.P. Mahalik, Sung-Cheal Byun, See-Moon Yang, and Byung-Ha Ahn</i> | |
| Modeling of Nonlinear Static System Via Neural Network Based Intelligent Technology | 207 |
| <i>Dongwon Kim, Jang-Hyun Park, Sam-Jun Seo, and Gwi-Tae Park</i> | |
| Bayesian Inference Driven Behavior Network Architecture for Avoiding Moving Obstacles | 214 |
| <i>Hyeun-Jeong Min and Sung-Bae Cho</i> | |
| Loss Minimization Control of Induction Motor Using GA-PSO | 222 |
| <i>Dong Hwa Kim and Jin Ill Park</i> | |

Emotional Intelligence and Smart Systems

| | |
|---|-----|
| Context-Restricted, Role-Oriented Emotion Knowledge Acquisition and Representation | 228 |
| <i>Xi Yong, Cungen Cao, and Haitao Wang</i> | |
| User Preference Learning for Multimedia Personalization in Pervasive Computing Environment | 236 |
| <i>Zhiwen Yu, Daqing Zhang, Xingshe Zhou, and Changde Li</i> | |
| Emotion-Based Smart Recruitment System | 243 |
| <i>Rajiv Khosla and Chris Lai</i> | |
| Evolvable Recommendation System in the Portable Device Based on the Emotion Awareness | 251 |
| <i>Seong-Joo Kim, Jong-Soo Kim, Sung-Hyun Kim, and Yong-Min Kim</i> | |

| | |
|--|-----|
| Emotional Extraction System by Using the Color Combination | 258 |
| <i>Keiko Sato, Yasue Mitsukura, and Minoru Fukumi</i> | |

| | |
|--|-----|
| Research on Individual Recognition System with Writing Pressure Based on Customized Neuro-template with Gaussian Function | 263 |
| <i>Lina Mi and Fumiaki Takeda</i> | |

Context-Aware Evolvable Systems

| | |
|---|-----|
| Context-Aware Evolvable System Framework for Environment Identifying Systems | 270 |
|---|-----|

Phill Kyu Rhee, Mi Young Nam, and In Ja Jeon

| | |
|---|-----|
| Context-Aware Computing Based Adaptable Heart Diseases Diagnosis Algorithm | 284 |
|---|-----|

Tae Seon Kim and Hyun-Dong Kim

| | |
|---|-----|
| Multiple Sensor Fusion and Motion Control of Snake Robot Based on Soft-Computing | 291 |
|---|-----|

Woo-Kyung Choi, Seong-Joo Kim, and Hong-Tae Jeon

| | |
|---|-----|
| Human Face Detection Using Skin Color Context Awareness and Context-Based Bayesian Classifiers | 298 |
|---|-----|

Mi Young Nam and Phill Kyu Rhee

| | |
|---|-----|
| Adaptive Gabor Wavelet for Efficient Object Recognition | 308 |
| <i>In Ja Jeon, Mi Young Nam, and Phill Kyu Rhee</i> | |

| | |
|---|-----|
| An Evolvable Hardware System Under Uneven Environment | 319 |
| <i>In Ja Jeon, Phill Kyu Rhee, and Hanho Lee</i> | |

| | |
|---|-----|
| An Efficient Face Location Using Integrated Feature Space | 327 |
| <i>Mi Young Nam and Phill Kyu Rhee</i> | |

Intelligent Fuzzy Systems and Control

| | |
|--|-----|
| Fuzzy Predictive Preferential Dropping for Active Queue Management | 336 |
| <i>Lichang Che and Bin Qiu</i> | |

| | |
|---|-----|
| A Fuzzy Method for Measuring Efficiency Under Fuzzy Environment | 343 |
| <i>Hsuan-Shih Lee, Pei-Di Shen, and Wen-Li Chyr</i> | |

| | |
|--|-----|
| Anytime Iterative Optimal Control Using Fuzzy Feedback Scheduler | 350 |
| <i>Feng Xia and Youxian Sun</i> | |

| | |
|--|-----|
| A Coupled Fuzzy Logic Control for Routers' Queue Management over TCP/AQM Networks | 357 |
| <i>Zhi Li and Zhongwei Zhang</i> | |

- Iris Pattern Recognition Using Fuzzy LDA Method 364
*Hyoun-Joo Go, Keun-Chang Kwak, Mann-Jun Kwon,
and Myung-Geun Chun*

- Precision Tracking Based-on Fuzzy Reasoning Segmentation
in Cluttered Image Sequences 371
Jae-Soo Cho, Byoung-Ju Yun, and Yun-Ho Ko

- Fuzzy Lowpass Filtering 378
Yasar Becerikli, M. Mucteba Tutuncu, and H. Engin Demiray

- Fuzzy Logic Based Intelligent Tool for Databases 386
Sevinc İlhan and Nevcihan Duru

Knowledge Representation and Its Practical Application in Today's Society

- Modelling from Knowledge Versus Modelling from Rules Using UML 393
Anne Häkansson

- Meeting the Need for Knowledge Management in Schools
with Knowledge-Based Systems – A Case Study 403
Anneli Edman

- Aspects of Consideration When Designing
Educational Knowledge Based Hypermedia Systems 410
Narin Mayiwar

- Semantic Tags: Evaluating the Functioning of Rules
in a Knowledge Based System 416
Torsten Palm

- Knowledge Management for Robot Activities in a Real World Context.
A Case for Task Pattern Analysis (TAPAS) 422
Lars Oestreicher

- Temporal Knowledge Representation and Reasoning Model
for Temporally Rich Domains 430
Slobodan Ribarić

- Reciprocal Logic: Logics for Specifying, Verifying, and Reasoning
About Reciprocal Relationships 437
Jingde Cheng

Approaches and Methods into Security Engineering III

- A New Paradigm Vertical Handoff Algorithm
in CDMA-WLAN Integrated Networks 446
Kyung-Soo Jang, Jang-Sub Kim, Jae-Sang Cha, and Dong-Ryeol Shin

| | |
|--|-----|
| Efficient Revocation of Security Capability in Certificateless Public Key Cryptography | 453 |
| <i>Hak Soo Ju, Dae Youb Kim, Dong Hoon Lee, Jongin Lim, and Kilsoo Chun</i> | |
| A Study on Privacy-Related Considerations in Ubiquitous Computing Environment | |
| (A Focus on Context Aware Environment Applied in Intelligent Technology) | 460 |
| <i>Jang Mook Kang, Jo Nam Jung, Jae-Sang Cha, and Chun su Lee</i> | |
| Optimal Operation for Cogenerating System of Micro-grid Network | 464 |
| <i>Phil-Hun Cho, Hak-Man Kim, Myong-Chul Shin, and Jae-Sang Cha</i> | |
| An Efficient and Secured Media Access Mechanism Using the Intelligent Coordinator in Low-Rate WPAN Environment | 470 |
| <i>Joon Heo and Choong Seon Hong</i> | |
| Pilot-Symbol Aided SFBC-OFDM Channel Estimation for Intelligent Multimedia Service | 477 |
| <i>Sang Soon Park, Juphil Cho, and Heung Ki Baik</i> | |
| Cryptographic Protocol Design Concept with Genetic Algorithms | 483 |
| <i>Kyeongmo Park and Chuleui Hong</i> | |
| An Efficient Backoff Scheme for IEEE 802.11e EDCF Differential Service | 490 |
| <i>Ho-Jin Shin, Jang-Sub Kim, and Dong-Ryeol Shin</i> | |
| Communicative Intelligent I | |
| Some Properties of Grounding Modal Conjunctions in Artificial Cognitive Agents | 500 |
| <i>Radosław Piotr Katarzyniak</i> | |
| Multi-agent System for Web Advertising | 507 |
| <i>Przemysław Kazienko</i> | |
| A Mobile Agent Approach to Intrusion Detection in Network Systems | 514 |
| <i>Grzegorz Kolaczek, Agnieszka Pieczynska-Kuchtiak, Krzysztof Juszczyszyn, Adam Grzech, Radosław Piotr Katarzyniak, and Ngoc Thanh Nguyen</i> | |
| Non-textual Document Ranking Using Crawler Information and Web Usage Mining | 520 |
| <i>Maciej Kiewra and Ngoc Thanh Nguyen</i> | |
| A Propagation Strategy Implemented in Communicative Environment | 527 |
| <i>Dariusz Król</i> | |
| Using Recommendation to Improve Negotiations in Agent-Based Systems | 534 |
| <i>Mateusz Lenar and Janusz Sobecki</i> | |

| | |
|--|-----|
| Fault Diagnosis of Discrete Event Systems Using Place Invariants | 541 |
| <i>Iwan Tabakow</i> | |

Intelligent Watermaking Algorithms and Applications

| | |
|---|-----|
| A Robust-Fragile Dual Watermarking System in the DCT Domain | 548 |
| <i>Moussa Habib, Sami Sarhan, and Lama Rajab</i> | |

| | |
|---|-----|
| A Data Hiding Scheme to Reconstruct Missing Blocks for JPEG Image Transmission | 554 |
| <i>Jia Hong Lee, Jyh-Wei Chen, and Mei-Yi Wu</i> | |

| | |
|--|-----|
| Adaptive Selection of Coefficient's Portions in the Transform Domain Watermarking | 560 |
| <i>Yoon-Ho Kim, Hag-hyun Song, and Heau Jo Kang</i> | |

| | |
|---|-----|
| Copyright Authentication Enhancement of Digital Watermarking Based on Intelligent Human Visual System Scheme | 567 |
| <i>YangSun Lee, Heau Jo Kang, and Yoon-Ho Kim</i> | |

| | |
|---|-----|
| Image Retrieval Based on a Multipurpose Watermarking Scheme | 573 |
| <i>Zhe-Ming Lu, Henrik Skibbe, and Hans Burkhardt</i> | |

| | |
|---|-----|
| Compressed Domain Video Watermarking in Motion Vector | 580 |
| <i>Hao-Xian Wang, Yue-Nan Li, Zhe-Ming Lu, and Sheng-He Sun</i> | |

| | |
|--|-----|
| Analysis of Quantization-Based Audio Watermarking in DA/AD Conversions . . . | 587 |
| <i>Shijun Xiang, Jiwu Huang, and Xiaoyun Feng</i> | |

| | |
|---|-----|
| A Lossless Watermarking Technique for Halftone Images | 593 |
| <i>Ping-Sung Liao, Jeng-Shyang Pan, Yen-Hung Chen, and Bin-Yih Liao</i> | |

Intelligent Techniques and Control

| | |
|--|-----|
| Implementation of Current Mode Fuzzy-Tuning PI Control of Single Phase UPS Inverter Using DSP | 600 |
| <i>Emine Doğru Bolat and H. Metin Ertuṅç</i> | |

| | |
|---|-----|
| Knowledge-Based Fuzzy Control of Pilot-Scale SBR for Wastewater Treatment . . | 608 |
| <i>Byong-Hee Jun, Jang-Hwan Park, and Myung Geun Chun</i> | |

| | |
|--|-----|
| Finely Tuned Cascaded Fuzzy Controllers with VHDL – A Case Study for Linerization of V-I Characteristics of a Convertor | 615 |
| <i>Avinash G. Keskar, Kishor Kadbe, Nikhil Damle, and Pooja Deshpande</i> | |

| | |
|--|-----|
| Control System for Optimal Flight Trajectories for Terrain Collision Avoidance . | 622 |
| <i>Tapan Sharma, Cees Bil, and Andrew Eberhard</i> | |

| | |
|---|-----|
| Optimal Remediation Design in Groundwater Systems by Intelligent Techniques . | 628 |
| <i>Hone-Jay Chu, Chin-Tsai Hsiao, and Liang-Cheng Chang</i> | |

| | |
|---|-----|
| Choquet Integral-Based Decision Making Approach for Robot Selection | 635 |
| <i>E. Ertugrul Karsak</i> | |

| | |
|---|-----|
| Fuzzy Logic and Neuro-fuzzy Modelling of Diesel Spray Penetration | 642 |
| <i>Shaun H. Lee, Bob R.J. Howlett, Simon D. Walters, and Cyril Crua</i> | |

e-Learning and ICT

| | |
|--|-----|
| Integrating Architecture of Digital Library and e-Learning Based on Intelligent Agent | 651 |
| <i>Sun-Gwan Han and Hee-Seop Han</i> | |

| | |
|---|-----|
| A Pedagogical Overview on e-Learning | 658 |
| <i>Javier Andrade, Juan Ares, Rafael García, Santiago Rodríguez, María Seoane, and Sonia Suárez</i> | |

| | |
|---|-----|
| Modeling Understanding Level of Learner in Collaborative Learning Using Bayesian Network | 665 |
| <i>Akira Komedani, Tomoko Kojiri, and Toyohide Watanabe</i> | |

| | |
|--|-----|
| Dynamic Generation of Diagrams for Supporting Solving Process of Mathematical Exercises | 673 |
| <i>Yosuke Murase, Tomoko Kojiri, and Toyohide Watanabe</i> | |

| | |
|---|-----|
| MOLEAS: Information Technology-Based Educational Software Framework | 681 |
| <i>Su-Jin Cho and Seongsoo Lee</i> | |

| | |
|--|-----|
| A Web-Based Information Communication Ethics Education System for the Gifted Elementary School Students in Computer | 688 |
| <i>Woochun Jun and Sung-Keun Cho</i> | |

| | |
|---|-----|
| Design of a Web Based Lab Administration System | 694 |
| <i>Sujan Pradhan and Hongen Lu</i> | |

| | |
|---|-----|
| Experiences with Pair and Tri Programming in a Second Level Course | 701 |
| <i>Maryam Purvis, Martin Purvis, Bastin Tony Roy Savarimuthu, Mark George, and Stephen Cranefield</i> | |

Logic Based Intelligent Information Systems

| | |
|--|-----|
| An Intelligent Safety Verification Based on a Paraconsistent Logic Program | 708 |
| <i>Kazumi Nakamatsu, Seiki Akama, and Jair Minoro Abe</i> | |

| | |
|---|-----|
| Paraconsistent Artificial Neural Network: An Application in Cephalometric Analysis | 716 |
| <i>Jair Minoro Abe, Neli R.S. Ortega, Maurício C. Mário, and Marinho Del Santo Jr.</i> | |

| | |
|---|-----|
| Non-alethic Reasoning in Distributed Systems | 724 |
| <i>Jair Minoro Abe, Kazumi Nakamatsu, and Seiki Akama</i> | |

| | |
|---|-----|
| A Connectionist Model for Predicate Logic Reasoning Using Coarse-Coded Distributed Representations | 732 |
| <i>Sriram G. Sanjeevi and Pushpak Bhattacharya</i> | |
| A General-Purpose Forward Deduction Engine for Modal Logics | 739 |
| <i>Shinsuke Nara, Takashi Omi, Yuichi Goto, and Jingde Cheng</i> | |
| A Deductive Semantic Brokering System | 746 |
| <i>Grigoris Antoniou, Thomas Skylogiannis, Antonis Bikakis, and Nick Bassiliades</i> | |
| Uncertainty Management in Logic Programming: Simple and Effective Top-Down Query Answering | 753 |
| <i>Umberto Straccia</i> | |
| Specifying Distributed Authorization with Delegation Using Logic Programming | 761 |
| <i>Shujing Wang and Yan Zhang</i> | |
| Intelligent Agents and Their Applications I | |
| The Design and Implementation of SAMIR | 768 |
| <i>Fabio Zambetta and Fabio Abbattista</i> | |
| Intelligent Data Analysis, Decision Making and Modelling Adaptive Financial Systems Using Hierarchical Neural Networks | 775 |
| <i>Masoud Mohammadian and Mark Kingham</i> | |
| Electricity Load Prediction Using Hierarchical Fuzzy Logic Systems | 782 |
| <i>Masoud Mohammadian and Ric Jentzsch</i> | |
| MEDADVIS: A Medical Advisory System | 789 |
| <i>Zul Waker Al-Kabir, Kim Le, and Dharmendra Sharma</i> | |
| Towards Adaptive Clustering in Self-monitoring Multi-agent Networks | 796 |
| <i>Piraveenan Mahendra rajah, Mikhail Prokopenko, Peter Wang, and Don Price</i> | |
| Shared Learning Vector Quantization in a New Agent Architecture for Intelligent Deliberation | 806 |
| <i>Prasanna Lokuge and Damminda Alahakoon</i> | |
| Patterns for Agent Oriented e-Bidding Practices | 814 |
| <i>Ivan Jureta, Manuel Kolp, Stéphane Faulkner, and T. Tung Do</i> | |
| Innovations in Intelligent Agents | |
| Innovations in Intelligent Agents | 821 |
| <i>Jeff Tweedale and Nikhil Ichalkaranje</i> | |

| | |
|---|-----|
| Multi-agent Systems: New Directions | 825 |
| <i>Nikhil Ichalkaranje and Jeff Tweedale</i> | |
| Agent Technology for Coordinating UAV Target Tracking | 831 |
| <i>Jisun Park, Karen K. Fullam, David C. Han, and K. Suzanne Barber</i> | |
| Cognitive Hybrid Reasoning Intelligent Agent System | 838 |
| <i>Christos Sioutis and Nikhil Ichalkaranje</i> | |
| Beyond Trust: A Belief-Desire-Intention Model of Confidence in an Agent's Intentions | 844 |
| <i>Bevan Jarvis, Dan Corbett, and Lakhmi C. Jain</i> | |
| Reasoning About Time in a BDI Architecture | 851 |
| <i>Bevan Jarvis, Dan Corbett, and Lakhmi C. Jain</i> | |
| A Delegation Model for Designing Collaborative Multi-agent Systems | 858 |
| <i>Stéphane Faulkner and Stéphane Dehoussé</i> | |

Ontologies and the Semantic Web

| | |
|---|-----|
| An Interactive Visual Model for Web Ontologies | 866 |
| <i>Yuxin Mao, Zhaohui Wu, Huajun Chen, and Xiaoqing Zheng</i> | |
| RDF-Based Ontology View for Relational Schema Mediation in Semantic Web . . | 873 |
| <i>Huajun Chen, Zhaohui Wu, and Yuxin Mao</i> | |
| Essentialized Conceptual Structures in Ontology Modeling | 880 |
| <i>Patryk Burek</i> | |
| Turning Mass Media to Your Media: Intelligent Search with Customized Results . | 887 |
| <i>Jun Lai and Ben Soh</i> | |
| Improving Search on WWW.HR Web Directory by Introducing Ontologies . . . | 894 |
| <i>Gordan Gledec, Maja Matijašević, and Damir Jurić</i> | |
| Designing a Tool for Configuring an Intelligent and Flexible Web-Based System . | 901 |
| <i>Diego Magro and Anna Goy</i> | |
| Location-Sensitive Tour Guide Services Using the Semantic Web | 908 |
| <i>Jong-Woo Kim, Ju-Yeon Kim, Hyun-Suk Hwang, and Chang-Soo Kim</i> | |
| Semantic Discovery of Web Services | 915 |
| <i>Hongen Lu</i> | |

Knowledge Discovery in Data Streams

| | |
|--|-----|
| Making Sense of Ubiquitous Data Streams – A Fuzzy Logic Approach | 922 |
| <i>Osnat Horovitz, Mohamed Medhat Gaber, and Shonali Krishnaswamy</i> | |

| | |
|---|------|
| σ -SCLOPE: Clustering Categorical Streams Using Attribute Selection | 929 |
| <i>Poh Hean Yap and Kok-Leong Ong</i> | |
| Extraction of Gene/Protein Interaction from Text Documents with Relation Kernel | 936 |
| <i>Jae-Hong Eom and Byoung-Tak Zhang</i> | |
| Combining an Order-Semisensitive Text Similarity and Closest Fit Approach to Textual Missing Values in Knowledge Discovery | 943 |
| <i>Yi Feng, Zhaoxi Wu, and Zhongmei Zhou</i> | |
| Support for Internet-Based Commonsense Processing – Causal Knowledge Discovery Using Japanese “If” Forms | 950 |
| <i>Yali Ge, Rafal Rzepka, and Kenji Araki</i> | |
| APForecast: An Adaptive Forecasting Method for Data Streams | 957 |
| <i>Yong-li Wang, Hong-bing Xu, Yi-sheng Dong, Xue-jun Liu, and Jiang-bo Qian</i> | |
| Finding Closed Itemsets in Data Streams | 964 |
| <i>Hai Wang, Wenyuan Li, Zengzhi Li, and Lin Fan</i> | |
| Computational Intelligence Tools Techniques and Algorithms | |
| An Efficient Schema Matching Algorithm | 972 |
| <i>Wei Cheng, Heshui Lin, and Yufang Sun</i> | |
| A Divisive Ordering Algorithm for Mapping Categorical Data to Numeric Data | 979 |
| <i>Huang-Cheng Kuo</i> | |
| A Mutual Influence Algorithm for Multiple Concurrent Negotiations – A Game Theoretical Analysis | 986 |
| <i>Ka-man Lam and Ho-fung Leung</i> | |
| Vulnerability Evaluation Tools of Matching Algorithm and Integrity Verification in Fingerprint Recognition | 993 |
| <i>Ho-Jun Na, Deok-Hyun Yoon, Chang-Soo Kim, and Hyun-Suk Hwang</i> | |
| Algorithms for CTL System Modification | 1000 |
| <i>Yulin Ding and Yan Zhang</i> | |
| A Robust Approach for Improving Computational Efficiency of Order-Picking Problems | 1007 |
| <i>Yu-Min Chiang, Shih-Hsin Chen, and Kuo-Chang Wu</i> | |
| An Efficient MDS Algorithm for the Analysis of Massive Document Collections | 1015 |
| <i>Yoshitatsu Matsuda and Kazunori Yamaguchi</i> | |

Approaches and Methods to Security Engineering IV

| | |
|--|------|
| (SE-33) Intelligent ID-Based Threshold System by an Encryption and Decryption from Bilinear Pairing | 1022 |
| <i>Young Whan Lee and Byung Mun Choi</i> | |
| Development of an Intelligent Information Security Evaluation Indices System for an Enterprise Organization | 1029 |
| <i>Il Seok Ko, Geuk Lee, and Yun Ji Na</i> | |
| A Study on the Centralized Database of the Multi-agents Based Integrated Security Management System for Managing Heterogeneous Firewalls | 1036 |
| <i>Dong-Young Lee</i> | |
| Adaptive Modulation and Coding Scheme for Wireless Mobile Communication System | 1043 |
| <i>Jae-Sang Cha and Juphil Cho</i> | |
| Performance Analysis of a Antenna Array System Using a New Beamforming Algorithm in the CDMA2000 1X Wireless Communication | 1050 |
| <i>Sungsoo Ahn, Minsoo Kim, Jungsuk Lee, and Dong-Young Lee</i> | |
| Intelligent Tool for Enterprise Vulnerability Assessment on a Distributed Network Environment Using Nessus and OVAL | 1056 |
| <i>Youngsup Kim, Seung Yub Baek, and Geuk Lee</i> | |

| | |
|--|------|
| Design and Implementation of SMS Security System for Wireless Environment . | 1062 |
| <i>Yan-Ha, Hea-Sook Park, Soon-Mi Lee, Young-Whan Park, and Young-Shin Han</i> | |

| | |
|--|------|
| Intelligent Method for Building Security Countermeasures by Applying Dr. T.H. Kim's Block Model | 1069 |
| <i>Tai-hoon Kim and Seung-youn Lee</i> | |

Watermaking Applications I

| | |
|--|------|
| Print and Generation Copy Image Watermarking Based on Spread Spectrum Technique | 1076 |
| <i>Ping Chen, Kagenori Nagao, Yao Zhao, and Jeng-Shyang Pan</i> | |
| Audio CoFIP (Contents Fingerprinting) Robust Against Collusion Attack | 1083 |
| <i>Kotaro Sonoda, Ryouichi Nishimura, and Yōiti Suzuki</i> | |
| A Low Cost and Efficient Sign Language Video Transmission System | 1090 |
| <i>Mohsen Ashourian, Reza Enteshari, and Ioannis Lambadaris</i> | |

| | |
|--|------|
| A New Watermark Surviving After Re-shooting the Images Displayed on a Screen | 1099 |
| <i>Seiichi Gohshi, Haruyuki Nakamura, Hiroshi Ito, Ryousuke Fujii, Mitsuyoshi Suzuki, Shigenori Takai, and Yukari Tani</i> | |
| Semi-fragile Watermarking Based on Zernike Moments and Integer Wavelet Transform | 1108 |
| <i>Xiaoyun Wu, Hongmei Liu, and Jiwu Huang</i> | |
| Shadow Watermark Extraction System | 1115 |
| <i>Feng-Hsing Wang, Kang K. Yen, Lakhmi C. Jain, and Jeng-Shyang Pan</i> | |
| Development of Nearly Lossless Embedding Technology of Contactless Sensible Watermarks for Audio Signals | 1122 |
| <i>Toshio Modegi</i> | |
| SVG-Based Countermeasure to Geometric Attack | 1129 |
| <i>Longjiang Yu, Xiamu Niu, and Sheng-He Sun</i> | |
| Watermaking Applications II | |
| Watermarking Protocol Compatible with Secret Algorithms for Resisting Invertibility Attack | 1134 |
| <i>Xinpeng Zhang and Shuzhong Wang</i> | |
| System Architecture Analysis of a Hybrid Watermarking Method | 1145 |
| <i>Chaw-Seng Woo, Jiang Du, Binh Pham, and Hamud Ali Abdulkadir</i> | |
| Audio Secret Sharing for 1-Bit Audio | 1152 |
| <i>Ryouichi Nishimura, Norihiro Fujita, and Yôiti Suzuki</i> | |
| Watermarking with Association Rules Alignment | 1159 |
| <i>Jau-Ji Shen and Po-Wei Hsu</i> | |
| A Reversible Watermark Scheme Combined with Hash Function and Lossless Compression | 1168 |
| <i>YongJie Wang, Yao Zhao, Jeng-Shyang Pan, and ShaoWei Weng</i> | |
| Improved Method of Spread Spectrum Watermarking Techniques Using Pixel-Correlations | 1175 |
| <i>Zheng Liu</i> | |
| Apply Semi-fragile Watermarking to Authentication of Compressed Video Data . | 1183 |
| <i>Tsong-Yi Chen, Da-Jinn Wang, Chih-Cheng Chiu, and Chien-Hua Huang</i> | |
| Multimedia Retrieval I | |
| An Approach of Multi-level Semantics Abstraction | 1190 |
| <i>Hongli Xu and De Sun Zhijie Xu</i> | |

| | |
|---|------|
| Effective Video Scene Detection Approach Based on Cinematic Rules | 1197 |
| <i>Yuliang Geng, De Xu, and Aimin Wu</i> | |
| 3-DWT Based Motion Suppression for Video Shot Boundary Detection | 1204 |
| <i>Yang Xu, Xu De, Guan Tengfei, Wu Aimin, and Lang Congyan</i> | |
| Neural Network Based Image Retrieval with Multiple Instance Learning Techniques | 1210 |
| <i>S.C. Chuang, Y.Y. Xu, and Hsin-Chia Fu</i> | |
| Shot Type Classification in Sports Video Using Fuzzy Information Granular | 1217 |
| <i>Congyan Lang, De Xu, Wengang Cheng, and Yiwei Jiang</i> | |
| Method for Searching Similar Images Using Quality Index Measurement | 1224 |
| <i>Chin-Chen Chang and Tzu-Chuen Lu</i> | |
| Edge Projection-Based Image Registration | 1231 |
| <i>Hua Yan, Ju Liu, and Jiande Sun</i> | |
| Automated Information Mining on Multimedia TV News Archives | 1238 |
| <i>P.S. Lai, S.S. Cheng, S.Y. Sun, T.Y. Huang, J.M. Su, Y.Y. Xu, Y.H. Chen, S.C. Chuang, C.L. Tseng, C.L. Hsieh, Y.L. Lu, Y.C. Shen, J.R. Chen, J.B. Nie, F.P. Tsai, H.C. Huang, H.T. Pao, and Hsin-Chia Fu</i> | |
| Soft Computing Approach to Industrial Engineering | |
| An Emergency Model of Home Network Environment Based on Genetic Algorithm | 1245 |
| <i>Huey-Ming Lee and Shih-Feng Liao</i> | |
| A Distributed Backup Agent Based on Grid Computing Architecture | 1252 |
| <i>Huey-Ming Lee and Cheng-Hsiung Yang</i> | |
| A Dynamic Supervising Model Based on Grid Environment | 1258 |
| <i>Huey-Ming Lee, Chao-Chi Hsu, and Mu-Hsiu Hsu</i> | |
| An Intelligent Extracting Web Content Agent on the Internet | 1265 |
| <i>Huey-Ming Lee, Pin-Jen Chen, Yao-Jen Shih, Yuan-Chieh Tsai, and Ching-Hao Mao</i> | |
| A Rendering System for Image Extraction from Music and Dance | 1272 |
| <i>Chihaya Watanabe and Hisao Shiizuka</i> | |
| Trend of Fuzzy Multivariate Analysis in Management Engineering | 1283 |
| <i>Junzo Watada</i> | |
| Kansei Engineering for Comfortable Space Management | 1291 |
| <i>Motoki Kohritani, Junzo Watada, Hideyasu Hirano, and Naoyoshi Yubazaki</i> | |

Experience Management and Information Systems

| | |
|---|------|
| Fuzzy Logic Experience Model in Human Resource Management | 1298 |
| <i>Zhen Xu, Binheng Song, and Liang Chen</i> | |
| Development of Business Rule Engine and Builder for Manufacture Process Productivity | 1305 |
| <i>Hojun Shin, Haengkon Kim, and Boyeon Shim</i> | |
| Automatic Detection of Failure Patterns Using Data Mining | 1312 |
| <i>Youngshin Han, Junghee Kim, and Chilgee Lee</i> | |
| Logic Frameworks for Components Integration Process | 1317 |
| <i>Haeng-Kon Kim and Deok-Soo Han</i> | |
| Automatic Classification Using Decision Tree and Support Vector Machine | 1325 |
| <i>Youngshin Han and Chilgee Lee</i> | |
| Opportunity Tree Framework Design for Quality and Delivery of Software Product | 1331 |
| <i>Sun-Myung Hwang and Ki-won Song</i> | |
| Breeding Value Classification in Manchego Sheep: A Study of Attribute Selection and Construction | 1338 |
| <i>M. Julia Flores and José A. Gámez</i> | |
| Learning Method for Automatic Acquisition of Translation Knowledge | 1347 |
| <i>Hiroshi Echizen-ya, Kenji Araki, and Yoshio Momouchi</i> | |
| Author Index | 1355 |

Table of Contents, Part III

Intelligent Agent Ontologies and Environments

| | |
|---|----|
| Agent-Based Approach for Dynamic Ontology Management | 1 |
| <i>Li Li, Baolin Wu, and Yun Yang</i> | |
| A Novel Approach for Developing Autonomous and Collaborative Agents | 8 |
| <i>Nora Houari and Behrouz Homayoun Far</i> | |
| The Effect of Alteration in Service Environments with Distributed Intelligent Agents | 16 |
| <i>Dragan Jevtic, Marijan Kunstic, and Denis Ouzecki</i> | |
| Managing Collaboration in a Multiagent System | 23 |
| <i>John Debenham and Simeon Simoff</i> | |
| Learning Plans with Patterns of Actions in Bounded-Rational Agents | 30 |
| <i>Budhitama Subagdja and Liz Sonenberg</i> | |
| Roles of Agents in Data-Intensive Web Sites | 37 |
| <i>Ali Ben Ammar, Abdelaziz Abdellatif, and Henda Ben Ghezala</i> | |
| Probabilistic Reasoning Techniques for the Tactical Military Domain | 46 |
| <i>Catherine Howard and Markus Stumptner</i> | |

Intelligent Multimedia Solutions and the Security in the Next Generation Mobile Networks

| | |
|---|----|
| A Network Service Access Control Framework Based on Network Blocking Algorithm | 54 |
| <i>Jahwan Koo and Seongjin Ahn</i> | |
| 3-D Building Reconstruction Using IKONOS Multispectral Stereo Images | 62 |
| <i>Hong-Gyoo Sohn, Choung-Hwan Park, and Joon Heo</i> | |
| Heuristic Algorithm for Estimating Travel Speed in Traffic Signalized Networks | 69 |
| <i>Hyung Jin Kim, Bongsoo Son, Soobeam Lee, and Sei-Chang Oh</i> | |
| Home Network Observation System Using User's Activate Pattern and Multimedia Streaming | 74 |
| <i>Kyung-Sang Sung, Dong Chun Lee, Hyun-Chul Kim, and Hae-Seok Oh</i> | |
| Determination of Optimal Locations for the Variable Message Signs by the Genetic Algorithm | 81 |
| <i>Jaimu Won, Sooil Lee, and Soobeam Lee</i> | |

| | |
|--|-----|
| Estimation of the Optimal Number of Cluster-Heads in Sensor Network | 87 |
| <i>Hyunsoo Kim, Seong W. Kim, Soobeam Lee, and Bongsoo Son</i> | |
| Development of Integrated Transit-Fare Card System in the Seoul Metropolitan Area | 95 |
| <i>Jeonghyun Kim and Seungpil Kang</i> | |
| Efficient Migration Scheme Using Backward Recovery Algorithm for Mobile Agents in WLAN | 101 |
| <i>Dong Chun Lee</i> | |
| Intelligent E-Mail Analysis, News Extraction and Web Mining | |
| Using Similarity Measure to Enhance the Robustness of Web Access Prediction Model | 107 |
| <i>Ben Niu and Simon C.K. Shiu</i> | |
| Intelligent Financial News Digest System | 112 |
| <i>James N.K. Liu, Honghua Dai, and Lina Zhou</i> | |
| An Incremental FP-Growth Web Content Mining and Its Application in Preference Identification | 121 |
| <i>Xiaoshu Hang, James N.K. Liu, Yu Ren, and Honghua Dai</i> | |
| Similarity Retrieval from Time-Series Tropical Cyclone Observations Using a Neural Weighting Generator for Forecasting Modeling | 128 |
| <i>Bo Feng and James N.K. Liu</i> | |
| Web Access Path Prediction Using Fuzzy Case Based Reasoning | 135 |
| <i>Simon C.K. Shiu and Cody K.P. Wong</i> | |
| Multiple Classifier System with Feature Grouping for Intrusion Detection: Mutual Information Approach | 141 |
| <i>Aki P.F. Chan, Wing W.Y. Ng, Daniel S. Yeung, and Eric C.C. Tsang</i> | |
| Design and Implement a Web News Retrieval System | 149 |
| <i>James N.K. Liu, Weidong Luo, and Edmond M.C. Chan</i> | |
| Semantic Integration and Ontologies | |
| An Ontology for Integrating Multimedia Databases | 157 |
| <i>Chull Hwan Song, Young Hyun Koo, Seong Joon Yoo, and ByeongHo Choi</i> | |
| Integrating Service Registries with OWL-S Ontologies | 163 |
| <i>Kyong-Ha Lee, Kyu-Chul Lee, Dae-Wook Lee, and Suk-Ho Lee</i> | |
| Data Integration Hub for a Hybrid Paper Search | 170 |
| <i>Jungkee Kim, Geoffrey Fox, and Seong Joon Yoo</i> | |

| | |
|---|-----|
| Effective Information Sharing Using Concept Mapping | 177 |
| <i>Keonsoo Lee, Wonil Kim, and Minkoo Kim</i> | |
| Ontology Supported Semantic Simplification of Large Data Sets of Industrial Plant CAD Models for Design Review Visualization | 184 |
| <i>Jorge Posada, Carlos Toro, Stefan Wundrak, and André Stork</i> | |
| EISCO: Enterprise Information System Contextual Ontologies Project | 191 |
| <i>Rami Rifaieh and Nabila Aïcha Benharkat</i> | |
| Mapping Fuzzy Concepts Between Fuzzy Ontologies | 199 |
| <i>Baowen Xu, Dazhou Kang, Jianjiang Lu, Yanhui Li, and Jixiang Jiang</i> | |
| Computer Vision, Image Processing and Retrieval | |
| Similarity Estimation of 3D Shapes Using Modal Strain Energy | 206 |
| <i>Soo-Mi Choi and Yong-Guk Kim</i> | |
| 3D-Based Synthesis and 3D Reconstruction from Uncalibrated Images | 213 |
| <i>Sang-Hoon Kim, Tae-Eun Kim, Mal-Rey Lee, and Jong-Soo Choi</i> | |
| 3-D Pose Tracking of the Car Occupant | 219 |
| <i>Sang-Jun Kim, Yong-Guk Kim, Jeong-Eom Lee, Min-Soo Jang, Seok-Joo Lee, and Gwi-Tae Park</i> | |
| Face Recognition by Multiple Classifiers, a Divide-and-Conquer Approach | 225 |
| <i>Reza Ebrahimpour, Saeed Reza Ehteram, and Ehsanollah Kabir</i> | |
| Shape Comparison of the Hippocampus Using a Multiresolution Representation and ICP Normalization | 233 |
| <i>Jeong-Sik Kim, Yong-Guk Kim, Soo-Mi Choi, and Myoung-Hee Kim</i> | |
| A Fast Image Retrieval Using the Unification Search Method of Binary Classification and Dimensionality Condensation of Feature Vectors | 240 |
| <i>Jungwon Cho, Seungdo Jeong, and Byunguk Choi</i> | |
| Semantic Supervised Clustering to Land Classification in Geo-Images | 248 |
| <i>Miguel Torres, G. Guzman, Rolando Quintero, Marco Moreno, and Serguei Levachkine</i> | |
| Communicative Intelligence II | |
| Towards an Intelligent Web Service for Ontology-Based Query-Answering Dialogues | 255 |
| <i>In-Cheol Kim</i> | |
| Using the Geographic Distance for Selecting the Nearest Agent in Intermediary-Based Access to Internet Resources | 261 |
| <i>Leszek Borzemski and Ziemowit Nowak</i> | |

| | |
|---|-----|
| Mining Internet Data Sets for Computational Grids | 268 |
| <i>Leszek Borzemski</i> | |

| | |
|---|-----|
| Towards Integration of Web Services into Agents for Biological Information Resources | 275 |
| <i>In-Cheol Kim and Hoon Jin</i> | |

| | |
|--|-----|
| Learning Within the BDI Framework: An Empirical Analysis | 282 |
| <i>Toan Phung, Michael Winikoff, and Lin Padgham</i> | |

| | |
|---|-----|
| How to Make Robot a Robust and Interactive Communicator | 289 |
| <i>Yoshiyasu Ogasawara, Masashi Okamoto, Yukiko I. Nakano, Yong Xu, and Toyoaki Nishida</i> | |

| | |
|--|-----|
| Analysis of Conversation Quanta for Conversational Knowledge Circulation | 296 |
| <i>Ken Saito, Hidekazu Kubota, Yasuyuki Sumi, and Toyoaki Nishida</i> | |

Approaches and Methods to Security Engineering V

| | |
|---|-----|
| An Intelligent Approach of Packet Marking at Edge Router for IP Traceback | 303 |
| <i>Dae Sun Kim, Choong Seon Hong, and Yu Xiang</i> | |

| | |
|---|-----|
| A Covert Timing Channel-Free Optimistic Concurrency Control Scheme for Multilevel Secure Database Management Systems | 310 |
| <i>Sukhoon Kang and Yong-Rak Choi</i> | |

| | |
|---|-----|
| Secure Password Authentication for Keystroke Dynamics | 317 |
| <i>YeongGeun Choe and Soon-Ja Kim</i> | |

| | |
|--|-----|
| The Efficient Multipurpose Convertible Undeniable Signature Scheme | 325 |
| <i>Sung-Hyun Yun and Hyung-Woo Lee</i> | |

| | |
|---|-----|
| A New Efficient Fingerprint-Based Remote User Authentication Scheme for Multimedia Systems | 332 |
| <i>Eun-Jun Yoon and Kee-Young Yoo</i> | |

| | |
|--|-----|
| A Study on the Correction of Gun Fire Error Using Neural Network | 339 |
| <i>Yang Weon Lee and Heau Jo Kang</i> | |

Multimedia Retrieval II

| | |
|--|-----|
| An Efficient Moving Object Extraction Algorithm for Video Surveillance | 346 |
| <i>Da-Jinn Wang, Thou-Ho Chen, Yung-Chuen Chiou, and Hung-Shiuan Liau</i> | |

| | |
|---|-----|
| An Experimental Comparison on Gabor Wavelet and Wavelet Frame Based Features for Image Retrieval | 353 |
| <i>Yu-Long Qiao, Jeng-Shyang Pan, and Sheng-He Sun</i> | |

| | |
|--|-----|
| Robust Video Retrieval Using Temporal MVMB Moments | 359 |
| <i>Duan-Yu Chen, Hong-Yuan Mark Liao, and Suh-Yin Lee</i> | |

| | |
|--|-----|
| Precise Segmentation Rendering for Medical Images Based on Maximum Entropy Processing | 366 |
| <i>Tsair-Fwu Lee, Ming-Yuan Cho, Chin-Shiuh Shieh, Pei-Ju Chao, and Huai-Yang Chang</i> | |
| A Hardware Implementation for Fingerprint Retrieval | 374 |
| <i>Yongwha Chung, Kichul Kim, Min Kim, Sungbum Pan, and Neungsoo Park</i> | |
| Fast Video Retrieval via the Statistics of Motion Within the Regions-of-Interest | 381 |
| <i>Jing-Fung Chen, Hong-Yuan Mark Liao, and Chia-Wen Lin</i> | |
| Information Theoretic Metrics in Shot Boundary Detection | 388 |
| <i>Wengang Cheng, De Xu, Yiwei Jiang, and Congyan Lang</i> | |
| Design of a Digital Forensics Image Mining System | 395 |
| <i>Ross Brown, Binh Pham, and Olivier de Vel</i> | |
| Multimedia Compression | |
| Side-Match Predictive Vector Quantization | 405 |
| <i>Zhen Sun, Yue-Nan Li, and Zhe-Ming Lu</i> | |
| Improved Image Coding with Classified VQ and Side-Match VQ | 411 |
| <i>Hsiang-Cheh Huang, Kang K. Yen, Yu-Hsiu Huang, Jeng-Shyang Pan, and Kuang-Chih Huang</i> | |
| Fast Multiple Reference Frame Motion Estimation for H.264 Based on Qualified Frame Selection Scheme | 418 |
| <i>Tien-Ying Kuo and Huang-Bin Chen</i> | |
| Block Standstill and Homogeneity Based Fast Motion Estimation Algorithm for H.264 Video Coding | 425 |
| <i>Feng Pan, H. Men, and Thinh M. Le</i> | |
| Fast Rate-Distortion Optimization in H.264/AVC Video Coding | 433 |
| <i>Feng Pan, Kenny Choo, and Thinh M. Le</i> | |
| Improving Image Quality for JPEG Compression | 442 |
| <i>Chin-Chen Chang, Yung-Chen Chou, and Jau-Ji Shen</i> | |
| Low-Power MPEG-4 Motion Estimator Design for Deep Sub-Micron Multimedia SoC | 449 |
| <i>Gyu-Sung Yeon, Chi-Hun Jun, Tae-Jin Hwang, Seongsoo Lee, and Jae-Kyung Wee</i> | |
| Multimedia Signal Processing | |
| Real-Time 3D Artistic Rendering System | 456 |
| <i>Tong-Yee Lee, Shaur-Uei Yan, Yong-Nien Chen, and Ming-Te Chi</i> | |

| | |
|--|-----|
| Index LOCO-I: A Hybrid Method of Data Hiding and Image Compression | 463 |
| <i>Wei-Soul Li, Wen-Shyong Hsieh, and Ming-Hong Sun</i> | |

| | |
|--|-----|
| Feature-Constrained Texturing System for 3D Models | 469 |
| <i>Tong-Yee Lee and Shaur-Uei Yan</i> | |

| | |
|--|-----|
| Dynamic Integrated Model for Distributed Multimedia System | 476 |
| <i>Ya-Rong Hou and Zhang Xiong</i> | |

| | |
|---|-----|
| Joint Detection for a Bandwidth Efficient Modulation Method | 483 |
| <i>Zhonghui Mei, Lenan Wu, and Shiyuan Zhang</i> | |

| | |
|--|-----|
| An Efficient and Divisible Payment Scheme for M-Commerce | 488 |
| <i>Yong Zhao, Zhen Han, Jiqiang Liu, and Zhigang Li</i> | |

| | |
|--|-----|
| Speech Authentication by Semi-fragile Watermarking | 497 |
| <i>Bin Yan, Zhe-Ming Lu, Sheng-He Sun, and Jeng-Shyang Pan</i> | |

Emergence and Self-organisation in Complex Systems

| | |
|--|-----|
| On Engineering Smart Systems | 505 |
| <i>E.V. Krishnamurthy and V. Kris Murthy</i> | |

| | |
|---|-----|
| Distributed Web Integration with Multiagent Data Mining | 513 |
| <i>Ayahiko Niimi, Hitomi Noji, and Osamu Konishi</i> | |

| | |
|---|-----|
| Self-adjusting Programming Training Support System Using Genetic Algorithm | 520 |
| <i>Eiji Nunohiro, Kenneth J. Mackin, Masanori Ohshiro, and Kazuko Yamasaki</i> | |

| | |
|---|-----|
| Waste Incinerator Emission Prediction Using Probabilistically Optimal Ensemble of Multi-agents | 526 |
| <i>Daisuke Yamaguchi, Kenneth J. Mackin, and Eiichiro Tazaki</i> | |

| | |
|---|-----|
| Cooperative Control Based on Reaction-Diffusion Equation for Surveillance System | 533 |
| <i>Atsushi Yoshida, Katsuji Aoki, and Shioichi Araki</i> | |

| | |
|--|-----|
| Comparison of the Effectiveness of Decimation and Automatically Defined Functions | 540 |
| <i>D.T. Nanduri and Vic Ciesielski</i> | |

| | |
|---|-----|
| Absolute Capacities for Higher Order Associative Memory of Sequential Patterns | 547 |
| <i>Hiromi Miyajima and Noritaka Shigei</i> | |

Soft Computing Techniques and Their Applications III

| | |
|--|-----|
| Finding Hidden Hierarchy in Reinforcement Learning | 554 |
| <i>Geoff Poulton, Ying Guo, and Wen Lu</i> | |

| | |
|---|-----|
| On-Line Reinforcement Learning Using Cascade Constructive Neural Networks | 562 |
| <i>Peter Vamplew and Robert Ollington</i> | |
| Node Exchange for Improvement of SOM Learning | 569 |
| <i>Tsutomu Miyoshi</i> | |
| Using Rough Set to Reduce SVM Classifier Complexity and Its Use in SARS Data Set | 575 |
| <i>Feng Honghai, Liu Baoyan, Yin Cheng, Li Ping, Yang Bingru, and Chen Yumei</i> | |
| A SVM Regression Based Approach to Filling in Missing Values | 581 |
| <i>Feng Honghai, Chen Guoshun, Yin Cheng, Yang Bingru, and Chen Yumei</i> | |
| Recognizing and Simulating Sketched Logic Circuits | 588 |
| <i>Marcus Liwicki and Lars Knipping</i> | |
| Automatic MLP Weight Regularization on Mineralization Prediction Tasks | 595 |
| <i>Andrew Skabar</i> | |
| Information Engineering and Ubiquitous Computing | |
| Integrated Process Modeling for Dynamic B2B Collaboration | 602 |
| <i>Je Yeon Oh, Jae-yoon Jung, Nam Wook Cho, Hoontae Kim, and Suk-Ho Kang</i> | |
| Assessment Methodology on Maturity Level of ISMS | 609 |
| <i>Choon Seong Leem, Sangkyun Kim, and Hong Joo Lee</i> | |
| CSFs for HCI in Ubiquitous Computing Environments | 616 |
| <i>Hong Joo Lee, Sangkyun Kim, and Choon Seong Leem</i> | |
| Practical Design Recovery Techniques for Embedded Operating System on Complying with RTCA/DO-178B and ISO/IEC15408 | 621 |
| <i>Minhyung Kim, Sangkyun Kim, and Myungwhan Choi</i> | |
| Information Privacy Engineering in ubiComp | 628 |
| <i>Tae Joong Kim, In Ho Kim, and Sang Won Lee</i> | |
| Design and Implementation of Home Media Server for Personalized Broadcasting Service in Ubiquitous Environment | 635 |
| <i>Chang-ho Hong, Jong-tae Lim, Chang Sohn, and Ha-eun Nam</i> | |
| A Distributed Approach to Musical Composition | 642 |
| <i>Michael O. Jewell, Lee Middleton, Mark S. Nixon, Adam Prügel-Bennett, and Sylvia C. Wong</i> | |

Location and Context-Based Systems

| | |
|--|-----|
| Efficient Mobility Management Using Dynamic Location Register in IMT-2000 Networks | 649 |
| <i>Il-Sun Hwang, Gi Sung Yoo, and Jin Wook Chung</i> | |
| SWSD: A P2P-Based System for Service Discovery from a Mobile Terminal | 655 |
| <i>Darije Ramljak and Maja Matijašević</i> | |
| An Efficient Eye Location Using Context-Aware Binarization Method | 662 |
| <i>Jo Nam Jung, Mi Young Nam, and Phill Kyu Rhee</i> | |
| Design and Implementation of Context-Awareness Processor for Multiple Instructions in Mobile Internet Environment | 670 |
| <i>Seungwon Na and Gu-Min Jeong</i> | |
| Integrated Management of Multi-level Road Network and Transportation Networks | 677 |
| <i>Jun Feng, Yuelong Zhu, Naoto Mukai, and Toyohide Watanabe</i> | |
| Music Plagiarism Detection Using Melody Databases | 684 |
| <i>Jeong-Il Park, Sang-Wook Kim, and Miyoung Shin</i> | |
| News Video Retrieval Using Automatic Indexing of Korean Closed-Caption | 694 |
| <i>Jungwon Cho, Seungdo Jeong, and Byunguk Choi</i> | |
| Classification and Skimming of Articles for an Effective News Browsing | 704 |
| <i>Jungwon Cho, Seungdo Jeong, and Byunguk Choi</i> | |

e-Based Systems in Education, Commerce and Health

| | |
|---|-----|
| Intelligent Tutoring System with 300-Certification Program Based on WIPI | 713 |
| <i>Youngseok Lee, Jungwon Cho, and Byunguk Choi</i> | |
| ECA Rule Based Timely Collaboration Among Businesses in B2B e-Commerce | 721 |
| <i>Dongwoo Lee, Seong Hoon Lee, and YongWon Kim</i> | |
| The Searching Methods of Mobile Agents in Telemedicine System Environments | 728 |
| <i>Hyuncheol Jeong and Inseob Song</i> | |
| Knowledge-Based RDF Specification for Ubiquitous Healthcare Services | 735 |
| <i>Ji-Hong Kim, Byung-Hyun Ha, Wookey Lee, Cheol Young Kim, Wonchang Hur, and Suk-Ho Kang</i> | |
| A Time Judgement System Based on an Association Mechanism | 742 |
| <i>Seiji Tsuchiya, Hirokazu Watabe, and Tsukasa Kawaoka</i> | |

- Response-Driven Web-Based Assessment System 749
Sylvia Encheva and Sharil Tumin

- Intelligence-Based Educational Package on Fluid Mechanics 756
KwokWing Chau

Computational Biology and Bioinformatics

- Generalized Composite Motif Discovery 763
Geir Kjetil Sandve and Finn Drabløs

- Protein Motif Discovery with Linear Genetic Programming 770
Rolv Seehuus

- Bayesian Validation of Fuzzy Clustering for Analysis of Yeast Cell Cycle Data 777
Kyung-Joong Kim, Si-Ho Yoo, and Sung-Bae Cho

- Rule Generation Using NN and GA for SARS-CoV Cleavage Site Prediction 785
Yeon-Jin Cho and Hyeoncheol Kim

- A Hybrid Approach to Combine HMM and SVM Methods
for the Prediction of the Transmembrane Spanning Region 792
*Min Kyung Kim, Chul Hwan Song, Seong Joon Yoo,
Sang Ho Lee, and Hyun Seok Park*

- Agents in Bio-inspired Computations 799
V. Kris Murthy

Complex Adaptive Systems

- Altruistic Punishment, Social Structure and the Enforcement of Social Norms 806
David Newth

- WISDOM-II: A Network Centric Model for Warfare 813
Ang Yang, Hussein A. Abbass, and Ruhul Sarker

- Adaptation on the Commons 820
Richard M. Kim and Simon M. Kaplan

- The Emergence of Order in Random Walk Resource Discovery Protocols 827
Ricky Robinson and Jadwiga Indulska

- Supporting Adaptive Learning with High Level Timed Petri Nets 834
Shang Gao, Zili Zhang, Jason Wells, and Igor Hawryszkiewycz

- Exploring the Effective Search Context
for the User in an Interactive and Adaptive Way 841
Supratip Ghose, Jason J. Jung, and Geun-Sik Jo

Communicative Intelligent III

| | |
|--|-----|
| Generating CG Movies Based on a Cognitive Model of Shot Transition | 848 |
| <i>Kazunori Okamoto, Yukiko I. Nakano, Masashi Okamoto, Hung-Hsuan Huang, and Toyoaki Nishida</i> | |
| Analyzing Concerns of People Using Weblog Articles and Natural Phenomena | 855 |
| <i>Toshihiro Murayama, Tomohiro Fukuhara, and Toyoaki Nishida</i> | |
| Sustainable Memory System Using Global and Conical Spaces | 861 |
| <i>Hidekazu Kubota, Satoshi Nomura, Yasuyuki Sumi, and Toyoaki Nishida</i> | |
| Entrainment of Rate of Utterances in Speech Dialogs Between Users and an Auto Response System | 868 |
| <i>Takanori Komatsu and Koji Morikawa</i> | |
| Locomotion Control Technique for Immersive Conversation Environment | 875 |
| <i>Rai Chan, Jun Takazawa, and Junichi Hoshino</i> | |
| Presentation of Human Action Information via Avatar: From the Viewpoint of Avatar-Based Communication | 883 |
| <i>Daisaku Arita and Rin-ichiro Taniguchi</i> | |
| Analysis and Synthesis of Help-Desk Responses | 890 |
| <i>Yuval Marom and Ingrid Zukerman</i> | |

Speech Processing and Robotics

| | |
|---|-----|
| A Talking Robot and Its Singing Skill Acquisition | 898 |
| <i>Mitsuhiko Nakamura and Hideyuki Sawada</i> | |
| Development of a New Vocal Cords Based on Human Biological Structures for Talking Robot | 908 |
| <i>Kotaro Fukui, Kazufumi Nishikawa, Shunsuke Ikeo, Eiji Shintaku, Kentaro Takada, Hideaki Takanobu, Masaaki Honda, and Atsuo Takanishi</i> | |
| An Adaptive Model for Phonetic String Search | 915 |
| <i>Gong Ruibin and Chan Kai Yun</i> | |
| Ontology Modeling and Storage System for Robot Context Understanding | 922 |
| <i>Eric Wang, Yong Se Kim, Hak Soo Kim, Jin Hyun Son, Sanghoon Lee, and Il Hong Suh</i> | |
| Intelligent Two-Way Speech Communication System Between the Technological Device and the Operator | 930 |
| <i>Maciej Majewski and Wojciech Kacalak</i> | |
| Activity-Object Bayesian Networks for Detecting Occluded Objects in Uncertain Indoor Environment | 937 |
| <i>Youn-Suk Song, Sung-Bae Cho, and Il Hong Suh</i> | |

| | |
|--|-----|
| Design of a Simultaneous Mobile Robot Localization and Spatial Context Recognition System | 945 |
| <i>Seungdo Jeong, Jonglyul Chung, Sanghoon Lee, Il Hong Suh, and Byunguk Choi</i> | |

Data Mining and Soft Computing Applications I

| | |
|---|-----|
| Mining Temporal Data: A Coal-Fired Boiler Case Study | 953 |
| <i>Andrew Kusiak and Alex Burns</i> | |
| Mining Classification Rules Using Evolutionary Multi-objective Algorithms | 959 |
| <i>Kalyanaraman Kaesava Kshetrapalapuram and Michael Kirley</i> | |
| On Pruning and Tuning Rules for Associative Classifiers | 966 |
| <i>Osmar R. Zaïane and Maria-Luiza Antonie</i> | |
| Using Artificial Neural Network Ensembles to Extract Data Content from Noisy Data | 974 |
| <i>Szymon K. Szukalski, Robert J. Cox, and Patricia S. Crowther</i> | |
| Identification of a Motor with Multiple Nonlinearities by Improved Genetic Algorithm | 981 |
| <i>Jung-Shik Kong and Jin-Geol Kim</i> | |
| Program Simplification in Genetic Programming for Object Classification | 988 |
| <i>Mengjie Zhang, Yun Zhang, and Will Smart</i> | |
| An Ontology-Supported Database Refurbishing Technique and Its Application in Mining GSM Trouble Shooting Rules | 997 |
| <i>Bong-Horng Chu, In-Kai Liao, and Cheng-Seen Ho</i> | |

Multimedia Security and Stegnography

| | |
|--|------|
| Develop Secure Database System with Security Extended ER Model | 1005 |
| <i>Xin Liu, Zhen Han, Jiqiang Liu, and Chang-xiang Shen</i> | |
| An Inference Detection Algorithm Based on Related Tuples Mining | 1011 |
| <i>Binge Cui and Dixin Liu</i> | |
| A Preliminary Design for a Privacy-Friendly Free P2P Media File Distribution System | 1018 |
| <i>Ron G. van Schyndel</i> | |
| Analysis of Parity Assignment Steganography in Palette Images | 1025 |
| <i>Xinpeng Zhang and Shuozhong Wang</i> | |
| A New Steganography Scheme in the Domain of Side-Match Vector Quantization | 1032 |
| <i>Chin-Shiuh Shieh, Chao-Chin Chang, Shu-Chuan Chu, and Jui-Fang Chang</i> | |

| | |
|--|------|
| Method of Hiding Information in Agglutinative Language Documents Using Adjustment to New Line Positions | 1039 |
| <i>Osamu Takizawa, Kyoko Makino, Tsutomu Matsumoto, Hiroshi Nakagawa, and Ichiro Murase</i> | |

| | |
|---|------|
| Hiding Biometric Data for Secure Transmission | 1049 |
| <i>Yongwha Chung, Daesung Moon, Kiyoung Moon, and Sungbum Pan</i> | |

Steganography

| | |
|--|------|
| VQ Image Steganographic Method with High Embedding Capacity Using Multi-way Search Approach | 1058 |
| <i>Chin-Chen Chang, Chih-Yang Lin, and Yu-Zheng Wang</i> | |

| | |
|---|------|
| Securing Mobile Agents Control Flow Using Opaque Predicates | 1065 |
| <i>Anirban Majumdar and Clark Thomborson</i> | |

| | |
|--|------|
| A Verifiable Fingerprint Vault Scheme | 1072 |
| <i>Qiong Li, Xiamu Niu, Zhifang Wang, Yuhua Jiao, and Sheng-He Sun</i> | |

| | |
|---|------|
| The Research on Information Hiding Based on Command Sequence of FTP Protocol | 1079 |
| <i>Xin-guang Zou, Qiong Li, Sheng-He Sun, and Xiamu Niu</i> | |

| | |
|---|------|
| Data Hiding in a Hologram by Modified Digital Halftoning Techniques | 1086 |
| <i>Hsi-Chun Wang and Wei-Chiang Wang</i> | |

| | |
|---|------|
| A Secure Steganographic Scheme in Binary Image | 1093 |
| <i>Yunbiao Guo, Daimao Lin, Xiamu Niu, Lan Hu, and Linna Zhou</i> | |

| | |
|---|------|
| A Reversible Information Hiding Scheme Based on Vector Quantization | 1101 |
| <i>Chin-Chen Chang and Wen-Chuan Wu</i> | |

| | |
|---|------|
| Zero-Based Code Modulation Technique for Digital Video Fingerprinting | 1108 |
| <i>In Koo Kang, Hae-Yeoun Lee, Won-Young Yoo, and Heung-Kyu Lee</i> | |

Soft Computing Approach to Industrial Engineering II

| | |
|--|------|
| Studies on Method for Measuring Human Feelings | 1115 |
| <i>Taki Kanda</i> | |

| | |
|--|------|
| Data Mining Method from Text Database | 1122 |
| <i>Masahiro Kawano, Junzo Watada, and Takayuki Kawaura</i> | |

| | |
|--|------|
| The Air Pollution Constraints Considered Best Generation Mix Using Fuzzy Linear Programming | 1129 |
| <i>Jaeseok Choi, TrungTinh Tran, Jungji Kwon, Sangsik Lee, and Abdurrahim El-keib</i> | |

| | |
|---|------|
| Ranking Functions, Perceptrons, and Associated Probabilities | 1143 |
| <i>Bernd-Jürgen Falkowski</i> | |
| Directed Mutation Operators – An Overview | 1151 |
| <i>Stefan Berlik and Bernd Reusch</i> | |
| A General Fuzzy Min Max Neural Network with Compensatory Neuron Architecture | 1160 |
| <i>A. V. Nandedkar and P.K. Biswas</i> | |
| An Analysis on Accuracy of Cancelable Biometrics Based on BioHashing | 1168 |
| <i>King-Hong Cheung, Adams Kong, David Zhang, Mohamed Kamel, Jane You and Toby, and Ho-Wang Lam</i> | |

| | |
|--|------|
| Condition Monitoring Capability Developed Through a Knowledge Transfer Partnership Between a Small Company and a University | 1173 |
| <i>Robert Howlett, Gary Dawe, and Terry Nowell</i> | |

Medical Text Mining and Natural Language Processing

| | |
|--|------|
| Extraction of Lexico-Syntactic Information and Acquisition of Causality Schemas for Text Annotation | 1180 |
| <i>Laurent Alamarguy, Rose Dieng-Kuntz, and Catherine Faron-Zucker</i> | |
| An Approach to Automatic Text Production in Electronic Medical Record Systems | 1187 |
| <i>Torbjørn Nordgård, Martin Thorsen Ranang, and Jostein Ven</i> | |
| gProt: Annotating Protein Interactions Using Google and Gene Ontology | 1195 |
| <i>Rune Sætre, Amund Tveit, Martin Thorsen Ranang, Tonje S. Steigedal, Liv Thommesen, Kamilla Stunes, and Astrid Lægreid</i> | |

| | |
|---|------|
| Physiological Modeling and Simulation for Aerobic Circulation with Beat-by-Beat Hemodynamics | 1204 |
| <i>Kenichi Asami</i> | |

| | |
|---|------|
| Collaborative and Immersive Medical Education in a Virtual Workbench Environment | 1210 |
| <i>Yoo-Joo Choi, Soo-Mi Choi, Seon-Min Rhee, and Myoung-Hee Kim</i> | |

Knowledge Based Intelligent Systems for Health Care

| | |
|--|------|
| Extraction of Risk Factors by Multi-agent Voting Model Using Automatically Defined Groups | 1218 |
| <i>Akira Hara, Takumi Ichimura, Tetsuyuki Takahama, and Yoshinori Isomichi</i> | |
| Representing Association Classification Rules Mined from Health Data | 1225 |
| <i>Jie Chen, Hongxing He, Jiuyong Li, Huidong Jin, Damien McAullay, Graham Williams, Ross Sparks, and Chris Kelman</i> | |

LXXVIII Table of Contents, Part III

| | |
|---|------|
| Leximancer Concept Mapping of Patient Case Studies | 1232 |
| <i>Marcus Watson, Andrew Smith, and Scott Watter</i> | |
| Barrier to Transition from Paper-Based to Computer-Based Patient Record: Analysis of Paper-Based Patient Records | 1239 |
| <i>Machi Suka and Katsumi Yoshida</i> | |
| Preprocessing for Extracting Information from Medical Record to Add XML Tags | 1246 |
| <i>Yoshiaki Kurosawa, Akira Hara, Machi Suka, and Takumi Ichimura</i> | |
| A Scheduling Method of Data Transmission in the Internet Communication by Recurrent Neural Network | 1253 |
| <i>Norio Ozaki and Takumi Ichimura</i> | |
| Health Support Intelligent System for Diabetic Patient by Mobile Phone | 1260 |
| <i>Takumi Ichimura, Machi Suka, Akihiro Sugihara, and Kazunari Harada</i> | |
| Proposal of Food Intake Measuring System in Medical Use and Its Discussion of Practical Capability | 1266 |
| <i>Yoshihiro Saeki and Fumiaki Takeda</i> | |
| Intelligent Learning Environment | |
| Simple Web Mail System That Makes the Best Use of the Senior Citizens Social Experience | 1274 |
| <i>Kiichirou Sasaki, Yurie Iribe, Masato Goto, Mamoru Endo, Takami Yasuda, and Shigeki Yoko</i> | |
| Evaluating Navigation History Comparison | 1281 |
| <i>Koichi Ota and Akihiro Kashihara</i> | |
| A Visualization System for Organizing and Sharing Research Information | 1288 |
| <i>Youzou Miyadera, Naohiro Hayashi, Shoichi Nakamura, and Setsuo Yokoyama</i> | |
| The Learning System of Shinshu University Graduate School of Science and Technology on the Internet | 1296 |
| <i>Hisayoshi Kunimune, Masaaki Niimura, Katsumi Wasaki, Yasushi Fuwa, Yasunari Shidama, and Yatsuka Nakamura</i> | |
| Automatic Generation of Answers Using Solution Network for Mathematical Exercises | 1303 |
| <i>Tomoko Kojiri, Sachio Hosono, and Toyohide Watanabe</i> | |
| Assisting Construction of Meta-cognitive Competence by Scaffolding Discovery of Plans in Problem-Solving | 1310 |
| <i>Kohji Itoh, Eisuke Mihara, Kenji Hasegawa, Masahiro Fujii, and Makoto Itami</i> | |

| | |
|---|------|
| Knowledge Level Design Support for SCORM2004-Conformed Learning Contents – Ontological Consideration on Platforms for Intelligent Educational Systems | 1317 |
| <i>Mitsuru Ikeda and Yusuke Hayashi</i> | |
| Intelligent Data Analysis and Applications | |
| Analyzing Domain Expertise by Considering Variants of Knowledge in Multiple Time Scales | 1324 |
| <i>Jun-Ming Chen, Gwo-Haur Hwang, Gwo-Jen Hwang, and Carol H.C. Chu</i> | |
| A New Algorithm to Discover Page-Action Rules on Web | 1331 |
| <i>Heng-Li Yang and Qing-Fung Lin</i> | |
| Efficient Remining of Generalized Association Rules Under Multiple Minimum Support Refinement | 1338 |
| <i>Ming-Cheng Tseng, Wen-Yang Lin, and Rong Jeng</i> | |
| Mining Association Rules from Distorted Data for Privacy Preservation | 1345 |
| <i>Peng Zhang, Yunhai Tong, Shiwei Tang, and Dongqing Yang</i> | |
| Mining Linguistic Mobility Patterns for Wireless Networks | 1352 |
| <i>Tzung-Pei Hong, Cheng-Ming Huang, and Shi-Jinn Horng</i> | |
| Individualized Product Design by Evolutionary Algorithms | 1359 |
| <i>Maik Maurer and Udo Lindemann</i> | |
| Fuzzy Similarity Measure and Fractional Image Query for Large Scale Protein 2D Gel Electrophoresis | 1366 |
| <i>Daw-Tung Lin, Juin-Lin Kuo, En-Chung Lin, and San-Yuan Huang</i> | |
| Building the Fuzzy Control System Based on the Pilot Knowledge | 1373 |
| <i>Michał Łower, Dariusz Król, and Bogusław Szlachetko</i> | |
| Author Index | 1381 |

A Method for Optimal Division of Data Sets for Use in Neural Networks

Patricia S. Crowther and Robert J. Cox

School of Information Sciences and Engineering,
University of Canberra, ACT 2601, Australia
trishc@webone.com.au, Robert.Cox@canberra.edu.au

Abstract. Neural Networks are used to find a generalised solution from a sample set of a problem domain. When a small sample is all that is available, the correct division of data between the training, testing and validation sets is crucial to the performance of the resultant trained network. Data is often divided uniformly between the three data sets. We propose an alternative method for the optimal division of the data, based on empirical evidence from experiments with artificial data. The method is tested on real world data sets, with encouraging results.

1 Introduction

Artificial neural networks (ANNs) are used to find a generalised solution with a subset of data from a problem domain. When training an ANN network, the data is divided into three distinct subsets; train, the data that is used to actually train the network, test, which is used to stop the training to prevent overfitting thus ensuring a generalised solution, and validation, which measures the accuracy of the resultant neural network. The validation set must be independent of the training and test sets.

In many cases, particularly in the medical field, the amount of available data from a given problem domain is very limited. Dividing the available data three ways further reduces the amount of data that is available to actually train the network.

Various ensemble techniques, such as boosting [1] and bagging [2] have been used to compensate for the lack of available data. N-way reseampling and n-way cross validation [3] are also used.

In the absence of such techniques, a practitioner must decide how to sub-divide the available data. Often it is divided into thirds. Haykin [4] suggests splitting the available data between a training set and a testing set (the latter corresponds to our validation set) then splitting the training set into an estimation and a validation set (our train/test sets). He goes on to recommend an 80/20 split for the latter, based on Kearns [5], who worked data sets of 5000 or more points. It is unclear as to whether his testing set (corresponding to our validation set) is 50% or less of the original data.

It is our hypothesis that the relatively arbitrary way in which ANN practitioners divide data into train, test and validation sets may not lead to neural networks that are optimally generalised and trained.

In this paper we explore, with artificial and real world data sets, the effect that altering the ratio of training and test data has on the performance of the network. Specifically, we are concerned that a relatively common ratio of 80/20 (train/test) is inappropriate and may lead to non-generalised networks. Additionally, we note that a

50/50 split does not make any allowance for the efficiency of the training algorithm. It is generally accepted, though rarely documented, that the training of an ANN is not a completely efficient process. It is therefore accepted that the training set should be larger than the testing set to compensate for the inefficiency of training.

We propose an algorithm to determine the optimal split between train and test data that we have tested empirically on both artificial and real world data sets. It appears to give better results than a 50/50 split and is less risk-prone than an 80/20 split.

2 Methodology

The algorithm was developed on a series of artificially generated data sets with known data and error distributions using a traditional multi-layer perceptron (MLP) ANN trained using error back-propagation. We extended the experiments to real world data sets, testing the hypothesis that an optimal division of data between training and testing sets may be different from a 50/50 split.

For all experiments, the percentage of training data was varied between 5% and 95% in steps of 1% (corresponding testing data therefore varied from 95% to 5%).

We use two measures of accuracy. Observed accuracy (OAcc) is the percentage of correctly classified data that a trained neural network achieves when measured against the validation set - it is the classification accuracy reported by a practitioner. We also use true accuracy (TAcc) that relates only to the experiments with artificial data sets. It is based on the underlying mathematical function used to generate the data and is calculated by comparing the output of the ANN with the function used to generate the data. It is not possible to know the true accuracy unless data has been artificially generated with known error rates. TAcc effectively measures how well the ANN has found the discriminator that was deliberately put there when the data was generated.

2.1 Artificial Data Sets

Initial experiments were conducted on artificially generated data sets, an approach used by other researchers [6]. We generated data using known discriminator functions, introduced a known percentage of classification errors and trained neural networks on the resultant data. We used a data dimension of 2, with 2 classification outputs (above or below the discriminator). The domain of the data was in the range $0 \leq x, y \leq 1$. The classification outputs were given values of 1 and 2.

As with [7, 8], a data point was defined to be in error if it was classified as above the discriminator when it was actually below, or vice versa. The errors were uniformly distributed across the data. A validation set of 1000 data points was generated for each run. Three sets of experiments were conducted, each with a different discriminator function, as shown in figure 1.



Fig. 1. Underlying functions: Left - simple discriminator; middle - more complex discriminator right - discontinuous discriminator (three circles data set)

The simple discriminator is described by:

$$y = \frac{1}{2} \sin \frac{3\pi x}{2} + \frac{1}{2} \quad (1)$$

The more complex discriminator is described by:

$$y = 0.2 + 0.2 \cos(6\pi x) + 0.65x^2 \quad (2)$$

Within each set, a given number of points was generated and divided randomly between training and testing data. Each point on the graphs or in the tables represents the mean of 50 runs, each with different initial random weights (4550 runs per experiment). We used an automated training algorithm for MLP ANNs [7, 8], so each run could have different training parameters (nodes, epochs and training constant).

2.2 Real World Data Sets

In this part of the study we used Abalone, Cancer, Dermatology and Weedseed data sets. All input data was normalised into the range 0 to 1.

The Abalone data set [9, 10] consists of 4177 samples in which abalone shellfish are classified into one of three age related groups based on eight measurements.

The Wisconsin Breast Cancer data set [9, 11] consists of 699 instances, 16 of which have incomplete data and have been removed for the purposes of this study, leaving 683 instances. 10 attributes are listed, but the first is an id so has been discarded, leaving nine that are used to classify a tumor as malignant or benign.

The Dermatology data set [9, 12] consists of 366 instances, eight of which have unknown values for age and so have been disregarded for this study, leaving 358 instances with 34 attributes. Instances are classified into six cases, psoriasis, seborrheic dermatitis, lichen planus, pityriasis rosea, cronic dermatitis and pityriasis rubra pilaris.

The Weedseed data set [13] consists of 398 instances; it classifies weed seeds into one of ten types, based on seven measurements of dimensions of the seeds.

For the real world data sets, one third of the instances were randomly extracted for use as the validation data set. The remaining two thirds of the data was split randomly between training and testing in the same manner used with the artificially generated data. Each point on the graph (or in the tables) represents the mean of 20 runs, each with a different random selection of training, testing and validation sets. For instance, the value for Abalone at 70% training represents the mean observed accuracy of 20 runs (each with different initial random weights) with 2190 training instances, 938 testing instances and 1059 validation instances.

The mean of 20 rather than 50 runs was taken in order to reduce the running times of the experiments. Empirical testing showed that this was acceptable.

3 Results from Artificially Generated Data

We ran 36 experiments with artificially generated data sets. Results of two of the experiments are shown in figure 2. Note that true accuracy closely follows the observed accuracy except at extremes of range, where true accuracy falls off more sharply. This is significant as it tells us that while a practitioner could believe he or she had a high accuracy (based on OAcc) the ability of the neural network to find the

discriminator, as shown by TAcc could be quite a bit below optimum. This makes OAcc within this range less reliable as an indicator of network performance.

Looking at the results, we note that most data sets train well at the point 80/20, similar to the recommendation in Haykin. However, the right hand graph (35% errors, 200 data points) tails quite sharply as early as 70%. Consequently, we recommend that the training ratio should be no greater than 70/30. Accepting that training is inefficient, we recommend a train/test ratio within the range 50/50 to 70/30.

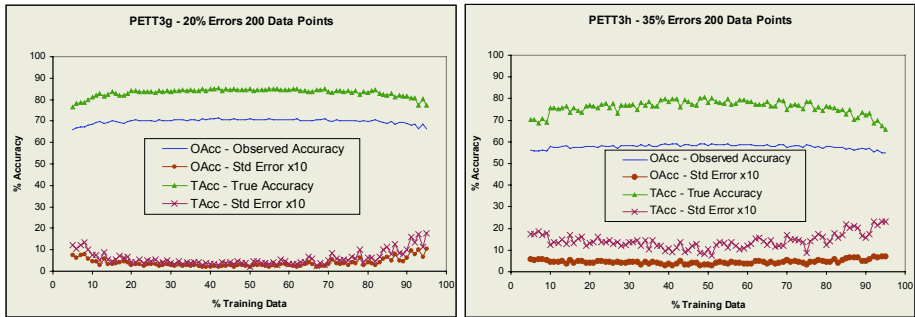


Fig. 2. More complex discriminator (2). 200 data points shared between training and testing. Left hand side 20% errors, right hand side 35% errors

Space precludes inclusion of graphs for all experiments. Tables 1-3 show the optimal split between testing and training for most experiments, OAcc and TAcc at this point, compared with those at the 50/50 mark. Excluded experiments are not materially different from those shown. In all but one case, searching for a better train/test split produced a better result than a straight 50/50 split.

Table 1. Peak performance for artificial data sets – Simple discriminator (1)

| Points in Test/Train set | Error Rate (%) | Peak Train (%) | OAcc at Peak (%) | TAcc at Peak | OAcc at 50/50 Split | TAcc at 50/50 Split |
|--------------------------|----------------|----------------|------------------|--------------|---------------------|---------------------|
| 100 | 10 | 50 | 81.8 | 89.7 | 81.8 | 89.7 |
| 100 | 20 | 66 | 71.9 | 86.6 | 69.7 | 82.9 |
| 100 | 35 | 61 | 57.3 | 73.9 | 56.3 | 70.9 |
| 200 | 10 | 69 | 86.33 | 95.5 | 85.5 | 94.3 |
| 200 | 20 | 69 | 75.13 | 92.0 | 74.2 | 90.1 |
| 200 | 35 | 52 | 59.33 | 81.1 | 58.6 | 79.5 |
| 300 | 10 | 55 | 87.5 | 96.8 | 86.4 | 95.4 |
| 300 | 20 | 55 | 76.5 | 93.9 | 76.0 | 93.1 |
| 300 | 35 | 33 | 60.65 | 85.5 | 59.6 | 81.7 |

4 Results from Real World Data

We tested our method on four real world data sets. Figure 3 shows the graphs for Dermatology and Weedseed. The Abalone and Cancer results did not show the characteristic tailing off at either extreme of the x-axis, probably due to the relatively large number of data points for each classification, so are not shown. The Dermatology

graph clearly shows the same tailing-off effect observed with the artificial data sets. A close examination of the Weedseed graph shows a much smaller ‘safe’ range – between 50% and 80% of data used for training, supporting our assertion that the ratio of train/test data should be in the range 50/50 to 70/30. In the case of Weedseed, the optimal point, as shown in table 4, occurs when the train/test ratio is 67/33. This data set has 398 points in 10 categories and is therefore a fairly sparse data set.

Table 2. Peak performance for artificial data sets – More Complex discriminator (2)

| Points in Test/Train set | Error Rate (%) | Peak Train (%) | OAcc at Peak (%) | TAcc at Peak | OAcc at 50/50 Split | TAcc at 50/50 Split |
|--------------------------|----------------|----------------|------------------|--------------|---------------------|---------------------|
| 100 | 10 | 54 | 78.0 | 85.0 | 77.1 | 84.1 |
| 100 | 20 | 48 | 69.9 | 83.6 | 69.4 | 82.2 |
| 100 | 35 | 39 | 57.5 | 74.8 | 56.8 | 73.6 |
| 200 | 10 | 64 | 78.9 | 86.0 | 78.1 | 85.3 |
| 200 | 20 | 42 | 71.2 | 85.4 | 70.9 | 85.1 |
| 200 | 35 | 41 | 59.1 | 79.9 | 58.3 | 78.2 |
| 300 | 10 | 44 | 79.1 | 86.2 | 78.4 | 85.8 |
| 300 | 20 | 73 | 71.6 | 85.8 | 71.2 | 85.6 |

Table 3. Peak performance for artificial data sets – Three Circles data set

| Points in Test/Train set | Error Rate (%) | Peak Train (%) | OAcc at Peak (%) | TAcc at Peak | OAcc at 50/50 Split | TAcc at 50/50 Split |
|--------------------------|----------------|----------------|------------------|--------------|---------------------|---------------------|
| 100 | 10 | 62 | 74.9 | 80.8 | 73.3 | 79.1 |
| 100 | 20 | 50 | 66.4 | 76.9 | 66.4 | 76.8 |
| 100 | 35 | 33 | 56.2 | 70.4 | 55.5 | 67.7 |
| 200 | 10 | 80 | 74.7 | 80.8 | 72.6 | 78.2 |
| 200 | 20 | 42 | 67.0 | 77.9 | 66.3 | 77.1 |
| 200 | 35 | 13 | 57.3 | 73.8 | 56.4 | 70.4 |
| 300 | 10 | 73 | 77.0 | 83.8 | 75.6 | 81.8 |
| 300 | 20 | 63 | 68.1 | 80.3 | 67.1 | 78.2 |

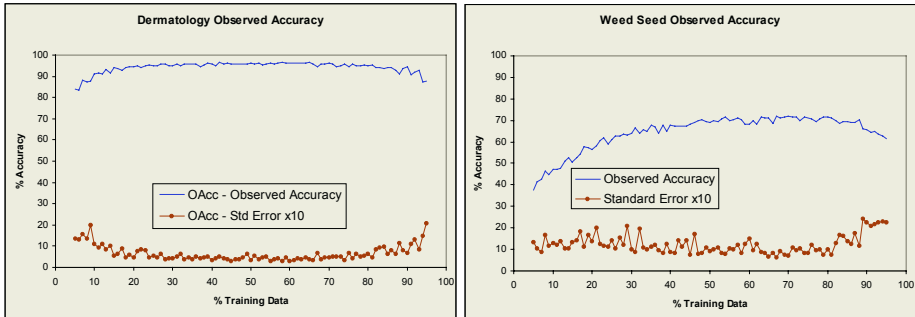


Fig. 3. Dermatology (left) and Weedseed (right)

Table 4 shows the optimal split between training and testing, along with peak observed accuracy for each of the four data sets, compared with OAcc at the 50/50 mark. It should be noted that the peak performance for Dermatology also occurred at

65% training data, but the standard error was slightly higher at 0.36, leading to the selection of the figures shown.

We note that in all cases, searching for a better training/testing split produced a better result than with a straight 50/50 split, confirming our hypothesis.

Table 4. Peak performance for Abalone, Cancer, Dermatology and Weedseed data sets

| Data Set | Peak Train% | Peak OAcc | Std Error at Peak | OAcc at 50/50 split |
|-------------|-------------|-----------|-------------------|---------------------|
| Abalone | 69% | 66.2% | 0.27 | 65.6% |
| Cancer | 49% | 97.3% | 0.2 | 96.9% |
| Dermatology | 58% | 96.6% | 0.31 | 96.1% |
| Weedseed | 67% | 72.1% | 0.6 | 66.9% |

5 Conclusion

We have shown the traditional 33/33/33 train/test/validation split can produce sub-optimal networks, especially when a data set has a small number of data points. We have also shown that Haykin's 80/20 split of the train/test data can be potentially unsafe, especially for small data sets.

We are convinced that for a data set with a large number of data points eg Abalone and Cancer, the exact train/test ratio is less important because there is sufficient data to support classification. With such data sets, practitioners can be comfortable with a ratio within the range 50/50 to 70/30.

We have demonstrated, using empirical tests, that when the non-validation data is divided between training and test data using a ratio in the range 50/50 – 70/30, the resultant accuracy, when graphed, produces a curve that peaks. The point at which it peaks represents a good ratio with which to split the data. Our recommended algorithm for splitting data is as follows:

- Remove one third of the data for validation.
- Of the remaining data, run a series of tests, splitting it between train and test in the ratio 50/50 through to 70/30 in steps of 1. (If 30 experiments are too many, increase the step size.) It may be necessary to run a number of experiments at each point, varying the initial random weights in order to produce a smooth enough curve to reliably identify the peak.
- From the above, choose the ratio that has the highest accuracy and use it to train the neural network.

References

1. Freund, Y, & Schapire, R.: Experiments with a New Boosting Algorithm. Proc 13th International Conference on Machine Learning 1996. Morgan Kaufmann pp148-156.
2. Breiman, L.: Bagging Predictors. Machine Learning 24(2) (1996) 123-140.
3. Weiss, S.M. & Kulikowski, C.A. Computer Systems That Learn, Morgan Kaufmann 1991.
4. Haykin, S., Neural Networks a Comprehensive Foundation 2nd Ed. Prentice Hall 1999.
5. Kearns, M. A Bound on the Error of Cross Validation Using the Approximation and Estimation Rates, with Consequences for the Training-Test Split. Advances in Neural Information Processing Systems 8, The MIT Press, pages 183–189, 1996.

6. Kuncheva, L. I. & Hadjitodorov, S. T., Using Diversity in Cluster Ensembles Proc. IEEE International Conf. on Systems, Man and Cybernetics, The Hague, The Netherlands, 2004.
7. Crowther, P., Cox, R. & Sharma, D. A Study of the Radial Basis Function Neural Network Classifiers using Known Data of Varying Accuracy and Complexity, Knowledge-Based Intelligent Information Systems 8th International Conference, KES 2004 Wellington, New Zealand, September 2004 Proceedings, Part III p 210-216, Springer-Verlag 2004.
8. Cox, R.J. & Crowther, P.S. An Empirical Investigation into the Error Characteristics of Neural Networks, Proceedings AISAT 2004 The 2nd International Conference on Artificial Intelligence in Science and Technology, Hobart, Australia, 21-25 November 2004 p 92-97
9. Machine learning repository: <http://www.ics.uci.edu/~mlearn/MLSummary.html>
10. Nash, Warwick J., Sellers, Tracy L., Talbot, Simon R., Cawthorn, Andrew J. & Ford, Wes B. The Population Biology of Abalone (*Haliotis* species) in Tasmania. I. Blacklip Abalone (*H. rubra*) from the North Coast and Islands of Bass Strait. Sea Fisheries Division Technical Report #48 (1994).
11. Mangasarian, O.L. & Wolberg, W.H. Cancer Diagnosis via Linear Programming. SIAM News, vol 23 no. 5, September 1990 p1 & p18.
12. Guvenir, H.A., Demiroz, G. & Ilter N. Learning Differential Diagnosis of Eryhemato-Squamous Diseases using Voting Feature Intervals. Artificial Intelligence in Medicine vol. 13, no. 3 (1998) pp 147-165.
13. Cox, R, Clark, D & Richardson, A. An Investigation into the Effect of Ensemble Size and Voting Threshold on the Accuracy of Neural Network Ensembles. Lecture Notes in Computer Science vol. 1747. Proceedings of the 12th Australian Joint Conference on Artificial Intelligence: Advanced Topics in Artificial Intelligence pp268-277 (1999).

Excluding Fitness Helps Improve Robustness of Evolutionary Algorithms

Matej Šprogar

Faculty of Electrical Engineering and Computer Science,
University of Maribor, Slovenia
matej.sprogar@uni-mb.si

Abstract. The article describes a variant of evolutionary algorithms, which avoids the usual explicit fitness based cycle. The idea is to exclude any presumptions about the problem at hand in the coding of the artificial evolution. In nature the fitness is implicit and we created a similar environment for genetic programming to solve practical engineering problems. Our attempt to avoid direct (explicit) fitness calculation showed positive effects on the robustness of the evolved solutions.

1 Introduction

Use of any sort of evolutionary algorithm (EA) as a search procedure is by now a well established process. Whether for artificial or real problems the EAs perform well. The recipe of how to apply the EAs is more or less straight – inspect the problem, define and code the evolutionary mappings (for example the gene-coding in GA) plus the fitness function, then run the system until some stopping criterion is met. The EA run itself however still includes many mysteries and dangers.

The first success of EAs in solving mathematical problems was an impulse to try and solve more complicated problems; today genetic programming is capable of human-competitive machine intelligence. We must not forget that the first EAs were used to find only a point in the search space, for example the correct value for a single variable. In time this search for a single point was not only expanded to several points, but to another level – a *learning* search for a program, that *calculates* this value. There was however no evolution in the process itself – most implementations and examples still use the proved inspect/code+fitness/run scenario. A problem in EAs is preferably solved by the tuning of the existing approach. For example, if the results are below expectations, the researcher normally invents a new or a “better” genetic operator or tunes the fitness function little more.

When we progress from the point-search to the learning (search) methods, as is the case in genetic programming (GP), the resulting programs are expected to work on unknown data, too. Kushch reports an increase in observations that solutions to learning problems may result in non-robust (or brittle) programs [1]. A much broader concept is generalisation, as it requires a formal methodology

for choosing the training and testing cases and evaluating and comparing the corresponding performances.

In this article we shall describe our observations of the behavior of a modified evolutionary algorithm. We excluded the conventional EA fitness-based approach, which assigns an explicit fitness score to each individual solution. Instead we simplified the evolutionary concepts. We applied a co-evolutionary search and we defined an interaction operator of the two opposing individuals. Co-evolution is a recognized evolutionary approach, easy to implement and apply in all environments. The problem of interaction of two individuals however has some pitfalls, which we address at the end.

2 Background

Hooper and Flann [2] suggest that GP, as an inductive learning method, can be expected to produce programs whose behaviour is applicable over all the input space and not just the training instances. They further state that when training and testing phases are adapted, improving the fitness function to prefer simpler expressions (i.e., smaller programs) may help to avoid over-fitting and obtain better predictive accuracy during the testing phases.

This kind of thinking reflects the usual attitude in EA community – if there’s something wrong with the algorithm, try tuning the fitness function first. We can only assume how a solution’s property affects the quality of the solution and base our fitness evaluation on this assumption. If the assumption is wrong we end up with a brittle solution that is over/under-fitted to the learning dataset. In both cases the solution will perform poorly on the previously unseen test data.

Koza devoted most of his GP book and examples to explicit genetic programming, only the chapter 28 is addressing the issue of emergence and “active” individuals [3]. This also reflects how much easier it is to use the explicit fitness-based EAs to solve engineering problems. Koza distinguishes between “passive” and “active” individuals – later have the ability to reproduce; the fact that they reproduce means that they are fit. Many accomplished the task of evolving self-replicating programs yet none of those experiments defines a simple method for solving other types problems; this is the strength of the explicit fitness based EAs.

Our approach tries to combine the advantages of both explicit and implicit fitness. We’ll try to create a method that is applicable to all sorts of problems (an excellent property of explicit-fitness based EAs) and also shows emergent properties (this is associated with self-replicating and evolutionarily self-improving computer programs).

2.1 Emergent Properties and Systems-Thinking

The EA approach itself is universal yet we always face search speed and efficiency problems. Use of faster and faster computers is not the solution of this problem. Therefore the GP community regards any approach with simple “binary” fitness

as immature; this is not enough to guide the subsequent search process [4]. All research is in the direction of more elaborate fitness measures and selection schemes. More elaborate gradual fitness function should hopefully make the EAs *faster*.

From the systems-thinking perspective [5] this is a problem. Every time we use EA we tune the algorithm to fit a specific problem and hence the final algorithm is impossible to port to another, although similar problem. A fitness evaluation is a kind of a “shortcut” that *exploits* our (probably) false understanding of the problem because it includes too-many presumptions. On the other hand, the simple binary fitness includes no *presumptions* about the (importance of) relative ordering of the individuals in the population, it simply says this individual is fit, this one is not. There’s no *ordering* of living creatures in the nature, nor are they given equal conditions. Ordering is a purely human invention. Darwin’s survival of the fittest should not be interpreted as “perform evaluation(!?) procedure, sort and select(!?) the survivors, kill the rest”, it is more of a “let them all have a try in life and the ‘fittest’ will turn out to have *more offspring*”! This is the main idea of our Autonomous EA (aEA).

2.2 The Idea

We constructed an evolutionary algorithm that avoids explicit fitness function. Because there’s no fitness function inside the algorithm we also need no fitness based selection. In the nature all living creatures are given a chance to live and have offspring. There are no assumptions, only a rough survival. Individual’s *life* is the one and only fitness function. In standard EAs the fitness function is a shortcut that allows EAs to pass judgements on individuals even *before* they have the chance to live/act. There’s no way EAs can correctly guess what kind of a life and how successful an individual would have been unless the individual is given a chance to live! From the theory of chaos we know that a small change inside a complex system may have dramatic effects on its long-term behavior. The complex system is always governed by a range of small interactions and influences between *all* (living) participants. But this is exactly what the fitness shortcut avoids – all the small but very important interactions. In extreme example, if a fitness designates one individual as bad, the selection operator will give to this individual no chance of survival. So this individual will make *no* impact on the evolution of the whole population. EAs try to compensate by using smart selection schemes, which also select worse individuals in order to maintain the genetic diversity. This is only a a mild cure that heals the symptoms, but does not remove the cause of the disease – the fitness shortcut.

Even the competitive fitness or other co-evolutionary fitness concepts suffer from this same problem – they always make a judgement without letting the individual *affect* the environment (the co-evolving population). Therefore even using the “perfect” fitness is problematic because it avoids all the small interactions between the living individuals, which define the contents of the new population.

3 Autonomous Evolutionary Algorithm – aEA

A human operator is needed to (1) design and (2) run the EA; in both phases many “errors” are possible that result in bad and/or brittle solutions. The true autonomous EA would need no human control in the run phase and would be more stable even if minor errors were made in the design phase. The name “autonomous EA” describes our intention to create the EA that is independent as much as possible of the human influence.

In order to build a more autonomous-like EA we hypothesized that it must co-evolve the solutions (individuals) together with the environment; environment is also a population of individuals. The individuals live and are not selected in any way and the environment also responds to improvements in individuals. It’s a closed system that incorporates both reinforcing and balancing dependencies between the participants.

3.1 Life of an Individual

One of the EA’s problems is that it doesn’t give an individual a chance to live. The system in EAs gives no respect to the interaction of individuals. In aEA we don’t make a fitness evaluation, but rather try an individual out in the environment. This *try* is a simple test whether the individual survives a *contact* with the environment. Because we decided for a co-evolving scenario, the environment is actually a second population, filled with individuals of a (possibly) different type. A contact is therefore a test which of the two individuals is “better”.

Sketch of the aEA life cycle

```

population<predator> P;           // individuals
population<prey> R;               // environment

while ( !P.empty() and !R.empty() )
{
    predator p; P >> p;           // fetch from P
    prey r; R >> r;               // fetch from R
    if (p > r) P << p.recombine(); // if p better-than r
    else R << r.recombine();       // insert offspring
}

```

The algorithm shows the aEA core loop stripped of details. There is no global selection process because there is no fitness. Instead we select a pair (p, r) and determine the winner using the special $>$ (better-than) operator. For example the predator is the winner if it “catches” the prey. Then the winner has a chance to multiply using the standard crossover operator. Important observation is that every individual in the environment must get its chance to survive and breed, no matter how good/bad it is. It is pure coincidence that governs the creation of pairs for the duels – sometimes a good predator will face a prey so advanced

that it is impossible to catch, or a lousy predator will find a prey that's crippled. This mechanism more closely resembles the nature's way to select the individuals for reproduction. The algorithmic process itself is *not* directed by the human understanding of the problem in any way!

3.2 Population Sizing

The draft algorithm above does not show how the library handles population sizing. If aEA would implement a core directly like this then without a special sizing control (used in EAs) either P or R would immediately get empty. There are two problems with such a control: (i) it encodes possibly erroneous human interpretation of the problem; (ii) it is problem-dependent and contradicts the autonomous nature of the aEA. In aEA we therefore chose to implement more complicated internal mechanisms that determine the number of offspring of each individual, based on its history and types of contacts it made with the environment and vice versa. The main idea is to regulate the population and environment sizes without any explicit numeric control function – it is self-regulated (it displays the behaviour of the natural systems, e.g. predator-prey model). If however either population P or environment R fall down to 0 then this is a sign that the opposing population was able to completely outperform the emptied population... This is also a simple stop criterion for the evolution.

This short aEA description does not cover all issues addressed by aEA. Details however can be seen in the library itself – the complete aEA library together with example projects is freely available under the terms of GNU GPL on the author's Web page at <http://rts.uni-mb.si/matej/aea>.

4 Example – Symbolic Regression

Problems of symbolic regression require finding a function, in symbolic form, that fits a given finite sampling of data points. The problem here is the target function $P(x) = x^4 + x^3 + x^2 + x$. For example the genetic programming excels in finding a suitable function given sample of 20 (x_i, y_i) data points, where the x_i come from the interval $[-1, +1]$. But this is all in a controlled environment, with no noise in the data, where fitness function is obvious and the problem is easy to code.

In our example test we'll compare the aEA against standard GP. For the GP implementation we used the *symbreg* project from the OpenBeagle GP library [6]. In order to test the robustness we extended the original learning data. New data included 41 fixed points in the interval $[-1, +1]$, sampled with a step size of 0.05. We also added a small amount of Gaussian noise with mean=0 and standard deviation=0.02 ($\mathcal{N}(0, 0.02)$) to a few randomly chosen y_i values.

In OpenBeagle the adjusted fitness measure is used. It is based on the error over all fitness points produced by the evolved function f . The fitness F is calculated using (1), where $f_i = f(x_i)$ and $P_i = P(x_i)$ and n is the number of fitness points (41):

$$F(f) = 1/(1 + \sqrt{\sum (f_i - P_i)^2/n}) \quad (1)$$

If the learning set was not disturbed by noise, the target function $P(x)$ would have had a perfect fitness score of 1. On our learning set the target's fitness was 0.936837. Both GP and aEA were equipped with the same function set: +, -, *, /, sin, cos, exp, log; a terminal set included only x as the independent variable. For the sake of comparison with GP the aEA was also “equipped” and measured with the described fitness.

4.1 Standard GP

The OpenBeagle's symbreg model has a vast number of available run-time options; we chose to change only the population size from 100 to 500 and to run the evolution for at least 500 generations. To evaluate one individual function a GP needs to evaluate it on all 41 learning samples. Therefore it performed $500 * 500 * 41 = 10.250.000$ function calculations in one run. The best-of-run individual was recorded. The 10 “best” functions from 10 independent runs had the mean fitness of 0.969185 with a standard deviation of 0.012355. The highest fitness score was 0.985981 and the lowest 0.948721. GP easily and quickly found functions with a fitness score higher than that of the target function $P(x)$, in fact the lowest score after 500 generations was always above $F(P)$.

To select the absolute winner from this set of 10 functions we need to observe also the size of the functions. The solution with the minimal fitness 0.948721 is also the smallest, with only 80 nodes. The “best” solution incorporated 306 nodes... It is obvious that severe over-fitting had occurred. We performed also a separate trial run set to stop at the limiting fitness score and as expected, quite soon after start, GP did evolve the target $P(x)$, but in the normal run it proceeded towards fitness 1. Fitness calculation is dependent only on the error, not on the size of the function as it is not trivial to specify such a criterion.

4.2 Autonomous EA

In order to run symbolic regression in aEA we need a GP coding of an individual function f and of an environment object r . We need an operator $>$ that tells us whether f is better-than r or not. In the example of symbolic regression it turns out that the simplest solution is to evolve two populations of functions one against the other. So we need an operator $f_1 > f_2$. The simplest implementation selects one random point from the learning dataset and compares the errors of both functions. The function that gets closer to the point's y value is the winner.

In each of the 10 separate runs aEA was set to evolve approximately for the same time on the same CPU as the GP (it is impossible to directly compare generations in GP with the iterations in aEA). The run could however end sooner if either of the two populations was emptied – this was the case in 3 runs. In 2 out of those 3 runs the aEA produced $P(x)$, and in the third one it found a function $f(x) = x + x * \sin(x) + x^3 * (\sin(x)/x + x)$, which scores 0.945239 and is very close to $P(x)$ also outside of the definition area $[-1, +1]$. If the evolution was

interrupted we selected the individual with the highest fitness for comparison with GP. The average score was 0.929419 with a standard deviation of 0.012315 in the range from 0.904932 up to 0.945239. While the standard deviation is almost identical to GP's the aEA's average fitness is much closer to the 0.936837 from $P(x)$. Actually the highest aEA's score was still lower than the lowest GP and closer to the optimal value.

5 Conclusions

In the original symbreg problem the GP outperforms aEA in terms of convergence speed. But when it comes to noisy data, where the fitness is difficult to define, aEA's simplistic design evolves more robust solutions. There are many details in aEA that still need to be fixed, including the problem with the start-up: we need continuous oscillations of the two populations, P and R ; depending on the problem coding a *premature* end of evolution is possible; this is usually because of different quality levels of initial random solutions. This way one population fully dominates the other right from the start, not because it evolved certain good properties. Another problem that needs attention is how to recognize (designate) the final solution from the population of solutions – for the symbolic regression example in this paper we just used the standard fitness approach. However, this is in contradiction with the main idea of the library and is one of the central issues to be resolved in our future work.

References

1. Kushch, I.: An evaluation of evolutionary generalisation in genetic programming. *Artificial Intelligence Review* **18** (2002) 3–14 Stanford University Computer Science Department technical report STAN-CS-90-1314.
2. Hooper, D., Flann, N.: Improving the accuracy and robustness of genetic programming through expression simplification. In Koza, J., Goldberg, D., Fogel, D., Riolo, R., eds.: *Genetic Programming 1996: Proceedings of the First Annual Conference*, MIT Press (1996) 428
3. Koza, J.: *Genetic Programming: On the Programming of Computers by Natural Selection*. MIT Press, Cambridge, MA (1992)
4. Banzhaf, W., Nordin, P., Keller, R., Francone, F.: *Genetic Programming, An Introduction*. Morgan Kaufmann, San Francisco (1998)
5. Bellinger, G.: Simulation is not the answer. <http://www.systems-thinking.org/> (2005)
6. Gagne, C., Parizeau, M.: Open BEAGLE: A new versatile C++ framework for evolutionary computation. In: *Proceeding of GECCO 2002, Late-Breaking Papers*, New York, NY, USA (2002)

Testing Voice Mimicry with the YOHO Speaker Verification Corpus

Yee W. Lau, Dat Tran, and Michael Wagner

School of Information Sciences and Engineering,

University of Canberra, ACT 2601, Australia

{Yee.Lau,Dat.Tran,Michael.Wagner}@canberra.edu.au

Abstract. The aim of this paper is to determine how vulnerable a speaker verification system is to conscious effort by impostors to mimic a client of the system. The paper explores systematically how much closer an impostor can get to another speaker's voice by repeated attempts. Experiments on 138 speakers in the YOHO database and six people who played a role as imitators showed a fact that professional linguists could successfully attack the system. Non-professional people could have a good chance if they know their closest speaker in the database.

1 Introduction

Voice mimicry is a simple technology form of attack requiring a lower level of expertise to investigate whether a speaker verification system is vulnerable to mimicry by an impostor without using any assistance of other technologies. Although reducing the false acceptance error rate of impostors has been investigated in speaker verification systems, there is still a potential of security threat concerns [4, 7]. There have been very few reports on attacks against speaker verification systems by human and speech synthesis mimicry. For instance, the vulnerability of speaker verification systems to threats by trainable speech synthesis technology has been investigated [1, 2, 3]. While speech synthesis may be employed to attack a system by copying a client's voice, this may not be practical in an operational system where minimum-processing time is required. Therefore, in this paper, we consider human voice mimicry to investigate whether a speaker verification system is vulnerable to mimicry without using speech synthesis technology. Furthermore, we want to find out whether professional linguists are helpful in deceiving an automatic speaker recognition system. We used a Gaussian mixture model (GMM)-based speaker verification system and the YOHO database for this investigation. Experimental results showed a fact that the professional linguists could successfully attack the system. Non-professional people could have a similar chance if they know their closest speakers in the database.

2 Speaker Verification

Let λ_0 and λ_i be the claimed speaker model and the background speaker model representing the speaker close (similar) to the claimed speaker, respectively. Let $P(X)$

$|\lambda_0)$ and $P(X | \lambda_i)$ be the likelihood functions for the claimed speaker and background speaker, respectively. For a given input utterance X , the claimed speaker's score $S(X)$ is used as follows

$$S(X) \quad \begin{cases} > \theta & \text{accept} \\ \leq \theta & \text{reject} \end{cases} \quad (1)$$

where θ is the decision threshold and the score $S(X)$ is calculated as [5]

$$S(X) = \log P(X | \lambda_0) - \log \left[\frac{1}{B} \sum_{i=1}^B P(X | \lambda_i) \right] \quad (2)$$

B is the number of background speaker models used to represent the population close to the claimed speaker.

3 The Yoho Voice Verification Corpus

The YOHO corpus was designed for speaker verification systems in office environments with limited vocabulary. There are 138 speakers, 108 males and 30 females. All waveforms are low-pass filtered at 3.8 kHz and sampled at 8 kHz. Speech processing was performed using HTK V2.0 [9]. The data were processed in 32 ms frames at a frame rate of 10 ms. Frames were Hamming windowed and pre-emphasized. The basic feature set consisted of 12th-order mel-frequency cepstral coefficients (MFCCs) and the normalized short-time energy, augmented by the corresponding delta MFCCs to form a final set of feature vector with a dimension of 26 for individual frames.

Gaussian mixture models (GMMs) are randomly initialized. Covariance matrices are diagonal, i.e. $[\sigma_k]_{ii} = \sigma_k^2$ and $[\sigma_k]_{ij} = 0$ if $i \neq j$, where σ_k^2 are variances $1 \leq k \leq K$. A variance limiting constraint was applied to all GMMs using diagonal covariance matrices [5]. This constraint places a minimum variance value $\sigma_{\min}^2 = 10^{-2}$ on elements of all variance vectors in the GMM in our experiments. There were 16 mixtures in each GMM and were trained in text-independent mode.

4 Testing Voice Mimicry

In our testing, there were two groups of imitators: professional and non-professional groups. The professional group comprised a female linguist (FL) and a male linguist (ML). The non-professional group comprised four people who had no specific expertise in voice mimicry: Australian female (AF), Australian male (AM), Chinese female (CF) and Chinese male (CM). The two Australian people are English speaking background and the two Chinese people are non-English speaking background. All of these six imitators were asked to imitate a selected speaker in the YOHO database after listening to that speaker's voice and speaking style.

To select the YOHO speaker for each imitator, we performed the following. Each imitator was required to speak 10 utterances picked up from the YOHO vocabulary in verification sessions. We then measured the average similarity scores between the imitator and the same-gender YOHO speakers. Let X be the 10 utterances spoken by

the imitator and λ_i be the model of the i th YOHO speaker, the similarity score was defined as the following log-likelihood function

$$S_i(X) = \log P(X | \lambda_i) \quad i = 1, \dots, 138 \quad (4)$$

Based on those scores, we chose the most similar YOHO speaker for each imitator. Now the imitators could start their voice mimicry testing. Each imitator listened to utterances in the YOHO verification sessions spoken by his/her most similar YOHO speaker three times then imitated that voice in three recording sessions. We performed the three recording sessions to consider the improvement of the imitator's voice mimicry. All of the three recordings were recorded using a high quality microphone and saved to 16-bit words and sampled at 8 kHz. The environment for recording was in a laboratory where the system was set up in a corner of the lab with a medium to low-level noise from the adjoining rooms, air-conditioning system, people walking through the corridor, and the fan in the Sun workstation. The same speech processing in Session 3 was applied to process the imitators' voice database.

The most similar YOHO speakers for the imitators FL, ML, AF, AM, CF and CM were 192, 176, 237, 176, 237 and 239, respectively.

5 Experimental Results

In order to evaluate the voice mimicry performance of the imitators, we computed false acceptance error rates obtained by the imitators and compared those with false acceptance and false rejection error rates obtained by the YOHO speakers.

5.1 Results for the Professional Group

Figure 1 shows the false acceptance error rates for the female linguist (FL) and her most similar YOHO speaker 192. It is found that even we set the threshold to 1 to get the 0% for overall false acceptance error rate, the speaker verification system still produces high false acceptance error rate (60%) for the female linguist.

In Figure 2, a similar result is obtained for the male linguist. However, the male linguist achieved only 10% for his false acceptance error if the threshold is set to 1. If the threshold is set to the equal error rate threshold (-0.2), the male linguist can achieve up to 70% for his false acceptance rate.

5.2 Results for the Non-professional Group

Both the Australian female and Chinese female had the same most similar YOHO speaker 237. The error rates for those speakers are shown in Figure 3. Their results are similar to the male linguist's result, the false acceptance error rate is about 20% for the Australian female and 30% for the Chinese female if the threshold is set to 1.

Figure 4 shows the verification error rate for the Australian male and his most similar YOHO speaker 176. The result is similar to that for the male linguist in Figure 2. However, the Chinese male had a better performance shown in Figure 5. He could achieve up to 60% false acceptance error rate if the threshold is set to 1.

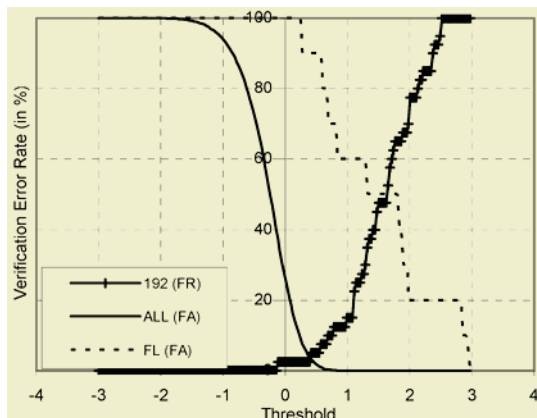


Fig. 1. Verification error rates (FR and FA) versus threshold for all YOHO speakers, the female linguist FL and her most similar speaker 192

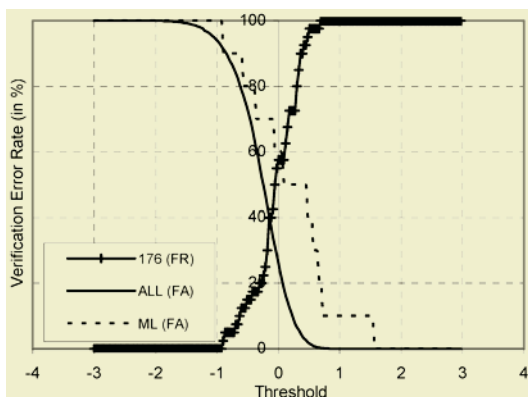


Fig. 2. Verification error rates (FR and FA) versus threshold for all YOHO speakers, the male linguist ML and his most similar speaker 176

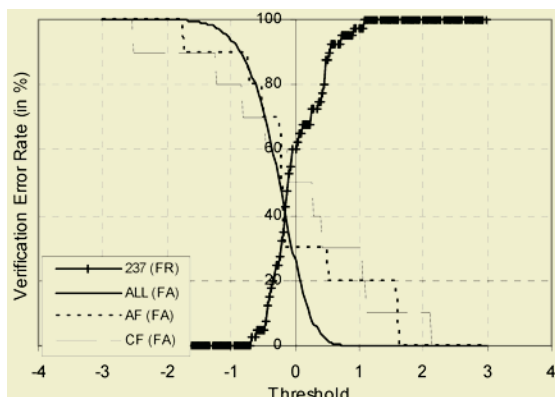


Fig. 3. Verification error rates (FR and FA) versus threshold for all YOHO speakers, the Australian female (AF), the Chinese female (CF) and their most similar YOHO speaker 237

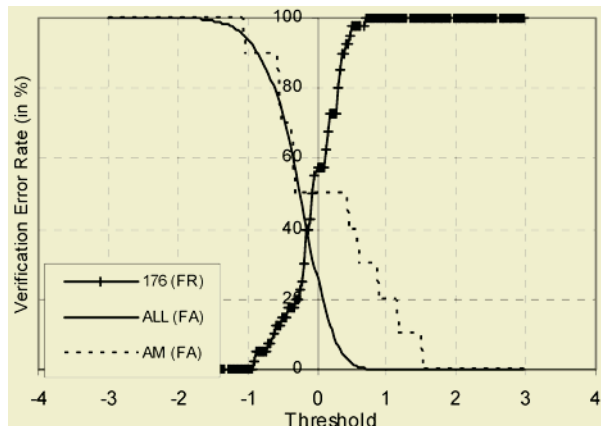


Fig. 4. Verification error rates (FR and FA) versus threshold for all YOHO speakers, the Australian male (AM) and his most similar YOHO speaker 176

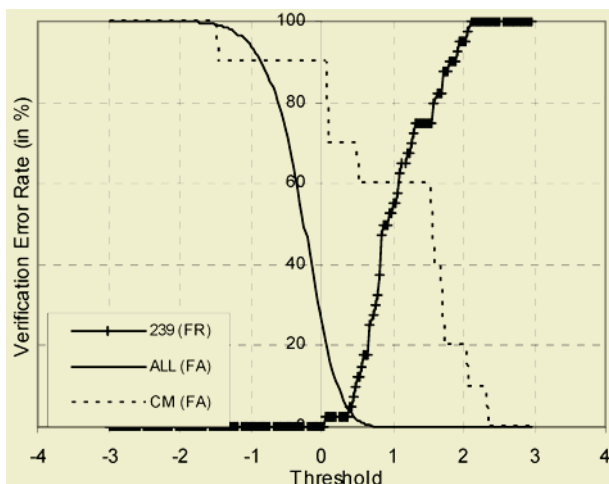


Fig. 5. Verification error rates (FR and FA) versus threshold for all YOHO speakers, the Chinese male (CM) and his most similar YOHO speaker 239

For all results shown in the above figures, we can find that the linguists did not achieve better voice mimicry performance than the non-professional imitators did. However, for voice mimicry performed on the claimed speaker who is not the most similar speaker, the linguists could perform better. Figure 6 shows the verification results for the female linguists.

If we set the threshold to 1 in both the figures, the female linguist could get 40% for her false acceptance error rate, higher than the Australian and Chinese females' false acceptance error rates (30%) although the YOHO speaker 237 was not the most similar speaker of the female linguist. However the male linguist did not achieve a higher error rate than the Australia and Chinese male did. This shows a fact that professional linguists could get a high chance to successfully attack the system.

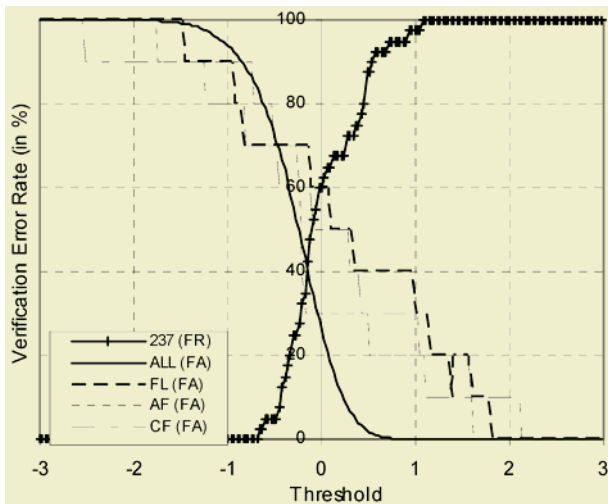


Fig. 6. Verification error rates (FR and FA) versus threshold for all YOHO speakers, the Australian female (AF), Chinese female (CF), their most similar YOHO speaker 237 and the female linguist (FL)

6 Conclusion

We have considered the voice mimicry with the Gaussian mixture model-based speaker verification system. Experimental results showed a fact that a non-professional impostor could get a high chance to successfully attack the system if that impostor knows the closest speaker in the database. A notable effect is that choosing speakers in the database whom are close to the client's voice and using their recording for impostor attempts will outperform the re-synthesis method [7].

References

1. Huang, X., Acero, A., Hon, H., Ju, Y., Liu, J., Meredith, S., Plumpe, M.: Recent Improvements on Microsoft's Trainable Text-to-Speech System: Whistler. Proc. of the Int. Conf. on Acoustics, Speech, and Signal Processing. Munich, Germany (1997)
2. Lindberg, J. and Blomberg, M.: Vulnerability in speaker verification. A study of technical impostor techniques" Proc of Eurospeech 99, (1999)1211-1214
3. Masuko, T., Tokuda, K. and Kobayashi, T.: Impostors using Synthetic Speech Against Speaker Verification Based on Spectrum and Pitch. Proc. ICSLP 2000.
4. Pellom, B.L., Hansen, J.H.L.: An Experimental Study of Speaker Verification Sensitivity to Computer Voice-Altered Impostors. IEEE ICASSP-99: Inter. Conf. on Acoustics, Speech, and Signal Processing, vol. 2, (1999)837-840
5. Reynolds, D.A.: Speaker identification and verification using Gaussian mixture speaker models. Speech Communication, vol. 17, (1995) 91-108
6. Satoh, T. Masuko, T. Kobayashi, T. Tokuda, K.: A robust speaker verification system against imposture using an HMM-based speech synthesis. Proc. 7th European Conference on Speech Communication and Technology, EUROSPEECH, Denmark, vol.2, (2001)759-762

7. Takashi, M., Keiichi, T., and Takao, K.: Imposture using synthetic speech against speaker verification based on spectrum and pitch. Proc. ICSLP-2000, vol. 2, (2000) 302-305.
8. Tran, D. and Wagner, M.: Fuzzy Gaussian Mixture Models for Speaker Recognition. Australian Journal of Intelligent Information Processing Systems (AJIIPS), vol. 5, no. 4, (1998) 293-300
9. Woodland, P. C., et. al.: Broadcast news transcription using HTK. Proceedings of ICASSP, USA (1997)

Image Multi-noise Removal via Lévy Process Analysis

Xu Huang¹ and A.C. Madoc²

¹ School of Information Sciences and Engineering,
University of Canberra, ACT, 2601, Australia
Xu.Huang@canberra.edu.au

² Center for Actuarial Studies, Department of Economics,
University of Melbourne, VIC 3051, Australia
a_c_m81@hotmail.com

Abstract. Almost every digital image is unavoidably contaminated by various noise sources. In our previous paper, we focused on Gaussian and Poisson noises. Unlike additive Gaussian noise, Poisson noise is signal-dependent and separating signal from noise is a difficult task. A wavelet-based maximum likelihood method for Bayesian estimator that recovers the signal component of the wavelet coefficients in original images by using an alpha-stable signal prior distribution is demonstrated to the discussed noise removal. Current paper is to extend out previous results to more complex cases that noises comprised of compound Poisson, Gaussian, and impulse noises via Lévy process analysis. As an example, an improved Bayesian estimator that is a natural extension of other wavelet denoising via a colour image is presented to illustrate our discussion.

1 Introduction

It is well known that noise degrades the performance of any image compression algorithm. In many cases it is degraded even before they are encoded. There are many noise sources such as Poisson noise (when you read a X-film), Gaussian noise (when you received a image from a communicated channel), impulse noise (when you check a ultrasonic diagram), and etc. If we could have information about the noises, it would be helpful for us to design a good filter. In this paper, we are going to extend our pervious research results [1, 14-16] to the noise sources consist of various major noise sources obeying compound Poisson and Gaussian distributions via Lévy process analysis. In particular [1] does not consider the impulsive noise even though the conditions of Levy process was investigated. Here a full investigation under the Levy process will be discussed.

In 1963, Mandelbort [2] firstly pointed out the drawback of Brownian motion as a stock price model and proposed an exponential non-Gaussian Lévy process. After that Madan and Senata [3] have proposed a Lévy process with the variance of the normal distribution is gamma distributed as a model for the logarithm of stock prices. Barndor-Nielsen [4] proposed an exponential normal inverse Gaussian Lévy process. Bertoin [5] discussed Lévy processes in his book. The fundamental properties of Lévy process are established by the basic conceptual building blocks such as its characteristic function, infinitely divisible distribution, and the Lévy measure. In our current paper, the definitions and conditions of our investigations and discussions will follow the statements by Bertoin [5] unless indicated otherwise.

If Y_i 's are independently identically distributed then Y would have a compound Poisson distribution with parameters $\Lambda = n\lambda_i$. As a consequence of the result the Lévy-Khintchine representation for the compound Poisson distribution is:

$$\begin{aligned} E[\exp\{i < \lambda, Y_1 >\}] &= E[\exp\{i \sum_{0 \leq s \leq t} < \lambda, \Delta s >\}] \\ &= \exp\{-\int_{\mathbb{R}^d} (1 - \exp\{i < \lambda, x >\}) \Lambda(dx)\} \end{aligned} \quad (1)$$

Here, a finite measure Λ on \mathbb{R}^d that gives no mass to the origin, let $\Delta = (\Delta t, t \geq 0)$ be a Poisson point process with characteristic measure Λ . The Lévy process $Y_t = \sum \Delta s$ with ($0 \leq s \leq t$) is well-defined. It was proved that the sum of independent Lévy processes is a Lévy process, thus, we can combine different “building blocks” to obtain a general characteristic function of the form same in the Lévy-Khintchine representation in the one-dimension case. For example, we can have the characteristic function of the stable (α, β, γ) distribution given by

$$\exp\{\gamma | \lambda |^\alpha [1 - i\beta \text{sgn}(\lambda) \tan(\pi\alpha/2)]\} \quad (2)$$

We are going to extend our method [1] for a stable (α, β, γ) distribution to the case contaminated by noises consisted of compound different Poisson distributions and together with a Gaussian distribution.

Several groups have discussed that wavelet subband coefficients have highly non-Gaussian statistics [7-16] and the general class of α -stable distributions has also been shown to accurately model heavy-tailed noise [10-11].

Wavelet transform as a powerful tool for recovering signals from noise has been of considerably interest [16-19]. In fact, wavelet theory combines many existing concepts into a global framework and hence becomes a powerful tool for several domains of application.

As mentioned by Achim *et al.* [21], there are two major drawbacks for thresholding. One is that choice of the threshold is always done in an ad hoc manner; another is that the specific distributions of the signal and noise may not be well matched at different scales.

In practice, the standard deviation can be readily estimated using the methods discussed in [11], [17]. Modelling the statistics of natural images is a challenging task because of the high dimensionality of the signal and the complexity of statistical structures that are prevalent.

In this paper it is carefully discussed that a wavelet-based maximum likelihood for Bayesian estimator that recovers the signal component of the wavelet coefficients in original images from contaminated images by compound Poisson noises and Gaussian noise via using an alpha-stable signal prior distribution.

Without loss of generality, in order to focus on major parameters we take the parameter, called skewness, $\beta \in [-1, 1]$ in above equation (2) to be unity. This is well known that the symmetric alpha-stable distribution.

2 Wave-Based Bayesian Estimator

Following our previous papers [1, 12-14], if we take the probability density of θ as $p(\theta)$; and the posterior density function as $f(\theta | x_1, \dots, x_n)$, then the updated probability density function of θ is as follows:

$$\begin{aligned}
f(\theta | x_1, \dots, x_n) &= \frac{f(\theta, x_1, \dots, x_n)}{f(x_1, \dots, x_n)} \\
&= \frac{p(\theta)f(x_1, \dots, x_n | \theta)}{\int f(x_1, \dots, x_n | \theta)p(\theta)d\theta}
\end{aligned} \tag{3}$$

If we estimate the parameters of the prior distributions of the signal s and noise q components of the wavelet coefficients c , we may use the parameters to form the prior PDFs of $P_s(s)$ and $P_q(q)$, hence the input/output relationship can be established by the Bayesian estimator, namely, let input/output of the Bayesian estimator = BE , we have:

$$BE = \frac{\int P_q(q)P_s(s)sds}{\int P_q(q)P_s(s)ds} \tag{4}$$

$P_s(s)$ is the prior PDF of the signal component of the wavelet coefficients of the ultrasound image and $P_q(q)$ is the PDF of the wavelet coefficients corresponding to the noise.

In order to be able to construct the Bayesian processor in (4), we can estimate the parameters of the prior distributions of the signal (s) and noise (q) components of the wavelet coefficients. Then, we use the parameters to obtain the two prior PDFs $P_q(q)$ and $P_s(s)$ and the nonlinear input-output relationship BE .

The left hand side of Figure 1 shows the simulation results of input/output of BE with Lévy process analysis. Here we put two different Poisson noises together with a Gaussian noise with $\eta = (\lambda_1 + \lambda_2)/2$, where “ λ ” is defined as a mean of a Poisson distribution. We allowed different noises to mix together, Poisson noise with mean equals to 10 and another Poisson noise with mean equals to 20 (we double the mean of first Poisson source to check how the mean, the key parameter of Poisson affect the output of the estimator, third one is Gaussian noise with $\sigma = 3.92$, $\mu = 35$ and $\mu = 15$. For this diagram we chose $\alpha = 1.5$ as our previous paper suggested [16] and with different γ/η values, i.e. 0.1, 1.0, 10, 20, and 30. We can see that the parameters did affect the outputs of the BE estimator. For example, when the means of Gaussian distributions shift, as shown the vertical axes in the left of Figure 1, the output “curves” give the different outputs for the same “inputs”. It is important to keep it in mind that according to the definition, the parameter η is the representation of the mean of Poisson distributions. It clearly presented the fact that, for the given case, the curves with $\gamma/\eta = 0.1, 1.0, 10, 20$, and 30 are approximately corresponding to the “hard”, “soft”, and “semisoft” functions respectively in comparison with results in [9,16].

Unlike the case contaminated by pure Gaussian noise [12-14], the mean of Poisson noise plays a role in a BE as shown in the left of Figure 1, where the parameters are the same as that in Figure 1 except for the mean of Poisson distribution is equal to 20 rather than 10, this is not rally surprised since if we keep the same symmetric parameter γ and bigger η , or bigger λ , will make smaller the ratio of γ/η , which leads the noise removal to be closer to the “soft” threshold values.

The right hand side of Figure 1, shows the input/out of BE with Lévy process analysis, where there are two parts, the first part is the same as the that shown in the left hand side of Figure 1, the second part is a impulsive noise is added in. We can see

that how the impulsive is affecting the input/output of a BE with a Levy process analysis. Here the impulse density was chose as 0.05. The means of Poisson distribution affect the identity axes as well as vertical axes. For the “curves” of $\gamma/\eta = 1$ and 10 there are some “vibrations”, some curves even the shapes are changed, for example, comparing with the curve of $\gamma/\eta = 10$ shown in the left hand side, the curve of $\gamma/\eta = 10$ in the right hand side is significant. The output of BE will be closer to soft when the related coefficients are larger the outputs will be closer to soft threshold values.

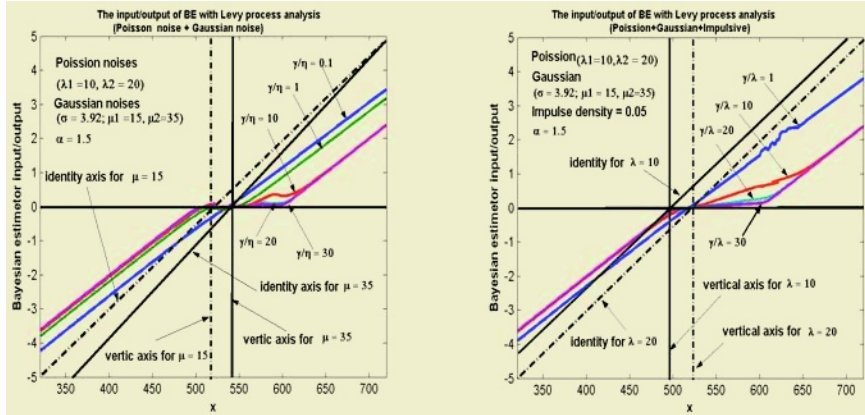


Fig. 1. The input/output of *BE* Levy process analysis. The left hand side is the charts of the input/output of *BE*, where there are multi-noises, two Poisson noises ($\lambda = 10$ and $\lambda = 20$) and two Gaussian noises ($\sigma = 3.92$, $\mu = 35$ and $\mu = 15$). The right hand side is the charts of the input/output of *BE*, where there are two parts, one is the same as that multi-noises shown in the left hand side and the second part is that it is added impulsive noise into the first part, where the impulse density is 0.05

Since the Levy process allows random noise to be discretely fluctuated, it is easy to describe the impulsive noise with other noises such as the continuing Gaussian noise and disserted Poisson noise. However, tt is important to remember that the parameters, α , β , and γ are playing their important role affecting the output of *BE*, which are discussed in the previous papers [1, 14-16]. In the next section, we shall take the values that make the input/output of *BE* obtaining an optimal result in the following examples. For example we took the previous suggestion of $\alpha = 1.5$ for different cases, such as $\gamma/\eta = 1$ for hard threshold-like and $\gamma/\eta = 30$ for soft threshold-like.

3 Some Examples

When we make noise removal, we have no information about the noise values of the image we obtained. We take the parameters $\alpha=1.5$, $\gamma/\text{mean} = 20$, in the case of *BE* with the Poisson 1 ($\lambda = 10$), Poisson 2 ($\lambda = 20$), Gaussian ($\sigma= 3.92$, $\mu = 15$) distributions and the impulsive noise with density = 0.05 (refer to Figure 1). In order to compare, we show the original image called “mountain” in the left hand side of Figure 2,

together with its contaminated one by Poisson noise, Gaussian noise and impulsive noise as shown in the right hand side of Figure 2. The Harr mother wavelet was used for this example. The output of denoised image from BE is shown in Figure 3.



Fig. 2. The input/output of BE with $\alpha = 1.5$ and Poisson 1 ($\lambda = 10$), Poisson 2 ($\lambda = 40$) and Gaussian ($\sigma = 3.92$, $\mu = 15$)

The left hand side of Figure 3 is the denoising results for the out/put of BE with the parameters $\alpha = 1.5$, $\gamma/\eta = 1$. The right hand side of Figure 3 is the denoising results for the out/put of BE with parameters $\alpha = 1.5$, $\gamma/\eta = 30$.

We have tried other methods; the results are shown in the table 1. Here the “1” means using “soft threshold”, “2” means using “Hard threshold”, “3” means using “Homomorphic Wiener” and “4” means BE with $\gamma/\eta = 30$.

Table 1. Comparison of denoising results with BE in signal to mean square error (S/MSE) in dB. Here 1 = soft thresholding; 2 = Hard thresholding; 3 = Homomorphic Wiener; 4 = BE ($\gamma/\eta = 20$ in Fig.1)

| Method | 1 | 2 | 3 | 4 |
|--------|-------|-------|-------|-------|
| S/MSE | 13.85 | 13.93 | 13.71 | 14.17 |



Fig. 3. The final results, a reasonable “clean picture” extracting from the contaminated image shown in the right hand side of Figure 2. The left hand side of Figure 3 is the input/out of BE with Levy process analysis with $a = 1.5$, $\gamma/\eta = 1$. The right hand side of Figure 3 is the input/out of BE with Levy process analysis with $a = 1.5$, $\gamma/\eta = 30$. The results clearly show that the Bayesian estimator works well

4 Conclusion

The technique uses the wavelet-based Bayesian estimator has been extended to the signal-dependent noise obeying Poisson distribution, Gaussian noise and impulsive noise via Lévy Process analysis. The final examples show that the statistician's Bayesian estimator theory is not only to simplify the selection of parameters and also in some situations to provide more precise images than other methods.

References

1. X. Huang, A.C. Madoc, and M. Wagner, "Noise Removal for Images by Wavelet-Based Bayesian Estimator via Levy Process," IEEE International Conference on Multimedia and Expo (ICME 2004), June 27-30, 2004, The Grand Hotel, Taipei, Taiwan. Final Program, pp. TP2-1.
2. B. Mandelbrot, "The variation of certain speculative prices" The Journal of Business 36, 1963, pp394-419.
3. D.B. Madan, and E. Seneta, "Chevyshev polynomial approximations and characteristic function estimation", Journal of the Royal Statistical Society Series B 49(2) 1987, pp.163-169.
4. D J Field, "What is the goal of sensory coding?", Neural Computation, vol.6, pp559-601, 1994.
5. E. Eberlein and K. Prause, "The generalized hyperbolic model: Financial derivatives and risk measures" FDM preprint 56, 1998, University of Freiburg.
6. J. Bertoin, "Lévy Processes", Cambridge University Press, Cambridge, U.K, 1996.
7. K. Sato "Lévy Processes and Infinitely Divisible Distribution", Cambridge University Press, Cambridge, U.K. 1999.
8. E.P. Simoncelli and E. H. Adelson, "Noise removal via Bayesian wavelet coring", IEEE Sig. Proc. Society, Third Int'l Conf. On Image Proc. Vol.I, pp379-382, Lausanne, 1996.
9. Y. XU, J.B. Weaver, D.M. Healy, and J. Lu, "Wavelet transform domain filtration technique", IEEE Transactions on Image Processing, vol. 3, 747-758, 1994.
10. S. G. Mallat, "A theory for multiresolution signal decomposition: The wavelet representation", IEEE Pat. Anal. Mach. Intell. Pp674-693, July 1989.
11. D. L. Donoho, "Denoising by soft-thresholding," IEEE Trans. Inform. Theory, vol. 41, pp613-627, May 1995.
12. M. Shao and C. L. Nikias, "Signal processing with fractional lower order moments: Stable processes and their applications", Proceeding of the IEEE, vol.81, no. 7, pp986-1010, July 1993.
13. D. L. Donoho and I. M. Johnstone, "Ideal spatial adaptation by wavelet shrinkage", Biometrika, Also Tech. Report of Statistics, July, 1992, revised April 1993.
14. X. Huang, A.C. Madoc, and A.D. Cheetham, "Multi-Noise Removal from Images by Wavelet-based Bayesian Estimator", IEEE Sixth International Symposium on Multimedia Software, Miami, FL, USA, December 13-15, 2004. pp.258-264.
15. X. Huang, A. C. Madoc, and A.D.Cheetham, "Wavelet-based Bayesian estimator for Poisson noise removal from images", IEEE International Conference on Multimedia and Expo, Maryland, U.S. July 6-10, 2003. Vol.I, pp593.
16. X. Huang and A. C. Madoc, "Maximum Likelihood for Bayesian Estimator Based on a stable for Image", IEEE International Conf. ICME2002, Proc. Vol.I, pp709-712, 2002.
17. E.P. Simoncelli, "Bayesian Denoising of Visual Image in the Wavelet Domain", pp291-308. vol.141, Springer-Verlag, New York, 1999.

18. Imola K. Fodor and Chandrika Kamath, "Denoising Through Wavelet Shrinkage: An Empirical Study", Lawrence Livermore national Laboratory technical report, UCRL-JC-144258, July 27, 2001.
19. D.L. Donoho and I.M. Johnstone, "Wavelet shrinkage: Asymptopia?", Journal of the Royal Statistical Society, Series B, vol. 57, 301-369, 1995.
20. D. L. Donoho, "Nonlinear wavelet methods for recovery of signals, densities, and spectra from indirect and noisy data", In Proceeding of Symposia in Applied Mathematic, American Mathematical Society vol. 00, 173-205, 1993.
21. A. Achim, A. Bezerianos, and P. Tsakalides, "An Alpha-stable based Bayesian algorithm for speckle noise removal in the wavelet domain," Proc. NSIP-01, June 03-06, 2001, Baltimore, Maryland USA.

Evaluating the Size of the SOAP for Integration in B2B

Alexander Ridgewell, Xu Huang, and Dharmendra Sharma

a_ridgewell@hotmail.com
Xu.Huang@canberra.edu.au
Dharmendra.Sharma@canberra.edu.au

Abstract. Web Services have become an important means of integration in an organisation and in business to business practices. Of particular interest is the large volumes of structured information that can result from a backup of data in a system, as part of a search requested on the stored data or from some other data exchange requirement. To be a viable in these areas the simple object acceptable protocol (SOAP) message used must be able to move the data in a secure and fault tolerant manner, but be able to do it in a fast and efficient manner. One of the largest problems in efficiency of using SOAP messages is in the large amount of information describing the structure and content of the message. This paper presents an examination of the size of SOAP document's used in data exchanges when compressed, which also compares the text based document, a comma separated value (CSV) file, containing the same information. Our results suggest significant size cost savings can be made when the SOAP message is compressed. Therefore, the SOAP message contains sufficient data entries this size cost saving makes to total size of the message comparable to the compressed CSV file.

1 Introduction

In recent years businesses have been moving strongly into the integration of systems [1-3]. Such integration is designed to make it easier for systems to communicate with each other within an organisation as well as with other organisations in a business to business relationship and can often require the exchange of large amounts of information.

In the last few years Web Services have emerged as a robust and flexible technology to enable system to system communication utilising open XML standards, generally created as ebXML messages within a SOAP envelope. As the SOAP messages are free text messages there is a need to look at how the messages are secured and how robust the messages are while being exchanged. Additionally the SOAP specification adds considerable overhead to the integration messages when compared to other wire formats and binary formats and this leads to longer encoding/decoding times and greater network bandwidth requirements [4].

Network bandwidth is a critical issue in the implementation of a Web Service based implementation plan with the integration frequently taking place over lower speed Wide Area Networks. To use Web services efficiently it is necessary to make the SOAP messages used in the process as compact as possible.

SOAP has a structure that needs to be used with its messages. This defines a minimum fixed size on the message content. On top of this the XML in the SOAP

body uses descriptive names for elements and attributes that provide information to a reader on what these things mean.

There are a number of ways to reduce the size of SOAP messages. The use of shorter names of elements and attributes in the SOAP body and the choices of where to use elements and attributes in the SOAP body can reduce the total size of the SOAP message, however these changes can reduce the readability of the message reducing it's robustness. The ability to use SOAP within an SMTP wrapper also allows for some of the SOAP body to be moved into an attachment file, often done for binary data elements such as images. However this can reduce the readability of the SOAP message, which again leads to lower robustness.

Another way to reduce the size of the ebXML message sent across the network would be to compress it [5]. This would increase the time taken to encode and decode the message; however this is likely to be a small cost with current hardware. Use of compression would also require that both the message producer and consumer can understand the compression algorithm used.

This paper will focus on the effect that compression algorithms have on the size of SOAP messages to determine if the decrease in size will relate to an appreciable improvement in the message transfer speed across a network. Our goal is to investigate if size cost reductions to the SOAP message are sufficient to make SOAP a valid format for large data exchanges. Hence, a compression algorithm could be further implemented in an open integration framework with the security and robustness required for business to business integration.

2 Experimental Design

To test the affect compression has on the size of SOAP messages several SOAP messages were created and the entire message was compressed with two different commercial compression programs, WinZip and WinRAR.

An empty SOAP message was created to show the minimum size a message can be (Listing 1). Additional SOAP messages were created to show how a message with a simple content structure would be affected with 1 (Listing 2), 2, 10, 20, 50 and 100 <ApplicationMessage> data entries.

```
<?xml version="1.0" encoding="UTF-8"?>
<SOAP-ENV:Envelope
  xmlns:SOAP-ENV="http://schemas.xmlsoap.org/soap/envelope/"
  xmlns:SOAP-ENC="http://schemas.xmlsoap.org/soap/encoding/"
  xmlns:xsi="http://www.w3.org/2001/XMLSchema-instance">
  <SOAP-ENV:Body SOAP-
    ENV:encodingStyle="http://schemas.xmlsoap.org/soap/encoding/">
  </SOAP-ENV:Body>
</SOAP-ENV:Envelope>
```

Listing 1

```
<?xml version="1.0" encoding="UTF-8"?>
<SOAP-ENV:Envelope
  xmlns:SOAP-ENV="http://schemas.xmlsoap.org/soap/envelope/"
  xmlns:SOAP-ENC="http://schemas.xmlsoap.org/soap/encoding/"
  xmlns:xsi="http://www.w3.org/2001/XMLSchema-instance">
  <SOAP-ENV:Body SOAP-
    ENV:encodingStyle="http://schemas.xmlsoap.org/soap/encoding/">
    <ApplicationMessages>
      <ApplicationMessage>
```

```

<Details>
  <Name>Someone</Name>
  <Date>01/01/2005</Date>
  <AnotherName>Someone Else</AnotherName>
  <AnotherDate>23/10/1945</AnotherDate>
</Details>
<Information>
  <Text>This is some text</Text>
  <IntegerData>9</IntegerData>
  <FloatingData>4.678</FloatingData>
  <Description>This is a descriptional field</Description>
  <AnotherInteger>413</AnotherInteger>
  <MoreDescriptiveText>This is another descriptional
field</MoreDescriptiveText>
</Information>
</ApplicationMessage>
</ApplicationMessages>
</SOAP-ENV:Body>
</SOAP-ENV:Envelope>

```

Listing 2

The information in the non-empty SOAP messages was also represented in simple Comma Separated Value (CSV) files. The CSV files represent the data in a textual format like SOAP, however the structure of the CSV file has a minimal size cost in the file. The size of the CSV file was then compared to the size of the far richer SOAP message under compression.

3 Experiment Results

The files were created and then compressed with both WinZip and WinRAR giving the following results.

Empty SOAP Message

| | Uncompressed file | WinZip compressed | WinRAR compressed |
|------|-------------------|-------------------|-------------------|
| SOAP | 363 bytes | 311 bytes | 279 bytes |

1 Data Entry

| | Uncompressed file | WinZip compressed | WinRAR compressed |
|----------------------|-------------------|-------------------|-------------------|
| SOAP | 1,136 bytes | 523 bytes | 564 bytes |
| SOAP, per data entry | 773 bytes | 212 bytes | 285 bytes |
| CSV | 138 bytes | 221 bytes | 187 bytes |

With a single data entry compressing the SOAP message results in a size reduction of about 50%, however it is still significantly larger than the CSV file.

2 Data Entries

| | Uncompressed file | WinZip compressed | WinRAR compressed |
|----------------------|-------------------|-------------------|-------------------|
| SOAP | 1,878 bytes | 622 bytes | 574 bytes |
| SOAP, per data entry | 758 bytes | 156 bytes | 148 bytes |
| CSV | 298 bytes | 271 bytes | 240 bytes |
| CSV, per data entry | 149 bytes | 136 bytes | 120 bytes |

With two data entries the size cost saving is up to 30%. The CSV file is still significantly smaller, particularly when similarly compressed.

10 Data Entries

| | Uncompressed file | WinZip compressed | WinRAR compressed |
|----------------------|-------------------|-------------------|-------------------|
| SOAP | 8,384 bytes | 1,484 bytes | 1,358 bytes |
| SOAP, per data entry | 802 bytes | 117 bytes | 108 bytes |
| CSV | 2,153 bytes | 933 bytes | 923 bytes |
| CSV, per data entry | 215 bytes | 93 bytes | 92 bytes |

With ten data entries the size cost saving is now around 18%. The CSV file is actually larger than the compressed SOAP file and the compressed CSV files offer only a small size cost improvement.

20 Data Entries

| | Uncompressed file | WinZip compressed | WinRAR compressed |
|----------------------|-------------------|-------------------|-------------------|
| SOAP | 16,623 bytes | 2,352 bytes | 2,175 bytes |
| SOAP, per data entry | 813 bytes | 102 bytes | 95 bytes |
| CSV | 4,572 bytes | 1,667 bytes | 1,654 bytes |
| CSV, per data entry | 229 bytes | 83 bytes | 83 bytes |

With twenty data entries the size cost saving is now 14% and there is decreased difference between the compressed SOAP document when compared to the compressed CSV file.

50 Data Entries

| | Uncompressed file | WinZip compressed | WinRAR compressed |
|----------------------|-------------------|-------------------|-------------------|
| SOAP | 41,426 bytes | 4,742 bytes | 4,515 bytes |
| SOAP, per data entry | 821 bytes | 89 bytes | 84 bytes |
| CSV | 11,915 bytes | 3,853 bytes | 3,851 bytes |
| CSV, per data entry | 238 bytes | 77 bytes | 77 bytes |

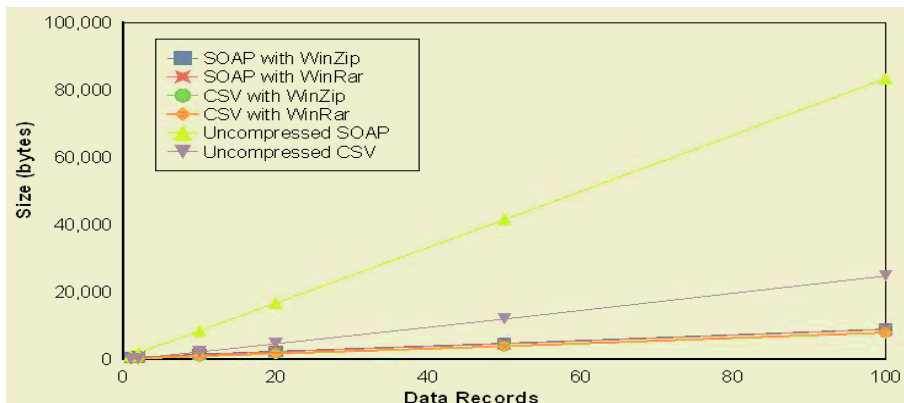
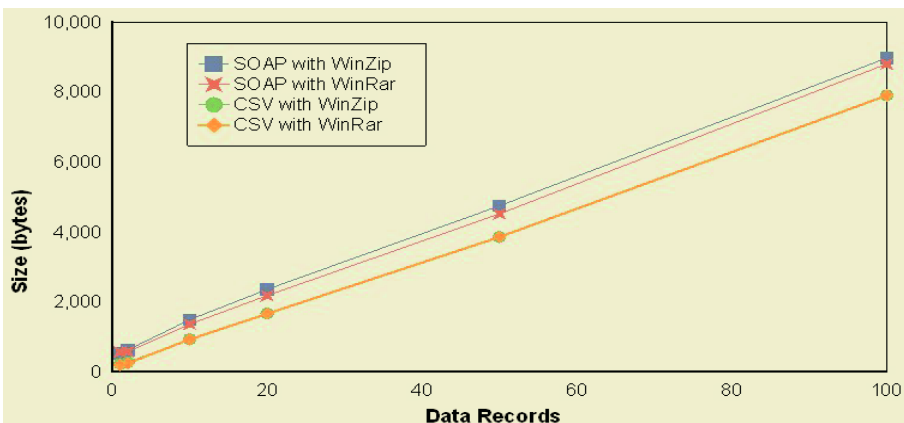
With fifty data entries the size cost saving is only 11%. The compressed SOAP document is now only about 12% larger than the compressed CSV file.

100 Data Entries

| | Uncompressed file | WinZip compressed | WinRAR compressed |
|----------------------|-------------------|-------------------|-------------------|
| SOAP | 83,320 bytes | 8,971 bytes | 8,798 bytes |
| SOAP, per data entry | 830 bytes | 87 bytes | 85 bytes |
| CSV | 24,708 bytes | 7,903 bytes | 7,900 bytes |
| CSV, per data entry | 247 bytes | 79 bytes | 79 bytes |

With one hundred data entries the size cost saving is still about 11%. The compressed SOAP document is now only about 9% larger than the compressed CSV file.

The difference in size for each of these points is illustrated in the figures below.

**Fig. 1.** Relative message sizes**Fig. 2.** Compressed message sizes

4 Discussion

Compression offers significant savings in the size of the SOAP message sent. As more data entries are added to the SOAP message the cost per data entry in a compressed SOAP document decreases to about 85 bytes a data entry.

The CSV file used showed a similar decrease in size when compressed, it is seen that as the number of data entries increase the compressed SOAP message will show greater size cost savings than the and the compressed CSV file and the total difference in size between the two becomes negligible. The greater savings found in the SOAP message compared to the CSV file is probably due to the compression efficiencies gained by the repetitive nature of the SOAP structure, with repeating element and attribute tags name. The negligible size difference between the compressed CSV and SOAP messages and the more richly described SOAP document structure make SOAP a preferable choice for the exchange of large data sets.

The tests were performed by compressing the entire SOAP message. In a practical implementation of compression in SOAP it could be advantages to keep the SOAP

header uncompressed to allow it to be more easily recognised by message subscribers. This would also allow the message to detail the compression algorithm used in the SOAP header, allowing messages to be decompressed outside the context of a business integration subscriber.

The use of compression will also require that the message's producer and consumer are able to compress and decompress the message easily. The simplest way for this to happen is if the message consumer can advertise to the message producer what algorithms it can accept and having the message producer compress the message with one of these. Similar encoding checks are currently used in HTTP [5] but it would be advantageous to perform such checks independently of the message's transport protocol.

5 Conclusion

In this paper we have presented how a SOAP message's size will change with compression. In order to show this squeezing SOAP is significant for integration in B2B, we have also compared it to similar compression made to a CSV formatted file, which are shown in Figures 1 and 2. The results of the evaluating the size of the SOAP for integration in B2B show that the compression of the SOAP message gives a significant reduction in the size of the SOAP message presented and, for a sufficient number of data entries in the message, the compressed SOAP message approaches the size of the compressed CSV file while maintaining the rich XML structure. This makes SOAP a useful format for use in the exchange of data between businesses. Further work needs to be carried out to determine what parts of the SOAP message should be compressed, how the compression should be performed and how it will fit in an integration framework. The other two important aspects of integration in B2B, namely the security and robustness, will be discussed in our coming papers.

References

1. Curbera, F. Duftler, M. Khalaf, R. Nagy, W. Mukhi, N and Weerawarana, S.: Unraveling the web services web: An introduction to SOAP, WSDL, UDDI. IEEE Internet Computing, 6(2): 86-93, March-April 2002.
2. Fan, M. Stallaert, J. and Whinston, A. B.: The internet and the future of financial markets, Communications of the ACM, 43(11):83-88, November 2000.
3. Rabhi, F.A. and Benatallah, B.: An integrated service architecture for managing capital market systems. IEEE Network, 16(1):15-19, 2002.
4. Kohlhoff, Christopher and Steele, Robert: Evaluating SOAP for High Performance Business Applications: Real-Time Trading Systems, 2003, <http://www2003.org/cdrom/papers/alternate/P872/p872-kohlhoff.html>, accessed 22 March 2005.
5. Goodman, Brian D.: Squeezing SOAP, GZIP enabling Apache Axis, IT Architect, IBM. 01 Mar 2003.

Personalised Search on Electronic Information

G.L. Ligon, Balachandran Bala, and Sharma Dharmendra

School of Information Sciences and Engineering, Division of Business,
Law and Information Sciences, University of Canberra, ACT 2601, Australia
g.ligon@student.canberra.edu.au
{bala.balachandran,dharmendra.sharma}@canberra.edu.au

Abstract. In the current world of Electronic Informatics, *Info Search* is more a relative term. General Search results have no relevance where people are looking for personalised, highly specific information. Generally, a user must revise a large number of uninteresting documents and consult several search engines before finding relevant information. Almost all search engines rely on text-based search algorithms and hence the probability of getting user desired information is heavily based on users ability to frame right *keywords* or *search strings*. This paper aims to address this problem by presenting a Personalized Search Agent (PSA) that generates effective keywords and also captures and organises different *areas of interests* of the user in a hierarchy that defines the user profile. The idea is to create a filter application, which applies a dual methodology of browsing and searching, that works between user and one or more commercial search engines specified by the user. This paper describes the design, architecture and the functional components of the PSA system and also describes how the system works thorough a scenario based approach.

1 Introduction

Undoubtedly, Internet is the most abundant source of information in the present world covering almost all domains of knowledge humans are ever exposed to. Moreover, the information available through Internet is constantly growing. As a result, the search of *interesting information* becomes a time-consuming and hectic task since this activity involves the analysis and separation of interesting pages from a great set of candidate pages [3]. Search engines are the most widely used tools for searching information on the web. Users provide a set of keywords to these search engines and wait for a set of *links to WebPages* in relation to those words. This mechanism is solely based on words (keywords) supplied by the user to the search engine. Therefore getting the desired information will highly depend on framing the most suitable keywords. The simpler the keywords are the more general (less precise) will be the results returned by the search engines. This causes inexperienced/novice users spend considerable amount of time searching for specific information. In terms of today's "*economy sensitive*" business world, this means waste of human resources, hardware/software resource, energy and time – making it a pullback force in productivity.

On the other hand, if the users try to make effective keywords, which would yield better results, they may end-up wasting time again, because the activity involves trial and error methods which eventually compromising on ease-of-use and efficiency. For example, imagine a user looking for web pages about software agents by typing keyword *agents*. This will result the search engine to return links to the WebPages containing information regarding, travel agents, marketing agents, software agents, insurance agents etc making it highly general to the user. If the user gives the keyword,

“software agents” he/she may get more specific results from a search engine, compromising on ease-of-use and efficiency.

This issue leads to the relevancy of middle-ware agents that can manage the situation. The idea is to organise user’s area of interests (we term it as *Knowledge Domains* in this paper) in a hierarchical order and then handle the user queries in conjunction with relevant knowledge domains, instead of direct submission to search engines. The middleware agent takes user queries, refines it with relevant field of interest (knowledge domain) and submits the refined keywords to search engines. This makes the search efficient, simple and personalised.

Our research objective is to provide an effective solution to the problems addressed above in a relatively simple way. The main goals of the current research are, to develop a filtering technique that would work between search engines and user for providing personalised search results, to use multiple search engines to find the relevant results for user queries and to capture user feedback and create a user profile based on it. A brief description on what follows in the paper.

In the coming sections of this paper we will be describing about a Personalised Search Agent, its architecture, main functionalities and user interactions based on activity- scenario.

2 Personalised Search Agent

The key concept behind the proposed Personalised Search Agent (PSA) is a hybrid pathway to fetch relevant information [2]. The two major pathways generally available are browsing and searching. Applying this heuristics, the PSA actually allows you to browse through high priority domains before submitting your search key. This not only greatly simplifies the search keyword but also make sure that the results will be from the intended field (domain) of interest; saving both time and energy [6, 7]. The browsing option (which is missed by most of the search engines) requires that a detailed set of interesting fields of knowledge (knowledge domains) needs to be categorised and organised in a hierarchical way. The aim is to develop a mechanism with which the user can select the field of interest before giving actual search keywords.

As stated earlier in this paper PSA acts as both pre and post-processor to one or more search engines. PSA tries to judge *preferred result* from the search results returned by the search engines based on the preference given by the user.

Knowledge domain and Knowledge sub-domains are the main resource for the personalised search method. Knowledge Domain (KD) is a branch of information field like science, commerce, space etc that is organised in a hierarchical way. Each KD is again branched to several Knowledge Sub Domains (KSD). Figure 1 is a simple structure depicting KD and KSD.

In the following section we describe the PSA architecture.

3 PSA Architecture

The architecture of PSA is illustrated Figure 2. PSA consist of 3 functional modules – GUI, Search Filter and Profile Filter. The GUI (Graphical User Interface) module interacts with the user; Search Filter module does the pre and post processing and Profile Filter module handles user profile database.

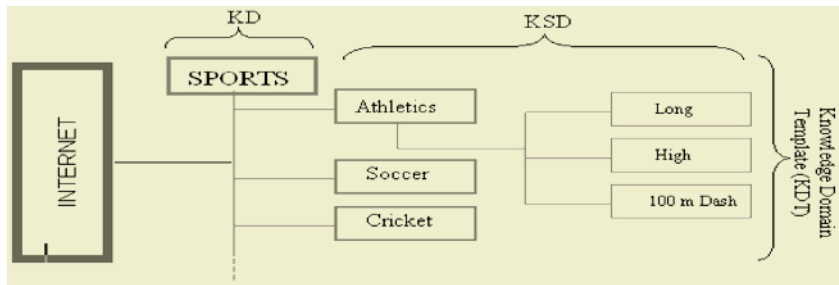


Fig. 1. Structure of knowledge domain template

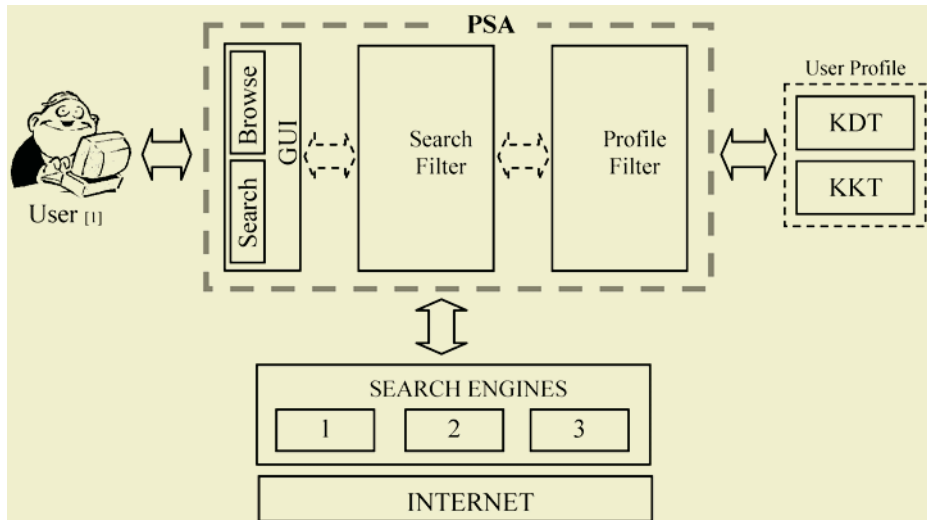


Fig. 2. PSA architecture

In the initial stage, the user will be supplied with a standard KD template that covers the most common domains and its sub domains. It could be a huge effort to form a general template incorporating all common domains but its only a one-time effort. Nevertheless, users can keep updating their KD template (KDT) on the go, by adding more KD/KSD.

User profile is a combination of different user preference values and feedback scores. The user explicitly defines some of them and some are implicitly learned by PSA.

Customised KDT: When a user first starts using PSA he/she is supplied with a KDT that they have to customise by selecting the preferred KSDs against each KD. For example the user will select, under a KD “sports” which KSDs would they prefer, like KSD “indoor games” under that KSD “badminton”. Customising KDT is a onetime effort and the user needs to reselect a KSD only on an event of a negative KD ranking. Also, the user need not customise the entire KDT in one instance, the PSA will ask the user for a KD/KSD preference in an ad-hoc basis when it is triggered with an event where no relative KD/KSD selection is available in the Keyword-KD table.

KD Ranking: When the user submits a query, the PSA submits it to a set of search engines after refining the keyword. The results from the search engines are then refined, organised and presented to the user leaving an option to feedback on the accuracy of a desired result. If the user gives a positive feedback, the related keyword-KD table entry is given a positive rank and vice-versa.

Keyword-KD Table (KKT): In the event of a search the user first browse through KD/KSD leaving their preference and then submits the keyword for search. This KD/KSD values are mapped against the search keyword and stored in a table for reuse.

Search Engine Ranking: PSA uses more than one popular search engines to squeeze information out of Internet. When the user selects a search result (which will be organised per search engine basis), PSA will record from which search engine the user got it's desired results and map it against keyword-KD table entry[5]. This greatly helps in prioritising the search results and prioritising the search engine to be used per keyword level and hence displaying the search results in the order of search engine ranking.

The PSA has three distinct functionalities as follows,

- Accepting user information and submitting it to the search engine: This involves capturing KD/KSD details and the search keyword on an event of search. Moreover, the keyword is further refined and submitted to the search engines.
- Retrieving information from search engine, personalise it and presented to the user: This subsystem consist of gathering information from different search engines for the submitted search string, extracting the links from the search engine result pages, organising it and presenting it to the user.
- Taking feedback from the user to update the user profile: This part consists of gathering user feedback and updating relevant ranking tables. Generally, two types of ranking and one table are maintained by PSA, which is briefly described earlier in this paper.

When the user gives a positive feedback the KKT is updated with the user selected link, search engine that returned the link, and both the Knowledge Domain Rank (KDR) and Search Engine Rank (SER) are incremented. These rankings are used by PSA to make decision on prioritising the results.

4 Sample User Interactions

The main functionalities of the system are analysed in a scenario-based approach. Diferent instance of user interaction, which would eventually explore the system functionalities are taken into consideration and explained below with sample outputs/ interfaces.

(Note: - The sample interfaces/outputs shown in this paper are indicative and not part of the real system, which is still under construction.)

Scenario 1: *User initiates a search process with a keyword, which has no related KKT entry*

Suppose, the user has entered a search string called “racket”. The PSA now matches it with all KKT entries and finds that there is no entry for keyword “racket”. PSA now presents KDT interface to the user to make a KD/KSD selection. A sample KDT interface is show in Figure 3.



Fig. 3. PSA sample search interface

Here the user has selected a KD named “Sports” and also selected two KSDs named “Indoor” and “Badminton” in the order of hierarchy. Please note the components in this interface are dynamic. That is, if the user has chosen KD that has a lot of KSD under its branch, the number and structure of components will change accordingly. Once the user has selected KD/KSDs, KKT is updated with a new entry.

PSA now concatenates KD/KSD to the search string and submits to different search engines as a single string (here as “sports indoor badminton racket”). If PSA fails to get any results back from any of the search engines, it refines the search string again by putting the least specific KD out of the main search string. (Eg. Sports “indoor badminton racket”).

Scenario 2: The user submitted query is refined and send it over to the search engine. The results are then presented to the user. User finds it's inappropriate and reports irrelevant result

A sample interface showing the search output would look like Figure 4.



Fig. 4. PSA sample output

If the user opted for more precise information, PSA will then try to refine the search keyword by replacing the least specific KSD. In this case it replaces the word sports out of the search string to make it like (sports “Indoor Badminton racket”). Table 1 shows all the possible trail words PSA generates on recurring error reports from the user.

Table 1. Possible keyword combinations generated by PSA

| TRAIL | KEYWORDS FORMED | COMMENTS |
|-------|----------------------------------|--|
| 1 | “Sports indoor badminton racket” | Putting least significant words out of main search string. |
| 2 | Sports “indoor badminton racket” | |
| 3 | Sports indoor “badminton racket” | |
| 4 | Sports indoor badminton “racket” | |
| 5 | “Indoor badminton racket” | Eliminating least significant KSDs |
| 6 | “Badminton racket” | |
| 7 | Sports indoor badminton racket | Putting KSD/KSDs and keyword as separate words. |
| 8 | Indoor badminton racket | |
| 9 | Badminton racket | |

Note that search string is not case sensitive and in all the possible combinations, the most significant KSD and the keyword are never eliminated. If user still reports error after trying all the above combinations, PSA will prompt the user for a potential change in the KDT (changes starting from the most significant KSD).

5 Conclusion and Future Work

This paper was an attempt to solve the problems of personalised information search in a simple and efficient way. The unique future of PSA is that it allows the user to browse and choose a specific domain before the actual search start. Moreover PSA updates user profiles based on user feedbacks also learns some user profile parameters in between this process (like search engine ranking). This makes PSA an adaptive tool, which becomes more powerful and effective with use. Most of our design were satisfactorily met and further work is continuing to address the issues of, *ranking methods needs more refinement and clarity, KK Table can potentially be normalised and same keyword different KSD Conflict.*

The system prototype is being evolved to address any arising limitations and future areas of potential refinement. Some of the future advancement plans are listed below.

- *Multi-user support:* Currently PSA is designed to use by a single user with single profile. PSA can potentially be enhanced as a multi-user support system with each user having their own login session and profile.
- A *roaming personal profile* by placing the profile database online? This could give PSA great accessibility. The personal profiles remains in a central repository (web server) and the PSA application will simply download one if it finds the local profile is outdated or there is no local profile.
- *Helping word rendering:* most of the search engines discard the helping words used with the search string like ‘and’, ‘about’, ‘is’ etc. But these are very good signals reflecting personal preference. Example if the user needs information regarding Abraham Lincoln, it’s more logical to type “about Abraham Lincoln” in-

stead of surfing around all those irrelevant information returned with keyword “Abraham Lincoln”. An efficient method to interpret helping words, which would enhance the PSA being more personal, is one of our future research tasks.

References

1. http://wqlc.ncf.ca/computer_user.GIF, 2005, “Computer User”, “System User”
2. Fiedler, W., *Managing Metadata in Web-based Information Systems with RDF*, in *Institute for Information Processing and Computer Supported New Media (IICM)*. January 2004, Graz University of Technology: Graz. p. 139.
3. Amandi, D.G.a.A., *PersonalSearcher: An Intelligent Agent for Searching Web Pages*. 2000.
4. Wooldridge, M., *An Introduction to MultiAgent Systems*. February 2002: John Wiley & Sons (Chichester, England). 340pp.
5. Bradley, Phil., *Internet power searching: the advanced manual*. 1999: Neal-Schuman Publishers (New York). 232 pp.
6. Oren Etzioni, Daniel S.Weld., *Intelligent agents on the Internet: Fact, Fiction and Forecast*. May 1995.
7. Jens E. Wolff, Holger Fl̄orke., *Searching and Browsing Collections of Structural Information*. April 1998.

Data Mining Coupled Conceptual Spaces for Intelligent Agents in Data-Rich Environments

Ickjai Lee

School of Information Technology,
James Cook University, Townsville, QLD4811, Australia
Ickjai.Lee@jcu.edu.au

Abstract. Conceptual spaces provide a robust conceptualized framework for many cognitive tasks within intelligent agents. As agents are asked to accomplish more complex tasks, an efficient and effective management of conceptual spaces has become an important issue. This paper proposes a data mining coupled conceptual spaces framework for the efficient management of concepts and properties in data-rich environments. This paper illustrates the working principle of data mining coupled conceptual spaces and demonstrates the efficacy and effectiveness of this framework.

1 Introduction

Recently, intelligent agents have been widely used in a variety of applications and have been one of active research topics in the AI community. Intelligent agents are computational software entities that are autonomous, collaborative, reactive and proactive [1]. They autonomously perform a series of actions to achieve their goals and objectives. They perceive facts from environments (knowledge acquisition and reactivity), build an internal model to represent learnt knowledge (knowledge representation), and autonomously reason with the internal model to achieve their goals (reasoning and proactiveness).

In this series of tasks, information (knowledge) representation is a core business in constructing intelligent agents. Proper internal representations lead to proper reasoning thus to the successful completion of goals. Traditionally, symbolic representation and associationism (in particular connectionism) have long been dominant approaches in knowledge representation. However, these approaches are exposing their limitations as data grows exponentially and cognitive tasks become extremely complex [2]. Connectionism is too fine-grained and symbolic representation is too coarse. An intermediate representation approach is required for some cognitive tasks [3].

A conceptual spaces approach is an intermediate way of representing information bridging between too detailed visual images (from sensory receptors) and too coarse symbolic knowledge representations [3]. They are conceptual representations providing flexible approaches for many reasoning activities such as concept formation, concept learning, inductive inferences, semantics, categorization and prediction [3–6]. This paper investigates an efficient management of

information (concepts and properties) and effective reasoning using data mining techniques within conceptual spaces. It explores how data mining can help various cognitive tasks within conceptual spaces and suggests suitable data mining techniques for each stage.

The remainder of this paper is organized as follows. Section 2 briefly introduces a conceptual space framework for representing information. Section 3 introduces how data mining approaches can support concept formation, concept learning, reasoning about concepts and properties, and association mining. Concluding remarks are followed in Section 4.

2 Conceptual Spaces Representation

In terms of representational granularity, there are three levels of information representations: subconceptual representation, conceptual representation and symbolic representation [3]. Subconceptual representation is concerned with the low level processing of raw data perceived from sensory inputs while symbolic representation is concerned with the high level expression of external world with predefined symbols. The former approximates external world with great details and the latter is seen as the highest abstraction. Thus, the former is seen as information-rich and theory-poor while the latter is seen as information-poor and theory-rich. Conceptual representation is an intermediate approach bridging subconceptual representation and symbolic representation. It is concerned with providing a suitable framework for conceptualizing information and it is required for various cognitive tasks [3].

Conceptual spaces provide a robust framework for conceptualizing and representing information. A conceptual space consists of a set $Q = \{q_1, q_2, \dots, q_l\}$ of quality dimensions that are used to assign various properties (qualities) to objects (O). Dimensions $Q' \subset Q$ where $\|Q'\| \geq 1$ are integral when an object $o_i \in O$ cannot be assigned to a value in one dimension $q_j \in Q'$. Integral dimensions are called a domain. Each domain is endowed with certain geometrical, topological or ordering structures. A conceptual space is seen as a collection of one or more domains. Objects are identified with points (also called knoxel [7]) within conceptual spaces, properties are represented by regions in domains and concepts are denoted by a collection of regions (properties) and their relations in conceptual spaces. Identifying categories and corresponding regions in domains, and finding relations among regions are important tasks within conceptual spaces.

Conceptual spaces are metric spaces, thus similarity can be measured by a certain distance function. The most popular dissimilarity function is the Minkowski metric that is defined as follows:

$$d_{L_p}(r, s) = (\sum |r_i - s_i|^p)^{1/p} \quad (p \in \Re \cup \{\infty\}, \& p \geq 1). \quad (1)$$

If $p = 1$, then $d_{L_1}(r, s) = |r_x - s_x| + |r_y - s_y|$ is the Manhattan metric. The Minkowski metric becomes the Euclidean metric when $p = 2$. The Manhattan metric is in use for inter domains while the Euclidean metric is in use for intra

domains [3]. This ease of measuring similarity robustly supports many cognitive tasks such as concept formation, concept learning, induction and semantics that are not easily supported by symbolic representation and associationism. Recently, the conceptual framework has been used in various applications including computer vision [7], cluster reasoning [8], representing dynamic actions [4, 5] and conceptual similarities of verbs [9]. In addition, managing concepts and categories in data-rich environments has been studied [2, 10, 11]. Details of conceptual spaces can be found [3].

3 Data Mining Coupled Conceptual Spaces

Data mining is an exploratory data analysis that efficiently finds unknown and useful patterns in data-rich environments. Three techniques (clustering, classification and association rules mining) are core methods in data mining. This section provides intelligent and efficient ways of managing conceptual spaces with these three techniques.

3.1 Concept Formation Using Clustering

Clustering consists of partitioning a set $P = \{p_1, p_2, \dots, p_n\}$ of objects into homogeneous groups so that it minimizes inter-cluster similarities and maximizes intra-cluster similarities. Since its learning is unsupervised it is a solid candidate for formulating concepts. In concept formation, effectiveness (quality clusters) is not only of interest, but efficiency. Various clustering methods have been proposed across different disciplines [12, 13]. However, traditional hierarchical clustering producing levels of different groupings typically requires $O(n^2)$ time that is too expensive in data-rich environments while traditional k -partitioning clustering requiring $O(n)$ time does not produce clusters as good as

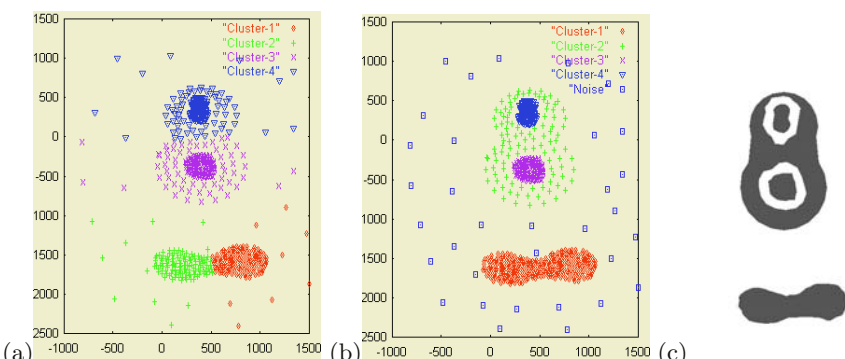


Fig. 1. Clustering with different approaches and polygonization ($\|P\| = 600$): (a) Partitioning clustering approaches (4 clusters); (b) Short-Long clustering (4 clusters); (c) Polygonizing of clusters

hierarchical clustering. Due to the advances in clustering in the data mining community, it is now possible to find quality clusters within $O(n \log n)$ time [8, 14] or even $O(n)$ time [15]. Fig. 1(a) and (b) illustrate two clustering results with the k -means clustering [16] requiring $O(n)$ time and Short-Long clustering [8] requiring $O(n \log n)$ time in 2D. These techniques can be used to quickly identify intra-similarity maximized concepts.

3.2 Reasoning with Concepts and Properties Using Postclustering

Note that, properties in conceptual spaces are regions in domains and a concept is a set of regions and their relationships. Thus, manipulating regions is an important task and Region Connection Calculus (RCC) [17] has been used to effectively manage properties and categories [2, 6, 10]. Since objects are points in conceptual spaces and clustering results are clusters that are basically sets of points. Converting clusters of points to polygonal regions will lead to ease reasoning about concepts and properties using the well-developed RCC. Fig. 1(c) depicts regions of clusters transformed by the polygonization process [18] that requires $O(n)$ time when the Delaunay Triangulation, requiring $O(n^{\lceil d/2 \rceil})$ time for $d > 3$ [19], is available. Now, qualitative spatial reasoning with RCC can be used for reasoning about transformed regions. For instance, the “8-like” cluster is discrete from the “helix-like” cluster ($DC(\text{“8-like”}, \text{“helix-like”})$).

3.3 Concept Learning Using Classification

Concept learning within conceptual spaces involves in tessellating a conceptual space into regions. The Voronoi diagram based prototype concept learning has been the most popular approach [3]. Here, a new object o is allocated to the most similar concept based on the similarity value measured by the Minkowski metric shown in Equation 1. This section compares the prototype-based concept learning to various classification methods and reports on the result with a dataset (IRIS) from the UCI repository [20]. The experimental result shows that data mining techniques improves classification accuracy which confirms the effectiveness of concept learning with data mining techniques. Accuracy is measured by recall and precision where recall is a proportion of positive examples that are

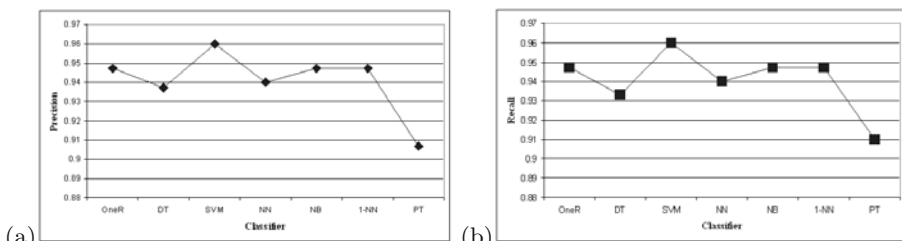


Fig. 2. Classification with different approaches: (a) Precision; (b) Recall

actually classified as positive and precision is a proportion of cases classified as positive that are indeed positive. Classification methods used are OneR, Decision Trees (DT), Support Vector Machines (SVM), Neural Networks (NN), Naive Bayes (NB), 1-Nearest Neighbor (1-NN) and ProtoType (PT) learning [3, 21]. Experiments are conducted with a 3-fold cross validation within WEKA [22]. Fig. 2 depicts that data mining methods are all superior to the prototype-based learning in this particular dataset.

3.4 Property Relations Using Association Rules Mining

Let us consider a conceptual space \mathcal{S} with a set $\mathcal{D} = \{D_1, D_2, \dots, D_n\}$ of domains and a set $\mathcal{O} = \{O_1, O_2, \dots, O_m\}$ of objects. \mathcal{O} forms a set $\mathcal{C} = \{C_1, C_2, \dots, C_l\}$ of concepts and $\mathcal{O}_k \subset \mathcal{O}$ forms a concept $C_k \in \mathcal{C}$ where $1 \leq k \leq l$. Here, we can apply Association Rules Mining (ASM) [23] to extract positive associations among objects and among domains to effectively manage properties and concepts [11].

Object-Level Associations. This refers to patterns of objects frequently co-occurring together within \mathcal{S} . For instance, a rule like “birds in black color are likely to be aggressive in nature”. Once this rule is revealed, then it is useful not only to identify the number of quality dimensions (or domains) in building conceptual spaces, but to provide implications of correlations such as interdependencies and causal relationships [11]. A $m \times n$ *object-domain relational table* that is similar to the traditional relational table can be easily constructed and used for this association mining. Here, rows are objects corresponding to transactions while columns are domains corresponding to items. Table 1(a) illustrates an example table with 4 domains.

Table 1. Various relational tables: (a) A $m \times 4$ object-domain relational table; (b) A $(l(l - 1)/2) \times 4$ concept-domain relational table

| | type | weight | height | colour |
|----------|----------|----------|----------|----------|
| O_1 | Canary | light | tall | yellow |
| O_2 | Swan | heavy | small | white |
| \vdots | \vdots | \vdots | \vdots | \vdots |
| O_m | Swallow | light | tall | black |

| | type | weight | height | colour |
|--------------|----------|--------------------|----------|----------|
| C_1C_2 | DC | PO | NTPP | TPP |
| C_1C_3 | DC | EQ | TPP | TPP |
| \vdots | \vdots | \vdots | \vdots | \vdots |
| C_lC_{l-1} | PO | NTPP ⁻¹ | EC | DC |

Domain-Level Associations. In conceptual spaces, how the regions in different domains are correlated and how different concepts are correlated are of great importance. For instance, rules like “concepts whose regions (properties) are partially overlap in a weight domain are likely to be discrete in a colour domain”. Especially these domain-level associations are useful for managing and defining concepts. Similar to the object-domain relational table, a *concept-domain relational table* can be constructed, where rows are pairs of concepts corresponding to transactions while columns are domains corresponding to items. Relations of

pairs of concepts are defined as one of the relations of RCC8: DC(DisCrete), EC(Externally Connected), PO(Partial Overlap), EQ(EQual), TPP(Tangential Proper Part), NTPP(Non-Tangential Proper Part), TPP⁻¹(Inverse of TPP) and NTPP⁻¹(Inverse of NTPP). Note that, other RCC family [17] can be used instead. In this table, the number of rows becomes $l(l-1)/2$ since any combination between concepts is possible. An example table is shown in Table 1(b).

4 Final Remarks

Intelligent agents are greatly demanding robust internal representations as they are required to solve and model complex real world problems. A conceptual space approach is an intermediate way of representing information bridging between detailed associationistic representations and coarse symbolic representations. This geometry and topology endowed conceptual space provides a robust framework for conceptualizing information and representing information for building intelligent agents. It has been widely used in various applications [4, 5, 7–9] and recently managing conceptual spaces has attracted a lot of attention in the AI community [2, 6, 8, 11]. However, the bottleneck is in efficient management. Data mining is a solid candidate to efficiently manage complex conceptual spaces. It is to extract interesting knowledge (rules, relationships, patterns, structures, regularities and constraints) from massive datasets [24]. Among many data mining techniques, clustering, classification and ARM are core techniques and most popular methods. This paper proposes a data mining coupled conceptual space framework for various cognitive tasks such as concept formation, concept learning, concept management and property reasoning. Experiments prove the efficiency and effectiveness of our framework.

References

1. Wooldridge, M.: *An Introduction to MultiAgent Systems*. John Wiley & Sons, West Sussex, England (2002)
2. Lee, I.: Fast Qualitative Reasoning about Categories in Conceptual Spaces. In Abraham, A., Köppen, M., Franke, K., eds.: Proc. of the 3rd Int. Conf. on Hybrid Intelligent Systems, Melbourne, Australia, IOS Press (2003) 341–350
3. Gärdenfors, P.: *Conceptual Spaces: The Geometry of Thought*. The MIT Press, Cambridge (2000)
4. Chella, A., Frixione, M., Gaglio, S.: Towards a Conceptual Representation of Actions. In Lamma, E., Mello, P., eds.: Proc. of the 5th Cong. of the Italian Asso. for Artificial Intelligence. LNCS 1792, Bologna, Springer (1997) 333–344
5. Chella, A., Frixione, M., Gaglio, S.: Symbolic and Conceptual Representation of Dynamic Scenes: Interpreting Situation Calculus on Conceptual Spaces. In Esposito, F., ed.: Proc. of the 7th Cong. of the Italian Asso. for Artificial Intelligence. LNCS 2175, Bari, Italy, Springer (2001) 333–343
6. Gärdenfors, P., Williams, M.A.: Reasoning about Categories in Conceptual Spaces. In Nebel, B., ed.: Proc. of the 17th Int. Joint Conf. on Artificial Intelligence, Washington, D.C., Morgan Kaufmann (2001) 385–392

7. Chella, A., Frixione, M., Gaglio, S.: Conceptual Spaces for Computer Vision Representations. *Artificial Intelligence Review* **16** (2001) 137–152
8. Lee, I., Williams, M.A.: Multi-level Clustering and Reasoning about Its Clusters Using Region Connection Calculus. In Whang, K.Y., Jeon, J., Shim, K., Srivastava, J., eds.: Proc. of the 7th Pacific-Asia Conf. on Knowledge Discovery and Data Mining. LNAI 2637, Seoul, Korea, Springer (2003) 283–294
9. Lagus, K., Airola, A., Creutz, M.: Data Analysis of Conceptual Similarities of Finnish Verbs. In: Proc. of the 24th Annual Meeting of the Cognitive Science Society, Virginia (2002) 566–571
10. Lee, I.: Hybrid Soft Categorization in Conceptual Spaces. In Ishikawa, M., Hashimoto, S., Paprzycki, M., Barakova, E., Yoshida, K., Köppen, M., Corne, D.W., Abraham, A., eds.: Proc. of the 4th Int.l Conf. on Hybrid Intelligent Systems, IEEE Computer Society (2004) 74–79
11. Lee, I.: Efficient Management of Conceptual Spaces Using Data Mining Techniques. In Mohammadian, M., ed.: Proc. of the Int. Conf. on Computational Intelligence for Modelling Control and Automation, Gold Coast (2004) 492–499
12. Aldenderfer, M.S., Blashfield, R.K.: Cluster Analysis. Sage Publications, Beverly Hills (1984)
13. Jain, A.K., Murty, M.N., Flynn, P.J.: Data Clustering: A Review. *ACM Computing Surveys* **31** (1999) 264–323
14. Sander, J.: Generalized Density-Based Clustering for Spatial Data Mining. PhD thesis, Computer Science, University of Munich, München, Germany (1998)
15. Sheikholeslami, G., Chatterjee, S., Zhang, A.: WaveCluster: A Wavelet Based Clustering Approach for Spatial Data in Very Large Databases. *The Int. Journal on Very Large Data Bases* **8** (2000) 289–304
16. MacQueen, J.: Some Methods for Classification and Analysis of Multivariate Observations. In: Proc. of the 5th Berkeley Symp. on Maths and Statistics Problems. Volume 1. (1967) 281–297
17. Cohn, A.G., Bennett, B., Gooday, J., Gotts, N.M.: Qualitative Spatial Representation and Reasoning with the Region Connection Calculus. *GeoInformatica* **1** (1997) 275–316
18. Lee, I., Estivill-Castro, V.: Fast Cluster Polygonization and Its Applications in Data-Rich Environments. (*GeoInformatica*) In press.
19. Okabe, A., Boots, B.N., Sugihara, K., Chiu, S.N.: Spatial Tessellations: Concepts and Applications of Voronoi Diagrams. Second edn. John Wiley & Sons, West Sussex (2000)
20. Blake, C., Merz, C.: UCI repository of machine learning databases (1998)
21. Mitchell, T.M.: Machine Learning. WCB/McGraw-Hill, New York (1997)
22. Witten, I.H., Frank, E.: Data Mining. Morgan Kaufmann Publishers, San Mateo, CA (2000)
23. Agrawal, R., Imielinski, T., Swami, A.N.: Mining Association Rules between Sets of Items in Large Databases. In Buneman, P., Jajodia, S., eds.: Proc. of the Int. Conf. on Management of Data, Washington, D.C., ACM Press (1993) 207–216
24. Han, J., Kamber, M.: Data Mining: Concepts and Techniques. Morgan Kaufmann Publishers, San Francisco, C.A. (2000)

An Evolutionary Algorithm for Constrained Bi-objective Optimization Using Radial Slots

Tapabrata Ray¹ and Kok Sung Won²

¹ School of Aerospace, Civil and Mechanical Engineering,
University of New South Wales,
Australian Defense Force Academy
t.ray@adfa.edu.au

² Temasek Laboratories, National University of Singapore,
5 Sports Drive 2, Singapore 117508
tslwks@nus.edu.sg

Abstract. In this paper, we introduce an evolutionary algorithm for constrained, bi-objective optimization. The objective space is divided into a predefined number of radial slots and solutions compete with members in the same slot for existence. The procedure creates a uniform spread of solutions across the slots and they collectively form the nondominated front. Constraints are handled using a standard min-max formulation. We report the performance of our algorithm on a set of seven constrained, bi-objective test problems (CTP1 to CTP7) which have been known to pose difficulties to *all* existing multiobjective algorithms.

1 Introduction

A number of evolutionary algorithms have been proposed in recent years and many of them have been successfully applied to solve multiobjective problems. A comprehensive review of multiobjective optimization (MO) algorithms appears in [1–3]. In order to study the performance of various MO algorithms, [4] proposed a set of seven tunable constrained, bi-objective test problems named CTP1 to CTP7. All existing state of the art MO algorithms have faced difficulties in solving these problems.

Jimenez et al., [5] introduced an algorithm called ENORA (An Evolutionary Algorithm of Nondominated Sorting with Radial Slots) and reported its performance on the set of above test problems. The results were indeed good, but a number of parameters were not listed which made it difficult to compare its results. In this paper, we present our version of the algorithm along similar lines of those presented by [5] with complete details of the parameters and all the mechanisms involved. The remainder of this paper is organized as follows: Sect. 2 provides the detailed description of the mathematical background for the algorithm. Section 3 showcases the numerical results culled from the simulation runs and Sect. 4 provides a summary and conclusion on the proposed MO algorithm.

2 Mathematical Details

A constrained, bi-objective optimization problem in the context of minimization can be presented as follows,

$$\text{Minimize: } \mathbf{f} = [f_1(\mathbf{x}) \quad f_2(\mathbf{x})]^T. \quad (1)$$

Where $\mathbf{x} = [x_1, x_2, \dots, x_n]^T$ is the vector of n design variables and $f_1(\mathbf{x})$ and $f_2(\mathbf{x})$ need to be minimized. Subject to:

$$g_i(\mathbf{x}) \geq a_i, i = 1, \dots, q. \quad (2)$$

Where q is the number of inequality constraints. The constraint vector \mathbf{c} for each solution can be represented as, $\mathbf{c} = [c_1, c_2, \dots, c_q]^T$. Where $c_i = 0.0$ if the constraint is satisfied and $c_i = a_i - g_i(\mathbf{x})$ if the constraint is violated. The pseudo-code of the algorithm is presented below.

```

Initialize a Population of m Solutions. (Set Eval=m,
Number of Radial Slots=d)
Evaluate the Solutions of the Population.
Assign Solutions to the Radial Slots.
While Eval < MaxEvals
    Select Two Parents Using Uniform Random Sampling.
    Create Two Children Using Crossover and Mutation.
    Evaluate the Children.
    Survive or Die: The Children either Survives or Die.
End While

```

2.1 Assigning Slots

Given a set of m solutions, their corresponding objective vectors and a predefined number of radial slots d , the assignment process is as follows:

1. Identify f_1^{Min} , f_1^{Max} , f_2^{Min} , and f_2^{Max} where they correspond to the minimum and the maximum value of objective 1 and objective 2 respectively.
2. The objective vector of each solution $\mathbf{f} = [f_1(\mathbf{x}) \quad f_2(\mathbf{x})]^T$ is scaled to yield a scaled objective vector as follows:

$$\mathbf{sf} = [s f_1(\mathbf{x}) \quad s f_2(\mathbf{x})]^T = \left[\frac{f_1(\mathbf{x}) - f_1^{\text{Min}}}{f_1^{\text{Max}} - f_1^{\text{Min}}} \quad \frac{f_2(\mathbf{x}) - f_2^{\text{Min}}}{f_2^{\text{Max}} - f_2^{\text{Min}}} \right]^T.$$

3. Compute $\tan(\theta) = \frac{1-s f_1(\mathbf{x})}{1-s f_2(\mathbf{x})}$.
4. If $0 \leq \theta < \frac{\pi}{2d}$: the solution belongs to slot 1, if $\frac{\pi}{2d} \leq \theta < \frac{\pi}{d}$: the solution belongs to slot 2 and so on.

2.2 Creation of Children

Two children are created from the two selected parents. The steps involved in each child creation are as follow:

1. Select the parents P_1 and P_2 and perform crossover.
 - (a) If $Q \leq P_{\text{UniCross}}$: use uniform crossover to create child 1 and child 2.
 - (b) If $Q > P_{\text{UniCross}}$: use arithmetic crossover to create child 1 and child 2.
2. For every variable in child 1 and child 2, check and perform mutation.
 - (a) If $S > P_{\text{Mut}}$: do not mutate the variable.
 - (b) If $S \leq P_{\text{Mut}}$ and $T \leq P_{\text{UniMut}}$: use uniform mutation to mutate the variable and set flag = 0.
 - (c) If $S \leq P_{\text{Mut}}$; flag $\neq 0$ and $R \leq P_{\text{NonUniMut}}$: use non-uniform mutation to mutate the variable and set flag = 0.
 - (d) If $S \leq P_{\text{Mut}}$ and flag $\neq 0$: use minimum mutation to mutate the variable.

Where Q, R, S, T are uniform random numbers. The probabilities of uniform crossover, mutation, uniform mutation, and non-uniform mutation are defined as P_{UniCross} , P_{Mut} , P_{UniMut} , and $P_{\text{NonUniMut}}$ respectively.

Uniform Crossover. Each variable of child 1 is inherited either from parent 1 or parent 2 based on a uniform random selection and the remaining set of variables is assigned to child 2.

Arithmetic Crossover. Each variable of child 1 and child 2 is created as follows: $C_i^1 = P_i^1 \times d + (1 - d) \times P_i^2$ and $C_i^2 = P_i^2 \times d + (1 - d) \times P_i^1$, where C_i^1 denotes the i^{th} variable of child 1, d is a random number from a uniform distribution between 0 and 1, P_i^1 and P_i^2 are the i^{th} variable of parent 1 and parent 2 respectively.

Uniform Mutation. Each variable of child 1 and child 2 is mutated as follows: $C_i^1 = x_i^l + (x_i^u - x_i^l) \times d$ where d is a random number from a uniform distribution lying between 0 and 1.

Non-uniform Mutation. Each variable of child 1 or child 2 is mutated as follows:

1. If $R > 0.5$ then $C_i^1 = C_i^1 + (x_i^u - C_i^1) \times a$.
2. If $R \leq 0.5$ then $C_i^1 = C_i^1 - (C_i^1 - x_i^l) \times a$.

Where R 's are random numbers from a uniform distribution lying between 0 and 1, and a is the perturbation scalar defined as: $a = 1 - d^{(1-t/T)^2}$. Where d is a random number between 0 and 1, T is the maximum number of solutions to be evaluated and t denotes the solution being evaluated.

Minimum Mutation. Each variable of child 1 and child 2 is mutated as follows:

1. If $R > 0.5$ then $C_i^1 = C_i^1 + (x_i^u - C_i^1) \times a$.
2. If $R \leq 0.5$ then $C_i^1 = C_i^1 - (C_i^1 - x_i^l) \times a$.

Where R 's are random numbers from a uniform distribution lying between 0 and 1, and a is the perturbation scalar defined as: $a = 1 - d^\epsilon$. Where d is a random number between 0 and 1, and ϵ is set to $1e-05$.

2.3 Replace or Die

This is the most important mechanism in the algorithm that accounts for diversity and collectively generates the nondominated front. Every child either fills an empty slot, replaces an existing individual or gets killed.

1. If the child is infeasible and the population of m solutions has infeasible solutions: eliminate the worst infeasible solution among $m + 1$ solutions. Fitness of an infeasible solution is determined by the maximum value of an element in the constraint vector \mathbf{c} .
2. If the child is infeasible and the population of m solutions has no infeasible solutions: the child is killed.
3. If the child is feasible and the population of m solutions has no infeasible solutions:
 - (a) Child has objective 1 less than f_1^{Min} or objective 2 less than f_2^{Min} : child survives, objective spaces are re-scaled using $m + 1$ solutions and the solutions are re-slotted. The solution from the densest slot that has the worst nondominance ranking is killed. If all the solutions in the densest slot are nondominated, a random one is killed.
 - (b) If the objective function values of the child is within f_1^{Min} , f_1^{Max} , f_2^{Min} , and f_2^{Max} , find the slot that the child belongs to. Add this child to the solutions belonging to that slot and replace the solution with the worst nondominance ranking. If all the solutions are nondominated, replace a random one.

3 Numerical Examples

The expressions for CTP1 to CTP7 used in this study are as follow:

CTP1

$$\text{Min. } f_1(\mathbf{x}) = x_1 . \quad (3)$$

$$\text{Min. } f_2(\mathbf{x}) = g(\mathbf{x}) \exp(-f_1(\mathbf{x})/g(\mathbf{x})) . \quad (4)$$

Subject to: $f_2(\mathbf{x}) - a_j \exp(-b_j f_1(\mathbf{x})) \leq 0$, $j = 1, 2$, $g(\mathbf{x}) = 1 + x_1$. Where $0 \leq x_i \leq 1$, $i = 1, \dots, 4$, $a_1 = 0.858$, $a_2 = 0.728$, $b_1 = 0.541$, and $b_2 = 0.295$.

CTP2–7

$$\text{Min. } f_1(\mathbf{x}) = x_1 . \quad (5)$$

$$\text{Min. } f_2(\mathbf{x}) = g(\mathbf{x}) \left(1 - \sqrt{\frac{f_1(\mathbf{x})}{g(\mathbf{x})}} \right) . \quad (6)$$

Subject to: $g(\mathbf{x}) = 1 + x_1$, $\cos(\theta)(f_2(\mathbf{x}) - e) - \sin(\theta)f_1(\mathbf{x}) \geq a|\sin(b\pi(\sin(\theta)(f_2(\mathbf{x}) - e) + \cos(\theta)f_1(\mathbf{x}))^c)|^d$. Where $0 \leq x_i \leq 1$, $i = 1, \dots, 4$, and the parameters for CTP2 to CTP7 are listed in Table 1.

Table 1. Parameters for the Test Problems CTP2 to CTP7

| | θ | a | b | c | d | e |
|------|------------|-------|------|-----|-----|-----|
| CTP2 | -0.20π | 0.20 | 10.0 | 1 | 6.0 | 1 |
| CTP3 | -0.20π | 0.10 | 10.0 | 1 | 0.5 | 1 |
| CTP4 | -0.20π | 0.75 | 10.0 | 1 | 0.5 | 1 |
| CTP5 | -0.20π | 0.75 | 10.0 | 2 | 0.5 | 1 |
| CTP6 | 0.10π | 40.00 | 0.5 | 1 | 2.0 | -2 |
| CTP7 | -0.05π | 40.00 | 5.0 | 1 | 6.0 | 0 |

The source code for NSGA-II was downloaded from <http://www.iitk.ac.in/kangal/soft.htm> which is the recommended version dated 10th April 2005. A population size of 100 was used for all the runs and 50,000 function evaluations were allowed for both algorithms. We have used four variables for all the test problems. The probabilities of crossover, mutation, uniform crossover, uniform mutation, non-uniform mutation, and minimum mutation were set to 0.6, 0.6, 0.5, 0.2, 0.5, and 0.3 respectively. As for NSGA-II, a simulated binary crossover [6] with $\eta_c = 20$, and polynomial mutation operator [6] with $\eta_m = 20$ was used. A crossover probability of 0.9 and mutation probability of 0.25 were chosen, as suggested in [4]. It is worth noting that the results reported in [4] are for five variables while that of [5] is for four variables.

Figure 1(a) shows the results obtained for test problem CTP1. For CTP1 with the presence of both constraints, about two-third portion of the original unconstrained Pareto-optimal region is now infeasible. Hence the constrained Pareto-optimal front has a kink at around $f_1 = 0.3$, and this is exactly what our algorithm has obtained, and the solutions have a good distribution along the front. On the other hand, NSGA-II failed to locate the Pareto-optimal front at the left one-third region, with its solutions falling into the infeasible region instead.

Figure 1(b) shows the nondominated solution front obtained by our algorithm for test problem CTP2. Both our algorithm and NSGA-II could obtain the Pareto front. Next we consider the test problem CTP3, as pointed out by [4], an MO algorithm will face difficulty in finding the discrete Pareto solutions because of the changing nature from continuous to discontinuous feasible space near the Pareto vicinity. From Fig. 1(c), it can be seen that our algorithm managed to locate all the discrete single Pareto solutions.

When we increase the value of parameter a from 0.1 to 0.75, this has an effect of making the transition from continuous to discontinuous feasible region far away from the Pareto-optimal region. Thus the MO algorithm would now have to travel through a longer narrow feasible “tunnel” in search of the single discrete solution at the end of the “tunnel”. Fig. 1(d) shows that our algorithm failed to locate the Pareto-optimal solutions. However, we note that the algorithm has successfully identified all the discrete discontinuous feasible regions just that it was not able to proceed out of the “tunnel” towards the Pareto-optimal solution at the end of it. NSGA-II performed slightly worse as it failed to locate all the all the discrete discontinuous points.

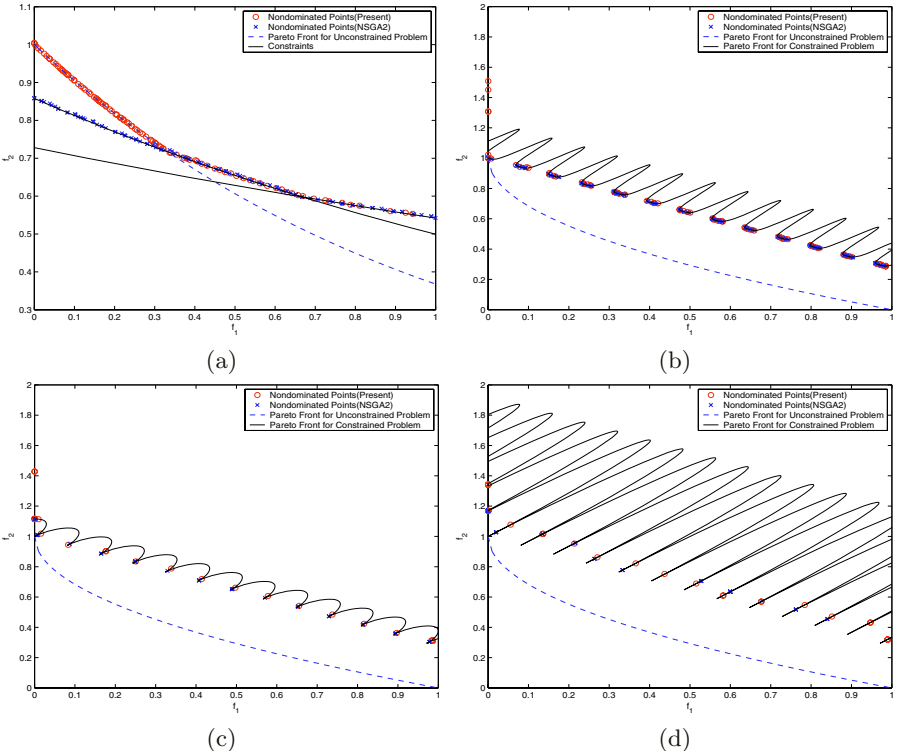


Fig. 1. (a) Nondominated Solutions obtained on Test Problem CTP1 (b) Test Problem CTP2 (c) Test Problem CTP3 (d) Test Problem CTP4

Test problem CTP5 posed another difficulty in terms of clustering of Pareto-optimal solutions. By adjusting the value of parameter c , we can obtain a Pareto front with the solutions more closely packed towards one end of the Pareto front. Figure 2(a) shows the results obtained by our algorithm and NSGA-II, although the Pareto-optimal solutions are more clustered towards the right side, our algorithm managed to identify all of them. Test problem CTP6 was an easier challenge with our algorithm locating the Pareto-optimal front and at the same time maintaining a good distribution of nondominated solutions along the front. However, we wish to make a note that, both our algorithm and NSGA-II were not able to generate any results for CTP6 using the definition of the g function given. Thus only for CTP6, we defined g as the Rastrigin's function instead, given by: $g = 31 + \sum_{i=1}^3 (x_i^2 - 10 \cos(2\pi x_i))$. The results with this new definition are shown in Fig. 2(b).

The final test problem CTP7 has infeasible solutions of differing widths towards the Pareto-optimal region. Since an MO algorithm has to overcome a number of such infeasible holes before coming to the region containing the Pareto-optimal front, many algorithms may face difficulty in solving this problem. More-

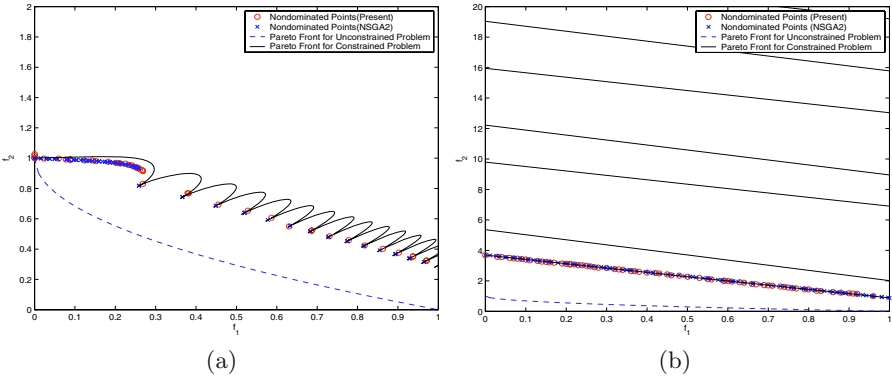


Fig. 2. (a) Nondominated Solutions obtained on Test Problem CTP4 (b) Test Problem CTP5

over, the unconstrained Pareto-optimal region is now infeasible. Figure 3 shows the nondominated solutions obtained by our algorithm, it can be seen that the entire Pareto-optimal front has been located.

4 Summary and Conclusion

In this paper, we have presented a variant version of the algorithm along similar lines of those presented by [5] with complete details of the parameters and mechanisms involved. The results, however, were not so satisfactory in more complicated test problems, like those treated herein. However for other test problems (e.g. CTP2), the proposed algorithm was able to simultaneously identify the Pareto front and also to maintain a good distribution along the front. The success of which has been fundamentally due to the slots assignment technique used.

The algorithm proposed incorporates a problem independent constraints satisfaction technique together with a powerful diversity mechanism which permits the identification of multiple nondominated solutions distributed uniformly along the Pareto-optimal fronts. The experimental results in test problems designed specifically to evaluate such algorithms show a considerable improvement on those obtained to date using other recently created algorithms, however for test problems CTP4 and CTP5, more research work need to be done to identify a more robust methodology in handling such difficult situations.

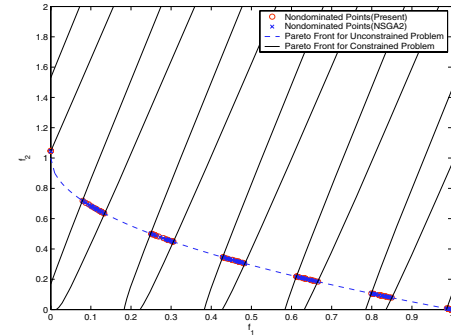


Fig. 3. Nondominated Solutions obtained on Test Problem CTP7

References

1. Deb, K., (2001), *Multi-Objective Optimization Using Evolutionary Algorithms*, John Wiley & Sons.
2. Coello Coello, C. A., Van Veldhuizen, D. A., and Lamont, G. B., (2002), *Evolutionary Algorithms for Solving Multi-Objective Problems*, Kluwer Academic Publishers, New York.
3. Marler, R. T. and Arora, J. S., (2004), “Survey of Multi-objective Optimization Methods for Engineering,” *Structural Multidisciplinary Optimization*, Vol. 26, pp. 369–395.
4. Deb, K., Pratap, A., and Meyarivan, T., (2001), “Constrained Test Problems for Multi-objective Evolutionary Optimization,” *Proceeding of the First International Conference on Evolutionary Multi-Criterion Optimization* (EMO-2001), 7–9 March, Zurich, Switzerland, pp. 284–298.
5. Jimenez, F., Gomez-Skarmeta, A. F., Sanchez, G., and Deb, K., (2002), “An Evolutionary Algorithm for Constrained Multi-objective Optimization,” *Proceedings of IEEE World Congress on Computational Intelligence*, Congress on Evolutionary Computation (CEC 2002), Hawaii, 12–17 May.
6. Deb, K. and Agrawal, R. B., (1995), “Simulated Binary Crossover for Continuous Search Space,” *Complex Systems*, Vol. 9, pp. 115–148.

An Optimization Approach for Feature Selection in an Electric Billing Database

Manuel Mejía-Lavalle, Guillermo Rodríguez, and Gustavo Arroyo

Instituto de Investigaciones Eléctricas, Reforma 113, 62490 Cuernavaca, Morelos, México
`{mllavalle,gro,garroyo}@ie.org.mx`

Abstract. Feature or attribute selection is a crucial activity when knowledge discovery is applied to very large databases. Its main objective is to eliminate irrelevant or redundant attributes to obtain a computationally tractable problem, without affecting the classification quality. In this article a novel optimization approach is evaluated. This method uses concave programming to minimize the number of attributes to input to the mining algorithm and also, to minimize the classification error. This technique is evaluated using a billing data base from the national electric utility in Mexico. The results are compared against those obtained by traditional techniques. From this experimentation, several improvements to the optimization approach are suggested.

Keywords: Knowledge discovery, Applications in power.

1 Introduction

Data mining is mainly applied to large amounts of stored data to look for the implicit knowledge hidden within this information. To take advantage of the enormous amount of information currently available in many databases, algorithms and tools specialized in the automatic discovery of hidden knowledge within this information have been developed. This process of non-trivial extraction of relevant information that is implicit in the data is known as Knowledge Discovery in Databases (KDD), where the data mining phase plays a central role in this process.

It has been noted, however, that when very large databases are going to get mined, the mining algorithms get very slow, requiring too much time to process the information and sometimes making the problem intractable. One way to approach this problem is to reduce the amount of data before applying the mining process [1]. In particular, the pre-processing method of feature selection applied to the data before mining has shown to be successful because it eliminates the irrelevant or redundant attributes that cause the mining tools to become inefficient, but the classification quality of the mining algorithm is preserved [2].

In this article, optimization techniques used for attribute or feature selection are evaluated, as an alternative to the methods traditionally proposed. Particularly, an interesting and novel approach is evaluated as proposed by Bradley and Mangasarian [3] which utilizes concave programming to minimize the classification error and, at the same time, minimizing the number of attributes for the mining task.

To cover these topics, the article is organized as follows: section 2 describes the application domain of the data base; section 3 details the experiments, and conclusions are offered in section 4. Although our work is focused on electric billing data, the real world lessons learned can be used to attack similar problems.

2 The Problem of Illicit Energy Use Characterization

One of the main objectives that Comision Federal de Electricidad (CFE) has is to distribute to its customers electricity produced at different generating plants in Mexico. Related to distribution, CFE faces different problems that prevent it to recover certain amount of “lost income” from the 100% of the total energy for sale. At present CFE loses approximately 21% of the energy for distribution. These losses are mainly due to two problems: a) technical, and b) administrative. The technical energy losses are usually in the range of 10%. The other 11% of the losses are due to administrative control problems, where the big problem is the illicit use of energy, that is to say, people who steal the energy and do not pay for it.

CFE has faced this problem applying different actions and has managed to reduce the percentage due to illicit use losses, which represents a recovery of several million dollars. Since the problem has not been completely solved, it is important to attack it with other technologies and actions, using a KDD approach based on data mining to obtain patterns of behavior of illicit customers. This alternative solution does not require a great deal of investment and it has been proven to be effective in similar cases, like credit card fraud detection.

The subject information to analyze is a sample of the SICOM database, a legacy system developed with the COBOL language; it contains around twenty tables with information about contracts, invoicing, and collection from customers across the nation. This system was not designed with the illicit users discovery in mind; nevertheless, it contains a field called *debit-type* in which a record is made if the debit is due to illicit use of energy. After joining three tables, including the one that has the *debit-type* field, a “mine” with 2,770 instances was obtained with the following attributes: *Permanent customer registry (RPU)*, *Year*, *Month*, *debit-type*, *Digit*, *kWh*, *Energy*, *Cve-invoicing*, *Total*, *Status*, *Turn*, *Tariff*, *Name*, *Installed-load*, *Contract-load*, and others that altogether add up to 21 attributes. One of the values that the attribute *debit-type* can be assigned is “9”, which indicates an illicit use, and it is our class attribute.

With this mine, we perform a series of experiments to evaluate the proposed Bradley’s approach [3] and to compare it against different ranking and wrapper methods; these experiments are subsequently described.

3 Concave Programming Evaluation

3.1 Implementation Details

Mangasarian and Bradley have extensively worked in the search and application of optimization methods to data mining for industry problems. Among these works, their approach to classify and select attributes is significant, since it obtained excellent results when compared against a method based on Support Vector Machines (SVM). The evaluation presented here is built on the model as it appears in [3]. The essential idea of Bradley’s model called *Feature Selection via concave minimization* (FSV), is composed of two parts: the classification of instances and the attribute selection.

The classification part is formulated in such a way as to search for the minimization of the distances between the instances incorrectly classified and the classification line, plane or hyper plane.

The attribute selection part of the objective function is to minimize the number of attributes required to carry out a good class separation, under the assumption that it is possible to obtain a (hyper) plane with less dimensions than the original data, and keep classification acceptable. This is mathematically formulated in the following way (see details in [3]):

$$\begin{array}{ll} \text{minimize}_{w, \gamma, y, z, v} & (1-\lambda) \left(\frac{e^T y}{m} + \frac{e^T z}{k} \right) + \lambda e^T (e - e^{-\alpha y}) \\ \text{subject to} & -Aw + e\gamma + e \leq y, \\ & Bw - e\gamma + e \leq z, \\ & y \geq 0, z \geq 0, -v \leq w \leq v \end{array}$$

We implemented these ideas [3], using a free optimization tool called General Algebraic Modeling System (GAMS) [10] (as opposed to Bradley that used CPLEX in his experiments). The GAMS implementation is called now FSV-GAMS.

3.2 Experimentation Details

The experimentation objective is to observe the FSV-GAMS behavior related to classification quality and response time with SICOM data. 25 experiments were designed in which the values of α and λ change. Although Bradley obtained good results with values of 5 and 0.05 respectively, he points out that these may vary with the application domain.

Additionally, we added three random variables to observe if FSV-GAMS was capable of eliminating such attributes. This idea is inspired in what is proposed in [11] where a single random variable is used as a decision threshold for attribute selection under a *ranking* approach where relevant attributes are separated from the irrelevant ones; we employ three, instead of one random variable, to avoid the introduction of a possible bias in the result due to the single random variable which in fact is a pseudo-random variable.

3.3 Experimental Results

Some of the results obtained as the parameters α and λ vary are shown in the Table 1: the selected number of attributes (#Att); the value of the objective function to minimize (ValObF.); the processing time in seconds (Time(sec)); the number of iterations required to arrive to the final solution (Iters), and the detail of the selected attributes.

From the experiment we can observe that:

- The selected number of attributes varies from 1 to 16, which indicates that α and λ particularly affect this FSV-GAMS result.
- 60% of the times, FSV-GAMS successfully removed the three random variables (variable numbers 22 to 24).
- The attribute number 6 is the one that was selected most often (23 times), and the attribute number 9 was never selected.
- The objective function value seems not to be seriously affected by α and λ neither is the number of iterations nor the processing time, which most of the time stayed between acceptable levels (around 5 minutes).

Table 1. Results for various values of α and λ

| α | λ | # | Att | ValObF | Time (sec) | Iters | 1 | 2 | 3 | 4 | 5 | 6 | 7 | 8 | 9 | 10 | 11 | 12 | 13 | 14 | 15 | 16 | 17 | 18 | 19 | 20 | 21 | 22 | 23 | 24 |
|------------|-----------|----|-----|--------|------------|-------|---|---|---|----|----|----|---|---|---|----|----|----|----|----|----|----|----|----|----|----|----|----|----|----|
| 0.1 | 0.01 | 15 | 15 | 0.6868 | 274.26 | 4521 | 1 | 1 | 1 | 1 | 1 | 1 | 1 | 1 | 1 | 1 | 1 | 1 | 1 | 1 | 1 | 1 | 1 | 1 | 1 | 1 | 1 | 1 | 1 | |
| 0.1 | 0.05 | 16 | 16 | 0.6628 | 265.29 | 5039 | 1 | 1 | 1 | 1 | 1 | 1 | 1 | | | | | 1 | 1 | 1 | 1 | 1 | 1 | 1 | 1 | 1 | 1 | 1 | 1 | |
| 0.1 | 0.20 | 11 | 11 | 0.5620 | 273.19 | 5205 | | | | 1 | 1 | 1 | 1 | | | | | 1 | 1 | 1 | 1 | 1 | 1 | 1 | 1 | 1 | 1 | 1 | 1 | |
| 1 | 0.01 | 15 | 15 | 0.6876 | 462.95 | 8354 | 1 | 1 | 1 | 1 | 1 | 1 | 1 | 1 | 1 | 1 | 1 | 1 | 1 | 1 | 1 | 1 | 1 | 1 | 1 | 1 | 1 | 1 | 1 | |
| 1 | 0.05 | 11 | 11 | 0.6729 | 269.52 | 5057 | 1 | 1 | 1 | 1 | 1 | 1 | | | | | 1 | 1 | 1 | 1 | 1 | 1 | 1 | 1 | 1 | 1 | 1 | 1 | 1 | 1 |
| 5 | 0.01 | 12 | 12 | 0.6965 | 288.51 | 5561 | 1 | 1 | 1 | 1 | 1 | | | | | 1 | 1 | 1 | 1 | 1 | 1 | 1 | 1 | 1 | 1 | 1 | 1 | 1 | 1 | 1 |
| 5 | 0.05 | 3 | 3 | 0.6975 | 186.31 | 2560 | | | | 1 | | 1 | | | | | | | | | | 1 | | | | | | | | |
| 20 | 0.01 | 12 | 12 | 0.7768 | 160.29 | 3554 | | | | 1 | 1 | 1 | 1 | 1 | | | 1 | 1 | | | 1 | 1 | 1 | | | | 1 | 1 | | |
| 20 | 0.05 | 8 | 8 | 0.7110 | 193.26 | 3013 | | | | | 1 | 1 | 1 | | | | | | | | 1 | 1 | 1 | 1 | | | | | 1 | |
| 20 | 0.20 | 1 | 1 | 0.7530 | 175.63 | 2626 | | | | | | | 1 | | | | | | | | | | | | | | | | | |
| 100 | 0.01 | 9 | 9 | 0.7647 | 275.78 | 10000 | | | | | | | 1 | 1 | 1 | | 1 | 1 | | | 1 | 1 | 1 | 1 | | | | | | |
| 100 | 0.05 | 4 | 4 | 0.7503 | 172.17 | 2559 | | | | | | | 1 | 1 | | 1 | | | | | | | | | | | | | 1 | |
| Averag/Tot | | | 8 | 1.0208 | 232.75 | 4425 | 7 | 9 | 5 | 21 | 15 | 23 | 3 | 3 | 0 | 9 | 4 | 5 | 6 | 1 | 14 | 20 | 6 | 18 | 10 | 5 | 2 | 1 | 8 | 10 |

Where the attribute number corresponds to the following description (to respect confidentiality): 1.year
 2.month 3.digit 4.kwh 5.energ 6.bill 7.total 8.status 9.tariff 10.InstLoad 11.ContLoad 12.cIMCC
 13.kwEen 14.toMcI 15.kwMen 16.toMen 17.toMkw 18.kwMcI 19.toMcC 20.cCEto 21.ciEen
 22.Random1 23.Random2 24.Random3

- The number of iterations contrasts with what Bradley reports, who mentions from 5 to 7 iterations. This is due to data base sizes he used which they were, in the best of the cases, three and a half times smaller than the one we used.

The next experimentation phase is to use only the data with the FSV-GAMS selected attributes as input to the decision tree induction algorithm J4.8 included in the Weka tool [12]. J4.8 is the last version of C4.5, which is one of the best-known induction algorithms used in data mining [6]. Some of the results are shown in Table 2: the generated tree size is the number of tree nodes (TrNod); the percentage of instances correctly classified using 10-fold cross validation (AccTest); the processing time required to generate the tree (Time(secs)).

The cost-benefit (C/Ben) is obtained assuming a +97.5 benefit when an “illicit” is correctly predicted and a -97.5 cost or loss otherwise. A +2.5 benefit when a “non-illicit” is correctly predicted (there are savings if an inspection is not needed) and a -2.5 cost or loss otherwise. The numbers 97.5 and 2.5 are arbitrary; they are assigned to reflect that finding an unknown illicit is very valuable. The last column (C/Ben 1000) is the normalized cost-benefit with respect to the cost-benefit as obtained when the 21 attributes are input to J4.8, that is, when there is no attribute selection.

In Table 2 we can observe that:

- The largest tree size is 55 nodes, while the smallest has only one node; nevertheless none of these two obtains the best classification quality.
- The percentage of instances correctly classified varies from 80 to 97%, that is, in all the experiments an acceptable prediction percentage was achieved.
- The processing time never went over 3.31 seconds (see Table 3).
- Four experiments achieved a cost-benefit very similar to the one obtained when using all the attributes.

Table 2. Results of J4.8 using FSV-GAMS selected attributes

| α | λ | TrNod | AccTest | Time (secs) | C/Ben | C/Ben1000 |
|----------------|-----------|--------------|--------------|-------------|----------------|--------------|
| 0.1 | 0.01 | 39 | 97.36 | 2.34 | 54630 | 996.8 |
| 0.1 | 0.05 | 39 | 97.36 | 2.52 | 54820 | 1000.3 |
| 0.1 | 0.2 | 15 | 95.37 | 1.66 | 52645 | 960.6 |
| 1 | 0.01 | 39 | 97.47 | 2.27 | 54835 | 1000.5 |
| 1 | 0.05 | 21 | 95.52 | 1.87 | 48105 | 877.7 |
| 5 | 0.01 | 21 | 95.52 | 1.9 | 48105 | 877.7 |
| 5 | 0.05 | 3 | 90.54 | 0.27 | 28035 | 511.5 |
| 20 | 0.01 | 55 | 90.18 | 1.33 | 24565 | 448.2 |
| 20 | 0.05 | 3 | 90.07 | 0.64 | 27780 | 506.9 |
| 20 | 0.2 | 3 | 90.18 | 0.04 | 27985 | 510.6 |
| 100 | 0.01 | 15 | 90.46 | 1.3 | 23655 | 431.6 |
| 100 | 0.05 | 3 | 89.96 | 0.75 | 24345 | 444.2 |
| Average | | 14.92 | 91.07 | 1.10 | 27410.2 | 500.1 |

3.4 Comparison Against Wrapper and Ranking Methods

To have an idea of the FSV-GAMS performance, in this section we compare the results presented in section 3.3 against the results produced by two well-known traditional methods, wrapper and ranking.

First we consider the process with an *exhaustive wrapper*. In this case, we will obtain that 7.12 months would be required to conclude such a process, which is not practical. Although there are less costly wrapper variations, these do not guarantee to obtain the optimum attribute subset.

Second, we compare the computational cost of the application of filter-ranking methods to select features of a VLDB. We use Elvira [13] and Weka [12] tools, since they provide suitable and updated platforms for the easy execution of multiple experiments in a PC environment. In the presentation of the experiments the processing time has been left out because it was always very small (less than one second). We apply different ranking methods to the electric billing data base. A detailed explanation of these methods can be found in [7] and [8].

Next, the selected attributes were input to the J4.8 classifier. Table 3 samples the obtained results. The measured aspects are the same as the ones used in Table 2.

In Table 3, we observe that most of the methods obtain a reduction in the number of attributes greater than 0.50 and reduce the mining algorithm processing time in an order of magnitude.

Table 3. Results of ranking methods and induction of trees with J4.8

| Método | #Ats. | TrNod | AccTest | Time(secs) | C/Ben 1000 |
|--------------------|-------|-------|---------|------------|------------|
| All attributes | 21 | 41 | 97.25 | 3.31 | 1000 |
| Mutual Information | 4 | 9 | 90.10 | 0.40 | 444 |
| Euclidean distance | 4 | 5 | 93.89 | 0.39 | 520 |
| Matusita distance | 3 | 3 | 90.21 | 0.26 | 507 |
| Kullback-Leibler 1 | 4 | 9 | 90.10 | 0.37 | 444 |
| Kullback-Leibler 2 | 9 | 33 | 97.50 | 0.46 | 1001 |
| Shannon entropy | 18 | 45 | 93.71 | 3.03 | 876 |
| Bhattacharyya | 3 | 3 | 90.21 | 0.30 | 507 |
| Relief | 4 | 5 | 93.89 | 0.38 | 520 |
| OneR | 9 | 23 | 95.95 | 0.49 | 892 |
| Chi-Square | 20 | 33 | 97.43 | 3.21 | 1004 |

With respect to the size of the discovered knowledge, it is observed that almost all the methods produce trees smaller than the complete case. On the other hand, although apparently all the methods do not affect the accuracy of the discovered knowledge too much, the cost-benefit column highlights those methods that better impact on the prediction of the illicit energy use patterns.

4 Conclusions and Future Work

From the experimentations presented we conclude that:

- a) FSV-GAMS selects relevant attributes (without affecting the prediction quality). Since the number of these varies with α and λ parameters, it is necessary to carry out several experiments (we did 25) to find the right combination of these parameters.
- b) The size of the generated knowledge, using the FSV-GAMS selected attributes, is comparable to that obtained by applying ranking methods and substantially drops the mining algorithm processing time.
- c) The cost-benefit achieved by FSV-GAMS, is similar or slightly better than if all the attributes were used to carry out the induction, although this is not consistent all the time, since it varies with α and λ . For our study case (illicit energy use), the FSV-GAMS processing time was reasonable (around 5 minutes) as compared with the wrapper approach that typically requires hours or days of execution; however the results suggest that for bigger data bases, the FSV-GAMS execution time will grow exponentially with the number of instances.

Given the previous comments, some future research issues arise with respect to FSV-GAMS improvement. For example:

- a) Instead of finding a (hyper) plane to decisively separate the classes, re-formulate FSV in terms of a fuzzy classification such that the penalty for the badly classified instances be gradual with respect to its distance-proximity to the fuzzy (hyper) plane separating the classes.
- b) It would also be important to re-formulate FSV-GAMS in such a way that it would not require to carry out thousands of iterations to arrive to the solution. This would be possible by applying methods as the interior point or by a linear re-formulation of the mathematical model (to substitute the exponential expression of the formulation by an equivalent lineal one). In its present formulation, FSV does not consider the cost-benefit aspect in the classification process, this is an important issue in real world applications.
- c) Finally, it would be important to re-formulate FSV so that it can classify more than two classes, handle mixed attributes (continuous and discrete), and generate explicit knowledge that is “understandable” by the human expert of the domain.

References

1. Pyle, D., Data preparation for data mining, Morgan Kaufmann, San Francisco, California, 1999.
2. Guyon, I., Elisseeff, A., An introduction to variable and feature selection, Journal of machine learning research, 3, 2003, pp. 1157-1182.

3. Bradley, P., Mangasarian, O., Feature selection via concave minimization and support vector machines. Machine learning, 15th int. conference ICML '98, SnFco., Calif. 1998, pp. 82-90.
4. Mitra, S., et.al., Data mining in soft computing framework: a survey, IEEE Trans. on neural networks, vol. 13, no. 1, January, 2002, pp. 3-14.
5. Kohavi, R., John, G., Wrappers for feature subset selection, Artificial Intelligence Journal, Special issue on relevance, 1997, pp. 273-324.
6. Quinlan, J., Unknown attribute values in ID3, Int. conf. Machine learning, 1989, pp. 164-168.
7. Piramuthu, S., Evaluating feature selection methods for learning in data mining applications, Proc. 31st annual Hawaii Int. conf. on system sciences, 1998, pp. 294-301.
8. Molina, L., Belanche, L., Nebot, A., Feature selection algorithms, a survey and experimental evaluation, IEEE Int. conf. on data mining, Maebashi City Japan, 2002, pp. 306-313.
9. Domingos, P., When and how to subsample, SIGKDD, Vol. 3, Issue 2, 2001, pp. 74-75. S.
10. General Algebraic Modeling System, GAMS IDE, Rev. 135, 2003.
11. Stoppiglia, H., Dreyfus, G., et.al., Ranking a random feature for variable and feature selection, Journal of machine learning research, 3, 2003, pp. 1399-1414.
12. www.cs.waikato.ac.nz/ml/weka, 2004.
13. www.ia.uned.es/~elvira/, 2004.

Integrating Relation and Keyword Matching in Information Retrieval

Tanveer J. Siddiqui¹ and Uma Shanker Tiwary²

¹ J.K. Institute of Applied Physics and Technology
Department of Electronics & Communication
University of Allahabad, Allahabad -211002, India
tjs@jkinstiute.org

² Indian Institute of Information Technology, Allahabad-211011
ust@iita.ac.in

Abstract. We propose an information retrieval (IR) model that combines relation and keyword matching. The model relies on a novel algorithm for relation matching. The algorithm takes the advantage of any existing relational similarity between document and query to improve retrieval effectiveness. If query concepts(terms) appearing in a document exhibit similar relationship then the proposed similarity measure will give high rank to the document as compared to those in which query terms exhibit different relationship. A conceptual graph (CG) representation has been used to capture relationship between concepts. In order to keep the approach computationally simple a simplified form of CG matching has been used instead of graph derivation. Structural variations have been captured during matching through simple heuristics. CG similarity measure proposed by us is simple, flexible and scalable and can find application in many related tasks like information filtering, question answering, document summarization etc.

1 Introduction

Most of the human knowledge is expressed in natural language and IR mainly deals with textual records written in a particular language. However, it is difficult to use natural language as knowledge representation language for computer systems. Most of the existing retrieval systems follow keyword representation for documents, in which the content of documents is represented as a set of unrelated terms and the relationship that exists between terms is ignored. Most of the earlier research was focused on refining and developing keyword matching algorithm [4]. In late 1980s and early 1990s it was felt by researchers that keyword matching approach have reached their maximum attainable performance and no significant improvement is possible using these methods[11]. The advent of WWW gave a new life to research in keyword matching. Regardless of all these research efforts the effectiveness of retrieval system is still rather low[15]. This motivates researchers to explore new directions for IR. Researchers do believe that improvement in IR performance can be achieved through improved search procedure[16]. One of the disadvantages of the keyword-based systems is that these systems perform retrieval merely on the presence or absence of keywords in the documents. However, meaning does not come merely by sticking words together. There can be sentences comprising the same set of words

involved in different relationships. As an example consider the following two sentence fragments:

The farmer exploits worker... and
Exploitation of farmers and workers ...

A ‘bag of word’ approach will fail to distinguish between these two. It is the relationship existing between words that gave them different meaning. It makes sense, therefore, that considering relationships in the matching process can improve retrieval effectiveness.

One of the ways of using relations is to expand query by adding terms using different types of relation e.g. synonyms or hypernym/hyponym relation. The term driving can be expanded using:

Synonyms: traveling, steering etc.
Hyponyms: motoring
Object: car, truck, vehicle, etc.

Other approaches include the use of proximity search and multi-word phrases. Proximity search approach is based on the assumption that words that are related tend to appear close together. But words appearing together may express different relationship as in the case of “Junior School” and “School Junior”. Multi-word phrase matching is simpler and existing methods for single term matching can be applied to multi-words. However it has not been found to be more effective than single word terms [7]. A number of researchers have used syntactic relation matching. The results reported with syntactic relation matching, however, are not very encouraging [13]. Syntactic relations may fail to identify similarity existing between terms expressed using different syntactic structures. This suggests that the use of semantic relations can provide better results. The DR-LINK project [5] was probably the first serious attempt in this direction. In DR-LINK project documents were represented using Conceptual Graphs (CGs). Conceptual graphs are very closely related to natural language and were originally developed to represent meaning of natural language text. Such a representation is capable of extracting more information from documents by explicitly capturing logical relationship between terms; unlike word-statistical approaches that merely count nouns and noun phrases. This makes CGs a useful formalism for tasks like information retrieval, database interfaces and natural language processing. Some researchers have concentrated on particular type of semantic relations[6],[3]. In [6] the work was focused on case relations whereas Khoo [3] concentrated on cause-effect relations and reported small but significant improvement in retrieval result.

Realizing the difficulty in identifying semantic relations we propose a retrieval model that combines relation and keyword matching. The proposed retrieval model is simple and flexible. It takes the advantage of any existing relational similarity between a document and a query, otherwise performs retrieval based on vector similarity. For relational similarity we have proposed a new CG similarity measure. The structure of the paper is as follows. Section 2 introduces conceptual graphs. Section 3 illustrates our retrieval model and relational similarity measures. An illustrative example is given in section 4, while in section 5 we investigate our model experimentally and discuss results. Finally we conclude in section 6.

2 Conceptual Graphs

CGs have evolved out of conceptual structures theory as set down by John F. Sowa and are based on the logic of Charles Sanders Peirce, Tesíñerés dependency graphs and the Semantic networks of AI. Conceptual graphs (CGs) are the basic building blocks of conceptual structures. Sowa [14] describes conceptual graphs as the logical form that state relationships between concepts and thus represents meaning

2.1 Definition and Notation

A conceptual graph is a finite, bipartite graph. It has two types of nodes - concept nodes and relation nodes [14]. In the graph concept nodes represent entities, attributes, states and events and relation nodes show how concepts are interconnected. Concept nodes have two types of field – referent field and type field. Two fields are separated with a colon. Concept nodes are represented using boxes and relation nodes using circles. Types of concepts (type labels) are organized into a type hierarchy.

CGs can be represented in three different forms. These are linear form, display form (DF) and conceptual graph interchange form (CGIF). Linear Form (LF) is a compact readable form which is normally followed in text. In the linear form (LF), concepts are represented by square brackets instead of boxes, and the conceptual relations are represented by parentheses instead of circles. Both DF and LF are designed for communication with humans or between humans and machines. CGIF was developed for communication between machines that use CG as their internal representation. CGIF has a concrete syntax which makes it usable for implementation. In CGIF co-reference labels are used to represent the arcs.

Example: Consider the sentence:

A cat is on a mat.

The DF representation is shown in fig. 1.

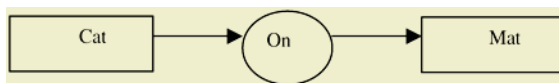


Fig. 1.

LF representation will be –

$[Cat] \rightarrow (On) \rightarrow [Mat]$

In CGIF the above sentence can be represented as:

$[Cat: *x] [Mat: *y] (On ?x ?y)$

The symbols $*x$ and $*y$ are called defining labels. The matching symbols $?x$ and $?y$ are the bound labels that indicate references to the same instance of a cat x or a mat y . For communication with systems that use other internal representations, CGIF can be translated to another logic-based formalism called the Knowledge Interchange Format (KIF): $(\exists x \text{ Cat} (\exists y \text{ Mat}) (\text{On } ?x ?y))$

Any statement expressed in any one of these notations can be automatically translated to a logically equivalent statement in any other form.

2.2 Why Conceptual Graphs?

Conceptual graphs form a knowledge representation language based on linguistics, psychology and philosophy[14] and were initially designed to facilitate natural language analysis and understanding. Since they are similar to semantic networks, they have also been applied to knowledge representation. CGs express meaning in a precise, readable and computable way. This makes them applicable for more effective information and knowledge processing.

2.3 Conceptual Graph Matching

Most of the research work on CG has focused on graph theory and graph algorithms which have been considered the essence of CG theory [2]. Researchers have proposed sound and complete graph derivation with respect to first order logic semantics and graph theory [1]. But these graph derivation algorithms are non-deterministic which is clearly undesirable for IR applications. Some efficient graph algorithms have been proposed[1],[10] based on CG normal form. But there is a widespread opinion that any reasonably complete method of structural comparison is not computationally affordable [10].

A number of researchers attempted to use CGs in information retrieval and proposed computationally tractable CG matching algorithms [5],[8],[9]. While the general sub-graph isomorphism problem is known to be computationally intractable, matching CGs containing conceptual information seems to be practical. None of these methods however, attempt to integrate relation matching with existing statistical similarity measures used commonly in information retrieval.

3 The Proposed Retrieval Model

Our model performs retrieval based on term(keyword) similarity and relational similarity. Vector and CG-based representation of documents has been used for identifying term and relational similarity respectively. These two similarity scores are then combined to perform retrieval.

3.1 Vector Space Representation

In vector space model both the document and query is represented as a vector whose elements denote the weights assigned to terms appearing in them. The document collection as a whole is represented as an $m \times n$ matrix, where m is the number of terms identified for representing the document collection and n is the number of documents in the collection. The inner product between query and document vector is used to give a term similarity score. The steps followed in vector representation of documents are:

- (i) Extract individual words and their frequencies in each document
- (ii) Eliminate stop words.
- (iii) Reduce words to their stems. (Porter's stemmer has been used)
- (iv) Assign weights to each term and prepare term-document matrix.

Many term-weighting schemes have been proposed in IR community over the years. Most of them consider term frequency(tf), inverse document frequency(idf) and document length factors to assign weights to term. The form of term weighting scheme used by us is doc="atn" and query = "ntc" [12]. Where the three letter combination has usual meaning representing the form of tf, idf and document length components respectively. This scheme uses following expression to assign term weights:

$$\text{Document-term weight ("atn")}: w_{ij} = (0.5 + 0.5 \times \frac{tf_{ij}}{\max tf_j}) \times (\log \frac{n}{n_i})$$

$$\text{Query-term weight ("ntc")}: w_{ik} = \frac{wl_{ik}}{\sqrt{\sum_{i=1}^m wl_{ik}^2}} \quad \text{Where, } wl_{ik} = tf_{ik} \times \log(\frac{n}{n_i})$$

$$\text{Query-document similarity } SV(j,k): \sum w_{ij} \times w_{ik}$$

Where, w_{ij} is weight of i^{th} term in document j
and $SV(j,k)$ is similarity between document j and query k.

3.2 CG-Based Representation

The CG-based representation of documents is prepared by extracting relationships. Query and document CGs are compared quantitatively to get a relational similarity score. The relationship considered include 'SUBJ', 'OBJ', 'ATTR', 'MNR', 'NUM', 'MOD' and 'PMOD'. The steps followed to construct CGs are:

The documents are first tagged using TnT tagger.

Tagged output is then processed to

- (i) normalize some of the noun phrases, for example the phrase "New method of computation of square root" will be transformed into "new square root computation method".
- (ii) rewrite compound statements involving "which" as two simple fragments by substituting referring instances. We have extracted syntactic rules for this purpose. When we applied these rules on CACM collection approximately 70% out of the 1442 statements involving "which" were reduced correctly to simple fragments. We feel that the exceptional cases will not create much problem as queries will also go under identical treatment.
- (iii) delete determiners, wh-determiners, wh-pronouns, reflexives and patterns like "as well as" (replaced by "and"), and "such as" etc.

Conceptual graphs are then constructed for the remaining fragments. Detail semantic interpretation has not been done as deep and complete understanding of the text is not necessary for information retrieval. This helps in keeping the approach computationally simple. The CGs are stored in the form of triplets as:

(rel c1 c2).

Where 'rel' is the relation and 'c1' and 'c2' are concepts participating in this relation.

Example: The tagged representation of the fragment "An efficient storage system for conceptual graphs" will be:

an {DT} efficient {JJ} storage {NN} system{NN} for{IN} conceptual {JJ} graphs {NNS}.

Its CG representation will be:

(attr storage efficient) (mod system storage) (pmod system graph) (attr graph conceptual)

For each sentence of each document such triplets are identified and stored. For each document the frequency of most frequent triple is obtained.

In order to keep our approach simple and practically feasible, no type hierarchy has been considered during CG representation of documents in the collection. This is because maintaining a type hierarchy for a general task like IR is difficult. Use of existing lexical resources for this purpose may yield sufficiently large number of relation triples which might result in low precision. In order to cover disjoint concepts that share similar meaning, the type hierarchy has been utilized to yield alternate relation triples for query. These alternate representations can be presented to the user and her acceptance can be obtained. Syntactic variations have been captured through simple heuristics. For example, when the root of a concept is a verb then a match with “obj” relation will be accepted for a triple involving “mod” relation provided the participating concepts and their order is same. This heuristic will allow “information retrieval” to be matched with “retrieve information”.

3.3 Retrieval Method

In order to perform retrieval we identify relational similarity and vector similarity. To get relational similarity between a query and a document, the query CG is matched with the document CG. This matching is done for each textual unit. Textual unit can be a single sentence, a window containing predetermined number of sentences or the whole document. In this study we have evaluated two CG similarity measures for identifying relational similarity between a query and a document, considering entire document as a textual unit. The first CG similarity measure (CGSim I) proposed by us to get relational similarity (SR), between query k and document j is as follows:

$$SR(j, k) = \frac{\sum_i (\text{match}(QTRPL[k], dtrpl[i, j]) \times dtrpl_freq[i, j])}{m \times \max_i (dtrpl_freq[i, j])}$$

where, QTRPL is a vector containing query triples of query k.

$\text{match}(QTRPL[k], dtrpl[i, j])$ is a function that returns a value 1 if i^{th}

triple in the document matches with any of the query triple, otherwise 0.

$dtrpl_freq[i, j]$ is frequency of i^{th} triple in the document j

$\max_i(dtrpl_freq[i, j])$ is maximum frequency of any triple in document j.

& m = query length (i.e. the number of triples in the query CG)

The vector similarity between document j and query k is computed as inner product of query and document vector.

$$SV(j, k) = \sum w_{ij} \times w_{ik}$$

These two similarity measure are then combined to get a single score as:

$$S = \alpha \times SV + \beta \times SR \text{ where } 0 \leq \alpha, \beta \leq 1$$

The values of α and β have been set empirically by us. When $\beta = 0$ only vector similarity will contribute to document score. By setting $\alpha=0$ we can do pure relational matching. The similarity measure is thus flexible enough to allow us to control degree of similarity. Further by varying the definition of textual unit this similarity measure can be fine tuned for different information retrieval related tasks.

However, there is a problem in the first similarity measure in cases of expanded query. When we add a new query triple automatically for searching the relevant document (say for “text retrieval” one can add “information retrieval”), the query length increases. This reduces the value of the relational similarity in the above equation which is not correct. To handle this problem we propose another CG similarity measure (CGSim II) in which the denominator term consists of the length of largest CG fragment (m_f) in the query. The exact expression used is as follows:

$$SR(j, k) = \frac{\sum_l (\text{match}(QTRPL[k], dtrpl[i, j]) \times dtrpl_freq[i, j]))}{m_f}$$

4 Example

Consider following text fragments:

1. *Comparing linear and graphic notation for conceptual graphs*
2. *Comparison of conceptual graphs*
3. *Flexible comparison of conceptual graphs*
4. *Matching conceptual graphs*
5. *Comparing co-occurrence graph of concepts*

and the query “*Comparison of conceptual graphs*”.

The stemmed terms, along with their weights, used in vector representation are:

1. *compar 0.402321 conceptu 0.364529 graphic 0.440113 linear 0.440113 notat 0.440113 graph 0.352362*
2. *comparison 0.621607 conceptu 0.563216 graph 0.544419*
3. *comparison 0.514024 conceptu 0.465739 flexibl 0.562309 graph 0.450195*
4. *conceptu 0.542961 match 0.655543 graph 0.524840*
5. *compar 0.432049 graph 0.378399 occur 0.472634 concept 0.472634*

The relationship triples identified are:

1. *(obj comapre notation) (attr notation linear) (attr notation graphic) (pmod notation graph) (attr graph conceptual)*
2. *(mod comparison graph) (attr graph conceptual)*
3. *(attr comparison flexible) (mod comparison graph) (attr graph conceptual)*
4. *(obj match graph) (attr graph conceptual)*
5. *(obj comapre graph) (mod graph co-occurrence) (mod graph concept)*

and the scores for these fragments are: 1.619, 2.729, 2.42, 2.06, 1.308 respectively.

We have given equal weight to relational and vector similarity in above calculation (i.e. $\alpha = \beta = 1.0$). The order in which the documents are ranked by the above similarity measure is 2, 3, 4, 1 and 5. If we consider vector similarity only then the ranking obtained will be 2, 3, 1, 4, 5. Though the fragment 4 is more relevant to the query but

it has been ranked low as compared to fragment 1. This is because vector similarity simply looks at term similarity only and fails to capture the semantics of concepts.

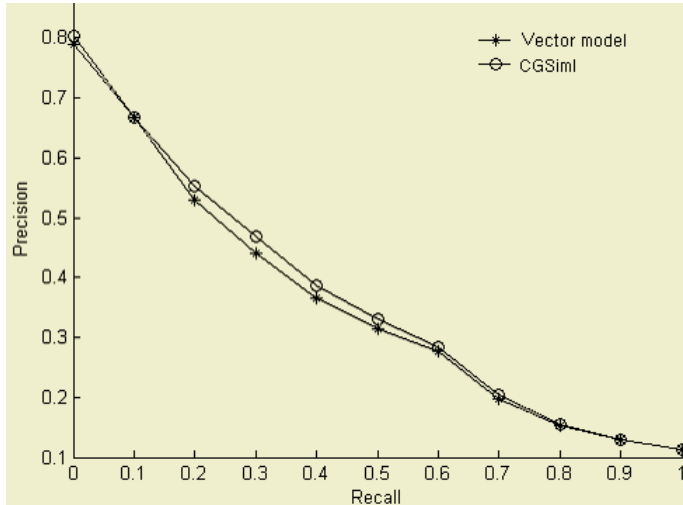


Fig. 2. Recall-Precision curve for CACM collection (averaged over 64 queries) for vector model and our retrieval model using CG similarity measure I

5 Experiment and Results

5.1 The Experiment

In order to investigate the usefulness of our approach we performed an experiment on CACM-3204 document collection. This collection has 3204 documents and 64 queries with known relevance judgments. The objective is to compare the retrieval performance of our model using the proposed relational similarity measures with that of vector space model. We first performed retrieval using vector similarity only and then performed retrieval using combined similarity. Figure 2 compares the recall-precision curve for our model using first CG similarity measure (CGSim I) with that of vector model. 11-point interpolated average precision (averaged over 64 queries of the collection) has been used. The performance of our model with second similarity measure (CGSim II) has been shown in figure 3.

5.2 Results and Discussions

As shown in figure 2 the performance of our model is found better than vector space model. Setting $\alpha = 1$ we varied β in the range of 0 to 1. The maximum mean average precision was found to be 37.22(%) for $\beta = 1.0$, representing an increase of 3.1% over vector model(36.10%). The term appearing in the denominator of our first similarity measure dampens the effect of relational similarity in cases when new triples are being added. It yields a maximum value of 1 when the only query triple matches

with the highest frequency triple in the document(a rare case). As alternate triples add to query, it increases query length and usually a document will be using only one of these alternate triples. This increases the value of the term appearing in denominator which contributes to low performance gain. In order to improve this situation we tried another similarity measure (CGSim II) in which relational similarity was obtained by dividing by the length of largest query CG fragment. The maximum mean average precision observed using CGSim II is 38.76% for $\alpha = 1$ and $\beta = 0.4$, representing an improvement of 7.37% which is quite significant.

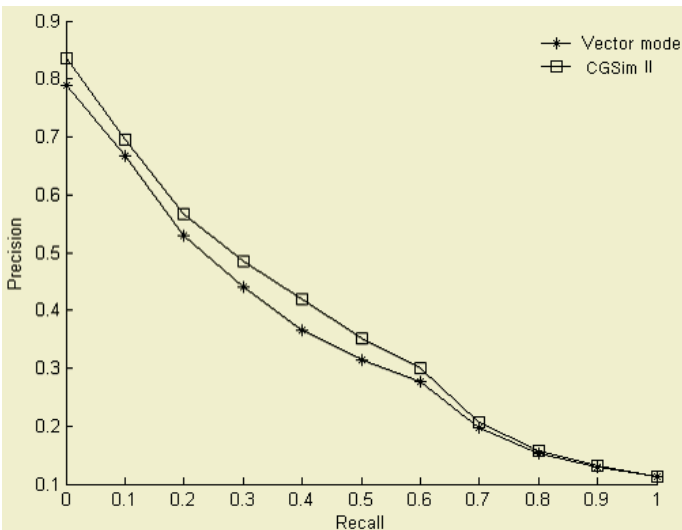


Fig. 3. Recall-Precision curve for CACM collection (averaged over 64 queries) for vector model and our retrieval model using CG similarity measure II

6 Conclusions

We proposed a retrieval model that combines relational and keyword similarity for information retrieval. A computationally simple CG matching algorithm has been proposed for measuring relational similarity. The algorithm is flexible enough to be tuned to match the requirement of specific user by merely setting parameters. Further by varying the definition of textual unit the scope of relation matching (i.e. the context) can be varied from sentence level to document level or any appropriately defined textual window. The relation matching through CGs brings semantics in the retrieval process resulting in improved ranking. The CG representation used by us is easily scalable.

Acknowledgement

Thanks to Thorsten Brants for providing license to use Trigrams'n'Tags (TnT) tagger.

References

1. Amati, G., Ounis, I.: Conceptual Graphs and First Order Logic, *The Computer Journal*, 43:1 (2000)
2. Chein, Michael et Mugnier, Marie-Laure(1995) Conceptual graphs are also graph. Research Report, 95-004, LIRMM
3. Khoo, Christopher S. G., Myaeng, S. H., Oddy, R. N.: Using cause-effect relations in text to improve information retrieval precision, *Information Processing and Management*, vol. 37, (2001) 119-145.
4. Khoo, Christpoher, Soo-Guan: The Use of Relation matching in Information Retrieval, LIBRES: Library and Information Research, 7:2, (1997)
5. Liddy E. D., Myaeng S. H.: DR-LINK: a system update for TREC-2. Second Text REtrieval Conference (TREC-2) (NIST-SP 500-215) NIST, Washington, DC, USA(1994), 85-99
6. Liu, G. Z.: Semantic vector space model: Implementation and evaluation. *Journal of American Society for Information Science*. 48(5) (1997) 395-417.
7. Mittendorf, E., Mateev, B., Schäuble, P.: Using the co-occurrence of words for retrieval weighting. *Information Retrieval*, 3, (2000) 243-251.
8. Montes-y-Gómez M., López-López, A., Gelbukh A.,: Comparison of conceptual graphs, Cario O, Sucar LE, Cantu FJ (Eds.) MICAI 2000: Advances in Artificial Intelligence. Lecture notes in Springer –Verlag, (2000) 548-556
9. Montes-y-Gomez, Gelbukh, Lopez-Lopez, Baeza-Yates: Flexible comparison of Conceptual Graphs. Lecture notes in computer science 2113. Springer-Verlag, (2001)
10. Mugnier M. L.: On Generalization/Specialization for Conceptual Graphs. *Journal of Experimental and theoretical Artificial Intelligence*, vol. 7, (1995) 325-344
11. Salton, G., Buckley, C., Smith, M.: On the application of syntactic methodologies in automatic text analysis.*Information Processing and Management*, 26(1), (1990)73-92.
12. Savoy J., Picard P.: Retrieval effectiveness on the Web, *Information Processing and Management*, 37(4), (2001)643-569
13. Smeaton, A.F., O'Donnell, R., Kelledy, F.: Indexing structures derived from syntax in TREC-3: System description. In D.K. Harman (Ed.), Overview of the Third Text REtrieval Conference (TREC-3) NIST SP-500-225 (1995), 55-67. Gaithersburg, MD: NIST
14. Sowa, J. F.: Conceptual structures- Information processing in mind and machine, (1984) Addison –Wesley
15. Sparck Jones, K.:Summary performance comparisons TREC-2, TREC-3,TREC-4, TREC-5 (1997) In TREC-5 Proceedings.
<http://wwwnlpir.nist.gov/TREC/trec5.papers/sparckjones.ps>
16. Xu, Y., Benaroch, M.: Information retrieval with a hybrid automatic query expansion and data fusion procedure. *Information Retrieval*. 7, (2004) 1-25.

Production Testing of Spark Plugs Using a Neural Network

Simon D. Walters, Peter A. Howson, and Bob R.J. Howlett

Engineering Research Centre, School of Engineering
The University of Brighton, Brighton, UK

s.d.walters@brighton.ac.uk
<http://www.brighton.ac.uk>

Abstract. Despite nearly 150 years' evolution, there have been relatively few advances in the design, and methods of production testing, of spark plugs. For years, an ingenious yet relatively simple "go/no go" batch test has been favoured, yet this testing solution exhibits some major disadvantages.

This paper describes an alternative method of spark plug testing, offering elementary diagnosis of faults as well as detection. In this functional test regime, spark voltage waveforms are classified using a neural network.

The promising results of this experimental work indicate that neural networks may offer considerable potential for the future of spark plug testing.

1 Introduction

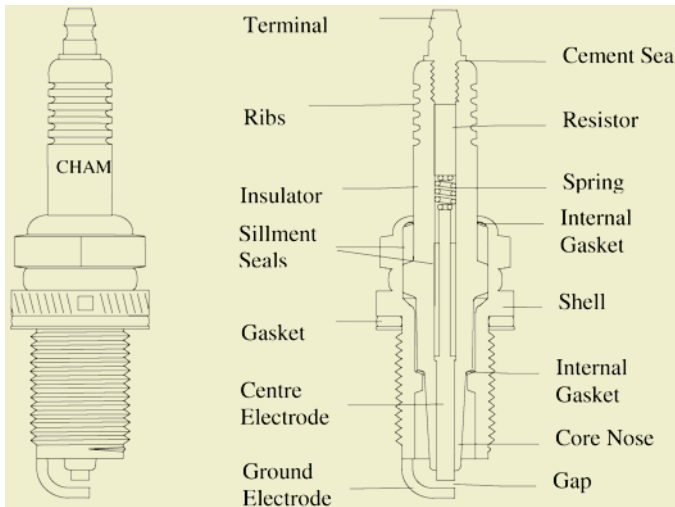
Since spark plugs were invented in 1860, there have been few major changes in their construction. Similarly, there have been apparently few advances in the methods of production testing of spark plugs [1], [2], [3]. Even in recent years, an ingenious yet relatively simple "go/no go" batch test has been a favoured production test, yet this relies on subjective human opinion to discern often minute differences in the output display; it also has health and safety issues, [2].

This paper describes an alternative method of spark plug testing. The objectives were to: (1) Investigate the potential of spark voltage waveforms as indicators of the physical and functional health of production spark plugs; (2) Evaluate a neural network as a means for detection and diagnosis of production faults in spark plugs. Neural networks have been successfully applied to other spark analysis projects [4].

Spark plugs are described in the literature [5], [6], [7]; they are required to reliably ignite fuel-air mixture within gasoline engines, whilst working under conditions of high voltage and high temperature. The production process of spark plugs is somewhat complex, offering many opportunities for errors or damage during assembly. This paper features tests on a batch of 80 RN7YC spark plugs; 40 "faulty", exhibiting various faults and 40 "good", as per Table 1. The physical and electrical implications of each fault may be gauged by referring to the diagram of a spark plug, (Fig. 1), and later text, respectively. A Multi-layer Perceptron (MLP) neural network architecture was trained using a custom-written cumulative back-propagation algorithm, implemented in the C language [8]. MLP neural networks have been recently applied to diverse pattern classification and modelling tasks, [9], [10]. The neural network was believed to be better suited for progression to increasingly complex classification, to be undertaken in later work, compared with other methods.

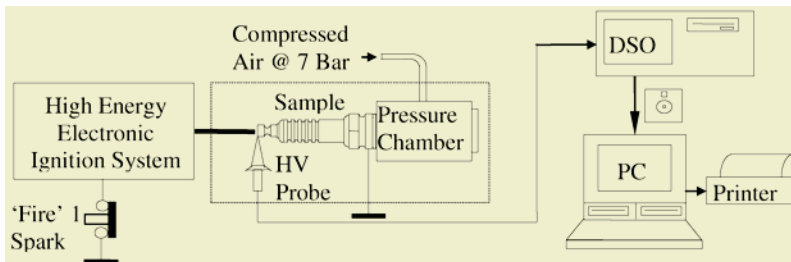
Table 1. Spark Plug Test Categories Prepared for this Work

| <u>No.</u> | <u>Class</u> | <u>Fault Description (Test Sample Used)</u> |
|------------|---------------|--|
| 40 | Good | None (RN7YC - Good) |
| 10 | Fault1 | Wrong plug type (N7YC - Good) |
| 10 | Fault2 | Resistor missing (RN7YC - 1 Springs, 0 Resistors) |
| 10 | Fault3 | Resistor missing & extra spring (RN7YC - 2 Springs, 0 Resistors) |
| 10 | Fault4 | Spring missing (RN7YC - 0 Springs, 1 Resistor) |

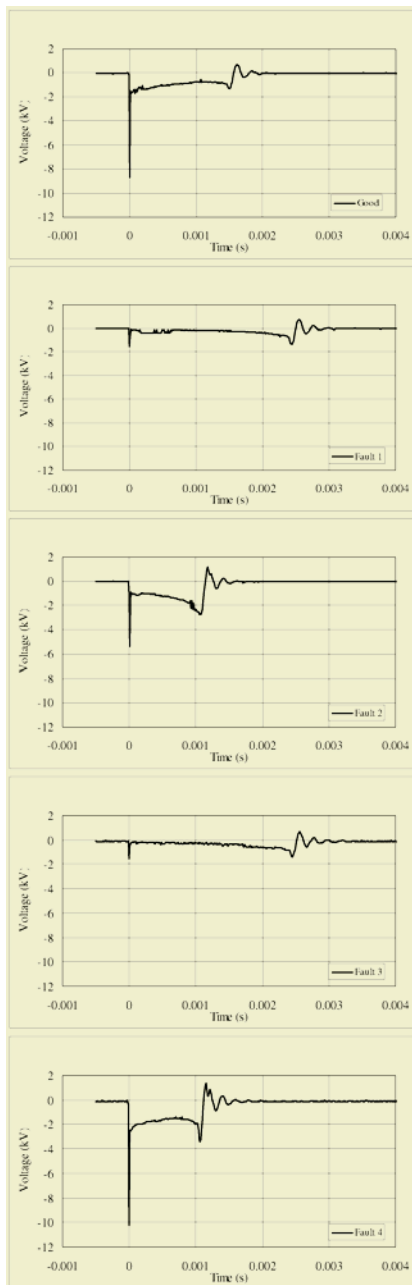
**Fig. 1.** Cross-section View of a Typical Spark Plug (Not To Scale)

2 Acquisition of Spark Voltage Waveforms

Experimental data for the investigation was prepared as described below: The batch of test spark plugs was prepared as described in Table 1. Equipment was set up according to Fig. 2.

**Fig. 2.** Air-quenched-gap Voltage Waveform Test - Experimental Arrangement

Each spark voltage waveform was stored by firing the ignition; the resulting spark triggered the oscilloscope which then captured the waveform. The stored waveform data was then transferred to computer disk. Fig. 3 depicts typical raw data waveforms.

**Good:**

The waveform of a “good RN7YC” spark plug exhibited a fairly high overall voltage – the presence of the resistor gave the characteristic sweeping upward curve of the glow discharge phase of the waveform.

Fault1:

The “good N7YC” spark plug effectively had a shorting link instead of the resistor. The lower spark plug voltage meant energy was dissipated at a slower rate, resulting in a longer spark waveform.

Fault2:

The “No resistor” spark plug had a large internal air gap, where the resistor would have been. This led to a high overall discharge voltage and rapid expenditure of energy, hence a shorter discharge.

Fault3:

The “no resistor, two springs” spark plug effectively exhibited a situation midway between Fault1 and Fault2; a lower spark plug voltage with slow energy dissipation rate, resulting in a long spark waveform.

Fault4:

The “no spring” spark plug had a resulting small internal air gap. This, coupled with the present resistor, led to a high overall discharge voltage and rapid expenditure of energy, hence a shorter discharge.

Fig. 3. Typical Spark Waveform Data

After storage, the waveforms were modified using MATHCAD. Modification entailed: Extracting the Y-axis (voltage) information, normalising these data with respect to a fixed maximum voltage, filtering of data points from 400 to 45, and adding

appropriate “desired output” data for each input data set. The modified data files were split into two groups: (a) Training data files (Training Sets) and (b) Recall data files.

3 Neural Network Fault Detection in RN7YC Samples

Training. The neural network was trained using the described training file and network parameters (Training Rates, Momentum, etc.) as per Table 2; the parameters were sourced by experimentation.

Recall. MATHCAD was used to pre-process and store the recall data in the same way as for the training data – except that no “desired output” data were added. The neural network was tested using individual recall data files.

Table 2. Neural Network Parameters

| Parameter | Value | Parameter | Value |
|-------------------------|-------|------------------------|-------|
| Input Nodes | 45 | Learning Rate (Hidden) | 0.80 |
| Hidden Nodes | 10 | Learning Rate (Output) | 0.20 |
| Output Nodes | 1 | Momentum | 0.80 |
| Training Sets (In File) | 40 | | |

The trained neural network was tested using new, previously unseen recall data. All desired results were either '0' for Fail or '1' for Pass. The “pass-mark” was set at 50%, or 0.5. A summary of the results is given in Table 3. For completeness, Fig. 4 shows full results for the Pass/Fail detection test.

Table 3. Fault Detection – Recall Data Performance Summary

| | |
|----------------------------------|--------------|
| GOOD detected: | 5/5 |
| FAULTY detected: | 20/20 |
| Total Correct Detections: | 25/25 |

Despite this being an early pilot test of the Neural Network as a spark waveform analyser, the results were conclusive, in that all Recall Data examples were correctly identified as good or faulty as applicable. The Neural Network was well suited to this application in a "Pass/Fail" test system. The next progression for the system was to distinguish between individual types of fault.

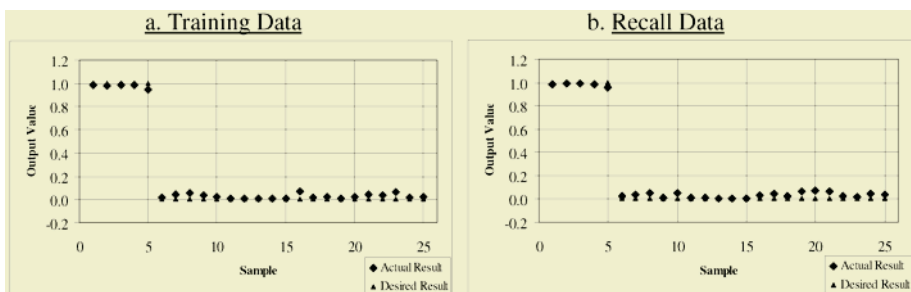


Fig. 4. Fault Detection Test Results

4 Neural Network Fault Diagnosis in RN7YC Samples

Training. Training data and recall data were prepared as described in Section 3, except that in this case, a new training file was produced with equal numbers of each class of spark plug. The neural network was trained, using identical parameters to those used for the “detection” test of Section 3, except for the number of output nodes being raised to 5 (one for each class of data) and the number of training sets being reduced to 25 (5 exemplars for each class of data). The resulting training file was smaller than the original “detection” test counterpart, so a change of training accuracy was expected.

Recall. The neural network was tested using individual recall data files.

All desired results were either '0' for FAIL or '1' for PASS. The “pass-mark” was set at 50%, or 0.5. A summary of the results is given in Table 4. For completeness, Fig. 5 shows full results for this diagnosis test; (Note: in Fig. 5, “y” and “d” represent “actual” and “desired” outputs, respectively).

Table 4. Fault Diagnosis – Recall Data Detection & Diagnosis Performance

| Detection | | Diagnosis | |
|----------------------------------|--------------|------------------------------------|--------------|
| GOOD detected: | 5/5 | GOOD Correctly Diagnosed: | 5/5 |
| FAULTY detected: | 20/20 | FAULT1 Correctly Diagnosed: | 3/5 |
| | | FAULT2 Correctly Diagnosed: | 5/5 |
| | | FAULT3 Correctly Diagnosed: | 4/5 |
| | | FAULT4 Correctly Diagnosed: | 5/5 |
| Total Correct Detections: | 25/25 | Total Correct Diagnoses: | 22/25 |

The results indicated that the difference between Good and Faulty examples was still discernable, despite the reduced number of training sets. Three misdiagnoses were made; confusion arose between Fault 1 and Fault 3 - faults producing very similar waveforms. The waveforms were similar because the faults produce effectively very similar electrical equivalent circuits. The fact that only three misdiagnoses were made suggests that even the subtle differences between Fault 1 and Fault 3 waveforms are not beyond the wit of the neural network classifier.

Further optimisation of the neural network settings and data capture method would be expected to yield improved discrimination between categories (i.e.: increasing training sets, by having more manufactured test spark plugs available, for example).

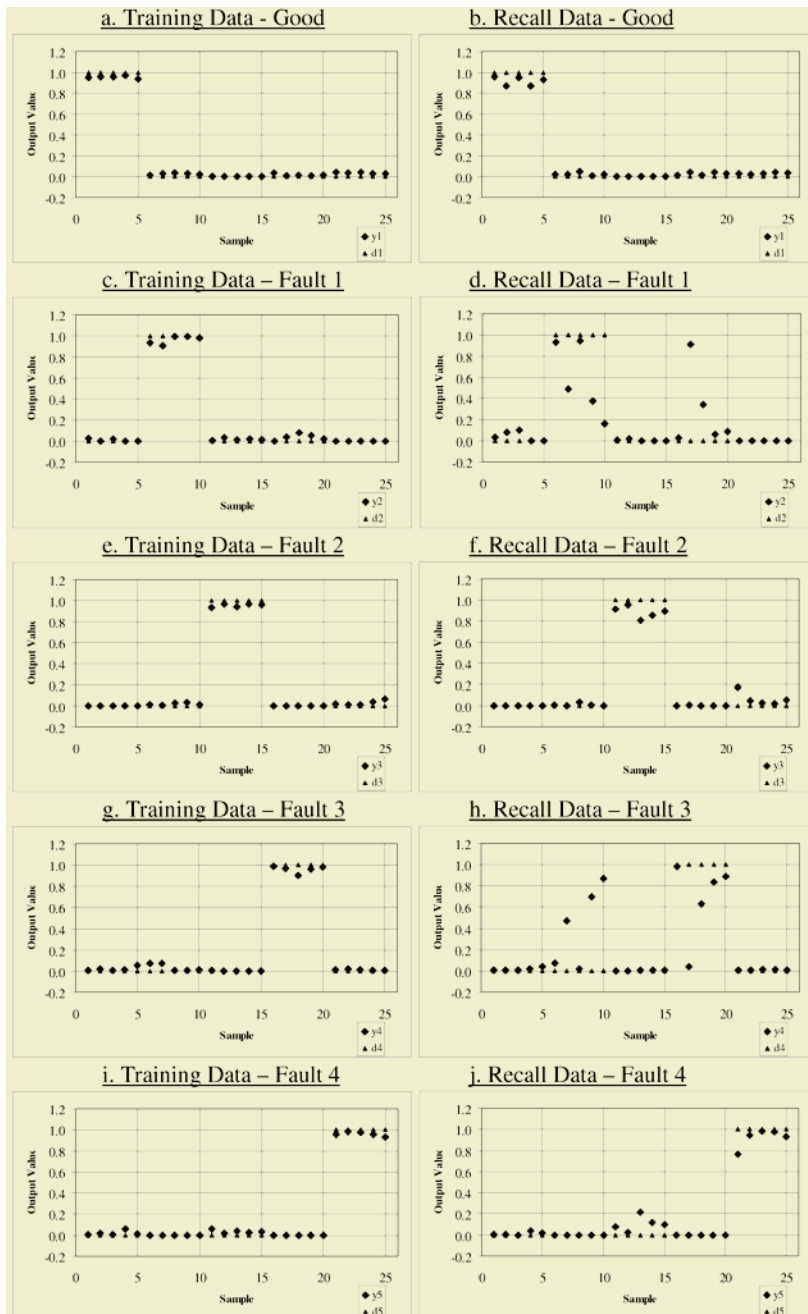
5 Conclusions

A novel method of testing spark plugs has been demonstrated in this paper.

High voltage ignition sparks were used to provide a suitable spark plug test waveform; the detection and diagnosis of faults was performed by a neural network.

Feasibility studies were undertaken, using real spark waveform data, which led to the MLP type of neural network being adopted for further spark plug testing studies.

In both tests a 100% success rate was achieved in PASS/FAIL fault detection; A slightly lower success rate was recorded for detailed fault diagnosis (88%), but suggestions were proffered for yielding improvements.

**Fig. 5.** Fault Diagnosis Test Results

The complexity of the described procedure was such that testing was slow and cumbersome; the principles of operation were, however, successfully proved.

Further work has increased the speed, reliability and applicability of the testing process, whilst shedding light on the electrical and physical science underpinning it.

Acknowledgement

The Author is grateful to Champion Spark Plug U.K. for their financial and technical support which was offered during this investigation into spark plug testing.

References

1. Walters, S. D.: Characterization and Analysis of Kettering-type Automotive Ignition Systems and Electrical Spark Profiles, Ph.D Thesis, University of Brighton, in Association with Champion Spark Plug (Europe), (1998).
2. Champion: Private Communication, Champion Spark Plug, (U.K.), (1994).
3. SAE ARP159A Standard: Dielectric Testing of Spark Plugs, SAE, (1994).
4. Walters, S. D., Howson, P. A., Howlett, R. J., Ryder, D. M., Miller, R.: Inverse Analysis of Electrical Discharge Phenomena by Neural Network, 30th UPEC, Procs., Vol. 2, pp. 850-853, University of Greenwich, (1995).
5. Champion: Straight Talk about Spark Plugs, Champion Spark Plug, (1987).
6. NGK: Engineering Manual for Spark Plugs, NGK Spark Plug Co. Ltd., OP-0076-9105, (1991).
7. Bosch: Spark Plugs, Robert Bosch GmbH., Delta Press, (1985 and 1999).
8. Haykin, S.: Neural Networks, Macmillan College Pub. Co. Inc., (1999).
9. Thompson, S., Fueten, F., Bockus D.: Mineral Identification using Artificial Neural Networks and the Rotating Polarizer Stage, Computers and Geosciences, Vol. 27, pp 1081-1089, (2001).
10. Howlett, R. J., De Zoysa, M. M., Walters S. D.: Monitoring IC Engines using Neural Networks, Paper: SAE-NA 2003-01-09, Procs., 6th International Conference on Engines for Automobiles, Capri, (2003).
11. Lippman, R. P.: An Introduction to Computing with Neural Networks, IEEE ASSP Magazine, Vol. 4, pp. 4-22, (1987).
12. Hush, D. R., and Horne, B. G.: Progress in Supervised Neural Networks, IEEE Signal Processing Magazine, pp. 8-39, (1993).
13. "Spark Plug Defects and Tests", National Advisory Committee for Aeronautics, Report No. 51, Washington Govt. Printing Office, (1920).

Variable Neighborhood Search with Permutation Distance for QAP^{*}

Chong Zhang^{1,2}, Zhangang Lin^{1,2}, and Zuoquan Lin^{1,2}

¹ School of Mathematical Sciences

² Key Laboratory of Pure and Applied Mathematics

Peking University, Beijing 100871, China

{zc,linzg,lz}@is.pku.edu.cn

Abstract. QAP is a famous \mathcal{NP} -Hard[1] combinatorial optimization problem. Many theoretical and real-life problems could be modeled as it. VNS is a recent metaheuristic and shows good performance in dealing with QAP[2]. In this paper, a new concept distance called *permutation distance* is proposed and exploited in detail. With permutation distance ready, we combine the hamming distance with it and propose a group of new neighborhood structures in QAP for VNS. Numerical tests running on the standard benchmark library QAPLIB[3] show that this approach would dramatically improve the performance of VNS for QAP. It surpasses some famous metaheuristics and belongs to the most efficient metaheuristics for QAP.

1 Introduction

Quadratic Assignment Problem(QAP) is a well-known \mathcal{NP} -Hard[1] combinatorial optimization problem. A large variety of applications could be modeled as it, which include CAD, hospital layout, image processing, typewriter keyboard design, and campus planning. Detailed information about its application could be found in [4].

Let's take a real-life example of QAP. There are n computer components which should be placed into n positions on a computer backboard. The so-called optimal wiring is to minimize the total length of interconnecting wiring and could be modeled as QAP. In general, QAP could be formalized as follows. Let \mathcal{P}_n be the set of permutations of $\{1, 2, \dots, n\}$. Consider two $n \times n$ matrix $A = (a_{ij}), B = (b_{ij})$. QAP is to look for a permutation $p \in \mathcal{P}_n$ that minimizes the function

$$f(A, B, p) = \sum_{i=1}^n \sum_{j=1}^n a_{ij} \times b_{p(i)p(j)} \quad (1)$$

To this day, solving QAP with size $n > 30$ optimally is not a trivial task. Metaheuristics, therefore, are widely adopted to deal with it. These methods

* Partially supported by a NKBRPC (2004CB318000) and NSFC (60373002, 60496322).

include tabu search[5, 6], ant colony[7–9], genetic algorithm[10], GRASP[11], simulated annealing[12], guided local search[13] and VNS[2].

Variable Neighborhood Search is a recent metaheuristic[14–16] and has shown success in dealing with many problems such as p-median problem[17], p-center problem[18], graph coloring[19], and vehicle routing problem[20, 21].

VNS needs a group of neighborhood structures $\mathcal{N}_k(k = 1, \dots, max)$ in the solution space \mathcal{S} and a sub search strategy. During the searching process, VNS gradually selects the starting points from \mathcal{N}_1 to \mathcal{N}_{max} of the current local minimum and searches using the sub search strategy. Each time when a better local minimum is encountered, the current will be replaced by the new one. This process will not stop until a stopping condition is met. When VNS is applied to QAP[2], the hamming distance is used to determine the neighborhood structures; the steepest descend method is employed as the searching strategy. Let $p^* \in \mathcal{P}_n$, the neighborhood structures \mathcal{N}_d induced by hamming distance could be defined as:

$$\mathcal{N}_d(p^*) = \{p | Ham(p^*, p) = d, p \in \mathcal{P}_n\} \quad d \in [2, 3, \dots, n] \quad (2)$$

where Ham stands for the hamming distance function. Although this form of VNS for QAP is simple and straightforward, it produces interesting experimental results[2]. Inspired by it, a more sophisticated form of VNS for QAP is developed with the help of some new concepts and improvements to this basic one.

This paper is structured as follows. Section 2 introduces a new concept distance named *permutation distance*. Section 3 combines the above two distances together and proposes a group of new neighborhood structures in QAP. Meanwhile, robust tabu search is used to replace the steepest descend method. With these things ready, an advanced VNS for QAP is introduced. Section 4 runs numerical experiments on QAPLIB[3] under different conditions and reports its performance. Section 5 completes the paper with some conclusions.

2 Permutation Distance

Pairwise exchange operation is the most basic operation used by many metaheuristics for QAP. This drives us to define a new distance concept according to it. Let's take a simple example first. $p = \{1, 2, 3, 4, 5\}$ and $p' = \{3, 2, 1, 5, 4\}$ are two points in \mathcal{P}_5 and their hamming distance is 4. But we could see that at least 2 pairwise exchange operations are needed from p to p' .

$$\{1, 2, 3, 4, 5\} \xrightarrow{\rho_{13}} \{3, 2, 1, 4, 5\} \xrightarrow{\rho_{45}} \{3, 2, 1, 5, 4\}$$

Therefore, we could say some distance between p and p' is 2.

We call $L_n = \{l | l \subseteq \{1, 2, \dots, n\}\}$ as the location set, and $E_n = \{e | e \subseteq \{1, 2, \dots, n\}\}$ as the element set. Considering any $p \in \mathcal{P}_n$, $l \in L_n$, we define $\pi(p, l) : \mathcal{P}_n \times L_n \rightarrow E_n$ as:

$$\pi(p, l) = e, \quad e = \{p(i) | i \in l\} \quad (3)$$

Definition 1. Let $p, p' \in \mathcal{P}_n$, $l \in L_n$. If $\pi(p, l) = \pi(p', l)$, l is a **covering set** of p and p' .

Definition 2. Let l be a covering set of p and p' . If $\forall l' \subset l$ exists $\pi(p, l') \neq \pi(p', l')$, l is a **minimum covering set** of p and p' .

Minimum covering set has two very interesting features¹.

Lemma 3. Given $p, p' \in \mathcal{P}_n$, m is a minimum covering set of p, p' ; $i \neq j \in m$. If $\hat{p} = p' \oplus \rho_{ij}$ ², m will split into two minimum covering sets m_1, m_2 of p, \hat{p} . This means $m = m_1 \cup m_2$, $m_1 \cap m_2 = \emptyset$.

Lemma 4. Given $p, p' \in \mathcal{P}_n$, m_1, m_2 are two minimum covering sets of p, p' ; $i \in m_1, j \in m_2$. If $\hat{p} = p' \oplus \rho_{ij}$, m_1, m_2 will combine into one minimum covering set m of p, \hat{p} . This means $m = m_1 \cup m_2$.

With these features ready, we could introduce the *permutation distance* and its properties.

Definition 5. Given $p, p' \in \mathcal{P}_n$, the **permutation distance** between them is defined as $n - m$, where m is the number of minimum covering sets of p, p' . This is denoted as $Pd(p, p') = n - m$

We can prove that this definition satisfies the three properties of generic distance. It's also consistent with the above example. Given $p, p' \in \mathcal{P}_n$ and $Pd(p, p') = d$ ($0 \leq d \leq n - 1$), $\hat{p} = p' \oplus \rho_{ij}$ ($i \neq j \in [1, 2, \dots, n]$). According to Lemma 3 and Lemma 4, we can conclude that $Pd(p, \hat{p}) = d - 1$ when i, j are in the same minimum covering set of p, p' or $Pd(p, \hat{p}) = d + 1$ when i, j are in different ones. We denote

$$\hat{p}_k = \begin{cases} p' \oplus \rho_{i_1 j_1} \oplus \rho_{i_2 j_2} \oplus \dots \oplus \rho_{i_k j_k} & 1 \leq k \leq d \\ p' & k = 0 \end{cases} \quad (4)$$

If $[i_k, j_k]$ ($1 \leq k \leq d$) is in different minimum covering sets of \hat{p}_{k-1} , a sequence of pairwise exchange operations $\{\rho_{i_1 j_1}, \rho_{i_2 j_2}, \dots, \rho_{i_k j_k}\}$ ($1 \leq k \leq d$) will decrease the minimum covering sets between p and p' by k and make $Pd(p, \hat{p}_d) = 0$ or $p = \hat{p}_d$ after d steps. Therefore, the permutation distance between $p, p' \in \mathcal{P}$ means the lower bound of pairwise exchanges needed when transforming one to another.

The hamming distance has an advantage that there exists an $\mathcal{O}(n)$ algorithm for computing the distance between any $p, p' \in \mathcal{P}_n$. Although permutation distance seems more complex than hamming distance, we find an $\mathcal{O}(n)$ algorithm for any $p, p' \in \mathcal{P}$. It will be described in detailed in an upcoming paper.

¹ For the limitation of space, the proofs of the two lemmas are omitted

² $p' \oplus \rho_{ij}$ means to exchange the i th and j th elements in p'

3 New Neighborhood Structures in QAP for VNS

Following what is done in (2), we could induce a group of neighborhood structures based on permutation distance. Let $p^* \in \mathcal{P}_n$, they could be defined as:

$$\mathcal{N}_d(p^*) = \{p | Pd(p^*, p) = d, p \in \mathcal{P}_n\} \quad d \in [1, 2, \dots, n-1] \quad (5)$$

We could immediately substitute these for the traditionally used neighborhood structures induced by hamming distance. But the numerical experiments show that each method has its own strong point and no one could surpass another on the whole. For example, neighborhood structures induced by permutation distance are better on instances like chr25a and tai40b than those induced by hamming distance, but worse on els19 and rou20.

To get the advantages of the two distance concepts, we propose a group of new neighborhood structures with the help of them. We introduce a notation $\{\alpha, \beta\}$, where α represents the hamming distance between $p, p' \in \mathcal{P}_n$ and β , the permutation distance. $\{\alpha_1, \beta_1\} > \{\alpha_2, \beta_2\}$ means $\alpha_1 > \alpha_2$ or $\alpha_1 = \alpha_2, \beta_1 > \beta_2$. The new neighborhood structures are defined as:

$$\mathcal{N}_{\{\alpha, \beta\}}(p^*) = \{p | Ham(p^*, p) = \alpha, Pd(p^*, p) = \beta, p \in \mathcal{P}_n\} \quad (6)$$

where $\alpha \in [2, n]$, $\beta \in [\alpha - \lfloor \alpha/2 \rfloor, \alpha - 1]$. It could be seen that the number of neighborhood structures will increase from $\mathcal{O}(n)$ to $\mathcal{O}(n^2)$ according to this definition. These structures provide the sub search strategy with a power to search the solution space more systematically and thoroughly. Although it seems to consume more time, the following numerical tests will show us that the overall performance is clearly promoted.

Besides the new neighborhood structures, we select the *robust tabu search*[6] as our sub search strategy. Till now, it's considered as one of the most effective methods dealing with QAP. The reason why we combine tabu search and VNS together could be stated as follows. For tabu search, designing the so-called "intensification" and "diversification" strategy is a key factor influencing its efficiency and effectiveness. However, there is lack of good general approaches for designing this strategy. VNS, by introducing some well-defined topological structures into the solution space, creates a systematic way to do intensification/diversification. This property can surely help their hybrid become more robust and effective. The following test results testify this thought.

Listing 1.1 describes the pseudo code of this advanced VNS(AVNS). It could be considered as a hybrid of VNS and tabu search. It uses the VNS as the main framework and tabu search as its sub search strategy. Works introduced in [22] provides another form of hybridization. It is an extended concentric tabu for QAP whose basic form could be regarded as taking tabu search as its main frame and a VNS-like strategy to construct its tabu rules.

4 Result of Numerical Experiments

In this section, some numerical experiments are designed to test the performance of AVNS. The QAP instances are selected from the QAPLIB[3]. All the test

```

1   $p = \text{RandomlyGet}(\mathcal{P})$ ;
2  while (!StopingCondition)
3  {
4      for ( $i = 2$ ;  $i \leq n$ ;  $i++$ )
5          for ( $j = i - \lfloor i/2 \rfloor$ ;  $j < i$ ;  $j++$ )
6          {
7               $p' = \text{RandomlyGet}(\mathcal{N}_{\{i,j\}}(p))$ ;
8               $\hat{p} = \text{RoTS}(p')$ ;
9              if ( $f(\hat{p}) < f(p)$ ) )
10                  $p = \hat{p}$  ,  $i = 2$  ,  $j = i - \lfloor i/2 \rfloor$  ;
11             }
12     }

```

Listing 1.1. Basic Scheme of Advanced VNS

programs are coded in ANSI C and complied with gcc-3.2 on Red Hat Linux 9.0. Optimization level “-O3” is used. The hardware platform is a single 2.4GHz Pentium4 machine with 512M Memory.

In the numerical experiments, each algorithm is always run on certain instance for 20 times. We denote $Q_x = (q_x - BKV) * 100/BKV[\%]$, where BKV is the best known value of this instance and q_x is the x percentile of the 20 results. The sub search function returns if no improvement is made in the last $4 * n$ steps, where n is the size of the current QAP instance.

We first compare the performance of AVNS with its two variations:

- HVNS: the same as AVNS in Listing 1.1 with neighborhood structures induced by hamming distance and substitute $\mathcal{N}_{\{i\}}(p)$ for $\mathcal{N}_{\{i,j\}}(p)$
- PVNS: the same as AVNS in Listing 1.1 with neighborhood structures induced by permutation distance and substitute $\mathcal{N}_{\{j\}}(p)$ for $\mathcal{N}_{\{i,j\}}(p)$

The test results are shown in Table 1. The Q_{10} and Q_{50} are used to measure the solution quality. The q_{90}/q_{10} is used to measure the stability of the current method. From Table 1 we could see that AVNS surpasses two other methods greatly.

The second experiment compares the performance of AVNS and the robust tabu search. This is meaningful for two reasons. First, robust tabu search is one of the most powerful metaheuristics for QAP. Secondly, we could see from the result whether the improvement in performance shown in Table 1 is merely gained by the power of robust tabu search.

For each instance, AVNS runs first and its consuming time is recorded. The following robust tabu search will be given the same amount of time. Test results are reported in Table 2 and Fig. 1 to Fig. 4. These figures illustrate the results of the two methods over 20 times running on certain instance.

From the result, we could see the performance of AVNS surpasses the robust tabu search dramatically, both in terms of solution quality and stability. We can conclude that the increase in performance isn’t merely brought by robust tabu search. It’s the result of all improvements made above.

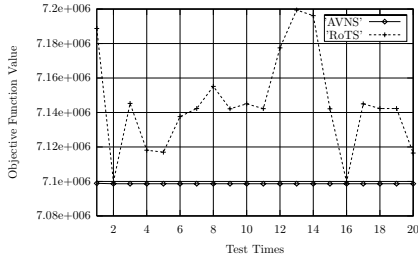
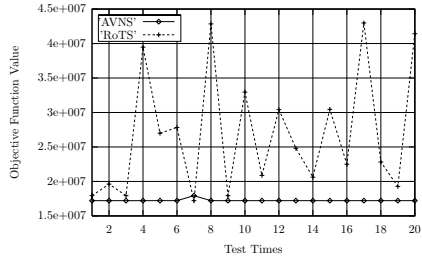
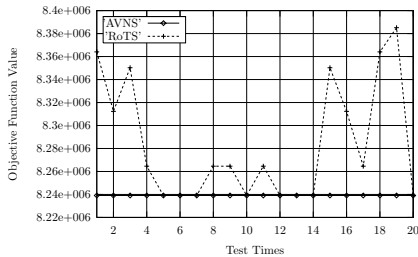
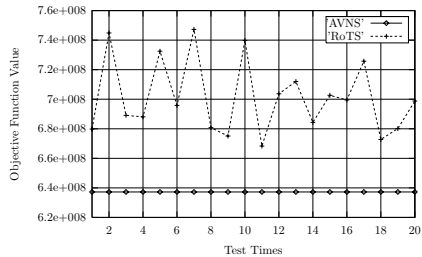
Table 1. Comparison of Three Methods

| Instance | | | AVNS | | | HVNS | | | PVNS | | |
|----------|------|-----------|----------|----------|-----------------|----------|----------|-----------------|----------|----------|-----------------|
| Name | Size | BKV | Q_{50} | Q_{10} | q_{90}/q_{10} | Q_{50} | Q_{10} | q_{90}/q_{10} | Q_{50} | Q_{10} | q_{90}/q_{10} |
| bur26h | 26 | 7098658 | 0 | 0 | 1 | 0 | 0 | 1.0001 | 0.003 | 0 | 1.0002 |
| chr22a | 22 | 6156 | 0 | 0 | 1.0185 | 1.706 | 0 | 1.0291 | 1.933 | 0 | 1.0415 |
| chr25a | 25 | 3796 | 2.055 | 0 | 1.0669 | 10.327 | 0.184 | 1.1619 | 5.638 | 0.184 | 1.1679 |
| els19 | 19 | 17212548 | 0 | 0 | 1.0379 | 0 | 0 | 1.0453 | 4.209 | 0 | 1.1769 |
| esc16b | 16 | 292 | 0 | 0 | 1 | 0 | 0 | 1 | 0 | 0 | 1 |
| had20 | 20 | 6922 | 0 | 0 | 1 | 0 | 0 | 1 | 0 | 0 | 1 |
| kra30a | 30 | 88900 | 0 | 0 | 1.0120 | 1.338 | 0 | 1.0156 | 1.119 | 0 | 1.0160 |
| lipa40a | 40 | 31538 | 0 | 0 | 1 | 0 | 0 | 1.0096 | 0 | 0 | 1.0093 |
| nug30 | 30 | 6124 | 0 | 0 | 1 | 0.065 | 0 | 1.0036 | 0.065 | 0 | 1.0015 |
| rou20 | 20 | 725522 | 0 | 0 | 1.0001 | 0.008 | 0 | 1.0031 | 0.080 | 0 | 1.0025 |
| scr20 | 20 | 110030 | 0 | 0 | 1 | 0 | 0 | 1 | 0 | 0 | 1.0059 |
| ste36c | 36 | 8239110 | 0 | 0 | 1 | 0 | 0 | 1.0135 | 0.011 | 0 | 1.0045 |
| tai20b | 20 | 122455319 | 0 | 0 | 1 | 0 | 0 | 1.0904 | 0.453 | 0 | 1.0999 |
| tai40b | 40 | 637250948 | 0 | 0 | 1 | 1.005 | 0 | 1.0464 | 0 | 0 | 1.0259 |
| tho30 | 30 | 149936 | 0 | 0 | 1 | 0 | 0 | 1.0029 | 0 | 0 | 1.0023 |

Table 2. Comparison of the AVNS and Robust Tabu Search(RoTS)

| Instance | | | AVNS | | | RoTS | | |
|----------|------|-----------|----------|----------|-----------------|----------|----------|-----------------|
| Name | Size | BKV | Q_{50} | Q_{10} | q_{90}/q_{10} | Q_{50} | Q_{10} | q_{90}/q_{10} |
| bur26h | 26 | 7098658 | 0 | 0 | 1 | 0.615 | 0.039 | 1.0132 |
| chr22a | 22 | 6156 | 0 | 0 | 1.0123 | 1.251 | 0.032 | 1.0491 |
| chr25a | 25 | 3796 | 3.451 | 0 | 1.0877 | 5.216 | 2.055 | 1.0869 |
| els19 | 19 | 17212548 | 0 | 0 | 1 | 38.353 | 4.209 | 2.3809 |
| esc16b | 16 | 292 | 0 | 0 | 1 | 2.055 | 0.685 | 1.0340 |
| had20 | 20 | 6922 | 0 | 0 | 1 | 0.376 | 0 | 1.0038 |
| kra30a | 30 | 88900 | 0 | 0 | 1 | 0 | 0 | 1.0142 |
| lipa40a | 20 | 31538 | 0 | 0 | 1 | 0 | 0 | 1 |
| nug30 | 30 | 6124 | 0 | 0 | 1.0006 | 0 | 0 | 1.0006 |
| rou20 | 20 | 725522 | 0 | 0 | 1.0001 | 0 | 0 | 1 |
| scr20 | 20 | 110030 | 0 | 0 | 1 | 0 | 0 | 1.0085 |
| ste36c | 36 | 8239110 | 0 | 0 | 1 | 0.309 | 0 | 1.0152 |
| tai20b | 20 | 122455319 | 0 | 0 | 1.0041 | 9.986 | 0.045 | 1.3667 |
| tai40b | 40 | 637250948 | 0 | 0 | 1 | 9.422 | 5.613 | 1.1060 |
| tho30 | 30 | 149936 | 0 | 0 | 1 | 0 | 0 | 1 |

We also compare the solution quality of AVNS with some other algorithms based on their solution quality report. These algorithms are tested with the comparable conditions which guarantee the platform difference could be omitted. The result is optimistic: AVNS is better than ant colony algorithms in [7, 8], GRASP in [11] and guided local search in [13]; and is in the same level with ant colony algorithm in [9] and genetic algorithm in [10]. Considering our work

**Fig. 1.** bur26h**Fig. 2.** els19**Fig. 3.** ste36c**Fig. 4.** tai40b

improving the performance by introducing some topological structures in the solution space of QAP, rather than adjusting the algorithm itself, our work could supplement with above well-performed approaches and produce more powerful methods for QAP.

5 Conclusion

In this paper, we propose a new concept distance called permutation distance in the solution space of QAP. With hamming and permutation distance, well-defined topological structures are introduced into VNS and help to enhance the robustness and effectiveness of low level tabu search. Numerical tests show this will lead to great improvement in performance and make the resulting method one of the most effective and efficient metaheuristics for QAP.

References

1. Sahni, S., Gonzalez, T.: P-complete approximation problems. *Journal of the ACM* **23** (1976) 555–565
2. Taillard, E., Gambardella, L.M.: Adaptive memories for the quadratic assignment problems. Technical Report IDSIA-87-97, Dalle Molle Institute for Artificial Intelligence (1997)
3. Burkard, R.E., Karisch, S., Rendl, F.: Qaplib - a quadratic assignment problem library. *European Journal of Operational Research* **55** (1991) 115–119

4. Cela, E.: The Quadratic Assignment Problem. Volume 1 of Combinatorial Optimization. Kluwer Academic Publishers (1998)
5. Misevicius, A.: A tabu search algorithm for the quadratic assignment problem. *COMPUTATIONAL OPTIMIZATION AND APPLICATIONS* **30** (2005) 95–111
6. Taillard, E.: Robust taboo search for the quadratic assignment problem. *Parallel Computing* **17** (1991) 443–455
7. Gambardella, L., Taillard, E., Dorigo, M.: Ant colonies for the quadratic assignment problem. *Journal of the Operational Research Society* **50** (1999) 167–176
8. Talbi, E., Roux, O., Fonlupt, C., Robillard, D.: Parallel ant colonies for the quadratic assignment problem. *Future Generation Computer Systems* **17** (2001) 441–449
9. Maniezzo, V., Colorni, A., Dorigo, M.: The ant system applied to the quadratic assignment. *IEEE TRANSACTIONS ON KNOWLEDGE AND DATA ENGINEERING* **11** (1999) 769–778
10. Misevicius, A.: An improved hybrid genetic algorithm: new results for the quadratic assignment problem. *KNOWLEDGE-BASED SYSTEMS* **17** (2004) 65–73
11. OLIVEIRA, C.A., PARDALOS, P.M., RESENDE, M.: Grasp with path-relinking for the quadratic assignment problem. *EXPERIMENTAL AND EFFICIENT ALGORITHMS LECTURE NOTES IN COMPUTER SCIENCE* **3059** (2004) 356–368
12. Misevicius, A.: A modified simulated annealing algorithm for the quadratic assignment problem. *INFORMATICA* **14** (2003) 497–514
13. Mills, P., Tsang, E., Ford, J.: Applying an extended guided local search to the quadratic assignment problem. *ANNALS OF OPERATIONS RESEARCH* **118** (2003) 121–135
14. Hansen, P., Mladenović, N.: Variable neighborhood search: Principles and applications. *European Journal of Operational Research* **130** (2001) 449–467
15. Hansen, P., Mladenović, N.: Variable neighborhood search. *Computers and Operations Research* **24** (1997) 1097–1100
16. Hansen, P., Mladenović, N. Handbook of Metaheuristics. In: *Variable Neighborhood Search*. Kluwer Academic Publishers (2003) 621–757
17. García-López, F., Melián-Batista, B., Moreno-Pérez, J.A., Moreno-Vega, J.M.: The parallel variable neighborhood search for the p-median problem. *Journal of Heuristics* **8** (2002) 375–388
18. Mladenovic, N., Labb  , M., Hansen, P.: Solving the p-center problem with tabu search and variable neighborhood search. *NETWORKS* **42** (2003) 48–64
19. Avanthay, C., Hertz, A., Zufferey, N.: A variable neighborhood search for graph coloring. *EUROPEAN JOURNAL OF OPERATIONAL RESEARCH* **151** (2003) 379–388
20. Br  sy, O.: A reactive variable neighborhood search for the vehicle-routing problem with time windows. *INFORMS JOURNAL ON COMPUTING* **15** (2003) 347–368
21. Bouthillier, A.L., Crainic, T.G.: A cooperative parallel meta-heuristic for the vehicle routing problem with time windows. *COMPUTERS AND OPERATIONS RESEARCH* **32** (2005) 1685–1708
22. Drezner, Z.: The extended concentric tabu for the quadratic assignment problem. *EUROPEAN JOURNAL OF OPERATIONAL RESEARCH* **160** (2005) 416–422

Using Rough Set to Induce Comparative Knowledge and Its Use in SARS Data

Honghai Feng^{1,2}, Cheng Yin³, Mingyi Liao⁴, Bingru Yang², and Yumei Chen⁵

¹ Urban & Rural Construction School, Hebei Agricultural University,
071001 Baoding, China

fenghonghai@sina.com

² Information Engineering School, University of Science and Technology Beijing,
100083 Beijing, China

³ Modern Educational Center, Hebei Agricultural University,
071001 Baoding, China

⁴ Department of Economic & Information, Dongbei University of Finance & Economics,
116023 Dalian, China

⁵ Tian'e Chemical Fiber Company of Hebei Baoding,
071000 Baoding, China

Abstract. Comparative knowledge is the main and important knowledge in our knowledge-box with which we differentiate things or get the difference between things. Using rough set we can induce not only the classification rules but also the comparative knowledge. For example, in comparison with men who do not smoke, the women who too do not smoke are more susceptible to suffer from lung cancer. From our SARS data set, using rough set theory we have induced the comparative knowledge such as: when the attribute hemoglobin's values of the patients are the same, and if the patients' states of illness are 3 (3 means that the state of illness is critical), then the attribute lymph's values are mostly smaller than the ones of the patients whose states of illness are 2(2 means that the state of illness is serious) and so on.

1 Introduction

Usually we use rough set to induce the classification rule that is a kind of causality knowledge [1], while in the real world information table, there are various kinds of knowledge such as comparative knowledge. The classification knowledge is the sameness or similitude knowledge with which we classify things. The classification knowledge is generated based on the sameness or similitude of the things and the comparative knowledge is induced based on the difference between things. Comparative knowledge is the main and important knowledge in our knowledge-box with which we get the difference of the things. For example, in comparison with men who do not smoke, the women who too do not smoke too are more susceptible to suffer from lung cancer. With the conventional rough set methods we cannot get this kind of knowledge. In this paper, we propose a rough set based algorithm for generating comparative knowledge, namely enlightened by the discernibility matrix, we introduce an indiscernibility matrix to measure the similitude between any two examples, and then induce the comparative

knowledge hidden in the information system. Generating comparative knowledge is the advantage of the rough set theory. Other machine learning theories such as SVM [2], ANN [3] and Bayesian networks cannot be used in this case.

2 Basic Concepts of Rough Set Theory

Rough set theory is a mathematical tool to deal with incomplete or imprecise information. It has been used in machine learning, knowledge discovery, decision support systems and pattern recognition. The methodology of rough sets addresses the problem of discovery of functional dependencies in empirical data.

A rough set method can produce a set of reduced decision rules from a decision table by attribute reduction and value reduction.

2.1 Decision Table

Data are often presented as a table, columns of which are labeled by attributes, rows by objects of interest and entries of the table are attribute values. Such tables are known as information systems, decision tables, or information tables.

A decision table is composed of a 4-tuple $DT = \langle U, A, V, f \rangle$, where $U = \{x_1, x_2, \dots, x_n\}$, is a nonempty, finite set called the universe; A is a nonempty, finite set of attributes; $A = C \cup D$, in which C is a finite set of condition attributes and D is a finite set of decision attributes; $V = \bigcup_{a \in A} V_a$, where V_a is a domain (value) of the attribute a , and $f : U \times A \rightarrow V$ is called the information function such that $f(x, a) \in V_a$ for every $a \in A, x_i \in U$.

2.2 Indiscernibility Relation

In a decision table $DT = \langle U, A, V, f \rangle$, to every subset of attributes $B \subseteq A$, a binary relation, denoted by $IND(B)$, called the B -indiscernibility relation, is associated and defined as follows:

$$IND(B) = \{(x_i, x_j) \in U \times U : a \in B, f(x_i, a) = f(x_j, a)\} \quad (1)$$

2.3 Reduction

In a decision table $DT = \langle U, A, V, f \rangle$, the reduction of condition attribute C means a nonempty subset $R \subset C$ satisfied by the following condition:

- 1) $IND(R) = IND(C)$
- 2) There is no subset of $R' \subset R$, which is satisfied by $IND(R') = IND(C)$

The reduced set of attributes provides the same ability of classification as the original set of attributes

2.4 Discernibility Matrix

Discernibility matrix of DT , denoted $M_{DT}(m_{ij})$ a $n \times n$ matrix is defined as

$$m_{ij} = \left\{ \begin{array}{l} \left\{ a \in C : f(x_i) \neq f(x_j, a) \wedge \left(d \in D, f(x_j, d) \neq f(x_i, d) \right) \right\} \\ 0, d \in D, f(x_i, d) = f(x_j, d) \\ \phi, f(x_i, a) = f(x_j, d) \wedge \left(d \in D, f(x_i, d) \neq f(x_j, d) \right) \end{array} \right\} \quad (2)$$

Where $i, j = 1, 2, \dots, n$.

Thus entry m_{ij} is the set of all attributes that classify objects x_i and x_j into different decision classes in U . From formula (2), all of the distinguishing information for attributes is contained in above discernibility matrix.

3 Algorithm

(1) Based on the indiscernibility of examples to construct the indiscernibility matrix following the methods of discernibility matrix.

$$m_{ij} = \left\{ \begin{array}{l} \{a \in C : f(x_i, a) = f(x_j, a)\} \\ \phi, f(x_i, a) \neq f(x_j, a) \end{array} \right\}$$

(2) Eliminate the constituents in the matrix whose amount of the attributes is 1 and $n - 1$ (n denotes the total amount of the attributes including condition and decision attributes).

(3) For the constituents whose amount of the attributes is not 1 and $n - 1$, generate the comparative rules.

4 Illustrative Examples

Given an information system in Table 1, where U is the universe, a, b, c, d and e are the attributes, here we do not divide the attributes into condition attributes and decision ones. Table 2 is the indiscernibility matrix generated from Table 1.

Table 1. An information table

| U | a | b | c | d | e |
|-----|-----|-----|-----|-----|-----|
| 1 | 1 | 0 | 0 | 1 | 1 |
| 2 | 1 | 0 | 0 | 0 | 1 |
| 3 | 0 | 0 | 0 | 0 | 0 |
| 4 | 1 | 1 | 0 | 1 | 0 |
| 5 | 1 | 1 | 0 | 2 | 2 |
| 6 | 2 | 1 | 0 | 2 | 2 |
| 7 | 2 | 2 | 2 | 2 | 2 |

Table 2. The indiscernibility matrix of Table 1

| | 1 | 2 | 3 | 4 | 5 | 6 | 7 |
|---|--------|-------|------|-------|-------|---|---|
| 1 | | | | | | | |
| 2 | $abce$ | | | | | | |
| 3 | bc | bcd | | | | | |
| 4 | acd | ac | ce | | | | |
| 5 | ac | ac | c | abe | | | |
| 6 | c | c | c | bc | cde | | |
| 7 | | | | de | ade | | |

For $m_{12} = abce$, due to the fact that the amount of attributes is $n - 1$, we cannot induce any comparative knowledge. For $m_{16} = m_{26} = m_{35} = m_{36} = c$, due to the

fact that the amount of attributes is 1, so we cannot induce any comparative knowledge either. For $m_{13} = bc$, we can hold that $b = 0 \wedge c = 0 \wedge (a = 1 \text{ to } a = 0) \rightarrow (d = 1 \text{ to } d = 0)$; or $b = 0 \wedge c = 0 \wedge (a = 1 \text{ to } a = 0) \rightarrow (e = 1 \text{ to } e = 0)$ or $b = 0 \wedge c = 0 \wedge (d = 1 \text{ to } d = 0) \rightarrow (e = 1 \text{ to } e = 0)$; for $m_{23} = bcd$, we can conclude that $b = 0 \wedge c = 0 \wedge d = 0 \wedge (a = 1 \text{ to } a = 0) \rightarrow (e = 1 \text{ to } e = 0)$. The rest may be deduced by analogy.

5 Experiments

5.1 Hand Written Chinese Character Recognition

We have generated the feature vectors of 4 hand written Chinese characters, where the values 1, 2, 3 and 4 of Y denote the 4 different hand written Chinese characters, and after discretization and attribute reduction we got Table 3.

Table 3. The information table after discretization and attribute reduction

| U | X_1 | X_2 | X_3 | Y |
|-----|-------|-------|-------|-----|
| 1 | 17 | 8 | 5 | 1 |
| 2 | 18 | 8 | 5 | 1 |
| 3 | 17 | 9 | 5 | 2 |
| 4 | 17 | 9 | 5 | 2 |
| 5 | 18 | 7 | 6 | 3 |
| 6 | 18 | 8 | 6 | 3 |
| 7 | 15 | 8 | 5 | 4 |
| 8 | 16 | 8 | 5 | 4 |

Some of the comparative knowledge induced from Table 3 is as follows:

$$X_1 = 17 \wedge (Y = 1 \text{ to } Y = 2) \rightarrow (X_2 = 8 \text{ to } X_2 = 9);$$

$$X_1 = 18 \wedge (Y = 1 \text{ to } Y = 3) \rightarrow (X_3 = 5 \text{ to } X_3 = 6).$$

Obviously from the comparative knowledge we can conclude that: When $X_1 = 17$, the difference between the $Y = 1$ and $Y = 2$ is caused by the difference between $X_2 = 8$ and $X_2 = 9$. The rest may be deduced by analogy.

5.2 SARS Data Experiments and Results

We have obtained clinical data from 524 SARS patients from Beijing. Using the indiscernibility matrix based algorithm mentioned above we have induced the following comparative knowledge.

- 1) If the ages of patients are more than 40 and the patients are infected by bacteria, then the highest body temperature of the patients who are not dead is below 39.5°C in comparison with the patients who died of various viscera failure or breath failure.
- 2) If the highest body temperature is the same, and the states of the patients are from 3 to 2 and then to 1, then the mean values of the lymph (%) are from 6.7 to 16.8 and then to 25.2

6 Discussion

The rough set theory can generate easier understudied rules than ANN, SVM etc, but due to the fact that the rules are used to classify the examples, they are generalized and simplified as soon as possible, and so would not be very clear for us to understand any relations among the examples. The comparative knowledge induced by our algorithm may not be so simple and generalized as rough set rules, but the knowledge reflects the local information of the system, and gives us a more concrete and easier understudied comparative information of the examples.

References

1. Z. Pawlak: Rough Sets: Theoretical Aspects of Reasoning About Data. Kluwer Academic Publisher, Norwell, MA, (1991)
2. V.N. Vapnik: Statistical Learning Theory. John Wiley & Sons, (1998).
3. S.B.Cho. "Pattern recognition with neural networks combined by genetic algorithm", Fuzzy sets and systems 103: 339-347, 1999

Mining Class Association Rules with Artificial Immune System

Tien Dung Do, Siu Cheung Hui, and Alvis C.M. Fong

School of Computer Engineering, Nanyang Technological University
Nanyang Avenue, Singapore
{pa0001852a,asschui,ascmfong}@ntu.edu.sg

Abstract. Associative classification, which is based on association rules, has shown great promise over many other classification techniques. However, the very large search space of possible rules may cause performance degradation in the rule mining process as well as classification accuracy. In this paper, we propose a new approach known as AIS-AC, which is based on Artificial Immune System (AIS), for mining class association rules for associative classification. Instead of massively searching for all possible association rules, AIS-AC will only find a subset of association rules that are suitable for effective associative classification in an evolutionary manner.

1 Introduction

Associative classification, which is based on association rules [1], has achieved high accuracy in comparison with other classification approaches [2,3,4]. However, the problem of AC, which is also the problem of association rule mining, is the very large search space of rules which may consequently cause performance degradation in the rule mining process. In this paper, we propose a new approach for mining association rules for AC. The idea is that, instead of massively searching for all association rules, an effective subset of association rules can be found for AC. The proposed approach is based on an *artificial immune system* (AIS) [5,6] model to search for a targeted set of association rules based on some constraints. By using the evolutionary search, the proposed approach is able to overcome the drawbacks of the conventional AC approach.

2 Associative Classification

An association rule R is an implication $X \Rightarrow Y$ occurring in a transactional database, where X and Y are sets of items or *itemsets*. Conventionally, a rule is considered mainly based on the *support* and *confidence* measures [1]. Association rule mining aims to find all rules, of which the support and confidence greater than or equal to the predefined minimum support and confidence thresholds respectively. Although many effective algorithms have been proposed to solve this problem, there are still computational problems related to the large number of itemsets and the size of the itemsets themselves [7].

Associative classification (AC) [2,3,4] uses association rules for classification. It consists of three major processes: rule generation, rule selection and classification.

Firstly, in the *rule generation* process, the set of association rules is mined from a training dataset based on the support and confidence thresholds. The set of association rules is mined in the form of $iset \Rightarrow c$ where $iset$ is an itemset and c is a class. Next, the *rule selection* process evaluates the generated association rules and selects the subset of rules, which will give the best classification accuracy. Finally, in the *classification* process, to classify a test sample d , the rule $R: iset \Rightarrow c$ with the highest confidence value that *matches* with d (i.e. d contains $iset$) is selected. The test sample d is then assigned to the class c of R . The *confidence* measure, say 80%, guarantees the reliability of the classification decision. The test sample is classified into the class c as most of the transactions (80%) that contain the $iset$ fall into the class c .

Association rule mining, which is based on the support and confidence measures, extracts high quality rules that can accurately generalize the training dataset. A rule with a high support value can then be considered as a general pattern that can be used to predict missing data or summarize the dataset. On the other hand, a rule with a high confidence value determines an accurate prediction. However, association rules and classification are two very different processes and it is not easy to integrate them [8]:

- *Classification is an ill-defined and non-deterministic task.* The support and confidence threshold values for generating the best set of association rules for classification may vary depending on the nature of the dataset. In contrast, association rule mining is a well-defined, deterministic task which requires predefined support and confidence thresholds.
- *It is important for the classification process to handle the overfitting/under-fitting issue.* However, this issue is mostly ignored in association rule mining as it simply finds rules satisfying the support and confidence constraints regardless of whether or not the rules would be overfitting/underfitting the data.

To tackle these problems, the rule selection process can be acted as a bridge to select from deterministically generated and possibly overfitting/underfitting association rules to form a more flexible and less overfitting/underfitting subset of rules that is suitable for classification task. In the rule generation process, the support and confidence thresholds should be set low enough so that most of the good class association rules are obtained. This enables the rule selection process to select an effective set of rules for the classification task. However, if the thresholds are set low, the rule generation process may also generate many redundant rules, which will lead to longer runtime and the need for higher memory usage.

3 Rule Mining Constraints

Apart from support and confidence, another factor that affects the accuracy of an associative classifier is the proportion of data samples from a dataset that can be classified by the set of association rules. We define the *coverage* measure of a set of classification association rules *CARs* for a dataset D as the percentage of the data samples in D , in which there is at least one rule in *CARs* matching with each data sample. The coverage measure is defined in (1).

$$\text{cover}(\text{CARs}, D) = \frac{|\{d \mid d \in D \wedge \exists \text{car} : \text{car} \in \text{CARs} \wedge \text{car matches_with } d\}|}{|D|} \quad (1)$$

Basically, three factors, namely support, confidence and coverage can influence the quality of association rules mined for AC. They can be considered as constraints for mining a set of CARs for AC with a training dataset D . The three constraints are given as follows:

$$\text{cover}(\text{CARs}, D) \geq \text{minCoverage} \quad (2)$$

$$\text{supp}(R, D) \geq \text{minSupport} \text{ for every } R \in \text{CARs} \quad (3)$$

$$\text{conf}(R, D) \geq \text{minConfidence} \text{ for every } R \in \text{CARs} \quad (4)$$

In conventional AC, all rules satisfying the support and confidence measures are generated. It means that, for most of the data samples, the optimal prediction (by the rule(s) with highest confidence) is obtained. In our proposed approach, to avoid massively searching the rule space, only a subset of rules satisfying the support and confidence thresholds is gathered. It is, therefore, important that the generated subset should contain most of the highest confidence rules so that the classification accuracy is comparable to the conventional AC. As such, we need to increase the confidence threshold (i.e. *minConfidence*) as high as possible, as long as we can find a set of rules CARs satisfying the three constraints. Note that equation (4) is equivalent to (5). Thus, our association rule mining for AC becomes searching for a set of rules CARs that satisfy constraints (2) and (3), and maximize the minimal confidence value of the rules in CARs.

$$\min\{\text{conf}(R, D) \mid R \in \text{CARs}\} \geq \text{minConfidence} \quad (5)$$

4 Artificial Immune Systems

Artificial immune systems (AIS) are developed based on metaphors from natural immune systems. The current AISs observe and adopt immune functions, principles and models, and apply them to solve problems in computing, engineering and other research areas [5,9]. In [6], an algorithm called CLONALG that focused on the clonal selection principle and affinity maturation process of adaptive immune response was proposed. The schematic representation of CLONALG is depicted in Figure 1. The algorithm starts with an initial set of population P_r and an empty memory set M (in step 1). The *selection* process then selects n best cells to generate a new population P_n according to the affinity principle (in step 2). The *clonal* process reproduces from these P_n cells, giving rise to a population of clones C (in step 3). This step produces more offspring for higher affinity cells. The affinity *maturation* process (similar to the mutation operator in genetic algorithms) mutates the cells to create the population C^* (in step 4). During mutation, it assigns a lower mutation rate for higher affinity cells than low affinity cells. The idea is that the cells close to a local optimum need only be fine-tuned, whereas cells far from an optimum should move larger steps towards an optimum or other regions of the affinity landscape [9]. The *reselection* process then reselects the improved cells from C^* and updates the memory set M (in step 5). The *diversity introduction* process replaces d cells with new ones N_d (in step 6). In this step, the lower affinity cells will have higher probability of being replaced.

5 The AIS-AC Approach

In AIS-AC, association rules are considered as immune cells. Constraints of the rules are adapted into parameters in the AIS-AC approach as follows. Firstly, in each gen-

eration, the support constraint is used for rule selection. Secondly, the confidence values of the rules are used for memory update that selects and moves the best rules to the memory. Finally, the coverage measure is considered as the termination condition. The coverage measure is calculated based on the memory rules to decide whether the process should continue with another generation or be terminated when the coverage value exceeds a specified threshold. The diversification feature of an immune system enables the mining of a set of rules with high coverage values. The diversity of rules means the diversity of the itemsets of the rules, which in turn implies a higher number of data samples that the set of rules has matched.

Similar to the approach described in [2], the proposed AIS-AC algorithm will mine association rules for each class separately. Figure 2 gives the proposed AIS-AC algorithm, which follows the general framework of the clonal selection algorithm CLONALG. The population P is first initialized by the set of all 1-itemset rules (i.e. $\{item\} \Rightarrow c$). The selection process (in lines 4-7) filters specific rules with support values below the support threshold. The actual affinity selection is carried out by retaining the highest confidence rules of population P . Then, the processes of cloning, mutation and diversity introduction are carried out (line 8-10). Finally, the best rules which satisfy the support and confidence constraints are moved to the memory pool. The confidence threshold (i.e. $minConfidence$) is initially set to a high value, which is subsequently reduced after a certain number of generations until the rules found can cover the dataset. The subsequent deduction of the confidence threshold during the evolutionary process helps to obtain the confidence threshold that is close to the optimal value. In line 9, the mutation rate is equal to “one item” for every rule. That is, when a rule is mutated, the newly produced rules will differ from the parent rule only by one item. The reason is that cells are rules with relatively small number of items (mostly 2, 3 or 4). Two rules with two or more different numbers of items may mean different implications or have no relation at all. The maturation of itemset $iset$ is done by randomly removing, changing or adding one item into the $iset$.

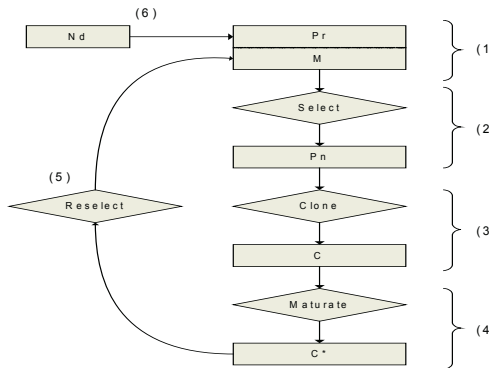


Fig. 1. The schematic representation of the CLONALG model

In the current implementation of AIS-AC, we have adopted a hash-tree structure used in the Apriori algorithm [1] for fast support and confidence counting. At the same time, the coverage of the memory pool is also calculated. This means that AIS-AC conducts a single scan of the dataset for each generation.

Input:

- 1: c - a class in the dataset for classification
- 2: I - the set of items in the dataset
- 3: $minSupport, minCoverage$ - minimum thresholds for the support and coverage measures
- 4: $noOfGenerations, selectionNumber, clonalRate$ - parameters for clonal selection theory

Output:

- 1: M - memory set containing a set of association rules for AC

Method:

- 1: Initialize $M = \emptyset$, $generationCount = 0$, $minConfidence=100\%$
- 2: Initialize $P = \{\{item\} \Rightarrow c \mid item \in I\}$
- 3: **do** $\//$ begin a generation
- 4: **forall** rule R in P **do** $\//$ selection
- 5: **if** $supp(R) < minSupport$ **then** remove R from P **endif**
- 6: **endfor**
- 7: Set $P =$ first $selectionNumber$ highest confidence rules in P
- 8: Clone P with $clonalRate$ $\//$ cloning
- 9: Mutate P $\//$ maturation
- 10: Diversify P $\//$ diversity introduction
- 11: **forall** rule R in P **do** $\//$ memory selection
- 12: **if** $and supp(R) \geq minSupport$ **and** $conf(R) \geq minConfidence$
- 13: **then** move R into M **endif**
- 14: **endfor**
- 15: Recalculate $minConfidence$
- 16: Set $generationCount = generationCount + 1$
- 17: **while** $cover(M) < minCoverage$ **and** $generationCount < noOfGenerations$
- 18: **Return** M

Fig. 2. The proposed AIS-AC algorithm

6 Performance Evaluation

We have conducted an experiment on a 1.4GHz Pentium PC with 400MB of memory running with MS Windows 2000. The datasets used in the experiment are obtained from the UCI Machine Learning Repository. In this experiment, we have selected largest datasets from the repository for testing, namely *Adult*, *Digit*, *Letter* and *Nursery*, with each consisting of more than 10,000 transactions. Table 1 lists the properties of the four datasets.

We have implemented the AIS-AC algorithm and CBA algorithm [2] with multiple class support thresholds (denoted as AC) for comparison. In the implementation of the AIS-AC algorithm, the clonal rate is set to 20 and the population is set to 200. The number of new rules for diversity introduction and the maximum number of generations are both set to 40. The coverage threshold is set to 100%. Figure 3 shows the performance results, based on precision (in bar chart) and runtime (in line chart), of the experiment on the two approaches using the four datasets. The performance of AIS-AC is obtained from 10 runs for each dataset with different support thresholds.

From the performance results, we have observed that the runtime of AIS-AC is quite steady and constant. In contrast, the runtime of AC is increased exponentially when the support threshold is decreased (for the first three datasets). It is because the number of frequent itemsets satisfying the support constraint has increased exponentially. However, this does not apply to the *Nursery* dataset as it contains only a rather

small set of 27 items compared with more than a hundred items in other datasets. Thus, when the support value is reduced, the number of itemsets does not increase significantly as the other datasets. Further, the performance of AC with small support values is not shown in Figure 3. This is because we are unable to obtain the performance results for the corresponding support values. The reason is that the runtime is too long or the number of possible rules is too large that the system has run out of memory during the rule mining process. The ability of mining rules with small support values gives AIS-AC an advantage in dealing with very large datasets.

Table 1. Datasets used in the experiment

| Dataset | No. of items (features) | No. of classes | No. of samples | Training set | Testing set |
|---------|-------------------------|----------------|----------------|--------------|-------------|
| Adult | 147 | 2 | 48842 | 32561 | 16281 |
| Digit | 151 | 10 | 10992 | 7494 | 3498 |
| Letter | 256 | 26 | 20000 | 13333 | 6667 |
| Nursery | 27 | 5 | 12960 | 8640 | 4320 |

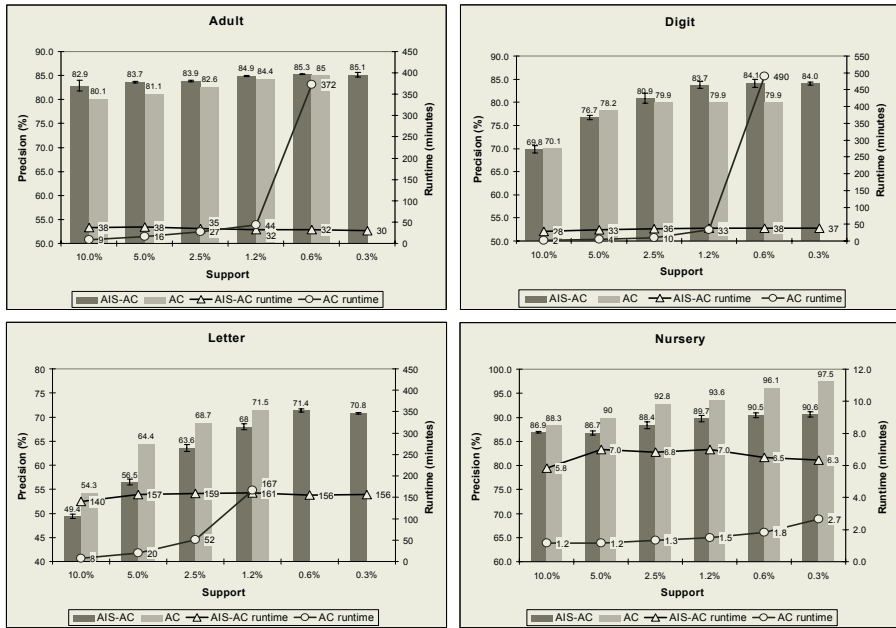


Fig. 3. Performance results

In principle, the AC algorithm has obtained the complete set of association rules. It should, therefore, be more accurate than AIS-AC with the same support threshold value. However, the performance results from the *Adult* and *Digit* datasets have shown that AIS-AC has surprisingly outperformed AC with most of the threshold values. One of the possible reasons is that AIS-AC with the flexible confidence (can be different among the classes) and coverage constraints can obtain a balance of rules for each class. In the dataset *Letter*, AC seems to perform better than AIS-AC. In fact, the best performance of AIS-AC is when the support value is 0.6%, and in AC, it is

1.2%. The precision is similar (71.4% vs. 71.5%) whereas the runtime of AIS-AC is faster. In the dataset *Nursery*, the AC approach performs better than AIS-AC. The reason, as mentioned before, is that in a small search space of association rules in this dataset, AIS-AC, therefore, loses its advantages.

7 Conclusion

In this paper, we have proposed an approach for searching association rules directly for AC by formulating a set of constraints, which can be used to determine an effective set of association rules for classification. By doing this, we can avoid the computationally expensive process of conventional association rule mining. The proposed algorithm is known as AIS-AC, which is based on an artificial immune system model for searching association rules for AC. In the evolutionary search of AIS-AC, the parameters of candidate rules can be evaluated after each generation. This enables the AIS-AC algorithm to check the constraints on the targeted rule set, and to refine them accordingly. This makes the algorithm more flexible in searching for an appropriate set of association rules from different datasets or domains.

References

1. R. Agrawal and R. Srikant, "Fast algorithms for mining association rules", In Proc. of the 20th Int'l Conf. on Very Large Databases (VLDB '94), Santiago, Chile, pp. 487-499, June 1994.
2. B. Liu, W. Hsu and Y. Ma, "Integrating classification and association rule mining", In Proc. of the Fourth International Conference on Knowledge Discovery and Data Mining, pp. 80-86, New York, NY, 1998.
3. W. Li, J. Han, and J. Pei., "CMAR: Accurate and efficient classification based on multiple class-association rules", In Proc. of ICDM, 2001.
4. B. Liu, Y. Ma and C.K. Wong, "Classification Using Association Rules: Weaknesses and Enhancements". In Vipin Kumar et al., Data mining for scientific applications, 2001.
5. L.N. de Castro and F.J. Von Zuben, "Artificial Immune Systems: Part I – Basic Theory and Applications", Technical Report – RT DCA 01/99, 1999.
6. L.N. de Castro and F.J. Von Zuben, "The Clonal Selection Algorithm with Engineering Applications", In Proc. of GECCO'00, Workshop on Artificial Immune Systems and Their Applications, pp. 36-37, 2000.
7. M. Hegland, "Algorithms for association rules", Advanced lectures on machine learning, Springer-Verlag New York, Inc., New York, NY, 2003.
8. A.A. Freitas, "Understanding the crucial differences between classification and discovery of association rules: a position paper", ACM SIGKDD Explorations Newsletter, Vol 2, No 1, p.65-69, June, 2000.
9. L. N. de Castro and J. I. Timmis, "Artificial Immune Systems as a Novel Soft Computing Paradigm", Soft Computing, Vol 7, No 8, pp.526-544, 2003.

Discovering Fuzzy Association Rules with Interest and Conviction Measures

K. Sai Krishna¹, P. Radha Krishna¹, and Supriya Kumar De²

¹ Institute for Development and Research in Banking Technology,

Masab Tank, Hyderabad –500057, Andhra Pradesh, India

ksaikrishna@mtech.idrbt.ac.in, prkrishna@idrbt.ac.in

² XLRI- Jamshedpur, C.H.Area (E), Jamshedpur –831001, Jharkhand, India

skde@xli.ac.in

Abstract. Association rule mining forms an important research area in the field of data mining. The theory of fuzzy sets can be used over relational databases to discover useful, meaningful patterns. In this paper, we propose an algorithm to mine fuzzy association rules over relational databases using Interest and Conviction measures. In the present work, we introduce fuzzy interest and fuzzy conviction measures and eliminate the rules, which have negative correlation. The experiments are conducted on an insurance database using our approach. The presented approach is very useful and efficient when there are more infrequent itemsets in a database.

1 Introduction

Association Rule mining is a process of finding association rules in a dataset. Association rule is of the form $A \rightarrow B$ where A and B are disjoint subsets having minimum user specified support and confidence level. The ‘support’ is the amount of times the rule appears with respect to the entire dataset, while ‘confidence’ is the degree or measure of times the consequent occurs with respect to the antecedents. Agrawal et al [1] proposed an Apriori algorithm in 1993 to generate association rules. In the literature, several algorithms have been proposed for finding association rules in the databases [8,11,13]. Association rules find its major role in market basket analysis but it is also interesting when quantitative or categorical data is considered [12].

Association Rules can be divided based on itemsets of interest as Positive and Negative [4,16]. Positive association rules simply called as association rules describe about interestingness and usefulness of a rule. These rules are of the form $A \rightarrow B$. Negative association rules are of the forms $A \rightarrow \neg B$. These association rules are also useful in some cases where infrequent itemsets of interest is more.

Another classification of association rules is Boolean, Quantitative and Fuzzy association rules [2,6,7,10,15]. Boolean Association Rules are used to find associations among attributes in a dataset, which have values either 0 or 1. In general, all datasets contain quantitative attributes rather than Boolean attributes. Quantitative and categorical attributes define the quantitative association rules. Mining quantitative association rules, introduced by Agrawal et. al [12], discretize the quantitative attributes domain into different intervals. Discovered rules from these intervals were not informative for domain experts as the intervals were not concise and meaningful. On the other hand, fuzzy logic can be used to get meaningful, understandable and concise

patterns from a database [5]. Fuzzy logic is a superset of conventional logic that has been extended to handle the concept of partial belongingness. Fuzzy membership function describes the degree to which an element belongs to a fuzzy set. Instead of using intervals, linguistic terms can be used to represent rules and these rules are easy to understand by human experts. In the literature, several attempts were made to represent knowledge in terms of fuzzy linguistic summaries. Application of fuzzy linguistic summaries in data mining has been discussed in [3].

Fuzzy association rules solve the problem of sharp boundaries. Each itemset in the fuzzy association rule is specified as a set of <attribute, linguistic term> pairs. In this paper, we present fuzzy interest and fuzzy conviction measures to discover interesting fuzzy association rules for a given minimum fuzzy support and fuzzy confidence. The rest of the paper is organized as follows. In section 2, we present an algorithm for mining fuzzy association rules considering fuzzy interest and fuzzy conviction measures. In section 3, we present an example to explain our approach. Experimental results on insurance dataset have been shown in section 4. Finally, we conclude in section 5.

2 Fuzzy Association Rule Mining

In this section, we present a novel algorithm, to represent the regularities and patterns having positive correlations in a database using linguistic terms. Initially, we applied k-means [9] clustering algorithm on each attribute to find the k- means of k clusters. Here, k is the number of desired clusters. The means of each cluster is used to compute the membership values. After fuzzification, the k clusters will become the k linguistic terms for that attribute. Each attribute value is mapped to a value in the range of [0,1] based on the membership function. In this work, we used triangular membership function. Apriori algorithm [1] is used to generate rules with user specified minimum fuzzy support and fuzzy confidence. The input to find frequent item sets is the attribute-linguistic term table. The fuzzy support and fuzzy confidence are calculated as given below:

$$FSupport(A_iL_j) = \frac{\sum_d A_iL_j}{\sum_{m=1 \text{ to } z} \sum_d A_iL_m}$$

$$FSupport(A_iL_k, A_jL_r) = \frac{\sum_d \min(A_iL_k, A_jL_r)}{\sum_{a=1..p} \sum_{b=1..n} \sum_d \min(A_iL_a, A_jL_b)} \quad \text{where } i \neq j$$

$$FConfidence(A_iL_k \rightarrow A_jL_r) = \frac{Fsupport(A_iL_k, A_jL_r)}{Fsupport(A_iL_k)}$$

Here, A_iL_j represents i^{th} attribute's j^{th} linguistic term, z represents number of linguistic terms defined for the attribute A_i and d represents all rows in attribute-linguistic term table. Usually, interesting rules found within fuzzy support and fuzzy confidence framework may contain negative correlations among attributes. Fuzzy interest and fuzzy conviction measures are introduced to find the dependency among itemsets in order to generate interesting and meaningful fuzzy association rules. The fuzzy interest measure is defined as follows:

$$F\text{Interest } (A_iL_k \rightarrow A_jL_r) = \frac{F\text{Support}(A_iL_k, A_jL_r)}{F\text{Support}(A_iL_k) * F\text{Support}(A_jL_r)}$$

Here three cases may arise based on the fuzzy interest value as given below:

1. If $F\text{Interest}=1$ then A_iL_k, A_jL_r are independent.
2. If $F\text{Interest}>1$ then A_jL_r is positively dependent on A_iL_k
3. If $F\text{Interest}<1$ then A_jL_r is negatively dependent on A_iL_k

Fuzzy interest measure removes negatively dependent rules from the set of generated association rules. Consider two rules $A_iL_k \rightarrow A_jL_r$ and $A_iL_k \rightarrow A_mL_n$ and assume fuzzy confidence of rules as 0.5 and 0.6 respectively and fuzzy support of A_jL_r and A_mL_n as 0.25 and 0.75 respectively. The probability of A_jL_r increases when A_iL_k is assumed (it is increasing from 0.25 to 0.5), whereas the probability of A_mL_n decreases in the same circumstances (it is decreasing from 0.75 to 0.6). It means attribute A_jL_r is positively correlated with A_iL_k whereas A_mL_n is negatively correlated with this attribute. For avoiding this kind of negative correlations, we use fuzzy conviction measure as defined below:

$$F\text{Conviction } (A_iL_k \rightarrow A_jL_r) = \frac{1 - F\text{Support}(A_jL_r)}{1 - F\text{Confidence}(A_iL_k \rightarrow A_jL_r)}$$

Algorithm: Fuzzy Association Rules

- Input:** D = Database of size $M \times N$ and $\langle A_1, A_2, A_3 \dots A_n \rangle$ are the set of attributes.
 M_i = Number of means for each attribute i
 Min Fsup = Minimum Fuzzy Support
 Min Fconf = Minimum Fuzzy Confidence
 Lno = Level number
1. Initialize M_i 's, Min Fsup , Min Fconf , Lno (Lno initial value is 2).
 2. Calculate M_i number of means for each attribute i.
 3. Construct attribute-linguistic table using fuzzy membership functions.
 4. Apply Apriori algorithm on attribute-linguistic table to find frequent 1 itemset that are having user specified Min Fsup using $F\text{Support}$ measure.
 5. Find frequent Lno level itemsets from ($Lno-1$) level that are having user specified Min Fsup using $F\text{Support}$ measure.
 6. Find set of frequent rules having Min Fconf using $F\text{Confidence}$ measure.
 7. Remove negative dependent rules using $F\text{Interest}$ measure.
 8. Remove rules with negative correlations using $F\text{Conviction}$ measure.
 9. $Lno \leftarrow Lno + 1$
 10. Repeat steps 5-9 until Itemset in ($Lno-1$) level is empty
 11. End
 12. End

Fig. 1. Algorithm for fuzzy association rules

The nature of $F\text{Conviction } (A_iL_k \rightarrow A_jL_r)$ can be specified by using following relations:

- a) $0 < F\text{Conviction } (A_iL_k \rightarrow A_jL_r) < \infty$
- b) A_iL_k and A_jL_r are independent if $F\text{Conviction } (A_iL_k \rightarrow A_jL_r) = 1$
- c) $0 < F\text{Conviction } (A_iL_k \rightarrow A_jL_r) < 1$ if and only if A_jL_r is negatively correlated with A_iL_k
- d) $1 < F\text{Conviction } (A_iL_k \rightarrow A_jL_r) < \infty$ if and only if A_jL_r is positively correlated with A_iL_k

The Fuzzy conviction measure mainly refers to the strength of the directed associations among the $\langle \text{attribute}, \text{linguistic term} \rangle$ sets. The detailed algorithm is given in Fig 1 and an example is given in the next section to explain our approach.

3 An Example

Consider a sample table shown in Table 1. For each attribute, we applied k-means algorithm to find means of clusters. In the k-means approach, the cost is based on the sum of squares of distance between elements and its corresponding cluster center. The cost is minimized by taking means as the sum of elements of the cluster divided by number of elements in the cluster. Initially k-Means algorithm initializes k mean values with k elements for each attribute. Each element is assigned to the closest cluster. The sum of the values of the cluster divided by number of the elements in the cluster for the next iteration is computed. The process is repeated until the difference between the means in the successive iterations is negligible.

Table 1. Sample Table

| | A ₁ | A ₂ | A ₃ |
|---|----------------|----------------|----------------|
| 1 | 9 | 9 | 30 |
| 2 | 10 | 10 | 9 |
| 3 | 11 | 30 | 10 |
| 4 | 30 | 31 | 11 |
| 5 | 31 | 32 | 9 |
| 6 | 32 | 30 | 10 |

Table 2. Attribute Linguistic Term Table

| | A ₁ L ₁ | A ₁ L ₂ | A ₂ L ₃ | A ₂ L ₄ | A ₃ L ₅ | A ₃ L ₆ |
|---|-------------------------------|-------------------------------|-------------------------------|-------------------------------|-------------------------------|-------------------------------|
| 1 | 1.0 | 0.0 | 1.0 | 0.0 | 0.0 | 1.0 |
| 2 | 1.0 | 0.0 | 0.976 | 0.023 | 1.0 | 0.0 |
| 3 | 0.952 | 0.047 | 0.035 | 0.964 | 0.99 | 0.009 |
| 4 | 0.047 | 0.952 | 0.0 | 1.0 | 0.94 | 0.059 |
| 5 | 0.0 | 1.0 | 0.0 | 1.0 | 1.0 | 0.0 |
| 6 | 0.0 | 1.0 | 0.035 | 0.964 | 0.99 | 0.009 |

On applying k-means algorithm to Sample table 1, the cluster means computed are 10, 31 for A₁; 9.5, 30.75 for A₂ and 9.8, 30.0 for A₃ when k (=total number of clusters) value is 2. Fuzzy membership functions for two clusters for first attribute are defined as given below:

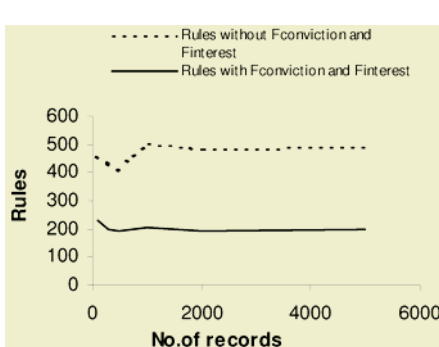
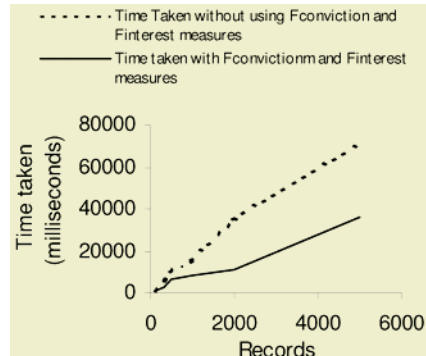
$$MF_1(x)=\begin{cases} 1 & \text{if } x \leq 10 \\ \frac{31-x}{21} & \text{if } 10 < x < 31 \\ 0 & \text{if } x \geq 31 \end{cases} \quad MF_2(x)=\begin{cases} 0 & \text{if } x \leq 10 \\ \frac{x-10}{21} & \text{if } 10 < x < 31 \\ 1 & \text{if } x \geq 31 \end{cases}$$

Based on the membership functions attribute linguistic term table can be formed as shown in table 2. Using fuzzy support and fuzzy confidence framework, fuzzy association rules generated are shown in table 3. The fuzzy support and fuzzy confidence threshold used for generating association rules are 0.1 and 0.3 respectively. Table 3 consists of some of the negatively dependent and negatively correlated rules. These rules can be removed using fuzzy interest and fuzzy conviction measures. Rules that have fuzzy interest greater than 1 are said to be positively dependent. Rules that have fuzzy conviction greater than 1 are said to be positively correlated.

Table 3. Rules generated with fuzzy support and fuzzy confidence framework

| | Rule | Fuzzy support of itemsets | Fuzzy confidence of rule |
|----|-------------------------------------|---------------------------|--------------------------|
| 1 | $A_1L_1 \rightarrow A_2L_3$ | 0.33139 | 0.66279 |
| 2 | $A_2L_3 \rightarrow A_1L_1$ | 0.33139 | 0.97133 |
| 3 | $A_1L_1 \rightarrow A_2L_4$ | 0.1686 | 0.3372 |
| 4 | $A_1L_1 \rightarrow A_3L_5$ | 0.327 | 0.654 |
| 5 | $A_3L_5 \rightarrow A_1L_1$ | 0.327 | 0.39879 |
| 6 | $A_1L_2 \rightarrow A_2L_4$ | 0.48837 | 0.9767 |
| 7 | $A_2L_4 \rightarrow A_1L_2$ | 0.48837 | 0.741279 |
| 8 | $A_1L_2 \rightarrow A_3L_5$ | 0.487 | 0.974 |
| 9 | $A_3L_5 \rightarrow A_1L_2$ | 0.487 | 0.5938 |
| 10 | $A_2L_3 \rightarrow A_3L_5$ | 0.17336 | 0.508 |
| 11 | $A_1L_1, A_2L_3 \rightarrow A_3L_5$ | 0.1625 | 0.49 |
| 12 | $A_1L_1, A_3L_5 \rightarrow A_2L_3$ | 0.1625 | 0.4969 |
| 13 | $A_2L_3, A_3L_5 \rightarrow A_1L_1$ | 0.1625 | 0.937 |

Table 4 shows fuzzy interest and fuzzy conviction measures for rules listed in table 3. Rules 3, 4, 5, 10 and 11 of table 4 have fuzzy interest less than one and fuzzy conviction less than one. We can eliminate these rules. In this sample example, rules 3, 4, 5, 10 and 11 are infrequent by both fuzzy conviction and fuzzy interest measures, but for large databases these measures may produce different infrequent rules. These rules can be eliminated easily by both measures and produce useful and positively correlated rules. Rules 1, 2, 6, 7, 8, 9, 12, 13 are the resultant positive correlated rules of the table 4.

**Fig. 2.** Comparison between association rules generated with and without fuzzy Interest and fuzzy conviction measures**Fig. 3.** Time comparison between with and without fuzzy interest and fuzzy conviction measures

4 Experimental Results

We applied our proposed fuzzy association rules algorithm with fuzzy interest and fuzzy conviction measures on insurance data [14]. Data set consists of 86 attributes. We experimented on 5000 randomly selected records with seven attributes namely, customer subtype, Number of houses, average size household, average age, married,

average income, number of mobile home policies. While applying k-Means algorithm over these seven attributes, number of clusters values (or k) considered 3, 2, 3, 3, 2, 4 and 2 respectively. The minimum fuzzy support and fuzzy confidence are considered 0.2 and 0.2 respectively for generating fuzzy association rules. Figure 2 shows the comparison between numbers of generated association rules with and without Fuzzy conviction and fuzzy interest measures. For example, one of the obtained rules is “(Customer subtype, large), (Number of houses, less), (average size household, more), (average income, average)→(mobile home policies, no), this can be described as “If Customer subtype is large, Number of houses is less, average size household is more and average income is average, then they are not interested to take mobile home policies”.

Table 4. Generated Rules and their measures

| | Rule | Fuzzy support of itemset | Fuzzy confidence of rule | Fuzzy interest of rule | Fuzzy conviction of a rule |
|----|-------------------------------------|--------------------------|--------------------------|------------------------|----------------------------|
| 1 | $A_1L_1 \rightarrow A_2L_3$ | 0.33139 | 0.66279 | 1.9426 | 1.9537 |
| 2 | $A_2L_3 \rightarrow A_1L_1$ | 0.33139 | 0.97133 | 1.9426 | 17.44 |
| 3 | $A_1L_1 \rightarrow A_2L_4$ | 0.1686 | 0.3372 | 0.5118 | 0.5147 |
| 4 | $A_1L_1 \rightarrow A_3L_5$ | 0.327 | 0.654 | 0.797 | 0.52 |
| 5 | $A_3L_5 \rightarrow A_1L_1$ | 0.327 | 0.39879 | 0.797 | 0.8316 |
| 6 | $A_1L_2 \rightarrow A_2L_4$ | 0.48837 | 0.9767 | 1.4825 | 14.67 |
| 7 | $A_2L_4 \rightarrow A_1L_2$ | 0.48837 | 0.741279 | 1.4825 | 1.932 |
| 8 | $A_1L_2 \rightarrow A_3L_5$ | 0.487 | 0.974 | 1.1877 | 6.943 |
| 9 | $A_3L_5 \rightarrow A_1L_2$ | 0.487 | 0.5938 | 1.1877 | 1.231 |
| 10 | $A_2L_3 \rightarrow A_3L_5$ | 0.17336 | 0.508 | 0.619 | 0.365 |
| 11 | $A_1L_1, A_2L_3 \rightarrow A_3L_5$ | 0.1625 | 0.49 | 0.5979 | 0.35298 |
| 12 | $A_1L_1, A_3L_5 \rightarrow A_2L_3$ | 0.1625 | 0.4969 | 1.4565 | 1.3096 |
| 13 | $A_2L_3, A_3L_5 \rightarrow A_1L_1$ | 0.1625 | 0.937 | 1.8749 | 7.997 |

In our algorithm, filtering of some rules is done using fuzzy conviction and fuzzy interest measures during generation of association rules. Thus, computation time decreases as compared to simple fuzzy support and fuzzy confidence framework. Figure 3 shows time comparison between with and without using fuzzy conviction and fuzzy interest measures. As it is evident from the graph that time required for execution is decreasing as well as useful rules are only being generated using our proposed algorithm.

5 Conclusion

Fuzzy association rules are useful for finding patterns in databases to take business decisions. These rules are meaningful with its linguistic representation. This paper presents an algorithm to find fuzzy association rules with positive correlation using fuzzy conviction and fuzzy interest measures. The number of association rules obtained is less than the number of rules generated by traditional algorithms. The time taken to generate these rules is also less than the traditional algorithms. The proposed algorithm has been tested on an insurance dataset, to discover interesting rules containing quantitative attributes.

References

1. Agrawal, R., Imieliński, T., Swami, A.: Mining association rules between sets of items in large databases. In the Proceedings of ACM SIGMOD international conference on Management of Data (1997) .207-216.
2. Au, Wai-Ho., Keith, Chan, C.C.: Mining Fuzzy Association Rules in a Bank-Account Database. TFS 11(2) (2003) 238—248.
3. Barro, S., Bugarin, A.J., Carinena, P., Diaz-Hermida, F.:A framework for fuzzy quantification models analysis. In IEEE Trans on Fuzzy Systems, Vol 11 (2003) 89-99.
4. Cock, M. De., Cornelis, C., Kerre, E..E.: Elicitation of fuzzy association rules from positive and negative examples. Fuzzy Sets and Systems 149 (2005) 73–85.
5. Delgado, M., Marin, N., Vila, Maria-Amparo.:Fuzzy Association Rules:General Model and Applications. IEEE Transactions on fuzzy systems, Vol. 11(2003) 238-248.
6. Graaf, J.M.de., Kosters, W.A., Witteman,J.J.W.: Interesting Fuzzy Association Rules in Quantitative Databases, In the 5th European Conference on Principles of Data Mining and Knowledge Discovery), Freiburg, Germany (2001) 140-151.
7. Hong, Tzung-Pei., Lin, Kuei-Ying., Wang, Shyue-Liang.: Fuzzy data mining for interesting generalized association rules, Fuzzy Sets and Systems, v.138 (2003) 255-269.
8. Han, J., Fu, Y.: Discovery of multi-level association rules from large databases. In proceedings of the 21st International Conference on Very Large Data Bases (1995) 420-431.
9. Jain, A. K., Dubes,R. C.: Algorithms for Clustering Data. Prentice Hall, New Jersey, 1988.
10. Kuok, C. M., Fu, A., Wong, M. H.: Mining Fuzzy Association Rules in Databases, SIGMOD Record, Vol. 27, No. 1 (1998) 41-46.
11. Park, J.S., Chen, M.S., Yu, P.S.: An efficient hash based algorithm for mining association rules. In proceedings of the ACM SIGMOID International Conference on management of Data (1995) 175—186.
12. Srikant, R., Agrawal, R.: Mining quantitative association rules in large relational tables. In: H.V. Jagadish and I.S. Mumick, (eds): Proceedings of the ACM SIGMOID International Conference on Management of Data (1996) 1-12..
13. Toivonen, H.: Sampling large databases for association rules. In Proceedings of the 22nd International Conference on Very Large Databases (1996) 134-145.
14. Van der Putten, P., Someren, M.van. (eds).: The Insurance Company Case. Published by Sentient Machine Research, Amsterdam. Also a Leiden Institute of Advanced Computer Science Technical Report (2000).
15. Zhang, W: Mining Fuzzy Quantitative Association Rules, 11th IEEE International Conference on Tools with Artificial Intelligence (2000) 99 – 102.
16. Zhang, C., Zhang, S.: Association Rule Mining Models and Algorithms. Springer-Verlag Berlin Heidelberg (2002).

Automatic Generation of Operation Manuals Through Work Motion Observation

Satoshi Hori¹, Kota Hirose¹, and Hirokazu Taki²

¹ Monotsukuri Institute of Technologists

333 Maeya, Gyoda 361-0038 Japan

hori@iot.ac.jp

<http://www.iot.ac.jp/manu/HORI.html>

² Wakayama University

930 Sakaedani, Wakayama 640-8510 Japan

Abstract. When a service technician repairs an air-conditioning system, or a factory worker operates a robot system, there exists an appropriate and efficient work process. A better work process is realized through the skills that workers acquire by experience. It is desirable that the improved work process be documented in manual form and shared among other workers. However documenting a work process is a time-consuming task. To automate the documentation, we have developed a method of observing a worker's motion with IC accelerometers and we have built a program that automatically generates a manual from the recorded work process.

1 Introduction

Firstly the scope and objective of our research are outlined. A service technician or worker moves as he checks and repairs machinery. He walks, pushes switches, and looks at meters. The behavior of an experienced technician is more efficient than that of a novice, and we can learn a lot by observing the work process of a well-trained and experienced worker. An efficient work process should be documented as a manual and shared among other workers, because good operation manuals improve work productivity. There is a keen demand for manual generation systems because documenting a work process is a time-consuming task. This is the motivation of our research. We are working on developing a method and system that can observe a person's behavior and store it as explicit knowledge using electronic media. The system enables us to share the knowledge and experience of other persons, so that we can improve work productivity and efficiency in tasks such as those involved in maintenance and servicing.

1.1 Brief Review of Motion Observation

Motion observation has attracted the attention of many researchers. A century ago, Gilbreth established Motion Study [1] as a method for designing better work processes. Since then, various terms, e.g. behavior, motion, and work, have been used to describe human behavior.

In this paper, we use terms which are defined as follow:

➢ **Body movement:** Movement and motion of a worker's body.

- **Motion data:** Sample data from observing *body movement*. This data consists of continuous and time-varying signals.
- **Basic motions:** A *basic motion* is a meaningful and key action, e.g., walking, sitting, grabbing hold of something, etc. A *basic motion* is extracted from the observed *motion data*.
- **Work:** Work is a series of *basic motions*. A worker performs a task when carrying out the work.

Most motion observation is performed according to the following steps:

- Step-1. **Motion sensing:** Electronically measure human *body movement*. Data is sampled and stored in numerical form.
- Step-2. **Motion labeling:** Observed *motion data* is continuous data. Split the data into segments and label the segments in order to pick up *basic motions*.
- Step-3. **Work recognition:** Infer how work is performed from the series of *basic motions*.

1.2 Outline of Our System

Figure 1 shows the outline of our system, which consists of two subsystems, (1) a wearable sensor system that observes the body movement and vision range of a worker, and (2) a manual-generator that generates a manual from the motion data recorded by the wearable sensor system.

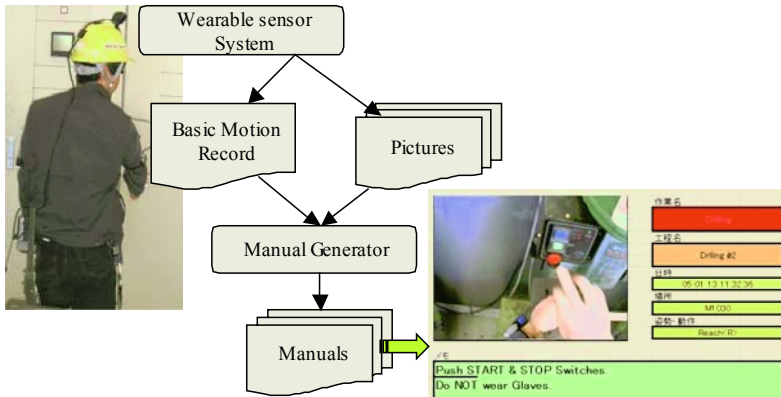


Fig. 1. Manual-Generation Procedure

2 Related Research

Motion has attracted the attention of many researchers, because (1) recent advances in electronic sensor technology have enabled us to capture human motion, and (2) we have become aware of the importance of intelligence that cannot be described in verbal form.

This section briefly reviews the related work of Nakayama [5] and the Industrial Engineering (I.E.) Motion Study of Gilbreth [1] from the viewpoints of motion sensing, motion labeling, and work recognition.

2.1 Nakayama's Behavior Recognition

Nakayama's work [5] is one of the first attempts to recognize human body movements by computer. He reported that his method recognized movement with a success rate of more than 63%. His method is useful in tagging video streams etc., but he did not fully describe what his behavior recognition method is used for. The method is as follows:

- Motion sensing: Observe human body movement using a commercial motion capture system.
- Motion labeling: Classify observed data into 5 categories by calculating movement correlations among arms and legs. This classified data is called “motion print”. Then split the movement sequence at points where the correlations change greatly. This process is called “motion chopping”. Finally name the segments.
- Work recognition: Compare the sequence of the segments. Recognize behaviors by assuming that similar segment sequences represent similar behaviors.

2.2 Industrial Engineering (I.E.) Motion Study

I.E., provides a strategy for finding the preferred method of doing Work, this is called Motion Study [1]. Frank and Lillian Gilbreth did pioneering work and established Motion Study in the beginning of the 20th century. Gilbreth noticed that most work is done with two hands, and all manual work consists of relatively few fundamental motions that are performed over and over again. “Get” or “pick up” and “place” or “put down” are two of the most frequently used groups of motions in a manufacturing line. Gilbreth developed subdivisions or events, which he considered common to all kinds of manual work. He coined the word *therblig* to refer to any of the seventeen elementary subdivisions.

- Motion sensing, Motion labeling, and work recognition: an I.E. engineer observes what a worker is doing on a manufacturing line. He understands the worker's movements and writes down the series of the basic motions using *therblig* symbols. He then establishes how the work is done. Figure 2 describes an example.
- Use of observed motion: The record of basic motions is analyzed and used for designing a better work procedure.

The I.E. Motion Study is expensive because it manually analyzes the worker's movement.

| <i>Therblig</i> | Description of Motion |
|-------------------------|------------------------------------|
| 1. TE: Transport Empty | Reach for pen. |
| 2. G: Grasp | Take hold of pen. |
| 3. TL: Transport Loaded | Carry pen to paper. |
| 4. P: Position | Position pen on paper for writing. |
| 5. U: Use | Sign the paper |
| 6. TL: Transport Loaded | Return pen. |

Fig. 2. Example of Motion Study: Task of “signing a paper”

3 Our Method of Motion Observation

As mentioned above, Figure 1 depicts the outline of our system. The system consists of two subsystems, (1) a wearable sensor system that observes the body movement and vision range of a worker, (2) a manual-generator that generates a manual from the motion data recorded by the wearable sensor system.

3.1 Wearable Sensor System

We employed IC accelerometers to measure a technician's motion. A CCD camera is also used to record what he sees because the series of basic motions is not enough to teach a novice what to do.

Recording Technician's Vision with a Camera

A CCD camera is used to record what a technician sees while doing a job. The camera is attached to the helmet worn by the technician so it can monitor his range of vision.

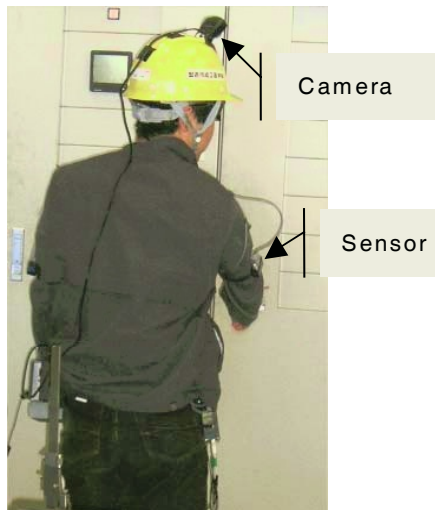
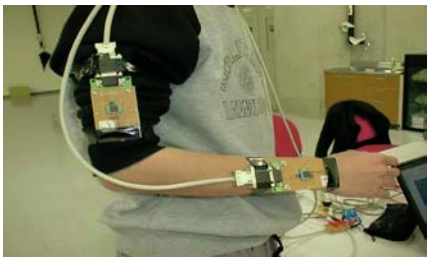
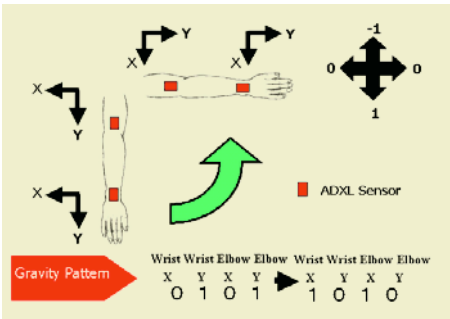


Fig. 3. Wearable Sensor System that Measures what a Technician does

Motion Observation with IC Accelerometers

We employed IC accelerometers to measure motion [2]. The sensors are attached to the arms and legs of a service technician. This section describes IC accelerometers and their signal processing. Analog Device's ADXL202 is employed as an accelerometer. The ADXL202 are low cost, low power, complete 2-axis accelerometers with a measurement range of ± 2 g. ADXL sensors attached to a right arm are shown in Figure 4 shows. Figure 5 demonstrates how "reach" motion is detected intuitively from the output of a wrist ADXL. "Reach" motion often occurs when a technician operates switches. The right hand is first extended close to the right leg. In the "reach" motion, the hand is raised and lowered.

**Fig. 4.** Accelerometers on Right Arm**Fig. 5.** Wrist Accelerometer's Output for Reach Motion

To detect a basic motion, the output signal is processed as follow:

Step-1. Measure raw X, Y acceleration data with a 50 msec sampling rate.

$$x_1^0, x_2^0, \dots, x_N^0; y_1^0, y_2^0, \dots, y_N^0$$

where N denotes the size of sample data.

$$x_i^0 : \text{Superscript 0 denotes raw data.}$$

Subscript i denotes i-th data point on X-axis.

Step-2. Eliminate noise by taking the moving average of each of five samples. Thus the cutoff frequency becomes 1.8 Hz.

$$x_i^1 = \frac{x_{i-2}^0 + x_{i-1}^0 + x_i^0 + x_{i+1}^0 + x_{i+2}^0}{5}$$

Step-3. Data labeling: Classify each data item into 3 bins labeled -1, 0, and 1. This data set is described as a gravity pattern.

Step-4. Motion labeling: Prepare a table that maps a gravity pattern change to a basic motion. As an example, when an arm's gravity pattern changes from 0101 to 1010, we determine that "reach" motion is occurring (see Figure 5).

4 Manual Generation

The wearable sensor system generates two types of files. One is the basic motion record file, a CSV file whose raw data consists of date and time, basic motion symbol, and the names of the picture files as in Figure 6. The other is the picture file. When the system detects any basic motion, it adds one line to the basic motion record file, while at the same time, five pictures are taken every second and saved as BMP files.

The manual-generation program reads the basic motion record file and generates one manual page when designated basic motion has occurred. Each page consists of five pictures, the corresponding occurrence times, and the basic motion codes. To complete the manual, all that is required is to fill in the title and an optional short description. Figure 7 shows an example of a generated manual. Thus this system saves a considerable amount of time in the reparation of manuals.

| Date & Time | Motion | Pictures |
|-------------------|----------|------------------------------------|
| 05 01 13 11 31:47 | Walk | pict.bmp¥2005-01-13 11-31-47-5.bmp |
| 05 01 13 11 31:51 | Reach | pict.bmp¥2005-01-13 11-31-51-5.bmp |
| 05 01 13 11 32:22 | Reach | pict.bmp¥2005-01-13 11-32-22-5.bmp |
| 05 01 13 11 32:36 | Walk | pict.bmp¥2005-01-13 11-32-36-5.bmp |
| 05 01 13 11 32:54 | Sit | pict.bmp¥2005-01-13 11-32-54-5.bmp |
| 05 01 13 11 33:39 | Walk | pict.bmp¥2005-01-13 11-33-39-5.bmp |
| 05 01 13 11 33:48 | Reach<R> | pict.bmp¥2005-01-13 11-33-48-5.bmp |

Fig. 6. Basic Motion Record File**Fig. 7.** Generated Manual Page

5 Conclusions

A human being moves his or her arms and legs when doing a job. For example, when a service technician checks and repairs machinery, he walks, pushes a switch, and looks at a meter. Since the behavior of an experienced technician is more efficient than that of a novice, the latter can learn new skills by observing the well-trained and experienced technician's movement.

We have developed a wearable sensor system employing IC accelerometers and a CCD camera, we have demonstrated that the sensor system can record meaningful motions, i.e., basic motions. An operation manual with pictures can be automatically generated from the recorded data.

Our system can save much effort in preparing manuals, and can support the storing and sharing of machine operation skills and facility repair experience. As mentioned in Section 1, information sharing of this kind improves productivity in maintenance services and manufacturing.

Further research will consider the following:

1. Improvement of the resolution of the IC accelerometers so that more complex and subtle work movements can be measured.
2. Since determination of what constitutes a basic motion is a very subjective matter, a computer algorithm is needed that can automatically segment basic motions from continuous observed data and can determine what basic motions occur at each work step.

References

1. Barnes, "Motion and Time Study", John Wiley & Sons, Inc., (1968).
2. S.Hori, K.Hirose, H.Taki, "Acquiring After-Sales Knowledge from Human Motions", KES2004, LNAI3214, pp.188-194 (2004).
3. B.Kuiper: "Qualitative Simulation" Artificial Intelligence Vol.2 pp.289- 338 (1986).
4. S.Kobayashi, K.Nakamura, "Knowledge Compilation and Refinement for Fault Diagnosis", IEEE Expert, Vol.6, No.5, pp.39-46, Oct. (1991).
5. T. Nakata, "Automatic Generation of Expressive Body Movement Based on Cohen-Kestenberg Lifelike Motion Stereotypes," Journal of Advanced Computational Intelligence and Intelligent Informatics, Vol.7 No.2, pp.124-129, (2003).
6. J. R. Quinlan: "Decision Trees and Decision making", IEEE Trans. on Systems, Man and Cybernetics, Vol.20, No.2, pp.339-346 (1990).
7. Seon-Woo Lee, Mase: "Activity and location recognition using wearable sensors", IEEE Pervasive Computing, Vol.1, Iss.3, pp.24-32 (2002).
8. Song, Goncalves, Perona,: "Unsupervised learning of human motion", IEEE Transactions on Pattern Analysis and Machine Intelligence, Vol.25, Iss.7, pp.814-827 (2003).

A Method of Controlling Household Electrical Appliance by Hand Motion in LonWorks

Il-Joo Shim, Kyung-Bae Chang, and Gwi-Tae Park

ISRL, Korea University, 1, 5ga Anam-dong Sungbuk-Gu, 136-713 Seoul, South Korea
{ijshim, lslove, gtpark}@korea.ac.kr
<http://control.korea.ac.kr>

Abstract. We investigate the method for many people to deliver home automation using the EMG that has been used for the sake of diagnosis of neurogenic and myogenic diseases. In order to compute characteristics of the EMG more easily, we use the well-known FFT. With characteristics obtained from FFT method, we propose the motion classifier for functional matching in network and to show the feasibility of home automation by the motion classifier, we have designed that basic household electrical appliance is run by operator's motion in on-line.

1 Introduction

The EMG is an electrical signal that appears neuromuscular action about contracting muscle and is a current that generates from flowing ion between muscle fiber membranes. It has a property that is non-stationary and very feeble. Moreover, as parts of observation in human body, it is a random. So the signal had to amplifier itself and analyze stochastically. At the middle of the 1960's, the appearance of OP-AMP (Operational Amplifier) brought about changes of studying the EMG. Because the signal could amplifier more effortlessly, many kinds of experiments were able to do for proofs. In the 1970's, the main stream of studies was the analysis of the signal's pattern by using stochastic processes [1]-[6]. To analysis the EMG that has a random characteristic like non-stationary and non-prediction [11], many researchers used a method like autocorrelation or power spectral density [1]. But Makhoul suggested that the autoregressive model based on modeling a signal as a linear combination of past value and the present, can be used to estimate a nonstationary process if that process can be classified as local stationary [10][12]. The autoregressive (AR) model is given by the equation.

$$X(n) = -\sum_{k=1}^P a_k X(n-k) + e(n) \quad (1)$$

Where $X(n)$ denotes the recorded signal at discrete time n , a_k are the AR parameters, P is the model order, and $e(n)$ is the noise. In the 1980's, many kinds of the analysing method were introduced [2] [7] [8]. Using the stochastic variables like zero crossings and variance, Sardis tried classifying the signal's pattern in accordance with real action [9]. Blake used the short time Fourier analysis for an analysis about fast movement and constant contraction [13].

In despite of many studies, there are many problems in development (especially, welfare-related) apparatus for using in real life. Because it is difficult to recognize motion from characteristics of the EMG and previous works have shown an analysing algorithm or method for their classifier in an off-line state. For this reason, some researchers have proposed an on-line learning method [17]. Forearm motion classifier, which generates learning data according to an operator's intention, is designed [16]. But, their method is also focused in prosthetic hand controller. So, we have investigated a method for realizing home automation by the EMG at on-line. In order to realize entire system more easily, the LabVIEW software is used and for application of home automation, we selected the LonWorks. For experiments of home automation, air conditioner, television, and light were employed. Entire system consisted of two parts. One is signal-processing area and the other is home automation area. In this paper, we call the part classifying motion the Signal Processing Area and the part realizing home automation from the result the Home Automation Area. It shows in Fig. 1.

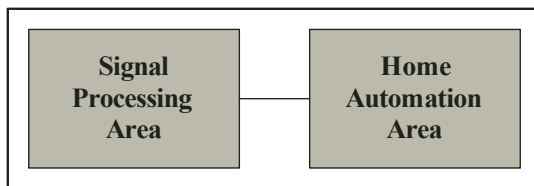


Fig. 1. Entire system

2 Signal Processing Area

2.1 Hardware

The EMG extracted from forearm was recorded using surface EMG electrodes manufactured by KENDALL and was a 33mm-diameter disk. Basically, a set of differential recording electrodes was placed over the forearm. To reduce noise, shielded and twisted pair wire was used and EMG amplifier was designed by method based on [9][14]. The EMG signals were amplified at gains between 1000 and 1500. A range of bandpass filter was from 7 Hz to 517 Hz. For the data acquisition, we used DAQ device (USBDAQ 9100MS, ADLINK Technology). Initial sampling was at 1000 Hz.

2.2 Software

With Software (LabVIEW 6i, National Instruments, Austin, TX), the signal processing was realized. It consisted of four parts. Each part is following (Fig. 2). [15]

I/O Interface: In order to process the EMG that comes in and out DAQ device, we employed the I/O VI (Virtual Instrument) usable in LabVIEW.

Data Positioning: We use a spectrum analysis so that define the frequency domain representation of time domain signal. But if the sequence that we want to extract is not within a defined a size (1000ms), it could not analyze precisely. To solve this problem, a method that the sequence can come in window is designed.

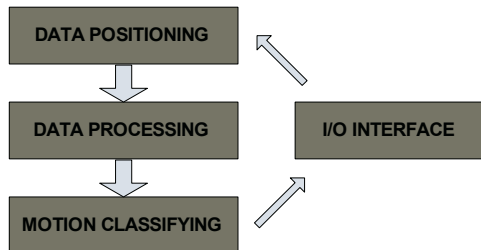


Fig. 2. Block diagram of Signal Processing Area

Data Processing: For analysis of the signal, the ‘FFT (Mag-Phase)’ and ‘NEUMERIC INTEGRATION’ modules in LabVIEW are used. FFT were computed at frequencies from 0 Hz to 1000 Hz at intervals (sampling rate/window width) of 1 Hz. But very little signal occurred above 250 Hz. We excluded components above 250 Hz. And the window that we used was Hanning.

Motion Classifying: With integrating value of the processed signal, we determined which Motion was activated.

2.3 Experimental Condition

The EMG data was measured from electrodes placed on the skin above the muscles controlling the movement. For measurement, we used two motions and the place that electrodes attached is extensor carpi ulnaris. The used motion was EX (Extension) and PR (Pronation). To measure PR, Pronator teres or Pronator quadratus relate to PR has to use. [19][20] But we determined to use only one place for reducing the number of electrode. Measuring the EMG, room temperature is set from 20 to 25C°. Posture is following; sitting an armchair, flexing elbow to 90 degrees and fixing the elbow at the armchair.

2.4 Frequency Analysis of Two Motions

At first, we performed experiment about EX and PR movement in time domain (Fig. 3) and in frequency domain (Fig. 4). From Fig. 3, we found that it is difficult to classify each of the movements. To search for characteristic that each of the motion can be classified, we compared signals in time domain with signals in frequency domain about same data. With comparing time domain with frequency domain, we found possibility that waveforms of frequency domain could be used for classifying each of the movements. As waveforms were not fixed but changed randomly, we obtained the value that averaged a data from each movement in five times. This experiment was performed in two states as WEAK and STRONG. But any distinction was not found in STRONG state. To realize Motion Classifier, we decided to use movements in WEAK state. A comparison that represents EX and PR in WEAK and STRONG state shows in Fig. 5, Fig. 6. In WEAK state, EX shows up-and-downstream from 47 Hz to 52 Hz and from 71 Hz to 77 Hz. Conversely, PR shows down-and-upstream. Of course, although there was the area that shows up-and-downstream or down-and-upstream state, we selected the area appeared symmetrically.

2.5 Design of Motion Classifier

From the results of analysis in frequency, we designed Motion Classifier. For classification, integrating value of two areas was used. With the computed value, we processed functionally. It shows in Fig. 7. Integrating value of the area represented from 47 Hz to 52 Hz was calculated statistically and threshold value was decided from it. And integrating value about from 71 Hz to 77 Hz also was calculated and threshold value was decided. In Fig. 6, V_{t1} is the former and V_{t2} is the latter. If integrating value about the former is greater than V_{t1} and integrating value about the latter is greater than V_{t2} , then it will be classified EX. If one of two integrating values is less than V_{t1} or V_{t2} , then it will be classified PR.

2.6 Performance Test

For performance analysis, three subjects participated in experiment. The threshold value that we decided was $V_{t1}=7.86$, $V_{t2}=11.86$. Changing the threshold value, we observed the performance of system that we designed. It was adjusted from 7.86 and 11.86 to 7.83 and 11.83. EX and PR motion were acted during 2 minutes at intervals of 2 seconds. As long as the value changes from 7.86 to 7.83, recognition ration of all subjects increased. Especially, when V_{t1} changes from 7.84 to 7.83, the recognition ration of subject B increases largely. (Fig. 8) When V_{t1} changes from 7.84 to 7.83, the recognition ration of subject C increases largely. (Fig. 9) Finally, we can search for the V_{t1} value that is able to use commonly by many subjects. But we do not have to overlook the nature that power noise is generated periodically. Generating the power noise, a performance of the range from 7.84 to 7.83 increases largely.

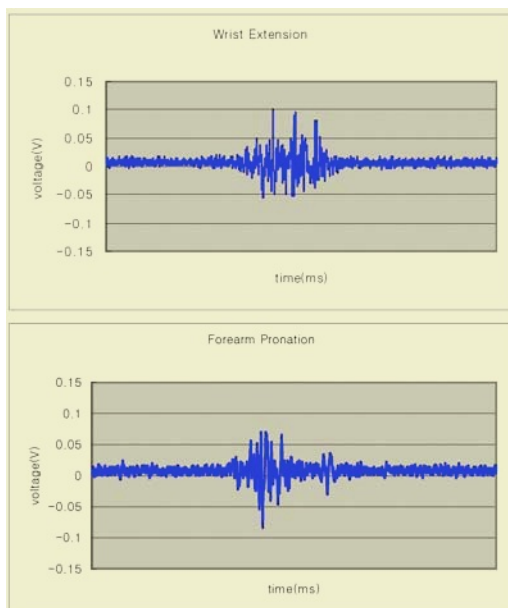


Fig. 3. Extension and Pronation in time domain

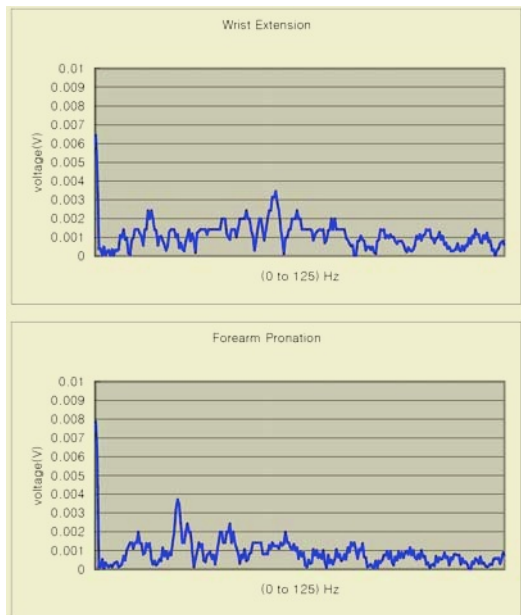


Fig. 4. Extension and Pronation in frequency domain

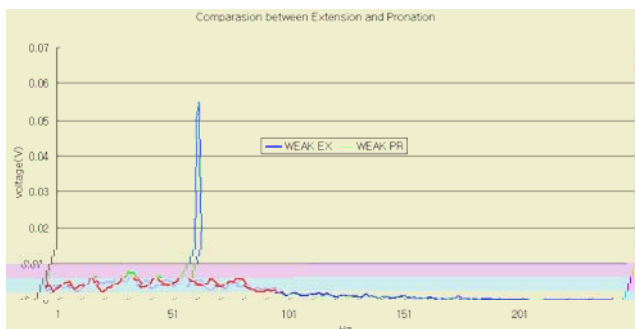


Fig. 5. Comparison of EX and PR in WEAK

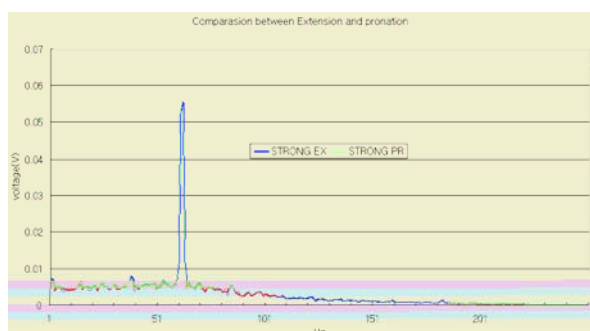
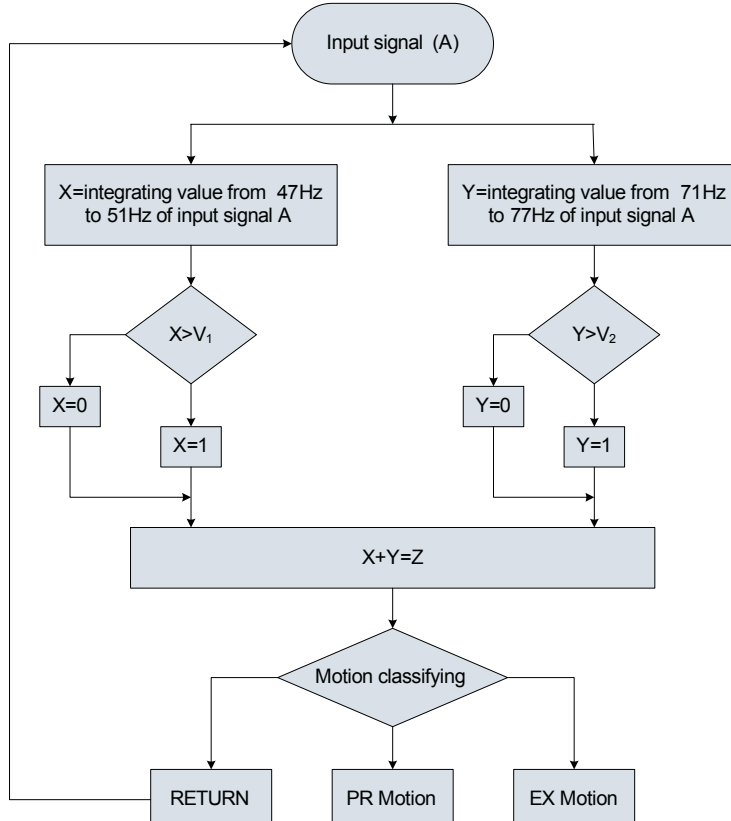
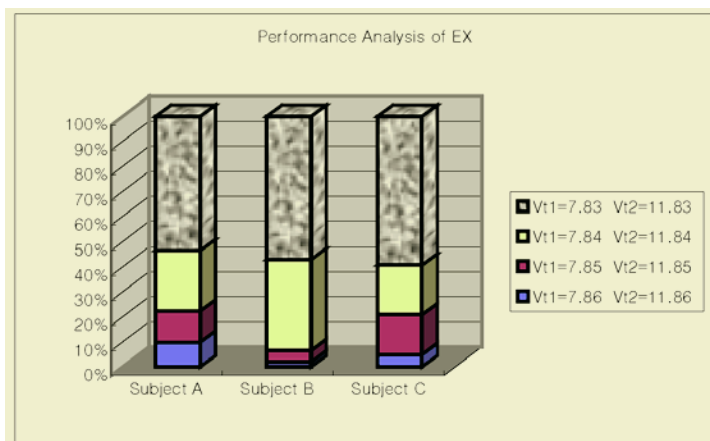


Fig. 6. Comparison of EX and PR in STRONG

**Fig. 7.** Flow chart of Motion Classifier**Fig. 8.** Performance Analysis of EX

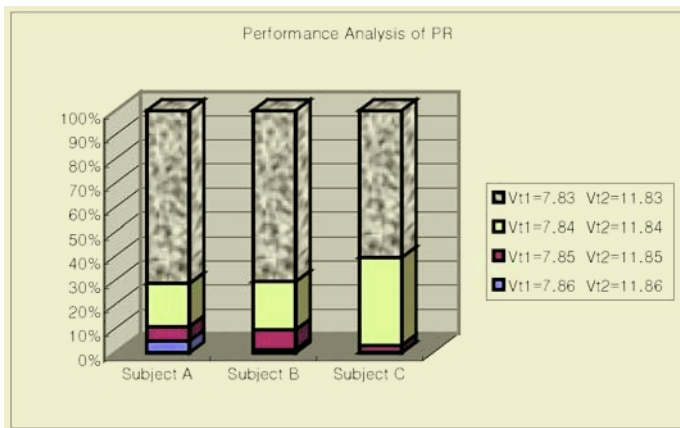


Fig. 9. Performance Analysis of PR

3 Home Automation Area

From the above results, we built demonstration room consisted of three household electrical appliance; Air conditioner, Television, and Light. In order to network each of the appliances, we employed LonPoint module (DI, DO) in LonWorks. Fig. 10 shows home automation area.

After the signal from Signal Processing Area comes in LonPoint Module running in LonWorks, Household Electrical appliance is operated according to defined function. To define a function in LonWorks, we used ‘LonWorks for Window’. The connection of defined function shows in Fig. 11.

Television and light was turned on/off by connected DI 2. And Air conditioner was turned on /off by connected DI 1. DO 2 and DO 3 were the output ports of result that we acted EX motion and DO 1 was the output port of result that we acted PR motion. The operated Household Electrical appliance shows in Fig. 12 and Fig. 13.

In Fig. 12, A is a light and B is a Television. In Fig 13, C is air conditioner and D is a posture of PR.

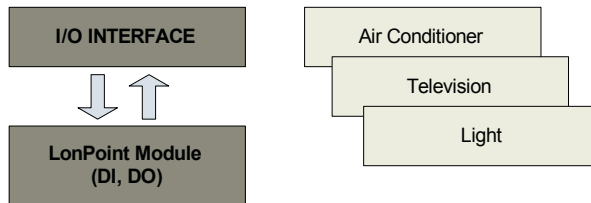
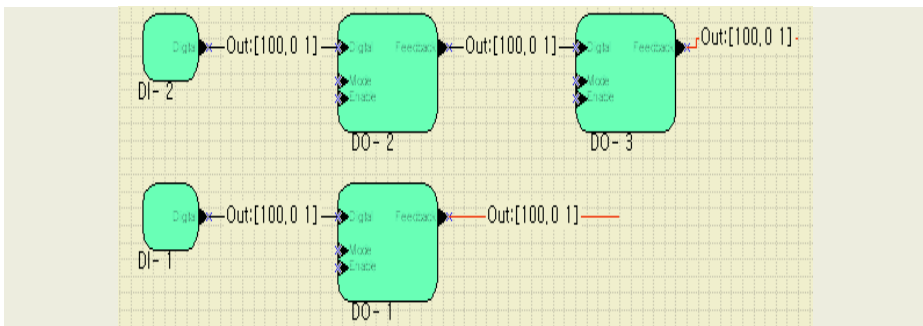
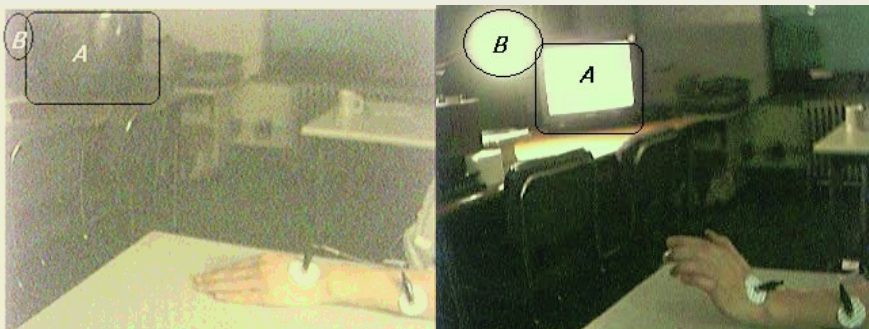
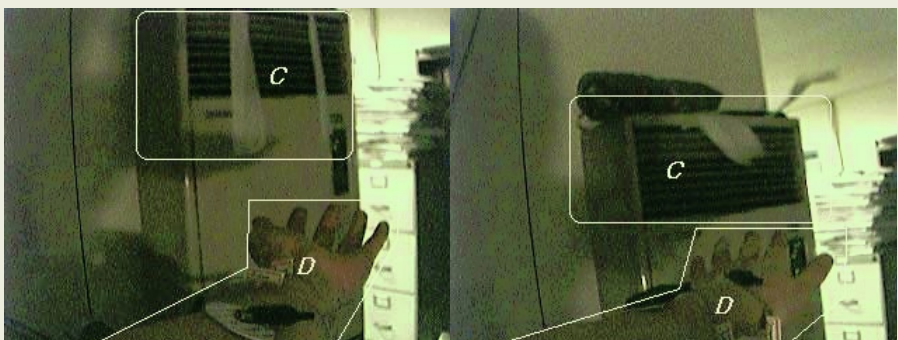


Fig. 10. Block diagram of Home Automation Area

4 Conclusions

In this thesis, the EMG that had used for diagnosis of neurogenic or myogenic diseases was studied for the purpose of applying another field. In other words, due to the

**Fig. 11.** Connection of defined function**Fig. 12.** Television and Light operation from EX**Fig. 13.** Air conditioner operation from PR

growth of Ethernet and development of network technology, the applications in many fields have diversified and complicated gradually. But, it is difficult for people who are congenital or acquired deformities like hemiplegia or paralysis to use above technique. So, to solve this problem, we designed Motion Classifier so that they might control household electrical appliance in real life. For application, we performed the experiment. And from the result, we found feasibility that many people could control household electrical appliance in real life. We will have future work for increasing recognition ratio and reducing power noise.

References

1. H. G. Kwantny et al., "An application of signal processing techniques to the study of myoelectric signals," *IEEE Trans. Biomed. Eng.*, vol. BME-7 (1970) 303-312
2. D. Graupe and W. K. Cline, "Functional Separation of EMG Signals via ARMA Identification Methods for Prosthesis Control Purposes," *IEEE Trans. Systems, Man and Cybernetics*, Vol. SMC-5 (1975) 252-259
3. P. Lago and N. B. Jones, "Effect of motor-unit firing time statistics on e.m.g. spectra," *Med. Biol. Eng. Comput.*, vol. 15 (1977) 648-655
4. R. S. Le Fever and C. J. De Luca, "The contribution of individual motor units to the EMG power spectrum," in proc. 29th ACEMB, vol. 56 (1976)
5. E. Shwedky, R. Balasubramanian, and R. N. Scott, "A nonstationary model for the electromyogram," *IEEE Trans. Biomed. Eng.*, vol. BME-24 (1977) 417-424
6. C. J. Luca, "Physiology and Mathematics of Myoelectric Signals," *IEEE Trans. Biomed. Eng.*, vol. BME-26 (1979) 313-325
7. M. H. Sherif, R. J. Gregor, and J. Lyman, "Effects of Load on Myoelectric Signals: The ARIMA Representation," *IEEE Trans. Biomed. Eng.*, vol. BME-28 (1981) 411-416
8. O. Paiss and G. F. Inbar, "Autoregressive Modeling of Surface EMG and Its Spectrum with Application to Fatigue," *IEEE Trans. Biomed. Eng.*, vol. BME-34 (1987) 761-770
9. G. N. Sardis and T. P. Gootee, "EMG Pattern Analysis and Classification for a Prosthetic Arm," *IEEE Trans. Biomed. Eng.*, vol. BME-29 (1982) 403-412
10. J. Makhoul, "Linear Prediction: A Tutorial Review," proceedings of the IEEE, vol. 63 (1975) 561-580
11. E. Shwedky, R. balasubramanian, and R. N. Scott, "A Nonstationary Model for the Electromyogram," *IEEE Trans. Biomed. Eng.*, vol. BME-24(1977) 417-424
12. G. Hefftner and G. Jaros, "The Electromyogram (EMG) as a Control Signal for Functional Neuromuscular Stimulation-Part I: Autoregressive Modeling as a Means of EMG Signature Discrimination," *IEEE Trans. Biomed. Eng.*, vol. BME-35 (1988) 230-237.
13. B. Hannaford and S. Lehman, "Short Time Fourier Analysis of the Electromyogram: Fast Movements and Constant Contraction," *IEEE Trans. Biomed.*, vol. 33 (1986) 1173-1181
14. G. V. K. Prasad, S. Srinivasan, and K. M. Patil, "A New DSP-Based Multichannel EMG Acquisition and Analysis System," *Computers and Biomedical Research* (1996) 395-406
15. J. P. Giuffrida and P. E. Cargo, "Reciprocal EMG Control of Elbow Extension by FES," *IEEE. NEURAL SYSTEMS AND REHABILITATION Eng.*, vol. 9 (2001) 338-345
16. D. Nishkwa et al., "On-line learning based electromyogram to forearm motion classifier with motor skill evaluation," *JSME Journal.*, vol. 43, no. 4, Series C (2000) 906-915
17. Fukuda, O., Tsuji, T., and Kaneko, M., "An EMG Controlled Robotic Manipulator Using Neural Networks," *Proc. Of IEEE Int. Workshop on Robot and Human Communication* (1997) 442-447, 1997
18. M. A. L. Daniels and C. Worthingham, Muscle Testing techniques of manual examination, 5th Ed. Philadelphia: W.B. Saunders Company (1986) 122-129
19. F. Edward and M. D. Delagi, Anatomic Guide for the Electromyographer. 2nd Ed. Illinois: CHARLES C THOMAS (1981) 34-63

Contribution of Biological Studies to the Understanding and Modeling of Skilled Performance: Some Examples

Atsuko K. Yamazaki¹ and J. Rudi Strickler²

¹ Department of Manufacturing Technologists, Institute of Technologists,
333 Maeya Gyoda-shi, Saitama, Japan 361-0038
atsuko@iot.ac.jp

² University of Wisconsin-Milwaukee, Great Lakes WATER Institute,
600 E. Greenfield Ave, Milwaukee, WI 53204, USA
jrs@uwm.edu

Abstract. A “skilled performance” by a human involves the automatization of a skill, which in turn is closely related to sensory-motor processing. Behavioral patterns of invertebrate animals are often described in relation to their simple sensory systems. Following biological observations, skill-based models for animal behaviors have been constructed to explore the fundamental systems of adaptive skill acquisition. This paper describes the underlying properties of “skilled performance” and how biological studies on animals that are less complex than humans can contribute to the understanding of task-based performance. The creating of a model for the skill is discussed by giving some examples.

1 Introduction

The learning theory of *automaticity* has been applied to performance-based tasks such as music conducting [1] and the sub-skills of drawing [2]. A study of skilled performance suggests that the brain creates a model for the performance of a particular task. The model becomes a guide for the brain to control the movements of muscles. Performing the tasks becomes *automatized* and the brain doesn't need to use its higher center of thinking for each task, once the skill is mastered. In automatic processing, a small number of specific brain sites related to sensory-motor processing become responsible for the activity [3]. Studies on automatic and controlled processes in human behavior also indicate that the automatization of a skill can be developed through consistent mapping to repeated stimuli, in which the response to the stimulus is consistent across extended periods of time for a certain task. The model for an automatized skill evolves under controlled mapping responses to various stimuli and performance improvement occurs through many trials in a controlled process. Hence, these studies indicate that constructing a model to describe a skill, as well as the process of acquiring a skill, is important for the study of skilled performance [3].

Non-verbal knowledge works as a basis of meaningful behavior in many cases where it functions for achieving a certain goal. An animal gathers information about its environment, and makes predictions from the information to perform a meaningful behavior to cope with the challenges of its environment. The stage of repeated trials

in the automation process of skilled performance can be interpreted as information gathering and computation under a certain environmental condition [4]. The information is stored in a certain form to give a cue for an effective response to an environmental change. In this sense, a key to illustrate a skill requires the understanding of its basic mechanism for obtaining, storing, and utilizing non-verbal knowledge as useful information. Neurological studies of learning suggest that flexible synaptic connections in the brain are involved in learning [5]. This may indicate that knowledge associated with skilled performance can be acquired by creating and changing a connection model of the brain.

2 Biological Input to Skilled Performance Research

Human behavior and human brain function are among the most complex in animals. At the other end of the complexity spectrum, behavior displayed by many invertebrates has been studied to understand what underlies animal behavior [6]. They do not show any sort of behavior derived from intellectual cognition like humans. They do not use spoken language for communication. However, they often show extraordinary degrees of learning and use knowledge they obtained from their environment to perform a meaningful task. They exhibit changes in their behavior to comply with their surroundings and these behaviors are often closely related to skilled movements and adaptive sensory filtering. The crayfish brain, as one kind of the arthropod brain, is sometimes referred as a "micro-brain" [7]. Although it contains relatively a small number of nerve cells compared with the vertebrate brain, crayfish show a variety of complex behaviors including locomotion, escape reactions, threatening and copulation, as well as their adaptive motions by learning.

A group of planktonic animals, the copepods (they are the most abundant members of the zooplankton community), are often referred as cousins of crayfish since they are microscopic crustaceans. Most copepods are between about 0.5 and 10 millimeters in size. They have antennae that allow them to sense food and environmental changes, as well as to distinguish mates from prey and predators. These zooplankters move autonomously and react to the various changes in their environment, contrary to the meaning of the word, "plankton". They constantly alter their behavior in response to environmental conditions [8]. The behavior of planktonic copepods has been studied in relation to their environment and their sensory systems. Sensory input, central processing, with behavior as the output in this research area have been extensively examined [9]. Because of the relative simplicity of their nervous systems, their body plans and the great diversity of their ecologically relevant behaviors, they can be considered appropriate animals for neuro-ecological studies.

In his microscopic studies, Strickler [8] has shown that copepods choose paths according to their environment. Koehl and Strickler [10] found that a copepod managed to catch food by moving its mouth parts while generating a flow around the parts. This catching movement was made only when food was within a certain volume in front of the animal. It also used its current-generating "skills" to navigate food into this volume. Hwang and Strickler [11] conducted an experiment on copepod behavior to examine whether copepods can differentiate prey from predator hydro-mechanically. Their results show that copepods can distinguish between hydro-mechanical signals generated by an external source and those created by its own feed-

ing current. The data also suggests that they may recognize simple patterns specific to signal sources. These observational studies reveal that copepods use information from flow currents surrounding them and even use their knowledge of flow currents in order to produce a meaningful flow around them.

Doall et al. [12] discovered that both male and female copepods swim with a normal speed of about 10 millimeters a second. But when the male crosses the track where a female has just swam, he changes course to follow her track, accelerating to speeds of 30 or 40 millimeters a second in order to catch up with her. Moreover, while tracking her chemical trail, the male will disturb the signal skillfully to prevent that another mate or a predator could follow the trail as well [13]. These observational results reveal that the fast and skillful performances of copepods appear to be very complex despite their rather simple sensory systems.

A copepod typically displays normal swimming behavior with a hop-and-sink pattern. The animal executes about one hop per second using the time between hops to perceive hydro-dynamical and chemical signals. In his recent study of fish preying on copepods, Strickler et al. (in press) [14] suggests that copepods may alter their sequence of swimming patterns to escape from the predators. Fish, on the other hand, may learn the swimming patterns to efficiently catch the food. The patterns may differ according to species of copepods and a certain species may have a certain pattern. An experiment on blue jays' food searching patterns by Bond and Kamil [15] suggests that polymorphisms in the searching pattern may have contributed to the evolution of moths. Both studies indicate that knowledge for survival involves perceptual and sensory capabilities, and cognition associated with learning should be studies from the perspective of a biological system.

3 Skill-Based Behavior Models Inspired by Biological Studies

Modeling of task-based behaviors has been done to simulate or to account for biological observational results on animals of lesser complexity. Yamazaki and Kamikowski [16] illustrated constructing models to simulate the behavior of zooplankton and phytoplankton in relation to their external and internal changes, based on results from observational studies on their behaviors. Even though the adaptive parts of the models were still limited, comparison of the results from the simulations with the ones from the observational studies showed that fine-tuning the different relations among the internal states can be a good basis for simulating the adaptive nature of behavior. The study also indicated the need for a scheme in which simple behavior can be simulated as an outcome from interactions among small components associated with observable behaviors. Their view of behavior modeling characterizes animal behavior as the inter-connection among internal and external factors formulated in explicit rules. Yet, the outcome of the system should be emergent, and not governed only by upper-level rules.

Behavioral experiments on hawk moth showed that they learned to detect both the color and the position of artificial flowers for which they received the reward. They used a strategy based on color information, which can be considered as a stimulus response of the moth, in the first phase of a learning session and then shifted to use position information obtained in the phase. Balkenius et al. [17] constructed a computational model based on behavioral data and on the sensitivities of the moth photore-

ceptors obtained in the experiments. The model consists of a number of interacting behavior systems that are triggered by specific stimuli and control specific behaviors. The ability of the moth for learning and its adaptive strategies for searching flowers were reproduced accurately by the model.

From the same prospective on behavior modeling, Beer [18] introduced the concept of *minimally cognitive behavior*, which he defined as the simplest agent-environment system. Beer and his colleagues implemented this concept in their experiments [19]. They experimented with an agent with short-term memory and a narrow visual range to show that the perception of body-scaled affordance can evolve to more complex affordance.

4 Discussion

Neural systems, even in small animals contain ascending pathways through which sensory information reaches the “brain”, and descending pathways relay motor commands from the “brain” to the motor neurons. This schema is far simpler than the process of acquisition and performance of a skill by a person. However, if we look at a complex process as an integrated coordination of much more primitive biological functions, the study of behavioral components, as seen in lower organisms, should provide models for the functional components. Additionally, the behavior modeling experiments described above indicate that the description of underlying behavior pattern is necessary to understand and illustrate more complex behaviors, and understanding its sensory-motor processing can give cues to illustrating a skilled performance. Research results from observing and modeling the behavior of simpler animals will provide the framework of how to illustrate each piece of the integrated components. When a person performs an automatized skill, real-time decision making derived by motor-sensory system is required [3]. Quick responses produced by the sensory system of a primitive organism, such as a crayfish, a zooplankter, or an insect should be considered as examples for constructive elements in a more complex sensory-motor system. Also, behavior schemata observed in organisms of less complexity can give keys for creating modules to be integrated to illustrate skilled performance.

References

1. Lonis, D. J.: Development and Application of a Model for Teaching of Conducting Gestures. Ed. D. Diss., University of Illinois, (1993)
2. Bloom, B.S.: Automaticity - the hands of feet of genius: Educational Leadership. Vol. 43. No.5. (1986) 70-77
3. Schneider, W., J.M. Chein: Controlled and automatic processing: behavior, theory, and biological mechanisms. Cognitive Science, Vol. 27. (2003) 525-559
4. Tzelgov, J., V. Yehene, L. Kotler, A. Alon: Automatizing algorithmic processing: The learning of linear ordering relations. Journal of Experimental Psychology: Learning, Memory, and Cognition, Vol. 26. (2000). 103-120
5. Kandel, E.R., J.H. Schwartz, T.M. Jessell: Principles of Neural Science, 4th ed. McGraw-Hill Companies, Inc, New York (2000)
6. Griffin, D. R.: Animal Thinking. Harvard University Press, Cambridge, MA (1984)

7. Mizunami, M., F. Yokohari, M. Takahata: Exploration into adaptive design of the arthropod "microbrain". *Zoological Science*. Vol. 16. (1999) 703-709
8. Strickler, J.R.: Feeding currents in calanoid copepods: Two new hypotheses, In: Laverack, M. S. (ed.): *Physiological adaptations of marine animals*, Symposium of Society for Experimental Biology, Vol. 39. (1985) 459-458
9. Weatherby, T.M., P.H. Lenz: Mechanoreceptors in calanoid copepods: designed for high sensitivity, *Arthropod Structure & Development*, Vol. 29, (2000) 275-288
10. Koehl, M.A.R., J.R. Strickler: Copepod feeding currents: Food capture at low Reynolds number. *Limnol. Oceanogr.*, Vol. 26 (1981) 1062-1073
11. Hwang J-S, J.R. Strickler: Can Copepods differentiate Prey from Predator Hydromechanically?. *Zoological Studies*, Vol. 40(1) (2001) 1-6
12. Doall, M.H., S.P. Colin, J. Yen, J.R. Strickler: Locating a mate in 3D: The case of *Temora longicornis*. *Phil. Trans. R. Soc. Lond. B* 353, (1998) 681-690
13. Yen, J., A.C. Prusak, M. Caun, M. Doall, J. Brown, J.R. Strickler: Biomimicry: Signaling during Mating in the Pelagic Copepod, *Temora Longicornis*, In: Seuront, L. and Strutton, P. G. (eds.): *Handbook of Scaling Methods in Aquatic Ecology*, CRC Press, London, (2003) 149-159
14. Strickler, J.R., J. Marino, N. Radabaugh, J. Ziarek, A. Nihongi: Visibility as a Factor in the Copepod - Planktivorous Fish Relationship. *Scientia Marina*, (in press)
15. Bond, A.C., Kamil, A.B.: Apostatic selection by Blue Jays produces balanced polymorphism in virtual prey. *Nature*, Vol. 395. (1998) 594-596
16. Yamazaki, A.K, D. Kamykowski: Modeling Planktonic Behavior as a Complex Adaptive System, In: Seuront, L. and Strutton, P. G. (eds.): *Handbook of Scaling Methods in Aquatic Ecology*, CRC Press, London, (2003) 543-557
17. Balkenius, A., A. Kelber, C. Balkenius: A Model of Selection between Stimulus and Place Strategy in a Hawkmoth, *Adaptive Behavior*, Vol. 12, No. 1, (2004) 21-35
18. Beer, R.D.: Toward the evolution of dynamical neural networks for minimally cognitive behavior, In: Maes, P. et al. (eds): *From Animals to Animats 4: Proc. 4th Int. Conf. on Simulation of Adaptive Behavior*, MIT Press, Cambridge, MA, (1996) 421-429
19. Slocum, A.C., D.C. Down, R.D. Beer: Further experiments in the evolution of minimally cognitive behavior: From perceiving affordances to selective attention, In: Mayer, J. A. et al. (eds): *6th Int. Conf. on Simulation of Adaptive Behavior*, MIT Press, Cambridge, MA, (2000) 430-439

Measurement of Human Concentration with Multiple Cameras

Kazuhiko Sumi, Koichi Tanaka, and Takashi Matsuyama

Graduate School of Informatics, Kyoto University, Kyoto 606-8501, Japan

sumi@vision.kueee.kyoto-u.ac.jp

<http://vision.kueee.kyoto-u.ac.jp/>

Abstract. We propose a new method to estimate human change of concentration from multiple camera views of the human. In our method, human state of concentration is observed as self-load, defined as energy injected in a period to keep and manipulate his/her body. If a person is concentrating to a certain task, he/she will brace himself/herself for better results, and energy consumption will increase. To confirm our idea, we developed a method to calculate self-load from multiple view of the human. We conducted an experiment in which test subjects have different level of complexity of task. Self-load of the subjects showed the positive correlation with the complexity of the task. We have convinced that self-load can be used to characterize the concentration of person being observed.

1 Introduction

One of the big difference between human-to-human interaction and human-to-computer interaction is timing. We human can measure timing to start conversation with another human. Measuring timing is a very sophisticated social action, which is not achieved by a computer yet. To realize such a behavior, it is important to have a good sensing systems to observe the human action and his/her internal state. In this research we focus on sensing human internal state, such as concentration, interest and frustration.

So far, many studies on human observation were carried out. Most of them are recognizing intentional signal in communication. Such researches include gesture recognition, facial expression recognition, lip reading, and voice recognition. Those methods are quite reasonable when the person is already interacting with a computer. On the other hand, if a person is not involved in communication, but is engaging in other personal jobs, the channel of communication is not established. In such cases, a computer should estimate the human interest, intention and feeling through one-way observation. This will often happen when assisting a human involved in a work, such as driving a car, operating a machine, traveling in an unfamiliar places, looking for something, and so on. If the person is doing something in concentration, it is not a good manner to offer help. But if the person is wondering, it might better to support him/her. Thus observing a human without interaction is a challenging subject.

Human internal state such as stress or frustration can be measured through a various sensors. Picard developed wearable sensors for human observation[4] using galvanic skin response, blood volume pressure, and electromyograph. Fernandez applied the system to measure frustration of a human using a computer[5]. However, wearing such a device may not be comfortable, and sensing from outside of a human is preferred. Mota analyzed learner's interest level by measuring 2D pressure distribution between a human and a chair under the human[6]. This system provides better comfort, but, still need to be contacting toward something. To realize non-contact human observation in a free space, we are interested in observing a human from cameras.

Cameras can be used to observe a human through various cues of human behaviors, such as, eye and sight[8], expression[7], gesture[2], and body posture[3]. To understand a human better, it is preferred to get a close up view of the human. However, in a ordinary room, it is not easy to get a close up view of his/her face all the time. Thus we are interested in observing a human only with cameras with wide field of view.

In this research, we estimate the concentration, in other words, how much is the human is occupied by the task he is doing. We use multiple cameras surrounding the human to be observed. To achieve a quantitative analysis we introduce new measure, which is referred to as self-load. Self-load is a energy consumption per unit time. The energy consumption is derived from static and dynamic posture of the observed human.

In the following section, first we define self-load and its derivation from his/her posture in Section 2. Then, we explain the pose estimation method using multiple cameras in Section 3. To confirm the effectiveness of our proposal, two series of experiments are carried out in Section 4. Finally, we conclude our proposal in Section 5.

2 Calculation of Self-load Using Cylindrical Human Body Model

In human body condition, compared with the state of doing nothing, thus no stress in his/her muscle, the work load which supplies the energy per unit time to the present body expression is calculable. The amount of energy consumption is referred to as self-loads. Although self-load is a physical amount of energy and is not a mental state, it is reasonable to assume that there is a high correlation between physical energy consumption and mental concentration.

First, the amount of energies needed about maintenance of a certain body posture and operation is defined by potential energy, movement energy, and posture maintenance energy. Posture maintenance energy is the energy required in order to maintain the posture and to keep muscles tension. If the joint is in the neutral position, posture maintenance energy is zero. It is expressed with the difference from the neutral state. If a person is putting his/her part on a structure, posture maintenance energy should be deducted, because he/she can save stress of his/her muscle. However, it is difficult to measure a force between

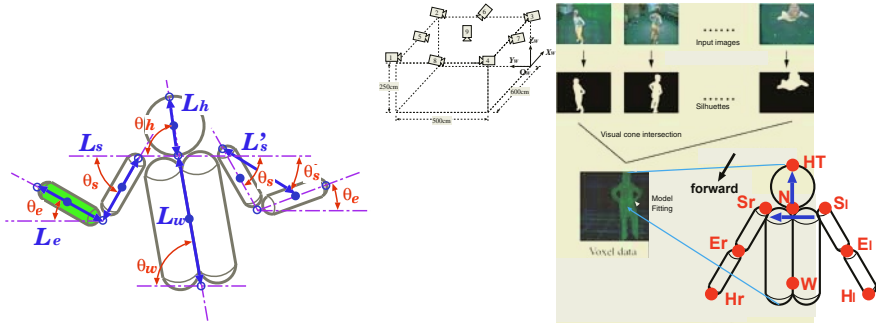


Fig. 1. A cylindrical human body model and parameters of its parts (left), and schematic diagram of human upper pose estimation from multiple camera images via 3D volume of a human (right)

the body and the structure, we will not consider the case in this research. Instead, we only treat a human with stable supporting energy.

In this chapter, we will apply Hill's muscle model[9], which considers an actuator pulling two springs with dumper, to calculate the sum of the energy consumed by a body part at a certain angle. Also, we assume that muscle actuation is iso-tensional, and the tension is only caused by gravity. This assumption is not satisfied when a person is pressing or pulling a hard structure with his muscle or when he is stressing his body. We don't consider such invisible cases in this study. Thus, we will consider visible part of posture maintenance energy which is expressed by the gravitation moment on a body part.

We model a human body by a set of cylinders shown in Figure. 1(left). A unit part of the body model is a single cylindrical part. Instantaneous self-load of the unit \$sl_e\$, lower arm for example, is the sum of potential energy \$sl_e^p\$, motion energy \$sl_e^m\$, and posture maintenance energy \$sl_e^k\$ shown in Equation 1.

$$sl_e = sl_e^p + sl_e^m + sl_e^k = m_e g h_e + \frac{1}{4} m_e L_e \omega_e(t)^2 + sl_e^k \quad (1)$$

where \$g\$, \$L_e\$, \$m_e\$, \$h_e\$, \$\omega_e(t)\$ are G-forces, length of the arm, mass of the arm, height of the arm center from the lowest position, and angular velocity of the arm at time \$t\$, respectively. Posture maintenance energy of the lower arm \$sl_e^k\$ is:

$$sl_e^k = m_e g \frac{L_e}{2} \cos\left(\frac{\theta_e}{2}\right) - sl_e^k_{init} \quad (2)$$

And its initial value is \$sl_e^k_{init} = \frac{1}{2} m_e g L_e\$. We can calculate self-load of upper arms \$sl_{sl}\$, \$sl_{sr}\$, and that of chest \$sl_w\$ in the same way. Instantaneous self-load of the whole upper body \$sl\$ is the sum of self-load of all the parts:

$$sl = sl_{el} + sl_{er} + sl_{sl} + sl_{sr} + sl_w \quad (3)$$

Self-load of the body SL is defined by the temporal average of the instantaneous self-load during the time interval T :

$$SL = \frac{1}{T} \sum_{t=0}^T sl \quad (4)$$

3 Pose Estimation from 3D Volumetric Representation

We estimate the pose parameters required for self-load calculation from the 3D volumetric representation. The 3D volumetric representation is derived by the intersection of visual cones[11]. For each visual cone, its top vertex is the camera center and its base plane is the silhouette of the body taken by the camera. This step is show in Figure.1(right). The model of upper body consists of 6 parts.

In the fitting process, the characteristic point of the body, head peak **HT** is searched first. Then from **HT**, center of neck **N**, right shoulder **S_r**, and left shoulder **S_l** are searched in this order. From the neck **N**, trunk of the body is scanned and waist center **W** is located. From the shoulders **S_r** and **S_l**, each arm is scanned toward hand, and elbow joint **E_l**, **E_r**, and hand tips **H_l**, **H_r** are located.

4 Experiment

To confirm our idea, we conducted three experiments. First, we have examined the pose estimation accuracy of our method using life size figure of a human. Our experiments were carried out in a laboratory shown in Figure. 1(left) with 9 cameras. This multiple camera system was calibrated in advance, and its voxel resolution is 2cm, its frame rate is 9 fps. The pose estimation result shows the worst angular error of arms, waist, and head are 13.8deg, 7.0deg, and 6.0deg respectively. This error is acceptable for self-load estimation. However, the fitting algorithm sometimes failed when arms are contacted in parallel to trunk of the body. More robust fitting algorithm are required for future work.

4.1 Self-load Measurement

In this experiments, we evaluated correlation between task complexity and self-load measure. We designed two scenarios. Each of them has three different levels of complexity. Total 7 subjects participated in the experiments. The set up is shown in Figure 2(left). Due to limitation of the 3D reconstruction space, the pose of the subject is limited to a sitting pose and we couldn't fit lower body in this setup.

Before the real experiment, the subject are required to wait until the experiment is ready. During this period, which is 28sec long, a TV program is displayed on the PC screen and neutral pose are measured. From the measurement, we calculated the initial self-load for each subject.

In the first experiment, which we refer to as “clap test”, a white box in the black background on another PC screen appeared 4 times during the 28sec

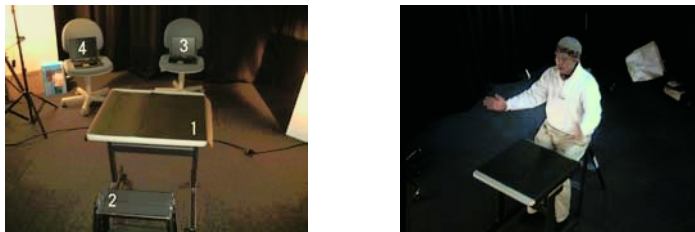


Fig. 2. Self-load measurement set up. (left) – 1: Desk, 2: Stool, 3: Task Screen, 4: TV Screen –, and a snap shot of the clap test



Fig. 3. Screen shown to the subject during clap test

session. A subject was requested to clap his/her hands, when he/she recognize a white box before it disappears. The duration of white box is same in a session but it becomes shorter, shown in Figure. 3, and the task becomes harder. Each subject performs three sessions and self-load is measured for each session. Figure. 2(right) shows one of the snapshot during this experiment.

In the second experiment, which we refer to as “catch test”, a button with “START” mark and a moving box with “CATCH” mark, shown in Figure. 4(left), are displayed on the screen. A session starts when the subject clicks the mouse on “START”, then “CATCH” starts running on the screen. The subject is requested to follow the moving box and click the mouse when it is on “CATCH” mark. The subject is requested to catch as many box as possible during the 28 sec session. The moving box randomly changes its direction but the velocity is the same within a session. The velocity increases 200, 400, 600 (pixel/sec) as the level of session increases. During the session, each subject performs three sessions with different complexity and self-load is measured. Figure 4(right) is a snap shot during this experiment.



Fig. 4. Screen shown to the subject during the catch test (left) and a snap shot of the experiment (right)

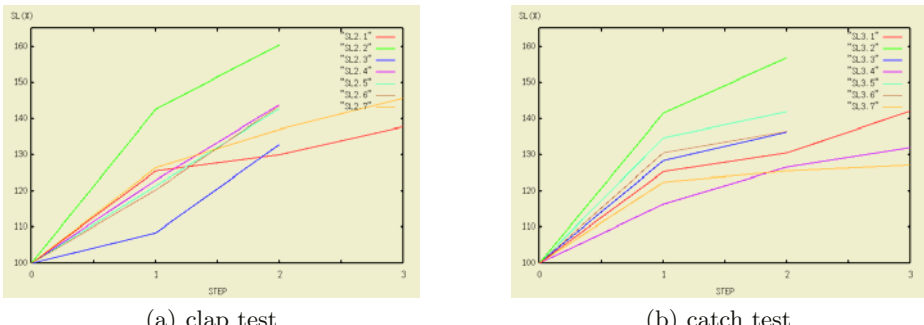


Fig. 5. Complexity of test and self-load $SL(\%)$

4.2 Result and Discussion

The initial self-load sl_0 measured before the experiment is distributed from 400 to 474. As we discussed in Section 2, the initial self-load depends on the body shape and initial pose of the subject and it does not have importance. In the following two experiments, self-load SL is normalized, and replaced by $SL' = SL/sl_0$.

Figure 5 (A) and (B) show the relationships of *SL* measure and complexity level of clap test and catch test respectively. Both of the figures show the strong correlation between *SL* and the complexity level, suggesting that *SL* can be used as the index of concentration.

In both tests, there are several subjects whose SL drops at level 3 complexity. However, it proved that some of them are moving their hand so fast and the system cannot recover the 3D volume due to the motion blur. The rest of them are those who gave up performing the requested task and not involved any more. So, those samples, which look conflicting with our estimation, do not conflict actually. Such samples are rejected from the Figures.

The difference between clap test and catch test is that catch test requires the subject continuous motion in proportion to the complexity. This implies contribution of kinetic energy to self-load increases as the complexity increases. However, we found that most of the dominant increase is posture maintaining energy. This suggests that concentration will appear as leaning forward pose. The result will match the previous work by Mota[6].

5 Conclusion

A feasibility study on observing human concentration with multiple cameras is described. A new measure, which is referred to as self-load, is proposed. Self-load is a energy consumption of the observed human keeping the same pose and motion. The pose is estimated from the 3D volumetric representation of the observed human and it is derived from 3D shape reconstruction technique like visual hull.

Through two scenarios of evaluation, we confirmed strong correlation between self-load and concentration. Also, we discovered leaning forward pose is

appearing when a human is concentrating to a task. Currently, the situation in which we can measure self-load is limited due to the limitation of pose fitting and invisible force of the observed human. Never the less, it is a epoch that estimating human internal state with images is feasible.

Further study will include wider range of scenario to observe human concentration, estimation of human state other than concentration, and integration with other modality such as face recognition, sight line recognition, and speech recognition.

References

1. L. R. Rabiner and B. H. Juang, "Fundamentals of Speech Recognition", Prentice Hall, 1993
2. Andrew Wilson, Aaron Bobick. "Learning Visual Behavior for Gesture Analysis". IEEE Trans. PAMI, vol. 21, no. 9, pp.884-900, 1999
3. T.B. Moeslund and E. Granum. "A Survey of Computer Vision-Based Human Motion Capture," CVIU, vol.81, no.3, pp.231–268, 2001
4. R. W. Picard and J. Healey, "Affective Wearables," Personal Technologies, Vol. 1, No. 4, pp. 231-240, 1997
5. R. Fernandez and R. W. Picard, "Signal Processing for Recognition of Human Frustration," Proceedings of ICASSP98. MIT MediaLag TR 447. 1997
6. S. Mota and R. W. Picard (2003), "Automated Posture Analysis for Detecting Learner's Interest Level." Workshop on Computer Vision and Pattern Recognition for Human-Computer Interaction, CVPR HCI, June, 2003
7. Michael J. Lyons, Julien Budynek, and Shigeru Akamatsu, "Automatic Classification of Single Facial Images", IEEE Trans. PAMI, Vol.;21, no.12, pp.1357-1362, 1999
8. Seki Makito, Shimotani Mitsuo, Sumi Kazuhiko, Measurement of Driver's Facial Direction, proc. IMEKO XV World Congres, pp.51-56, June, 1999
9. A.V. Hill, "First and last experiments in muscle mechanics", London, Cambridge University Press, 1970
10. D.M.Gavrila and L.S.Davis. 3-D model-based tracking of humans in action: a multi-view approach. in Proc. IEEE Computer Vision and Pattern Recognition, San Francisco, 1996.
11. Takashi Matsuyama, X. Wu,Takeshi Takai, and Toshikazu Wada: Real-Time Dynamic 3D Object Shape Reconstruction and High-Fidelity Texture Mapping for 3D Video, IEEE Trans. on Circuits and Systems for Video Technology, Vol.CSVT-14, No.3, pp.357-369, 2004

Constructive Induction-Based Clustering Method for Ubiquitous Computing Environments

Takeshi Yamamoto¹, Hirokazu Taki¹, Noriyuki Matsuda¹,
Hirokazu Miura¹, Satoshi Hori², and Noriyuki Abe³

¹ Graduate school of Systems Engineering, Wakayama University

² Institute of Technologists

³ Faculty of Computer Science and Systems Engineering, Kyushu Institute of Technology

Abstract. This paper describes a classification criteria-structuring method for handling exception cases. Clustering technology is utilized to classify large amounts of data effectively. In current clustering technology, however, it is impossible for a system to classify all data completely, due to exceptions in the data. In an ubiquitous computing environment, exceptions arise due to changes in the environment. We propose an architecture in which the system changes classification criteria and rules using constructive induction.

1 Introduction

Enormous amounts of data are produced in the modern information-oriented society, and as a result, effective selection technology is required for extracting necessary data from the huge quantities available. Clustering technology methods provide one type of solution to this problem. Data mining technology, which extracts relationships from large quantities of data, is also useful. Here, we consider clustering methods developed to process data in ubiquitous computing environments into meaningful sets. Because the produced data in the sensor network of the ubiquitous computing environments have many kinds of characters. We also consider current data mining methods and criteria for selecting important relations for use in clustering technology.

Clustering technology interprets data according to application needs, such as image or sound recognition, classifying data by using meaningful parameters according to the data situation. Current clustering technology uses given criteria or conditions learned from examples. In such cases, the technology-user needs to provide in advance the criteria for segmenting the data. However, where exceptions occur, correct segmentation may not be possible, due to the difficulty of defining all cases. Therefore, in an ubiquitous computing environment, the system must be able to reconstruct classification criteria flexibly.

Current clustering methods classify the original data set (e.g., image data) into some classes using classification criteria (shown in Fig. 1). In Fig. 1, the system can use data shape or color to make a correct classification. However, when the system classifies a new datum having a triangular shape and red color, if it uses shape only to select the class, it will fail to classify correctly. Sometimes, current classification criteria are not suitable for new data. To solve such problems, the system must have a dynamic criteria-changing function.

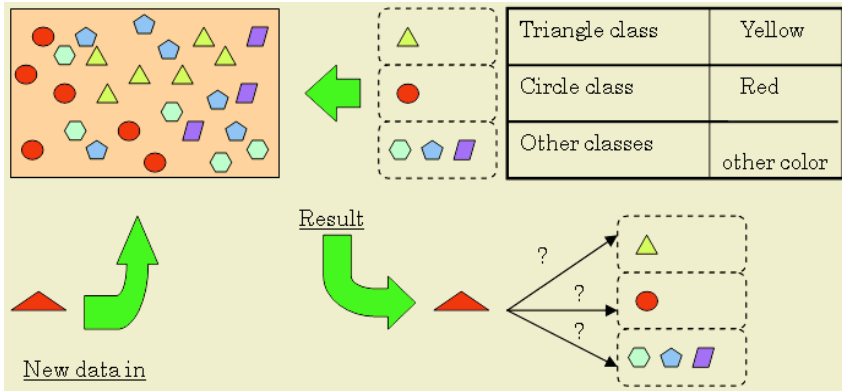


Fig. 1. An example of segmentation of an image

We propose a reconstruction method for changing clustering criteria. The method consists of three major components: the first is an induction learning module to formulate classification criteria, the second, a map function to change the feature space of data, and the third, a constructive induction function for selecting new features in order to classify exceptions into correct classes.

2 Related Studies

2.1 Problems of Clustering with Exceptions

The basic idea of clustering technology is to classify mixed data into classes based on criteria (or rules) defined according to the observations of the user. Since this cannot produce complete criteria for all future data, we need new clustering technology that can provide suitable criteria for cases where exceptions are found. An exception is a special case when the clustering system cannot classify it correctly from lacks of suitable criteria.

2.2 Applications of Learning with an Instructor

This section concerns learning clustering rules from classified examples [1], [2], [3]. Learning with an instructor involves finding rules from sets of objects that are classified by the instructor. Classification criteria are learned according to the instructor's selection rules. Learning clustering rules from classified examples is useful in forming classification criteria, rule conditions, or classification functions.

The clustering system, which uses clustering rules from classified examples, operates in two stages: a learning stage and a segmenting stage, as shown in Fig.2. In the learning stage the system learns clustering criteria from sets of classified data and gets rules for segmenting data. In the segmenting stage it calculates segmentation estimates for treating exceptions to rules. In this way, it learns classification rules and produces new criteria for segmenting data with exceptions.

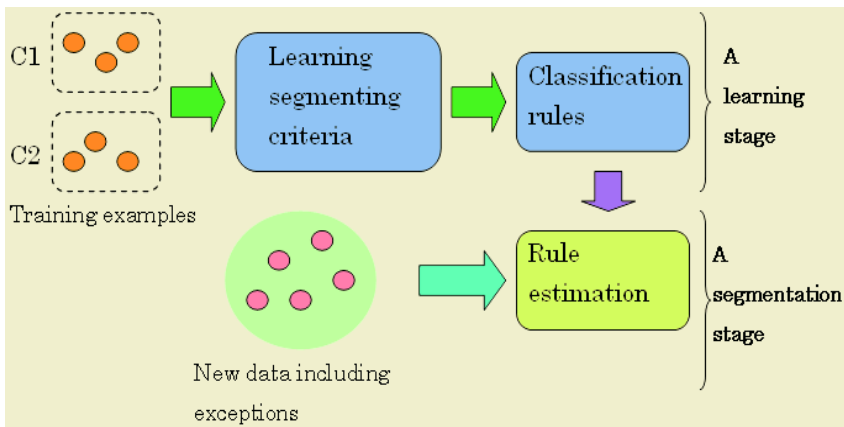


Fig. 2. Process for learning clustering rules through classification

2.3 Problems in Learning Clustering Rules

The learning method discussed here makes classification criteria from classified data. At present, this method does not have an incremental learning function, so it cannot produce complete criteria for new data with exceptions. Weak points in the method are as follows.

(1) Estimates are mainly done using hierarchical clustering strategies, such as the nearest neighbor method, and partitioning-optimization methods, such as k-means. However, exceptions which are very similar to a classified set cannot be dealt with (as shown in Fig. 3) because all estimates are done using distance based on classification criteria.

In Fig. 3, although the new instance (X_7) should belong to C_1 , X_7 is similar to C_3 and is thus classified into C_3 according to current criteria. This is an incorrect classification. Here, in order to enable a correct selection rules corresponding to X_7 only must be added.

New rules:

IF X is near X_7 THEN X is classified into C_1 .

IF X is not near X_7 THEN current selection function is used.

The X_7 selection range is located in C_3 (shown in Fig. 3). The new range of the C_3 selection area is doughnut shaped.

(2) Constructive Induction for Clustering

When the system cannot manage or find classification criteria, new viewpoints (features and attributes) must be added to the existing criteria. In the conventional learning method, if there is an inconsistency in the rules, the logical function is not useful for clustering. An inconsistency may occur when selection is carried out using only one suitable attribute. For example, similarly shaped flowers colored blue and red cannot be properly classified using only the shape attribute. By adding color as a new attribute, the system becomes able to classify the flowers as blue or red. It is important that when the system adds a new attribute it also re-structures the logical or numerical condition rules.

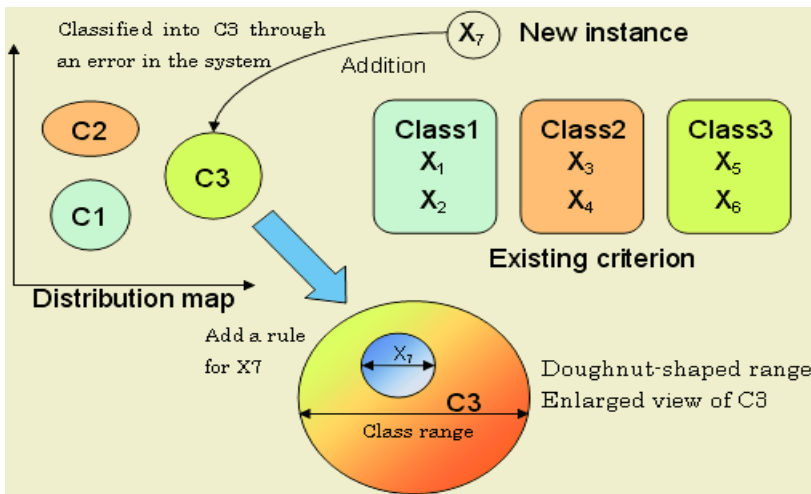


Fig. 3. The appearance of a similar exception instance

3 Clustering Technology Architecture for Ubiquitous Computing Environments

3.1 Clustering Process for Exceptions

Current clustering systems don't deal with data exceptions and have the following weak points:

- (1) Failure of classification of similar examples (as shown in Fig. 3).
The system cannot treat new exception data that are not different from classified data.
- (2) Failure of classification when the distribution map is not linear (as shown in Fig. 4).
In order to use current linear distribution methods the system must use mapping functions to classify data using linear criteria.
- (3) Failure of classification due to lack of features.
The system must add new features to classification criteria using constructive induction.

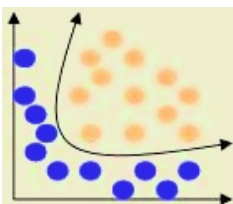


Fig. 4. A non-linear distribution map

We propose a clustering system architecture to solve these three weak points.

3.2 Three-Layered Structure

The system consists of a three-layered structure based on three methods to solve inconsistencies when exceptions occur. The three-layered structure consists of a rule-making layer, a mapping layer and a constructive induction layer, as shown in Fig. 5.

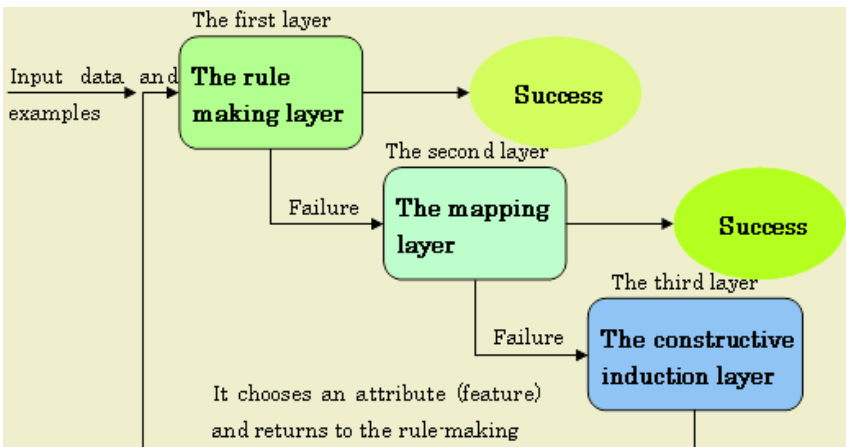


Fig. 5. Three-layered structure in the clusstering architecture

(1) The rule-making layer

The system selects attributes and parameters to automatically form range criteria, and picks up exceptions. A rule is defined in Boolean (AND/OR) and numerical range expressions. The applicability conditions for the rule are made through induction learning and are estimated by evaluating new data.

(2) The mapping layer

In mapping a linear distribution from a non-linear one, the system uses several mapping function techniques. If the system finds an exception, it uses other mappings, ignoring the exception. In Fig. 6, when it used "Grey level", linear separation was not possible in processing all the screens like A-1 distribution map, but by using screen separation, the system could classify data using linear distributions like B-3 distribution map.

(3) Constructive induction layer

The attributes selection problem is very difficult because the system cannot select useful attributes before it finds exceptions. The attribute selection method for exceptions is the Relief [6] algorithm. The Relief algorithm chooses an example (a vector) at random in a set of given data and selects positive and negative examples according to which is closest to the data. It then calculates the average of an attribute, i , and can select an attribute related to the concept.

3.3 Algorithm for Each Processing Part in Three Layers

The algorithm used in the three layers and collaboration between the three layers is now discussed.

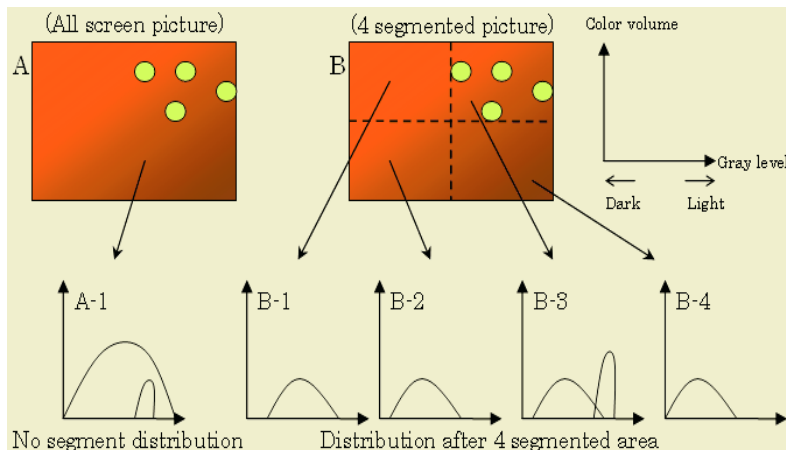


Fig. 6. Example of mapping of linear distribution from non-linear distribution

When a new example is inputted, the first or rule-making layer initially processes it. If the instance corresponds to data in the rule-making layer, processing is finished, and the new condition is added to the rules. If there is no correspondence, the second or mapping layer selects a suitable mapping function to classify the new data. If there is no correspondence with the exceptions in the mapping layer, constructive induction adds a new attribute (feature) to the third layer and goes back to the first layer (the rule-making layer) again. The process is then repeated to classify all data completely.

4 Summary

We have discussed the weak points of conventional clustering and also new clustering methods with changing criteria functions for an ubiquitous computing environment. In addition, we considered the problems of exception data in clustering, and described restructuring rules and selection features. We are now planning to use our clustering method for natural human behavior understanding. To classify the many variations of human behavior, we use this information as an ubiquitous interface. This system can recognize any type of behavior to automatically form clustering criteria.

We will carry out evaluations in order to study the effectiveness of confirming exceptions, measuring the exception detection rates from graphical images of artificial data, and then evaluating the effectiveness of the system functions with natural data. We intend to use our method for two applications: image clustering for detecting irrigable form conditions in agriculture, and patient situation detection in hospitals.

References

1. T. Kamishima, F. Motoyoshi, S. Akahori, "Learning from Cluster Examples—Employing Attributes of Clusters", Transactions of the Japanese Society for Artificial Intelligence, vol. 18, no. 2, pp. 86-95, (2003) (in Japanese).
2. T. Kamishima, F. Motoyoshi, S. Akahori, "Learning from Cluster Examples", Journal of the Japanese Society for Artificial Intelligence, vol. 12, no. 2, pp. 276-284 (1997) (in Japanese).

3. T. Kamishima and F. Motoyoshi, "Learning from Cluster Examples", *Machine Learning*, vol. 53, pp. 199-233 (2003) .
4. H. Tsuda, "What is support vector machine", *Journal of the Institute of Electronics, Information and Communication Engineers*, 83, 6, pp. 460-466, 2000 (in Japanese).
5. S. Sugaya, E. Suzuki, "Normal form conversion and object recognition by Support Vector Machines", *Proceedings of the Japanese Society for Artificial Intelligence National Conference*, pp. 476-479, June ,1999 (in Japanese).
6. K. Kira, L. Rendell: "A practical approach to feature selection", in *Proceedings of the 9th International Conference on Machine Learning* (1992).
7. H. Taki, "Constructive Inductive Learning and Bias", *Journal of the Japanese Society for Artificial Intelligence*, Vol. 9, no. 6, pp. 818-822 (1994) (in Japanese).

Indoor Location Determination Using a Topological Model

Junichi Sakamoto¹, Hirokazu Miura¹, Noriyuki Matsuda¹, Hirokazu Taki¹,
Noriyuki Abe², and Satoshi Hori³

¹ Graduate school of Systems Engineering, Wakayama University

² Faculty of Computer Science and Systems Engineering, Kyushu Institute of Technology

³ Institute of Technologists

Abstract. Context-aware computing that recognizes the context in which a user performs a task is one of the most important techniques for supporting user activity in ubiquitous computing. To realize context-aware computing, a computer needs to recognize the user's location. This paper describes a technique for location detection inside a room using radio waves from a user's computer. The proposed technique has to be sufficiently robust to cater for dynamic environments and should require only ordinary network devices, such as radio signal emitters, without the need for special equipment. We propose a topological model representing the structure of rooms in a building, and describe a room-detection method using this model.

1 Introduction

Context-aware computing [1] which offers services based on the context in which a user is performing a task is one of the most important techniques in supporting user activities in ubiquitous computing. In context-aware computing, a computer needs to recognize the user's environment, e.g., the user's current location, the time at which a service is requested and the user's activities. To recognize activities, the computer has to know where the user/computer are located. In this paper, we focus on techniques for detecting the location of a user/computer.

Considerable work has been done in the research field of indoor location determination systems [2], [3]. The systems described need special hardware and communication interfaces such as infra-red radiation and ultrasonic wave signals, and the exact location, i.e., the coordinates of the user device, has to be calculated. To improve performance, it is necessary that a large number of devices be arranged in the space concerned (e.g., building, room, etc.). Thus, the achievement of good performance with these systems is very expensive. To reduce the costs involved, systems using ordinary network devices that are widely used for wireless communications between computers, such as radio, are proposed [5]-[7]. But these systems are weak where signal conditions change, due to shadowing, fading, etc.

APIT [10] has been proposed to solve these problems. In this approach, the system does not detect the user's location by the change in signal strength from the user's radio device; rather it detects location by the signal strength. The system can decide whether the user is inside a room or not, without calculating the coordinates. This means that APIT is robust in dynamic environments. However, in the case where the

user is inside a building that has many floors, there may be some errors. This is because APIT does not take the 3-dimensional structure of rooms in a building into account, and, as a result, indoor location determination cannot be effectively carried out.

In this paper, we propose an indoor location determination method, making use of APIT and a topological model. A topological model represents the hierarchical structure of rooms in a building. With the topological model, this location determination method will enable context-aware computing with good performance from the viewpoint of tracking changes in a user's location.

The remainder of this paper is organized as follows: Section 2 discusses previous work in the area; Section 3 describes our proposed technique for indoor location determination; Section 4 presents various applications of our scheme; finally, we describe our conclusions and discuss future work in Section 5.

2 Related Work

There have been several reports of work on location determination techniques. Active bat [2] and Cricket [3] determine location by the use of sensor devices such as infrared or ultrasonic wave signal devices. The performance of these systems depends on how many devices can be arranged in the space considered. To achieve good performance with these systems, a large number of devices is needed, e.g., 720 devices for every 1000 square meters. Thus it is very expensive to maintain good performance and practical implementation is difficult. We believe that what is really required is a method which relies only on ordinary network devices that are widely used for wireless communications between computers, e.g., Wireless LAN, Bluetooth, Zigbee and Mote [4].

Almost all the systems that use radio signals [5]-[7] calculate the location coordinates of the object concerned, which means that the system is very complicated. With indoor location, it is necessary to determine which room the computer is located in, i.e., it is more important to know the boundary between the rooms than coordinates. In these systems, however, the estimation error is large, leading to mistaken results. In the case shown in Figure 1, the computer is originally located in room Y, but the system may estimate that it is located in room X because of the large error. These systems use the formula given in [8] for a wireless model, but there are many cases where real world radio signals cannot be modeled with the formula.

Ogawa et al. [9] have proposed a location determination method using radio signals from base stations, with supervised learning. In their work, the assumption is made that change of environment does not occur, i.e., the device does not move. Thus, with their system it is difficult to determine the location of a mobile device.

The APIT (Approximation of the Perfect PIT Test) which is robust in dynamic environments has been proposed in [10]. In APIT, the wireless mobile node has a 2-dimensional map and determines its own location by communicating with anchor nodes. Anchor nodes are aware of their own coordinates beforehand. The node looks for other nodes and anchor nodes to which it can communicate. If it finds them, it determines their ID, before plotting anchor coordinates in the map and drawing a triangular area connecting anchor to anchor. The node determines that its own position is inside these triangular areas. This allows it to narrow down the area where it

can potentially reside. An overview of APIT is shown in Figure 2. The center of gravity of shaded area indicates the node's coordinates.

We describe how APIT determines whether a node is inside these triangular areas or not. In Figure 3 and 4, node M, 1, 2, 3 are mobile nodes and node A, B and C are anchor nodes. Each node measures the signal strength from each anchor. Node M compares the signal strength which it receives from the anchor nodes with the signal strength which neighbor nodes receive. If no neighboring node of M is further from or closer to all three anchor nodes simultaneously, node M assumes that it is inside the ΔABC . Otherwise, M assumes that it is outside the ΔABC . Figure 3 presents a scenario where M will assume that it is inside the ΔABC . In Figure 4, node 1 will report to node M that it is further away from A, B and C than M. Figure 4 shows the case where it is outside the triangle ABC.

On the other hand, in the case where the user is inside a building that has many floor, there can be some error in the system as we mentioned above. This is because the 3-dimensional structure of rooms is not taken into account. In some cases, the device may receive signals from lower or upper floors, leading to misdetection. Therefore, in this paper we propose an indoor location determination technique using a topological model representing the hierarchical structure of rooms in the building.

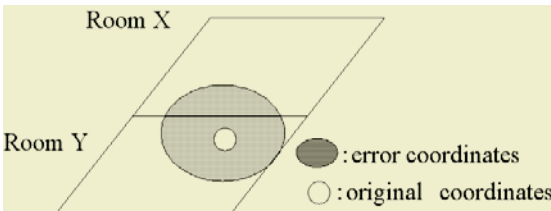


Fig. 1. Problem of indoor determination

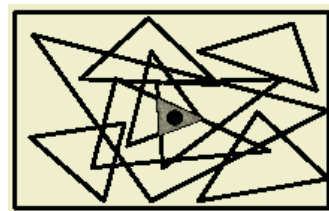


Fig. 2. APIT overview [10]

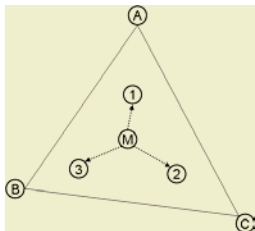


Fig. 3. APIT inside case

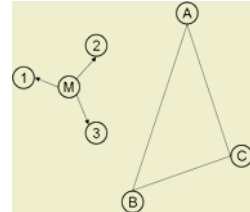


Fig. 4. APIT outside case

3 Closed-Region Discrimination and Topological Model

In this section, we describe the detailed operation of the proposed technique. Our proposal makes use of CRD (Closed-Region Discrimination) and a topological model [11]. CRD consists of algorithms based on APIT with some modification added. The topological model represents the hierarchical structure of the rooms in the building. Our proposal uses the ordinary network devices without special equipment and does not calculate location coordinates. Thus, our system is inexpensive and simple. We explain CRD and the topological model in the following section.

3.1 CRD (Closed-Region Discrimination)

The method we use in CRD is based on APIT with some modification added. The following assumptions are made.

- The node in our CRD solves its own location by location name rather than by possessing a 2-dimentional map. This is different from APIT.
- Anchor nodes in CRD are aware of their location names and the number of anchor nodes which have the same location name, and do not move – i.e., anchor placement is fixed.
- Anchor nodes are arranged at the corners of a room.
- The mobile node and neighbor nodes share the common anchor nodes.

The procedure used in CRD is as described below. In Figure 5, node M, 1, 2, 3 are mobile nodes and node A, B, C, D, E, F, G, H, I are anchor nodes. A-D are arranged at the corner of room 101, other anchors are in room 102. The node M estimates its own location by the following steps.

- Step1. The mobile node M, the neighboring nodes 1, 2 and 3 receive signals from anchors and obtains the information such as the anchor IDs, the location name and signal strengths.
- Step2. The node looks for neighbor nodes with which it can communicate.
- Step3. Node M collects the information (obtained by Step 1) from neighbor nodes. The node constructs a table grouped by the same location (shown in Table 1).
- Step4. The node looks for a neighbor node that has a consistently larger or smaller signal strength than its own signal strength from all the anchor nodes in the same room in Table 1. If such a neighbor node is found, the node is outside the room consisted of anchors. Otherwise, the node resides inside the room. From Table 1, node M compares its own signal strength with node 1's signal strength from anchor E-H. Node M is outside room 102 because all values of node 1 in room 102 are consistently smaller than M. However, such a case is not found in room 101. This is because that Node M is inside room 101.

Table 1. Table of signal strengths from anchor nodes

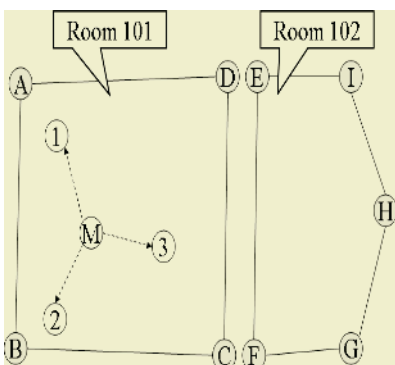


Fig. 5. Node placement

| Location name | Anchor ID | Signal Strength | | | |
|---------------|-----------|-----------------|--------|--------|--------|
| | | Node M | Node 1 | Node 2 | Node 3 |
| Room 101 | A | 14.5 | 17.0 | 12.0 | 11.5 |
| | B | 14.0 | 12.5 | 17.0 | 12.0 |
| | C | 12.5 | 9.5 | 12.0 | 15.0 |
| | D | 11.5 | 12.0 | 9.0 | 13.0 |
| Room 102 | E | 11.5 | 10.5 | 6.0 | 12.5 |
| | F | 11.0 | 8.5 | 10.5 | 14.0 |
| | G | 8.5 | 5.5 | 7.0 | 11.0 |
| | H | 7.0 | 5.5 | 5.0 | 10.0 |
| | I | 8.0 | 7.0 | 5.0 | 10.0 |

3.2 Topological Model

In the case where our algorithm is applied to a building with many floors, there may be some error in indoor detection. Figure 6 shows a building that has several rooms and stairs, with the rooms indicated by numbers. In the CRD algorithm, anchors are arranged in each room. When there is a node at the point marked X in Figure 6, the node can receive signals from the anchor nodes in rooms 101 and 202. As a result, the node cannot determine whether the location is in room 101 or 202. This leads to a mis-estimation of the location. To prevent this happening, we use a topological model and history of the location of the mobile node. The topological model represents relationships between abstract spaces in a building, such as “near”, “contains”, etc. Figure 7 shows an overview of the topological model which represents the hierarchical structure of the room in the building in Figure 6. The bottom layer of this model indicates the room number or stairs/elevator.

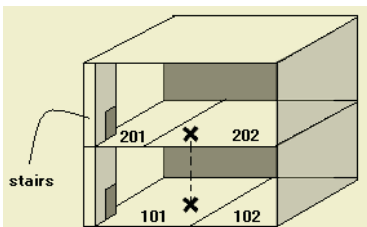


Fig. 6. Problem conditions

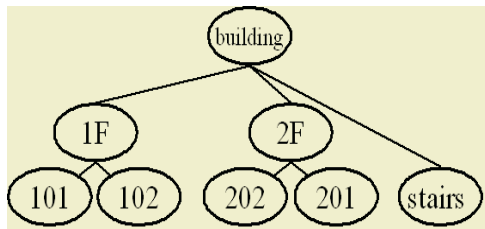


Fig. 7. Example of topological model

We now describe how to use the topological model and estimated history. If the node cannot decide whether it is located in room 101 or 202 from the result of CRD, the topological model and history data are used. If the history data indicates that the previous location was in room 102, the node can estimate that the current location is in room 101. If the history indicates that the node moved to the stairs from room 102, the current location is in room 202.

4 Applications

This section describes applications using our proposed technique. There are three kinds of applications. The first is where the user wishes to use nearby computer peripherals, such as a printer in an office. A simple message is sent to printers connected in a wireless network as follows: “Print this document using the printer in the place where I am now located”. Printers receiving this message sense their own location and that of the user. A printer is found in the place where user is and the user’s document is printed. As another example, if the user requests information concerning shops in a shopping complex, a computer provides relevant information arranged according to shop proximity.

The second application we consider is where a location administrator communicates with users inside its location area. For instance, since our system enables judgment as to whether a user is inside or outside a designated location, user input of working hours in an office or school can be automated. When the user enters his/her office, the system starts to record, and when the user leaves the office, the system

stops recording. Another example would be where only those persons inside a specific location, such as a library, would be able to browse an e-book free of charge. This is based on the premise that only people inside the library have the right to consult the library books.

The third application is where others want to know the location of a user. In cooperative work using mobile computers, it is often not possible to know where others are located – building, car, train, etc. This problem is solved by using our proposed technique so that a user can be made aware of another user's location. Additionally, it is possible to provide a user's location while taking privacy into account, by applying inclusion relations in the topological model.

Thus, our proposed technique can be used in a varied range of applications.

5 Conclusions and Future Work

We have described an indoor location determination technique consisting of Closed-Region Discrimination, topological models and estimated history. The advantage of our technique is that it does not use coordinates, special hardware is not required, and it is simple and robust in dynamic environments. Future work will investigate required signal strengths and how many nodes and anchors are needed. For this purpose, we are preparing a simulation program that will utilize various parameters.

References

1. B. Schilit, N. Adams, and R. Want, Context-Aware Computing Applications, *Proceedings of Workshop on Mobile Computing Systems and Applications IEEE*, Santa Cruz, CA, US, December 1994.
2. Andy Harter, Andy Hopper, Pete Steggles, Andy Ward, Paul Webster, The Anatomy of a Context-Aware Application, *Proceedings of the Fifth Annual ACM/IEEE International Conference on Mobile Computing and Networking (MOBICOM'99)*, pp. 59-68, Seattle, Washington, USA, August 1999.
3. N. B. Priyantha, A. Chakraborty, and H. Balakrishnan, The Cricket location-support system, *the 6th Annual ACM/IEEE International Conference on Mobile Computing and Networking (MobiCom 2000)*, pp. 32.43, Boston, MA, USA, Aug. 2000.
4. Mote, <http://www.tinyos.net/>
5. Akiko Iwaya, Nobuhiko Nishio, Masana Murase, and Hideyuki Tokuda, GOMASHIO: Proximity Based Localization, *Wireless Ad-Hoc Sensor Networks, IPSJ SIG Mobile Computing and Ubiquitous Networking*, Vol.108 pp.23-30, Nov. 2001 (in Japanese).
6. Teruaki Kitasuka, Tsuneo Nakanishi, and Akira Fukuda, Wireless LAN based Indoor Positioning System WiPS and Its Simulation, *2003 IEEE Pacific Rim Conference on Communications, Computers and Signal Processing (PACRIM'03)*, pp. 272-275, Aug. 2003..
7. N. Bulusu, J. Heidemann and D. Estrin, GPS-less Low Cost Outdoor Localization for Very Small Devices, *IEEE Personal Communications Magazine*, Vol. 7, No. 5, pp. 28-34, October 2000.
8. Deepak Ganesan, Deborah Estrin, Alec Woo, David Culler, Complex Behavior at Scale: An Experimental Study of Low-Power Wireless Sensor Networks, In *Technical Report UCLA/CSD-TR 02-0013*, 2002.

9. Tomoaki OGAWA, Shuichi YOSHINO and Masashi SHIMIZU, The In-door Location Determination Method Using Learning Algorithms with Wireless Active Tags, *IPSJ Ubiquitous Computing Systems(UBI)*, Vol. 2004, No66, pp31-38, 2004 (in Japanese).
10. Tian He, Chengdu Huang, B. M. Blum, John A. Stankovic, and Tarek F. Abdelzaher, Range-Free Localization Schemes in Large Scale Sensor Networks, *the Ninth Annual International Conference on Mobile Computing and Networking (MobiCom 2003)*, San Diego, CA, September 2003.
11. B. Brumitt, and S. Shafer, Topological World Modeling Using Semantic Spaces, *Workshop Proceedings, UbiComp 2001*, pp.55-62, 2001.

Lightweight Agent Framework for Camera Array Applications

Lee Middleton, Sylvia C. Wong, Michael O. Jewell,
John N. Carter, and Mark S. Nixon

School of Electronics and Computer Science, University of Southampton, UK
`{ljm, sw2, moj, jnc, msn}@ecs.soton.ac.uk`

Abstract. This paper describes a lightweight middleware agent framework (LAF) for coordinating a large array of computers with attached cameras to construct high resolution video-rate image sequences. Compared to existing camera middleware, LAF provides more than a remote sensor access API. The use of an agent framework allows reconfigurable and transparent access to cameras, as well as software agents capable of intelligent processing. It also eases maintenance by encouraging code reuse. Other features include an automatic discovery mechanism at startup, and multiple language bindings. Performance tests showed the lightweight nature of the framework while validating its correctness and scalability. Two different camera agents were implemented to provide access to a large array of distributed cameras. Correct operation of these camera agents was confirmed via several image processing agents.

1 Introduction

Increasingly, large arrays of high quality cameras are used for capture and analysis of motion. Kanade et al. mounted 49 cameras in a room to capture motion for virtualised reality [1]. Wilburn et al. built a dense CMOS camera array to achieve high resolution and framerate capturing of image data [2]. Zhang et al. built a large self configuring camera array capable of rendering novel views of scenes in near real time [3]. In all these works multiple cameras are employed to produce a higher quality image than would be possible with a single camera. Specifically, we seek to deploy high resolution video-rate data captured from multiple cameras for the analysis of human gait.

In this paper we propose a middleware framework for a camera data acquisition system. The aim is to allow transparent and reconfigurable access to visual data while minimising maintenance by encouraging code reuse. Real time streaming is not required because gait analysis requires high resolution data. Additionally, the complexity of the algorithms employed make it impossible to do on-the-fly processing. The middleware facilitates communication between dedicated camera computers and image/gait processing software. It has the following features: (i) *Zeroconf*: This allows agents to automatically locate middleware components in a network. (ii) *Multi language support*: This allows users to exploit the benefits of the different languages. (iii) *Lightweight*: The algorithms used in gait analysis are CPU intensive, thus the middleware must not be an additional adverse drain on resources. (iv) *Service discovery*: Agents can query the middleware to discover and utilise services provided by other agents. (v) *Locking*: Cameras are stateful devices. It is important that processes cannot be interrupted mid-session.

Hori et al. [4] also implemented a middleware for networks of computers with attached cameras. Here, cameras were accessed as if they were a local device. This is similar to player/stage [5], which provides software abstraction for robot sensors. However, these systems are not suitable for our application as their goals are to provide direct access to sensor data over a network. In contrast, we want intelligent agents in our framework, where researchers can provide agents that perform complex algorithms. Multi-camera tracking systems [6, 7] also study the same problem. Here, camera agents not only act as capture devices, but also perform processing on the image data. The middleware is highly focused on the task of tracking. Thus the messages are high level commands like location of objects. The middleware is also responsible for coordinating the movement and focus of the cameras to achieve a goal. In comparison, the middleware in our application has to be more general purpose. This is because researchers have different requirements from the image data. For example, in our research group, there are people who work with raw image data, silhouettes [8], and 2D and 3D models [9]. A final approach to this camera coordination problem is to leverage an existing middleware such as CORBA [10] or XML-RPC [11]. However, both systems require lot of resources to run. Many features not required in our application are included by default, and they cannot be optionally switched off. Also, there is a steep learning curve before researchers can add their existing code to this framework.

Our proposed solution contains some of the features from all the approaches outlined above, while being easy to use and lightweight. The paper is organised as follows: Section 2 provides an overview of the Lightweight Agent Framework (LAF). Section 3 introduces the two camera agents essential to our camera data acquisition system. Section 4 presents results from performance tests. Finally, Section 5 describes application agents that employ the services provided by the camera agents.

2 System Overview

Figure 1 shows an overview of LAF. The system has been simultaneously developed on C++, Java, and Python. Central to the system is the *router*. It is the main point of communication and coordination. All *messages* between components (except streamers) are sent via the router. Also, it acts as a broker for agents providing and requiring services. Agents are providers of services. Remote agents are clients of services provided by agents. To use the service provided by an agent, a remote agent requests a *lock* on the agent from the router. However, LAF is not restricted to a simple model of clients (remote agents) and servers (agents). An agent can contain one or more remote agents, thus allowing it to be both a client and a server at the same time. Ports are inputs and outputs of agents. Streamers are direct socket connections, mediated via the router. This allows video information to be sent directly between agents without the traffic passing through the router.

Ports and Streamers. There are two types of ports in LAF: input and output. Input ports are used to pass data to an agent. They can be optional or non-optional. Processing cannot proceed until all non-optional ports are *set*. Output ports are used to pass data to remote agents. In applications involving a large array of cameras, a large amount of data is generated. If this data is to be sent via the router, the router may fail. For this

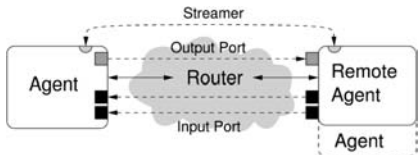


Fig. 1. An overview of how the middleware and agents fit together

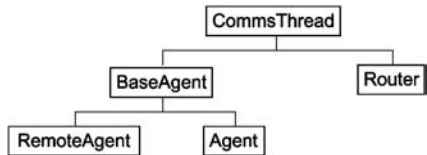


Fig. 2. Diagram showing the interrelation of the software objects

reason, streamers were implemented. A streamer is a direct socket connection between an agent and a remote agent. The router is responsible for instigating this connection, so address information is not required ahead of time.

Messages. LAF employs XML messages for communication between the router, agents and remote agents. Broadly, there are three classes of messages – status, router and agent. Status messages give feedback about the success of an action. Router messages are actions that only the router can perform. Agent messages are communications, via the router, between agents and remote agents. They deal with control and communication.

Router. The router, agent and remote agent are implemented via a common class hierarchy, as shown in Figure 2. The router is responsible for agent subscription, message re-direction, and agent selection. It employs a plugin system which makes it simple to extend its functionality. Upon starting, the router registers itself as a multicast DNS service (mDNS) in zeroconf. The mDNS service allows information to be passed to any subscriber of the service. In this case the port and IP address of the router are passed via mDNS. Essentially this means that connection to the router by any agent is potentially an automatic process.

The subscription process of an agent from the perspective of the router begins when a SUBSCRIBE message is received. This message contains the *type* of agent which is being subscribed. The type of an agent is purely a descriptive name describing the service it provides. When the subscription is received the router assigns a unique name for the agent. This is made up of the type and a unique id number. Once an agent is subscribed, it is added to two lists (connected agents and free agents) which are maintained in the router. If an agent unsubscribes or dies, the router removes it from both lists. All messages pass through the router. As a result of this the router can perform filtering of the messages. For example, some messages are permitted only if the sender has a lock on the target. If the sender does not have the required lock, the router returns an NOK message to the sender. In most cases however the extent of the routers manipulation of the message is handling acknowledgements and passing it onward to the appropriate target. The last function of the router is the agent selection process. This is used when a remote agent attempts to lock an agent. The selection mechanism currently employed is a naive one. A handle to the first agent of the correct type on the free agent list is returned to the remote agent. The selected agent is also removed from the free agent list.

Agents and Remote Agents. Users writing agents for LAF will need to create a derived class of Agent. The Agent class provides the underlying networking and messag-

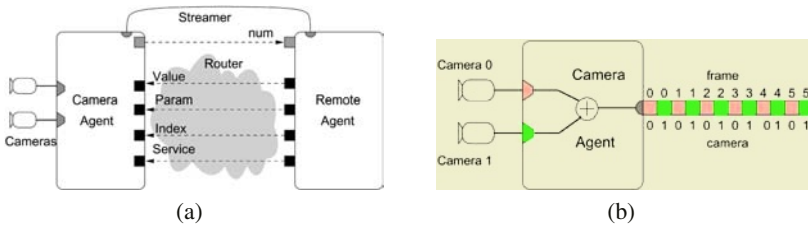


Fig. 3. (a) Configuration of camera agent. (b) Sending image data with a streamer

ing required for all agents. The derived class will minimally need to (a) provide type, ports, and streamers in the constructor, and (b) overwrite the `action()` method. Type is a descriptive name of the service provided. Ports and streamers provide the inputs and outputs of this agent. The `action` method is the engine of the agent. The user writes their own action method to provide the agents' functionality. Users writing remote agents will need to create a derived class of `RemoteAgent`. The derived class will need to specify the name(s) of the agent(s) it wishes to lock, set the agent's input ports and call the `action()` method. Agents and remote agents can connect to LAF either automatically or manually. Automatic connection is performed using zeroconf while manual connection uses environment variables.

3 Camera Agents

Figure 3(a) illustrates the specific ports and general configuration for a camera agent. Only the `service` port is compulsory. The service port exposes the features of the cameras controlled by the agent, such as grab image and set shutter speed. The other input ports were employed to set required parameters. The `streamer` is used to transmit image data over the network directly to remote agents. The video data is sent a frame at a time with the frame from each camera interleaved as shown in figure 3(b).

The camera agent provides access to the camera array on a per PC basis. However, accessing and controlling a large number of cameras can be cumbersome using camera agents alone. For instance to access 6 cameras which are connected in pairs to each of three PCs the user needs to maintain three separate camera agents. As a result, a super camera agent was written to provide a single collated image data stream to image processing applications. The configuration for a super camera agent is shown in Figure 4(a). It contains a number of remote agents for locking camera agents connected to the router. Thus, the super camera agent is both a remote agent and an agent. Image data is transmitted to the super camera agent via a number of streamers. These are demangled into a single output stream for other other remote agents to consume (Figure 4(b)).

4 Performance Testing

Four tests were carried out to evaluate the performance of LAF. Figure 5 shows that connection and disconnection times to LAF do not increase with an increasing number of registered agents. The second test measures the overhead of messaging. One hundred

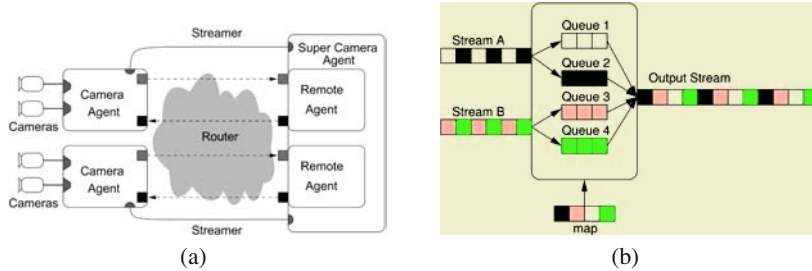


Fig. 4. (a) Configuration of super camera agent. (b) Demangling of image streams

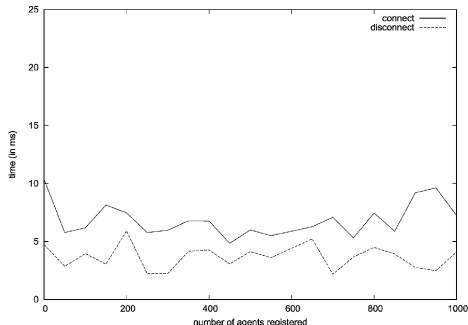


Fig. 5. Connection and disconnection time against number of agents registered

Table 1. Time (in ms) to perform 100 string concatenation operations

| agents | remote agents | |
|--------|---------------|--------|
| | C++ | Python |
| C++ | 943 | 1771 |
| Python | 1596 | 2158 |

Table 2. Startup time

| | time (ms) |
|---------------------|-----------|
| C++ agent | 263 |
| C++ remote agent | 291 |
| Python agent | 512 |
| Python remote agent | 604 |

separate operations were invoked against an agent with two mandatory inputs and a single output. The result is shown in Table 1. The third test measures the average startup times of agents and is illustrated in Table 2. The slower start up times of the remote agents is the overhead due to locking. The messaging test and the startup time test demonstrate the lightweight nature of LAF. The fourth test examined the streaming performance. For a camera agent we achieved an average of 661 Mbit/s with a gigabit network. This means we can directly (640 × 480, 30fps) stream video data from 9 camera.

5 Application Agents

As an example of the system in operation three application agents are described here. Firstly, an agent was designed to allow remote configuration of cameras (see Figure 6). Secondly, an image mosaicing agent was designed. Figure 7(a) shows a composite image created by this agent. Finally, a background subtraction agent was developed. It locks a single camera and statistically computes a reference background when no subject is in view. When the subject is in the scene, the reference is used to find portions of the image that have changed. Figure 7(b) shows an example output frame.

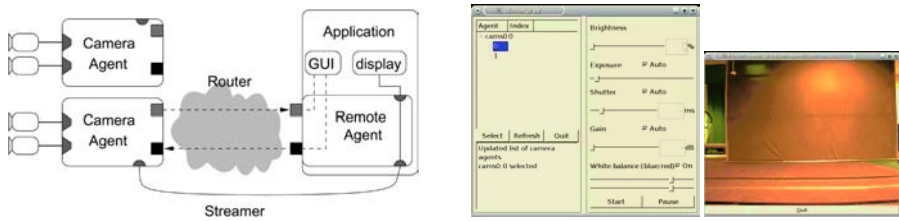


Fig. 6. Camera control application agent

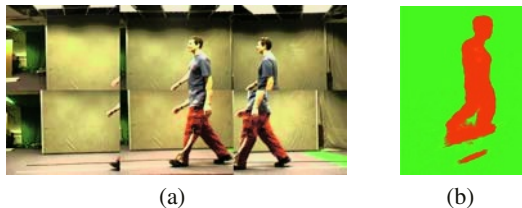


Fig. 7. (a) Creation of an uncalibrated image mosaic from six cameras on three PCs using the image mosaicing agent. (b) Output from the background subtraction agent

6 Conclusions

This paper described the development of a middleware, LAF, for the control of a large array of cameras. LAF consists of a router, and superclasses for agents (service providers) and remote agents (clients). Since agents can contain remote agents, LAF is not limited to a simple client/server model. LAF provides transparent access to camera control. Additionally, it facilitates access and reuse of intelligent agents that provide a variety of image processing operations. Other features of LAF include minimal computational overhead, zeroconf for automatic discovery of components in the framework, locking, and multiple language support. This paper also presented performance tests and applications of LAF. By measuring the connection and disconnection times of agents on an increasingly loaded router, scalability was demonstrated. Messaging tests showed the overhead of communication, in either C++ or Python, was small. Measured startup times showed the registration process to be short. Video streaming tests validated that the throughput in the designed system was sufficient to stream 9 cameras. Three application agents were also demonstrated in this paper. These applications validated the correctness of the design and demonstrated the ease of implementation of image processing applications.

References

1. Kanade, T., Saito, H., Vedula, S.: The 3d-room: Digitizing time-varying 3d events by synchronized multiple video streams. Technical report, Carnegie Mellon University (1998)
2. Wilburn, B., Joshi, N., Vaish, V., Levoy, M., Horowitz, M.: High speed video using a dense camera array. In: Proceedings International Conference on Computer Vision and Pattern Recognition. (2004)

3. Zhang, C., Chen, T.: A self-reconfigurable camera array. In: Eurographics Symposium on Rendering. (2004)
4. Hori, T., Nishada, Y., Yamasaki, N., Aizawa, H.: Design and implementation of a reconfigurable middleware for sensorized environments. In: Proceedings of the IEEE/RSJ International Conference on Intelligent Robots and Systems. Volume 2. (2003) 1845–1850
5. Gerkey, B., Vaungan, R.T., Howard, A.: The player/stage project: Tools for multi-robot and distributed sensor systems. In: Proceedings of the 11th International Conference on Advanced Robotics. (2003) 317–323
6. Sato, K., Maeda, T., Kato, H., Inokuchi, S.: CAD-based object tracking with distributed monocular camera for security monitoring. In: Proceedings of the Second CAD-Based Vision Workshop. (1994) 291–297
7. Orwell, J., Massey, S., Remagnino, P., Greenhill, D., Jones, G.A.: A multi-agent framework for visual surveillance. In: International Conference on Image Analysis and Processing. (1999) 1104–1107
8. Veres, G., Gordon, L., Carter, J., Nixon, M.: What information is important in silhouette-based gait recognition. In: Proceedings of IEEE Computer Vision and Pattern Recognition conference. (2004)
9. Wagg, D.K., Nixon, M.S.: On automated model-based extraction and analysis of gait. In: Proceedings of 6th International Conference on Automatic Face and Gesture Recognition. (2004) 11–16
10. Henning, M., Vinoski, S.: Advanced CORBA Programming with C++. Addison Wesley (1999)
11. Tang, J., Tong, W., Ding, J., Cai, L.: MOM-G: message-oriented middleware on grid environment based on OGSA. In: International Conference on Computer Networks and Mobile Computing. (2003) 424–427

The Location of Optimum Set-Point Using a Fuzzy Controller

Li Yan and Bin Qiu

School of Computer Science and Software Engineering,
Monash University, Vic 3800, Australia
{lyan,bq}@csse.monash.edu.au

Abstract. This paper presents an intelligent algorithm using fuzzy set and fuzzy logic theory to select an adaptive initial set-point of the bottleneck buffer to complement a recently proposed delay-based end-to-end congestion avoidance scheme. The set-point is self-tuned from an initial value to an optimum value according to the requirement of the control system. If the initial set-point is far from the optimum set-point, especially when the size of the bottleneck buffer equals to the value of the bandwidth-delay product, the loss ratio and the delay and delay jitter must be increased. Aimed at improving all parameters of QoS regardless of the properties of the network such as the buffer size and the link speed, this paper derives a fuzzy controller to select the initial set-point based on the measured maximum queuing delay to make the initial set-point close to the optimum value. As a result, parameters of QoS are not degraded when bottleneck links have different buffer sizes and link speeds. The proposed algorithm is tested through the use of extensive simulations to prove its capability to improve network performance in comparison with existing algorithms.

1 Introduction

The Internet has been experiencing an exponential growth of multimedia applications, which include real-time and non real-time applications. They have stringent requirements for quality of service (QoS) in terms of loss ratio, delay, delay jitter and throughput. However, it is well-known that loss-based TCP congestion control algorithms for delivering multimedia applications have many limitations in the current Internet. Moreover, large deployment of these applications using UDP transport protocol could result in server inter-protocol unfairness against TCP-based traffic and possible even congestion collapse [1].

In recent years, many end-to-end congestion algorithms have been proposed, such as TCP/Sack, TCP/Tahoe, TCP/Reno, TFRC, TCP/Vegas, Novel TCP and FAST TCP. They aim at making the improvement on QoS at one or two parameters, but are unable to improve the overall network performance. In contrast, a delay-based end-to-end congestion avoidance (DECA) scheme was recently proposed for improving the overall network performance including all QoS parameters for all type of applications without any assistance from routers [2][3].

The DECA deploys a fuzzy proportional and derivative controller to adjust the sending rate of sources according to the feedback information after a round-trip time (RTT). A fuzzy controller is designed to tune control gains based on the sending rate variations proportion. Meanwhile, as the control target, an adaptive set-point of the bottleneck buffer was derived to assist the controller to stabilize the sending rate when the control gains can not be adjusted. The scheme produces a significant and effective improvement on overall network performance when the bottleneck buffer size has small size. However, when the bottleneck buffer size equals to the value of bandwidth-delay product, the degree of reducing the mean delay and delay jitter is not ideal, even if the mean delay is lower compared with the use of TCP/Sack.

Furthermore, router buffers are sized today based on the well-known rule $B = (\overline{RTT} \times C)$. This rule leads to very high buffer size selected in high speed networks. However, an investigation in [4] found that large buffer size might be a constraint in high speed routers. On the other hand, the buffer size is very important for delay-sensitive applications, since the TCP flows could also result in higher queuing delay with high variance. Some studies in [4][5][6] suggested that using small buffers can still maintain higher utilization in high speed networks and small buffers enable effective operation of delay-sensitive applications over IP networks. Since buffer sizes are selected by router vendors, applications might be delivered along connection paths via bottleneck links with different buffer sizes and link speeds. Whatever happen, it is an important work for the DECA to do the best reducing the mean queuing delay and delay jitter under various network conditions.

This paper will present an intelligent algorithm using fuzzy theory to allow selecting an initial set-point based on the measured maximum queuing delay and adaptive to different buffer sizes and link speeds at bottleneck links. As a result, QoS parameters are not degraded when applications experience bottleneck links with the different buffer sizes and link speeds. Simulation results demonstrate that the F-DECA maintains lower loss ratio, mean delay and delay jitter compared with the DECA and the TCP/Sack.

2 The Proposed Algorithm

The DECA scheme designed a fuzzy proportional plus derivative controller to adjust the sending rate of sources according to the delay information. The aim of the control system is to maintain the bottleneck buffer size at a suitable range so that the overall network performance can be improved. To avoid the sending rate oscillation, the set-point can be increased or decreased as soon as the control gains of the controller can not be adjusted to reach the predefined target rate derivation proportion (RDP). Then, the initial set-point is 0.5 (half buffer size) in order to balance between the utilization and loss ratio.

It is noticed that the final set-point is an optimum set-point for the current network condition for maintaining the target RDP. However, if the initial set-point 0.5 is far from the optimum set-point, the control system had to take more

time to reach the optimum value so that the network performance must suffer more. Thus, we will address this problem to define a suitable initial set-point instead of the static set-point, aimed at reducing the distance between the initial set-point and the optimum set-point.

In this section, an intelligent algorithm deploying a fuzzy controller will be introduced to derive an adaptive initial set-point. Firstly, maximum queuing delay will be discussed before a fuzzy controller is described.

2.1 Maximum Queuing Delay

It has been proved by simulation results that the optimum set-point is related to the buffer size and the link speed at the bottleneck link. When the buffer size is large, the optimum set-point is smaller compared with the small buffer size. Also with high link speed, the optimum set-point is larger than with low link speed. It could be concluded that the optimum set-point is inverse proportional to the buffer size and direct proportional to the link speed.

Due to the properties of the network such as the buffer size and the link speed unknown by end sides, the relationship between the optimum set-point and them can be replaced with the relationship between the set-point and the maximum queuing delay, since the maximum queuing delay reflects the relationship among the buffer size and the link speed at the bottleneck link along a connection. From simulation results, it is shown that larger maximum queuing delay results in the optimum set-point smaller than that with smaller maximum queuing delay. The maximum queuing delay from theoretical view is defined as follows.

$$D_{queuing} = \frac{BufferSize}{C} \quad (1)$$

Here $D_{queuing}$ is the maximum queuing delay along a connection path, C represents the link speed at the bottleneck; and $BufferSize$ is the buffer size at the bottleneck. However, the $D_{queuing}$ can not be obtained since end sides have not any router information. But the maximum queuing delay could be roughly measured by the maximum RTT and the minimum RTT, and they are represented as follows.

$$MD_{queuing} = RTT_{max} - RTT_{min} \quad (2)$$

Here, $MD_{queuing}$ is the measured maximum queuing delay at end sides along a connection path. The $MD_{queuing}$ is not equal to the $D_{queuing}$, since the MD includes one packet processing time at all routers along its connection path. In this paper, we assume that the processing time is much less than the $D_{queuing}$ so that the $MD_{queuing}$ can represent the $D_{queuing}$.

As we know, if the initial set-point is close to the optimum set-point, then the network performance has obvious benefits. Since the accurate relationship between the maximum queuing delay and the optimum set-point cannot be expressed by an equation up to now, we design a fuzzy controller to tune the the initial set-point based on the maximum queuing delay.

2.2 A Proposed Fuzzy Controller

Fuzzy control systems are used to address unknown system dynamics and uncertainty of environment in an effective manner [7]. Since the set-point cannot be expressed or modeled by exact mathematical equations and precise numerical values, a fuzzy controller is designed for on-line selection of the initial set-point according to previous research experiences and preliminary simulations.

In this study, triangular membership functions are adopted for both input and output linguistic variables. The input to the fuzzy logic controller is the measured maximum queuing delay $MD_{queuing}$, which is fuzzified into five fuzzy sets: extra small (ES), small (S), medium (M), large (L) and extra large (EL). The membership value is 1.0 if the maximum queuing delay value is over 0.25 or under 0.05. The output of the fuzzy controller is the value of *set – point*, which is defined within the range of $[0.05, 0.5]$ in order to avoid buffer starvation and buffer overflow. The shape, support and position of these membership functions are largely based on simplicity and previous experience. The output membership values are represented by five fuzzy sets with the same notation.

The inference engine for selecting the initial *set – point* works as follows:

- if $MD_{queuing}$ is *extrasmall*, then *set – point* is *extralarge*;
- if $MD_{queuing}$ is *small*, then *set – point* is *large*;
- if $MD_{queuing}$ is *medium*, then *set – point* is *medium*;
- if $MD_{queuing}$ is *large*, then *set – point* is *small*;
- if $MD_{queuing}$ is *extralarge*, then *set – point* is *extrasmall*;

The input membership functions of these fuzzy sets for the $MD_{queuing}$ are shown in Fig.1(a). The output membership functions for these fuzzy sets are shown in Fig.1(b).

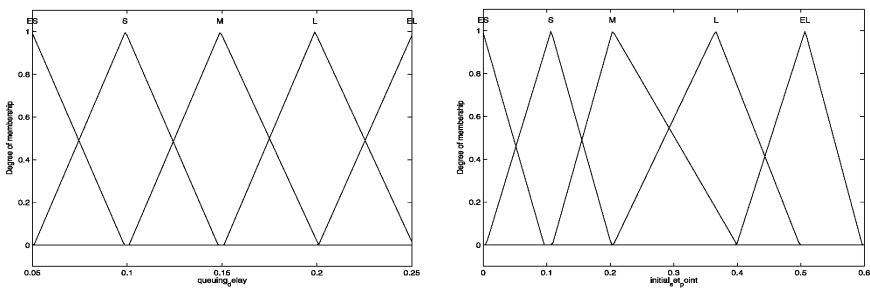


Fig. 1. Fuzzy Controller

3 Simulation Results

The proposed algorithm, namely F-DECA, has been implemented and evaluated with the *ns2* network simulator[8]. The simulation results provide us with evidence that this intelligent algorithm has the capability to optimize the initial

set-point so that there is a significant reduction on the loss ratio, mean delay and delay jitter when the bottleneck has large buffer sizes compared with the use of previous DECA and the loss-based TCP/Sack. In this section, the simulation results are discussed.

In the simulation a dumbbell topology consists of a bottleneck link with n sources and destinations connected. The bottleneck link is 10Mb/s and the links at source end and destination end have the capacity of 100Mb/s. The link round-trip time is defined as 250ms. Routers in the bottleneck use the FIFO drop mechanism. In order to test the performance of the F-DECA controller for different buffer sizes, we vary the buffer size from 100% bandwidth-delay product to 10% bandwidth-delay product. The simulation results for 50 100 150 200 250 connections are given. Simulations execute the static number of connections, where each connection has the same propagation delays. The simulation runs 250s in total. The simulation obtains parameters in network utilization, loss ratio, delay and delay jitter for three schemes for the purpose of comparison, i.e. F-DECA, DECA and TCP/Sack.

3.1 Utilization and Loss Ratio Comparison

It can be seen in Fig.2(a) that when the buffer size is large with 400 packet sizes that the network utilization is very high over 95% among the F-DECA and the DECA and the TCP/Sack regardless the number of connections. However, Fig.2(b) shows when the buffer size is small with 40 packet sizes, the utilization by the use of TCP/Sack mechanism is lower than other two mechanisms. However, both the F-DECA and the DECA still have high utilization over 95%. Therefore, the utilization by the use of loss-based TCP is sensitive to the buffer size, whereas the F-DECA and the DECA result in high utilization and are not sensitive to buffer sizes.

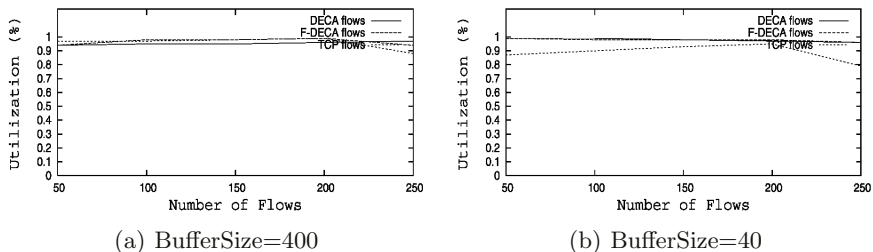


Fig. 2. Utilization

Meanwhile, it can be noted that in Fig.3(a) the loss ratio with the F-DECA is around 0.5%, which is much lower than with the DECA and the TCP/Sack when the buffer size is 400 packet sizes. Fig.3(b) shows that when the buffer size is 40 packets, the loss ratio by the use of F-DECA is lower than using the DECA, and is much lower than the use of TCP/Sack. In most cases, the F-DECA with

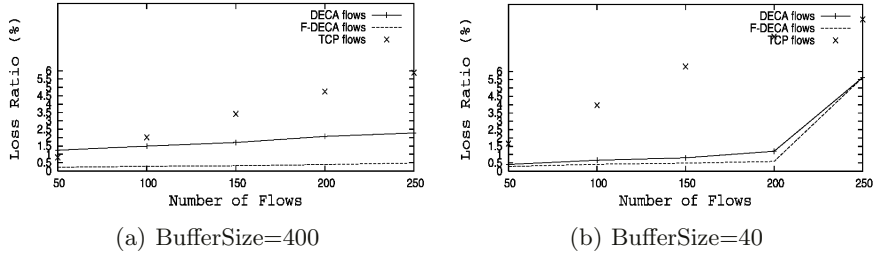


Fig. 3. Loss Ratio

adaptive set-point can effectively and significantly maintain the lower loss ratio. In contrast, the TCP/Sack can produce high loss ratio and increase the loss ratio with buffer size decreased.

3.2 Mean Delay and Its Jitter Comparison

Fig.4 and Fig.5 present the mean queuing delay with its standard deviation using different mechanisms. The queuing delay is measured at the bottleneck where the average queue size is divided by its link speed. The mean queuing delay and its standard deviation link represents the mean delay and delay jitter. It can be seen in Fig.4 that the mean queuing delay with the F-DECA is reduced by 50ms and 2ms respectively than the DECA when the buffer size is set to 400 and 40 packets, whereas delay jitter with the F-DECA is reduced by 50ms and

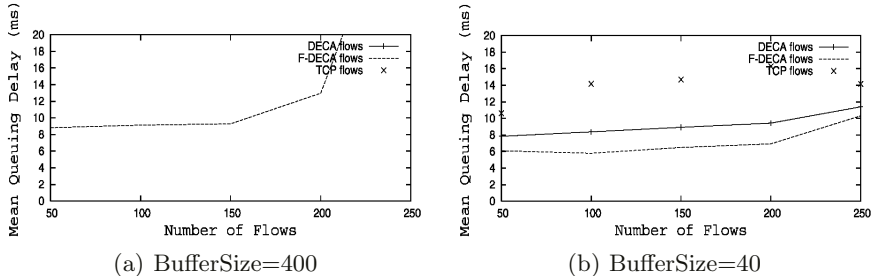


Fig. 4. Mean Queue Size

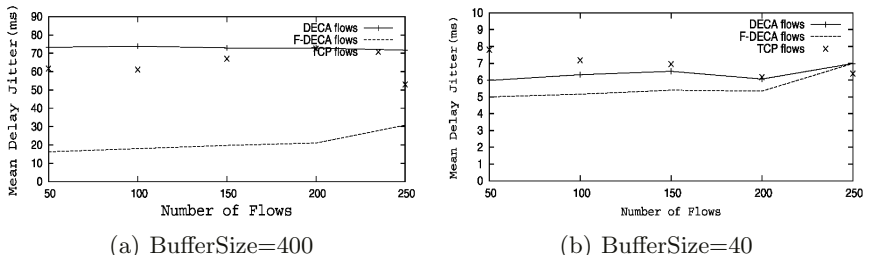


Fig. 5. Queue Size Std

1ms respectively than that with the DECA when the buffer size is selected as 400 and 40 packets. Meanwhile, it can also be seen that the TCP/Sack produces higher mean queuing delay than the other mechanisms. Delay jitter with the TCP/Sack is lower than with the DECA and higher than with the F-DECA when the buffer size is 400 packets in Fig.5(a), whereas with 40 packets buffer delay jitter with the TCP/Sack is higher than that with the other mechanisms in Fig.5(b). When the flow number is 250, delay jitter is a little lower than the other mechanisms because it has higher mean queuing delay. We have more simulation results by varying the link speed. The trends are the same as discussed above. Therefore, the adaptive initial set-point based on the maximum queuing delay is advantageous.

4 Conclusion

The proposed algorithm (F-DECA) deploys a fuzzy controller to adjust the initial set-point so that the initial set-point is close to the optimum set-point. Simulation results prove that this algorithm is capable of achieving overall performance improvement. The future enhancement of the fuzzy logic controller will be some automated methods to assist with the selection of shape, support and position of membership functions for optimum output.

References

1. R.Rejaiae and M.Handley, "Quality Adaptation for Congestion Controlled Video Playback over the Internet", *SIGCOMM*, pp. 189-200, 1999.
2. L. Yan, B. Qiu, and L. Che, "A delay-based End-to-End Congestion Avoidance Scheme for Multimedia Network", *Advances in Multimedia Information Processing-PCM2004*, vol. 3332, pp. 389-396, 2004.
3. L. Yan and B. Qiu, "An intelligent algorithm for QoS improvement in a delay-based End-to-End Congestion Avoidance Scheme", Accept by IEEE ICITA'2005.
4. D.Barman, G.Smaragdakis, and I. Matta, "The Effect of Router Size on HighSpeed TCP Performance", In Proc. Globecom2004
5. G. Appenzeller, I.Keslassy and N. McKeown, "Sizing Router Buffers", In *Pro. ACM SIGCOMM '04*, August /September 2004.
6. S. Gorinsky, A. Kantawala, and J. Turner, "Selecting the BufferSize for an IP Network Link", *WUCSE-2004-50*, Washington University in St.Louis.
7. C. C. Lee, "Fuzzy logic in Control systems: Fuzzy logic controller, Part II," *IEEE Trans. on Systems, Man, and Cybernetics*, vol. 20, pp. 419-435, Mar. 1990.
8. "The network simulator -ns2." <http://www.isi.edu/nsnam/ns/>.

Genetic Modeling: Solution to Channel Assignment Problem

Preeti Bajaj^{1,*}, Avinash G. Keskar^{2,*}, Amol Deshmukh, S. Dorle, and D. Padole

¹ Electronics Dept, G.H.Raisoni College Of Engineering, Nagpur, India
preetib123@yahoo.com

² Electronics Dept, Visvesvaraya National Institute of Technology

Abstract. Interference in wireless/mobile communications can be reduced by deploying efficient radio subsystems and by **making use of channel assignment techniques**. The number of frequencies assigned to each base station must be chosen large enough to satisfy the given demand in the corresponding cell. In this paper, authors made an attempt to combine advantages of all existing individual techniques, which results legal frequency assignments without any interference. The main optimization work with the genetic algorithm is done to search for an optimal call list and not to directly find an optimal frequency assignment. The application of our combined genetic algorithm method to very different frequency-assignment problems has revealed that it is possible to get very good results **without any parameter adjustment**.

1 Introduction

The tremendous growth of the wireless/mobile users' population coupled with the bandwidth requirements of multimedia applications requires efficient **REUSE** of the scarce radio spectrum allocated to wireless/mobile communications. Interference can be reduced by deploying efficient radio subsystems and by **making use of channel assignment techniques**. Thereby, it is important to avoid possible interferences between different mobile users. At the same time, the number of frequencies assigned to each base station must be chosen large enough to satisfy the given demand in the corresponding cell. Regarding these two requirements, formulation of the frequency-assignment problem as a discrete optimization problem has been derived. Many researchers had attended the channel assignment problem and results are being presented [1-5]. It was reported that the time needed to compute an optimal solution increases exponentially with the size of the problem. The authors tried to focus the nature of problem, need for optimization and based on that a new method to give better performance. Existing published approaches can be divided into two different groups. The algorithms, which first determine an ordered list of all call in the whole system and then assign frequencies to the calls following a deterministic assignment strategy. Secondly, the formulation of a cost function which evaluates for example the number of interference constraints violated by a given frequency assignment and then try to minimize this cost function.

* Professor and Head

1.1 Call Orderings

This approach consists in the idea of first generating a list of all calls in the system. First, all calls are continuously numbered and then these numbers are entered in a list. This list is then identified with a corresponding vector, which contains the different call numbers. Once given such a list of calls, some authors propose to assign the frequencies to the calls following a deterministic strategy. Such a well-known assignment algorithm was for example the so called “frequency exhaustive assignment (FEA) strategy”[6]. Starting at the top of list, this algorithm assigns to each call the lowest possible frequency consistent with previous assignments, i.e., without violating the interference constraints. It is then obvious that the number of frequencies, which is necessary to allocate a proper channel for each call, depends significantly on the order of the calls within the list. Unfortunately, even such a process of sorting in general does not lead to an optimal order of the calls and consequently no optimal frequency assignments can generally be found this way.

1.2 Minimization of Cost Functions

A conventional approach of neural network approach for the minimization of the cost function consists of danger of getting stuck in local minima. A much more powerful approach to cope with the problem of local minima is **genetic algorithms**. In the case of large and difficult frequency-assignment problems, with GA, it is nearly impossible to find a solution, which fulfills all given constraints. This means that the value of the cost function cannot be minimized to zero.

1.3 Combined Genetic Algorithm

Combining the advantages of both the algorithms into a new algorithm (Combined Genetic Algorithm –CGA), is proposed as shown in Fig.1. Here, an optimal call list is determined first and only then frequencies are assigned with the FEA strategy. This assures to legal frequency assignments without any interference. This leads to a desirable reduction of the search space and therefore significantly facilitates the optimization problem.

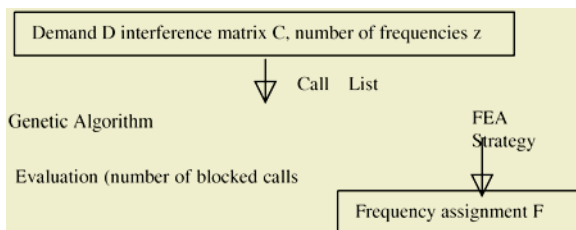


Fig. 1. Combined Genetic Algorithm (CGA)

1.4 CGA Execution

Apply genetic algorithm to generate new call lists and then the FEA strategy is used to evaluate the quality of the generated call lists. Here, for each single call list ‘L’ the FEA strategy is applied in order to determine the number of calls without an allocated

frequency, i.e., it is checked that how many calls have to be blocked because for the given number of frequencies ‘Z’ the FEA strategy can not assign a proper frequency without violating the interference constraints. Denoting the number of blocked calls by ‘b’, a low value of ‘b’ then corresponds to a high-solution quality in the context of the evaluation process needed within the genetic algorithm.

Based on these derived evaluations genetic algorithm then generates new, hopefully better, call lists during the next iteration. This process is then repeated until the application of the FEA strategy to a proper call list leads to a frequency assignment with the desired minimum number of frequencies.

In the whole process to minimize the total available number of frequencies ‘Z’ a solution is also provided by first estimating the number of frequencies, which is at least necessary to solve the optimization problem. Such estimation can easily be determined by the application of LOWER BOUNDS. Therefore, first a value equal to the computed lower bound is chosen and the CGA method is started with this assumed number of frequencies.

2 Design Approach

Authors have applied the proposed algorithm to 21-cell problem [7]. The cellular layout of the considered 21-cell system is depicted in Fig. 2. Assuming the demand vector shown in Table 1 and considering different interference conditions, derivates the frequency-assignment problem.

Table 1. Derivation of Vector D2

| | d1 | d2 | d3 | d4 | d5 | d6 | d7 | d8 | d9 | d10 | |
|----|-----|-----|-----|-----|-----|-----|-----|-----|-----|-----|-----|
| D2 | 5 | 5 | 5 | 8 | 12 | 25 | 30 | 25 | 30 | 40 | |
| | d11 | d12 | d13 | D14 | d15 | d16 | d17 | d18 | d19 | d20 | d21 |
| D2 | 40 | 45 | 20 | 30 | 25 | 15 | 15 | 30 | 20 | 20 | 25 |

Considering the conditions on frequencies to be assigned a value of **two** in the corresponding column of Table 2 implies ACC (Adjacent Channel Constraint) that the neighbored frequencies cannot be used simultaneously in **adjacent cells**. Additionally, different values of the so-called Cosite Constraint (CSC) are assumed in the investigated benchmark problems. This value corresponds to the **minimum distance between two frequencies used in the same cell**. Finally, a cluster size of seven has been assumed for all presented problems of Table II. This means that the same frequency can be assigned to two base stations, if these stations are separated by at least two other cells. The resulting interference matrices C can then be derived by the given information and the cellular layout shown in Fig.1.

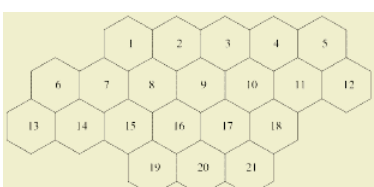


Table 2. Frequency Demand for the 21 Cell problem

| | |
|----------------|----|
| Problem Number | 6 |
| ACC | 2 |
| CSC | 5 |
| Demand Vector | D2 |

Fig. 2. 21 Cell System

3 Simulation and Experimental Results

The simulation of above 21-cell problem to verify the CGA approach is being done using Matlab and GEBT toolbox of genetic algorithm. A main file ChannelAssign.m is created to call other functions. CMaint.m file contains the compatibility matrix, which has been generated according to the constraints. AssignCell.m file is used to do frequency assignment. In Channel.m file, GA functions are called. The graphical output, which is generated at the end of execution, is also a result of this file. FitConstraint.m checks the assigned frequencies for the criteria of assignment and if the criterion is satisfied then only assignment takes place. Rule_Adapt.txt stores output in text format.

3.1 Output of Simulation 1

Demand Vector used: Default (As shown in GUI window)

Max Freq. used=321

| Derived Channel Assignment For a Given Problem | | | | | | | | | | | | | | | | | | | | | | | | | | | |
|--|----|----|----|----|-----|-----|-----|-----|-----|-----|-----|-----|-----|-----|-----|-----|-----|-----|-----|-----|-----|-----|-----|-----|-----|-----|----|
| 1 | 3 | 5 | 7 | 3 | 3 | 5 | 7 | 9 | 3 | 5 | 7 | 3 | 9 | 7 | 3 | 5 | 9 | 3 | 5 | 7 | 3 | 5 | 9 | 3 | 5 | 7 | |
| 11 | 13 | 15 | 17 | 11 | 11 | 13 | 15 | 17 | 11 | 13 | 15 | 11 | 17 | 15 | 11 | 13 | 17 | 11 | 13 | 17 | 11 | 13 | 15 | 11 | 13 | 15 | |
| 19 | 21 | 23 | 25 | 19 | 19 | 21 | 23 | 25 | 19 | 21 | 23 | 19 | 25 | 23 | 19 | 21 | 25 | 19 | 21 | 25 | 19 | 21 | 23 | 19 | 21 | 23 | |
| 27 | 29 | 31 | 33 | 27 | 27 | 29 | 31 | 33 | 27 | 29 | 31 | 27 | 33 | 31 | 27 | 29 | 33 | 27 | 29 | 33 | 27 | 29 | 31 | 27 | 29 | 31 | |
| 35 | 37 | 39 | 41 | 35 | 35 | 37 | 39 | 41 | 35 | 37 | 39 | 35 | 41 | 39 | 35 | 37 | 41 | 35 | 37 | 41 | 35 | 37 | 39 | 35 | 37 | 39 | |
| 0 | 0 | 0 | 47 | 43 | 43 | 45 | 47 | 49 | 43 | 45 | 47 | 43 | 49 | 47 | 43 | 45 | 49 | 43 | 45 | 49 | 43 | 45 | 47 | 45 | 47 | 47 | |
| 0 | 0 | 0 | 0 | 53 | 51 | 51 | 53 | 55 | 57 | 51 | 53 | 55 | 51 | 57 | 55 | 51 | 53 | 57 | 51 | 53 | 57 | 51 | 53 | 55 | 51 | 53 | 55 |
| 0 | 0 | 0 | 0 | 59 | 61 | 59 | 61 | 63 | 65 | 59 | 61 | 63 | 59 | 65 | 63 | 59 | 61 | 65 | 59 | 61 | 65 | 59 | 61 | 63 | 59 | 61 | 63 |
| 0 | 0 | 0 | 0 | 67 | 67 | 69 | 71 | 73 | 67 | 69 | 71 | 67 | 73 | 71 | 67 | 69 | 73 | 67 | 69 | 73 | 67 | 69 | 71 | 67 | 69 | 71 | |
| 0 | 0 | 0 | 0 | 75 | 75 | 77 | 79 | 81 | 75 | 77 | 79 | 75 | 81 | 79 | 75 | 77 | 81 | 75 | 77 | 81 | 75 | 77 | 79 | 75 | 77 | 79 | |
| 0 | 0 | 0 | 0 | 83 | 83 | 85 | 87 | 89 | 83 | 85 | 87 | 83 | 89 | 87 | 83 | 85 | 89 | 83 | 85 | 89 | 83 | 85 | 87 | 83 | 85 | 87 | |
| 0 | 0 | 0 | 0 | 91 | 91 | 93 | 95 | 97 | 91 | 93 | 95 | 91 | 97 | 95 | 91 | 93 | 97 | 91 | 93 | 97 | 91 | 93 | 95 | 91 | 93 | 95 | |
| 0 | 0 | 0 | 0 | 0 | 99 | 101 | 103 | 105 | 99 | 101 | 103 | 99 | 105 | 103 | 99 | 101 | 105 | 99 | 101 | 105 | 99 | 101 | 103 | 99 | 101 | 103 | |
| 0 | 0 | 0 | 0 | 0 | 107 | 109 | 111 | 113 | 107 | 109 | 111 | 107 | 113 | 111 | 107 | 109 | 113 | 107 | 109 | 113 | 107 | 109 | 111 | 107 | 109 | 111 | |
| 0 | 0 | 0 | 0 | 0 | 115 | 117 | 119 | 121 | 115 | 117 | 119 | 115 | 121 | 119 | 115 | 117 | 121 | 115 | 117 | 121 | 115 | 117 | 119 | 115 | 117 | 119 | |
| 0 | 0 | 0 | 0 | 0 | 123 | 125 | 127 | 129 | 123 | 125 | 127 | 123 | 129 | 127 | 0 | 0 | 129 | 123 | 125 | 127 | 0 | 0 | 129 | 123 | 125 | 127 | |
| 0 | 0 | 0 | 0 | 0 | 131 | 133 | 135 | 137 | 131 | 133 | 135 | 131 | 137 | 135 | 0 | 0 | 137 | 131 | 133 | 135 | 0 | 0 | 137 | 131 | 133 | 135 | |
| 0 | 0 | 0 | 0 | 0 | 139 | 141 | 143 | 145 | 139 | 141 | 143 | 139 | 145 | 143 | 0 | 0 | 145 | 139 | 141 | 143 | 0 | 0 | 145 | 139 | 141 | 143 | |
| 0 | 0 | 0 | 0 | 0 | 147 | 149 | 151 | 153 | 147 | 149 | 151 | 147 | 153 | 151 | 0 | 0 | 153 | 147 | 149 | 151 | 0 | 0 | 161 | 155 | 157 | 159 | |
| 0 | 0 | 0 | 0 | 0 | 155 | 157 | 159 | 161 | 155 | 157 | 159 | 155 | 161 | 159 | 0 | 0 | 161 | 155 | 157 | 159 | 0 | 0 | 169 | 0 | 0 | 167 | |
| 0 | 0 | 0 | 0 | 0 | 163 | 165 | 167 | 169 | 163 | 165 | 167 | 0 | 169 | 167 | 0 | 0 | 169 | 0 | 0 | 169 | 0 | 0 | 167 | 0 | 0 | 175 | |
| 0 | 0 | 0 | 0 | 0 | 171 | 173 | 175 | 177 | 171 | 173 | 175 | 0 | 177 | 175 | 0 | 0 | 177 | 0 | 0 | 177 | 0 | 0 | 175 | 0 | 0 | 175 | |
| 0 | 0 | 0 | 0 | 0 | 179 | 181 | 183 | 185 | 179 | 181 | 183 | 0 | 185 | 183 | 0 | 0 | 185 | 0 | 0 | 185 | 0 | 0 | 183 | 0 | 0 | 183 | |
| 0 | 0 | 0 | 0 | 0 | 187 | 189 | 191 | 193 | 187 | 189 | 191 | 0 | 193 | 191 | 0 | 0 | 193 | 0 | 0 | 193 | 0 | 0 | 191 | 0 | 0 | 191 | |
| 0 | 0 | 0 | 0 | 0 | 195 | 197 | 199 | 201 | 195 | 197 | 199 | 0 | 201 | 199 | 0 | 0 | 201 | 0 | 0 | 201 | 0 | 0 | 199 | 0 | 0 | 199 | |
| 0 | 0 | 0 | 0 | 0 | 203 | 0 | 207 | 203 | 205 | 207 | 203 | 0 | 207 | 0 | 0 | 207 | 0 | 0 | 207 | 0 | 0 | 0 | 0 | 0 | 0 | 0 | |
| 0 | 0 | 0 | 0 | 0 | 209 | 0 | 213 | 209 | 211 | 213 | 0 | 213 | 0 | 0 | 0 | 213 | 0 | 0 | 213 | 0 | 0 | 0 | 0 | 0 | 0 | 0 | |
| 0 | 0 | 0 | 0 | 0 | 215 | 0 | 219 | 215 | 217 | 219 | 0 | 219 | 0 | 0 | 0 | 219 | 0 | 0 | 219 | 0 | 0 | 0 | 0 | 0 | 0 | 0 | |
| 0 | 0 | 0 | 0 | 0 | 221 | 0 | 225 | 221 | 223 | 225 | 0 | 225 | 0 | 0 | 0 | 225 | 0 | 0 | 225 | 0 | 0 | 0 | 0 | 0 | 0 | 0 | |
| 0 | 0 | 0 | 0 | 0 | 227 | 0 | 231 | 227 | 229 | 231 | 0 | 231 | 0 | 0 | 0 | 231 | 0 | 0 | 231 | 0 | 0 | 0 | 0 | 0 | 0 | 0 | |
| 0 | 0 | 0 | 0 | 0 | 0 | 0 | 0 | 0 | 233 | 235 | 237 | 0 | 0 | 0 | 0 | 0 | 0 | 0 | 0 | 0 | 0 | 0 | 0 | 0 | 0 | 0 | |
| 0 | 0 | 0 | 0 | 0 | 0 | 0 | 0 | 0 | 239 | 241 | 243 | 0 | 0 | 0 | 0 | 0 | 0 | 0 | 0 | 0 | 0 | 0 | 0 | 0 | 0 | 0 | |
| 0 | 0 | 0 | 0 | 0 | 0 | 0 | 0 | 0 | 245 | 247 | 249 | 0 | 0 | 0 | 0 | 0 | 0 | 0 | 0 | 0 | 0 | 0 | 0 | 0 | 0 | 0 | |
| 0 | 0 | 0 | 0 | 0 | 0 | 0 | 0 | 0 | 251 | 253 | 255 | 0 | 0 | 0 | 0 | 0 | 0 | 0 | 0 | 0 | 0 | 0 | 0 | 0 | 0 | 0 | |
| 0 | 0 | 0 | 0 | 0 | 0 | 0 | 0 | 0 | 257 | 259 | 261 | 0 | 0 | 0 | 0 | 0 | 0 | 0 | 0 | 0 | 0 | 0 | 0 | 0 | 0 | 0 | |
| 0 | 0 | 0 | 0 | 0 | 0 | 0 | 0 | 0 | 263 | 265 | 267 | 0 | 0 | 0 | 0 | 0 | 0 | 0 | 0 | 0 | 0 | 0 | 0 | 0 | 0 | 0 | |
| 0 | 0 | 0 | 0 | 0 | 0 | 0 | 0 | 0 | 269 | 271 | 273 | 0 | 0 | 0 | 0 | 0 | 0 | 0 | 0 | 0 | 0 | 0 | 0 | 0 | 0 | 0 | |
| 0 | 0 | 0 | 0 | 0 | 0 | 0 | 0 | 0 | 275 | 277 | 279 | 0 | 0 | 0 | 0 | 0 | 0 | 0 | 0 | 0 | 0 | 0 | 0 | 0 | 0 | 0 | |
| 0 | 0 | 0 | 0 | 0 | 0 | 0 | 0 | 0 | 281 | 283 | 285 | 0 | 0 | 0 | 0 | 0 | 0 | 0 | 0 | 0 | 0 | 0 | 0 | 0 | 0 | 0 | |
| 0 | 0 | 0 | 0 | 0 | 0 | 0 | 0 | 0 | 287 | 289 | 291 | 0 | 0 | 0 | 0 | 0 | 0 | 0 | 0 | 0 | 0 | 0 | 0 | 0 | 0 | 0 | |
| 0 | 0 | 0 | 0 | 0 | 0 | 0 | 0 | 0 | 297 | 0 | 0 | 0 | 0 | 0 | 0 | 0 | 0 | 0 | 0 | 0 | 0 | 0 | 0 | 0 | 0 | 0 | |
| 0 | 0 | 0 | 0 | 0 | 0 | 0 | 0 | 0 | 303 | 0 | 0 | 0 | 0 | 0 | 0 | 0 | 0 | 0 | 0 | 0 | 0 | 0 | 0 | 0 | 0 | 0 | |
| 0 | 0 | 0 | 0 | 0 | 0 | 0 | 0 | 0 | 309 | 0 | 0 | 0 | 0 | 0 | 0 | 0 | 0 | 0 | 0 | 0 | 0 | 0 | 0 | 0 | 0 | 0 | |
| 0 | 0 | 0 | 0 | 0 | 0 | 0 | 0 | 0 | 315 | 0 | 0 | 0 | 0 | 0 | 0 | 0 | 0 | 0 | 0 | 0 | 0 | 0 | 0 | 0 | 0 | 0 | |
| 0 | 0 | 0 | 0 | 0 | 0 | 0 | 0 | 0 | 321 | 0 | 0 | 0 | 0 | 0 | 0 | 0 | 0 | 0 | 0 | 0 | 0 | 0 | 0 | 0 | 0 | 0 | |

Fig. 3. Output of simulation 1

3.2 Output of Second Simulation

Max Freq. used =272

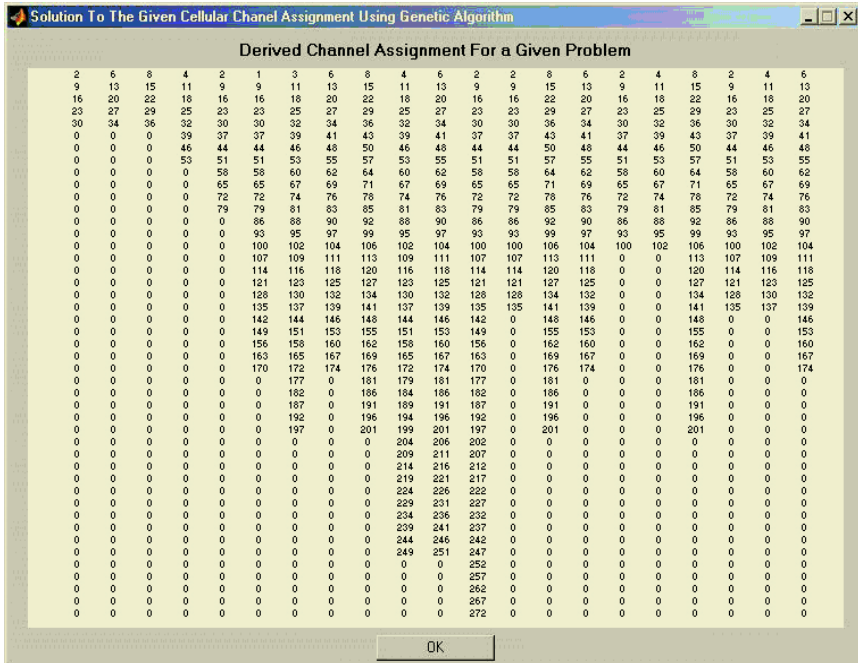
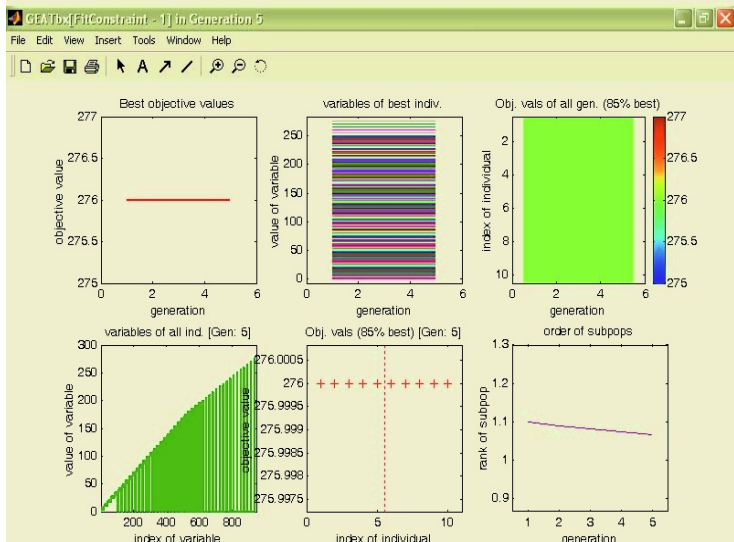


Fig. 4. Output of simulation 2

3.3 Graphical Status of Genetic Operations



4 Conclusion

The work includes simulation for different outputs with respect to different demand vectors. Even though the size of the CHROM has been kept fixed the demand vector has been made variable to facilitate the visualization of the derived channel assignment for a demand vector other than the one mentioned in problem. This combined approach constitutes an important improvement for the successful application of genetic algorithms to the frequency assignment problem.

A further significant decrease of the computing time can be reached by a possible parallelization of our algorithm. The presented CGA-strategy is very well suited for a parallel implementation because nearly 95% of the computing time is spent within the algorithm in order to evaluate the call lists by the FEA strategy. But the evaluations of these call lists within each iteration can be executed at the same time by different processors because there does not exist any dependence between the evaluations of the single vectors. The proposed parallel implementation would nearly accelerate the computation by a factor of ten if we generate ten new solutions in each iteration. Finally, the procedures of selection, mutation and crossover might be further improved and adjusted to the frequency assignment problem in order to accelerate the convergence behavior and reduce the computing time this way.

References

1. D. Kunz, "Channel assignment for cellular radio using neural networks," *IEEE Trans. Veh. Technol.*, vol. 40, pp. 188–193, Feb. 1991.
2. N. Funabiki and Y. Takefuji, *IEEE Trans. Veh. Technol.*, vol. 41, pp. 430–437, Nov. 1992.
3. J. S. Kim, S. H. Park, P. W. Dowd, and N. M. Nasrabadi, *IEEE Trans. Veh. Technol.*, vol. 46, pp. 957–967, Nov. 1997.
4. Frank Yeong-Sung Lin, National Taiwan University, January 1998
5. C. Y. Ngo and V. O. K. Li, "Fixed channel assignment in cellular radio networks using a modified genetic algorithm," *IEEE Trans. Veh. Technol.*, vol. 47, pp. 163–172, Feb. 1998
6. Yang Wang, Thomas Kunz, "A Dynamic Assignment Problem in a Mobile System with Limited Bandwidth" January 2003

On Self-organising Diagnostics in Impact Sensing Networks

Mikhail Prokopenko¹, Peter Wang¹, Andrew Scott²,
Vadim Gerasimov¹, Nigel Hoschke², and Don Price²

¹ CSIRO Information and Communication Technology Centre
Locked bag 17, North Ryde 1670, Australia

{Mikhail.Prokopenko,Peter.Wang,Vadim.Gerasimov}@csiro.au

² CSIRO Industrial Physics
Locked bag 17, North Ryde 1670, Australia
{Andrew.Scott,Nigel.Hoschke,Don.Price}@csiro.au

Abstract. Structural health management (SHM) of safety-critical structures requires multiple capabilities: sensing, assessment, diagnostics, prognostics, repair, etc. This paper presents a capability for *self-organising diagnosis* by a group of autonomous sensing agents in a distributed sensing and processing SHM network. The diagnostics involves acoustic emission waves emitted as a result of a sudden release of energy during impacts and detected by the multi-agent network. Several diagnostic techniques identifying the nature and severity of damage at multiple sites are investigated, and the self-organising maps (Kohonen neural networks) are shown to outperform the standard k-means algorithm in both time- and frequency domains.

1 Introduction

Structural health management (SHM) of complex, safety-critical structures such as aero-space vehicles will ultimately require the development of intelligent systems – systems that can process the data from large numbers of sensors; evaluate and diagnose detected damage; form a prognosis for the damaged structure; make decisions regarding response to or repair of the damage; initiate the required actions and monitor their effectiveness. CSIRO, with support from NASA, is investigating approaches to such sensor networks based on complex multi-agent systems principles that are expected to provide the desirable characteristics of robustness, reliability and scalability [1, 12]. The transition from conventional “hot spot” monitoring, which uses relatively few sensors and treats damage detection as a separate task from data analysis and prognosis, to comprehensive SHM employing very large numbers of diverse sensors integrated into the material microstructure, will necessitate the handling of massive amounts of diverse data, leading to potential failures due to information and communications loss, and information overload. In order to solve this problem, we propose an innovative multi-cellular sensor and communication network, with self-monitoring and self-diagnosing capabilities, leading to distributed self-assessment. Data will be processed locally, and only information relevant to other regions of the structure will be communicated.

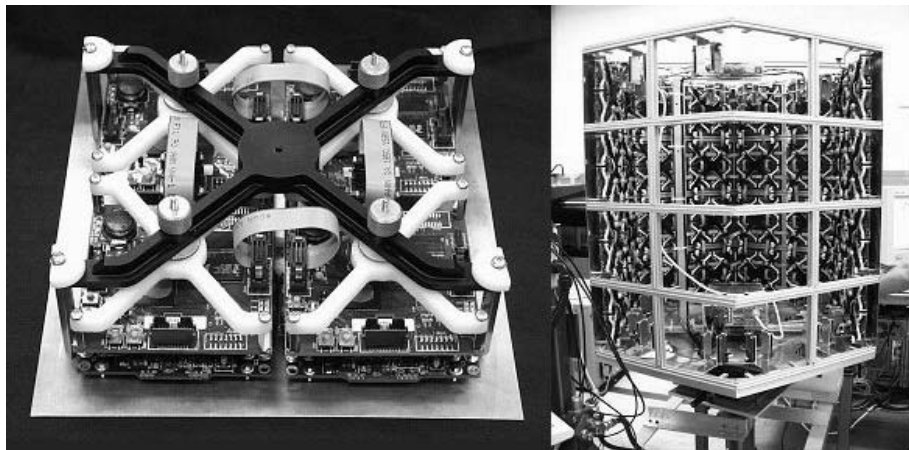


Fig. 1. A single aluminium panel with 4 cells (left) and a general view of the Concept Demonstrator (right), with four of the six sides populated

Thus, the focus of our current research is on developing a capability for *self-organising diagnosis* by a group of autonomous sensing cells in a distributed sensing and processing network, and on demonstrating the outcomes on a large-scale hardware test-bed – the “Ageless” Aerospace Vehicles (AAV) Concept Demonstrator (CD). The AAV-CD consists of “cells”, that not only form a physical shell for an aerospace vehicle, but also have sensors, logic, and communications. Currently, each cell contains 4 passive piezoelectric polymer sensors, consisting of a $110\ \mu\text{m}$ -thick film of PVDF (polyvinylidene fluoride) coated on both sides with a conductive gold layer, bonded to an aluminium skin panel in order to detect the elastic waves generated in the structure by impacts. The present structure of the AAV-CD is a hexagonal prism. A modular aluminium frame is covered by 220 mm x 200 mm, 1-mm thick aluminium panels that form the outer skin of the structure. Each such panel contains four cells, and each of the six sides of the prism contains eight of these panels. The entire AAV Concept Demonstrator contains 48 panels, 192 cells, and a total of 768 sensors in the initial system (Figure 1).

Some of the distributed processing involves only interactions between local agents, while other processing requires the emergence of dynamic hierarchical structures. An example of the former is emergent spatial organisation, such as our previously reported work on the formation of impact boundaries [6, 7], evolvable recovery membranes [15] and impact networks around damaged areas [14], which can be used to characterize the extent of damage. The focus of this paper is to investigate diagnostic techniques identifying the nature and severity of damage at multiple sites, but at this stage, not identifying either the causes of damage or the required remedial actions. In particular, we consider the self-organising maps (SOMs or Kohonen neural networks) [9, 10], the Principal Component Analysis (PCA) technique [8], and their combinations. Each considered technique involves collecting input-vectors for several impact signal categories, a training phase using a half of the input-vectors and producing a clustering,

and a testing phase when the other half is diagnosed by mapping to produced clusters. Appropriate metrics, e.g. recall and precision, are used to characterise the techniques performance.

At this stage, the diagnostic models are centralised: all the detected inputs are collected prior to the training and testing phases, so that processing is carried out outside the AAV-CD. Eventually, these techniques will be decentralised and embedded in the AAV-CD multi-cellular array, enabling an on-line assessment of damage type and severity. Our main objective is to evaluate the concept of self-organising diagnostics in the context of a self-monitoring impact sensing network. The following Section briefly reviews some background research. Section 3 describes the employed techniques, followed by experimental set-up and diagnostics results (Section 4) and conclusions (Section 5).

2 Background

Acoustic emission (AE) is an ultrasonic wave emitted as a result of a sudden release of energy during a deformation and failure process [3]. The released energy can be detected by sensors sensitive to displacement or velocity. A subsequent analysis of the arrival times of the signals at different sensor locations along with knowledge of the velocity of sound propagation can be used to triangulate the location of the damage mechanism [2, 13]. In some cases, detailed analysis of the acoustic emission signals can also provide information about the nature and severity of the damage. For example, AE methods are being investigated for on-board impact detection for the Space Shuttle — following the Columbia Shuttle accident which resulted from damage to the Shuttle wing’s leading edge, caused by impact of foam insulation that broke off of the external tank during ascent [13].

Recently, neural networks have been successfully used in clustering and identifying damage-related AE signals in a highly noisy environment, achieving very good classification results for crack-related signals in the presence of strong time-varying noise and other interference [5] — in particular, the Kohonen network (SOM) was applied for this purpose. Artificial Neural Networks (ANN) and Support Vector Machines (SVM) were also recently considered as approaches to build classifiers in order to assess the structural integrity of shafts and pins based on ultrasonic signatures [11]. It is generally observed that a combination of classifiers may produce a more informative classification. Thus, a sequence of PCA and SOM is used in [5], while a hybrid ANN-SVM classifier is found more informative in [11].

3 Self-organising Maps

The very popular SOM algorithm was originally devised by Teuvo Kohonen [9, 10] as a model of the self-organisation of neural connections, with the ability to produce organisation starting from possibly total disorder. The Kohonen algorithm for self organising feature maps stores prototypes $\vec{w}_{i,j}$ (also known as codebook vectors) of the input-vectors of an euclidian input space X , \vec{x} , in the neurons (cells) of a neural layer R (a 2D grid). The prototype vectors $\vec{w}_{i,j}$ are usually initialized with random values. At each

iteration $t \geq 0$, there are M updates: one for each input-vector $\overrightarrow{x(m)}$, $1 \leq m \leq M$ (we shall denote an update with an index $\tau = tM + m$). Every stimulus $\overrightarrow{x(m)}$ is mapped to the “winner” neuron with the position (i, j) in the neural layer R , which has the prototype vector $\overrightarrow{w_{i,j}}$ with the minimal euclidian distance in input space:

$$\|\overrightarrow{x(m)} - \overrightarrow{w_{i,j}(\tau)}\| = \min_{(k,l) \in R} (\|\overrightarrow{x(m)} - \overrightarrow{w_{k,l}(\tau)}\|),$$

where $\|\cdot\|$ denotes the euclidian distance in input space. The winner neuron corresponds to the highest neural activity, being the “center of excitation”. The prototype vector of the winner neuron is updated, becoming more sensitive to that type of input. This allows different cells to be trained for different types of data. The neighbors of the winner neuron adjust their prototype vector towards the input vector as well, but in a lesser degree, dependent on their distance from the winner. Usually a neighbourhood function $\eta_{(i,j),(k,l)}(t)$ that decreases both with time and distance between positions (i, j) and (k, l) on the planar neural layer (e.g., a radial symmetric Gaussian neighbourhood function), is used for this purpose:

$$\overrightarrow{w_{k,l}(\tau+1)} = \overrightarrow{w_{k,l}(\tau)} + \alpha(t) \eta_{(i,j),(k,l)}(t) [\overrightarrow{x(m)} - \overrightarrow{w_{k,l}(\tau)}].$$

The function $\alpha(t)$, such that $0 < \alpha(t) < 1$ determines the speed of learning and can be reduced during the learning process. The radius of the neighbourhood $\rho(t)$ decreases with each iteration as follows:

$$\rho(t) = \rho_0 e^{-\frac{t \ln \rho_0}{N}}$$

with N being the maximal number of iterations. In our experiments, a linear neighbourhood function outperformed the Gaussian function.

Since prototype vectors, whose neurons with positions (k, l) are close to the winner with the position (i, j) , are always updated together, a topology preservation is achieved — neurons that are closer in the neural layer tend to respond to inputs that are closer in the input space. In other words, SOM learns a smooth mapping of the input space to the neural layer. However, the solutions obtained by SOM might be different due to different trajectories through the search space, and therefore the input-vectors can be reused many iterations (“epochs”) during the training phase, in different orders.

4 Experimental Results

In order to carry out and evaluate self-organising diagnostics in the AAV impact sensing network, we collected the data containing the transients (voltage vs time) from PVDF transducers attached to a separate aluminium panel that is subject to laser or mechanical impacts, with high or low energy. Laser impacts have been produced by pulses with either the energy of 300 mJ or 30 mJ using a Q-switched Nd:YAG laser focused onto the surface to simulate particle impacts by ablating material from the aluminum. Impacts did not pierce the skin, but left a significant crater in the aluminum surface. The outputs were detected by four receivers while the laser impact site is changed over the panel in a specific pattern (Figure 2). The sensors were in quadrant α only, at positions

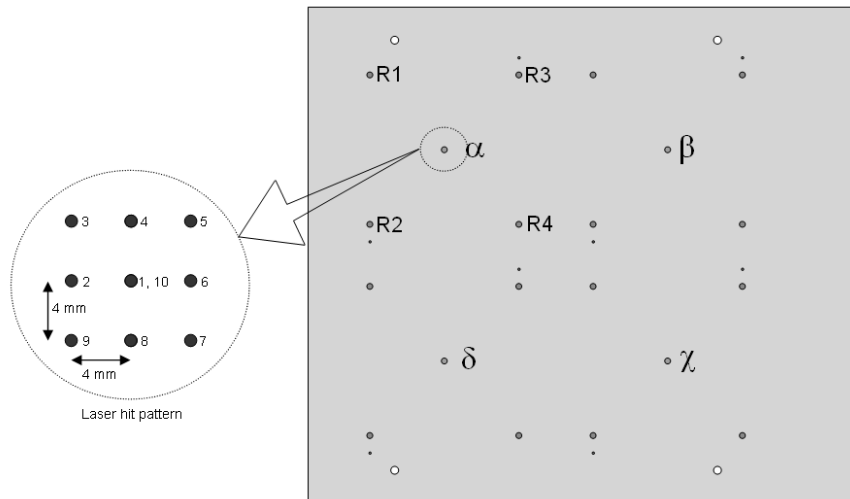


Fig. 2. A pattern of laser impacts

$R1$, $R2$, $R3$ and $R4$. Ten laser impacts, for each energy level, were aimed near the centre of each quadrant equidistant from each, with each subsequent impact moving 4-mm in the sequence, indexed from 1 to 10, so that the first and the tenth strike at the centre.

The mechanical impacts resulted from a stainless steel-tipped pendulum bob. Again, the outputs were detected by four receivers, while striking the panel ten times at each quadrant. Ten pendulum impacts, for each energy level, were aimed at the centre of each quadrant — unlike laser shots, they were not moved around on a 4-mm grid.

The goal of clustering and diagnostics is to identify and distinguish between different impact types (laser vs pendulum) and different impact energies (high vs low) — the distances to impacts are not intended to be determined. In other words, the process of varying impact locations in the laser experiments does not pursue the goal of representing different distances in the data-set, but has a rather practical purpose of avoiding the panel fatigue from repeated laser impacts.

The collected data present a number of challenges for clustering and diagnostics. First of all, there are different impact types and different energy levels, creating 4 objective categories. For example, a high-energy impact from the quadrant β may be very similar to a low-energy impact from the quadrant α — especially if the signals of the same impact, detected by four sensors, are treated separately from each other. Laser impacts, in addition, vary due to the shifting impact locations: for instance, impacts at locations 1 and 10 differ from those at 3,5,7,9, and from those at 2,4,6,8. Moreover, there are signal reflections from the panel's edges. More precisely, in all of these signals, the first arrival corresponds to the S_0 Lamb wave (the lowest order extensional wave), whose faster low frequency components propagate at $5.3 \text{ mm}/\mu\text{s}$ in this material. This is followed by the A_0 (flexural) wave, for which the higher frequency modes propagate faster than the lower frequency components, at the Rayleigh wave velocity

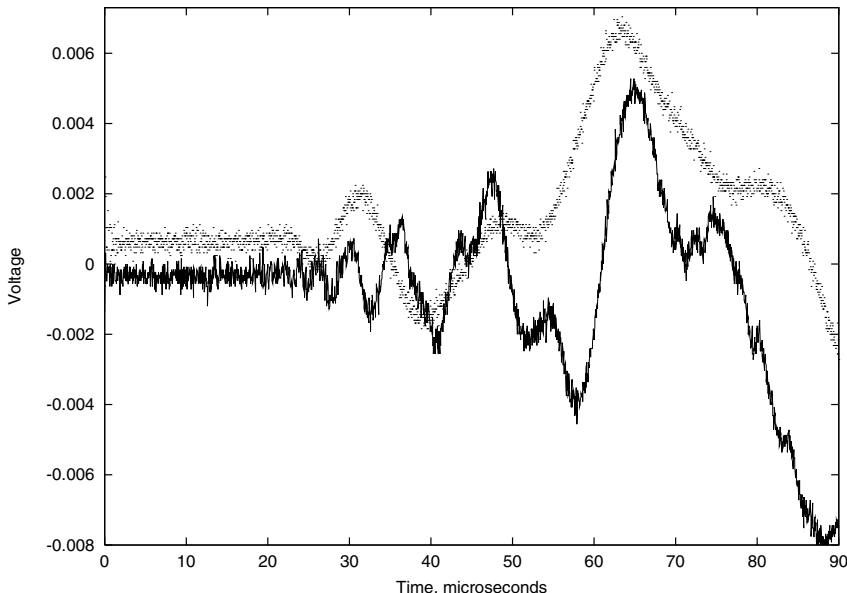


Fig. 3. A laser signal (high energy) in quadrant β , location 5, detected by sensor $R2$ is shown with solid lines. A pendulum signal (low energy) in quadrant α detected by sensor $R1$ is shown with dots

($3 \text{ mm}/\mu\text{s}$ in aluminum). The presence of both waves in the signal makes the laser impacts quite hard to cluster and properly diagnose. Figure 3 shows two signals: a laser with high energy, and a pendulum with low energy. Finally, the training set is relatively small containing 80 impacts detected by 4 sensors.

Each signal contains 2048 time-domain points. Moreover, the signals from the same impact detected by four sensors were concatenated into one input-vector — to better account for the varying distances. In practice such merging can be easily achieved after an AAV cell determines that its four sensors detected the same signal. The training (clustering) phase used signals corresponding to the impact locations from 6 to 10, leaving locations from 1 to 5 to the testing (diagnostics) phase.

In order to comparatively evaluate SOM performance, we used k-means clustering algorithm [4], augmented either with the Principal Component Analysis (PCA) [8], or Discrete Fourier Transform. The PCA transforms a data-set into a new coordinate system in such a way that the new first coordinate axis has the greatest possible variance of the data-set projection, the second axis has the second greatest possible variance of the projections, etc. The ordered new coordinates are called the Principal Components (PCs). In many applications the corresponding variance rapidly decreases from the first to the last PC. A reduction of data-set dimensionality with minimal information loss can be achieved by using only a few first PCs to represent the data. This is a common technique in image compression and pattern recognition. The PCA helps to improve performance and reduce memory demand of data processing algorithms. However, this technique is not optimized for clustering, which, in combination with the information

loss, degrades the quality of the clustering results. Although the PCA is frequently used as a part of a processing sequence in data classification, the true reason to include it is not to improve the classification results, but to reduce the computational demands of the algorithms that follow the PCA. In our experiments we used Singular Value Decomposition (SVD) based algorithm to calculate the PCA.

The Discrete Fourier Transform (DFT) also changes the way the data-set is distributed. It does not guarantee a better clustering either. But if the data-set represents acoustic or electromagnetic signals, the spectral representation of the signals may lead to a better discrimination between different classes of the signals. This was the case with the data-set in our experiments. The K-means algorithm applied to the DFT-processed data-set led to slightly better results than the same algorithm applied to the raw data. To calculate the DFT we used the Fast Fourier Transform (FFT) algorithm embedded in Matlab.

In summary, the clustering was done with a) k-means algorithm applied to the input space; b) k-means algorithm applied to the PCA space; c) k-means algorithm applied to the frequency domain (using Fourier Transform of the input-vectors, FFT) d) SOM of the input space; e) SOM of the FFT space. A comparison between a) and b) is expected to show the benefits of using PCA as a preliminary step, while a comparison between a) and c) would highlight the benefits of FFT. On the other hand, a comparison between a) and d), as well as between c) and e) may support the usage of SOMs in diagnostics.

Input-vectors are labelled with 4 categories (“laser-high”, “laser-low”, “pendulum-high”, “pendulum-low”), and these labels are propagated to resultant clusters (using majority-voting), enabling diagnostics and its evaluation. We used several metrics for each scenario: recall, precision and effectiveness. The recall measures how many test input-vectors x were successfully matched to the correct cluster category out of y existing test vectors from this category: $\delta_i = x_i/y_i$. The precision measures how many test vectors were attracted to each clustered category in relation to the total size of the cluster: $\pi_i = x_i/z_i$, where z_i is the number of all test vectors placed in the cluster. For example, if the cluster 3 attracted $z_3 = 25$ vectors, out of which $x_3 = 19$ vectors belonged to the correct category (which contains $y = 20$ vectors in total), then $\delta_3 = 19/20 = 0.95$ and $\pi_3 = 19/25 = 0.76$. In other words, 95% of the test vectors from this category are correctly recalled (diagnosed) with the precision of 76%. The effectiveness is defined as a harmonic mean of recall and precision: $q_i = 2\delta_i\pi_i/(\delta_i + \pi_i)$, and we use the average effectiveness $q = \sum_{i=1}^4 q_i/4$ in the comparative analysis.

The results of diagnostics are summarised in table 1. The k-means algorithm applied to the PCA-processed data-set had inferior results comparing to the same algorithm applied to the original data. The number of clusters maximising the effectiveness was quite large with or without the FFT step ($k = 50$ and $k = 60$ respectively). FFT helped only marginally — however, there is a clear benefit in using it in the presence of noise. We trained 20 SOMs in the time-domain, each having a square layer of 400 neurons, with a linear neighbourhood function, and calculated the mean recall and precision over these 20 runs, followed by the effectiveness of these mean values (shown in the table). The average performance of these SOMs approached the best result of k-means, while the best SOM out of the trained set exceeded this result. The SOMs applied in the frequency domain have also shown only a marginal improvement, and their best

Table 1. Diagnostics: results of testing

| Technique | Laser | | | | Pendulum | | | | q | |
|------------------------------|------------|---------|------------|---------|------------|---------|------------|---------|--------|--|
| | High | | Low | | High | | Low | | | |
| | δ_1 | π_1 | δ_2 | π_2 | δ_3 | π_3 | δ_4 | π_4 | | |
| a) k-means: k=6, no PCA | 0.15 | 1.0 | 1.0 | 0.28 | 0.25 | 1.0 | 0.0 | 0.0 | 0.2739 | |
| k-means: k=60, no PCA | 0.4 | 1.0 | 0.95 | 0.76 | 1.0 | 1.0 | 0.90 | 0.67 | 0.7955 | |
| b) k-means: k=32, 35 PCs | 0.35 | 1.0 | 0.65 | 0.65 | 1.0 | 0.91 | 0.90 | 0.58 | 0.7067 | |
| c) k-means: k=50, FFT | 0.45 | 1.0 | 0.85 | 0.77 | 1.0 | 1.0 | 1.0 | 0.69 | 0.8116 | |
| d) SOM: linear η , mean | 0.42 | 0.95 | 0.83 | 0.61 | 0.99 | 0.98 | 0.93 | 0.80 | 0.7817 | |
| SOM: linear η , maximum | 0.55 | 1.0 | 0.95 | 0.68 | 1.0 | 1.0 | 0.95 | 0.90 | 0.8570 | |
| e) SOM-FFT: mean | 0.44 | 0.95 | 0.88 | 0.60 | 0.97 | 0.98 | 0.88 | 0.81 | 0.7814 | |
| SOM-FFT: maximum | 0.55 | 1.0 | 0.95 | 0.70 | 1.0 | 1.0 | 1.0 | 0.91 | 0.8676 | |

SOM has also outperformed k-means with the FFT step. Thus, we can conclude that SOM technique is quite appropriate when the training set is small and in the presence of noise.

5 Conclusions

In this paper we evaluated several techniques aimed at self-organising diagnostics in impact sensing networks. The self-organising maps (Kohonen neural networks) have shown to be more promising, outperforming the standard k-means algorithm in both time- and frequency domains, and suggesting a way to embed self-organising diagnostics in distributed and decentralised SHM systems. The common feature of all experiments was a difficulty in recalling the “Laser-High” category. In fact, a better account of this category was a distinguishing contributor to the overall success of the SOM. It can be observed that the signals from this category are mostly placed in the “Laser-Low” category, reducing its precision. In other words, the energy levels are harder to recognise in the higher-velocity signals detected by remote sensors. This observation calls for a comprehensive analysis of optimal sensor density and layout, which is another subject of future work.

References

- Abbott, D., B. Doyle, J. Dunlop, T. Farmer, M. Hedley, J. Herrmann, G. James, M. Johnson, B. Joshi, G. Poulton, D. Price, M. Prokopenko, T. Reda, D. Rees, A. Scott, P. Valencia, D. Ward, and J. Winter. Development and Evaluation of Sensor Concepts for Ageless Aerospace Vehicles. Development of Concepts for an Intelligent Sensing System. Technical Report NASA/CR-2002-211773, Langley Research Center, Hampton, VA, 2002.
- Abbott, D., J. Dunlop, G. Edwards, T. Farmer, B. Gaffney, M. Hedley, N. Hoschke, P. Isaacs, M. Johnson, C. Lewis, A. Murdoch, G. Poulton, D. Price, M. Prokopenko, I. Sharp, A. Scott, P. Valencia, P. Wang, and D. Whitnall. Development and Evaluation of Sensor Concepts for Ageless Aerospace Vehicles. Report 5. Phase 2 — Implementation of the Concept Demonstrator. CSIRO Telecommunications and Industrial Physics. Confidential Report No. TIPP 2056, April 2004.

3. Drouillard, T. F. A history of acoustic emission. *Journal of Acoustic Emission*, vol. 14, no. 1, 1–34, 1996.
4. Elkan, C. Using the Triangle Inequality to Accelerate k-Means. In Proceedings of the 20th International Conference on Machine Learning, 147–153, Washington, DC, 2003.
5. Emamian, V., M. Kaveh, and A. Tewfik. Robust Clustering of Acoustic Emission Signals using the Kohonen Network. In Proceedings of the 25th IEEE International Conference on Acoustics, Speech and Signal Processing, Istanbul, Turkey, 2000.
6. Foreman, M., M. Prokopenko, and P. Wang. Phase Transitions in Self-organising Sensor Networks. In Banzhaf, W., Christaller, T., Dittrich, P., Kim, J.T. and Ziegler, J. (Eds.) *Advances in Artificial Life - Proceedings of the 7th European Conference on Artificial Life*, 781–791, LNAI 2801, Springer Verlag, 2003.
7. Lovatt, H., G. Poulton, D. Price, M. Prokopenko, P. Valencia, and P. Wang. Self-organising Impact Boundaries in Ageless Aerospace Vehicles. In Proceedings of the Second International Joint Conference on Autonomous Agents and Multi-Agent Systems, 249–256, Melbourne, 2003.
8. Jolliffe, I.T. *Principal Component Analysis*. New York, Springer, 1986.
9. Kohonen, T. Self-organized formation of topologically correct feature maps. *Biological Cybernetics*, 43, 59–69, 1982.
10. Kohonen, T. Analysis of a simple self-organizing process, *Biological Cybernetics*, 44, 135–140, 1982.
11. Lee, K., V. Estivill-Castro. A Hybrid Classification Approach to Ultrasonic Shaft Signals. In G.I. Webb, X. Yu (Eds.) *AI 2004: Advances in Artificial Intelligence, 17th Australian Joint Conference on Artificial Intelligence, Cairns, Australia, December 4-6, 2004, Proceedings*, LNCS 3339, 284–295, Springer 2004.
12. Price, D., A. Scott, G. Edwards, A. Batten, T. Farmer, M. Hedley, M. Johnson, C. Lewis, G. Poulton, M. Prokopenko, P. Valencia, and P. Wang. An Integrated Health Monitoring System for an Ageless Aerospace Vehicle. *Structural Health Monitoring 2003: From Diagnostics & Prognostics to Structural Health Management*, F.-K. Chang (Ed.), DEStech Publications, 310–318, 2003.
13. Prosser, W.H., S.G. Allison, S.E. Woodard, R.A. Wincheski, E.G. Cooper, D.C. Price, M. Hedley, M. Prokopenko, A. Scott, A. Tessler and J.L. Spangler. Structural health management for future aerospace vehicles. In Proceedings of the 2nd Australasian Workshop on Structural Health Monitoring, Melbourne, Australia, December 2004.
14. Wang, P., P. Valencia, M. Prokopenko, D. Price, and G. Poulton. Self-reconfigurable sensor networks in ageless aerospace vehicles. In Proceedings of the 11th International Conference on Advanced Robotics, 1098–1103, Coimbra, Portugal, 2003.
15. Wang, P., and M. Prokopenko. Evolvable Recovery Membranes in Self-monitoring Aerospace Vehicles. In Proceedings of the 8th International Conference on Simulation of Adaptive Behaviour, 509–518, Los Angeles, USA, July 2004.

A Coevolutionary Algorithm with Species as Varying Contexts

Myung Won Kim, Joung Woo Ryu, and Eun Ju Kim

School of Computing, Soongsil University 1-1, Sangdo 5-Dong, Dongjak-Gu, Seoul, Korea
mkim@comp.ssu.ac.kr, ryu0914@orgio.net, blue7786@bineee.pe.kr

Abstract. A coevolutionary algorithm is an extension of the conventional genetic algorithm that incorporates the strategy of divide and conquer in developing a complex solution in the form of interacting co-adapted subcomponents. It takes advantage of the reduced search space by evolving species associated with subsets of variables independently but cooperatively. In this paper we propose an efficient coevolutionary algorithm combining species splitting and merging together. Our algorithm conducts efficient local search in the reduced search space by splitting species for independent variables while it conducts global search by merging species for interdependent variables. We have experimented the proposed algorithm with several benchmarking function optimization and have shown that the algorithm outperforms existing coevolutionary algorithms

1 Introduction

Evolutionary algorithm is a general and efficient optimization method and it is successfully applied to various problems including resource management, scheduling, and pattern recognition. However, one of the common problems of the algorithm is that search time grows exponentially as the dimension of search space expands.

Recently, attempts have been made to improve the search speed of the evolutionary algorithm. Potter and DeJong have proposed the cooperative coevolutionary algorithm which improves the search speed significantly [1]. In the algorithm a complete solution is divided into a set of subcomponents corresponding to a single variable called species each of which evolves independently but cooperatively. Each species evolves independently using its own evolution strategy and it corresponds to the search of the 1-dimensional space of a single variable and consequently it allows efficient search. In the algorithm, however, each species cooperates with other species in such a way that an individual of the species is evaluated by evaluating a complete chromosome that is assembled from itself and the best individuals of other species. In this way species evolves independently but cooperatively. In this approach we can view species as local solutions with the fixed contexts and evolution process is a search through the context space with delicate contextual guides. The algorithm shows especially good results when it is applied to the problems of concept learning and the task assignment problem between agents [2,3,4]. But the method can be even less efficient than ordinary algorithms in particular cases that there are lots of Nash equilibrium points and that variables are strongly interdependent. In order to overcome this problem, K. Weicker and N. Weicker proposed adaptive cooperative coevolution algorithm with which they solved the problem by combining species representing vari-

ables if there is variable interdependency [5]. But when most variables are interdependent with one another and after combining all species representing the variables, evolutionary speed sharply decreases as it does in ordinary algorithms due to the rapid expansion of search space.

In this paper we propose a new coevolutionary algorithm as an improvement of Weickers' algorithm. In our algorithm species are not only merged but also split into subcomponent species if necessary. Merging species allows more global but slow evolutionary search while splitting species allows local but fast evolutionary search. Efficiency can be achieved by combining species merging and splitting appropriately. We use variable interdependency as a decision criterion for dynamically controlling species merging and species splitting. In our algorithm species are split when variables are independent while species are merged when variables are interdependent.

2 Existing Coevolutionary Algorithms

2.1 Cooperative Coevolution

Conventional genetic algorithm, proposed by John Holland is a general and global search method based on the natural selection and evolution mechanism. Genetic algorithm initializes and maintains a population of chromosomes that encode potential solutions to a given problem. Each chromosome is generally a fixed length sequence of bits put in order

Potter and DeJong proposed the cooperative coevolutionary genetic algorithm (CCGA) improving the conventional genetic algorithm, which suffers from slow evolution when search space is large. In CCGA each chromosome is divided into its subcomponents each of which corresponds to partial solutions associated with one or more variables involved in the objective function to be optimized. We call a collection of such a specified subcomponent a species. In the algorithm each species evolves independently but cooperatively in such a way that each chromosome of a species is evaluated by assembling it together with representative chromosomes of the other species. In this way each species evolves independently while it collaborates with the other species for evaluation. In CCGA each species is associated with a single variable and by allowing each species evolve independently the algorithm reduces the search space significantly.

Although its evolution speed is fast, CCGA can be less efficient than the ordinary algorithm for problems in which there are strong variable interdependency such that there are lots of Nash equilibrium points [6]. Potter and DeJong also proposed a variant (CCGA2) of the original CCGA (CCGA1) to alleviate the local optimum problem of the original CCGA, particularly when there is strong variable interdependency. The evolution method of CCGA2 is similar to that of CCGA1 but it differs from CCGA1 in that it uses the different evaluation method.

2.2 ACC (Adaptive Cooperative Coevolution)

The Adaptive Cooperative Coevolution Algorithm (ACC) is similar to CCGA except that species can be merged in ACC. During evolution in ACC, variable interdependency is computed and represented by a dependency matrix, and it is used to control

species merging. Two species are merged if variable interdependency between their associated variables (or variable sets) exceeds a given threshold [5].

3 SMCA: Species Splitting and Merging Coevolutionary Algorithm

When it is applied to problems in which variables are strongly interdependent, ACC is no longer efficient because species are merged into a large species as evolution progresses and the evolution speed gets slow down since the search space expands rapidly. To solve this problem of ACC, we propose a new coevolution algorithm called SMCA in which species are not only merged but also split if necessary.

In SMCA, species are merged in a similar way in ACC. SMCA starts with the set of base species each of which is associated with a single variable. During evolution process, interdependencies between species are maintained by a dependency matrix. Two species are merged when their associated interdependency value exceeds a given threshold. A merged species is split into a set of base species if it fails to improve its elite chromosome within a certain period of time. Split species can be merged again based on interdependency between species. Merged species allow more global search, however, they slow down the search speed while split species speed up the search but it may suffer from local search. SMCA combines local but fast search and global but slow search by combining merging and splitting of species appropriately.

3.1 Species Merging

In SMCA its merging method is similar to that of ACC. In case species $S_{V(t)}$ is a merged species that created from species $S_{V_j(t)}$ and $S_{V_k(t)}$ when $V = V_j \cup V_k$, the population of the new species $S_{V(t)}$ is determined as in Eq. 1. $c_i^{S_{V(t)}}$ the i -th chromosome of the new population $S_{V(t)}$ is determined as follows.

As the result, the merged species $S_{V(t)}$ consists of four different kinds of chromosomes created by merging species chromosomes in four different ways; (1) the elite chromosomes of both species, (2) the elite chromosome of species $S_{V_j(t)}$ and randomly chosen chromosomes of species $S_{V_k(t)}$, (3) randomly chosen chromosomes of species $S_{V_j(t)}$ and the elite chromosome of species $S_{V_k(t)}$, and (4) randomly chosen chromosomes of both species. Here, we set the size of population of each kind of chromosomes except (1) to be one third of the population of the merged species. As in ACC, a species is merged when the value of species interdependency in the dependency matrix exceeds a given threshold.

$$c_i^{S_{V(t)}} = \begin{cases} c_{elite}^{S_{V_j}(t)} \circ c_{elite}^{S_{V_k}(t)} : \text{if } i=1, \\ c_{elite}^{S_{V_j}(t)} \circ c_{rand}^{S_{V_k}(t)} : \text{if } 2 \leq i \leq \left\lceil \frac{n}{3} \right\rceil, \\ c_{rand}^{S_{V_j}(t)} \circ c_{elite}^{S_{V_k}(t)} : \text{if } \left\lceil \frac{n}{3} \right\rceil < i \leq \left\lceil \frac{2n}{3} \right\rceil, \\ c_{rand}^{S_{V_j}(t)} \circ c_{rand}^{S_{V_k}(t)} : \text{otherwise} \end{cases} \quad (1)$$

3.2 Species Splitting

Species splitting is to speed up evolution by reducing the search space. If a merged species does not improve the fitness of its elite chromosome within a certain period of time, we consider that the search point places where search is slow and we try to split species for speeding up evolution by chance. Let $\text{proj}(c_i^{S_{V_k}(t)}, V)$ represent a function of extracting genes that encode variables in set V from the i -th chromosome $c_i^{S_{V_k}(t)}$ of species $S_{V_k}(t)$, corresponding to variable set $V_k(t)$, when there exists species $S_{V_k}(t)$, and $V \subseteq V_k$. In this case, if $P = \{U_1, U_2, \dots, U_m\} \left(\bigcup_{i=1}^m U_i = V_k, U_i \cap U_j = \emptyset (i \neq j) \right)$ is a partition of variable set V_k , $S_{U_i}(t)$, the i -th species split from species $S_{V_k}(t)$, and $c_j^{U_i(t)}$, the j -th chromosome of species $S_{U_i}(t)$, are determined as follows.

$$\begin{aligned} \text{split}(S_{V_k}(t), P) &= \{S_{U_1}(t), S_{U_2}(t), \dots, S_{U_m}(t)\} \\ S_{U_i}(t) &= (c_1^{S_{U_i}(t)}, c_2^{S_{U_i}(t)}, \dots, c_n^{S_{U_i}(t)}) \end{aligned} \quad (2)$$

$$c_j^{S_{U_i}(t)} = \text{proj}(c_j^{S_{V_k}(t)}, U_i) : 1 \leq i \leq n, 1 \leq j \leq m \quad (3)$$

In other words, the original species is split into a set of different species each of which corresponds to a set of variables. Apparently many different ways of splitting are possible depending on how the set of variables associated with the species to split is partitioned. In this paper, to make our algorithm simple, we split a species into a set of single variable species.

4 Experiments

We experimented with our algorithm on some of the benchmark function optimization problems including the Ackley function, the Rosenbrock function, and the Schwefel function. For comparison purposes, we used each function in its original form and in its coordinate rotated form to introduce variable interdependency [7]. Parameters and methods used in our function optimization experiments are shown in Table 1.

Table 1. Experiment Parameter Values

| parameters | value |
|------------------|-----------------------|
| population size | 100 |
| bits/variable | 16 |
| crossover rate | 0.6 |
| mutation rate | 1/(chromosome length) |
| selection method | fitness proportionate |
| crossover method | 2 point crossover |

We compare the average performance over 10 runs of our algorithm and others as shown in Figs. 1, 2, and 3.

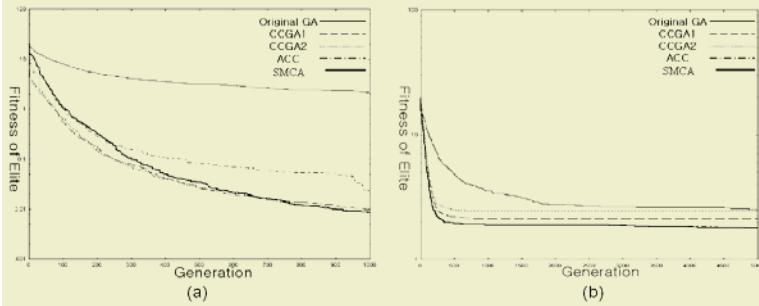


Fig. 1. (a): Ackley and (b): Rotated Ackley

The original form of the Ackley function is defined as

$$F(\vec{x}) = -20 \exp\left(-0.2 \sqrt{\frac{1}{n} \sum_{i=1}^n x_i^2}\right) - \exp\left(\frac{1}{n} \sum_{i=1}^n \cos(2\pi x_i)\right) + 20 + e, -20 \leq x_i \leq 20 \quad (4)$$

The global optimum of the function is $F(\vec{x}) = 0$ at $\vec{x} = (0, 0, \dots, 0)$. The Ackley function does not have variable interdependency in its original form but its rotated form has variable interdependency. In our experiment n (dimension) is fixed to 30.

The Rosenbrock function is given as in Eq. 5 and it has a weak variable interdependency in its original form.

$$F(\vec{x}) = \sum_{i=1}^{n/2} [100(x_{2i} - x_{2i-1}^2)^2 + (1 - x_{2i-1})^2], -2.048 \leq x_i \leq 2.048 \quad (5)$$

The Rosenbrock function has its global minimum at the point $\vec{x} = (1, 1, \dots, 1)$. An interesting characteristic of this function is that variable interdependency exists only between variables x_{2i} and x_{2i-1} when $0 < i \leq n/2$.

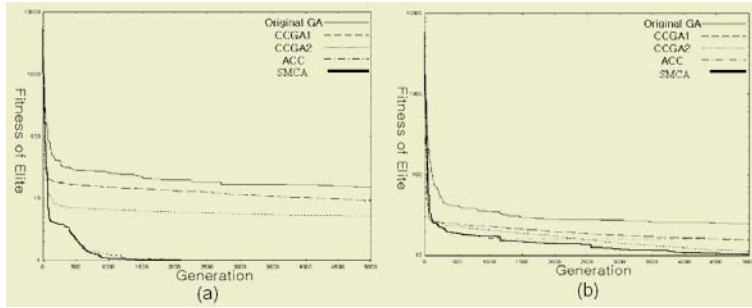


Fig. 2. (a): Rosenbrock and (b): Rotated Rosenbrock

The Schwefel function has a term that contains the sine function and oscillation is getting larger as it moves outward from the center $\vec{x} = (0, 0, \dots, 0)$. The original form of the function is defined as

$$F(\vec{x}) = \sum_{i=1}^n [-x_i \cdot \sin(\sqrt{|x_i|})], -500 \leq x_i \leq 500 \quad (6)$$

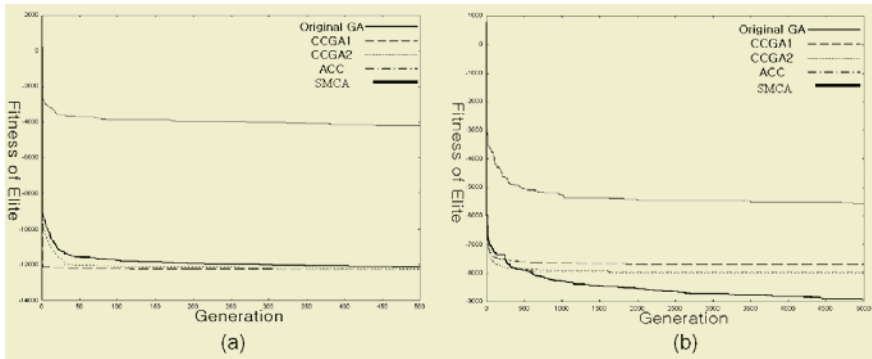


Fig. 3. (a): Schwefel and (b): Rotated Schwefel

The global optimum of this function is $\vec{F}(\vec{x}) = -n \cdot 418.9829$ at the point $\vec{x} = (420.9687, 420.9687, \dots, 420.9687)$.

In summary, CCGAs are efficient when no variable interdependency exists, however, otherwise they are not efficient. ACC is efficient even when variable interdependency exists, however, it quickly saturates when strong variable interdependency exists. The experiment results clearly show that SMCA is all-time efficient no matter how much variable interdependency exists.

5 Conclusion

In this paper we described a new coevolutionary algorithm that improves the existing coevolutionary algorithms. In CCGA species corresponding to a single variable evolve independently by cooperatively, which significantly reduces the search space and consequently results in fast evolution. However, CCGA suffers from the problem of local optimum when variable interdependency exists. To overcome this problem ACC was proposed and it merges species associated with interdependent variables. Merging species allows more global search than splitting species. However, ACC also suffers from slow evolution when variables are strongly interdependent. In this case species are quickly merged into a larger species, causing the expanded search space. SMCA, however, combines species merging and splitting appropriately in order to take advantage both of fast evolution of CCGA and of global search of ACC. One interesting point is that in the coevolutionary algorithm we can view species as local solutions with the fixed contexts and evolution process is searching through the context space. Our experiment results have shown that SMCA outperforms existing evolutionary algorithms.

Acknowledgement

This work was financially supported from the project of Super Intelligence Chip and Applications (the grant no. 00013078) of the Korea Ministry of Industry and Energy (MIE).

References

1. M. A. Potter and K. A. DeJong, "A cooperative coevolutionary approach to function optimization," Proc. of the Third Conference on Parallel Problem Solving from Nature, Springer-Verlag, pp.249-257, 1994.
2. M.A. Potter and K.A DeJong, "Cooperative Coevolution: An Architecture for Evolving Co-adapted Subcomponents," Evolutionary Computation 8(1), MIT press, pp.1-29, 2000.
3. M. Mundhe and S. Sen, "Evolving agent societies that avoid social dilemmas," Proc. Of GECCO-2000, Las Vegas, Nevada, pp.809-816, July 2000.
4. L. Pagie and M. Mitchell, " A Comparison of Evolutionry and Coevolutionary Search," Journal of Computational Intelligence and Applications, Vol. 2, No. 1, pp. 53-69, 2002.
5. K. Weicker and N. Weicker, "On the improvement of coevolutionary optimizers by learning variable interdependencies," Congress on Evolutionary Computation (CEC99), pp.1627-1632, 1999.
6. J. Nash, *Non-cooperative games*, Annals of Mathematics 5(2), pp. 286-295, 1951.
7. R. Salomon, "Reevaluating genetic algorithm performance under coordinate rotation of benchmark functions," BioSystems 39, pp.210-229, 1996

Hybrid Filter Fusion for Robust Visual Information Processing

Mi Young Nam and Phill Kyu Rhee

Dept. of Computer Science & Engineering
Inha University, Yong-Hyun Dong, Incheon, South Korea
rera@im.inha.ac.kr, pkrhee@inha.ac.kr

Abstract. This paper proposes a preprocessing filter fusion for efficient face recognition. Since no priori knowledge of system working environment can be assumed. The proposed method can decide an optimal configuration of filter by exploring the filter fusion to unknown illumination conditions. In this paper, we propose to investigate how to preprocess an input face image for the task of robust face recognition, especially in changing illumination environment (bad illumination). We found that the performance of each preprocessing method for compensating illumination is highly affected by working illumination environment. Changing illumination poses a most challenging problem in face recognition. A previous research for illumination compensation has been investigated. The illumination filter includes Retinex filter, end-in contrast stretching and histogram equalization filter. The proposed method has been tested to robust face recognition in varying illumination conditions (our lab, FERET DB). We made in illumination cluster using combined FART and RBF, K-means algorithm. Extensive experiment shows that the proposed system can achieve very encouraging performance in varying illumination environments. We furthermore show how this algorithm can be extended towards face recognition across illumination.

1 Introduction

Face recognition technologies have been motivated from the application area of physical access, face image surveillance, people activity awareness, visual interaction for human computer interaction, and humanized vision. Face recognition becomes an important task in computer vision, and one of the most successful application areas recently. Even though many algorithms and techniques are invented, the task of face recognition still remains a difficult problem yet, and existing technologies are not sufficiently reliable. Dynamically changing illumination in a real world application poses one of the most challenging problem in face recognition systems. In this paper, we made context modeling from illumination condition.

The most crucial problem in a face recognition is to eliminate or bypass the effect of changing illumination [1]. As shown in Fig.1, the same person looks very much different with varying illumination environments. Recently, several researchers have tried to attack this problem. Liu and Wechsler[2] have introduced EP (Evolutionary Pursuit) for face image encoding, and have shown its successful application.

The proposed the filter fusion guided by an evolutionary approach has been employed to adapt the system for variations in illumination. The proposed approach

employs filter fusion, which is generated from the retinex algorithm. Even though the Gabor wavelet provides the nice properties for face recognition as discussed above, they cannot provide sufficiently reliable solution in changing environments such as variations in illumination. The proposed recognition system adopts the adaptive strategy. The illumination filter fusion adapts itself by reorganizing its structure and parameters. The proposed system has been tested using face images which exposed to different illumination environments. The feasibility and effectiveness of the proposed face recognition system are investigated. We achieved very encouraging experimental results. The outline of this paper is as follows. In section 2, we present the previous illumination compensation methods. In section 3, we present the proposed adaptive filter bank for illumination image and the architecture of the proposed face recognition. We give experimental results in section 4. Finally, we give concluding remarks.



Fig. 1. The face images which shows the variances in varying illumination

2 Illumination Compensation Components

2.1 Histogram Equalization Filter

To improve contrast of image, histogram equalization is used. If the distribution of gray level was biased to one direction or scaled value was not uniformly distributed, histogram equalization is a good solution for image enhancement. The result of histogram equalization is achieved by following three steps [5].

- 1) Count the number of occurrence for each gray scale levels and draw histogram.
- 2) Find the normalized cumulative histogram.
- 3) Find the new contrast value by mapping normalized cumulative histogram to gray scale.



Fig. 2. The histogram equalization result under varying illumination

2.2 Ends-in Contrast Stretching

The contrast stretching of the image is distribution of light and dark pixels and applied to an image to stretch a histogram to fill the full dynamic range of the image [5].

$$output(x) = \begin{cases} 0 & \text{for } x < low \\ 255 \times (x - low) / (high - low) & \text{for } low \leq x \leq high \\ 255 & \text{for } high < x \end{cases} \quad (1)$$

Contrast stretching is scaled so that image fills the entire dynamic range. Ends-In Contrast stretching is possible intensities but have a pixel concentration in one part of the histogram.



Fig. 3. Contrast stretching result under varying illumination

2.3 Retinex

Color constancy is excellent for all forms of the retinex but color rendition was elusive as a result of the gray world assumption implicit to the retinex computation. A color restoration was developed and applied after the multi scale retinex in order to overcome this color loss but with a modest dilution in color constancy.

The single-scale retinex is given by [4,5,6,7].

$$R_i(x, y) = \log I(x, y) - \log[F(x, y) \times I_i(x, y)] \quad (2)$$

Where,

$I_i(x, y)$: Image distribution,

i_{th} : Color band,

$F(x, y)$: The normalized surround function

This characteristic provides for general purpose and automatic application of the method and for simple construction of a multi-scale retinex as. Fig.4 is shown Retinex results of face preprocessing examples in FERET fafc dataset.



Fig. 4. The retinex preprocessing result under varying illumination

3 Face Recognition Using Selective Preprocessing and Adaptive Gabor Feature Space

3.1 Proposed Method for Face Image Preprocessing

The proposed method has been tested to adapt the system for image processing in varying illumination condition. The system learns the changing environment, and adapts by restructuring its structure and parameters. The flow diagram of image processing is given in Fig.5. From figure illumination condition is generated using genetic algorithm. Combination filter is gain enhanced face recognition ratio.

We adopt FuzzyART and RBF methods for achieving an optimal illumination clustering. The clustering result is shown Fig.6.

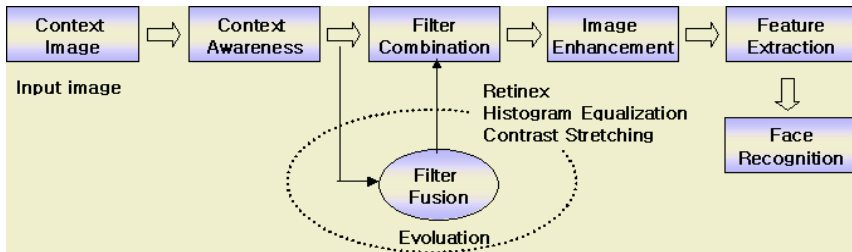


Fig. 5. Filter fusion based face recognition architecture

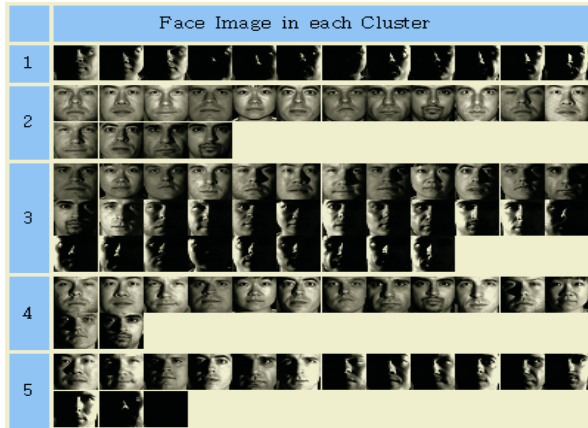


Fig. 6. Face illumination clustering by proposed method

As shown Fig.7, the details of face recognition process using the proposed adaptive filter block is given in the following:

1. Perform filtering, and derives Gabor representation $F(\vec{x})$ for each fiducial point, and normalized it.
2. Concatenate the Gabor representations for fiducial points to generate total Gabor vector.

$$V = (F^{(k)}(\vec{x}_1) \ F^{(k)}(\vec{x}_2) \dots \ F^{(k)}(\vec{x}_n)) \quad (3)$$

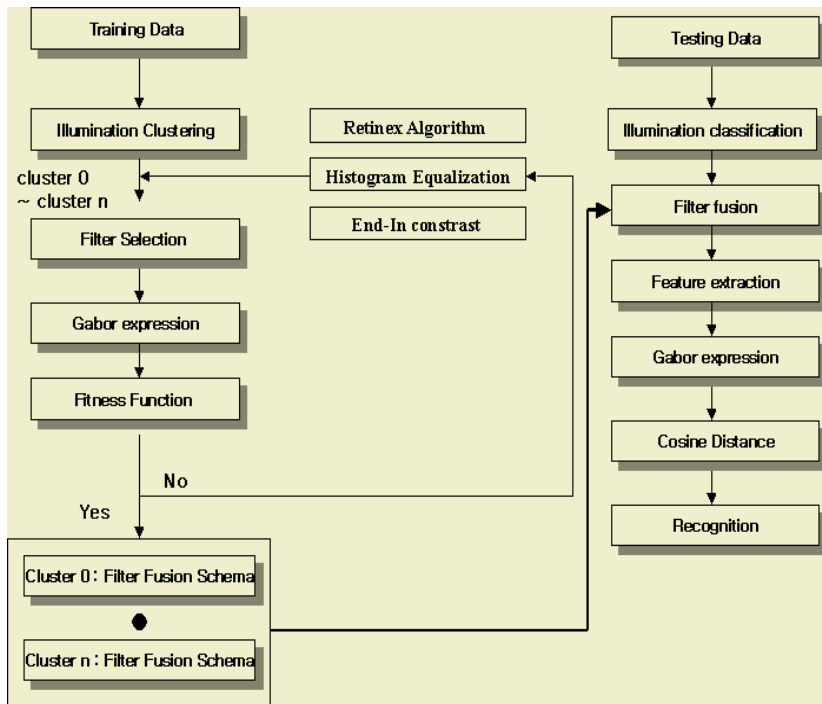


Fig. 7. The proposed face recognition method using filter fusion

3. Begin the classifier architecture optimization until a criterion is met, where the criterion is the performance does not improve anymore or the predefined maximum trial limitation is encountered.
 - 1) Generate an initial filter block configuration and parameters.
 - 2) Evaluate the performance evaluation function, $\eta(V) = \lambda_1 \eta_1(V) + \lambda_2 \eta_2(V)$ for the newly adapted filter block.
 - 3) Search for the new filter block configuration and parameters that maximize the evaluation function.
 - 4) Applying GA's genetic operators to generate new population of Gabor feature space. Go to Step 3.
4. Perform recognition using the constructed new filter block from Step 3.

Preprocessing is performed for providing nice quality images as much as possible using image filtering techniques discussed in the previous session [11].

3.2 Feature Description Using Gabor Wavelet

Feature space is represented by Gabor wavelet. Gabor wavelet efficiently extracts orientation selectivity, spatial frequency, and spatial localization. It is a simulation or approximation to the experimental filter response profiles in visual neurons [8]. Gabor wavelet is used for image recognition due to its biological relevance and computational properties. Gabor wavelet is one of the successful models that simulate biologi-

cally motivated receptive fields. A receptive function can be defined for different classes of visual neurons. The receptive fields of the neurons in the primary visual cortex of mammals are oriented and have characteristic frequencies. These could be modeled 2-D Gabor filter. The Gabor filter is known to be efficient in reducing redundancy and noise in images [9]. Gabor wavelet is biologically motivated convolution kernels in the shape of plane waves restricted by Gabor kernel. The Gabor wavelet has shown to be particularly fit to image decomposition and representation. The convolution coefficients for kernels of different frequencies and orientations starting at a particular fiducial point are calculated. The Gabor kernels for a fiducial point are defined as follows:

$$\phi_{\mu,\nu}(\vec{x}) = \frac{||\vec{k}_{\mu,\nu}||^2}{c^2} \exp^{-\frac{||\vec{k}_{\mu,\nu}||^2 + ||\vec{x}||^2}{2c^2}} [\exp i(\vec{k}_{\mu,\nu} \cdot \vec{x} - \exp^{-\frac{\sigma^2}{2}})] \quad (4)$$

where μ and ν denote the orientation and dilation of the gabor kernels, $(\vec{x}) = (x, y)$, $\|\cdot\|$ denotes the norm operator, and the wave vector $(\vec{k})_{\mu,\nu}$ is defined as follows:

$$(\vec{k})_{\mu,\nu} = (k_\nu \cos \phi_\mu, k_\nu \sin \phi_\mu)^t \quad (5)$$

where $k_\nu = 2^{-\nu+2}$ and $\phi_\mu = \pi\mu/8$.

The family of Gabor kernels is similar each other since they are generated from one mother wavelet by dilation and rotation using the wave vector $(\vec{k})_{\mu,\nu}$. Each kernel is a product of a Gaussian envelope and a plane wave. The first term in the brackets in Eq. (4) determines frequency part of the kernel and the second term compensates for the DC value, which makes the kernels DC-free. The effect of the DC term vanishes when the parameter σ has sufficiently high values, where σ determines the ratio of the Gaussian window width to wavelength.

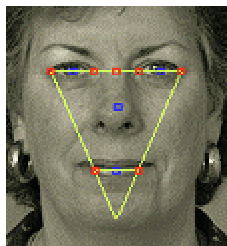
Gabor wavelet is usually used at five different frequencies, $\nu = 0, \dots, 4$, and eight orientations, $\mu = 0, \dots, 7$ [10]. The kernels show desirable characteristics of spatial locality and orientation selectivity, a suitable choice for face image feature extraction for classification.

4 Experimental Results

In this paper, image which we use where face images are exposed to lighting variant fafc dataset of FERET DB [12] as show to Fig.8. Fig.8 gives an example of images under varying illuminant.

The dataset1 is the fafc dataset of FERET database is gray scale facial image and dataset2 is our lab dataset where face images are exposed to illumination variation and noise. As shown in Fig.9, we extracted 9 feature points. Therefore, size of the feature vector is 9×40 . We change two dimensions to one dimension of 1×360 size. Facial landmarks are encoded with sets of complex Gabor wavelet coefficients called jets.

Table 1, 2, 3 and 4 shows examples from the database before and after processing with our proposed method. From the experiments show in Table 1, 2, 3 and 4, we find that normal images show a best performance Retinex algorithm and histogram equalization. Dark images (fafc dataset) show best performance using Retinex for system. Table 5 shows face recognition using filter fusion each cluster by discrimination FART and RBF.

**Fig. 8.** Experimental Dataset**Fig. 9.** The nine feature space (feature extraction for face recognition)**Table 1.** Face recognition for 9 feature points each person in Our Lab dataset

| Lab Data | No filter | H.E. | Retinex |
|-----------------------------|-------------|-------------|-------------|
| # of correct classification | 1210 / 1259 | 1221 / 1259 | 1142 / 1259 |
| % of correct classification | 96.10 % | 96.98 % | 90.70 % |

Table 2. Face recognition for 9 feature points each person in FERET fafb dataset

| fafb | No filter | H.E. | Retinex |
|-----------------------------|------------|------------|------------|
| # of correct classification | 915 / 1195 | 951 / 1195 | 231 / 1195 |
| % of correct classification | 76.56 % | 79.58 % | 19.33 % |

Table 3. Face recognition for 9 feature points each person in FERET fafc dataset

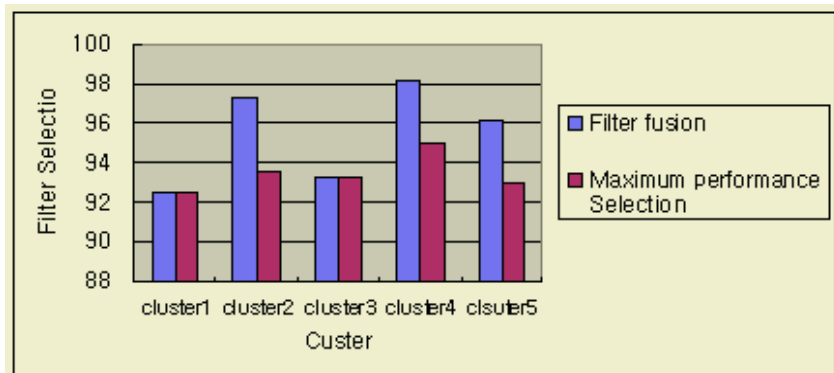
| FERET fafc | No filter | H.E. | Retinex |
|-----------------------------|-----------|----------|-----------|
| # of correct classification | 8 / 194 | 33 / 194 | 161 / 194 |
| % of correct classification | 4.12 % | 17.9 % | 82.98 % |

Table 4. Face recognition ratio using multiple preprocessing methods

| Dataset\Methods | Retinex + H.E | H.E + Retinex | Contrast stretching |
|--------------------|---------------|---------------|---------------------|
| FERET fafc dataset | 19.07% | 72.68% | 28.35% |
| Our lab dataset | 97.30% | 93.01% | 97.06% |

Table 5. Face recognition ratio for each 5 cluster (as shown Fig.7)

| Cluster | Filter fusion | Maximum Performance Filter |
|-----------|---------------|----------------------------|
| Cluster 1 | 92.5 | 92.5(Retinex) |
| Cluster 2 | 97.3 | 93.5 |
| Cluster 3 | 93.3 | 93.3 (Retinex) |
| Cluster 4 | 98.2 | 95 |
| Cluster 5 | 96.2 | 93 |



As shown Table5, the retinex single filter shows good performance in bad illumination and filter fusion is good performance other illumination. This paper could correct recognition rate of occasion that handle Retinex and histogram equalization paratactically was high each different dataset under varying illumination, that Retinex algorithm is effective in performance in image for illumination. The experimental result of Retinex method shows the recognition rate of 82.98% in fafc dataset and 90.70% in our lab dataset. Different algorithm or sequence that compare with experiment result in system is as following [15]. From Tables, it becomes apparent that selected image filter method shows good recognition performance while general illuminant filter single filter do. This can interpret use existence and nonexistence and parameter of each image filter using genetic algorithm, because general filtering may appear result that flow image filter unconditionally, and drops preferably quality of original above zero because suitable parameter control is impossible.

5 Concluding Remarks

In this paper, we address an efficient processing filter for efficient face recognition under varying illumination. Changing illumination poses a most challenging problem in face recognition. Most existing image processing technologies for robust face recognition are not sufficiently reliable under changing illumination. The proposed method image preprocessing performs well especially in changing illumination environments since it can adapt itself to external environment. The proposed method can decide an optimal configuration of filter block by exploring the filter combination and the associated parameters to unknown illumination conditions. Extensive experiment shows that the proposed system can achieve very encouraging performance in varying illumination environments.

References

1. Seung Yonng Lee, Illumination Direction and Scale Robust Face Recognition using Log-polar and Background Illumination Modeling, Thesis, Inha University, Korea, (2002)
2. H. Liu et. al.: Illumination Compensation and Feedback of Illumination Feature in Face Detection. Proc. International Conferences on Information-technology and Information-net, Beijing, Vol. 3. (2001) 444-449
3. Rafael C. Gonzalez and Richard E. Woods, Digital Image Processing, Addison-Wesley, (1992)
4. Andrew Moore.: Real-time Neural System for color Constancy. IEEE Transactions on Neural Networks, Vol. 2. no.2, (1991)
5. Funt, B.V., Ciurea, F., and McCann, J. Retinex in Matlab. In *Proc. of IS&T/SID Eighth Color Imaging Conference*, (2000) 112– 121.
6. Daniel J. Jobson, Zia-ur Rahman, Glenn A. Woodell,: The Spatial Aspect of Color and Scientific Implications of Retinex Image Processing.
7. Brian Funt, Kobus Barnard.: Luminance-Based Multi-Scale Retinex. rmalize proceedings AIC Colour 97 8th Congress of the International Colour Association, (1997)
8. Bossmayer, T.R.J.: Efficient image representation by Gabor functions - an information theory approach. in J.J. Kulikowsji, C.M. Dicknson, and I.J. Murray(Eds.), Pergamon Press, Oxford, U.K. 698-704
9. Marios Savvides, B.V.K. Vijaya Kumar, P.K. Khosla, "Robust, Shift-Invariance Biometric Identification from Partial Face Images," presented at Proc of SPIE, Biometric Technologies for Human Identifications (OR51), Orlando, FL, (2004)
10. Marios Savvides, B.V.K. Vijaya Kumar.: Quad Phase Minimum Average Correlation Energy Filters for Reduced Memory Illumination Tolerant Face Authentication. *Lecture Notes in Computer Science, Springer-Verlag*, Vol. 2688. (2003) 19-26
11. A. S. Georghiades, P. N. Belhumeur, and D. J. Kriegman,: From Few to Many: Illumination One Models for face recognition under Variable Lighting and Pose. IEEE Trans. on PAMI, Vol. 23. no.6, June(2001) 643-660
12. P.Phillips.: The FERET database and evaluation procedure for face recognition algorithms. Image and Vision Computing, Vol. 16. no.5, (1999) 295-306.
13. FRVT 2000 Evaluation Report, by D.M. Blackburn, J.M. Bone, and P.J. Phillips. February (2001)

Edge Detection in Digital Image Using Variable Template Operator

Young-Hyun Baek¹, Oh-Sung Byun¹, Sung-Ryong Moon¹, and Deok-Soo Baek²

¹ Department of Electronic Engineering Wonkwang University,
344-2 Sinyong-Dong, Iksan, Korea
{neural176,boss0019,srmoon}@wonkwang.ac.kr
<http://newslab.wonkwang.ac.kr>

² Department of Electronic Engineering Iksan National College,
194-5 Ma-Dong, Iksan, Korea
{dsbaek}@iksan.ac.kr

Abstract. This paper discusses an approach for detecting a new edge in color images. The color image is to be represented by a vector field, and the color image edges are detected as differences in the local vector statistics. This method is based on the calculation for the vector angle between two adjacent pixels. Unlike Euclidean distance in RGB space, the vector angle distinguishes the differences in chromaticity, independent of luminance or intensity. The proposed approach can easily accommodate concepts, such as variable template edge detection, as well as the latest developments in vector order statistics for color image processing. In this paper, it is used not a conventional fixed template operator but a variable template operator. The variable template is implemented and experimental results for digital color images are included.

1 Introduction

The In the computer vision, the detection and interpretation of edge features have found to play essential parts in extracting specific information from scene images. The latest advances in color edge detection apply vector order statistics to spatially locate edges in color images. There exists a number of equivalent three-dimensional color spaces with varying characteristics [1].

One group of spaces uses cartesian coordinates to represent points in the space. Examples include the three primary illumination colors RGB, the complementary colors CMY, and the opponent color representation YCbCr. An alternative set of spaces employ polar coordinates and include the HIS and HSV spaces. This work presents a class of variable template operators designed to detect the location and orientation of edges in color images[2,3].

For color images, a number of approaches have been proposed. Most approaches have used the RGB space for their processing.

The Sobel template operator has been applied successfully to all three planes in the RGB space and the gradients were summed to obtain the resultant edges in [4,5].

The Sobel template operator was also applied to each component of the HIS space, and the individual results were combined using a trade-off parameter between hue and intensity [6].

Certain transformations such as YUV and YCbCr can be performed very quickly while others such as HIS and CIE LUV are very complex.

In this paper, we propose a variable template operator for the obtaining illumination (Y) information for the purposes of intensity invariant segmentation from the RGB image.

The experiment results show that the variable template operator is fast exactly and is less affected the Sobel and other conventional fixed template.

2 Background Materials

2.1 RGB Color Model

The RGB color space consists of the three additive primaries: red, green, and blue. The spectral components of these colors combine additively to produce a resultant color. The RGB model is represented by a 3-dimensional cube with red, green, and blue at the corners on each axis (Fig. 1). Black is at the origin. White is at the opposite end of the cube. The gray scale follows the line from black to white. In a 24-bit color graphics system with 8 bit per color channel, red is (255,0,0). One the color cube, it is (1,0,0). The RGB model simplifies the design of computer graphics systems but is not ideal for all applications. The red, green, and blue color components are highly correlated. This makes it difficult to execute some image processing algorithms. Many processing techniques, such as histogram equalization, work on the intensity component of an image only. These processes are easier implemented using the HIS color model and YCbCr color model[7].

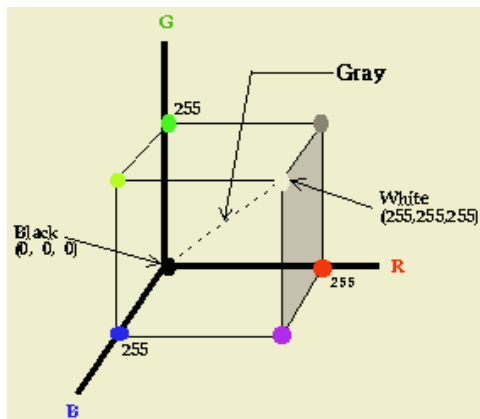


Fig. 1. RGB color cube

2.2 YCbCr Color Model

YCbCr is another color space that separates the luminance from the color information. The luminance encoded in the Y and the blueness and redness encoded in CbCr. It is very easy to convert from RGB to YCbCr.

$$\begin{aligned}
 Y &= 0.29900R + 0.58700G + 0.11400B \\
 Cb &= -0.16874R - 0.33126G + 0.50000B \\
 Cr &= 0.50000R - 0.41869G - 0.08131B
 \end{aligned} \quad (1)$$

3 Proposal Variable Template Operator for Edge Detection

Let $D(i, j)$ denote the first derivation of the color image $X(i, j)$, such that [8].

$$D(i, j) = \begin{bmatrix} \frac{\partial X_R(i, j)}{\partial i} & \frac{\partial X_R(i, j)}{\partial j} \\ \frac{\partial X_G(i, j)}{\partial i} & \frac{\partial X_G(i, j)}{\partial j} \\ \frac{\partial X_B(i, j)}{\partial i} & \frac{\partial X_B(i, j)}{\partial j} \end{bmatrix} \quad (2)$$

Variable template (VT) are defined to simplify the expression

Step1: Convert from RGB to YCbCr.

$$\begin{aligned}
 Y(i, j) &= 0.29900 \frac{\partial X_R(i, j)}{\partial i} * \frac{\partial X_R(i, j)}{\partial j} \\
 &\quad + 0.58700 \frac{\partial X_G(i, j)}{\partial i} * \frac{\partial X_G(i, j)}{\partial j} \\
 &\quad + 0.11400 \frac{\partial X_B(i, j)}{\partial i} * \frac{\partial X_B(i, j)}{\partial j}
 \end{aligned} \quad (3)$$

Step 2: By using Y

$$VT = \begin{bmatrix} -Y(i, j) & -Y(i, j+1) & -Y(i, j+2) \\ Y(i+1, j) & (i, j) & Y(i+1, j+2) \\ Y(i+2, j) & -Y(i+2, j+1) & Y(i+2, j+2) \end{bmatrix} \quad (4)$$

It is each pixel yard of according to difference of data value as variable 3x3 template created. And Y parameter is luminance, i column and j row is shown in equation (4).

4 Simulation Result and Analysis

The proposed template has been implemented and applied to several color images. In this paper, it is confirmed that the result of an edge detection applying is variable template operator better than of the conventional Sobel operator. The test images use 20 pictures, 20 pictures have various object size.

The proposed template detects the region of a edge applying the Variable Template to YCbCr model in the quantizing 16, 32, 64 bit.

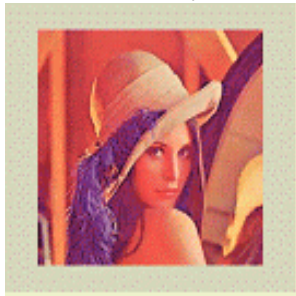
The original test image is shown in Fig. 2. In Fig. 3, each converting from original test image to YCbCr image.



(a)Butterfly



(b)House

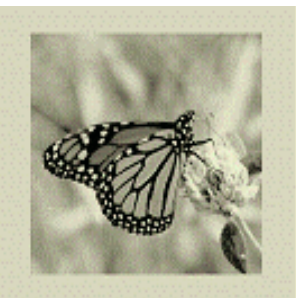


(c)Lena



(d)Road

Fig. 2. Original image: (a)Butterfly, (b)House, (c)Lena, (d)Road



(a)Butterfly



(b)House



(c)Lena



(d)Road

Fig. 3. Converting from original test image to YCbCr image: (a)Butterfly, (b)House, (c)Lena, (d)Road

In a computer simulation, we use the scalar sobel operator on the Y component of this color image. The edge map generated by Sobel vector operator is shown in fig. 4: (a), (c), (e), (g). Figure 4: (b), (d), (f), (h) show the edge map generated by the variable template matching operator. These indicate that the variable template matching operator offers performance advantages over the conventional template matching operator for the color image.

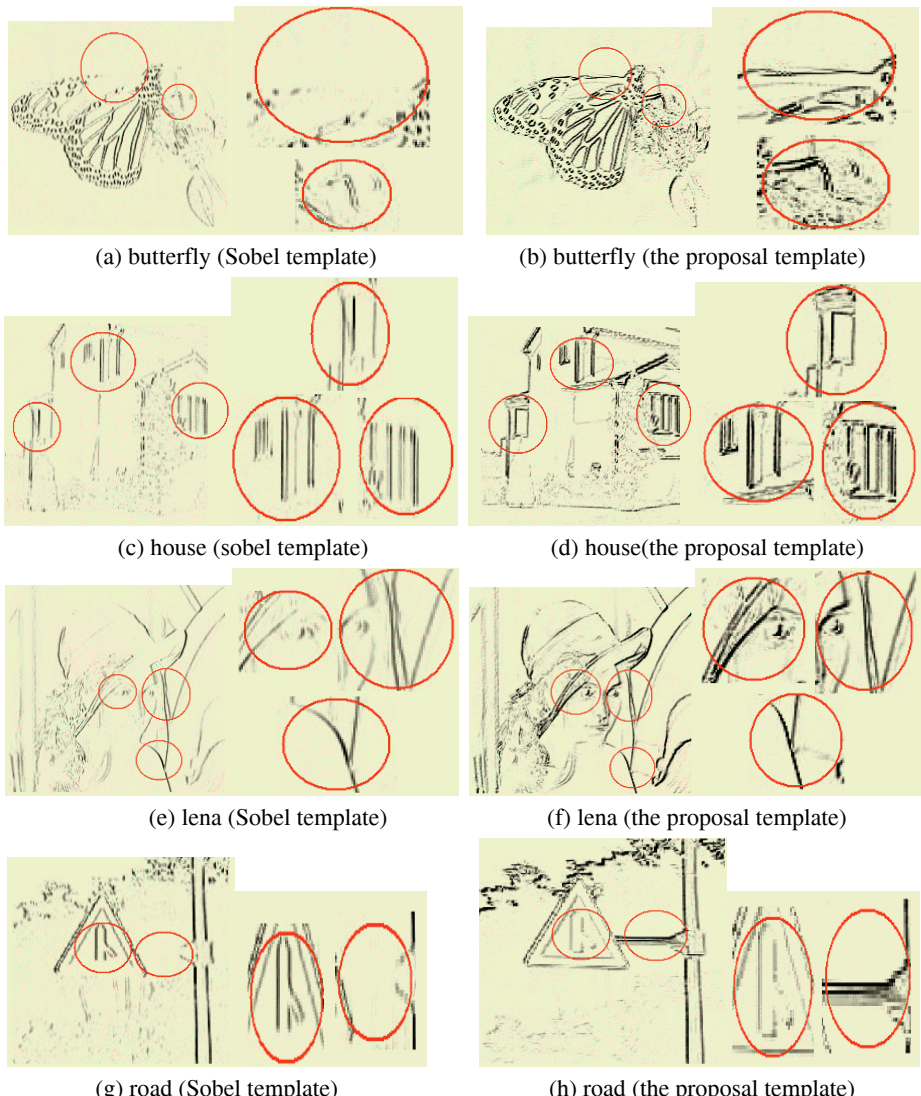


Fig. 4. Edge detection on Sobel template operator: (a), (c), (e), (g), edge detected using proposed variable template operator: (b), (d), (f), (h)

5 Conclusion

This paper applied the variable template operator, using the YCbCr model in color image.

The consuming computational time for the variable template operator matching is less than that of the conventional template operator method.

Especially, it is confirmed that the correct edge can be detected when be close to each edges, and the better result can be got at the place of having smoothly curved line. Here after, the proposal template operator will enhance edge or detect edge in image included noise.

References

1. R.Nevatia, "A color edge detector and its use in scene sementation," IEEE Trans. On PAMI, vol. SMC-7, no. 11, Nov. 1977.
2. R. Gonzalez and R. Woods, Digital Image Processing, Addison-Wesley Publishing Company, 1992.
3. H. Levkowitz, Color Theory and Modeling for Computer Graphics, Visualization, and Multimedia Applications. Kluwer Academic Publishers, 1977.
4. P. Trahanias and A. N. Venetsanopoulos, "Color edgedetection using vетor statistics," IEEE Trans. On Image Processing, vol. 2, pp. 259-264, April 1993
5. Y. Yang, "Colour edge detection and segmentation usi-ing vector analysis," Master's thesis, Electrical and Computer Engineering, University of Toronto, ON, Canada, 1955.
6. T. Carron and H. Yan, "Sementation of color image using 1 and color spa ce information," Journal of Electronic Imageing, vol. 1, pp. 374-380, October 1922.
7. Crane, A simplified approach to Image Processing, Prentice-Hall, 1997.
8. T. W. Anderson, An introduction to multivariate statistical analysis, Wiley, New York, 1984

Combining Demographic Data with Collaborative Filtering for Automatic Music Recommendation

Billy Yapriady and Alexandra L. Uitdenbogerd

School of Computer Science and Information Technology, RMIT University
GPO Box 2476V, Melbourne 3001, Australia
alu@cs.rmit.edu.au

Abstract. It has been shown in several studies that demographics such as gender, socio-economic background and age affect one's musical tastes. In this work we combine these factors with traditional collaborative filtering techniques in order to improve recommendation precision. We propose a simple measure for combining the data and show that it has potential for this application.

1 Introduction

Ever since the Web began to be used by a large sector of the community, there has been development of tools for filtering the abundance of content available. Initially developed for filtering news, collaborative filtering has since been applied to a wide variety of content. Systems that use the technique — often called *recommender systems* — have become an important component of on-line retail as well as being a tool for assisting users to find interesting content. However the quality of the recommendations produced by these systems needs to be improved. With this aim we have examined the possibility of combining user demographic data with collaborative filtering.

Several kinds of evidence can be used for recommending music to a user: ratings of content by other users, information intrinsic to the user such as personality, implicit ratings from users based on browsing habits, and content similarity. Currently in the music domain, systems use explicit or implicit ratings in order to recommend material. Content-based recommendation is currently under-developed, and *User-specific* information is unexplored for music recommendation. Several studies have shown that demographics such as gender, socio-economic background and age are correlated with one's musical taste (surveyed in [8]). In this work we combine these factors with traditional collaborative filtering techniques in order to improve recommendation precision. We propose a simple measure for combining the data and show that it has potential for this application.

2 Collaborative Filtering

A collaborative filtering based recommender collects feedback from users about what they like, groups users into neighbourhoods with similar tastes, and recom-

mends items for a given user based on what their neighbours prefer. Typically this involves storing lists of users and items, as well as ratings for each item by each user. The *active user* is one for whom the task of the recommender is to generate predictions, which can be in two forms: a number expressing the level of confidence that an item will be liked by the active user, or a list of top- N items that the active user will like the most.

The recommender finds a set of users who have a history of agreeing with the active user. This set of users is known as *neighbours* of the active user. The recommender then combines the preferences of neighbours to produce a prediction or top-N recommendations for the active user. This widely-used technique is also known as the *nearest-neighbour* or user-based collaborative filtering algorithm.

The GroupLens research group was the first to introduce an automated collaborative filtering recommender [4]. Their system automated the filtering process for selection of Netnews, by determining users with similar tastes based on their previous ratings [2]. They used the Pearson Correlation coefficient to determine the neighbourhoods. Using all available correlated neighbours, the system made predictions by calculating the weighted average of deviation from the mean rating of the neighbours.

With the Ringo music recommender Shardanand and Maes [7] experimented with various techniques to measure distance between users. Ringo imposed a threshold on the neighbourhood correlation coefficient, only selecting those with greater similarity for the neighbourhood. Higher thresholds resulted in greater accuracy but lessened the number of items for which the system could generate predictions. Shardanand proposed the Constrained Pearson Correlation Coefficient, which was claimed to offer more accurate and better performance than the original algorithm used by GroupLens.

Breese et al. [1] showed that Pearson correlation performed better than information retrieval measures such as vector cosine. Intelligent techniques that have been explored for recommender systems include the clustering of users based on their click-stream data [5], the use of reasoning for movie recommendation based on semantic features [6], and applying ontological inference for academic paper recommendations [3].

3 Experiments

The aims of our experiments were to verify the effectiveness of existing techniques within our experimental framework, and to determine whether demographic information could improve music recommendations.

We created a new data set by presenting users with a questionnaire in which they were asked to enter their gender, age and nationality, and to rate a list of 100 recordings. Where people gave more than one nationality or indicated their ethnicity, we used the nationality that was given first. If both the ethnicity and nationality were given, we used the ethnicity. Invalid ratings were discarded. As the recordings were identified by name only, participants only rated those that they knew, resulting in 4451 ratings. The 83 users represented a broad range of ages, and nationalities (see Figure 1). The users were mostly students

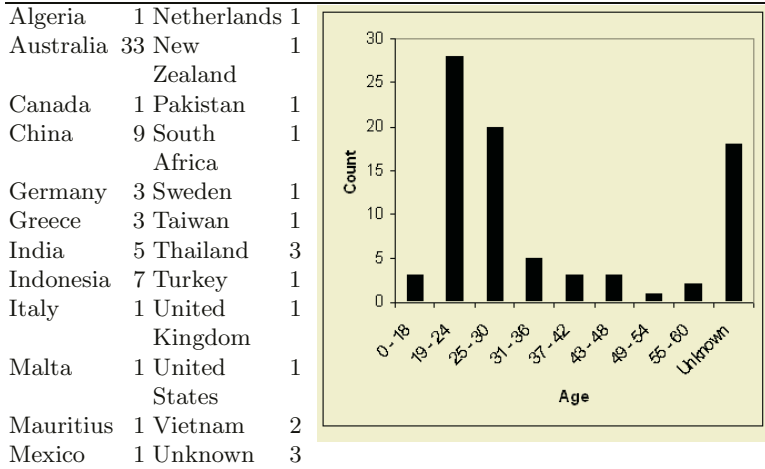


Fig. 1. Distribution of users' nationalities and ages

and staff of educational institutions. Some of them have musical backgrounds and are actively involved in musical activities. The number of unknown users' ages is very high, showing the reluctance felt about revealing age. There were more male (55%) than female (33%) users, and 12% of the users omitted gender information.

We applied two criteria to compare the quality of the collaborative filtering algorithms: Mean Absolute Error, and Standard Deviation of Errors. These were applied across all ratings as well as to the extreme ratings values only, that is, strong likes and dislikes.

For each user we randomly divided the ratings into a test dataset of 25% of their ratings, and a source dataset containing the other 75% of ratings. Predictions for the test dataset were then calculated using the source dataset.

3.1 Algorithms

In this section we use the following definitions: $r_{u,i}$ is the rating given by user x for item i ; n is the total number of users in the database, a as a subscript represents the active user, and u any other user. Standard deviations are indicated with σ , and means with a bar over the item (for example \bar{r}).

The base-line algorithm, *Average*, consisted of finding the mean rating for each item and using that as its predicted rating.

The *Pearson correlation coefficient* between user a and u ($W_{a,u}$), used for the GroupLens system [2], is defined as:

$$W_{a,u} = \frac{\sum_{i=1}^n (r_{a,i} - \bar{r}_a) \times (r_{u,i} - \bar{r}_u)}{\sigma_a \cdot \sigma_u} \quad (1)$$

The algorithm uses both negative and positive correlations to make predictions. The predicted value for an item for the active user is given by:

$$P_{a,i} = \bar{r}_a + \frac{\sum_{u=1}^n (r_{u,i} - \bar{r}_u) \times W_{a,u}}{\sum_{u=1}^n W_{a,u}} \quad (2)$$

The constrained Pearson correlation coefficient between user a and u ($W_{a,u}$), used in the Ringo system [7] is defined as:

$$W_{a,u} = \frac{\sum_{i=1}^n (r_{a,i} - r_m) \cdot (r_{u,i} - r_m)}{\sigma_a \cdot \sigma_u} \quad (3)$$

where r_m is the mid-point of the rating scale. Ringo used a seven-point rating between 1 and 7. Our project used a five-point rating between 1 and 5. Therefore the rating mid-point was 3. Like the Pearson algorithm above, the prediction is calculated as the mean weighted average of all users rating the item.

For this preliminary work on the use of demographics information, we concentrate on just three parameters: age, gender and nationality. The *demographics similarity weight* between the active user and all other users in the neighbourhood are defined as:

$$D_{a,u} = \max \left\{ \frac{\frac{Age_{a,u} + Sex_{a,u} + National_{a,u}}{3}}{1} \right\} \quad (4)$$

where:

$$Age_{a,u} = \begin{cases} \frac{40 - |Age_a - Age_u|}{20} & : |Age_a - Age_u| \leq 40 \\ 0 & : |Age_a - Age_u| > 40 \end{cases}, \quad (5)$$

$$Sex_{a,u} = \begin{cases} 1 & : Sex_a = Sex_u \\ 0 & : Sex_a \neq Sex_u \end{cases} \quad (6)$$

and:

$$National_{a,u} = \max \left\{ \begin{array}{ll} 2 & : Nation_a = Nation_u \\ 1 & : Continent_a = Continent_u \\ 0 & : \end{array} \right. \quad (7)$$

Where all demographic data was missing we assigned the middle value (0.5) for the demographics similarity weighting. Where only some demographic data was missing, we assigned middle values to the missing fields based on the ratio within a maximum sum of 3. Thus $Age_{a,u}$, $Sex_{a,u}$, and $National_{a,u}$ were assigned the middle values 0.6, 0.3 and 0.6 respectively. The predicted value for an item for the user is the mean weighted average of all users rating for the item.

$$P_{a,i} = \bar{r}_a + \frac{\sum_{u=1}^n (r_{u,i} - \bar{r}_u) \times D_{a,u}}{\sum_{u=1}^n D_{a,u}} \quad (8)$$

The new combined algorithm that we call the *Demographics and Pearson Correlative Coefficient* algorithm calculates the predicted value for an item for the active user using the following equation:

$$P_{a,i} = \bar{r}_a + \frac{\sum_{u=1}^n (r_{u,i} - \bar{r}_u) \times W_{a,u} \times D_{a,u}}{\sum_{u=1}^n W_{a,u} \times D_{a,u}} \quad (9)$$

Only using ratings from users who are very positively correlated with the active user, a technique known as *thresholding*, may lead to more accurate predictions, at the cost of fewer items that can be recommended. In the experiments reported here we applied a threshold of 0.5 to constrained Pearson, Demographics, and the combination algorithm.

3.2 Discussion

Table 1 shows a summary of the mean and standard deviation of errors across all data and across extreme values. The best results occur when combining constrained Pearson using a threshold of 0.5 with demographics data. Purely using demographics works surprisingly well.

The overall distribution of errors in rating predictions by the base algorithm shown in Figure 2 almost forms the preferred bell-shaped curve centered at 0. However, it performs less well on extreme values (the dark bars in the same graph), where we see two bell-shaped curves instead of one. As a result, this

Table 1. Summary of results

| Algorithms | Mean Absolute | Standard Deviation of Errors | | |
|--|---------------|------------------------------|---------|------|
| | Errors | All | Extreme | All |
| Average | 1.07 | 1.43 | 1.26 | 1.53 |
| Pearson | 1.02 | 1.33 | 1.21 | 1.55 |
| Constrained Pearson | 0.90 | 1.13 | 1.12 | 1.33 |
| Constrained Pearson (threshold 0.5) | 0.89 | 1.12 | 1.11 | 1.33 |
| Demographics | 0.90 | 1.14 | 1.12 | 1.33 |
| Demographics (threshold 0.5) | 0.90 | 1.13 | 1.12 | 1.33 |
| Demographics and Constrained Pearson | 0.89 | 1.13 | 1.12 | 1.33 |
| Demographics and Constrained Pearson (threshold 0.5) | 0.90 | 1.11 | 1.10 | 1.30 |

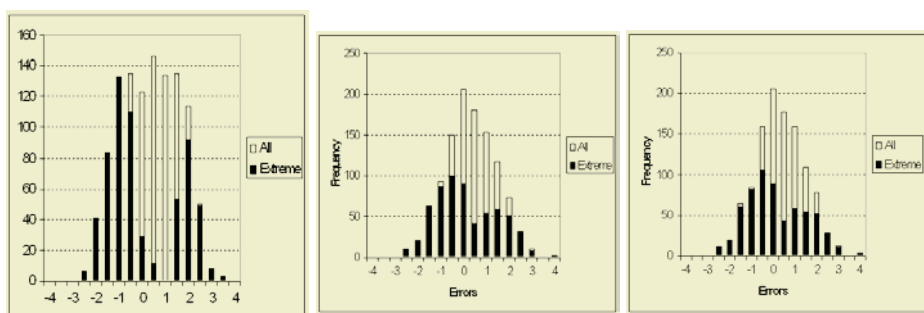


Fig. 2. The distribution of errors for the base Average algorithm (left), the Constrained Pearson correlation coefficient algorithm (center), the Demographics Similarity Weighting algorithm (right)

algorithm has a tendency to perform better in cases where the target value is close to the mid-point of the rating scale. Therefore, in practical application, where users are most interested in extreme values, the base algorithm would be suboptimal. However, it does have the advantage that it can generate predictions for almost all target values. The various formulations of Pearson correlation-based recommendation attempt to improve these extreme values. For example, see the distribution of errors in Figure 2. The shape is much closer to a single bell curve for extreme values.

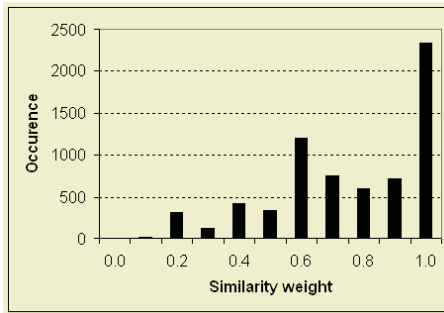


Fig. 3. The distribution of demographics similarity weights

Figure 3 shows the distribution of the demographics similarity weights between all users that were generated in our experiments. The distribution shows that many users scored the maximum demographic similarity and no pair of individuals were so different in age, gender and nationality to score 0. The distribution of errors across all values for the demographics algorithm (Figure 2) has a nice bell-shaped curve. For extreme values, the curve is also almost bell-shaped.

When thresholding is applied, the shapes of the distributions for both all values and extreme values are very similar to those shown in Figure 2.

In summary, errors are minimised for both constrained Pearson and Demographic techniques as well as their variants. However, the differences are fairly small. That is, all techniques shown would result in an average error of about one position displacement on the rating scale from 1 to 5 for recommendations. However, the results show that applying demographic data to the problem is promising, given the size and shape of the distribution of errors.

4 Conclusions

We set out to verify the effectiveness of existing collaborative filtering techniques, and to compare these to new techniques that encode demographical information. Based on our study we conclude that knowledge of users' age, gender, and nationality, can be used to improve the performance of music recommenders. It is

likely that the combination of demographics and the constrained Pearson correlation coefficient will produce superior results to either algorithm on its own. There is potential for refining the demographics approach further for greater efficacy, however, in its current form it can already present recommendations to users before they have provided many ratings.

Acknowledgements

The authors thank the MRS development team and Arran Stewart. This research was supported by RMIT School of Computer Science and Information Technology grants.

References

1. J. Breese, D. Heckerman, and C. Kadie. Empirical analysis of predictive algorithms for collaborative filtering. In *Proceedings of the Fourteenth Conference on Uncertainty in Artificial Intelligence*, Madison, WI, USA, July 1998. Morgan Kaufmann.
2. J. Herlocker, J. A. Konstan, A. Borchers, and J. Riedl. An algorithmic framework for performing collaborative filtering. In *Proc. ACM-SIGIR International Conference on Research and Development in Information Retrieval*. ACM, August 1999.
3. S. E. Middleton, N. R. Shadbolt, and D. C. De Roure. Ontological user profiling in recommender systems. *ACM Trans. Inf. Syst.*, 22(1):54–88, 2004.
4. B. Miller, J. Riedl, and J. Konstan. Experiences with GroupLens: Making Usenet useful again. In *Proceedings of the Usenix Winter Technical Conference*, January 1997.
5. B. Mobasher, H. Dai, T. Luo, and M. Nakagawa. Improving the effectiveness of collaborative filtering on anonymous web usage data. In S. Anand and B. Mobasher, editors, *Workshop Intelligent Techniques for Web Personalization, IJCAI*, pages 53–60, 2001.
6. R., P. S. Dutta, and S. Sen. Movies2go - a new approach to online movie recommendation. In S. Anand and B. Mobasher, editors, *Workshop Intelligent Techniques for Web Personalization, IJCAI*, 2001.
7. U. Shardanand and P. Maes. Social information filtering: Algorithms for automating word of mouth. In *ACM Conference on Computer Human Interaction (CHI)*, 1995.
8. A. L. Uitdenbogerd and R. G. van Schyndel. A review of factors affecting music recommender success. In M. Fingerhut, editor, *Third International Conference on Music Information Retrieval*, pages 204–208, Paris, France, October 2002.

Different Perspectives on Modeling Workflows in an Agent Based Workflow Management System

Bastin Tony Roy Savarimuthu, Maryam Purvis, and Martin Purvis

Department of Information Science, University of Otago,

PO Box 56, Dunedin, New Zealand

{tonyr, tehrany, mpurvis}@infoscience.otago.ac.nz

Abstract. Most workflows are modeled from the point of view that the entire workflow can be perceived, modeled and executed as a single entity. While this is true in scenarios involving manufacturing industries it is not the same in e-business scenarios, which would involve various participants such as buyers, sellers, etc. In these scenarios it is difficult to explicitly model and use a single process model (with hierarchical sub processes). In these cases, a model of the interactions can be specified using Interaction Protocols (IPs). In this paper we discuss how our agent based workflow system supports process specific workflow models and the workflows based on interaction protocol models. The process modeler has the option of choosing one of these approaches of modeling or a combination of these approaches to model a workflow.

1 Introduction

Most of the commercially available workflow management systems do not offer sufficient flexibility for distributed organizations that participate in the global market. These systems have rigid, centralized architectures that do not operate across multiple platforms [3-5]. Employing a distributed network of autonomous software agents that can adapt to changing circumstances would result in an improved workflow management system. In the past, WfMS were used in well-defined activities, such as manufacturing, where the processes tend to be more established and stable. But in the current climate WfMS may be used for more fluid business processes, such as e-commerce, or in processes involving human interactions, such as the software development process. In such situations, it is not always possible to predict in advance all the parameters that may be important for the overall processes. This gives rise to the need of adaptive systems. Our previous works [10, 11] describe the advantages of our agent-based framework JBees [9], such as distribution, flexibility and ability to dynamically incorporate a new process model.

The process models that a workflow modeler designs for our system consists of the entire workflow model and the resources that are needed to perform various tasks associated with that model. While this is the typical scenario in most of the production oriented workflows, there are certain workflow scenarios in which Interaction Protocol (IP) models would be suitable than a overall workflow model. In this paper, we discuss how various agents that participate in an e-business scenario can use Interaction Protocols. The workflow modeler has the option to choose from two approaches of modeling, the process centric workflow or the workflow based on interaction pro-

ocols. The paper is organized as follows. A brief background of our work is given in Section 2. Section 3 describes how process centric workflows are used in our workflow system. In the Section 4 we explain how our agent-based architecture can be used for design and execution of interaction protocols. Section 5 provides some recommendations for choosing one of the mechanisms to model processes. The concluding remarks are presented in Section 6.

2 Background

2.1 Coloured Petri Nets (CPNs)

We use CPN as a formalism to model workflows in our system. The sound mathematical foundation behind the Coloured Petri nets (CPNs) makes it a very useful tool for modeling distributed systems. Petri nets consist of four basic elements namely *tokens*, *places*, *transitions* and *arcs*. A detailed description of CPNs can be found in [2].

2.2 Interaction Protocols (IPs)

Interaction protocols [1] are the specifications that allow a certain kind of conversation or exchange of messages between two agents. This reduces the search space of possible responses to an agent message. These interaction protocols can be used to model workflow scenarios in which agents are used to execute the process models and send messages to appropriate agents to perform a particular task. Each agent has the interaction protocol describing how to communicate with the other agent and what actions to perform when a new message arrives.

2.3 Existing Architecture

Our research is focused on developing an agent-based WfMS, where the work associated with running a WfMS has been partitioned among various collaborating agents that are interacting with each other by following standard agent communication protocols [7]. JBees is based on Opal [8] and uses the CPN execution tool JFern [6]. The processes are modeled using CPNs [2]. A first description of JBees can be found in our previous papers [9-11]. Our enhanced system consists of seven Opal agents, which provide the functionality to control the workflow. The manager agent provides all functionality the workflow manager needs, such as creation and deletion of tasks, roles and process definitions, instantiation of new process instances and creation of resource agents. The process agent executes a process instance. Each resource in the system has its own resource agent. Every resource in the system gets registered to one of the broker agents that allocate the resources to the process. The storage agent manages the persistent data that is needed. The monitor agent collects all the process specific data and sends them to the storage agent. The control agent continuously looks for anomalies to the criteria specified by the human manager and reports the violations to these criteria to the manager agent. The manager agent provides information to the human manager, which can be used for a feedback mechanism.

3 Mechanism 1: Demonstrating the Process Perspective Models Using an Example

Most workflow systems model application based on a single sequence of workflow process model such as fault processing system or diamond processing system. Our architecture described in the previous section is suitable for modeling from this perspective.

Figure 1 shows an order entry process for purchasing a book designed from a process perspective. The tasks include order entry, inventory check, credit check, evaluation, approval, billing, shipping, archiving and the task associated with writing a rejection letter. A task can be represented as a sub process and linked to the main process model forming a hierarchy of process models. Each task will be assigned to an appropriate resource agent. More details on how our system supports the process perspective can be found in our previous works [9-11].

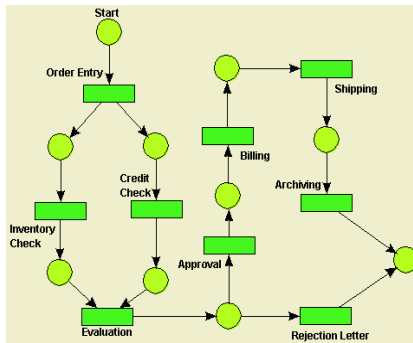


Fig. 1. The Order Entry process

4 Mechanism 2: Using Interaction Protocols (IPs) to Model Workflows

The reasons for using IPs for agents are manifold [1]. Interaction protocols are better intuitive models of how agents will interact than the message based communication between two agents. This conversation can be modelled as the interaction protocol between agents using Colored Petri nets. The advantage is of using an IP is that an agent is aware of the overall model. Some of the error handling mechanisms and global data handling mechanisms could be assigned to the agent. This gives a clear picture of various conversations an agent could be involved in.

Conversation structures are separated from the actions that are taken when an agent is involved in a conversation, facilitating the reuse of conversations in multiple contexts. The transitions that represent the actions can be implemented accordingly (by static binding or dynamic binding) depending upon the requirements.

Figure 2 shows the interaction protocols that each agent executes in a car insurance claim scenario. The car insurance workflow is expressed using the interaction protocols. The agents involved in the workflow scenario are the customer agent, insurance company manager agent (ICManager agent) and the panel beater agent. The customer

captures different images of the damaged car and sends the photograph to the manager of insurance company. The insurance company manager forwards the photographs to the panel beater to get an estimate of the damage. The panel beater assesses the damage and sends a report to the insurance company manager. The insurance manager decides the insurance amount that has to be paid to the customer and informs the customer.

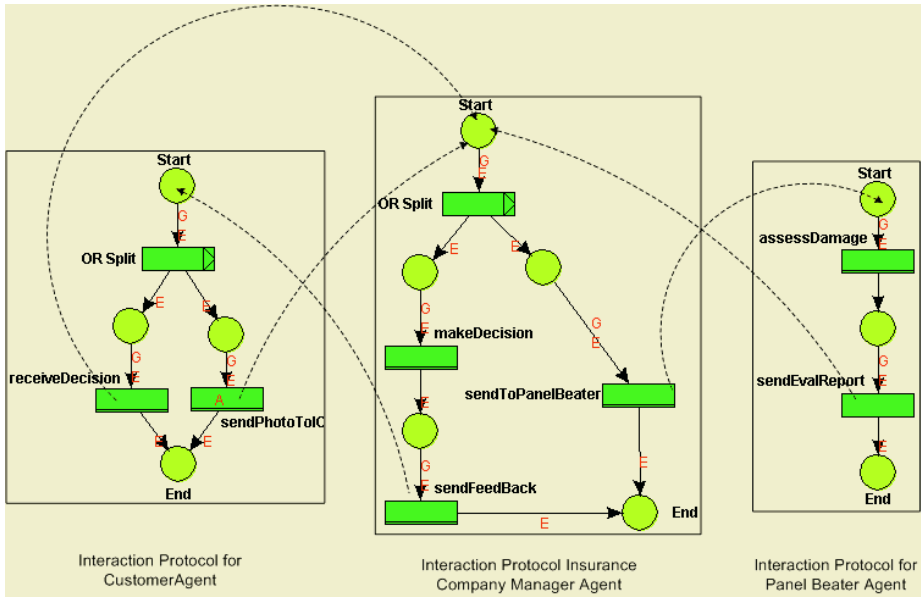


Fig. 2. Interaction protocols for car insurance claim scenario

4.1 Architectural Support for Interaction Protocols

Each agent in the scenario described above is an instance of a process agent. The process agent is capable of executing process models. In this case, we have three process agents that are capable of executing interaction protocols. The dotted arrows that emanate from the transitions in the interaction protocols show that the agent that executes the transition sends the messages. The arrowheads point to the start of an interaction protocol. This interaction protocol is executed when a message reaches a particular agent. For example when the insurance manager receives the images of the damaged car from the customer, the *ICManager* agent sends an email to the panel beater agent. When the message reaches the panel beater agent, it prompts the user of the system (the actual panel beater), to read the email. Then, the panel beater agent executes the interaction protocol. After the damage has been assessed, the agent sends a report to the *ICManager* agent. The sample code for sending this message encoded in the *sendToPanelBeater* transition is given below

```

JobToken jt = (JobToken) get ("X");
if(jt.getAttribute(CarInsuranceOntology.TO_PANEL_BEATER))
{ sendMessageToPanelBeater(); }

```

Before the execution of any protocol, a job token (assume, X) is created. This job token consists of certain attributes that enable the firing of various transitions. The attributes are stored in name and value pairs in a map. For the transition named *sendToPanelBeater* to fire, the job token should have a value corresponding to the name TO_PANEL_BEATER in the car insurance ontology. In this simple scenario, there has not been a need for additional resource agents to perform certain tasks. But more complex examples might need resource agents similar to the ones described in Section 3. For simplicity reasons, the not understood performative has not been shown in all the interaction protocols in figure 2. Our system also supports the dynamic changing of interaction protocols similar to the changing of process centric models.

5 Choosing Process Models

From workflow perspective, it is desirable to choose process centric way of process modeling. But from an agent perspective it might be desirable to have more autonomy to the agent by using the interaction protocol models for each agent. We feel that though both these perspectives are correct, the nature of the process that is being dealt with should be of importance when one thinks about choosing which way to go. In an application like fault processing system, the entire workflow is well defined and in this case, process centric approach would be easier to design and execute. But for fluid processes which might involve many alternative interactions between agents and that involves multiple agents interaction protocols need to be used. The car insurance workflow described in the previous section uses the interaction protocols. But the same workflow could also be modelled as a process centric model shown in figure 3.

The differences between the two approaches are given below.

- a) Process centric approach is the widely used approach in workflow systems. The agents are prescribed about what to do, rather than being more autonomous.
- b) The interaction protocol approach provides more autonomy to the agents in the workflow system and the interaction protocol approach has been widely used in the agent-based systems.
- c) Interaction protocol approach provides detailed description of interactions between agents as opposed to the process centric approach. It can be observed from figure 3 that the process centric approach hides most of the agent interaction details explicitly in the process model even though it has been implemented programmatically.

It can also be argued that both these approaches can be used together under certain circumstances. The process model shown in figure 3 provides only an overview of the workflow and hides the transition level details from the user. At each transition in the process model, there is some form of information exchange between two agents. For example in the transition *sendRequestToAssessor*, the *ICManager* sends a request to the panel beater to assess the level of damage and send a report. In this case, the process agent that executes this transition can instantiate two agents that adhere to the interaction protocols shown in Figure 2.

Thus, by combining both the ways of modeling, the user is able to understand the workflow in a better way. This provides a richer meaning to the scenario which both these models had failed provide individually, in certain cases.

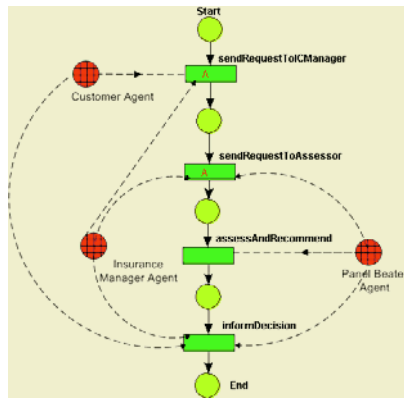


Fig. 3. Process model of the car insurance scenario (process centric approach)

Assume that we now have an e-business workflow scenario such as the English auction, which involves an auctioneer agent, seller agent and the buyer agents. In this case the workflow modeler should choose one of the approaches described in the previous sections. We believe that for this particular scenario the interaction protocol approach would be much more suitable than the process centric approach as the emphasis of the scenario is more on how the interactions between agents take place (bidding, accepting bid etc.) rather than the execution/completion of a particular task. In cases where most of the participants/agents are distributed, the interaction protocol is quite useful, as it would explicitly show the state of each of the participants. In the auction scenario, the state of any of these conversations can be easily traced using an IP model. Though this is possible in the process centric approach, the users will not have an explicit graphical clue to identify the state of the participants.

We would like to mention that when the workflow is oriented more towards processes and completion of various tasks by different roles then the process centric process modelling should be undertaken and for the workflows that have a heavy focus on interactions then the interaction protocol approach should be taken. In cases where the overall process model as well as individual exchanges are important then both mechanism should be used together to provide a richer understanding of the problem at hand. The workflow modelers should understand the different perspectives of modeling mechanisms the system provides and take advantage of them to provide a model that is meaningful to the user of the system.

6 Conclusion

We have presented the two ways of modeling processes, the process centric way and the interaction protocol way. We have also discussed the architectural support for both of these mechanisms in our workflow system. Using a scenario we have described what are the different ways in which a workflow process model can be designed. When the process model has a focus of overall process, the process-centric model is suitable and when the interactions of each participant is important then the modeling should be undertaken based on interaction protocols. When there is a need for understanding both the overall model and the individual interactions, then both

models should be used as discussed in section 5. In future we have planned to examine both approaches by using complex models and applying both mechanisms of process modeling and comparing the advantages and the disadvantages.

References

1. R. Scott Cost, Ye Chen, Timothy W. Finin, Yannis Labrou, Yun Peng, Using Colored Petri Nets for Conversation Modeling, *Issues in Agent Communication*, p.178-192, 2000
2. Jensen, K., Coloured Petri Nets - Basic Concepts, Analysis Methods and Practical Use, Vol. 1: Basic Concepts. EATCS Monographs on Theoretical Computer Science. 1992, Heidelberg, Berlin: Springer Verlag GmbH. 1-234.
3. S. Meilin, Y. Guangxin, X. Yong, and W. Shangguang, 'Workflow Management Systems: A Survey.' in Proceedings of IEEE International Conference on Communication Technology, 1998.
4. J.W. Shepherdson, S.G. Thompson, and B. Odgers, 'Cross Organisational Workflow Coordinated by Software Agents', in CEUR Workshop Proceedings No 17. Cross Organisational Workflow Management and Coordination, San Francisco, USA, (1998)
5. W.M.P van der Aalst and K. van Hee, *Workflow Management: Models, Methods, and Systems*, MIT Press, 2002.
6. Mariusz Nowostawski. JFern – Java based Petri Net framework, 2003.
7. FIPA, FIPA Communicative Act Library - Specification. 2002.
<http://www.fipa.org/specs/fipa00037>
8. Martin K. Purvis, Stephen Cranefield, Mariusz Nowostawski, and Dan Carter, 'Opal: A multi-level infrastructure for agent-oriented software development', The information science discussion paper series no 2002/01, Department of Information Science, University of Otago, Dunedin, New Zealand, (2002).
9. Martin Fleurke, Lars Ehrler, and Maryam Purvis, 'JBees - an adaptive and distributed framework for workflow systems', in Workshop on Collaboration Agents: Autonomous Agents for Collaborative Environments (COLA), Halifax, Canada, pp. 69–76.
10. Savarimuthu, B.T.R., Purvis, M. and Fleurke, M. (2004). 'Monitoring and Controlling of a Multi-agent Based Workflow System' In Proc. Australasian Workshop on Data Mining and Web Intelligence (DMWI2004), Dunedin, New Zealand. CRPIT, 32. Purvis, M., Ed. ACS. 127-132.
11. Savarimuthu, B.T.R and Purvis M.A, 'A Collaborative mulit-agent based workflow system.' In: M. G. Negoita, R. J. Howlett, L. C. Jain (eds.), *Knowledge-Based Intelligent Information and Engineering Systems*, 8th International Conference, KES2004, Wellington, New Zealand, September 2004, Proceedings, Part II, Springer LNAI 3214, pp. 1187-1193, 2004.

An Agent-Enhanced Workflow Management System

Bastin Tony Roy Savarimuthu*, Maryam Purvis,
Martin Purvis, and Stephen Cranfield

Department of Information Science, University of Otago,
P O Box 56, Dunedin, New Zealand

{tony, tehrany, mpurvis, scranefield}@infoscience.otago.ac.nz

Abstract. The overall goal of the research is to address the problems in traditional workflow management systems by developing a distributed and adaptable workflow management system. This paper discusses the research objectives and the work that has been carried out in the development of a workflow management system, JBees, which uses agent-based infrastructure as the building block. We also outline the work under progress and our future plans on enhancing our workflow system.

1 Introduction

Traditional workflow management systems [9-11] suffer from disadvantages such as the lack of dynamic incorporation/modification of process models, lack of adaptability of process models during run time and the lack of support for the integration of distributed process models. The overall goal of the research is to address these problems by developing a distributed and adaptable workflow management system. Employing a distributed network of autonomous software agents [21] that can adapt to changing circumstances is our solution to address this problem. These changes would be triggered by market changes and the process improvements due to continuous process re-engineering. The agent-based system, JBees [3] would facilitate the distribution of process models and the dynamic changing of process models during run time.

In the context of WfMSs, agent technology has been used in different ways [25]. In some cases the agents fulfil particular roles that are required by different tasks in the workflow. In these cases the existing workflow is used to structure the coordination of these agents [26, 27]. An example of this approach is the work by Nissen in designing a set of agents to perform activities associated with the supply chain process in the area of e-commerce [27]. In other cases, the agents have been used as part of the infrastructure associated with the WfMS itself in order to create an agent-enhanced WfMS [28, 29]. These agents provide an open system with loosely coupled components, which provides more flexibility than the traditional systems. Some researchers

* Bastin Tony Roy Savarimuthu, the primary author of this paper is a PhD student at the department of Information Science at the University of Otago, Dunedin, New Zealand. The co-authors of this paper are his supervisors Dr. Maryam Purvis, Prof. Martin Purvis and Dr. Stephen Cranfield. This paper describes the work that has been carried out so far and the future plans towards the primary author's PhD degree

have combined both of these approaches [30], where an agent-based WfMS is used in conjunction with specialized agents that provide appropriate application-related services. In our framework, JBees [3], the WfMS is partitioned among various interacting agents following the interaction protocols. The model associated with a business process is represented using the Coloured Petri net formalism and is executed by a specially designed agent. This agent-based environment facilitates the dynamic incorporation of changed models into the system and thereby assists process re-engineering. Advantages of employing agents include the facilitation of inter and intra organizational co-operation and flexibility in choosing processes on the fly and controlling process parameters.

The paper is organized as follows. The research objectives of our work are given in Section 2. Section 3 provides a summary of the work that has been carried out, the work under progress and our future plans. The concluding remarks are presented in Section 4.

2 Research Objectives

We propose to achieve our final goal by refining the work into three objectives. Our first objective is to enhance the agent-based architecture by providing support for the creation and execution of process models and the changing of process models during runtime. The architecture will include a simulation engine to model, study and evaluate executions prior to run time. The architecture will also include components for monitoring and controlling the system. Rapid growth and availability of services in the Internet can be well made use of, by the workflow systems. Modern workflow systems should provide appropriate mechanisms to connect and use these freely available web services as well as web services that are proprietary to businesses. The architecture of our system will be extended to support the service-oriented architecture of web services.

The second objective is to build a society of agents that can work in a collaborative fashion to solve problems. This social network of agents would provide mechanisms for negotiation to perform tasks and also for sharing workload. Each society will comprise of its own norms and rules. There would be a repository for ontologies specific to the workflow system as well as repositories for domain specific application. We would also be developing a mechanism for intelligent resource allocation.

The final objective is to develop practical examples of workflow systems (with many workflow societies) from different domains, which will be used to validate our system and also demonstrate the capabilities of the system.

3 Summary of the Work

Our research is focused on developing an agent-enhanced WfMS, where the work associated with running a WfMS has been partitioned among various collaborating agents that are interacting with each other by following a standard agent communication protocol, FIPA [23]. JBees is based on Opal [4] and uses the CPN execution tool JFern [5]. A first description of JBees can be found in the previously published papers [1] and [2].

3.1 Architecture of the Agent Based Workflow System

Our first research objective is to build an agent based infrastructure for the workflow management system. According to Sycara [21], there are several benefits for using multi-agent systems for building complex software. For example, multi-agent systems can offer a high level of encapsulation and abstraction. Because agents are independent, every agent can decide, which is the best strategy for solving a particular problem. Different developers can build the agents simultaneously as long as they understand the communication between the agents that they develop. A second important benefit is that multi-agent systems offer distributed and open platform architecture. Agents can support a dynamically changing system without the necessity of knowing each part in advance.

Our work builds on the work done by Ehrler, Fleurke and Purvis [1, 2] on multi-agent based workflow system. Figure 1 shows the enhanced architecture of our agent based system, JBees [6, 7]. The manager agent provides all functionality the workflow manager needs such as creation and deletion of tasks, roles and process definitions, instantiation of new process instances and creation of resource agents. The process agent executes a process instance. Each resource in the system has its own resource agent. These resource agents may be interfaces to the human agents as well as devices such as scanners and printers. Every resource in the system gets registered to one of the broker agents that allocate the resources to the process. The storage agent manages the persistent data that is needed. The monitor agent collects all the process specific data and sends them to the storage agent. The control agent continuously looks for anomalies to the criteria specified by the human manager and reports the violations to these criteria to the manager agent. The manager agent provides information to the human manager, which can be used for the feedback mechanism.

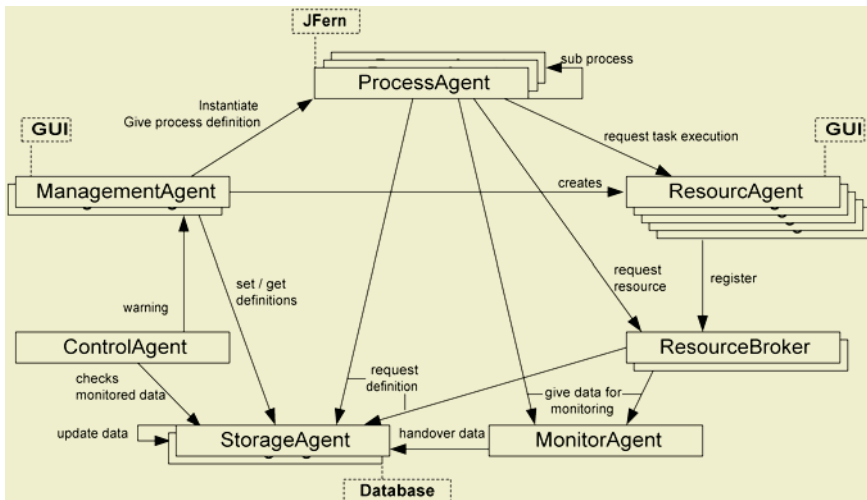


Fig. 1. The current architecture of JBees

To the enhanced architecture shown in figure 1, we intend to integrate the Web Services. Web Services are software components available on the Internet, which

provide certain services that may be of general interest, such as weather monitoring services, currency converters, etc. A large fraction of the web services are used within companies protected within their own firewalls. These web services can be accessed for day-to-day business transactions. Examples of these web services include banking services and air ticket booking. The workflow process modeller can integrate web services with the existing workflow system. For example, a process model associated with the travel plan of a tourist may depend upon environmental factors, such as the weather conditions. The task associated with finding the weather condition can be provided using a web service. We have implemented the basic infrastructure that helps in incorporating the web services by wrapping a web service as an agent. Our work on integration of web services to the framework can be found in our works [19, 20, 24].

We are currently modifying the architecture of the system to incorporate composition of web services. The Coloured Petri Net (CPN) [12] formalism that we use for modelling processes will be used for the composition of web services as well. With the incorporation of the web service agents the resource agents provide the interfaces to human agents, devices as well as web services.

3.2 Conceptualisation and Implementation of Workflow Institutions/Societies

In order to achieve the goals of a collaborative environment in a workflow system, the agents in the system form societies. The inspiration for this work has been drawn from the previous research in the area of agent institutions/societies [13-17]. The new architecture would include the libraries that specify the norms of the society. Each society will comprise of its own norms and rules. There would be a repository for ontologies specific to the workflow system as well as repositories for domain specific application (software development, medical information system etc). The resource agents possess similar capabilities within a given society. The resource brokers allocate resources depending upon the manager's request. The resource brokers negotiate with the resources to identify and allocate the best possible resource that suits the task to be performed. The resource broker will also consider the reputation of resource agents during the allocation of a task. We are currently implementing the architecture that we proposed in our previous work [18].

3.3 Creation of Practical Examples to Validate the Functionalities System

Finally, to validate the overall working of the workflow management system we intend to develop several practical examples of workflow systems with all the features described in the previous sub-sections. So far, we have used examples from different domains such as auctions, online book purchasing, car insurance and diamond processing industry in our previous works. These examples would be enhanced with the new features that will be developed, validated and demonstrated.

4 Conclusions

In this paper we have described our research objectives in the development of agent-enhanced workflow management system, JBees. We have discussed the work that has

been undertaken and the work under progress. We have also explained the future work that would be carried out.

References

1. Martin Fleurke. JBees, an adaptive workflow management system - an approach based on petri nets and agents. Master's thesis, Department of Computer Science, University of Twente, P.O. Box 217, 7500 AE Enschede, The Netherlands, 2004.
2. Martin Fleurke, Lars Ehrler, and Maryam Purvis, 'JBees - an adaptive and distributed framework for workflow systems', in Workshop on Collaboration Agents: Autonomous Agents for Collaborative Environments (COLA), Halifax, Canada, eds., Ali Ghorbani and Stephen Marsh, pp. 69–76, <http://www.cs.unb.ca/~ghorbani/cola/proceedings/NRC-46519.pdf>, (2003). National Research Council Canada, Institute for Information Technology.
3. Department of Information Science University of Otago. JBees. <http://jbees.sourceforge.net>, 2004.
4. Martin K. Purvis, Stephen Cranefield, Mariusz Nowostawski and Dan Carter, 'Opal: A multi-level infrastructure for agent-oriented software development', The information science discussion paper series no 2002/01, Department of Information Science, University of Otago, Dunedin, New Zealand, (2002).
5. Mariusz Nowostawski. JFern – Java based Petri Net framework, 2003.
6. Savarimuthu, B.T.R., Purvis, M. A. and Fleurke, M. (2004), "Monitoring and Controlling of a Multi-agent Based Workflow System", Proceedings of the Australasian Workshop on Data Mining and Web Intelligence (DMWI2004), Conferences in Research and Practice in Information Technology, Vol. 32, Australian Computer Society, Bedford Park, Australia (2004) 127-132.
7. Ehrler, L., Fleurke, M., Purvis, M. A. and Savarimuthu, B.T.R., "Agent-Based Workflow Management Systems (Wfmss): JBees- A Distributed and Adaptive WFMS with Monitoring and Controlling Capabilities", to be published in a special issue of the Journal of Information Systems and e-Business on Agent-Based Information (2005).
8. Savarimuthu, B.T.R., Purvis, M. and Fleurke, M. (2004). Towards a multi-lingual workflow system – a practical outlook. In Proc. Australasian Workshop on Data Mining and Web Intelligence (DMWI2004), Dunedin, New Zealand. CRPIT, 32. Purvis, M., Ed. ACS. 127-132.
9. S. Meilin, Y. Guangxin, X. Yong, and W. Shangguang, 'Workflow Management Systems: A Survey.' in Proceedings of IEEE International Conference on Communication Technology, (1998).
10. J.W. Shepherdson, S.G. Thompson, and B. Odgers, 'Cross Organisational Workflow Coordinated by Software Agents', in CEUR Workshop Proceedings No 17. Cross Organisational Workflow Management and Coordination, San Francisco, USA, (1998)
11. W.M.P van der Aalst and K. van Hee, Workflow Management: Models, Methods, and Systems, MIT Press, 2002.
12. Jensen, K., Coloured Petri Nets - Basic Concepts, Analysis Methods and Practical Use, Vol. 1: Basic Concepts. EATCS Monographs on Theoretical Computer Science. 1992, Heidelberg, Berlin: Springer Verlag GmbH. 1-234.
13. Dastani, M.M., Dignum, M.V., & Dignum, F.P.M. (2003). Role-Assignment in Open Agent Societies. In (Ed.), *Proceedings of the Second International Conference on Autonomous Agents and Multiagent Systems (AAMAS'03)* Melbourne: ACM Press.
14. Mario Verdicchio, Marco Colombetti: A Logical Model of Social Commitment for Agent Communication. Workshop on Agent Communication Languages 2003: 128-145

15. Marco Colombetti, Nicoletta Fornara and Mario Verdicchio.(2002) The Role of Institutions in Multiagent Systems *Ottavo Convegno Associazione Italiana per l'Intelligenza Artificiale AI*IA*, Siena, Italy
16. Dignum, V, Weigand, H 'Toward an Organization-Oriented Design Methodology for Agent Societies' Intelligent Agent Software Engineering. 2003, London, Idea publishing group. 191-212.
17. Huang, P. and Sycara, K, 'A computational model for online agent negotiation ', in Proceedings of 35th Hawaii International Conference on System Sciences, (2002).
18. Savarimuthu B.T.R., and Purvis, M. 'Collaborative multi-agent based workflow system'. In Knowledge-Based Intelligent Information and Engineering Systems (KES), pages 1187–1193. Springer, 2004.
19. Purvis, M. and Savarimuthu, B.T.R., 'A multi-agent based workflow system embedded with web services', in Workshop on Collaboration Agents: Autonomous Agents for Collaborative Environments (COLA), Halifax, Canada, eds., Ali Ghorbani and Stephen Marsh, 2004, Beijing, China.
20. Savarimuthu, B.T.R., Purvis, M.A, Purvis, M.K, Cranefield S., 'Agent-Based Integration of Web Services with Workflow Systems', Accepted to be published in Autonomous Agents and Multi-agent Systems (AAMAS), 2005, Enschede, Netherlands.
21. Wooldridge, M.J., *Intelligent Agents*, in *Multiagent Systems*, G. Weiss, Editor. 1999, MIT Press: Cambridge. p. 27-77
22. Sycara, K.P., *Multiagent Systems*. AI magazine, 1998. 19(2)
23. FIPA, *FIPA Communicative Act Library - Specification*. 2002.
<http://www.fipa.org/specs/fipa00037/>
24. Savarimuthu, BTR., Purvis, M.A., Purvis, M.K., and Cranefield, S., "Agent-Based Integration of Web Services with Workflow Management Systems", Information Science Discussion Paper Series, Number 2005/05, ISSN 1172-6024, University of Otago, Dunedin, New Zealand (2005).
25. G. Joeris. Decentralized and Flexible Workflow Enactment Based on Task Coordination Agents. In 2nd Int'l. Bi-Conference Workshop on Agent-Oriented Information Systems (AOIS 2000 @ CAiSE*00), Stockholm, Sweden, pages 41–62. iCue Publishing, Berlin, Germany, 2000.
26. N.R. Jennings, P. Faratin, T.J. Norman, P. O'Brien, and B. Odgers. Autonomous Agents for Business Process Management. Int. Journal of Applied Artificial Intelligence, 14(2):145–189, 2000.
27. M.E. Nissen. Supply Chain Process and Agent Design for E-Commerce. In 33rd Hawaii International Conference on System Sciences, 2000.
28. H. Stormer. AWA - A flexible Agent-Workflow System. In Workshop on Agent-Based Approaches to B2B at the Fifth International Conference on Autonomous Agents (AGENTS 2001), Montral, Canada, 2001.
29. M. Wang and H. Wang. Intelligent Agent Supported Flexible Workflow Monitoring System. In Advanced Information Systems Engineering: 14th International Conference, CaiSE 2002, Toronto, Canada, 2002.
30. Q. Chen, M. Hsu, U. Dayal, and M.L. Griss. Multi-agent cooperation, dynamic workflow and XML for e-commerce automation. In fourth international conference on Autonomous agents, Barcelona, Spain, 2000.

Knowledge Sharing Between Design and Manufacture

Sean D. Cochrane, Keith Case, Robert I. Young, Jenny A. Harding, and Samir Dani

Wolfson School of Manufacturing Engineering, Loughborough University,
Leicestershire, LE11 3TU, UK
s.d.cochrane@lboro.ac.uk

Abstract. The aim of this research is to develop a representation method that allows knowledge to be readily shared between collaborating systems (agents) in a design/manufacturing environment. Improved mechanisms for interpreting the terms used to describe knowledge across system boundaries are proposed and tested. The method is also capable of handling complex product designs and realistic manufacturing scenarios involving several parties. This is achieved using an agent-architecture to simulate the effects of individual manufacturing facilities (e.g. machine tools and foundries) on product features. It is hypothesised that knowledge sharing between such agents can be enhanced by integrating common product and manufacturing information models with a shared ontology, and that the shared ontology can be based largely on The Process Specification Language (PSL).

1 Introduction

Manufacturability analysis allows cost/performance optimisations to be made early in the design process with minimum rework; and many organisations have deployed Knowledge Based Systems (KBS) to improve the consistency of this analysis. Typically KBS work well in isolation. There is however, a growing requirement to share knowledge between systems. This is driven in part, by a need to do more than move problems along a supply chain. Such holistic analysis requires intimate knowledge of all the processes used to manufacture a product, and with the growing use of subcontractors, no single party is now likely to provide this. The development and maintenance of knowledge bases can also be expensive, and knowledge sharing distributes these costs between collaborating parties.

Knowledge sharing is not however straightforward. Existing systems typically use bespoke models of entities and relationships, and implied terms for stating rules, constraints and objectives. These make it difficult for knowledge to be mapped between systems. Recent research tackles these issues by formally defining lexicons of terms, referred to as *ontologies*. An explicit ontology provides a starting point for the mapping process. Ontology mapping has however proven difficult to achieve on an industrial case scale. Ontologies often use different terms to describe similar concepts and similar terms to describe different concepts. Different taxonomies and conflicting definitions add further complexity. Mapping techniques include shared ontologies which define terms relevant to multiple systems. Shared ontologies are however difficult to define beyond generic concepts. The specific terms used to describe actual products and processes (e.g. nuts, bolts, milling, and drilling) still need to be defined; and their inclusion leads to large lexicons, with complex taxonomies that are difficult to apply and adapt to specific application. The question arises as to whether specific

terms can be fully defined by instantiating generic concepts? A set of generic concepts (and associated models) for manufacturability analysis would be required for this purpose.

The aim of this research is to develop representation methods that improve knowledge sharing between collaborating systems in design/manufacturing environments. Improved mechanisms for interpreting the terms used to describe knowledge across system boundaries are required. The method should also be capable of handling complex product designs and realistic manufacturing scenarios involving several parties. Section 2 discusses the research literature relevant to knowledge sharing, and section 3 describes the knowledge sharing approach proposed by this research. Conclusions and further work are discussed in section 4.

2 Information Models and Ontologies

The use of object-oriented models to structure shared information in design environments is widely discussed in the research literature. Proposed models include separate product and manufacturing hierarchies [1], where classes represent entities such as product features and manufacturing processes. These structures have also been extended for knowledge representation. The Factory Data Model (FDM) [2] for example, extends the Manufacturing Model [1] with a strategy hierarchy for manufacturing rules, constraints and objectives. Even the FDM however, does not specify the terminology used to describe rules. This is left to bespoke extensions of the basic model. The interpretation of rules will therefore be specific to the model deployed by each KBS. This makes it difficult for systems to directly apply knowledge from other systems.

Ontologies have been proposed as a way of overcoming these issues. Ontologies are “*a formal description of the entities within a given domain: the properties they possess, the relationships they participate in, the constraints they are subject to, and the patterns of behaviour they exhibit*” [3]. Explicitly defining the terms used by a KBS to describe rules makes it easier to map between systems (figure 1: left). There are however, significant issues involved with mapping ontologies, including: extraneous clauses (e.g. synonyms), and conflicting inferences. Techniques such as combinator logic [4] have been demonstrated as a means of resolving conflicting inferences under certain conditions. These techniques are rigorous, but potentially difficult to scale to industrial case examples involving several collaborating parties.

Shared ontologies have been proposed as a way of simplifying ontology mapping (figure 1: right). This is analogous to using English to communicate across national boundaries, even when no native English speakers are present. In practice however, establishing a shared ontology is difficult when several parties are involved. Ideally, a pre-existing ontology would be available, and several have recently emerged. These include: *The Process Specification Language* (PSL) [5], and the Suggested Upper Ontology (SUO) [6].

PSL targets process-centric environments (e.g. manufacturing and construction), and defines generic terms for most (if not all) processes. PSL has been used to exchange project planning information [7], describe process inputs and outputs [8], and model process flows, e.g. painting [9]. The need for a shared set of terms for interpreting product/manufacturing models, and the potential application of PSL to this issue

has also been recently highlighted [10]. SUO defines a large lexicon, which incorporates PSL, and more specific concepts for manufacturing (and other) environments, e.g. material removal and cutting. The more detailed concepts needed to describe specific environments are not included in SUO (e.g. casting cylinders, and drilling holes). These invariably require bespoke augmentation for specific applications.

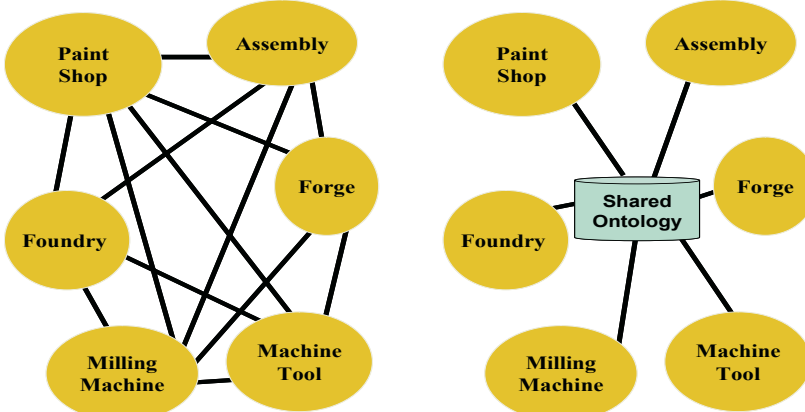


Fig. 1. Ontology Mapping Approaches

PSL and SUO highlight a limit of shared ontologies. Agreement on generic concepts may be achievable, but the specific customised concepts required by all applications are unlikely to be included. A “one-size-fits-all” approach would be highly cumbersome, and so ontologies such as PSL and SUO are recommended as starting points for more detailed, application specific ontologies. Customisation however, leads to the previously described issues of synonyms and conflicting inferences. Point to point mappings (figure 1: left) will also be required, as bespoke terms fall outside the operation of the shared structure.

3 Multi-agent Systems

Agents are software modules capable of applying knowledge to a particular task (essentially a form of KBS). Agents (in simplified form) support goals (i.e. an idea of what they are trying to achieve), have a defined perception of their environment and the information they receive from their environment, hold beliefs about how they should behave and interact with their environment, and be capable of executing actions or action sequences (i.e. plans) that meet goals [11]. An agent’s perceptions, goals, beliefs and actions will usually be expressed in terms of rules; and ontologies can be applied to expressing the rules deployed by agents. Multiple Agent Systems address a number of inter-related tasks through the operation and interaction of several agents. Such architectures have been applied to many environments, including product design, and are supported by bespoke ontologies for detailed design tasks, materials, and quality standards [12].

Returning to our manufacturability analysis problem; figure 1 can be seen as several agents representing facilities (e.g. machine tools), collaborating in the manufac-

ture of a product. Each agent can be owned and developed by participants in the supply chain, and the problem of knowledge sharing (as previously described) can be seen in terms of agent communication and interaction. The knowledge bases of each agent may use terms that have similar or conflicting meanings. These issues have been tackled using a mediator agent [13] to manage the mapping of terms between systems.

4 Hypothesis and Research Platform

This research sets out to share knowledge between several parties in a manufacturing supply chain. This is achieved using an agent-architecture to simulate the effects of individual manufacturing facilities (e.g. machine tools) on product features. It is hypothesised that knowledge sharing between agents can be enhanced by integrating a common information model with a shared ontology, and that the shared ontology can be based largely on PSL. Specific terms can also be modelled by instantiating entities and relationships defined by the shared-generic ontology. This allows specific terms to be interpreted by other agents. The questions that need to be addressed in developing this hypothesis include: what PSL concepts are relevant to manufacturability analysis, and what additional shared concepts are required? Mechanisms for handling the specific terms are also required.

Figure 2 shows the research platform designed to explore these issues. The Manufacturability Analysis Platform (MAP) uses agents, called Process Agents, to simulate the behaviour of manufacturing facilities. Each process agent manipulates the shared product and manufacturing information models according to the processes they are capable of performing. Higher level controlling agents referred to as Strategy (or Complex Process) Agents create and match manufactured features as closely as possible to the required features of a product. Strategy agents hold beliefs relating to how processes should be combined (e.g. drilling precedes boring), and a perception of the whole product being manufactured (not just individual features). Strategy agents effectively simulate the effects of multiple processes, and these simulations can (and should) include a final comparison of required and manufactured features.

Process agents (guided by messages from strategy agents) manipulate the resource usage profile and initial process plan (via the shared model). These outputs directly support manufacturability analysis, and are monitored by the shared model for conflicting inferences, e.g. errors in the logic of the process plan, and insufficient resource allocations. Errors will also be reported if manufactured features (in the final comparison) fall short of requirements.

Process agent perceptions include required and manufactured features (e.g. holes) and their attributes (e.g. diameter tolerances). An agent's goal will be to improve the correlation between required and manufactured feature attributes. In the case of a "drill-hole" process, this includes the creation of the manufactured feature itself. Alternatively a "bore-hole" process would search for a pre-existing manufactured hole, with the aim of improving its diameter tolerance. Beliefs include the relationship between facility parameters and manufactured feature attributes, resource demands, and how process durations relate to product features (e.g. milling rate * surface area). The actions supported by an agent include the manipulation of manufactured features,

process plans and resource profile. A process agent will also interpret messages from a strategy agent, e.g. "bore-hole (list-of-holes)", and "ream-hole (list-of-holes)".

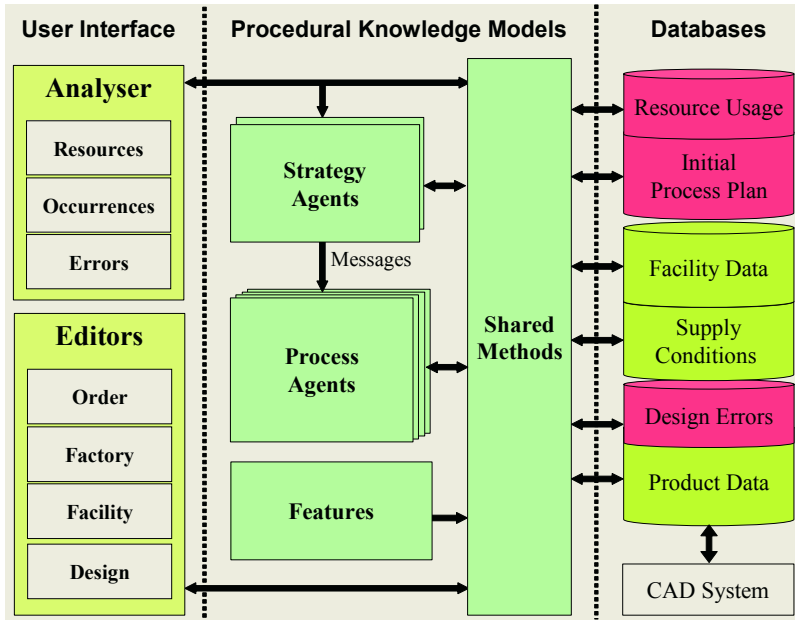


Fig. 2. The Manufacturability Analysis Platform (MAP)

5 The Shared Ontology

This section discusses the requirements of the shared terms, and how they can be derived (where ever possible) from existing ontologies and standards. A distinction is drawn between the shared-generic concepts relevant to all systems and the bespoke lexicon that only needs to be shared between agents in a particular environment.

As agents need to manipulate a common process plan, terms for describing processes, and their inter-relationships are required. PSL supports this extremely well. Processes can be modelled as "activity-occurrences"; and process hierarchies can be described using PSL terminology, e.g. "boring_hole15" is a "sub-activity-occurrence" of "machining-my-product". PSL also allows sequencing rules to be applied, e.g. "drilling" is "possible" after "drill-setting", and for process durations, beginnings, endings, and resource demands to be described in a consistent (shared) manner.

The naming of processes and resources requires consideration, as this falls outside the PSL ontology, and forms part of the bespoke-shared lexicon. Parent process names almost certainly need to be interpreted across system boundaries e.g. "machining-my-product", as these form part of a Strategy Agent's perception, and are likely to use multiple process agents to achieve their goals. Individual sub-process names will also need to be shared if two or more agents need to declare rules relating to each other. Drilling-Hole15 and Boring-Hole15, may for example, be performed by different machine tools. Process names can be handled within the shared model and enforced in a consistent fashion across all systems.

As multiple agents are likely to process the same features, a shared set of concepts for describing features is required. This should include numerical representations (e.g. real numbers and integers), along with geometries (e.g. m, m2, m3, and gram), and enumerated properties (e.g. colour: blue, red, and green). A shared understanding of the features themselves is also required. Each feature includes a set of attributes (e.g. a holes diameter and associated tolerances), and rules for setting attributes (e.g. a hole must be associated with a solid structure such as a block or cylinder). The basic concepts of numbers and geometries are included in SUO, and many detailed feature definitions are provided by STEP AP224 [14]. A shared understanding of Blocks, Cones, Cylinders, Holes, Taps, and Countersinks can therefore be defined according to existing standards. The names of individual features (e.g. Hole15), are however an additional part of the bespoke/shared lexicon. The shared model can be used to enforce the consistent use of feature names across all connecting agents (reporting errors if different names are used by different agents).

6 Conclusions and Further Work

This work focuses on knowledge representation for manufacturability analysis in design. This was chosen due the perceived benefits of sharing knowledge between several parties involved in the manufacture of a product (e.g. holistic analysis). The work has demonstrated the integration of a product and manufacturing information model, with a shared ontology based on PSL. The resulting “shared model” acts as a platform for sharing knowledge between problem solving agents collaborating in the manufacturability analysis of complex products. A structure for building process agents (based on perceptions, goals, beliefs, and actions) has also been proposed and tested. Obvious extensions of the work include the sharing of costing and failure effects knowledge. These use much of the same knowledge of manufacturing processes, and could be represented using similar methods.

Acknowledgements

This work is part of the “Knowledge Representation and Reuse for Predictive Design and Manufacturing Evaluation”, project, funded under EPSRC GR/R64483/01. Further information can be found on: <http://www-staff.lboro.ac.uk/~mmsdc>.

References

1. Molina A, Bell R, 1999. A Manufacturing Model representation of a flexible manufacturing facility. *Journal of Engineering Manufacture: Proceedings of the Institution of Mechanical Engineers*, Vol 213, Part B, pp.225-246.
2. Harding J, Popplewell K, 2001. Enterprise design information: the key to improved competitive advantage. *Int. J. Computer Integrated Manufacturing*, 2001, V. 14, No. 6, 514-521.
3. Uschold, M, Gruninger M, 1996. Ontologies: Principles, Methods, and Applications. *Knowledge Engineering Review*, 1996, Vol. 11, pp. 96-137.
4. Correa da Silva F, Vasconcelos W, Robertson D, Brilhante V, Melo A, Finger M, Agusti J, 2002. On the insufficiency of ontologies: problems in knowledge sharing and alternative solutions. *Knowledge Based Systems* 15 (2002) 147-167.

5. Schlenoff C, Gruninger M, Tissot F, Valois J, Lubell J, Lee J. The Process Specification Language (PSL) Overview and Version 1.0 Specification. Accessed 03/Oct/03: <http://ats.nist.gov/psl>
6. Niles I, Pease, A, 2001. Towards a Standard Upper Ontology. In Proceedings of the 2nd International Conference on Formal Ontology in Information Systems (FOIS-2001), Maine, October 17-19, 2001. Accessed 03/Oct/03: <http://suo.ieee.org>
7. Gruninger M, Sriram R, Cheng J, Law K. Process Specification Language for Project Information Exchange. Int. J. of IT in Architecture, Engineering & Construction, 2003.
8. Bock, C., Gruninger, M., 2004. Inputs and Outputs in PSL NISTIR 7152, NIST, Gaithersburg, MD, 2004. Web Accessed 17th Feb 05: www.nist.gov.
9. Bock, C., Gruninger, M., 2004. PSL: A Semantic Domain for Flow Models. Software and Systems Modeling Journal, 2004. Web Accessed 17th Feb 05: www.nist.gov.
10. Cutting-Decelle, A, Young R, Anumba C, Baldwin A, Bouchlaghem N. The Application of PSL in Product Design across Construction and Manufacturing. CERA Journal, Vol. 11, No.1, March 2003.
11. Arazy O, Woo C, 2002. Analysis and design of agent-oriented information systems. The Knowledge Engineering Review, Vol. 17:3, 215–260.
12. Chira O, Chira C, Tormey D, Brennan A, and Roche T, 2004. A Multi-agent Architecture for Distributed Design. Lecture Notes in Computer Science. Volume 2744 / 2004 Title: Holonic and Multi-Agent Systems for Manufacturing. ISBN: 3-540-40751-0. Chapter: pp. 213 – 224. Online Date: January 2004.
13. Zhang J, Zhang A, Chen C, Wang B, 2003. Semantic Interoperability Based on Ontology Mapping in Distributed Collaborative Design Environment. Lecture Notes in Computer Science. Volume 2663 / 2003 Title: Advances in Web Intelligence: First International Atlantic Web Intelligence Conference AWIC 2003, Madrid, Spain, May 5-6, 2003. Proceedings Chapter: pp. 208 – 217. Online Date: August 2003.
14. Sharma, R, Gao J, 2002. Implementation of STEP Application Protocol 224 in an automated manufacturing planning system. Proceedings of the Institute of Mechanical Engineers, Vol 216 Part B: Journal of Engineering Manufacture.

Toward Improvement-Oriented Reuse of Experience in Engineering Design Processes

Michalis Miatidis¹ and Matthias Jarke^{1,2}

¹ Informatik V (Information Systems), RWTH Aachen University, Germany
{miatidis,jarke}@cs.rwth-aachen.de

² Fraunhofer FIT, Schloss Birlinghoven, Sankt Augustin, Germany

Abstract. Engineering design processes are hard to support. The creativity, complexity and unpredictability characterizing them complicate the identification and formalization of their fine-grained process knowledge. Process support should therefore alleviate this shortcoming by eliciting new engineering ways of working and improving the existing ones based on substantial experiences captured during process execution. This paper discusses a process improvement approach pointing toward this direction. An adapted experience factory infrastructure, by continuously monitoring the process execution, infers new ways of working using a case-based approach and provides improvement support on both a project and a corporate basis. The presented solution integrates ideas from case-based reasoning, requirements engineering and software engineering.

1 Motivation

Engineering design is a business process that covers the early phases from the conceptual idea of a product until its final production. It is arguably one of the most complex, labor- and capital-intensive tasks undertaken by engineers, and determines the competitiveness of the final product. Because of its inherent creative nature, it is a special case of business process. It is poorly structured and, as a rule, evolves in an unpredictable manner. In such highly dynamic settings with continuously changing requirements, the overwhelming majority of the engineering *ways of working* are not properly formalized, but are heavily based on the experience knowledge of the human performers.

As a consequence, cooperative design environments providing process support to such creative and knowledge-intensive processes have further to deal with the systematic collection of experience from previous project cycles and its dissemination and utilization from analogous problem solving contexts in the future.

Traceability, always advocated but rarely adequately practiced in engineering, becomes an absolute necessity now, although it is even more difficult than ever. In the short term, it empowers human performers to reuse existing product and process experiences. In the long term, it provides accountability of good or bad practices, as well as lessons learned.

2 Background

In the last years, we have designed and implemented a process support environment for engineering design processes. This environment is built on top of the *PRIME* (Process-Integrated Modeling Environments) framework that empowers method guidance through process-integrated tools [1], [2].

Technically, PRIME is an object-oriented implementation framework organized around a process metamodel for requirements engineering that has been defined in the *NATURE* project [3]. This metamodel is based on the assumption that in highly creative processes the human performers tend to react contextually according to their accumulated experience and in analogy with previous similar cases they have been involved in.

The *NATURE*-based process metamodel explicitly represents *situations* and *intentions*. A *context* represents the process knowledge of how to reach a specific intention in a given situation and can be refined into three kinds of chunks. *Executable contexts* describe pieces of the process that can be automated and are usually applied by tool actions. *Choice contexts* capture the most creative parts where a decision among several alternatives is demanded. Strategies and systematic plans are defined by *plan contexts* that may iteratively contain other contexts of all three types.

This generic process metamodel offers a powerful ontology that is able to adequately describe the formalized knowledge of a process, as well as its experience knowledge. A domain-specific *guidance metamodel* is built around this metamodel to identify the generic process patterns that define the well-established practices (knowledge) in a particular domain. Similarly, a *traceability metamodel* extending the original process metamodel is employed to organize the recorded design history (experience) in trace chunks according to the contextual decomposition schema.

Since process knowledge and experience stem from the same metamodel, they are comparable and any process discrepancies between them can establish the foundation for an experience-based process improvement.

3 Experience Factory Integration

Because of its inherent creativity, engineering design cannot be fully prescribed in advance. Effective process support through method guidance can only be based on the *explicit knowledge* of well-understood *process fragments* where a precise way of working dominates the engineering practice.

The recorded traces, on the other hand, describe the entire process execution lifecycle in a systematic way. Thus, they further capture the fuzzy process parts where the selection of a way of working is arbitrary and solely based on the so-called *tacit knowledge* that the human performer carries in his mind.

The left part of Fig. 1 shows in a schematic way the chain of the process support that our environment offers to engineering design processes by utilizing engineering knowledge. At the top starting point of the chain reside the domain

experts. They comprise the engineering groups that define the specifications, requirements and design methodologies for the addressed scenarios. This domain knowledge is formalized into concrete engineering ways of working using the guidance metamodel. Their definitions are further enriched with Petri-Net control semantics and get mechanically interpreted by a process engine that provides automated process support to the human performers. Simultaneously, design history is captured and organized into trace chunks according to the concrete traceability model. Finally, the trace chunks are stored in a repository.

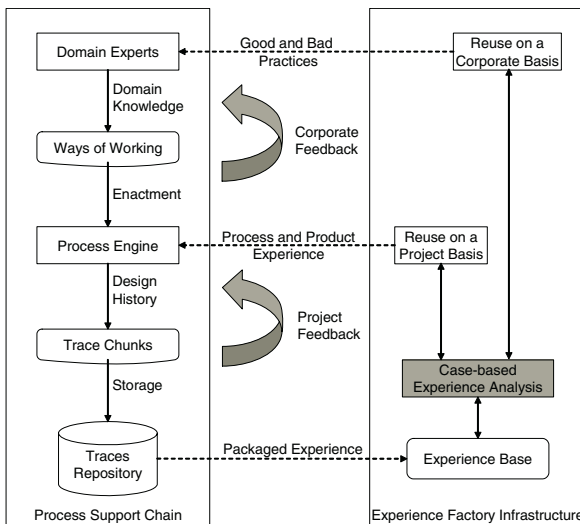


Fig. 1. Experience factory based extension to process support chain

Several process improvement paradigms exist in the literature that strive for higher final product quality and increased productivity [1]. Out of all the existing contributions, we distinguish the *quality improvement paradigm* that provides an intelligent mechanism for continuous quality improvement through reuse and modification of life cycle experiences and products [4]. The quality improvement paradigm is applied by an *experience factory* organization that supports the synthesis of process knowledge through analysis of captured experience, and supplies it on demand.

We have extended our original process support chain according to such an experience factory infrastructure that continuously monitors the accumulated experience (traces) of the process support chain (right part of Fig. 1). In this context, the traces repository plays the role of the *experience base* that integrates experience models in a dynamically evolving memory structure.

The cornerstone of this infrastructure is an analysis component that can on demand evaluate recorded practices and elicit new ways of working employing the *case-based reasoning* (CBR) paradigm. CBR has proven a powerful weapon

for the utilization of the specific knowledge of previously experienced problem situations (*cases*) [5]. Any new case is solved by reusing solutions from similar cases from the past.

The very essence of a case is captured in our basic process metamodel and through it is disseminated to both the guidance and traceability metamodels. Namely, a case comprises:

- the *situation* that describes the subjectively perceived state of the process execution when the case occurs,
- the *intention* that reflects the goal to be achieved after the case occurs,
- the *context* which describes a meaningful relation between a situation and an intention and thus encapsulates the derived solution to the case, and
- the *products* that are being transformed during the case enactment.

Based on the intimate representation of a case using the above constituents, we promote the contextualized nature of the life cycle experience hidden behind a case. This knowledge can be reused in order to provide process improvement on both a project (“*in the small*”) and a corporate (“*in the large*”) basis. In the next section, we describe the case-based reuse on a project basis. The second variant is identified as a future research topic in the concluding section of this paper.

4 Reuse on a Project Basis

The reuse of experience on a project basis provides improvement support directly to individual human performers during their process execution. It is materialized through a *project feedback cycle* that can on demand suggest solutions for the cases behind highly creative and fuzzy parts of the process where no formalized way of working exists.

In such cases, the human performer can be supported by a context-based retrieval of information about design experiences clustered in cases from the past. This experience can provide solutions to problems behind questions of the form: “*how should I proceed in order to achieve my goal?*” or “*what are the possible ways of proceeding in the current situation?*”. Additionally, since the cases contain descriptions of the characteristics of the products transformed during their enactment, the human expert can benefit by learning from or even reusing successful practices in product design from the past.

Design experience reuse results to a reduced design overhead, avoidance of useless iterations over costly process parts, and increased final product quality. As a side effect, the human expertise is effectively utilized for the learning process of trainees.

Our approach has been evaluated in the collaborative research center *SFB 476 IMPROVE* [6]. In this project, in cooperation with other computer science and engineering groups, we have created an integrated design environment for the early phases of the *nylon* production, the so-called conceptual design and basic engineering.

This integrated support is provided through an adaptation of the aforementioned process support chain. Chemical and plastics engineering groups cooperating with us have formalized the well-known methodologies dominating the design practice of our addressed scenario using the guidance metamodel.

During the engineering design, the actual situation of the enactment is continuously monitored by the process engine and the actions of the human performer are traced in the repository. Whenever a well-known situation is traced with a modeled way of working, the process engine automatically interprets its definition and guides the human performer according to it.

In the case of a situation that no well-known way of working exists, the human performer can on demand request experience-based support. This support is then given through the four processes comprising the CBR cycle [5].

Initially, the CBR analysis module *retrieves* suitable cases from the experience base that can be applied to the new situation. These cases are represented as collections of objects corresponding to the basic elements identified in the previous section. The similarity comparison of the current case with the retrieved ones is made using similarity measures for object-oriented case representations, as defined in [7].

The retrieved cases (if any) are then displayed in a *process tracer* visualization tool. Inside this tool, the recorded traces are organized chronologically and hierarchically according to the contextual decomposition and linked to the achieved goals. The performer can *explore* these cases by navigating through them and select the most appropriate ones.

The selected cases can be either followed exactly by the human performer or *revised*. In the case that a human performer decides to revise a proposed case, he can document his decision using a *decision editor* that represents the execution path (*position*) that the human performer has selected for achieving his goal (*issue*), according to an *IBIS* (Issue-Based Information System) model [1]. Old and new position can be ranked by *arguments* that support or object to it. As a consequence, the *design rationale* behind a case is accumulatively captured and is successively communicated to human performers of analogous cases in the future.

Any revised cases are *retained* by automatically recording their enactment and storing its trace chunk into the experience base. From now on, they also constitute pieces of experience that can be provided for support to analogous cases in the future.

The products produced, consumed or transformed during the design process, as a rule for the chemical engineering domain we are tackling with, are characterized by their rich *multimedia* content (e.g. 3D simulation results or CAD drawings). In such cases, only a real-time visualization enables both the novice and experienced experts to evaluate a design alternative and judge its appropriateness with respect to the actual goals and their relevant obstacles.

Drawing on the analogy of the well-known phenomenon of “zapping” rapidly across television channels to find interesting ones, we have developed a tool which allows *semantic zapping* among multimedia products according to goals

and domain ontologies. This tool is called *TRAMP* (Tool for Representation and Annotation of Multimedia content in Plastics engineering) and has been prototypically implemented for the visualization of multimedia simulation traces in plastics engineering.

TRAMP builds on the XML structure of a trace database whose multimedia objects are organized both, according to the *MPEG-7* multimedia metadata standard and according to goal hierarchies and domain models [8].

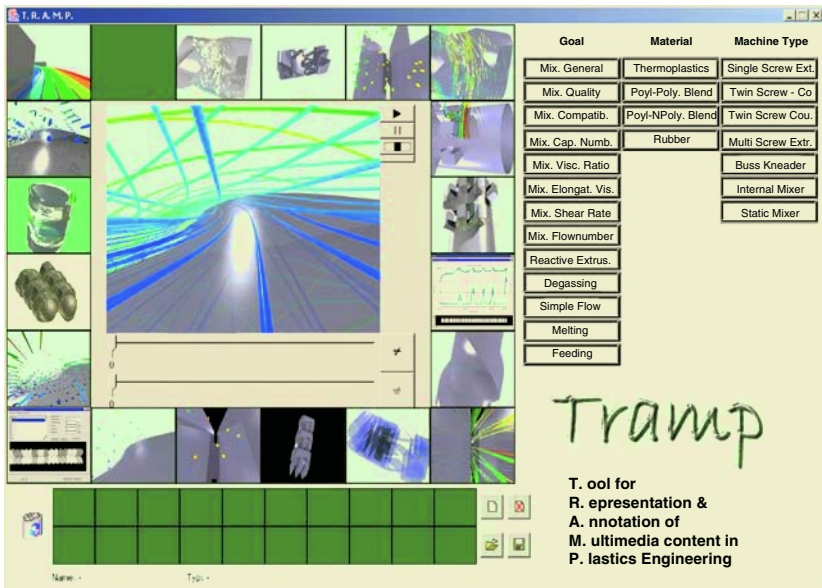


Fig. 2. Semantic zapping across multimedia traces based on ontologies and goals

Fig. 2 shows a screenshot of *TRAMP*. The three columns of buttons on the right were generated from the domain models. The left column contains a list of relevant goals (tertiary effects) to be achieved, whereas the other columns refer to the domain categories of materials and device types. By selecting a combination of buttons, the thumbnail gallery gets filled with visualizations of 1D and 3D simulation results relevant to the indicated combination of goals, materials and device types. By dragging one of these thumbnails into the center, the corresponding multimedia object gets enlarged and (if a video) played, thus enabling *human judgment*. When changing the center object, the context also shifts, so new similar objects can appear in the thumbnail gallery, old ones can vanish and slowly the context of goal, materials and device metadata can shift as well. Alternatives, that the engineer finds particularly interesting (in a positive or negative sense), can be drawn into the personal collection at the bottom left of the tool and get annotated with arguments linking them to positions in the decision editor.

5 Summary and Future Outlook

In this paper, we outlined a process improvement approach tailored for the support of engineering design processes. This approach has been exploited through the extension of the process support chain of our PRIME-based environment with an experience factory infrastructure. By this extension, our original linear process support chain becomes cyclical and engineering processes are not only *defined*, *guided* and *traced* as in the past, but also *improved* based on a case-based analysis and reuse of recorded experiences.

We focused on the experience reuse on a project basis. The experience reuse on a corporate basis will be addressed in our future research. In this case, through a *corporate feedback cycle* (Fig. 1) feedback is provided back to the enterprise in order to improve its *know-how*. To this end, we are planning to develop a methodology for the bottom-up capitalization of knowledge by abstracting from individual experiences across several project instantiations (*high level cases*). Inadequate methodologies can be detected by the observation of certain ways of working that perform poorly according to qualitative metrics, whereas new ones can elaborate with a statistical analysis of frequent process violations and discrepancies.

Acknowledgements

This work was carried out in the Collaborative Research Center 476 IMPROVE, which is funded by the Deutsche Forschungsgemeinschaft (DFG). Thanks are due to all our project colleagues.

References

1. Pohl, K.: Process-Centered Requirements Engineering. Research Studies Press (1996)
2. Pohl, K., Weidenhaupt, K., Dömges, R., Haumer, P., Jarke, M., Klamma, R.: PRIME—Toward Process-Integrated Modeling Environments. ACM Transactions of Software Engineering Methodology **8** (1999) 343–410
3. Jarke, M., Rolland, C., Sutcliffe, A., Dömges, R., eds.: The NATURE of Requirements Engineering. Shaker Verlag (1999)
4. Basili, V.R., Caldiera, G., Rombach, H.D.: The Experience Factory. In: Encyclopedia of Software Engineering. John Wiley & Sons (1994) 469–476
5. Aamodt, A., Plaza, E.: Case-Based Reasoning: Foundational Issues, Methodological Variations, and System Approaches. AI Communications **7** (1994) 39–59
6. Marquardt, W., Nagl, M.: Workflow and Information Centered Support of Design Processes—The IMPROVE Perspective. Computers and Chemical Engineering **29** (2004) 65–82
7. Bergmann, R., Stahl, A.: Similarity Measures for Object-Oriented Case Representations. In: Proceedings of the 4th European Workshop on Case-Based Reasoning. (1998)
8. Spaniol, M., Klamma, R., Jarke, M.: Data Integration for Multimedia E-Learning Environments with XML and MPEG-7. In: Proceedings of the 4th International Conference on Practical Aspects of Knowledge Management. (2002)

A Hybrid Approach to Determining the Best Combination on Product Form Design

Yang-Cheng Lin¹, Hsin-Hsi Lai¹, Chung-Hsing Yeh², and Chen-Hui Hung³

¹ Department of Industrial Design, National Cheng Kung University, Tainan, 701, Taiwan
lyc0914@cm1.hinet.net, hsinhs@mail.ncku.edu.tw

² School of Business Systems, Monash University, Clayton, Victoria 3800, Australia
ChungHsing.Yeh@infotech.monash.edu.au

³ Department of Chinese Literature, National Cheng Kung University, Tainan, 701, Taiwan
superpurse@yahoo.com.tw

Abstract. This paper presents a hybrid approach, using a grey relational analysis (GRA), neural networks (NNs), and a tabu search (TS) algorithm, to determining the best combination of product form design. The GRA model is used to identify the most influential elements of product form. The NN model is used in conjunction with the GRA model, in order to predict and suggest the best form design combination. The TS is applied to search for the best global solution. The hybrid approach provides useful insights to help product designers work out the best combination of product form design for matching the given product image.

1 Introduction

Whether consumers choose a product, depends largely on their perception of the product image [1]. Based on the relationship between the product form and the product image perceived by consumers, design support models [6] and consumer oriented technologies [9] have been developed as “translating technology of a consumer’s feeling and image of a product into design elements”. They help designers realize consumers’ perception to design product form for the given product image.

In this paper, we develop a hybrid approach [12] to addressing this issue, by combining the grey relational analysis (GRA) [3], the neural networks (NNs) [10], and the tabu search (TS) [4, 5] algorithm. The hybrid approach can be used to help product designers determine the best combination of product form design for achieving the desirable product image. In other words, if needed, the hybrid approach help product designers focus on the desirable product image, and the model will work out the best combination of the product form elements for it. In subsequent sections, we first illustrate the structure of the hybrid approach, and then describe the procedure of the hybrid approach. To examine how the hybrid approach works, an experimental study on mobile phones is conducted as mobile phones are currently the most popular consumer product and exhibit a wide variety of product forms.

2 The Structure of the Hybrid Approach

We first present a brief outline of the hybrid approach as shown in Fig.1. The GRA model is used to examine the relationship between product form elements and product

image, thus identifying the most influential elements of product form for a given product image. The NN model is used in conjunction with the GRA model, in order to predict and suggest the best form design combination. Based on the notion, the product design is known to be a hard combinational optimization problem, in particular, the product form and the product image. Hence, the TS is applied to search for the best form design combination.

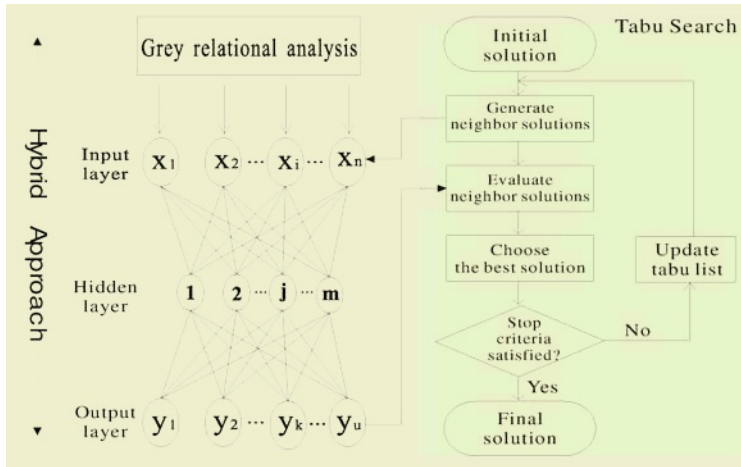


Fig. 1. The structure of the hybrid approach

3 The Procedure of the Hybrid Approach

This procedure comprises the following six steps, described with emphasis on the concept description:

Step 1: Extracting Representative Experimental Samples

First, we should decide what products are chosen as the object of the experimental study. We should then focus on investigating and categorizing of various products in the consuming market. The experimentalists or subjects separate the chosen experimental product samples into several groups by the product samples' similarity degree using the KJ method [2]. Based on the KJ results, we build a similarity matrix from the separation result. Subsequently, we apply the multidimensional scaling (MDS) analysis and then perform the cluster analysis or the factor analysis based on the MDS result. We can obtain the cluster tree diagram or the scatter diagram as shown in Fig.2. We can extract the representative experimental samples from Fig.2.

Step 2: Morphological Analysis of Product form Elements

The morphological analysis [6] is used to extract the form elements of the representative experimental product samples (ex. the mobile phones) by surveying product design experts. In this paper, the product form included not only the outline shapes, but also the product elements. The morphological analysis can involve two primary processes. In the first process, the experts were asked to write down the influential form

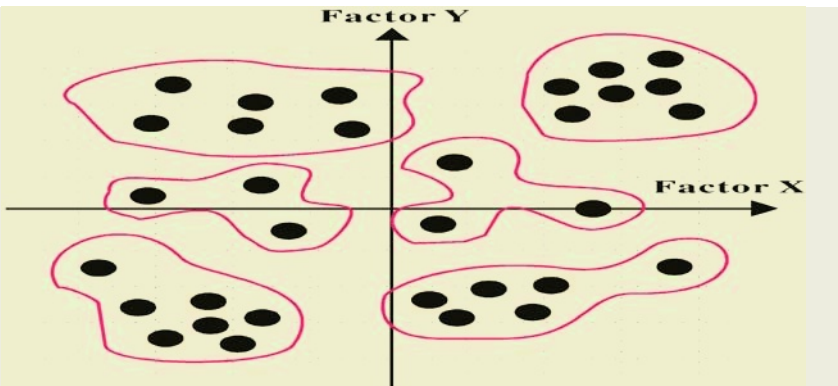


Fig. 2. The scatter diagram based on the MDS result

elements of the experimental product samples individually according to their knowledge and experience. The survey result was separated into two parts, the “form feature” and the “form treatment” [1]. The “form feature” indicated the size and shape of outline components that make up the mobile phones, such as buttons, icons, a screen or a body shell. The “form treatment” described the relationship between the outline components, for example, the equidistance arrangement of the buttons. In the second process, the same experts formed a focus group to discuss and examine the survey result. The similar components or opinions were combined or discarded. The result of the morphological analysis was reported in our prior studies [7, 8]. Table 1 shows the extracted result of form elements of mobile phones.

Step 3: Evaluating Product Image of Experimental Samples

To evaluate the degree to which the experimental samples match a given product image, subjects of the expert group are involved in the experimental evaluation. This purpose is conducted to grasp the consumer's perception or psychological feeling about a new product using the semantic differentials (SD) method [11]. Pairs of image words (such as simple-complex) are often used to describe the consumer's image of the product in terms of ergonomic and psychological estimation. In this paper, the image word pair used is simple-complex (S-C) and the design elements used are the form elements of mobile phones as identified in Table 1. The 15 subjects used seven scales (1-7) of the SD method to evaluate 33 representative mobile phones for their value of the S-C image, with 1 being the simplest and 7 being the most complex. Table 2 provides a numerical data source for applying the grey system and neural network techniques in this paper.

Step 4: Experimental Analysis of GRA

The GRA model calculates the grey relational degree between each comparison series x_i and the reference series x_0 . In this paper, the comparison series x_i ($i = 1, 2, \dots, 9$) are the product form elements. The reference series x_0 are the values of product images. The procedure of GRA involves the following seven steps: (1) Represent the original data series. (2) Normalize the data series. (3) Calculate $|x_0(k) - x_i(k)|$. (4) Calculate $\max\{|x_0(k) - x_i(k)|\}$ and $\min\{\min|x_0(k) - x_i(k)|\}$. (5) Set the distinguishing coefficient $\xi = 0.5$.

(6) Calculate the grey relational coefficient of the data series by (1). (7) Calculate the grey relational degree of the data series by (2), and obtain the value of $r(x_0, x_i)$, as shown in Fig. 3.

Table 1. Extracted form elements of mobile phones

| Items | Type 1 | Type 2 | Type 3 | Type 4 |
|----------------------------------|-------------------|--|-------------------|-----------|
| 1. Top shape | Line | Curve | Arc | Irregular |
| 2. Body shape | Parallel line | Raised curve | Concave curve | |
| 3. Bottom shape | Line | Curve | Arc | |
| Length and width ratio of body | Wide ratio 2:1 | Middle ratio 2.5:1 | Slender ratio 3:1 | |
| Function buttons style | With large button | Symmetry style | Other style | |
| Number of buttons arrangement | Regular | Irregular | | |
| 7. Screen size | TV ratio 4:3 | Movie ratio 16:9 | Other ratio | |
| Screen mask and function buttons | Independence | Function buttons dependence on screen mask | Interdependence | |
| 9. Outline division style | Normal division | Rim division | Special division | |

The result shows that the “top shape” element (x_1) affects the simple-complex image the most, followed by the “function buttons style” element (x_5) and the “length and width ratio of body” element (x_4). This implies that the designers should focus their attention more on these most influential elements, when the objective of designing a mobile phone is to achieve a desirable simple-complex image. The GRA model can be used to simplify the NN model for helping product designers focus on more influential form elements. In our prior study [7], the result implies that excluding less influential form elements from a NN based model, according to the GRA model, may have no impact on the prediction performance.

Step 5: Experimental Analysis of the NN Model Based on the GRA Model

A typical three-layer network consists of an input layer, an output layer, and one hidden layer. In the NN, the learning algorithm has two processes, including the training process and the test process [10]. We develops the NN model based on the GRA model, called the GRA-NN model to determine the best combination of product form elements for matching a set of desirable product image. The procedure of GRA-NN



Fig. 3. The result of GRA

model involves the following three steps: (1) Building the GRA-NN model. For all input variables, we use the type value of 1 to indicate that the input variable is characterized by the type of the corresponding form element. If the input variable has no type characterization, its type value is set to 0. The evaluation average values of the product image are used as the output neuron, ranging between 1 and 7, as specified in the experimental study. The number of neurons of the hidden layer is dependent on the ideal solution of each model, and varies in each case. (2) Training the GRA-NN model. All experimental samples are used as the training samples. When the root of mean square (RMS) errors is convergent, the training process is completed. (3) Performance evaluation of the GRA-NN model. In order to examine if the GRA-NN model can be applied to new samples, the test samples are used. The new subjects are involved in the test process, using the SD method with a 7-point scale (1-7). We can calculate the model's corresponding RMS errors to compare the performance of the model. The evaluation results suggest that the NN based model should be used to help product designers determine the best combination of mobile phone form elements. In situations where product designers would like to focus on fewer form elements in the design process, the result of GRA model can be used to simplify the NN model, without greatly compromising its performance [7].

Step 6: Tabu Search for the Optimal Combination of Product form Design

In applying tabu search to solving a specific problem, neighborhood structure, tabu list, and search strategy are crucial for improving the performance. The prediction image values of the output neurons of the GRA-NN model are inputted to the TS algorithm as the initial solution. The solution space is all the combinations of design form elements according to the morphological analysis. As a result, a form design database consisting of different combinations of product form elements together with their associated product images can be built. In this approach, a move is the operation of changing the value at a given position to the next possible value, that is, a move change from 1 to 2, 2 to 3, 3 to 4, 4 to 1, and so on. For example, for the initial solution of 1234, the neighborhood of a solution is obtained by applying the move to all the positions: 2234, 1334, 1244, and 1231. A candidate list is the part of the neighborhood that is evaluated to determine the solution for the next iteration. In this approach, the complete neighborhood is included in the candidate list. All the solu-

tions of the candidate list are evaluated and the best solution is the current one. With the aim of choosing good moves, the aspiration criterion requires that the solution is better than the current best solution. The process is terminated if no improvement is achieved for a specified number of iterations or if the number of steps exceeds the maximum.

Table 2. Consumer perception for 33 selected mobile phones

| Phone No | X1 | X2 | X3 | X4 | X5 | X6 | X7 | X8 | X9 | S-C |
|----------|----|----|----|----|----|----|----|----|----|-------|
| 1 | 2 | 2 | 1 | 3 | 2 | 2 | 1 | 2 | 1 | 4.467 |
| 2 | 2 | 3 | 1 | 2 | 3 | 2 | 1 | 2 | 3 | 3.133 |
| 3 | 1 | 3 | 2 | 1 | 2 | 1 | 2 | 3 | 1 | 2.867 |
| 4 | 3 | 3 | 1 | 2 | 2 | 1 | 3 | 1 | 1 | 5.533 |
| 5 | 4 | 1 | 1 | 2 | 3 | 2 | 3 | 1 | 2 | 5.533 |
| 6* | 1 | 2 | 1 | 2 | 2 | 1 | 1 | 3 | 1 | 6.400 |
| 7 | 2 | 2 | 1 | 2 | 2 | 1 | 2 | 2 | 3 | 6.867 |
| 8 | 4 | 1 | 2 | 3 | 2 | 2 | 1 | 2 | 3 | 6.800 |
| 9 | 2 | 2 | 1 | 1 | 1 | 1 | 2 | 1 | 2 | 4.600 |
| 10 | 2 | 3 | 1 | 2 | 2 | 1 | 1 | 1 | 1 | 6.200 |
| 11* | 3 | 2 | 3 | 3 | 2 | 2 | 1 | 1 | 2 | 6.600 |
| 12 | 2 | 1 | 1 | 2 | 2 | 1 | 2 | 3 | 1 | 4.533 |
| 13 | 1 | 2 | 1 | 2 | 1 | 1 | 3 | 3 | 1 | 3.933 |
| 14 | 3 | 2 | 2 | 3 | 1 | 1 | 2 | 3 | 3 | 6.933 |
| 15 | 2 | 2 | 1 | 3 | 1 | 1 | 1 | 3 | 1 | 5.600 |
| 16* | 1 | 1 | 1 | 3 | 1 | 1 | 1 | 1 | 1 | 2.733 |
| 17 | 1 | 1 | 1 | 2 | 3 | 1 | 2 | 2 | 3 | 4.333 |
| 18 | 2 | 2 | 1 | 2 | 1 | 1 | 2 | 3 | 3 | 2.533 |
| 19* | 2 | 3 | 2 | 2 | 1 | 1 | 2 | 1 | 2 | 4.533 |
| 20 | 2 | 2 | 2 | 2 | 1 | 1 | 1 | 2 | 1 | 3.200 |
| 21 | 2 | 2 | 2 | 2 | 2 | 1 | 1 | 2 | 1 | 5.533 |
| 22 | 2 | 2 | 2 | 2 | 3 | 1 | 1 | 1 | 1 | 6.867 |
| 23 | 2 | 2 | 1 | 2 | 2 | 2 | 1 | 2 | 3 | 4.467 |
| 24 | 2 | 2 | 1 | 2 | 2 | 1 | 2 | 2 | 1 | 3.667 |
| 25 | 3 | 3 | 1 | 2 | 1 | 1 | 2 | 2 | 3 | 3.067 |
| 26 | 3 | 3 | 3 | 3 | 2 | 1 | 2 | 3 | 1 | 4.533 |
| 27 | 3 | 2 | 1 | 3 | 2 | 2 | 1 | 2 | 1 | 3.600 |
| 28* | 1 | 2 | 2 | 2 | 1 | 2 | 1 | 2 | 3 | 4.600 |
| 29 | 2 | 2 | 2 | 3 | 1 | 1 | 1 | 1 | 1 | 4.933 |
| 30 | 1 | 3 | 1 | 3 | 1 | 1 | 1 | 1 | 1 | 5.333 |
| 31 | 2 | 3 | 3 | 1 | 1 | 1 | 1 | 3 | 3 | 3.733 |
| 32 | 2 | 3 | 3 | 2 | 1 | 2 | 2 | 3 | 2 | 3.533 |
| 33 | 2 | 1 | 3 | 2 | 2 | 1 | 2 | 2 | 2 | 3.733 |

The TS algorithm can apply for the GRA-NN model to search for the best product form combination in terms of a desired product image. To illustrate the hybrid approach, Table 3 shows the best form combination for a given product image represented by the S-C value of 4. The combination of form elements given in Table 3 has its S-C value being 4.086, which is the closest among all the form combinations.

Table 3. The best combination of product form elements

| X ₁ | X ₂ | X ₃ | X ₄ | X ₅ | X ₆ | X ₇ | X ₈ | X ₉ |
|----------------|----------------|----------------|----------------|----------------|----------------|----------------|----------------|----------------|
| | | | | | | | | |

4 Conclusion

In this paper, we have presented a new hybrid approach, using a grey relational analysis (GRA), neural networks (NNs), and a tabu search (TS) algorithm, for determining the best combination on product form design. The hybrid approach would help the product designers better understand consumers' perception of product form with respect to the corresponding product images. This paper provides useful insights in designing form elements of a product for matching a given product image. Although this paper is focused on product form design, the approach can be applied to other products with various design elements.

References

1. Chuang, M.C., Chang, C.C., Hsu, S.H.: Perceptual Elements Underlying User Preferences Toward Product Form of Mobile Phones. *International Journal of Industrial Ergonomics* **27** (2001) 247-258
2. Cross, M.: *Engineering design methods*. John Wiley, London (1994)
3. Deng, J.L.: Control problems of grey system. *System and Control Letters* **1** (1982) 288-294
4. Glover, F.: Tabu search: Part I. *ORSA Journal on Computing* **1** (1989) 190-206
5. Glover, F.: Tabu search: Part II. *ORSA Journal on Computing* **2** (1990) 4-32
6. Hsiao, S.W., Chen, C.H.: A Semantic and Shape Grammar Based Approach for Product Design. *Design Studies* **18** (1997) 275-296
7. Lai, H.H., Lin, Y.C., Yeh, C.H.: Form Design of Product Image Using Grey Relational Analysis and Neural Network Models. *Computers and Operations Research* **32** (2005) 2689-2711
8. Lin, Y.C., Lai, H.H., Yeh, C.H.: Consumer Oriented Design of Product Forms. *Lecture Notes in Computer Science* **3174** (2004) 898-903
9. Nagamachi, M.: Kansei Engineering As a Powerful Consumer-Oriented Technology for Product Development. *Applied Ergonomics* **33** (2002) 289-294
10. Nelson, M.: *Illingworth WT. A Practical Guide to Neural Nets*. Addison-Wesley, NY 1991
11. Osgood, C.E., Suci, C.J.: *The Measurement of Meaning*. Urbana: University of Illinois Press (1957)
12. Smith, K., Palaniswami, M., Krishnamoorthy, M.: A Hybrid Neural Approach to Combinatorial Optimization. *Computers and Operations Research* **23** (1996) 597-610

Utilizing Active Software to Capture Tacit Knowledge for Strategic Use

Jenny Eriksson Lundström

Department of Information Science, Computer Science Division

Uppsala University, Sweden

jenny.eriksson@dis.uu.se

Abstract. Knowledge on the organization's own work-strategies for carrying out regular tasks are now being recognized as an increasingly more valuable resource. However, due to the complexity of eliciting the distributed, fragmented and partly tacit knowledge inherent in best practice and "know-how", tools to handle this need seem systematically unaccounted for. This paper outlines an approach on extracting this knowledge by utilizing an augmented active software framework. Our focus in this paper is how this approach provides a beneficiary way of employing the knowledge generated by active software during a session. We illustrate the relevance of this approach by a sample scenario extending a real-world example taken from the software engineering domain.

Topic: Knowledge Representation and Management, Intelligent Agents

Keywords: Intelligent Agents, Active Software, Knowledge Management, Knowledge Elicitation Methodology, Tacit Knowledge

1 Introduction

In the knowledge-centered organization's of today, improving the overall achievement by learning from co-workers' experiences on efficient and successful ways of performance *i.e. best-practices*, constitute a strategic process for facilitating higher performance and streamlined work-flows [2, 7]. Moreover, operational structure transparency secure key knowledge within the organization and facilitate the realization of strategic goals. As a result, eliciting and strategically transferring internal best-practices throughout the organization could be a source of competitive advantage [11].

1.1 Transferring Tacit Knowledge

A large part of the desired knowledge is distributed and consists of the "know-how" of several actors within and external to the organization. This experience-based or *tacit knowledge* is highly contextual and bound to firm processes experienced by the individual [5]. The nature and origin of tacit knowledge makes it less conducive to formalization and thus, transferring "know-how" is traditionally conducted on a human-to-human basis where experienced colleagues serve

as mentors (*e.g.* in medical training). So, how could one elicit this experience in a more systematic way, capture it in a system and render it operational for strategic evaluation?

1.2 Digital Advisors – A Feasible Solution

In the beginning of the 80s, digital advisors in the form of critiquing expert systems evolved as the solution to computerized mentors (*e.g.* the ATTENDING-family by Miller [8], Langlotz and Shortliffe's ONCOCIN [6], Fischer's JANUS [3], for an extensive survey see *e.g.* Silverman [12]). Providing expert assistance to the user, the expert critiquing system made the advice or critique the central aspect of its functionality. The aim was to provide explanations from the user's own perspective and in some implementations, to help the user to refine his/her own solution to the level of an expert. At the time, in most cases these systems failed to meet the demands placed on industry-viable products [1, 4].

Today, the situation is changing. The complexity of technology solutions drives the complexity of the organization's processes [1] and intelligent user interface approaches like tutors, coaches, wizards and user interface agents have been developed to meet these needs (for a comparative study see *e.g.* Robbins [10]). In addition, increasingly more reliant on individual "know-how" and performance, organizations recognize the need for improving terms of process, quality and common terminology by adopting a consistent way to work across the organization [13].

In this paper we address the problem of capturing best-practice and "know-how" of organizations by presenting an augmented active software-framework. The paper is organized as follows: Section 2 provides a background on the use of active software as an advisor, explaining its usefulness in relation to our concept. In Section 3, the augmented active software-framework and its contributions in reaching our objective are presented. Section 4 elaborates on a real-world software engineering project in a leading financial service-provider. We show how active software supports the user in his/her task and extends this scenario to an illustration on the gain of using the augmented active software framework in capturing tacit knowledge for strategic use. Finally, in Section 5 the paper is concluded.

2 Active Software

Providing its user with qualified assistance in accomplishing a given task, active software implemented as a multi-agent system offers a competitive approach on digital assistance [4]. Consisting of several independent agents, working together but still accomplishing their own task according to the design objectives, each agent is able to perceive and adapt to its environment with a proactive, *i.e. goal-oriented*, behavior [14]. Automatically, the system is able to see what knowledge is necessary to model, and where and how it best could be provided.

As its primary aim, the active software in the role of advisor captures actions and knowledge of a user, reasons on this knowledge and automates the

application of this knowledge to the user’s task [4]. In addition, the organization’s strategic objectives, *e.g.* enforcing standards and training the employees, could be facilitated using active software. As an example, by employing the use of active software in a software development process, the management could streamline processes and secure the quality of the artifacts produced.

Considering that best-practice and “know-how” constitute valuable competence to realize organizational goals, the incorporation of this knowledge in active software seem desirable. Achieving this improvement however, implies that such capability could be captured and transferred. As previously stated, humans have a problem of making explicit their mental models and of providing a comprehensive presentation of the sub-processes from which they compose their routine-work [9]. Thus, in order to make the tacit knowledge of best-practices and “know-how” available through active software, the inverse transfer of knowledge, from the user to the system must be accomplished.

3 Transferring Tacit Knowledge by Augmented Active Software

The multi-agent architecture of active software is augmented by the introduction of a second intelligent agent-layer. The meta-layer introduced acts and evaluates the users’ actions and the critique generated by the underlying active software. While emphasizing the organization’s perspective, the data extracted is thought to be suitable for strategic analysis, since it holds the extension of the user’s mental model for addressing and acting on a real task performed in an actual work situation.

3.1 An Augmented Active Software Framework and Its Interrelations

Here we present an integrated approach using a flexible knowledge base. However, as an alternative, the active software could be an embedded part of a knowledge-based system. In either case, both the meta-layer and the active software are required to be a fully integrated part of the supported environment. In addition, the active software must provide the functionality of a digital advisor, or at least an analytical critic which could provide critique on a restricted part of the underlying system or task at hand.

The architecture is comprised by the following parts:

user interface The user interaction is conducted through the artifact development environment. This enables “learning by doing” in a realistic setting.

meta-layer The meta-layer consists of a multi-agent system utilizing the knowledge and critique of the active software as well as the user actions while reasoning. The evaluation is conducted with a differentiated view and for several levels of granularity. Thus, the meta-layer must be configurable to adapt to the organization’s goals.

active software The active software tool captures, reasons and automatizes the application of the captured knowledge to the artifact produced [4]. Since the active software generates qualitative information on the users actions, the environment and needed knowledge for comparison, this information is utilized by the meta-layer in detecting valuable data.

artifact development environment The layer holding all development tools, such as management applications, languages, development models and databases.

artifact The artifact being produced.

3.2 The Meta-layer Design

The overall goal of the meta-layer is to provide transparency to the organizations own processes, “know-how” and best-practices; and to serve as a tool for extracting tacit knowledge for strategic use. The meta-layer is modelled as a deliberative multi-agent system integrated on top of the active software layer. The symbolic representation of deliberative agents allows for the design of intelligent behavior needed to reason on the outcome of the underlying active software layer. Incorporating a proactive feature, the latter knowledge on possible errors are augmented by the knowledge available from the different agents in the active software.

For a given agent of the meta-layer, a set *services* of rules express the abilities of the agent, while the representation of the agent’s goals, memory and abilities are defined by the set *self*. Moreover, the conceptual model holds a representation of agent’s and domain ontologies *onto* and the control module. The ontologies are utilized for interpretation of incoming messages according to the communication protocol. The component *environment* holds the representation of the knowledge of all underlying layers of the architecture as well as the other agents. In addition, the component *objectives* holds additional information on the domain-specific features desirable according to the predefined goal, as well as knowledge on counter-productive patterns and their interrelations, extending the error model component of the underlying active software layer.

4 Active Software Supporting Software Implementation – An Illustration

The field of software implementation is illustrative in exploring the benefits of the augmented active software presented since the success of the organization in a given project highly relies on the individual software developer’s “know-how”. Moreover, normally the extraction of best-practices in this field becomes complex due to its highly dynamic and agile nature.

When implementing Rational Unified Process (RUP), one of the largest financial service providers in Scandinavia, here referred to as A-bank, utilized an agent-based active software placed on top of IBM’s RUP and Rational Rose XDE

Developer [4]. The idea was to provide the software developers with dynamic assistance and suggestions from the perspective of the actual project and their own work-processes. As an instrument for evaluating its 840-head IT department a Balanced Score Card was used. The criteria include efficiency, quality, economics, human resources and partnership with the business units [13].

4.1 An Active Software Scenario

The following scenario is based on Jacobson and Bylund [4]:

A software developer participates in a session with the active software tool. In creating a Use Case Model for a given artifact, the developer interacts with the unobtrusive active software tool, receiving feedback through suggestions, explanations, iteratively refining the Use Case Model until the developer's goals are reached.

During the session the meta-level registers the software developer's actions as well as the interaction with the underlying active software. The software developer's actions, chosen process structures, common errors as well as unusual solutions for finalizing the Use Case Model are registered by the meta-level for further processing. The registration phase is followed by an analysis phase where the software developer's reoccurring errors, linked actions, received feedback and altered performance is analyzed based on the utilization of the error model of the underlying active software and an additional knowledge base holding data on organization-specific objectives.

Now, the data emanating from the analysis performed on the individual software developer's session are analyzed against earlier collected data in a similar way as in the primary analysis phase. The purpose of this second analysis is to enable comparison of the work-processes of several software developers. The augmented active software thus provide data for analysis of different levels of the organization's work processes. In our sample scenario it enables a view on Use Case Model creation processes, which is lifted from the project context, while still emanating from the actions performed by the software developer according to their idea of addressing the task. Thus, the individual software developer's actual actions based on his/her mental model of the situation are captured as the basis for strategic analysis. Whereas the information can be utilized for trimming the active software in an educational sense as well as for organizational management, the resulting actions are based on the actual way the organization's own software developers are working and not on an idea of how the work is conducted.

4.2 How Could A-Bank Benefit from an Augmented Active Software?

By analyzing the active software generated critique and context in the augmented framework, reasoned opinions of ways of working are captured for a given A-bank artifact. From a strategic perspective, A-bank's own interesting work-patterns, how best-practices differ from less competitive used for the strategic analyzes. By

utilizing the team-members' own work-processes visible in the organization's own projects as examples, this knowledge could serve as a basis for change management and to realize strategic goals according to A-bank's Balanced Score Card discussed in the introduction of Section 4. The captured knowledge serves as a technical driver for collaboration and communication, and thus, A-bank could use the extracted knowledge for *enhancing partnership*. By providing a possibility for the individual employee to improve and evaluate the own work strategies from the organizational benefit, the employee could enhance his or her competence and identify the own significance for the large organization. Thus, *human resources are more efficiently and sociable utilized*. In addition, by enhancing the overall performance by the enforcement of best-practices, the quality of the work could improve. This also affects the users own work strategies and releases the employee from routine work and frustrating problems due to counter-productive work-processes. Streamlining of processes will of course *cut costs* and *increase efficiency*. Moreover, by enhancing the overall performance by best-practice the *quality of the work will improve*. Using the own knowledge strategically, helps A-bank to realize strategic goals as formulated in the Balanced Score Card.

5 Conclusion

We have proposed an approach addressing the need of organizations to capture and visualize tacit knowledge for strategic use. A meta-agent structure for capturing and reflecting on procedural and tacit knowledge augments an active software framework. By enriching the active software with the perspective of the organization, the framework provides a beneficiary way of utilizing the knowledge which is generated for a given user and collected by the active software during a session. Humans are not good at explaining their mental processes and thus, the main advantage of this approach is that it facilitates the elicitation of tacit knowledge as a help to realize organizational goals. The captured tacit knowledge could be utilized to customize and train the active software structures, but more importantly, provide the corporation with important information on how to accomplish its strategic goals.

6 Perspectives

Enhanced overall competence is the enabler of higher productivity, lower costs and higher quality [4]. Employing software-solutions as facilitators of knowledge transfer when enriching business solutions with user best-practices, will provide benefits to the organization. By allowing these best practices to turn into strategic information for evaluating the organizational needs, a comprehensive and competitive view on the strategic ways of reaching these objectives is provided.

However, it is important to recognize that the extracted data only could be used for evaluating and creating strategic knowledge – it is not strategic knowledge *a priori*. Moreover, it could not make employees superfluous. It merely

serves as an enabler of creativity and to improve the overall performance [1]. Conclusively, by being aware and by using the knowledge of how the best-practices of the organization's own processes actually are composed and executed, development of the artifacts will be fast and comparatively low-cost. Minimizing frustrating work and maximizing employee satisfaction enable competitive advantage. In this way active software provides transparency for discovering the organizations own way of doing business. It becomes a way of exploiting the organization's own intelligence, for strategic use.

References

1. A. Bowles: Active Software Tools for Application Development - Maximizing the Potential, *Robert Frances Group, IT Agenda, Business Advisors to IT Executives*, October 2003.
2. G. T. Ferguson and S. J. Taylor: Innovation: Bold New World, *Outlook Special Edition*, May 2004.
3. G. Fischer, A. C. Lemke and T. Mastaglio: Using Critics to Empower Users, *Proceedings of the Conference on Human Factors in Computing Systems (CHI'90)*, 1990.
4. I. Jacobson and S. Bylund: *A Multi-Agent System Assisting Software Developers*, Jaczone.
5. C. Jimes and L. Lucardie: Reconsidering the Tacit-explicit Distinction - A move toward Functional (Tacit) Knowledge Management, *Electronic Journal of Knowledge Management*, Volume 1, Issue 1, pp 23-32, 2003.
6. C. Langlotz and E. Shortliffe: Adapting a Consultation System to Critique User Plans, *International Journal of Man-Machine studies*, Vol 19, pp. 479-496, 1983.
7. B. Liautaud and M. Hammond: *E-Business Intelligence: Turning Information into Knowledge into Profit*, Mc Graw-Hill, New York, pp.6-10, 2000.
8. P. Miller: *A Critiquing Approach to Expert Computer Advice: ATTENDING*, Pitman Publishing Ltd, London, England, 1984.
9. I. Nonaka and H. Takeuchi: *The Knowledge Creating Company*, Oxford University Press, Oxford, 1995.
10. J.E.Robbins: *Design Critiquing Systems* Tech Report UCI-98-41, University of California, Irvine, 1998.
11. G. P. Shaw and D. Y. Smith: Don't let Knowledge and Experience Fly Away: Leveraging Scarce Expertise to Support Ongoing Competitiveness in the Aerospace and Defense Industry *Accenture, Electronics & High Tech IT Research and Insights*, 2004.
12. B. G. Silverman: Survey of expert critiquing systems: practical and theoretical frontiers, *Communications of the ACM*, v.35 n.4, p.106-127, April 1992.
13. Swedbank implements RUP with Jaczone WayPointer, *Jaczone*, 2004.
14. M. Wooldridge and N. Jennings: Agents Theories, Architectures and Languages: A Survey, *Lecture Notes in Artificial Intelligence*, Springer-Verlag, 1995.

A Bandwidth Efficiency of Lempel-Ziv Scheme for Data Authentication

Chin-Chen Chang^{1,2}, Tzu-Chuen Lu², and Jun-Bin Yeh

¹ Feng Chia University, Taichung, Taiwan, 40724, R.O.C.

ccc@cs.ccu.edu.tw

<http://www.cs.ccu.edu.tw/~ccc>

² National Chung Cheng University, Chiayi, Taiwan, 621, R.O.C.

Abstract. This paper extends the bandwidth of Lempel-Ziv-Welch (LZW) and Lempel Ziv Fiala Greene (LZFG) compression schemes to hide information in the compressed codes for compressed data authentication. The proposed schemes are designed for two objectives; one is to compress a text file; the other is to hide secret information to warrant its authenticity. According to the results of experiment, the proposed scheme could easily and efficiently reach the objective of hiding secret information and only with negligible degradation in compression performance. In addition, the proposed scheme can be even used to hide secret information in medical images without distorting the image quality.

1 Introduction

The growing development of the Internet helps us to conveniently share and transmit digital medium, such as digital image, video, and text, on the Internet. However, the convenience also brings some problems like illegal copying, tampering, or non-authenticated invasion that we would need an appropriate mechanism, such as cryptography or watermarking, to protect intellectual property rights and copyright or to ensure the completeness of the data [4, 10, 11]. Watermarking technique has been widely used on images, videos, and audios, but not on text files or medical images. Although watermarking has been a common method to modify the content of the medium by hiding watermark in medium, there are still some exceptions that a text files or medical image could not be done in the same way. Hence, a proper mechanism based on characteristics of text file to ensure the integrity of the file is needed [5, 6, 8, 15]. In addition, in order to handle rapid growth of data and solve bottleneck of Internet efficiency, engineers and computer scientists usually use the techniques of data compression to filter redundant data before transmitting them on Internet. The hidden information in the compressed file might also be filtered after compressed processing [7, 9]. Lempel-Ziv (LZ) coding is one of the famous lossless compression methods among those [2, 18]. In terms of the text-compressed process of LZ, we notice that some compressed codes can be wisely used to hide information. Therefore, in this paper, we shall propose a scheme of authentication which hides information on host files in LZ compressed form for integrity protection and ownership

verification. The proposed scheme will not modify the contents of the host file. The rest of this paper is organized as follows: In Section 2, some related works would be reviewed. Then, in Section 3 and Section 4, our new schemes will be presented in detail. After that, Section 5 shows the experimental results to demonstrate our new schemes. Finally, conclusions are drawn in Section 6.

2 Related Works

The methods of lossless text compression can be roughly classified into two categories (1) statistical-based methods, such as Huffman coding, arithmetic coding, and (2) dictionary-based methods, such as Lempel-Ziv coding. Lempel-Ziv coding [17], called LZ-77, was proposed by Abraham Lempel and Jakob Ziv in 1977 on the purpose of compressing text files. It is assumed that $T = \{T_1, T_2, \dots, T_t\}$ is a text file over an alphabet Σ , and T_i is the i -th symbol in T ; the length of T is t and $T_{i,\ell} = \{T_i, T_{i+1}, \dots, T_{i+\ell-1}\}$ is the pattern of size ℓ from T_i to $T_{i+\ell-1}$ in T , where $1 \leq i \leq t$. Let $T_{i,\ell}$ is the current processing pattern. Assume the first $i-1$ symbols of T have been compressed. The compressed string is formed as $Z = (P_0, L_0, C_0), (P_1, L_1, C_1), \dots, (P_{i-1}, L_{i-1}, C_{i-1})$, where $(P_k, L_k, C_{k+L_\ell}) = \max\{(p_0, \ell_0, T_{k+\ell_0}), (p_1, \ell_1, T_{k+\ell_1}), \dots, (p_j, \ell_j, T_{k+\ell_j})\} \in (I, I, \Sigma)^t$; $\{(p_0, \ell_0, T_{k+\ell_0}), (p_1, \ell_1, T_{k+\ell_1}), \dots, (p_j, \ell_j, T_{k+\ell_j})\}$ is the set of candidate matches; (P_k, L_k, C_{k+L_ℓ}) is one of the candidate matches with the longest L_k ; P_k represents a match to the current processing pattern at an offset of P_k the length of the match is L_k ; and C_k is following character $T_{k+\ell}$ of the processing pattern at the $(i + \ell)$ -th position of T .

In order to enhance the efficiency of LZ-77, Atallah and Lonardi have developed an improved version LZ-78 algorithm in 1978 [18]. In LZ-78, a dictionary was created to record the previously encoded patterns. The compressed code in LZ-78 is formed as a pair of an index and a symbol. The index is corresponding to the dictionary entry, which was the longest match to the processing pattern. The symbol is the following character of the processing pattern. If there is no match found in front of the string, then the new pair is appended into the dictionary. Many variants have been proposed, such as LZR, LZSS, LZB, LZH, LZFG, LZW, LZC, LZT, LZMS, and LZJ, to enhance the efficiency of the LZ-77 and LZ-78 algorithms [12, 13, 16]. The most well-known improved algorithm of LZ-78 family is Lempel-Ziv-Welch (LZW) proposed by Terry Welch in 1984 [16]. LZW has been generally used by a number of formats, including GIF, TIFF, PostScript, PDF, Unix Compress, and V.42bis. Another hybrid variant Lempel Ziv Fiala Greene (LZFG) was proposed by Fiala and Greene in 1989 that combines the ideas of LZ-77 and LZ-78 [10]. The LZFG algorithm uses the dictionary building technique from the original LZ-78, but stores the data in a modified tree of data structure, and the standard of sliding window, which used in LZ-77, is used to remove the oldest entries from the dictionary. It usually runs faster than other improved algorithms.

In order to ensure the authenticity of the text file in the compressed form, Atallah and Lonardi proposed an authentication scheme, Lzs-77, which hides

secret message within the LZ-77 compressed document [1, 2]. The scheme is based on the unpredictability of a certain class of pseudo-random generator [3]. In Lzs-77 authentication scheme, when a sender wants to send a text file T to a receiver, she/he has to embed a secret message (M) in the compressed codes of T in order to ensure that the received text file is authentic and integral. The text file after hidden M is called stego file. If the extracted message from the stego file is the same as M , then the receiver could make sure that the received file is integral. Instead of selecting the match, which has the longest L_k among the candidate matches, the Lzs-77 algorithm selects the more proper match according to M . It is assumed that the current processing pattern is $T_{i,\ell}$. First, they search the longest match (P_k, L_k, C_{k+L}) and look further back to check whether there is any other match which is the same as (P_k, L_k, C_{k+L}) . Second, they permute the order of matches in the longest matches of $T_{i,\ell}$ by using BBS [3]. Third, they build a complete binary tree to store the matches in the reorder set. In the binary tree, each leaf node represents a match of the reorder set, and has a unique code identified by the path from the root to the node. Finally, they use the bits of M to choose one of the leaf nodes to encode $T_{i,\ell}$. They travel the binary tree by using the longest pattern of M that ends up in a node marked with $T_{i,\ell}$. Although the Lzs-77 algorithm would not have an influence on LZ-77's internal structure, however, it still has several disadvantages that the Lzs-77 algorithm based on LZ-77 algorithm, which uses a triple to represent a compressed code, is inefficient, especially in the condition that the characters of the text file occur infrequently. In addition, the hiding capacity of the Lzs-77 algorithm is limited by the content of the text file. Since the secret messages only could be hidden in the compressed codes of the processing pattern, the number of matches is more than 1, where $q > 1$. Hence, they usually need to append some more irrelevant data to T for hiding secret message that, somehow, will decrease the compression rate. In order to solve the disadvantages of the Lzs-77 algorithm, this paper is going to propose two schemes of hiding information that embeds secret message in the compressed codes of LZW and LZFG algorithms for authenticating the compressed data. The hiding scheme based on LZW algorithm is called LZWS-05, and the scheme based on LZFG is called LZFGS-05.

3 The LZWS-05 Algorithm

LZW scheme uses a dictionary to record the occurred pattern. In this way, the dictionary has to be primed with all the characters of Σ . The processing characters would be accumulated as a pattern $T_{i,\ell}$ as long as it is contained in the dictionary. If the addition of another character γ , which is not in the dictionary, results in a pattern $T_{i,\ell+1} = T_{i,\ell} + \gamma$, the compressed code of $T_{i,\ell}$ would be the corresponding index of $T_{i,\ell}$ in the dictionary. Then, the pattern $T_{i,\ell+1}$ is appended to the dictionary, and we start to accumulate another pattern with the start character γ . This subsection modifies the LZW algorithm to be able to embed a secret message. An LZWS-05 encoder is used to encode the transmitted text file and embed secret message, and an LZWS-05 decoder is used to

decode the text file and extract the hidden message. We assume that a sender wants to transmit a text file $T = \{T_0, T_1, \dots, T_t\}$ integrally and authentically to a receiver. They need to ensure that T cannot be forged or reused. Hence, the sender hides a ciphertext or watermark $M = \{M_0, M_1, \dots, M_n\}$ on the compressed codes of T . In order to keep M secretly, both the sender and the receiver have to have a secret key K to hide and extract the secret message. The secret key K should be sent on a secure channel. We generate a pseudo-random sequence $f(K) = (k_1 k_2 \dots k_n)$ in binary format by using a pseudo-random number generator (PRNG) seeded with K . If the currently processing message bit M_j is equal to k_j , the currently processing pattern $T_{i,\ell+1} = T_{i,\ell} + \gamma$ would be normally encoded by its corresponding index in the dictionary. Otherwise, we would have to encode the last pattern $T_{i,\ell-1}$ with its corresponding index in the dictionary, and start to accumulate another pattern with the initial character γ . The embedding rules of LZWS-05 are shown as below:

- The secret message would only be hidden while $Idx(T_{i,\ell}) \geq |\Sigma|$, where function Idx returns the corresponding index of $T_{i,\ell}$ in the dictionary, and $|\Sigma|$ the number of alphabets in Σ .
- If $k_j = M_j$, then $T_{i,\ell}$ is normally encoded by using LZW algorithm.
- If $k_j \neq M_j$, then encodes $T_{i,\ell-1}$ by $Idx(T_{i,\ell-1})$.

When the receiver receives the compressed codes, he/she uses the LZWS-05 decoder to decode the original text and extract the hidden message. The LZWS-05 encoder would not affect the resultant compression in LZW. In other words, the decompressed text contents of the LZWS-05 are the same as that of the LZW. Hence, the compressed codes generated by LZWS-05 encoder also could be decoded by the standard LZW decoder. If the hidden message needs to be extracted from the compressed codes, we only need to check whether the pattern has existed in the dictionary or not. If the pattern exists in the dictionary, then the secret bit is 1. Otherwise, the secret bit is 0.

4 The LZFGS-05 Algorithm

In LZFG, an input pattern could be classified into one of two categories: Literal or Copy. The pattern which is classified to Literal category means that LZFG is not able to discover any match in the previously encoded sequence in a slide window, or the match is not long enough. The compressed code of the pattern classified to Literal category is represented as a pair ('0000', $|T_{i,\ell}|$) following with the pattern which is represented in the binary format. Here '0000' in the pair indicates that the pattern is Literal, and $|T_{i,\ell}|$ is the length of the pattern. LZFG uses eight bits to encode the pair and each character in the pattern. The pattern classified to Copy category means that LZFG is able to discover a match in the previously encoded sequence which is long enough to be matched. The compressed code of the pattern classified to Copy category is represented as a pair ($|T_{i,\ell}|, \delta$). LZFG uses sixteen bits to encode the pattern. First four bits are used to indicate $|T_{i,\ell}|$, and the following twelve bits are used to indicate the

displacement δ , which is the distance between $|T_{i,\ell}|$ and the longest match. One principle to determine whether the match is long enough is to engage with the length of the match. If $|T_{i,\ell}| \geq 2$, we could assume that the match is long enough and the pattern would be classified into Copy category. Otherwise, it is classified into Literal category.

We shall modify LZFG to be able to embed a secret message. The proposed scheme is called LZFGS-05. An LZFGS-05 encoder is used to encode the transmitted T and embed M , and an LZFGS-05 decoder is used to decode the text file and extract the hidden message. It is assumed that the first i characters has been encoded, and the current processed pattern is $T_{i,\ell} = T_{i,\ell-1} + \gamma$, which is used to hide information. The LZFGS-05 embedding rules are shown as below:

- The secret message is able to be hidden while $|T_{i,\ell}| \geq 2$ for Literal category, or $|T_{i,\ell}| \geq 4$ for Copy category.
- If $k_j = M_j$, then $T_{i,\ell}$ is normally encoded by using LZFG algorithm.
- If $k_j \neq M_j$, then encodes $T_{i,\ell-1}$ by using LZFG algorithm.

When the receiver receives the compressed codes, he/she could use either standard LZFG decoder to decode original text or the LZFGS-05 decoder to decode original text and extract hidden message. The main idea for extracting hidden message is to check if the first byte of the currently decoded pattern could be encoded in the previous pattern or not. If the decoded pattern could be encoded in the previous pattern, then the secret bit is 1. Otherwise, the secret bit is 0.

5 Experiments

Two systems which compress and hide data based on LZWS-05 and LZFGS-05 were developed on an AMD 1.4 GHz personal computer with 512 Ram, and tested on the uncompressed text files. Several standard text files were used to compress and hide in evaluating the performance of the proposed systems. The standard is the Calgary Corpus that developed in 1997, provided a set of 14 files, bib, book1, book2, news, paper1, paper2, paper3, paper4, paper5, paper6, progc, progl, progp and trans, with various characteristics [14]. Table 1 shows the hiding capacities of the LZWS-05 system, the LZFGS-05 system, and the LZS-77 system. The column labeled as "File Size" is the size of the text file in bytes. In the LZWS-05 system, the table sizes were 1024, 2048, and 4096. In Table 1, the greater the table size is, the less the number of bytes could hide. Table size of LZW is one factor about the number of patterns. The greater table size will cause the longer match pattern and less number of patterns, but it also needs more bits for a single pattern. It should be aware that our scheme needs more number of patterns to hide more secret message, so it would be a trade-off with the size of table and the number of hidden bits. For some special cases, like geo, obj1, obj2, they don't really follow the result that because the pattern in the file is independent and the number of indices is increased, so we could not easily find longer match pattern. Although it could not work well for the ratio of compression, but it is good for hiding secrete message. According to

Table 1. The hiding capacity of various schemes

| File Name | File Size | LZWS-05 | | | LZFGS-05 | | LZS-77 |
|-----------|-----------|---------|--------|--------|----------|--------|--------|
| | | 1024 | 2048 | 4096 | | | |
| bib | 111,261 | 6,510 | 5,709 | 5,056 | 1,503 | 1,721 | |
| book1 | 768,771 | 45,818 | 41,669 | 36,931 | 12,500 | 14,524 | |
| book2 | 610,856 | 34,225 | 31,843 | 28,890 | 9,272 | 10,361 | |
| geo | 102,400 | 3,893 | 3,926 | 4,866 | 684 | 4,101 | |
| news | 377,109 | 21,104 | 21,061 | 19,627 | 5,064 | 5,956 | |
| obj1 | 21,504 | 564 | 581 | 643 | 291 | 353 | |
| obj2 | 246,814 | 2,838 | 3,119 | 6,018 | 3,359 | 3,628 | |
| paper1 | 53,161 | 2,771 | 2,554 | 2,480 | 810 | 937 | |
| paper2 | 82,199 | 4,943 | 4,261 | 3,795 | 1,297 | 1,551 | |
| paper3 | 46,526 | 2,731 | 2,493 | 2,241 | 722 | 893 | |
| paper4 | 13,286 | 759 | 676 | 666 | 204 | 249 | |
| paper5 | 11,954 | 679 | 608 | 605 | 184 | 210 | |
| paper6 | 38,105 | 2,078 | 1,818 | 1,771 | 579 | 738 | |
| pic | 513,216 | 5,945 | 5,982 | 5,744 | 4,813 | 3,025 | |
| progC | 39,611 | 1,907 | 2,017 | 1,987 | 591 | 736 | |
| progI | 71,646 | 3,748 | 3,365 | 2,951 | 897 | 1,106 | |
| progP | 49,379 | 2,288 | 2,134 | 1,972 | 624 | 741 | |
| trans | 93,695 | 4,469 | 4,789 | 4,353 | 1,143 | 1,201 | |

the experimental results shown in Table 1, LZWS-05 could hide more information than LZS-77, but the compression performance of LZWS-05 is smaller than that of LZS-77. It could be applied on the situation while the announcements of some special organization have to be passed through public channel. Fig. 1 shows the comparisons of hiding capacity among LZWS-05, LZFGS-05 and LZS-77. Hence, LZWS-05 outperforms than LZFGS-05 and LZS-77. Fig. 2 shows the hide ratio comparison between LZWS-05 and LZFGS-05. The ratio is computed by $\frac{HP}{HP+NP}$, where HP is the number of patterns, which we hide the information into its compressed codes, and NP is the number of patterns, which we are not able to hide the information into its compression codes. According to the experimental results we can summarize that the hiding capacity of LZWS-05 is higher than those of LZFGS-05 and LZS-77. However, the compression performance of LZFGS-05 is better than that of LZWS-05.

6 Conclusions

This paper proposes two lossless information-hiding schemes LZWS-05 and LZFGS-05, which are based on LZW and LZFG, respectively. LZWS-05 provides larger hiding capacities and allows complete recovery of the original host signal and hidden information. The hidden capacity of LZFGS-05 is less than LZWS-05, but the ratio of compression is higher than LZWS-05 and LZS-77. The average time of the LZWS-05 and LZFGS-05 systems to compress a character

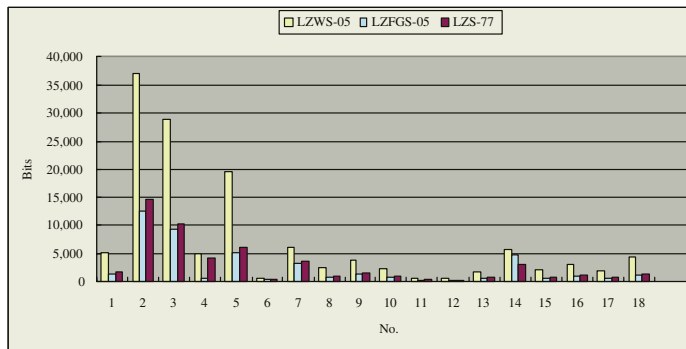


Fig. 1. The comparisons of hiding capacity among LZWS-05, LZFGS-05 and LZS-77

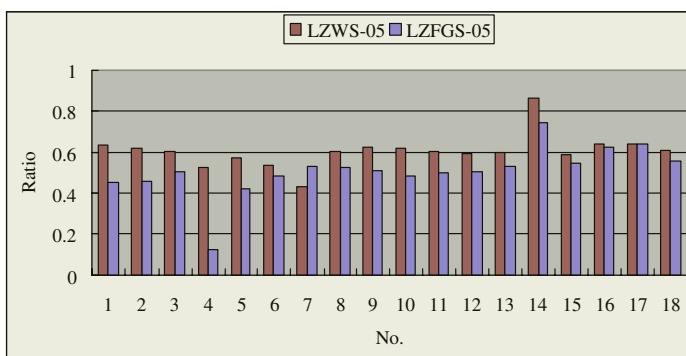


Fig. 2. The comparison of the hide ratio between the LZFGS-05 and LZWS-05

is 5.1337 microseconds, which represents that the average number of processed characters is 190K in one second. From the experimental results, it is obvious to observe that LZWS-05 and LZFGS-05 is indeed an efficient and effective scheme for compressing host signal and hiding secret information.

References

1. Atallah, J.: Handbook on Algorithms and Theory of Computation. CRC Press, Florida (1998)
2. Atallah, M. J. and Lonardi, S.: Authentication of LZ-77 Compressed Data. Proceedings of the ACM Symposium on Applied Computing. (2003) 282–287
3. Blum, L, Blum, M. and Shub, M.: A Simple Unpredictable Pseudo-random Number Generator. SIAM Journal on Computing. **15** (1986) 364–383
4. Chang, C. C. and Chan, C. S.: A Watermarking Scheme Based on Principal Component Analysis Technique. Informatica. **14** (2003) 431–444
5. Huang, D. and Yan, H.: Interword Distance Changes Represented by Sine Waves for Watermarking Text Images. IEEE Transactions on Circuits and Systems for Video Technology. **11** (2001) 1237–1245

6. Hwang, M. S., Chang, C. C. and Hwang, K. F.: Digital Watermarking of Images Using Neural Networks. *Journal of Electronic Imaging.* **9** (2000) 548–555
7. Johnson, N. F., Duric, Z. and Jajodia, S.: *Information Hiding: Steganography and Watermarking – Attacks and Countermeasures*, Kluwer Academic Publishers. Boston. Massachusetts (2001)
8. Katzenbeisser, S. and Petitcolas, A. P.: *Information Hiding Techniques for Steganography and Digital Watermarking*. Boston. Artech House (2000)
9. Low, S. H., Maxemchuk, N. F. and Lapone, A. M.: Document Identification for Copyright Protection Using Centroid Detection. *IEEE Transactions on Communications.* **46** (1998) 372–383
10. Lu, C. S. and Liao, H. M.: Structural Digital Signature for Image Authentication: an Incidental Distortion Resistant Scheme. *IEEE Transactions on Multimedia.* **5** (2003) 161–173
11. Mukherjee, D. P., Maitra, S. and Acton, S. T.: Spatial Domain Digital Watermarking of Multimedia Objects for Buyer Authentication, *IEEE Transactions on Multimedia.* **6** (2004) 1–15
12. Sayood, K.: *Introduction to Data Compression*. Academic Press, Morgan Kaufmann Publishers. SanDiego. CA (2000)
13. Sedgewick, R.: *Algorithms*. 2nd ed. Addison-Wesley Publishing Company (1988)
14. The test files courtesy of T. Bell and M. Powell may be found at <http://corpus.canterbury.ac.nz/index.html>
15. Welch, T. A.: A Technique for High Performance Data Compression. *IEEE Transactions on Computers.* **17** (1984) 8–19
16. Ziv, J. and Lempel, A.: A Universal Algorithm for Sequential Data Compression. *IEEE Transactions on Information Theory.* **23** (1997) 337–342
17. Ziv, J. and Lempel, A.: Compression of Individual Sequences via Variable-Rate Coding. *IEEE Transactions on Information Theory.* **24** (1978) 530–536

Research on Confidential Level Extended BLP Model*

Xin Liu^{1,2}, Zhen Han¹, Ke-jun Sheng^{1,2}, and Chang-xiang Shen^{1,3}

¹ Research Center of Information Security Architecture,

Beijing Jiaotong University, Beijing, China

j fz97@sohu.com, zhan@center.njtu.edu.cn

² Department 4, Naval University of Engineering, Wuhan, China

³ The Naval Compute Technology Institute, Beijing, China

Abstract. The rule of “No-Down-Write” of BLP model restrict its applying in application system because “Down-Write” is often necessary in real life. A new access control model based on Confidential level extended BLP model was researched because of the conflicts. A range of Confidential level is given to the subjects and a confidential rule set is established to endow the subject with the capability of writing down in a bound when it satisfied the confidential rules. The model enforces MAC. The definitions, security check rules, axioms of the model are illustrated in the paper. The model was applied in a multilevel secure DBMS development. The implementation is introduced in short at last.

1 Introduction

Mandatory Access Control is a control policy to protect the multilevel sensitive information resources from the illegal access or modification. It is based on BLP model [1]. There are four components in the model: subjects (active entities such as users, processes), objects (passive entities such as files, data), access mode (read only, append, write, execute) and security. System defines some sensitivity levels in a partial order. For an example, the levels are Unclassified, Confidential, Secret and Top Secret in an order $U < C < S < TS$. The security level of a subject reflects the authorization of the subject to the information. The maximum level is its security clearance. The security level of an object is its security class that reflects the protection requirement to that object. The access properties are summarized as “No-Up-read” and “No-Down-Write” rules.

This paper presents a formal security model for MAC and applied it in a MLS DBMS development. The organization of the paper is as follows: Chapter 1 summarizes some of the current secure models and their deficiencies, then gives the ideas of the new model. The formal definitions and rules of the model are described in chapter 2 followed by the applying of the model in a MLS DBMS development. The advantages of the new model and the directions of the next work are introduced in chapter 3.

1.1 Some Current Security Models

The most popular multilevel secure model at present is BLP model whose basic rules can be abstracted as Non-Up-Read and Non-Down-Write. The two rules are adopted

* The paper is supported by 973 project of China (Grant No. TG1999035801)

in almost all security models those enforce Mandatory access control policy [1]. The information flow must be controlled by satisfying the two rules in order to prevent the subjects from accessing the objects without corresponding clearances.

The Biba model is an integrity security model and its rules are Non-Down-Read and Non-Up-Write [2].

The SeaView model combines the MAC and DAC policies to control the data access in databases [3]. Every subject is assigned a bound of confidentiality and integrity levels for its operations. They are C_{\min} , I_{\min} , C_{\max} , I_{\max} to separate the read level and write level for subjects. It integrate the rules of BLP and Biba models and add a execute rules.

1.2 Disadvantages of the Above Models

As classical MAC model, the rules in BLP model are too strict to avoid conflicts with the actual requirements. For example, a subject with high security level may want to write object with lower level. The inconsistency can be illustrate by following example:

Suppose price and purpose are two fields in a table equipments, the level of price is unclassified while the level of purpose is secrecy. Then such a operation are forbidden:

```
UPDATE equipment
SET price=price*1.1
Where purpose =”missle test”
```

The SeaView model introduced polyinstance conception to maintain the database integrity and to avoid convert channel. It decompose the multilevel relations into single levels the stores them in different tables, so the efficiency was sacrificed.

So a new multilevel secure model for database is presented for the purpose to solve the conflicts and to enforce MAC in this paper.

The new model takes account of both confidentiality and integrity of the information in database.

1.3 The New Model Overview

A new security level is defined in the new model to extend confidential clearance by giving a subject a highest and a lowest confidential clearance. So we modify the “a” and “w” rules. The subjects in this model permit writing down in certain range. The model is more flexible and practical.

1.3.1 The Definition of Security Level

A security level has three components: Confidential classification /clearance, integrity classification/ clearance and a set of categories. All the security levels in a system form a set. A category set is a subset of all categories defined for the system. A category is an additional sensitivity assignment based on need-to-know.

1.3.2 Read / Write Clearance of Subjects

Every subject has a bound of write confidential clearance, denoted by C_{\min} , C_{\max} , Then its Write confidential clearance is pairs $\langle C_{\min}, C_{\max} \rangle$, its read clearance is C_{\min} .

A subject is considered as trusted if its read confidential clearance dominate its lowest confidential clearance strictly; A trusted subject is authorized to write down some data to the objects whose classification are dominated by it but not lower than a certain value if it satisfies the confidential rule2 in sect. 2.2. The subject can't propagate information down at this situation.

1.3.3 Security Check Rules

The check rules for *appending* operations (a) are as follows: (1) ①the current confidential clearance of subject is dominated by the Confidential classification of an object; ②the integrity clearance of the subject dominates the integrity classification of an object ③The object's category set contains the subject's category set OR (2) ①the Confidential classification of an object is belong to the write confidential clearance bound of the subject. ②③the same with (1);④satisfies the Confidential Rule.(Rule 2 in 2.2).

The check rules for *reading* operations (r) are as follows: ①The current confidential clearance of the subject dominate the Confidential classification of the object; ②The integrity clearance of the subject is dominated by the integrity classification of the object; ③The subject's category set contains the object's category set.

The check rules for *reading and writing* operations (w) are as follows: (1) ①The current confidential clearance of the subject is equal to the Confidential classification of the object; ②the integrity clearance of the subject is equal to the integrity classification of the object. ③The subject's category set is equal to the object's; OR (2) ①the Confidential classification of an object is belong to the write confidential clearance bound of the subject. ②③the same with (1);④satisfies the Confidential Rule.

Here a new concept of **Confidential Rule** is introduced. It is responsible for the confidential check in the condition that the confidential classification of an object is belong to the write confidential clearance bound of the subject.

2 Formal Description of the New Model

2.1 Definitions

Suppose S is the set of subjects, O of objects, A of access manners, C of confidential levels, I of integrity levels, CAT of categories, Sec_L of security levels, Sec_L: ={(c,i,ct)|c ∈ C, i ∈ I, ct ⊆ CAT}.

Definition 1. System state v: $v \in V = (B \times M \times F \times I \times CT \times H)$

Current Access Set B: $B \subseteq (S \times O \times A)$

Access mode Set A: $A = \{r, w, e, a\}$, “r”present only read,“a”only write,“w”both read and write“e”neither read nor write.

Access Control Metrix M: $M = \{M | M \text{ is metrix and its element } m_{ij} \text{ is the set of rights of } S_i \text{ have on } O_j\}$

Confidential function F: composed of four parts: subject's highest confidential clearance function f_{max} , f_{min} subject's lowest confidential clearance function

f_{\min} , subject's current confidential clearance function f_c , Object' Confidential levelification function f_o

Integrity function I: similar to Confidential function.

Category function CT: subject's Category function ct_s , $ct_s(s) \subseteq CAT$, and object's Category function ct_o

H is current objects hierarchy .

Definition 2. Confidential rule set CVP: $cvp \in CVP$ is a mapping of objects to {Yes,No}, Yes=1, present accord with the rules, or No=0.

Function k: is a mapping of CVP to Sec_L. $\forall cvp \in CVP$, has one $k(cvp) \in Sec_L$ only.

For security level $sec_l \in Sec_L$ there is a $sec_l_cvp = \{cvp \mid k(cvp) = sec_l, cvp \in CVP\}$.

Definition 3. Deputy of security set DS: $DS = \{DS \mid DS \subseteq S\}$

Function m: m is a one to one mapping of DS to Sec_L. $\forall ds \in DS$, exist and exist unique $k(ds) \in Sec_L$; $\forall sec_l \in SEC_L$, exist and exist unique $m^{-1}(sec_l) \in DS$;

Deputy of security ds: the ds corresponding to $sec_l = (c, i, ct)$ is $ds = m^{-1}(sec_l)$ and $f_c(ds) = c$, $i_c(ds) = i$, $ct_s(ds) = ct$, $f_{\max}(ds) = TS$, $i_{\max}(ds) = C$ or $f_{\min}(ds) = U$, $i_{\min}(ds) = U$.

Definition 4. We call confidential level c belong to write confidential clearance pairs (C_{\min}, C_{\max}) if $C_{\min} \leq c \leq C_{\max}$.

2.2 Rules

$rq(S_i, O_j, \underline{x})$ presents the \underline{x} access requirement from subject S_i to object O_j .

Rule 1

For every $b = (s, o, \underline{x}) \in B$:

$\underline{x} = a \rightarrow f_c(s) \leq f_o(o), i_c(s) \geq i_o(o), ct_s(s) \subseteq ct_o(o)$; OR

$f_{\min}(s) \leq f_o(o) \leq f_c(s), i_c(s) \geq i_o(o), ct_s(s) \subseteq ct_o(o)$ and satisfy Rule 2;

$\underline{x} = w \rightarrow f(s) = f_o(o), i_c(s) = i_o(o), ct_s(s) = ct_o(o)$ OR

$f_{\min}(s) \leq f_o(o) \leq f_c(s), i_c(s) = i_o(o), ct_s(s) = ct_o(o)$ and satisfy Rule 2;

$\underline{x} = r \rightarrow f_c(s) \geq f_o(o), i_c(s) \leq i_o(o), ct_s(s) \supseteq ct_o(o)$;

(4) $\underline{x} = e \rightarrow f_{\max}(s) \geq f_o(o), i_{\max}(s) \geq i_o(o), ct_s(s) \supseteq ct_o(o)$

Rule 2

At state (b, M, f, i, ct, H) , $a \in M_{ij} \subseteq M$, if $f_{\min}(s) \leq f_o(o) \leq f_c(s), i_c(s) \geq i_o(o), ct_s(s) \subseteq ct_o(o)$, for $rq(S_i, O_j, a)$:

S_i activate O_j' , security level of O_j' is $sel_11 = (f_o(O_j'), i_o(O_j'), ct_o(O_j'))$ and $f_o(O_j') = f_c(S_i)$, $i_o(O_j') = i_c(S_i)$, $ct_o(O_j') = ct_s(S_i)$. Authorize $rq(S_i, O_j', a)$ and form $b_1^* = \{(S_i, O_j', a)\} \cup b$, enter the state (b_1^*, M, f, i, ct, H) .

The corresponding confidential rules set of $sel_12 = (f_o(O_j), i_o(O_j), ct_o(O_j))$ is sel_12_cvp .

If $\forall cvp \in SEC_L2_ivp$, $cvp(O_j') = YES$

Then turn to step (3)

Else S_i delete object O_j' , deny $rq(S_i, O_j, a)$.

From f^* let $f_o(O_j') = f_o(O_j)$.

The deputy of security of sel_12 is S_i'

Authorize $rq(S_i', O_j', r)$, form $b_2^* = \{(S_i', O_j', r)\} \cup b_1^*$, enter state $(b_2^*, M, f^*, i, ct, H)$.

Authorize $rq(S_i, O_j, a)$, form $b_3^* = \{(S_i, O_j, a)\} \cup b_2^*$, enter state $(b_3^*, M, f^*, i, ct, H)$

S_i' delete object O_j' .

2.3 Theorems and Corollary

Theorem 1. The subject can write to the object indirectly while the object's Confidential classification is belong to the subject's write confidential clearance, object's integrity classification is dominated by subject's, the two category sets are equal exactly, and the content that the subject write to the object is accord with the confidential rules in the security level of the object.

Proof. Suppose when the subject has $rq(S_i, O_j, a)$ request, the content which the subject S_i want to write into the object O_j is $ContentW_{ij}$, the content which the subject S_i read out from the object O_j is $ContentR_{ij}$ and the content of the object O_j is $Content_j$.

At the state (b, M, f, i, ct, H) , $a \in M_{ij} \subseteq M$, $f_c(S_i) \leq f_o(O_j)$, $i_c(s) \geq i_o(o)$, $ct_s(s) \subseteq ct_o(o)$, the content which S_i write into O_j is $ContentW_{ij}$.

According to step (1) of rule 2, after granting the activated object O_j' the right of $rq(S_i, O_j', a)$, $ContentW_{ij} = ContentW_{ij'} = Content_{j'}$.

According to step(2) of rule 2, if $Content_{j'}$ is accord with the confidential rule set sec_l2_cvp , after granting object O_j' the right of $rq(S_i', O_j', r)$ in step(5) of rule 2, $ContentR_{ij'} = Content_{j'}$.

According to step(6) of rule 2, after granting object O_j the right of $rq(S_i', O_j, a)$, $ContentW_{ij'} = ContentR_{ij'}$.

Due to a) b) c), we get $ContentW_{ij} = ContentW_{ij'}$. It proves that the subject S_i can write into the object O_j by a deputy if the content which S_i writes into O_j is accord with the confidential rules.

Corollary 1. If the state (b, M, f, i, ct, H) satisfies the BLP Axiom, then the state (b_3^*, M, f, i^*, H) in rule 2 satisfies the BLP Axiom.

Corollary 2. Rule 1 satisfies the BLP Axiom.

Corollary 3. The model accords with BLP model.

Corollary 4. The model accords with Biba model.

The proofs of the above corollaries are omitted here. The key component in the new model is the confidential rule set CVP.

3 Applying the Model in MLS DBMS Development

The security module is composed of a Mandatory Access Control model in the lower layer and a Discretionary Access Control model in the upper layer to enforce the MAC.

The implementation of security label including the expression and definition of security levels, the storage of multilevel relations/tuples, the extension of data dictionary and the extension of SQL sentences should be considered when applying the model in MLS DBMS development. The multilevel tuples can be stored in one table other than in some single level tables. So the join operation of tables in query operations are decreased much greatly and the efficiency of the system is increased. We create sensitivity label attribute (MLSLAB) for every tuple in tables. We add correspond mechanism in the DDL and DML update sentences to use the labels to execute the security functions.

4 Conclusions

Too strict are the rules of the current security models the conflicts between work demands and security constraints are arisen and much inconvenience in work is resulted in. For example, one can't alternate from one role to another role to acquire different security levels. It not only increases the burden of SSO but also decreases the security of the system. It makes the strict security model lose its effect. The new model in this paper is worked out because of above problems. The model enforces mandatory access control and satisfies the criteria of class B1 in TCSEC. The advantages is that separation of the read and write confidential level and extension the level to a bound improves the flexibility and practicability of the model.

The future work will focus on the decision policy of establishing the confidential rules set.

References

1. Bell, D.E., and La Padula, L.J. "Secure Computer Systems: A Refinement of the Mathematical Fundations" [J], ESD-TR-73-278, Vol.III, AD 780 528, Electronic Systems Division, Air Force System Command, Hanscom AFB, Bedford, Massachusetts, November. 1974
2. Biba, K.J., "Integrity Considerations for Secure Computer Systems" [J], ESD-TR-76_372, Hanscom AFB, MASS.:Air Force Electronic Systems Division, 1977.
3. Dorothy E. Denning, Teresa F.Lunt "The SeaView Security Model", Security and Privacy, 1988. Proceedings., 1988 IEEE Symposium, April 1988 Pages:218 - 233

Secure Tamper Localization in Binary Document Image Authentication

Niladri B. Puhan and Anthony T.S. Ho

Center for Information Security, School of Electrical and Electronic Engineering
Nanyang Technological University, Singapore, 639798
etsho@ntu.edu.sg

Abstract. In this paper, we propose a novel method for secure tamper localization in binary document images using erasable watermarks. For binary images, watermarking with pixel flipping approach is a difficult task, because it can bring noticeable visual distortion. In localization, finding sufficient number of low-distortion pixels in a block to embed the cryptographic signature and their blind detection is more difficult. Also, an imperceptible watermark cannot be embedded in white regions of the document image, making such regions insecure against hostile attacks. In the proposed new method, an erasable watermark is embedded in each block of a document image independently for secure localization. The embedding process introduces some background noise; however the content in the document can be read or understood by the user, because human vision has the inherent capability to recognize various patterns in the presence of noise. After verifying the content of each block, the exact copy of original image can be restored at the blind detector for further analysis. In the proposed method, the tamper localization accuracy is significantly improved as compared to the method proposed by Kim and Queiroz. Simulation results show that an erasable watermark of necessary data length can be embedded in individual blocks of various document images to attain cryptographic security.

1 Introduction

Digital watermarking is the art of securing multimedia data by embedding a proprietary mark which may be easily retrieved by the owner of the data to verify about ownership and authenticity. There have been different types of watermarking methods proposed in the literature, designed for various applications [1]. Digital documents and images can be easily and maliciously modified using readily available image processing tools. Thus the need for image authentication methods to establish the integrity and authenticity of digital data is necessary and important. The authentication method is useful in, for example, electronic commerce, legal applications and medical archiving to determine whether the digital data in question has integrity or not. Integrity and authenticity of digital media can be guaranteed through the use of watermarks in conjunction with cryptographic signature. In authentication watermarking, the advantage of having the cryptographic signature hidden inside the digital data rather than appended to it is obvious. Lossless format conversion of the watermarked data does not render it inauthentic though the representation of the data is changed. Another advantage is that if authentication information is localized, then it is possible to achieve the capability to localize the modifications after tampering by a malicious

attacker. Secure fragile watermarking schemes combined with cryptography have been proposed in [2], [3] as a means to verify image authenticity.

There has been a growing interest in the authentication watermarking of binary document images such as text, circuit diagrams, signature, financial and legal documents. For such images in which the pixels take on only a limited number of values, hiding significant amount of data for authentication purpose without causing visible artifacts becomes more difficult. As such, many watermarking algorithms use the perceptual model to select low-distortion contour pixels for high watermark capacity [4], [5]. The only method for tamper localization using cryptographic signature in binary document images has been reported by Kim and Queiroz in [6]. In this method, the original image is divided into many sub-images and each sub-image is watermarked independently. A two-layer watermark is embedded imperceptibly using a block-wise data hiding technique to verify the integrity of watermarked image and localizing any modification in it. The disadvantage of the method is that the size of each sub-image is 128x128 pixels; so its localization accuracy is not good. The block-wise embedding used in this method also suffers from parity attack. The parity attack arises because the signature is embedded by considering the parity of the blocks, i.e. the number of white pixels. If two pixels that belong to the same block change their values, the parity of this block may not change and so this modification will pass undetected. To overcome these shortcomings, we propose an algorithm that is feasible and effective for secure tamper localization in binary documents.

One of the first tamper localization methods was proposed by Wong in [7]. In this scheme, an image is divided into non-overlapping blocks and the watermarking is performed for each block independently. The seven most significant bits of all pixels in a block are hashed using a secure key. The hash output is then XORed with a chosen binary logo and inserted into the LSBs of the same block. At detector, the watermark verification proceeds in the reverse order. However the algorithm suggested by Wong cannot be directly applied in case of binary documents because each pixel has only one bit. By modifying any pixel to embed a watermark would affect the signature of the block and the authentication test would fail. The challenging problem is how to divide a block into two parts such that the above idea of embedding the authentication signature can be applied. While imperceptibly and securely embedding the authentication signature in a block, the number of low-distortion pixels should be high and the watermark detection process should be blind. In a reasonable block-size such as 32x32 pixels, there is insufficient number of low-distortion pixels available. The blind detection requirement of these pixels adds to the difficulty in achieving 128-bit watermark capacity for each block. Further, an imperceptible watermark cannot be embedded in white regions of the image. Thus, the white regions are particularly vulnerable to content alteration by the attacker. Due to these shortcomings, it is evident that unless the block size is large, imperceptible watermarking may not be suitable to obtain secure localization in document images.

So we turn our attention to the possibility of embedding the signature in other such pixels that brings visual distortion in watermarked image, but the resulting distortion due to embedding process can be erased entirely at the blind detector. After erasing the embedded watermark, the exact copy of the original image can be restored at the blind detector. This particular concept is known as erasable watermarking in literature and the watermark thus embedded is termed as an erasable watermark. The algorithm

proposed by Fridrich *et al* in [8] for exact authentication of natural images is of particular interest to this paper. Let A represent the information that is altered in the cover image when we embed a message of N bits. Fridrich *et al* showed that the erasability is possible provided A is compressible. If A can be losslessly compressed to M bits, $N-M$ additional bits can be erasably embedded in the cover work. In the implementation of this algorithm for natural images, it is observed that the neighboring pixels are highly correlated. Thus some bit planes in the whole image can be sufficiently compressed to implement an erasable watermark. In case of binary document images each pixel is represented by one bit and it can be considered that there is only one bit plane in the image. If all pixels in the bit plane are losslessly compressed to construct the erasable watermark, then the compressed block does not have perceptual correlation with the original. Therefore, creating an erasable watermark by directly compressing the bit plane is not relevant in document images. Within a block if a set of suitable pixels with high correlation can be found, they can be losslessly compressed and an erasable watermark can be constructed. This motivation is addressed in the next section by proposing a new localization method for binary document images. The paper is organized as follows: in Section 2 the proposed localization method is described. Simulation results and discussion are presented in Section 3. Finally some conclusions are given in Section 4.

2 Proposed Localization Method

In this section, we shall propose a localization method for embedding the authentication signature as an erasable watermark in each block of the document image. In the proposed method, after embedding an erasable watermark there will be visible noise in the watermarked image made available for different users. In the embedding process, the relevant information contained in the binary document is preserved so that the user can read or understand the documents. The user can verify the authenticity of such available images and localize any tampering if occurred after watermarking with high probability and accuracy. The watermark can then be erased from the authentic images to retrieve the distortion-free original images for further analysis and application. In the proposed method we find a set of pixels in each block such that; (1) there exists a high correlation among the pixels and the number of such pixels is high (2) the same set of pixels can be found at blind detector and (3) the relevant information is preserved after the embedding process.

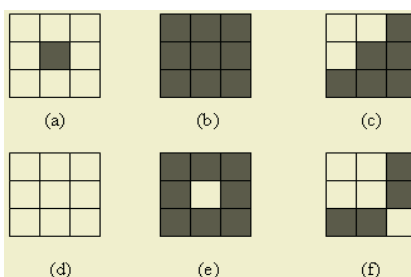


Fig. 1. Different categories of pixels in a binary document image based on their 8-neighborhood

As shown in Figure 1 (a)-(f), there can be six categories of pixel neighborhood in such images. Pixels whose neighborhoods have both white and black pixels are contour pixels like in (c) and (f) and they convey maximum information in the document image. The center pixel in (b) is called a *foreground* pixel and the center white pixel in (e) can represent a hole, so these pixels convey some information. The black pixel whose all neighbor pixels are white is termed as an *isolated* pixel like in (a). These pixels are perceived as noise in a sharply-contrasted binary image. As shown in (d), a white pixel whose all neighbor pixels are white is termed as a *background* pixel. The isolated and background pixels do not convey important information within document images. If these pixels are altered, a background noise will be formed in the image which is similar to the salt-and-pepper noise found in case of natural images. In document images, we obtain information by recognizing various patterns such as symbols, lines and curves etc. It is known that human vision has remarkable ability to recognize such patterns even in the presence of noise. So after embedding an erasable watermark in these pixels, the user can still obtain relevant information about the document. The background pixels occur in long sequences and isolated pixels occur in between them with less probability. So such a set of pixels can be significantly compressed using the run-length coding scheme. Flipping of a background pixel creates an isolated pixel and vice-versa in an image; so blind detection of the embedded pixels is possible. We shall outline the proposed method for tamper localization in following steps.

Embedding

1. The whole image is divided into non-overlapping blocks of $Y \times Z$ pixels. Watermarking is performed for each block independently and in a sequential order starting from left to right and top to bottom of the image.
2. In each block, an ordered set of *insignificant* pixels are searched in a sequential scanning order. Pixels which are in the border with other blocks are not included in this search to maintain block independence. A pixel is defined to be in the insignificant pixel set if the conditions are satisfied in following order.
 - a) The pixel is either a background pixel or an isolated pixel.
 - b) If there is no other pixel in its 8-neighborhood that has already been decided as an insignificant pixel.
 - c) After flipping, any new insignificant pixel should not be created among already scanned 8-neighborhood pixels.
 Condition (b) is necessary because any pixel previously found to be insignificant shall remain so after its flipping. Condition (c) is necessary because the newly created insignificant pixel will lead to wrong detection.
3. The insignificant pixel set is losslessly compressed using the run-length coding scheme. Authentication signature ‘S’ is computed from the block according to the following equation.

$$S = H(C_b, K, I_b, I_K) . \quad (1)$$

where H , C_b , K , I_b and I_K denote hash function, current block in the original image, secret key, block index and image index, respectively.

The block index is used in the computation of signature to resist block-swapping by hostile attacker and the image index is necessary to resist the collage attack [9]. The compressed data and authentication signature are concatenated to create the

message ' m ', which is embedded in the insignificant pixel set. The embedding is performed pixels-wise; so an insignificant pixel holds one bit of m and its pixel value is set equal to the signature bit it holds. Likewise all blocks in the image are watermarked.

Detection

4. To verify each block, the message m is extracted by finding the insignificant pixel set like in steps (1) and (2). Its component pieces, the compressed version of insignificant pixel set and the authentication signature are also extracted. The compressed version of the insignificant pixel set together with the watermarked block is used to reconstruct the original block. The authentication signature of the reconstructed block is computed and compared with the extracted signature.
5. If the two signatures match, the reconstructed block is authentic. Verification of each block is done independently to localize any tampering in the watermarked image.

3 Results and Discussion

In this section, we present simulation results by creating the erasable watermark for our proposed block-wise localization method. The authentication signature to be used in this algorithm is the Hashed Message Authentication Code (HMAC). The HMAC is found by computing the one way hash function of the data string that is a concatenation of the pixel set and secret key. In our method, provable security against content modification is obtained by using the cryptographic hash function. In the implementation, we have used MD5 [10] hash function to compute the HMAC. The output 128-bit HMAC is used as the authentication signature and the message ' m ' is constructed for each block as described in the proposed method. First ten bits of m represents the size of the compressed data. While compressing the insignificant pixel set by run-length coding, 10-bit representation is used for the number of white pixels and 1-bit for the number of black pixels. This is because there cannot be two consecutive isolated (black) pixels in the insignificant pixel set. First ten bits and the run-length encoded data represent the compressed data in m . We have chosen a block size of 32x40 pixels and the block-size can be suitably modified if length of the authentication signature is changed in any case, e.g. 64 or 96 bits.

Figure 2 shows the original and the watermarked image after pixel-wise embedding of m in each block. It is observed that although background noise is present in the watermarked images, the text can still be read and understood by the user. In the watermarked image, it is observed that the background noise appears to be more random and different well-structured patterns can be recognized due to the inherent ability of human vision. Without any tampering, all blocks in the watermarked images are verified. After verification, the exact copy of original image can be restored at the blind detector. The watermark erasing process is shown in Figure 3. For secure embedding, each block in the original image should have sufficient capacity. The capacity of a block is the number of bits that can be embedded within it. To analyze the performance of the proposed method in different images, we define the term *redundancy* (R) in Eq. 2 as number of bits available in a block to accommodate the signature.

The recent development of various methods of modulation such as PCM and PPM which exchange bandwidth for signal-to-noise ratio has intensified the interest in a general theory of communication. A basis for such a theory is contained in the important papers of Nyquist and Hartley on this subject. In the present paper we will extend the theory to include a number of new factors, in particular the effect of noise in the channel, and the savings possible due to the statistical structure of the original message and due to the nature of the final destination of the information.

The recent development of various methods of modulation such as PCM and PPM which exchange bandwidth for signal-to-noise ratio has intensified the interest in a general theory of communication. A basis for such a theory is contained in the important papers of Nyquist and Hartley on this subject. In the present paper we will extend the theory to include a number of new factors, in particular the effect of noise in the channel, and the savings possible due to the statistical structure of the original message and due to the nature of the final destination of the information.

Fig. 2. Top: original image of 320x440 pixels. Bottom: watermarked image after embedding the erasable watermark in each block

The recent development of various methods of modulation such as PCM and PPM which exchange bandwidth for signal-to-noise ratio has intensified the interest in a general theory of communication. A basis for such a theory is contained in the important papers of Nyquist and Hartley on this subject. In the present paper we will extend the theory to include a number of new factors, in particular the effect of noise in the channel, and the savings possible due to the statistical structure of the original message and due to the nature of the final destination of the information.

Fig. 3. The watermark erasing process is shown in which 44 blocks out of 110 blocks have been restored to its original content

$$R = \text{Size of the insignificant pixel set} - \text{Compressed data size}. \quad (2)$$

In an ideal case, each block of the original image should have $R \geq 128$. In Figure 4, it is shown that most blocks in the image have sufficient redundancy for embedding

m . If R is less than 128 bits in a block, e.g. 120 bits, then first 120 bits of HMAC is used to construct m and authenticate the current block. Similarly at detector, the comparison between computed and extracted signature is done only for first 120 bits. We perform two alterations in the watermarked image; the first character ‘ H ’ in line-7 and the only word ‘*information.*’ in last line is deleted as shown in Figure 5. The detection is performed on the attacked image. The detector correctly localizes the tampered blocks in the attacked image.

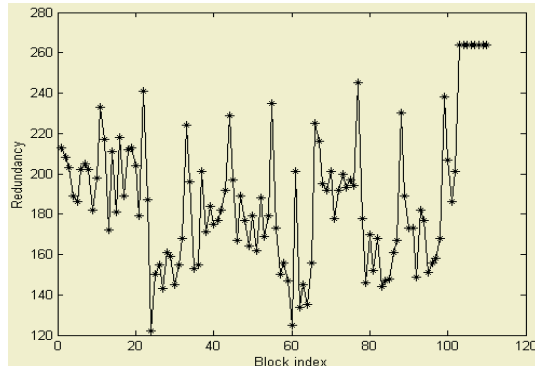


Fig. 4. Redundancy (R) for each block of the original image. Except two blocks, all the blocks have $R \geq 128$

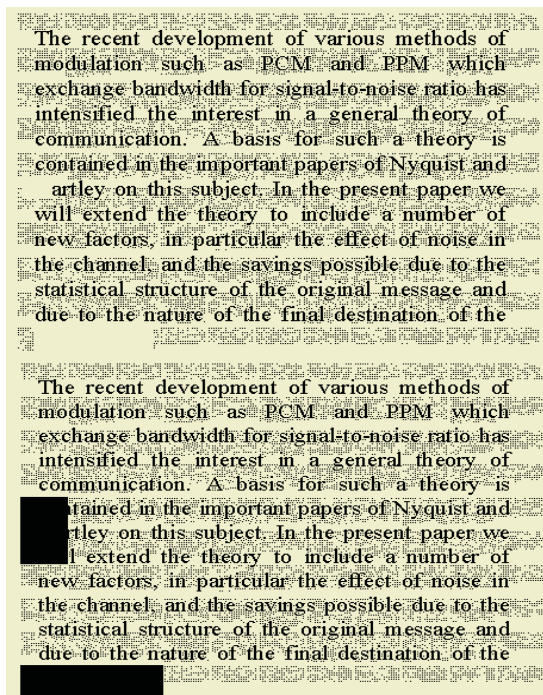


Fig. 5. Top: attacked image. Bottom: image showing tamper localization

Though the localization accuracy and cryptographic security offered by the block-wise localization method is high, its block-wise independence was used by Holliman and Memon to design a counterfeiting attack known as collage attack in [9]. To counteract this attack, Wong and Memon suggested including a unique image index while computing the signature in [11]. The use of a unique image index in Eq. 1 for computing the signature removes the possibility of collage attack entirely. Such an approach is feasible for some practical applications; however it may not be always possible because managing such indices brings extra burden to the user. We are currently investigating to suitably extend the proposed method to counteract collage attack in case of binary document images without using image index. To test the effectiveness of proposed method further, a total of 10 binary test images containing text, formulae, drawing and tables are generated. The dimension of the test image is chosen to be the multiple of 32x40 pixel block size. In Table 1, R_{mean} for each test image is given, where R_{mean} the mean of redundancy for all the blocks in a test image. The R_{mean} values for all test images are nearly or above 190 bits. From the Table, it can be shown that using the new method it is possible to securely embed the erasable watermark of necessary length in various document images for tamper localization.

Table 1. Redundancy in test images

| Number | Size | R_{mean} (bits) |
|--------|----------|-------------------|
| 1 | 480x560 | 196.62 |
| 2 | 448x520 | 187.02 |
| 3 | 448x520 | 190.36 |
| 4 | 480x 480 | 195.20 |
| 5 | 608x480 | 188.84 |
| 6 | 480x480 | 189.80 |
| 7 | 576x480 | 191.66 |
| 8 | 640x480 | 205.15 |
| 9 | 608x520 | 206.91 |
| 10 | 512x520 | 191.19 |

The performance of the proposed algorithm can be compared with the previous method [6]. In this method, the localization accuracy was approximately at the block size of 128x128 pixels. In the proposed method it has been significantly improved to approximately the block-size of 32x40 pixels as shown. The block-wise embedding in the previous method suffers from parity attacks as discussed in Section 1. The possibility of parity attack is not present in the proposed method because each message bit is embedded in an insignificant pixel instead of a block. The ability of the proposed method for localizing any type of content alteration in the watermarked image is equivalent to the security of cryptographic authentication. In the present method the embedded watermark needs to be erased from the watermarked image for further use, additionally. However, this does not create any bottleneck to the user, because the implementation process is computationally fast. Since the proposed method is relatively simple and no complex perceptual model is necessary, it is possible to obtain fast implementation that is useful for many practical applications of document authentication.

4 Conclusion

In this paper, we proposed a new watermarking method that is useful in localizing content alteration in binary document images using erasable watermarks. The proposed method can localize any kind of content alteration in the image with high probability and accuracy. For this purpose, an ordered set of insignificant pixels was selected and then compressed using the run-length coding scheme. An erasable watermark was constructed by combining the compressed data and HMAC of the block in the original image. After embedding process, the user could easily interpret the document in the presence of noise due to the inherent ability of human vision. After verifying the authenticity, the user could restore the exact copy of the original image for further analysis. The localization accuracy of the proposed method is significantly improved and does not suffer from any parity attack.

References

1. M. D. Swanson, M. Kobayashi, A. H. Tewfik: Multimedia Data-Embedding and Watermarking Technologies. Proc. of the IEEE, vol. 86, no. 6, (1998)
2. M. Yeung, F. Mintzer: An Invisible Watermarking Technique for Image Verification. Proc. IEEE Int. Conf. Image Processing, Santa Barbara, CA, (1997), 680-683
3. P. W. Wong: A Public Key Watermark for Image Verification and Authentication. Proc. IEEE Int. Conf. Image Processing, Chicago, IL, (1998), 425-429
4. M. Wu, E. Tang, B. Liu: Data hiding in digital binary images. Proc. IEEE Int. Conf. on Multimedia and Expo, Jul 31-Aug 2, (2000), New York
5. A.T.S. Ho, N. B. Puhan, P. Marziliano, A. Makur, Y. L. Guan: Perception Based Binary Image Watermarking. IEEE International Symposium on Circuits and Systems (ISCAS), Vancouver, Canada, 23-26 May (2004)
6. H. Y. Kim, R. L. de Queiroz: Alteration-Locating Authentication Watermarking for Binary Images. Proc. Int. Workshop on Digital Watermarking, Seoul, LNCS-2939, (2004)
7. P. Wong: A Watermark for Image Integrity and Ownership Verification. Proc. IS&T PIC, Portland, Oregon, (1998)
8. J. Fridrich, M. Goljan, M. Du: Invertible Authentication. Proc. of SPIE, Security and Watermarking of Multimedia Contents, (2001)
9. M. Holliman, N. Memon: Counterfeiting attacks on oblivious block-wise independent invisible watermarking schemes. IEEE Trans. Image Processing, vol. 9, no. 3, 432-441, March (2000)
10. R. L. Rivest: RFC 1321: The MD5 Message-Digest Algorithm. Internet Activities Board, (1992)
11. P.W. Wong, N. Memon: Secret and public key image watermarking schemes for image authentication and ownership verification. IEEE Trans. Image Processing, vol. 10, no. 10, October (2001)

A Seal Imprint Verification with Rotation Invariance

Takenobu Matsuura and Kenta Yamazaki

Department of Communications Engineering, Tokai University,
1117 Kitakaname, Hiratsuka, Kanagawa, 259-1292 Japan
matsuura@dt.u-tokai.ac.jp

Abstract. This paper discusses on a seal imprint verification method with rotation invariance. The rotation invariant feature is represented by the absolute value of Fourier coefficients of seal imprint on circles with different radii. The impulse response of finite impulse response (FIR) system having the absolute value of Fourier coefficients of seal imprint on circles with different radii as the input and output is calculated. The resultant impulse response of the FIR system is used here as the feature of seal imprint. Seal imprint can be verified evaluating the distance between the impulse responses of the reference and imprint to be verified. Seal imprint verification experiments are given to show the effectiveness of the proposed method.

1 Introduction

Although biometrics has been applied in many areas, seal imprint verification has been commonly used in Japan and some Asian countries as a personal confirmation. Most of seal imprint verifications have been made by visual confirmation of human being. Seal imprints appear on many types of documents, such as bank cheques, receipts and so on. In order to make the verification for large numbers of seal imprints automatically, some methods have been proposed [1],[2],[3], which are mainly based on a matching of skeletons of character strokes. In those methods an adjustment of rotation angle for seal imprint was required in the matching process. It is not so easy to make the adjustment of rotation angle. It is desirable to realize a simple verification system without the adjustment of rotation angle. As a method without any adjustment of rotation angle a method using the Zernike moments was proposed [4]. However it was difficult to obtain a good approximation from seal imprint with complicate character because of complex computation of the moments. Another method [5] was reported that the seal imprint verification by a personal computer provided better results than those by human being, but no discussion was made about the rotation of seal imprint. While a technique of treating seal as in three-dimensions (3D) was proposed [3]. In the method, it is not easy and very complicate to adjust rotation angle and consideration about stained seal imprint still remain as future work. In order to improve the disadvantage mentioned above a seal imprint verification method

with rotation invariance was proposed [6]. In the method good verification results were obtained for rotation and stains of seal imprint, however it was not able to obtain better results for blurred imprints in comparison with rotation and stains of seal imprint. In this paper, in order to improve the disadvantage mentioned above a seal imprint verification method with rotation invariance is proposed. The rotation invariant feature is represented by the absolute value of Fourier coefficients of the image of seal imprint on circles with different radii. The impulse response of finite impulse response (FIR) system is calculated to characterize seal imprint using the absolute value of Fourier coefficients of the seal imprint on circles with different radii as the input and output of the system, respectively. The resultant impulse response of the above FIR system is used here as the feature of seal imprint. Seal imprint can be verified evaluating the distance between the impulse responses of the reference and imprint to be verified.

2 Feature Extraction

In this section, first, after a seal imprint has been represented as an image of 64 x 64 pixels with 256 gray levels by digital scanner, the seal imprint is represented by 2D continuous function in Cartesian coordinate as

$$f(x, y) = \sum_{n=0}^Q \sum_{m=0}^Q f(n, m) \phi(x - n, y - m) \quad (1)$$

where

$$\phi(x, y) = \frac{\sin \pi x}{\pi x} \cdot \frac{\sin \pi y}{\pi y} \quad (2)$$

and Q is an integer related to the image size. $f(n, m)$ is a gray level at a pixel (n, m) on the seal imprint. Then the following function is defined by letting $x = r \cos t$, $y = r \sin t$ in (1) as

$$\hat{f}(r, t) = f(r \cos t, r \sin t) \quad (3)$$

where, $0 \leq r \leq R$, $0 \leq t \leq 2\pi$ and $\hat{f}(r, t)$ is defined inside of the circle of radius R . An example of a polar image of seal imprint on circles with different radii is shown in Fig.1. Furthermore it is assumed here that without loss of generality, $\hat{f}(r, t)$ is a periodic function as

$$\hat{f}(r, t) = \hat{f}(r, t + 2m\pi) \quad (4)$$

for any integer m . Under the assumption the polar image $\hat{f}(r, t)$ is expanded into the truncated Fourier series by letting $r = r_k$ (constant) as

$$\hat{f}(r_k, t) \simeq \sum_{m=-M}^M a_m^{(k)} e^{jmt} \quad (5)$$

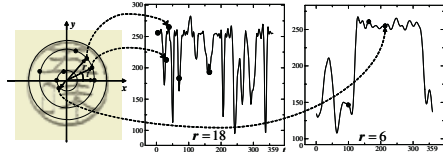


Fig. 1. Polar image of seal imprint on circles with different radii

where

$$a_m^{(k)} = \frac{1}{2\pi} \int_0^{2\pi} \hat{f}(r_k, t) e^{-jmt} dt \quad (6)$$

An example of Fourier series approximation for the polar image shown in Fig.1 is given in Fig.2. Let $\hat{g}(r, t) = \hat{f}(r, t + \alpha)$ be the rotated seal imprint of $\hat{f}(r, t)$ by

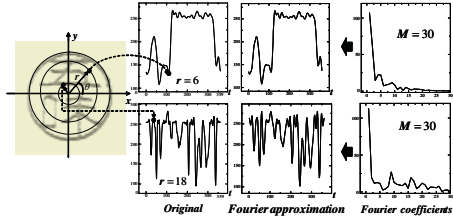


Fig. 2. Fourier approximation of polar image and Fouriercoefficients

angle α about its origin. Then it can be seen that the Fourier coefficients $b_m^{(k)}$ of $\hat{g}(r_k, t)$ is given as

$$b_m^{(k)} = a_m^{(k)} e^{jma\alpha}. \quad (7)$$

Thus we have the following relation:

$$u_m^{(k)} \equiv |b_m^{(k)}| = |a_m^{(k)}| \quad (8)$$

It can be seen from (8) that the absolute value of Fourier coefficients $|u_m^{(k)}|$, of seal imprint on circles with different radii are rotation invariant. Then the following vector is defined as

$$\mathbf{u}_k^T = [u_0^{(k)}, \dots, u_M^{(k)}], \quad (k = 1, \dots, K) \quad (9)$$

where \mathbf{u}_k^T is the transposition of \mathbf{u}_k .

3 Impulse Response of FIR System Characterizing Seal Imprint

In this section it is assumed that the FIR system can be described as

$$\hat{u}_n^{(j)} = \sum_{m=0}^L h_m^{(j,k)} u_{n-m}^{(k)}, \quad (n = 0, 1, \dots, M) \quad (10)$$

where $h_m^{(j,k)}$ is the impulse response, and $u_n^{(k)}$ and $\hat{u}_n^{(j)}$ are the input and output of the FIR system, respectively. In order to represent the relation between the absolute value of Fourier coefficients, $u_m^{(k)}$ and $\hat{u}_m^{(j)}$, of seal imprint on circles with different radii, the impulse response, $h_m^{(j,k)}$, of the FIR system defined in (10) is determined such that

$$J = \sum_{n=0}^M \left(u_n^{(j)} - \sum_{m=0}^L h_m^{(j,k)} u_{n-m}^{(k)} \right)^2 \quad (11)$$

is minimized. Then the optimal impulse response in the least square sense can

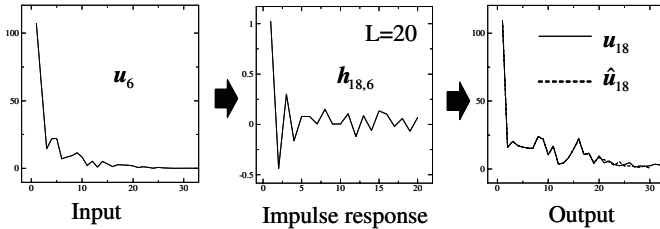


Fig. 3. Input,impulse response and output of FIR system from left

be obtained as

$$\mathbf{h}_{jk} = (U_k^T U_k)^{-1} U_k^T \mathbf{u}_j, \quad (j = 1, \dots, K) \quad (12)$$

where

$$\mathbf{u}_j^T = [u_0^{(j)}, \dots, u_M^{(j)}] \quad (13)$$

$$\mathbf{h}_{jk}^T = [h_0^{(j,k)}, \dots, h_L^{(j,k)}] \quad (14)$$

$$U_k = \begin{bmatrix} u_0^{(k)} & 0 & 0 & \cdots & 0 \\ u_1^{(k)} & u_0^{(k)} & 0 & \cdots & 0 \\ u_2^{(k)} & u_1^{(k)} & u_0^{(k)} & \cdots & 0 \\ \vdots & \vdots & \vdots & \ddots & \vdots \\ u_i^{(k)} & u_{i-1}^{(k)} & u_{i-2}^{(k)} & \cdots & u_{i-L}^{(k)} \\ \vdots & \vdots & \vdots & \ddots & \vdots \\ u_M^{(k)} & u_{M-1}^{(k)} & u_{M-2}^{(k)} & \cdots & u_{M-L}^{(k)} \end{bmatrix} \quad (15)$$

The impulse response of the FIR system having the absolute value of Fourier coefficients, \mathbf{u}_6 and \mathbf{u}_{18} given in Fig.2, of seal imprint on circles with different radii, $r = 6$ and $r = 18$, as the input and output respectively and the output $\hat{\mathbf{u}}_{18}$ of the FIR system are shown in Fig.3.

4 Seal Imprint Verification Algorithm

It is assumed here that the impulse response \mathbf{h}_{jk} ($j = 1, \dots, K$) of the FIR system determined for a particular seal imprint (reference) and the threshold value η have been evaluated before going to the seal verification algorithm. Then the seal imprint verification algorithm is given as follows :

(Algorithm)

- 1). Represent a given seal imprint as 2D continuous function

$$g(x, y) = \sum_{n=0}^Q \sum_{m=0}^Q g(n, m) \phi(x - n, y - m) \quad (16)$$

and define $\hat{g}(r, t) = g(r \cos t, r \sin t)$.

- 2). Compute the Fourier coefficients $b_m^{(k)}$ of the polar image $\hat{g}(r_k, t)$.

$$b_m^{(k)} = \frac{1}{2\pi} \int_0^{2\pi} \hat{g}(r_k, t) e^{-jmt} dt, \quad (m = 0, \dots, M) \quad (17)$$

- 3). Define the vector representing the rotation invariant feature of the given seal imprint.

$$\mathbf{v}_j^T = [v_0^{(j)}, \dots, v_M^{(j)}], \quad (j = 1, \dots, K) \quad (18)$$

where $v_m^{(k)} \equiv |b_m^{(k)}|$

- 4). Compute the impulse response of FIR system having \mathbf{v}_k and \mathbf{v}_j as the input and output respectively.

$$\mathbf{w}_{jk} = (V_k^T V_k)^{-1} V_k^T \mathbf{v}_j, \quad (j = 1, \dots, K; j \neq k) \quad (19)$$

where

$$\mathbf{w}_{jk}^T = [w_0^{(j,k)}, \dots, w_L^{(j,k)}], \quad (j = 1, \dots, K) \quad (20)$$

$$V_k = \begin{bmatrix} v_0^{(k)} & 0 & 0 & \dots & 0 \\ v_1^{(k)} & v_0^{(k)} & 0 & \dots & 0 \\ v_2^{(k)} & v_1^{(k)} & v_0^{(k)} & \dots & 0 \\ \dots & \dots & \dots & \dots & \dots \\ v_i^{(k)} & v_{i-1}^{(k)} & v_{i-2}^{(k)} & \dots & v_{i-L}^{(k)} \\ \dots & \dots & \dots & \dots & \dots \\ v_M^{(k)} & v_{M-1}^{(k)} & v_{M-2}^{(k)} & \dots & v_{M-L}^{(k)} \end{bmatrix} \quad (21)$$

- 5). Verify the seal imprint with \mathbf{w}_{jk} as true if

$$\sum_{j=1, j \neq k}^K \| \mathbf{h}_{jk} - \mathbf{w}_{jk} \|^2 < \eta$$

otherwise false,
where $\| \cdot \|$ means Euclidean norm.

5 Experiments

In our experiment, 1020 seal imprints belonging to 34 classes with variations such as rotation, stains with ink, blur and so on were used. As the experimental results, verification error rate was 0.05%. Seal imprint is represented as image of pixels with a pixel of 8 bits. Some examples of the seal imprints are shown in Fig.4. The absolute value of Fourier coefficients of seal imprint on circle with a

| | original | rotation | stained | blurred |
|--------|----------|----------|---------|---------|
| Seal 1 | | | | |
| Seal 2 | | | | |
| Seal 3 | | | | |
| Seal 4 | | | | |
| Seal 5 | | | | |
| Seal 6 | | | | |

Fig. 4.

radius (the left figure) and the impulse response of the FIR system having the absolute value of Fourier coefficients of seal imprint on circles with different radii as the input and output (the right figure) are shown in Fig.5 through Fig.9. It should be noted that the seal imprints shown in Fig.5 through Fig.7 should be verified as same in usual verification. On the other hand the seal imprints shown in Fig.8 and Fig.9 should be verified as different. It can be seen from Fig.5 that not only the absolute value of Fourier coefficients of seal imprint on circle with a radius but also the impulse response of the FIR system having the absolute value of Fourier coefficients of seal imprint on circles with different radii as the input and output are rotation invariant. The Fig.6 shows that the impulse response of the FIR system for given seal imprints is more suitable for describing the feature of seal imprint than the absolute value of Fourier coefficients. Because

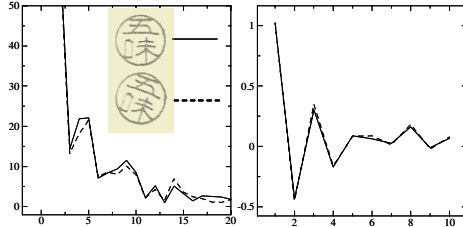


Fig. 5. Original and rotated seal imprints from left

in Fig.6 the absolute value of Fourier coefficients for given seal imprints are slightly different from each other, however the impulse responses are very close. The absolute value of Fourier coefficients and the impulse response of the FIR

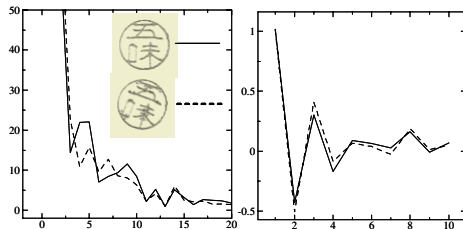


Fig. 6. Original and stained seal imprints from left

system for seal imprints with blur are shown in Fig.7. Also it can be seen from Fig.7 that the impulse response of the FIR system for given seal imprints is more suitable for describing the feature of seal imprint than the absolute value of Fourier coefficients. In comparison with the previous method[6] the present method provides better results for blurred seal imprints. In Fig.8 the absolute

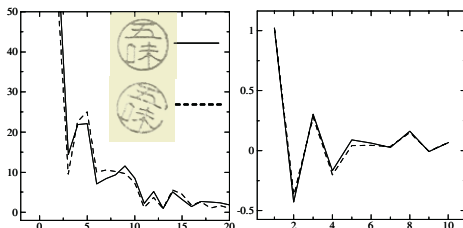


Fig. 7. Original and blurred seal imprints from left

value of Fourier coefficients and the impulse response of the FIR system for seal imprints with same characters and different fonts are shown. It can be seen from Fig.8 that the absolute value of Fourier coefficients and the impulse response of the FIR system are quite different. In Fig.9 the absolute value of Fourier

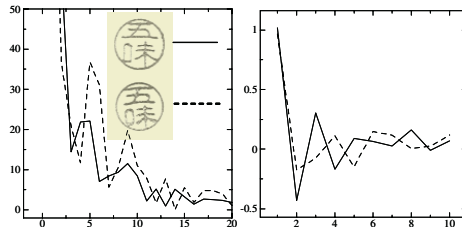


Fig. 8. Seal imprints with same characters and different fonts

coefficients and the impulse response of the FIR system for seal imprints with different characters shown. It can be seen from Fig. 9 that the absolute value of Fourier coefficients and the impulse response of the FIR system are quite different. It also can be seen from Figs. 5-9 that the impulse response of the FIR

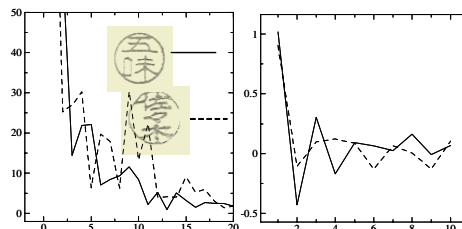


Fig. 9. Seal imprints with different characters

system having the absolute value of Fourier coefficients of seal imprint on circles with different radii as the input and output is effective for verification of seal imprints with rotation, stains and blur. An example of seal verification with the impulse responses is given in Fig. 10.

6 Conclusion

This paper proposed a seal imprint verification method with rotation invariance. The rotation invariant feature is represented by the absolute value of Fourier coefficients of seal imprint on circles with different radii. The impulse response of FIR system, whose input and output are the absolute value of Fourier coefficients of seal imprint on circles with different radii, is used as a feature of seal imprint. Seal imprints were verified by evaluating the distance between the impulse responses for a particular(reference) and given seal imprints. It was found from the seal imprint verification experiments that the impulse response of the FIR system having the absolute value of Fourier coefficients of seal imprint on circles with different radii as the input and output is effective for seal imprint verification.

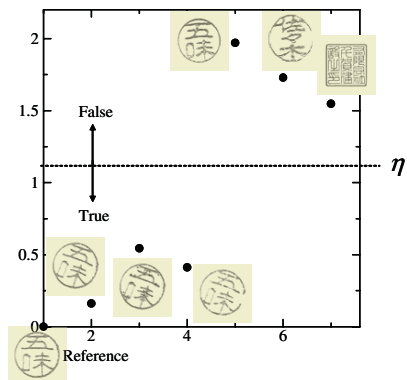


Fig. 10.

References

1. Lee.S.W, and Kim.J.H: "Attributed stroke Graph Match-ing for Seal Imprint Ver-ification", Pattern Recognition Lett..Vol.9,No.2,pp.137-145,Feb,1989
2. Hiroshi MIENO: "An Experiment of Identification of Seal Impression by pattern Matching", Mar.1975
3. Ryoji HARUKI,Takahiko HORIUCHI: "Automatic Seal Impression Identification Using 3-Dimensional Reference Seals",IEICE,,D-II.J82-D-II No.11 pp.2000-2007 Nov .1999.
4. T.matsuura and K.mori: "Rotation Invariant Seal Imprint Verification Method", ICECS2002,Vol.3,pp.955-958,Sep,2002
5. Katsuhiko UEDA: " Experimental Analysis of Factors Influencing the seal-Imprint Verification" IEICE,D-II Vol.J72-D-II ,No.1, pp.66-75 Jun . 1989
6. T.matsuura and K.Yamazaki: "Seal Imprint Verification Method with Rotation invariance",APCCAS2005,IEEE pp.597-600 ,2004.12

Robust Authenticated Encryption Scheme with Message Linkages

Eun-Jun Yoon and Kee-Young Yoo*

Department of Computer Engineering, Kyungpook National University,
Daegu 702-701, South Korea
ejyoon@infosec.knu.ac.kr, yook@knu.ac.kr

Abstract. An authenticated encryption scheme is a message transmission scheme, which sends messages in a secure and authentic way. In large message transmission, traditional authenticated encryption scheme has the disadvantage that the communication and the computation costs are too high. In 2002, Tseng-Jan proposed an efficient authenticated encryption scheme with messages linkage; that is, only a random number was used and the communication costs and the computational complexity were better than previously proposed schemes. The current paper, however, points out that Tseng-Jan's scheme suffers from serious security faults such that any adversary can easily forge valid signature blocks and pass the receiver's verification, and the scheme does not provide forward secrecy and non-repudiation. We also propose an improvement to the scheme to overcome the weaknesses.

Keywords: Cryptography, Authenticated encryption, Message linkage, Signature

1 Introduction

A digital signature is very important in modern electronic data processing systems. A digital signature is analogous to an ordinary hand-written signature and establishes both of sender authenticity and data authenticity. The signer uses his private key to generate a signature for the given message, and the verifier uses the signer's public key to verify the signature.

The notion of a signature scheme with message recovery was introduced by Nyberg and Rueppel [1][2]. Subsequently, Horster et al. [3] proposed an authenticated encryption scheme that is a modification of Nyberg-Rueppel's scheme. In an authenticated encryption scheme, the signer may generate the signature for a message and then send it to a specified receiver, and only the specified receiver can recover and verify the message. Therefore, an authenticated encryption scheme can be regarded as the combination of a data encryption scheme and a digital signature scheme.

* Corresponding author: Kee-Young Yoo (yook@knu.ac.kr)
Tel.: +82-53-950-5553; Fax: +82-53-957-4846

An authenticated encryption scheme is a message transmission scheme, which sends messages in a secure and authentic way. Basically, an authenticated encryption scheme should satisfy the following properties [1][2][4]:

- (1) **Confidentiality:** it is computationally infeasible for an adaptive adversary to obtain any secret information from a ciphertext.
- (2) **Authenticity (unforgeability):** it is computationally infeasible for an adaptive adversary to masquerade as the sender in sending a message.
- (3) **Non-repudiation:** it is computationally feasible for a third party to settle a dispute between the sender and the receiver in the event where the sender denies the fact that he is the originator of the message.

In order to recover the message from the signature, the message cannot be hashed to reduce the message size. If the message is large, it must be divided into a sequence of message blocks, and each message block is encrypted and signed individually. Unfortunately, this approach has a disadvantage; an intruder can reorder or delete some signature blocks so that the recipient does not know whether the message blocks have been rearranged or deleted. This disadvantage can be remedied by employing a redundancy mechanism to create linkages among message blocks, but it increases the communication costs.

As the public space and the communication costs can be reduced with message recovery to a large message, Tseng et al. [5] proposed an efficient authenticated encryption scheme with message linkage for message flows, which link up the message blocks to avoid the message block being reordered, replicated, or partially deleted during transmission. In this scheme, only a random number was used and the communication costs and the computational complexity were better than in previously proposed schemes [6][7][8].

The current paper, however, demonstrates the vulnerability of Tseng-Jan's authenticated encryption scheme that suffers from serious security faults such that any adversary can easily forge the valid signature blocks and pass the receiver's verification. Moreover, Tseng-Jan's scheme does not provide forward secrecy and non-repudiation [9]. We propose an improvement to the scheme to overcome these weaknesses. Compared with the Tseng-Jan's scheme, only one more exponentiation value is required in the improved scheme. Therefore, the proposed scheme preserves the main merits inherent in Tseng-Jan's authenticated encryption scheme.

The remainder of this paper is organized as follows: In Section 2, a brief review of the Tseng-Jan's scheme with message linkages is given, and then our cryptanalysis is proposed in Section 3. The improved scheme is presented in Section 4, while Section 5 discusses the security of the proposed protocol. Our conclusions are presented in Section 6.

2 Review of Tseng-Jan's Scheme

In this section, we briefly review Tseng-Jan's authenticated encryption scheme with message linkage and low communication costs. Tseng-Jan's proposed scheme

is divided into three phases: a system initialization phase, a signature generation phase, and a message recovery phase.

System Initialization Phase: In the system initialization phase, the system authority (SA) chooses a large prime number p such that $p - 1$ has a large prime factor q . Let g be a generator with order q in $GF(p)$. SA also selects a secure one-way hash function $f(\cdot)$. Then, SA publishes p , q , g and $f(\cdot)$. Each user in the system, U_i , selects a secret key x_i in Z_q and computes the corresponding public key $y_i = g^{x_i} \bmod p$.

Signature Generation Phase: Without loss of generality, assume that signer U_a wants to send message M to a specified receiver U_b . Message M is made up of the sequence $\{M_1, M_2, \dots, M_n\}$, where $M_i \in GF(p)$. Thus, signer U_a carries out the following procedure to generate the signature blocks for message M .

- (1) Choose a random number $k \in GF(q)$.
- (2) Compute $r_i = M_i \cdot f(r_{i-1} \oplus y_b^k) \bmod p$ for $i = 1, \dots, n$ and $r_0 = 0$, where “ \oplus ” denotes the exclusive or operator.
- (3) Compute $s = k - r \cdot x_a \bmod q$, where $r = f(r_1 || r_2 || \dots || r_n)$, f is a one-way hash function and “ $||$ ” denotes concatenation.

Finally, U_a sends $(n + 2)$ signature blocks $(r, s, r_1, r_2, \dots, r_n)$ to U_b in a public way. Note that r_i is used as a linking parameter to generate the i th and $(i + 1)$ th message blocks.

Message Recovery Phase: After receiving the set $(r, s, r_1, r_2, \dots, r_n)$, U_b performs the verification procedure to recover the message blocks $\{M_1, M_2, \dots, M_n\}$.

- (1) Compute $r' = f(r_1 || r_2 || \dots || r_n)$ and check whether $r' = r$ holds.
- (2) Compute

$$y_b^k = y_b^s \cdot y_{ab}^r \bmod p, \quad (1)$$

where $y_{ab} = y_a^{x_b} \bmod p$.

- (3) Recover the message blocks $\{M_1, M_2, \dots, M_n\}$ as follows:

$$M_i = r_i \cdot f(r_{i-1} \oplus y_b^k)^{-1} \bmod p, \quad (2)$$

for $i = 1, \dots, n$ and $r_0 = 0$.

3 Cryptanalysis of Tseng-Jan's Scheme

In this section, we point out that Tseng-Jan's authenticated encryption scheme suffers from serious security faults such that any adversary can forge valid signature blocks and pass the receiver's verification, and that the scheme does not provide forward secrecy and non-repudiation.

Forgery Attack: Suppose that adversary E intercepts the signature blocks $(r, s, r_1, r_2, \dots, r_n)$ sent from U_a to U_b , and that E chooses a random number r_n^* and changes r_n to r_n^* . Finally, E computes $r^* = f(r_1 || r_2 || \dots || r_n^*)$ and sends the modified signature blocks $(r^*, s, r_1, r_2, \dots, r_n^*)$ to the receiver. After receiving the modified signature blocks $(r^*, s, r_1, r_2, \dots, r_n^*)$, U_b performs the following verification procedure to recover the message blocks $\{M_1, M_2, \dots, M_n\}$:

- (1) Compute $r' = f(r_1 || r_2 || \dots || r_n^*)$ and check whether $r' = r^*$ holds. Obviously, the modified signature blocks will pass the checking process.
- (2) Compute $y_b^k = y_b^s \cdot y_{ab}^{r^*} \pmod{p}$, where $y_{ab} = y_a^{x_b} \pmod{p}$.
- (3) Recover the message blocks $\{M_1, M_2, \dots, M_n\}$ as follows:

$$M_i = r_i \cdot f(r_{i-1} \oplus y_b^k)^{-1} \pmod{p}, \text{ for } i = 1, \dots, n^* \text{ and } r_0 = 0.$$

Since an unreasonable y_b^k is computed by $y_b^s \cdot y_{ab}^{r^*} \pmod{p}$ in Step (2), there is no verification value in the modified signature blocks to check whether an unreasonable y_b^k is correct or not. As a result, since the recovered message is obviously not the signer's original message M , Tseng-Jan's scheme is vulnerable to the forgery attack.

Forward Secrecy Problem: Tseng-Jan's scheme does not provide forward secrecy as the Nyberg-Rueppel scheme does. When the secret key x_a of U_a is revealed by accident or is stolen, anyone can compute the Diffie-Hellman key $y_{ab} = y_b^{x_a} = y_a^{x_b} \pmod{p}$. Thus, all past communicated messages from U_a to U_b will lose confidentiality.

Non-repudiation Problem: Tseng-Jan's scheme does not satisfy non-repudiation property. As a signature scheme, if there are some disputes over the message signed, the signer or the receiver should be able to convince a third party that the signature is valid. Just like a signature scheme, a possible solution to this problem is to use the zero-knowledge protocol for the simultaneous discrete logarithms in [10]. The receiver U_b reveals y_b^k to a third party and proves that $r_i = M_i \cdot f(r_{i-1} \oplus y_b^k) \pmod{p}$ for $i = 1, \dots, n$, and $r = h(r_1 || r_2 || \dots || r_n)$. However, with the knowledge of y_b^k , a third party can derive Diffie-Hellman key y_{ab} from the equation $(y_b^k y_b^{-s})^{r^{-1}} \pmod{p}$. Therefore, for any ciphertext, the third party can recover the message from Equation (1) and (2).

4 Proposed Scheme

In this section, we present an improvement of Tseng-Jan's scheme. Since the signature blocks do not contain any verification value to check whether the signature blocks are transmitted from the legal signer or not, a forgery attack can succeed in Tseng-Jan's scheme. Additionally, the forward secrecy and non-repudiation problems occur because the Diffie-Hellman key y_{ab} is used to recover the signer's original message M . To overcome the weaknesses of Tseng-Jan's scheme, the signer U_a needs to send $(n + 2)$ signature blocks $(s, v, r_1, r_2, \dots, r_n)$ to

U_b as follows. The system initialization phase is the same as the one presented in Section 2. In the following, we only describe the other two phases. The proposed authenticated encryption scheme is illustrated in Figure 1.

Signature Generation Phase: Without loss of generality, let us assume that signer U_a wants to send message M to a specified receiver, U_b . Message M is made up of the sequence $\{M_1, M_2, \dots, M_n\}$, where $M_i \in GF(p)$. Thus, signer U_a carries out the following procedure to generate the signature blocks for message M .

- (1) Choose a random number $k \in GF(q)$.
- (2) Compute $r_i = M_i \cdot f(r_{i-1} \oplus y_b^k) \bmod p$ for $i = 1, \dots, n$ and $r_0 = 0$.
- (3) Compute $v = g^k \bmod p$ and $s = k \cdot v - r \cdot x_a \bmod q$, where $r = f(r_1 || r_2 || \dots || r_n)$.

Finally, U_a sends $(n + 2)$ signature blocks $(s, v, r_1, r_2, \dots, r_n)$ to U_b in a public way.

Message Recovery Phase: After receiving the set $(s, v, r_1, r_2, \dots, r_n)$, U_b performs the verification procedure to recover the message blocks $\{M_1, M_2, \dots, M_n\}$.

- (1) Compute $r' = f(r_1 || r_2 || \dots || r_n)$.
- (2) Check whether

$$v^v = g^s y_a^{r'} \bmod p \quad (3)$$

holds.

- (3) Compute $y_b^k = v^{x_b} \bmod p$.
- (4) Recover the message blocks $\{M_1, M_2, \dots, M_n\}$ as follows:

$$M_i = r_i \cdot f(r_{i-1} \oplus y_b^k)^{-1} \bmod p, \quad (4)$$

for $i = 1, \dots, n$ and $r_0 = 0$.

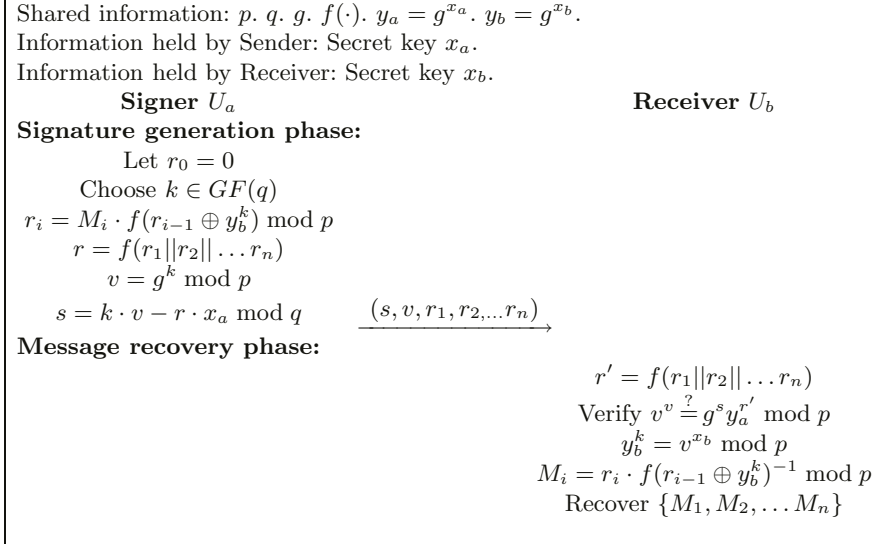
In the proposed message recovery phase, the message blocks $\{M_1, M_2, \dots, M_n\}$ can be correctly recovered and verified, since the verification equation (3) holds. Its validity is easy to see in that the left-hand side is

$$v^v = g^{k \cdot v} \bmod p$$

and the right-hand side is

$$\begin{aligned} g^s y_a^{r'} \bmod p &= g^{k \cdot v - r \cdot x_a} g^{x_a \cdot r'} \bmod p \\ &= g^{k \cdot v - r \cdot x_a + x_a \cdot r'} \bmod p \\ &= g^{k \cdot v} \bmod p, \end{aligned}$$

where $s = k \cdot v - r \cdot x_a \bmod q$ and $r = f(r_1 || r_2 || \dots || r_n)$. As a result, since $r_i = M_i \cdot f(r_{i-1} \oplus y_b^k) \bmod p$, M_i can be obtained by equation (4).

**Fig. 1.** Proposed authenticated encryption scheme

5 Security Analysis

In this section, we provide a security analysis of the proposed authenticated encryption scheme. First, we define the security terms [11] needed for providing the security of the proposed scheme as follows:

Definition 1. A secure one-way hash function $y = f(x)$ is one in which given x to compute y is easy and given y to compute x is hard.

Definition 2. The discrete logarithm problem (DLP) is the following: given a prime p , a generator g of Z_p^* , and an element $\alpha \in Z_p^*$, find the integer α , $0 \leq \alpha \leq p-2$, such that $g^\alpha \equiv \beta \pmod{p}$.

In light of the above definitions, we analyze the security of the proposed scheme as follows:

- (1) Adversary E tries to derive a user's secret key x_i from the corresponding public key $y_i = g^{x_i} \bmod p$. E will face the difficulty of computing the discrete logarithm problem by Definition 2. It is also difficult to derive the secret key x_i from $s = k \cdot v - r \cdot x_a \bmod q$, because the equation has two unknown variables.
- (2) If the signature blocks are changed by adversary E , i.e., r or both r and v are illegally changed by adversary E , it will lead to the relation $v^v = g^s y_a^{r'} \bmod p$ not hold. For this forgery attack to succeed, E should compute valid $s = k \cdot v - r \cdot x_a \bmod q$ that can be hold the verification equation (3). However,

with the signature blocks $(s, v, r_1, r_2, \dots, r_n)$, E cannot derive the signer's secret key x_a from s , since the equation contains two unknown variables, k and x_a , and k is protected under the secure one-way hash function and the DLP assumptions. Therefore, the receiver can easily check whether the signature blocks are transmitted from the legal signer U_a by Step (2) of the message-recovery phase. As a result, the proposed scheme can resist forgery attack.

- (3) Adversary E may try to forge (including reorder, delete and substitute etc.) a signature for new messages by using a valid signature. Without a loss of generality, we assume that E tries to substitute M'_i for M_i . Since f cannot be inverse due to the secure one-way hash function property by Definition 1, E must compute $r_i^* = M_i^* \cdot f(r_{i-1} \oplus y_b^k) \bmod p$. However, the probability of $f(r_1 \parallel \dots \parallel r_i \parallel \dots \parallel r_n) = f(r_1 \parallel \dots \parallel r_i^* \parallel \dots \parallel r_n)$ is negligible because $f(\cdot)$ is strong collision resistant by Definition 1.
- (4) When the secret key x_a of U_a is revealed, anyone can compute the Diffie-Hellman key $y_{ab} = y_b^{x_a} = y_a^{x_b} \bmod p$. However, unlike Tseng-Jan's scheme, the Diffie-Hellman key y_{ab} is useless to recover the signer's original message M in the proposed message recover phase. Therefore, there are no forward secrecy problems or non-repudiation property problems in the proposed scheme.
- (5) If there are some disputes over the message signed, the signer or the receiver should have a way to convince a third party that the signature is valid. The receiver U_b reveals y_b^k to the third party and proves that $r_i = M_i \cdot f(r_{i-1} \oplus y_b^k) \bmod p$ for $i = 1, \dots, n$, and $r = h(r_1 \parallel r_2 \parallel \dots \parallel r_n)$. However, with the knowledge of y_b^k , the third party cannot derive $y_b^{k'}$ to recover message M' from the values $r'_i = M'_i \cdot f(r'_{i-1} \oplus y_b^{k'}) \bmod p$, $v = g^{k'} \bmod p$ and $s = k \cdot v - r \cdot x_a \bmod q$ because the third party cannot know the random number $k' \in GF(q)$ from $v = g^{k'} \bmod p$ to compute $y_b^{k'}$. That is, the third party will face the secure one-way hash function property and the difficulty of computing the discrete logarithm problem by Definition 1 and Definition 2, respectively. Therefore, for any ciphertext, the third party cannot recover the signer's other message M' .

6 Conclusion

The current paper demonstrated the vulnerability of Tseng-Jan's authenticated encryption scheme, which suffers from serious security faults that any adversary can easily forge the valid signature blocks and pass the receiver's verification, and the scheme does not provide forward secrecy and non-repudiation. We proposed an improvement to the scheme to overcome these weaknesses. Compared with the Tseng-Jan's scheme, only one more exponentiation value is required in the proposed scheme. Therefore, the proposed scheme preserves the main merits inherent in Tseng-Jan's authenticated encryption scheme.

Acknowledgements

We would like to thank the anonymous reviewers for their helpful comments to improve our manuscript. This research was supported by the MIC (Ministry of Information and Communication), Korea, under the ITRC (Information Technology Research Center) support program supervised by the IITA (Institute of Information Technology Assessment).

References

1. Nyberg, K., Rueppel, R.A.: Message Recovery for Signature Schemes Based on the Discrete Logarithm. *Advances in Cryptology – EUROCRYPT’94*. Springer-Verlag. (1994) 175-190
2. Nyberg, K., Rueppel, R.A.: Message Recovery for Signature Schemes Based on the Discrete Logarithm. *Designs, Codes and Cryptography*. Vol. 7. (1996) 61-81
3. Horster, P., Michels, M., Petersen, H.: Authenticated Encryption Schemes with Low Communication Costs. *Electronics Letters*. Vol. 30. (1994) 1212
4. Lee, M., Kim, D., Park, K.: An Authenticated Encryption Scheme with Public Verifiability. *Japan-Korea Joint Workshop on Algorithms and Computation (WAAC2000)*. (2000) 49-56
5. Tseng, Y.M., Jan, J.K.: An Efficient Authenticated Encryption Scheme with Message Linkages and Low Communication Costs. *Journal of Information Science and Engineering*. Vol. 18. (2002) 41-46
6. Hwang, S.J., Chang, C.C., Yang, W.P.: Authenticated Encryption Schemes with Message Linkages. *Information Processing Letters*. Vol. 58. (1996) 189-194
7. Lee, W.B., Chang, C.C.: Authenticated Encryption Scheme without using a One-way Hash Function. *Electronics Letters*. Vol. 31. (1995) 1656-1657
8. Lee, W.B., Chang, C.C.: Authenticated Encryption Schemes with Linkage between Message Blocks. *Information Processing Letters*. Vol. 63. (1997) 247-250
9. Chen, B.H.: Improvements of Authenticated Encryption Schemes With Message Linkages for Message Flows. *Computers and Electrical Engineering*. Vol. 30. (2004) 465-469
10. Boyar, J., Chaum, D., Damgard, I., Pederson, T.: Convertible Undeniable Signatures. *Crypto’90*. Springer-Verlag. (1991) 189-205
11. Menezes, A.J., Oorschot, P.C., Vanstone, S.A.: *Handbook of Applied Cryptograph*. CRC Press. New York. (1997)

BPCS-Steganography – Principle and Applications

Eiji Kawaguchi

Keio University, Research Institute for Digital Media and Content

2-15-45 Mita, Minato-ku, Tokyo 108-8345 Japan

e - kawagu@alto.ocn.ne.jp

Abstract. The abstract should summarize the contents of the paper and should Steganography is a technique to hide secret information in some other data (we call it a vessel) without leaving any apparent evidence of data alteration. All of the traditional steganographic techniques have limited information-hiding capacity. This is because the principle of those techniques was either to replace a special part of the frequency components of the vessel image, or to replace all the least significant bits of a multi-valued image with the secret information. Our new steganography uses an image as the vessel data, and we embed secret information in the bit-planes of the vessel. This technique makes use of the characteristics of the human vision system whereby a human cannot perceive any shape information in a very complicated binary pattern. We can replace all of the “noise-like” regions in the bit-planes of the vessel image with secret data without deteriorating the image quality. We termed our steganography “BPCS-Steganography,” which stands for Bit-Plane Complexity Segmentation Steganography.

1 Introduction

Internet communication has become an integral part of the infrastructure of today’s world. In some Internet communication it is desired that the communication be done in secrete. Encryption provides an obvious approach to information security, and encryption programs are readily available. However, encryption clearly marks a message as containing “interesting” information, and the encrypted message becomes subject to attack. Furthermore, in many cases it is desirable to send information without anyone even noticing that information has been sent.

Steganography presents another approach to information security. In steganography, data is hidden inside a vessel or container that looks like it contains only something else. A variety of vessels are possible, such as digital images, sound clips, and even executable files. In recent years, many steganographic programs have been posted on Internet Web pages. Most of them use image data for the container of the secret information. Some of them use the least significant bits of the image data to hide secret data. Other programs embed the secret information in a specific band of the spatial frequency component of the carrier. Some other programs make use of the sampling error in image digitization. However, all those steganographic techniques are limited in terms of information hiding capacity. They can embed only 5-15 % of the vessel image at the best. Therefore, traditional steganography is more oriented to water marking of computer data than to secret person-person communication applications.

We have invented a new technique to hide secret information in a color image. This is not based on a programming technique, but is based on the property of human

vision system. Its information hiding capacity can be as large as 50% of the original image data. This could open new applications for steganography leading to a more secure Internet communication age.

Some other aspect of the new steganography is that it is very fragile, i.e., the embedded information is easily destroyed even by a small vessel alteration. This is not a weak point, but it is a strong point when we apply it to a document-alteration detective system.

Digital images are categorized as either binary (black-and-white) or multi-valued pictures despite their actual color. We can decompose an n-bit image into a set of n binary images by bit-slicing operations [1][2]. Therefore, binary image analysis is essential to all digital image processing. Bit slicing is not necessarily the best in the standard binary coding system (We call it Pure-Binary Coding system (PBC)), but in some cases the Canonical Gray Coding system (CGC) is much better [3].

2 The Complexity of Binary Images

The method of steganography outlined in this paper makes use of the complex regions of an image to embed data. There is no standard definition of image complexity. Kawaguchi discussed this problem in connection with the image thresholding problem, and proposed three types of complexity measures [4][5][6]. In the present paper we adopted a black-and-white border image complexity.

2.1 The Definition of Image Complexity

The length of the black-and-white border in a binary image is a good measure for image complexity. If the border is long, the image is complex, otherwise it is simple. The total length of the black-and-white border equals to the summation of the number of color-changes along the rows and columns in an image. For example, a single black pixel surrounded by white background pixels has the boarder length of 4.

We will define the image complexity α by the following.

$$\alpha = \frac{k}{\text{The max. possible B - W changes in the image}} \quad (1)$$

Where, k is the total length of black-and-white border in the image. So, the value ranges over

$$0 \leq \alpha \leq 1. \quad (2)$$

(1) is defined globally, i.e., α is calculated over the whole image area. It gives us the global complexity of a binary image. However, we can also use α for a local image complexity (e.g., an 8×8 pixel-size area). We will use such α as our local complexity measure in this paper.

3 Analysis of Informative and Noise-Like Regions

Informative images are simple, while noise-like images are complex. However, this is only true in cases where such binary images are part of a natural image. In this sec-

tion we will discuss how many image patterns are informative and how many patterns are noise-like. We will begin by introducing a “conjugation” operation of a binary image.

3.1 Conjugation of a Binary Image

Let P be a $2^N \times 2^N$ size black-and-white image with black as the foreground area and white as the background area. W and B denote all-white and all-black patterns, respectively. We introduce two checkerboard patterns W_c and B_c , where W_c has a white pixel at the upper-left position, and B_c is its complement, i.e., the upper-left pixel is black (See Fig. 1). We regard black and white pixels as having a logical value of “1” and “0”, respectively.

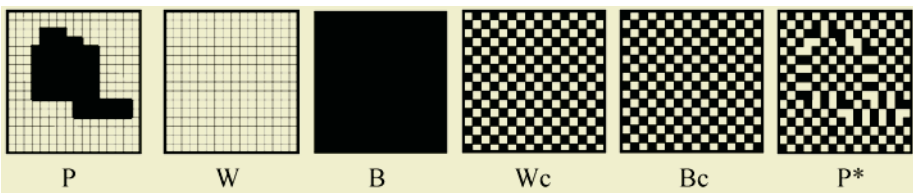


Fig. 1. Illustration of each binary pattern ($N=4$)

P is interpreted as follows. Pixels in the foreground area have the B pattern, while pixels in the background area have the W pattern. Now we define P^* as the conjugate of P which satisfies:

1. The foreground area shape is the same as P .
2. The foreground area has the B_c pattern.
3. The background area has the W_c pattern.

Correspondence between P and P^* is one-to-one, onto. The following properties hold true and are easily proved for such conjugation operation. “ \oplus ” designates the exclusive OR operation.

$$A) P^* = P \oplus W_c \quad (3)$$

$$B) (P^*)^* = P \quad (4)$$

$$C) P^* \neq P \quad (5)$$

$$D) \text{Let } \alpha(P) \text{ be the complexity of a given image } P, \text{ then we have,} \quad (6)$$

$$\alpha(P^*) = 1 - \alpha(P).$$

It is evident that the combination of each local conjugation (e.g., 8×8 area) makes an overall conjugation (e.g., 512×512 area). (6) says that every binary image pattern P has its counterpart P^* . The complexity value of P^* is always symmetrical against P regarding $\alpha = 0.5$. For example, if P has a complexity of 0.7, then P^* has a complexity of 0.3.

3.2 Criterion to Segment a Bit-Plane into Informative and Noise-Like Regions

We are interested in how many binary image patterns are informative and how many patterns are noise-like with regard to the complexity measure α .

Firstly, as we think 8×8 is a good size for local area, we want to know the total number of 8×8 binary patterns in relation to α value. This means we must check all 2^{64} different 8×8 patterns. However, 2^{64} is too huge to make an exhaustive check by any means. Our practical approach is as follows. We first generate as many random 8×8 binary patterns as possible, where each pixel value is set random, but has equal black-and-white probability. Then we make a histogram of all generated patterns in terms of α . This simulates the distribution of 2^{64} binary patterns.

Fig.2 shows the histogram for 4,096,000 8×8 patterns generated by our computer. This histogram shape almost exactly fits the normal distribution function as shown in the figure. We would expect this by application of the central limit theorem. The average value of the complexity α was exactly 0.5. The standard deviation was 0.047 in α . We denote this deviation by σ ("sigma" in Fig. 2)

Secondly, our next task is to determine how much image data we can discard without deteriorating the image quality, or, rather at what complexity does the image data become indispensable.

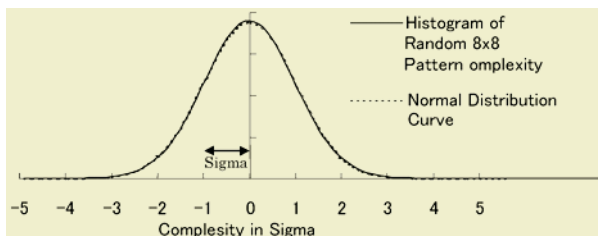


Fig. 2. Histogram of randomly generated 8×8 binary patterns

To discard data means to replace local image areas in a bit-plane with random noise patterns. If we replace all the local areas having complexity value $\alpha_L \leq \alpha$, yet the image still maintains good quality, then perhaps we can discard more. If the quality is no longer good, then we can not discard that much. If $\alpha = \alpha_L$ is the minimum complexity value to be good, such α_L is used as the threshold value.

To be indispensable, or rather "informative," for an image means the following. If the image data is still "picture-like" after we have discarded (randomized) a certain amount of image data for such an α that $\alpha \leq \alpha_U$, and if we discard more, then it becomes only noise-like. Then, that α_U is regarded as the limit of the informative image complexity.

If α_L and α_U coincide ($\alpha_0 = \alpha_L = \alpha_U$), we can conclude α_0 is the complexity threshold to divide informative and noise-like regions in a bit-plane.

We made a "random pattern replacing" experiment on a bit-plane of a color image. Fig. 3 illustrates the result.

Fig. 3 shows that if we randomize regions in each bit-plane which are less complex than $0.5 - 8\sigma$, the image can not be image-like any more. While, we can randomize the more complex regions than $0.5 - 8\sigma$ without losing much of the image information. This means the most of the informative image information is concentrated in between 0 and $0.5 - 8\sigma$ in complexity scale. Surprising enough, it is only 6.67×10^{-14} % of all 8×8 binary patterns. Amazingly, the rest (i.e., 99.999999999999333%) are mostly noise-like binary patterns.

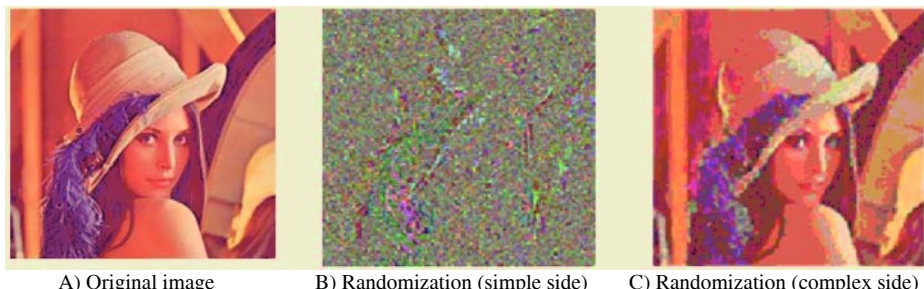


Fig. 3. Randomization of the less and the more complex than $\alpha = 0.5 - 8\sigma$

The conclusion of this section is as follows. We can categorize the local areas in the bit-planes of a multi-valued image into three portions (1) Natural informative portions (2) Artificial informative portions (3) Noise-like portions. The reason we categorize the excessively complicated patterns as “informative” is based on our experiments [7].

The most important fact here is that replacing a noise-like portion with any noise-like 8×8 binary blocks doesn't produce any visual change on the vessel.

4 BPCS-Steganography

Bit-Plane Complexity Segmentation Steganography (BPCS-Steganography) is our new steganographic technique, which has a large information hiding capacity. As have shown in the previous section, the replacement of the complex regions in each bit-plane of a color image with random binary patterns is invisible to the human eye. We can use this property for our information hiding (or, embedding) strategy. The term information embedding capacity is the same as information hiding capacity.

In our method we call a carrier image a “vessel” or “dummy” image. It is a color image in BMP file format, which embeds the secret information (files in any format). We segment each secret file (already compressed form) to be embedded into a series of blocks having 8 bytes of data each. These blocks are regarded as 8×8 image patterns. We call such blocks the secret blocks. We embed these secret blocks into the vessel image using the following steps.

1. Convert the vessel image from PBC to CGC system.
This conversion is executed by the exclusive-or operation [3].
2. Segment each bit-plane of the vessel image into informative and noise-like regions by using a threshold value (α_0). A typical value is $\alpha_0 = 0.25$.
3. Group the bytes of the secret file into a series of secret blocks.
4. If a block (S) is less complex than the threshold (α_0), then conjugate it to make it a more complex block (S^*). The conjugated block must be more complex than α_0 as shown by equation (6).
5. Embed each secret block into the noise-like regions of the bit-planes (or, replace all the noise-like regions with a series of secret blocks). If the block is conjugated, then record this fact in a “conjugation map.”
6. Also embed the conjugation map as was done with the secret blocks.
7. Convert the embedded vessel image from CGC back to PBC.

The Decoding algorithm (i.e., the extracting operation of the secret information from an embedded vessel image) is just the reverse procedure of the embedding steps.

The novelty in BPCS-Steganography is itemized in the following.

- A) Segmentation of each bit-plane of a color image into “Informative” and “Noise-like” regions.
- B) Introduction of the B-W border based complexity measure (α) for region segmentation.
- C) Introduction of the conjugation operation to convert simple secret blocks to complex blocks.
- D) Using CGC image plane instead of PBC plane.
- E) There are many variations in implementing a BPCS-Steganography program.
Such variation can be put into an embedding/extraction key. This key is neither included in the program, nor hidden in the vessel image.

5 Examples of Embedding

5.1 Embedding Capacity

We have developed a BPCS-Steganography program for Windows. In that program, we took an 8×8 square as the local image size. Fig. 4 (A) is an example of an original vessel image (800x600, 24bit BMP color). (B) is the same image after embedding all the files in Fig. 5 (A). As indicated in the table, the embedded information includes several image files in JPEG format, a technical paper in PDF, a video clip in MPEG, and a plain text file. These files were automatically compressed when embedded. However, JPEG files were not any more compressed because they were already compressed in its JPEG file format. PDF and MPEG files were not so much compressed. Only the plain text file was compressed by almost 50% when embedded. The actual embedding ratio in this example was a little less than 50%. The embedding capacity changes by the “complexity threshold value” to segment each bit-plane into noise-like or informative region. If the threshold is set small, the capacity increases, but become more easy to deteriorate the vessel.

The embedding operation does not increase the size of the vessel image by even a single byte. Yet, even when viewed on the computer monitor, the images before and after embedding are almost indistinguishable from one another.

Another example of embedding is shown in Fig. 6. It is a multiple embedding of BMP files with different sizes. First, Renoir-4 was embedded in Renoir-3, then it was embedded in Renoir-2, then in Renoir-1, and all were finally embedded in Renoir-0.

5.2 General Property of BPCS-Steganography

The property of BPCS-Steganography is summarized as follow.

- 1) The embedding capacity is very large compared with traditional steganography methods.
- 2) Embedded information is fragile.
- 3) Embedded data adhere to the vessel image.
- 4) Embedding/extracting operation is fast in time.



(A) Original vessel image (1.407MB, BMP) (B) Embedded vessel image (1.407MB, BMP)

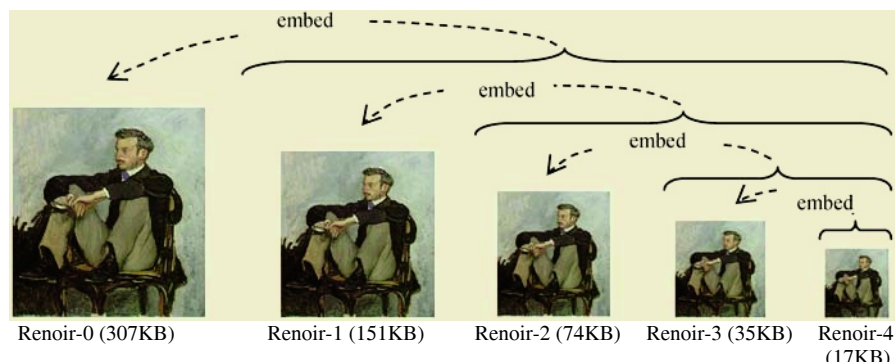
Fig. 4. Example of a vessel image

| File Name | File Size (KB) |
|---------------|----------------|
| article.pdf | 114 |
| astronaut.jpg | 35 |
| millet.jpg | 8 |
| lena.jpg | 52 |
| moglie.mpg | 286 |
| mona_lisa.jpg | 77 |
| text.txt | 176 |
| Total | 748 |

(A) Summary of embedded data



(B) Embedded pictures

Fig. 5. Files embedded in Fig 4(B)**Fig. 6.** Multiple embedding using BMP image files

The property 3) means the embedded information is always carried by the vessel image. They are never separated and the embedded data will not be removed.

The property 4) is based on the fact that the basic BPCS algorithm is implemented by operations such as addition, subtraction, comparison in integer, character matching, etc. No complicated computation is needed.

6 Applications of BPCS-Steganography

Traditional steganography has been regarded as a technique to hide secret information as well as its location to keep it confidential. No other applications were discussed in deep till today. BPCS-Steganography, in the mean time, can be applied to more.

BPCS-Steganography applications are categorized into several types according to its property shown above.

6.1 Confidential Data Storage and Communication

This application category makes use of the property 1 of BPCS-Steganography. They are all straightforward applications.

For confidential data storage, secret data are embedded in a group of vessel images and they are stored in a computer disk. For confidential communication, a secret message is embedded in an innocuous-looking vessel image, and it is attached to an ordinary e-mail message. The sender and the receiver must negotiate which common key they will use before they start communication.

A web-based communication scheme is one of the most hard-to-detect methods. A common key is used, too. Fig. 7 illustrates the scheme. The communication proceeds as follows, where A and B are two persons having a respective home-page on the Web.

Step-1: A and B decide a common key.

Step-2: A embeds his secret message that is addressed to B in A's image

Step-3: A uploads the message-embedded image onto A's home-page

Step-4: B downloads the image and extracts the message by using the key and receive the message

Step-5: B embeds his reply-message in B's image

Step-6: B uploads the image onto B's home-page

Step-7: A downloads the image and extract the reply-message to read the reply-message

Thus, it is extremely difficult to know who are corresponding to whom.

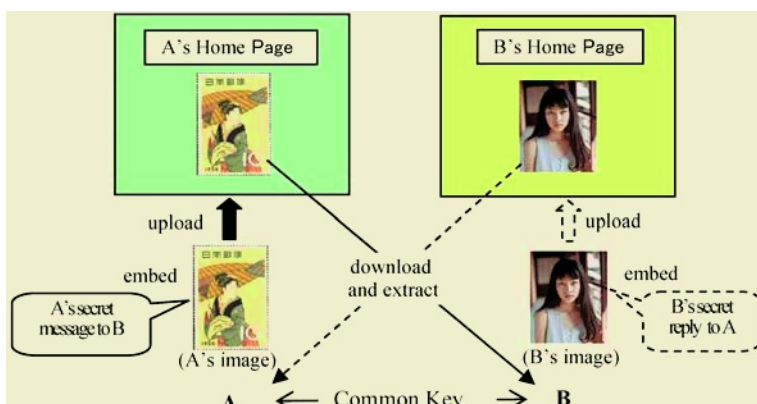


Fig. 7. Web-based mutual communication scheme

6.2 Forgery Detection of Digital Certificate Document

This application category makes use of the general property 2 of BPCS-Steganography. Currently, an original certificate document is “written” or “printed” on a paper surface or on a plastic card. No computer documents can serve as a certificate. This is because every computer document today has a “single-layered information structure” in the sense that all information there is just as it looks. No unseen information is included. It is alterable by a document editor. (A PDF file is not very easy to alter, but still editable.) So, digital documents are all forgeable and it is impossible to tell if a given document is real or fake by itself. This is the reason why we can’t e-mail a digital certificate document over the Internet. A digital signature system is necessary, and is available, to make a digital document authentic. However, that system is based on an extra information-infrastructure, namely, human authentication bureau. This method is not very easy for daily use. Therefore, if someone invents some computer data that works as a digital certificate document without any external framework, it is revolutionary.

We will firstly classify the types of certificate-document forgery into two categories [8].

Type-1 Forgery: Altering a part of an authentic certificate

This is attempted on a driver’s certificate, credit card, passport (photo), student transcript (grading score), etc.

Type 2 Forgery: Creating a new fake certificate

Examples of this category are on PhD diploma, pedigree, expert evidence, medical certificate, etc.

A fragile steganography, like BPCS, can be used for protecting both types of forgery in a digital form.

Digital documents generally include several data-types such as plain texts, graphics, images, and even motion pictures in some special case. When people see them on a computer monitor, they look all image information. People don’t care if the original data consist of several different types or just one image data. So, we will convert the digital document data into image data. However, this converted image has a single layered information structure, and still remains being forgeable.

A multi-layered information structure is as follows. It has an external layer which is visible and an internal layer which is invisible (unseen) for human eye. The internal layer can further be structured as sub-external and sub-internal layers. This multi-layered information structure is easily implemented by steganographic information hiding technique, BPCS or not.

In order for a digital document to serve as a certificate (to protect both types of forgeries), we will do the following.

Step-1: Convert a given digital document consisting of several data types into one single image data.

We call this conversion “vessel image creation.” The data size will increase significantly by this conversion.

Step-2: Embed the original document data in the created vessel image according to a steganography program.

This process needs a large data-embedding capacity. BPCS method has such

a large capacity. The external view of the embedded vessel-image is the external information layer, and the embedded original document is the internal information layer. The internal information can be extracted according to an extracting program of the steganography if it is not damaged.

As is clear from the step-2, the external and the internal layer have the same visual information. In order for someone to alter this multi-layered digital document successfully, he/she must alter both the external and the internal information at the same time. However, this is impossible from the natural nature of steganography in general. On top of that, once he/she tries to alter a part of the external layer, it will instantly damage the internal layer because the embedded data is so fragile, especially the BPCS case is. Once the internal layer is damaged, the internal layer will never be extracted.

Type-1 Forgery Detection

Deciding if a given digital certificate document having multi-layered information structure is authentic or not in the type-1 sense is very easy. If the internal data extraction fails, the digital certificate document is forged. If extracted successfully, but some discrepancy found between the external and the extracted visual information, the certificate document is forged. Otherwise, the document is authentic.

Type-2 Forgery Detection

A type-2 forgery protective digital certificate needs some additional scheme. It is a “one-way scrambled key” to embed the original document data, and also to extract it. The detailed scheme is described in the other paper [8].

The forgery detection capability depends on the fragileness of the steganography that we use. In order to boost up the fragileness of BPCS-Steganography, we have employed additional Cross-Bit-Planes EOR (Exclusive OR operation) operations before embedding. However, the topic is too much detailed for this paper.

6.3 Media Database System Application

Most database system has varieties of metadata within itself. They are used for data retrieving. A media database system today handles the media data and its metadata in separate categories, but tightly associates each other within the DBMS. One troublesome problem here is as follows. When someone creates and edits metadata, he/she must work under a dedicated editing system that is a part of the DBMS. This means the work place for metadata handling is limited within that DBMS. So, editing metadata “off-line” is very difficult.

Another problem is the difficulty of a local database re-organization. This happens when someone wants to download a set of specially localized media data from a large database system and tries to re-organize or merge with other local database. He/she may able to collect and down load the media data, but may not able to download the associated metadata as he/she wants.

These are caused by the fact that media data and the metadata are separately located in the system and associated with each other under the control of the DBMS.

One solution to this problem is that each media data carries its own metadata as well as some additional data that may be used in some other system in an embedded

form by a steganography like BPCS. This application of BPCS-Steganography makes use of its general property 3. Our research group started a new project to implement a “metadata included media database system” in Keio University.

7 Conclusions and Future Work

The objective of this paper was to describe the principle and applications of our BPCS-Steganography, which is based on a property of the human visual system. The most important point for this technique is that humans can not see any information in the bit-planes of a color image if it is very complex. We have discussed the following points and showed our experiments.

- (1) We can categorize the bit-planes of a natural image as informative areas and noise-like areas by the complexity thresholding.
- (2) Humans see informative information only in a very simple binary pattern.
- (3) We can replace complex regions with secret information in the bit-planes of a natural image without changing the image quality. This leads to our BPCS-Steganography.
- (4) Gray coding provides a better means of identifying which regions of the higher bit planes can be embedded.

We are very convinced that this steganography is a very strong information security technique, especially when combined with encrypted embedded data. It will be applied to secret data storage and confidential communications. Furthermore, it can be applied to many other areas like digital document forgery detection and database applicatins. Future research will include the application to vessels other than 24-bit images, implementing a specific digital certificate document system which we explained in section 6.2.

References

1. Hall, Ernest L., *Computer Image Processing and Recognition*, Academic Press, New York, 1979.
2. Jain, Anil K., *Fundamentals of Digital Image Processing*, Prentice Hall, Englewood Cliffs, NJ, 1989.
3. Kawaguchi, E., Endo, T. and Matsunaga, J., “Depth-first picture expression viewed from digital picture processing”, *IEEE Trans. on PAMI*, vol.5, no.4, pp.373-384, 1983.
4. Kawaguchi, E. and Taniguchi, R., “Complexity of binary pictures and image thresholding - An application of DF-Expression to the thresholding problem”, *Proceedings of 8th ICPR*, vol.2, pp.1221-1225, 1986.
5. Kawaguchi, E. and Taniguchi, R., “The DF-Expression as an image thresholding strategy”, *IEEE Trans. on SMC*, vol.19, no.5, pp.1321-1328, 1989.
6. Kamata, S., Eason, R. O., and Kawaguchi, E., “Depth-First Coding for multi-valued pictures using bit-plane decomposition”, *IEEE Trans. on Comm.*, vo.43, no.5, pp.1961-1969, 1995.
7. Kawaguchi, E. and Niimi M, “Modeling Digital Image into Informative and Noise-Like Regions by Complexity Measure”, in *INFORMATION MODELLING AND KNOWLEDGE BASES XV*, IOS Press, pp.255-265, 1998.
8. Nozaki, K., Noda, H., Kawaguchi, E. and Eason, R., “A Model of Unforgeable Digital Certificate Document System”, in *INFORMATION MODELLING AND KNOWLEDGE BASES XVI*, IOS Press, pp.203-210, 2005.

Improved Video Watermark Detection Using Statistically-Adaptive Accumulation

Isao Echizen¹, Yasuhiro Fujii¹, Takaaki Yamada¹,
Satoru Tezuka¹, and Hiroshi Yoshiura²

¹ Systems Development Laboratory, Hitachi, Ltd.,
890 Kashimada, Saiwai-ku, Kawasaki, 212-8567, Japan

{iechizen,fujii,t-yamada,tezuka}@sdl.hitachi.co.jp

² Faculty of Electro-Communication, The University of Electro-Communications,
1-5-1, Chofugaoka, Chofu, 182-8585, Japan

yoshiura@hc.uec.ac.jp

Abstract. Redundant coding is a basic method that embeds watermarks repeatedly in every frame or region and thus can prevent errors by the accumulation of the frames or the regions in watermark detection. It would not always be effective, however, because many kinds of image processing would remove watermarks from specific frames or regions and then remaining watermarks would be attenuated by the accumulation procedure of the frames or the regions from which watermarks were removed. We therefore propose a detection method preventing this attenuation by estimating bit-error rate from each watermarked region and selecting the regions so that the region accumulating the selected regions has the minimal bit-error rate. Experimental evaluations have shown that the new method can improve watermark survivability after MPEG encoding by an average of 15.5% and can be widely used in statistically based watermarking.

Keywords: video watermarking, improving detection, bit-error rate

1 Introduction

Watermarking can be used to embed copyright and copy-control information in video pictures and will therefore be used in DVD players and recorders as well as in digital broadcasting equipment such as set-top boxes. Video providers subject the watermarked pictures to various kinds of image processing—such as compression (using MPEG or other compression technology), resizing, filtering, and D/A or A/D conversion—and these image processing procedures can also be exploited by illegal users who want to remove the embedded information. The watermarks should nonetheless be robust enough to be reliably detected after any of these kinds of processing. Watermark (WM) survivability is thus essential and methods for improving WM survivability have been studied in both the pixel and frequency domains. Methods using redundant coding [1–3] and spread spectrum coding [4] of the embedded information have been established, as have methods

for embedding information in perceptually insignificant parts of the pictures [5] and in elements that will be little affected by the expected image processing [6].

The redundant coding is a basic method that embeds watermarks repeatedly in every frame or regions and thus can prevent errors by accumulating the frames or the regions coded repeatedly in watermark detection. It, however, would not be always effective after image processing procedures that can remove WMs on the specific frames or regions because the remaining WMs would be attenuated by the simple accumulation procedure of the frames or regions from which WMs were removed. The detection methods should therefore use a measure of the degree of remanence of WMs in each region of frame and should control accumulation according to this measure (*e.g.*, by not accumulating regions or frames having a low degree of WM remanence).

We thus propose a detection method that estimates the bit-error rate of WMs in each watermarked region on the frame by using inferential statistics and that selects the regions so that the region accumulating the selected regions has the minimal bit-error rate. Section 2 of this paper describes one of the previous methods and the problem with it. Section 3 describes our proposed method, Section 4 reports experimental evaluations confirming that the proposed method can withstand image processing, and Section 5 concludes the paper.

2 Previous Method

The redundant coding methods can be classified into the following two types:

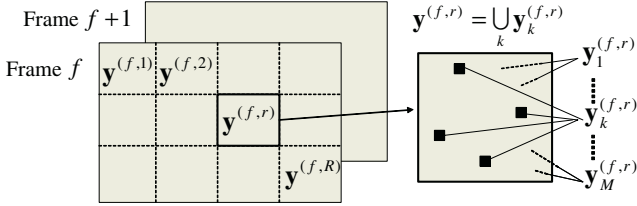
- (a) **Redundant coding within a frame:** Watermark embedding is done by dividing the frame picture into several regions and applying the same watermark in each region. In WM detection, WMs are extracted by accumulating all the divided pictures in a frame [1, 2].
- (b) **Redundant coding over frames:** WM embedding is done by applying the same watermark in each consecutive frame of the video. In WM detection, WMs are extracted by accumulating all the frames or a specific number of sequential frames [2, 3].

Among these methods, the method [2] is one of the basic WM schemas employing both of types (a) and (b). We briefly describe the previous method [2] and the problem with it.

WM Embedding. The luminance set of the f th frame consisting of N pixels is $\mathbf{y}^{(f)} = \{y_i^{(f)} \mid 1 \leq i \leq N\}$. The process flow of the M -bit-WM embedding is described below:

Step E1: Do the following steps over $f = 1, 2, \dots$

Step E2: Divide $\mathbf{y}^{(f)}$ into RM regions $\mathbf{y}_k^{(f,r)}$ s ($r = 1, \dots, R, k = 1, \dots, M$) consisting of the corresponding pixels: $\mathbf{y}_k^{(f,r)} = \{y_{k,i}^{(f,r)} \mid 1 \leq i \leq \lfloor N/(RM) \rfloor\}$, which satisfies $\mathbf{y}^{(f)} = \bigcup_{r,k} \mathbf{y}_k^{(f,r)}$, $\mathbf{y}_k^{(f,r)} \cap_{r \neq r'} \mathbf{y}_{k'}^{(f,r')} = \emptyset$, and $\mathbf{y}_k^{(f,r)} \cap_{k' \neq k} \mathbf{y}_{k'}^{(f,r)} = \emptyset$ (See example shown in Fig. 1).

**Fig. 1.** Example of video partitioning

Step E3: Generate each watermarked region $\mathbf{y}_k'^{(f,r)}$ by adding the WM pattern $\mathbf{m}_k = \{m_{k,i} \in \{-1, +1\} \mid 1 \leq i \leq \lfloor N/(RM) \rfloor\}$ comprising a pseudo random array ± 1 s into the original region $\mathbf{y}_k^{(f,r)}$:

$$y_{k,i}'^{(f,r)} = \begin{cases} y_{k,i}^{(f,r)} + \mu^{(f,r)} m_{k,i} & \text{if } b_k = 1 \\ y_{k,i}^{(f,r)} - \mu^{(f,r)} m_{k,i} & \text{if } b_k = 0, \end{cases}$$

where $\mu^{(f,r)}$ is WM strength of the region $\mathbf{y}^{(f,r)}$.

WM Detection. Calculate M statistical values v_k s of the accumulated frame for each region by using the following procedure to correlate the WM pattern \mathbf{m}_k with the accumulated watermarked regions:

Step D1: Do the following steps over $f_0 = 1, F+1, 2F+1, \dots$

Step D2: For each k ($k = 1, \dots, M$), accumulate FR regions $\mathbf{y}_k'^{(f,r)}$ s ($f = f_0, \dots, f_0 + F - 1, r = 1, \dots, R$) in the region $\mathbf{a}'_k = \{a'_{k,i} \mid 1 \leq i \leq \lfloor N/(RM) \rfloor\}$. The $a'_{k,i}$ of the accumulated region \mathbf{a}'_k is given by

$$a'_{k,i} = \frac{1}{FR} \sum_{f=f_0}^{f_0+F-1} \sum_{r=1}^R y_{k,i}'^{(f,r)}.$$

Step D3: Calculate the set consisting of the M statistical values $\mathbf{v} = \{v_k \mid 1 \leq k \leq M\}$. The statistical value v_k is obtained by correlating the WM pattern \mathbf{m}_k with the accumulated region \mathbf{a}'_k . That is,

$$v_k = \frac{1}{\lfloor N/(RM) \rfloor} \sum_{i=1}^{\lfloor N/(RM) \rfloor} m_{k,i} a'_{k,i} = \frac{1}{FR \lfloor N/(RM) \rfloor} \sum_{f,r,i} m_{k,i} y_{k,i}'^{(f,r)} \pm \mu, \quad (1)$$

where μ is given by $\mu = 1/FR \sum_{f,r} \mu^{(f,r)}$. Since $m_{k,i} y_{k,i}'^{(f,r)}$ is considered to be an independent stochastic variable with mean 0 [7], each v_k follows the normal distribution if the number of $m_{k,i} y_{k,i}'^{(f,r)}$ s, $FR \lfloor N/(RM) \rfloor$ is large enough. That is,

$$v_k \sim \begin{cases} N(\mu, \sigma^2) & \text{if } b_k = 1 \\ N(-\mu, \sigma^2) & \text{if } b_k = 0. \end{cases}$$

Step D4: Determine M embedded bits b_k s by comparing v_k with a threshold value $T(> 0)$:

$$b_k = \begin{cases} 1 & \text{if } v_k \geq T \\ 0 & \text{if } v_k \leq -T \\ \text{"not detected"} & \text{if } -T < v_k < T. \end{cases}$$

Because watermarked pictures are subjected to wide varieties of image processing procedures, the WMs on pictures must be able to survive various kinds of image processing procedures. The accumulation operation of Step D2, however, would not always be effective because the signal of WMs could be attenuated by accumulating regions from which WMs were removed during the image processing. For example, accumulating two regions, the noise of a region σ is approximately reduced to $1/\sqrt{2}\sigma$. The signal of WMs μ , however, is approximately reduced to $1/2\mu$ if WMs on a region out of two is removed. Consequently S/N ratio is getting worse by the accumulation. The accumulation operation of the previous method could thus cause the signal of WMs μ to decrease so much that the embedded bits could not be detected reliably.

To solve this problem, the WM method needs to preserve the watermark strength μ when detecting WMs. We therefore propose a detection method that prevents the WM strength from being decreased by the accumulation operation.

3 Using Statistically-Adaptive Accumulation to Improve the Detection of Video Watermarks

3.1 Principle of the Proposed Method

The proposed WM detection method can prevent the decrease of WM strength in the accumulated regions by estimating the bit-error rates (BERs) of each region and using these estimates to control the accumulation operation in a way that minimizes the BERs of the accumulated regions. The process of the proposed WM detection comprises the following functions:

BER estimation: Estimates the BER from the statistical values of the region.

Sorting operation: Sorts the regions (actually, the corresponding set of statistical values) by the corresponding BERs.

Accumulation control: Accumulates, one by one, regions (set of the statistical values) in ascending order of the corresponding BER and re-estimates the BER of the accumulated region in each accumulation step. Selects the accumulated region having the smallest BER.

Bit-value determination: Determines bit-values by comparing the threshold value with the set of the statistical values of the accumulated regions selected by the accumulation control.

The proposed method can be applied to various kinds of the statistical-based WM schema described in Section 2.

3.2 Process Flow

The process flow of the proposed WM detection method is shown in Fig. 2. Steps D2 and D3 respectively represent the flows of the BER estimation and the sorting operation, and Steps D4 and D5 represent the flow of the accumulation control. Step D6 represents the flow of the bit-value determination.

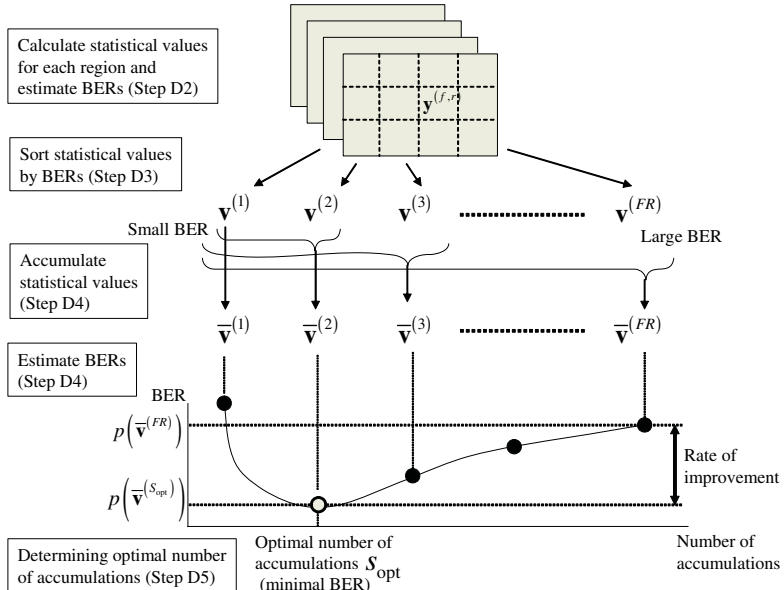


Fig. 2. Overview of the proposed method

Step D1: Do the following steps over $f_0 = 1, F + 1, 2F + 1, \dots$

Step D2: For each region $\mathbf{y}'^{(f,r)} = \bigcup_k \mathbf{y}'_k^{(f,r)}$ ($f_0 \leq f \leq f_0 + F - 1, 1 \leq r \leq R$), calculate the set consisting of the M statistical values, $\mathbf{v}^{(f,r)} = \{v_k^{(f,r)} \mid 1 \leq k \leq M\}$ and estimate BER $p(\mathbf{v}^{(f,r)})$ from the set $\mathbf{v}^{(f,r)}$. The statistical value $v_k^{(f,r)}$ of the region $\mathbf{y}'_k^{(f,r)}$ is given by correlating the WM pattern \mathbf{m}_k with the region $\mathbf{y}'_k^{(f,r)}$. That is,

$$v_k^{(f,r)} = \frac{1}{[N/(RM)]} \sum_{i=1}^{\lfloor N/(RM) \rfloor} m_{k,i} y_{k,i}^{(f,r)} = \frac{1}{[N/(RM)]} \sum_i m_{k,i} y_{k,i}^{(f,r)} \pm \mu^{(f,r)}, \quad (2)$$

Doing the above process over FR regions ($f = f_0, \dots, f_0 + F - 1, r = 1, \dots, R$), we get FR sets $\mathbf{v}^{(f_0,1)}, \dots, \mathbf{v}^{(f_0+F-1,R)}$ and the corresponding FR BERs $p(\mathbf{v}^{(f_0,1)}), \dots, p(\mathbf{v}^{(f_0+F-1,R)})$.

Step D3: Sort the FR sets $\mathbf{v}^{(f_0,1)}, \dots, \mathbf{v}^{(f_0+F-1,R)}$ by the corresponding BERs and rename the suffixes of the sets and the BERs in ascending order of the BERs. Thus we get the FR sets $\mathbf{v}^{(1)}, \dots, \mathbf{v}^{(FR)}$ that satisfy $p(\mathbf{v}^{(1)}) \leq \dots \leq p(\mathbf{v}^{(FR)})$.

Step D4: Generate the accumulated sets $\bar{\mathbf{v}}^{(s)}$ s ($s = 1, \dots, FR$) from the FR sets by $\bar{\mathbf{v}}^{(s)} = 1/s \sum_{i=1}^s \mathbf{v}^{(i)}$ and estimate the BERs $p(\bar{\mathbf{v}}^{(s)})$ ($s = 1, \dots, FR$) from the FR accumulated sets.

Step D5: Select the set of the statistical values having the smallest BER $\bar{\mathbf{v}}^{(s_{\text{opt}})}$, where s_{opt} represents the optimal number of accumulations:

$$s_{\text{opt}} = \arg \min_{1 \leq s \leq FR} p(\bar{\mathbf{v}}^{(s)}).$$

Step D6: Determine M embedded bits b_k s by comparing $\bar{v}_k^{(s_{\text{opt}})}$ with a threshold value $T (> 0)$ as is the case with Step D4 in Section 2.

Note that the set $\bar{\mathbf{v}}^{(FR)}$ of Step D4 is equal to the set \mathbf{v} of Step D3 in Section 2 and thus that $p(\bar{\mathbf{v}}^{(FR)})$ represents the BER of the proposed method.

3.3 Estimation of BER

The basic method of the BER estimation described in Section 3.1 was proposed by Echizen *et al.* [8]. This method can estimate the BER from a watermarked still picture after image processing by using the inferential statistics. We expand this method to the BER estimation of the regions employed by the proposed method.

BER of Region. To estimate the BER for each region of watermarked pictures, we use the M statistical values $v_k^{(f,r)}$ of the set $\mathbf{v}^{(f,r)}$ in formula (2) introduced in the proposed WM detection. As mentioned in Step D3 in Section 2, each statistical value $v_k^{(f,r)}$ follows the normal distribution if the number of $m_{k,i} y_{k,i}^{(f,r)}$ s, $\lfloor N/(RM) \rfloor$ is large enough. That is,

$$v_k^{(f,r)} \sim \begin{cases} N(\mu^{(f,r)}, \sigma^{2(f,r)}) & \text{if } b_k = 1 \\ N(-\mu^{(f,r)}, \sigma^{2(f,r)}) & \text{if } b_k = 0. \end{cases}$$

Thus the bit error rate of the region $\mathbf{y}'^{(f,r)}$ for an arbitrary embedded bit is

$$p(\mathbf{v}^{(f,r)}) = \int_{-\infty}^{-T} \phi(v; \mu^{(f,r)}, \sigma^{2(f,r)}) dv. \quad (3)$$

As shown in formula (3), the mean $\mu^{(f,r)}$ and variance $\sigma^{2(f,r)}$ of the normal distribution should be used to estimate bit error rate. The information we get from the watermarked region $\mathbf{y}'^{(f,r)}$ at hand is, however, not the normal distribution but is M statistical values $v_k^{(f,r)}$ that independently follow either $N(\mu^{(f,r)}, \sigma^{2(f,r)})$ or $N(-\mu^{(f,r)}, \sigma^{2(f,r)})$ according to the embedding bit. The $\mu^{(f,r)}$ and $\sigma^{2(f,r)}$ should thus be estimated from these statistical values.

EM Algorithm. The expectation-maximization (EM) algorithm is a representative maximum-likelihood method for estimating the statistical parameters of a probability distribution [9]. In the case of the mixture normal distribution comprising two normal distributions (i.e., $N(\mu^{(f,r)}, \sigma^{2(f,r)})$ and $N(-\mu^{(f,r)}, \sigma^{2(f,r)})$) that the statistical values $v_k^{(f,r)}$ follow, the EM algorithm can estimate the probability $w_k^{(f,r)}$ that each $v_k^{(f,r)}$ follows $N(\mu^{(f,r)}, \sigma^{2(f,r)})$, $\mu^{(f,r)}$, and $\sigma^{2(f,r)}$. The relation between $w_k^{(f,r)}$, $\mu^{(f,r)}$, and $\sigma^{2(f,r)}$ is given by

$$\begin{aligned}\mu^{(f,r)} &= \frac{1}{M\alpha^{(f,r)}} \sum_k w_k^{(f,r)} v_k^{(f,r)}, \\ \sigma^{2(f,r)} &= \frac{1}{M\alpha^{(f,r)}} \sum_k w_k^{(f,r)} v_k^{(f,r)2} - \mu^{(f,r)2},\end{aligned}$$

where $\alpha^{(f,r)} = 1/M \sum_k w_k^{(f,r)}$ is the weighting factor of $N(\mu^{(f,r)}, \sigma^{2(f,r)})$ to the mixture normal distribution. These parameters are sequentially updated from initial values by the iterative calculation and $\mu^{(f,r)}$ and $\sigma^{2(f,r)}$ are used as estimates when they are converged. See Ref. [9] for the details of this calculation.

4 Experimental Evaluation

The ability of the proposed method to detect watermarks after MPEG encoding was compared experimentally with that of the previous method by using the standard motion picture “Walk through the square” (three hundred 720×480 -pixel frames) [10].

4.1 Procedure

A WM pattern representing 256-bit information ($M = 256$) was generated by using the pseudo-random generator [11] and was embedded in each of four 360×240 -pixel regions ($R = 4$) of every frame by using the procedures described in Section 2.1. After MPEG-2 encoding and decoding with three different bit rates (2, 3, 4 Mbps), 256-bit information was sequentially detected in 30-frame segments of the 300 frames of the watermarked pictures ($F = 30$; the number of detecting points is $300/30 = 10$) and the BERs measured using the proposed detection method described in Section 3.2 were compared with those measured using the previous detection method described in Section 2. The above procedure was done using 100 different random WM patterns.

4.2 Results

The average values (over 100 WM patterns) of the measured BERs obtained using the proposed and the previous methods are shown for each bit rate in Fig. 3(a), where the horizontal axis represents the detecting points from 1 to 10 and the vertical axis represents the average BERs. We can see that the proposed

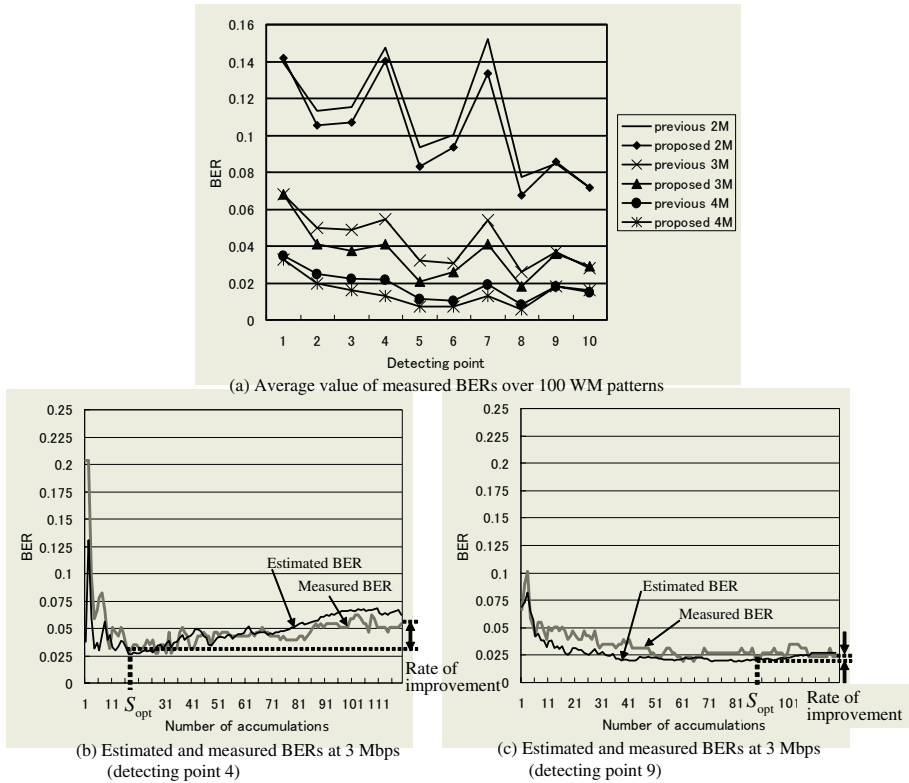


Fig. 3. Evaluation results

method could reduce the BERs at each bit rate and most detecting points. At all bit rates the average ratio of the proposed BER to the previous BER is 0.845. The proposed method thus yielded an average improvement of 15.5%.

Example transitions of the BERs estimated by the proposed method (corresponding to Fig. 2) are shown in Figs. 3(b) and 3(c), where the horizontal axes represent the number of accumulations (the order of the accumulation follows the ascending order of the estimated BERs) and the vertical axes represent the estimated (black line) and measured (gray line) BERs at the detecting points. From Figs. 3(b) and 3(c), we can see that the estimated BERs are roughly consistent with the experimentally measured BERs. In Fig. 3(b) (detecting point 4), the BER tends to increase with the number of accumulations and the rate of improvement is about 2.5%. At all bit rates similar trends were also found for the detecting points 2 through 8, where most parts of the neighboring frames were messy or moving. We can infer that the strengths of WMs in the regions having various picture properties were varied by MPEG-2 encoding and thus the BERs of the regions increased with the number of accumulations as a result of the sorting operation of the proposed method.

In Fig. 3(c) (detecting point 9), on the other hand, the plot of BER against the number of accumulations is flat and the rate of improvement is nearly 0. At all bit rates similar trends were also found for the detecting points 1 through 10, where most parts of the neighboring frames were static. We also can infer that the strengths of WMs in the regions were not varied by MPEG-2 encoding and thus the BERs of the regions were not changed by the sorting operation.

For all MPEG-2 bit rates evaluated, the proposed method could give lower or equal BERs dependant on the picture properties and yielded an average improvement of 15.5%. The proposed method can thus improve watermark detection.

5 Conclusion

This paper proposes a watermark detection method, for use with redundant coding, that can prevent watermark strength from being decreased by the accumulation operation. It estimates the bit-error rate by using the expectation-maximization algorithm from inferential statistics. Experimental evaluations have shown that the new method can improve watermark detection after MPEG-2 encoding by an average of 15.5% and can be widely used in statistically based watermarking.

References

1. Lin *et al.*: Spatial Synchronization Using Watermark Key Structure, *Proc. SPIE*, vol. 5306, pp. 536–547, 2004.
2. Kalker *et al.*: Video watermarking system for broadcast monitoring, *Proc. SPIE*, vol. 3657, pp. 103–112, 1999.
3. Kusanagi *et al.*: An Image Correction Scheme for Video Watermarking Extraction, *IEICE Trans. Fundamentals*, vol. E84-A, no. 1, pp. 273–280, 2001.
4. Cox *et al.*: Secure Spread Spectrum Watermarking for Multimedia, *IEEE Trans. on Image Processing*, vol. 6, no. 12, pp. 1673–1687, 1997.
5. Hsu *et al.*: Hidden Digital Watermarks in Images, *IEEE Trans. on Image Processing*, vol. 8, no. 1, pp. 58–68, 1999.
6. Seo *et al.*: A Digital Watermarking Algorithm Using Correlation of the Tree Structure of DWT Coefficients, *IEICE Trans. Fundamentals*, vol. E87-A, no. 6, pp. 1347–1354, 2004.
7. Bender *et al.*: Techniques for data hiding, *Proc. SPIE*, Vol. 2020, pp. 2420–2440 1995.
8. Echizen *et al.*: Estimating the Bit-error rate in Digital Watermarking Using Inferential Statistics, *J. IPS Japan*, vol. 42, no. 8, pp. 2006–2016, 2001.
9. Redner *et al.*: Mixture densities, maximum likelihood and the EM algorithm, *SIAM Review*, vol. 26, pp. 195–239, 1984.
10. The Institute of Image Information and Television Engineers: Evaluation video sample (standard definition).
11. Matsumoto *et al.*: Mersenne Twister: A 623-dimensionally equidistributed uniform pseudorandom number generator, *ACM Trans. on Modeling and Computer Simulation* vol. 8, no. 1, pp. 3–30, 1998.

Comparison of Feature Extraction Techniques for Watermark Synchronization

Hae-Yeoun Lee¹, Heung-Kyu Lee¹, and Junseok Lee²

¹ Department of EECS, Korea Advanced Institute of Science and Technology,
Guseong-dong, Yuseong-gu, Daejeon, 305-701, Republic of Korea
hytoiy@casaturn.kaist.ac.kr

² Digital Contents Research Division, Electronics and Telecommunications Research Institute,
Gajeong-dong, Yuseong-gu, Daejeon, 305-700, Republic of Korea

Abstract. This paper evaluates feature extraction techniques in aspect of watermark synchronization. Most watermarking algorithms suffer from geometric distortion attacks that desynchronize the location of the inserted watermark. The process of synchronizing the location for watermark insertion and detection is crucial to design robust watermarking. One solution for watermark synchronization is to use features. This paper reviews feature extraction techniques in feature-based watermarking: the Harris corner detector and the Mexican Hat wavelet scale interaction method. We evaluate the scale-invariant keypoint extractor in comparison with others. After feature extraction, the set of triangles is generated by Delaunay tessellation. These triangles are the location for watermarking. Redetection ratio of triangles is measured against geometric distortion attacks and signal processing attacks. Experimental results show that the scale-invariant keypoint extractor is appropriate for robust watermarking.

1 Introduction

During the last decades, digital technologies have grown, wherein all kinds of multimedia have been digitalized. However, digital multimedia can be copied, manipulated, and reproduced illegally without any quality degradation and protection.

Digital watermarking is a method for copyright protection. Copyright information is inserted into contents itself and used as evidence of ownership. Previous watermarking algorithms show severe weakness to geometric distortion attacks that desynchronize the location of the inserted copyright information and prevent watermark detection. To resist geometric distortion attacks, watermark synchronization, a process for finding the location for watermark insertion and detection, should be performed. We call this location *the patch*. One solution for watermark synchronization is to use features. Features represent an invariant reference for geometric distortion attacks so that referring features can solve synchronization problems.

Kutter *et al.* [1] describe a feature-based synchronization method. First, they extract feature points using the Mexican Hat wavelet scale interaction method. Then, the feature points are used to segment the image using a Voronoi diagram. The spread-spectrum watermark was inserted into each segment. Bas *et al.* [2] extract feature points using the Harris corner detector and then decompose the feature points into a set of disjoint triangles by Delaunay tessellation. These triangles are watermarked by an additive spread-spectrum method on the spatial domain. Nikolaidis and Pitas [3]

consider a segmentation-based synchronization method. First, they extract regions by applying an adaptive k-mean clustering technique. Then, the bounding rectangles of regions are used for watermarking. Tang and Hang [4] extract feature points using the Mexican Hat wavelet scale interaction method. Disks of fixed radius R whose center is each feature point are normalized, because objects in the normalized image are invariant to distortions. Normalized disks are watermarked on the frequency domain.

From watermark synchronization using features, feature extraction is important to design robust watermarking. This paper reviews feature extraction techniques used in feature-based watermarking and evaluates the scale-invariant keypoint extractor in comparison with other techniques. We measure redetection ratio of the patches. Results show that the scale-invariant keypoint extractor is useful and robust against geometric distortion attacks as well as signal processing attacks.

In Section 2, we review feature extraction techniques and describe the scale-invariant keypoint extractor. Section 3 explains how to synchronize the watermark. Evaluation results are shown in Section 4 and Section 5 concludes this paper.

2 Feature Extraction Techniques

Bas *et al.* [2] compared major feature extraction techniques: the Harris corner detector, the Susan corner detector, and the Achard-Rouquet detector. The Harris corner detector outperformed. However, they just focus on the redetection of each feature point, not the patches for watermarking. Segmentation is commonly used for feature extraction. However, features from segmentation depend on contents. Moreover, their location is severely sensitive to distortions [3]. The Mexican Hat wavelet scale interaction method is an intensity-based feature extraction technique and has been used for robust watermarking [1, 4]. This section reviews two feature extraction techniques: the Harris corner detector and the Mexican Hat wavelet scale interaction method and then describes the scale-invariant keypoint extractor.

2.1 Harris Corner Detector

The Harris corner detector uses differential features of images. This detector generate the second moment matrix using image gradients and then combines eigenvalues of the moment matrix to compute a corner-strength, whose local maximums indicate corner positions. The second moment matrix $E_{x,y}$ is defined by

$$E_{x,y} = (x, y)H(x, y)^T \text{ with } H = \begin{bmatrix} D_{x,x} & D_{x,y} \\ D_{x,y} & D_{y,y} \end{bmatrix}. \quad (1)$$

$E_{x,y}$ can be considered as an auto-correlation function with a shape factor H . D represents image gradient of x - and y -axis. The corner-strength R_H is acquired by combining the eigenvalues as follows.

$$R_H = \text{Det}(H) - k\text{Tr}^2(M) \text{ where } \text{Tr}(H) = D_{xx} + D_{yy}, \text{Det}(H) = D_{xx}D_{yy} - D_{xy}^2. \quad (2)$$

k is an arbitrary constant. Corner points are extracted by searching local maximums on this corner-strength of R_H . This detector shows high accuracy in corner positions. However, the set of feature points is sensitive to image noise.

2.2 Mexican Hat Wavelet Scale Interaction Method

The Mexican Hat wavelet scale interaction method uses intensity features of images. This method determines feature points by identifying significant intensity changes that occur at different scaled versions of the same image. First, two different scales of Mexican Hat wavelet are applied to the same image. Then, a scale interaction image is acquired by the following quantities.

$$P_{ij}(\vec{x}) = \left| M_i(\vec{x}) - \gamma \cdot M_j(\vec{x}) \right|, \quad (3)$$

$M_i(\vec{x})$ represents the response of the Mexican Hat wavelet at the image location \vec{x} for scale i and j , respectively. γ is a normalizing constant. $P_{ij}(\vec{x})$ is the scale interaction between two different scales i and j . Local maximums of the scale interaction image $P_{ij}(\vec{x})$ are determined as the set of feature points. This method is robust to image noise. It is also invariant to rotation because Mexican Hat wavelet has a circularly symmetric frequency response.

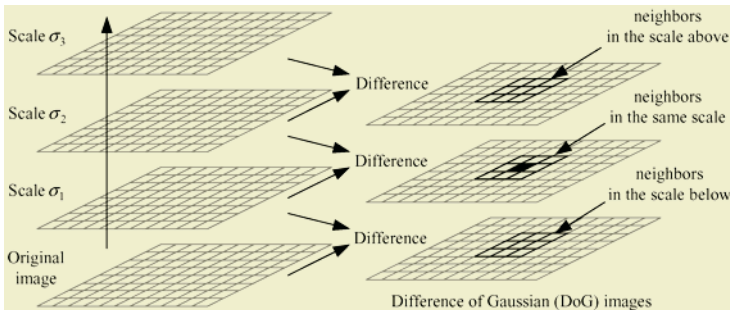


Fig. 1. Scale-space from Difference of Gaussian function and the closest neighborhoods

2.3 Scale-Invariant Keypoint Extractor

In object recognition and image retrieval applications, affine-invariant features have been recently researched [5, 6, 7]. These features are highly distinctive and matched with high probability against a large case of image distortions. We explain the scale-invariant keypoint extractor that is proposed by Lowe [5] and proved to be invariant to image rotation, scaling, illumination changes, and projective transform.

Basic idea of the scale-invariant keypoint extractor is detecting feature points through a staged filtering approach that identifies stable points in the scale-space. To extract the set of candidate feature points, they generate a scale-space using a Difference of Gaussian function, in which an image is filtered by Gaussian functions of different scales and then difference images are calculated. All local maximums and minimums are searched by checking eight closest neighborhoods in the same scale and nine neighborhoods in the scale above and below (see Fig. 1). These locations are invariant to changes of image scale.

After candidate points are found, the points that have a low contrast or are poorly localized are removed by measuring the stability at its location and scale. The stability of each point is calculated from a 2 by 2 Hessian matrix H as follows.

$$Stability = \frac{(D_{xx} + D_{yy})^2}{D_{xx}D_{yy} - D_{xy}^2} < \frac{(r+1)^2}{r} \text{ where } H = \begin{bmatrix} D_{xx} & D_{xy} \\ D_{xy} & D_{yy} \end{bmatrix}. \quad (4)$$

r is the ratio between the largest and smallest eigenvalues and controls the stability. D represents image gradient of x - and y -axis.

Orientation of each feature point is assigned by considering local image properties. Orientation histogram is formed from gradient orientations at all sample points within the circular window of a feature point. Peak in this histogram corresponds to dominant direction of the feature point. Gradient orientation θ are computed by using pixel differences as follows.

$$\theta = \tan^{-1}(L_{x,y+1} - L_{x,y-1})/(L_{x+1,y} - L_{x-1,y}). \quad (5)$$

L is a Gaussian filtered image with the closest scale in which each feature point is found. Scale-invariant keypoints obtained through this process are invariant to rotation, scaling, translation and partly illumination changes of images. Therefore, scale-invariant keypoints may be useful to design robust watermarking.

3 Watermark Synchronization Using Feature Extraction

Watermarking algorithms are composed of two processes: watermark insertion and detection. Watermark insertion is a process of inserting the watermark into contents. Watermark detection is a process of detecting the inserted watermark to prove ownership. Fig. 2 shows general framework of feature-based watermarking.

The first step for watermark insertion and detection is analyzing contents to extract features and then features are relatively related to generate the patches. During watermark insertion, the watermark is inserted into all patches. During watermark detection, all patches are tried to detect the watermark. The ownership can be proved successfully if the watermark is correctly detected from at least one patch.

Delaunay tessellation is commonly used to extract patches by decomposing the feature points into a set of disjoint triangles. Given a set of feature points, Delaunay tessellation is the straight line dual of the corresponding Voronoi diagram, which partitions the image into segments such that all points in one segment are closer to the location of the feature points.

The distribution of feature points is an important factor to design robust watermarking. In other words, the neighborhood size of feature points should be designed carefully. If the size is too small, the distribution of the feature points is concentrated on textured areas. If the size is too large, feature points become isolated. To obtain the homogeneous distribution of feature points, we apply a circular neighborhood constraint, in which the feature points whose strength is the largest are selected [2]. The neighborhood size D is dependent on image dimension and quantized by r as follows.

$$D = (w + h)/r. \quad (6)$$

w and h represent the width and height of images. r is a constant to control the size. Circle diameter depends on image dimensions to be against changes of image scale. For each feature extraction method described in Section 2, Fig. 3 shows the extracted patches against additive uniform noise, rotation 10°, and scaling 1.1x. First row is

from the Harris corner detector. Second row is from the Mexican Hat wavelet scale interaction method. Last row is from the scale-invariant keypoint extractor. Although attacks result in different tessellation by modifying relative position of feature points, there are several corresponding patches. Therefore, we can synchronize successfully.

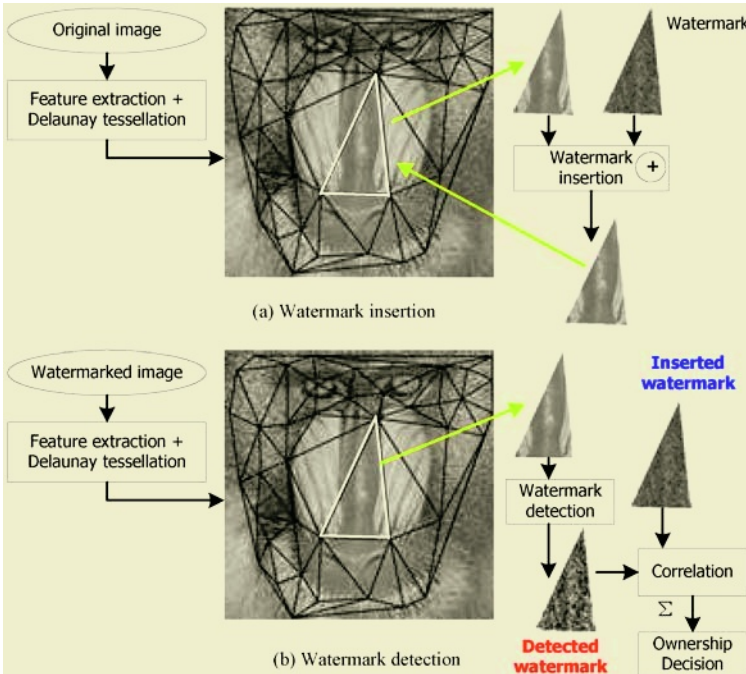


Fig. 2. Framework for watermark insertion and detection

4 Evaluation Results

We evaluated three feature extraction methods in aspect of watermark synchronization: the Harris corner detector (method 1), the Mexican Hat wavelet scale interaction method (method 2), and the scale-invariant keypoint extractor (method 3). We used 15 images whose size was 512 by 512 pixels (Baboon, Boat, Lake, Bridge, Couple, Pepper, Lena, Indian, Plane, Pentagon, Girl, IKONOS, KOMPSAT, SPOT1, and SPOT2). Because our research focuses on applying watermarking into remote-sensing fields, we include satellite images. Differently from other images, satellite images contain considerable noise, similar patterns are repeated multiple times and that make feature extraction difficult. Details of experimental setups and results refer author's website (<http://mmc.kaist.ac.kr/~hytoiy/IHMSP2005.htm>).

We applied signal processing attacks (median filter, Gaussian filter, additive uniform noise, and JPEG compression) and geometric distortion attacks (rotation, scaling, and cropping) listed in Stirmark 3.1. For each method, the number of extracted patches is shown in Table 1. Averaged numbers from method 1, method 2, and method 3 were 73 patches, 79 patches, and 71 patches, respectively.

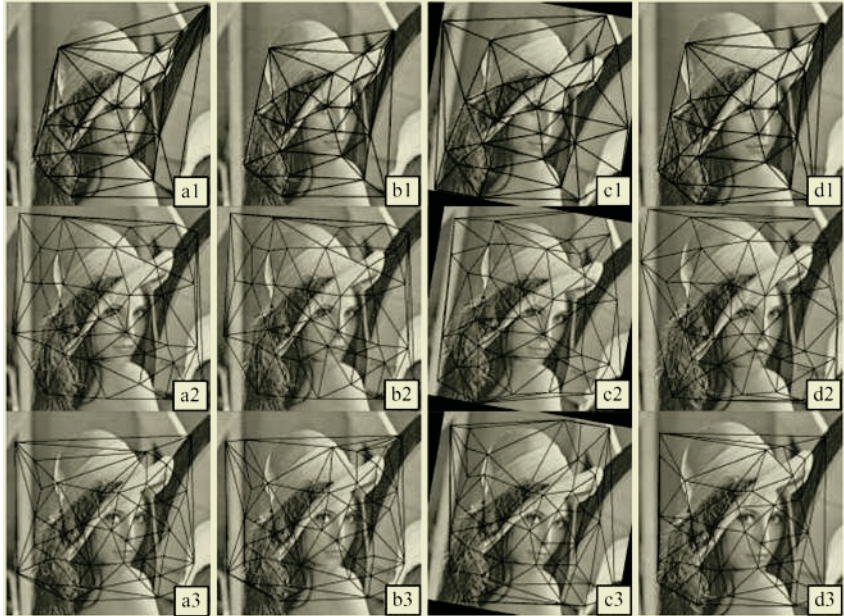


Fig. 3. Patches for watermark insertion and detection: (a) original image, (b) image with additive uniform noise, (c) image with rotation 10°, and (d) image with scaling 1.1x

Table 1. Number of extracted patches for each method

| | Babo. | Boat | Lake | Brid. | Coup. | Pepp. | Lena | In-dian | Plane | Penta. | Girl | Ik-ono. | Kom. | Spot1 | Spot2 |
|---------|-------|------|------|-------|-------|-------|------|---------|-------|--------|------|---------|------|-------|-------|
| Method1 | 67 | 63 | 86 | 89 | 58 | 61 | 40 | 60 | 53 | 60 | 41 | 81 | 114 | 113 | 102 |
| Method2 | 60 | 73 | 86 | 79 | 71 | 72 | 67 | 77 | 71 | 106 | 66 | 90 | 98 | 80 | 87 |
| Method3 | 57 | 46 | 65 | 69 | 56 | 71 | 65 | 77 | 56 | 55 | 51 | 81 | 122 | 91 | 97 |

We measured redetection ratio of the patches. This represents how many patches that have been detected in the original image are correctly redetected in the attacked images. Prior to comparison, we reversed the coordinates of patches in attacked images into the coordinates in the original image by applying inverse transform.

Table 2 shows redetection ratios under signal processing attacks and geometric distortion attacks. We represent the results of several images in details. Last column represents averaged detection ratios of 15 images. Against signal processing attacks, method 2 outperformed because the Mexican Hat wavelet scale interaction method was not affected by small intensity distortions. The Harris corner detector use differential features that are sensitive to image noise. Therefore, method 1 showed relatively low performance and worked poorly when images had complex textures like Baboon or contained many noise factors. Method 3 using scale-invariant keypoints showed higher performance than method 1, but lower performance than method 2. Against most geometric distortion attacks except scaling attacks, method 3 performed well, although the performance differences were small to be ignorable. In scaling attacks, method 1 worked better than others because differential features of images were preserved well in changes of image scale. Method 2 showed severe weakness in scaling attacks. As the image scale changes, the response from the Mexican Hat

wavelet is different. Therefore, the feature points are extracted in different position. Method 3 showed relatively lower performance than method 1 in scaling attacks. However, overall performance is acceptable for watermarking purposes, because we can prove the ownership if the watermark is detected from at least one patch.

Table 2. Redetection ratios under signal processing and geometric distortion attacks (%)

| | | Baboon | Lake | Bridge | Lena | Indian | Plane | Penta. | Ikonos | Komp. | Spot2 | Total |
|--------------------------|---------|--------|------|--------|------|--------|-------|--------|--------|-------|-------|-------|
| Median 2x2 | Method1 | 25 | 35 | 25 | 58 | 28 | 47 | 35 | 20 | 21 | 50 | 34 |
| | Method2 | 50 | 57 | 76 | 85 | 88 | 77 | 56 | 82 | 68 | 78 | 73 |
| | Method3 | 40 | 51 | 39 | 46 | 21 | 45 | 36 | 36 | 24 | 48 | 41 |
| Median 3x3 | Method1 | 39 | 33 | 28 | 55 | 35 | 17 | 28 | 25 | 13 | 52 | 35 |
| | Method2 | 50 | 64 | 67 | 66 | 64 | 77 | 53 | 70 | 54 | 90 | 66 |
| | Method3 | 19 | 17 | 36 | 29 | 27 | 55 | 36 | 17 | 37 | 32 | 34 |
| Gaussian filter | Method1 | 57 | 42 | 34 | 53 | 67 | 43 | 25 | 33 | 38 | 45 | 44 |
| | Method2 | 90 | 77 | 92 | 85 | 78 | 90 | 64 | 84 | 92 | 90 | 85 |
| | Method3 | 75 | 62 | 59 | 74 | 51 | 86 | 58 | 54 | 52 | 62 | 64 |
| Uniform noise | Method1 | 45 | 38 | 30 | 58 | 25 | 28 | 27 | 23 | 35 | 43 | 41 |
| | Method2 | 72 | 78 | 81 | 75 | 75 | 79 | 71 | 78 | 86 | 91 | 81 |
| | Method3 | 42 | 62 | 51 | 72 | 44 | 59 | 29 | 52 | 57 | 47 | 53 |
| JPEG comp. 50 | Method1 | 48 | 47 | 37 | 60 | 37 | 32 | 37 | 32 | 41 | 56 | 46 |
| | Method2 | 87 | 85 | 81 | 69 | 88 | 100 | 82 | 89 | 91 | 93 | 87 |
| | Method3 | 72 | 57 | 51 | 77 | 64 | 88 | 55 | 62 | 62 | 81 | 65 |
| JPEG comp. 70 | Method1 | 45 | 42 | 38 | 58 | 45 | 47 | 37 | 27 | 39 | 55 | 45 |
| | Method2 | 97 | 81 | 91 | 88 | 87 | 100 | 78 | 89 | 91 | 93 | 90 |
| | Method3 | 74 | 63 | 59 | 52 | 58 | 86 | 56 | 54 | 63 | 78 | 64 |
| JPEG comp. 90 | Method1 | 52 | 38 | 43 | 60 | 48 | 43 | 40 | 31 | 46 | 48 | 47 |
| | Method2 | 98 | 78 | 95 | 90 | 77 | 100 | 81 | 92 | 90 | 93 | 90 |
| | Method3 | 74 | 72 | 61 | 72 | 58 | 82 | 58 | 54 | 57 | 79 | 67 |
| Crop 5% | Method1 | 34 | 27 | 30 | 40 | 25 | 34 | 40 | 10 | 26 | 28 | 30 |
| | Method2 | 18 | 22 | 25 | 31 | 23 | 21 | 19 | 24 | 27 | 24 | 25 |
| | Method3 | 25 | 38 | 42 | 42 | 23 | 63 | 38 | 27 | 39 | 51 | 38 |
| Crop 15% | Method1 | 22 | 23 | 18 | 38 | 28 | 23 | 38 | 4 | 19 | 25 | 24 |
| | Method2 | 7 | 15 | 19 | 15 | 14 | 7 | 13 | 8 | 13 | 17 | 14 |
| | Method3 | 19 | 28 | 20 | 26 | 17 | 43 | 25 | 14 | 32 | 30 | 25 |
| Crop 25% | Method1 | 9 | 16 | 11 | 38 | 18 | 15 | 32 | 1 | 18 | 23 | 18 |
| | Method2 | 3 | 5 | 5 | 6 | 12 | 3 | 6 | 6 | 7 | 9 | 6 |
| | Method3 | 9 | 18 | 17 | 15 | 13 | 29 | 20 | 10 | 20 | 21 | 17 |
| Rotation 1.0° +Cropping | Method1 | 31 | 21 | 28 | 40 | 32 | 34 | 23 | 25 | 18 | 35 | 32 |
| | Method2 | 52 | 50 | 56 | 52 | 40 | 44 | 44 | 43 | 54 | 59 | 50 |
| | Method3 | 47 | 38 | 38 | 42 | 38 | 61 | 44 | 51 | 33 | 44 | 42 |
| Rotation 5.0° +Cropping | Method1 | 34 | 16 | 15 | 40 | 33 | 40 | 25 | 12 | 18 | 32 | 29 |
| | Method2 | 27 | 33 | 34 | 39 | 39 | 23 | 26 | 29 | 44 | 40 | 33 |
| | Method3 | 32 | 26 | 35 | 46 | 25 | 36 | 35 | 32 | 25 | 35 | 32 |
| Rotation 10.0° +Cropping | Method1 | 33 | 21 | 27 | 33 | 27 | 26 | 22 | 11 | 19 | 22 | 25 |
| | Method2 | 23 | 22 | 25 | 36 | 34 | 25 | 23 | 26 | 21 | 34 | 27 |
| | Method3 | 21 | 23 | 35 | 38 | 21 | 45 | 47 | 41 | 25 | 33 | 33 |
| Rotation 30.0° +Cropping | Method1 | 25 | 17 | 19 | 40 | 23 | 30 | 25 | 14 | 12 | 34 | 24 |
| | Method2 | 17 | 15 | 22 | 28 | 25 | 17 | 23 | 24 | 24 | 26 | 23 |
| | Method3 | 26 | 18 | 17 | 23 | 18 | 21 | 29 | 33 | 16 | 25 | 23 |
| Scaling 0.8× | Method1 | 10 | 10 | 6 | 20 | 3 | 15 | 42 | 11 | 4 | 19 | 19 |
| | Method2 | 0 | 0 | 0 | 0 | 0 | 0 | 2 | 0 | 0 | 0 | 0 |
| | Method3 | 11 | 9 | 13 | 8 | 8 | 11 | 13 | 12 | 7 | 8 | 10 |
| Scaling 0.9× | Method1 | 33 | 20 | 18 | 23 | 40 | 34 | 35 | 22 | 6 | 37 | 29 |
| | Method2 | 0 | 0 | 0 | 1 | 1 | 0 | 8 | 0 | 1 | 0 | 1 |
| | Method3 | 19 | 22 | 30 | 12 | 5 | 11 | 35 | 23 | 11 | 21 | 19 |
| Scaling 1.1× | Method1 | 27 | 15 | 30 | 45 | 25 | 43 | 32 | 19 | 11 | 36 | 27 |
| | Method2 | 5 | 0 | 13 | 4 | 1 | 3 | 24 | 0 | 4 | 6 | 5 |
| | Method3 | 25 | 9 | 26 | 38 | 12 | 29 | 29 | 16 | 7 | 22 | 20 |
| Scaling 1.2× | Method1 | 12 | 15 | 13 | 43 | 22 | 30 | 17 | 4 | 5 | 25 | 20 |
| | Method2 | 0 | 0 | 4 | 0 | 0 | 0 | 5 | 0 | 2 | 0 | 1 |
| | Method3 | 11 | 11 | 7 | 15 | 5 | 11 | 13 | 4 | 5 | 7 | 8 |

5 Conclusion and Future Works

Watermark synchronization is crucial to design robust watermarking. One solution to find the location for watermark insertion and detection against image attacks is to use features. In feature-based watermarking, feature extraction method should be selected carefully. This paper reviewed major feature extraction techniques: the Harris corner detector and the Mexican Hat wavelet scale interaction method. We evaluated the scale-invariant keypoint extractor in comparison with other techniques in aspect of watermark synchronization. We measured redetection ratio of the patches against geometric distortion attacks as well as signal processing attacks. The scale-invariant keypoint extractor showed acceptable performance for robust watermarking. Nevertheless, the redetection ratio in scaling attacks was relatively low. Our future research focuses on increasing robustness against these attacks.

References

1. M. Kutter, S.K. Bhattacharjee, T. Ebrahimi: Towards second generation watermarking schemes. Proc. of ICIP, Vol. 1, (1999) 320-323
2. P. Bas, J-M. Chassery, B. Macq: Geometrically invariant watermarking using feature points. IEEE Trans. on Image Processing, Vol. 11 (2002) 1014-1028
3. A. Nikolaidis, I. Pitas: Region-based image watermarking. IEEE Trans. on Image Processing, Vol. 10 (2001) 1726-1740
4. C.W. Tang, H-M. Hang: A feature-based robust digital image watermarking scheme. IEEE Trans. on Signal Processing, Vol. 51 (2003) 950-959
5. D.G. Lowe: Distinctive image features from scale-invariant keypoints. International Journal of Computer Vision, Vol. 60 (2004) 91-110
6. K. Mikolajczyk, C. Schmid: Scale and affine invariant interest point detectors. International Journal of Computer Vision, Vol. 60 (2004) 63-86
7. T. Tuytelaars, L.V. Gool: Matching widely separated views based on affine invariant regions. International Journal of Computer Vision, Vol. 59 (2004) 61-85

Reversible Watermarking Based on Improved Patchwork Algorithm and Symmetric Modulo Operation

ShaoWei Weng¹, Yao Zhao¹, and Jeng-Shyang Pan²

¹ Institute of Information Science, Beijing Jiaotong University, P.R. China

² National Kaohsiung University of Applied Sciences, Taiwan

Abstract. Modulo operations are often used in reversible watermarking scheme. However, the modulo operations would cause an annoying visual artifact similar to the “salt-and-pepper” noise when pixel value close to the maximally allowed value are flipped to zero and vice versa. To prevent the “salt-and-pepper” noise, the paper presents reversible watermarking scheme using improved patchwork and an improved modulo operation. The improved modulo operation called symmetric modulo operation effectively avoids “salt-and-pepper” noise by the reasonably reducing the flipping distance. Experimental results show that correctly watermark bits can be retrieved by the patchwork algorithm without the original image and that the original image can be restored perfectly while the perceptual degradation of the watermarked signal remained acceptable.

1 Introduction

In some applications, especially for some critical applications such as the fields of the law enforcement, medical and military image system, it is crucial to restore the original image without any distortions after the watermarked data are retrieved for any legal or other considerations. The watermarking techniques satisfying those requirements are referred to as the reversible watermarking.

Reversible watermarking puts emphasis on the reversible recovery of the original image and correctly extracts the watermark in order to judge whether the image has been attacked or modified. The concept of reversible watermark firstly appeared in the patent owned by Eastman Kodak[1]. Modulo operation is a kind of simply reversible operation. Fridrich et al[3] proposed another reversible watermarking data embedding scheme, which embeds data in the saved space of some losslessly compressed bit-planes in the spatial domain. Tian[5] proposed a reversible data embedding approach based on expanding the pixel value difference between neighboring pixels which will not overflow or underflow after the expansion .De Vleeschouwer et al[4] proposed a lossless data hiding algorithm based on patchwork theory.

The patchwork algorithm[2] is applied in the reversible watermark in order to correctly detect the watermark sequence without the original image. However, the methods are not satisfactory. Owing to the practice application, some image

blocks can not satisfy the assumption the patchwork algorithm based on, which introduces the possibility of wrong judgment and reduces the embedding bits. The modulo operations[3] easily introduce the “salt-and-pepper” noise, which heavily impacts on and destroys the effect of the image.

The paper put forward an improved approach—symmetric modulo operation to resolve the problems mentioned above and use the improved patchwork algorithm successfully in reversible watermarking for images.

In section 2, some relevant knowledge are reviewed, in Section 3 embedding process and extracting process are presented respectively, in Section 4, we give the experimental results and Section 5 concludes the paper.

2 Relevant Knowledge

The patchwork is an excellent watermarking algorithm proposed for images [2]. Bender, Gruhl, Morimoto, and Lu proposed the core idea. The modulo operations are simply lossless operations. To describe our scheme later, some relevant knowledge of the patchwork algorithm and modulo operation is briefly introduced.

2.1 The Review of the Patchwork Algorithm

The algorithm is based on the following assumptions: (i) the sample populations are uniformly distribution.(ii) the sample means are all the same.

The two major steps in the algorithm are (i) choose two patches pseudo-randomly and (ii) add the small constant value to the sample values of one patch and subtract the same value from the sample values of another patch . Mathematically speaking:

$$\alpha_i = a_i + \delta, \beta_i = b_i - \delta \quad a_i \in A, b_i \in B \quad (1)$$

Let S_n be defined as:

$$S_n = \sum_{i=1}^n (\alpha_i - \beta_i) \quad a_i \in A, b_i \in B \quad (2)$$

According to the assumption the patchwork algorithm based on, the expected value of S_n is 0.

Let S'_n be defined as:

$$S'_n = \sum_{i=1}^n ((\alpha_i + \delta) - (b_i - \delta)) = 2n\delta + \sum_{i=1}^n (\alpha_i - \beta_i) \quad a_i \in A, b_i \in B \quad (3)$$

From Equ.(3), we know that we can embed a watermark bit into the patch pair by slightly modifying the original sample values. The detection process starts with subtraction of the sample values between the patches. In extraction, we can detect whether the original image is watermarked or not by comparing $E[\alpha_i - \beta_i]$ with the threshold $M = n\delta$.

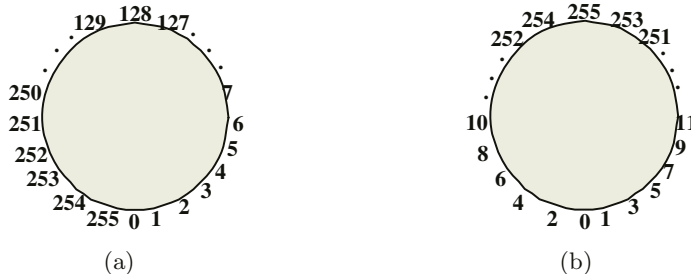


Fig. 1. Modulo operations. (a) Traditional modulo 255 addition; (b) Symmetric modulo operation

2.2 The Review of Modulo Operations

The invertible modulo operations[3] from the above paragraph can be represented using the following permutation: $0 \rightarrow 1, 1 \rightarrow 2, \dots, 254 \rightarrow 255, 255 \rightarrow 0$ shown in Fig. 1.(a). The formula for this invertible addition is:

$$j \bigoplus (k) = C[j/C] + \text{mod}((j + k), C) \quad (4)$$

where $[x]$ stands for the integer part of x and C is the cycle length. The invertible subtraction is defined as

$$j - k = j \bigoplus (-k) \quad (5)$$

where i is the grayscale value, k is the concrete watermark value, \bigoplus is modulo operation.

3 Proposed Reversible Watermarking Approach

A basic frame of our proposed scheme is presented in Fig.2, based on the improved patchwork algorithm and symmetric modulo operation, where x is an original image block, x_w is the watermarked version of x , Key is a secret key, WM represents the watermark sequence.

x_p is represented as the image block after pseudo-randomly selection process which consists of the patch A and B . x_{oe} is represented as the image block after the patch A and B are divided into four sets A_o, A_e, B_o, B_e . A_o which the positions tagged with “x” represents consists of odd pixel values, while A_e which the positions tagged with “*” represents consists of the even pixel values. B_o, B_e are similar to A_o, A_e . If watermark bit is equal to 1, the grayscale values of A rotate clockwise C times and the grayscale values of B rotate anti-clockwise C times according to symmetric modulo operation and constant embedding level C , The patchwork B is similar to the patch A .

3.1 Symmetric Modulo Operation

From the formula [4], grayscale 255 is flipped to grayscale 0 and vice versa. Those flipping pixels introduce the “salt-and-pepper” artifact. Although the modulo 225 addition may completely restore the original image, but it would cause the

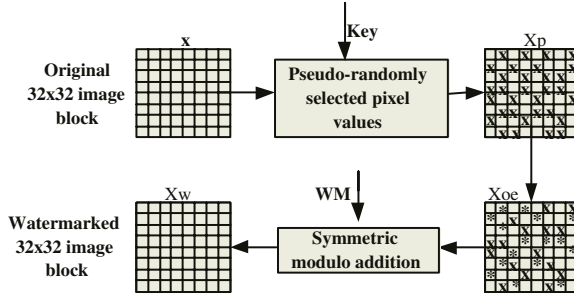


Fig. 2. Embedding process for 32x32 block

heavily visual distortion, and those flipping points would increase the possibility of wrong judgment which is analyzed in detail in the Section 3.3

Modulo operation is represented as the following permutations: $0 \rightarrow 1, 1 \rightarrow 3, \dots, 253 \rightarrow 255, 255 \rightarrow 254, \dots, 4 \rightarrow 2, 2 \rightarrow 0$, shown in Fig.1.(b). Odd and even grayscale values symmetrically spread around the circle. The method may guarantee all neighbors correspond to close grayscale values. It prevents “salt-and-pepper” artifact.

3.2 Improved Patchwork Algorithm

The original patchwork algorithm adds the small constant value δ to the sample values of one patch and subtracts the same value δ from the sample values of another patch, but the symmetric modulo operation would make odd pixel values add δ and even pixel values subtract δ respectively in the patch A and B . The value of $E[\alpha_i - \beta_i] \alpha_i \in A, \beta_i \in B$ is nearly not changed. The original patchwork algorithm combining with symmetric modulo operation do not work, so the paper improves the patchwork algorithm. The method is presented as follows:

Calculate the sample means $\bar{a}_o = 1/n \sum_{i=1}^n (a_o)$, $\bar{a}_e = 1/n \sum_{i=1}^n (a_e)$, $\bar{b}_o = 1/n \sum_{i=1}^n (b_o)$, $\bar{b}_e = 1/n \sum_{i=1}^n (b_e)$ and of sets A_o, A_e, B_o, B_e and the difference d_1 of the sample means between the set A_o, A_e and the difference d_2 between B_o, B_e . Owing to patch A and patch B are pseudo-randomly selected, the expected value of the difference ($d_1 - d_2$) is 0 whatever A or B is according to the original patchwork algorithm. After embedding process completed, generally d would become larger and is larger than $8 \times C$.

The extracting process which is similar to the embedding process is presented in Fig. 3. Here, introduce the extracting method: first calculate the difference of the sample means between the set A_o and A_e , and the difference d_2 between B_o and B_e . Compare the value $d = (d_1 - d_2)$ with threshold $M = 4*C$ (constant embedding level). When $d > M$, “1” is embedded. When $d < -M$, “0” is embedded. Second by watermark bits, the original image is reversibly restored. If watermark bit is equal to 1, the grayscale values of A rotate anti-clockwise C times and the grayscale values of B rotate clockwise C times according to symmetric modulo operation to restore the original image.

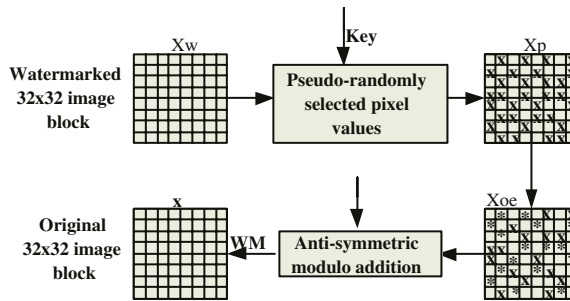


Fig. 3. Extracting process for 32x32 block

3.3 The Analysis of the Problematic Blocks

In general, the mean of the sample pixels belonging to patch A are close to the mean of the sample pixels belonging to patch B before embedding. This is highly probable, since the blocks have equal sizes and are pseudo-randomly selected. But in practical application, some image blocks can not satisfy those assumptions, that is the difference of the sample mean values between patch A and patch B is larger. Even after embedding watermark, the distance is too large to correctly detect the watermark. Now the paper takes an example to explain that drawback. Assume $w_k = 0$. Calculate $S'_n = \sum_{i=1}^n ((b_{1i} + \delta) - (b_{0i} - \delta)) = 2n\delta + \sum_{i=1}^n (b_{1i} - b_{0i})$, $b_{0i}, b_{1i} \in B$. Assume $\sum_{i=1}^n (b_{1i})$ is less than $\sum_{i=1}^n (b_{0i})$ and the difference is very larger. If $(\sum_{i=1}^n (b_{1i} - b_{0i}))$ is less than $(-\delta n)$, then $(2\delta n + \sum_{i=1}^n (b_{1i}) < \delta n)$. Where δn is equal to the threshold value M .

According to the above analysis, S'_n is less than threshold value, so the watermark sequence can not be correctly extracted. The paper calls those blocks as bad blocks. If the number of bad blocks is very larger, it would heavily impact the number of the embedding bits. Add the value of δ to reduce the situation, but the visual quality would become bad, so δ can not be too larger. To correctly detect these blocks, the receiver needs additional knowledge to reverse the embedding.

If the difference between b_{1i}, b_{0i} is fewer, but after embedded watermark information, the difference is still fewer. For such blocks, the method of resolving the problem is not to embed watermark. When extracted, one can reverse the watermark and the original image without additional knowledge for the receiver. We call such blocks as useless blocks.

4 Experimental Results

The test 256-grayscale image ‘‘Lena’’ with size 256×256 is divided into 32×32 pixel block.

From the above Fig. 4, you may easily notice those flipping points, which cause the salt-pepper-noise. Those heavily influence the quality of the image. For



Fig. 4. Original image and watermarked image with modulo 255 addition. (a) The original image ; (b) A part of the watermarked image

Table 1. It shows the results with the modulo 255 addition and the patchwork algorithm. It partitions the distribution of the image blocks into three categories. The category contains the regular blocks, the second is the bad block avoided by adding the embedding depth. and the last blocks can not bring nothing to capacity. The embedding level is the constant C

| Image | Block Size | Regular Size | Bad Size | useless Size |
|-------|-----------------------|--------------|----------|--------------|
| Lenna | $16 \times 16(C = 4)$ | 219 | 24 | 13 |
| | $32 \times 32(C = 4)$ | 60 | 0 | 4 |

those disadvantages, we present an improved method: symmetric modulo operation. The method may eliminate “salt-and-pepper” noise.

Fig. 5 and Table 2 show the experimental results of adopting the symmetric modulo operation and improved patchwork algorithm. There are not any flipping points in Fig. 5. The visual quality is largely improved.



Fig. 5. It shows the watermarked image with the different embedding levels by the patchwork algorithm and symmetric modulo operation. The constant C is the fixed embedding level. (a) Watermarked image ($C = 2$); (b) Watermarked image ($C = 4$)

Table 2. Number of blocks used to infer the capacity. The last two columns respectively correspond to the regular blocks and the bad blocks

| Image | Block Size | Regular Size | Bad Size | useless Size |
|-------|-----------------------|--------------|----------|--------------|
| Lenna | $32 \times 32(C=2)$ | 62 | 2 | 0 |
| | $32 \times 32(C = 4)$ | 0 | 0 | 0 |

5 Conclusion

The paper applies the patchwork algorithm and modulo 255 addition to reversibly restore original image, but the methods have some drawbacks, for example “salt-and-pepper” noise and bad blocks. In order to resolve that disadvantage, the paper presents symmetric modulo addition by constant embedding level in advance to avoid the “salt-and-pepper”. With larger embedding level, for instance from 2 to 4, the number of the bad blocks become fewer or none, but the quality of the image become a little worse. In practice, we may choose different embedding level for different situation.

References

1. C. W. Honsinger, P. Jones, M. Rabbani, and J. C. Stoffel: Lossless Recovery of an Original Image Containing Embedded Data. US patent, No 77102/E-D,(1999)
2. Bender W, Gruhi D, Morimoto N, et al: Techniques for data hiding[J]. IBM System Journal. (1996), 35(4,5):313-336
3. J.Fridrich,J.Goljan, and R.Du: Invertible Authentication. In Proceedings of SPIE, Security and Watermarking of multimedia Content, San Jose, January (2001)
4. C.De Vleeschouwer, J.F.Delaigle and B.macq: Circular Interpretation of Histogram for Reversible Watemarking. Proceedings of IEEE Workshop on Multimedia Signal Processing, Cannes, France, pp. 345 -350,(2001)
5. J.Tian: Reversible watermarking by difference expansion. Proceedings of Workshop on Multimedia and security,19-22,Dec,(2002)

Spatial Knowledge-Based Applications and Technologies: Research Issues

Elisa Bertino¹ and Maria Luisa Damiani²

¹ Department of Computer Sciences, Purdue University, West Lafayette, Indiana, USA

² Dipartimento di Informatica e Comunicazione, Università degli Studi di Milano,
Via Comelico 39/41, 20135 Milano, Italy

Abstract. Spatio-temporal data and knowledge have become increasingly important in the last years. In this paper, which introduces the session on *Knowledge Engineering Techniques for Spatio-temporal Applications*, we outline some issues in geo-spatial research and applications for which the use of innovative knowledge, tools and methodologies is crucial.

1 Introduction

In the last decade we have witnessed significant evolutions of data, knowledge and applications in the geo-spatial domain. Such evolutions have been pushed by the availability of wireless networks and portable devices that have enabled the development of significant location-based services. Moreover, new important application areas have emerged, such as homeland security and mobile-commerce, which pose new interesting challenges. In particular, what is most striking in many of these innovative applications is the increasing pervasiveness of spatial information. Whereas until few years ago, only a limited number of organizations were able to afford a geographical information system (GIS) because of its high cost and complexity, nowadays geo-spatial information is going to be integrated into the business processes of a variety of different enterprises, even not directly involved in geographical-related sectors. Geo-spatial information has become the basic ingredient of applications that are or are going to be of common use, such as location based services, user navigation and ubiquitous computing. Increasingly thus geo-spatial information is deployed in heterogeneous contexts and used by people that often have little familiarity with geo-spatial concepts.

It can be also observed that current spatially-aware applications often deal with increasingly larger geographical areas. In contrast with early applications that were mostly concerned with local geographical phenomena, such as cadastre management and urban planning, new emerging applications may scale up to a continental or world-wide dimension and involve a large number of players spread across large geographical areas. Applications related with the development of Spatial Data Infrastructures are a significant example of such a trend. A Spatial Data Infrastructure (SDI) can be defined as infrastructure consisting of IT systems and policies that facilitate the availability of and access to spatial data. In the SDI Cookbook [1], a SDI is defined as “a basis for spatial data discovery, evaluation, and application for users and providers within all levels of government, the commercial sector, the non-profit sector, and academia and

by citizens across different jurisdictions". A SDI thus aims at establishing a bulk of rules and knowledge to be shared across cultural and administrative boundaries. The establishment of an infrastructure for spatial information at European scale has been recently approved by the European Commission [3]. For the realization of a SDI, however, like for all the applications based on the cooperation of different communities of users, it is fundamental to ensure the interoperability among the sources of geo-spatial information, that may differ for example in resolution and spatial and thematic content.

Another characteristic of current applications is that the notion of space has also evolved. We can distinguish among different kinds of space: besides the *data space*, that is, the space populated by observations of the real world, there is a *meta-data space* populated by meta-objects, representing spatial resources such as geo-spatial data sources and user communities. Since the spatial resources may be characterized by a position and evolve in time, they can be considered as themselves embedded in a space and be possibly spatially interrelated. An example of spatial relationship at the metadata level is that of nearness between cadastral data sources. Finally, space can also consist of the *artificial space*. Examples of artificial spaces are the virtual landscapes built using virtual reality and videos. Note that there are applications in which all these spaces need to coexist.

For the development of spatially aware applications characterized thus by novel kinds of users and services, extended geographical scope and information dissemination, the technology has to deal with a number of challenges. In what follows we briefly discuss some research themes in which spatial knowledge can play an important role. Finally we focus on a possibly reference application area in which these technological advances would find a social and economic motivation.

2 Research Challenges

2.1 Geographical Ontologies

A classical and well-known issue in geo-spatial data management is data integration. Geo-spatial data are inherently heterogeneous simply because the real world can be observed from multiple points of views. However, nowadays the problem is further exacerbated by the need of integrating geo-spatial information across cultural and administrative boundaries, as requested for example by SDIs. Whereas the standardization initiatives that started in 1994 with the constitution of OpenGIS Consortium (now Open-Geospatial Consortium), has contributed to solve the problem of physical heterogeneity by defining common software specifications and interfaces, the issue of semantic heterogeneity of spatial information is still open. One aspect of such heterogeneity is the different conceptualization of spatial objects. An interesting example of such a diversity in conceptualization is reported by Bennet in [2]. In particular, this paper discusses the concept of *forest* and presents different interpretations of this term and how these interpretations can affect the determination of the spatial extensions of the spatial objects classified as forests. In order to deal with the semantic heterogeneity of spatial information, the development of geographical ontologies is crucial. A geographical ontology (geo-ontology) defines the spatial concepts that are shared by a community of users, representing thus the semantic reference for users and applications that accept to align

their spatial data with such an ontology [10][6]. The formalization of geo-ontologies either for general purpose or for specific domains is thus a major technological challenge. In this view, a notable case study is the GEON project (Geo-sciences Network) currently under development in the US [5]: a major goal of the project concerns the development of domain-specific ontologies for geology and more in general for geo-sciences. Research issues related to the definition of ontologies include how to fuse information compiled using different ontologies possibly developed by multiple communities. In general, the mapping between ontologies is not automated and relies on the application of domain expertise. Recent approaches, however, try to automate such a process of geospatial information fusion [4].

2.2 Distributed Architectures for Geo-spatial Information Management

A second challenge concerns the development of distributed architectures for the management of geo-spatial information. Because the processing of spatial data and knowledge is complex and expensive, many computational functions that once were centralized in a GIS can now be made available in form of Web Services, thus as programs that can be accessed by clients through the Web. Web services may consist of simple functions such as those performing coordinate conversion or more complex ones such as those simulating spatial phenomena. At the same time, the development of portable devices has encouraged the development of spatially-aware applications for mobile users. Therefore mobile users can access Web services and download on portable devices geo-spatial information that can be further managed locally. In all these cases, however, the spatial information mainly flows from the centre, i.e. the server, towards the periphery, i.e. the client. A more innovative distributed architecture in which the information, being collected remotely, flows instead from the periphery to the centre is represented by geo-sensor networks. Geo-sensors, such as GPS-based devices, biosensors, cameras on board of static or mobile platforms typically acquire streams of geo-spatial data. The aggregation of a number of sensor nodes into a computational structure forms a geo-sensor network. Raw data is thus collected by the nodes of the network and possibly aggregated and analyzed. Data aggregation and analysis can be locally executed in real-time by sensor nodes, or off-line in several distributed or centralized repositories [9]. Because this area of research is recent, there is no a common accepted framework. From a knowledge engineering perspective, however, relevant open research issues include modelling and reasoning with geo-sensors.

2.3 Spatial Data Warehouses and Spatial Data Mining

In the near future large amounts of raw spatial data will become available, especially in the form of sensor data. At the same time the complexity of the decision making processes, involving geo-spatial data and knowledge, will increase. It is thus reasonable to expect that technologies for spatial knowledge discovery will become more and more relevant. Spatial data warehousing and spatial data mining are two complementary techniques for knowledge discovery. Spatial data warehousing mainly focuses on the development of extended and spatial-based multidimensional data models to support spatial data aggregation and user navigation. Spatial data aggregation is an opera-

tion providing a synthetic view of a geographical phenomenon, whereas navigation is a functionality allowing the user to interactively inspect and analyze data through a set of spatially aware operators (Spatial OLAP) [7]. In contrast, spatial data mining deals with the development of algorithms for the discovery of complex spatial knowledge, such as spatial clustering and spatial association rules. Because of the increasing number of mobile communication devices, a challenging knowledge discovery task is the extraction of knowledge in the form of space-time trajectories of these personal devices [8]. These trajectories contain detailed information about personal and vehicular mobile behaviour, and therefore offer interesting practical opportunities to find patterns to be used, for instance, in traffic and sustainable mobility management, e.g., to study the accessibility to services. A further research issue is the integration of multidimensional data modelling, OLAP and data mining in a comprehensive system able to deal with the different aspects of data modelling, user interaction and complex knowledge extraction.

3 An Application Scenario

Finally we would like to pose the question of which kinds of application domains are best representative of the next generation spatial applications and thus where the above technologies could be best exploited. We believe that the recent natural disasters should make researchers reflect about the relevance of issues such as natural risk and disaster management. Disasters like floods, storms, earthquakes, represent a serious disruption for the human society and can compromise the social and economic stability of several countries. To mitigate their effects, disaster management strategies are needed based on an interdisciplinary approach and accounting for organizational, social and technological aspects. The use of spatial technologies in disaster management is a growing field with limited published information to date. From a technological and an information engineering point of view, this domain offers several challenges. First, this is an application area in which many types of information have both a spatial and a temporal component. Moreover, relevant data are spread on the territory, and are acquired by many diverse technologies, including real-time sensor data from satellites and networks on the Earth. Further, in these applications the interaction with the available data spatial infrastructures is essential. The general architecture that can be envisaged is thus a highly distributed architecture enabling the cooperation among geo-sensor networks, infrastructures such as SDIs and decision support systems. For example, sensor data related with other types of data, such as mapping and cadastral information from different countries, may provide a database from which hazard maps can be generated, indicating which areas are potentially dangerous. Similarly, knowledge patterns extracted from raw spatial data can be used together with simulation models for environmental surveillance and monitoring purposes. Geo-ontologies instead would represent the semantic glue for connecting all the application resources in some metadata space.

4 Conclusions

In this paper which introduces the session on knowledge engineering techniques for spatio-temporal applications we have outlined current trends in geo-spatial applications

for which the use of innovative knowledge tools and methodologies is crucial. We have also briefly discussed some relevant research issues; certainly our discussion is not exhaustive and many other relevant challenges can be identified, such as for example the development of security and privacy techniques for geo-spatial applications and location-aware services. We trust that the attendees will find many interesting ideas, concepts and research results in the papers presented in this session as well as challenging research directions.

References

1. Global Spatial Data Infrastructure: The SDI Cookbook, V2, Jan. 2004.
<http://www.gsdi.org/docs2004/Cookbook/cookbookV2.0.pdf>
2. Bennett B.: What is a Forest? on the vagueness of certain geographic concepts. *Journal Topoi*, 20 (2), pp 189-201, 2001.
3. Commission of the European Communities: Proposal for a Directive of the European Parliament and of the Council establishing an infrastructure for spatial information in the Community, 23 Jul. 2004. http://inspire.jrc.it/proposal/COM_2004_0516_F_EN_ACTE.pdf
4. Duckham, M. and Worboys, M. F.: An algebraic approach to automated geospatial information fusion Accepted for publication in International Journal of Geographical Information Science, 2005
5. Kuij L., Ludaescher B.: A System for Semantic Integration of Geologic Maps via Ontologies. In the Proc. of the Workshop on Semantic Web Technologies for Searching and Retrieving Scientific Data (SCISW), Sanibel Island, Florida, 2003
6. Kuhn W.: Semantic reference systems. *International Journal of Geographical Information Science* 17(5): 405-409, 2003
7. Rivest S., Bédard, Y. and Marchand P.: Towards better support for spatial decision-making: defining the characteristics of spatial on-line analytical processing (SOLAP) *Geomatica, the Journal of the Canadian Institute of Geomatics*, 55:2001, 539–555, 2001
8. Meratnia, N. and de By, R.: Aggregation and Comparison of Trajectories. In the Proc. ACM GIS'02
9. Nittel S., Stefanidis A., Cruz I., Egenhofer M., Goldin D., Howard A., Labrinidis A., Madden S., Voisard A. and Worboys M. : Report from the First Workshop on Geo Sensor Networks. *SIGMOD record*, Special Issue on Sensor Network Technology Infrastructure, Security, Data processing, and Deployment, Ed.Vijay Kumar, March, 2004
10. Spaccapietra S., Parent C., Cullot N., and Vangenot C.: On Spatial Ontologies. In the Proc.of GeoInfo 2004, VI Brazilian Symposium on GeoInformatics, Campos do Jordao, 2004

Managing Spatial Knowledge for Mobile Personalized Applications*

Joe Weakliam¹, Daniel Lynch¹, Julie Doyle¹, Helen Min Zhou¹,
Eoin Mac Aoidh¹, Michela Bertolotto¹, and David Wilson²

¹ Department of Computer Science, University College Dublin
{joe.weakliam,daniel.b.lynch,julie.doyle,min.zhou,
eoin.macaoih,michela.bertolotto}@ucd.ie

² Department of Software and Information Systems,
University of North Carolina at Charlotte
davils@uncc.edu

Abstract. The continuing explosion in the amount of readily available spatial data has given rise to significant problems in accessing the most task-relevant spatial information. At the same time, advances in mobile computing have yielded handheld platforms powerful enough to deliver spatial information interactions, but with usability issues in interfacing and wireless data transmission. We are developing techniques to manage information overload in mobile interactions with spatial knowledge repositories. In this paper we outline a novel application called CoMPASS (Combining Mobile Personalized Applications with Spatial Services) that incorporates knowledge management and spatial modeling approaches to provide end-users with spatial data tailored to their immediate requirements and long-term spatial preferences. CoMPASS presents spatial data in the form of personalized vector maps, based on user models, which enhance both application quality and efficiency by delivering the most relevant information and map content.

1 Introduction

When browsing the World Wide Web, users face the well-documented problems of information overload and irrelevant content due to the sheer volume of data that has become available in recent years. A similar problem is being faced in GIS (Geographic Information Systems) applications with the continuing explosion of available spatial data. GIS users can access spatial data in a variety of formats based on current requirements, e.g. a cartographer may want 3-dimensional data displaying the aspect of the surrounding environment, while for a tourist a scanned city map would be sufficient. The majority of GIS applications present spatial data in the form of area maps, such as in the popular driving directions and tourist guides. However, these datasets are typically more detailed than necessary. This can be a problem in the mobile environment where

* The support of the Informatics Research Initiative of Enterprise Ireland is gratefully acknowledged

clients attempt to download spatial information on devices with more limited capabilities. Spatial databases in general contain massive amounts of spatial data representing diverse geographic areas. A large proportion of such data is of little use to a high percentage of users trying to locate specific detail satisfying their current interests. In many mobile GIS applications, if two users with complementary interests regarding spatial content both request a map of the same region, no attempt is made to present the users with contrasting map representations: the users are presented with the same default map composed of standard map content. Developing user models or profiles [1] and employing personalization techniques such as collaborative filtering [2], can provide a more effective way to manage spatial knowledge by more precisely tailoring spatial information to user needs. Presenting only on-point spatial information helps to focus user task activities and reduces the data communication overhead, both of which are crucial in mobile applications because of limited screen size, computational power, and communication bandwidth.

In this paper we introduce a mobile GIS environment called CoMPASS that models user interests related to spatial content and utilizes user profiles to return the most relevant spatial content in map format. Section 2 discusses related work in knowledge management and spatial modeling in GIS. Novel approaches employed by CoMPASS addressing some of the limitations encountered in mobile GIS applications are described in section 3. An evaluation of the performance of CoMPASS is given in section 4. Section 5 concludes and outlines future work.

2 Related Work

Research in tailoring spatial information in GIS applications typically focuses on the presentation of spatial content and/or the spatial context related to the user's location. Zipf and Richter [3] propose producing maps where the user's attention is directly drawn to the area of the map that is currently of interest to them. Maps divided into distinct zones with each zone containing different levels of detail are generated. Interest zones are those holding the greatest detail but much of this detail may not be relevant to the current user. While maps with detailed spatial content are delivered to the user, no attempt is made to personalize the map content. In [4] neural networks are used to elicit user preferences regarding geographical and semantic information in Web GIS. The neural network is refined by system learning processes combining spatial and semantic criteria and the information provided to users is continuously adapted by monitoring the users' actions and the system recommendations. However, such work deals solely with image schemata and is also heavily reliant on explicit user input. Zipf [5] proposes the dynamic creation of more personalized tourist maps based on a wide range of variables including spatial and personal context; however the ideas in [5] are at a conceptual level and have yet to be implemented. The notion of representing geographic maps as aspect maps is outlined in [6]. Aspect maps are described as spatial organization structures in which one or more aspects of geographic entities are represented. While the authors present a novel approach for spatial modeling, they fail to consider possible user prefer-

ences related to spatial interests. Finally, GeoNotes [7] describes an annotating mechanism enabling users to annotate physical coordinates, and uses collaborative filtering to return annotations entered by other users that are relevant to the current user. With GeoNotes, users can associate annotations according to physical location. The user has the ability to set the filters, and search explicitly. In contrast to the systems described above, CoMPASS provides users with personalized vector maps containing spatial content, at varying levels of detail and tailored to a user's individual requirements, without requiring any explicit input. CoMPASS achieves this by monitoring user-map interactions and using information inherent in these implicit actions to develop models of user preferences.

3 System Overview

CoMPASS is a mobile GIS providing users with spatial information tailored to their personal requirements. It addresses current problems of quality and efficiency related to superfluous information in mobile GIS by aligning task-based user models and personalization of spatial information with Progressive Vector Transmission (PVT) [8][9]. Using PVT in conjunction with personalization is very effective as the size of the data set necessary for rendering the personalized map is reduced significantly. User models are derived implicitly, over the course of normal map interactions. The CoMPASS client has currently been fully implemented on a Tablet PC, and we are developing a simplified version for an iPaq Pocket PC.

3.1 Map Personalization

Map personalization is an approach to generating area maps containing specific spatial content, in terms of map features and spatial annotations, based on a user's individual preferences. Map personalization is realized by monitoring user interactions with maps during sessions and these interactions are analysed to construct a profile modeling the user's spatial content preferences. User preferences are then employed to infer the most appropriate spatial information for subsequent delivery. In CoMPASS we consider two types of personalization: personalization of map annotations, and personalization of map feature content.

CoMPASS allows a user to annotate spatial data sets with multimedia information; this is used to model the kind of map-related information relevant to the user. As the user navigates a physical region, relevant annotations are considered for presentation based on several criteria: a location filter surrounding the user is created where the user's trajectory alters the shape of this filter, e.g. if the user moves in a straight line then the filter is altered to return more annotations ahead of the user's location. This generates a spatial relevance boundary within which annotations are returned. Annotations are also associated with specific map features and if a feature holds no relevance to the user, annotations linked to that feature will not be returned, even if they fall within the relevance boundary. Relevant textual annotations are retrieved according to their keywords with

traditional IR search techniques incorporated to eliminate superfluous annotations from the results set. Collaborative filtering is employed to improve the relevance score of annotations. The authors of annotations returned in the keyword search populate the set of similar users. The averages of the scores linked to annotations rated by these “similar” users are then calculated and the results are normalized to generate a relevance score.

The first step in personalizing map feature content is to deliver a “best-fit” map to the user based on their current position and existing spatial preferences (profile). Every action performed by the user for the entire map session is recorded in a log file, (e.g. pan, zoom, toggle feature on/off, etc.) Knowledge about map features and regions of interest are then inferred from the map actions executed by the user. Finally, all of the user’s preferences related to spatial content for the current session are recorded, with significant updates being propagated to the user model for future sessions. Analyzing the content of the log files enables the system to elicit knowledge about core user interests related to features and regions of significance for any particular session. The features and regions that the user interacted with are then evaluated based on several criteria including:

1. Feature presence in frames: if a feature is visible inside a frame, then this indicates interest rather than disinterest in that feature as the user has the option of removing that feature from the map.
2. Map actions executed: some actions indicate more interest in features than others, e.g. highlighting a feature indicates explicit interest whereas panning the map discloses no real interest in a feature.

3.2 Mobile Interface

In CoMPASS when a user requests a map, a GML file, containing those features of relevance to the user, is created at the server. This dataset is transmitted over the wireless network to a Tablet PC client. As GML is concerned only with describing map content, it is necessary to render the GML graphically to view the data in a map format. In CoMPASS, maps are visualized by parsing the GML file and transforming the GML entities to Java objects, which are displayed within the GUI. Using GML enables fast processing of spatial data and allows us to model the data using an open standard. When designing an interface for mobile applications it is important to design a flexible multimodal interface allowing for various types of interaction [10]. Users in the field can interact with the system via the pen/keyboard of the mobile device. Alternatively, a speech interface is provided which can be useful in hands-busy eyes-busy environments. Fig. 1 shows a screenshot of the CoMPASS mobile interface.

3.3 Progressive Vector Transmission

When a map request is made, CoMPASS takes the user’s current location and profile detail to ascertain map features of highest relevance for the current session. We use maps in vector format (instead of raster maps) as they are more

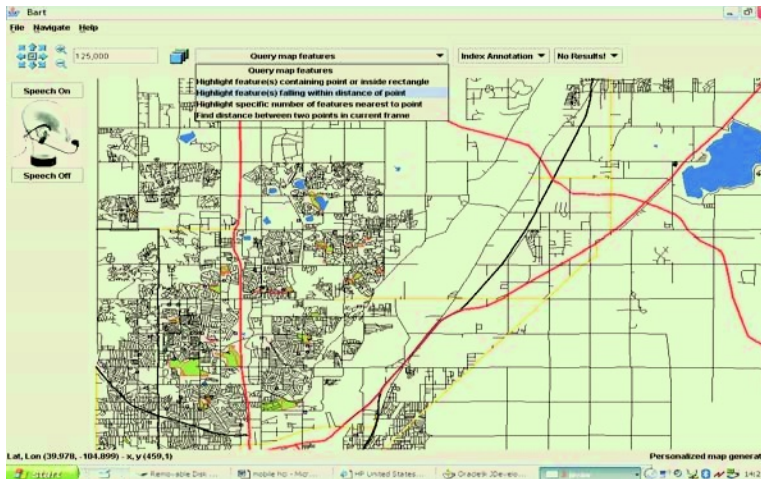


Fig. 1. Mobile Interface for Tablet PC

versatile for manipulation and analysis. However, downloading vector maps from a server to a thin client is time consuming, even through fast communication links, as vector datasets are typically large due to the complex geometry of real world objects. This coupled with the fact that users generally receive more detailed maps than were requested results in unacceptable performance times. Progressive Vector Transmission (PVT) [8][9] enables us to model and “personalize” spatial data by adapting it to the level of detail desired by the user.

A general approach for PVT pre-computes a sequence of consistent multiple representations at lower levels of detail (LoD) from a fully detailed map on the server. This sequence is then transmitted in order of increasing detail to the mobile client. Once the set of session interest map features has been established, the coarsest LoD, representing the spatial data associated with each feature, is transmitted first and displayed at the client. The detail at the client is then progressively substituted by subsequent finer feature detail until users are satisfied or a fully detailed map is completely transmitted. This is extremely important when sending data to mobile devices due to restrictions inherent in these devices.

4 Evaluation

An initial evaluation has been carried out to assess the performance and quality of spatial modeling provided by CoMPASS, using vector data describing Adam County and Arapahoe County, Colorado, USA (obtained from the US Census Bureau). Spatial modeling was assessed both on a map personalization basis, and on the efficiency of vector data transfer.

In order to evaluate our personalization approach 6 users participated in an initial experimental study. The users were each assigned 20 tasks related to locating specific detail contained within maps. The users had the freedom of

interacting with the maps in any manner, i.e. they could execute any map action at any time, but ultimately had to realize the individual session goal assigned at the outset of each session. There are potentially 30 features visible in a map frame at any time with which the user can interact. The following outlines some representative examples of the 20 tasks assigned to the users:

1. Locate the nearest park because you want to go walking.
2. Locate a lake that is situated near a major road, as you want to go fishing.
3. Locate a park that contains a lake to take your children to feed the ducks.

The 20 tasks assigned to the 6 users were all related to parks, lakes, major roads or some combination of these features. The reason for assigning predetermined mapping tasks is to enable the system to correlate different users who can potentially interact with maps in contrasting manners. All 6 users were instructed to request detail for each of the 20 sessions from the same starting positions.

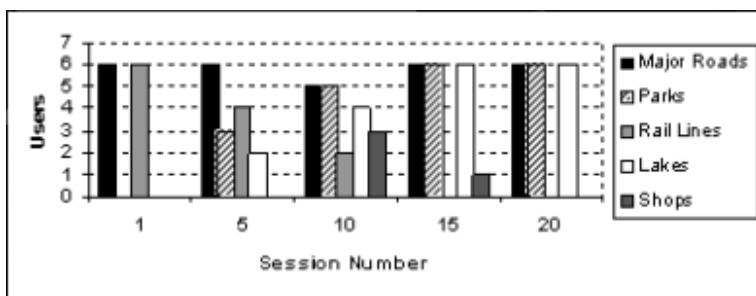


Fig. 2. Graph showing results of map personalization

The aim of the experimental study was to show that CoMPASS can effectively learn user preferences over time and make improved recommendations each time the user requests a new map. In the experimental study carried out, the users were all assigned fixed tasks to reveal the results of spatial modeling for a group of users rather than simply for one single user. For each user making their first request, the same set of features was presented to each as all maps were requested from the one location. Fig. 2 shows the graph of results obtained. The detail in the graph shows that as the number of sessions increases so does the level of personalization. CoMPASS recommends parks, lakes, and major roads for all sessions after session 15 for each of the 6 users as they interacted with these features heavily as per the session goals. On the other hand CoMPASS does not recommend shops and rail lines because the users do not interact with these features with any sense of regularity due to the session goals.

We have also carried out a second evaluation testing the efficiency of our system. This evaluation reveals that progressive transmission is particularly useful when transmitting large vector data sets.

5 Conclusion

The problems of information overload and irrelevant information are widespread in mobile GIS. Spatial modeling and knowledge management are two ways to address these issues. In this paper we introduce a mobile GIS called CoMPASS that delivers personalized maps based on users' preferences related to spatial content and makes use of existing knowledge management techniques such as personalization and collaborative filtering to model spatial data both at the client and at the server. There is much scope for future work with CoMPASS: we intend to use spatial data mining techniques to mine patterns of user interest in map regions and features, and collaborative filtering to group users with interest in the same features and regions.

References

1. B. Mobasher, H. Dai, T. Luo, Y. Sun, and J. Zhu. Discovery of Aggregate Usage Profiles for Web Personalization. In *Proceedings of the Web Mining for E-Commerce Workshop (WEBKDD 2000)*, pages 61–82, Boston, August 2000.
2. D. Goldberg, D. Nichols, B. Oki, and D. Terry. Using Collaborative Filtering to Weave and Information Tapestry. *Communications of the ACM*, 35(12):61–70, December 1992.
3. A. Zipf and K-F. Richter. Using Focus Maps to Ease Map Reading. In *In: Künstliche Intelligenz (KI)*, pages 35–37, April 2002.
4. Y. Yang and C. Claramunt. User Preference Elicitation and Refinement in Web Geographical Information Systems. In *Proceedings of W2GIS 2004*, pages 27–44, Goyang, South Korea, November 2004.
5. A. Zipf. User-adaptive Maps for Location Based Services (LBS for Tourism. In *Proceedings of the 9th International Conference for Information and Communication Technologies in Tourism*, pages 329–338, Innsbruck, Austria, 2002.
6. B. Berendt, B. Barkowsky, and C. Freksa. Spatial Representation with Aspect Maps. In *Proceedings of Spatial Cognition: An Interdisciplinary Approach to Representing and Processing Spatial Knowledge*, pages 157–175.
7. F. Persson, P. Espinoza, A. Fagerberg, R. Sandin, and T. Coster. GeoNotes: A Location-based Information System for Public Spaces. In *In: Designing Information Spaces: the Social Navigation Approach*, pages 151–173, 2003.
8. M. Bertolotto and M. Egenhofer. Progressive Transmission of Vector Map Data over the World Wide Web. *GeoInformatica*, 5(4):345–373, 2001.
9. B.P. Buttenfield. Transmitting Vector Geospatial Data across the Internet. In *Proceedings of GIScience*, pages 51–64, 2002.
10. S. Oviatt. User-Centered Modeling for Spoken Language and Multimodal Interfaces. *IEEE Multimedia*, 13(4):26–35, 1996.

Geospatial Clustering in Data-Rich Environments: Features and Issues

Ickjai Lee

School of Information Technology,
James Cook University, Townsville, QLD4811, Australia
Ickjai.Lee@jcu.edu.au

Abstract. Geospatial clustering must be designed in such a way that it takes into account the special features of geoinformation and the peculiar nature of geographical environments in order to successfully derive geospatially interesting global concentrations and localized excesses. This paper examines families of geospatial clustering recently proposed in the data mining community and identifies several features and issues especially important to geospatial clustering in data-rich environments.

1 Introduction

As the size of data grows tremendously, we are witnessing the great need of data mining in many disciplines. Similar to other areas, data mining has been applied to the geographical context. Many attempts have been made to derive valuable hidden patterns in large geospatial¹ databases. Among several data mining techniques, clustering is one of the most widely and frequently used techniques. Clustering is a series of processes grouping a set of point data, $P = \{p_1, p_2, \dots, p_n\}$ in some study region R , into smaller homogeneous clusters with similar characteristics so that inter-cluster similarity is minimized and intra-cluster similarity is maximized. Numerous clustering approaches have been suggested within the machine learning (using self organizing maps), data mining (using mathematical summaries or indexing), spatial databases (using densities), image processing (using transformations), statistics (using sampling or mixture model) and GIS communities (using spatial dependence).

This paper examines families of geospatial clustering techniques recently proposed to efficiently handle large geospatial databases in the data mining community and in the GIS community. The main aim of this paper is to identify some features (that make geospatial data special) crucial for designing geospatial clustering and to discuss some issues involved². This paper attempts to fill the gap between the data mining community (concerning more about computational efficiency) and the GIS community (concerning more about “special characteristics of geospatial data”).

¹ In this paper, geospatial, geo-referenced and spatial are used interchangeably

² This paper is not to provide a comprehensive survey of state-of-the-art clustering methods. Also due to the space limit, references to various clustering methods are not included unless necessary

2 Background

It is well noted that space can make a difference and it is important to consider some special characteristics of geospatial data in geospatial analysis. Several attempts [1, 2] have been made to emphasize the importance of special characteristics of geospatial data in geospatial analysis. Recently, geospatial analysis in data-rich environments has attracted a lot of attention and has become a main focus of several specialized research meetings and conferences [3–5]. Few attempts [6–8] have been made to identify some peculiar geospatial characteristics needed to be considered for geospatial data mining.

Clustering is one of core techniques in data mining [9]. A large number of clustering methods have been proposed within the data mining and the GIS community. See [10–15] for various clustering approaches and details. Different clustering methods have been shown to offer different capabilities, different domains of applicability, different optimization functions, and different computational requirements. Note that, clusters are on the eye of beholder. Different inductive inferences will result in different clustering [16]. Obviously, no particular clustering method has been shown to be superior to all its competitors in all aspects. Despite the wealth of research in geospatial clustering, little attention has been paid to some features that must be considered in geospatial clustering and issues that are crucial to geospatial clustering.

3 Features and Issues for Geospatial Clustering

Geospatial clustering partitions geo-referenced data into smaller homogeneous subgroups with similar characteristics due to contiguity (spatial proximity). These geo-referenced datasets encapsulate the inherent and peculiar characteristics of geospatial data what makes them special [1]. These special characteristics of geoinformation require specialized clustering methods that incorporate the geo-referenced nature in order to identify high-quality patterns of geospatial concentrations. In addition to typical requirements of clustering in data mining (scalability to dimensionality and size of data, ability to deal with different types of attributes, discovery of clusters with non-convex shape, minimal domain knowledge to determine input parameters, ability to deal with noisy data, insensitivity to input order, and ability to incorporate user-defined constraints) [9], geospatial clustering needs to take the followings into account to detect geospatially meaningful concentrations.

Consideration of spatial dependence: Spatial dependence is a well-known special characteristic of geo-referenced data expressed in the First of Law of Geography. Anselin discussed spatial dependence along with spatial heterogeneity [1]. His proposition saying “the phenomenon where locational similarity is matched by value similarity” emphasizes the importance of spatial dependence among nearby neighbors. This spatial dependence is in opposition to the principle (or assumption) of independence underlying traditional statistics. In particular, this property is of great importance for detecting geospatially aggregated clusters. How to model this is explained in the next consideration.

Unambiguous modelling of spatial adjacency: Geospatial clustering is strongly tied to the discrete $\text{is_nearby_neighbor} \subset P \times P$ relation since nearby neighbors tend to form geospatial clusters. Thus, geospatial clustering becomes the matter of modelling and capturing geospatial adjacency and proximity. In order to capture spatial dependence between nearby neighbors, we need to concisely define who the neighbors are and how far they are. Most geospatial clustering methods utilize traditional raster-like modelling or vector-like modelling. However, these modelling approaches do not adequately handle the geospatial adjacency of discrete point data [17, 18]. More seriously, they constitute argument-dependent neighboring approaches that produce different neighboring information depending on argument values. These arguments are the cell size for raster-like modelling, and the number of neighbors and the radius for vector-like modelling (for instance, k -nearest neighboring and d -distance neighboring). Geospatial clustering must consider this ambiguity and inconsistency caused by these modelling approaches. Clustering results should not be brittle to those ambiguities. Note that, user-supplied arguments inhibit the possibility of exploratory derivation of arguments from the data. In addition, finding best values for arguments in argument-dependent modelling is time consuming in data-rich environments.

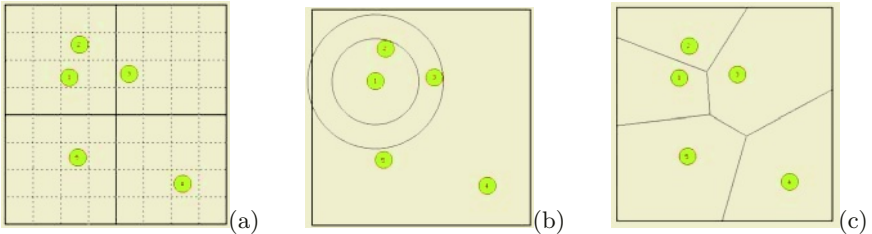


Fig. 1. Various neighbor modellings ($\|P\| = 5$): (a) The raster approach; (b) The vector approach; (c) The Voronoi approach

Fig. 1 illustrates the ambiguity caused by raster and vector modelling. The first source of ambiguity in the raster model is the shape of pixels and the pattern of neighbors. Each point shown in Fig. 1(a) could have 4-connectivity neighbors (considering N, S, E and W cells) or 8-connectivity neighbors (considering N, S, E, W, NE, NW, SE and SW cells). Furthermore, the adjacency relationship also heavily depends on the size of cell. In Fig. 1(a), if the cell size (volume) becomes 16 times bigger (considering now solid lines, rather than dotted lines), then neighboring becomes different. Similarly, it is a difficult task to define topological relationships of point data with vector models. This is because points do not have extent (0-dimensional objects), but only have location. Thus, points do not exhibit topological relationships such as “adjacent”, “touch” or “intersect” unless they coincide. Often, metric relationships such as d -distance concepts are used to overcome this problem. Points lying within a certain distance are regarded as neighbors. This works in some sense. However, this adjacency relationship still

presents inconsistencies similar to the problems mentioned in the raster model. The Voronoi approach overcomes this inconsistency to some degree and uniquely defines neighborhood as shown in Fig 1(c). One drawback of this approach is that it requires $O(n^{[d/2]})$ time for $d > 3$ [19].

Consideration of local interactions and global interactions: When there is no interaction or no correlation among the phenomena registered at data points, the points do not form clusters. However, interactions result in data points that may either attract or repulse one another. Both attraction and repulsion will likely produce either clustered or regular distributions (note that physical models of attraction and/or repulsion are used for producing nice graph drawings [20]). If two points represent phenomena that attract each other, then locations for events of the phenomena become closer. The two data points belong to the same cluster. In graph drawings, if all end-points of interactions repel one another equally, then the resulting distribution is regular. Inversely, strong attraction among a certain number of points may bring about isolated points, those too far become unattracted. Also, powerful repulsion causes clusters. All this implies that isolated points (noise and other data points not belonging to a cluster) are not only generated by repulsion with cluster members, but also by attraction among other points in the dataset. It is now obvious that both clusters and noise points are generated not only by interactions between their neighbors, but also other members in the dataset. A combination of local influence and global influence is the effect that shapes clusters. Note that, the behavior of spatial phenomena is the result of a combination of both local interactions (interactions confined to nearby neighbors) and global interactions (all the interactions over the study region) [21, 22].

Relative proximity rather than absolute proximity: Spatial heterogeneity implies that each location in R has intrinsic uniqueness [21]. That is, conditions vary from place to place. Statistical properties including mean, variance and covariance are dependent on absolute location and have different interpretations over R . Although relative locations (distances) are the same, their relative interpretations may differ. Fig. 2 depicts a minimum spanning tree with 9 points.

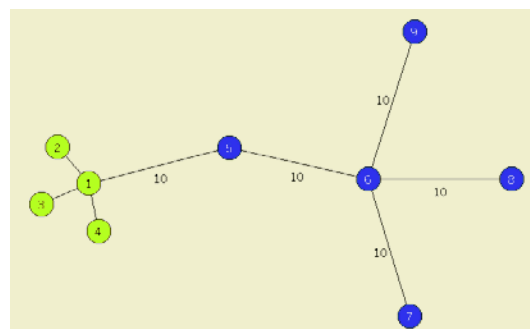


Fig. 2. Data that illustrates the importance of relative proximity in geospatial clustering ($\|P\| = 9$)

The two points, p_1 and p_6 , are both equidistant from p_5 . Clustering based on absolute distance will have the same grounds to place p_1 and p_6 in a cluster with p_5 . However, the length of edge $e_{1,5} = (p_1, p_5)$ seems to be relatively long with respect to the length of edge $e_{5,6} = (p_5, p_6)$ because of other points that create an heterogeneous perspective of the study region. Thus, p_5 is likely to belong to the same cluster as p_6 , but not to the cluster of p_1 . Although the lengths of the edges $e_{1,5}$ and $e_{5,6}$ are equal, they have different relative interpretations (relative to other points in R). Now, it is clear that relative proximity is more important than absolute proximity in geo-referenced settings and thus in geospatial clustering.

Non-stationary analysis: The geographical property of non-stationarity also implies that local variations at one place are not the same as variations elsewhere. When analyzing a point p_i and the region surrounding it, considering local interactions and global interactions deals with how much to take into account those points close to p_i and how much to take into account those points far from p_i . Relative proximity is about considering distances in relation to other points. Non-stationarity means that these decisions can not remain static across the study region and that is somewhat the dataset has to dictate how to account for them dynamically as the focus of analysis varies in the study region. An example of stationary analysis is the use of global values as thresholds for geospatial clustering. This not only ignores local variations, but disregards spatial heterogeneity. Thus, geospatial clustering approaches using global values as thresholds will easily fail to identify locally aggregated sparse concentrations that are also of importance as well as high-density concentrations. For instance, they are unable to report two distinct groups (dense (p_1, p_2, p_3 and p_4) and sparse (p_5, p_6, p_7, p_8 and p_9)) simultaneously in the dataset shown in Fig. 2.

Exploratory rather than confirmatory: Since clustering is to identify geospatial clusters without apriori knowledge, we do not know how many clusters exist, where they are, how close they are and how big they are prior to clustering. These information should be derived from data, which underpins exploratory data analysis and the principle to “let the data speak for themselves” [23, 24]. Openshaw [24] stresses that constraints and preconditions should be minimized in exploratory data analysis and geographical data mining. Hypotheses should be uncovered from the data, not from the user’s prior knowledge and/or assumptions. Minimizing the need to adjust arguments reduces the risk of tampering with the analysis tools. It also promises higher user friendliness. Traditional clustering methods share a need for user-specified arguments and prior knowledge to produce their best results. Such information needs are supplied as density threshold values in density-based clustering, merge or split conditions in hierarchical clustering, number of parts in partitioning clustering, prior probabilities and assumptions about the distribution of continuous attributes within classes in model-based clustering, or edge-cut thresholds in graph-based clustering. This parameter-tuning is extremely expensive and inefficient for huge datasets because it demands pre-processing and/or several trial and error steps. The need to find best-fit arguments in wide-spread semi-automatic clustering is not the

only concern, slight changes of values of arguments produce totally different clustering results. This sensitivity to user-supplied arguments raises serious questions regarding the validity of results.

Versatility (multi-purpose): The popular way of modelling real-world geospatial data is McHarg's multi-layer view of the world [25]. In this view, each geographical layer captures something unique to it. Thus, many heterogeneous types of features are stored in GIS including 2-dimensional point data, 3-dimensional point data, obstacle data (rivers, mountains or political boundaries). There is also a diversity in scales or contexts, such as data from urban areas where the Manhattan metric is more applicable and data on a large scale where the Euclidean metric is more suitable. In data-rich environments, GIS consists of hundreds of layers that may contain thousands or millions of points. A sophisticated versatile geospatial clustering that is generic to much of this diversity is in demand for such data-rich environments to handle many heterogeneous clustering settings such as clustering 2D point data in the presence of river obstacles in the Manhattan distance and grouping 3D point data in the absence of obstacles in the Euclidean distance.

Consideration of background information: Since geographical layers are thematically, geospatially and temporally correlated, incorporating background information to clustering may produce unexpected interesting patterns. A classical approach is the consideration of a layer of population-at-risk but an obstacle layer is also a possible candidate for background information. For instance, one approach is to consider obstacles as background information [6, 26]. In many spatial settings, obstacles (rivers, mountains, lakes and political boundaries) prevent traversing the straight path between two points, and thus influence interactions among objects.

4 Final Remarks

Bailey and Gatrell [21] remark “space can make a difference”. Data mining promises more precise and meaningful output with the incorporation of spatial dimensions. For instance, ‘crime incidents of urban areas are increasing and those of rural areas are decreasing’ is more precise and meaningful than ‘crime incidents are increasing or decreasing’. Considering peculiar features of geoinformation is of great importance in order to detect both geospatially aggregated high-density concentrations and local excesses.

References

1. Anselin, L.: What is Special About Spatial Data? Alternative Perspectives on Spatial Data Analysis. Technical Report 89-4, National Center for Geographic Information and Analysis, University of California (1989).
2. Egenhofer, M.J.: What's Sepcial about Spatial? Database Requirements for Vehicle Navigation in Geographic Space. In: Proc. of the 1999 SIGMOD Conf., Washing, D.C., ACM Press (1993) 398–402

3. Fong, J., Ng, M.K.: Proc. of the 5th Pacific-Asia Conf. on Knowledge Discovery and Data Mining. University of Hong Kong, Hong Kong (2001)
4. Böhlen, M.H., Jensen, C.S., Scholl, M.O.: Spatio-Temporal Database Management. Springer, Berlin, Germany (1999)
5. Roddick, J.F., Hornsby, K.: Temporal, Spatial, and Spatio-Temporal Data Mining. Springer, Berlin, Germany (2000)
6. Lee, I.: Multi-Purpose Boundary-Based Clustering on Proximity Graphs for Geographical Data Mining. PhD thesis, School of Electrical Engineering and Computer Science, University of Newcastle, Newcastle, Australia (2002)
7. Openshaw, S.: Geographical Data Mining: Key Design Issues. In: Proc. of the 4th Int. Conf. on Geocomputation. (1999)
8. Shekhar, S., Huang, Y., Wu, W., Lu, C.T.: What's Special about Spatial Data Mining: Three Case Studies. In: Data Mining and Engineering Applications. Kluwer Academic Publisher (2001)
9. Han, J., Kamber, M.: Data Mining: Concepts and Techniques. Morgan Kaufmann Publishers, San Francisco, C.A. (2000)
10. Aldenderfer, M.S., Blashfield, R.K.: Cluster Analysis. Sage Publications, Beverly Hills (1984)
11. Dubes, R., Jain, A.K.: Clustering Techniques: The User's Dilemma. Pattern Recognition **8** (1976) 247–260
12. Han, J., Kamber, M., Tung, K.H.: Spatial Clustering Methods in Data Mining. In: Geographic Data Mining and Knowledge Discovery. Cambridge University Press, Cambridge, UK (2001) 188–217
13. Hartigan, J.A.: Clustering Algorithms. John Wiley & Sons (1975)
14. Jain, A.K., Dubes, R.C.: Algorithms for Clustering Data. Prentice-Hall (1988)
15. Kolatch, E.: Clustering Algorithms for Spatial Databases: A Survey (2000).
16. Estivill-Castro, V.: Why So Many Clustering Algorithms: A Position Paper. SIGKDD Explorations **4** (2002) 65–75
17. Ahuja, N.: Dot Pattern Processing Using Voronoi Neighborhoods. IEEE Transactions on Pattern Analysis and Machine Intelligence **PAMI-4** (1982) 336–343
18. Gold, C.M.: Problems with Handling Spatial Data - The Voronoi Approach. Canadian Institute of Surveying and Mapping Journal **45** (1991) 65–80
19. Okabe, A., Boots, B.N., Sugihara, K., Chiu, S.N.: Spatial Tessellations: Concepts and Applications of Voronoi Diagrams. John Wiley & Sons, West Sussex (2000)
20. Eades, P., X., L., Tamassia, R.: An Algorithm for Drawing a Hierarchical Graph. Int. J. of Computational Geometry and Applications **6** (1996) 145–155
21. Bailey, T.C., Gatrell, A.C.: Interactive Spatial Analysis. Longman Scientific & Technical, Harlow, UK (1995)
22. Tobler, W.R.: A Computer Movie Simulating Urban Growth in the Detroit Region. Economic Geography **46** (1970) 234–240
23. Gould, P.: Letting the Data Speak for Themselves. Annals of the Association of American Geographers **71** (1981) 166–176
24. Openshaw, S.: Two exploratory space-time-attribute pattern analysers relevant to GIS. In: Spatial Analysis and GIS. Taylor & Francis, London (1994) 83–104
25. McHarg, I.L.: Design with Nature. Natural History Press, New York (1969)
26. Tung, A.K.H., Hou, J., Han, J.: Spatial Clustering in the Presence of Obstacles. In: Proc. of the 17th Int. Conf. on Data Engineering, Heidelberg, Germany, IEEE Computer Society (2001) 359–367

Spatio-temporal Modeling of Moving Objects for Content- and Semantic-Based Retrieval in Video Data

Choon-Bo Shim¹ and Yong-Won Shin²

¹ School of Information & Communication Engineering,

Sunchon National University, Sunchon, Jeonnam 540-742, South Korea

cbsim@sunchon.ac.kr

² Dept. of Healthcare Management, Catholic University of Pusan, Busan 609-757, South Korea
kevin@cup.ac.kr

Abstract. The general aim of this paper is to study the spatio-temporal representation scheme which can efficiently model moving objects' trajectories in video data. Our scheme deals with not only the single moving object but the multiple (two or more) moving objects. The traditional schemes only consider direction property, time interval property, and spatial relationship property for modeling moving objects' trajectories. But, our scheme also takes into account on distance property, conceptual location information, and related object information (e.g. player name having a soccer ball) so that we may improve a retrieval accuracy to measure a similarity between two moving objects as well as them. The proposed spatio-temporal representation scheme supports content-based retrieval using moving objects' trajectories and supports semantics-based retrieval using concepts which are acquired through the conceptual location information of moving objects. Finally, we show from our experiment that our scheme is superior to existing related work about 10-20% in terms of retrieval effectiveness.

1 Introduction

Recently, a lot of interests in content-based (or similarity-based) retrieval have been increased in multimedia database applications. Unlike image data, the most important feature in video data is the trajectory of moving objects. The trajectory of a moving object can be represented as a spatio-temporal relationship which combines spatial properties between moving objects in each frame with temporal properties among a set of frames. It also plays an important role in video indexing for content- and semantic-based retrieval. A user query for content-based retrieval using the trajectory of moving objects in video databases is as follows: "*Find all video shots whose trajectory is similar to the trajectory sketched in a graphic user interface.*" In some multimedia applications, we can extract semantics from the location information of moving objects. For example, in case of soccer video databases, we can approximately obtain semantics such as corner kick, penalty kick, and free kick from a sequence of locations of a soccer ball. Thus, it is necessary to support both content- and semantic-based retrieval using a sequence of locations of moving objects.

The initial research issues on the content-based video retrieval have highly concentrated on data representation schemes which can efficiently model content itself extracted from video data [1,2,3,4]. However, for handling a large amount of multimedia data, it is required to provide schemes with good retrieval performance on a

variety of user queries. Thus, we propose a new spatio-temporal representation scheme which can efficiently model moving objects' trajectories in video databases. Our scheme deals with a single moving object as well as multiple (two or more) moving objects. The traditional schemes only consider direction property, time interval property, and spatial relationship property for modeling moving objects' trajectories. However, our scheme also takes into account on distance property, conceptual location information, and related object information (e.g. player name having a soccer ball) so that we may improve retrieval accuracy to measure a similarity between two moving objects as well as them. Therefore, the proposed spatio-temporal representation scheme can support content-based retrieval using moving objects' trajectories as well as semantics-based retrieval using concepts which are acquired through the conceptual location information of moving objects. Finally, in our performance study, our scheme yields substantially better retrieval performance compared to existing related work in term of retrieval effectiveness.

This paper is organized as follows: Section 2 briefly introduces the related work on video retrieval using moving objects' trajectories; A new spatio-temporal representation scheme for modeling moving objects' trajectories is presented in Section 3; Based on our representation scheme, the content- and concept-based retrieval in video databases is described in Section 4; the experimental results of our scheme is shown in Section 5; and Section 6 covers conclusion with brief summary.

2 Related Work

There have been some researches on content-based video retrieval using spatio-temporal relationships in video data. First, when assuming a moving object is a salient one moving over time, Li et al. [5] represented the trajectory of a moving object as eight directions such as North(NT), Northwest(NW), Northeast(NE), West(WT), Southwest(SW), East(ET), Southeast(SE), and Southwest(SW). They represented as (S_i, d_i, I_i) the trajectory of a moving object A over a given time interval I_i where S_i is the displacement of A and d_i is a direction. They also represented as $A(\alpha, \beta, I_k)B$ the spatio-temporal relationships between moving objects A and B over time interval I_k . Here α is one of eight topological relationships: Disjoint(DJ), Touch(TC), Equal(EQ), Inside(IN), Coverd_by(CB), Contains(CT), Covers(CV), Overlap(OL). β is the directional relationship between moving objects A and B. Therefore, the spatio-temporal relationships between moving objects A and B can be represented as a list of motions, like $A < (\alpha_1, \beta_1, I_1), (\alpha_2, \beta_2, I_2), \dots, (\alpha_n, \beta_n, I_n) > B$.

Secondly, Shan and Lee [6] represented the trajectory of a moving object as a sequence of segments, each being expressed as the slope ranging from 0 to 360 degree for the single moving object's trajectory. In order to represent the multiple moving object' trajectories, they simply used the 2D string scheme proposed by Chang [7]. So, the multiple moving objects' trajectories consist of a set of symbol objects, each being represented as a 2D string. Figure 1(a) shows the video shot "*A policeman is chasing the car*". This shot includes the trajectories of two salient objects, 'policeman' and 'car'. Using the 2D string, the 2D-string representation of the multiple moving objects' trajectories is shown in Figure 1(b). However, in the 2D-string scheme, it is difficult to express the spatio-temporal relationships between moving objects precisely.

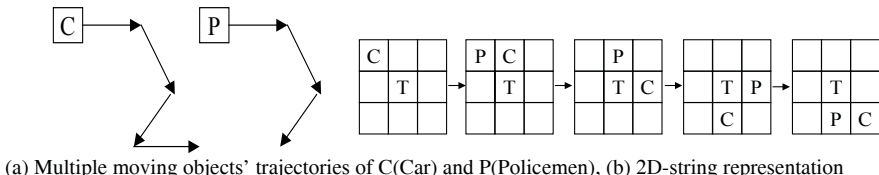


Fig. 1. Example for Multiple Trajectories and 2D string representation

3 Spatio-temporal Modeling for Moving Objects in Video Data

Moving objects are salient objects which are continuously changing its locations over time interval. To effectively deal with moving objects, it is necessary to consider both spatial and temporal relationships. Existing schemes, like Li's scheme and Shan's scheme, consider only directional and topological information for modeling the trajectory of moving objects. But, our representation scheme takes into account distance information in addition. The trajectory is defined as a set of motions of moving objects over time interval. We first define a spatio-temporal representation scheme for modeling a single moving object's trajectory and multiple moving objects' trajectories respectively.

[Definition 1] For a given ordered list of time interval I_0, I_1, \dots, I_{n-1} , the single trajectory of a moving object A, $ST(A)$, is defined as follows:

$$ST(A) = MPS(A) + SPS(A)$$

Where $MPS(A) = \{M_i(A) | i = 0, \dots, n-1\}$ is a motion property information for a moving object A over all the time intervals, each of which $M_i(A) = (R_i(A), D_i(A), I_i(A))$ is motion property for a moving object A over time interval I_i , $R_i(A)$ is a moving direction over time interval $I_i (= [t_i, t_{i+1}])$ and is represented as a real angle with a range of 0 to 360 degree. $D_i(A)$ is a moving distance over I_i and is described as an absolute Euclidean distance or a relative distance. $I_i(A)$ means a time interval from the start time to the end time while the moving object A is moving. $SPS(A) = \{S_i(A) | i = 0, \dots, n\}$ is a stationary property information for a moving object A over all the time instances, each of which $S_i(A) = ([L_i(A)], [O_i(A)])$ is a stationary property for a moving object A at time t_i , $L_i(A)$ is a location information of the moving object A. The location information basically describes a real location in coordinates or a semantic-based location according to a real application, e.g., 'penalty area' or 'goal area' in the soccer game. $O_i(A)$ is an object information related with the moving object A, e.g., 'actor' or 'owner' having the moving object A. Here, $[]$ means an optional operator.

We define multiple trajectories as the trajectories of two or more moving objects. However, since the multiple trajectories can be represented by the combination of the trajectory between two moving objects, we first define a relationship trajectory between two objects.

[Definition 2] Let at least one of object A and object B be a moving object. For a given ordered list of time interval I_0, I_1, \dots, I_{n-1} , the relationship trajectory between A and B, $RT(A, B)$, is defined as follows:

$$RT(A, B) = MPM(A, B) + SPM(A, B)$$

Where $MPM(A, B) = \{M_i(A, B) | i = 0, \dots, n-1\}$ is a motion property information for A and B over all the time interval when at least one of object A and object B is a

moving object, each of which $M_i(A, B) = (D_i(A, B), I_i(A, B))$ is a motion property for A and B over time interval $I_i([t_i, t_{i+1}])$, $D_i(A, B)$ is a relative moving distance of A to B over I_i and is ranged from 0 to 100. That is, $D_i(A, B)$ is 50 in case the moving distance of A is the same as that of B. $D_i(A, B)$ is ranged from 51 to 100 in case the moving distance of A is greater than that of B while it is near to 0 as the moving distance of A is less than that of B. $I_i(A, B)$ is the same as single trajectory. $SPM(A, B) = \{S_i(A, B) | i = 0, \dots, n-1\}$ is a stationary property information for A and B over all the time instances, each of which $S_i(A, B) = ([L_i(A)], [O_i(A)], [L_i(B)], [O_i(B)], T_i(A, B), R_i(A, B))$ is a stationary property for A and B at time t_i , $L_i(A)$ and $L_i(B)$ are the location information of moving object A and B, respectively. $O_i(A)$ and $O_i(B)$ are the actors having moving objects A and B, respectively. $T_i(A, B)$ is a spatial (topological) relations on XY-coordinates from A to B, being represented as one of seven topological relations operator: FA(FarAway), DJ(DisJoint), ME(MEEet), OL(OverLap), CL(is-inCLuded-by), IN(Include), and SA(Same). Finally, $R_i(A, B)$ means a directional relations from A to B and is ranged from 0 to 360 degree.

Based on Definition 1 and 2, the multiple trajectory of two or more moving objects, $MT(A_1, A_2, \dots, A_n)$, can be represented by a combination of the relationship trajectory (RT) and the single trajectory (ST).

[Definition 3] Among objects A_1, A_2, \dots, A_n , let i be the number of moving objects and j be the number of stationary objects, i.e., $n=i+j$. The multiple trajectory of A_1, A_2, \dots, A_n , $MT(A_1, A_2, \dots, A_n)$, is defined as follows:

$$MT(A_1, A_2, \dots, A_n) = \{ST(A_p) | p = 1, \dots, i\} + \{RT(A_q, A_{q+1}) | q = 1, \dots, k\}, k = n - j$$

Here $ST(A_i)$ is the single trajectory of an object A_i . $RT(A_k, A_{k+1})$ is the relationship trajectory between object A_k and A_{k+1} where k is the number of relationship trajectories between two moving objects as well as between a moving object and a stationary object.

Figure 2 shows an example of the multiple trajectory of three objects: Car(C), Building(B), and Motorcycle(M). The C object and the M object are moving objects ($i=2$) and the B object is a stationary object ($j=1$). Thus, k is 3 and $MT(C, M, B) = \{ST(C), ST(M), ST(B)\} + \{RT(C, M), RT(C, B), RT(M, B)\}$.

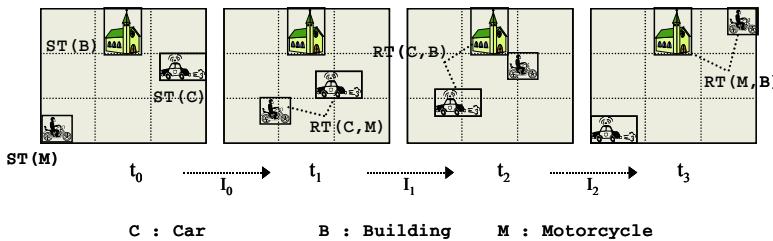


Fig. 2. Multiple trajectories for Car, Building, and Motorcycle

4 Content- and Semantic-Based Retrieval Based on Moving Objects

In order to show content- and semantic-based retrieval using the proposed spatio-temporal representation scheme, we apply the proposed scheme to a soccer video

database as its application. Since the soccer video data have a lot of motion information based on a soccer ball being a salient object, it is very useful to extract the trajectories of the soccer ball as well as semantics which are acquired through the locations of the soccer ball's trajectories in a soccer ground field. We present a user query processing in terms of contents- and semantic-based retrieval.

At first, to support a user query for content-based retrieval efficiently, we define the location information of a soccer ground field, as shown in Figure 3 by using soccer ground field in Figure 4. Here, a query for content-based retrieval means a user query which can be answered based on trajectories of moving objects. The model shows the location information of a soccer ground field for salient objects' trajectories (i.e., soccer ball's and soccer players' trajectories). Figure 3 explains the names of locations in the model of a soccer ground field which is designed for content-based retrieval in soccer video data. A user query for content-based retrieval is as follows: *"Find all video shots whose trajectory is similar to the trajectory sketched by a user."* For the content-based retrieval query, it is necessary to make use of a convenient graphic user interface to describe the query. For example, we can produce a content-based query Q in a soccer ground field, as shown in Figure 4. To answer the query Q, we first represent the query Q as our spatio-temporal representation scheme. Secondly, we search the soccer video database and we finally retrieve all of the video shots having similar trajectories to Q. The following shows the spatio-temporal representation of the query Q.

$$\begin{aligned}
 ST(Q) &= MPS(Q) + SPS(Q) \\
 &= \{L_0(Q), \text{Object A}, L_1(Q), \text{Object A}, L_2(Q), \text{Object A}, L_3(Q), \text{Object A}, L_4(Q), \text{Object A}, L_5(Q)\} + \{M_0(Q), M_1(Q), M_2(Q), M_3(Q), M_4(Q)\} \\
 &= (\text{LRT}, \text{Object A}, \text{LCM}, \text{Object A}, \text{LCT}, \text{Object A}, \text{LLT}, \text{Object A}, \text{LLP}, \\
 &\quad \text{Object A}, \text{LGP}) + \{(240, 19, I_0), (105, 19, I_1), (150, 12, I_2), (280, 32, I_3), (135, 16, I_4)\}
 \end{aligned}$$

| | | |
|----|----------------------|----------|
| 1 | Left Upper Goal | LUG(RUG) |
| 2 | Left Lower Goal | LLG(RLG) |
| 3 | Left Bottom Penalty | LBP(RBP) |
| 4 | Left Lower Penalty | LLP(RLP) |
| 5 | Left Upper Penalty | LUP(RUP) |
| 6 | Left Top Penalty | LTP(RTP) |
| 7 | Left Left Bottom | LLB(RRB) |
| 8 | Left Left Top | LLT(RRT) |
| 9 | Left Center Bottom | LCB(RCB) |
| 10 | Left Center Middle | LCM(RCM) |
| 11 | Left Center Top | LCT(RCT) |
| 12 | Left Right Top | LRT(RLT) |
| 13 | Left Right Middle | LRM(RLM) |
| 14 | Left Right Bottom | LRB(RLB) |
| 15 | Left Top Sideline | LTS(RTS) |
| 16 | Left Bottom Sideline | LBS(RBS) |
| 17 | Left Bottom Corner | LBC(RBC) |
| 18 | Left Top Corner | LTC(RTC) |
| 19 | Left Top Goalline | LTG(RTG) |
| 20 | Left Bottom Goalline | LBG(RBG) |
| 21 | Left Penalty Point | LPP(RPP) |
| 22 | Left Goalpost Line | LGL(RGL) |
| 23 | Left Goalpost Inside | LGI(RGI) |
| 24 | Left Goalpost Over | LGO(RGO) |
| 25 | Center Circle Point | CCP |
| 26 | Half Line | HFL |
| 27 | Center Circle Area | CCA |
| 28 | Left Goal Area | LGA(RGA) |
| 29 | Left Penalty Area | LPA(RPA) |
| 30 | Left Bottom Area | LBA(RBA) |
| 31 | Left Middle Area | LBA(RBA) |
| 32 | Left Top Area | LTA(RTA) |
| 33 | Left Left Area | LLA(RRA) |
| 34 | Left Right Area | LRA(RLA) |

Fig. 3. Location information of a soccer ground field for content-based retrieval

Secondly, using a soccer ball's trajectories, it is possible to extract some semantics, such as 'corner kick', 'penalty kick', 'goal kick', 'throw in', 'free kick', and 'centering'. Therefore, we can support semantic-based retrieval using important concepts in the soccer video database. As a result, we can improve the precision of retrieval to user query and provide a user with conveniences. A user query for semantic-based

retrieval is as follows: "*Find all video shots that include scenes of 'free kick' or 'shooting'.*" When a user wants to make a query with some semantics, we first transform the given semantic-based query into its corresponding spatio-temporal representation and then search the soccer video database, like content-based query.

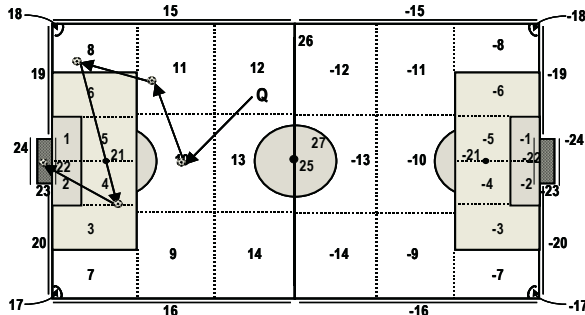


Fig. 4. The example of a content-based query

Table 1 briefly depicts the important semantics in the soccer video database and their corresponding spatio-temporal representations. We only consider the left side of the soccer ground field and the right side is similar to it. Here, '&', '|', '?', and '[]' operators mean *and*, *or*, *don't care*, and *all*, respectively. In addition, we can support an actor-based query based on soccer players having the soccer ball. The user queries are as follows: "*Find all of the video shots which include the scenes of 'player A' having the ball*" and "*Find all of the video shots with the scenes in which 'player B' does shooting*."

Table 1. Main semantics and their spatio-temporal representations

| Semantics | Spatio-temporal representations |
|--------------|---|
| Goal Kick | (LGA LPA, [!(LGA&LPA)]) + {(0~90 270~360, ?, I ₀)} |
| Penalty Kick | (LPP, LPG LBG LGO LGI) + {(90~270, ?, I ₀)}(LPP, LPL, LGA LPA) + {(90~270, ?, I ₀), (0~90 270~360, ?, I ₁)} (LPP, LPL, LGA LPA) + {(90~270, ?, I ₁)} |
| Free Kick | (LLB LLT LBA LMA LTA, LGA LPA) + {(90~270, ?, I ₀)} |
| Centering | (LLB LLT LCB LCCT, LGA LPA) + {(90~270, ?, I ₀)} |
| Corner Kick | (LTC, LLT LGA LPA LTG LGL LGI) + {(270~360, ?, I ₀)}(LBC, LLB LGA LPA LBG LGL LGI) + {(0~90, ?, I ₀)} |
| Throw In | (LBS, [!LBS]) + {(0~180, ?, I ₀)}(LTS, [!LTS]) + {(180~360, ?, I ₀)} |
| Goal In | (?, ..., LGI) + {(?, ?, I ₀), ..., (?, ?, I _{n-1})} (?, ..., LGI) + {(?, ?, I ₀), ..., (?, ?, I _{n-1})} |
| Goal Out | (?, ..., LTG LBG) + {(?, ?, I ₀), ..., (?, ?, I _{n-1})} (?, ..., LTG LBG) + {(?, ?, I ₀), ..., (?, ?, I _{n-1})} |

5 Experimental Results

In order to verify the usefulness of our representation scheme for both the single trajectory and the multiple trajectories, we do the performance analysis by using real soccer video data. Since soccer video data have many trajectories of soccer balls, i.e., salient objects, it is necessary to extract the trajectories of moving objects from the soccer ball. Table 2 depicts the experimental data used for our performance analysis.

Most of video data, formatted as MPEG file, which are used in our experiment, include a shot of 'getting a goal'. We extract the trajectories of a soccer ball by manually tracing the ball in a ground field. For our experiment, we make forty query trajectories consisting of twenty in 'the right field' and twenty in 'the left field' from the half line of the ground field.

Table 2. Experimental data for performance analysis

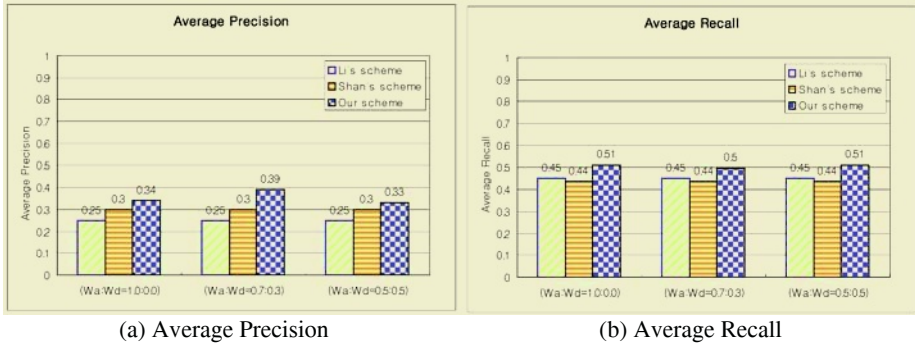
| Parameters | Data Set | |
|---------------------------------------|--------------------------|-------------------------------|
| | Single Trajectory | Multiple Trajectories |
| Data domain | Soccer Video Data | |
| Salient moving object | Soccer Ball | Soccer Ball and Player |
| # of data | 350 | 200 |
| The avg. motion # of data trajectory | 8.4 | 8.9 |
| # of query | 40 | 10 |
| The avg. motion # of query trajectory | 3.8 | 3.1 |

For our performance analysis, we compare our scheme with the Li's scheme and Shan's scheme in terms of retrieval effectiveness, that is, average precision and recall measures. Let RD (Relevant data in Database) be the number of video data relevant to a given query which are selected from the database, RQ (Retrieved data by Query) be the total number of data retrieved by a given query, and RR (Relevant data that are Retrieved) be the number of relevant data retrieved by a given query. In order to obtain RD , we make a test panel which selects relevant data manually from the database. The test panel is composed of 10 graduate school students from our computer engineering department. The precision measure is defined as the proportion of retrieved data being relevant, that is, RR/RQ and the recall measure is defined as the proportion of relevant data being retrieved, that is, RR/RD .

For our performance comparison, we adopt the 11-point measure [8], which is most widely used for measuring the precision and recall. For a single trajectory, we consider the weight of angle (W_a) and the weight of distance (W_d) separately since we use both angle and distance for modeling the trajectory of moving objects. Figure 5 shows the retrieval effectiveness of our scheme, Li's scheme, and Shan's scheme. In case we do our performance analysis based on only the angle property ($W_a=1.0$ and $W_d=0.0$), it is shown that our scheme achieves about 5-10% higher precision than that of Li's and Shan's schemes while it holds about the same recall. In case we consider the weight of angle about two times greater than that of distance ($W_a = 0.7$ and $W_d=0.3$), it is shown that our scheme achieves about 10-15% higher precision than that of Li's and Shan's schemes while it holds about the same recall. In case we consider the importance of the angle and that of the distance equally ($W_a=0.5$ and $W_d=0.5$), it is shown that our scheme is better than Li's and Shan's schemes in terms of both precision and recall measures.

For multiple trajectories, we consider the weight of angle (W_a), the weight of distance (W_d) and the weight of topological relations (W_t) according to modeling the trajectory of multiple moving objects. Figure 6 depicts the performance results for multiple trajectories in our scheme, Li's scheme, and Shan's scheme. In case we consider the angle and the topological relation about two times more importantly than the distance ($W_a=0.4$, $W_d=0.2$, and $W_t=0.4$), it is shown that our scheme achieves about

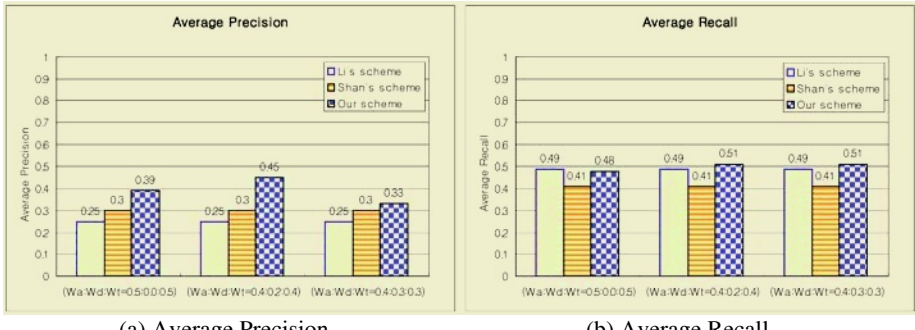
15-20% higher precision than that of Li's and Shan's schemes while it holds about the same recall.



(a) Average Precision

(b) Average Recall

Fig. 5. Experimental results for single trajectory



(a) Average Precision

(b) Average Recall

Fig. 6. Experimental results for multiple trajectories

From our experiment, we finally show that our scheme achieves better performance on average precision than Li's and Shan's schemes while it holds about the same recall in the single trajectory and multiple trajectories. Particularly, in case of the single trajectory, the performance of our scheme is the best when the weight of angle is over two times than that of distance ($W_a=0.7$ and $W_d=0.3$). In case of the multiple trajectories, the performance of our scheme is the best when the weight of angle and topology is over two times than that of distance ($W_a=0.4$, $W_d=0.2$ and $W_t=0.4$).

6 Conclusions

We proposed a new spatio-temporal representation scheme which can efficiently model moving objects' trajectories in video databases. In order to improve retrieval accuracy to measure a similarity between two moving objects, our scheme took into account on distance property, conceptual location information, and related object information (e.g. player name having a soccer ball) while the traditional schemes only consider direction property, time interval property, and spatial relations property for modeling moving objects' trajectories. The proposed scheme supported content-based

retrieval using moving objects' trajectories and supported semantics-based retrieval using concepts which are acquired through the location information of moving objects. Finally, from the experimental results, our scheme is superior to existing related work like Li's and Shan's scheme when the weight of angle is over two times greater than that of distance.

References

1. J. R. Smith, S. F. Chang, "VisualSEEk: a Fully Automated Content-Based Image Query System," in Proceedings of ACM Multimedia 96, pp. 87-98, 1996.
2. G. Ahanger, D. Benson, and T. D. C Little, "Video query formulation," in Proceedings of SPIE Electronic Imaging Science and Technology, pp. 280-291, 1995.
3. A. Yoshitaka, M. Yoshimitsu, M. Hirakawa, and T. Ichikawa, "V-QBE: Video database retrieval by means of example motion of objects," in Proceedings of IEEE International Conference on Multimedia Computing and Systems, pp. 453-457, 1996.
4. Z. Aghbari, K. Kaneko, and A. Makinouchi, "Modeling and Querying Videos by Content Trajectories", In Proceedings of the International Conference and Multimedia Expo, pp. 463-466, 2000.
5. J. Z. Li, M. T. Ozu, and D. Szafron, "Modeling Video Temporal Relationships in an Object Database Management System," in Proceedings of Multimedia Computing and Networking(MMCN97), pp. 80-91, 1997.
6. M. K. Shan and S. Y. Lee, "Content-based Video Retrieval via Motion Trajectories," in Proceedings of SPIE Electronic Imaging and Multimedia System II, Vol. 3561, pp. 52-61, 1998.
7. S. K. Chang, Q. Y. Shi, and C. W. Yan, "Iconic Indexing by 2D Strings," IEEE Trans. Pattern Analysis, Machine Intelligence, Vol. 9, No. 3, pp. 413-428, 1987.
8. G. Salton and M. McGill, An introduction to Modern Information Retrieval, McGraw-Hill, 1993.

Calendars and Topologies as Types

A Programming Language Approach to Modelling Mobile Applications

François Bry, Bernhard Lorenz, and Stephanie Spranger

Institute for Informatics, Univ. Munich, Germany

spranger@pms.ifi.lmu.de

<http://www.pms.ifi.lmu.de>

Abstract. This article introduces a programming language approach to modelling spatio-temporal data using *calendars* and *topologies* specified as types. Calendric and topologic data appearing in Web applications are most often rather complex, sometimes involving different calendars and/or topologies. The basic principle is to model spatio-temporal data by means of *predicate subtyping*. This principle is used to define calendric and topologic data types representing granularities as well as conversions between those data types. A thesis underlying this work is that calendars and topologies are more conveniently expressed with dedicated language constructs and that calendar and topology data are more efficiently processed with dedicated reasoning methods than with general purpose “axiomatic reasoning” of e.g. ontology languages or theorem provers.

1 Introduction

This article introduces a programming language approach to modelling spatio-temporal data using *calendars* and *topologies* specified as types. Calendars are human abstractions of the physical flow of time. They enable to measure time in *time granularities* like day, week, working day, and teaching term. Topologies are human abstractions of (schematised) geographic objects and their relationships. Similarly to time granularities in a calendar, geographic objects in a topology may have different *location granularities* like city, district, and street. More abstractly, calendars and topologies both are finite collections of granularities related to each other, in general, in different manners.

The authors of the work reported about in this article claim that a programming language approach to calendars and topologies has similar advantages as types (res. objects) and type checking in functional (resp. object-oriented) programming. Types complement data with machine readable and processable semantics. Type checking is a very popular and well established “lightweight formal

Acknowledgment: This research has been funded in part by the PhD Program Logics in Computer Science (GKLI) and the European Commission and by the Swiss Federal Office for Education and Science within the 6th Framework Program project REWERSE number 506779 (cf. <http://rewerse.net>).

method” to ensure program and system behavior and to enforce high-level modularity properties. Types and type checking enhance efficiency and consistency of (modern) programming and modeling languages. Specific aspects of calendars and topologies make type checking with calendars and topologies an interesting challenge: a mobile application listing pharmacies in the surrounding of a (mobile) user will preferably only mention those that are currently open. Such an application refers to various topologic and calendric data. Types give such data their intended semantics, e.g. that some data refer to days. Static type checking ensures certain semantics on the data when processing them, e.g. to find an open pharmacy. The calendric data involved in such mobile applications are most often rather complex, sometimes involving different calendars (e.g. cultural calendars like the Gregorian and the Islamic and professional calendars) with various regulations and lots of irregularities (e.g. leap years). The topologic data involved often refer to different topologies like buildings or cities and to connections between such topologies. Furthermore, calendar data such as dates are probably more than any other data domain a subject to user interpretation: e.g. the date “12/02/2005” is interpreted in France as 12th February 2005 while it is interpreted as 2nd December 2005 in the US. Many traditional Web sites and pages refer explicitly or implicitly to such calendar data. In the current Web, such data can hardly be interpreted by computers. The vision of the Semantic Web is to enrich the current Web with well-defined meaning and to enable computers to meaningfully process such data.

This paper is devoted to a unifying view of calendars and topologies: time and location granularities are modelled as data types and are related in calendars and topologies, themselves specified as types. The basic principle of the programming language approach to modelling spatio-temporal data is *predicate subtyping* [1]. Predicate subtyping with predicate types is a stronger form of typing and subtyping enabling to encode more information in types, because the elements of a predicate type are described by a predicate set. Predicate sets are used to declaratively define (possibly infinite) sets. Predicate types have been widely investigated in type theory, logics, proof assistants, and theorem proving. The typing approach to calendars and topologies presented in this article uses predicate types in a different manner and not for theoretical, but instead practical purposes: predicate subtyping is used to define calendric and topologic data types representing granularities as well as conversions between those data types. A thesis underlying the work reported about in this article is that calendars and topologies are more conveniently expressed with dedicated language constructs and that calendar data and expressions are more efficiently processed with dedicated reasoning methods than with “axiomatic reasoning” of ontology languages like RDF and OWL.

2 Advantages of Types and Static Type Checking

Static type checking (i.e. verifying at compile time whether expressions and definitions in a program obey the typing rules of the language) is a very popular

and well established “lightweight formal method” to ensure program and system behaviour and to enforce high-level modularity properties [1].

Types and static type checking is as useful and desirable with calendric data types and topologic data types as it is with whatever other data type: it catches a significant number of errors before a program runs. Types are a valuable form of program documentation that rarely becomes outdated. They simplify locating definitions in libraries. Furthermore, typed languages gain in efficiency, because functions need not verified during run time. Types are backbones for module systems yielding in abstraction. Specific aspects of calendars and topologies make static type checking for such data an interesting challenge. Some basic problems not only of theoretical but also of practical importance concerning calendric and topologic data can be solved: (i) The problem of granularity conversion (discussed for calendric types in [2]), i.e. to cast the elements of one granularity (e.g. day) to those of another granularity (e.g. working day) is solved with the concept of *predicate types*. (ii) *Context-aware* modelling of calendars and topologies is possible, i.e. the type checker statically verifies according to which calendar/topology some data have to be interpreted. A type checking approach with calendric types is proposed in [3]. (iii) Constraint solving on calendric and topologic data is performed *independently, efficiently* and *without loss of semantics* of the data. The reason for this is that predicate types specify a conversion from one data type to another, coincidentally obtaining some level of abstraction by means of granularities. Constraint solving on calendric data with different calendric types by means of conversion constraints is introduced in [2].

3 A Unifying View of Calendars and Topologies

This section is a mathematical prolog that formally introduces the notion of granularity.

Definition 1. *An n-dimensional space is a pair $(\mathcal{A}^n, <_{\mathcal{A}^n})$ where \mathcal{A}^n is an infinite set (isomorphic to \mathbb{R}^n) and $<_{\mathcal{A}^n}$ is a total order on \mathcal{A}^n such that \mathcal{A}^n is not bounded for $<_{\mathcal{A}^n}$. An element $a = (a_1, \dots, a_n)$ of \mathcal{A}^n is called **n-point**.*

Note that since \mathcal{A} is totally ordered (recall that it is isomorphic to \mathbb{R}), the total order is preserved over the Cartesian product of $\mathcal{A} \times \dots \times \mathcal{A}$.

Definition 2. *Let $(\mathcal{A}^n, <_{\mathcal{A}^n})$ be an n-dimensional space.*

A generalised subspace s over $(\mathcal{A}^n, <_{\mathcal{A}^n})$ is a (finite or infinite) collection of pairwise disjoint, totally ordered right-open subspaces $[a^-, a^+)$, $a^-, a^+ \in \mathcal{A}^n$ such that $a^- <_{\mathcal{A}^n} a^+$ and $a \in [a^-, a^+)$ iff $a \in \mathcal{A}^n$ and $a^- \leq_{\mathcal{A}^n} a <_{\mathcal{A}^n} a^+$.

In the following, $S_{\mathcal{A}^n}$ denotes the set of all generalised subspaces over $(\mathcal{A}^n, <_{\mathcal{A}^n})$.

Definition 3. *Let $(\mathcal{A}^n, <_{\mathcal{A}^n})$ be an n-dimensional space.*

*Let $G = \{g_i \mid i \in \mathbb{Z}\}$ be a set isomorphic to \mathbb{Z} . Let call the elements of G **granules**. A **granularity** is a (non-necessarily total) function \mathcal{G} from G into $S_{\mathcal{A}^n}$ such that for all $i, j \in \mathbb{Z}$ with $i < j$*

1. if $\mathcal{G}(g_i) \neq \emptyset$ and $\mathcal{G}(g_j) \neq \emptyset$, then for all $a_i = (a_{i_1}, \dots, a_{i_n}) \in \mathcal{G}(g_i)$ and for all $a_j = (a_{j_1}, \dots, a_{j_n}) \in \mathcal{G}(g_j)$, then $a_i <_{\mathcal{A}^n} a_j$, and
2. If $\mathcal{G}(g_i) = \emptyset$, then $\mathcal{G}(g_j) = \emptyset$.

According to Definition 3, granules of a same granularity are totally ordered and non-overlapping. The first condition of Definition 3 induces from the ordering of the n-point (of the n-dimensional space) the common-sense ordering on granules. The second condition of Definition 3 is purely technical: it makes it possible to refer to the *infinite* set \mathbb{Z} also for *finite* sets of granules.

Examples of granularities are *time granularities* [4] over $(\mathcal{A}, <_{\mathcal{A}})$ *location granularities* over $(\mathcal{A}^2, <_{\mathcal{A}^2})$.

Granularities can be defined by specifying subtype relations (in terms of predicates). Two subtype relations, *aggregation of* and *inclusion of*, have been defined for (one-dimensional) time granularities in [4]. E.g. a type “working day” is an inclusion (in the common set-theoretic sense) of the type “day” since the set of working days is a subset of the set of days; the type “week” is an aggregation of the type “day” since each week can be defined as a time interval of days.

Similar to the subtype relations, aggregation and inclusion, between time granularities, aggregations and inclusions are defined between location granularities as follows.

Definition 4. Let \mathcal{G} and \mathcal{H} be location granularities.

\mathcal{G} is an **inclusion subtype of** \mathcal{H} , denoted $\mathcal{G} \subseteq \mathcal{H}$, i.e. every granule of \mathcal{G} is a granule of \mathcal{H} .

For example, the location granularity “subway station” is an inclusion subtype of the location granularity “station”, selecting only those stations with subway connection.

Definition 5. Let \mathcal{G} and \mathcal{H} be location granularities.

\mathcal{G} is an **aggregation-enclosure subtype of** \mathcal{H} , denoted $\mathcal{G} \preceq \mathcal{H}$, if every granule of \mathcal{G} is a 2-dimensional space over \mathcal{H} and every granule of \mathcal{H} is included in (exactly) one granule of \mathcal{G} .

\mathcal{G} is an **aggregation-connection subtype of** \mathcal{H} , denoted $\mathcal{G} \prec \mathcal{H}$, if every granule of \mathcal{G} is a 2-dimensional space over \mathcal{H} and every granule of \mathcal{H} is included in (at least) one granule of \mathcal{G} .

For example, the location granularity “train network” is an aggregation-enclosure subtype of the location granularity “train connection”, aggregating a set of train connections into a network. And a “train connection” itself is an aggregation-connection subtype of “station”, connecting several stations to a train line. Note that connections are not necessarily disjoint, because the same station may participate in different train lines, for example.

The two subtype relations, inclusion subtype and aggregation subtype, are corner stones of modeling granularities as types that, to the best of the knowledge of the authors, have not been proposed elsewhere. As the examples given below show, they are very useful in modeling calendars and topologies. Indeed, they reflect widespread forms of common-sense reasoning with calendric and topologic data.

4 Modelling Calendars as Types in CaTTS

CaTTS is a generic modelling language [4] for data modelling and reasoning with calendars. CaTTS consists of two languages, a *type definition language*, CaTTS-DL, and a *constraint language*, CaTTS-CL, of a (common) parser for both languages, and of a language processor for each language. CaTTS-DL provides with CaTTS-TDL (for type definition language), a tool to define calendars and CaTTS-FDL (for format definition language), a tool to define calendar data, in particular dates to give calendar data well-defined meanings. CaTTS-CL provides a means to express a wide range of temporal constraints over calendar data referring to the types defined in calendar(s) specified in CaTTS-DL.

In CaTTS-DL, one can specify in a rather simple manner more or less complex, cultural and professional calendars. Irregularities like leap seconds or Hebrew leap months can be easily expressed in CaTTS-DL. In particular, CaTTS-DL provide a means to define time granularities as *calendric data types* by means of predicate types. E.g. the Gregorian calendar can be modelled in CaTTS-DL as follows:

```
calendar Gregorian =
  cal
    type second;
    type minute = aggregate 60 second @ second(1);
    ...
    type month = aggregate
      31 day named january,
      alternate month(i)
        | (i div 12) mod 4 == 0 &&
          ((i div 12) mod 100 != 0 || (i div 12) mod 400 == 0) -> 29 day
        | otherwise
          -> 28 day
    end named february, ..., 31 day named december @ day(1);
    type year = aggregate 12 month @ month(1);
    type weekend-day = select day(i) where
      relative i in week == 6 || relative i in week == 7;
    type working-day = day \ weekend-day;
  end
```

The above calendar specification binds a calendar (between the keywords `cal` and `end`) to the identifier `Gregorian`. This CaTTS-DL calendar specification consists of a set of type definitions (each identified by the keyword `type` followed by an identifier). The first type defined is `second`. It has no further properties. The type `minute` is defined from the type `second` by specifying a predicate. The CaTTS language processor interprets this recursive type definition as an *aggregation subtype* of the type `second` such that each of its elements comprises 60 seconds¹ (denoted `aggregate 60 second`) and that the minute that has index 1, i.e. `minute(1)` comprises all seconds between `second(1)` in `second(60)` (denoted `@ second(1)`). Any further type definition follows the same pattern. The definitions are straightforward following the rules of the Gregorian calendar [5]. Since Gregorian months have different lengths, a CaTTS type `month` is defined with a repeating pattern of the twelve months. The months February, which is one day longer in each Gregorian leap year is defined by an additional

¹ In CaTTS-DL, it is possible to define a type `minute` that considers leap seconds, as well

pattern which specifies the leap year rule for the Gregorian calendar using the CaTTS language construct `alternate...end`. The type definition of the type `weekend_day` is derived from that of the type `day`. The CaTTS language processor interprets this type definition as an *inclusion subtype* of the type `day` such that each of its elements must be relatively to a week either the 6th or the 7th day (denoted `relative i in week == 6 || relative i in week == 7`). The type `working_day` is also an inclusion subtype of `day`, selecting those days which are not weekend days (denoted `day \ weekend_day`).

The above exemplified CaTTS-DL calendar specification defines a calendar as a “type” that can be used, in principle, in *any* language (e.g. XQuery, XSLT, XML Schema), using calendar data enriched with type annotations after this CaTTS-DL calendar. CaTTS’ type checker [3] is used to check the calendar data typed after a CaTTS-DL calendar in such programs or specifications, thus, providing a means to interpret such data.

Note further that particularities like time zones can be easily expressed in a CaTTS-DL calendar definition. Calendar definitions of other cultural calendars in CaTTS-DL, in particular the Islamic and Hebrew calendars and variations of the Gregorian calendar like the Japanese calendar as well as date format specifications using CaTTS-FDL are given in [4, 6, 7].

5 Topological Types

In many cases, location reasoning pertains to routing and navigation tasks which rely on network infrastructures. Here, we use networks as a straightforward example for a topology, knowing that more complicated topologies might require further research. However, this example shows that a holistic model of the real world is rarely necessary. E.g. a journey involving the public underground system can be planned without any information about the *geographic* composition of the subway network.

Knowledge about schedules and the *topologic* structure suffices to find an optimal connection between two stations. Expressing such information in a location type language would provide both an abstraction from geographic coordinates and a means to enable reasoning on location data. Let us consider a part of Munich’s subway and suburban train network defined in a topology type system.

```
type subway_station = collect
  Sendlinger_Tor, Hauptbahnhof, Marienplatz, Stiglmaierplatz, ...
type train_station = collect Hauptbahnhof, Karlsplatz, Marienplatz, ...
type station( subway_station | train_station );
type U1 = connect Sendlinger_Tor - Hauptbahnhof - Stiglmaierplatz - ...
type U3 = connect Sendlinger_Tor - Marienplatz - Odeonsplatz - ...
type S2 = connect Hauptbahnhof - Karlsplatz - Marienplatz - ...
type network = collect U1, U3, S2;
```

A network such as the one in figure 1 can be defined as shown above. The type `subway_station` is defined as a collection of named subway stations. A collection



Fig. 1. Network section

is an ordered set of entities which satisfy certain constraints, in this case denoting a subway station. The definition of `train_station` is analogous. The common supertype `station` is a union of both (not necessarily disjoint) sets. A subway line (U_1, U_3 , etc.) is defined as an ordered connection of subway stations. If there is a subway train servicing station A, B, and C (in this order), then these stations are connected with each other to form a line. Therefore, a line is directed, i.e. a service is usually comprised by two lines operating in different directions. This is especially useful for modelling different time tables and changing services for off-peak operation, etc. A network is in turn a collection of lines.

The approach sketched above provides a means for modeling topological data required in many applications pertaining to routing problems. Map representations are facilitated by linking the topological information to spatial data, e.g. sets of coordinates (polygons) which denote areas. This linking also facilitates the use of established calculi like RCC8 [8]. Furthermore, this approach allows for symbolic queries, such as finding out which stations lie in a certain quarter of the city or which district office is in charge of a road segment. Linked data is also necessary whenever for example polygons cannot be *directly* represented as location granularities, which is only possible in special cases (e.g. when areas can be regularly divided into same-size cells.)

6 Conclusion and Perspectives

This article has reported on a new approach introducing a unifying view of calendars and topologies in which time and location granularities are modelled as data types. Further work will be devoted to the refinement the idea of bridging between temporal and spatial modelling and reasoning techniques and their application to typical problems in common scenarios.

References

1. Pierce, B.C.: *Types and Programming Languages*. MIT Press (2002)
2. Bry, F., Rieß, F.A., Spranger, S.: A Type Language for Calendars. submitted to publication (2005)
3. Bry, F., Rieß, F.A., Spranger, S.: A Reasoner for Calendric and Temporal Data. submitted to publication (2005)
4. Bry, F., Rieß, F.A., Spranger, S.: CaTTS: Calendar Types and Constraints for Web Applications. In: Proc. 14th Int. World Wide Web Conference, Japan. (2005)
5. Dershowitz, N., Reingold, E.: *Calendrical Calculations: The Millennium Edition*. Cambridge University Press (2001)
6. Bry, F., Spranger, S.: Towards a Multi-calendar Temporal Type System for (Semantic) Web Query Languages. In: Proc. 2nd Int. Workshop Principles and Practice in Semantic Web Reasoning. LNCS 3208, Springer-Verlag (2004)
7. Bry, F., Haußer, J., Rieß, F.A., Spranger, S.: Cultural Calendars for Programming and Querying. In: Proc. 1st Forum on the Promotion of European and Japanese Culture and Traditions in Cyber Society and Virtual Reality, France. (2005)
8. Randell, D.A., Cui, Z., Cohn, A.: A Spatial Logic Based on Regions and Connection. In: Proc. 3rd Int. Conf. Principles of Knowledge Representation and Reasoning, USA. (1992) 165–176

Moving Object Detection in Dynamic Environment

M. Julius Hossain, Kiok Ahn, June Hyung Lee, and Oksam Chae*

Department of Computer Engineering, Kyung Hee University,
1 Seochun-ri, Kiheung-eup, Yongin-si, Kyunggi-do, Korea, 449-701
mdjulius@yahoo.com, blackeroica@mg.co.kr
ljhyung7@kdc.ac.kr, oschae@khu.ac.kr

Abstract. This paper presents an edge extraction based automatic algorithm for detection of moving objects that have been specially developed to deal with the variations in illumination and background. We develop an efficient approach for background edge generation as well as update and robust method of edge matching that is able to effectively reduce the risk of false alarm. The proposed method can be successfully realized in various monitoring systems like intrusion detection as well as video surveillance. Experiments with real image sequences are presented, along with comparisons with some other existing methods, illustrating the advantages of the proposed algorithm.

1 Introduction

Advanced video surveillance technologies as well as intrusion detection systems are pursued for varied security, law enforcement, and military applications. One of the most significant demands from such systems is to isolate the events of potential interest from a large volume of redundant image data. However, existing machine vision approaches are also prone to unacceptably high false alarm rates from a wide range of phenomena, including camera motion, illumination variations in both natural and artificial lighting and only a few of the existing approaches deal with the environment where background scene changes frequently [1,2]. These problems are extensively investigated in our study and we try to strengthen existing vision approach, which is less susceptible to these phenomena.

Existing algorithms use different principles to approach moving object detection. In simple differencing approach [3,4], the difference in brightness between a reference image and input image results the difference image and the resultant image is thresholded with a value, chosen empirically to obtain new objects. This method exhibits low complexity but it is very sensitive to noise and variations in illuminations and does not consider the local consistency of image. In statistical segmentation approaches [5], changes in brightness in each pixel of a reference image and an input image are mapped on the two-dimensional plane for the analysis of their distribution. This method concerns with discriminating between changes due to illumination variations and those due to scene content change [3]. It solves part of the problems due to the change of illumination but lacks the ability to obtain the structure or number of moving objects; shows only whether they exist or not. Moving edge extraction method [6] uses the difference in edge pixels between a reference image and an input image instead of their difference in brightness to adapt system to the changes in illumination. For this method, the edge of a reference image should be thick enough to

* Corresponding Author

include the background edge of the input image. However, most of the existing methods still suffer from changes in illumination and are not suitable for a dynamic environment like parking lot, where background scene changes frequently.

Proposed method conserves the edge extraction approach [2,7] and tries to remedy the aforementioned drawbacks. In our method, edges are extracted from image as a unit of segment and reference edges are updated automatically. This update of the reference edges adapts our detection approach to the change in background scene. Flexible conformity between corresponding edge segments of input image and reference image solves part of the camera calibration error, which helps to reduce the false alarm rate. Representation of edge segment reduces the affect of noises as noises are found sparse and in a small group of points [5,6] which are simply ignored in edge extraction step.

2 Structure of the Proposed Method

Proposed algorithm, depicted in Figure 1, includes three stages: generation of initial reference edge list, detection of moving object and update of edge lists. Initial reference edges are obtained by accumulating the training set of background images. Input edges are extracted from current image, each edge segment is searched in the reference edge list and symmetric edges are eliminated from the input edges. Moving objects are detected from the remaining edge segments if any, after the application of local processing [8]. Finally, temporary reference edge list and temporary edge list are updated by changing the weight values associated with them. In object detection mode, the reference edge list consists of two separate lists: initial reference edge list and temporary reference edge list shown in Figure 1. Initial reference edges are static having no weight value associated with them for update. Temporary reference edge list is formed by including moving edges staying in a fixed position for long duration and updated according to its associated weight value. To include a new edge segment in temporary reference edge list, a temporary edge list is maintained along with a weight value for each edge reflecting the stability of the moving edge. We extract pieces of edge information from images and represent them as efficiently designed edge classes [9]. The representation of edge segments helps to strengthen the conformity process between two edges and facilitates generating more accurate model of detected moving objects. The use of object oriented design principles provides a flexible platform for implementing a broad set of image processing and easily manageable code, sharing common resources. The representation of edge helps to remove sparse and small group of noise pixels and each edge can be accessed independently for conformity.

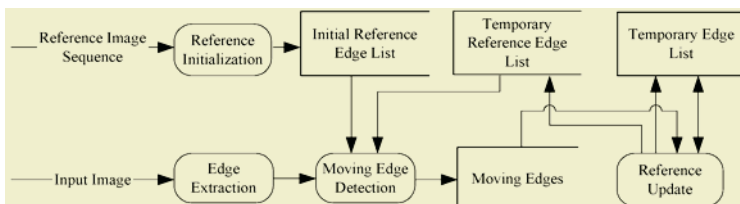


Fig. 1. Structure of the proposed algorithm

3 Implementation

3.1 Generation of Initial Reference Edge List

In a particular illumination, some of the edges of background may disappear from the scene. For this reason, if reference edge list is formed from a single background image, false alarm can be generated when new edges of background appear due to the change of illumination. So, we generate initial reference edge list from a set of training images, taken in different operational environments and thus it includes more background edges. Figure 2 shows the algorithm proposed in this study to form initial reference edge list. Training images are read out one by one followed by figuring out the gradient magnitude with the application of edge operator. Quantization is applied to the gradient image to remove the remaining background and weak edges. For each image, quantized values are accumulated to an accumulation array and normalized that finally generates a gradient image having impact of all the training images. The procedure is accomplished with extraction of reference edges by applying Canny edge extraction algorithm [10]. Figure 3(a) and Figure 3(b) are two samples of background images with different illumination and the corresponding edge images are shown in Figure 3(c) and Figure 3(d), respectively. These two edge lists are accumulated with rest of the edge images of training set to generate initial reference edges, which are shown in Figure 3(e). It can be observed that there are some edges, which are not found in any of the given samples and thus they are contributed from other sample images of background. It can also be noticed that some weak edges disappear in accumulated reference edge image, though they exist in one of the two sample edge images. These edges are rarely found in rest of the training images.

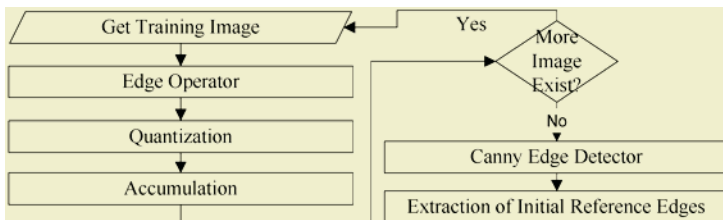


Fig. 2. Generation of initial reference edge list

3.2 Detection of Moving Objects

Figure 4 shows proposed method for detection of moving object. Input edge segments are extracted from current image and each of the extracted input edge segments is searched in reference edge list. If there exist a similar edge segment in the reference list, then corresponding input edge is removed from input edge image. In this case, weight of the reference edge is increased, if it is a temporary reference edge and its weight is less than the predetermined threshold value. To find a match between two edge segments, we applied a flexible conformity method [2], which allows little bit of disparity between two edge segments, thus tolerates minor change in camera focus. Conformity method is used to remove the corresponding reference edge segments from the edges of input image. However, the remaining edge segments are not com-

plete because of noise, breaks in the edge from non-uniform illumination and other effects that introduce spurious intensity discontinuities. We use local processing [8] to assemble edge pixels into meaningful edges where all the points that are similar according to a set of predefined criteria are linked, forming an edge of pixels and thus result moving edge segments.

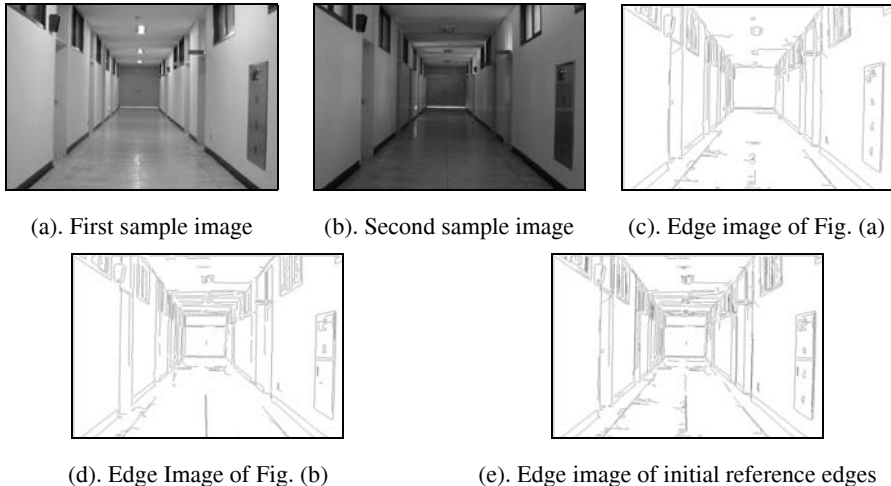


Fig. 3. Generation of initial reference edges

3.3 Update of Reference Edge List

Update of reference edges is important to detect moving objects in dynamic environment. To facilitate this, a temporary edge list is maintained which stores the edge segments of moving object with a weight for each segment. If a moving edge is found in next frame at same location, the weight of that segment is incremented else it is decremented. If weight of any edge segment of the temporary edge list reaches the specified threshold value, then it is moved to the temporary reference edge list. An edge segment is also removed from the temporary edge list if the weight of the edge reaches zero. In similar fashion, if a temporary reference edge segment is not found in the input edge list then the weight of the temporary reference edge is decreased. An edge segment is removed from temporary reference edge list when its weight is zero.

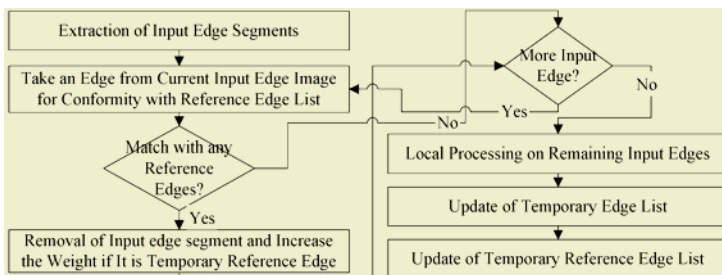


Fig. 4. Detection of moving object

4 Results

We applied the proposed method on images of size 740 x 500 and illumination range 0-255 that were picked from a corridor and an indoor parking lot with various changes in constituents and illumination, using a digital camcorder. We used a system, which included processor of AMD Athlon XP 2100+, RAM of 512MB. Visual C++ 6.0 and MTES [11], an image processing environment tool were used as environment tools which process 5 frames per second.

Proposed method is adaptive to the change in illumination. Figure 5 shows a sample frame selected from the set of 32 training images with various illuminations that were picked in different operational environments. All of these images are accumulated to form initial reference edge list so that resultant list includes more information regarding background image. A man is found in Figure 6, where the illumination is relatively high. The difference image is shown in Figure 7, which reflects that image-differencing approach is not suitable for intrusion detection in dynamic environment. The removal of reference edges by the proposed method results the edge segments of the moving object and detects the intended man, shown in Figure 8.

We compared the result of proposed method with the result by shading model method [12,13]. Figure 9 reflects a sample background image where Figure 10 shows the image containing a moving object in different illumination. Figure 11 and Figure 12 depict the resultant edge image of moving object by proposed method and modified shading model method, respectively. The result shows that propose method is suitable in dynamic environment and less prone to false alarm due to illumination change. The flexible methods for updating reference edge and robust method for edge matching facilitate to have these better results in fast change in illumination.



Fig. 5. A sample of background images in dark state



Fig. 6. Input image with moving object in light state



Fig. 7. Difference image



Fig. 8. Detected moving object by proposed method

**Fig. 9.** A sample of background images**Fig. 10.** Input image with moving object**Fig. 11.** Detected moving object by proposed method**Fig. 12.** Detected moving object by modified shading model method

5 Conclusions and Future Works

In this paper, we present a novel method for moving object detection based on extracted edge information, effective for dynamic environment. Our algorithm adapts background statistics to slow or fast change in the scene constituents and illumination. Proposed method has been tested on numerous real scenes with various changes of illumination. The results of our experiments show that proposed algorithm is adaptive to the changes of illumination as well as constituents of background. This approach can be tested to realize robust measurement for traffic monitoring system and to detect the suspicious activities of people and car in parking lot.

References

1. Lee, W.: A Framework for Constructing Features and Models for Intrusion Detection Systems. ACM Transactions on Information and System Security, Vol. 3 No. 4 (2000) 227 - 261
2. Hossain, M.J., Lee, J.W., Chae, O.S.: An Adaptive Video Surveillance Approach for Dynamic Environment. IEEE International Symposium on Intelligent Signal Processing and Communication System, Seoul, Korea, (2004) 84-89
3. Rosin, P.L.: Thresholding for Change Detection", Computer Vision and Image Understanding, Vol. 86, No. 2, (2002) 79-95
4. Chae, O. S., Kang, S.H.: Intruder Detection in Difference Image using the Region Growing based on Shape Features. CISST, Vol. I (2001) 449-459
5. Young, S., Forshaw, M., Hodgetts, M.: Image Comparison Methods for Perimeter Surveillance. International Conference on Image Processing and Its Applications Vol. 2 (1999) 799-802

6. Makarov, A., Vesin, J.M., Kunt, M.: Intrusion Detection using Extraction of Moving edges. Proceedings of the 12th IAPR International Conference on Computer Vision & Image Processing, Vol. 1 (1994) 804-807
7. Ahn, Y.H., Ahn, K., Chae, O.S.: Detection of Moving Objects Edges to Implement Home Security System in a Wireless Environment. Lecture Notes in Computer Science 3043, Part 1, (2004) 1044-1051
8. Gonzalez, R.C., Woods, R.E.: Digital Image Processing. Second Edition, Printice-Hall Inc. (2002) 585-586
9. Ahn, K.O., Hwang, H.J., Chae, O. S.: Design and Implementation of Edge Class for Image Analysis Algorithm Development based on Standard Edge. Proceeding of The 30th KISS Autumn Conference, (2003) 589-591
10. Canny, J.: A Computational Approach to Edge Detection. IEEE Transactions on PAMI, 8-6, (1986) 679-698
11. Chae, O.S., Lee, J.H., Ha, Y.H.: Integrated Image Processing Environment for Teaching and Research. Proceedings of International Workshop on Information & Electrical Engineering, South Korea (2002) 23-27
12. Zeljkovic, V., Popovic, M.: Detection of moving objects in video signal under fast changes of scene illumination. Proceedings of International Conference of Telecommunications in Modern Satellite. Vol. 2 (2001) 411 – 414
13. Skifstad, K., Jain, R.: Illumination Independent Change Detection for Real World Image Sequences. Computer Vision, Graphics, and Image Processing, Vol. 46 (1989) 387-399

A General Framework Based on Dynamic Constraints for the Enrichment of a Topological Theory of Spatial Simulation

Mehul Bhatt¹, Wenny Rahayu¹, and Gerald Sterling²

¹ Department of Computer Science

La Trobe University

Melbourne, Australia 3086

+61-3-94791280

{mbhatt, wenny}@cs.latrobe.edu.au

² Air-Operations Division, DSTO

PO Box 4331 Melbourne

Australia 3001

+61-3-96267728

Gerald.Sterling@dsto.defence.gov.au

Abstract. Qualitative spatial representation and reasoning has emerged as a major sub-field of AI in the past decade. An important research problem within the field is that of integrated reasoning about various spatial aspects such as distance, size, topology etc - an important application here being the qualitative simulation of physical processes. Approaches based on topology alone fail to provide an explicit account of other important aspects of spatial change thereby also not utilizing dynamically available information pertaining to them. Our work in this paper is based on the idea that a general theory of spatial simulation based on topological changes alone can be enriched by the inclusion of sub-theories relevant to other aspects of spatial change. We propose a general framework consisting of dynamic constraints for the enrichment of a topological theory of spatial changes. We propose the utilisation of such dynamic constraints for the incorporation of dynamically available information relevant to various aspects of space thereby making that aspect explicit in the theory. As an example of the proposed approach, we integrate dynamically available information pertaining to motion and size with the topological theory of RCC-8 using our framework of dynamic constraints.

1 Introduction

Qualitative reasoning about space and time - *reasoning at the human level* - promises to become a fundamental aspect of future systems that will accompany us in daily activities [1]. Indeed, the past decade has witnessed the growth of research in qualitative spatio-temporal representation and reasoning and its emergence as an active sub-field of AI [2, 3]. Dealing with uncertainty in space-time has yielded a much more developed research trend [1] – that of *spatial envisionment* or motion extrapolation, an important application of such envisionment being the *qualitative simulation of physical processes*

[4–7]. The aim here is to simulate the spatio-temporal behavior of, in general, solid objects or more simply to predict the result of motion. Within the context of qualitative representational formalisms, the most commonly applied technique is that of a *Continuity Network* or *Conceptual Neighbourhood Diagram* (CND), a term originating from [8]. Given a relational theory for representing spatial information, a CND associated with that theory is essentially a graph that tries to systematically capture the continuity of a change of relation between spatial objects – with the nodes representing primitive relations from the theory and edges representing direct, continuous transitions between them. For example, Fig. 1 shows the direct transitions possible for a topological theory of spatial changes, namely the Region Connection Calculus (RCC) [9]. It consists of the following set of eight jointly exhaustive and pair-wise disjoint (JEPD) relations: DC – *disconnected*, EC – *externally connected*, PO – *partially overlapping*, EQ – *equal*, and TPP – *tangential proper-part* & NTPP – *non-tangential proper-part* along with their respective inverses. In essence, two spatial relations are neighbours in a CND if a continuous change can yield a direct transition from one relation (node) to the other. This idea of the continuity of spatial change, with respect to a background theory for representing spatial information, inherent in the CND has been exploited towards qualitative reasoning about spatial changes in [5, 10, 11].

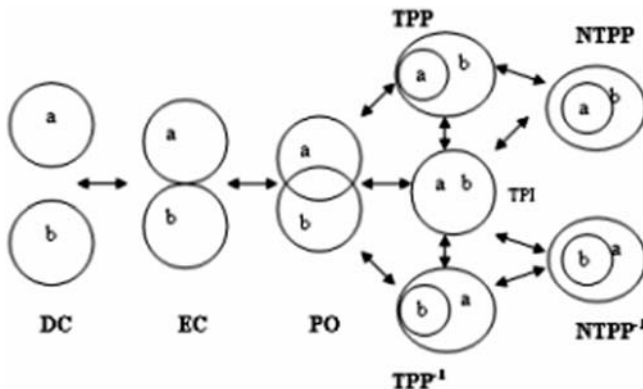


Fig. 1. Direct Topological Transitions for RCC8 Relations

Notice that the topological transitions in Fig. 1 are implicitly subject to the satisfaction of various constraints over the spatial objects involved. For example, consider a scenario pertaining to the motion of objects in a $n - \text{dimensional}$ space: assume two disconnected (DC) regions, atleast one of them moving towards the other. If they collide, we have EC holding between them. If they bounce or brush off, we return to DC. Otherwise, they go through each other and we have PO. At this point, we have four possibilities for the next spatial relation: EC, EQ, TPP or TPP⁻¹. Exactly which transition happens next depends upon the *relative motion and sizes* of the objects. Furthermore, each of these constraints can be classified on the basis of the spatial aspect that it deals with; the spatial aspect that has been left implicit in the theory of topological changes.

For example, consider motion that has not been treated explicitly in the transition network of RCC-8 [5]. Likewise, relative size constraints between regions too have not been accounted for in the direct topological transitions between RCC-8 relations. This paper contains two main contributions: **(a)** We propose a general framework consisting of dynamic constraints for the enrichment of a topological theory of spatial changes. We propose the utilisation of such dynamic constraints for the incorporation of dynamically available information relevant to various aspects of space such as distance, size, position etc, thereby making that aspect explicit in the theory. **(b)** Within the context of our framework, we incorporate motion and size constraints into the topological theory of spatial changes based on RCC. Motion in this paper is based on a simple notion of time-varying distances whereas size is based on primitive comparison relations between the n -dimensional measures of the regions involved.

2 Sub-theories Based on Dynamic Constraints

2.1 The General Framework

We propose a general framework consisting of a suite of sub-theories, each encompassing a different aspect of spatial change such as distance, size, motion etc, within a theory of spatial changes that is based on topology alone. A constraint (see Def. 1) is dynamic in the sense that it can only be satisfied when dynamic information, pertaining to distance, size, position etc, is available.

Definition 1. A *Dynamic Constraint* within our framework is a n -ary temporal predicate that may or may not hold a certain point in time. Dynamic constraints are of the form $\phi(arg_1, \dots, arg_n)$ and every such constraint has an implicit temporal argument t . A *Dynamic Constraint Set*, denoted as $\Theta_{subtheory}$, is a set consisting of a finite number of such dynamic constraints.

All dynamic constraints in this paper are binary (temporal argument not included) and will be of the following form: $\phi(arg_1, arg_2, t)$. For clarity, we may omit the temporal argument in certain cases. Every dynamic constraint set $\Theta_{subtheory}$ characterizes a sub-theory pertaining to a certain aspect of spatial change that needs to be explicitly modelled so as to complement the basic theory of topological changes. As an example consider the sets Θ_M and Θ_S in section 3, which denote the class of motion and size constraints that have been included within the theory of topological changes. The inclusion of these constraints has the effect of providing an explicit account of the the relative motion and sizes of the objects involved.

Definition 2. A *Dynamic Constraint Suite*, denoted by Σ , is the set consisting of all dynamic constraint sets to be included as sub-theories with the framework. More formally, $\Sigma \equiv \{\Theta_1, \Theta_2, \dots, \Theta_n\}$, where each of the Θ_i represents dynamic constraints relevant to a certain aspect of spatial change being modelled within the framework.

We refer to a collection of such sub-theories as a dynamic constraint suite. Important, from a computational viewpoint, is the idea of the satisfiability of a set of dynamic constraints $\Theta_{subtheory}$, or Σ – *Satisfiability* in general. Within the context of our framework, the same has been stated more precisely in Def. 3 below:

Definition 3. Satisfiability - A set of dynamic constraints, given by $\Theta_{\text{subtheory}}$, on a transition between two qualitative states is satisfiable iff $\forall \phi \text{ holds}(\phi, t)$, where $\phi \in \Theta_i$. Here, $\text{holds}(\phi, t)$ should be interpreted as the successful validation of the constraint ϕ based on the dynamically available information at time point t . Likewise, satisfiability of all dynamic constraints within our framework Σ is defined to be the satisfiability of every dynamic constraint set $\Theta_{\text{subtheory}}$ contained therein.

2.2 Constraints on Topological Transitions

Def. 1 – 3, which provide a general representational framework for the specification of the dynamic constraints, will be used to formalise the incorporation of dynamic constraints within the theory of topological changes. We introduce the idea of a **transition constraint** - A transition constraint is essentially a dynamic constraint, but one that is imposed on a certain transition between two topological relations. The satisfiability criteria for a transition constraint is similar to that of a dynamic constraint expressed in **Def. 3**. Again, intuitively the satisfiability entails that a certain relational transition with respect to the base topological theory is consistent with the dynamically available (for e.g. sensory) information relevant to the respective spatial aspect that the constraint is supposed to model. A more precise formulation is presented in the following.

Let \mathbf{R} denote the set of JEPD relations included in the RCC-8 theory – $\mathbf{R} \equiv \{dc, ec, po, eq, tpp, ntpp, tpp^{-1}, ntp^{-1}\}$. Let \mathbf{T} be a set consisting of ordered pairs of the form $< r_i, r_j >$ (a binary relation on \mathbf{R}). For clarity, we refer to such a ordered pair using the predicate $\text{trans}(r_i, r_j)$. Its intended semantics is that a direct, continuous transition from r_i to r_j is legal (though not necessarily possible). Note that the set \mathbf{T} can be easily defined by simple enumeration on the basis of the transition network of RCC-8 shown in Fig. 1. Also, the scope of the universally quantified region variables x and y in the definition \mathbf{P} below is understood to be the subset of regions that are related by r_i at time point t_1 . The following is the formal definition for a transition constraint:

$$\begin{aligned} (\mathbf{P}) \text{ poss}(< r_i, r_j >, t) \equiv & [(\forall x, y) (\exists t_1 t_2)] \\ & (t_1 < t_2) \wedge (t_2 < t) \wedge \text{holds}(r_i, x, y, t_1) \wedge \phi_1(x, y, t_2) \wedge \dots \wedge \phi_k(x, y, t_2). \\ \text{where } < r_i, r_j > & \in \mathbf{T}, \text{ and } \phi_1 \dots \phi_k \in \Theta \text{ from } \Sigma \end{aligned}$$

The intended interpretation for \mathbf{P} defined above is that a direct, continuous and legal transition from r_i to r_j is *possible* at time point t if regions x and y have the relation r_i between them at some time-point t_1 before t and that at other time-point t_2 between t_1 and t , the dynamic constraints imposed on the the legal transition $\text{trans}(r_i, r_j)$ can be *satisfied* on the basis of the dynamically available information pertaining to the spatial aspect being modelled by the respective constraint.

2.3 Minimal and Σ -Consistency

The idea of **minimal and Σ -consistency** has been informally defined below in Def. 4. Minimal consistency essentially entails that absolutely no transition constraints have been imposed on the direct topological changes possible between RCC-8 relations. It

can be easily verified that the concept of Σ -Consistency is much more richer than the minimal/general account of spatial changes provided by the RCC-8 direct topological transitions. This is because depending on the number and nature of the additional sub-theories included within Σ , additional information that is dynamically available will be utilised whilst simulating the physical system.

Definition 4. Consistency of an Envisionment - An envisionment¹ of a physical system, either partial or complete, is **minimally consistent** iff the transitions between qualitative states (topological relations between objects) of the system are solely based on the direct topological transitions possible wrt the RCC-8 conceptual neighbourhood diagram. Similarly, the envisionment is **maximally consistent**², also referred to as ' Σ -Consistent', iff the transitions between the states satisfy every set of constraints included in the Σ , in addition to being consistent with the RCC-8 CND.

A formal account of the Σ -Consistency of transitions between qualitative states or a complete envisionment of a physical system can be derived by generalizing the definition of a transition constraint \mathbf{P} given in section 2.2. Precisely, the definition of $\text{poss}(r_i, r_j)$ entails the consistency of a single transition, for e.g., from *DC* to *EC*, involving two objects. This definition needs to be generalised for an arbitrary chain of legal transitions r_0, r_1, \dots, r_n involving more than two objects. Such a chain of transitions is Σ -Consistent iff $\text{poss}(r_i, r_{i+1})$ is true for all $< r_i, r_{i+1} >$. These definitions can easily be extended to handle domains consisting of an arbitrary number of objects. However, the definitions already presented are sufficient for the purposes of this paper.

3 Motion and Size Constraints on Topological Transitions

In this section, we illustrate how the formal framework developed in Section 2 can be applied - we illustrate the incorporation of dynamically available information pertaining to the relative movement and sizes of objects. Note that this paper does not attempt to provide a full-scale treatment of motion or relative sizes of spatial objects. Our use of motion and size constraints in this section is only exemplary of the manner in which the proposed framework involving dynamic constraints is to be utilised.

- (A1) $DC(x, y) \equiv_{\text{def}} \text{dist}(x, y) > \delta$
- (A2) $EC(x, y) \equiv_{\text{def}} \text{dist}(x, y) \leq \delta \wedge \text{dist}(x, y) \neq 0$
- (A3) $Co(x, y) \equiv_{\text{def}} \text{dist}(x, y) = 0$

We define a class of motion constraints Θ_M (see Def. 5) that are based on a simple notion of time-varying distances between objects. These constraints are in turn based on three dyadic relations, DC - disconnected, EC - externally connected and CO - coalesce, between pairs of regions expressed using the function $\text{dist}(x, y)$ (see A1-A3). For e.g., two regions are *disconnected* if the degree of displacement between them is greater a

¹ An envisionment is a temporal partial ordering of all the qualitative states a modelled physical system can evolve into given some indexed/initial state [12]

² Of Course, within the context of our theory of dynamic constraints

certain δ , where δ is a domain dependent parameter. We sometimes use the primitive function $dist(x, y)$ with a temporal argument, as in $dist(x, y, t)$, to denote the distance between x and y at time-point t . The distance function can be intuitively understood as the size of the shortest line connecting any two points in the two region boundaries. The concept of distance should be understood as a qualitative notion of displacement, i.e., the accurate measurements are not important [13], but how the distance between regions varies with time so as to capture their relative movement.

Definition 5. *The class of **motion constraints** Θ_M includes dynamic constraints of the form discussed in Def. 1. Specifically, Θ_M consists of the five motion relations based on the primitive notion of distance between two regions that are defined axiomatically in C1-C5: $\Theta_M \equiv \{\phi_{ap}, \phi_{re}, \phi_{sp}, \phi_{co}, \phi_{st}\}$.*

- (C1) $\phi_{ap}(x, y, t) \equiv_{def} [(\exists t_1 t_2)] (t_1 < t) \wedge (t < t_2) \wedge holds(DC, x, y, t_1) \wedge \neg holds(CO, x, y, t_2) \wedge dist(x, y, t_1) > dist(x, y, t_2)$
- (C2) $\phi_{re}(x, y, t) \equiv_{def} [(\exists t_1 t_2)] (t_1 < t) \wedge (t < t_2) \wedge [holds(DC, x, y, t_1) \vee holds(EC, x, y, t_1)] \wedge dist(x, y, t_1) < dist(x, y, t_2)$
- (C3) $\phi_{sp}(x, y, t) \equiv_{def} [(\exists t_1 t_2)] (t_1 < t) \wedge (t < t_2) \wedge [holds(DC, x, y, t_2) \vee holds(EC, x, y, t_2)] \wedge holds(CO, x, y, t_1)$
- (C4) $\phi_{co}(x, y, t) \equiv_{def} [(\exists t_1 t_2)] (t_1 < t) \wedge (t < t_2) \wedge [holds(DC, x, y, t_1) \vee holds(EC, x, y, t_1)] \wedge holds(CO, x, y, t_2)$
- (C5) $\phi_{st}(x, y, t) \equiv_{def} [(\exists t_1 t_2)] (t_1 < t) \wedge (t < t_2) \wedge dist(x, y, t_1) = dist(x, y, t_2)$

The following interpretation holds for the motion constraints defined in Θ_M : $\phi_{ap}(x, y, t)$ – x & y are approaching each other at time-point t , $\phi_{re}(x, y, t)$ – x & y are receding from each other, $\phi_{sp}(x, y, t)$ – x & y are splitting, $\phi_{co}(x, y, t)$ – x & y are coalesce, and $\phi_{st}(x, y, t)$ – x & y are static.

We also define a class of size constraints Θ_S (see Def. 6) that are based on primitive comparison relations between the sizes of the regions involved. Similar to [14], we assume that the size of a n-dimensional region corresponds to its n-dimensional measure. For example, the size of a sphere in R^3 corresponds to its volume. The function $size(x)$ will be used to denote the size of an region given by x .

Definition 6. *The class of **size constraints** Θ_S includes the following dynamic constraints that relate the size of two regions at a certain time point: $\Theta_S \equiv \{\phi_<, \phi_>, \phi_\leq, \phi_\geq, \phi_= \}$. Each of the size constraints is of the form $\phi_{size_rel}(x, y, t)$, where $\phi_{size_rel} \in \Theta_S$. For notational convenience, the interpretation of $\phi_{size_rel}(x, y, t)$ is explained with an example: $\phi_<(x, y, t)$ should be interpreted as ' $size(x) < size(y)$ ' at time t , where $size(x)$ is the size of region x , and $size(y)$ is the size of region y .*

We now have a dynamic constraint suite $\Sigma \equiv \{\Theta_M, \Theta_S\}$. Dynamic constraints that make up the theory Σ can now be used for the definition of transition constraints, i.e., dynamic constraints imposed on the topological transitions (see section 2.2). The precise representational form of the transition constraints definable within the context of our theory Σ will follow the generic definition in P.

- (T1) $\text{poss}(\text{trans}(dc, ec), t) \equiv [(\forall x, y) (\exists t_1 t_2)]$
 $(t_1 < t_2) \wedge (t_2 < t) \wedge \text{holds}(dc, x, y, t_1) \wedge [\phi_{ap}(x, y, t_2)]$
- (T2) $\text{poss}(\text{trans}(ec, dc), t) \equiv [(\forall x, y) (\exists t_1 t_2)]$
 $(t_1 < t_2) \wedge (t_2 < t) \wedge \text{holds}(dc, x, y, t_1) \wedge [\phi_{re}(x, y, t_2)]$
- (T3) $\text{poss}(\text{trans}(po, eq), t) \equiv [(\forall x, y) (\exists t_1 t_2)]$
 $(t_1 < t_2) \wedge (t_2 < t) \wedge \text{holds}(po, x, y, t_1) \wedge [\phi_{co}(x, y, t_2) \wedge \phi_{=}(x, y, t_2)]$
- (T4) $\text{poss}(\text{trans}(po, tpp), t) \equiv [(\forall x, y) (\exists t_1 t_2)] (t_1 < t_2) \wedge (t_2 < t)$
 $\wedge \text{holds}(po, x, y, t_1) \wedge [\neg\phi_{co}(x, y, t_2) \wedge \phi_{<}(x, y, t_2) \wedge \neg\phi_{sp}(x, y, t_2)]$

For parsimony of space, we only illustrate a subset of the transition constraints that are definable by way of the axioms **T1-T4** above. The dynamic constraints from our framework that are imposed on the transitions are highlighted in the brackets. As an example, consider transition constraint **T4** – $\neg\text{poss}(\text{trans}(po, tpp), t)$. It enforces the condition that a legal transition between two regions from *po* to *tpp* is *possible* at time-point *t* iff at some time-point $t_1 < t$, *x* and *y* were *po* at t_1 , and at another time-point t_2 , such that $t_1 < t_2 < t$, the dynamic constraints imposed on the transition are *satisfiable*. Notice how this simple axiom integrates three differing aspects of spatial change – topology, motion & size. A similar discussion applies for other transition constraints as well and will be left out.

4 Discussion and Further Work

The overall context of our work is centered around the idea of an envisionment based qualitative simulation program [12]. The work in [5] utilizes the same approach and is based on a logical theory of topological changes alone. Although their work utilizes constraints, they are used in a static and domain dependent manner in the form of inter & intra-state constraints. Motion, size or any other aspect of space is not treated explicitly and dynamically available information has not been utilized. Using our approach, the specification of some of the domain specific constraints becomes redundant – for r.g., Consider two regions *a* and *b*, such that $\text{size}(a) < \text{size}(b)$ at all times. Since *a* is smaller than *b*, one constraint that always needs to be maintained (an inter-state constraint) is that *b* can never be a tangential or non-tangential proper-part of *a*. Since size constraints are explicitly accounted for in the form of transition constraints in our theory, no domain specific constraint to the effect needs to be specified by the domain modeller.

The formulation of motion constraints in Section 3 is based on the idea of defining connectedness between two objects using the primitive notion of displacement between them. This idea arises from [13], though in a somewhat different context. Using this formulation, the relation of *partial overlap* (PO) between two regions cannot be expressed when connectedness is defined using the primitive notion of distance (see A1 – A3). As such, dynamic constraints on $\text{trans}(ec, po)$ or $\text{trans}(po, ec)$ are not definable. This, however, reflects the lack of expressivity of the manner in which motion is defined. Dealing with such inadequacies or providing a full-scale treatment of

motion, which is beyond the scope of our research interests, has already been treated elsewhere [11].

Non-determinism or ambiguity is represented in RCC's transition network in the form of multiple edges emanating from one node to other. This ambiguity can be reduced (atleast partially) by making use of dynamically available of information pertaining to relative motion and sizes – dynamic constraints can be used to restrict the simulation to a certain region of the state space. Ofcourse, this assumes the presence of a sub-theory for motion, sizes etc within the spatial simulation framework to complement the theory of spatial changes based on topology alone. With this motivation, our long-term research goal is to investigate integrated ways to represent & reason about various spatial aspects such as distance, topology, size, orientation, motion etc. We consider a dynamic constraint based approach to be a suitable candidate contributing toward such a goal. The main idea here being that of utilising the dynamically available information relevant to various spatial aspects whilst simulating a system.

References

1. Vieu, L.: Spatial representation and reasoning in AI. In Stock, O., ed.: *Spatial and Temporal Reasoning*, Kluwer Academic Publishers (1997) 5–40
2. Cohn, A.: Qualitative spatial representations. In: *Working Notes of IJCAI'99 Workshop on Adaptive Spatial Representations of Dynamic Environments*. (1999) 33–52
3. Hernandez, D.: *Qualitative Representation of Spatial Knowledge*. Springer-Verlag New York, Inc. (1994)
4. Kuipers, B.J.: Qualitative simulation. *Artif. Intell.* **29** (1986) 289–338
5. Cui, Z., Cohn, A.G., Randell, D.A.: Qualitative simulation based on a logical formalism of space and time. In: *Proceedings of AAAI-92*, AAAI Press (1992) 679–684
6. Randell, D.A., Cohn, A.G., Cui, Z.: Naive topology: Modelling the force pump. In Struss, P., Falttings, B., eds.: *Advances in Qualitative Physics*. MIT Press (1992) 177–192
7. Kuipers, B.: Qualitative reasoning: modeling and simulation with incomplete knowledge. MIT Press (1994)
8. Freksa, C.: Conceptual neighborhood and its role in temporal and spatial reasoning. In Singh, M., Travé-Massuyès, L., eds.: *Decision Support Systems and Qualitative Reasoning*, North-Holland, Amsterdam (1991) 181–187
9. Randell, D.A., Cui, Z., Cohn, A.: A spatial logic based on regions and connection. In Nebel, B., Rich, C., Swartout, W., eds.: *KR'92. Principles of Knowledge Representation and Reasoning: Proceedings of the Third International Conference*. Morgan Kaufmann, San Mateo, California (1992) 165–176
10. Hernandez, D.: Reasoning with qualitative representations: Exploiting the structure of space. In Carrete, N., Singh, M., eds.: *Qualitative Reasoning and Decision Technologies*, Barcelona: CIMNE (1993) 493–502
11. Galton, A.: Towards an integrated logic of space, time and motion. In: *IJCAI*. (1993) 1550–1557
12. Weld, D.S., de Kleer, J.: *Readings in Qualitative Reasoning about Physical Systems*. Morgan Kaufmann Publishers (1989)
13. Santos, P., Shanahan, M.: From regions to transitions, from transitions to objects. In Baral, C., McIlraith, S., eds.: *AAAI-02 Cognitive Robotics Workshop, Working notes of the AAAI Workshop on Cognitive Robotics*. (2002)
14. Gerevini, A., Renz, J.: Combining topological and size information for spatial reasoning. *Artif. Intell.* **137** (2002) 1–42

Automatic Geomorphometric Analysis for Digital Elevation Models

Miguel Moreno, Serguei Levachkine, Miguel Torres,
Rolando Quintero, and G. Guzman

Geoprocessing Laboratory-CIC-National Polytechnic Institute, Mexico City, Mexico
{marcomoreno, sergei, mtorres, quintero, jguzmanl}@cic.ipn.mx
<http://geo.cic.ipn.mx>, <http://geopro.cic.ipn.mx>

Abstract. We present an approach to perform geomorphometric analysis for Digital Elevation Models (DEM) to obtain the *Cartographic Knowledge Domain (CKD)* of the landscapes. CKD is oriented to represent the essential properties of DEM by means of concepts. These properties are obtained by analyzing the terrain topography. This analysis is based on two classifications: landform and topographic ruggedness. The approach involves the following raster layers: slope, profile curvature and plan curvature (primary attributes), which have been built to identify the intrinsic properties of the landscape. We use a *multi-valued raster* to integrate the primary attributes of DEM to generate the landform classification layer in order to find the terrain characteristics of the water movement. The topographic ruggedness is used to express the amount of elevation difference between adjacent cells of DEM. The topographic ruggedness is presented by means of Terrain Ruggedness Index (TRI). This work is oriented to support subsequent processes. The method has been implemented into Geographical Information System - ArcInfo, and applied for Tamaulipas State, Mexico.

1 Introduction

Nowadays, the Digital Elevation Models (DEM) are playing an increasingly important role in many technical fields of Geographical Information Systems (GIS) development, including earth and environmental sciences, hazard reduction, civil engineering, landscape planning, and commercial display [1]. DEM is a particular type of raster geo-images. The geometric characteristics of DEM are the following: resolution, origin of coordinates, number of rows and columns. This raster describes thematic aspects of the terrain, which are represented by attributes. Furthermore, DEM has been incorporated in geomorphometric analysis. This is the measurement of geometry of the landforms¹ to analyze distribution and concentration of certain spatial objects and has traditionally been applied to watersheds, drainages, hillslopes and other groups of terrain objects. Contrasting with the traditional topographic map methods, the GIS approaches are relatively easy to apply in a consistent way on large landscape areas, because they allow summation of terrain characteristics for any re-

¹ Landform is the result of various processes acting on the surface has also the function of a static boundary condition for processes in geomorphology, hydrology, meteorology and others

gion. The advantage of DEM analysis is that just one static parameter has to be captured to describe landscape processes. The characteristics of terrain are distinguished by spatial relationships among different geographic objects. They can be characterized by both its composition and configuration. We usually note that DEMs are directly computed from the elevation model and *secondary compound attributes*, which involve combination of primary attributes and constitute physically the spatial variability of specific processes that are presented in the landscape [2], while *primary attributes* include slope, aspect, plan and profile curvature. Most of these topographic attributes are computed from directional derivatives of a topographic surface. The slope affects the overall rate of movement downslope. The *Profile curvature* impacts the acceleration and deceleration of the water flow. Therefore, it influences in the erosion and the deposition processes. The *Plan curvature* affects convergence and divergence of the water flow [3].

We propose the *Cartographic Knowledge Domain (CKD)* as a finite space of attributive, topological, logical and spatial data, which are associated with raster cartographic objects and patterns. These patterns are represented by a set of concepts [4]. For instance, attributive data such as type of border, landform, surface, population, administrative unit, among others, geometric data like contours, coordinates, etc.

In this work, we propose a method to perform spatial analysis based on geo-image processing by means of Spatial Analyzer Module (SAM). In Section 2 we present the description of SAM and describe its functionality. Additionally, we describe how raster layers have been obtained. Section 3 sketches out the construction of CKD. Some results are shown in Section 4. Section 5 outlines our conclusions.

2 Spatial Analyzer Module

SAM is a special module, which has been designed to perform the spatial analysis procedures. SAM uses geographic data to make the spatial analysis. This module has been implemented using Arc Macro Language (AML) to ensure portability between computer platforms executing ArcInfo 7.0 or later. The present analysis consists of using different spatial data related to the case of study. SAM contains two components: *Analysis Block*, which is composed of a set of processes to make data analysis; *List of Procedures* that stores the sequence of steps to execute the processes. More details of SAM are described in [5].

2.1 Analysis Block

It contains the functions to perform the spatial analysis. The functions are the following:

Grid Functions. They contain the set of functions for cell analysis, which includes operations of the map algebra and functions to compute primary topographic attributes such as slope, aspect, plan and profile curvature and upslope contributing area.

- *Map Algebra Functions.* They consist of the set of functions for cell analysis that includes operations of the map algebra. In this case the functions are considered to compute the square root (*SQRT*) and square (*SQR*) respectively in the input grid [6].

- **Slope Function (CALC_SLOPE):** Slope identifies the maximum rate of change in value from each cell to its neighbors. An output slope grid can be computed as percent slope or degree of slope. Conceptually, the slope function fits a plane to the z-values (altitudes) of a 3 x 3 cell neighborhood around the processing or center cell. The direction of the plane (x,y-values) faces is the aspect for the processing cell. The slope for the cell is computed from the 3 x 3 cell neighborhood by using the average maximum technique [7]. This function is described with more detailed in [1]. The formulas to compute the slope are the following:

$$\text{Rise_Run} = \sqrt{\sqrt{dz/dx} + \sqrt{dz/dy}} , \quad (1)$$

$$\text{Slope} = \text{Atan}(\text{Rise_Run}) * 57.29578 , \quad (2)$$

where dz/dx and dz/dy are calculated by using a 3x3 window as described in Eqn. 3 and 4:

$$dz/dx = ((a+2d+g)-(c+2f+i))/(8 * X_mesh_spacing) , \quad (3)$$

$$dz/dy = ((a+2b+c)-(g+2h+i))/(8 * Y_mesh_spacing) , \quad (4)$$

- **Curvature Functions:** These functions compute the curvature in a DEM. The curvature functions can be used to describe the physical characteristics of a drainage basin to understand erosion and runoff processes. Two types of curvatures can be obtained by using SAM. 1) *Profile curvature (CALC_PROFILE_CURVATURE)* is the curvature of topography from a cross-section view (perpendicular to contour lines). 2) *Plan curvature (CALC_PLAN_CURVATURE)* is the curvature of topography from a map view (following contour lines). The curvature of a surface is computed by a cell-by-cell. For each cell, we use a fourth-order polynomial of the form [1]:

$$Z = Ax^2y^2 + Bx^2y + Cxy^2 + Dx^2 + Ey^2 + Fxy + Gx + Hy + I , \quad (5)$$

Eqn. 5 is used to fit a surface composed of a 3 x 3 window. The coefficients from A to I are calculated from this surface. The relationships between the coefficients and the nine values of elevation for every cell numbered are shown in Fig. 1 and described in [6]. The output of the *CURVATURE* function is the second derivative of the surface (i.e., the slope of the slope), which is defined in Eqn. 6.

$$\text{Curvature} = -2(D+E)*100 , \quad (6)$$

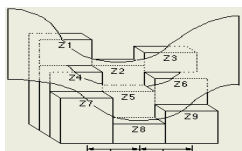


Fig. 1. Elements to compute the curvature

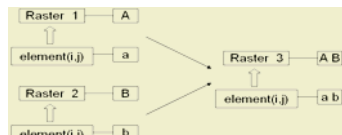


Fig. 2. Data schema of multi-valued rasters

- **Overlay Function (OVERLAY).** This operation has been designed to generate *multi-valued raster*, which can be used to combine different geo-images. It is to count rasters with more than one attribute and assign values to these attributes for each raster elements [6]. The representation schema of the data structure is shown in Fig. 2. It is important to note that two rasters can only be overlaid if they have the same geometry.

2.2 List of Procedures

List of procedures stores the set of functions for each one of the analysis processes, and it describes the required data type and the constraints. In this paper we propose two processes: Ruggedness Index and Landform Clasification. SAM has a wide range of applications, not only to make *geomorphometric analysis* but also to perform the detection of *landslide* and *flooding* areas [5].

2.2.1 Topographic Ruggedness

Topographic Ruggedness is represented by means of Terrain Ruggedness Index (TRI). TRI is a measurement developed by Riley to represent the amount of elevation difference between adjacent cells of a DEM [8]. The process essentially computes the difference in elevation values from the center cell and the eight cells surrounding it immediately. This process squares each of the eight elevation difference values to make them all positive and averages the values (squares). Therefore, TRI is derived by taking the square root of this average, and it corresponds to the elevation average change between any point into a grid cell and its surrounding area. The authors of the TRI propose the classification for the values obtained by the index (see Table 1). The pseudo-code [8] to generate TRI layer is:

```
program TRI { de-Input Grid; tmp1-Standard elevation difference;
tmp2-TRI; tmp3- adjust TRI range; ri-Output grid
tmp1(X,Y) := ((SQR(dem(x,y)-dem(x-1,y-1)) + (SQR(de(x,y)-de(x,y-1)) +
SQR(de(x,y)-de(x+1,y-1)) + (SQR(de(x,y)de(x+1,y)) + (SQR(de(x,y)-de(x+1,y+1)) +
(SQR(de(x,y)-de(x,y)) + (SQR(de(x,y)-de(x-1,y+1)) + (SQR(de(x,y)-de(x-1,y)))
tmp2(X,Y) :=SQR(tmp1(x,y))
tmp3(X,Y) :=If (tmp2(x,y)>=5000) then tmp3(x,y) :=5000 Else tmp3(x,y) :=tmp2(x,y)
if (0>=tmp3(x,y)<= 80) then ri(x,y) :=1; if (81>=tmp3(x,y)<=116) then ri(x,y) :=2;
if (117>=tmp3(x,y)<=161) then ri(x,y) :=3; if (162>=tmp3(x,y)<=239) then ri(x,y) :=4
if (240>=tmp3(x,y)<=497) then ri(x,y) :=5; if (498>=tmp3(x,y)<=958) then ri(x,y) :=6
if (959>=tmp3(x,y)<=5000) then ri(x,y) := 7 )}
```

Table 1. Terrain Ruggedness Index Classification

| TRI | Interval (m) | Represent |
|-----|--------------|-------------------------------|
| 1 | 0-80 | Level terrain surface |
| 2 | 81-116 | Nearly level surface |
| 3 | 117-161 | Slightly rugged surface |
| 4 | 162-239 | Intermediately rugged surface |
| 5 | 240-497 | Moderately rugged |
| 6 | 498-958 | Highly rugged |
| 7 | 959-4367 | Extremely rugged surface |

2.2.2 Landform Classification

Primary and *secondary attributes* have been used to classify DEM into different landforms. A method by Pennock described in [3] was implemented to automatize the classification. The slope, profile curvature and plan curvature are used to classify eleven different landforms (see Table 2). The landform classification is considered to evaluate the probable water movement and concentrations. Watershed is an area that drains water and other substances to common outlet as concentrated drainage. This area is normally defined as the total area flowing to a given outlet or pour point [3]. These areas are detailed by *WATERSHED* function (Arc/Info). The following pseudo-code has been designed to generate the *landform classification*:

```

program LFC{ dem - Input Grid; slope - slope; profcurv - profile curvature;
plancurv - plan curvature; watershead - watershead area;
otgrd0 - Aux grid; otgrd1- Aux grid; landform-landform classification;
slope:=CALC_SLOPE(dem); profcurv:=CALC_PROFILE_CURVATURE(dem);
plancurv:=CALC_PLAN_CURVATURE(dem); otgrd0:=OVERLAY(profcurv, plancurv);
otgrd1:=OVERLAY(slope, watershead); landform:=OVERLAY(otgrd0, otgrd1);
classify (landform,landformgrid) }

```

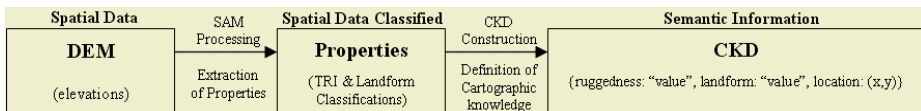
Table 2. Classification of landform elements for a DEM

| Landform Elements | Acronym | Slope | Profile Curvature | Plan Curvature | Water-head |
|----------------------|---------|-------|-------------------|----------------|------------|
| Divergent Shoulder | DHS | >0 | >0.1 | >0.1 | NA |
| Planar Shoulder | PSH | >0 | >0.1 | >0.1 >-0.1 | NA |
| Convergent Shoulder | CSH | >0 | >0.1 | >0.1 | NA |
| Divergent BlackSlope | DBS | > 3.0 | >-0.1 <0.1 | >0.1 | NA |
| Planar BackSlope | PBS | > 3.0 | >-0.1 <0.1 | >0.1 >0.1 | NA |
| Convergent BackSlope | CBS | > 3.0 | >-0.1 <0.1 | >0.1 | NA |
| Divergent FootSlope | DFS | >0 | >0.1 | >0.1 | NA |
| Planar FootSlope | PFS | >0 | >-0.1 | >0.1 >0.1 | NA |

3 Cartographic Knowledge Domain Implementation

To generate the *Cartographic Knowledge Domain (CKD)*, it is important to consider the values of the classification, which are denoted by cartographic patterns. Let P_{DEM} be the recognized pattern by a computer system into DEM. P_{DEM} involves attributive, geometric and topologic data, which are known in the knowledge context. These data are used to define the *CKD* that is considered the subject domain of the application. The most important terrain information is the following: coordinate system, elevation, ruggedness, shape, etc. We use this information to recognize and assign a concept from *CKD* (e.g. “Planar FootSlope” and “Moderately rugged”) to subsequent processing.

On the other hand, to build *CKD*, it is necessary to obtain the “essential properties” of DEMs. These properties describe the spatial semantics of DEM representation. The mechanism proposed for *CKD* consists of structures, which determine the *a priori* knowledge about DEMs. The retrieval process related to these structures is used to extract concepts by means of the *CKD*. Fig.3. depicts the process to group the characteristics of DEMs into *CKD*.

**Fig. 3.** Implementation of Cartographic Knowledge Domain

For instance, $P_{DEM} = \{ruggedness: "Moderately"; landform: "Planar FootSlope"; Location (100,240)\}$. This structure belongs to *CKD*; furthermore, it is possible to locate characteristics that involve DEMs. These characteristics are denominated *cartographic patterns* such as: “Moderately rugged”, “Planar FootSlope” and so on.

In our work, *CKD* is used in hydrological network generalization, because the terrain-form defines the behavior (*cartographic patterns*) of the networks (rivers, drain,

bodies of water, etc). In addition, in this context the adequate parameters to describe functions to line simplification are required in the process. These functions will be able to use different values according to the landform and ruggedness².

4 Results

By using SAM, we construct *terrain ruggedness index* and *landform classification* layers. Some results of this approach are presented in this section. The methods have been applied to Tamaulipas State, Mexico covered by DEM at two resolutions, 10 x 10 m and 100 x 100 m generated in GEOLAB, interpolating line contours.

Fig. 4a shows the original DEM (100 meter resolution) composed of 8000 rows and 2478 columns. The minimum value is 0 m, maximum value is 3496, mean value of this layer is 227.40 m and the standard deviation is 498.469. Fig. 4b shows the *terrain ruggedness* layer constructed by SAM, and the TRI classification of this area. The *TRI* layer has the following values; mean is 2.386 m and the standard deviation is 2.457. This means that Tamaulipas State has slightly rugged areas in its territory. The extremely rugged areas are principally concentrated at the southwestern part of Tamaulipas State.

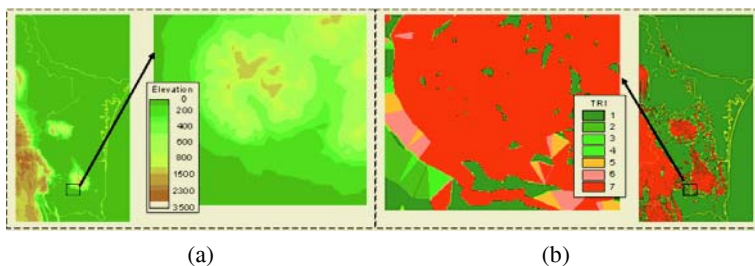


Fig. 4. a) Digital Elevation Model with resolution of 10 m, b) Terrain Ruggedness layer

To test the landform classification, we use two DEMs of the same area in two resolutions: 1) 1925 rows and 2410 columns (10 meter resolution), 2) 190 rows and 239 columns (100 meter resolution); see Fig 5. In Fig. 5a we appreciate the DEM prior to classification. Fig. 5b and 5c depict the landform classification of the DEM. The differences between these figures are due to the resolutions. Fig. 5b has more level of detail than Fig 6c. The favorite value in both classifications is Planar Back Slope, this means that the terrain is mainly planar (this is its semantics).

5 Conclusion

In this work, we propose the Spatial Analyzer Module integrated into GIS-application to analyze *geomorphometric characteristics* of geo-images. SAM generates primary attributes of DEM to detect landform elements in raster image data. In this approach, spatial and attributive data are used to generate raster.

² The parameter values for planar and rough areas should be different because the terrain-form defines the simplification degree of the lines

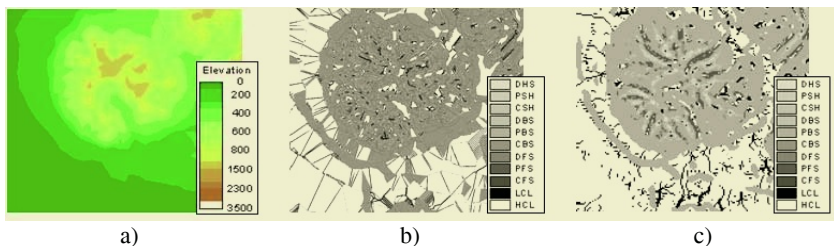


Fig. 5. a) DEM with resolution of 10 m, b) Landform classification of DEM with resolution of 10 m, c) Landform classification of DEM with resolution of 100 m

The geomorphometric analysis is traditionally performed by using the methods based on topographic map-processing in manual way. Our approach significantly decreases the amount of time and effort required to quantify selected terrain characteristics. Other methods are designed to evaluate additional characteristics, which are different to the properties proposed in our approach. However, these methods can be integrated into SAM.

The geomorphometric analysis facilitates the extraction-information of the spatial properties that can be used in other cartographic processes such as hydrological balance, automatic map description, map generalization, etc. Moreover, the *landform classification* approach is used to identify flooding areas and the path of the hydrological flows. CKD represents the properties of a specific area by means of concept. Also, we can catch the *semantics*, which is represented by a set of properties that involves the DEM.

Acknowledgments

The authors of this paper wish to thank the CIC, CGPI, IPN and CONACYT for their support.

References

1. Moreno, M., Levachkine, S., Torres, M. & Quintero, R.: Landform Classification in Raster Geo-Images, In: Sanfeliu, A., Martínez-Trinidad, F., Carrasco-Ochoa, J.A.(eds): Progress in Pattern Recognition, Image Analysis and Applications, LNCS, Vol. 3287, Springer-Verlag, Berlin Heidelberg (2004) 558-565
2. Wilson, J.P., Gallant, J.C. Terrain Analysis- Principles and Applications. John Wiley & Sons, USA, (2000)
3. Pennock, D.J., ZebARTH, B.J. and de Jong, E.: Landform classification and soil distribution in hummocky terrain, Saskatchewan, Canada, Geoderma. 40, (1997), 297-315. Bonk, R: Scale-dependent Geomorphometric Analysis for Glacier Mapping at Nanga Parbat
4. Torres, M., Levachkine, S.: Semantics Definition to Represent Spatial Data. In: Levachkine, S., Ruas, A., Bodansky, E. (eds.), Proc. International Workshop on Semantic Processing of Spatial Data (GEOPRO 2002), 3-4 December 2002, Mexico City, Mexico (2002)
5. Torres, M., Moreno, M., Menchaca, R. and Levachkine, S.: Making Spatial Analysis with a Distributed Geographical Information System, International Conference on Databases and Applications (DBA'2003), IASTED, (2003), 1245-1256

6. Molenaar, M.: An Introduction to the theory of spatial object modelling for GIS. Taylor & Francis, U.K. (1998)
7. Burrough, P.A.. Principles of Geographical Information Systems for Land Resources Assessment. Oxford University Press, New York, (1986)
8. Riley, S. J., DeGloria, S. D., and Elliot, R.: A terrain ruggedness index that quantifies topographic heterogeneity. Intermountain Journal of Sciences, Vol. 5 (1999) 23-27

The Study of Electromagnetism-Like Mechanism Based Fuzzy Neural Network for Learning Fuzzy If-Then Rules

Peitsang Wu¹, Kung-Jiuan Yang², and Yung-Yao Hung¹

¹ Department of Industrial Engineering and Management
I-Shou University, Taiwan 840, R.O.C.
{pwu,d9320001}@isu.edu.tw

² Department of Information Management,
Fortune Institute of Technology, Taiwan 842, R.O.C.
kjyang@center.fjtc.edu.tw

Abstract. In this paper, a meta-heuristic algorithm (electromagnetism-like mechanism, EM) for fuzzy neural network training is introduced. Electromagnetism-like mechanism simulates the electromagnetism theory of physics by considering each sample point to be an electrical charge. The EM algorithm utilizes an attraction-repulsion mechanism to move the sample points towards the optimum. Besides, the electromagnetism-like mechanism is not easily falling into local optimum. Therefore, the purpose of this study is to use the electromagnetism-like mechanism to develop the fuzzy neural networks (EMFNN), and employ this EMFNN to train fuzzy if-then rules. According to the case, the EMFNN could successfully generalize new fuzzy if-then rules.

1 Introduction

Fuzzy neural networks (FNN), associates the fuzzy logic with neural networks, has been used to learn the fuzzy if-then rules. There are many literatures address the architectures of fuzzy neural networks [4], [5], [8], [9]. And each of them has different capability for problem solving. Since the experts' knowledge is quite subjective, the fuzzy logic attempts to capture the experts' knowledge. The fuzzy neural network is used to learn fuzzy if-then rules which can represent the qualitative factors.

Recently, the genetic algorithm combined with fuzzy neural network has been proposed in [2], [3], [6], [7], and the performances of genetic algorithm combined with fuzzy neural network were better than the conventional fuzzy neural network. Although the genetic algorithm is good for fuzzy neural network training the performances of other meta-heuristic algorithm such as Electromagnetism- like Mechanism (EM) for fuzzy neural network training is what we want to investigate.

Electromagnetism-like Mechanism (EM) is a meta-heuristic algorithm for global optimization, which was first proposed by Birbil and Fang in 2003 [1]. EM simulates the electromagnetism theory of physics by considering each sample point to be an electrical charge. Wu et al. [10] was the first to use the EM for training neural network with saving on the computation memories and time, and the results indicate that the EM performed much better than the genetic algorithm in find optimal solution globally. However, the electromagnetism-like mechanism for fuzzy neural network training hasn't yet investigated. Therefore, the authors are motivated to systematically study the work.

In this paper, the authors attempt to propose a fuzzy neural network that is able to learn the fuzzy IF- THEN rules and introduce a meta-heuristic algorithm (Electromagnetism-like Mechanism, EM) to develop an EM based fuzzy neural network (EMFNN).

2 Fuzzy Neural Networks

Ishibuchi et al. [4] proposed fuzzy neural networks (FNN) architecture with symmetric triangular fuzzy inputs, weights, and outputs. Kuo and Xue [8] replaced the triangular fuzzy numbers with asymmetric Gaussian functions since it can speed up the convergence. The input-output relation of the mentioned FNN is discussed in the following. First, the operations of fuzzy numbers are presented.

The proposed FNN learning algorithm is similar to EBP-type learning algorithm. Some assumptions should be clarified before discussing the algorithm: 1. Fuzzify a four layers feedforward neural network with n_I input units, n_H hidden units, and n_O output units (i.e. input vectors, target vectors connection weights and thresholds are fuzzified). 2. The input vectors are non-negative fuzzy numbers whose lower and upper bounds are larger than zero. 3. These fuzzy numbers are asymmetric Gaussian shaped fuzzy numbers.

The input-output relation of the proposed FNN is defined by the extension principle [8] and can be written as follows:

Input layer:

$$\tilde{O}_{pi}[\alpha] = \tilde{X}_{pi}[\alpha], \quad i=1, 2, \dots, n_I \quad (1)$$

Hidden layer:

$$\tilde{O}_{ph}[\alpha] = f(\widetilde{Net}_{ph}[\alpha]), \quad h=1, 2, \dots, n_H \quad (2)$$

$$\widetilde{Net}_{ph}[\alpha] = \sum_{i=1}^{n_I} \tilde{W}_{hi}[\alpha] \cdot \tilde{O}_{pi}[\alpha] + \tilde{\Theta}_h[\alpha] \quad (3)$$

Output layer:

$$\tilde{O}_{pk}[\alpha] = f(\widetilde{Net}_{pk}[\alpha]), \quad k=1, 2, \dots, n_O \quad (4)$$

$$\widetilde{Net}_{pk}[\alpha] = \sum_{h=1}^{n_H} \tilde{W}_{kh}[\alpha] \cdot \tilde{O}_{ph}[\alpha] + \tilde{\Theta}_k[\alpha] \quad (5)$$

The objective is to minimize the cost function defined as:

$$E_p = \sum_{\alpha} \sum_{k=1}^{n_O} \alpha (E_{k(\alpha)}^L + E_{k(\alpha)}^U) = \sum_{\alpha} E_{p(\alpha)}, \quad (6)$$

where

$$\sum_{\alpha} E_{p(\alpha)} = \sum_{k=1}^{n_O} \alpha (E_{k(\alpha)}^L + E_{k(\alpha)}^U), \quad (7)$$

$$E_{k(\alpha)}^L = \frac{1}{2} (T_{pk}[\alpha]^L - O_{pk}[\alpha]^L)^2, \quad (8)$$

$$E_{k(\alpha)}^U = \frac{1}{2} (T_{pk}[\alpha]^U - O_{pk}[\alpha]^U)^2, \quad (9)$$

where $E_{k(\alpha)}^L$ and $E_{k(\alpha)}^U$ can be viewed as the squared errors for the lower boundaries and the upper boundaries of the α -cut sets of a fuzzy outputs and fuzzy targets. Other α -cut sets of a fuzzy weight are independently modified to reduce $E_{p(\alpha)}$.

Otherwise, the fuzzy numbers after modifications are distorted. Therefore, each fuzzy weight is updated in a similar but still different way from the approach of [8]. That is, in the proposed FNN, the membership functions are asymmetric Gaussian functions (i.e. a general shape), which are represented as:

$$\tilde{A}(x) = \begin{cases} \exp\left(-\frac{1}{2}\left(\frac{x-\mu}{\sigma^L}\right)^2\right) & x < \mu, \\ 1, & x = \mu, \\ \exp\left(-\frac{1}{2}\left(\frac{x-\mu}{\sigma^R}\right)^2\right) & \text{otherwise.} \end{cases} \quad (10)$$

Thus, the asymmetric Gaussian fuzzy weights are specified by their three parameters (i.e., center right width and left width). The gradient search method is derived for each parameter. It is the amount of adjustment for each parameter using the cost function $E_{p(\alpha)}$ as follows:

$$\Delta\mu_{kh}(t) = -\eta \frac{\partial E_{p(\alpha)}}{\partial \mu_{kh}} + \beta \Delta\mu_{kh}(t-1), \quad (11)$$

$$\Delta\sigma^R_{kh}(t) = -\eta \frac{\partial E_{p(\alpha)}}{\partial \sigma^R_{kh}} + \beta \Delta\sigma^R_{kh}(t-1), \quad (12)$$

$$\Delta\sigma^L_{kh}(t) = -\eta \frac{\partial E_{p(\alpha)}}{\partial \sigma^L_{kh}} + \beta \Delta\sigma^L_{kh}(t-1). \quad (13)$$

A detail derivation of above equation was in [8].

3 Electromagnetism-Like Mechanism

In this section, a new heuristic algorithm of global optimization method will be introduced, which is named the Electromagnetism-like Mechanism (EM) [1]. The algorithm has a mechanism that encourages the points to converge to the highly attractive valleys, and contrarily, discourages the points to move further away from steeper hills. This idea is similar to the attraction–repulsion mechanism of the electromagnetism theory. In the approach, the charge of each point relates to the objective function value, which we are trying to optimize. The principle of superposition states that the electromagnetic force on a charged particle caused by any number of other particles can be calculated by adding together vectorially the forces from each of the other particles calculated separately. The points observing better objective values would signal the other points to converge to the global or local minimizes. In the algorithm, each sample point is treated like a charged particle. This charge basically determines the magnitude of attraction or repulsion of the point over the population, and attraction directs the points towards better regions, whereas repulsion allows particles to exploit the unvisited regions [1].

In the general scheme of EM is illustrated in Table 1.

In this algorithm, there are four procedures: “Initialization”, “Local search”, “Total force calculation”, and “Move along the total force”. “Initialization” is used to sample m points from the feasible region. A typical way for initialization is sampling the points from the feasible region uniformly. The next procedure, “Local search”, is used to search around the neighborhood information to get better solutions. The major procedures of the EM algorithm are the “Total force calculation” and “Move along the total force” procedures. The “Total force calculation” procedure is used for calculating the total force exerted on each point, whereas “Move along the total

force" procedure is used for moving the sample points along the direction of the total force [10].

Table 1. General scheme of EM.[1]

| Algorithm EM (m , MAXITER, LSITER, δ) |
|--|
| m : number of sample points |
| MAXITER: maximum number of iterations |
| LSITER: maximum number of local search iterations |
| δ : local search parameter, $\delta \in [0,1]$ |
| <ol style="list-style-type: none"> 1. Initialize() 2. iteration $\leftarrow 1$ 3. while (iteration < MAXITER) do 4. Local(LSITER, δ) 5. F \leftarrow CalcF() 6. Move(F) 7. iteration \leftarrow iteration +1 8. end_while |

By incorporating the electromagnetism-like mechanism, we now have our fuzzy neural network learning algorithm as following:

Step 1: Initialize the weights randomly through the EM, there are $3*n$ dimensional hyper-cube if the neural network with n fuzzy weights.

Step 2: Evaluating each sample point in the population in terms of objective value using E_p of fuzzy neural networks.

Step 3: If termination conditions are met, go to step 7.

Step 4: The procedure of local search is used to find a better point in the neighborhood. If the new point y observes a better point in fixed iterations, the sample point x^i is replaced by this new point y . And the neighborhood search ends. Hence the current best point is updated.

Step 5: This charge is evaluated by using the objective function value of the point, x^i , relative to the objective function value of the current best point. After determining the charge of each point on x^i , the total force F^i is calculated.

Step 6: After evaluating the total force F^i , the point is moved towards the direction of the force by a random step length. Return to step 2.

Step 7: Stop, return the best point and translate it into the fuzzy weights of FNN. This iterative process leads to the improved performance of candidate set of fuzzy weights.

Step 8: After the above procedures, the trained fuzzy weights is treated as the initial fuzzy weights for EMFNN training.

4 Case Study

In our study, we quote the training patterns form [6] for testing our proposed model. The data are collected form a nationally well-known CVS franchise company provides the daily sales data. Since the forecasting pattern is divided into two categories, general pattern and special pattern, the data collection is also comprised of two parts:

1. Time series data: The company provides the daily sales of 500c.c. papaya milk. The total number of the data points is 379. The sudden increase of sales indicates that the promotion is conducting. Totally there are five times of promotion. The time period lasts from 7/1/2004 to 7/14/2004. For the purpose of testing, these 379 data points are further divided into training set and testing set. The front one has 334 data points while the latter one having forty-five data points.
2. Expert questionnaire: To survey all the possible factors of promotion and their effects on the sales, this study employs fuzzy Delphi method. The questionnaire's setup is based on the company's practical requirements. Thus, some factors are included. The procedures are based on the modified fuzzy Delphi method.

After discussing with the company's senior managers, all the factors are divided into three dimensions. The first dimension represents the methods of promotion, while the types of advertising media are presented in the second dimension. The third dimension represents the competitors' actions. Table 2 presents the fuzzy number of each event from [6]. The network topology with three inputs (three dimensions) and one output that representing the promotion effect on sales is utilized for learning fuzzy IF-THEN rules. In the proposed fuzzy IF-THEN rules, the membership functions are asymmetric Gaussian functions.

Thus, totally there are only 42 ($3 \times 7 \times 2$) IF-THEN rules for training the EMFNN. The setup of the electromagnetism-like mechanism is as follows:

1. The number of sample points: 30.
2. Local search iterations (LS): 5 and 10.
3. Step length parameter (δ): 0.1 and 1.
4. The number of generations: 10.
5. The number of hidden nodes: 3, 4, and 5.

Table 2. The Fuzzy Number of Each Event [6]

| Factors | Events | $\sigma^L = \frac{l-\mu}{3}$ | μ | $\sigma^U = \frac{u-\mu}{3}$ |
|---------------------|------------------------------------|------------------------------|-------|------------------------------|
| Promotion methods | 10 dollars discount | 0.2000 | 8.600 | 0.2333 |
| | 5 dollars discount | 0.2333 | 4.900 | 0.3000 |
| | Buy 2 get 1 free | 0.2000 | 6.800 | 0.3000 |
| Advertising media | At night on TV | 0.2667 | 7.600 | 0.3000 |
| | At noon on TV | 0.1667 | 2.500 | 0.3333 |
| | In the evening on TV | 0.1333 | 3.100 | 0.4667 |
| | Radio | 0.2667 | 4.500 | 0.4000 |
| | Newspaper | 0.1667 | 3.800 | 0.5000 |
| | POP notice | 0.1000 | 6.500 | 0.4333 |
| | Poster | 0.2000 | 6.600 | 0.3000 |
| Competitor's action | Related products without promotion | 0.2000 | 7.600 | 0.4000 |
| | Related products with promotion | 0.1000 | 4.500 | 0.3333 |

Table 3 presents the computational results of EM. Basically, step length parameter (δ) equals to 1 can provide better results compared to those of 0.1. From EM, we can obtain 30 sets of initial weights. The best sets are used as the initial weights of FNN in order to find the final solution. Table 4 lists the final results.

Table 3. The results of EM

| Network Structure | LS | δ | Min_MSE |
|-------------------|----|----------|----------|
| 3-3-3-1 | 5 | 0.1 | 0.047619 |
| | 5 | 1 | 0.045739 |
| | 10 | 0.1 | 0.046947 |
| | 10 | 1 | 0.046005 |
| 3-4-4-1 | 5 | 0.1 | 0.046862 |
| | 5 | 1 | 0.046187 |
| | 10 | 0.1 | 0.047784 |
| | 10 | 1 | 0.046086 |
| 3-5-5-1 | 5 | 0.1 | 0.048948 |
| | 5 | 1 | 0.046422 |
| | 10 | 0.1 | 0.046635 |
| | 10 | 1 | 0.046620 |

5 Conclusion

This paper has studied a meta-heuristic algorithm, Electromagnetism-like Mechanism (EM) [1] for global optimization. The authors apply the electromagnetism-like mechanism on the fuzzy neural network training. This article also studied the architecture and learning algorithm of conventional fuzzy neural network. In order to evaluate the performance of EM for fuzzy neural network training, the authors have established a system for EMFNN by C++.

In this paper, an Electromagnetism-like Mechanism will be applied to generate the initial weights for FNN. This can prevent the network getting stuck to a local minimum. For our case, the step length parameter (d) is a main factor of EMFNN for decreasing the network error. The lower error will take place when the step length parameter equals to 1. The Computational Result of FNN is better when the learning rate and momentum are both set to be 0.7. Besides, it should be noticed that if the sample points, the number of local search iterations and the range of weights increase, the search time would also increase.

In future works, more real world problems could be applied for EMFNN training, and the parameter design for performance measures could be carried out carefully. Applying the EM for other architectures of fuzzy neural network training could also be done. And the comparison of EMFNN and other optimization methods based fuzzy neural network could be implemented.

Acknowledgment

This research was supported by the NSC of R. O. C. (NSC 92- 2213-E-214-023).

References

1. Birbil, S. I., Fang, S. C.: Electromagnetism-like Mechanism for Global Optimization. Journal of Global Optimization 25 (2003) 263-282.
2. Buckley, J.J.; Reilly, K.D.; Penmetcha, K.V.: Backpropagation and Genetic Algorithms for Training Fuzzy Neural Nets. IEEE International Conference on Fuzzy Systems 1 (1996) 2-6.

3. Hsiao, S. W., Tsai, H. C.: Applying a hybrid approach based on fuzzy neural network and genetic algorithm to product form design. *International Journal of Industrial Ergonomics* 35 (5) (2005) 411-428.
4. Ishibuchi, H., Kwon, K., Tanaka, H.: A Learning Algorithm of Fuzzy Neural Networks with Triangular Fuzzy Weights. *Fuzzy Sets and Systems* 71 (1995) 277-293.
5. Ishibuchi, H., Manabu N.: Numerical analysis of the learning of fuzzified neural networks from fuzzy if-then rules. *Fuzzy Sets and Systems* 120 (2001) 281-307.
6. Kuo, R. J., Wu, P., Wang, C. P.: Fuzzy Neural Networks for Learning Fuzzy If-Then Rules. *Applied Artificial Intelligence* 14 (2000) 539-563.
7. Kuo, R. J., Wu, P., and Wang, C. P.: An Intelligent Sales Forecasting System through Integration of Artificial Neural Networks and Fuzzy Neural Networks with Fuzzy Weight Elimination. *Neural Networks* 15 (2002) 909-925.
8. Kuo, R. J., and Xue, K. C.: Fuzzy Neural Networks with Application to Sales Forecasting. *Fuzzy Sets and Systems* 108 (1999) 123-143.
9. Liu, P., Li, H.: Approximation analysis of feedforward regular fuzzy neural network with two hidden layers. *Fuzzy Sets and Systems* 150 (2) (2005) 373-396.
10. Wu, P., Yang, W. H. and Wei, N. C.: An Electromagnetism Algorithm of Neural Network Analysis -An Application to Textile Retail Operation. *Journal of the Chinese Institute of Industrial Engineers* 21(1) (2004) 59-67.

Statistical Data Analysis for Software Metrics Validation

Ming-Chang Lee

Department of Information Management, Fooyin University, Taiwan
Sc114@mail.fy.edu.tw

Abstract. A metrics validation process is defined that integrates quality factors and quality functions. It proposes a comprehensive metric validation methodology that has validity criteria, which support the quality function and activities conducted by software organization for the purpose of achieving project quality goals. In this paper, valid metrics are assessing differences in quality, assessing relative quality, control quality (discrimination between high quality and low quality), control quality (tracking changes), and prediction quality. The criteria are defined and illustrated by association, consistency, discriminative power, tracking. Statistical methods such as Mann-Whitency, Wilcoxon Rank Sum test, Wald-Wolfowitz, and Discriminate Analysis play an important role in evaluating metrics against the validity criterion.

Keywords: Metrics validation methodology, quality functions, validity criteria, nonparametric statistical methods

1 Introduction

Software metrics are tressed as part of an engineering discipline – metrics should be evaluated to determine whether they measure what they purpose to measure prior to use them. There are fours metrics methodologies that have been validation analyses performance on specific metrics or metric system. Among these validations are the following: Function points are derived using an empirical relationship based on countable (direct) measures of software information domain and assessments of software complexity [1]. The function is interpreted to be probability that a defect is detected by time γ . $R(\gamma)$ is the probability that is no failure during the time interval of length of γ , where $R(\gamma) = 1 - F(\gamma)$ [2]. Halstead uses the primitive measure to develop expressions for the overall program length; potential minimum volume for an algorithm; the actual volume (number of bits required to specify); the program level (a measure of software complexity); language level (a constant for a given language); and other features such as development effort, development time, and even the projected number of faults in the software ([8], [11]). Evaluation of metrics against syntactic complexity is properties [11].

In this paper, software measurements have the following characteristics: (1) it has mathematically defined criteria, which can be applied to measure software quality. (2)The criteria are: consistency, association, discriminative power and Tracking [3]. It is developed from the point of view of the metric user who has requirements for assessing, controlling, and predicting quality [4]. It defines a metrics validation process that integrates quality factor, metric, and functions [5].

2 Quality Factor, Quality Metric and Validated Metric

2.1 Quality Factor

A quality factor F is an attribute of software that contributes to its quality [6], where software quality is defined as the degree to which software processes a desired combination of attributes [3]. For example portability is a quality factors. A factor can have values such as the errors counts F_1, F_2, \dots, F_n in a set of software quality components. We define F to be a type of metric that provides a direct measure of software quality (quality assessment, quality control and quality prediction) [3].

2.2 Quality Metric

A quality factor M (e.g., cyclomatic complexity) is a function whose inputs are software data (elementary software measurements). Cyclomatic complexity $M = e - n + p$ where e is the number of edge, n is the number of nodes, and p is the number of connected components in the flow graph. M can be interpreted as the degree to which software possesses a given attribute that may affect its quality (e.g., relativity) [10]. It is known that M to be an indirect measure of software quality [1]. It is important to recognize that in general there can be many-to-many relationships, one-to many or one-one relationship between F and M [6].

2.3 Validated Metric (Measured Metrics)

Validated Metric is one whose values have been shown to be statistically associated with corresponding factor values. For example, on Discriminative power factor with quality controlling use Mann-Whitney statistically method comparison of average ranks of two group of components.

3 Validity Criteria with Statistical Methodology

Each validity criteria support one or more of the quality functions assessment, control and prediction, which were described above. The validity criteria contain association, consistency, discriminative power, tracking, and repeatability.

3.1 Association

This criterion assesses whether there is a sufficient linear association between F and M to warrant using M (dependent variable) as an indirect measure of F (independent variable). For example, a study was determined the relationship between the unique variable count (vars) and total program length (N) for a sample set of C++ program. Furthermore, the relationship appears to be linear; the formula $N = a + b \text{ Vars}$. The appropriateness of the model or the strength of the relationship can then be analyzed using other quantitative methods.

(1) Correlation Coefficient

The strength of a relationship between two sets of measures can often be evaluated using correlation coefficient. The Pearson product-moment correlation is often used to

assess the strength of the linear relationship between two sets of measures [4]. The symbol of the correlation coefficient is r , whereas the symbol for the corresponding parameter of the population is ρ . To determine the significance of correlation coefficient, the null hypothesis is general that there is no correlation between the two populations: $H_0: \rho = 0$. The alternative is then $H_1: \rho \neq 0$

The correlation coefficient r between F and M must be exceed a specified threshold, or

$$R > \beta_\alpha, \text{ with specified } \alpha \quad (1)$$

(2) Determination Coefficient

The measure R^2 is called determination coefficient. This may be interpreted as the percentage of variance in one measure accounted for by the other. R^2 must exceed a specified threshold, or

$$R^2 > \beta_\alpha, \text{ with specified } \alpha. \quad (2)$$

(3) Factor Analysis

If it employs correlation to examine the relationship between several independent variables and a dependent variable, it usually finds that some of the independent variables are strongly related to each other (Conte, 1986). For example, let us suppose that data has been gathered about the programming process at a particular company in which we have information on a dependent variable (such as programming time) and some ten independent variables, which for this example will call simply x_1, x_2, \dots, x_{10} . We may decide to perform regression analysis, which may produce a regression equation involving all ten independent variable.

3.2 Consistency

This criterion assesses whether there is sufficient consistency between the ranks of F and the rank of M to warrant using an indirect measure of F [4].

(1) Spearman Rank Correlation Coefficient [9]

When data can be ranked in ordinal scale, a pearman rank correction is often used. The symbol for this correction coefficient is r_s and is defined as follows.

$$r_s = 1 - \frac{6}{(n^3 - n)} \sum_{i=1}^n d_i^2 \quad (3)$$

Where the symbol n represents the sample size and d_i represents the difference in rank of the i^{th} pair of data. It is also possible to test whether the relationship r_s is significant.

The null hypothesis is $H_0: \rho_s = 0$ (no population correlation between ranks)

The alternative hypothesis is then $H_1: \rho_s \neq 0$ (population correlation between ranks)

The r_s value must exceed a specified threshold, or

$$r_s > r_\alpha, \text{ with significance level } \alpha. \quad (4)$$

We can conclude that the performance for two groups is different, with H_0 rejected at level α .

(2) The nonparametric Mann-Whitney U test

Mann-Whitney U test can be used to determine whether the two samples are from identical populations [4]. The U test is the most useful alternative to the parametric t test. After the ranks are established, compute $U = \min(U_1, U_2)$ where

$$\begin{aligned} U_1 &= n_1 n_2 + \frac{n_1(n_1+1)}{2} - R_1 \\ U_2 &= n_1 n_2 + \frac{n_2(n_2+1)}{2} - R_2 \end{aligned} \quad (5)$$

The null hypothesis is H_0 : The performance for two groups is same

The alternative hypothesis is then H_1 : The performance for two groups is different

The U value must exceed a specified threshold, or

$$U < U_\alpha \text{ with significance level } \alpha. \quad (6)$$

We can conclude that the performance for two groups is different, with H_0 rejected at level α .

3.3 Discriminative Power

Software metrics research may yield data that one can only say comes from a nominal scale. Examples of nominal scale data are presence or absence of defects in software modules, the use or non-use of structured programming techniques in software development, or the use of one of the language VB, C++, or VB for implementation. It is still possible to perform some statistical tests even such nominal data, the best known of which is Wilcoxon Rank Sum Test.

3.4 Tracking

This criterion assesses whether M is capable of tracking changes in F (e.g., as a result of design changes) to a sufficient degree to warrant using M as an indirect measure of F . If M_i' is validated, then $M_i'(T_1), M_i'(T_2), \dots, M_i'(T_m)$ of component i measured at time T_1, T_2, \dots, T_m . For example, if complexity M_i' is valid for tracking error count F_i' . We use an appropriate statistical method (e.g., Wald-Wolfowitz Runs Test).

3.4.1 Wald-Wolfowitz Runs Test

The data consists of two samples, mutually independent of each other. One sample M_1, M_2, \dots, M_m is of size m and the other F_1, F_2, \dots, F_n is of size of n [5].

H_0 : M 's is capable of tracking in F' , that is the M 's and the F ' have identical distribution function. H_1 : M 's is not capable of tracking in F' .

The W value must exceed a specified threshold, or $W > W_\alpha$ with significance level α , or

$$W > W_{\frac{\alpha}{2}} \quad (7)$$

Where

$$W_{\frac{\alpha}{2}} = \frac{2nm}{m+n} + 1 + Z_{\frac{\alpha}{2}} \sqrt{\frac{2mn(2mn - m - n)}{(m+n)^2(m+n-1)}} \quad (8)$$

W is the total number of runs

4 Nonparametric Statistical Methods for Metrics Validation

Nonparametric statistical methods are used to support metrics validation, because these methods have important advantages over parametric methods. Nonparametric metric methods allow us to develop very useful order relations concerning the relative quality and control quality. The validity criteria, which use nonparametric methods, are shown in Table1.

Table 1. The validity criteria properties and nonparametric methods

| Criterion | Scale | Nonparametric methods | Properties |
|----------------------|---------|---|----------------|
| Consistency | Ordinal | Spearman rank correlation coefficient Man-Whitney U test | Higher / Lower |
| Discriminative power | Nominal | Wilcoxon Rank Sum Test | High / Low |
| Tracking | Nominal | Wald-wolfowitz Runs Test | Increment |

4.1 Spearman Rank Correlation Coefficient

For example, a study was made to determine the relationship between the unique variable count (V) and total program length (N) for a sample set of Pascal program.

The sum of d^2 is 21.9. Using equation (3), we have $r_s = 0.9$, $n = 24$. From Critical values for the Spearman Rank Correlation Coefficient table, If $\alpha = 0.02$, we calculate $\alpha/2 = 0.01$, $r_{0.01} = 0.485$, $r_s (= 0.9) > (r_{0.01} = 0.485)$, we will reject H_0 . Therefore, we can conclude that there is a strong linear relationship between the ranks of variable count (V) and total program length (N), with H_0 rejected at the 0.05 levels.

4.2 The Nonparametric Mann-Whitney U Test

For example, a group of subjects had been instructed to solve the same problem (Sort Experiment) in C++, while another group of subjects had been instructed to solve the same problem in Pascal. Table 2 shows the ranks programming times for the Sorting Experiment. Using equation (5), in our example, $R_1 = 183.5$ (C++) and $R_2 = 281.5$ (PASCAL). Consequently, $U_1 = 161.5$ and $U_2 = 63.5$, leading to $U = 63.5$. From Critical values for the Critical Values for the Mann-Whitney table, If $\alpha = 0.05$, we calculate $U_{0.05} = 64$, $U = 63.5 < (U_{0.05} = 64)$, we will reject H_0 . Therefore, we can conclude the performance for the two languages are different, with H_0 rejected at the 0.05 levels.

4.3 Wilcoxon Rank Sum Test

We suppose a software engineer wants to compare executive time on FORTRAN language with PASCAL language program. Table 3 shows the executive time for each program are measured.

Table 2. Shows the ranks programming times for the Sorting Experiment

| Subject | C++ | Rank | PASCAL | Rank | Subject | C++ | Rank | PASCAL | Rank |
|---------|-----|------|--------|--------|---------|-----|------|--------|------|
| 1 | 12 | 1 | 20 | 5 | 9 | 28 | 13 | 39 | 24 |
| 2 | 13 | 2 | 21 | 6.5 | 10 | 30 | 14 | 40 | 26.5 |
| 3 | 14 | 3 | 25 | 8.510 | 11 | 32 | 16 | 41 | 26.5 |
| 4 | 19 | 4 | 26 | 15 | 12 | 34 | 17 | 42 | 26.5 |
| 5 | 21 | 6.5 | 31 | 1820.5 | 13 | 36 | 19 | 42 | 29 |
| 6 | 25 | 8.5 | 35 | 20.5 | 14 | 42 | 26.5 | 42 | |
| 7 | 27 | 11.5 | 38 | 22 | 15 | 46 | 30 | 44 | |
| 8 | 27 | 11.5 | 38 | 23 | | | | | |

Table 3. The executive time for each program are measured

| FORTRAN | Rank | PASCAL | Rank | FORTRAN | Rank | PASCAL | Rank |
|---------|------|--------|------|---------|------|--------|------|
| 1.96 | 4 | 2.11 | 6 | 1.62 | 1 | 2.50 | 10 |
| 2.24 | 7 | 2.43 | 9 | 1.93 | 3 | 2.84 | 12 |
| 1.71 | 2 | 2.07 | 5 | | | 2.88 | 13 |
| 2.42 | 8 | 2.71 | 11 | | | | |

H_0 : The two populations of executive times corresponding to A (FORTRAN) and B (PASCAL) have identical probability distribution

H_1 : The probability distribution for population A is shifted to the right or left of the probability distribution corresponding to for B.

Test statistic: The test statistic is T_A , the rank sum of task A's executive time.

Rejection region: the rejection region corresponding to $\alpha = 0.05$. We will reject H_0 for

$T_A \leq T_L$ or $T_A \geq T_U$. From table 3, we calculate $T_A = 25$. From the table (Critical Values of T_L and T_U for the Wilcoxon Rank Sum Test) for the chosen two-tailed value α , $T_L = 28$ and $T_U = 56$. Since $T_A \leq (T_L =) 28$ or $T_A \geq (T_U =) 56$. Thus we will reject H_0 .

4.4 Wald-Wolfowitz Runs Test

For example, a group of subjects had been instructed to solve the same problem (Sort Experiment) in C++, while another group of subjects had been instructed to solve the same problem in Pascal. For sample pieces of executive time were collected in A (Pascal), and five sample pieces of executive time were collected in B (C++). Table 4 shows origin of piece and ranks.

Table 4. Origin of piece execution time and ranks

| | | | | | | | | | |
|--------------------------------|---|---|---|---|---|---|---|---|---|
| Origin of piece execution time | A | A | A | B | A | B | B | B | B |
| Rank | 1 | 2 | 3 | 4 | 5 | 6 | 7 | 8 | 9 |

The null hypothesis to be test is H_0 : A and B have identical distribution function, (Pascal is capable of tracking in C++). The alternative hypothesis is then H_1 : A and B have not identical distribution function. Under $n_1 = 4$, $n_2 = 5$, $\alpha = 0.05$, using equation (7) and (8), we have $W = 4$.

$W_{\frac{\alpha}{2}} = 4$. We may accept the null hypothesis at a α level of 0.05 and conclude that Pascal is capable of tracking in C++.

5 Conclusion

We described and illustrated a comprehensive metrics validation methodology that has validity criteria, which support the quality functions of assess relative quality, control quality (discriminate between high and low), control quality (tracking changes), and predict quality. The criteria are defined and illustrated: association, consistency, discriminative power, tracking. We indicate why parametric or nonparametric statistical methods are applicable to and compatible with the validity criteria. Statistical method such as Mann-Whitency, Wilcoxon Rank Sum test, Wald - Wolfowitz, and Discriminate Analysis play an important role in evaluating metrics against the validity criterion.

References

1. J. Albrecht, and J. E., Gaffney: Software function, source lines of code, and development error prediction: a software science validation”, IEEE trans. Software Engineering, Nov, 639-648, 1983.
2. V. R. Basili, R. W Selbt, and T. Y., Phillips, Metric analysis and data validation across Fortran projects, IEEE trans. Software Engineering, Nov, pp. 652-663,1983.
3. N. E. Bush and N. E. Fenton,: Software Measurement: A conceptual Framework, Journal system Software, Vol. 12, pp.223-231, 1990.
4. S. D. Conte, H. E. Dunsmore, and V. Y. Shen, Software Engineering Metrics and Models, The Benjamin / Cmming publishing, C. Inc., 1986.
5. W. J., Conover, Practical Nonparametric Statistics, Macmillan Publishing Company, 1992.
6. Deutsch, M. S. and Wills, R. R.,: Software Quality Engineering: A total technical and management approach, Prentice – Hall, Inc., Maxwell Macmillan Publishers, 1988.
7. R. A. Fenton,,,: Software Measurement: Theory, Tools and Validation, Software Engineering Journal, Vol 5 (1), 1990.
8. Fitzsimmons and T. Love, A review and Evaluation of Software Science, ACM Computing Surveys, vol. 10, no. 1, March, pp. 3-18, 1978.
9. R. V., Hogg and J. Ledolter, Applied Statistics for Engineers and Physical Scientists, Macmillan Publishing Company, 1992.
10. Porter, and Seiby, R. W., Empirically guided software development using metric-based classification tress, IEEE Software Eng., vol.7, Mar., pp. 46-54, 1990.
11. E. J Weyuker, Evaluating software complexity measures, IEEE Software Eng., vol. 14, Sept., pp.1357-1365, 1998.

A Multi-stage Fuzzy-Grey Approach to Analyzing Software Development Cost

Tony C.K. Huang¹, Gwo-Jen Hwang², and Judy C.R. Tseng³

¹ Department of Information Management, National Central University
Chung-Li 320, Taiwan, ROC.
ckhuang@mgt.ncu.edu.tw

² Department of Information and Learning Technology, National University of Tainan
Tainan, Taiwan 700, R.O.C.
gjhwang@mail.nutn.edu.tw

³ Department of Computer Science and Information Engineering, Chung Hua University
Hsinchu, 300, Taiwan, R.O.C.
judycrt@chu.edu.tw

Abstract. Analysis of software development cost is an important issue for both the academic and the commercial circles. There have been many methods proposed to analyze benefits and costs of software development. However, in practical applications, these methods are usually not applicable owing to various unpredictable factors, such as depression, which may affect the budget of software development, the changes of computer techniques, which may affect the cost of software development, and the adoption of different management concept, which may affect the enterprise's willingness of investing in software development. On the other hand, it is hoped that software development cost could be controlled appropriately while considering multiple requirements. In this paper, we proposed a Multi-Stage Fuzzy-Grey (MSFG) method to cope with these problems. A case study for the development of an e-training system is also given to demonstrate the benefits of our approach.

1 Introduction

Considerable research attention is now directed at gaining a better understanding of the software development process as well as constructing and evaluating software development cost analysis tools (Kemerer 1987). Several aspects need to be considered in software engineering, including software project management, software quality control, software configuration management, and assessment for cost and time of software development (Pressman 2001).

Among these aspects, software development cost analysis is the most critical challenge for most information system (IS) managers. Since the early 1950's, many researchers have proposed algorithmic models for measuring software development costs (Abdel-Hamid 1990). Constructive Cost Model (COCOMO) (Boehm 1981) and function point (FP) (Albrecht 1979) are two popular methods for software development cost analysis. These methods and tools have been applied practically to the planning and control of software projects (Kemerer 1987, 1993). Software development cost includes labor and capital costs, code and documentation costs, develop-

ment and maintenance cost, or other distributions of cost by phase or activity (Boehm 1988). Not only over- but also under-analysis may result in opportunities lost, non-productive projects, low quality software, less profitable products, waste of resources, increased cost, and even break-down of the IS project in mid-stream.

In this paper, we propose a Multi-Stage Fuzzy-Grey (MSFG) approach to cope with the software development problems. In our approach, fuzzy (Feng and Xu 1999) and grey (Deng 1989) theories are employed to assist the domain experts to make decisions for each software development phase. Experimental results showed that nearly 20 % cost could be reduced while all of the software requirements were completely met by applying our approach.

2 Multi-stage Approach to Software Development Cost Analysis

Figure 1 illustrates the flow chart of our approach, which is initiated by dividing the IS functions into several disjoint components by applying the UML (Fowler 1999) tool with CORBA (Mowbray and Malveau 1997) standard. Consequently, relevant historical data are collected from other enterprises or software suppliers, which are very useful for estimating the possible range of cost for the entire project. In this step, fuzzy technology is employed to estimate the cost range, which is one of the important factors for deciding whether the information system should be outsourcing.

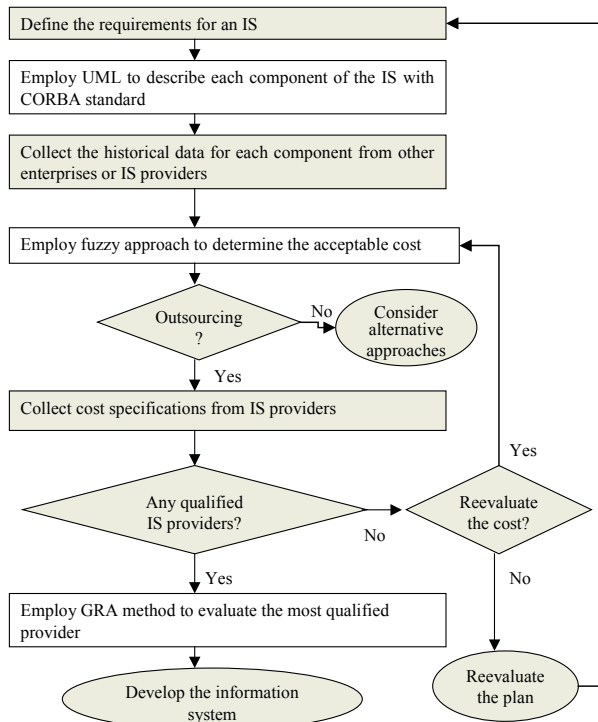
Outsourcing often means that an organization trusts all the activities associated with its information systems, including development of new systems, to another company. Lacity et al. (1996) has proposed a method to determine whether outsourcing or in-house development should be adopted for each component of a software system. If the company decides to outsource the information system to some information system provider, the Grey Relational Analysis (GRA) method is then employed to choose the most qualified provider. If no qualified provider can be found, the estimated cost and the proposed requirements have to be re-evaluated until a satisfactory system development solution is reached.

3 Fuzzy Cost Evaluation Model

Once the requirements can be clearly described, the cost of each component of the software system can be estimated and evaluated such that the best development strategy can be proposed to meet both the functional requirements and the economical consideration. Our Fuzzy Cost Evaluation Model consists of the following six steps:

Step 1: Collect the historical data of software development costs from other enterprises or software providers

To demonstrate the benefits of applying our approach, we collected historical data of software development costs from 20 enterprises located in Taiwan, including Internet content providers, e-training companies, electronic device companies, and Internet service providers. Those historical data are illustrated in Table 1, where A, B... T represent the enterprises who provide historical software development data, and the target enterprise who is planning to develop a new software is represented as Z.

**Fig. 1.** MSFG flow chart**Table 1.** Historical data of software development costs provided by twenty enterprises

| Enterprise | Cost | Enterprise | Cost | Enterprise | Cost | Enterprise | Cost |
|------------|-------|------------|-------|------------|-------|------------|-------|
| A | 3,776 | F | 4,535 | K | 4,413 | P | 5,237 |
| B | 4,258 | G | 4,629 | L | 4,315 | Q | 5,378 |
| C | 4,383 | H | 4,804 | M | 4,318 | R | 5,539 |
| D | 4,540 | I | 4,715 | N | 4,553 | S | 5,491 |
| E | 4,526 | J | 4,475 | O | 4,825 | T | 5,368 |

Step 2: Define the universe of discourse

By analyzing the historical data of software development costs, the maximum and minimum costs can be obtained. Assume that the maximum cost is D_{max} and the minimum cost is D_{min} . By defining the universe of discourse U to represent the acceptable cost range, we have $U=[D_{min}-D_1, D_{max}+D_2]$, where D_1 and D_2 are the revision values for D_{min} and D_{max} , respectively. In the example given in Table 1, we have $D_{min}=3776$ and $D_{max}=5539$. To adjust boundaries of the universe of discourse to fit the partition with length 300, i.e., $U=[3600, 5700]$, we have $D_1=176$ and $D_2=161$.

Step 3: Determining the number of fuzzy partitions

By assuming that the length of each cost interval is 300, seven cost intervals $u_1, u_2, u_3, u_4, u_5, u_6$ and u_7 could be determined, where $u_1=[3600, 3900]$, $u_2=[3900, 4200]$, $u_3=[4200, 4500]$, $u_4=[4500, 4,800]$, $u_5=[4800, 5100]$, $u_6=[5100, 5400]$, $u_7=[5400, 5700]$.

Step 4: Defining fuzzy sets to describe cost intervals

A linguistic variable A_i ($i=1, 2, \dots, n$) is used to describe the status of each cost interval. In the previous case, we have $n = 7$, and the fuzzy linguistic terms are A_1 = “Very Low”, A_2 = “Low”, A_3 = “More or less Low”, A_4 = “Average”, A_5 = “More or less High”, A_6 = “High” and A_7 = “Very High”, which are defined to describe $u_1, u_2, u_3, \dots, u_7$, respectively. Without loss of generality, we have Very Low: $A_1=\{u_1/1, u_2/0.5, u_3/0, u_4/0, u_5/0, u_6/0, u_7/0\}$, Low: $A_2=\{u_1/0.5, u_2/1, u_3/0.5, u_4/0, u_5/0, u_6/0, u_7/0\}$, More or less Low: $A_3=\{u_1/0, u_2/0.5, u_3/1, u_4/0.5, u_5/0, u_6/0, u_7/0\}$, Average: $A_4=\{u_1/0, u_2/0, u_3/0.5, u_4/1, u_5/0.5, u_6/0, u_7/0\}$, More or less High: $A_5=\{u_1/0, u_2/0, u_3/0, u_4/0.5, u_5/1, u_6/0.5, u_7/0\}$, High: $A_6=\{u_1/0, u_2/0, u_3/0, u_4/0, u_5/0.5, u_6/1, u_7/0.5\}$ and Very High: $A_7=\{u_1/0, u_2/0, u_3/0, u_4/0, u_5/0, u_6/0.5, u_7/1\}$.

Step 5: Constructing the vector

In this step, a vector is constructed for each software component to describe the vague acceptance degrees of the cost intervals. A fuzzy subset B of a universe of discourse X is defined as $B = \{(\mu_B(x), x) | x \in X\}$, where $\mu_B: X \rightarrow [0,1]$ is the membership function of fuzzy subset B and $\mu_B(x)$ is the degree of membership for x to belong to B . Assuming that $B=\{u_1/0, u_2/0.1, u_3/0.2, u_4/0.6, u_5/0.1, u_6/0, u_7/0\}$, which implies the degree of membership is 0, 0.1, 0.2, 0.6, 0.1, 0 and 0 if the development cost is in u_1 [3600, 3900], u_2 [3900, 4200], u_3 [4200, 4500], u_4 [4500, 4800], u_5 [4800, 5100], u_6 [5100, 5400] and u_7 [5400, 5700], respectively.

Step 6: Determining the final cost interval

The Max-Min composition operation is employed to determine the most reasonable cost interval of a component for enterprise Z:

$$Y = [0 \ 0.1 \ 0.2 \ 0.6 \ 0.1 \ 0 \ 0] \circ \begin{bmatrix} 1 & 0.5 & 0 & 0 & 0 & 0 & 0 \\ 0.5 & 1 & 0.5 & 0 & 0 & 0 & 0 \\ 0 & 0.5 & 1 & 0.5 & 0 & 0 & 0 \\ 0 & 0 & 0.5 & 1 & 0.5 & 0 & 0 \\ 0 & 0 & 0 & 0.5 & 1 & 0.5 & 0 \\ 0 & 0 & 0 & 0 & 0.5 & 1 & 0.5 \\ 0 & 0 & 0 & 0 & 0 & 0.5 & 1 \end{bmatrix} = [0.1 \ 0.2 \ 0.5 \ 0.6 \ 0.5 \ 0.1 \ 0]$$

The maximum value in Y is u_4 , which implies that the most feasible interval of the software development cost for enterprise Z is between 4500 and 4800 dollars.

4 GRA Approach for Software Vender Selection

A software provider can be one of the candidates if the proposed price conforms to the acceptable cost interval. A group of decision makers is then responsible for selecting a best-fit software provider from those candidates. Table 2 shows the GRA decision table for the e-training case study, where criteria C_1, C_2, \dots, C_{11} denote “Stability”, “Functionality”, “Usability”, “Feasibility”, “Maintainability”, “Performance”, “Documentation”, “Correctness”, “Sharable Requirement”, “Security” and “Price”, respectively; P001, P002, ..., P005 represent five software providers; the integer below each criterion represents the weight of that criterion.

Table 2. The GRA decision table for selecting the software providers

| | C ₁ | C ₂ | C ₃ | C ₄ | C ₅ | C ₆ | C ₇ | C ₈ | C ₉ | C ₁₀ | C ₁₁ |
|------|----------------|----------------|----------------|----------------|----------------|----------------|----------------|----------------|----------------|-----------------|------------------|
| | 4 | 1 | 1 | 1 | 1 | 2 | 1 | 3 | 3 | 2 | 1 |
| P001 | Low | 10 | Easy | 2 | 5 | Very Good | Clear | Bad | 0.4 | 0.6 | Very Satisfied |
| P002 | Very High | 4 | Not Easy | 3 | 5 | Good | Neutral | Good | 0.2 | 0.8 | Satisfied |
| P003 | Mid | 8 | Very Easy | 3 | 4 | Neutral | Very Clear | Neutral | 0.8 | 0.4 | Very Unsatisfied |
| P004 | High | 6 | Easy | 1 | 4 | Very Good | Neutral | Very Good | 0.2 | 0.2 | Very Unsatisfied |
| P005 | Low | 13 | Easy | 2 | 2 | Neutral | Neutral | Neutral | 1.0 | 0.6 | Satisfied |

The decision-making process of applying GRA is given as follows:

(1) Convert original data to numeric values (as illustrated in Table 3).

Table 3. Illustrative example of a converted GRA decision table

| | C ₁ | C ₂ | C ₃ | C ₄ | C ₅ | C ₆ | C ₇ | C ₈ | C ₉ | C ₁₀ | C ₁₁ |
|------|----------------|----------------|----------------|----------------|----------------|----------------|----------------|----------------|----------------|-----------------|-----------------|
| | 4 | 1 | 1 | 1 | 1 | 2 | 1 | 3 | 3 | 2 | 1 |
| P001 | 0.25 | 10 | 0.66 | 2 | 5 | 1.0 | 0.75 | 1.0 | 0.4 | 0.6 | 4 |
| P002 | 1.0 | 4 | 0.33 | 3 | 5 | 0.75 | 0.5 | 3.5 | 0.2 | 0.8 | 2 |
| P003 | 0.5 | 8 | 1.0 | 3 | 4 | 0.5 | 1.0 | 2.0 | 0.8 | 0.4 | 1 |
| P004 | 0.75 | 6 | 0.66 | 1 | 4 | 1.0 | 0.5 | 5.0 | 0.2 | 0.2 | 1 |
| P005 | 0.25 | 13 | 0.66 | 2 | 2 | 0.5 | 0.5 | 2.0 | 1.0 | 0.6 | 2 |

(2) Find the maximum value for each criterion in the decision table (see Table 4).

Table 4. Maximum value of each criterion

| Criteria for software components | C ₁ | C ₂ | C ₃ | C ₄ | C ₅ | C ₆ | C ₇ | C ₈ | C ₉ | C ₁₀ | C ₁₁ |
|----------------------------------|----------------|----------------|----------------|----------------|----------------|----------------|----------------|----------------|----------------|-----------------|-----------------|
| The maximum value | 1.0 | 13 | 1.0 | 3 | 5 | 1.0 | 1.0 | 5.0 | 1.0 | 0.8 | 4 |

(3) Normalize the values of each criterion by dividing the values by the maximum value in the same column (as illustrated in Table 5).

Table 5. Normalized GRA decision table

| | C ₁ | C ₂ | C ₃ | C ₄ | C ₅ | C ₆ | C ₇ | C ₈ | C ₉ | C ₁₀ | C ₁₁ |
|-------------|----------------|----------------|----------------|----------------|----------------|----------------|----------------|----------------|----------------|-----------------|-----------------|
| | 4 | 1 | 1 | 1 | 1 | 2 | 1 | 3 | 3 | 2 | 1 |
| $\chi_0(k)$ | 1.0 | 1.0 | 1.0 | 1.0 | 1.0 | 1.0 | 1.0 | 1.0 | 1.0 | 1.0 | 1.0 |
| P001 | $\chi_1(k)$ | 0.25 | 0.77 | 0.66 | 0.67 | 1.0 | 1.0 | 0.75 | 0.2 | 0.4 | 0.75 |
| P002 | $\chi_2(k)$ | 1.0 | 0.31 | 0.33 | 1.0 | 1.0 | 0.75 | 0.5 | 0.7 | 0.2 | 1.0 |
| P003 | $\chi_3(k)$ | 0.5 | 0.62 | 1.0 | 1.0 | 0.8 | 0.5 | 1.0 | 0.4 | 0.8 | 0.5 |
| P004 | $\chi_4(k)$ | 0.75 | 0.46 | 0.66 | 0.33 | 0.8 | 1.0 | 0.5 | 1.0 | 0.2 | 0.25 |
| P005 | $\chi_5(k)$ | 0.25 | 1.0 | 0.66 | 0.67 | 0.4 | 0.5 | 0.5 | 0.4 | 1.0 | 0.75 |

(4) Compute the difference of the series by $\Delta_{ij}(k)=\|\chi_0(k)-\chi_i(k)\|$, where $i=1, 2, \dots, 5$ and $k=1, 2, \dots, 11$. That is, $\Delta_{01}=(0.75, 0.23, 0.34, 0.33, 0, 0, 0.25, 0.8, 0.6, 0.25, 0, 0)$, $\Delta_{02}=(0, 0.69, 0.67, 0, 0, 0.25, 0.5, 0.3, 0.8, 0, 0.5)$, $\Delta_{03}=(0.5, 0.38, 0, 0, 0.2, 0.5, 0, 0.6, 0.2, 0.5, 0.75)$, $\Delta_{04}=(0.25, 0.54, 0.34, 0.67, 0.2, 0, 0.5, 0, 0.8, 0.75, 0.75)$ and $\Delta_{05}=(0.75, 0, 0.34, 0.33, 0.6, 0.5, 0.5, 0.6, 0, 0.25, 0.5)$.

- (5) Compute the maximum difference $\text{Max} \{ \text{Max}_i (\|\chi_0(k)-\chi_i(k)\|) \}$. That is, $\text{Max} \|\chi_0(k)-\chi_1(k)\| = \Delta_{01}(8) = 0.8$, $\text{Max} \|\chi_0(k)-\chi_2(k)\| = \Delta_{02}(9) = 0.8$, $\text{Max} \|\chi_0(k)-\chi_3(k)\| = \Delta_{03}(11) = 0.75$, $\text{Max} \|\chi_0(k)-\chi_4(k)\| = \Delta_{04}(9) = 0.8$ and $\text{Max} \|\chi_0(k)-\chi_5(k)\| = \Delta_{05}(1) = 0.75$. Therefore, the maximum difference $\Delta_{\max} = 0.8$. Similarly, the minimum difference can be found by applying $\text{Min}\{\text{Min}(\|\chi_0(k)-\chi_i(k)\|)\}$. That is, $\text{Min} \|\chi_0(k)-\chi_1(k)\| = \Delta_{01}(6) = 0$, $\text{Min} \|\chi_0(k)-\chi_2(k)\| = \Delta_{02}(1) = 0$, $\text{Min} \|\chi_0(k)-\chi_3(k)\| = \Delta_{03}(3) = 0$, $\text{Min} \|\chi_0(k)-\chi_4(k)\| = \Delta_{04}(6) = 0$ and $\text{Min} \|\chi_0(k)-\chi_5(k)\| = \Delta_{05}(2) = 0$; and hence the minimum difference $\Delta_{\min} = 0$
- (6) Compute the grey relational coefficient $\gamma_{0i}(k) = \zeta \Delta_{\max} / (\Delta_{0i}(k) + \zeta \Delta_{\max})$ by setting $\zeta = 0.5$. That is, $\gamma_{01} = (0.35, 0.64, 0.54, 0.55, 1, 1, 0.62, 0.33, 0.4, 0.62, 1)$, $\gamma_{02} = (1, 0.37, 0.37, 1, 1, 0.62, 0.44, 0.57, 0.33, 1.0, 0.44)$, $\gamma_{03} = (0.44, 0.51, 1, 1, 0.67, 0.44, 1, 0.4, 0.67, 0.4, 0.35)$, $\gamma_{04} = (0.62, 0.43, 0.54, 0.37, 0.67, 1, 0.44, 1, 0.33, 0.35, 0.35)$ and $\gamma_{05} = (0.35, 1, 0.54, 0.55, 0.4, 0.44, 0.44, 0.4, 1, 0.62, 0.44)$.
- (7) Compute the grey relational coefficient $\gamma_{0i}(k) = \zeta \Delta_{\max} / (\Delta_{0i}(k) + \zeta \Delta_{\max})$ by setting $\zeta = 0.5$. That is, $\gamma_{01} = (0.35, 0.64, 0.54, 0.55, 1, 1, 0.62, 0.33, 0.4, 0.62, 1)$, $\gamma_{02} = (1, 0.37, 0.37, 1, 1, 0.62, 0.44, 0.57, 0.33, 1.0, 0.44)$, $\gamma_{03} = (0.44, 0.51, 1, 1, 0.67, 0.44, 1, 0.4, 0.67, 0.4, 0.35)$, $\gamma_{04} = (0.62, 0.43, 0.54, 0.37, 0.67, 1, 0.44, 1, 0.33, 0.35, 0.35)$ and $\gamma_{05} = (0.35, 1, 0.54, 0.55, 0.4, 0.44, 0.44, 0.4, 1, 0.62, 0.44)$.
- (8) Compute the relational coefficient by the following formula, and then rank the relational sequence. As $\Gamma_{0i}(k) = \frac{1}{n} \sum_{k=1}^n \beta_k \gamma_{0i}(k)$, we have

$\Gamma_{01} = 4(0.35)+0.64+0.54+0.55+1+2(1)+0.62+3(0.33)+3(0.4)+2(0.62)+1 = 1.02$. Similarly, we have $\Gamma_{02} = 1.23$, $\Gamma_{03} = 1.02$, $\Gamma_{04} = 1.09$ and $\Gamma_{05} = 1.01$, and hence the final ranking is $\Gamma_{02} > \Gamma_{04} > \Gamma_{03} = \Gamma_{01} > \Gamma_{05}$, which implies that software provider P002 is the most feasible candidate.

5 Conclusions

Cost analysis as well as vendor selection is known to be an important and challenging issue in developing software systems. In this paper, we propose a Multi-Stage Fuzzy-Grey (MSFG) approach to cope with this problem. The novel cost analysis method is developed based on the object-oriented concept, which is helpful to the project manager in controlling the software development budget for small- or medium- scale enterprises. Although the MSFG approach seems to be promising, there are some limitations of applying it: (1) Sufficient historical data must be available so that the cost analysis procedure can make precise prediction; (2) Participants must have the same ability and experiences in judging the importance of each criterion. Consequently, this issue is worth further studying.

Acknowledgement

This study is supported by the National Science Council of the Republic of China under contract numbers NSC-93-2524-S-260-001 and NSC-93-2524-S-009-004-EC3.

References

1. Barreiro, J.M., Caraca, J.P., Fernández, A., López-Illescas, A., Montes, C., Olmo, J.: ISODEPOR: System for the Interpretation of Isoquinetics. Resúmenes de Comunicaciones del IV Congreso Internacional de Entrenamiento Deportivo, Tecnología y Entrenamiento, León (1997)
2. Abdel-Hamid, T.K.: On the Utility of Historical Project Statistics for Cost and Schedule Analysis: Results from a Simulation-based Case Study. *Journal of Systems and Software*, 13(1) (1990) 71–82
3. Boehm, B.W., and Papaccio, P.H.: Understanding and Controlling Software development costs. *IEEE Transactions on Software Engineering*, 14(10) (1988) 1462–1477
4. Deng, J.L.: Introduction to Grey System Theory. *the Journal of Grey System*, Vol. 1 (1989) 1–24
5. Feng, S. and Xu, L.D.: Decision support for fuzzy comprehensive evaluation of urban development. *Fuzzy Sets and Systems*, Vol. 105 (1999) 1–12
6. Fowler, M., and Scott, K.: UML Distilled: a Brief Guide to the Standard Object Modeling Language. 2nd ed., Addison Wesley (1999)
7. Kemerer, C.F.: An Empirical Validation of Software development cost Analysis Models. *Communications of the ACM*, 30(5) (1987) 416–429
8. Kemerer, C.F.: Reliability of Function Points Measurement: a Field Experiment. *Communications of the ACM*, 36(2) (1993) 85–97
9. Lacity, M.C., Willcocks, L.P., and Feeny, D.F.: The Value of Selective IT Sourcing, *MIT Sloan Management Review*, 39(3) (1996) 13–25
10. Mowbray, T.J., and Malyeas, R.C.: CORBA Design Patterns, New York: Wiley Computer (1997)
11. Pressman, R.S.: Software Engineering: a Practitioner's Approach, New York: McGraw-Hill (2001)

A Two-Phased Ontology Selection Approach for Semantic Web

Tzung-Pei Hong¹, Wen-Chang Chang², and Jiann-Horng Lin²

¹ Department of Electrical Engineering, National University of Kaohsiung
tphong@nuk.edu.tw

² Department of Information Management, I-Shou University
m9122020@stmail.isu.edu.tw, jhlin@isu.edu.tw

Abstract. In this paper, we attempt to propose a two-phased ontology selection approach. Users can describe their requirements through a two-level requirement analysis model. The coarse-level analysis model is quite simple, only used for describing the main domains covered by the desired ontology and for selecting a fixed number of promising candidate source ontologies. The fine-level analysis model then refines the coarse-level model by defining the details in each domain. It is used to find the best matched ontology from the candidates from phase 1. The token extraction module and the WordNet system are also used to help for flexible match. The proposed selection approach can help easily find an appropriate ontology for a new application.

1 Introduction

Due to the wide usage of internet in this decade, the need of sharing and exchanging knowledge is dramatically increasing. Recently, the concept of semantic webs has been widely used to help make machines read and understand the web pages in different domains. Especially, ontology plays an important role on performing semantic webs [2]. Neches *et al.* defined an ontology as the basic terms and relations comprising a vocabulary [7]. Gruber took an ontology as a specification of a conceptualization [4]. Uschold and Gruninger thought an ontology might take a variety of forms, but it would necessarily include a vocabulary of terms and some specification of their meaning [8]. We could thus define an ontology as an explicit formal specifications of concepts, relationships and terms to represent domain knowledge. Several approaches were proposed to help build ontology [1][3][5][6]. However, when a new application or requirement occurs, efficiently and easily selecting an existing ontology to use, instead of building a new ontology, can save much time in building an intelligent semantic-web system. In this paper, we thus attempt to propose a two-phased ontology selection approach. Users first describe their requirements through a two-level requirement analysis model and the proposed approach will find out the best matched ontology according to the requirements. The token extraction module and the WordNet system are also used to help for flexible match.

2 Coarse-Level Requirement Analysis

The requirement analysis for helping select an appropriate ontology consists of two levels: a coarse level and a fine level. The coarse-level analysis model is quite simple,

only used for describing the main domains covered by the desired ontology and for selecting a fixed number of promising candidate source ontologies. The process for users to build an analysis model in the coarse level is shown in Figure 1.

According to the objective of the desired ontology, the requirement analysis phase begins by asking users to input the desired domain names or the most important concept names into the first row of a table, called the coarse-level relation table. The contents in the first row are then automatically copied in the first column. Next, the users specify the relationships between input names in the relation table. Each relationship represents a name in the first column implies to its corresponding name in the first row. If no relationship exists between two names, the corresponding cell remains blank.

After the coarse-level relation table is built, it can easily be converted into a graphical analysis model. The model is composed of two components – objects (by circles) and relationships (by arrows). Each object represents a domain name from the relation table. Each relationship represents the associations between two objects. It is a simple and clear model for users to understand the main objective of the built ontology.

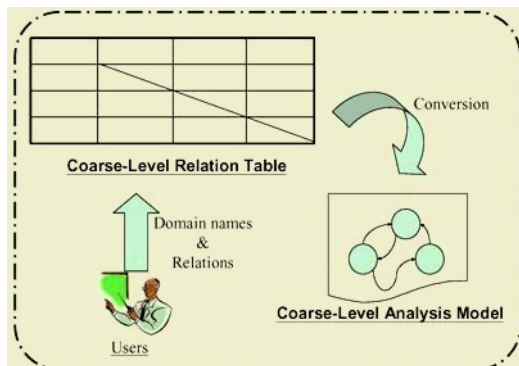


Fig. 1. The process of building a coarse analysis model

3 Fine-Level Requirement Analysis

The coarse-level analysis model is quite simple, only used for describing the main objective of an ontology and for selecting appropriate source ontologies. Thus, the fine level refines the coarse-level model by defining the details in each domain. The process for users to build an analysis model in the fine level is shown in Figure 2.

In this process, each finer concept related to a domain name in the coarse level is further designated by users. The concepts for the same domain may be organized into a hierarchy according to the assignment of level numbers from the user interface. Some related but not hierarchical concepts can also be provided by the expert. All these concepts are then used to further select the relevant ontologies. The fine-level analysis model thus provides more detailed information for selecting the best matched ontology.

4 Coarse Selection

After requirement analysis, the remaining work is to select the best match ontology for being used in an application. There are two phases: coarse selection and fine selection,

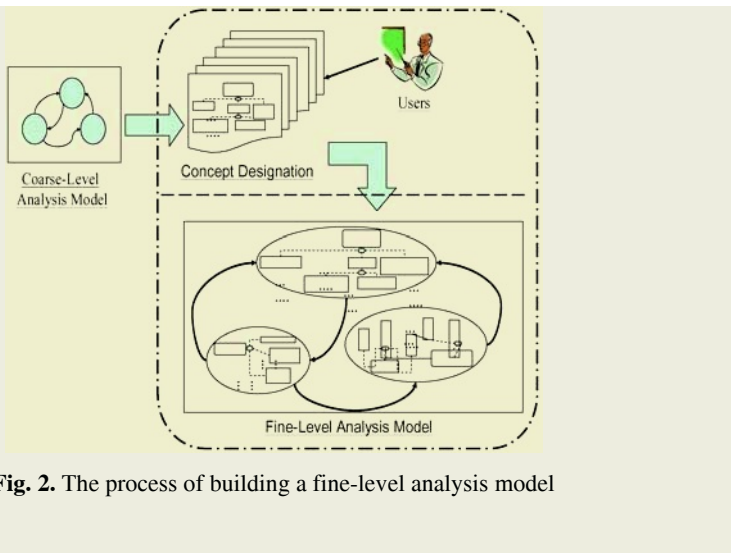


Fig. 2. The process of building a fine-level analysis model

for achieving this purpose. The coarse selection phase uses the coarse-level analysis model to filter the source ontologies and find some candidates for Phase 2. Then the fine selection phase uses the fine-level analysis model to decide which candidate ontology will be selected for usage in a new application. The coarse selection approach is described in this section. Figure 3 shows the process of selecting relevant candidate ontologies according to the coarse-level specification.

In the process, the ontology match table shown in Table 1 is used to keep the match degrees among the candidate ontologies and the coarse-level analysis model.

The domain names in the coarse-level analysis model are put in the first row, and the names of source ontologies to be selected are put in the first column. If a source ontology matches a domain name, the corresponding cell is marked with a match score.

In addition, the module for token extraction is designed to cut out the tokens in a compound domain name for later match. For example, the domain name “department of medicine” is a compound name since it has three tokens. The module will remove blanks, punctuations, prepositions and articles, and save nouns, verbs and adjectives as the keywords (terms). The WordNet system is then used to replace the terms by synonyms for flexible match. The entire procedure for selecting relevant candidate ontologies is stated as follows.

The Procedure for Selecting Relevant Candidate Ontologies

INPUT: Source ontologies and a coarse-level analysis model.

OUTPUT: Relevant candidate ontologies.

STEP 1: Create the initial ontology match table by putting the domain names in the coarse-level analysis model in the first row and the names of source ontologies in the first column.

STEP 2: For each domain name, do STEPs 3 to 5.

STEP 3: Call the token-extraction procedure to parse the domain names into terms. If it is a compound domain name, more than one term may be extracted. If it is not, the domain name itself is a term.

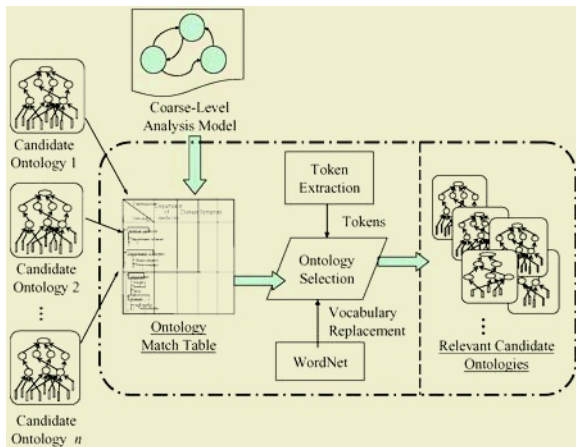


Fig. 3. The process of selecting relevant candidate ontologies

Table 1. The match table

| Domain Name Source Ontology \ | Domain Name 1 | Domain Name 2 | Domain Name 3 | ... | Domain Name m |
|----------------------------------|---------------|---------------|---------------|-----|---------------|
| Ontology 1 | | | | | |
| Ontology 2 | | | | | |
| Ontology 3 | | | | | |
| ⋮ | | | | | |
| Ontology n | | | | | |

- STEP 4: Get the synonyms of each term from the WordNet lexical library.
- STEP 5: Match each ontology with the terms or their synonyms. Each term and its synonyms can only be counted one if they are matched multiple times with an ontology. If r terms (or their synonyms) from a domain name with s terms are matched with an ontology, the match degree is r/s .
- STEP 6: For each ontology, calculate its match degree as the summation of its matched degrees with all the domain names divided by the number of domain names m .
- STEP 7: Select the ontologies with their match degrees satisfying the system requirement as the relevant candidates.

Note that the system requirement may be a limited number, a match threshold or both. It can be flexibly set up by users.

5 Fine Selection

The fine selection phase uses the fine-level analysis model further to find the best matched ontology for usage in a new application. Figure 4 shows the process of calculating the match degree between a relevant candidate ontology and the given fine-level analysis model.

In the process, an intra-ontology match table as shown in Table 2 is used to keep the match degrees among the terms of a relevant candidate ontology and the concepts in the fine-level analysis model. The concepts appearing in the fine-level analysis model are put in the first row, and the terms appearing in a coarse selected source ontology are put in the first column. If a term appearing in a relevant candidate ontology matches a concept, the corresponding cell is marked with a score.

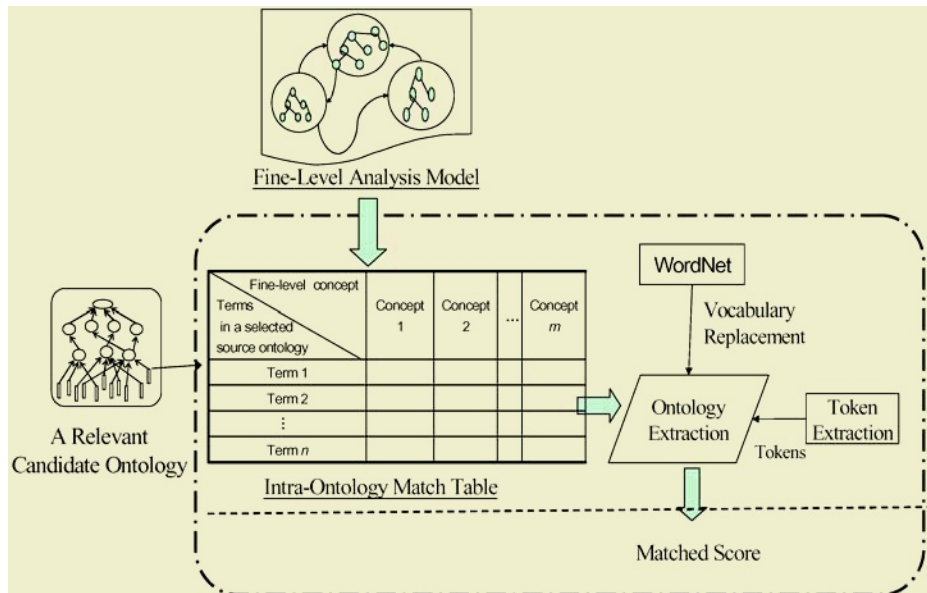


Fig. 4. The process of calculating the match degree between a relevant candidate ontology and the given fine-level analysis model

The token extraction procedure as in Phase 1 is used to cut out the tokens in a compound concept name for later match. The WordNet system is also used to replace the tokens by synonyms for flexible match. The entire procedure for finding the best matched ontology is stated as follows.

Table 2. The intra-ontology matching table

| Fine-level concept Terms in a selected source ontology | Concept 1 | Concept 2 | Concept 3 | ... | Concept m |
|---|-----------|-----------|-----------|-----|-----------|
| Term1 | | | | | |
| Term2 | | | | | |
| Term3 | | | | | |
| : | | | | | |
| Termn | | | | | |

The Procedure for Selecting the Best Matched Ontology

INPUT: The relevant candidate ontologies and a fine-level analysis model.

OUTPUT: The best matched ontology.

- STEP 1: For each candidate ontology, do STEPs 2 to 9.
 - STEP 2: Create the initial intra-ontology match table by putting the concept names of the fine-level analysis model in the first row and the terms of the source ontology in the first column.
 - STEP 3: For each concept name, do STEPs 3 to 5.
 - STEP 4: Call the token-extraction procedure to parse the concept names into tokens. If it is a compound concept name, more than one token may be extracted. If it is not, the domain name itself is a token.
 - STEP 5: Get the synonyms of each token from the WordNet lexical library.
 - STEP 6: Match each term in the selected source ontology with the tokens or their synonyms. If r tokens (or their synonyms) from a concept name with s tokens are included in a term, the match degree is r/s .
 - STEP 7: For each term, calculate its match degree as the summation of its matched degrees for all the concept names divided by the number of concept names m .
 - STEP 8: For any path connecting two matched terms, calculate its match degree as the average match degree of the nodes on the path. That is, if a path consists of nodes n_l to n_p , then its match degree is $(\sum_{i=l}^p d_i) / p$, where d_i is the match degree of n_i .
 - STEP 9: Calculate the match degree of the candidate ontology with the given final-level analysis model as:
- $$w_1 \sum_{i \in \text{matched nodes}} d_i + w_2 \sum_{i,j \in \text{matched nodes}} p_{ij},$$
- where w_1 and w_2 are the weighting factors, d_i is the match degree of node i and p_{ij} is the match degree of path (i, j) .
- STEP 10: Select the ontology with the highest match degree as the desired one.

6 Conclusions

In this paper, we have proposed a two-phased selection approach to help find an appropriate ontology from existing ones and to avoid re-inventing the wheels. The proposed approach is based on a two-level requirement analysis from users. The coarse-level analysis model is quite simple, only used for describing the main objectives of the desired ontology and for selecting appropriate source ontologies as candidates. The fine-level analysis model then refines the coarse-level model by defining the details and is used for selecting the best matched ontology. In the coarse selection, an ontology match table is used to keep the match degrees among the source ontologies and the coarse-level analysis model. The module for token extraction and the WordNet system are also used to help for flexible match. In the fine selection, an intra-ontology match table is used to keep the match degrees among the terms of a relevant candidate ontology and the concepts in the fine-level analysis model. The ontology with the highest match score among all the candidates is then output as the desired one.

References

1. Gómez-Pérez, "Some ideas and examples to evaluate ontologies," *The IEEE Eleventh Conference on Artificial Intelligence Applications*, Washington, USA, 1995, pp. 299-305.
2. Gómez-Pérez and O. Corcho, "Ontology languages for the semantic web," *IEEE Intelligent Systems*, Vol. 17, 2002, pp. 54-60.
3. N. Guarino and R. Poli, "The role of formal ontology in the information technology," *International Journal of Human-Computer Studies*, Vol. 43, 1995, pp. 623-624.
4. T. Gruber, "A translation approach to portable ontology specifications," *Knowledge Acquisition*, Stanford, California, Vol. 5, 1993, pp. 199-220.
5. T. Gruber, "Towards principles for the design of ontologies used for knowledge sharing," *International Journal of Human-Computer Studies*, MN, USA, Vol. 43, 1995, pp. 907-928.
6. Y. F. Kao, Y. H. Kuo, C. S. Lee and I. H. Meng, "A domain ontology learning approach based on soft-computing techniques," *National Computer Symposium*, Taiwan, 2003.
7. R. Neches, R. E. Fikes, T. Finin, T. R. Gruber, T. Senator and W. R. Swartout, "Enabling technology for knowledge sharing," *AI Magazine*, Vol. 12, 1991, pp. 36-56.
8. M. Uschold and M. Gruninger, "Ontologies: principles, methods and applications," *The Knowledge Engineering Review*, Vol. 2, 1996, pp. 93-155.

A Method for Acquiring Fingerprint by Linear Sensor

Woong-Sik Kim and Weon-Hee Yoo

Department of Computer Science & Information Engineering Inha University
#253 YongHyun Dong, Nam Ku, Incheon, South Korea
wskim1@software.or.kr, whyoo@inha.ac.kr

Abstract. The method for acquiring fingerprint by using a linear fingerprint sensor comprises the steps of: capturing a fingerprint image sequentially through the fingerprint sensor; dividing scanned fingerprint image as a predetermined segments according to a constant time and speed; detecting the optimum overlap region by comparing each image strip and its segment with the next image strip; calculating the value of mean image variation through the overlap region; and mixing the entire image by applying the mean image variation value to each image strip.

According to the present invention, the method for acquiring fingerprints by a linear fingerprint sensor in accordance with the present invention can improve the correct recognition rate greatly by estimating and compensating for the scanned image by the fingerprint sensor and accurately restoring the same to the original image.

1 Introduction

The present invention relates to a method for acquiring fingerprints by a linear fingerprint sensor, and more particularly, to a method for acquiring fingerprints by a linear fingerprint sensor by which a fingerprint image captured by the linear sensor is acquired by the estimation and restoration of the fingerprint image.

As is generally known, fingerprints have been recently adapted to many fields since the modern fingerprinting method was established by Edward R. Henry. Particularly, fingerprints are widely used as strong personal authentication means in the fields of pay, personnel, banking, criminal investigation, security, etc.

In case of using a linear sensor as a method for recognizing fingerprints in the prior art, a plurality of image strips are captured, and thus a method for combining captured image strips is required.

The image restoration method disclosed in the US Patent No. 6,002,815 has a problem that it cannot suggest a method for compensating for a pressure difference for a sensor of a finger and horizontal and rotational directions.

2 Description

Linear sensor capable of restoring a precise fingerprint image by dividing a fingerprint image into a plurality of regions, estimating the optimum matching point of each divided region and compensating for the fingerprint image deformed based on the matching point.

Preferably, the captured fingerprint image is divided a plurality of segments in which the width of each segments is the same as the height of each image strip.

Preferably, the achieve overlap rate of each image strip of about 50% each parameter has a optimal value as follows;

$$[\Delta x]_{opt} \approx \frac{N}{2M}, [\Delta y]_{opt} \approx \frac{M}{2}, [\Delta \alpha]_{opt} \approx \frac{M}{2N}.$$

Preferably, in the step of capturing the fingerprint image, the capturing rate according to the speed of movement of fingerprint is controlled by using the following speed change formula applied the limitation value of each parameter, where the formula,

$$v_{i+1} = \max\left(\frac{2v_i \Delta y_i}{M}, \frac{2Mv_i \Delta x_i}{N}, \frac{2Mv_i \Delta \alpha_i}{N}\right).$$

Preferably, a degree of inclination to the image variation is calculated by using the following formula under the superposed fingerprint image, where the formula,

$$\tan(\Delta \alpha) = \frac{M * \tan(\alpha_y)}{N + M * \tan(\alpha_x)}.$$

Preferably, the step of mixing the entire image further comprises the steps of: summing the variation value of local coordinates (horizontal, vertical, degree of inclination) from the referenced image strip through the following formulas; and estimating a global coordinate, where the formulas,

$$\begin{aligned} A_{i+1} &= A_i + \Delta \alpha \\ X_{i+1} &= X_i + \Delta x * \cos(A_{i+1}) - \Delta y * \sin(A_{i+1}) \\ Y_{i+1} &= Y_i + \Delta x * \sin(A_{i+1}) + \Delta y * \cos(A_{i+1}) \end{aligned}$$

3 Method

The fingerprint sensor generates continuous image strips, and estimates a variable value between the strips by using an overlap region between two sequential strips. Each strip has at least two rows consisting of discrete points and pixels. With the image strips acquired by the sensor, the distance between the strips is estimated and the image strips are combined to produce a composite image.

More specifically, assuming that the movement direction of the finger, which is an object moving on the upper surface of the fingerprint sensor, and the pressure applied on the fingerprint sensor by the finger are different from each other, a produced image is affected by the movement characteristic of the finger.

Therefore, in the method for acquiring fingerprints of the present invention, sequentially acquired image strips are captured so that they can be combined, and a set of coordinate variables (x, y coordinates) for each image is generated.

In the present invention, when each image segment is combined to be generated as the full image, the coordinate set provides the accurate position of the corresponding

image strip. In addition, in the method for acquiring fingerprints of the present invention, added information about the combination of fingerprint images, such as the start and end position of an image, the loss state of synchronization, etc. are acquired and the adaptive capturing rate is calculated and produced by the movement amount of each image strip.

For this purpose, in the method for acquiring fingerprints according to the present invention, (x, y, α) is used for the local coordinate system between two adjacent strips of a captured fingerprint image, and (X, Y, A) is used for the global coordinate system for the full image. The coordinate difference of the local coordinate system is represented as $(\Delta x, \Delta y, \Delta \alpha)$.

At this time, a sensor region consists of N columns and M rows as illustrated. Since the sensor is a linear sensor, it is assumed that $N \geq M^2$. The image strips acquired by this sensor have the same size as the sensor region.

That is, the method for acquiring an image by the combination of images according to the present invention includes a series of processes for acquiring image strips. In order to estimate the movement amount of an image according to a movement value of the relative coordinate, as illustrated, the central movement amount of the image strips and the rotational movement value thereof are calculated by comparison of the image strips.

At this time, in order to compare a plurality of image strips, it is necessary that an overlap region where the image strips are overlapped is present. Thus, the capturing rate of the fingerprint sensor is controlled according to the speed change of the finger so that the image strips are overlapped with one another.

Strips S_i and S_{i+1} are captured at speed V_i and V_{i+1} at time t_i and t_{i+1} .

That is, as illustrated, the image strip is divided into M segments, which is the same as the height of each image strip, in order to detect the transition value of the image strip.

Then, based on the segment of the first image strip S_1 of all the image strips, the optimum overlap region in the segment region of the next image strip S_2 is detected.

In addition, a angle of rotation and a degree of vertical/horizontal deformation are estimated between the first image strip S_1 and the next image strip S_2 , and simultaneously the mean weight value is given to each variable value, for thereby combining the image strips. That is, Δx_{ij} and Δy_{ij} are calculated based on the optimum matching point, and Δx_i , Δy_i and $\Delta \alpha_i$ of S_i are obtained by the mean square linear approximation with a weighting factor.

In other words, as illustrated, the image is captured so that a plurality of image strips having M segments can be formed, the overlap region of the image strips is adapted to calculate a vertical and horizontal displacement values.

By this, as illustrated, the overlap regions of the image strips forms an approximate value in the global coordinate system. Local (x, y) movement values Δx_j and Δy_j indicate the position of the minimum value of the differential function of the corresponding segment. The mean square linear approximation with a weighting value is

used to estimate sloping side $\Delta\alpha$, tangential displacement Δy and parallel displacement Δx .

At this time, as illustrated, isometric approximation is adapted to acquire a degree of inclination of $\Delta x_j = \Delta x(j)$ and $\Delta y_j = \Delta y(j)$ and Δx and Δy . The displacement of Δx and Δy is acquired by the approximate function value at the center of the first image strip.

Therefore, when the overlap region is estimated from the image strip divided into a plurality of segments which is captured as the finger moves, as illustrated, the image displacement is represented which is the same as the displacement of each segment with a constant sloping side.

The degree of inclination for the image displacement of the segment will be expressed by mathematical formula 1.

$$\tan(\Delta\alpha) = \frac{M * \tan(\alpha_y)}{N + M * \tan(\alpha_x)} \quad (1)$$

As illustrated, three parameters for the movement amount of fingerprints are presented between segments of a plurality of overlapped image strips. Those parameters includes tangent line, parallel displacement amount and angle of rotation. By using the thusly calculated parameter set in the local coordinate system, the image strips are compared with one another, and then are combined in the global coordinate system, for thereby acquiring a complete image.

Strips S_{i+1} (local coordinate) are accumulated in the appropriate position of the full image buffer (global coordinate system) by using Δx_i , Δy_i and $\Delta\alpha_i$. When the buffering is completed, the corresponding full image is stored. At this time, it is judged whether scanning is completed.

If the scanning is not completed, it is necessary to control the capturing rate according to the change of the movement speed of the finger so that certain regions of the image strips are overlapped. To change the capturing rate, at least one of the coordinate parameters has to be spaced as long as a predetermined marginal value.

$$[\Delta x]_{opt} \approx \frac{N}{2M}, [\Delta y]_{opt} \approx \frac{M}{2}, [\Delta\alpha]_{opt} \approx \frac{M}{2N}. \quad (2)$$

The marginal value of each parameter described in Mathematical Formula 2 is adapted so that approximately 50% of the image strips can be overlapped with one another. At this time, the capturing rate Δv_{i+1} of the sensor can be calculated by analogy of Mathematical Formula 2.

That is, assuming that Δy_{i+1} converges to $\frac{M}{2}$, when $\Delta v_i * \Delta y_i \sim \text{const}$ and $\Delta v_{i+1} * \Delta y_{i+1} \sim \text{const}$, the displacement of y of v_{i+1} ($v_{i+1} = \frac{2v_i \Delta y_i}{M}$) can be calculated. Likewise, if x and α are calculated in the same manner, the following capturing rate is obtained.

$$v_{i+1} = \max\left(\frac{2v_i \Delta y_i}{M}, \frac{2Mv_i \Delta x_i}{N}, \frac{2Mv_i \Delta \alpha_i}{N}\right). \quad (3)$$

The fingerprint image shows a variety of types according to a variable value for each movement as illustrated. The value of the corresponding parameter is different according to each of the types.

At this time, since X , Y and A fully define the position of the current image strip on the global image coordinate, the global coordinate (image coordinate) is performed on the local coordinate (coordinate of the sensor) by a recursive procedure such as the following formula.

$$\begin{aligned} A_{i+1} &= A_i + \Delta\alpha \\ X_{i+1} &= X_i + \Delta x * \cos(A_{i+1}) - \Delta y * \sin(A_{i+1}) \\ Y_{i+1} &= Y_i + \Delta x * \sin(A_{i+1}) + \Delta y * \cos(A_{i+1}) \end{aligned} \quad (4)$$

That is, as expressed in Mathematical Formula 4, A_{i+1} , X_{i+1} and Y_{i+1} can calculate the global coordinate and produce the composite image by summing the parameters A_i , X_i and Y_i of the previous image strip and variable values thereof.

The fingerprint recognition system of the present invention restores a scanned fingerprint image by image estimation and restoration algorithm as illustrated.

4 Experimental Results

Estimator makes coordinate estimations for the horizontal, vertical shifts and rotations of subsequent strips relative to the previous ones.

Two subsequent stripes usually have very small angle difference, but this difference might be reasonable between first and last strip on the image. That means that in Estimator we may use kind of skew instead of the real rotation – the angle between two consecutive stripes is small. And in Re-constructor we are forced to use rotations, but for the small angles we may use skew. The reason is that skew is much faster technique than rotation.

<Describe that delta_y, delta_alpha issue and how to get delta_x from them>

Tests on 256*32 8-bpp strip placed into 256*128 output image buffer:

- 1) One rotation (float point, interpolation, plus shifts): 12 ms
- 2) One rotation (float point, but with no interpolation): 7 ms (~2 times faster)

The test has been done four times with sensor <a>, using the algorithm and , not using the algorithm and total 16 fingerprints; 6-left loop, 4-right loop, 3-hole and 3-double loop. And for the person himself 96times, for stranger, tested 120times.

The rejection rate during enrolling the finger image is important factor for evaluating the sensor and technology [3], [5]. But, in case of sensor <a>, the rate for capturing image and even the quality of image showed much better than sensor . For the algorithm test of three different ones, the sensor showed worst identification rate [8], [9].

< Matching result with various sensors and algorithms >

| | <a> Sensor Image | Sensor Image |
|------------------------------|---|---|
| Algorithm (Minutiae) | FMR = 11 / 96 FNMR = 0 / 120 REJECT = 0 | FMR = 20 / 96 FNMR = 0 / 120 REJECT = 6 |
| Algorithm (Non-minutiae) | FMR = 29 / 96 FNMR = 0 / 120 REJECT = 1 | FMR = 28 / 96 FNMR = 0 / 120 REJECT = 2 |
| A Corp. algorithm | FMR = 0 FNMR = 0 REJECT = 0 | FMR = 0 FNMR = 0 REJECT = 6 |

5 Conclusion

Most of linear sensors have inferior image restoration than the general optical sensor due to the skill of user and negligence. However, with the price and slim shape of the sensors, it has been applied in several fields such as mobile phone and others, and if the ensuing research could improve the image restoration for even more, there would be slim shape and the economic benefit to contribute to the development of bio-recognition industry.

In this thesis, the method to capture the fingerprint image by maintaining consistent speed like the fax machine or copier is applied to the vertical movement, horizontal movement and rotation theories, and the algorithm is proposed to make easy access to the easy inputting of fingerprint that the result of captured image result is applied for algorithm of minutiae method algorithm to the sensor. And the case of applying the algorithm for non-minutiae method, and the experiment was made with the case of applying the algorithm with the example of recuperation office [6], [7], [8].

As in the case of the result through the experiment is shown to be better than the experimental video quality of algorithm or the rate of recognition proposed in this thesis.

References

1. Dario Mario and David Maltoni, "Direct Gray-Scale Minutiae Detection in Fingerprints," IEEE Trans. Pattern Analysis and Machine Intelligence, Vol. 19, No. 1, pp. 27-39, Jan., 1997.
2. Lin Hong, Yifei Wan, and Anil Jain, "Fingerprint Image Enhancement: Algorithm and Performance Evaluation," IEEE Trans. Pattern Analysis and Machine Intelligence, Vol. 20, No. 8, pp. 777-789, Aug., 1998.
3. A.K. Jain, L. Hong, and R. Bolle, "On-Line Fingerprint Verification," IEEE Trans. Pattern Analysis and Machine Intelligence, Vol. 19, No. 4, pp. 302-313, April., 1997.
4. A.K. Jain, S. Prabhakar, L. Hong, and S. Pankanti, "Filterbank-based fingerprint matching," IEEE Trans. on Image Processing. 9(5):846-859, May 2000.

5. K. Nalini, and A.K. Jain, "A Real-Time Matching System for Large Fingerprint Database," IEEE Trans., Pattern Analysis and Machine Intelligence, Vol. 18, No. 18, pp. 799-813, Aug., 1996.
6. Xudong Jiang and Wei-Yun Yau, "Fingerprint Minutiae Matching Based on the Local and Global Structures," International Conference on Pattern Recognition (ICPR'00), Vol. 2, No. 18, pp. 1038-1042, Sep., 2000.
7. T. Maeda, M. Matsushida and K. Sasakawa, "Identification Algorithm Using a Matching Score Matrix," IEICE Trans. INF. & SYST., Vol. E-84-D, No. 7, pp. 819-824, July 2001.
8. Xudong Luo, Jie Tian and Yan Wu, "A Minutia Matching algorithm in Fingerprint Verification," International Conference on Pattern Recognition (ICPR'00), Vol. 4, No. 18, pp. 4833-4841, Sep., 2000.
9. J. D. Stoszand and L. A. Alyea, "Automated Systems for Fingerprint Authentication Using Pores and Ridge Structure," Proceedings of SPIE, Automatic Systems for the Identification and Inspection of Humans (SPIE Vol. 227 7), San Diego, 1994, pp. 210- 223.

Evaluation and NLP*

Didier Nakache^{1,2} and Elisabeth Metais¹

¹ CEDRIC /CNAME: 292 rue Saint Martin - 75003 Paris, France
datamining@wanadoo.fr, metais@cnam.fr

² CRAMIF: 17 / 19 rue de Flandre - 75019 Paris, France

Abstract. F-measure is an indicator used since 25 years to evaluate classification algorithms in textmining, from precision and recall. For classification and information retrieval, some ones prefer to use the break even point. Nevertheless, these measures have some inconvenient: they use a binary logic and don't allow applying a user (judge) assessment. This paper proposes a new approach of evaluation. First, we distinguish classification and categorization from a semantic point of view. Then, we introduce a new measure: the K-measure, which is an overall of F-measure and break even point, and allows applying user requirements. Finally, we propose a methodology for evaluation.

Keywords: evaluation, measure, classification, categorization, NLP, F-measure.

1 Introduction

Natural language processing produces many algorithms for classification, categorization and information retrieval. The performance of these algorithms is computed from several measures, like precision and recall. To make easier the reading of performance, [Van Rijsbergen 79] created a synthetic measure: the F-measure, which is a combination of these two indicators. Today, needs are diversified, problems are more complex, but we keep the same indicator since 25 years [Sparck Jones 2001]. This usage is it still justified? Without renouncing existing scales, how to integer new needs? In several domains, like in medicine, some users may consider that a medium result is a bad result, or inappropriate. So, we had to find an indicator able to answer this problem, without losing qualities of existing measures.

To do this, we introduce our paper by precising the main concepts: evaluation, classification, categorization, and information retrieval. We will propose a definition for each one (section 2). Section 3 presents the state of the art for evaluation and main indicators. Finally, after analysis of the F-measure properties (section 4), we will propose a new approach of evaluation, adapted for each case, and allowing to integrate user's requirements (section 5).

2 Etymology and Definitions

Terms 'classification' and 'categorization' have different histories and origins. No scientific definition could be found, except in Webster dictionary which gives two meanings for the word classification: 'taxonomy' and "category".

* This work is partially financed by the French "Ministere de l'education nationale, de l'enseignement et de la recherche"

According to the history of these two terms and their actual meaning, we propose to define **classification** as being action of arranging a whole set into hierarchical or ordered structure, in existing classes or not, or the result of this action, and **categorization** as being action (or its result) of grouping elements with common characteristics. Nevertheless, in a classification, it will be possible to quantify or valorize difference between proposition and requirement. We could consider an answer as being partially true, and associate a metric to the difference. Finally, **information retrieval** is different from classification and categorization by a great set of enabled answers (potentially infinite), by missing of referential, and often obligation of human evaluation. Classical application would be a web crawler, or AI answers to a request. With so different task, evaluation methods and indicators can be different.

3 State of the Art

3.1 What Is Evaluation?

Evaluation consists of measuring the difference between result and requirement. No metric is associated, but we use to generate a number between 0 and 1 without unity. Some elements are very subjective and can't be automated. Tefko Saracevic [Saracevic 70] insists on the main role of judge.

3.2 Indicators and Measures: Toward the F-Measure

A system can answer to a request according to the following model:

| | Pertinent | Not pertinent | Total |
|-----------------------------|-----------|---------------|-----------|
| Found (or proposed) | a | b | a+b |
| Not found (or not proposed) | c | d | c+d |
| | a+c | b+d | a+b+c+d=N |

From this contingency table, NLP community computes several distances:

$$\text{precision} = a/(a+b), \text{recall} = \frac{a}{a+c}, \text{pertinence} = \frac{a+d}{a+b+c+d},$$

$$\text{error} = \frac{b+c}{a+b+c+d}, \text{fallout} = \frac{b}{b+d}, \text{silence} = \frac{c}{a+c}, \text{specificity} = \frac{d}{b+d},$$

$$\text{noise} = \frac{b}{a+b}, \text{overlap} = \frac{a}{a+b+c} \text{ and generality} = a/N$$

Finally, 4 single measures (a, b, c, d) generate 10 basic indicators, themselves combined to generate other measures. In most of cases, we only use precision and recall. From these different measures, several synthetic indicators have been created, but the most famous is the F-Measure from [Van Rijsbergen 79]:

$$\text{F-Measure} = ((1+\beta^2)*\text{Precision}*\text{Recall}) / ((\beta^2*\text{Precision})+\text{Recall}), \text{with usually } \beta^2 = 1$$

We can notice that this measure doesn't take care of pertinence and is binary: an answer is good or 'not good'

4 Analysis of F-Measure

First, we demonstrated that the F-measure is only harmonic average of precision and recall. Then, we watch its properties. When precision has the same value than recall, we get: Precision = Recall = F1-measure. So, the result is comprehensive and we try to maximize it by maximization of both precision and recall (like for ‘Break Even Point’ approach). Indeed, it would be difficult to evaluate an algorithm which would have a good precision and a bad recall (or reverse).

Let’s compute harmonic mean M of precision P and recall R:

$$\frac{2}{M} = \frac{1}{P} + \frac{1}{R} \text{ so } \frac{2}{M} = \frac{P+R}{P*R}, \text{ and } \frac{M}{2} = \frac{P*R}{P+R}. \text{ Finally, we get: } M = \frac{2*(P*R)}{P+R} = F1$$

We notice that F1-measure is only a harmonic mean of precision and recall. Nothing can justify this choice from a mathematical point of view. Nevertheless, harmonic mean has an interesting property which is: the result strongly decreases when only one of its components decreases. At the opposite, it grows strongly when the parameters are both high. This property is interested because it would give a low result for algorithms which would improve precision or recall exclusively in prejudice of the other one.

We can demonstrate that property for the F1-measure: we have $F1=2*P*R/(P+R)$, with precision=P and recall=R. Let’s have $S=P+R$ and $D=P-R$. Our problem becomes: how to improve F-measure when S increase (so precision AND recall are high) and D is minimized (keeping precision and recall closed). We have: $S^2 - D^2 = (S+D)(S-D) = (P+R+P-R) \times ((P+R)-(P-R)) = 2P \times 2R = 4PR$

$$\text{And finally: } F1 = \frac{2 * P * R}{P + R} = \frac{S^2 - D^2}{2S} = \frac{S}{2} - \frac{D^2}{2S}; \text{ that's the reason why F-measure is}$$

improved when S increase, and decreased when D increase. If one of the components is low, the resulting mean is low too. The F_n measure has another interesting property: it allows to modify importance of precision or recall.

5 Proposition of a New Indicator: Toward K-Measure

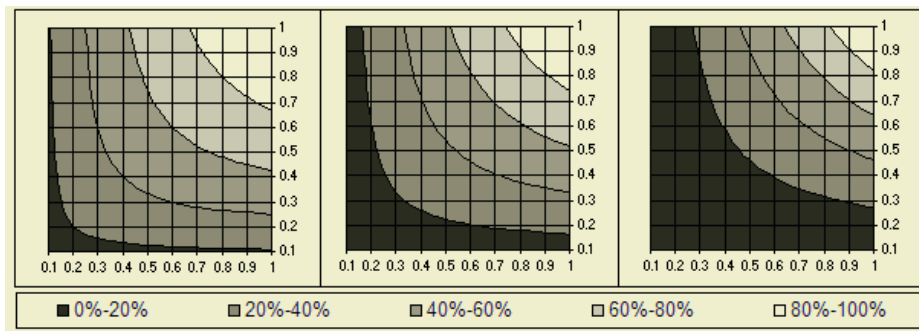
In section 1, we tried to define classification and distinguish it from categorization and information retrieval. Now, we are going to find a new measure, with more possibilities for evaluation.

Case of Categorization

From empirical research, we found a formula which could integrate those needs and introduce **K-Measure**, based on F-measure:

$$\mathbf{K-Measure = (1+\beta^2)*(Precision*Recall)^{\alpha} / ((\beta^2*Precision)+Recall)}$$

First, we can see that if $\alpha=1$, then K-measure is equal to F-measure. If $\alpha=1$ and $\beta^2=1$, we get the usual F1-measure. So, the K-measure is a generalization of the F-measure. This is particularly useful because we can keep the history. Now, let’s see properties when $\beta^2=1$, and α parameter is varying with values 1, 1.2, and 1.6:



We notice that when α parameter increases, the requirement level is increasing too. For example, if precision=recall=0.4, F-measure = 0.4, and k-measure = 0.13 with $\alpha=1.6$ (three times less). This result will be considered as bad, while F-measure considers it as medium. So, we can formalize a requirement level, just increasing α parameter. We can observe that favor precision or recall is preserved, by increasing β parameter. In conclusion, K-measure has properties very interesting for evaluation:

- It is an overall of F measure which keep its properties,
- It allows to express a judge requirement level,
- It can represent too a Break Even Point approach when $\alpha=0.5$.

It is a formula of convergence, and an overall of different approaches used nowadays.

Case of Classifications

As proposed in section 1, a classification distinguishes from categorization because we can use a distance measure between classes. [Budanitsky 2001] demonstrated that the best measure of semantic distance was Jiang and Conrath's measure:

$$d = \text{Dist}_{JC}(c1 : c2) = 2 \log(p(\text{lso}(c1 : c2))) - (\log(p(c1)) + \log(p(c2)))$$

with $\text{lso}(c1 : c2)$ = largest common group.

If we call 'd' that distance (with $d=1$ when classes are very far), then precision and recall can be defined like this:

Precision = a / B et Recall = a / c

a = Count of pertinent and proposed classes (= correct classification)

B = proposed class but not pertinent: we consider the distance 'd' with the nearest correct class. Then compute $(1-d)$ to have B near 1 when distance is weak.

c = Count of not proposed and pertinent classes

It is then possible to use K-measure.

Case of Information Retrieval (IR)

Information retrieval is different from classification and categorization because of large possible answers. Example of classical application would be a web crawler.

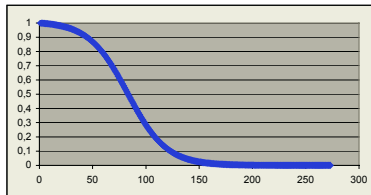
To find a good indicator, we started from score used by [Vooheres 2003] $\frac{1}{Q} \sum_{i=1}^Q \frac{n}{i}$, where n represents the number of good answers in range i, Q is the number of question. To represent a requirement level (for example: "I want that good answers are in the first 30, because it is the length of a web page", we need to modulate the initial Boolean and linear approach by integrating a sigmoid function. After empirical researches, we could find a coefficient W_i which solves our problem:

$$w_i = \frac{1 + e^{(l-k)}}{1 + e^{(-k(\frac{N-i+1}{N})-l)}}$$

With k and l, two parameters (default values are k=15, and l=0.7), N represents the number of answer, and i the range of the answer.

Let's see the properties of that equation when k and l are varying (in our example, we have N=273)

$$K=15, l=0.7$$



We can see that if the required answer doesn't appear in top 50, the score is strongly down, and quite null if higher than 150. The l parameter moves inflection point (right and left), and k changes the slope.

The two parameters allow generating any requirement level. This score favor fact of giving good answers in first. To compute final indicator, we just multiply weight by pertinence. For automatic computing, we can use a Boolean approach: 1 for a good answer, otherwise 0. But for human evaluation, each judge can give a percentage. Global evaluation indicator becomes:

$$D \text{ Mesure} = \frac{\sum_{i=1}^N \text{Pertinence}_i * w_i}{\sum_{i=1}^N w_i} = \frac{\sum_{i=1}^N \text{Pertinence}_i * \frac{1 + e^{(l-k)}}{1 + e^{(-k(\frac{N-i+1}{N})-l)}}}{\sum_{i=1}^N \frac{1 + e^{(l-k)}}{1 + e^{(-k(\frac{N-i+1}{N})-l)}}}$$

6 Conclusion

In this paper, we first defined classification and categorization. The first case we can measure the distance between classes, not in second case because it is binary. The F-measure, which created 25 years ago, has established as a standard of evaluation. Since, the needs evolves but not evaluation. Analysis of F-measure helps us to create a new measure: K-measure, an overall of F-measure able to integrate requirements.

We demonstrate how to use k-measure for classification as well to integrate the distance between the results. Finally, we propose a new measure for information retrieval which enhances finding good answers first and allow the expression of needs.

K-measure provide the following advantages: a meta measure of convergence between Van Rijsbergen's F-measure and Joachims's break even point. It has mathematical properties which allow creating a synthetic indicator from whatever other measure. Finally, it allows integrating the judge approach of Saracevic and formalizing the required levels. So, we can say it's a measure which converge the three approaches without modifying any of their properties.

In our future works, we will experiment these measures, particularly their impacts on classical measures.

Special Thanks

We want to thanks:

- OutcomeRea Association and its president professor Jean François Timsit for the work we done together,
- Professor Jacky Akoka and laboratory Cedric - CNAM of Paris,
- Pierre Kebaili and Jacques Tonner (CRAMIF: Caisse Régionale d'Assurance Maladie d'Ile de France) for supporting us.

References

- [Budanitsky 2001] A. Budanitsky and G. Hirst: "Semantic distance in WordNet: An experimental, application-oriented evaluation of five measures" Department of Computer Science Univ. of Toronto.
- [Saracevic 70] T. Saracevic, "Introduction to Information Science", 111-151. New York: R.R. Bowker, 1970. Chap. 3: The concept of "relevance" in information science: A historical review.
- [Sparck Jones. 2001] K. Sparck Jones. "Automatic language and information processing: Rethinking evaluation". Natural Language Engineering, 7(1):29–46. 2001.
- [Van Rijsbergen 79] K. Van Rijsbergen, "Information Retrieval", (2nd Ed.) Butterworths, London. www.dcs.gla.ac.uk/Keith/Preface.html.
- [Voorhees 2003] E. M. Voorhees: "Evaluating the Evaluation: Edmonton", May-June 2003. Main Papers, pp. 181-188. Proceedings of HLT-NAACL 2003.

A Handwriting Tool to Support Creative Activities

Kazuo Misue and Jiro Tanaka

Graduate School of Systems and Information Engineering,
University of Tsukuba,
1-1-1 Tennoudai, Tsukuba, 305-8573 Japan
{misue, jiro}@cs.tsukuba.ac.jp

Abstract. Handwriting in computer environments satisfies many requirements that are necessary to support creative activities, as it is easy to use, natural, flexible, and informal. This article proposes a tool to support creative activities using handwriting. The tool has the following features: (1) It is targeted for use in processing diagrams with logical structures. (2) It provides a handwriting input interface. (3) It maintains the handwritten feel of diagrams. (4) It supports creative activities intellectually and actively. The architecture and the behavior of the tool are explained using some screen shots of a prototype.

1 Introduction

Computers augment human creativity with their information processing capability. Many tools have been developed to support human creative activities [1]. Most of them are focused on providing a variety of advanced functions.

However, human creativity is very delicate. It contains some factors that we cannot control by ourselves. Most tools developed so far seem to have given careless consideration to the aspects of feelings and impressions, which may influence human creative activities. As a result, designers often use paper (or a whiteboard) and a pen in the early stages of their creative activities even though a lot of tools with advanced functions are available [2].

Recently, user interfaces of computers have been changing into forms that are appropriate for activities in the real world. For example, pens (or styluses) and large screen displays are becoming popular. Such interfaces have enabled several kinds of handwriting, such as a pen as an input device and sketching as an input method.

Handwriting in computer environments satisfies many creative needs by being easy to use, natural, and flexible. Additionally, the informality provided by handwriting seems to benefit human creative activities. Therefore, we propose a tool to support creative activities that exploits the features of handwriting. The tool is especially targeted to support creative activities involving logical structures.

2 Use of Handwriting to Support Creative Activities

2.1 Externalize Information Using Drawings

In this article “creation” is defined as making something that is conceptually new. Examples of creative activities include developing a computer system, making web sites, constructing a building, and so on. Such creative activities contain operations of concept in their upstream. It is important to organize and/or to integrate information that is disorganized or fragmentary. We may do such operations in our head when there are only a few concepts to be handled. However, we often externalize information in our head using drawings; we express concepts with words, symbols, or diagrams, and connect them with lines, enclose them with circles, and so on. Drawing diagrams with logical structures and looking at them objectively accelerates the creative activities, especially when there are a lot of concepts, as well as complex relationships between them.

2.2 Requirements for Tools to Support Creative Activities

The externalizing processes in creative activities do not occur only once but require a lot of trial and error repetition. Pen and paper are not very convenient for repetition, so computers are the logical choice to support such processes. Therefore, it is important to develop tools that support externalization efficiently and appropriately.

When we get an idea, we often forget it soon after. The idea is often vague and ambiguous. It is rarely a complete idea; usually it is partial and imperfect. Therefore, it is important to write down such fragile, vague, partial, or incomplete information efficiently. Moreover, it is also important to write it down appropriately. Excluding ambiguity from the information and converting it into a more formal style for computer input might cause us to lose the intrinsic point of view, resulting in a misunderstanding. Consequently, it is necessary to achieve the following objectives when designing tools to support creative activities.

- To be able to write down ideas quickly and easily.
- To be able to write down ideas without having to deal with useless or indirect operations.
- To be able to write down ideas freely in the order we get them.
- To be able to write down vague, partial, or incomplete ideas appropriately.

2.3 Handwriting in Computer Environments

We think that handwriting in the computer environment satisfies some of the following requirements for input devices, input methods and expression forms.

- i) **Input device:** Pen-type devices are used for input. Styluses for PDAs or tablet PCs are pen-type devices that are widely used. Typical monitors used with these devices are liquid crystal or plasma screens that have touch panels.

- ii) **Input method:** Sketching or gestures are used as input methods. Sketching adopts the tracks of a pointing device as ink data. Gestures are similar to sketching but interpret tracks of pointing devices as commands.
- iii) **Expression form:** Curves drawn freehand or that seem to be drawn freehand are used to express forms. This requirement depends on the character of the expression. Thus, the expression of the so-called “handwritten style” also satisfies this requirement.

2.4 Merits of Handwriting in Supporting Creative Activities

Handwriting offers several merits in supporting creative activities. Here we explain the merits according to the requirements described above.

i) Pen-type device (input device)

Easy: Pen-type devices are simple to use; they are similar to normal ink pens that people are used to using, so they are easy to operate. This ease of use enables quick input of ideas.

Natural: Input is very natural using a pen. We can input directly at the operating position of the device and can move the operating position quickly and directly to a target position on the screen. Such features also contribute to quick input of ideas.

ii) Sketching input (input method)

Flexible: We can write/draw anything by sketching it; characters, expressions, diagrams, pictures, and so on. Sketching input doesn't require any input modes, so we can write/draw anything in the order we prefer.

Direct: We can write/draw what we want anywhere we want to in a direct way. We do not need to worry about such things as learning how to use drawing tools, templates of shapes, Chinese character conversion, etc.

iii) Freehand drawings (expression form)

Informal: Body type fonts, geometric figures, and regular arrangements tend to give a formal and “hard” impression, while drawings done by hand tend to give an informal and “soft” impression. Furthermore, the former style often gives the impression of being regular, static, stable, complete, elaborate and consistent, while hand-drawn images often give the impression of being disorderly, unsteady, dynamic, unstable, incomplete and ambiguous.

The KJ-method developed by Jiro Kawakita is one of the most famous methods developed to enhance creative activities [3]. handwritten diagrams prepared using the KJ-method give very different impressions when they are compared with diagrams automatically generated by computer. The KJ-method seems to exploit the informality of hand-drawn diagrams to benefit thinking processes [4].

3 A Handwriting Tool to Support Creative Activities

In this section, we give an outline of a handwriting tool designed to support creative activities. The tool is presented using screen shots of a prototype. We also describe the technical challenges of developing such a tool.

3.1 Overview of the Handwriting Tool for Logical Drawing

The features of the proposed tool are as follows.

- The main processing objects of the tool are diagrams with logical structures.
- The tool provides a freehand sketching interface.
- The tool maintains the feel and ambiguity of drawings done by hand.
- The tool supports drawing intellectually and actively.

Here, the diagrams with logical structures are not diagrams in which arrangement in coordinates and geometrical shapes are essentially important, but are diagrams where logical relationships such as connective relationships and inclusion relationships are important. Examples include system configuration diagrams, flow charts, concept maps, and network topology diagrams.

The tool provides integration of the handwriting environment and drawing support for diagrams with logical structures. It aids in drawing efforts using handwriting by analyzing the logical structures of diagrams and using these structures for layout constraints or automatic layouts of the diagrams. It not only exploits handwriting as an input method but also preserves the handwritten “feel” of the image and supports redrawing of the images.

3.2 Architecture and Technical Challenges

Figure 1 shows the architecture of the tool; it consists of five functional parts. The “gesture recognizer” deals with the user’s sketching input as gestures or interprets it as ink data. The “spatial parser” analyzes diagrams consisting of ink data to grasp logical structures of the diagrams. The “constraint solver” solves some constraints according to the logical structure of the diagram. The “layout modifier” computes new layouts of the diagrams, and then the “handwritten style generator” modifies the shapes of the diagrams to preserve the handwritten feel of the original diagrams.

To develop the prototype tool, we used the SATIN toolkit [5] to recognize standard gestures and to make a spatial parser. The spatial parser constructs graph structures of diagrams [6]. Isolated shapes are interpreted as nodes, and shapes connecting to other shapes are interpreted as edges. The other functional parts are written in Java without any toolkit. The constraint solver works to preserve connections between nodes and edges. Moving the nodes influences the positions and shapes of connected edges. The handwritten style generator modifies shapes of the influenced edges.

To further evolve and improve the tool, the rules handled by the five functional parts should be reconsidered. The parsing rules should cover more complex diagrams, and the rules of the constraint solver should be extended to handle various transformations of diagrams. Some of the techniques used in the image-editing program ScanScribe [7] might be used for this purpose.

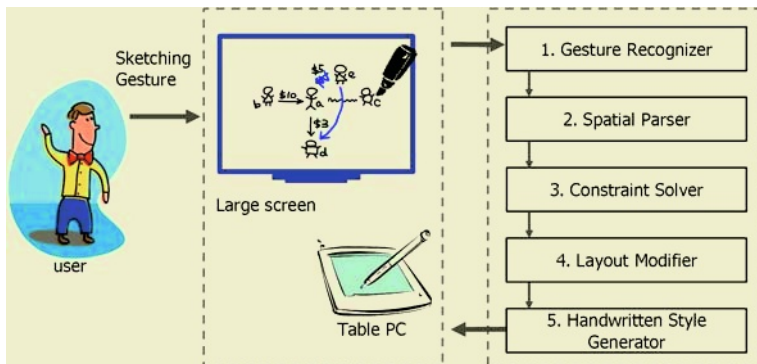


Fig. 1. Architecture of the proposed tool

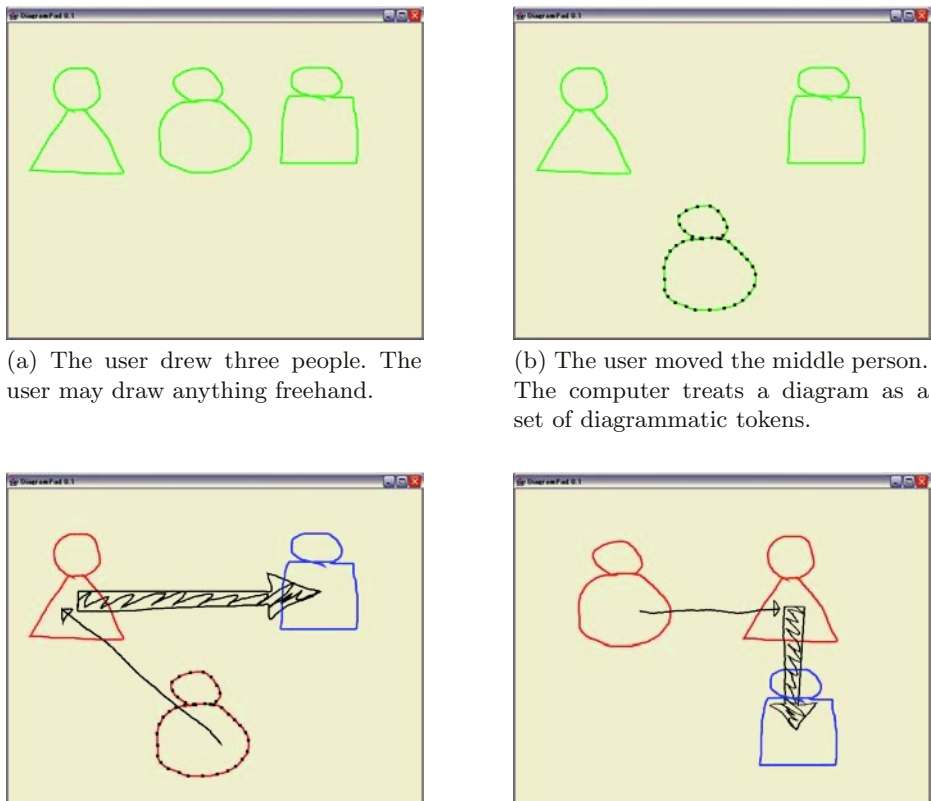


Fig. 2. Sample screens of handwriting tool intended for a logical domain

3.3 Behavior of the Prototype Tool

We introduce the behavior of the tool by referring to some screen shots. In Figure 2(a) the user had drawn three people freehand, and in Figure 2(b) the user moved the middle person. The tool treats a diagram as a set of diagrammatic tokens, which are semantic units. In Figure 2(c) the user added two arrows representing relationships between the people. The arrows were also drawn freehand without a template. At that time, the tool understood that the arrows expressed logical relationships between the people. In Figure 2(d) the positions of the people have been moved by the user. The tool automatically changed the positions and the shapes of the arrows according to the movement of the people.

By using some other existing tools, logical relationships can also be expressed between unit shapes. However, an important point here is that the tool extracts logical structures from handwritten diagrams drawn freely and transforms the diagrams while preserving the feel of handwritten diagrams.

4 Related Works

We make the position of the proposed tool clear by introducing some related tools that use handwriting.

Tivoli [8] is an electronic whiteboard application targeted to run on the Xerox LiveBoard. It is designed to support informal workgroup meetings and uses handwriting input with a pen-type device. Electronic Cocktail Napkin [9, 10] and Flatland [11] are also tools aimed to develop informal features of the whiteboard.

Pegasus [12] is a drawing system for rapid geometric design. It “receives” the user’s free hand strokes and beautifies them by considering geometric constraints among segments. Teddy [13] is a 3D modeling system that provides a sketching interface for designing 3D freeform objects.

Silk [10, 14] is a tool focusing on the design support of GUI. It combines the advantages of sketching on paper with the advantages of using computer-based tools. DENIM [2] is a system that helps web site designers in the early stages of design.

Knight [15] is a whiteboard system for software development. It is designed to use the best features of the whiteboard and the CASE tool.

Domains of the tools can be characterized along the dimensions shown in Figure 3. The horizontal axis represents the target area of the tool. The vertical axis represents the form of the target information in creative activities. The

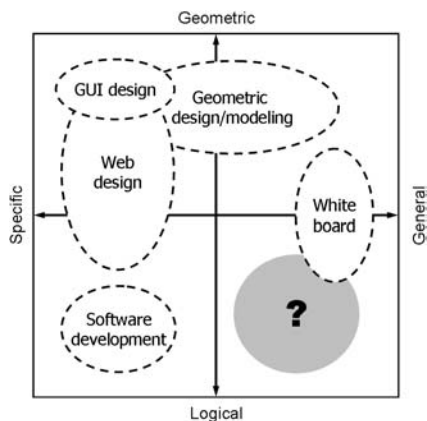


Fig. 3. Target domains of creative activity support

lower right area marked with “?” is a domain for which handwriting has not been used up to now. The tool we proposed in this article targets this domain.

5 Concluding Remarks

In this article we proposed a handwriting tool to support creative activities. The tool is intended for logical structures, which are useful in the upstream of creative processes. Handwriting, which the tool exploits, benefits human creative activities. We illustrated the position of the tool by introducing some other tools that use handwriting. We also described some technical problems were described in this article. Another issue that needs to be evaluated is how handwriting influences and affects thinking.

References

1. Kunifuiji, S. et al.: Trend of research and development of knowledge creation support system and current state of development in JAIST, Report of the 1st symposium on knowledge creation support (2004) 1–10 (in Japanese)
2. Lin, J., Newman, M. W., Hong, J. I., Landay, J. A.: DENIM: Finding a Tighter Fit Between Tools and Practice for Web Site Design, CHI 2000 (2000) 510–517
3. Kawakita, J.: The KJ-method, Chuokoron-sha (1967) (in Japanese)
4. Misue, K., Sugiyama, K.: Freehand-like drawing of compound graphs: A fundamental technique for computer aided abduction, Proc. 37th Conf. Information Processing Society of Japan, 4H-7 (1988) 1304–1305 (in Japanese)
5. Hong, J. I., Landay, J. A.: SATIN: A Toolkit for Informal Ink-based Applications, Proc. UIST 2000 (2000) 63–72
6. Baba, A., Tanaka, J.: Eviss: A Visual System Having a Spatial Parser Generator, APCHI'98 (1998) 158–164
7. Saoud, E., Fleet, D., Larner, D., Mahoney, J.: Perceptually-Supported Image Editing of Text and Graphics, UIST '03 (2003) 183–192
8. Pedersen, E. R., McCall, K., Moran, T. P., Halasz, F. G.: Tivoli: An Electronic Whiteboard for Informal Workgroup Meetings, INTERCHI '93 (1993) 391–398
9. Gross, M. D., Do, E. Y.-L.: Ambiguous Intentions: a Paper-like Interface for Creative Design, UIST '96 (1996) 183–192
10. Hearst, M. A., Gross, M. D., Landay, J. A., Stahovich, T. E.: Sketching Intelligent Systems, IEEE Intelligent Systems, Vol. 13, No. 3 (1998) 10–19
11. Mynatt, E. D., Igarashi, T., Edwards, W. K., LaMarca, A.: Flatland: New Dimensions in Office Whiteboards, CHI '99 (1999) 346–353
12. Igarashi, T., Matsuoka, S., Kawachiya, S., Tanaka, H.: Interactive Beautification: A Technique for Rapid Geometric Design, UIST 97 (1997) 105–114
13. Igarashi, T., Matsuoka, S., Tanaka, H.: Teddy: A sketching interface for 3d freeform design, SIGGRAPH 1999 (1999) 409–416
14. Landay, J. A., Myers, B. A.: Sketching Interfaces: Toward More Human Interface Design, IEEE Computer, March (2001) 56–64
15. Damm, C. H., Hansen, K. M., Thomsen, M.: Tool Support for Cooperative Object-Oriented Design: Gesture Based Modeling on an Electronic Whiteboard, CHI 2000 (2000) 518–525

Natural Storage in Human Body

Shigaku Iwabuchi, Buntarou Shizuki, Kazuo Misue, and Jiro Tanaka

Department of Computer Science, University of Tsukuba
1-1-1 Tennoudai, Tsukuba City, Ibaraki, 305-8573, Japan
{shigaku,shizuki,misue,jiro}@iplab.cs.tsukuba.ac.jp
<http://www.iplab.cs.tsukuba.ac.jp/>

Abstract. We propose using the human body for “storing” data used in devices for the imminent ubiquitous computing era. In the future, people will use information appliances as powerful creativity tools, using them for taking pictures, recording ideas, and recording voices. Removable medium are now widely used with such devices to record the data. However, data stored on a physical medium is troublesome to handle and thus hinders smooth knowledge creation. Natural storage using the human body would eliminate the physical burden.

1 Introduction

Storage devices that enable the user to store and carry digital data have played an important role in computing. Today, both removable media (e.g. compact disks, memory cards, and floppy disks) and fixed media embedded in a device (e.g. hard disks) are widely used.

In the upcoming era of ubiquitous computing, people will live in an environment where information appliances[1], i.e. tools in which computers are embedded, are distributed. Appliances that produce and/or replay digital data, such as digital cameras and portable voice recorders, will be particularly useful for organizing ideas. These appliances, however, will still require storage capability.

While removable media are fairly convenient for storing digital content, their weight and bulk impose a physical burden. In addition, breakage or theft of the media results in loss of data. While there has been research into storage for use in the ubiquitous environment, the systems proposed so far use physical (i.e. visible) media. They thus have the same problems inherent to conventional removable media. For example, the tangible file systemm[2] connects the ID on a sheet of paper to digital data. The personal server[3] is a mobile device that enables the user to carry personal storage in a ubiquitous environment.

We propose using the human body as a “storage device” by creating an illusion of data being stored in the body. We call this concept **natural storage**. Natural storage eliminates the problems of size, weight, etc. of conventional removable medium. Actualizing this concept requires developing appliances that give the user the illusion that data is stored in the user’s body. We developed prototypes of two such appliances to demonstrate this concept.

2 Concept of Natural Storage

The fundamental concept of natural storage is using the human body for storing digital data. Natural storage is used with appliances that need access to data in everyday life. It requires less knowledge of computers or data storage concepts as compared with current removable media. Natural storage does not require complicated knowledge, such as the path of files, the size of files, and the capacity limit of storage.

An example scenario of using natural storage is as follows. Today, we enjoy watching images taken with digital still cameras. To watch the images, we first insert a memory card into a camera to record the image data, and then we display the images on a computer screen or print them out to paper. When natural storage is applied to this situation, the images generated by the digital camera appear to be stored in the user's body. And when an appliance for outputting the data, such as a printer or a display, the data is directly output from the body (Figure 1).

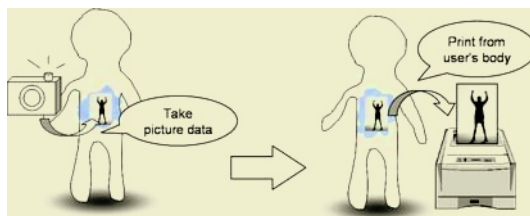


Fig. 1. Use of natural storage with appliances, capturing and printing out still images

It is also possible to apply natural storage to an appliance like a microphone for recording voice. When a user holds the microphone and speaks, the sound is recorded into the user's body. Then, using an appliance like a headphone, the user can listen to the stored sounds.

These appliances could be widely distributed for public use, enabling people to record or retrieve ideas. As people carry a pen and paper for recording and organizing their ideas today, these appliances will support creativity in the ubiquitous environment.

Using the human body for storage has three advantages in particular.

1. Carrying data imposes no burden because natural storage has neither weight nor size.
2. Data cannot be lost due to physical breakage.
3. The media cannot be forgotten. Since the data is stored in the user's body, the person always has it.

The first two still hold even in comparison to storing data in small and/or wearable devices such as cellular phones. As long as physical objects external to the user's body are used as media, there is still a burden. Even if the media is fully miniaturized, there is still the risk of the media being lost.

3 Design of Appliances

The key to the natural storage concept is giving the user the illusion of storage being in the user's body. This is done by implementing two functions in the appliance. (1) The appliance detects the user's ID and associates it with the user's actual storage in a network. (2) The appliance gives the user feedback as if natural storage is in the user's body.

To enable data to be carried and stored like data on removable media, the appliance associates the user's ID with actual storage in a network. Since networking is available anywhere in a ubiquitous environment, the storage associated with a user can be accessed anywhere. The implementation of storage in this way means that the access authority is attached while restrictions on the storage capacity can be concealed. The information needed for association is stored to a database. When the appliance is activated, the appliance sends the user's ID to the database and requests the location of the actual storage.

To create the illusion that the user's body is a storage device, the appliance gives the user feedback as if the data were actually being stored in and retrieved from his or her body as the user uses the appliance. Considering the interactions between a user and a storage device will help clarify the interfaces between the appliance and user. When storage is used, there are two interactions:

Addressing. Addressing specifies the storage to be used. This corresponds, for example, to the insertion of a floppy disk or the specification of a URL.

Feedback. Feedback presents the user the existence of storage. Feedback includes, for example, the blink of a pilot lamp and the sound and vibration of a spinning disk.

Note that a user cannot actually see what is happening between an appliance and the actual storage. The user grasps the image of storage using only the information acquired from interactions with the appliance. Therefore, the interface of an appliance should have two interactions, addressing and feedback, that give the user the illusion of data storage. Figure 2 illustrates how the user images natural storage. An appliance identifies the ID of the user(1), accesses the user's actual storage(2), and returns the result to the user(4). The addressing interaction corresponds to detecting the user's ID. The feedback interaction corresponds to presenting the result. Both of interactions, (1) and (4), cause the user to image the natural storage(3). The designs of each interaction are as follows:

- For ID identification, the appliance should support biometric identification methods, such as fingerprint and iris pattern recognition, because such methods actively involve the human body. The best method to use depends on the type of appliance. For example, fingerprint recognition is effective for handheld appliances, such as microphones and digital cameras. Camera-based ID verification is suitable for appliances used at a distant.

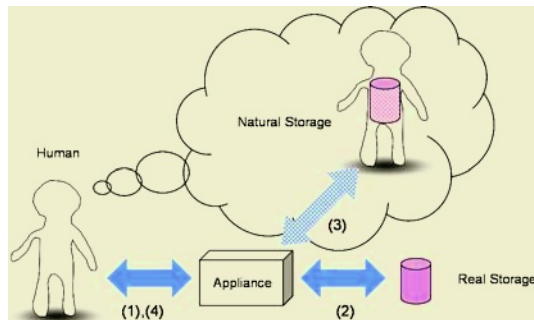


Fig. 2. The user images natural storage, not a real storage, from the interaction with the appliance

- The interface supporting feedback interaction should also use the user's body. For example, an access lamp attached on the user's body can help create an illusion of storage. The illusion is enhanced by providing virtual sounds and vibration associated with using natural storage.

4 Prototypes

We are developing two appliances that use natural storage.

4.1 Natural Storage Camera

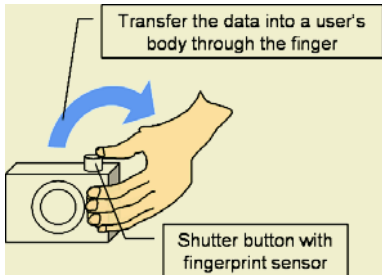
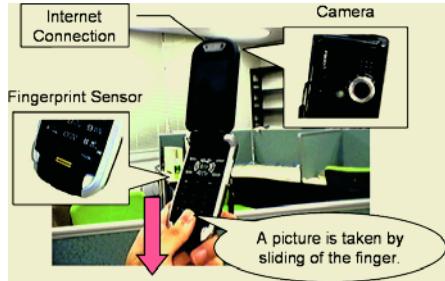
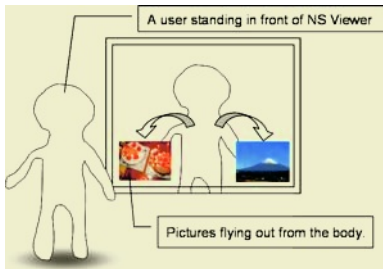
Our natural storage camera (NS camera) is a digital camera that uses natural storage. A fingerprint sensor functions as the shutter button. The data for pictures taken with the camera are virtually stored in the body of the person who presses the shutter button (Figure 3). Consequently, the camera does not need removable media to record picture data.

We are using NTT Docomos F900iT cellular phone for the prototyping. The F900iT has a camera, fingerprint sensor, and wireless internet connection. These functions are controlled by a program written in Java. Moreover, its size and portability are similar to those of a typical digital camera. Figure 4 shows an overview of the prototype.

The functions are as follows. When the user slides his or her finger on the fingerprint sensor, the camera takes a picture. Simultaneously, the camera obtains the user's ID from the fingerprint and acquires the network path to the actual storage from a database on the server. The picture data is then uploaded to the actual storage associated with the ID. From the user's viewpoint, it appears as if the data was saved inside his or her body through the finger.

4.2 Natural Storage Viewer

Our natural storage viewer (NS viewer) appliance is a kind of mirror for looking at pictures stored in a user's body. Figure 5 shows an idealized image of the NS

**Fig. 3.** NS camera overview**Fig. 4.** Prototype of NS camera (F900iT)**Fig. 5.** NS viewer overview**Fig. 6.** Prototype of NS viewer

viewer. It consists of a display and a camera. When the user stands in front of NS viewer, not only is the user's body mirrored but so are the pictures stored in the body. The pictures appear to fly out of the body and then circle along the user's image in the screen. The scale of the pictures changes with the distance between the viewer and the user. To look at the pictures more closely, the user approaches the viewer.

Figure 6 shows a picture of the NS viewer prototype. It consists of a plasma display and a 110,000-pixel resolution camera. The camera is attached to the upper part of the plasma display so that the scene in the front of the camera can be captured. In the present version, a square marker is attached to the user to enable the user's ID to be detected and to determine the user's location.

NS viewer works as follows. First, one frame in the video stream from the camera is captured, and the ID of the marker and its position in the frame are detected using the ARToolKit[4]. Next, the location of the storage associated with the ID is obtained from the database. In the present version, the location of the storage is represented by a URL. Picture files are downloaded from the directory to the location designated by the URL and superimposed around the marker in the frame. The plasma display then shows the resulting image. The image is flipped horizontally like in an actual mirror.

From the user's viewpoint, the operations inside the system, which were described above, are not visible. The interaction between the viewer and the natural storage appears simple. Standing in front of the plasma display corre-

sponds to the addressing interaction. The pictures circling the body, as reflected on the screen, correspond to the feedback interaction. Together, the addressing and feedback interactions give the user the illusion of the storage being in the user's body.

5 Discussion and Future Work

There are several approaches to making natural storage practical.

One possible approach is to embed in the user a memory device that can wirelessly access by radio. While embedding RFID tags in the body is already practical[5], it still carries a physical risk and can create mental anxiety. Our approach of associating storage with a personal ID results in virtual realization, so there is no risk or anxiety.

Storing data and carrying data between appliances can be done using network sharable storage (e.g. NFS on Linux), which does not require a removable storage device. There is thus no physical burden, similar to natural storage. However, from the user's viewpoint, storage on the network is a logical concept with no shape. Natural storage uses a concrete object, the human body, as imaginary storage.

Theoretically, many types of data could be stored using natural storage. How to handle a large amount of data in natural storage, i.e. scalability, is a major issue. As the amount of data increases, the need for managing the data also increases. Conventional removable storage devices and file systems use physical media, enabling the user to understand the location of the data intuitively. To enable the user to intuitively recognize data stored in natural storage, we could store the different types of data in different body parts. For example, text data could be stored in the left hand, pictures in the right hand, and music in the ears. With an appliance like NS viewer, the user could recognize the different types visually.

An appliance that accesses natural storage needs to be in an environment in which there is a radio network. Candidate locations include spaces where a computer is omnipresent, such as Active space[6]. A limited space, like a classroom or office, may also be suitable.

We plan to enhance our prototypes. For example, the present prototype of NS viewer recognizes a user's ID by detecting a marker attached to the user's body. Personal recognition using image processing would be more efficient.

6 Related Work

Some systems assign IDs to objects and associate online data with those IDs. mediaBlocks [7] uses a wooden block attached to an RFID tag, called a "tangible bit", as a container for online data. IconSticker[8] transfers an icon on a computer desktop to the real world as a paper icon printed as a barcode. This enables treating data as real-world objects. Pick and Drop[9] moves data between a computer and real-world objects by using the barcode. The prototype enables

data to be transferred from paper to a computer, apparently with a pen-type device. All of these systems involve real-world objects or an exclusive-use device. Consequently, they impose the same physical burden as removable media. In contrast, natural storage, which appears to use the human body for storage, imposes no such burdens.

7 Conclusion

In this paper, we proposed natural storage that seemingly exists in the human body. It eliminates the physical burden of conventional removable storage. For its application, natural storage enable people to record ideas anywhere at anytime with information appliances. The appliance interface should have two interactions, addressing and feedback, that give the user the illusion of data storage and retrieval. Two prototypes, a natural storage camera and a natural storage viewer, have demonstrated this concept.

References

1. Norman, D.A.: *The Invisible Computer*. MIT Press (1998)
2. Karypidis, A., Lalis, S.: The tangible file system. In: Proceedings of the 23rd International Conference on Distributed Computing Systems Workshops (ICDCSW'03). (2003) 268–273
3. Want, R., Pering, T., Danneels, G., Kumar, M., Sundar, M., Light, J.: The Personal Server: Changing the Way We Think about Ubiquitous Computing. In: Proceedings of Ubicomp 2002: 4th International Conference on Ubiquitous Computing. (2002) 194–209
4. (ARToolKit) URL: <http://www.hitl.washington.edu/artoolkit/>.
5. (VeriChip) URL: <http://www.4verichip.com/>.
6. Roman, M., Hess, C.K., Cerqueira, R., Ranganathan, A., H, R.: Gaia: A middleware infrastructure to enable active spaces. In: IEEE Pervasive Computing. (2002) 74–83
7. Ullmer, B., Ishii, H., Glas, D.: mediaBlocks: Physical Containers, Transports, and Controls for Online Media. In: SIGGRAPH'98. Computer Graphics Proceedings, ACM (1998)
8. Siio, I., Mima, Y.: IconStickers: Converting Computer Icons into Real Paper Icons. In: Human-Computer Interaction, Ergonomics and User Interfaces. Volume 1 (HCI International '99). (1999) 271–275
9. Rekimoto, J.: Pick-and-drop: A direct manipulation technique for multiple computer environments. In: Proceedings of UIST'97. (1997) 31–39

Computerized Support for Idea Generation During Knowledge Creating Process*

Xijin Tang¹, Yijun Liu^{1,2}, and Wen Zhang^{1,2}

¹ Institute of Systems Science, Academy of Mathematics and Systems Science
Chinese Academy of Sciences, Beijing 100080 P.R. China

² Graduate School, Chinese Academy of Sciences, Beijing 100039 P.R. China
`{xjtang, yijunliu, zhangwen}@amss.ac.cn`

Abstract. In daily life, people spend a lot of time in group activities, such as communication, debate, collaboration and consensus achieving for problem solving where creative ideas are expected to be generated by active interaction and stimulation between participants. In this paper, we focus on exploring effective computerized support for group argumentation, mainly on group brainstorming for idea generation. Versatile aids are explored, such as visualization of expert opinion structure, text-mining of external information, clustering of contributed opinions and various analysis about participation, etc. and integrated into a group argumentation environment (GAE), to support the emergence of a *ba* for knowledge creation. We apply such an environment to top-level small-scale academic conferences (Xiangshan Science Conference) on frontiers of science and technology in China.

Keywords: Idea generation, knowledge creation, meta-synthesis, *ba*, Xiangshan Science Conference

1 Introduction

In daily life, people spend a lot of time in group activities, such as communication, debate, negotiation, collaboration and consensus building. Group argumentation, especially held in most expert meetings, academic seminars, etc, is regarded as a convenient way to acquire ideas or knowledge from experts for new options or solutions towards complex problems. To facilitate group argumentation for idea generation, heavy endeavors have been engaged in computerized support with social cognitive perception of human creativity and tremendous advances of information technologies. Research on human creativity provides conceptual models for creativity support systems (CSS) or similar tools. Famous models about creativity proposed by western scholars are 4-stage model by G. Wallas in 1926 [1] and 2-space transformation model by M. Boden [2]. Continual refinements or extensions of both models have been applied and brought out many CSS or idea processors [3, 4]. On the other hand, by deep thinking over oriental epistemology creativity while absorbing western thoughts, eastern people also proposed conceptual framework of creativity or knowledge creation. Japanese scholar I. Nonaka proposed SECI model about organizational

* Supported by Natural Science Foundation of China (Grant No. 79990580 & 70221001)

knowledge creating process based on Polanyi's distinction between tacit knowledge and explicit knowledge and related 4 distinguished kinds of *ba* for different phases of SECI process [5, 6]. *Ba* can be viewed as a platform where knowledge is created, shared, and exploited. So how to develop a right *ba* for exploiting and creating knowledge effectively and efficiently is a major concern. Most computerized support tools for group work can provide help for effective interaction between participants under different levels or facets during knowledge creating process, such as communication, information sharing, argumentation or even sense making, such as AIDE [7], and many other lab or business products.

In early 1990s, Chinese system scientist X. S. Qian proposed meta-synthesis approach (MSA) and the concept of Hall of Workshop for Meta-Synthetic Engineering (HWMSE) which serves as a test bed of meta-synthetic support for unstructured problem solving by utilization of breaking advances in information technologies [8, 9]. The essential idea of MSA can be simplified as "confident hypothesizing, rigorous validating", i.e. quantitative knowledge arises from qualitative understanding. MSA accepts Chinese philosopher's distinction of qualitative facet and quantitative facet of human intelligent capability and calls for man-machine collaboration during problem solving process, and emphasizes the active roles of human beings during human-machine collaboration, which is beyond traditional decision support systems (DSS) where machine plays active roles during human-machine interaction. For unknown or new issues, new knowledge is often needed for a creative and practical solution. Creative solutions may refer to wisdom. Then HWMSE is expected to enable knowledge creation and wisdom emergence. Moreover HWMSE could be treated as a *ba* for knowledge creating [10, 11].

In this paper, we concentrate on computerized support for group argumentation for idea generation during problem solving process, which is supposed as a knowledge creating process. The basis of our work is MSA and HWMSE in consideration of both western and eastern models in creativity and rich achievements in CSS. Versatile computerized aids have been developed, such as visualization of expert opinion structure, text-mining of external information, clustering of contributed opinions and evaluation of subjective participation, etc. and integrated into a group argumentation environment (GAE), to support the emergence of a *ba* for knowledge creation. An application of GAE to top-level small-scale academic conferences (Xiangshan Science Conference) on frontiers of science and technology in China is given and future works are indicated.

2 Computerized Support for Meta-synthetic Support for Idea Generation

For hypothesis (scenarios or multiple perspectives) towards unknown issues during problem solving process, creative ideas are always desired especially for different perspectives development. Idea generation is always applied during divergent thinking process and usually starts with a topic, which is the anchor for creative thinking and insights of the topic are expected to be acquired or for further investigation from a variety of expanding aspects. In this section, the framework of our developing versatile aids for group working process is given.

2.1 Framework of Computerized for Group Argumentation

Fig. 1 shows the three layers (interfacing, function and data services) of the functional structure of the integrated group argumentation environment (GAE) which is based on client/server framework and mainly includes an online electronic brainstorming argumentation room (BAR).

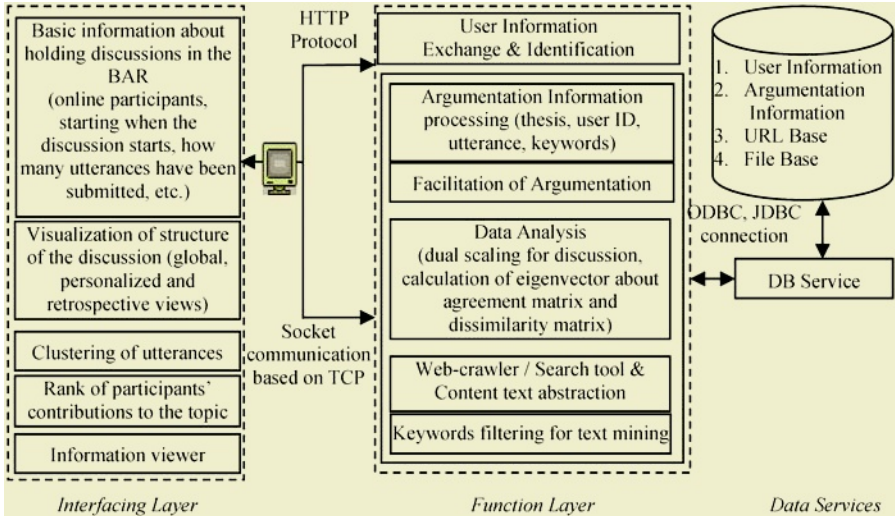


Fig. 1. Functional Framework of Group Argumentation Environment

Interfacing layer shows what can be achieved at client window of BAR, and function layer is services provided at server side. Firstly, GAE can be regarded as a group support system. Furthermore, by providing visualized thinking structure during the group working process together with a variety of analytical mechanism about the process and participants, it aims to support emergence of a dynamic originating *ba* and evaluation of its effectiveness which is one of core issues in providing meta-synthetic support for unstructured problem solving [12]. Follows introduce some salient functions.

2.2 Visualized Shared Memory for Group Argumentation

As shown in Fig 2(a), the main client window for visualized shared memory (as depicted at the interfacing layer in Fig. 1) is consisted of event record area, dialoguing area and visualizing area.

Both common viewer and personal viewer provide timely updated visualized global structure about relationships between participants and their keywords/utterances in the session at the shared visualized area and help to acquire a whole perspective about the discussed topic which may expose some structured elements of an unstructured issue.

Fig. 2(b) shows retrospective analysis which applies same mechanism as both viewers and provides participants to “drill down” the discussing process for visualized

partial perspectives. Further analysis of pieces of discussion such as selected intervals of discussion or combination of any selected participants may be helpful to detect the existence or formulating process of a micro community and acquire further understanding about participants' thinking structure.

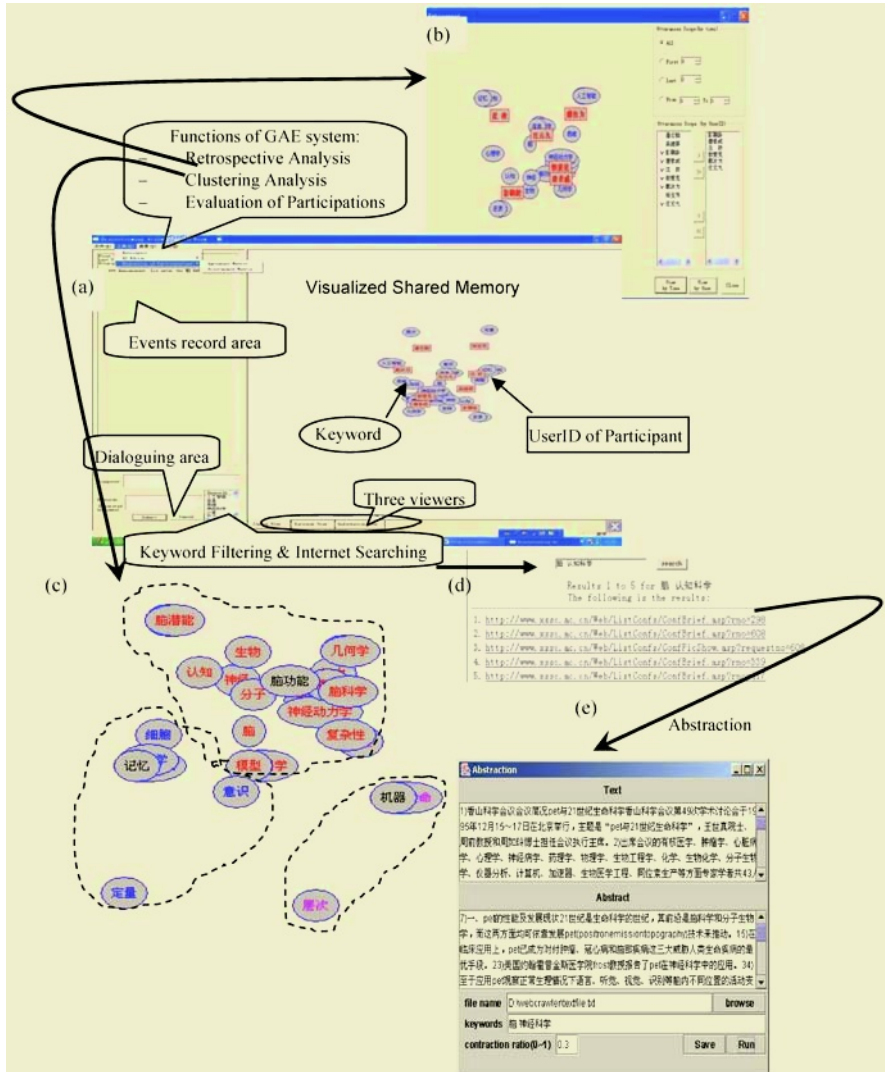


Fig. 2. Client Window of BAR (a) Main client window, (b) Retrospective viewer, (c) Clustering analysis ($K=3$), (d) Selected keyword searching, (e) Text abstraction

2.3 Information Support

Currently there are two ways to provide external information for participants in the course. One is to search Internet directly via any searching engines. Another is sup-

ported by text mining techniques. Here three tools are provided, web-crawler, search tool and content text abstraction. The web-crawler is tailored to collect the web pages automatically from WWW which are relevant with concerned topic; search tool provide access to relevant information (web) pages collected via web-crawler according to selected keywords; and content text abstraction extracts the information page into an outline by Luhn method [13].

2.4 Outcome of Argumentation and Evaluation of Participation

Besides basic functions of visualization of expert opinion structure during argumentation process for expanding both individual and group thinking spaces, some work has also been undertaking by synthesizing practical requirements, psychological models and algorithms when more concerns go to procedural rationality of group working process. Currently, two kinds of supports are available in evaluation of a session. 1) Automatic summarizing of experts ideas, which is mainly based on KJ method. There are two ways based on visualized spacial relations. One is to map the 2-dimension structure into 16×16 grids. Those utterances which fall into same cell is regarded as one cluster. Another uses K-means clustering method to get k centroids, where k is an assumed number of clusters. The closest keyword to the centroid could be regarded as cluster label. 2) Evaluation of participation by calculation of eigenvectors about agreement matrix and dissimilarity matrix. Both matrixes are constructed by the number of keywords shared or different between all participants.

Next we apply our tool to analyze Xiangshan Science Conference (XSSC, www.xssc.ac.cn), which is initiated in 1993 in similar to Gordon Research Conferences and denotes as the general designation of a series of small-scale academic meetings which bring together a group of scientists working at the frontier of research of a particular area and enable them to discuss in depth all aspects of the most recent advances in the field and to stimulate new directions for research in China.

3 GAE Practice in Xiangshan Science Conference

In this experiment, all those conferences whose main theme is about ‘brain & mind’ are selected from over 200 conferences. The chairpersons and people who give plenary speeches are participants and the titles of their talks are utterance. Then we have 9 participants. Fig. 2 shows basic analysis taken in this test. Fig. 2(a) is a whole perspective of all concerned scientists’ contributions among those concerned conferences. It shows participants who share more common keywords locate closer in the 2-dimension space. Fig. 2(c) shows 3 clusters by K-means clustering method, where keywords   and  are acquired as the label (centroid) of each cluster.

Table 1 lists the evaluation of participation based on agreement and discrepancy matrixes. It is shown that user  holds highest rank based on both eigenvectors, which may be justified by his active role as one of chairpersons or plenary speech contributors among those conferences, which furthermore exposes his big influence in neuroscience field in China.

Table 1. Evaluation of 9 Participants

| | |
|---|--|
| Maximum eigenvector of agreement matrix: | (0.3761, 0.0914, 0.3082, 0.6179, 0.2522, 0.3618, 0.3125, 0.1937, 0.1092) 郭爱克 > 汪云九 > 唐孝威 > 彭聃龄 > 戴汝为 |
| Rank of the top five participants: Meaning of the indicator: | which expert holds more common concerns during the brainstorming session |
| Maximum eigenvector of discrepancy matrix: | (0.3438, 0.2799, 0.3437, 0.4088, 0.3482, 0.3274, 0.3628, 0.2839, 0.2783) 郭爱克 > 彭聃龄 > 沈政 > 汪云九 > 戴汝为 |
| Rank of the top five participants: Meaning of the indicator: | which expert's perspectives are more diverse than those of other people during the brainstorming session |

It is expected such kind of further analysis about users' participation could provide more information about the performance assessment of group argumentation, and for further testing of some assumptions about individual impacts towards group behaviors.

4 Concluding Remarks

In this paper, we focus on computerized support for group argumentation for idea generation. Research on creativity and knowledge creation together with computerized supports provides basis for our research, which is mainly on man-machine collaborative meta-synthetic support for complex problem solving. What we are exploring is not only a computerized support tool for idea generation, but also expecting to support the emergence of originating *ba* during group interacting process. Our developed group argumentation environment exhibits our ideas in combining SECI model and concept of HWMSE.

Our current work is still at very initial stage from both research and practice [11, 14, 15]. From the research perspective, currently we mainly concentrate on divergent thinking process supporting for confident hypothesis formulation, a basic step of meta-synthesis approach [8]. The aim of GAE is to support dynamic emergence of a knowledge creation environment (*ba*). Lots of further work are under exploration, such as better human-machine interaction, opinion synthesis in consideration of expert's background, and evolving process of keyword network to detect the pathway of knowledge creation, etc. More experiments will also be undertaken for verification and validation of GAE in practice. XSSC is a rich land for such kind of tests.

References

1. Wallas, W.: Art of Thought. London: J. Cape, (1926)79-107
2. Stefik, M., Smolar S. (eds.): The Creative Mind: Myths and Mechanisms: six reviews and a response. Artificial Intelligence, Vol. 79, No.1(1995) 65-67
3. Chen, Z.: Toward a better understanding of idea processors. Information and Software Technology, Vol.40, No.10 (1998) 541-553
4. Aihara, K., Hori K.: Enhancing creativity through reorganizing mental space concealed in a research notes stack. Knowledge-Based Systems, Vol. 11, No. 7-8 (1998) 469-478
5. Nonaka, I., Takeuchi, Y.: Knowledge Creating Company. Oxford University Press, New York (1995)

6. Nonaka, I., Konno, N., Toyama, R.: Emergence of ‘*Ba*’. In: Nonaka, I., Nishiguchi, T.(eds.): *Knowledge Emergence*, Oxford University Press, New York (2001) 13-29
7. Mase, K., Sumi, Y., Nishimoto, K.: Informal Conversation Environment for Collaborative Concept Formation. In: Ishida, T. (eds.): *Community Computing: Collaboration over Global Information Networks*, Wiley (1998)
8. Qian, X. S., Yu, J.Y., Dai, R.W.: A new Discipline of Science - the Study of Open Complex Giant System and its Methodology. *Chinese Journal of Systems Engineering & Electronics*, Vol. 4, No. 2 (1993) 2-12
9. Qian, X. S.: *Establishing Systematology*. Shanxi Science and Technology Press, Taiyuan (2001) (in Chinese)
10. Tang, X. J.: Towards Meta-Synthetic Support to Unstructured Problem Solving. In: Chen, G. Y. et al. (eds.): *Proceedings of the Fourth International Conference on Systems Science and Systems Engineering*. Global-Link Publisher, (2003) 203-209
11. Tang, X. J., Liu, Y. J.: Computerized Support for Idea Generation during Knowledge Creating Process. In Cao, C.G., Sui, Y.F. (eds.): *Knowledge Economy Meets Science and Technology (KEST'2004)*, Tsinghua University Press, Beijing, (2004) 81-88
12. Tang, X. J., Liu, Y. J.: Exploring computerized support for group argumentation for idea generation. In: Nakamori, Y. et al. (eds.): *Proceedings of the fifth International Symposium on Knowledge and Systems Sciences*, Japan (2004) 296-302
13. Luhn, H.: The automatic creation of literature abstracts. *IBM Journal of Research and Development*, Vol. 2, No. 2 (1958)159-165
14. Tang, X. J., Liu, Y. J.: A Prototype Environment for Group Argumentation. In the Proceedings of the 3rd International Symposium on Knowledge and Systems Sciences, Shanghai (2002) 252-256.
15. Liu, Y. J., Tang, X. J.: A Visualized Augmented Tool for Knowledge Association in Idea Generation. In Gu, J. F. et al. (eds): *Knowledge and Systems Sciences: Toward Meta-Synthetic Support for Decision Making (KSS'2003)*, Global-Link Publishers (2003)19-24

Awareness in Group Decision: Communication Channel and GDSS

Hitoshi Koshiba¹, Naotaka Kato², and Susumu Kunifugi¹

¹ Japan Advanced Institute of Science and Technology, Ishikawa, Japan
{hkoshiba,kuni}@jaist.ac.jp

² Industrial Research Institute of Ishikawa, Ishikawa, Japan
kato@irii.go.jp

Abstract. This paper presents the effects of “Awareness”¹ in group decisions. The important objectives of this study are: (1) to analyze the group-decision process from the viewpoint of “awareness”. (2) to analyze and compare the effects of using group decision support system (GDSS), and (3) to analyze the decision-making process using a high-performance video conferencing system (involving high resolution and real-size pictures) as well as a general video conferencing system.

1 Introduction

Researches on computer supported cooperative work (CSCW) and Groupware have received considerable attention from many researchers. Further, GDSS is a common area of research by both CSCW and Groupware.

Information technology has advanced in recent years and has introduced several communication channels into our society. It is considered to be one of the essential and noteworthy technologies that has changed our daily life and is rapidly becoming an integral part of modern society. It is not only changing our communication style in terms of the use of GDSS but is also providing new platforms and environments. In the past, GDSS was used only in a face-to-face environment[1]; however, new advanced technologies have made it possible to use GDSS in face-to-face as well as distributed environments.

Research in the realm of CSCW and Groupware indicates that “awareness” is closely related to both the communication channel and collaborative work. Therefore, CSCW and Groupware researchers are increasingly paying more attention to “awareness.” At present, researches on GDSS are focusing only on the changes in communication channels [2, 3] and limited research works are available on the issue of “awareness.”

In this paper, we discuss the importance of “awareness” in using GDSS and its impact on the consensus-building process. Further, we discuss the differences in decision making due to the use of different communication channels.

¹ In this paper “awareness” means, important information in cooperative working, such as general information that we are usually unaware of. It is tacit knowledge. For example, WYSIWIS (What You See Is What I See), eye contact, etc.

The primary focus of this study is to understand the manner in which “awareness” can be used for effective and efficient decision making. We attempted to achieve this through experiment and analysis. We studied the effect of “awareness” on decision making in certain communication channels with and without the GDSS.

In this experiment, we used the following communication channels: a face-to-face environment and two different types of distributed environments, namely, a simple and convenient video conferencing system and a high-quality video conferencing system. The reason for considering two different distributed environments was that they allowed us to experiment with a variety of video conferencing systems. An example of a simple and convenient video conferencing system is NetMeeting, a Microsoft product, which is commonly used in distributed environments. On the other hand, the high-performance video conferencing system uses high resolution and real-size pictures. The scope, size, and quality of the pictures are known to be closely related to the “awareness” levels. Thus, the use of two different distributed environments would enable us to distinguish between the simple and convenient and the high-quality video conferencing systems.

In this paper, the environment that employs a simple and convenient video conferencing system is referred to as the “distributed environment” and the other that employs a high-performance video conferencing system is referred to as the “virtual face-to-face environment.”

2 Experiment

2.1 Experimental Condition

In this experiment, we settled a problem by group decision making. The theme chosen for group decision was “choice of destination for the transfer of national capital functions.” This theme is a real project conducted by the Japanese government. The reason for selecting this theme was as follows: 1. Subjects may have been interested in the theme. 2. Subjects may not have felt much about the theme.

The same theme for decision was considered in all the environments. All subjects performed each experiment independently and under different conditions.

Study subjects comprised 40 graduate students who were divided into 20 pairs. For the experiments using GDSS, subjects comprised 22 graduate students who were divided into 11 pairs, including 3 pairs that were subjected to the face-to-face environment, 4 pairs to the distributed environment, and 4 pairs to the virtual face-to-face environment.

On the other hand, for the experiments that did not use GDSS, the subjects comprised 18 graduate students who were divided into 9 pairs, including 3 pairs that were subjected to the face-to-face environment, 3 pairs to the distributed environment, and 3 pairs to the virtual face-to-face environment.

2.2 Experimental Process

First, the subjects were made to read a document for 10 minutes. Subsequently, they participated in a group decision-making. In the case of experiments that did not use

GDSS, the subjects participated in an uninhibited decision making, while in the case of the experiments using GDSS, subjects accomplished decision making by following the steps shown in Fig. 1.

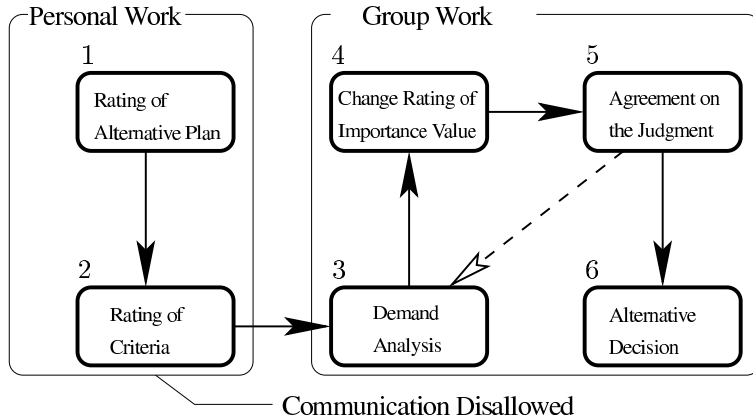


Fig. 1. Group Decision Process

2.3 Experimental Environment

Face-to-Face Environment: The subjects were seated facing each other across the table. A distance of approximately 1 m was maintained between them. In the case of experiments using GDSS, a 15-inch display was placed on the table for the purpose of GDSS.

Distributed Environment: The subjects were directed to a room that was equipped with a 15-inch display and a mobile PC placed on the table. GDSS was displayed on the 15-inch display and NetMeeting was run on the mobile PC (equipped with a USB camera and microphone). This setup established the simple and convenient video conferencing system. The picture had a QCIF resolution of 176×144 pixels. The subjects were attempted to communicate using this setup.

Virtual Face-to-Face Environment: The subjects were directed to different rooms that was equipped with a 15-inch display and a 90-inch projector. The 15-inch display was provided for GDSS, and the 90-inch projector was meant to be used with PCS-1 (a Sony product) for communication. This setup constituted the high-quality video conferencing system. The picture had a XVG resolution of 1280×768 pixels. The subjects attempted to communicate using this setup.

Snapshots of the experiments of using GDSS environments are shown in Figs. 2-4.

2.4 Experimental System

A existing GDSS-Group Navigator[4] was used in this research. The Group Navigator was designed as a decision-making support system for alternative evaluation.

We improvised the Group Navigator by modifying certain functions and adding the TCP/IP communication function. The features of the Group Navigator are as follows:



Fig. 2. Face-to-Face Environment



Fig. 3. Distributed Environment



Fig. 4. Virtual Face-to-Face Environment

1. Its design is based on WYSIWIS (What You See Is What I See), which enables sharing of viewpoints.
2. It supports mutual understanding.
3. On the basis of the subjective judgment capability acquired by alternative evaluation decision-making process, suggestions on new approaches of consensus-building support by using sensitivity analysis are provided.

A group comprised 4 to 5 persons, and face-to-face and distributed environments were used as communication channels. The previous study reported employed only face-to-face environment[4].

A screenshot of the system is shown in Fig. 5.

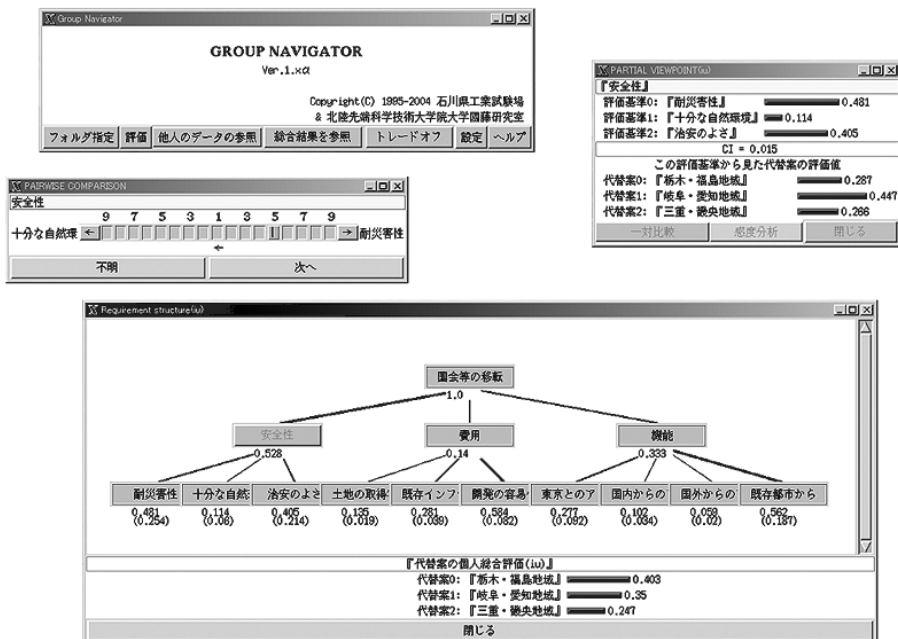


Fig. 5. Screenshots of Group Navigator

2.5 Evaluation Index

Qualitative evaluations were made on the basis of an interview and a 13-item questionnaire on decision and communication. Quantitative evaluations were based on speech times, percentage of tagging speech², duration of the group decision-making process, etc.

3 Results

The 6 conditions considered in this study are listed in Table. 1. The table presents remarkable excerpts selected from the data of the results obtained. Further, it provides a relative comparison.

Table 1. Experiment Result (excerpts of data)

| | | Satisfaction of Decision Process | Satisfaction of Result | Consent of Result | Communication Stress-less | Percentage of Tagging Speech | Percentage of Face viewing |
|-------------------------|--|--|----------------------------------|----------------------------------|------------------------------------|----------------------------------|----------------------------------|
| Face-to-Face | Using GDSS Without GDSS using | C A | C B | C B ⁺ | C B | A B | A ⁺ C |
| | Using GDSS Without GDSS using | C ⁺ B | A C ⁺ | B ⁺ B ⁺ | B ⁺ C ⁺ | B ⁺ C ⁺ | C ⁺ B ⁺ |
| Virtual Face-to-Face | Using GDSS Without GDSS using | B ⁺ A ⁺ | B ⁺ A ⁺ | A A ⁺ | A A ⁺ | A ⁺ C | B A |
| | | A ⁺ :Highest B ⁺ :Upper Middle C ⁺ :Low | | | A:High B:Low Middle C:Lowest | | |

4 Discussion

4.1 Effects of Change in Communication Channel

Changes in the communication channel are associated with “realistic presence awareness,” which involves actions similar to those involved in “atmosphere awareness.” It includes some “awareness” about one’s line of sight, motion, emotion, etc. It is a scale to measure “how much does it resemble a face-to-face environment?” when an environment is not a face-to-face environment. Therefore, the “realistic presence awareness” level was estimated for all the communication channels used in this study, namely, face-to-face environment, virtual face-to-face environment, and distributed environment.

There are several published studies available on “awareness” and communication channels. The novel conclusions obtained from our experiments are as follows:

1. Each subject in the virtual face-to-face environment has a more agreeable impression of the group decision-making process.
2. He/she may exert a positive influence on the group decision-making process if it is held in the middle course of “realistic presence awareness.”

Therefore, our approach that used a simple and convenient video conferencing system and a high-performance video conferencing system was justified.

² We transcribe speech to character using video and tag it

4.2 Effects of the Use of GDSS

The satisfaction and consent of subjects are limited in most communication channels; however, in our experiment using GDSS, tagging speech exhibited an improvement of 3% to 11% in all communication channels. High percentage of tagging speech implies a high-quality discussion[5]. We believe that this was caused by “knowledge awareness[6]” and “context awareness” supports provided by GDSS.

4.3 Communication Channel and Group Decision

In the face-to-face environment, subjects of the groups using GDSS were stressed out. This suggests that a face-to-face environment has low affinity for GDSS. Hence, if negotiation professionals are carrying out group decision making using advanced tactics, we suggest that the face-to-face environment without GDSS be considered. However, if a negotiation professional is not involved and a rational discussion is desired, we suggest that a distributed environment with GDSS be used as it has high affinity for GDSS. Further, if a friendly discussion is desired, we suggest that a virtual face-to-face environment with GDSS be considered because it supports friendly discussion and has a high affinity for GDSS. Incidentally, a low percentage of tagging speech was observed in the virtual face-to-face environment without GDSS, which supports the possibilities of divergent-thinking support.

4.4 Awareness in the Group Decision Process

The following important types of “awareness” in group decision have been proposed by us: “realistic sensitive awareness,” “knowledge awareness,” and “context awareness.” Our hypothesis aims to include “awareness” in this group decision process. In the group decision support process shown in Fig. 1, steps 2 to 4 depict the externalization of the sense of values of the GDSS user, making the concept of “knowledge awareness” congenial. Steps 3 to 5 indicate that figure indicate repeated discussion and decision are essential in certain conditions, namely, value of consensus, mutual compromise, etc, making the concept of “context awareness” congenial. Steps 4 and 5 represent discussion. “Realistic sensitive awareness” is important in this case.

5 Conclusion

In this paper, we reveal important types of “awareness” in group decision using GDSS. Further, we also reveal the impact of “awareness” in the consensus-building process and the result of decision making with changes in the communication channels. The result helped us determine the manner in which “awareness” can be used more effectively in the decision-making process. Further, it also helped us select a communication channel for effective decision making.

References

1. J. F. Nunamaker, Alan R. Dennis, Joseph S. Valacich, Douglas Vogel, Joey F. George: Electronic Meeting System to Support Group Work, *Communication of the ACM*, Vol.34, No.7, pp.40-61, 1991
2. Jerry Fjermestad: An Analysis of Communication Mode in Group Support Systems Research, *Decision Support Systems*, Vol.37 No.2, pp.239-263, 2004
3. A. Obata, K. Ishigaki, S. Kunifuji: Effects of the Visual Channel on Remote Cooperative Work. *HCI International*, 2001
4. N. Kato, M. Chujo, S. Kunifuji: A Group Decision Support System by Externalizing, Sharing and Reflecting Individual Viewpoints. *INTERACT 1997*, 600-601, 1997
5. N. Kato: Group Decision Support System based on Sharing Individual Viewpoint in Consensus Building Processes, Doctoral dissertation, JAIST, 1998 (in Japanese)
6. T. Yamakami, Y. Seki: Knowledge Awareness in Asynchronous Information Sharing. Proc. of the IFIP TC8/WG8.4 ,Working Conference, pp.215-225, 1993

Aware Group Home: Person-Centered Care as Creative Problem Solving

Ryozo Takatsuka and Tsutomu Fujinami

School of Knowledge Science
Japan Advanced Institute of Science and Technology
1-1 Asahidai, Ishikawa, Japan
{ryozo-t,fuji}@jaist.ac.jp

Abstract. The population of elderly is rapidly increasing in Japan and we expect that almost eight percent of elderly people will suffer from dementia in 2015. The change suggests that we can no longer hospitalize them, but have to find some way to go along with them at home. Group Home is thought to be ideal form of caregiving in the sense that the inhabitants can keep their contacts with the locals and circumstance to feel at home. Managing Group Home may, however, often run into troubles due to the cognitive asymmetry between the elderly with dementia and caregivers. We address in this paper the problems we found in the communication between the people with dementia and caregivers and present design principles for Aware Group Home, which enhances the awareness of caregivers towards people with dementia using information technologies.

1 Introduction

The population of elderly is rapidly increasing in Japan and we expect that one fourth of our population are older than sixty-five years in 2015, which amounts to thirty three million people. The number of people with dementia, who need some types of care, is then estimated to be about two million five hundred thousand, which occupies almost eight percent of elderly people. The change suggests that we can no longer hospitalize them, but have to find some way to go along with them at home.

Group Home is a type of caregiving for the elderly with dementia, where a small group of people with dementia, normally limited to five to nine in Japan, live together in a house and live their lives at their best with an appropriate help from caregivers. Group Home is thought to be ideal form of caregiving in the sense that the inhabitants can keep their contacts with the locals and circumstance to feel at home.

Managing Group Home may, however, often run into troubles due to the cognitive asymmetry between the elderly with dementia and caregivers. The cognitive world of people with dementia is often inaccessible from cognitively normal people. Some people with dementia have provided us with their own witness[Boden 04], helping us understand what they think and how they feel.

We are, however, afraid that they are rather exceptional. Most caregivers are often stunned at the strange behaviors of people with dementia, before watching calmly what they are doing.

We address in this paper the problems we found in the communication between the people with dementia and caregivers and present design principles for Aware Group Home, which enhances the awareness of caregivers towards people with dementia using information technologies.

The paper is organized as follows. Section 2 addresses the problem in communication with people with dementia. Following sections 3 and 4 present our attempt to get an access to cognitive world of people with dementia. Section 5 explains some results and Section 6 makes our approach clear.

2 Understanding People with Dementia

Understanding a person with dementia (hereinafter PWD) is no more different than understanding a normal person. According to Situation Theory[Barwise 83], meaning is conveyed as follows: Suppose there exists an action, a_1 , by PWD. The action, a_1 , is then categorized into a particular type of act, T_1 . We realize the content of his action by categorizing a_1 into T_1 , which we express as $a_1 : T_1$, read as “ a_1 is of type T_1 .” A person who moves his legs repeatedly to push his body forward is, for example, understood to be ‘moving’. The distinction between a particular action and the type into which the action is categorized is of importance here.

Suppose that the PWD is a resident of a Group Home and he is moving to the entrance. His action then signals that he is going out, which we term as an action, a_2 . For a caregiver, the PWD’s action, a_2 , is categorized as ‘leaving’ home, which might lead to an accident. The caregiver, therefore, tries to stop him before his leaving home. The caregiver’s inference is schematically expressed as $(a_1 : \text{moving}) \Rightarrow (a_2 : \text{leaving})$ to be read as “moving means leaving.”

Let us now turn our attention to the cognitive world of PWD. Suppose that the PWD actually wanted to go home. His action of going out, a_2 , must be understood as ‘going home’ from his point of view. The PWD’s inference is thus as follows: $(a_1 : \text{moving}) \Rightarrow (a_2 : \text{going} - \text{home})$ to be read as “moving means going-home.”

We draw from the example above a conclusion that the caregiver and PWD are attuned to different sets of constraints, the constraints which give each action some meaning. Being attuned to different sets of constraints is a source of misunderstanding between them and the cause of troubles. The PWD is obviously angered if he is not allowed to go home no matter how well the caregiver tries to care the PWD. To understand PWDs fully, we have to attune ourselves to the same constraints to which PWDs attune themselves.

The difficulties in understanding PWD are addressed in two steps. The first step concerns the *categorization* of their behaviors and the second the set of *constraints* to which they attune themselves. We address each in the following sections.

3 Monitoring People with Dementia at Group Home

It is often difficult to categorize PWD's behaviors due to their limited cognitive abilities. Watching TV means, for example, to enjoy watching a broadcast program for normal people, but some PWDs lack the concept of broadcast and cannot distinguish things around them and events on-air on TV. The levels of cognitive abilities vary among PWDs, thus caregivers have firstly to observe PWDs as much as possible to understand how they perceive the state of affairs surrounding them.

It is desirable for caregivers to observe PWDs, but requires a particular care in doing so. Most PWDs may notice the attention directed toward them even if they are cognitively disabled to some extent. Caregiver's attention may disturb PWDs and lead to unwanted outcomes such as anxiety. As an attempt to keep out of the way each other, we have installed a set of video cameras on our Group Home for caregivers to observe PWDs unnoticed.

We have installed six cameras in total; camera1 toward the gate, camera2 toward the entrance hall, camera3 from the sitting room to the way of rest room and bathroom: that is, the dead space from kitchen, camera4 from the entrance hall to the corridor to the sitting room, camera5 toward the kitchen, and camera6 above the sitting room. Figure 1 shows cameras1 and 2 installed in the entrance hall. Six cameras covered the view of common places except those of rest rooms and bathroom. We have also installed two kinds of sensors at the entrance to detect a passer-by: that is, thermographic one and infrared one. The former one is used for all day and the latter one for night.

The images obtained through these six cameras are monitored on two 14 inch displays, one of which is installed at the entrance and the other in the sitting room. The display can show the images in four-divided, six-divided or individual scene. Four-divided scene containing four images available from camera1-4 is usually chosen, when the caregiver working in the kitchen utilizes the monitor the most frequently. The location-free display at 2.4GHz of wireless LAN is also utilized to catch the state of Group Home, when all hands of caregivers are full in a rest room or in a bathroom. The movies filmed via these six cameras are also stored in a hard-disk recorder and ready for viewing for a week.

4 Creating a Story People with Dementia Live

The second difficulty in understanding PWD is to understand the meaning of their behaviors from their own point of view. Our approach is to create a story a PWD lives, which is known as narrative-based care in the literature [Greenhalgh 98]. Here is an example of a male PWD, who often leaves our Group Home. Below is a case where the caregiver does not have an acquaintance with narrative-based care. The story is firstly narrated from PWD's point of view:

PWD's account: Now is the time my son comes back home from school. He will be in trouble if I am away from home because his mother has already died. I enjoyed my stay here quite a lot. I have to hurry up to



Fig. 1. Two cameras installed in the entrance hall

home now. Um... I am very tired and cannot walk. Eh, someone is calling me, but I cannot respond to him as I am in a hurry. He is telling me not to go, but I have to go. Oh, he is still following me. I have to run, but I cannot move my legs any more. God, I stumbled on a stone...

The same course of events can be narrated differently from a caregiver's point of view as follows:

Caregiver's account: The guy is recovering and can walk longer than before although he used to be in bed, rarely going out, when he was at his home. I believe that asking him to do some daily work at Group Home such as wiping the windows has improved his health. But he may stumble if I do not stop him now because he is not fully recovered so as to go back home on his foot. He is about to stumble, but he tries to run away when I call him. I wish if he stopped now. Oh my god, he stumbled. No wonder, he was too hurry to walk.

The above story explains why the PWD stumbled in response to the caregiver's behavior. The PWD receives the caregiver's behavior as a threat. The incident was caused by the caregiver's ignorance of the PWD's cognitive world. The caregiver does not realize that it was himself who caused the accident be-

cause he attunes himself to a different set of constraints from those to which the PWD are attuned.

The things may change if the caregiver knows the PWD's story. Suppose that he understands the reason why the PWD left the Group Home by turning to the story. He can then play a role of onlooker until the PWD reaches the point where he can no longer walk. Once the PWD stops for a break, it is the chance for the caregiver to interrupt him by playing a role of someone with goodwill. If he offers a help, the PWD is willing to follow his advice, namely, to walk together to 'his' home, which is in fact the Group Home he has just left.

We have created a number of stories to each PWD. Each story observes the five rules as stated in [Greenhalgh 98]:

1. Narrative has a beginning, a series of unfolding events, and an ending.
2. Narrative presupposes both a narrator and a listener.
3. The narrative is concerned with individuals.
4. The narrative provides items of information that do not pertain simply or directly to the unfolding of events.
5. The narrative is absorbing.

5 Results

Three months have passed since we started our project and preliminary investigation revealed some characteristics in the use of images available via cameras. A series of interview to five caregivers working at our Group Home found that caregivers with longer experience utilize the images more frequently than those with shorter experience. By 'longer' we mean the experience of more than four years. We call the caregivers with longer experience *skilled*, while those with shorter experience *novices*.

Through the series of interview, we understood the reason why the skilled utilize the images more frequently than novices. They are good at applying a story to understand the mental state of each PWD. They frequently take a glance at the images to know what residents are doing and how they feel, but not stare. As the scene in the monitor is familiar to skilled, she merely follows her narrative reinforced by the scenes. Novices, on the other hand, have little time to view the images. They have also difficulties in understanding the cognitive world of PWDs. We conclude from our observation that it depends on how well a caregiver can understand the meaning of PWD's behavior how well she can utilize the images. The story helps caregivers decide when they should interrupt PWDs.

6 Person-Centered Care as Creative Problem Solving

Before concluding the paper, we would like to make our approach clear by comparing ours with traditional one. People with dementia have traditionally been

regarded as sick and a target of therapy. We call this traditional approach *medical model*. The problem of medical model is typically observed as a restriction on PWD's behaviors for the sake of cure. They may even be tied down to the bed so as not to do a harm to themselves or others at worst.

The reality is, however, PWDs are incurable for the moment, thus, it does not make much sense to treat PWDs based on medical model. Alternative is to place PWDs within social context and treat them as a person. We call this alternative *social model*. Our target is the person itself and we help him live a spontaneous life to his best. We have to, however, ensure him from accidents. The difference between these two models is summarized in Table 1.

Table 1. Medial Model vs. Social Model

| | Medical Model | Social Model |
|------------|-----------------------|----------------------------|
| Target | sickness | personhood |
| Objectives | therapy | assistance |
| Problem | restricted activities | life-threatening accidents |

We argue that the caregiving for PWDs is a creative problem solving and no different from other scientific activities. As other scientific activities do, we start by collecting first-hand data by observing behaviors of PWDs directly or through cameras. Observing PWDs through cameras is preferred to direct observation on the spot because direct observation may change the behavior of observed, making it difficult for us to get an access to the real figures. We then make a hypothesis to explain why a PWD behaves that way, not the other way. With information available from other sources than cameras, e.g., a family history, we gradually construct a theory of his behavior or his mental model. The theory is expressed in a form of story, which is easy to memorize and share among caregivers. The theory is validated through practice of caregiving and monitoring the results. A circle of knowledge creation is then complete, followed by new circle.

7 Conclusion

We have addressed the problems in understanding people with dementia (PWD) at Group Home. Video cameras installed on our Group Home have been useful for observing their behaviors keeping out of the way each other, but one has to turn to a story to understand the meaning of PWD's behavior. A story allows caregivers to catch the best timing to interrupt PWDs for safety, thus contributing to PWDs' spontaneous lives. We found through a series of interview that experienced caregivers watch the images available via cameras more frequently than novices do. We think that creating and sharing stories among caregivers facilitate effective use of video images. We have also proposed to view caregiving as a creative problem solving process. We believe that technologies installed on Group Home should contribute to facilitating the process of creative problem solving as we described.

As a next step, we are concerned with families of PWDs. Keeping PWD and his family close may place him in broader social context. Distributing video images to families may strengthen their relationships and caregivers may also be benefited from their interactions by obtaining the information of PWD which may otherwise be unavailable. The more items of information caregivers obtain, the better story they can create of PWD. In the human society, person is the most affecting circumstance. Information technologies should be applied to facilitate to improve an awareness of caregivers for elderly with dementia on the basis of person-centered care [Kitwood 97], but not merely suit convenience to caregivers themselves.

Acknowledgement

Our research is partly supported by the fund from Ministry of Education, Culture, Sports, Science and Technology, JAPAN, under the name of Cluster for Promotion of Science and Technology in Regional Areas.

References

- [Barwise 83] Barwise, J. and Perry, J.: *Situation and Attitude*, MIT Press, Cambridge (1983)
- [Boden 04] Boden, C.: *Who will I be when I die?*, HarperCollins Publishers (2004)
- [Greenhalgh 98] Greenhalgh, T. and Hurwitz, B.: *Narrative Based Medicine: Dialogue and Discourse in Clinical Practice*, B M J Books (1998)
- [Kitwood 97] Kitwood, T.: *Dementia Reconsidered: The Person Comes First*, Taylor and Francis Open University Press (1997)

COLLECT-UML: Supporting Individual and Collaborative Learning of UML Class Diagrams in a Constraint-Based Intelligent Tutoring System

Nilufar Baghaei and Antonija Mitrovic

Intelligent Computer Tutoring Group

Department of Computer Science & Software Engineering

University of Canterbury, Private Bag 4800, New Zealand

{N.Baghaei, T.Mitrovic}@cosc.canterbury.ac.nz

Abstract. Automatic analysis of interaction and support for group learning through a distance collaborative learning system is at the forefront of educational technology. Research shows that collaborative learning provides an environment to enrich the learning process by introducing interactive partners into an educational system. Many collaborative learning environments have been proposed and used with more or less success. Researchers have been exploring different approaches to analyse and support the collaborative learning interaction. However, the concept of supporting peer-to-peer interaction in Computer-Supported Collaborative Learning (CSCL) systems is still in its infancy, and more studies are needed that test the utility of these techniques. This paper proposes an Intelligent CSCL system that uses Constraint-Based Modeling (CBM) approach, to support collaborative learning addressing both collaborative issues and task-oriented issues. The system supports the tertiary students learning Object-Oriented Analysis and Design using UML. The CBM approach is extremely efficient, and it overcomes many problems that other student modeling approaches suffer from [5]. CBM has been used successfully in several tutors supporting individual learning. The comprehensive evaluation studies of this research will provide a measure of the effectiveness of using CBM technique in Intelligent CSCL environments.

1 Introduction

E-learning is becoming an increasingly popular educational paradigm as more individuals who are working or are geographically isolated seek higher education. Support for collaboration is especially important in this context, because the lack of face-to-face interaction complicates the collaboration and students have few opportunities to practice collaborative skills [1]. There have been several definitions for collaborative learning. The broadest (but unsatisfactory) definition is that it is a *situation* in which *two or more* people *learn* or attempt to learn something *together* [2]. A more comprehensive definition given by [3] states as follows: "... a coordinated, synchronous activity that is the result of a continued attempt to construct and maintain a shared conception of a problem". Since effective collaborative learning includes both learning to effectively collaborate, and collaborate effectively to learn, the facilitator must be able to address social or collaboration issues as well as task-oriented issues [4]. Collaboration issues include the distribution of roles among students (e.g. critic, mediator, idea-generator), equality of participation, and reaching a common understanding, while task-oriented issues involve the understanding and application of key

domain concepts. The educational systems are responsible for regulating the interaction, and guiding the students towards effective collaboration and learning.

In the last decade, many researchers have contributed to the development of CSCL and advantages of collaborative learning over individualised learning have been identified. Numerous systems for collaborative learning have been developed (discussed in the following section); however, the concept of supporting peer-to-peer interaction in CSCL systems is still in its infancy.

This paper proposes an Intelligent CSCL system that uses Constraint-Based Modeling (CBM) approach, to support collaborative learning addressing both collaborative issues and task-oriented issues. The CBM approach is extremely efficient, and it overcomes many problems that other student modeling approaches suffer from [5]. The system supports the tertiary students learning Object-Oriented Analysis (OOA) and Object-Oriented Design (OOD) using UML.

Section 2 reviews some of the collaborative learning systems that have been developed. Section 3 outlines the objectives of this research followed by the intended approach in Section 4. Current and Future work is discussed in the last section.

2 Related Work

This section discusses examples of three types of CSCL systems, in the context of the collaboration management model [4]:

- *Reflecting Actions*: The most basic level of support a system may offer involves making the students aware of the participants' actions. Actions taken on shared resources or those that take place in private areas of a workspace may not be directly visible to the collaborators, yet they may significantly influence the collaboration. Raising awareness about such actions may help students maintain a representation of their team-mates' activities. The system described in [6] is an example.
- *Monitoring the State of Interactions*: Such systems fall into two categories: those that aggregate the interaction data into a set of high-level indicators, and display them to the participants, and those that internally compare the current state of interaction to a model of ideal interaction, but do not reveal this information to the users. In the former case, the learners are expected to manage the interaction themselves, having been given the appropriate information to do so. In the latter case, this information is either intended to be used later by a coaching agent, or analysed by researchers in an effort to understand the interaction [4]. MArCo [7] and EPSILON [8] are examples of such systems.
- *Offering Advice*: This will include the CSCL systems that analyse the state of collaboration using a model of interaction, and offer advice intended to increase the effectiveness of the learning process. The coach in an advising system plays a role similar to that of a teacher in a collaborative learning classroom. The systems can be distinguished by the nature of the information in their models, and whether they provide advice on strictly collaboration issues or both social and task-oriented issues. Examples of the systems focusing on the social aspects of collaborative learning include Group Leader Tutor [9] and DEGREE [10] and examples of the systems addressing both social and task-oriented aspects of group learning are LeCS [11], COLER [12] and COMET [13].

3 Research Objectives

The main objective of this research is to develop an intelligent collaborative system for the tertiary students learning object-oriented analysis and design using UML. It focuses on CBM, which uses constraints to represent the domain knowledge. Constraints are used to identify errors in the student solution. CBM technique will be used to model student/group knowledge, and represent the domain knowledge as a set of syntax and semantic constraints.

A number of evaluation studies will be conducted to test the feedback messages (both task-based and collaborative-based feedback), the pedagogical agent, and the usability of the interface.

The research will evaluate the possibility of giving advice with comparing student work with an expert solution *as well as* group solution, in contrast to the approach usually taken by previous studies that have either supported tutoring (teaching the domain concepts) or coaching the social interaction (encouraging the students to discuss and participate). Therefore, the proposed system can be considered as a learning environment that supports both individual and collaborative learning.

4 Research Approach

The project is divided into two main parts: support for problem solving and support for social interaction between group members. The system will support two or more students working together on a problem from networked machines. Communication windows are available so that students can send advice, suggest alternative actions, comment on their partner's actions, etc. One of the learners would act as moderator, who will be responsible for the final submission of the solution to the system after getting approval from all the group members. The following subsections provide more detailed information on individual components of the system.

4.1 Architecture

The system will use *distributed architecture* [14], where the tutoring functionally is distributed between the client and the server. The application server consists of a student modeler, which creates and maintains student models for all users, a domain module, a pedagogical module and a group modeler.

The user interface is Java-based and may perform some teaching functions. The architecture of the proposed system is illustrated in Figure 1. The system is being implemented in Allegro Common Lisp.

4.2 Interface

The interface of the system is divided into three main parts: the section on the right hand side will be the individual workspace, the one in the middle will be the shared workspace and the one on the left hand side will show the system feedback messages to the group members. The text of the problem is being displayed at the top and sentence openers and a chat area is provided at the bottom of the shared workspace to facilitate synchronous communication between the group members.

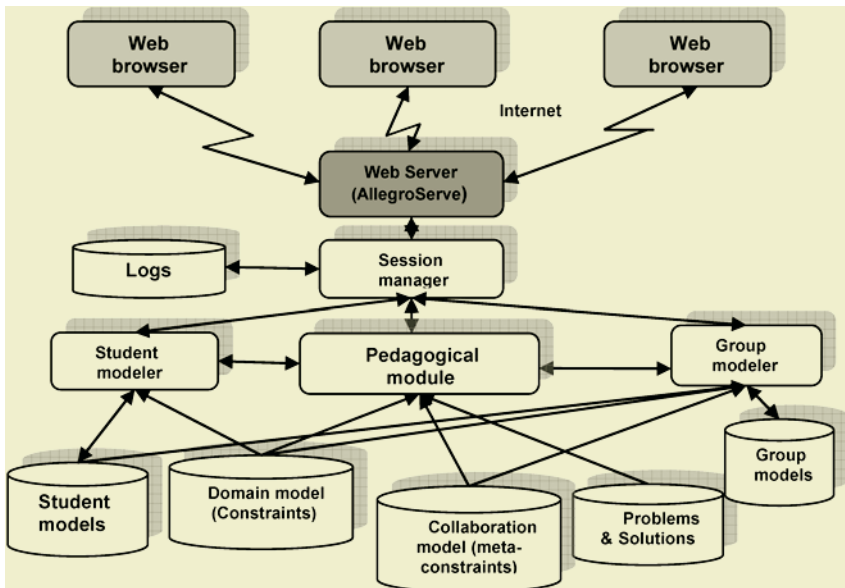


Fig. 1. The architecture for the proposed system

When a solution is submitted, the pedagogical module generates feedback on it, offers the possibilities of working on the same problem (if there were mistakes in the solution), logging off, or going on to the next problem, which will be selected by the system. The student is also able to view the history of the session, and specify the kind of feedback required. Both student's individual solution and group solution (submitted by the moderator) will be compared with ideal solution stored in the system.

The input data (for the system to further analyse) are: Shared workspace, Private work area (for individual members of the group), Chat facility with use of sentence openers and three buttons (OK, NO, Not sure) which will be used by each individual member to express their opinions whenever the shared workspace is updated. Only one student, the one who holds the pencil, can update the shared diagram at a given time. Figure 2 illustrates the current state of the interface implementation, supporting individual learning.

4.3 Group Modeller

A new component will be added to the system, which will be responsible for:

- Recording history of students' social interactions with each other through the chat facility,
- Proposing new learning tasks based on the learning needs of the group,
- Recording history of group technical knowledge as a whole; a group solution is considered the one that is submitted by one student as a representative (after all the team members agree on the solution being submitted).

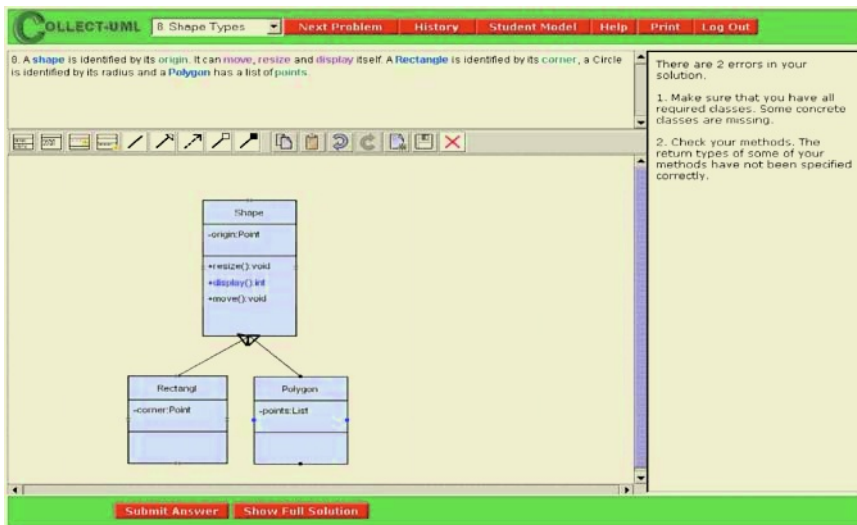


Fig. 2. The current state of COLLECT-UML interface

4.4 Pedagogical Module

The pedagogical module provides support for individual and collaborative learning:

- The student can work in the private area and submit his/her solution to the system; the solution will be compared with an ideal solution and the system provides feedback for improving their individual performance; feedback would be on demand and task-based in this case.
- The group members will collaborate and submit a final solution to the system; the solution is compared with expert solution and feedback will be provided. Feedback would be on demand and task-based.
- The group solution will be compared with each member's solution and discussion items based on the differences will be recommended. This will provide participation and negotiations between the group members.
- Feedback messages will be given to each group member (from time to time), encouraging them to discuss, participate, acknowledge, etc. The feedback messages will be generated based on student performance in chat area, agreement buttons and shared workspace.

4.5 Domain and Collaboration Model

The Domain model has already been implemented as a set of syntax and semantic constraints (88 semantic and 45 syntax constraints so far). Each constraint consists of a relevance condition, a satisfaction condition and a feedback message. The feedback messages are presented when the constraint is violated. It is common in any design problem to have two or more correct solutions for a problem, especially if the problem is complex. The system will contain only one correct solution to the problem. However, the system will be capable of recognizing alternative correct solutions, as

there are constraints that check for equivalent constructs in the student's and ideal solutions. Figure 3 illustrates an example of a semantic constraint for the UML domain.

```
(77
"Check your methods. You have method(s) of type non-static,
when it should be static."
(and (match IS METHODS (?* "@" ?tag ?name ?c_tag ?type_IS
                           ?access_IS ?static_IS ?*))
      (match SS METHODS (?* "@" ?tag ?name2 ?c_tag ?type_SS
                           ?access_SS ?static_SS ?*))
      (test IS ("yes" ?static_IS)))
(not-p (test SS ("no" ?static_SS)))
"methods"
(?tag))
```

Fig. 3. An example of a semantic constraint

Meta constrains compare student's interaction with an ideal model of interaction and will provide collaborative-based feedback messages; the social-interaction comments generated by the system can be discarded by the student. Meta-constraints will be evaluated from time to time by taking into account the content of chat area, contribution to the group diagram, and comparison of group and individual diagram.

5 Conclusions and Future Work

The single-user version of the system has already been designed and implemented. It will be extended to support collaborative learning as the next step. The enhancement process will include implementation of shared workspace, modification of pedagogical module to support both individual and group of users, designing and implementing the group modeling component and developing meta-constraints. The comprehensive evaluation of the system will be carried out at the University of Canterbury, in a second-year Software Engineering course. The evaluation studies of this research will provide a measure of the effectiveness of using CBM technique in intelligent computer supported collaborative learning environments.

References

1. Constantino-Gonzalez, M., and Suthers, D. Coaching Collaboration in a Computer Mediated Learning Environment. (CSCL 2002), (NJ, USA, 2002), pp.583-584.
2. Dillenbourg, P. What do you mean by "Collaborative Learning". In Dillenbourg, P. (Eds.), Collaborative Learning: Cognitive and Computational Approaches, Amsterdam: Elsevier Science. pp.1-19, 1999.
3. Roschelle, J. and Teasley, S.D. The construction of shared knowledge in collaborative problem solving. In O'Malley, C.E. (Eds), Computer-Supported Collaborative Learning. Berlin, pp. 69-197, 1995.
4. Jerman, P., Soller, A. and Muhlenbrock, M. From Mirroring to Guiding: A Review of State of the Art Technology for Supporting Collaborative Learning. In Dillenbourg, P., Eurelings, A and Hakkarainen, K. (Eds.), European Perspectives on CSCL (CSCL 2001), (Maastricht, Netherlands, 2001), pp.324-331.

5. Mitrovic, A., Mayo, M., Suraweera, P. and Martin, B. Constraint-based Tutors: a Success Story. 14th International Conference on Industrial and Engineering Applications of Artificial Intelligence and Expert Systems (IEA/AIE-2001), (Budapest, 2001), pp.931-940.
6. Plaisant, C., Rose, A., Rubloff, G., Salter, R. and Shneiderman, B. The design of history mechanisms and their use in collaborative educational simulations. (CSCL 1999), (California, USA, 1999), pp.348-359.
7. Tedesco, P. and Self, J. A. Using meta-cognitive conflicts in a collaborative problem solving environment. (ITS 2000), (Montreal, Canada, 2000), pp.232-241.
8. Soller, A. and Lesgold, A. Knowledge acquisition for adaptive collaborative learning environments. AAAI Fall Symposium: Learning How to Do Things, Cape Cod, MA, 2000.
9. McManus, M. and Aiken, R. Monitoring computer-based problem solving. International Journal of Artificial Intelligence in Education, 6(4). pp.307-336, 1995.
10. Barros, B. and Verdejo, M.F. Analysing student interaction processes in order to improve collaboration: The DEGREE approach. International Journal of Artificial Intelligence in Education, 11. pp.221-241, 2000.
11. Rosatelli, M., Self, J., and Thirty, M. LeCs: A collaborative case study system. (ITS 2000), (Montreal, Canada, 2000), pp.242-251.
12. Constantino-Gonzalez, M., and Suthers, D. A coached collaborative learning environment for Entity-Relationship modelling. 5th International Conference on ITSs (ITS 2000), (Montreal, Canada, 2000), pp.324-333.
13. Suebnukarn, S. and Haddawy, P. A Collaborative Intelligent Tutoring System for Medical Problem-Based Learning. International Conference on Intelligent User Interfaces, (Madeira, Portugal, 2004).
14. Mitrovic, A. An intelligent SQL tutor on the Web. International Journal of Artificial Intelligence in Education, 13 (2-4). pp.173-197, 2003.

Using Affective Learner States to Enhance Learning

Amali Weerasinghe and Antonija Mitrovic

Intelligent Computer Tutoring Group, Department of Computer Science,
University of Canterbury, Private Bag 4800, Christchurch, New Zealand
acw51@student.canterbury.ac.nz, tanja@cosc.canterbury.ac.nz

Abstract. A tutor's ability to adapt the tutorial strategy to a student's emotional and cognitive states is an important factor contributing to the effectiveness of human one-on-one tutoring. Even though tutoring systems were developed with the aim of providing the experience of human one-on-one tutoring to masses of students in an economical way, using learners' emotional states to adapt tutorial strategies have been ignored until very recently. This paper proposes an initial study to understand how human tutors adapt their teaching strategies based on the affective needs of students. The findings of the study will be used to investigate how these strategies could be incorporated into an existing tutoring system which can then adapt the tutoring environment based on the learner's affect and cognitive models.

1 Introduction

A number of empirical studies [6, 8] have shown that the performance of students who interact with an ITS improved significantly compared to those who learn in a traditional classroom setting. However, ITS have yet to reach the effectiveness of human one-on-one tutoring. The effectiveness of human one-on-one tutoring is largely due to the tutor's ability to adapt the tutorial strategy to the students' emotional and cognitive states. Even though users' emotional states were shown to strongly influence both reasoning and communication which in turn affect the learning process [11], using learners' emotional states to adapt tutorial strategies have been ignored until very recently. This paper outlines a study to investigate how a model of affect can be used to improve the objective performance of learners interacting with an ITS.

Related work is given in section 2. The next section explains the research goals. Section 4 presents the pilot study which is followed by the research outline.

2 Background

There have been various research attempts to incorporate models of affect into an ITS. These attempts can be categorised based on the methods used to assess the quality and the intensity of the affective states of the learners [4]: (i) self-report (ii) behavioral and cognitive indices (iii) psycho physiological indices.

2.1 Self-report

Self-report is the main method to assess the presence of emotions if we assume that emotional states are conscious. Self-report provides an opportunity for students to externalise their feelings or attitudes during the interaction with a learning environ-

ment. This makes it easier for the tutors to adapt their pedagogical actions to suit individual learners. de Vicente and Pain (1999) conducted an empirical study with students in order to investigate the feasibility of self-report in diagnosing motivation. They investigated whether self-report as a method was acceptable to students and whether the information obtained was reliable. It was concluded that self-report was generally well-received by students, and is a valid approach to diagnose motivation. However, it was also recommended that relying exclusively on self-report was not advisable, as sometimes students did not update the self-report facilities as frequently as the motivational states changed.

2.2 Behavioral and Cognitive Indices

Another means of measuring emotional states is to detect behavioral and cognitive patterns that are associated with them [4]. de Vincete and Pain (2002) conducted an empirical study to investigate whether it is feasible to detect a student's motivational state based on his/her interactions with an ITS. The participants (10 post graduate students with previous teaching experience) were asked to watch the recorded interactions of a student with MOODS (a prototype ITS for learning Japanese numbers with an added motivation self-report facility), and infer and comment on the motivational state of the student during the interaction. The inferences were based on the way a student performed the exercises such as the order in which she did the exercises, whether she gave up or not, mouse movements during an interaction etc. These inferences were then used to produce a set of motivation diagnosis rules and their validity is yet to be evaluated. The results suggest that it is feasible to infer motivation diagnosis knowledge based only on the information provided by the computer interactions in an intelligent tutoring system.

Conati and Zhou (2002) have developed a probabilistic model that assesses student emotional reaction during interaction with Prime Climb, an educational game designed to assist students learn number factorization. This model is based on the OCC cognitive theory of emotions. This model records how game events relate to the students' goals, as well as how these goals probabilistically depend on the students' traits and playing behaviour. This model is developed to assess students' affect during the interaction with the climbing instructor, an intelligent agent used to improve the pedagogical effectiveness of Prime Climb. The function of this agent is to provide hints that help the student reason about number factorization, without compromising her level of engagement. Evaluations were carried out to validate the accuracy of the model and is yet to be incorporated into the pedagogical activities of the agent.

2.3 Psycho Physiological Indices

It has been shown that that an emotional state modulates many physical changes in tandem: provoke specific facial actions, increase or decrease tension in muscle groups etc. A variety of psychophysiological indices such as heart rate, blood pressure, skin conductance, finger temperature, respiration can be used to detect emotions via sensors such as microphones, cameras, strain gauges applied to mouse buttons, special wearable devices etc. Use of such psychophysiological data may provide the most dynamic and objective approach for assessing changes in a person's affective state.

An empirical study was conducted to assess the performance of biometric signals in detecting user affective states of students interacting with Prime Climb (mentioned above) [2]. The biometric signals focused on are skin-conductivity (SC), electromyography (EMG) of the muscles involved in frowning and corrugating eyebrows, blood-volume pressure (BVP), and respiration (RESP). The study was carried in an uncontrolled environment in which students (from grade 2 to 10) interacted freely with Prime Climb. The objective of the study was to ascertain whether the four sensors could identify the six specific emotions currently modelled in the dynamic decision network (joy, distress, admiration, reproach, pride and shame). The level of noise in all the signals was high and all the sensors are sensitive to motion. Consequently the researchers had to focus on less noisy SC and EMG signals as it was difficult to detect meaningful patterns for RESP and BVP during the preliminary analysis. The results indicated that a sudden arousal can cause a startle response in the SC signal and that the relative amplitude of this pattern is in direct relation to the user's arousal level.

Haag and colleagues (2004) used data gathered from a set of biosensors to train a neural network classifier. It was then used to automatically detect the emotional state of a user in terms of arousal and valence values. The data was gathered from a single participant on different days and different times of the day. The standard photo set was used to elicit emotions. The participant's heart rate, BVP heart rate, BVP amplitude, EMG amplitude, skin conductivity, respiration amplitude, respiration rate were used to train the neural net. Two separate networks for valence and arousal each were trained. The results indicate that the estimation of the valence value is a much harder task than arousal.

3 Research Goals

As the research in field of affective tutoring systems is still at the very early stages, researchers still focus on the initial issues such as which emotions are most important for learning, how to assess the emotions of interest etc. Currently researchers focus on generating models and evaluating them. To the best of our knowledge, a model of affect is yet to be used to improve the objective performance of the learners.

According to Self (1990), it is more important to focus on using the student model to enhance the effectiveness of the pedagogical process, than building a highly accurate student model that models everything about the student. Therefore, we are interested in investigating how an affective model can be used to improve the objective performance of learners. One of the things that we choose to focus on using the affective model is to develop an effective problem selection strategy because most ITSSs employ adaptive problem selection based only on the cognitive model which may result in problems being too easy or too hard for students. This may occur due to factors like how much guessing was involved in generating the solution, how confident she was about the solution, how motivated she was etc., which are not captured in the cognitive model. Therefore, using both cognitive and affective models can potentially increase the effectiveness of a problem selection strategy, which in turn can improve the learners' motivation to interact with the system.

We are also interested in exploring the possibility of using the affect model to assist students to engage in deep learning. Self-explanation is described as an "*activity*

of explaining to one-self in an attempt to make sense of new information, either presented in a text or in some other medium” [1]. Self-explanation has been shown to be an effective teaching and learning meta-cognitive strategy which facilitates the identification and removal of misconceptions promoting reflection. If the ITS has the capability to identify instances where students need explicit assistance to engage in deep learning, the tutor can facilitate self-explanation. Therefore, the tutor facilitates self-explanation for students who will benefit from self-explanation without disrupting others. Thus self-explanation can be made adaptive based on the affect model. Therefore, in this research we propose to use the model of affect not only to help students gain domain-specific knowledge, but also meta-cognitive skills such as self-explanation, reflection etc.

Several ITSs have been developed by the Intelligent Computer Tutoring Group, at the University of Canterbury [9] based on constraint-based modeling [10], a student modelling technique which is becoming increasingly popular. Some of the tutors developed are SQL-Tutor for database querying, EER-Tutor for database modelling, NORMIT for database normalization and ERM tutor for database mapping [7]. We chose to use ERM tutor as ER mapping is a very well-defined task making it relatively easier to incorporate an affective model than an open-ended task such as database modelling. The current version of the ERM tutor does not have a sophisticated problem selection strategy or a strategy to facilitate adaptive self-explanation.

As we want to explore how emotional states of students could be used to adapt the tutoring strategies, we propose to conduct a study to understand how human tutors respond to learners' affective states.

4 Pilot Study

As a pilot study, we conducted an experiment with students enrolled for a computer studies course at the University of Canterbury. As it is a beginners' course, the students have different academic backgrounds. In this course students learn how to use MS-Office software and other basic computing skills like surfing the internet, file management etc. The students do lab tasks on their own, and the tutors help on demand. They are required to carry out the lab tasks in the order in which they are described in the book (some lab tasks can be carried out only after completing the previous one). Consequently, there was no opportunity for problem selection. However, this is not a major issue, because our main study will involve students interacting with existing tutoring systems which facilitate problems selection.

The study was carried out in March 2005 and eleven students were tutored by five professional tutors. Data was gathered from four different sources: video recordings of tutoring sessions, tutors' and students' comments after the session and answers to the email questionnaire from students. The maximum number of students tutored by one tutor was three. The average duration of a session was 38:16 minutes.

The data collected is still being analysed. Some of the findings are discussed here. As the tutor and the student had to sit closely, most tutors chose not to observe students' facial expressions to give enough personal space to students. Consequently the opportunity to gather how tutors react to students' facial expressions were lost. Even without observing students' facial expressions we could observe instances of tutor interventions based on self-report (in the form of students' questions), students' inter-

actions with the software and affective states. Some of the students' interactions that prompted tutor intervention were clicking on the same screen item repeatedly, or looking for a menu option in different menus. Student expressions that were acted upon were gaze at the screen without focus and frustration noises. Most students were happy with the timing of interventions. Less able students tend to benefit more from one-on-one sessions. They also seem to complete a lot more tasks than in a normal lab session. Some more able students prefer to attempt the task several times before actually asking for a tutor's help. Consequently, having a tutor observing all their attempts made them uncomfortable.

We also looked at how tutors decide the level of detail of feedback during the interventions. A key factor deciding the level of detail of feedback was the student's competency on the current task. i.e. if the student is struggling with the current task, then the tutor tends to provide minimum level of detail necessary to complete the task. This approach seems to be effective as all the students were satisfied with the level of detail of feedback received. Therefore, if we can use affective factors to recognise how difficult or easy the current task for the student, then we can combine this information with other interaction data such as the number of attempts, time required to complete the problem etc. to develop an effective strategy to tailor feedback for students.

5 Research Outline

As our goal is to incorporate an affective model into the ERM tutor, we propose to use existing tutoring systems as the learning environment in our next study. The objectives of this study are to understand how human tutors identify the emotional states of students learning using an ITS and how human tutors adapt tutoring strategies in each situation. Based on the study we want to explore how this adaptation of tutorial strategies can be incorporated into an intelligent tutoring system. As we want to explore general tutoring strategies, we plan to use four different tutoring systems (mentioned above) in the study. Participants will be students who are enrolled in an introductory database course in 2005 at the University of Canterbury. As these tutoring systems provide problem-solving environments and complement classroom instruction, the study will take place only after the students have learnt the relevant learning material in the classroom. Several tutors will work with the students on a one-on-one basis while the students interact with the system.

At the beginning of the study, the participants will be asked to sit a pre-test online, which can be used to understand their background knowledge. The participants will then be asked to use a selected tutor. In addition, the human tutors are expected to provide a one-on-one tutoring environment for each student based on their emotional states i.e. to guide the students towards the correct solutions using appropriate methods like asking questions at appropriate times etc. The problem sets in these tutoring systems are arranged according to the complexity by a human expert. However, the students have the freedom to select a different problem. Participants are expected to use the system for at least an hour. However, deciding when to stop using the system is left to students. At the end of the study, they will be asked to sit a post-test online which can be used to gain a measure of their improvement. All participants will be interviewed at the end of each session to understand their perceptions about the hu-

man tutoring and the system. They will also be asked to comment on the non verbal behaviour they received from the human tutors and how it affected their learning experience. At the end of the study, the human tutors will also be interviewed to understand their views on the tutoring sessions and the system. Students' interactions will be recorded by each tutoring system and all the sessions will be videotaped.

Initially, the researchers will go through the video recordings without the human tutors to investigate whether the tutoring strategies used by different tutors and the non verbal behaviour which triggered them could be understood. The researchers will also look for any similarities between the strategies. The extent to which this information can be extracted without the human tutors' assistance will provide a measure of the feasibility of incorporating the tutoring interventions into an ITS. As the second step, the video recordings will be analysed with the human tutors to understand the students' emotions detected by the human tutor and how the presence of these emotions helped the human tutor to decide what type of intervention is needed. For instance, how does a human tutor recognise that a student is frustrated because the current problem is too difficult for her, or what is the most appropriate question to ask in a situation where the student tries to guess the answer. The first example relates to how an effective problem selection strategy can be incorporated into an ITS, whereas the second one relates to how self-explanation can be facilitated in an ITS.

User logs will be analysed to obtain important behavioural data such as response times, no. of attempts required to arrive at the correct solution etc. We would then explore how this type of behavioural data can be used to adapt the tutorial strategies.

Students' performance on pre- and post-tests will also be analysed to understand how much they have improved. For instance, for each student using the ERM tutor, we plan to record the domain concepts or the steps of the mapping algorithm the students have problems with before interacting with the system, the tutoring strategy used to help them, and the effectiveness of the used strategy in terms of post-test scores and students' comments. If several students have difficulties with same domain concepts and have been tutored by different human tutors using different strategies, then the effectiveness of each strategy can be compared.

Video recordings, user logs, students' and tutors' comments and pre-and post-test performance will provide valuable insights to which emotions are vital to assess and how to detect their presence. Then we need to decide on how to assess the selected emotions through the available methods such as self-report, behavioural (interaction) patterns (such as response times, mouse movements etc.) and other data collected through bio-sensors. The next step is to develop an affect model which can be incorporated into the ERM tutor. It is crucial to carefully select the effective tutorial strategies to be incorporated into the tutor based on the study. We then need to design and implement the selected tutorial strategies based on the affect and the cognitive models. Finally, comprehensive evaluations studies are required to obtain a measure of the effectiveness of the implemented affective components and the tutorial strategies in the domain of database mapping.

References

- Chi, M. T. H. Self-explaining Expository Texts: The dual processes of generating inferences and repairing mental models. *Advances in Instructional Psychology*, 2000, pp. 161-238.

2. Conati, C., Chabbal, R. and Maclareen, H. A Study on Using Biometric Sensors for Monitoring User Emotions in Educational Games, Third Workshop on Affective and Attitude User Modeling, Assessing and Adapting to User Attitudes and Affect: Why, When and How in conjunction with User Modeling 2003.
3. Conati, C. and Zhou, X. Modeling Students' Emotions from Cognitive Appraisal in Educational Games In S. A. Cerro, G. Gouarderes and F. Paraguacuv (eds.) Proceedings of the International Conference on Intelligent Tutoring Systems, pp 944-954, Berlin: Springer, 2002.
4. Dalgleish, T. and Power, M. J. Handbook of Cognition and Emotion John Wiley & Sons Ltd, West Sussex, England, 1999.
5. Haag, A. Goronzy, S., Schaich, P. and Williams, J. Emotion Recognition Using Bio-sensors: First Steps towards an Automatic System In E. André et al. (eds.):Workshop of Affective Dialogue Systems, ADS 2004, Springer-Verlag Berlin Heidelberg pp. 36–48, 2004.
6. Koedinger, K. R., Anderson, J. R., Hadley, W. H. and Mark, M. A. Intelligent tutoring goes to school in the big city. International Journal of Artificial Intelligence in Education, 8 (1), 1997, pp. 30-43.
7. Marshall, M. ERM Tutor and ER-to-Relational Mapping Tutor Honours Report, University of Canterbury 2004.
8. Mitrovic, A. and Ohlsson, S. Evaluation of a Constraint-Based Tutor for a Database Language. International Journal on AIED, 10 (3-4), 1999, pp. 238-256.
9. Mitrovic, A., Suraweera, P., Martin, B. and Weersasinghe, A. (2004) DB-suite: Experiences with Three Intelligent, Web-based Database Tutors. Journal of Interactive Learning Research (JILR), vol. 15, no. 4, pp. 409-432, November 2004.
10. Ohlsson, S. Constraint-based Student Modeling. In: Greer, J. E. and McCalla, G. (eds.). Proceedings of Student Modeling: The Key to Individualized Knowledge-based Instruction, Berlin 1994, Springer-Verlag, pp. 167-189.
11. Picard R.W. Affective Computing MIT Press, Cambridge, Massachusetts, 1997.
12. Self, J. "Bypassing the intractable problem of student modelling", In *Intelligent Tutoring Systems: At the Crossroads of Artificial Intelligence and Education*. Frasson, C. and Gauthier, G. (Eds.), Norwood, NJ, Ablex Publishing Corporation, pp. 107-123.
13. de Vicente, A. and Pain, H. Motivation self-report in ITS. In Lajoie S.P. and Vivet, M. (eds.) proceedings of the Ninth World Conference on Artificial Intelligence in Education, Amsterdam 1999, IOS Press, pp. 648 -650.
14. de Vicente, A. and Pain, H. Informing the detection of students' motivational state: An empirical study. In S. A. Cerro, G. Gouarderes and F. Paraguacuv (eds.) Proceedings of the International Conference on Intelligent Tutoring Systems, pp 933-943, Berlin: Springer, 2002.

Three Foraging Models Comprised of Ants with Different Pheromone Sensitivities

Mari Nakamura

Research Institute for Cell Engineering (RICE),
National Institute of Advanced Industrial Science and Technology (AIST),
3-11-46 Nakoji Amagasaki, Hyogo 661-0974 Japan
[tagami-nakamura@aist.go.jp](mailto>tagami-nakamura@aist.go.jp)
<http://staff.aist.go.jp/tagami-nakamura/index.html>

Abstract. An ant colony shows collective behavior through signal patterns formed by individual ants communicating among themselves who behave according to local information. First, in this paper I devise a method for designing ant colony models that describes both the formation mechanism of signal patterns and the regulation mechanism of task allocation. Next, using the above method, I design three foraging models (trail, attraction and desensitization), by modifying a simple foraging model repeatedly, changing ant sensitivity to recruit pheromone, to improve foraging by regulating allocation of ants to sub-tasks. Out of them, the desensitization model shows the best foraging efficiency as a result of both proper allocation among subtasks and stable behavior.

1 Introduction

In previous studies, I proposed ant colony models that show macroscale collecting behavior as a result of the microscale behavior of individual ants through the formation of pheromone signal patterns [1, 2]. Ants respond to local cues in their environment, and indirectly communicate among themselves with pheromone signals. I studied the interaction between both the formation mechanism of signal patterns and the regulation mechanism of task allocation, focusing on ants' sensitivity to the signals.

As illustrated in Fig. 1, I have devised the method comprised of following three steps, to simplify the design of the collecting behavior of ant colony.

1. Introduction of subgroup structure: microscale behavior of individual ants is decomposed into several behavior modes, using a mode-transition rule common to all ants in the colony. Ants in the same mode behave in the same manner.
2. Introduction of spatial structure: The distribution of ants in each mode is estimated from their behavior, integrating ants in the mode. The distribution of pheromone signals is calculated by the distribution of ants laying pheromones.
3. Matching parameters: the macroscale behavior of an entire ant colony is comprised of the spatial distributions of ants in each mode and of the signal regions, using the same mode-transition rule.

In this paper, I apply this method to model ant colony's foraging. In foraging, ants spread widely to search for food sources (*food-search subtask*), bring it to the nest while leaving pheromone signals (*food-carry subtask*), and concentrate on the signals that lead them to the food source (*recruitment subtask*).

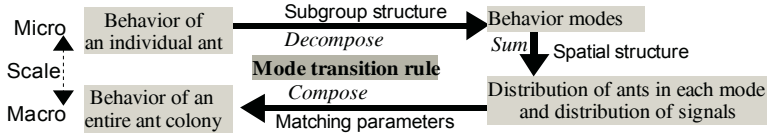


Fig. 1. Method for designing ant colony models

In section 2 of this paper, I use the above method and design three foraging models of an ant colony (*trail, attraction and desensitization*), repeatedly modifying the simplest one (the trail model) by changing ants' sensitivity to recruit pheromone (that is, by adding a new behavior mode to the mode-transition rule) to improve foraging efficiency by regulating allocation to the above subtasks. In section 3, results of foraging models' simulation are compared. The desensitization model shows balanced allocation, stable behavior, and the best foraging efficiency.

2 Designs of Three Foraging Models

2.1 Behavior of Signal Regions of Recruit Pheromone

When foraging, an ant carries a piece of food from the source to the nest leaving a trail of *recruit pheromone* on the ground. In these foraging models, the pheromone gradually evaporates and dissipates, as formulated in Eqs. 1 and 2, respectively, where $T(x, y)$ denotes the densities of the pheromone trail on the ground (*x-y plane*: $z=0$) and $P(x, y, z)$ represents the evaporated pheromone in the air.

$$(d/dt + \gamma_{ap})T(x, y) = 0 \quad (1)$$

$$\begin{aligned} \{d/dt - \gamma_{dif}(d^2/dx^2 + d^2/dy^2 + d^2/dz^2)\}P(x, y, z) &= 0 \quad (z > 0) \\ &= \gamma_{ap}T(x, y) \quad (z=0) \end{aligned} \quad (2)$$

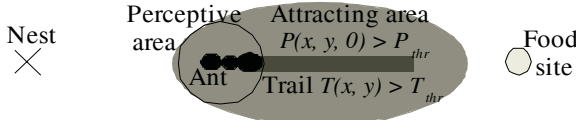


Fig. 2. Signal regions of recruit pheromone drawn by an ant carrying food

As illustrated in Fig. 2, ants use two kinds of recruit pheromone signals: *trail* and *attracting area* defined as regions where $T(x, y)$ is stronger than T_{thr} and where $P(x, y, 0)$ is stronger than P_{thr} , respectively. Here, T_{thr} and P_{thr} denote thresholds, or minimum perceptible pheromone densities on the ground and in the air.

2.2 Three Foraging Models: Trail, Attraction and Desensitization

Trail, attraction, and desensitization models are explained in the following sections and in Figs. 3, 4 and 5, respectively. They are simulated with parameters in Table. 1 and under a condition that “*after ants have consumed all the food units of one food site, a new food cluster of a predetermined size appears randomly within a 45 grid distance from the nest to maintain a constant number of existing food sites*”.

Table 1. Parameters used in three foraging models

Simulated space extends to $100 \times 100 \times 3$ grids. In pheromone diffusion, the ground is a reflecting boundary, and the others are absorbing ones.
The nest is located at the center of the ground.
Model colony is comprised of 600 ants moving on the ground.
One step is a period that an ant changes its action in response to a stimulus.
Radius of the perceptive field = traveling distance of an ant in a step = 1.5 grid.
Ants in search and wander modes randomly change direction at rate of 0.1 per step.

2.2.1 Trail Model: The Simplest Model

In this model, ants are only sensitive to trail. The colony is comprised of ants in *search*, *carry*, and *trace* modes (Fig. 3-1), which are allocated to food-search, food-carry, and recruitment subtasks, respectively. Their actions are defined as follows:

- A search-mode ant walks in a straight path, sometimes randomly changing direction. After finding a pheromone signal or food, it changes to trace or carry mode.
- A carry-mode ant leaves a pheromone trail while conveying one food unit from its source to the nest. When arriving at the nest, it drops the food unit into the nest, changes to trace mode and then randomly selects one of the trails around the nest.
- A trace-mode ant follows a trail in the opposite direction from the nest. After it reaches the food source, it changes to carry mode. If it loses the food source, it changes to search mode.

Trail model

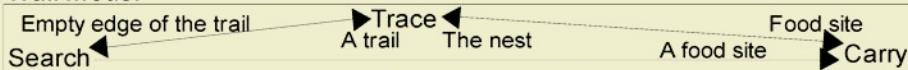
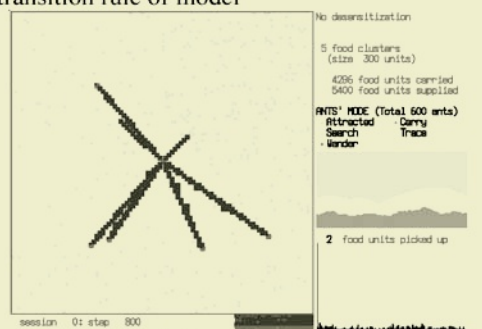
**Fig. 3.1.** Mode transition rule of model**Fig. 3.2.** Dynamics of model**Fig. 3.3.** Snapshot at step 800

Fig. 3. Explanation of trail model: Figs. 3, 4, and 5 illustrate mode-transition rules of three foraging models, outline their dynamics, and display their snapshots simulated with 300 units of food clusters constantly supplied at five food sites. Left-hand sides of the frames in snapshots display distributions of ants in each mode (gray dots), pheromone signals (dark-gray regions), the nest (black cross at the center), and food sites (large gray dots). Logs for the ant rate in each mode (from top to the bottom: wander, search, attracted, trace, and carry modes) and for the number of ants picking up a food unit (that is, food pickers) for the last 200 steps are displayed on the right-hand side of the frames in the snapshots

Time constant $\gamma_{vap} = 0.21$, threshold $T_{thr} = 0.01$ and amount of pheromone left by an ant in a step = 10.0 are determined to maintain trails for several steps.

This model shows stable recruitment to all existing food sites with small short-term fluctuations and dominance of the food-search subtask in allocation (Figs. 3-3).

2.2.2 Attraction Model: Intensifying Recruitment

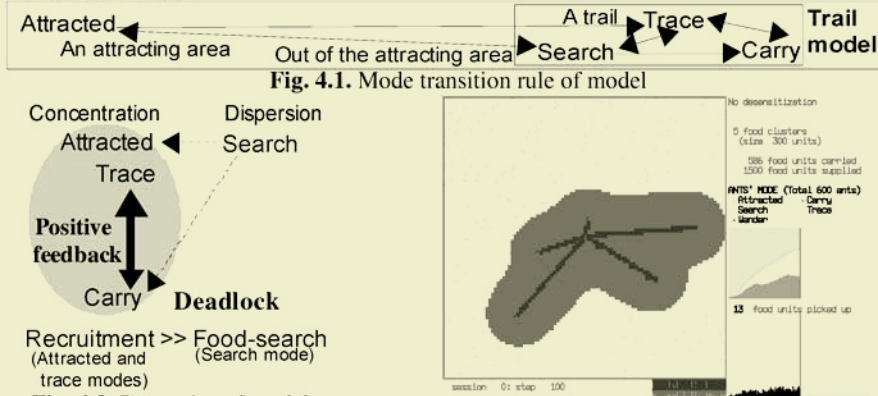
In this model, ants are sensitive to both the trail and attracting areas. To recruit more ants from a wider area, an attracting area is introduced, and *attracted* mode is appended to mode-transition rule (Figs. 4-1). The action of attracted-mode ants is defined as follows:

- If a search-mode ant finds an attracting area, it changes to attracted mode.
- An attracted-mode ant moves to a point where evaporated pheromone is strongest within its perceptive area. If it reaches a trail, it changes to trace mode. If it loses the attracting area, it changes to search mode.

Expansion of attracting areas is determined by the diffusion factor $\gamma_{dif} = 0.42$ and the thresholds $P_{thr} = 0.01$.

This model shows irregular and unstable long-term fluctuation in recruitment patterns caused by repeating deadlock (Fig. 4-3), as follows:

Attraction model



Recruitment >> Food-search
(Attracted and
trace modes)

Fig. 4.2. Dynamics of model

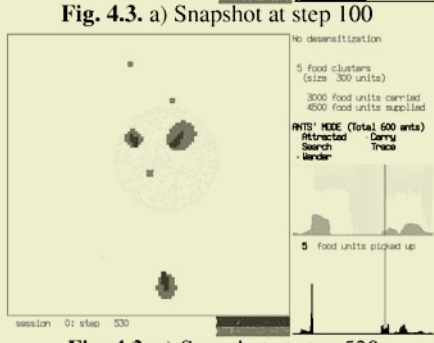
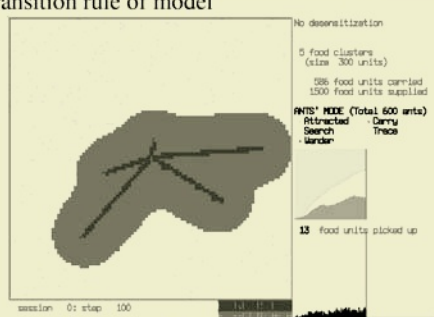
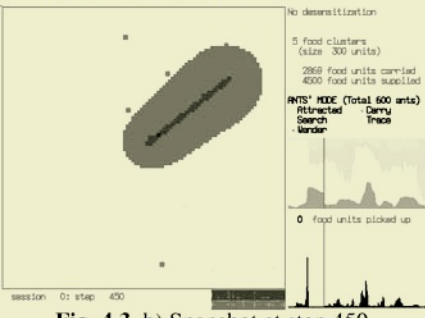


Fig. 4. Explanation of attraction model: Details are explained in the legend of Fig. 3

1. Search-decreasing stage (Fig. 4-3a): Recruitment to all food sites is observed. The rate of search-mode ants rapidly decreases because ants are caught within the signal regions. The number of food pickers shows modest fluctuations.
2. Enclosure stage (Fig. 4-3b): Almost all ants are enclosed within a few signal regions, and this impedes the search for new food sources. Recruited ants move in a group following signals quickly consuming marked food sites one after another. Then, the numbers of food pickers shows irregular, violent fluctuations.
3. Signal-vanishing stage (Fig. 4-3c): After deadlock, signals soon vanish, and ants enclosed within the signal regions return to search mode and spread over the ground. The number of food pickers is almost 0. Search-mode ants soon find new food sites and switch to carry mode, repeating the above cycle.

2.2.3 Desensitization Model: Avoiding Deadlock

In this model, ants lose their sensitivity to pheromone signals for a certain period. To avoid deadlock, desensitization is introduced, and *wander* mode is appended to the mode-transition rule (Fig. 5-1). The action of *wander*-mode ants is defined as follows;

- If a trace-mode ant reaches the end of a trail without locating a food source, it changes to *wander* mode, and loses its sensitivity to pheromone signals and food sources.
- During a desensitization period, a *wander*-mode ant walks in a straight path, sometimes randomly changing direction. After the desensitization period wears off, it returns to search mode.

The desensitization period is determined as 20 steps to disperse *wander*-mode ants outside signal regions.

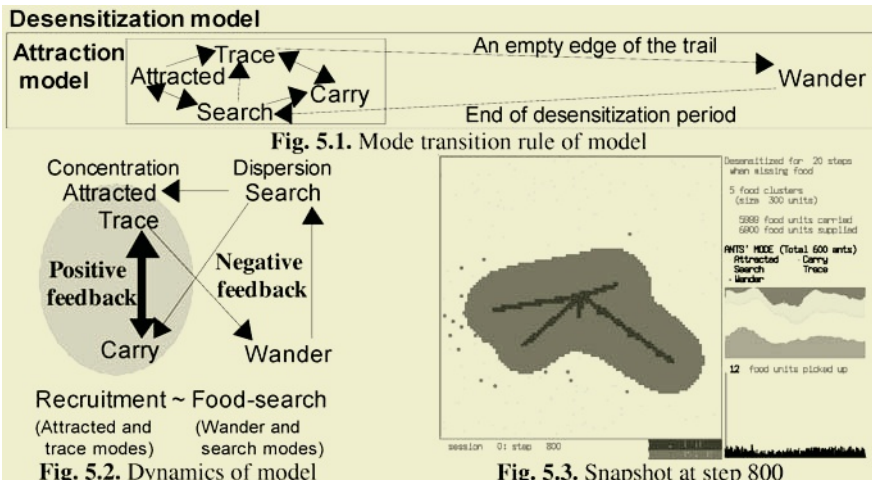


Fig. 5. Explanation of desensitization model: Details are explained in the legend of Fig. 3

This model shows stable recruitment to all food sites with moderate fluctuations, and proper allocation between food-search and recruitment subtasks (Figs. 5-3).

As outlined in Fig. 5-2, the interaction between the localized concentrations of ants attracted to pheromone signals and long-range lateral inhibition emulated by widespread desensitized ants functions according to the same mechanism as reaction-diffusion system.

3 Comparison of the Three Foraging Models' Behavior

3.1 Allocation Among Food-Search, Recruitment, and Food-Carry Subtasks

As indicated in Fig. 6, the trail model concentrates ants in the food-search subtask, and the attraction model concentrates ants in the recruitment subtask on time average. The foraging efficiencies of these models, which reflect allocation to food-carry subtask, mainly depend on the amount of work done by ants in minor subtask of food-carry or recruitment, because ants in major subtask waste time, raising the cost of foraging (as argued in foraging theory [5]). In contrast, the desensitization model circulates ants among three subtasks without large time loss, increasing allocation to food-carry subtask.

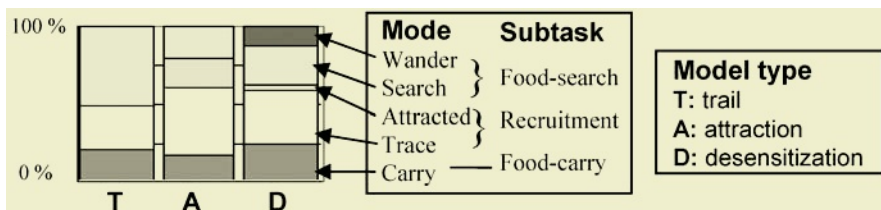


Fig. 6. Rate of ants in each mode in three foraging models, averaged for 5,000 steps, simulated with 300 units of food clusters constantly supplied at five food sites

3.2 Stability of Foraging Behavior

Figure 7 indicates time distributions from the appearance of a food site to its removal in each model. Compared with the others, distribution in the attraction model is prominently scattered, showing strong correlation to distance from the nest, because the enclosure of ants impedes the search for food sources far from the nest.

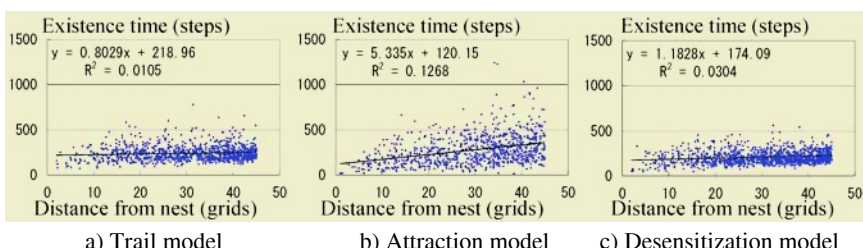


Fig. 7. Distributions of existence time of food sites in three foraging models, simulated under the same food supply condition as figure 6: Regression lines of the distributions and their residual sum of squares are indicated

3.3 Foraging Efficiency with Varying Food Supplies

Figure 8 indicates the foraging efficiency of each model: the number of food units carried by each model, with varying the sizes of supplied food clusters and the number of food sites. The following features of the three models are indicated.

- As the size of the supplied food clusters and the number of food sites increase, foraging efficiency increases in all three models.
- The desensitization model demonstrates the best foraging efficiency among them, despite changes in the size of supplied food clusters and the number of food sites.
- When the number of food sites is relatively small, the trail model's foraging efficiency is relatively low because trails cannot attract enough ants from wide areas.
- When relatively small size food clusters are supplied, the attraction model's foraging efficiency is relatively low because deadlock frequency increases.

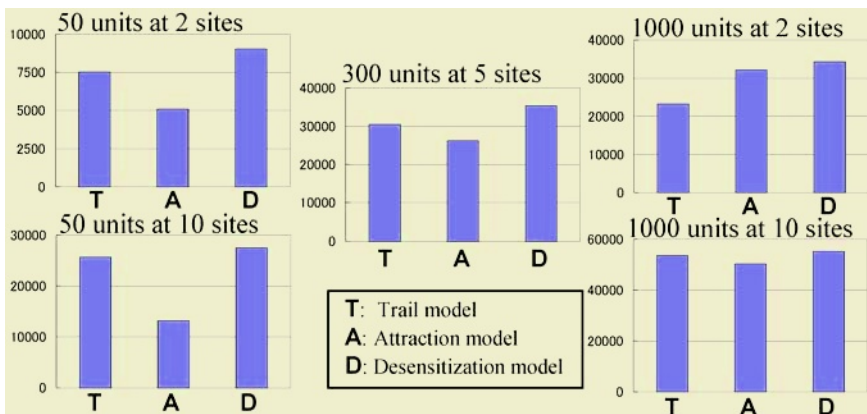


Fig. 8. Number of food units carried in each model at *5000 steps* averaged across *10 simulations* with varying number of food sites and sizes of supplied food clusters

4 Discussion

In the desensitization model of this paper, “noise” or “error” introduced by desensitization functions to avoid deadlock, as same as in the other foraging models [6].

In previous paper [2], I applied the method to a task-allocation model carrying out foraging and mound-piling tasks using independent signals for each task. Mode transition rule of the model is comprised of two modules for each task that are connected to each other through desensitized mode (as same as in other task allocation models [7]), not to concentrate ants in either of these tasks. Its simulation result indicates weak interaction between both tasks.

References

1. Nakamura M. and Kurumatani K. (1997) “Formation mechanism of pheromone pattern and control of foraging behavior of an ant colony”, In: Langton C. G. et al. (eds) *Artificial Life V*, The MIT Press, pp 64-77

2. Nakamura M. (2005) "Regulation mechanism of task-allocation and formation mechanism of ants' distribution pattern in collective behavior of ant colony models", *in proc. of 4th WSTST* (Muroran), pp 937-948 (in press)
3. Kurumatani K. and Nakamura M. (1997) "Qualitative analysis of causal graphs with Equilibrium type-transition", *in proc. of IJCAI'97* (Nagoya), pp. 542-548
4. Kurumatani K. (2000) "Macro-model generation for emergent cooperative behaviors in ant colony's foraging (1, 2)", *Journal of Japanese society of artificial intelligence*, pp. 829-843 (in Japanese)
5. Stephens D. W. and Krebs J. R. (1986) "Foraging theory", *Princeton University Press*
6. Deneubourg J.-L. et al. (1983) "Probabilistic Behavior in Ants; A Strategy of Errors?", *J. Theor. Biol.* 105:259-271
7. Gordon D. M. (1999) "Ants at work", *Free Press*

Emerging of an Object Shape Information Caused by Signal-Transmission Relay of Multi-robots

Sumiaki Ichikawa¹, Koji Hatayama², and Fumio Hara²

¹ Tokyo University of Science, Suwa, 500-1, Toyohira, Chino-shi, Ngano-ken, Japan 391-0292
ichikawa@rs.suwa.tus.ac.jp

² Tokyo University of Science, 1-3, Kagurazaka, Shinjukuku, Tokyo, Japan 163-8601

Abstract. This paper discusses emerging of object shape information by multi-robots. We carried out computer simulation studies and found that the significant shape information was emerged as the cyclic waveform pattern of signal frequency among the robots. Robots have local communication ability. When enough number of the robots distributed on an object, they established signal transmission relay around the object. The characteristics of the shape information were examined with respect to some simulation conditions. Then, we were able to obtain the conditions for enough classifying of different shape objects.

Keywords: Multi-robot system, Local communication, Shape information, Object classify

1 Introduction

A multi-robot system is one of the methodologies to give a certain ability to a robot system. This approach expects emerging of new abilities through just simple and small interactions among multiple robots. The new abilities are not expected in a single robot system. An emerged ability is expected in flexibility, adaptability robustness. Although many researchers who are interested in these ideas have investigated [1][2][3], almost all the research mainly focus on locomotion, formation or reconfiguration of multi-robot system. To expand probabilities and expectations for emergent robotics, on the other hand, we focus on sensing by multi-robot system. Sensing situations of robot system will be needed in its adaptive behavior, which is also including such locomotion, formation and reconfiguration.

We think that there are two interactions in a multi-robot system. One is physical interaction and the other is informational one. In this paper we want to focus on a robot function of optical signal communication, which can deliver an information within its local range. The optical signal has a significant character that can be intercepted by object shadow. That is, it is expected that a signal communication around an object is strongly influenced by the object shape.

In this paper, we will think about a situation that many robots are surrounding an object, which has geometrical shape with some convex parts. The robots, which are staying at their position, relay a communication signal by their signal transmission. Then, signal transmission relay is able to go around the object. This can be observed from the top view as frequency of transmitted signal. The changes in the frequency look like a waveform in time-line. We examine the characteristics of the observed waveform as a specific information of the object shape. We think that it is emerging of a shape information about an object shape.

A current work in this research is not how to recognize a shape information by robots themselves. The first aim of this paper is to show a potential of the emerged shape information in signal transmission relay. Therefore, the results and its meanings want to be watched carefully. In section 2, fundamental mechanism is explained in ideal position and the ideal number of robots. In section 3, the position of robots is improved into practical situation that each robot can move around and then contacts on a target object. In section 4, the potential of emerged shape information is evaluated with a method which is to reconstruct a shape from a shape information. In section 5, we include this paper.

2 Fundamental Mechanism of Emerging a Shape Information

It is assumed that the robots use an optical signal, which has two physical characteristics: One is enough directly straightforward transmission, and the other is that it is eclipsed by an object shape. Two illustrations in Fig. 1 are given to explain a fundamental mechanism of emerging an relevant shape information to an object. May robots are densely surrounding an object. Each illustration focuses on a partial circumference of the object which is approximated into an arc radius R_1 or R_2 respectively, where the radius R_1 is larger than the radius R_2 . It is additionally assumed that the transmitting direction among robots on the object is unidirectional along the object. This can be done by giving each robot the range limited to the left side toward the object direction.

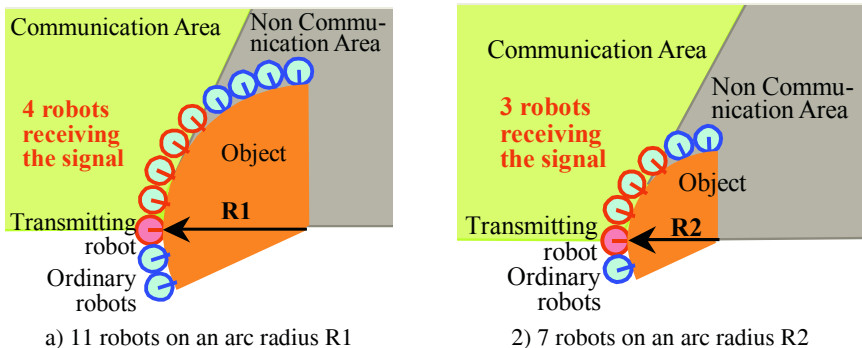


Fig. 1. Relation between the curvature of an object shape and the number of the robots which can receive a communication signal from transmitting robot. A partial radius R_1 is larger than that R_2

A communication signal was transmitted from the ‘ordinary robot’ in Fig. 1 and the transmitting robot, which is a dark circle on top of the left side of the object, has transmitted a signal. Then, the whole area around the object is separated into two areas. The left side area is communication area where robots can receive an optical signal from the transmitting robot without being covered by the object. On the other hand, the right side area is non-communication area, where robots can not receive communication signal because it is covered by the object. In the case of the lager radius R_1 , 4 robots are within the communication area of the transmitting robot. In the other case of the smaller radius R_2 , 3 robots are within that. The number of the robots

within the communication area simply depends on the curvature of the partial circumference. When the signal transmission relay goes around the object, the changes in the number of simultaneously transmitting robots will show a specific information of the object shape. In this paper we consider it as a specific shape information.

3 Simulation Studies for Emerging of a Shape Information

3.1 Behavior Rules for a Robot

A robot behaves along these two rules as action modes:

Mode 1: Disenabling signal receiving. A robot avoids a detected obstacle otherwise simply goes forward. When a robot detect a target object it turn its direction into the normal direction of the object surface and emits a signal once, and then it changes its action mode into Mode 2.

Mode 2: Enabling signal receiving. A robot stay at that position. Once a signal is received the robot emits a signal once and then the signal receiving is disabled for time τ to pass receiving a signal from the below robots in their communication signal relay.

3.2 Conditions for a Simulation Study

A simulation study was assigned. A target object is a convexity shown in Fig. 2. It has 4 corners ((2) (4) (5) (7) in Fig. 2), which are different curvature radius corners, and 3 straight edges ((1) (3) (6) in Fig. 2).

Robots, which behave along the Mode 1 in their initial state, move around the working space. In our previous work [4], it is known that these behaviors are corresponding to the random walk as long as enough number of robots are working.

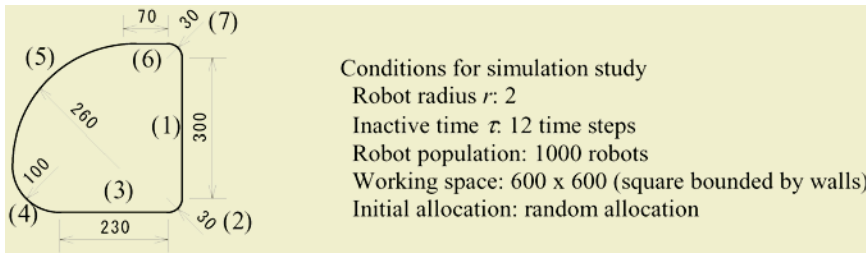


Fig. 2. A convexity, a target object which has 4 curved edges and 3 straight edges

3.3 Simulation Results

Here, it is assumed that a communication signal can be observed as a flush light and the number of these flashes can be counted from some farther position where all of the light flashes can be overlooked. We will investigate the changes in that count.

Fig. 3 shows results of the simulation study, where the horizontal axis means time step t and vertical axis means the count of emitting robots at that time step t . The changes in the count can form a waveform like these. In Fig. 3 a), which shows the

result of the time range for $t = 0 - 300$, it was found that the amplitude of the count was growing little by little over time steps. A sufficient cyclic waveform pattern emerged after $t = 700$ at last. The 5 cyclic waveform patterns were able to be seen for $t = 1700 - 1800$ in Fig. 3 b).

For the beginning of simulation, only the signal emitted by robots which had just contacted on the target object were observed. On the other hand, after a while enough number of robots distributed on the target object, the signals of transmission relay were frequently observed. Then a cyclic waveform of the count of the emitted signals was observed on the target object.

The indexes (1) - (7) in Fig. 2 and the indexes (1) - (7) in Fig. 3 b) are corresponding to each other. It is found that the changes in the count in Fig. 3 b) correlate well with the changes in the curvature angle on the target object shape in Fig. 2. That is, it is though that a single cycle of the waveform sufficiently shows a shape information of the target object.

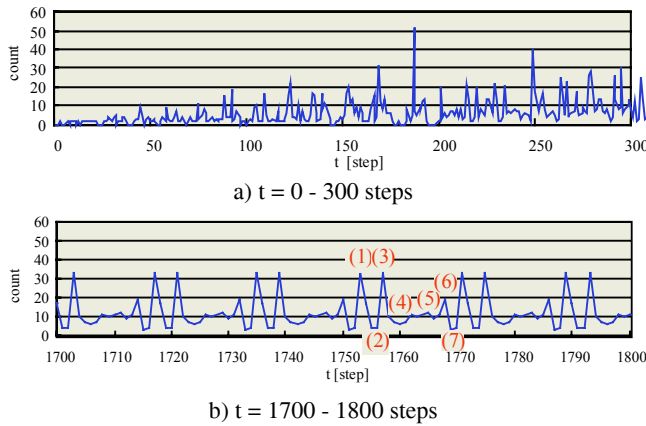


Fig. 3. Changes in the count of simultaneously emitting robot

4 Credibility of the Shape Information

With respect to an emerged shape information, we investigate the influences of the simulation conditions such as robot body size, robot population size, variation in robot position on the object, object shape and object size. And then, we examine an object shape calculated from the obtained shape information. Three representative values, such as ρ , Cc and Rr , are defined for the characteristics of these conditions of simulation study.

4.1 Representative Values for Simulation Conditions

Robots Density Around a Target Object

Robots density ρ is defined by the ratio the number of robots contacting around a target object to the maximum number of the robots in terms of geometric size, that is most dense numbers.

Characteristic Size of a Robot and an Object

Where the average radius of a target object is radius \bar{R} and the radius of a robot is r , the characteristic size of a robot and an object, Rr , is defined by the ratio the average of the object radius to the robot radius.

Characteristic Value of Object Shape

To investigate the characteristics of the shape information a 2-dimensional convexity consisting of curves is used in a simulation study. The variation of curvature around the convexity is represented in an index Cc , which is defined by the following:

$$Cc = \sum_{i=0}^N \frac{1/R_i}{1/\bar{R}} \cdot \frac{\theta_i}{2\pi}$$

R_i : Curvature of the i -th curve
 θ_i : Angle range of the i -th curve at the center of an object.
 L : Length of circumference of an object
 $\bar{R} : L/2\pi$

Where, the index i means the i -th curve of all ones to assume that the convexity consisting of N curves.

Here, we give an image to recognize Cc . Cc is 1 or larger value than 1. If Cc is the minimum value 1, it means the object is a pure circle. While, if Cc is the larger than 1, it means the object has the more spiny curves. Fig. 4 takes 5 target objects for instance: The circle of the left is $Cc = 1.00$, other target objects can be grouped by triangle group and by square group.

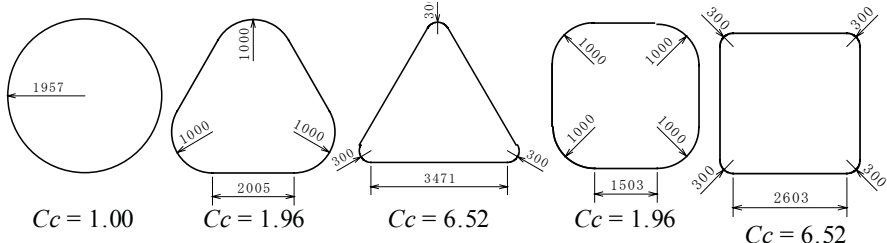


Fig. 4. Target objects with the characteristic value of object shape, triangle and square

4.2 Reconstruction from a Shape Information

The count of observed signal at a time has two informations. One is the curvature of a partial arc of the object shape at that position. The other is the length of the arc. The curvature and the length of the arc can be approximately and geometrically calculated from the observed count. How to reconstruct an object shape from a shape information is the following:

- Extracting a single cyclic waveform from of the signal count in time-line. If a target object has a shape of pure circle, a single cyclic waveform can not be extracted because the waveform is simply flat. But, in this case, a flat waveform means the shape of the target object is purely circle, therefore, the count shows the curvature and the diameter of the circle.
- Picking-up a count in the cyclic waveform at every time step. Calculating the curvature and the length of an arc corresponding to the picked-up count.

- iii) Connecting the calculated arcs in order of the time-line. At this moment, a curving line consisting of the connected arcs is not always closing between start point and end point because each calculated arc has discrete error within the resolution by the count of signals (See in Fig. 5 a)).
- iv) Applying a geometrical heuristics and correcting the curve line. The geometrical heuristics are the two followings: 1) an object perimeter have to be closed, 2) a start point and an end point are smoothly connected each other, that is, the total angle among the arcs have to be 360 degree. Applying these heuristics the accumulation of the arc errors is divided into each arc angle and arc length to close just on 360 degree (See in Fig. 5 b)).

Fig.5 shows an example of shape reconstruction of a target object in Fig. 2. The dots on curving line shows connecting point of the arcs. The little bigger dot in the bottom of Fig. 5 shows start point of connection. Fig.3 a) is a simply connected shape in the clockwise direction. It is not closed shape. On the other hand, Fig. 5 b) is a corrected shape, which is applied with the geometrical heuristics mentioned above.

In very carefully thinking of these results, it is said that the extracted cyclic waveform of signal count has a shape information of a target object, that is, a cyclic waveform can identify a target object.

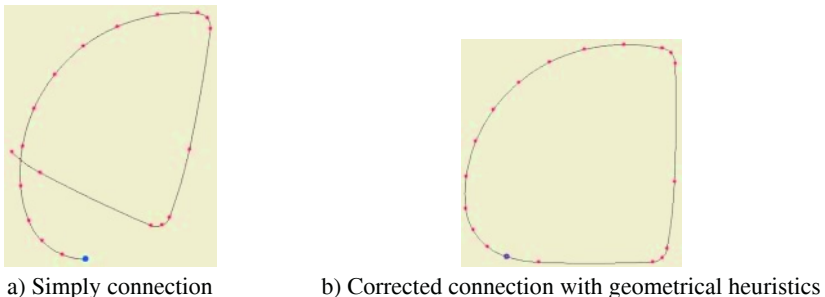


Fig. 5. An example of a reconstructed shape from the shape information of the object in Fig.2

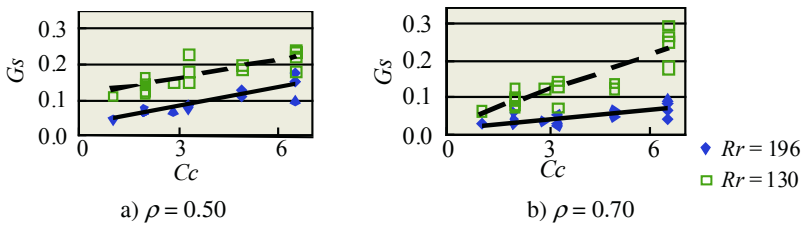
4.3 Characteristics of Shape Reconstruction

Computer simulation studies are carried out for following object shape with Cc :

Cc : 1.00 (circle), 1.96 (triangle, rectangle, pentagon), 2.80 (triangle, rectangle, pentagon), 3.26 (sector), 4.89 (triangle, rectangle), 6.52 (triangle, rectangle)

To evaluate accuracy of a shape reconstruction we examine the coherence between a reconstructed shape and an original shape. To examine it the center of the shapes are matched and then rotated until minimizing the area of the difference between the reconstructed shape and the original shape. Then, we focus on the ratio of the difference area to the original area. The index Gs shows the ratio.

In Fig. 6, the horizontal axis is Cc , the characteristic value of shape and vertical axis is Gs . Each Gs for Cc is examined in two Rr ($Rr = 196, 130$ ($r = 10, 60$)). The data in the same Rr are able to approximate to liner lines: data of $Rr = 130$ to doted line and data of $Rr = 196$ to solid line in Fig. 6. General tends of the results is that in the larger Cc the Gs was also increasing. The inclination of the Gs is strongly appeared in smaller Rr . The higher density ρ is almost decreasing Gs .

**Fig. 6.** The ratio of the difference area G_s

5 Conclusions

This paper discussed probabilities of emerging of a significant object-shape-information in signal transmission relay among multi-robots. This paper did not discuss about who recognizes the shape information but about the probabilities of the shape information at the first step. Fundamental mechanism of representation of shape was shown in section 2, which was under the ideal geometrical condition. While, in section 3 and 4, computer simulation studies were carried out in more practical condition, which is including the process of robot to contact on a target object. Then, it was found that the original shape could be reconstructed from a shape information of the frequency waveform but the reconstructed shape had little error from the original shape, and the error had variation in trials of robot's distribution around an object. Thus, we think the emerged object-shape-information has sufficient shape information, because it was shown by what was able to be reconstructed into original shape. It is the future work as the next step that how to recognize the information by robots themselves.

References

1. Masahiro Shimizu, Akio Ishiguro, et al., "Adaptive Shape Reconfiguration of a Decentralized Motile System Exploiting Molecular Dynamics and Stokesian Dynamics Methods", Journal of Robotics and Mechatronics, Vol. 16, No. 2, 3, (2004) pp. 271-277.
2. K. Sugawara and M. Sano, "Cooperative Behavior of Interacting Simple Robots in a Clock-face Arranged Field", Distributed Autonomous Robotic Systems 5 (2002) pp.331-339.
3. S. Ichikawa and F. Hara, "Effects of Static and Dynamic Variety in the Character of Robots on Group Intelligence of Multi-Robot System", Distributed Autonomous Robotic System 4, Springer-Verlag Tokyo, (2000).
4. S. Ichikawa and F. Hara, "Experimental Characteristics of Multiple-Robots Behaviors in Communication Network Expansion and Object-Fetching", Distributed Autonomous Robotic System 2, Springer-Verlag Tokyo, (1996) pp. 183 - 194.

Autonomous Synchronization Scheme Access Control for Sensor Network

Kosuke Sekiyama¹, Katsuhiro Suzuki¹, Shigeru Fukunaga², and Masaaki Date²

¹ Department of Human and Artificial Intelligence Systems, Fukui University

² OKI Electric Industry Co., Ltd., Ubiquitous System Laboratory,
Corporate Research & Development Center

Abstract. This paper describes a novel distributed communication timing control for wireless sensor networks. For collision avoidance among sensor nodes, communication slots are allocated with a centralized controller in TDMA, however, we propose Phase Diffusion Synch-Alliance model as a fully distributed communication timing control. This model is based on the coupled phase-oscillator dynamics to dynamically adjust communication timing where phase synchronization and repulsion are coordinated depending on the network topology.

1 Introduction

In this paper, we suppose a sensor network composed of more than hundreds of sensory devices, sensor nodes, with a function of wireless communication where each node periodically transmits data to neighboring nodes in the range of communication. Some issues arise in regard to the communication timing control. The collision avoidance is one of the classical but still the most important issue in the wireless communication. Because each node is assumed to be driven by a battery, repetition of data transmissions should be avoided to save unnecessary energy consumption. The communication range is also limited in the small range since the electric power consumption is in proportion to the 2 to 4th power of the distance of data transmission[1]. Among the standard protocols, TDMA[2, 3] guarantees collision-free communication, however it requires a base station for centralized access controls which make the whole system stiff and should be the final choice for the wireless sensor networks. Meanwhile, CSMA [4, 5] has been also used as a standard protocol as a fully distributed timing control, however, it is not efficient in that the throughput will substantially decline in the case that a number of nodes communicate in the network, and it causes disadvantages in the increasing costs of carrier sensing[6]. Also, the hidden terminal problem is left to be solved[4, 5]. As a peculiar problem in sensor networks, some nodes may occupy the timing slot for a long period which would cause imbalanced conditions in the communication network. Thus, we have many problems to solve in the issue of communication timing control. In order to cope with these problems, we propose *Phase Diffusion Synch-Alliance* method as a fully distributed wireless communication timing control for the sensor networks which is an extended model of our previously proposed method named *Phase Diffusion Time*

Division [7] based on self-organization in the coupled phase oscillator dynamics. The details are described in subsequent sections.

2 Phase Diffusion Synch-Alliance: PDSA

2.1 Approach in Phase Diffusion Synch-Alliance: PDSA

The phase dynamics in PDTD [7] is fully based on the repulsive force interactions which make each phase of oscillator apart from each other to achieve collision-free state. Where, some clusters of phase in sync emerge, but its process can be facilitated if the repulsive interaction and synchronization (attractive force) are well coordinated in the phase dynamics. Base on the same assumption in the case of PDTD, we introduce *node type* for each node as shown in fig.1 where the number of node represents node type. Node type is self-adjusted according to the network topology. While the phase of node *a* must be repulsive with phase of nodes in the interaction range in 2Hop area, it attempts to synchronize with the nodes of equivalent node type as shown in fig.2; thus, we expect more fast and effective phase pattern formation. A set of the equivalent node type for synchronization is named *synch-alliance*. The synch-alliance is not determined a prior, but it is organized according to the node-type selection. The method of PDSA provides followings; (i) node-type selection for sync-alliance formation, (ii) coupled phase dynamics unified repulsive and synchronizing interactions to form an effective phase difference pattern to facilitate collision-free state in fully distributed way.

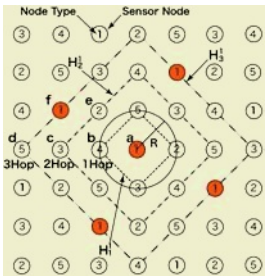


Fig. 1. Sensor Nodes and Node-type

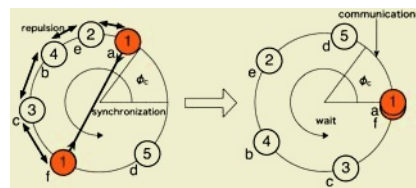


Fig. 2. Phase Difference Formation with Synch-Alliance

2.2 Collision Detection and Collision Rate

In this paper, we do not deal with actual data communications over the sensor networks; we focus on the timing control for collision avoidance for the present. However, the phase difference pattern is self-organized based on the interactions of pulse signals. If a node detects pulse signals from other nodes, each timing is encoded into the phase diagram; hence, if any two phases appear within the

phase interval, $0 \leq \theta < \phi_c$, which state is regarded as a collision. Note that this is not actual collision in the data communication, but a virtual detection of potential collision. The collision rate is given by c_i . The formal definition and evaluation of collision are described in [7].

3 Synch-Alliance Formation

3.1 Synch-Alliance with *Node-Type*

In PDSA, every node must form phase differences with neighboring nodes within the interaction range to avoid collision state, however, synchronization with some nodes which are not related to the collision will facilitate an efficient phase pattern. We refer to the group of nodes to be synchronized as synch-alliance which is discriminated from the other nodes based on *node-type*. Data containing node-type are referred to as type data. For this argument, we firstly define a peripheral node set as follows;

$$\partial_{n\text{Hop}}^i = \{\text{Nodes in the range of } n\text{Hop.}\} \quad (1)$$

Also, the node set within n Hop from node i , H_n^i , is given as follows;

$$\begin{cases} H_1^i = \{k \mid k \in \partial_{1\text{Hop}}^i\} & (n = 1), \\ H_n^i = \{k \mid k \in \partial_{n\text{Hop}}^i - \partial_{(n-1)\text{Hop}}^i\} & (n = 2, 3). \end{cases} \quad (2)$$

Then, node-type of node i is denoted as $\tau(i)$, and a set of type data within n Hop from node i is denoted as $\tau(H_n^i)$ which is defined as follows;

$$\tau(H_n^i) = \{\tau(k) \mid k \in H_n^i\} \quad (n = 1, 2, 3). \quad (3)$$

Looking back at fig.1, the neighboring node sets of 1Hop to 3Hop of node 1 is illustrated by H_1^1 to H_3^1 respectively. Also, we refer to the number of element in the set A by denoting $|A|$ for later discussions.

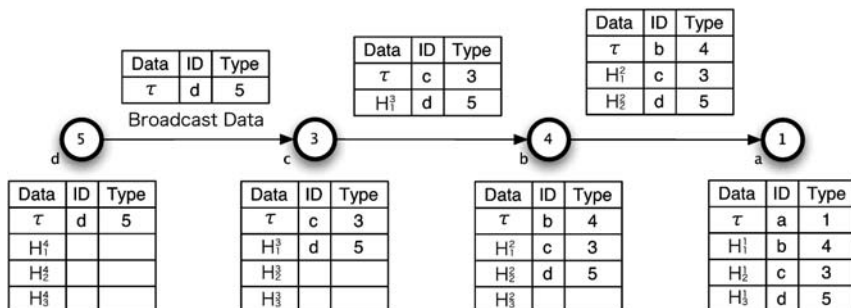


Fig. 3. Propagation Type data

3.2 Acquisition Method of Node-Type Data

Each node i is assumed to collect node-type data within 3Hop, $\tau(H_3^i)$ by means of multihop broadcast. We presume this data transmission is made by very short pulse signals and is negligible to the primary communication. Each node i broadcasts not only own node-type data, but also the data set of nodes within 2Hop neighborhood, $\tau(H_2^i)$. For example, as shown in fig.1, node a can obtain $\tau(H_3^a)$ where node-type data of node b, c , and d are included. In fig.3, propagation of node-type is illustrated where node is depicted with circle, and the suffix to the left represents node ID, and the number inside of the circle represents node-type. Also, the data structure is illustrated as a table by which data packet each node broadcasts to the neighbor nodes. In fig.3, node c receives the type data ($\tau(d) = 5$) from node d . Although the broadcast includes all the data sets received from the other peripheral nodes, fig.3 illustrates only a part of the data flow, from node d to node a . Furthermore, each node has a local time, and the time data is included in the type data when transmission. The time data is used as the criterion to check the latest data among received data.

3.3 Node-Type Selection

Let denote $C_2^i(\sigma)$ be a subset of $\partial_{2\text{Hop}}^i$ taking type $\sigma (\sigma \in 1, 2, \dots, 7)$, and define as;

$$C_2^i(\sigma) = \{k \mid k \in \partial_{2\text{Hop}}^i \text{ and } \tau(k) = \sigma\}. \quad (4)$$

Then, in the case that node i takes $\tau(i) = \sigma$, the fitness value F_i is introduced to evaluate degree as to how many nodes take the equivalent node-type to $\tau(i)$ within 2Hop from node i , ($\partial_{2\text{Hop}}^i$), which is defined as,

$$F_i(\sigma) = \exp \left(-\eta \cdot \frac{|C_2^i(\sigma)|}{|\partial_{2\text{Hop}}^i|} \right). \quad (5)$$

F_i takes the value between 0 and 1 according to the number of nodes taking the same type with node i ; it goes to 0 if all nodes take the equivalent type to node i , and vice versa. This implies the degree of potential risk of collision. Next, the parameter indicating feasibility for the node to select node-type σ is given by

$$f_i(\sigma) = 1 - \frac{a}{a + \exp(-\zeta \cdot |C_2^i(\sigma)|)}. \quad (6)$$

Where, ζ is given by $\zeta = 4 + 5 \cdot F_i$, and $a = 0.001$ is used for simulations. $f_i(\sigma)$ represents a sigmoid function which enables to escape initial convergence in the type selection while the fitness value takes low value. By eq.6, selection probability of node type σ is made by

$$P_i(\sigma) = \frac{f_i(\sigma)}{\sum_{\tau=1}^{N_i} f_i(\tau)}, \quad (7)$$

where N_i denotes the number of node-type which takes minimum 7, but is adjusted by the procedure in following section.

3.4 Self-tuning of the Number of Node-Type

This section describes self-adjustment procedure of the number of kind, hereafter denoted as $\#$, of node-type based on fitness value F_i of node i . Provided that nodes are arranged in a lattice form, $\#$ of node-type can be equivalent each other. When configuring sensor networks in practice, however, its network topology is supposed to be deformed rather than a regular grid form. Therefore, we presume the network topology as shown in fig.4(a) where the topology is perturbed based on the regular grid model. In the case of the perturbed gird model, $\#$ of node-type must be adjusted because the density of node differs depending on the part of the network; some crowded parts may require more node-types, while the other part may require less. Since information on the network topology is not available a prior, each node is required to cope with these problems automatically.

The recent history of fitness value F_i given by eq.5 is stored in queue M_i define as

$$M_i(t) = \{F_i(t), F_i(t - T_i), \dots, F_i(t - mT_i)\}. \quad (8)$$

where, $T_i = \frac{2\pi}{\omega_i}$ denotes the evaluation cycle of node i , and $m = 20$ is assumed in simulations. Maximum value of M_i is denoted as $\max M_i$, and $\#$ of elements is represented as $|M_i| (= 20)$. The designated time where $\max M_i$ is obtained is referred to t^* as follows;

$$t^* = \begin{cases} \max \left[\underset{t \in [t-kT_i, t]}{\operatorname{argmax}} M_i(t) \right], & \text{for } \max M_i = 1, \\ \min \left[\underset{t \in [t-kT_i, t]}{\operatorname{argmax}} M_i(t) \right], & \text{for } \max M_i < 1. \end{cases} \quad (9a)$$

$$(9b)$$

Where, $k = 1, \dots, m$. In the case of $\max M_i = 1$, time t^* will designate the latest time in $\max M_i$, meanwhile, it will designate the earliest time in the case of $\max M_i < 1$. Normalizing fitness value F_i with time decay, the stress value z_i is defined as;

$$z_i = 1 - \left(\frac{\sum_{k=1}^m \exp^{-b \cdot k} F_i(t - kT_i)}{\sum_{k=1}^m \exp^{-b \cdot k}} \right)^2. \quad (10)$$

Where, $b = 0.1$ is assumed in simulations. The stress value z_i is calculated every cycle T_i , and accumulated based on the following rule;

$$Z_i = \begin{cases} Z_i + z_i, & t - t^* \geq \hat{n}T_i, \\ Z_i, & t - t^* < \hat{n}T_i, \\ 0, & \text{if } \# \text{ of nodetype changes.} \end{cases} \quad (11)$$

Where, $\hat{n} = 3$ is assumed in simulations. If $\max M_i$ does not change its value during the fixed cycles \hat{n} , the stress value z_i is accumulated to Z_i . At the first stage of adaptation, the fitness F_i will take less than 1 every cycle, so the designated time t^* is likely to take the earliest time (smaller value) according to eq.9b; it implies that $t - t^*$ becomes larger and the stress value z_i will be frequently accumulated to Z_i . Meanwhile, if the fitness F_i converges to 1, since t^* will take

always the latest time, Z_i will remain unchanged. However, Z_i is refreshed to 0 whenever # of node-type is updated. Denoting N_i ($N_i \in 5, \dots, \bar{N}_i$) as the value of # of node-type, the update rule is given by the following probability;

$$N_i = \begin{cases} N_i - 1, & \left(\frac{\sum_{k=1}^m F_i(t-kT_i)}{|M_i|} = 1 \right) \text{ and } 5 < \tau(i) < \bar{N}_i, \\ N_i, & \left(\frac{\sum_{k=1}^m F_i(t-kT_i)}{|M_i|} < 1 \right), \\ N_i + 1 \text{ with probability } \frac{1}{2}, & Z_i > 1. \end{cases} \quad (12)$$

In the case that a state of $F_i = 1$ maintains for certain period mT_i , # of node-type will decrease in order to reduce redundant node-type. However, since the optimal # of node-type is known to be 5 in a regular grid, the minimum value is set to 5. Meanwhile, if Z_i takes larger than 1 which implies that the fitness F_i remains low, and it is difficult to improve the performance, # of node-type will increase to alleviate the situation. In other cases, N_i remains the same. This adjustment is implemented according to the congestion of node assignment in network topology.

4 Phase Dynamics

Coupled Stochastic Phase Dynamics: Outline. In this section, we describe the phase dynamics to self-organize a collision-free communication timing pattern. Each node interacts with the nodes inside of 3Hop (∂_3^i), and they are classified into two groups, *Synch-Alliance* to be synchronized and *Repulsive* node set to be kept away from the phase of node i . *Synch-Alliance* is defined as the nodes located in 3Hop from node i and taking the equivalent node-type of node i ; that is given by

$$A_3^i(\sigma) = \{k \mid k \in H_3^i \text{ and } \tau(k) = \sigma\}. \quad (13)$$

Where, we abbreviate denotation as $A_3^i(\tau(i)) (= A_3^i)$. On the other hand, *Repulsive* node set for node i is formally given by

$$B_2^i(\sigma) = \{k \mid k \in \partial_2^i \text{ and } \tau(k) \neq \sigma\}. \quad (14)$$

We also abbreviate notation as $B_2^i(\sigma) = B_2^i$. Note that as node-type selection is optimized, B_2^i will approach to ∂_2^i because there will be no equivalent node-type within 2Hop. Now, the coupled phase dynamics are defined as follows,

$$\dot{\theta}_i = \omega_i + \sum_{j \in A_3^i} G(\Delta\theta_{ij}) + \sum_{j \in B_2^i} R(\Delta\theta_{ij}) + \xi(S_i) \quad (15)$$

Let $\theta_i(t)$ ($0 \leq \theta_i < 2\pi$) be the phase of node i at time t . The phase difference between node i and node j is given by $\Delta\theta_{ij} = \theta_j - \theta_i$, ($\text{mod } 2\pi$). Where, ω_i is eigenfrequency of the oscillator, $R(\Delta\theta_{ij})$ is a phase response function of repulsion, $G(\Delta\theta_{ij})$ is a phase response function of synchronization and $\xi(S_i)$ is a stochastic function. This method repulses a phase with the node of the interaction range, and aims at formation of phase difference by synchronization a phase positively with the node which does not interfere in communication.

Phase Response Function: Synchronization. The node i also interacts with synch-alliance nodes in $A_3^i(\tau(i))$. The phase response function for synchronization is expressed as follows;

$$G(\Delta\theta_{ij}) = \begin{cases} \hat{\alpha}\Delta\theta_{ij} & (\Delta\theta_{ij} < \pi) \\ \hat{\alpha}\Delta\theta_{ij} - 2\pi & (\pi \leq \Delta\theta_{ij}) \end{cases} \quad (16)$$

Phase Response Function: Repulsive Interaction. The phase of node i must be repulsive to those in the node set B_2^i for collision avoidance. The phase response function for repulsive interaction is defined as following formula,

$$R(\Delta\theta_{ij}, p) = \begin{cases} \alpha \left(\Delta\theta_{ij} - \frac{2\pi}{p} \right), & \Delta\theta_{ij} \leq \frac{2\pi}{p}, \\ \beta \Delta\hat{\theta}_{ij}, & \frac{2\pi}{p} < \Delta\theta_{ij} < 2\pi - \frac{2\pi}{p} \text{ and } \Delta\hat{\theta}_{ij} < \frac{\pi}{p}, \\ \beta \left(\Delta\hat{\theta}_{ij} - \frac{2\pi}{p} \right), & \frac{2\pi}{p} < \Delta\theta_{ij} < 2\pi - \frac{2\pi}{p} \text{ and } \Delta\hat{\theta}_{ij} > \frac{\pi}{p}, \\ \alpha \left(\Delta\theta_{ij} - (p-1) \frac{2\pi}{p} \right), & 2\pi - \frac{2\pi}{p} \leq \Delta\theta_{ij}. \end{cases} \quad (17)$$

$$\beta = v(1 - c_i)^2. \quad (18)$$

Where $\Delta\hat{\theta}_{ij} = \Delta\theta_{ij}(\text{mod } \frac{2\pi}{p})$, and α, v are constant coefficient. Also p denotes the number of phase divisions, which must be chosen to satisfy $\frac{2\pi}{p} > \phi_c$ such that sufficient large phase margin are guaranteed for a collision free phase pattern. We also note that β is responsible for the stochastic adaptation, where the slope of $R(\Delta\theta_{ij})$ will change according to the collision rate c_i .

Stochastic Adaptation. The phase order relation of nodes cannot be interchanged only in an action of a phase response function. Therefore, stochastic fluctuation reflecting the collision rate is incorporated to the dynamics. Detail of this function is described in [7].

5 Simulation

5.1 Simulation Settings

Simulations are conducted to verify proposed method. The perturbed network is shown in fig.4(a) which deals with perturbed grid mode. In regard to the perturbed network, topology was configured from the regular grid by perturbation with uniform random values in $[-\frac{d}{2}, \frac{d}{2}]$. The initial value of each phase is randomly assigned in $[0, 2\pi]$, and node-type is also randomly given from $[1, \dots, 5]$. The other common parameters are listed in table.1.

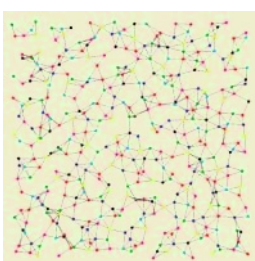
5.2 Simulation Results

Collision rate is employed for overall performance evaluation. The phase difference histogram is presented to illustrate how phase patterns are organized through the coupled phase dynamics with eq.(15). Fig.4 (b) shows a degree distribution of perturbed grid model, where Poisson distribution is observed as we

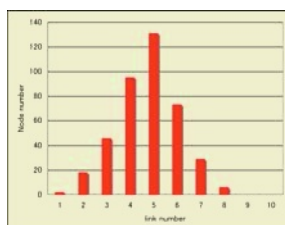
Table 1. Common simulation parameter set

| | | |
|------------------|--|-----------------------------------|
| i | Network size | 20×20 |
| P_i | Default number of node-type | 5 |
| α | Coefficient of phase reaction function | $1.0[\text{rad}/\text{s}]$ |
| $\hat{\alpha}$ | Coefficient of phase reaction function | $20.0[\text{rad}/\text{s}]$ |
| v | Coefficient of phase reaction function | $0[\text{rad}/\text{s}]$ |
| ω_i | Eigen frequency of a node | $10[\text{rad}/\text{s}]$ |
| n | Calculation cycle of a collision rate | 10 |
| \hat{n} | Calculation cycle of a stress rate | 3 |
| d | The node distance | 40[m] |
| p | The phase partition number | 11 |
| ϕ_c | The Phase margin | $\frac{2\pi}{p} - \frac{\pi}{30}$ |
| $\max P_i$ | Maximum Type number | 11 |
| $R(1\text{Hop})$ | Communication range | 56[m] |

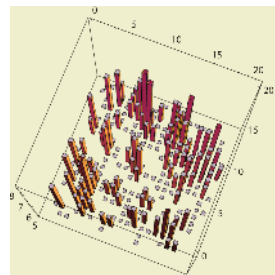
expected from the theory of random graph. As shown in fig.4 (c), the spatial distribution of degree (# of link for each node) is not uniform, which suggests there appear crowded and sparse areas in the network; hence, # of node-type



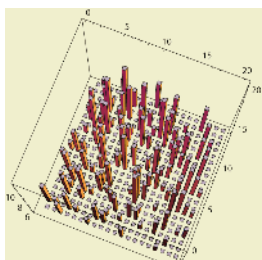
(a) Topology of networks



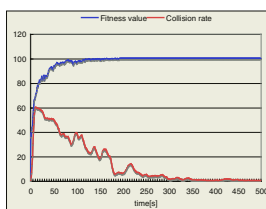
(b) Degree distribution



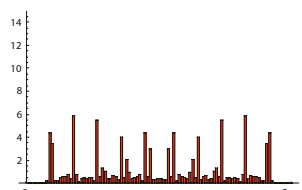
(c) The number of link for each node



(d) The number of Node-Type in the Convergent state



(e) Collision rate and Fitness value



(f) Phase division pattern t=500[s]

Fig. 4. Perturbed grid model

must be adjusted to deal with spatial randomness. As shown in fig.4 (d), the self-adjustment of # of node-type is successfully attained where crowded part has more node-types and sparse area has less. Collision-free state is also achieved as shown in fig.4 (e). Fig.4 (f) depicts average phase difference pattern, which seems deformed because of the topological irregularity.

6 Conclusions

Phase Diffusion Synch-Alliance was proposed as a novel distributed communication timing control in the sensor networks. Neighboring nodes are dynamically classified into a synch-alliance for synchronization and the other nodes for repulsive interactions through the node-type selection. The phase dynamics realizes that more than hundreds of nodes can cooperatively self-organize a time division pattern for collision free communication. As well as a regular grid model, we confirmed that PSDA is applicable to deformed random graph networks. Although this model illustrates satisfactory performance, some problems remain to be solved as a future work in regard to the convergence performance. In the phase dynamics, interference is sometimes observed in the interactions between repulsive and synchronization actions. It is also related to efficiency on node-type selection. in addition to these theoretical revisions, hardware experiment is also necessary.

References

1. Rabaey, J.M., Ammer, M.J., da Silva, J.L., Patel, D., Roundy., S.: Picoradio supports ad hoc ultra-low power wireless networking. *Computer* **33** (2000) 42–48
2. Falconer, D.D., Adachi, F., Gudmunson: Time division multiple access methods for wireless personal communications. *IEEE Communications Magazine* **33(1)** (1995) 50–57
3. Shih, E., Cho, S., Ickes, N., Min, R., Sinha, A., Wang, A., Chandrakasan, A.: Physical layer driven protocol and algorithm design for energyefficient wireless sensor networks. *ACM SIGMOBILE Conference on Mobile Computing and Networking and Roma and Italy* (2001) 272–286
4. KLEINROCK, L., TOBAGI, F.A.: Packet switching in radio channels: Part i-carrier sense multiple-access modes and their throughput-delay characteristics. *IEEE Transaction on Communications* **23** (1975) 1400–1416
5. Tobagi, F.A., Kleinrock, L.: Packet switching in radio channels: Part ii—the hidden terminal problem in carrier sense multiple-access and the busy-tone solution. *IEEE Transactions on Communications* **23** (1975) 1417–1433
6. S.G.Glisic: 1-persistent carrier sense multiple access in radio channels with imperfect carrier sensing. *IEEE Trans. Commun.* **39** (1991) 458–464
7. Sekiyama, K., Kubo, Y., Fukunaga, S., Date, M.: Self-organizing communication timing control for sensor network. *Proceeding of the 7th Asia-Pacific Conference on Complex Systems Cairns Convention Center, Cairns, Australian* (2004) 121–133

Supporting Design for Manufacture Through Neutral Files and Feature Recognition

T.J. Jones¹, C. Reidsema¹, and A. Smith²

¹ School of Mechanical and Manufacturing Engineering, UNSW, Australia
t.jones@student.unsw.edu.au

² GKN Aerospace Engineering Services, Port Melbourne, Australia

Abstract. To reduce the non-recurring design costs of creating a new product, Knowledge Based Engineering developers must strive to combine design tasks with downstream processes, including analysis, manufacturing appraisal, process planning and inspection activities. To facilitate the transfer of data between design companies and those involved in downstream activities we propose that the IGES neutral CAD format and a wireframe model is useful for supporting concurrent engineering objectives and enhancing contemporary Feature Recognition (FR) processes. This paper presents an Intelligent Design Advisor (IDA) in development; combining broad range FR with manufacturing knowledge has the potential to reduce design cycle time in the concurrent engineering environment. The IDA captures company knowledge and intellectual property from experts and supports designers by advising of manufacturing alternatives satisfying functional and economic measures.

1 Introduction

To be successful, an engineering company must aim to reduce the non-recurring design costs of creating a new product, without diminishing quality standards. To facilitate such a cost reduction, companies must combine the design task with downstream processes [1]. There are a number of computer-based tools in the industry with the purpose of reducing the ‘over the wall’ approach to engineering design, however they do not bridge the gap between downstream processes like manufacturing analysis and the upstream processes of conceptual design where the most impact can be realised. There is a need, therefore, for engineering companies to develop Knowledge Based Engineering (KBE) tools to automate the process of integrating design and analysis. This paper suggests a method for providing information about the product model to downstream processes, thereby reducing problems associated with interacting with product designs at the initial, or conceptual phase. Computer Aided Process Planning (CAPP) software automates the process of matching a product to a manufacturing process traditionally undertaken by a human expert. This process involves a number of key steps:

1. Interrogating and interpreting a product Computer Aided Design (CAD) model for its key features;
2. Selecting a machine capable of manufacturing these features, and;
3. Creating a sequence of activities to have the selected machines create the product described by the geometry of its CAD model.

CAPP software tools are useful for reducing demand on skilled human experts and ensuring the production of consistent process plans through eliminating redundancies

and conflicts that arise in complex designs. CAPP tools are, unfortunately, not as adept at dealing with variations in product topography as human experts. Additionally, manual feature recognition is a time consuming task. For the human expert, when experience and creativity are not capable of producing a viable manufacturing process plan, the original design must be modified. Contemporary CAPP software does not yet have the ability to interact with the engineering designer sufficiently early to reduce the chance of creating an uneconomic design or one that cannot be created. Additionally, CAPP software tends to be limited by restriction of manufacturing domains in terms of process planning and ability to recognise types of design features contained within the product CAD model. Salomans suggests that using knowledge of design features from CAD software used to create a product model, known as feature based design, involves the translation of feature information from one type to another and is inefficient [4]. From the perspective of feature-based design, an example might be the conversion of design features in the product model to manufacturing features useful to a CAPP system as described in Figure 1.



Fig. 1. Example of Design Features vs. Manufacturing Features

A new methodology is required to overcome the limitations of recognising features in complex problems and the limitations on manufacturing domain knowledge prevalent in current implementations of CAPP software FR techniques.

2 Feature Recognition

Feature recognition is an automated method for identifying and extracting features from a CAD product model for the purpose of finding manufacturing or analysis information about the product. Automating the extraction of design features from a CAD model has a positive effect on reducing lead-time of activities downstream of engineering design. The role of feature recognition in relation to manufacture is depicted in Figure 2. Mainstream contemporary computer aided design modelling software utilises a design by feature methodology. Automated recognition of the features of a design should therefore be a simple matter of citing the feature elements defined in the original CAD product model. The disadvantage of this approach is that, as shown in Figure 1, the features utilised within a product model may have different interpretations within different domains. For example, features that support manufacturing analysis differ from features that support stress analysis and so on [3]. Geometry, therefore, remains the most important characteristic of a product model in feature recognition processes, as it is consistent across all domains. This implies that there are no disadvantages in using a non-specific file format, for example neutral files such as IGES, over a proprietary CAD file format for the purpose of feature recognition. Current literature covering feature recognition highlights the difficulty associated with

developing a generic feature recognition method and the domain of a generic feature recognition tool is potentially vast, even if constrained to certain products and materials.

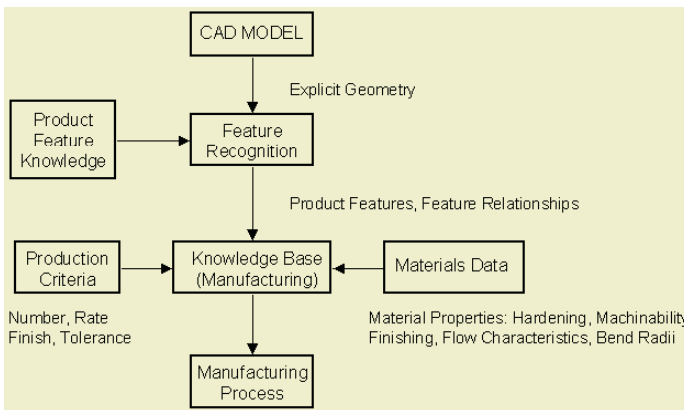


Fig. 2. Feature Recognition in Relation to Manufacturing Analysis

A number of solutions have been put forward to solve this problem that includes:

1. Development of new Design by Feature (DBF) CAD systems with more robust feature descriptions [3].
2. Application of rigorous naming conventions to track the interaction of different features [5].

Whilst these methods may go someway towards solving the problems associated with finding features in the first instance, they do restrict the software that may be used in terms of the focus of utilisation such as Design for Manufacture (DFM) or analytical or detail design. Additionally these methods do not deal with the problem of applying FR techniques to legacy product models, which are a source of valuable Intellectual Property (IP) retained by an organisation. What is required is a combination of various FR algorithms, each successful at solving a small aspect of the overall domain. This approach has the potential to create faster, more efficient, and more importantly, more robust solutions than are currently possible. For example, consider a product model in the conceptual design phase for which a basic appraisal of possible manufacturing processes is desired, but for which no detailed geometry exists. In order to facilitate the successful combination of independent FR algorithms, we propose that a common standard be used for examination by all FR routines applied to a problem. Such a standard would require:

1. Consistent input data;
2. Dependency on geometry only; and
3. An ability to retain and utilise legacy knowledge held by a company.

Such a standard would also alleviate problems associated with transferring product models between organisations. The feature recognition processes we are developing works in conjunction with wireframe product models and utilises knowledge of relationships between geometric entities in order to assemble product features.

Table 1. Example of Rules for identifying a Through Hole Feature

| Rule ID | Geometry Relationships |
|---------|--|
| 1 | Two planar circular curve groups |
| 2 | Normal vectors from planar circular curve groups (ID 1) must intersect |
| 3 | Planar circular curve groups (ID 1) must not lie on adjacent curve groups |
| 4 | Planar circular curve groups (ID 1) must each lie on a non-identical curve group |

Table 1 shows an example of a set of rules required to identify a through hole feature. Additional rules are required to separate individual features and are still in development, however each closed group of curves cannot be present in more than a limited number of feature types to avoid the problem of generating multiple feature types from identical geometry.

3 Data Exchange Issues

It is generally accepted that there are two methods of identifying features in a CAD model: capturing features as they are created and identification of features after creation, by post-processing. For companies whose focus is in providing engineering design services to a client, the latter method is often the preferred one. Such companies must cater for a wide variety of CAD formats whilst simultaneously ensuring a competitive resource profile in terms of carrying a high investment in manpower and CAD software skills and licenses. The design and manufacture of engineering products typically involves the transfer of information between designers and manufacturers, ordinarily located in different companies and often in different countries. Although each company will have different requirements of its software, the CAD product model is the most important embodiment of design and manufacturing knowledge of the product. The overhead that comes with conforming to the Product Data Management (PDM) system of another company may be overcome by the use of software independent formats for storing model geometry. The International Graphics Exchange Format (IGES) and Standard for Exchange of Product Model Data (STEP) are both non-proprietary international accepted standards and often referred to as neutral formats [6,7]. The use of neutral files offers a number of advantages to the KBE software developer. A company can remain independent of the CAD software used by a client or customer and utilise their core competencies related to their choice of engineering software. Additionally, neutral files offer independence of the modelling techniques that have been used to generate the product model geometry through rewriting the product feature tree with consistent geometry types and no parent/child relationships. Of particular benefit to feature recognition processes, this marshalling of product geometry into a structured format through the use of neutral files permits simpler aggregation of multiple smaller feature libraries. This is useful in decomposing the problem so that combined algorithms suitable for identifying the most suitable set of features of a geometric shape can be used.

Wireframe models are now seldom used for creation of complex solid models, even though they are easily generated by using neutral file formats like IGES and STEP. Unlike solid models, wireframe models are computationally undemanding to handle but, like surface models, they can become ambiguous when determining what is ‘solid’ and what is a removal volume. This ambiguity may be too difficult for an

automated feature recognition system to handle. However, the speed and simplicity of analysing a wireframe model is significant enough when compared to surface and solid based models to make this approach worthwhile.

4 Methodology

The employment of domain indefinite feature recognition processes and neutral file formats has the potential to assist development of KBE applications by reducing dependence between customer-client data management systems and reducing the computational resources and time required to extract broad ranging features from computer product models. These methods are being utilised in our current development of an Intelligent Design Advisor (IDA) for supporting the conceptual phase of engineering design [9]. An IDA, as seen in Figure 3, supports design processes in the context of concurrent engineering by matching design features of a CAD model with manufacturing process knowledge, providing feedback on manufacturing options to the designer. At the conceptual design phase, there is comparatively little information available to support product costing, however with knowledge of relative economics of manufacturing processes, product features and material combined with production batch sizes, the designer is able to focus detailed features of the design on the suggested manufacturing solution. A composition of feature recognition algorithms to support a design advisor must be augmented by:

1. A decision making mechanism;
2. A Program Interface for user feedback concerning product features; and
3. A knowledge base of manufacturing knowledge as it relates to features of design, together with relative cost differences between processes.

The decision-making system uses feature recognition processes to extract information from a product model and is passed to a user for confirmation of material, tolerance and batch sizes. Utilizing a knowledge base for manufacturing process capability we are developing an algorithm for assisting the engineering designer in selecting a manufacturing process satisfying functional criteria at lowest cost. If maintained by a manufacturing company, an Intelligent Design Advisor for manufacturing may allow the engineering designer to remain abreast of available production capability without the supplementary burden information gathering outside of their own discipline. The IDA will have the potential to reduce feedback time between manufacture and upstream conceptual design to minimize the overall design cycle time, particularly for design companies not directly involved with manufacture. Additionally, the IDA permits the capture of company knowledge and IP in the processes used by human experts to relate design to manufacture. Development of manufacturing knowledge sources is continuing, with assistance from academic and industry sources, together with a selection of broad domain feature recognition algorithms to support manufacturing evaluation. The selection of a Decision Support System (DSS) is yet to be made, however a number of options are available for solving complex problems like those inherent in the ‘fuzzy’ nature of design shape and manufacture evaluation.

The intelligence proposed through this solution is founded on the capture and instantiation of existing engineering knowledge and design intent as it applies to relationships between design features and manufacturing solutions, Table 2.

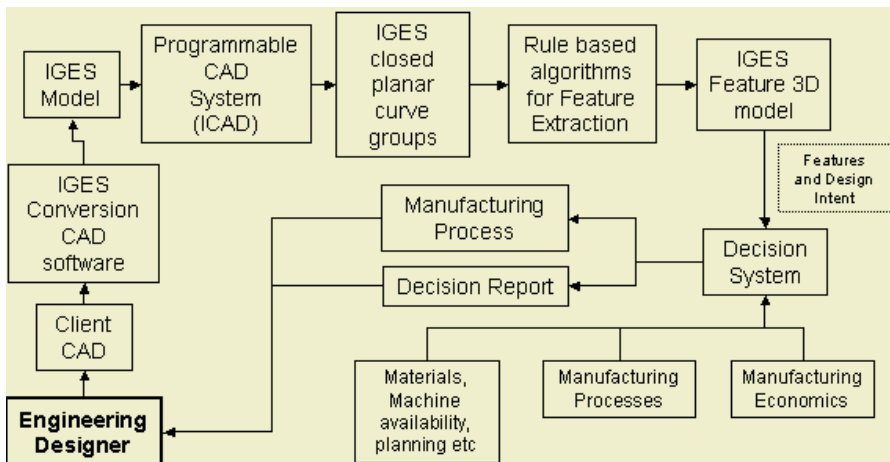


Fig. 3. Overview of Intelligent Design Advisor for Manufacturing

Table 2. Manufacturing Knowledge

| Process Type | Manufacturing Knowledge |
|------------------|--|
| 3 axis Machining | Square edged features only; slots, pockets, holes, bosses, stiffeners, etc |
| Casting/Forging | Presence of parting plane and drafts, internal cavities with limited access, no sharp corners or edges, low batch sizes. |

The DSS, uses sources of knowledge that includes:

1. Relationships between materials and manufacturing process capability;
2. Relative economics of manufacturing processes; and
3. Manufacturing process capability and availability.

An intelligent agent identifies a best-case solution to the problem of manufacturing process selection, using knowledge sources to satisfy the requirements of the input data. The complexity of this problem may be extended to include concepts like minimum weight or minimum tolerance in addition to satisfying functional and economic criteria. As a first step, case-based reasoning or rule-based approaches will be tested in preference to a more complex solution technique, for reasons of programming simplicity. The acceptance of a design aid for manufacturing can be foreseen when it minimizes disruption to the creative design process by being suitably time responsive to the requirements of the user. Thus, the technology that will be selected will be focused on this objective.

5 Conclusions

Commercial pressure within the global aerospace industry to reduce non-recurring engineering design costs has necessitated the integration of design with downstream applications like manufacturing process planning, analysis, assembly and inspection. Feature recognition is a process for identifying and extracting design features from a geometric CAD product model and may be used as the basis for developing KBE tools to automate the integration of design with downstream processes. The applica-

tion of rules to identify feature by the relationships between wireframe curve groups is fast and captures intelligent knowledge of design intent. The use of neutral file formats like IGES and STEP provides marshalling of the geometry components used to create a part, and thus makes the model independent of the parent CAD program and the CAD operator's hierarchy of design features used to build the product shape. When combined with a wireframe model, this design feature independence is a useful method of supporting generic feature recognition processes, particularly those not developed for application in a specific manufacturing domain. Feature recognition, as a core component of an Intelligent Design Advisor (IDA) for supporting the conceptual phase of engineering design has the potential to further reduce design cycle time within the framework of concurrent engineering. The intelligence of the decision system is supported by logical application of existing design knowledge in a new context, in a manner similar to intelligent agents like blackboard databases. An IDA capable of rapidly establishing an optimum manufacturing solution based on initial product geometry can support designers of engineering products, while retaining and re-applying company knowledge and intellectual property.

Acknowledgements

The authors would like to gratefully acknowledge the contribution from GKN Aerospace Engineering Services Australia in the areas of feature recognition and engineering design support, together with grant support from the Australian Research Council.

References

1. Ozturk, F. and Ozturk, N., 1999. *Feature-Based Environmental Issues: Neural Network-Based Feature Recognition*. International Journal of Vehicle Design, Vol. 21, No. 2, pp. 190-204.
2. Corbett J., Crookall J. R., (1986). Design for Economic Manufacture. *Annals of CIRP*, 1986, Vol. 35, No. 1 pp. 93-97.
3. Shah, J., Anderson, D., Kim, Y., Joshi, S., 2001. *A Discourse on Geometric Feature Recognition from CAD Models*. Journal of Computing and Information Science in Engineering, Vol. 1, pp. 41-51.
4. Salomons, O. W., 1994. *Computer Support in the Design of Mechanical Product: Constraint Specification and Satisfaction in Feature Based Design for Manufacturing*. PhD thesis, University of Twente, Netherlands, 1994.
5. Yan, X., Yamazaki, K., Liu, J., 2000. *Recognition of Machining Features and Feature Topologies from NC Programs*. Journal of Computer Aided Design, Vol. 32, pp. 605-616.
6. National Institute of Standards and Technology (USA). [online] <http://www.nist.gov/iges/>.
7. Standard for Exchange of Product Model Data: Int'l Standards Organisation, #10303.
8. Subrahmanyam, S. and Wozny, M. 1995. *An Overview of Automatic Feature Recognition Techniques for Computer-Aided Process Planning*. Computers in Industry, Vol. 26, pp1-21.
9. Jones, T. J., Reidsema, C., Smith, A., 2004. *Implementation Of Automated Manufacturing Process Planning In Engineering Design*. Proceedings of Asia-Pacific Industrial Engineering and Management Systems Conference, December 2004.

A Programmable Pipelined Queue for Approximate String Matching

Mitsuaki Nakasumi

Faculty of Economics, Komazawa University, 1-23-1 komazawa setagaya-ku Tokyo, Japan
nakasumi@komazawa-u.ac.jp

Abstract. Mining data streams is an emerging area of research given the potentially large number of business applications. A significant challenge in analyzing/mining data streams is the high data rate of the stream.

In this paper, we explain a Programmable Pipelined Queue to cope with the high data rate of incoming data streams. It can be added easily to general computer system. And we apply the Programmable Pipelined Queue to online string matching.

1 Introduction

Data stream mining must cope with the high data rate and deliver the analysis results in real time in resource constrained environments.

In many applications, the data of interest comprises multiple sequences that each evolve over time. These sequences are not independent: in fact, they frequently exhibit high correlations. Therefore, much useful information is lost if each sequence is analyzed individually. What we desire is to study the entire set of sequences as a whole, where the number of sequences in the set can be very large. For example, if each sequence represents data recorded from a network element in some large network, then the number of sequences could easily be in the several thousands, and even millions.

To make our task even more challenging, it is typically the case that the results of analysis are most useful if they are available immediately, based upon the portion of each sequence seen so far, without waiting for “completion” of data streams. In fact, these sequences can be indefinitely long, and may have no predictable termination in the future.

What we require is the capability to “repeat” our analysis over and over as the next element (or batch of elements) in each data sequence is revealed, so that accurate estimations of delayed/missing elements and/or up-to-date correlations are available quickly. And we have to do this on potentially very long sequences, indicating a need for analytical techniques that have low incremental computational complexity.

In this paper, we propose a novel approach that is able to mine data streams. Moreover, it is adaptable to memory, time constraints and data stream rate. We termed our approach as “programmable pipelined queue”. This approach has powerful data transfer mechanism.

2 Programmable Pipelined Queue

The system overview is shown in Figure 1. The system consists of general Processing Unit, Cache Memory and Main Memory. And furthermore, it contains Programmable

Pipelined Queue which includes input/pattern buffer as same as cache level memory hierarchy and Queue Manager. The Queue Manager component consists of a unit which executes instructions for data allocation and data access from I/O buffer area to the buffer. The input buffer contains data streams. The pattern buffer has strings to match. The input/pattern buffer is liner-addressable high throughput memory. And compiler allocates the address pointers to the input/pattern buffer. Queue Manager maintains the pointers of the input/pattern buffer.

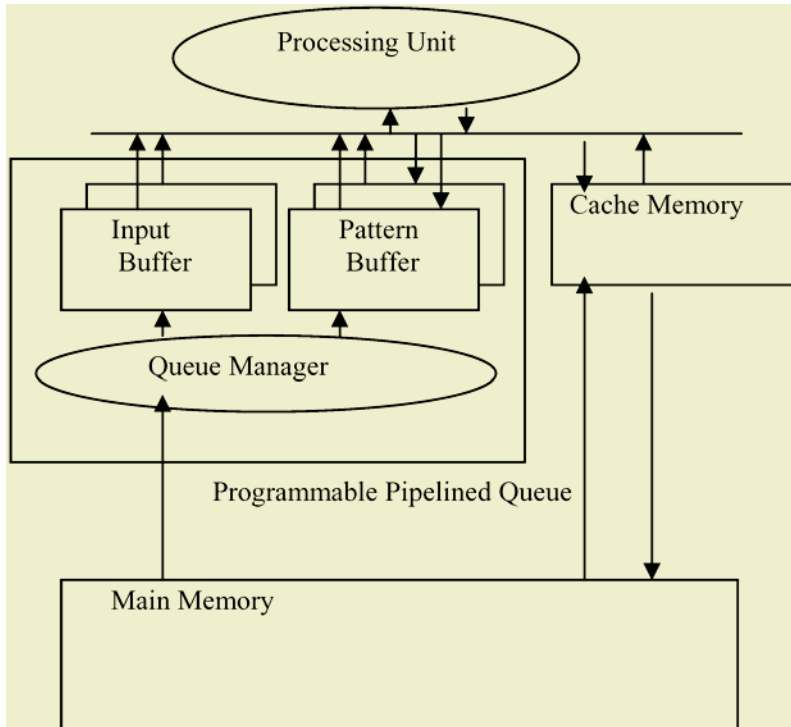


Fig. 1. System overview

The pointers of the input buffer are corresponded to I/O buffer addresses, and the pointers of the pattern buffer are corresponded to a part of address space. Since the buffers have been divided into many small banks, Processing Unit can access to the input/pattern buffer as pipelined.

The input buffer preloaded with the data stream from I/O buffer area on main memory. This allows the gap between the characters read from the buffer and the characters entering the buffer to vary as matches occur. Both the characters of data stream and pattern strings are supplied to the registers of Processing Unit. Queue Manager has the resource-aware logic that uses the data adaptation techniques to catch up with the high-speed data stream and at the same time to achieve the optimum accuracy according to the available resources. The process starts by checking the minimum data rate that could be achieved using data adaptation techniques with an acceptable accuracy.

If there is no match in the first character, the result of the second comparison is not considered. However, when the first comparison does match, the result of the second comparison is considered. This allows the system to use input characters faster than they enter into the buffer. This is important because when the comparison fails, the buffer stalls on the current character until all possible matching prefixes of the pattern are compared against. During this time, however, data continues to enter into the buffer. After the initial memory read, the memory essentially stands idle for the remainder of the cycle, and the combinational logic is idle until the completion of the memory read. Given this situation, pipelining is a general technique that is an obvious choice for increasing the speed of the system, but at first glance it seems unworkable. Pipelining generally does not make sense for single-character-oriented string matching architectures because we need to update the pointers each cycle based on results from the current cycle. The solution is parallel execution of two pattern matching. This solution increases the latency, but total performance will be better than stalled.

3 Pattern Matching Algorithm

A bit parallel pattern matching[10] is to simulate the non deterministic automaton, so that each row i of the automaton fits in a computer word R_i . For each new text character, all the transitions of the automaton are simulated using bit operations among the $k+1$ computer words. The formula to make the new R'_i values at text position j from the current R_i values is as follows:

$$\begin{aligned} R'_0 &= ((R_0 \ll 1) | 0^{m-1}) \& M[T_j], \\ R'_{i+1} &= ((R_{i+1} \ll 1) \& M[T_j]) | R_i | (R_i \ll 1) | (R'_i \ll 1), \end{aligned}$$

where $M[c]$ is a preprocessed mask table. The first bit of $M[c]$ is always set and the $(r+1)$ th bit is set whenever Pattern $P_r = c$. We start the search with $R_i = 0^{m-1} 1^{i+1}$. In the formula for R'_{i+1} are expressed, in that order, horizontal, vertical, diagonal and dashed diagonal arrows.

The algorithm is shown as following steps and Figure 2.

Figure 2 shows data flow of the algorithm. The following is the notation used in the figure. Let dotted line be the flow of data. Let box in the main memory be data block. The numbers in the figure are corresponded to following steps.

1. In preprocessing stage, A Matching table ($M[T_j]$) is build in the pattern buffer.
Each pattern is related with a character as pattern index.
2. Data items arrive in sequence with a data rate.
3. Queue Manager reads each characters and compares character with pattern index in matching table.
4. If pattern index matched, Queue Manager injects the pattern into allocated area in the input buffer (across the memory banks).
5. Processing Unit read the patterns from input buffer.
6. Processing Unit executes the formula to make the new R'_i .
7. If matching pattern within allowed error increase counter
8. Repeat 3 to 7.
9. If pattern buffer is full, then pattern string is migrated to data space by LRU algorithm.

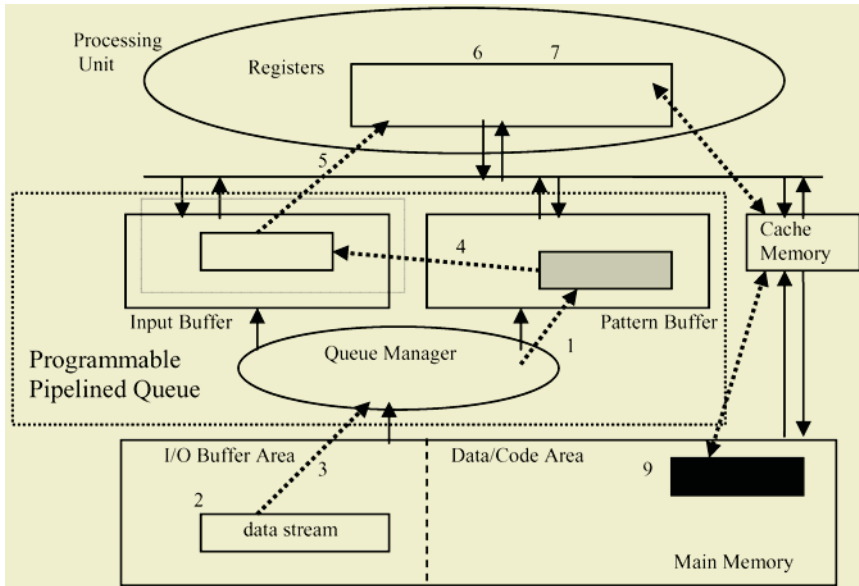


Fig. 2. Data flow of the algorithm

4 Cost Models for Proposed Scheme

In this section, we present our cost models for this system. The cost formulae are estimates of the response time for a given task using a specified architectural model when environmental factors are taken into consideration. We initially present the general cost model for approximate string matching. We then illustrate how the general model is mapped to the cost functions for our proposed system. The response time (expressed at a high level of abstraction) for approximate string matching is as follows:

$$T = t_p + t_m + t_{\text{overhead}} \quad (1)$$

where T is the processing clock cycle time, t_p is the clock cycle time taken to perform matching and preprocessing, t_m is the clock cycle time taken to perform memory and I/O access, and t_{overhead} is the scheduler latency.

Depending on the model used for and the approximate string matching different scenarios within each model, the factors which determine t_m will change. This results in a consequent change in the actual cost function that determines t_m .

In the following discussion, we present the different matching mechanisms and the cost functions to determine t_m for each case.

Traditional Paradigm

The $t_m^{\text{traditional}}$ for traditional paradigm is as follows:

$$t_m^{\text{traditional}} = \text{memory accesses} \times \text{cache miss rate} \times \text{miss penalty} \quad (2)$$

The larger cache block size reduces cache misses to takes advantage of spatial locality. One problem is that larger blocks can increase conflict and even capacity misses. Another is that larger blocks can increase miss penalty.

In this application, higher cache hit is expected approximate string matching process (with a few errors), but lower cache hit is expected to get string from data stream. Then, the total of cache hit rate in the approximate string matching is expected lower. The lower cache hit rate makes throughput lower.

We also consider scheduler latency, t_{overhead} . When a thread issues an I/O request via a kernel system call (such as a read() call), if the device driver that handles the system call cannot satisfy the request for data, it puts the thread on a wait queue. This puts the requesting thread to sleep so that it will not be eligible to run while waiting for the device to provide the data. The driver then insures that the I/O request will generate an interrupt when the device completes the request and then the driver returns control to the kernel. The requesting thread is asleep and the device is performing the requested I/O. After the I/O request is issued, the device will complete the request and interrupt. This will cause an interrupt service routine to run in the kernel, which runs the device driver's interrupt handler. The driver will figure out if the data from the device will satisfy the read request.

Proposed Paradigm

The t_m proposed for our proposed system is as follows:

$$t_m \text{ proposed} = \text{memory accesses} \times \text{queue stall rate} \times \text{queue stall penalty} \quad (3)$$

Since the queue manager maps I/O packets to data structure and injects the data into input buffer, it reduces the overhead of data copying from I/O buffer to main memory and from main memory to cache like memory(input buffer).

In this application, higher cache hit is expected approximate string matching process (with a few errors), and higher input buffer hit is expected to get string from data stream. Then, the total time of memory stall in the approximate string matching is expected lower. The lower memory stall makes throughput higher.

We also consider scheduler latency, t_{overhead} . When a thread issues an I/O request via a kernel system call (such as a read() call), if the queue manager that handles the system call cannot satisfy the request for data, the queue manager checks device status bits, periodically. The queue manager sets status bit on when arriving data to input buffer. Then the requesting thread is able to access input buffer without interrupt overhead.

5 Conclusions

This paper has shown a Programmable Pipelined Queue to cope with the high data rate of incoming data streams. There are three reasons to achieve high performance.

- 1) The queue manager can inject the many strings to the registers by pipelined data supply.
- 2) Since the queue manager maps I/O packets to data structure and injects the data into input buffer, it reduces the overhead of data copying from I/O buffer to main memory and from main memory to input buffer.
- 3) The requesting thread is able to access input buffer without interrupt overhead.

It is our future work to extend the prototype system so as to process those matching at high performance. In addition, it may improve the total performance to process several matching at a time, and to examine the possibility is also our future research topic.

References

1. Babcock B., Babu S., Datar M., Motwani R., and Widom J.: "Models and issues in data stream systems", In Proceedings of PODS (2002).
2. R. Rastogi, "Single-Path Algorithms for Querying and Mining Data Streams", In Proceedings of SDM2002,pp.43-48,2002.
3. V. Ganti, J. Gehrke, and R. Ramakrishnan: "DEMON: Mining and monitoring evolving data", In Proceedings of ICDE, pp.439-448, 2000.
4. B.-K. Yi, N. Sidiropoulos, T. Johnson, H. V. Jagadish, C. Faloutsos, and A. Biliris: "Online data mining for coevolving time sequences", In Proceedings of ICDE, pp.13-22, 2000.
5. R. Baeza-Yates and G. Navarro.: "Faster approximate string matching.", Algorithmica, 23(2):127-158, 1999.
6. T. Fawcett and F. J. Provost: "Activity monitoring: Noticing interesting changes in behavior", In Knowledge Discovery and Data Mining, pp.53-62, 1999.
7. R.J. Bayardo Jr., "Efficiently mining long patterns from databases", In Proc. of the 1998 ACM-SIGMOD Int'l Conf. on Management of Data, pp.85-93,1998
8. Sergey Brin, Rajeev Motwani, Jeffrey D. Ullman, and Shalom Tsur., "Dynamic itemset counting and implication rules for market basket data", In Proc. of the ACM-SIGMOD Int'l Conf. on Management of data, vol.26, pp.255-264,1997
9. Joseph M. Hellerstein, Peter J. Haas, and Helen J. Wang:"Online aggregation", SIGMOD'97,1997
10. R. Baeza-Yates.: "A unified view of string matching algorithms.", In Proceedings of Theory and Practice of Informatics (SOFSEM'96), LNCS 1175, pages 1-15, 1996.
11. R. Agrawal and R. Srikant."Fast algorithm for mining association rules", In Proceedings of the 20th Int'l Conf. on Very Large Databases, 1994
12. R. S. Boyer and J. S. Moore. "A fast string searching algorithm", Communications of the ACM, 20(10):pp.761-772, 1977.

A Framework for Mining Association Rules

Jun Luo¹ and Sanguthevar Rajasekaran^{2,*}

¹ Department of ECCS, Ohio Northern University, Ada, OH 45810

² Department of CSE, University of Connecticut, CT 06269-3155

Abstract. Association rule mining is one of important data mining problems. In this paper, a framework for efficiently calculating frequent itemsets in voluminous data is presented. The algorithm FIT [LR] is a practical implementation of the framework. A theoretical comparison between FIT and Eclat [ZPOW] is also explored. The analysis asserts that the performance of FIT is much more efficient than that of Eclat. Experimental results confirmed the assertion with data from [AS].

1 Introduction

The study of mining algorithms was initiated by Agrawal, Imielinski, and Swami [AIS] and since then quite a few papers have been written on the topic [HGN] [WHH][HC][HWLT]. An itemset that contains k items from an item set (I) is called a k -itemset. An itemset is frequent if the number of transactions in a database (D) that contain the itemset is no less than a user-specified minimum support ($minsup$). Some notations used in this paper are listed in Table 1. If the union of two itemsets, X and Y for example, is a frequent itemset then X and Y are defined to have a *strong association relation*. Otherwise, X and Y are said to have a *weak association relation*. If A represents a set or a list, then we let $|A|$ denote the number of elements in A .

Table 1. Notations

| Notations | Comments |
|-----------------|--|
| L_k | The collection of frequent k -itemsets and their attributes lists. |
| $CF_{L_k}^i$ | All the attributes lists that follow the i^{th} attribute list in L_k , for $1 \leq i \leq L_k $. |
| $G_{L_k}^{i,j}$ | The union of the attributes lists from the i^{th} attribute list to the j^{th} attribute list in L_k , for $1 \leq i < j \leq L_k $. |
| $F_{L_k}^{i,j}$ | All the attributes lists that are in $CF_{L_k}^j$ and have strong association relations with $G_{L_k}^{i,j}$, for $1 \leq i < j \leq L_k $. |

This paper is organized as follows: Section 2 discusses a framework for efficiently calculating frequent itemsets in voluminous data. Section 3 presents

* This author has been supported in part by the NSF Grants CCR-9912395 and ITR-0326155

the theoretical analysis of FIT. A comparison between FIT and Eclat is also explored. Section 4 illustrates sample experimental results. Finally, Section 5 presents conclusions.

2 A Framework for Calculating Frequent Itemsets

The attribute list of an itemset (X) is defined to be the set of the unique identification numbers of all the transactions that contain X . The support of X is the number of attributes in its attribute list. The support of the union of two itemsets (X and Y) can be calculated as follows: 1) calculate the intersection between X 's attribute list and Y 's attribute list; 2) count the number of attributes in the resulting attribute list. The intersection operation can be efficiently implemented using a hash table. For example, in order to intersect two attribute lists (l_1 and l_2), the hash table is initialized such that the i^{th} entry is set to 1 if i is contained by l_1 . Otherwise, the i^{th} entry is set to -1. Then, for each attribute (j) in l_2 , j will be kept in the resulting attribute list only if the j^{th} entry of the hash table is 1. To calculate the intersection between l_1 and each of n attribute lists, l_1 is scanned only once and the hash table is used for the subsequent calculations.

To calculate frequent itemsets from a given set of attribute lists (L_k), the attribute lists are logically divided into $\frac{|L_k|}{d}$ groups, in which $1 < d < |L_k|$. For convenience of discussion, $|L_k|$ is assumed to be a multiple integral of d . The groups are denoted as $G_{L_k}^{0,d-1}, G_{L_k}^{d,2d-1}, \dots$, and $G_{L_k}^{|L_k|-d,|L_k|-1}$. Starting with the first group until the last one, for each group $G_{L_k}^{id,(i+1)d-1}$, do the following: 1) The set $F_{L_k}^{id,(i+1)d-1}$ is calculated; 2) For each attribute list (l_g) in $G_{L_k}^{id,(i+1)d-1}$, the intersection between l_g and any of other attribute lists that either are in $F_{L_k}^{id,(i+1)d-1}$ or follow l_g in $G_{L_k}^{id,(i+1)d-1}$ are computed.

3 Performance Analysis

Compared to Eclat, FIT has computation advantages in two aspects: 1) FIT has fewer comparisons for each intersection operation between two attribute lists; 2) FIT can significantly reduce the total number of intersection operations.

Lemma 1 specifies the conditions under which the total number of intersections performed by FIT is less than that performed by Eclat.

Lemma 1. *Assume an L_k is divided into subgroups, and the size of each subgroup is denoted as d . If for each subgroup $G_{L_k}^{(i-1)d,id-1}$, in which $1 < i \leq \frac{|L_k|}{d}$, the inequality of $\frac{|F_{L_k}^{(i-1)d,id-1}|}{|CF_{L_k}^{id-1}|} < \frac{d-1}{d}$ is satisfied, then the algorithm FIT performs fewer intersection operations than the algorithm Eclat.*

The proof of Lemma 1 is as follows: Given an L_k , the total number of intersection operations performed by Eclat and FIT are given in Eq. (1) and Eq. (2), respectively.

$$N_1 = (|L_k| - 1) + (|L_k| - 2) + \cdots + 1 = \frac{|L_k|(|L_k| - 1)}{2} \quad (1)$$

$$\begin{aligned} N_2 &= \sum_{i=1}^{\frac{|L_k|}{d}-1} (|L_k| - id) + \sum_{i=1}^{\frac{|L_k|}{d}} \sum_{j=1}^d \left(d - j + F_{L_k}^{(i-1)d,id-1} \right) \\ &= \frac{|L_k| - d}{d} |L_k| - d \left(\frac{(\frac{|L_k|}{d} - 1 + 1)}{2} (\frac{|L_k|}{d} - 1) \right) + \\ &\quad \sum_{i=1}^{\frac{|L_k|}{d}} \left(F_{L_k}^{(i-1)d,id-1} d + \frac{(d-1)d}{2} \right) \\ &= \frac{|L_k|^2 - |L_k|d}{2d} + \frac{(d-1)|L_k|}{2} + d \sum_{i=1}^{\frac{|L_k|}{d}-1} F_{L_k}^{(i-1)d,id-1} \\ &= \frac{|L_k|^2 - 2|L_k|d + |L_k|d^2}{2d} + d \sum_{i=1}^{\frac{|L_k|}{d}-1} F_{L_k}^{(i-1)d,id-1} \end{aligned} \quad (2)$$

If FIT has fewer intersection operations, then Ineq. (3) must be satisfied.

$$(1) - (2) > 0$$

$$\begin{aligned} &\Leftrightarrow \frac{|L_k|(|L_k| - 1)}{2} - \frac{|L_k|^2 - 2|L_k|d + |L_k|d^2}{2d} - d \sum_{i=1}^{\frac{|L_k|}{d}-1} F_{L_k}^{(i-1)d,id-1} > 0 \\ &\Leftrightarrow \frac{|L_k|^2(d-1) - |L_k|d(d-1)}{2d} - d \sum_{i=1}^{\frac{|L_k|}{d}-1} F_{L_k}^{(i-1)d,id-1} > 0 \\ &\Leftrightarrow \frac{|L_k|(|L_k| - d)(d-1)}{2d} - d \sum_{i=1}^{\frac{|L_k|}{d}-1} F_{L_k}^{(i-1)d,id-1} > 0 \end{aligned} \quad (3)$$

Because each $F_{L_k}^{(i-1)d,id-1}$ contains at most $|L_k| - id$ attribute lists, in which $1 \leq i \leq \frac{|L_k|}{d}$, Ineq. (4) can be concluded as follows:

$$\begin{aligned} &d \sum_{i=1}^{\frac{|L_k|}{d}-1} F_{L_k}^{(i-1)d,id-1} \\ &\leq |d| \sum_{i=1}^{\frac{|L_k|}{d}-1} (|L_k| - id) = d|L_k|(\frac{|L_k|}{d} - 1) - \frac{d^2}{2}(\frac{|L_k|}{d} - 1 + 1)(\frac{|L_k|}{d} - 1) \\ &= |L_k|(|L_k| - d) - \frac{|L_k|(|L_k| - d)}{2} = \frac{|L_k|(|L_k| - d)}{2} \end{aligned} \quad (4)$$

The value of $\frac{|L_k|(|L_k|-d)}{2}$ is greater than that of $\frac{|L_k|(|L_k|-d)(d-1)}{2d}$ by $\frac{|L_k|(|L_k|-d)}{2d}$. In other words, if at least $\frac{|L_k|(|L_k|-d)}{2d}$ pairs of attribute lists have weak association relations with each other, FIT will perform fewer intersection operations than Eclat. For each subgroup $G_{L_k}^{(i-1)d,id-1}$, in which, $1 \leq i \leq \frac{|L_k|}{d}$, the maximum number of attribute lists that can have weak association relation with $G_{L_k}^{(i-1)d,id-1}$ is $|L_k| - id$. Whenever an attribute list has a weak association relation with $G_{L_k}^{(i-1)d,id-1}$, it can be removed, which saves d intersection operations performed by FIT in the next step. Assume that there are least c percent of $|L_k| - id$ attribute lists that have weak association relations with $G_{L_k}^{(i-1)d,id-1}$, then the total number of intersection operations saved for FIT equals to $\sum_{i=1}^{\frac{|L_k|}{d}-1} (d(|L_k|-id)c)$. FIT will have fewer intersection operations than Eclat if the value of $\sum_{i=1}^{\frac{|L_k|}{d}-1} (d(|L_k|-id)c)$ is greater than that of $\frac{|L_k|(|L_k|-d)}{2d}$. As a result, Ineq. (5) is concluded below:

$$\begin{aligned}
& \sum_{i=1}^{\frac{|L_k|}{d}-1} (d(|L_k|-id)c) > \frac{|L_k|(|L_k|-d)d}{2d} \\
& \equiv cd \frac{(|L_k|-d+d)}{2} \left(\frac{|L_k|}{d} - 1 \right) > \frac{|L_k|(|L_k|-d)}{2d} \\
& \equiv c \frac{L_k(L_k-d)}{2} > \frac{|L_k|(|L_k|-d)}{2d} \\
& \equiv c > \frac{1}{d}
\end{aligned} \tag{5}$$

So, Lemma 1 has been proved.

Lemma 2 below gives another observation about the efficiency of FIT.

Lemma 2. *Given an L_k , the number of intersections performed by FIT can be as least as $\frac{2}{\sqrt{|L_k|+1}}$ of the number of intersections performed by Eclat.*

The proof of Lemma 2 is as follows: From Eq. (1) and Eq. (2), Eq. (6) is obtained:

$$N_3 = \frac{\frac{|L_k|(|L_k|-1)}{2}}{\frac{|L_k|^2-2|L_k|d+|L_k|d^2}{2d} + d \sum_{i=1}^{\frac{|L_k|}{d}-1} F_{L_k}^{(i-1)d,id-1}} \tag{6}$$

The value of N_3 in Eq. (6) satisfies Ineq. (7).

$$\begin{aligned}
N_3 & \leq \frac{\frac{|L_k|(|L_k|-1)}{2}}{\frac{|L_k|^2-2|L_k|d+|L_k|d^2}{2d}} = \frac{d(1 - \frac{1}{|L_k|})}{1 - \frac{2d}{|L_k|} + \frac{d^2}{|L_k|}} \\
& = \frac{1 - \frac{1}{|L_k|}}{\frac{1}{d} - \frac{2}{|L_k|} + \frac{d}{|L_k|}}
\end{aligned} \tag{7}$$

Let

$$f(d) = \frac{1}{d} - \frac{2}{|L_k|} + \frac{d}{|L_k|} \tag{8}$$

Given an L_k , the value of $|L_k|$ is a constant. Therefore, N_3 in Ineq. (7) will have the maximum value when $f(d)$ in Eq. (8) has the minimum value. Assume d in Eq. (8) is a variable of real data type, and the domain of d is $[1, |L_k|]$, then $f(d)$ is a continuous function on d and the corresponding differential function can be calculated as follows:

Let

$$f'(d) = -\frac{1}{d^2} + \frac{1}{|L_k|} \quad (9)$$

Consider two conditions: 1) $1 < d \leq \sqrt{|L_k|}$; 2) $\sqrt{|L_k|} < d \leq |L_k|$.

When $1 < d \leq \sqrt{|L_k|}$, the value of $f'(d)$ in Eq. (9) is always negative, which means $f(d)$ in Eq. (8) is a decreasing function. So, N_3 in Ineq. (7) increases as d increases, and N_3 has the maximum value when $d = \sqrt{|L_k|}$. The maximum value of N_3 is specified in Ineq. (10).

$$N_3 \leq \frac{1 - \frac{1}{|L_k|}}{\frac{1}{\sqrt{|L_k|}} - \frac{2}{|L_k|} + \frac{\sqrt{|L_k|}}{|L_k|}} = \frac{\sqrt{|L_k|} + 1}{2} \quad (10)$$

When $\sqrt{|L_k|} < d \leq |L_k|$, the value of $f'(d)$ in Eq. (9) is always positive, which means $f(d)$ in Eq. (8) is an increasing function. Therefore, N_3 in Ineq. (7) decreases as d increases.

From the above discussion, it can be concluded that the number of intersections performed by FIT can be as least as $\frac{2}{\sqrt{|L_k|}+1}$ of that performed by Eclat. So, Lemma 2 has been proved.

For example, if a database D consists of 1000 distinct items, then Eclat performs exactly 499,500 intersection operations in order to calculate all the frequent 2-itemsets. On the other hand, in the best situations, FIT performs only 31,591 intersection operations to calculate the same set of frequent 2-itemsets.

Given two attribute lists, l_1 and l_2 , the pseudocodes to calculate intersections between l_1 and l_2 using FIT and Eclat are illustrated below:

```

void FITIntersection(int hb[], int l2[])
{
    j = 0;
    while(j < |l2|){
        m = l2[j];
        if(!hb[m])
            put l2[j] into the resulting attribute list;
        j++;
    }
}

```

```

void EclatIntersection(int l1[], int l2[])
{
    i = j = 0;
    while(i < |l1| && j < |l2|){
        if(l1[i] == l2[j]){
            put l1[i] into the resulting attribute list;
            i++; j++;
        }
        else if(l1[i] < l2[j])
            i++;
        else
            j++;
    }
}

```

As the information on l_1 is already stored in a hash table (hb) before the procedure FITIntersection() is called, l_1 is not used inside the procedure at all. In FITIntersection(), for each iteration of the loop, only one comparison is performed inside the loop body. Moreover, the while loop executes only $|l_2|$ times for each procedure call. On the other hand, in EclatIntersection, in the worst case, for each iteration of the loop, two comparisons are performed inside the loop body. The while loop might execute $|l_1| + |l_2| - 1$ times for a procedure call.

Given a set of n attribute lists (l_1, l_2, \dots, l_n) and assume that $|l_1| \geq |l_2| \geq \dots \geq |l_n|$, let N_4 and N_5 represent the worst case total number of comparisons performed by Eclat and FIT, respectively. Then, expressions for N_4 and N_5 are given in Eq. (11) and Eq. (12).

$$N_4 = \sum_{i=1}^{n-1} \sum_{j=i+1}^n 2(|l_i| + |l_j| - 1) = 2(n-1)(|l_1| + |l_2| + \dots + |l_n|) - n(n-1) \quad (11)$$

$$N_5 = \sum_{i=1}^{n-1} (|l_{i+1}| + \dots + |l_n|) = |l_2| + 2|l_3| + 3|l_4| + \dots + (n-2)|l_{n-1}| + (n-1)|l_n| \quad (12)$$

Because each attribute list has at least one attribute, the value of N_4 is always be greater than that of N_5 , which means FIT always has fewer comparisons than Eclat. If all the attribute lists have the same number of attributes, the ratio of $\frac{N_4}{N_5}$ will be near to 4. Theoretically, $\frac{N_4}{N_5}$ is upper-bounded by $\frac{4 \times |l_1|}{l_n}$, in which l_1 is the longest attribute list, and l_n is the shortest attribute list.

4 Experimental Results

We have implemented the algorithms Apriori [AS] and Eclat. To find out the efficiency of the pseudocode of FITIntersection, a program, called simple method, is also implemented. The simple method is the same as FIT except that it does not divide the attribute lists into subgroups. For the same reason mentioned in [HGN], we did not implement the algorithm FP-Growth [HPY]. Instead of trying

to implement as many other current algorithms as possible, we spent most of the time implementing Apriori more efficiently, since most papers compared their algorithms to Apriori. Also, in our implementation, Eclat was extended to calculate L_2 from L_1 . All the experiments were performed on a SUN UltraTM 80 workstation. Synthetic datasets were created using the data generator in [AS].

The synthetic datasets used in the experiments were $D1 = T10I4N10kD1000k$, $D2 = T10I4N100kD1000k$. The dataset $T10I4N10kD1000k$ means an average transaction size of 10, an average size of the maximum potentially frequent itemsets of 4, 10, 000 distinct items, and 1, 000, 000 generated transactions.

The first set of experiments was performed on $D1$, and the run time results are shown in Fig. 1. The second set of experiments was performed on $D2$, and the run time results are shown in Fig. 2. Fig. 3 shows the speedups of FIT over Apriori. Similarly, Fig. 4 illustrates the speedups of FIT over Eclat. In both experiments, set L_1 was divided into 3 levels of subgroups. The sizes were 120, 15, and 3. For any other set L_k , $k > 1$, the subgroup level was restricted to 1, and the size was set to 3.

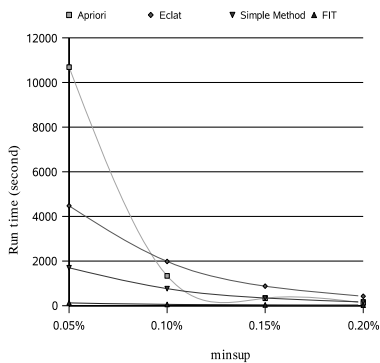


Fig. 1.

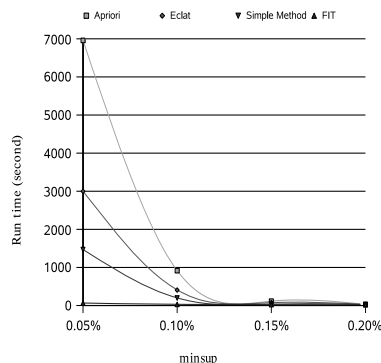


Fig. 2.

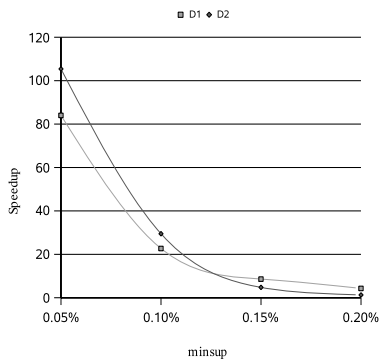


Fig. 3.

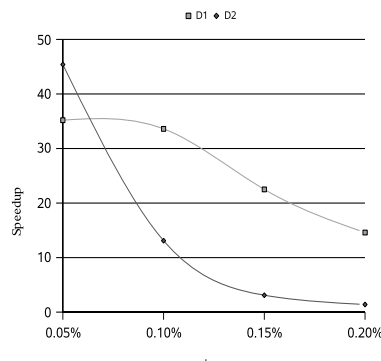


Fig. 4.

To see how effectively the simple method reduced the total number of comparisons performed by Eclat, two sample results are shown in Fig. 5 and Fig. 6. Both results came from the experiments on D2. Fig. 5 shows the total number of comparisons when minsup was set to 0.15 percent. Fig. 6 illustrates the total number of comparisons when minsup was set to 0.05 percent. In Fig. 5, the total number of comparisons performed by the simple method is about 23 percent of that performed by Eclat. In Fig. 6, the total number of comparisons performed by the simple method is about 31 percent of that performed by Eclat.

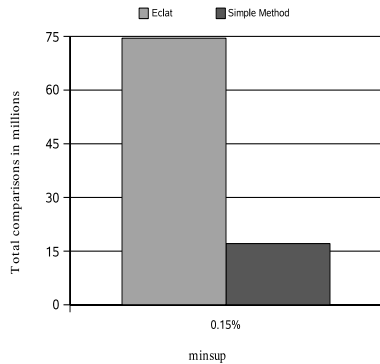
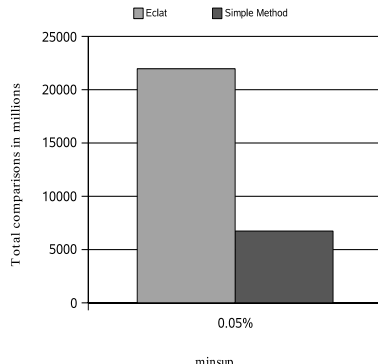
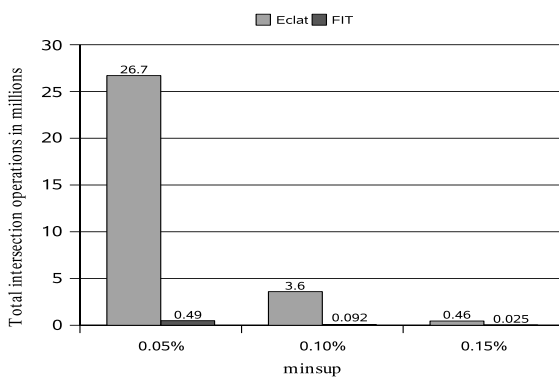
**Fig. 5.****Fig. 6.**

Fig. 7 compares the total number of intersection operations performed by FIT and Eclat. The results in Fig. 7 came from the experiments on *D2*. That FIT significantly cut down on the intersection operations performed by Eclat explains the results in Fig. 4 where FIT is much faster than Eclat.

**Fig. 7.**

We conducted extensive experiments on the simple method, FIT, Eclat, and Apriori. Other experimental results support the conclusions of this paper.

5 Conclusions

In this paper, a framework for efficiently calculating frequent itemsets in voluminous data was introduced. The analysis of FIT was discussed. The comparisons between FIT and Eclat were also explored. Both theoretical analysis and experimental results showed that FIT is an efficient algorithm.

References

- [AIS] R. Agrawal, T. Imielinski, and A. Swami: Mining Associations between Sets of Items in Large Databases. Proceedings of the ACM-SIGMOD 1993 International Conference on Management of Data, Washington D.C., USA, 1993.
- [AS] R. Agrawal and R. Srikant: Fast Algorithms for Mining Association Rules. Proceedings of the 20th International Conference on Very Large Databases, Santiago, Chile, 1994.
- [HC] J. D. Holt and S. M. Chung: Parallel Mining of Association Rules from Text Databases on a Cluster of Workstations. 18th International Parallel and Distributed Processing Symposium, Santa Fe, New Mexico, 2004.
- [HGN] J. Hipp, U. Guntezr, and G. Nakhaeizadeh: Algorithms for Association Rule Mining – A General Survey and Comparison. The Sixth ACM SIGKDD International Conference on Knowledge Discovery and Data Mining, Boston, MA, USA, 2000.
- [HPY] J. Han, and J. Pei, and Y. Yin: Mining Frequent Patterns without Candidate Generation, ACM SIGMOD International Conference on Management of Data, Dallas, TX, USA, 2000.
- [HWLT] J. Han, J. Wang, Y. Lu, and P. Tzvetkov: Mining Top-K Frequent Closed Patterns without Minimum Support. The 2002 IEEE International Conference on Data Mining, Maebashi City, Japan, 2002.
- [LR] J. Luo and S. Rajaskaran: FIT: A Fast Algorithm for Discovering Frequent Itemsets in Large Databases. KES2004 Eighth International Conference on Knowledge-Based Intelligence Information and Engineering Systems, Wellington, New Zealand, 2004.
- [WHH] K. Wang, Y. He and J. Han: Mining Frequent Itemsets Using Support Constraints (PDF). 2000 International Conference on on Very Large Data Bases, Cairo, Egypt, 2000.
- [ZPOW] M. J. Zaki, S. Parthasarathy, M. Ogihara, and W. Li: New Algorithms for fast discovery of association rules. Proceedings of the third International Conference On Kdd and Data Mining, Newport Beach, CA, USA, 1997.

Near-Optimal Fuzzy Systems Using Polar Clustering: Application to Control of Vision-Based Arm-Robot

Young-Joong Kim¹ and Myo-Taeg Lim¹

Department of Electrical Engineering, Korea University,
1, 5-ka, Anam-dong, Seoul 136-701, Korea
{kyjoong,mlim}@korea.ac.kr
<http://cml.korea.ac.kr>

Abstract. This paper presents a design algorithm to near-optimal fuzzy systems using polar clustering method for vision-based robot control systems. The complexity of the optimal fuzzy system for a vision-based control system is so great that it can not be applied to real systems or can not be useful. Therefore we generally use clustering method, to reduce the complexity of optimal fuzzy systems. In the class of near-optimal fuzzy systems, for more efficient use of clustering, we propose the polar clustering method using polar quantization. In order to verify the effectiveness of the proposed method, experimentally, it is applied to a vision-based arm robot control system.

1 Introduction

Fuzzy theory became the major field of researches in mathematics and control systems, since it was initiated by Lotfi A. Zadeh in 1965 [1]. In the 1970s, fuzzy decision making was proposed by Bellman and Zadeh [2], the foundation for fuzzy control was established by Zadeh, and he introduced the concept of linguistic variables and proposed to use fuzzy IF–THEN rules to formulate human knowledge [3]. Mamdani and Assilian established the basic framework of fuzzy controller and applied the fuzzy controller to control a stream engine. In the early 1980s, Japanese engineers, Sugeno, Nishida, Yasunobu, Miyamoto, etc., found that fuzzy controllers were very easy to design and worked very well for many problems [4]. Because fuzzy control dose not require a mathematical model of the process, it could be applied to many systems where conventional control theory could not be used due to a lack of mathematical models. Since it was encouraged at the success in Japan, fuzzy system was studied vigorously by many researchers in fuzzy mathematics, fuzzy logic and artificial intelligence, fuzzy systems, uncertainty and information, and fuzzy decision making. In addition, for effective design of such fuzzy systems, we generally use gradient descent training, recursive least squares, clustering, adaptive, etc. [5].

Specially, optimal fuzzy systems provide a very exact solution, but these are no longer a practical system when the number of input-output pairs is large,

because a number of fuzzy rules become also large. Due to such cost of applicant operations to actual systems are inefficient [5]. Therefore, generally the clustering is used for reduction of the complexity of optimal fuzzy systems. It is to design system by grouping the pairs of input-output and decreasing a number of fuzzy rules to overcome these shortcomings [6], [7]. However, the larger cluster is used, the lower accuracy of fuzzy system is gotten [5].

In the class of vision-based control systems, there are so many input-output pairs, because vision data is large. Therefore, the complexity of the optimal fuzzy system is so great that it can not be applied to real vision-based control systems or it can not be useful. In addition, much more accurate direction information is needed than distance information, because control systems are more sensitive to the error of direction rather than distance [9], [10], [11]. The reason why, we propose the use of the cluster that can be much weighted in direction information. In this paper, in order to improve the effectiveness of clustering method, we propose polar clustering method. The idea of polar clustering is the vector quantization in the polar coordinates. In addition, a new design algorithm of the near-optimal fuzzy system using nearest polar clustering is presented.

The contents of this paper are as follows. In the section 2, we introduce optimal fuzzy systems, and the polar clustering method is proposed, and a new algorithm of near-optimal fuzzy systems using polar clustering is presented. In the section 3, to verify our proposed method, we make an experiment to control for docking and homing of vision-based arm robot system. Finally, section 4 gives our conclusion.

2 Near-Optimal Fuzzy Systems Using Polar Clustering

2.1 Optimal Fuzzy Systems

Suppose that we are given N input-output pairs $(x_0^l; y_0^l)$, $l = 1, 2, \dots, N$, and N is small. Then, the optimal fuzzy system are represented as follows:

$$f^*(x) = \frac{\sum_{l=1}^N y_0^l \exp\left(-\frac{|x-x_0^l|^2}{\sigma^2}\right)}{\sum_{l=1}^N \exp\left(-\frac{|x-x_0^l|^2}{\sigma^2}\right)}, \quad (1)$$

where $x \in R^n$ is an input vector, $y \in R^m$ is a real output vector. The fuzzy system (1) is constructed from the N rules:

$$\text{Rule}^{(l)} = \text{IF } x_1 \text{ is } A_1^l \text{ and } \dots \text{ and } x_n \text{ is } A_n^l, \text{ THEN } y \text{ is } B^l \quad (2)$$

with

$$\mu_{A_i^l}(x_i) = \exp\left(-\frac{|x_i - x_{0i}^l|^2}{\sigma^2}\right), \quad (3)$$

and the center of B^l equal to y_0^l . In this paper, by the help of [4], [5], we use the general product inference engine, singleton fuzzifier, and center average defuzzifier.

The following theorem shows that by properly choosing the parameter σ , the fuzzy system (1) match all the N input-output pairs to any given accuracy.

Theorem 1: For arbitrary $\epsilon > 0$, there exists σ^* such that the fuzzy system (1) with $\sigma = \sigma^*$ has the property that

$$|f(x_0^l) - y_0^l| < \epsilon \quad (4)$$

for all $l = 1, 2, \dots, N$.

Proof: The proof of this theorem can be drawn from [5]. \diamond

The σ is a smoothing parameter. The smaller σ , the smaller matching error $|f(x_0^l) - y_0^l|$, but the less smooth $f(x)$ becomes. The optimal fuzzy system (1) uses one rule for one input-output pair, thus it is no longer a practical system when the number of input-output pairs is large. For these large sample problems, various clustering techniques can be used to group the input-output pairs so that a group can be represented by one rule. Clustering means partitioning of a collection of data into disjoint subsets or clusters, with the data in a cluster having some properties that distinguish them from the data in the other clusters [5].

2.2 Near-Optimal Fuzzy Systems Using Polar Clustering

Since vision-based robot control systems are more sensitive to the error of direction rather than distance, much more accurate direction information is needed than distance information. In this section, we propose the polar cluster that can be much weighted in direction information. The idea of polar clustering is the vector quantization in the polar coordinates.

In the Cartesian coordinates that consists of i -axis and j -axis, image data of any point is represented by $I(i, j)$. It is transformed into the one that is represented by $H(\rho, \theta)$ in the polar coordinates that consists of ρ -axis and θ -axis using the followings:

$$\rho = \sqrt{(i - i_c)^2 + (j - j_c)^2}, \quad (5)$$

$$\theta = \tan^{-1} \left(\frac{i - i_c}{j_c - j} \right), \quad (6)$$

where ρ is the radial distance from the center of image, and θ represents the angle (from 0 to 2π) subtended by any point (i, j) and the center of image. In (5)-(6), i_c and j_c are the centers of a image of Cartesian coordinates.

Next, $H(\rho, \theta)$ is vector quantized into disjoint subsets or clusters, and the near-optimal fuzzy system is designed using the following algorithm of nearest polar clustering.

Algorithm 1: Design of the near-optimal fuzzy system using nearest polar clustering

```

/* Start with the first input-output pair (x_0[1]; y_0[1]),
   where x_0[1] is a point in the Polar coordinates. */
x_c[1] = x_0[1]; /* Establish a cluster center */
M = 1;
r = Select_cluster_radius();
/* Consider the k-th input-output pair (x_0[k]; y_0[k]),
   where x_0[k] is a point in the Polar coordinates. */
for( k = 2; k <= N; k++ ) {
    for (l = 1; l <= M; l++ )
        D[l] = Distance( x_c[l], x_0[k] );
    Find_minimum( D );
    /* Suppose the minimum is D[L] */
    if ( D[L] > r ) {
        M = M + 1;
        x_c[M] = x_0[k]; /* Establish a new cluster center */
        Update_fuzzy_system( x_c[M], y_0[k] );
    }
    else
        Update_fuzzy_system( x_c[L], y_0[k] );
}

```

This vector quantization method can be applied to the fuzzy system that needs high accuracy of direction information for improving the effectiveness. In order to verify the effectiveness of polar clustering method, we compare the general clustering in Cartesian coordinates with the proposed clustering in polar coordinates by the measurement of quantization errors. Simulation results are shown in Table 1.

Table 1. Quantization errors of general clustering and polar clustering

| Coordinates | | Error | Maximum Value | Average Value |
|-------------|----------|---------------|------------------|---------------|
| Cartesian | Angle | 45 [Degrees] | 2.4288 [Degrees] | |
| | Distance | 20 [Pixels] | 7.5962 [Pixels] | |
| Polar | Angle | 4.5 [degrees] | 2.2333 [degrees] | |
| | Distance | 20 [Pixels] | 9.3778 [Pixels] | |

In this simulation, we use 100 clusters for general clustering in Cartesian coordinates and for proposed method in polar coordinates, respectively. Table 1 shows that the mean value of distance error of polar clustering is comparatively big, but the maximum value of angle error is quite small. Therefore, polar clustering method can be more effective to control of direction.

3 Experiment Result

In order to verify the effectiveness of the proposed method experimentally, it is applied to a vision-based arm robot control system. Since the modelling of this robot system is hard work, and many image processing procedures, explained in [8], are performed to search desirable data from images, we can not obtain the exact data of the robot position. Therefore, we design a near-optimal fuzzy system using polar clustering. We make use of an arm robot, objects and goal positions in figure 1.

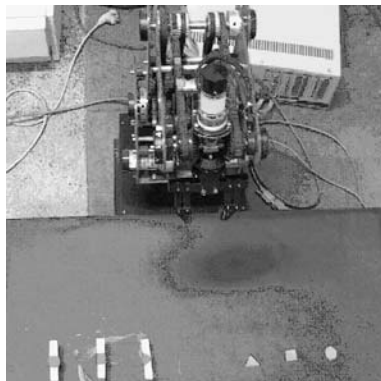


Fig. 1. An experimental system with a vision-based Arm robot, objects and goal positions

The near-optimal fuzzy system that decrease amounts of rules by polar clustering is designed as follows:

$$f(x) = \frac{\sum_{l=1}^N y_0^l \exp\left(-\frac{|x-x_c^l|^2}{\sigma^2}\right)}{\sum_{l=1}^N \exp\left(-\frac{|x-x_c^l|^2}{\sigma^2}\right)}, \quad (7)$$

where f is a near-optimal fuzzy system designed using Algorithm 1 and the centers, x_c^l , of polar clusters.

In the class of vision-based control systems, there are many image processing procedures to search desirable data from images. First, a color image is transformed into a binary image to search for feature colored objects using thresholding, and then we put labels on them for classification of objects and eliminate pixels having linkable elements below the desirable size and distinguish pixel sets having same linkable elements using size filtering, because binary images include various noisy elements. By the help of object recognition methods reported in [8], [11], we can recognize objects using characteristics of transformed signals and the positions of recognized object centers can be obtained. Finally, position data of recognized objects become inputs of a near-optimal fuzzy system using the proposed polar clustering method. In this paper, a near-optimal fuzzy system and image processors are implemented by Visual C++.

The positions in which failures of docking or homing occur using general clustering are illustrated in left figures, and the results of the proposed method are illustrated in right figures in Fig. 2, 3, 4, respectively. In the Fig 4, we use the 200 clusters for each method. We have no failure using proposed method. But, we see that there still exist failures of 7 times using general clusters.

4 Conclusion

In order to control of docking and homing for the vision-based arm robot system with uncertainties which are due to a lack of mathematical models, the concept of an optimal fuzzy system is introduced. To reduce the complexity of optimal fuzzy systems, we use clustering method. Specially, for more effective use of clustering, a polar clustering method and a new design algorithm of the near-

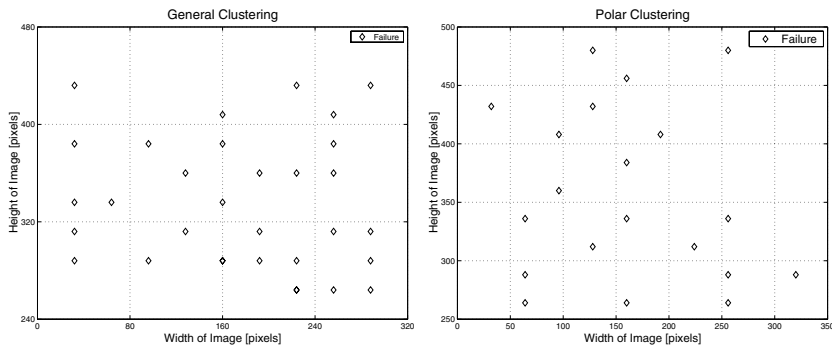


Fig. 2. (i) The positions of 32 failures using 100 clusters in Cartesian coordinates are pointed in left plot. (ii) The positions of 20 failures using 100 clusters in polar coordinates are pointed in right plot

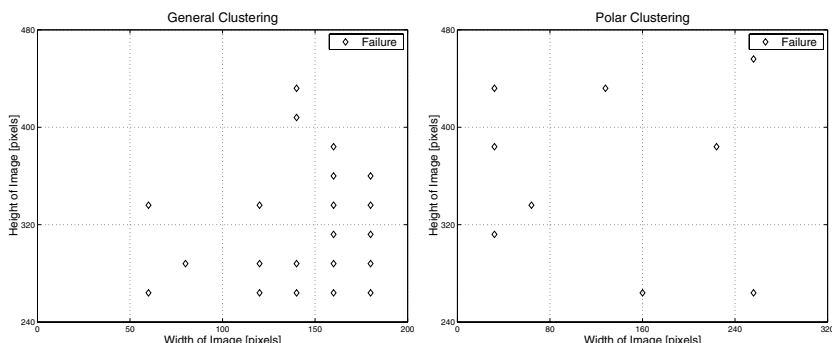


Fig. 3. (i) The positions of 21 failures using 150 clusters in Cartesian coordinates are pointed in left plot. (ii) The positions of 9 failures using 150 clusters in polar coordinates are pointed in right plot

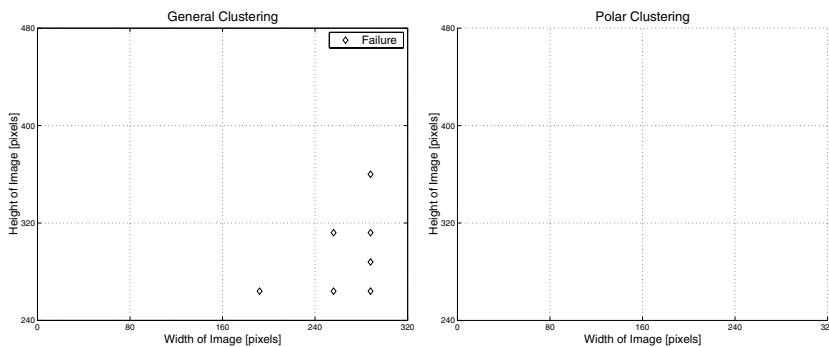


Fig. 4. (i) The positions of 7 failures using 200 clusters in Cartesian coordinates are pointed in left plot. (ii) There are no failure using 200 clusters in polar coordinates in right plot

optimal fuzzy system using nearest polar clustering are proposed. By simulations of quantization errors and experiments, efficiency of proposed polar clustering method is proven. The proposed method can be applied to the fuzzy system that needs high accuracy of direction information for improving the effectiveness.

References

1. Zadeh, L. A.: Fuzzy sets. *Informat. Control*, Vol. 8. (1965) 338–353
2. Bellman, R. E. and Zadeh, L. A.: Decision-making in a fuzzy environment. *Management Science*, Vol. 17(4). (1970) 141–164.
3. Zadeh, L. A.: Outline of a new approach to the analysis of complex systems ad decision processes. *IEEE Trans. System, Man, and Cybernetics*, Vol. 3(1). (1973) 28–44
4. Sugeno, M. and Nishida, M.: Fuzzy control of model car. *Fuzzy Sets and Systems*. (1985) 103–113
5. Wang L. X.: *A Course in Fuzzy Systems and Control*. Prentice-Hall Inc. (1997)
6. Baraldi, A. and Blonda, A.: A Survey of Fuzzy Clustering Algorithms for Pattern Recognition-Part I. *IEEE Trans. System, Man, and Cybernetics-Part B: Cybernetics*, Vol. 29(6). (1999) 778–786
7. Baraldi, A. and Blonda, A.: A Survey of Fuzzy Clustering Algorithms for Pattern Recognition-Part II. *IEEE Trans. System, Man, and Cybernetics-Part B: Cybernetics*, Vol. 29(6). (1999) 787–800
8. Gonzalez, R. C. and Woods, R. E.: *Digital Image Processing*. Prentice-Hall Inc. (2002)
9. Wilson, W.J., Williams Hulls, C.C. and Bell, G.S.: Relative End-Effector Control Using Cartesian Position Based Visual Servoing. *IEEE Trans. Robotics and Automation*, Vol. 12(5). (1996) 684–696
10. Chen, W., James K. Mills, Jiaxin Chu, and Dong Sun: A Fuzzy Compensator for Uncertainty of Industrial Robots. *Proc. IEEE Int. Conf. on Robotics and Automation*, May, Vol. 3. (2001) 2968–2973
11. Shakunaga, T.: An Object Pose Estimation System Using a Single Camera. *Proc. IEEE Int. Conf. on Intelligent Robots and Systems*, July, Vol. 2. (1992) 1053–1060

Door Traversing for a Vision-Based Mobile Robot Using PCA

Min-Wook Seo, Young-Joong Kim, and Myo-Taeg Lim

Department of Electrical Engineering, Korea University
1, 5-ka, Sungbuk-gu, Anam-dong, Seoul 136-701, Korea
{s1hanul,kyooong,mlim}@korea.ac.kr
<http://cml.korea.ac.kr>

Abstract. This paper presents a method that a vision-based mobile robot can find location of doors and can safely traverse the door in complex environments. A robot must be able to find the door in order that it achieves the behavior that is scheduled after traversing a door. In this paper, PCA (Principal Component Analysis) algorithm using a vision sensor is used for a mobile robot to find the location of door. In addition, a fuzzy controller using a sonar data is used for a robot to avoid obstacles and traverse the door.

1 Introduction

In recent years, various types of robots have been used in human assistance, welfare, amusement, etc. An intelligent robot should make decision behavior according to the facing environment, and it should require its perceptual and dynamic system. There are various kinds of actions that a mobile robot must achieve basically in order to achieve a big task in indoor environment. Since a mobile robot must record its position in order to find goal, it must be able to find and recognize strangers and specially doors for map building and navigation.

Usually, a shape of doors is a rectangle with a knob, and people can find a door easily by experience and direct observation in interior of building when people visit first time. Based on this fact, some methods were researched by this information. The doors are extracted from using dilation and afterwards with a very simple algorithm that enhances the columns merging those columns separated by very thin spaces [1]. There are some problems when not only the image of door is not columns separated by very thin spaces but also many column elements of image happen in off-door image. In additions, the problems that occur using a ‘simple’ polyhedral model of doors for detection and servoing are reported in [2]. The robust method to autonomously find doors in a corridor that is composed of cluttered environments is presented [3]. Specially, the PCA (Principal Component Analysis) method is a useful statistical technique that has found application in fields such as face recognition and image compression, and is a common technique for finding patterns in data of high dimension. Specially, eigen-space method reported in [4], [5], had been verified well for the recognition strategy.

Fuzzy logic approaches have been utilized in navigation systems for mobile robots over a decade. Early in 1991, Yen and Pfluger proposed a method of path planning and execution using fuzzy logic for mobile robot control [6]. The efficiency of using

fuzzy logic in mobile robot navigation systems has been demonstrated [7], [8], [9], [10]. A comprehensive study of fuzzy logic-based autonomous mobile robot navigation systems had been reported in [11]. Recently, several new solutions to the mobile robot navigation problem based on fuzzy logic in unknown environments have been proposed [12], [13], [14]. There also exist methods combining fuzzy logic with other algorithms, such as genetic algorithms [15], potential fields and neural networks [16].

To increase performance that a mobile robot finds a door, this paper proposes a method that a mobile robot finds location of doors in complex environments and safely traverses the door. In this paper, a PCA algorithm using a vision sensor is used for a robot to find the location of door, and a fuzzy controller using sonar data is used for a robot to avoid obstacles and traverse the door.

The organization of this paper is as follows. In Section 2, we present a door recognition method from image data using the PCA. In section 3, we present a fuzzy rule-base for a mobile robot using sonar. In section 4, we present results of the experiment with the Pioneer-2 mobile robot. Finally, we draw conclusions.

2 Door Recognition

Since the quantity of data in a image (640*480 pixels) per a frame that was entered through a CCD camera is very large, we use the reduced (160*120 pixels) image is used for recognition of doors in this paper. We can obtain some door images (Positive Image) and off-door images (Negative Image) in an office. Fig. 1 is a collection of positive images and Fig. 2 is a collection of negative images.



Fig. 1. Positive door images



Fig. 2. Negative door images

2.1 Eigenspace Mapping

Training images can be viewed as a vector. If the image's width and height are w and h pixels respectively, the number of components of this vector will be $w \cdot h$. Each pixel is coded by one vector component. The construction of this vector from image is performed by a simple concatenation of rows or columns. The main idea of the PCA is to find the vectors that best account for the distribution of training images within the entire image space.

Let the training set of images be $\Gamma_1, \Gamma_2, \Gamma_3, \dots, \Gamma_M$, ($\Gamma \in R^N$). The average of the set is defined as follows:

$$\Psi = \frac{1}{M} \sum_{n=1}^M \Gamma_n \quad (1)$$

where M means the number of images in the training set. Each training image differs from the average image by the following vector:

$$\Phi_i = \Gamma_i - \Psi \quad (2)$$

This set of large vector Φ is then subject to the Karhunen- Loeve expansion, to produce the M orthonormal vectors u_n , and their associated eigenvalues λ_n that optimally describe the distribution of the data in error sense of an RMS (Root Mean Square). The vector u_k and scalars λ_k are the eigenvectors and eigenvalues with respect to the C (covariance matrix) where the matrix $A = [\Phi_1, \Phi_2, \Phi_3, \dots, \Phi_M]$. Covariance matrix of Φ is calculated by the following equation:

$$C = \frac{1}{M} \sum_{n=1}^M \Phi_n \Phi_n^T = \frac{1}{M} A A^T \quad (3)$$

The matrix C , however, is N by N . And determining the N eigenvectors and eigenvalues is an intractable task for typical image sizes. We need a computationally feasible method to find these eigenvectors [4].

When the number of data points in the image space is less than the dimension of the space, ($M < N$), then, dimension of eigenvector will be only M rather than N . The remaining eigenvectors will have associated eigenvalues of zero. Fortunately we can solve the N by N dimensional eigenvectors in this case in terms of the eigenvectors of an M by M . Consider the eigenvectors v_i of $A^T A$ such that:

$$A^T A v_i = u_i v \quad (4)$$

Multiplying both side by A , we have:

$$A A^T A v_i = u_i A v_i \quad (5)$$

From which we see that $A \cdot v_i$ are the eigenvectors of $C' = A^T A$. A new image region is transformed into eigenspace representation by the following equation:

$$u_l = \sum_{k=1}^M v_{lk} \Phi_k \quad (6)$$

So, we calculate the eigenvalues and eigenvectors not from C but from C' . The result images from equation (6) are shown in Fig. 3. There are top 4 eigenspace images. Training images are consisted of 20 positive images and 40 negative images.



Fig. 3. Eigenspace ($\lambda_1 \sim \lambda_4$)

2.2 Door Recognition Method Using Eigenspace

Training image can be reunited using eigenspace image that is obtained through section 2.2. In other words, training images that are used in an experiment are represented by linear combination of eigenspace.

$$EW = A \quad (7)$$

E is eigenspace matrix and W is coefficient matrix. Because each column of E is orthonormal, we can find W_P and W_N from the following equation:

$$\begin{aligned} W_P &= E^T \cdot \text{Positive image} \\ W_N &= E^T \cdot \text{Negative image} \end{aligned} \quad (8)$$

Each weight group, W_P and W_N , is described as $W_P = [w_1, w_2, w_3, \dots, w_m]$, $w \in R^N$ and $W_N = [w_1, w_2, w_3, \dots, w_l]$, $w \in R^N$. When new image will be entered through CCD camera, we can find weight vector (w_k) of new image from the following equation:

$$w_k = E^T (\Gamma - \Psi) \quad (9)$$

According to the following Euclidian distance, we can know that new image belongs to the positive image group or belongs to the negative image group.

$$\varepsilon = \|w_i - w_k\|^2, (i = 1, 2, \dots, m+l) \quad (10)$$

When the smallest w_i of ε belongs to W_P , a new image is a door and if the smallest w_i of ε belongs to W_N , we can judge that the new image is not a door.

3 Fuzzy Logic Control System

Sonar sensors measure the time elapsed between the transmission of a signal and the receiving of an echo of the transmitted signal to determine the distance to an obstacle. The sonar sensors on mobile robots can be used to detect objects around the mobile robot and to avoid collision with unexpected obstacles.

The goal of navigation in this paper is to make the mobile robot avoid an obstacle and traverse a door. The motion of the mobile robot will be realized by the control of its linear velocity and heading angle. Therefore, the input fuzzy variables of the fuzzy controller are the forward distance of robot between mobile robot and obstacle, and the side distance that is difference between left distance and right distance. The output fuzzy variables are chosen as the heading angle, θ , and linear velocity, v .

Mobile robot and location of sonar sensor are presented in Fig. 4.

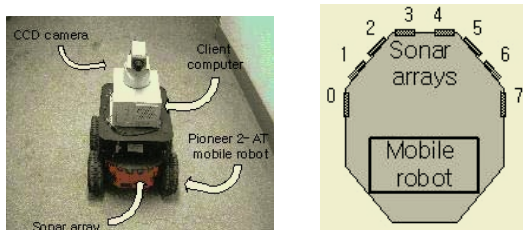


Fig. 4. Mobile robot system

Input fuzzy variables of control system are as follows:

$$\begin{aligned}
 D(k) &= \min(\text{sonar}(3), \text{sonar}(4)) \\
 L(k) &= \min(\text{sonar}(1), \text{sonar}(2)) \\
 R(k) &= \min(\text{sonar}(5), \text{sonar}(6)) \\
 SD(k) &= L(k) - R(k) \\
 SA(k) &= \text{sonar}(0) + \text{sonar}(7)
 \end{aligned} \tag{11}$$

where $D(k)$ is forward distance of the robot between the mobile robot and an obstacle, $L(k)$ is left distance of the robot, $R(k)$ is right distance of the robot, $SD(k)$ express difference between left distance and right distance of mobile robot, and $SA(k)$ is used in pass a door.

The rules of linear velocity for the robot are presented in Table 1.

Table 1. The rules for linear velocities

| \backslash | SD(k) | Negative | Zero | Positive |
|--------------|-------|----------|--------|----------|
| D(k) | Near | Slow | Medium | Slow |
| | Far | Medium | Fast | Medium |

When an obstacle or a wall is near to a mobile robot, θ will be increased and if that is away then, θ will be decreased. With this truth, heading angle rule table is composed. Heading angle rules of the fuzzy controller are presented in Table 2.

Table 2. The rules for heading angles

| \backslash | SD(k) | Negative | Zero | Positive |
|--------------|-------|-------------|------|------------|
| D(k) | Near | Large Right | Zero | Large Left |
| | Far | Small Right | Zero | Small Left |

The fuzzy control actions of v and θ are inferred using the Mamdani's compositional rule of inference. The defuzzification method is used center of gravity method. If θ is big at the moment that a mobile robot passes a door, then the mobile robot will be bumped to a door. We limited value of defuzzyfication of θ to solve this situation. From $SA(k)$, we can know the moment a mobile robot passes a door. A threshold, 40cm, is space that remains between a robot and a door when a robot passes door.

4 Experimental Result

In this section, a collection of images is shown in Fig. 1 and 2. Each image is captured with a CCD camera on the top of the robot, and it is used to learn. Maximum distance range of sonar sensor is limited to 3m according to an experiment space. The width of mobile robot is 50cm and the width of a door is 80cm.

While the mobile robot rotates 360° at positions a, b, and c in an office shown in Fig. 5, respectively, we have comparative tests with reported in [1] whether the mobile robot can find a door or not.

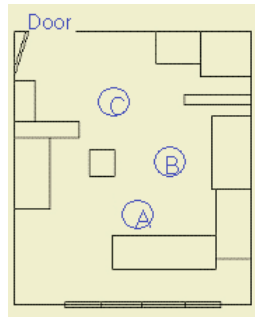


Fig. 5. Test positions of the mobile robot in an office

Experimental results of the comparative tests are shown in Table 3. The case A is the ratio of success when the robot looks a door. On the contrary, the case B is the ratio of failure when the robot does not look a door. Experimental results show that the proposed method is more effective.

Table 3. Experimental results

| Position | Case A: Door | | Case B: Not Door | |
|----------|-----------------|-----------------|------------------|-----------------|
| | Existing method | Proposed method | Existing method | Proposed method |
| a | 60% (6/10) | 90% (9/10) | 50%(15/30) | 0%(0/30) |
| b | 20% (2/10) | 90% (9/10) | 33%(10/30) | 0%(0/30) |
| c | 30% (3/10) | 80% (8/10) | 20%(6/30) | 0%(0/30) |

5 Conclusion

This paper presents a method that a mobile robot can find locations of doors in complex environment and safely traverses the door. The PCA algorithm has been tested on our mobile robot Pioneer-2 in a real office environment. According to experimental results, it should be confirmed that the proposed method using PCA provides the superior performance of door recognition. The proposed method can be used to intelligent mobile robots to increase the performance of other recognition processes.

References

- Monasterio, I., Lazkano, E.: Learning to Traverse Doors Using Visual Information. Mathematics and Computers in Simulation, Vol. 60. (2002) 347-356
- Eberst, C., Andersson, M.: Vision-Based Door-Traversal for Autonomous Mobile Robots. International Conf. on Intelligent Robots and Systems. (2000) 620-625
- Stoeter, A.: Real-time Door Detection in Cluttered Environments. International Symposium on Intelligent Control, Vol. 15, July (2000) 187-192
- Turk, M., Pentland, A.: Eigenfaces for recognition. J. Cognitive Neuroscience, Vol. 3(1) (1991) 71-86
- Kirby, M., Sirovich, L.: Application of The Karhunen-Loeve Procedure for The Characterization of Human Face. IEEE Trans. on PAMI, Vol. 12 (1990) pp. 103-108
- Yen, J., Pfluger, N.: Path Planning and Execution Using Fuzzy Logic. AIAA Guidance, Navigation and Control Conference, Vol. 3, New Orleans LA Aug. (1991) 1691-1698

7. Reignier, P.: Fuzzy Logic Techniques for Mobile Robot Obstacle Avoidance. *Robotics and Autonomous Systems*, Vol. 12. (1994) 143-153
8. Lee, P. S., Wang, L. L.: Collision Avoidance by Fuzzy Logic Control for Automated Guided Vehicle Navigation. *Journal of Robotics Systems*, Vol. 11. (1994) 743-760
9. Beaufrre, B.: A Mobile Robot Navigation Method Using A Fuzzy Logic Approach. *Robotica*, Vol. 13. (1995) 437-448
10. Yen, J., Pfluger, N.: A Fuzzy Logic Based Extension to Payton and Rosenblatt's Command Fusion Method for Mobile Robot Navigation. *IEEE Trans. Syst. Man, Cybern.*, Vol. 25(6) (1995) 971-978
11. Saffiotti, A.: The Uses of Fuzzy Logic in Autonomous Robot Navigation. *Soft Computing*, Vol. 1, (1997) 180-197
12. Montaner, M. B., Serrano, A. R.: Fuzzy Knowledge-based Controller Design for Autonomous Robot Navigation. *Expert Systems with Application*, Vol. 14, (1998) 179-186
13. Maaref, H., Barret, C.: Sensor-based Fuzzy Navigation of An Autonomous Mobile Robot in An Indoor Environment. *Control Engineering Practice*, Vol. 8, (2000) 747-768
14. Doitsodis, L., Valavanis, K. P., Tsourveloudis, N. C.: Fuzzy Logic Based Autonomous Skid Steering Vehicle Navigation. *IEEE Int. Conf. on Robotics and Automation*, Vol. 2. Washington, DC May (2002) 2171-2177
15. Pratihar, D. K., Dep, K., Ghosh, A.: A Genetic-Fuzzy Approach for Mobile Robot Navigation Among Moving Obstacles. *International Journal of Approximate Reasoning*, Vol. 20, (1999) 145-172
16. Wang, J. S., Lee, C. S.: Self-Adaptive Recurrent Neural-Fuzzy Control for An Autonomous Underwater Vehicle. *IEEE Int. Conf. on Robotics and Automation*, Vol. 2. Washington, DC May (2002) 1095-1100

Local Feature Analysis with Class Information

Yongjin Lee¹, Kyunghee Lee², Dosung Ahn¹,
Sungbum Pan³, Jin Lee¹, and Kiyoung Moon¹

¹ Biometrics Technology Research Team
Electronics and Telecommunications Research Institute
161 Gajeong-dong, Yuseong-gu, Daejeon, 305-350, Korea
{solarone,dosung,jinlee,kymoon}@etri.re.kr

² Department of Electrical Engineering
The University of Suwon, Korea
khlee@suwon.ac.kr

³ Division of Information and Control Measurement Engineering
Chosun University, Korea
sbpan@chosun.ac.kr

Abstract. In this paper, we propose a new feature extraction method for face recognition. This method is based on Local Feature Analysis (LFA), a local method for face recognition since it constructs kernels detecting local structures of a face. However, LFA has shown some problems for recognition due to the nature of unsupervised learning. Here, we point out the problems of LFA and propose a new feature extraction method with class information to overcome the shortcomings of LFA. Our method consists of three steps. First, using LFA, a set of local structures are extracted. Second, we select some extracted structures that are efficient for recognition. At last, we combine the selected local structures to represent them in a more compact form. This results in new bases which have compromised aspects between kernels of LFA and eigenfaces for face images. Throughout the experiments, our method has shown improvements on the face recognition over the previously proposed methods, LFA, eigenface, and fisherface.

1 Introduction

In face recognition, feature extraction is one of the most important steps and it represents high dimensional image data into low dimensional feature vectors. In feature extraction, there are two approaches, a global and a local method. Among the global methods, eigenface [1] and fisherface [2] are the two most representative methods, which use Principal Component Analysis(PCA) and Fisher Linear Discriminant(FLD) respectively. Both methods construct bases and the bases are named as *eigenfaces* and *fisherfaces*, and they are considered as models for faces, where the features are extracted by linearly projecting a face image onto the bases. The eigenfaces and fisherfaces describe the whole shape of a face rather than local structures of a face such as nose, eye, jaw-line, and cheekbone. While eigenfaces are constructed from the covariance matrix

of face images, fisherfaces are obtained from between-class scatter matrix and within-class scatter matrix. In other words, eigenface is an unsupervised method and fisherface is a supervised method. Previous experiments show that fisherface performs better than eigenface, and it is robuster to the variations of illumination and poses than eigenface [2]. However, fisherface is known to be prone to overfit to the classes whose data are used in basis construction [3]. Global methods are easy and fast but it is said that they are weak to such variations although fisherface somehow overcame the limitations.

On the contrary, it is known that local methods are robust to the variations. Local Feature Analysis(LFA) [4] is referred to as a local method since it constructs a set of kernels that detects local structures; e.g., nose, eye, jaw-line, and cheekbone, and the kernels are used as bases for feature extraction as in eigenface and fisherface. However, LFA requires feature selection step since the number of the constructed kernels is as the same as the dimension of input images, and it does not use any class information as in eigenface.

In this paper, we point out the problems of LFA and propose a new feature extraction method to overcome the shortcomings of LFA. We exploit class information to construct and select kernels that are useful for face recognition. The rest of the paper is organized as following: In Sec. 2, LFA will be briefly reviewed. In Sec. 3, we propose our method and experimental results are given to verify the efficiency of our method in Sec. 4.

2 Local Feature Analysis

Local Feature Analysis constructs kernels, which are basis vectors for feature extraction. Kernels are constructed using the eigenvectors of the covariance matrix of face images as in eigenface. However, unlike eigenface, kernels describe local structures of a face(see Fig. 3) rather than a whole face structure, and they are *topographic* since the kernels are indexed by spatial location [4] [3].

Let's suppose that there is a set of n d -dimensional sample images $\mathbf{x}_1, \dots, \mathbf{x}_n$. Hence, the covariance matrix, \mathbf{C} , of the images is computed as

$$\mathbf{C} = \frac{1}{n} \sum_{t=1}^n (\mathbf{x}_t - \mathbf{m})(\mathbf{x}_t - \mathbf{m})^T \quad (1)$$

where $\mathbf{m} = \frac{1}{n} \sum_{t=1}^n \mathbf{x}_t$. When there are N largest eigenvalues of \mathbf{C} , λ_r , and the corresponding eigenvectors, Ψ_r , a set of kernels, \mathbf{K} , is derived by enforcing topology into the eigenvectors. In addition, the outputs of kernels, \mathbf{O} , and the covariance of the outputs, \mathbf{P} , are written in a matrix form,

$$\mathbf{K} = \Psi \Lambda \Psi^T \quad (2)$$

$$\mathbf{O} = \mathbf{K}^T \mathbf{X} \quad (3)$$

$$\mathbf{P} = \Psi \Psi^T \quad (4)$$

where $\Psi = [\Psi_1 \dots \Psi_N]$, $\Lambda = \text{diag}\left(\frac{1}{\sqrt{\lambda_r}}\right)$, and $\mathbf{X} = [\mathbf{x}_1 \dots \mathbf{x}_n]$. Since \mathbf{K} is symmetric, we only consider the columns of \mathbf{K} as the bases. Note that the

number of kernels constructed by LFA is as the same as the dimension of input images, V . Hence, the dimension of the outputs is reduced by choosing a subset of kernels, \mathcal{M} . \mathcal{M} is a subset of indices of columns of \mathbf{K} . \mathcal{M} is constructed by iteratively adding a kernel whose output produces the biggest reconstruction error.

At each step, the point added to \mathcal{M} is chosen as the kernel corresponding to location, x ,

$$\arg \max_x \langle \|\mathbf{O}_t(x) - \mathbf{O}_t^{rec}(x)\|^2 \rangle \quad (5)$$

where subscript t and x in a parenthesis denote t^{th} input image and index of elements of vectors, respectively. That is, $\mathbf{O}_t(x)$ represents the output of x^{th} kernel for t^{th} input image. And $\mathbf{O}_t^{rec}(x)$ is the reconstruction of the output. The reconstruction of t^{th} output is

$$\mathbf{O}_t^{rec}(x) = \sum_{m=1}^{|\mathcal{M}|} \mathbf{Z}(m, x) \mathbf{O}_t(y_m) \quad (6)$$

where $\mathbf{Z}(m, x)$ is the reconstruction coefficient and $y_m \in \mathcal{M}$.

For all images, the reconstruction is written in a matrix form as follows.

$$\mathbf{O}^{rec} = \mathbf{Z}^T \mathbf{O}(\mathcal{M}, :) \quad (7)$$

$\mathbf{O}(\mathcal{M}, :)$ denotes the subset of \mathbf{O} corresponding to the points in \mathcal{M} for all n images. And, \mathbf{Z} is calculated from:

$$\mathbf{Z} = \mathbf{P}(\mathcal{M}, \mathcal{M})^{-1} \mathbf{P}(\mathcal{M}, :). \quad (8)$$

3 Proposed Method

In this section, we address the problems of LFA for recognition and propose a new feature extraction method based on LFA. Our method consists of three steps: construction, selection, and combination of the local structures.

In Eq 2, we can see that the kernels of LFA whiten the coefficients of the eigenvectors using the square root of the eigenvalues. \mathbf{C} can be rewritten as the covariance matrix of difference vectors [5].

$$\mathbf{C} = \frac{1}{2n^2} \sum_{t=1}^n \sum_{s=1}^n (\mathbf{x}_t - \mathbf{x}_s)(\mathbf{x}_t - \mathbf{x}_s)^T \quad (9)$$

Note that the mean of difference vectors is zero. In other words, it can be also considered that kernels whiten the coefficients of the eigenvectors for difference vectors. This means that kernels from LFA diminish the variations between two images, even if they are from different classes. For efficient recognition, feature extractors(i.e., bases) have to either maximize the variations from different people or minimize them from the same person. Different from LFA, our proposed

method constructs the kernels from intra-class covariance matrix to minimize the variations from the same person. For c classes, let there is a set of n_i samples in the subset \mathcal{X}_i labelled c_i . Then, the intra-class covariance matrix, \mathbf{C}_I , is defined as

$$\mathbf{C}_I = \frac{1}{\sum_{i=1}^c n_i^2} \sum_{i=1}^c \sum_{\mathbf{x}_t \in \mathcal{X}_i} \sum_{\mathbf{x}_s \in \mathcal{X}_i} (\mathbf{x}_t - \mathbf{x}_s) (\mathbf{x}_t - \mathbf{x}_s)^T \quad (10)$$

Here, \mathbf{C}_I is the covariance matrix of intra-difference vectors. Hence, the proposed new kernels are defined as,

$$\mathbf{K}_I = \mathbf{V} \mathbf{U} \mathbf{V}^T \quad (11)$$

where $\mathbf{V} = [\mathbf{v}_1 \dots \mathbf{v}_N]$, $\mathbf{U} = \text{diag}\left(\frac{1}{\sqrt{u_r}}\right)$, and u_r and \mathbf{v}_r denote r th largest eigenvalue and the corresponding eigenvector of \mathbf{C}_I . Therefore, the new kernels, \mathbf{K}_I , reduce the variations between images from the same person by whitening the coefficients of the eigenvectors for the intra-difference vectors. The more rigorous discussion related to the eigenvectors of \mathbf{C} and \mathbf{C}_I can be found in [5]. Fig. 3 shows that our new kernels show local properties similar to those of LFA. The output matrix, \mathbf{Q} , of the proposed kernels and the correlation matrix, \mathbf{R} , are written as

$$\mathbf{Q} = \mathbf{K}_I^T \mathbf{X} \quad (12)$$

$$\mathbf{R} = \mathbf{K}_I \mathbf{C} \mathbf{K}_I^T \quad (13)$$

where $\mathbf{Q} = [\mathbf{q}_1 \dots \mathbf{q}_t \dots \mathbf{q}_n]$ and $\mathbf{q}_t = \mathbf{K}_I^T \mathbf{x}_t$.

Anther shortcoming of LFA is in its feature selection method. As mentioned in previous section, LFA chooses a set of kernels whose outputs produce the biggest reconstruction error. Although mean reconstruction error is a useful criterion for representing data, there is no reason to assume that it must be useful for discriminating between data in different classes. This problem can be easily verified through an experiment with face images which include some background, i.e., Fig. 1. In this exemplary experiment, we used the first 200 eigenvectors to construct a set of kernels and selected 200 kernels which produced the biggest reconstruction errors. Dots are placed in the selected kernel's locations on the mean image of input images in Fig. 1(a), and the orders of the first 20 kernels added to \mathcal{M} are written in Fig. 1(b). In Fig. 1(a), it can be seen that kernels which belong to the outside of the face are also selected, which means that the kernel selection process aims at reducing reconstruction error on a whole picture not just on a face. Note that it is difficult to select kernels more than the number of eigenvectors used for kernel construction since the algorithm involves matrix inversion and may cause rank deficiency(Eq. 8).

Therefore, to overcome such inefficiencies of LFA, we use class information to select useful kernels for recognition. After constructing kernels from \mathbf{C}_I (Eq. 10), we calculate their Fisher Scores using the outputs of kernels(Eq. 12). Fisher Score is a measure of discriminant power which estimates how well classes are

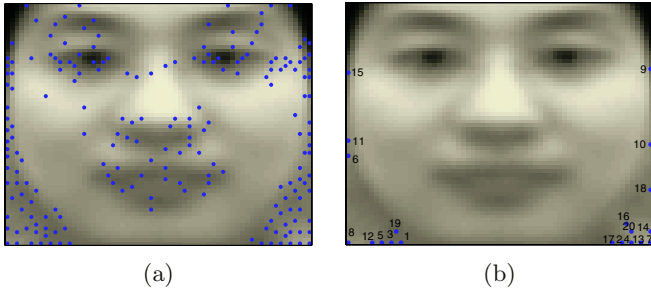


Fig. 1. (a) The locations of 200 kernels selected according to minimum reconstruction error. (b) The locations of the first 20 kernels and their orders of selection

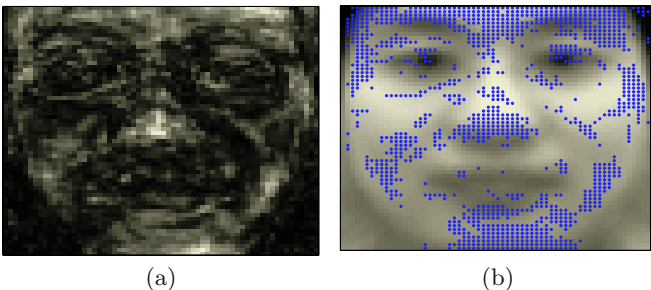


Fig. 2. (a) The Fisher Scores of the kernels. White color is corresponding with larger magnitude. (b) The locations of the first 1300 kernels selected according to Fisher Score

separated from each other by the ratio of the *between-class scatter*, S_B , and the *within-class scatter*, S_W [6]. Fisher Score of x th kernel, $J(x)$, can be defined as

$$J(x) = \frac{S_B(x)}{S_W(x)} = \frac{\sum_{i=1}^c n_i (\mathbf{m}_i(x) - \mathbf{m}(x))^2}{\sum_{i=1}^c \sum_{q \in \mathcal{X}_i} (\mathbf{q}(x) - \mathbf{m}_i(x))^2} \quad (14)$$

where $\mathbf{m}(x) = \frac{1}{n} \sum_{i=1}^c n_i \mathbf{m}_i(x)$ and $\mathbf{m}_i(x) = \frac{1}{n_i} \sum_{q \in \mathcal{X}_i} \mathbf{q}(x)$.

In Fig. 2(a), the score values are displayed on the location of the corresponding kernels. It shows that kernels belonging to the meaningful areas for recognition, such as eyebrow, nose, cheekbone, and jaw-line, received higher scores than the rest, hence such areas are brighter than the rest. This verifies the usefulness of Fisher Score for kernel selection. The locations of the first 1300 kernels selected according to Fisher Score are represented in Fig. 2(b). However, kernel selection by Fisher Score does not regard the redundancy between outputs of kernels. To cover the meaningful area of a face, a large number of kernels are required, which can be a serious burden for computation and storage. This problem can be solved by overlaying the set of local structures onto a single sheet. We call the above approach and the derived bases *composite template*, since the bases of our method consist of a set of local structures.

Suppose that we choose a subset, \mathcal{H} , of column vectors(i.e., kernels) from the matrix \mathbf{K}_I (Eq. 11) using Fisher Score(Eq. 14) and their elements are denoted by $\mathbf{K}_I(:, x_i)$. Hence, a *composite template*, \mathbf{g} , is composed by linear combination of local structures.

$$\mathbf{g} = \sum_{i=1}^{|\mathcal{H}|} w_i \mathbf{K}_I(:, x_i) \quad (15)$$

w_i is a linear combination weight and $x_i \in \mathcal{H}$. However, we do not want to lose information by combining the local structures. Hence, we select the combination weights in such a way that the entropy of the outputs of \mathbf{g} is maximized [7]. For simplicity, we assume Gaussian density for the outputs. Other criterions and density assumptions may be used for different combination strategies. Let a_t be the final output for the t th input, \mathbf{x}_t .

$$a_t = \mathbf{g}^T \mathbf{x}_t = \sum_{i=1}^{|\mathcal{H}|} w_i \mathbf{q}_t(x_i). \quad (16)$$

Without loss of generality, we assume zero mean for a .

$$p(a) = \frac{1}{\sqrt{2\pi}\sigma} \exp\left[-\frac{a^2}{2\sigma^2}\right] \quad (17)$$

where σ^2 is the variance of a . Maximization of the entropy of Eq. 17 is equivalent to the maximization of σ^2 , which can be rewritten as

$$\begin{aligned} \sigma^2 &= \frac{1}{n} \sum_{t=1}^n a_t^2 \\ &= \sum_{i=1}^{|\mathcal{H}|} \sum_{j=1}^{|\mathcal{H}|} w_i \mathbf{R}(x_i, x_j) w_j \\ &= \mathbf{w}^T \mathbf{R}(\mathcal{H}, \mathcal{H}) \mathbf{w} \end{aligned} \quad (18)$$

where $\mathbf{w}^T = [w_1 \dots w_{|\mathcal{H}|}]$. Since $\mathbf{R}(\mathcal{H}, \mathcal{H})$ is symmetric, the linear combination weights, \mathbf{w} , which maximizes Eq. 18 can be easily estimated if we constrain $\mathbf{w}^T \mathbf{w} = 1$. In this case, it is equivalent to carry out PCA for the outputs from \mathcal{H} . This makes it clear how many composite templates, \mathbf{g} , should be constructed. The maximum number of composite templates is N since a set of kernels, \mathbf{K}_I , the outputs, \mathbf{Q} , and the covariance matrix, $\mathbf{R}(\mathcal{H}, \mathcal{H})$, are all based on the N eigenvectors, i.e., their ranks are N .

Remark. The Fig. 3 shows eigenfaces (a), kernels of LFA (b), fisherfaces (c) [2], the proposed kernels (d), and *composite templates* (d). Similar to kernels of LFA, the proposed new kernels also show local properties. Eigenfaces and kernels of LFA are at the extreme cases, one is global and the other is local. Our *composite*

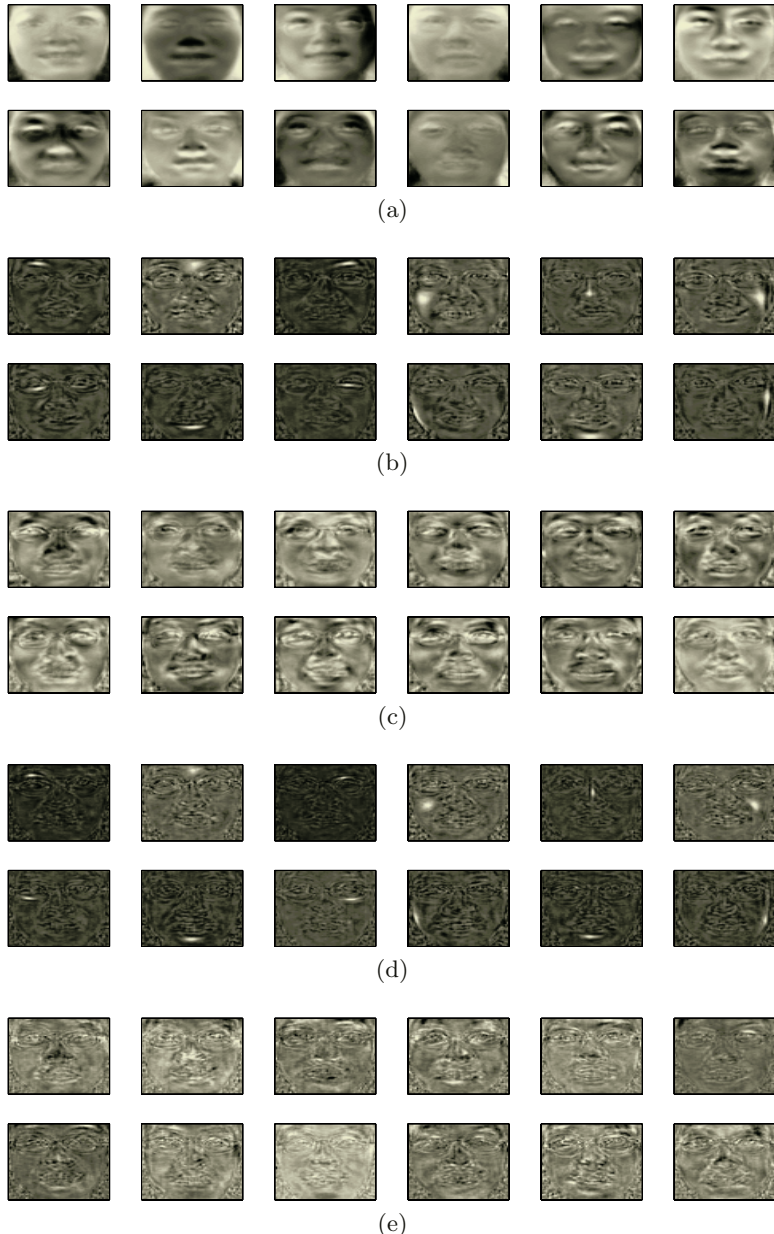


Fig. 3. (a) The first 12 eigenfaces. (b)The kernels of LFA selected manually. (c) The first 12 fisherfaces. (d) The proposed kernels. (e)The first 12 composite templates

templates, which are constructed by combining kernels, show intermediate aspects between kernels(local) and eigenfaces(global). Fisherfaces, which also use Fisher Score, are somehow similar to *composite templates*, however, it can be

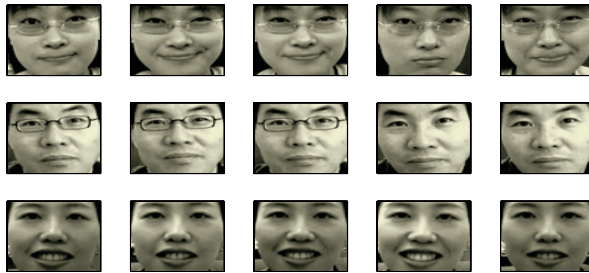


Fig. 4. Example faces in our database

thought that fisherfaces are constructed by combining the global structures(i.e., eigenfaces) since Fisher Liner Discriminant(FLD) is applied after the dimension of the images is reduced using PCA.

4 Experiments and Results

To verify the efficiency of our suggested method through face recognition experiments, we used images from a group of 55 people and a few images are shown in Fig. 4. For each person, 20 facial images were taken. To construct bases for feature extraction, the images of 20 randomly selected people from the group were used. Among the images that were not used in base construction, 10 images for each person were used for training (gallery), and the rest were used for testing (probe). The size of image is 64×64 , and the experiments were conducted using Euclidean distance.

Throughout the experiments, we have compared the results from the following feature extraction methods: (a) eigenface, (b) LFA, (c) fisherface, and (d) *composite template*. For LFA, 200 eigenvectors of \mathbf{C} (Eq. 1) were used to construct a set of kernels and 200 kernels were chosen among them (Fig. 1). For *composite template*, 250 eigenvectors of \mathbf{C}_I (Eq. 10) were used to construct a set of kernels and 1300 kernels were selected (Fig. 2). For fisherface, the dimension of the images was reduced into 120 using PCA, and the FLD was applied to the reduced dimension images. The bases constructed by each method are shown in Fig. 3.

Fig. 5 shows recognition rate with the increments of the number of features. For the rank 1, the best recognition rates of eigenface, LFA, fisherface, and composite template are 60.57%, 71.71%, 82.29%, and 94.29%, respectively (Table 1). Here, rank n means that the matching algorithm using different feature extraction methods finds the correct image within top n gallery images. To achieve the best recognition rate in each method, 178, 199, 17, and 158 features were needed. In LFA and fisherface, we increased the number of the eigenvectors, however, it did not show any improvements. Note that the number of fisherfaces is bounded on the number of classes(people), which are used in basis construction. By fixing the shortcomings of LFA, our proposed method showed the best performance

Table 1. Accuracy(%) which test images are matched within rank 1, 2, 3, 4, 5 using the number of features in the first row. The numbers in the first column are the minimum number of features with the best performance for the rank 1. (a) eigenface, (b) LFA, (c) fisherface, and (d)composite template

| Rank | (a): 178 | (b): 199 | (c): 17 | (d): 158 |
|------|----------|----------|---------|----------|
| 1 | 60.57 | 71.71 | 82.29 | 94.29 |
| 2 | 70.00 | 79.14 | 88.29 | 96.57 |
| 3 | 75.43 | 81.14 | 92.00 | 98.00 |
| 4 | 77.43 | 83.43 | 93.43 | 98.57 |
| 5 | 77.71 | 84.57 | 94.00 | 98.86 |

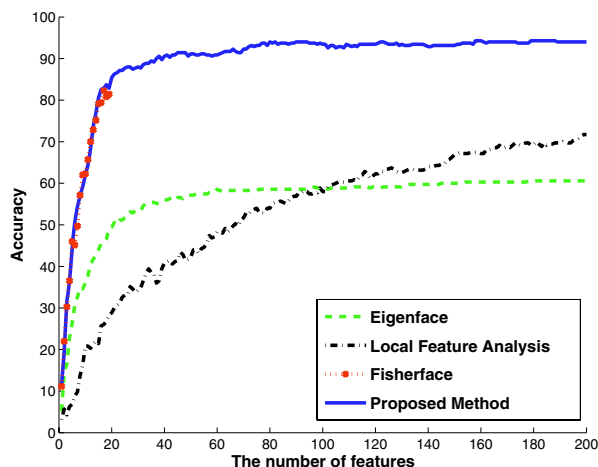


Fig. 5. Accuracy(%) which test images are matched at rank 1 with the increments of the number of features

among the tested methods. It can be also seen that the size of kernels chosen by Fisher Score was reduced effectively.

5 Conclusions

Based on LFA, we propose a new feature extraction method for face recognition. Our method consists of three steps. First we extract local structures using LFA. Second, we select a subset of them, which is efficient for recognition. Finally, we combine the local structures into composite templates. The composite templates represent data in a more compact form and show compromised aspects between kernels of LFA and eigenfaces. Although LFA is originally problematic for recognition, the proposed *composite template* method has shown better recognition performance than eigenface, LFA, and fisherface.

References

1. Turk, M.A., Pentland, A.P.: Face recognition using eigenface. In: Proc. of IEEE Conf. on Computer Vision and Pattern Recognition, Maui, Hawaii (1991)
2. Belhumeur, P.N., Hespanha, J.P., Kriegman, D.J.: Eigenfaces vs. Fisherfaces: Recognition using class specific linear projection. *IEEE Trans. Pattern Analysis and Machine Intelligence* **19** (1997) 711–720
3. Bartlett, M.: Face Image Analysis by Unsupervised Learning. Kluwer Academic Publisher (2001)
4. Penev, P., Atick, J.: Local feature analysis: A general statistical theory for object representation. *Network: Computation in Neural Systems* **7** (1996) 477–500
5. Wang, X., Tang, X.: Unified subspace analysis for face recognition. In: Proc. of IEEE Int. Conf. on Computer Vision. (2003)
6. Duda, R.O., Hart, P.E., Stork, D.G.: Pattern Classification. John Wiley & Sons (2001)
7. Principe, J.C., Xu, D., Fisher III, J.W.: Information-theoretic learning. In Haykin, S., ed.: *Unsupervised Adaptive Filtering: Blind Source Separation*. John Wiley & Sons, Inc. (2000) 265–319

Training of Feature Extractor via New Cluster Validity – Application to Adaptive Facial Expression Recognition

Sang Wan Lee¹, Dae-Jin Kim², Yong Soo Kim³, and Zeungnam Bien¹

¹ Department of Electrical Engineering and Computer Science, KAIST,
Daejeon, 305-701, Korea
bigbean@ctrssys.kaist.ac.kr, zbien@ee.kaist.ac.kr
<http://ctrsgate.kaist.ac.kr/~bigbean>

² Human-friendly Welfare Robot System Engineering Research Center, KAIST,
Daejeon, 305-701, Korea
djkim@ctrssys.kaist.ac.kr

³ Division of Computer Engineering, Daejeon University, Daejeon, 300-716, Korea
kystj@dju.ac.kr

Abstract. A lot of researches on classifiers, which can perform well with a given set of feature vectors, have been done. However, researches on feature vectors, which extract better feature vectors automatically, have not been done very much. We face two problems when we consider feature extraction process. One is how we can make a good feature extractor, and the other is what more separable features are. In this paper, we solved these two problems by proposing feature extractor-training methodology that uses new cluster validity as an objective function. By combining feature extractor to Fuzzy Neural Network Model, we achieve on-line adaptation capability as well as optimized feature extraction. The result shows recognition rate of 97% when on-line adaptation is being done.

1 Introduction

Facial Expression has various characteristics such as interconnection among components, vagueness, and subjectivity[1]. To consider these characteristics, researchers have used various classification techniques[1-5]. However, most of previous researches are focused on classification only, not feature extractor, so the complexity of interconnection increases as using more features. In this paper, to solve this problem and to exclude heuristics in selecting feature, we propose training method of feature extractor based on Levenberg-Marquardt concept.

So then, what is separable feature? And how can we make feature more separable? Various researches related with this question have been studied on the category of Fuzzy C-Means algorithm. To improve Bezdek[6] and Xie and Beni[7]'s concepts, Kim developed inter-cluster proximity[8]. Though it can evaluate validity of clusters, it cannot measure separability when there is no overlap.

Then the question, what are more better features guaranteeing separability, still remains unanswered. Therefore, to guarantee the separability of class vector from feature extractor, we propose novel cluster validity as an objective function for training. Also, we introduce adaptation for personalized facial expression recognition, specially using Fuzzy Neural Network Model[9] performing on-line adaptation. In section 2,

we introduce overall structure of Facial Expression Recognition System. In section 3, new cluster validity for training is introduced, and then training method of feature extractor is explained in section 4. The superiority of on-line adaptation capability is shown in section 5.

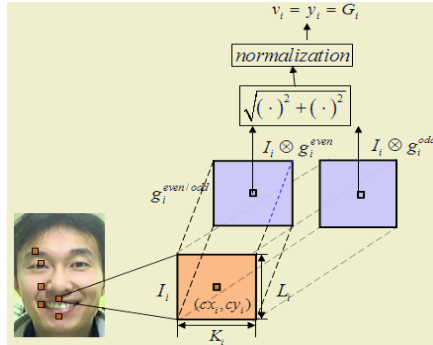


Fig. 1. Feature Extraction Process for given 6-facial feature points

2 Adaptive Facial Expression Recognition System

2.1 Feature Extraction Process via Gabor Wavelets [10]

Face and its each region are found by Haar-classifier using openCV library[11]. Because we can approach to each facial point in this manner, we focus on facial expression recognition process in this paper, rather than face detection process. In facial expression recognition process, the first step is a feature extracting layer which has a set of Gabor filters and normalization process[10](Fig. 1). Each feature vector, as follows, can show the rate of specific frequency and angle that sub image contains.

$$\vec{v} = [v_1, v_2, v_3, v_4, v_5, v_6]^T \quad (1)$$

2.2 Fuzzy Neural Network Model[9]

To organize adaptive classifier, output of feature extractor is applied to Fuzzy Neural Network Model[9] working in the unsupervised manner. In this algorithm, after performing initial iteration with training data, the centers of each cluster are converged, and then perform an on-line adaptation.

3 Proposed Cluster Validity for Training of Feature Extractor

In this section, we will introduce three kinds of criterions and total cluster validity consisted of them. To get more separable feature sets through the training process in section 4, proposed total cluster validity is used as an objective function, and so it has the form that is easy to differentiate.

Definition 1. Cluster Validity Based on Distance

Basically in this paper, conventional distance-based cluster validity, namely within and between class scatterness, are used. They are as follows.

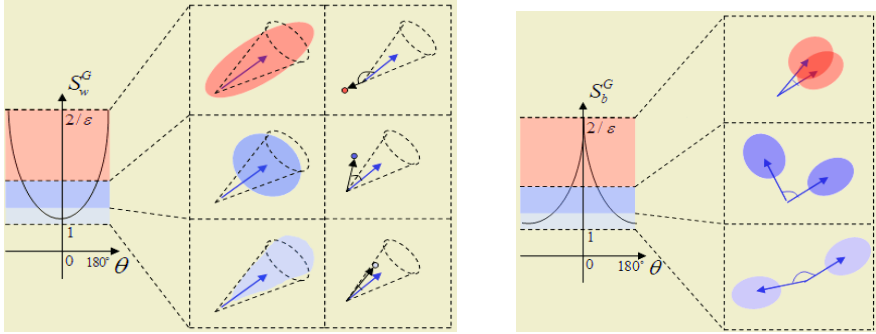


Fig. 2. Within-class guide $S_w^{G(j)}(n)$ about n-th point of class j and Between-class guide $S_b^{G(j,k)}$ about class j and k are shown. Both reflect separability of inner-class, and between classes

$$S_w = \frac{1}{J} \sum_{j=1}^J \frac{1}{N_j} \sum_{n=1}^{N_j} \left\{ \sum_{i=1}^6 (v_i^{(j)}(n) - M_i^{(j)})^2 \right\} \quad (2)$$

$$S_b = \frac{1}{J} \sum_{j=1}^J \left\{ \sum_{i=1}^6 (M_i^{(j)} - M_o)^2 \right\} \quad (3)$$

where $\bar{M}^{(j)} = \frac{\sum_{n=1}^{N_j} \bar{v}^{(j)}}{N_j}$, $\bar{M}_o = \frac{1}{J} \sum_{j=1}^J \sum_{n=1}^{N_j} \bar{v}^{(j)}$ is center of each and total class. N, N_j, J is number of training data, number of data per class, and number of class, respectively.

Definition 2. Proposed Cluster Validity Based on Angle

Because the scatterness in definition 1 considers trace of matrix only, additional criterion which considers scattering direction is needed. The most well-known criterion to fulfill this need is Mahalanobis distance and first term of Battacharyya distance. To apply these characteristics, we introduce a minimization problem based on vector concept. Minimizing cost function means that data are pulled from center of total class so that they can locate around center of their class.

$$\text{minimize } \angle(\bar{v}^{(j)}(n) - \bar{M}_o)(\bar{M}^{(j)} - \bar{M}_o) \equiv \text{minimize } \left| \cos^{-1} \left(\frac{(\bar{v}^{(j)}(n) - \bar{M}_o) \cdot (\bar{M}^{(j)} - \bar{M}_o)}{\|\bar{v}^{(j)}(n) - \bar{M}_o\| \|\bar{M}^{(j)} - \bar{M}_o\|} \right) \right| \quad (4)$$

Because cosine function is concave in $-180^\circ \sim 180^\circ$, we simplify above problem.

$$\text{minimize } 2/\left\{ \epsilon + 1 + \frac{(\bar{v}^{(j)}(n) - \bar{M}_o) \cdot (\bar{M}^{(j)} - \bar{M}_o)}{\|\bar{v}^{(j)}(n) - \bar{M}_o\| \|\bar{M}^{(j)} - \bar{M}_o\|} \right\} \quad (5)$$

where ϵ ($0 < \epsilon \leq 1$) means control parameter of concavity. From above, we define cost function to be minimized as a guidance of within-class.

$$S_w^{G(j)}(n) \triangleq \left(2/\left\{ \epsilon + 1 + \frac{(\bar{v}^{(j)}(n) - \bar{M}_o) \cdot (\bar{M}^{(j)} - \bar{M}_o)}{R^{(j)}(n) R_M^{(j)}} \right\} \right), \quad S_w^G \triangleq \frac{1}{J} \sum_{j=1}^J \frac{1}{N_j} \sum_{n=1}^{N_j} S_w^{G(j)}(n) \quad (6)$$

where j is class index and

$$R^{(j)}(n) \triangleq |\bar{v}^{(j)}(n) - \bar{M}_o|, \quad R_M^{(j)} \triangleq |\bar{M}^{(j)} - \bar{M}_o| \quad (7)$$

Secondly, maximizing problem is introduced as guidance among classes. Maximization of angle makes classes avoid each other in viewpoint of direction.

$$\text{maximize } \angle(\bar{M}^{(j)} - \bar{M}_o)(\bar{M}^{(k)} - \bar{M}_o) \equiv \text{maximize } \left| \cos^{-1} \left(\frac{(\bar{M}^{(j)} - \bar{M}_o) \cdot (\bar{M}^{(k)} - \bar{M}_o)}{\|\bar{M}^{(j)} - \bar{M}_o\| \|\bar{M}^{(k)} - \bar{M}_o\|} \right) \right| \quad (8)$$

By similar simplification as the first case, we can convert Eq. (8) to a maximization problem. In this manner, we define cost function to be minimized as a guidance of between-class.

$$S_b^G(j,k) \triangleq \left(2 / \left\{ \varepsilon + 1 - \frac{(\bar{M}^{(j)} - \bar{M}_o) \cdot (\bar{M}^{(k)} - \bar{M}_o)}{R_M^{(j)} R_M^{(k)}} \right\} \right), \quad S_b^G \triangleq \frac{1}{J C_2} \sum_{j=1}^J \sum_{k=1}^J S_b^G(j,k) \quad (9)$$

Definition 3. Additional Cluster Validity for Fuzzy Neural Network Model

To utilize FNNM[19], we need an additional condition, because FNNM performs vigilance test by fixed vigilance parameter. It means a variation of within-class scatterness. Therefore, it is similar to the covariance term of Battachayya distance.

$$S_b^V \triangleq \frac{1}{J} \sum_{j=1}^J (s_w^{(j)} - S_w)^2 \quad (10)$$

Definition 4. Proposed Total Cluster Validity

Criterions introduced through Def. 1 to 3 constitute total cluster validity as follows.

$$S_{\text{proposed}} \triangleq \begin{pmatrix} S_b^{\text{new}} & 0 & 0 \\ 0 & S_w^{\text{new}} & 0 \\ 0 & 0 & (1 + S_b^V) \end{pmatrix} \quad \text{where } S_b^{\text{new}} = \begin{pmatrix} S_b^{-1} & 0 \\ 0 & S_b^G \end{pmatrix}, S_w^{\text{new}} = \begin{pmatrix} S_w & 0 \\ 0 & S_w^G \end{pmatrix} \quad (11)$$

To evaluate and differentiate Eq. (11), we use a determinant.

$$\det(S_{\text{proposed}}) = S_b^{-1} S_b^G S_w S_w^G (1 + \beta S_b^V) = \det(S_b^{\text{new}}) \det(S_w^{\text{new}}) (1 + \beta S_b^V) \quad (12)$$

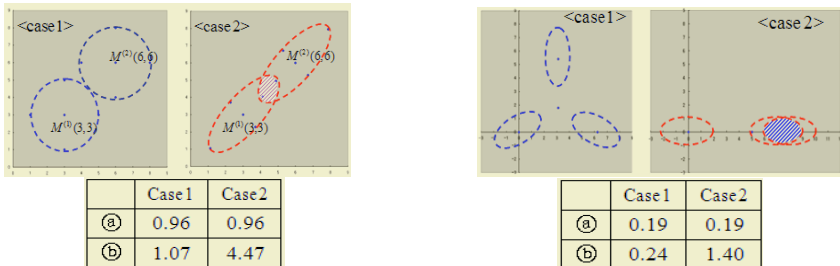


Fig. 3. Numerical Example ; Comparison between conventional cluster validity in Eq.(2,3) and proposed cluster validity in Eq. (11)

Now the training problem of feature extractor is determined to minimize Eq. (12). Figure 3 is a numerical example showing that the proposed method is superior to the conventional criterion as introduced in Eq. (2) and (3).

4 Training of Feature Extractor

We introduce training technique of feature extractor using proposed separability criterion in section 3. Basically, training methodology follows Levenberg – Marquardt(LM) concept[12,13]. First, partial derivatives of S_w, S_b are as follows.

$$\frac{\partial S_w}{\partial f_i} = \frac{2}{J} \sum_{j=1}^J \frac{1}{N_j} \sum_{n=1}^{N_j} (v_i^{(j)}(n) - M_i^{(j)}) \left\{ \frac{\partial v_i^{(j)}(n)}{\partial f_i} - \frac{\partial M_i^{(j)}}{\partial f_i} \right\} \quad (13)$$

$$\frac{\partial S_b}{\partial f_i} = \frac{1}{J} \sum_{j=1}^J 2(M_i^{(j)} - M_{oi}) \left\{ \frac{\partial M_i^{(j)}}{\partial f_i} - \frac{\partial M_{oi}}{\partial f_i} \right\} \quad (14)$$

where $\frac{\partial M_{oi}}{\partial f_i} = \frac{1}{J} \sum_{j=1}^J \left(\frac{\partial M_i^{(j)}}{\partial f_i} \right)$, $\frac{\partial M_i^{(j)}}{\partial f_i} = \frac{1}{N_j} \sum_{n=1}^{N_j} \frac{\partial v_i^{(j)}(n)}{\partial f_i}$

Secondly, partial derivative of S_w^G has a final numerical formula as follows.

$$\frac{\partial S_w^G}{\partial f_i} = \frac{1}{J} \sum_{j=1}^J \frac{1}{N_j} \sum_{n=1}^{N_j} \frac{\partial S_w^G(n)}{\partial f_i} \quad (15)$$

$$\begin{aligned} \frac{\partial S_w^G(n)}{\partial f_i} = & -\frac{\{S_w^G(n)\}^2}{2R^{(j)}(n)R_M^{(j)}} \cdot \left\{ \frac{(v_i^{(j)}(n) - M_{oi})}{(M_i^{(j)} - M_{oi})} R_M^{(j)} \frac{\partial R_M^{(j)}}{\partial f_i} + \frac{(M_i^{(j)} - M_{oi})}{(v_i^{(j)}(n) - M_{oi})} R^{(j)} \frac{\partial R^{(j)}}{\partial f_i} \right. \\ & \left. + \left(\epsilon + 1 - \frac{2}{S_w^G(n)} \right) \left(R^{(j)}(n) \frac{\partial R_M^{(j)}}{\partial f_i} + R_M^{(j)} \frac{\partial R^{(j)}(n)}{\partial f_i} \right) \right\} \end{aligned} \quad (16)$$

where $\frac{\partial R^{(j)}(n)}{\partial f_i} = \frac{(v_i^{(j)}(n) - M_{oi})}{R^{(j)}(n)} \left(\frac{\partial v_i^{(j)}(n)}{\partial f_i} - \frac{\partial M_{oi}}{\partial f_i} \right)$, $\frac{\partial R_M^{(j)}}{\partial f_i} = \frac{(M_i^{(j)} - M_{oi})}{R^{(j)}(n)} \left(\frac{\partial M_i^{(j)}}{\partial f_i} - \frac{\partial M_{oi}}{\partial f_i} \right)$

Also, partial derivative of S_b^G is given by computation similar to the case above.

$$\frac{\partial S_b^G}{\partial f_i} = \frac{1}{J C_2} \sum_{j=1}^J \sum_{k=1}^J \frac{\partial S_b^G(j,k)}{\partial f_i} = \frac{2}{J(J-1)} \sum_{j=1}^J \sum_{k=1}^J \frac{\partial S_b^G(j,k)}{\partial f_i} \quad (17)$$

$$\begin{aligned} \frac{\partial S_b^G(j,k)}{\partial f_i} = & \frac{\{S_b^G(j,k)\}^2}{2R_M^{(j)}R_M^{(k)}} \cdot \left\{ \frac{(M_i^{(j)} - M_{oi})}{(M_i^{(k)} - M_{oi})} R_M^{(k)} \frac{\partial R_M^{(k)}}{\partial f_i} + \frac{(M_i^{(k)} - M_{oi})}{(M_i^{(j)} - M_{oi})} R_M^{(j)} \frac{\partial R_M^{(j)}}{\partial f_i} \right. \\ & \left. - \left(\epsilon + 1 - \frac{2}{S_b^G(j,k)} \right) \left(R_M^{(j)} \frac{\partial R_M^{(k)}}{\partial f_i} + R_M^{(k)} \frac{\partial R_M^{(j)}}{\partial f_i} \right) \right\} \end{aligned} \quad (18)$$

Also, Partial derivative of additional cluster validity S_b^V is given as follows.

$$\frac{\partial S_b^V}{\partial f_i} = \frac{2}{J} \sum_{j=1}^J (S_w^{(j)} - S_w) \cdot \left(\frac{\partial S_w^{(j)}}{\partial f_i} - \frac{1}{J} \sum_{j=1}^J \frac{\partial S_w^{(j)}}{\partial f_i} \right) \quad (19)$$

$$\frac{\partial S_w^{(j)}}{\partial f_i} = \frac{2}{N_j} \sum_{n=1}^{N_j} (v_i^{(j)}(n) - M_i^{(j)}) \left\{ \frac{\partial v_i^{(j)}(n)}{\partial f_i} - \frac{\partial M_i^{(j)}}{\partial f_i} \right\} \quad (20)$$

Finally, partial derivative of $\det(S_{proposed})$ is calculated using Eq. (13) to (20).

$$\frac{\partial \det(S_{proposed})}{\partial f_i} = \left\{ \frac{\partial \det(S_b^{new})}{\partial f_i} \det(S_w^{new}) + \frac{\partial \det(S_w^{new})}{\partial f_i} \det(S_b^{new}) \right\} (1 + \beta S_b^V) + \beta \frac{\partial S_b^V}{\partial f_i} \det(S_b^{new}) \det(S_w^{new}) \quad (21)$$

where $\frac{\partial \det(S_b^{new})}{\partial f_i} = \frac{\partial S_b^G}{\partial f_i} S_b^{-1} - \frac{S_b^G}{S_b^2} \frac{\partial S_b}{\partial f_i}$, $\frac{\partial \det(S_w^{new})}{\partial f_i} = \frac{\partial S_w^G}{\partial f_i} S_w^{-1} - \frac{\partial S_w}{\partial f_i} S_w^G$. And all calculation process about θ is just the same.

Additionally, by using technique introduced in [10], we can get partial derivatives of feature extraction process, $\partial v_i / \partial f_i$, $\partial v_i / \partial \theta_i$. Hereby all calculations for Levenberg – Marquardt algorithm are completed so as to find best cluster validity.

5 Results

We used 42 images of EKMAN DB and 45 JAFFE DB to get a general classifier. The learning process was done for three expressions - happy, sad, and angry. To show the system's adaptation capability, BSCL DB was used. This database, which consisted of 5 individuals and totally 600 images, was collected by PC-CAM in real circumstances during 6 days. First 60 data of each user were used as training data to organize personalized classifier. Then another 60 data, collected during 5 days after first data set had been collected, were used as on-line test data.

Generalization performance for EKMAN and JAFFE DB is 74% and 89% each. Personalization(Off-line adaptation) test of BSCL DB is successful as shown in second column of Table 2. In this table, clustering rate averages 98.7% after initial clustering of FNNM when learning of feature extractor is done, whereas 80.2 % without learning. From this result, we can conclude that performance is improved by minimizing proposed cluster validity.

Table 1. Left table shows initial clustering result (98.7%), and right table shows on-line adaptation test after initial clustering (97% for new data)

| | FNNM only | Training of Feature Extractor + FNNM | | No Adaptation | On-line Adaptation |
|--------|-----------|--------------------------------------|--------|---------------|--------------------|
| USER#1 | 98.3 % | 100.0 % | USER#1 | 95.0 % | 100.0 % |
| USER#2 | 76.7 % | 100.0 % | USER#2 | 91.7 % | 96.7 % |
| USER#3 | 81.2 % | 100.0 % | USER#3 | 95.0 % | 98.3 % |
| USER#4 | 61.7 % | 98.3 % | USER#4 | 98.3 % | 98.3 % |
| USER#5 | 83.3 % | 95.0 % | USER#5 | 68.3 % | 91.7 % |

After organizing personalized GWNN, we continued to perform on-line adaptation with other 60 data during 5 days. Table 4 shows the results. The accuracy of 97.0% was obtained in average when performing on-line adaptation, whereas generalization performance of 89.7%, which does not utilize on-line adaptation.

6 Conclusion

Though previous researches considered various kinds of features and the interconnection among them by using various classification techniques, they have not been considered fundamental problem, feature extraction process itself. As the solution for this problem, a training method of feature extractor in Gabor Wavelet Neural Network for facial expression recognition has been proposed.

By using FNNM as an on-line adaptation, the system becomes to have capability of tracking user's change of facial expressions as time goes by without any supervisory manner. Therefore, the recognition rate can be improved when unlearned new user continues to use the system using adaptation process.

References

1. Park, G.-T.: A Study on Extraction of Emotion from Facial Image using Soft Computing Techniques. Ph.D Thesis, Dept. of Electrical Engineering and Computer Science, KAIST. (1998)
2. Kapoor, A., Yuan, Q., Picard, R.W.: Fully Automatic Upper Facial Action Recognition. IEEE International Analysis and Modeling of Faces and Gestures. (2003) 195 – 202.
3. Fasel, B.: Robust Facial Analysis using Convolutional Neural Networks. Proc. of the ICPR. (2002)
4. Guodong, G., Charles, R. D.: Simultaneuous Feature Selection and Classifier Training via Linear Programming: A Case Study for Face Expression Recognition. Proc. Of IEEE CVPR. (2003)
5. Ira Cohen et al.: Facial Expression Recognition From Video Sequences. ICME. (2002)
6. Bezdek, J.C.: Numerical taxonomy with fuzzy sets. J. Math. Biol vol 1. (1974) pp. 57-71.
7. Xuanli, L., Beni, G.: A Validity Measure for Fuzzy Clustering. IEEE Trans. on PAMI. Vol 13. (1991)
8. Kim, D.-W., Lee, K.H., Lee, D.H.: Fuzzy Cluster Validation Index based on Inter-Cluster Proximity. Pattern Recognition Letters. (2003)
9. Kim,Y.S., Ham,C.H., Baek, Y. S.: A Fuzzy Neural Network Model Solving the Underutilization Problem. Journal of Korea Fuzzy Logic and Intelligent Systems Society, Vol. 11. (2001) pp. 354-358.
10. Lee, S.W., Kim, D.-J., Kim, Y. S., Bien, Z.: An Adaptive Facial Expression Recognition System Using Fuzzy Neural Network Model and Q-learning, SCISISIS. Yokohama. Japan. (2004)
11. http://www.cs.bham.ac.uk/resources/courses/robotics/doc/opencvdocs/ref/OpenCVRef_Experimental.htm#decl_cvGetHaarClassifierCascadeScale
12. Ranganathan A.: The LM Algorithm, Report of BORG Lab. in Georgia Institute of Technology. (2004)
13. Edwin, K. P., Stanislaw H. Zak.: An Introduction to Optimization, John Wiley & Sons. (2001)

Adaptive Fuzzy Output-Feedback Controller for SISO Affine Nonlinear Systems Without State Observer

Jang-Hyun Park¹, Sam-Jun Seo², Dong-Won Kim³, and Gwi-Tae Park³

¹ Department of Control System Engineering, Mokpo National University,
61, Torim-ri Chonggye-myon, Muan-gun, Chonnam, Korea
jhpark72@mokpo.ac.kr

² Department of Electrical Engineering, Anyang University,
708-113, Anyang 5-dong, Manan-gu, Anyang-shi, Kyonggi-do 430-714, Korea
ssj@aycc.anyang.ac.kr

³ School of Electrical Engineering, Korea University
1, 5-ka, Anam-dong, Seongbuk-ku, Seoul 136-701, Korea
{upground,gtpark}@korea.ac.kr

Abstract. This paper proposes a new output-feedback adaptive fuzzy controller for SISO affine nonlinear systems. The previous output-feedback control algorithms are all based on the state observer (e.g., higher-order-observer) or additional low-pass filter to make the estimation error dynamics SPR, which makes the stability analysis of the closed-loop system and real implementation very complicated. The distinguished aspect of the proposed output-feedback control algorithm is that no state observer or low-pass filter is employed. Only the output error is used to generate control input and update laws for unknown fuzzy parameters. The stability analysis depends heavily on the universal function approximation property of the fuzzy system to estimate unknown function of the desired control input. It is shown that, combining this simple output-feedback control algorithm with an online self-structuring fuzzy system, the Lyapunov stability of the closed-loop system is globally guaranteed.

1 Introduction

After it was proven that fuzzy logic systems (FLSs) are universal function approximators [1], [2], the adaptive control algorithms of unknown or ill-defined nonlinear systems that employ FLSs have been intensively researched. The main advantages of using FLSs are that the exact model of the controlled system is not required and linear-in-the-parameters condition on unknown nonlinearities is not needed. Thus, the class of nonlinear systems to which the adaptive control scheme is applicable is enlarged by using FLSs.

In [3], [4], [5], [6], [7], [8], [9], [10], output-feedback control schemes based on an adaptive observer using UFAs were proposed. Subsequently, the condition of linear dependence upon unknown parameters has been removed by introducing UFAs such as fuzzy systems and neural networks in the observer structure. Their

schemes require strictly positive real (SPR) conditions on the estimation error dynamics so that they can use Meyer-Kalman-Yakubovic (MKY) lemma. The original observation error dynamics, which is not SPR in general, is augmented by a low-pass filter designed to satisfy the SPR condition of a transfer function associated with the Lyapunov stability analysis. However, this scheme results in the filtering of the regressor (or basis) vectors of UFAs, which makes the dynamic order of the observer very large. Moreover, the fixed structure of the UFAs results in an unnecessarily large dimension of basis vectors. The result in [10] is limited to systems that can be transformed into output feedback form, i.e., in which nonlinearities depend upon measurement only.

This paper proposes a new ouput-feedback adaptive fuzzy controller for SISO affine nonlinear systems. As mentioned earlier, the previous output-feedback control algorithms are all based on the state observer (e.g., higher-order-observer) or additional low-pass filter to make the estimation error dynamics SPR, which makes the stability analysis of the closed-loop system and real implementation very complicated. The distinguished aspect of the proposed output-feedback control algorithm is that no state observer or low-pass filter is employed. Only the output error is used to generate control input and update laws for unknown fuzzy parameters. The stability analysis depends heavily on the universal function approximation property of the fuzzy system to estimate unknown function of the desired control input. It is shown that, combining this simple output-feedback control algorithm with an online self-structuring fuzzy system, the Lyapunov stability of the closed-loop system is globally guarnateed.

2 Problem Formulation

We consider the following affine nonlinear SISO systems

$$y^{(n)} = a(y, \dot{y}, \dots, y^{(n-1)}) + b(y, \dot{y}, \dots, y^{(n-1)}) u \quad (1)$$

where y and u are the ouput and input of the system, respectively, $a(\mathbf{x})$, $b(\mathbf{x})$ are unknown nonlinear functions. Let $\mathbf{x} = [y \ \dot{y}, \dots, y^{(n-1)}]^T = [x_1 \ x_2 \ \dots \ x_n]^T$.be the state vector. Then, (1) can be rewritten as a state space model

$$\begin{aligned} \dot{x}_i &= x_{i+1}, i = 1, 2, \dots, n-1 \\ \dot{x}_n &= a(\mathbf{x}) + b(\mathbf{x}) u \\ y &= x_1. \end{aligned} \quad (2)$$

It is assumed that only the ouput y is measurable and $b(\mathbf{x}) > 0$ for all $\mathbf{x} \in \mathbf{R}^n$ for controllability.

Let the desired output be y_d and the desired state vector be $\mathbf{y}_d = [y_d \ \dot{y}_d \ \dots \ y_d^{(n-1)}]^T$. The tracking error is defined as $e = y_d - y$ and the tracking error vector is $\mathbf{e} = \mathbf{y}_d - \mathbf{x} = [e \ \dot{e} \ \dots \ e^{(n-1)}]^T$. A filtered tracking error is defined as

$$s = \left(\frac{d}{dt} + \lambda \right)^{n-1} e = \lambda^T \mathbf{e} \quad (3)$$

where $\lambda > 0$ is a design constant and $\lambda = [\lambda^{n-1} \ (n-1) \lambda^{n-2} \cdots (n-1) \lambda \ 1]^T$. The time derivative of s is derived as

$$\begin{aligned}\dot{s} &= \lambda_1^T \mathbf{e} + y_d^{(n)} - y^{(n)} \\ &= \lambda_1^T \mathbf{e} + y_d^{(n)} - a(\mathbf{x}) - b(\mathbf{x}) u \\ &= -a(\mathbf{x}) - \lambda_1^T \mathbf{x} - b(\mathbf{x}) u + y_d^{(n)} + \lambda_1^T \mathbf{x}_d \\ &= a_1(\mathbf{x}) - b(\mathbf{x}) u + v_1\end{aligned}\tag{4}$$

where $\lambda_1 = [0 \ \lambda^{n-1} \ (n-1) \lambda^{n-2} \cdots (n-1) \lambda]^T$, $a_1(\mathbf{x}) = -a(\mathbf{x}) - \lambda_1^T \mathbf{x}$, and

$$v_1 = y_d^{(n)} + \lambda_1^T \mathbf{x}_d.$$

The aim of this paper is to design an adaptive fuzzy controller for affine non-linear system (2) under the assumptions such that the estimated fuzzy parameters and tracking error are uniformly ultimately bounded (UUB).

3 Adaptive Fuzzy Controller Design

3.1 Optimal Controller Design

The proposed ideal controller is motivated by the one in [11].

Lemma 1. *For the system (1), if the control input is determined as*

$$u = k\lambda^{n-1}e + \frac{a_2(\mathbf{x}) + v(\mathbf{x}, v_1, v_2)}{b(\mathbf{x})}\tag{5}$$

where k is the positive design constant, $a_2(\mathbf{x}) = a_1(\mathbf{x}) - b(\mathbf{x}) k\lambda_2^T \mathbf{x}$, $v(\mathbf{x}, v_1, v_2) = v_1 + b(\mathbf{x}) v_2$, $v_2 = k\lambda_2^T \mathbf{x}_d$, and $\lambda_2 = [0 \ (n-1) \lambda^{n-2} \cdots (n-1) \lambda \ 1]^T$. Then, s converges to zero.

Proof. Consider the Lyapunov function $V_s = \frac{1}{2}s^2$. Taking the time derivative of V_s along (4) yields

$$\begin{aligned}\dot{V}_s &= s\dot{s} \\ &= s \left(a_1(\mathbf{x}) - b(\mathbf{x}) \left(k\lambda^{n-1}e + \frac{a_2(\mathbf{x}) + v}{b(\mathbf{x})} \right) + v_1 \right) \\ &= s \left(a_1(\mathbf{x}) - b(\mathbf{x}) \left(ks - k\lambda_2^T \mathbf{e} + \frac{a_2(\mathbf{x}) + v}{b(\mathbf{x})} \right) + v_1 \right) \\ &= s(-b(\mathbf{x}) ks + a_1(\mathbf{x}) - b(\mathbf{x}) k\lambda_2^T \mathbf{x} - a_2(\mathbf{x}) \\ &\quad + v_1 + b(\mathbf{x}) k\lambda_2^T \mathbf{x}_d - v) \\ &= -b(\mathbf{x}) ks^2\end{aligned}$$

According to the Lyapunov theorem, the result implies that $\lim_{t \rightarrow \infty} s = 0$.

We define the optimal unknown function $u_a^*(\mathbf{x}, v_1, v_2)$ as

$$u_a^*(\mathbf{x}, v_1, v_2) = \frac{a_2(\mathbf{x}) + v(\mathbf{x}, v_1, v_2)}{b(\mathbf{x})}$$

and employ a FLS to estimate the unknown function $u_a^*(\mathbf{x}, v_1, v_2)$ using universal function approximation property of the FLS as follows

$$u = k\lambda^{n-1}e + \hat{u}_a(\eta) \quad (6)$$

where $\hat{u}_a(\eta)$ is the output of the FLS and $\eta \in \mathbf{R}^m, m = n+2$ is the input vector to the FLS defined in the sequel.

3.2 Adaptive Fuzzy System

Brief Explanation of FLS and FBF. The FLS comprises four principle components: fuzzifier, fuzzy rule base, fuzzy inference engine and defuzzifier. Many different choices are available within each block, and in addition, many combinations of these choices can result in a useful subclass of FLSs. The FLSs viewed as nonlinear systems are potential candidates for modeling and control of nonlinear systems. As proved in [1],[2], the FLS has the universal function approximation property. We choose singleton fuzzifier, product inference engine, center-average defuzzifier and the triangular membership function described as

$$A_{i_j}^j(\eta_j, p_{i_j}, q_{i_j}) = \begin{cases} \frac{\eta_j - p_{i_j} + q_{i_j}}{q_{i_j}} & p_{i_j} - q_{i_j} \leq \eta_j < p_{i_j} \\ \frac{-\eta_j + p_{i_j} + q_{i_j}}{q_{i_j}} & p_{i_j} \leq \eta_j < p_{i_j} + q_{i_j} \\ 0 & \text{otherwise} \end{cases}$$

where $j \in \{1, 2, \dots, m\}$. and $i_j \in \{1, 2, \dots, k_j\}$ with k_j being the number of MFs for η_j . The p_{i_j} and q_{i_j} are the center and half width of the triangular MF, respectively.

Lemma 2. *Given $\varepsilon_\delta > 0$, there exists a set of bounded weights θ^* such that the nonlinear function $u_a^*(\mathbf{x}, v_1, v_2)$ can be approximated by a linear in parameters FLS*

$$u_a^*(\mathbf{x}, v_1, v_2) - \theta^{*T} \xi(\eta) = \delta(d, \mathbf{x}, v_1, v_2)$$

where

$$\eta(t) = [y(t) \ y(t-d) \ \dots \ y(t-(n-1)d) \ v_1(t) \ v_2(t)]^T$$

and $d > 0$ is a positive time delay, θ^* is a collection of the optimal fuzzy consequence parameters and $\xi(\eta)$ is a collection of fuzzy basis functions (FBFs),

$$|\delta(d, \mathbf{x}, v_1, v_2)| < \varepsilon_\delta$$

provided $\xi(\eta)$ is a suitable basis of activation functions over R^m .

Proof. Refer to [12].

By this Lemma, the output of the FLS can be written as the linear combination of the FBFs:

$$\hat{u}_a(\eta, \hat{\theta}) = \hat{\theta}^T \xi(\eta) \quad (7)$$

where $\hat{\theta}$ is a collection of the estimated fuzzy consequence parameters. The FLS in the form of (7) is the most frequently used one in control application.

Self-structuring Algorithm. For the FLS (7) to have approximation ability on the entire R^m space an infinite number of MFs and fuzzy rules are required. However, if we use triangular functions as MFs, only some of the fuzzy rules have nonzero values although the FLS has an infinite number of MFs and rules. Based on this fact, we propose a simple self-structuring algorithm as follows.

Step 1: Initially, for the given initial state $\eta_0 = [\eta_{01} \cdots \eta_{0m}]^T$, create two MFs for all $\eta_i, i = 1, \dots, m$ as illustrated in Fig. 1.

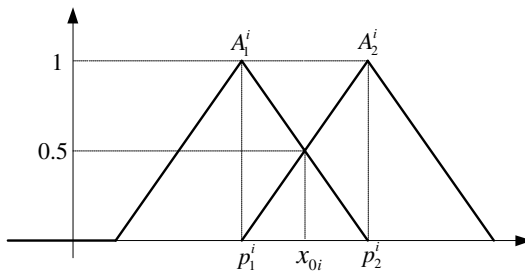


Fig. 1. Create initial MFs

Step 2: Create 2^m fuzzy rules which combine the generated MFs in Step 1 as follows.

- $R_1 : \text{IF } \eta_1 \text{ is } A_1^1, \dots, \text{ and } \eta_m \text{ is } A_1^m$
THEN \hat{u}_a is C_1
- $R_2 : \text{IF } \eta_1 \text{ is } A_1^1, \dots, \text{ and } \eta_m \text{ is } A_2^m$
THEN \hat{u}_a is C_2
- \vdots
- $R_{2^m} : \text{IF } \eta_1 \text{ is } A_2^1, \dots, \text{ and } \eta_m \text{ is } A_2^m$
THEN \hat{u}_a is C_{2^m}

The initial $\hat{\theta}_i$'s where $C_i(\hat{\theta}_i) = 1, i = 1, \dots, 2^m$ are set to zeros. With this FLS, controlling begins.

Step 3: In general, assume that the centers of the left- and right-most MFs of η_i are p_l^i and p_r^i , respectively. If the i th variable η_i moves into the outside of $[p_l^i \ p_r^i]$, create a new MF A_k^i as illustrated in Fig. 2.

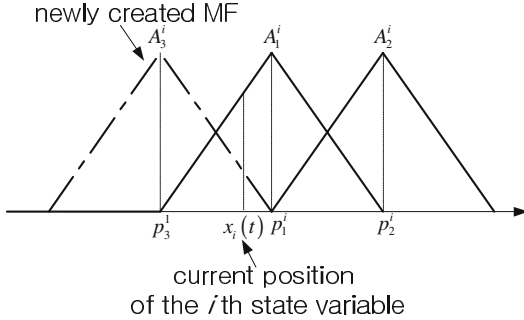


Fig. 2. Create new MF

Step 4: Assume that the other current state variables $\eta_j(t), i \neq j$ are in the range of $[p_{cl}^j \ p_{cr}^j]$ where p_{cl}^j and p_{cr}^j are the centers of the consecutive MFs. If the current number of fuzzy rules are l , 2^{m-1} fuzzy rules are newly added using the MF just created in step 3.

$$\begin{aligned}
 R_{l+1} : & \text{IF } \eta_1 \text{ is } A_{cl}^1, \dots, \text{ and } \eta_j \text{ is } A_k^j \dots \\
 & \quad \text{and } \eta_m \text{ is } A_{cl}^m \text{ THEN } \hat{u}_a \text{ is } C_{l+1} \\
 R_{l+2} : & \text{IF } \eta_1 \text{ is } A_{cl}^1, \dots, \text{ and } \eta_j \text{ is } A_k^j \dots \\
 & \quad \text{and } \eta_m \text{ is } A_{cr}^m \text{ THEN } \hat{u}_a \text{ is } C_{l+2} \\
 & \vdots \\
 R_{l+2^{m-1}} : & \text{IF } \eta_1 \text{ is } A_{cr}^1, \dots, \text{ and } \eta_j \text{ is } A_j^k \dots \\
 & \quad \text{and } \eta_m \text{ is } A_{cr}^m \text{ THEN } \hat{u}_a \text{ is } C_{l+2^{m-1}}
 \end{aligned}$$

The initial $\hat{\theta}_i$'s where $C_{l+j}(\hat{\theta}_i) = 1, j = 1, \dots, 2^{m-1}$ are also set to zeros.

Step 5: Repeat step 3 and step 4.

Using this simple scheme, one could start with a FLS having 2^m rules and gradually increases the number of MFs and fuzzy rules in response to the trajectories of the state variables. One can easily see that with this algorithm, there is the effect that the FLS has an infinitely large structure from the beginning. Note that the output of the FLS at time t consists of the contribution of 2^m fuzzy rules no matter how many fuzzy rules there are.

3.3 Adaptive Law and Stability Analysis

The adaptive law for the estimated parameters of the FLS is determined as the following lemma.

Lemma 3. *The update law for $\hat{\theta}$ is determined as*

$$\dot{\hat{\theta}} = -\gamma \left(e\xi + \sigma(t) |e| \hat{\theta} \right) \quad (8)$$

where γ is the positive learning rate and

$$\sigma(t) = \begin{cases} \frac{b_\xi}{\varepsilon_\theta} & \text{if } |\hat{\theta}| > \varepsilon_\theta \\ 0 & \text{otherwise} \end{cases}$$

with ε_θ is a design constant and $|e| \leq b_\xi$. Then $|\hat{\theta}| \leq \varepsilon_\theta$.

Proof. Consider the Lyapunov function $L_\theta = \frac{1}{2\gamma} \hat{\theta}^T \hat{\theta}$. The time-derivative of the function L_θ along (8) is derived as

$$\begin{aligned} \dot{L}_\theta &= \frac{1}{\gamma} \hat{\theta}^T \dot{\hat{\theta}} \\ &= \hat{\theta}^T \left(-e\xi - \sigma(t) |e| \hat{\theta} \right) \\ &\leq |e| |\hat{\theta}| b_\xi - \sigma(t) |e| |\hat{\theta}|^2 \\ &= -|e| |\hat{\theta}| \left(\sigma(t) |\hat{\theta}| - b_\xi \right) \end{aligned}$$

This leads that if $|\hat{\theta}| > \varepsilon_\theta$ then $\dot{L}_\theta \leq 0$.

Note that the switching function $\sigma(t)$ is adopted so that the FLS can keep the learned information. That is, all the previous update laws for FLS parameters [13], [14], [3], [15], [16], [17], [18] based on σ - or ε -modification of the conventional robust adaptive method [19], although they are adopted for the robustness and stability, lose their information since the updated parameters go to zero as time goes on. This is the serious demerit in the intelligent learning system. However, the adopted switching scheme prevents the information-losing situation if ε_θ is chosen large enough such that $\varepsilon_\theta > |\theta^*|$ while guarantees boundedness of the $|\hat{\theta}|$. Note also that the ε_θ is freely designed constant, that is why we used the ε -denotation.

We are now ready to present our main theorem.

Theorem 1. *Consider the system (1) with the control input (6) with (7). Then, the filetered tracking error s is globally UUB.*

Proof. From (4), the time derivative of the filetered tracking error can be derived as

$$\begin{aligned} \dot{s} &= a_1(\mathbf{x}) - b(\mathbf{x}) u + v_1 \\ &= a_1(\mathbf{x}) - b(\mathbf{x}) u + b(\mathbf{x}) u_a^* - b(\mathbf{x}) u_a^* + v_1 \\ &= -b(\mathbf{x}) u + b(\mathbf{x}) u_a^* + b(\mathbf{x}) k\lambda_2^T \mathbf{x} - b(\mathbf{x}) k\lambda_2^T \mathbf{x}_d \\ &= b(\mathbf{x}) \left(-k\lambda^{n-1} e - \hat{\theta}^T \xi - k\lambda_2^T \mathbf{e} + \hat{u}_a^* + \delta \right) \\ &= b(\mathbf{x}) \left(-ks - \hat{\theta}^T \xi + \delta \right) \end{aligned} \quad (9)$$

where $\tilde{\theta} = \hat{\theta} - \theta^*$. Now, consider the Lyapunov function $L_s = \frac{1}{2}s^2$. The time derivative of L_s along (9) is

$$\begin{aligned}\dot{L}_s &= s\dot{s} \\ &= b(\mathbf{x}) \left(-ks - \tilde{\theta}^T \xi + \delta \right) s \\ &\leq -b(\mathbf{x}) ks^2 + b(\mathbf{x}) (b_{\tilde{\theta}} b_{\xi} + \varepsilon_{\delta}) |s| \\ &\leq -b(\mathbf{x}) ks^2 + b(\mathbf{x}) (b_l^2 + 0.5s^2) \\ &= -b(\mathbf{x}) ((k - 0.5)s^2 - b_l^2)\end{aligned}$$

where $b_{\tilde{\theta}} = \varepsilon_{\theta} + |\theta^*|$, $b_l = b_{\tilde{\theta}} b_{\xi} + \varepsilon_{\delta}$. This means that if $|s| > b_l/\sqrt{k - 0.5}$, then $\dot{L}_s < 0$, that is, the s converges to the compact set

$$\Omega_s = \left\{ s | |s| \leq \frac{b_l}{\sqrt{k - 0.5}} \right\}$$

and the radius of the set can be arbitrary small by choosing sufficiently large k . This completes the proof.

The block diagram of the overall control system is illustrated in Fig. 3.

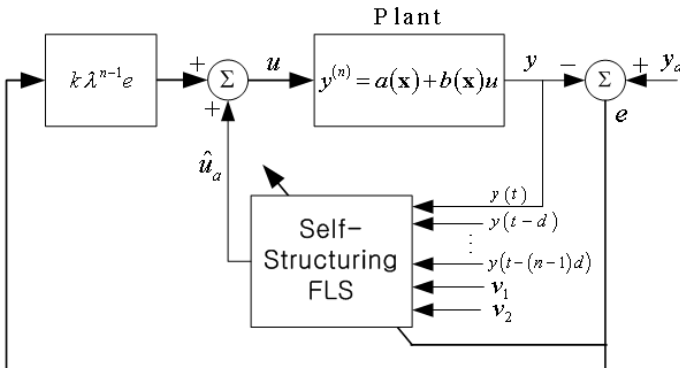


Fig. 3. Overall output-feedback adaptive fuzzy control system

4 Conclusions

This paper proposes a new output-feedback adaptive fuzzy controller for SISO affine nonlinear systems. The previous output-feedback control algorithms are all based on the state observer (e.g., higher-order-observer) or additional low-pass filter to make the estimation error dynamics SPR, which makes the stability analysis of the closed-loop system and real implementation very complicated. The distinguished aspect of the proposed output-feedback control algorithm is that no state observer or low-pass filter is employed. Only the output error is used to generate control input and update laws for unknown fuzzy parameters.

The stability analysis depends heavily on the universal function approximation property of the fuzzy system to estimate unknown function of the desired control input. It is shown that, combining this simple output-feedback control algorithm with an online self-structuring fuzzy system, the Lyapunov stability of the closed-loop system is globally guaranteed.

References

1. L.-X. Wang and J. M. Mendel, "Fuzzy basis functions universal approximation, and orthogonal least-squares learning," *IEEE Trans. Neural Network*, vol. 3, no. 5, pp. 807–814, 1992.
2. J. L. Castro, "Fuzzy logic controllers are universal approximators," *IEEE Trans. System, Man, and Cybernetics*, vol. 25, no. 4, pp. 629–635, 1995.
3. J.-H. Park, and S.-H. Kim, "Direct adaptive output-feedback fuzzy controller for nonaffine nonlinear system," *IEE Proceedings - Control Theory and Applications*, vol. 151, no. 1, pp. 65–72, 2004.
4. S. Tong, H.-H. Li, "Observer-based robust fuzzy control of nonlinear systems with parametric uncertainties," *Fuzzy Sets and Systems*, vol. 131, pp. 165–184, 2002.
5. L. Xiaodong, Z. Qingling, "New approaches to h^∞ controller design based on fuzzy observers for t-s fuzzy systems via lmi," *Automatica*, vol. 39, pp. 1571–1582, 2003.
6. N. Golea, A. Golea, K. Benmohammed, "Stable indirect fuzzy adaptive control," *Fuzzy Sets and Systems*, vol. 137, pp. 353–366, 2003.
7. Y.-G. Leu, T.-T. Lee, and E.-Y. Wang, "Observer-based adaptive fuzzy-neural control for nonlinear dynamical systems," *IEEE Trans. Syst. Man Cybern.-Part B: Cybern.*, vol. 29, no. 5, pp. 583–592, 1999.
8. ——, " h^∞ -observer based adaptive fuzzy-neural control for a class of uncertain nonlinear systems," in *Proceedings of the IEEE International Conference on Syst. Man Cybern.*, 1999, pp. 449–454.
9. Y.-H. Kim, F. L. Lewis, and C. T. Abdalla, "A dynamic recurrent neural-network-based adaptive observer for a class of nonlinear systems," *Automatica*, vol. 33, no. 8, pp. 1539–1543, 1997.
10. J. Y. Choi and J. Farrell, "Observer-based backstepping control using on-line approximation," in *Proceedings of the 1999 IEEE American Control Conference*, 2000, pp. 3646–3650.
11. S. N. Huang, K. K. Tan, and T. H. Lee, "Further results on adaptive control for a class of nonlinear systems using neural networks," *IEEE Trans. Neural Networks*, vol. 14, no. 3, pp. 719–722, 2003.
12. A. J. Calise and N. Hovakimyan and M. Idan, "Adaptive output feedback control of nonlinear systems using neural networks," *Automatica*, vol. 37, no. 1, pp. 1201–1211, 2001.
13. J.-H. Park and G.-T. Park, "Robust adaptive fuzzy controller for nonlinear system using estimation of bounds for approximation errors," *Fuzzy Sets & Systems*, vol. 133, no. 1, pp. 19–36, 2003.
14. ——, "Robust adaptive fuzzy controller for nonaffine nonlinear systems with dynamic rule activation," *Int. J. Robust and Nonlinear Control*, vol. 13, no. 2, pp. 117–139, 2003.
15. W. H. Yoo, "Adaptive fuzzy sliding mode control of nonlinear system," *IEEE Trans. Fuzzy Systems*, vol. 6, no. 2, pp. 315–312, 1998.

16. W.-Y. Wang, M.-L. Chan, C.-C. J. Hsu, and T.-T. Lee, “ h_∞ tracking-based sliding mode control for uncertain nonlinear systems via an adaptive fuzzy-neural approach,” *IEEE Trans. System, Man, and Cybernetics - Part B: Cybernetics*, vol. 32, no. 4, pp. 483–492, 2002.
17. C.-L. Hwang and C.-Y. Kuo, “A stable adaptive fuzzy sliding-mode control for affine nonlinear systems with application to four-bar linkage systems,” *IEEE Trans. Fuzzy Systems*, vol. 9, no. 2, pp. 238–252, 2001.
18. L. K. Wong, H. F. Leung, and P. K. S. Tam,, “A fuzzy sliding controller for nonlinear systems,” *IEEE Trans. Industrial Electronics*, vol. 48, no. 1, pp. 32–37, 2001.
19. P. A. Ioannou and J. Sun, *Robust Adaptive Control*. Englewood Cliffs, NJ:Prentice-Hall, 1996.

High-Speed Extraction Model of Interest Region in the Parcel Image of Large Size

Moon-sung Park¹, Il-sook Kim², Eun-kyung Cho³,
Young-hee Kwon³, and Jong-heung Park¹

¹ ETRI, Postal Technology Research Center, 305-700,
161 Ga-jung-dong Yousung-gu, Daejeon, Korea
{mspark,jpark}@etri.re.kr

² Chungnam National University, 305-764, 220 Gung-dong, Yuseong-gu, Daejeon, Korea
kimis@pcu.ac.kr

³ DaeDuk College, Department of Computer, Internet & Information, 305-715,
48 Jang-dong You-sung-gu Daejeon, Korea
{ekcho,yhkwon}@ddc.ac.kr

Abstract. This paper deals with a model for the high-speed extraction of ROI (Region Of Interest) during the process of logistics transported on conveyor belt. The objective of this paper is to extract various ROIs from large size image of logistics more than 4096 by 4096. For this purpose we propose two algorithms, a PIM (Picture Information Measure) and a Difference Block algorithm, and verified it by the experiments. Our experiments show that the proposed methods extract ROIs nearly 100 percent.

1 ROI Extraction Model

With the development of e-commerce, the volume of off-line logistics is rapidly increasing. So, it is required to develop new technologies for more effective classification and transportation of logistics. Two-dimensional barcode system is essential to provide various value-added services as well as to interpret barcode and to get the information of registered mails (including parcels) after acquiring parcel images[1,2]. In this paper, we propose a high-speed extraction model of the interest regions in large size parcel images by the characteristic examination. It is a preprocessing mechanism in order to extract not only non-uniform patterns of logistics, i.e. edges, label, address, and stamp area, but also uniform patterns such as barcode label area. Our model divides a large size image into smaller units (block), and applies a simple examine method into it so as to eliminate non-interest regions at earlier stage. Then, we divide each block into 4 units and perform the detailed examine methods on it. This model includes a mechanism to get more detailed information of the interested regions, detects wrong extraction region and made adjustment when objects to be extracted exist in the neighbor blocks. For this, we propose two algorithms. One is to use the difference between maximum and minimum value of blocks instead of examining all characteristics of the information. The other is to use the deviation and density information of the extracted blocks (Fig. 1.).

Currently, since the transporting speed of parcels is 6,500 parcels per hour, each parcel must be processed within 550ms. Previous research [2] can extract various informations exactly but it requires 900ms for the processing. It takes too much time

at the preprocessing stage. In this paper, we investigate on the image preprocessing method and the extraction of the candidate regions by the characteristics examination with the two-dimensional barcode.

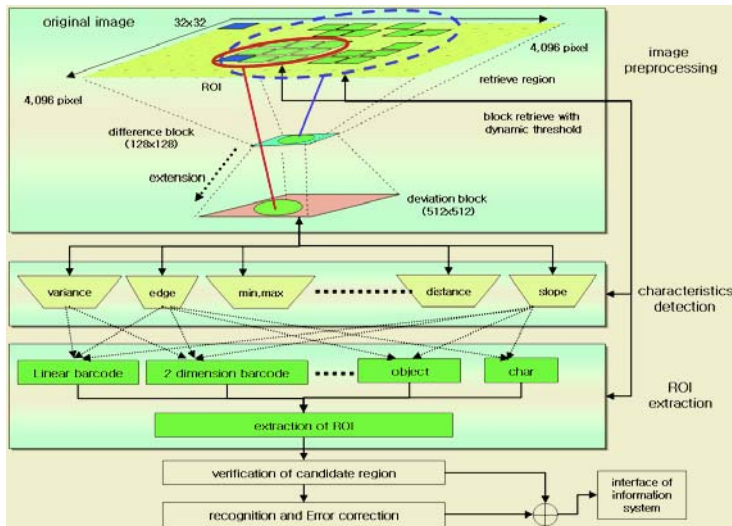


Fig. 1. Diagram for ROI Extraction

2 Preprocessing for Parcel Images

To minimize the preprocessing time, we propose a PIM (Picture Information Measure) and a difference block algorithm which use the difference between maximum and minimum value of block. The procedures and results of these two algorithms are explained in this section.

2.1 PIM (Picture Information Measure)

We propose a block examination method which can be extended to consider 512 by 512 blocks so as to improve the accuracy of ROI (region of interest) extraction at the preprocessing stage. At first, we need to set an optimal threshold value for the inspection of all blocks. For this, we extend "PIM" algorithm proposed by S-K Chang[3] because it doesn't consider spatial structure as a traditional quantitative metric. In this paper, we compute the entropy between pixels to get the characteristics of image data's and apply the PIM extension for the quantization of block images. The value of PIM is computed by subtracting the total number of pixels in blocks from the maximum histogram value. The equation for the PIM computation is as following (1).

$$PIM(f) = \sum_{i=0}^{L-1} h(i) - \max_i h(i) \quad , \quad i = \{0, \dots, L-1\} \quad (1)$$

$h(i)$: the number of pixels of the gray level i in a block.

When the histogram of entroypy has a broad range of values, the standard deviation value becomes large. Also when an image consists of relatively simple blocks,

the mean value of PIM becomes small. We can classify images by PIM values and can compute PIM by reducing quantization level. We get the information of entire areas after computing the mean and standard deviation value of blocks. After computing a PIM value for each block, we take blocks with higher entropy values. In other words, we exclude blocks with lower entropy value.

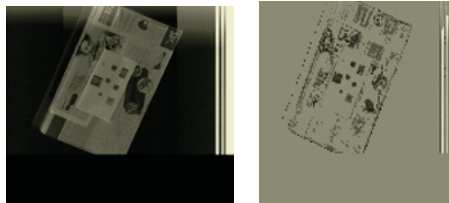


Fig. 2. Original image and the image applied PIM block

By applying above methods, we can extract the boundary area between parcels and the belt surface of conveyor. However, the accuracy of the extraction area mainly depends on the selection of high and low entropy values. So, it is required to get and to set the optimal values for the environments where images are acquired.

2.2 The Extraction of Difference Block

The processing time for the PIM requires 160ms to eliminate noninterest regions. In this subsection, we propose a method to reduce candidate regions for the examination. This method has 128 by 128 blocks, computes the difference between maximum and minimum value and eliminates blocks with lower difference values. The difference of block i , $diff_i$, is computed as shown in Equation (2).

$$diff_i = max_i - min_i \quad (2)$$

max_i : max value of i -th block, min_i : min value of i -th block

$$diff_{threshold} = LowDynamic_{threshold} = 0.3633(max_i - min_i) \cdot diff_i \geq diff_{threshold} \quad (3)$$

The low dynamic threshold value is equal to $diff_{threshold}$. The condition for $diff_{threshold}$ computation is same as that of low value computation in the blocks where the image signal transition from low to high is occurred. Since all blocks where black color turn to white color need not be considered for the examination, we examine lines with two or three pixel units (Equation (4)).

$$diff_i(max_i, min_i) = \sum_x^{32} \sum_{y=2}^{32-2} f_i(x, y) \quad (4)$$

Let $f_i(x, y)$ denote the pixel value for a coordinate (x, y) . The value of Equation (4) is same as that of Equation (3).

Even when y value is examined by three pixel line units, the result is also same. So, we apply Equation (4) in order to reduce the computational complexity in larger size images. As shown in Fig. 3, we can eliminate noninterest regions when we choose blocks whose value is larger than the minimum dynamic threshold value.

**Fig. 3.** Original and Block Image

3 Preprocessing for High-Speed ROI Extraction

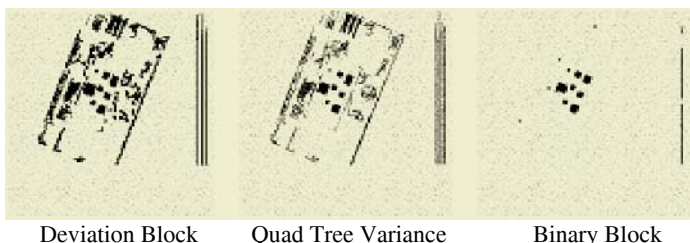
In this section, we explain methods to get the accurate information of ROI from the preprocessing result.

3.1 Barcode ROI Extraction with PIM

After the preprocessing with PIM, the characteristics examination is performed on the ROI candidate regions. This examination takes the following steps. ① ROI is extended 8-neighbor so as to avoid the elimination of blocks to be extracted. ② since a barcode region has a pattern of a series of black and white color, it will have large variation values (Equation (5)).

$$\text{BlockMean} = \frac{1}{M \times N} \sum_{x=0}^{M-1} \sum_{y=0}^{N-1} P(x, y), \quad \text{Variance} = \frac{1}{M \times N} \sum_{x=0}^{M-1} \sum_{y=0}^{N-1} (P(x, y) - \text{BlockMean})^2 \quad (5)$$

M: the length of block, N: height of block P: actual value of pixel,
BlockMean: mean value of block, Variance: variance of block

**Fig. 4.** The results of PIM based ROI Block Extraction at each stage

A block turns into a binary block image by whether its variance value is above dynamic threshold or not. With this, the size of ROI block is reduced into 1/4. By applying this process iteratively, the size of ROI is continuously reduced. ③ In binary coded areas, we extract block areas, compute the distance between pixels and get the directional information with the labeling. Also, the number of ROI is scanned in cross(+) type, count the maximum number of ROIs sequentially arranged at x and y axis, and excludes ROIs with lower value than dynamic thresholding value. ④ perform the projection with directional information as the verification of barcode area.

3.2 ROI Extraction Using Diff

As explained in the previous subsection, it requires a lot of time to extract barcode region and to read it. In this paper, we apply a mechanism to reduce the processing time for the proposed PIM and Difference block algorithm. The main computation complexity caused by the variance and mean computation, quad tree deviation computation, and ROI extraction after it is coded with binary value. These computation time should be minimized to improve the efficiency of the algorithms. For this, we divide a 32 by 32 pixel block into 8 by 8 pixel units and compute a standard deviation of j-th block as shown in Equation (6). Let $f_j(x,y)$ denote j-th image pixel in 8 by 8 pixels. This is to fix the minimum size of block instead of reducing sizes iteratively.

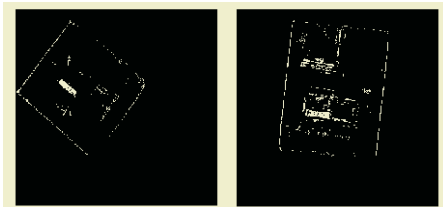
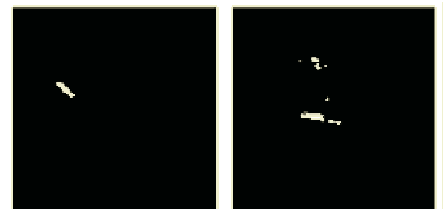
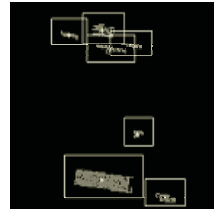
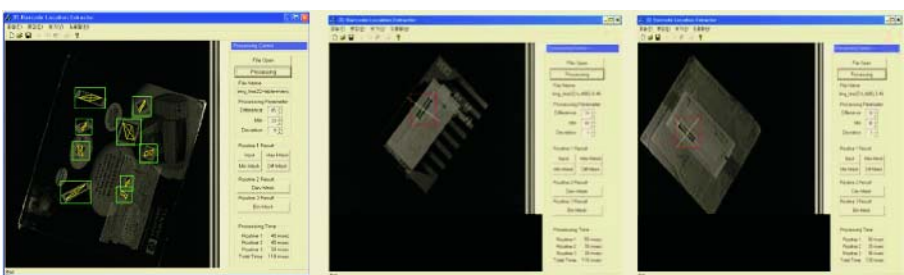
$$\text{mean}_j = \frac{1}{64} \sum_{x=0}^{M-1N-1} \sum_{y=0}^{N-1} f_j(x,y), \quad \text{dev}_j = \frac{1}{64} \sum_{x=0}^{M-1N-1} \sum_{y=0}^{N-1} |f_j(x,y) - \text{mean}_j| \quad (6)$$

And, the value $\text{diff}_{\text{threshold}}$ is set to the value of deviation ROI of j-th block if $\text{dev}_j \geq \text{LowDynamic}_{\text{threshold}}$ so as to apply the minimum dynamic thresholding.

The deviation ROI block contains more accurate barcode candidate regions but still left the boundary and letter regions too (Fig. 5). We divide the deviation block into 4 by 4 block and examine it for the elimination of non-interest regions and the reduction of labeling computation time. The block examination method is to draw cross-shaped(+) lines with 5 block, and excludes blocks which aren't arranged more than four blocks sequentially in each width, length and height. This replaces 512 by 512 blocks with 128 by 128 blocks. Since the size of each block is reduced, thus the processing time can also be reduced with binary ROI blocks. Compute the maximum length and width of ROIs. When this value is larger than one, this indicates that there exist some objects in the area. So, this is marked as ROI in 128 by 128 ROI blocks. By applying this process, most boundary areas and letters can be erased(Fig. 6).

Even though most noisy areas are erased in binary ROI block, some noisy areas may still exist when the distance between ROI block is too far and ROI is extracted with line type. For these, ① when a block is isolated, it should be eliminated in ROI. For this, first ROI 4-neighbor is checked and we exclude it in ROI blocks if there is no connectivity. ② For the elimination of the line shaped areas, we check 8-neighbor, and eliminate it if there is no connectivity. If the connectivity is 1, then it should be eliminated after performing 8-neighbor checks in neighboring blocks. ③ If the connectivity is two, we eliminate it since it is considered as salient part of ROI. The results after performing the above conditions are shown in Fig. 7. With these results, each center point and outer box is computed for each labeling areas.

For each center point, the center seed point can be computed for the region filling for the later steps from the deviation block. To deal with the empty areas in deviation blocks, the marked area of the deviation block which is get from a 3 by 3 pixel area of the center point is set to the connection point of the center coordination. The center seed point and coordination of outer boxes is necessary for the region filling of 4-neighbor blocks. The value used for filling in same area is the binary block label. As a result, we get the region filling ROI block. Fig. 8 shows the base axis and center axis computed from an actual image by applying the mechanism explained here.

**Fig. 5.** The difference of ROI block**Fig. 6.** Block of binary ROI**Fig. 7.** After noisy elimination of binary ROI block**Fig. 8.** Extracted Center point and outer box**Fig. 9.** ROI extraction results of two-dimensional barcode

4 Analysis

For the analysis of high-speed ROI extraction algorithm proposed in this paper, we perform experiments with actual parcels. For our experiments, we design 150 parcels and analyze the results. In experiments, we applied all information extracted from the surface of parcels. Also, we attach barcodes by considering the complexity of the parcel surface. As shown in Table 1, the Difference block method reduces about 163.73msec~522msec compare to PIM for ROI extraction.

Even though the maximum size of parcels is used and some complex information exist on parcel surface in our experiments, the extraction time for two-dimensional barcode and outer boundary extraction of parcels is done within 160msec~190msec. We also observed that the barcode decoding can be done within 10~20msec. This means that up to 18,000 parcels per hour can be processed since only 200 msec is required for the processing of each parcel.

Table 1. The processing time of PIM and Diff Method

| ROI extraction method | | processing time (msec) | | | |
|------------------------------|--------------------------|------------------------|---------|--------------|----------|
| | | PIM average | PIM max | Diff average | Diff max |
| PIM deviation, mean | Diff(max, min) | 106 | 160 | 29.27 | 36.02 |
| quad tree variance deviation | | 59.63 | 90 | | |
| Binarization labeling | 1 st labeling | 115.5 | 220 | 38.99 | 55.7 |
| | region filling | 59.63 | 90 | 17.25 | 25.56 |
| | 2 nd labeling | 91.5 | 150 | 11.31 | 16.25 |
| extraction of object edge | | 1.58 | 1.74 | 2.87 | 5.2 |
| | | | | 8.6 | 13 |
| total processing time | | 433.84 | 711.74 | 109.87 | 154.22 |

5 Conclusions

In this paper, we investigate on the high-speed ROI extraction mechanism in large size parcel images. For this, we propose a block based characteristic examination method. This is useful when the size of image is large and the density of interest region is high. However, the problem of the extraction of regions similar to barcode regions, of the distortion of barcode image, region adjustment for irregular diffused reflection, linear and two-dimensional barcode decoding, the label extraction and high-speed address extraction without labels is left for the future research areas.

References

1. Korea Post, "2001 Annual Report on Postal Service," consulted <http://www.koreapost.go.kr>.
2. Moon-sung Park, Il-sook Kim, Eun-kyoung Cho, Young-hee Kwon, "High Speed Extraction Model of ROI for Automatic Logistics System," Neural Information Processing 11th International Conference ICONIP 2004, LNCS Vol. 3316, pp.706-713, 2004. 11. 8.
3. Shi-Kuo Chang, "Principles pictorial Information Systems Design," Prentice-Hall, pp.43-81, 1996.
4. R. C. Gonzalez and R. E. Woods, "Digital Image Processing," Prentice Hall, 2002.
5. Jae-Beom Lee, Ju-Hyun Park, Hyuk-Jae Lee, and Woo-Chan Lee, "Error Concealment Based on Semantic Prioritization with Hardware-Based Face Tracking," ETRI Journal, vol.26, no.6, pp.535-544, Dec. 2004.
6. Jae-Gon Kim, Hyun Sung Chang, Jinwoong Kim, and Hyung-Myung Kim, "Threshold-Based Camera Motion Characterization of MPEG Video," ETRI Journal, vol.26, no.3, pp.269-272, June 2004.

Using Interval Singleton Type 2 Fuzzy Logic System in Corrupted Time Series Modelling

Dong-Won Kim and Gwi-Tae Park*

Department of Electrical Engineering, Korea University,
1, 5-ka, Anam-dong, Seongbuk-ku, Seoul 136-701, Korea
{upground, gtpark}@korea.ac.kr

Abstract. This paper is focused on modelling of time series data which are corrupted by noise using type 2 fuzzy logic system (FLS). Type 2 FLS in which premise or consequent membership functions are type-2 fuzzy sets, can handle rule uncertainties. Type-2 FLS is very similar to a type-1 FLS, the major structural difference being that the defuzzifier block of a type-1 FLS is replaced by the output processing block in a type-2 FLS. That block consists of type-reduction followed by defuzzification. In the simulation results, Box-Jenkin's gas furnace time series will be demonstrated and we also compare the results of the type-2 fuzzy logic approach with the results of using only a traditional type-1 fuzzy logic approach.

1 Introduction

It is obvious that forecasting activities play an important role in our daily life. We usually forecast many things concerned with our daily life, such as the economy, stock market, population growth, weather, etc. Forecasting with 100% accuracy may be impossible, but we can do our best to reduce forecasting errors [1]. Many techniques for time-series analysis have been developed assuming linear relationships among the series variables. Unfortunately, many real-world applications involve nonlinearities between environmental variables [2]. In addition, we can rarely avoid uncertainty. At the empirical level, uncertainty is an inseparable companion of almost any measurement, resulting from a combination of inevitable measurement errors and resolution limits of measuring instruments [3]. When training data is corrupted by measurement noise, uncertainty can occur. To handle these uncertainties directly, type-2 fuzzy logic system (FLS) is introduced [4-5]. The concept of a type-2 fuzzy set was introduced by Zadeh as an extension of the concept of an ordinary fuzzy set (henceforth called a type-1 fuzzy set) [6]. Type-2 fuzzy sets have grades of membership that are type-1 fuzzy sets. A type-2 membership grade can be any subset in $[0,1]$ -the primary membership; and, corresponding to each primary membership, there is a secondary membership (which can also be in $[0,1]$) that defines the possibilities for the primary membership. A type-1 fuzzy set is a special case of a type-2 fuzzy set; its secondary membership function is a subset with only one element-unity. They are very useful in circumstances where it is difficult to determine an exact membership function for a fuzzy set; hence, they are useful for incorporating uncertainties. Type-2 fuzzy sets and FLS have already been used successfully in a variety of applica-

* Corresponding author

tions [7]. However, there still exist other applications not yet evaluated. Investigating applicability of the type-2 fuzzy logic system to noisy time series data modelling is highly demanded.

In this study, interval singleton type-2 fuzzy logic system [8] is first applied to model noisy Box-Jenkin's gas furnace data. The well known Box-Jenkin's gas furnace data will be demonstrated to show the performance of the type-2 FLS. We also compare the results of the type-2 approach with the results of using only ordinary fuzzy logic system. Thus it can be considered type-2 approach is much more successful in producing accurate ability of noisy series.

2 Interval Singleton Type 2 Fuzzy Logic System [8]

Since the type-2 fuzzy logic system (FLS) is applied to the Box-Jenkin's gas furnace data, its fundamentals are briefly explained. The detailed descriptions and formulations are can be found in [5]. A general FLS is depicted in Fig. 1. Type-2 FLS is very similar to a type-1 FLS. The major structural difference being that the defuzzifier block of a type-1 FLS is replaced by the output processing block in a type-2 FLS. The block consists of type-reduction followed by defuzzification. Type-2 FLS includes fuzzifier, rule base, fuzzy inference engine, and output processor. The output processor includes type-reducer and defuzzifier; it generates a type-1 fuzzy set output from the type-reducer or a crisp number from the defuzzifier. A type-2 FLS is characterized by IF-THEN rules, but its premise or consequent sets are now type-2 [5].

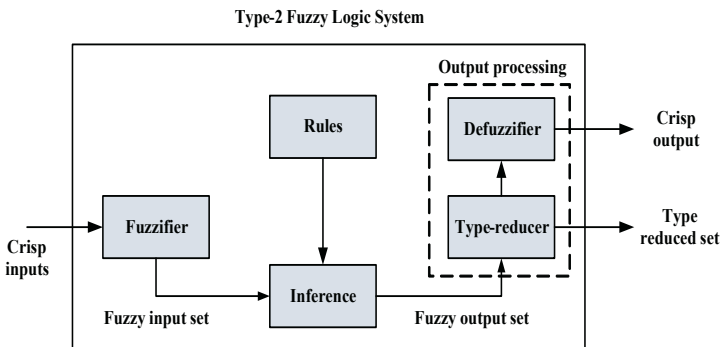


Fig. 1. Structure of type-2 FLS

2.1 Type-2 Membership Functions

When the circumstances are so fuzzy that we have trouble determining the membership grade even as a crisp number in $[0,1]$. Then we use fuzzy sets of type-2, a concept that was first introduced by Zadeh in 1975. Consider the case of a fuzzy set characterized by a Gaussian membership function with mean m and a standard deviation that can take values in $[\sigma_1, \sigma_2]$, i.e.

$$\mu(x) = \exp\left[-\frac{1}{2}\left(\frac{x-m}{\sigma}\right)^2\right] \quad (1)$$

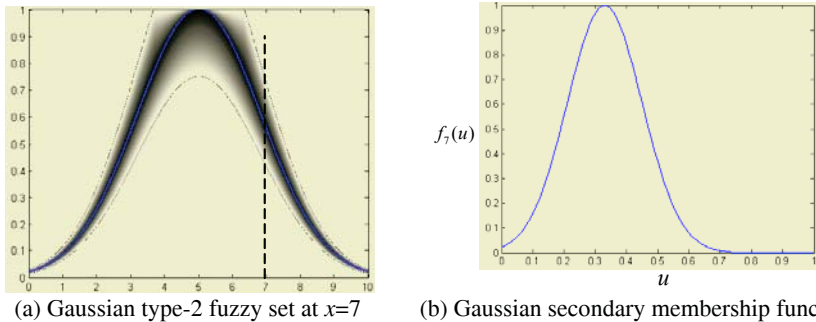


Fig. 2. Gaussian type-2 fuzzy set and secondary membership function. A type-2 fuzzy set represents a type-1 set with uncertain deviation

Corresponding to each values of σ , we will get a different membership curve. So the membership grade of any particular x can take any of a number of possible values depending on the value of σ , i.e. the membership grade is not a crisp number, it is a fuzzy set [9]. Fig. 2 shows the domain of the fuzzy set associated with $x=7$ and its corresponding Gaussian secondary membership function at $x=7$.

Uncertainty in the primary membership grades of a type-2 MF consists of a bounded region, which is called as *footprint of uncertainty* (FOU) of a type-2 MF. It is the union of all primary membership grades. An upper MF and a lower MF are two type-1 MFs which are bounds for the FOU of an interval type-2 MF. The upper MF is a subset which has the maximum membership grade of the FOU and, the lower MF is a subset which has the minimum membership grade of the FOU [5]. General type-2 FLSs are computationally intensive because type-reduction is very intensive. So we employed interval type-2 FLS. When the secondary MFs are interval sets (secondary memberships are either 0 or 1), it is called as interval type-2 FLS.

2.2 Fuzzy Rules

In the type-1 case, we generally have IF-THEN rules of the following form

$$R^l: \text{IF } x_1 \text{ is } F_1^l \text{ and } \dots \text{ and } x_p \text{ is } F_p^l, \text{ THEN } y \text{ is } G_l, l=1,\dots,M$$

Consider a type-2 FLS having p inputs $x_1 \in X_1, \dots, x_p \in X_p$ and one output $y \in Y$. As in the type-1 case, we assume there are M rules, but l th rule has the following form

$$R^l: \text{IF } x_1 \text{ is } \tilde{F}_1^l \text{ and } \dots \text{ and } x_p \text{ is } \tilde{F}_p^l, \text{ THEN } y \text{ is } \tilde{G}_l, l=1,\dots,M$$

This rule represents a type-2 relation between the input space $X_1 \times \dots \times X_p$, and the output space, Y , of the type-2 FLS.

2.3 Fuzzy Inference Engine

In a type-1 FLS the inference engine combines rules and gives a mapping from input type-1 fuzzy sets to output type-1 fuzzy sets. Multiple premise in rules are connected by the t-norm. The membership grades in the input sets are combined with those in

the output sets using the sup-star composition. Multiple rules may be combined using the t-conorm operation or during defuzzification by weighted summation. In type-2 case the inference process is very similar. The inference engine combines rules and gives a mapping from input type-2 fuzzy sets to output type-2 fuzzy sets.

Fig. 3 (a) shows input and premise operations of the interval singleton type-2 FLS for a two premise-single consequent rule, singleton fuzzification, and minimum t-norms. (b) depicts consequent operations for the interval singleton type-2 FLS

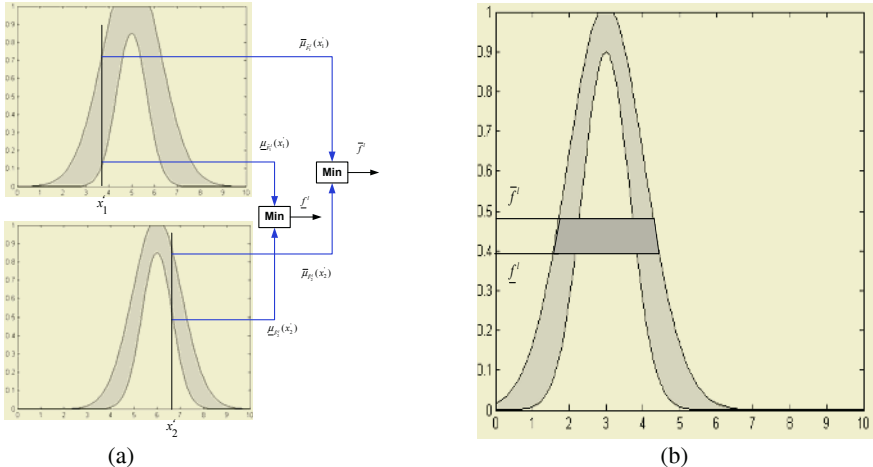


Fig. 3. (a) Input and premise operations and (b) consequent operation for interval singleton type-2 FLS

2.4 Type-Reduction and Defuzzification

In a type-1 fuzzy system, where the output sets are type-1 fuzzy sets, we perform defuzzification in order to get a number, which is in some sense a crisp (type-0) representative of the combined output sets. In the type-2 case, the output sets are type-2; so we have to use extended versions of type-1 defuzzification methods. Since type-1 defuzzification gives a crisp number at the output of the fuzzy system, the extended defuzzification operation in the type-2 case gives a type-1 fuzzy set at the output. Since this operation takes us from the type-2 output sets of the fuzzy system to a type-1 set, we can call this operation type reduction and the type-1 fuzzy set so obtained a type-reduced set. The type-reduced fuzzy set may then be defuzzified to obtain a single crisp number; however, in many applications, the type-reduced set may be more important than a single crisp number. There exist many kinds of type-reduction, such as centroid, center-of-sets, height, and modified height, the detailed descriptions of which are given in [4].

3 Simulation Results

We evaluate the performance of interval singleton type-2 fuzzy logic system applying it to the modelling of noisy Box-Jenkin's gas furnace time series. In addition, we compare the performance of the type-2 FLS with that of singleton FLS.

Box and Jenkin's gas furnace is a famous example of system identification. The well-known Box-Jenkins data set consists of 296 input-output observations, where the input $u(t)$ is the rate of gas flow into a furnace and the output $y(t)$ is the CO_2 concentration in the outlet gases. The delayed terms of $u(t)$ and $y(t)$ such as $u(t-2)$, $u(t-1)$, $y(t-2)$, and $y(t-1)$ are used as input variables to the type-2 FLS. The actual system output $y(t)$ is used as target output variable for this model. The performance index (PI) is defined as the root mean squared error

$$PI = \sqrt{\frac{1}{m} \sum_{i=1}^m (y_i - \hat{y}_i)^2} \quad (2)$$

where y_i is the actual system output, \hat{y}_i is the estimated output of each node, and m is the number of data.

We present the noise-free data which is four input variables of the Box-Jenkin's gas furnace time series in Fig. 4. In the figure, (a) and (b) are the delayed terms of methane gas flow rate $u(t)$ and carbon dioxide density $y(t)$, respectively. But the noise-free signals are corrupted by white Gaussian noise of 5 dB uniformly distributed signal and the corrupted time series in Fig. 5 will be employed as new input variables to the interval singleton type-2 fuzzy logic system.

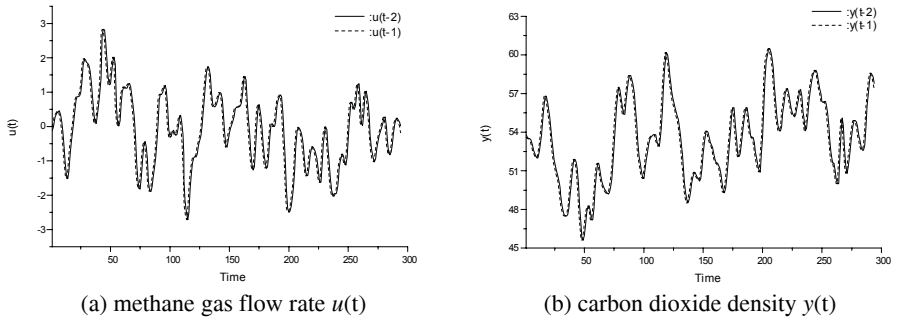
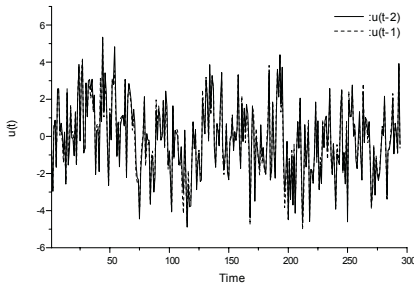
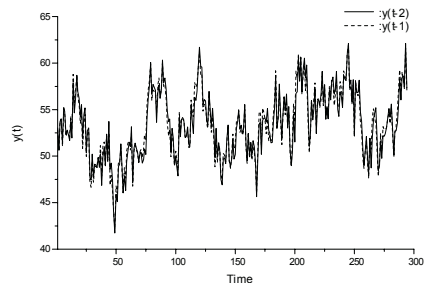
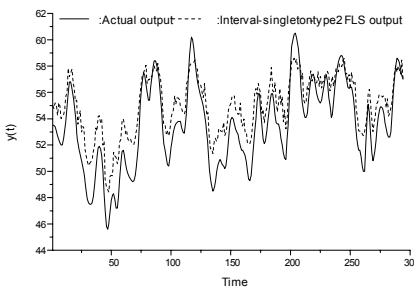


Fig. 4. Noise-free Box-Jenkin's gas furnace time series

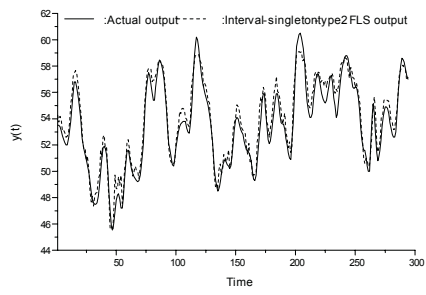
For the simulation, we used four input variables, namely, $u(t-2)$, $u(t-1)$, $y(t-2)$, and $y(t-1)$ and to predict $y(t)$. We also assigned two or three fuzzy sets for each inputs. So the number of fuzzy rules varies from 16 to 36.

Fig. 6 (a) shows the modelling results of the interval singleton type-2 FLS which contains 14 fuzzy rules with two MFs for each input variables. In this case, the value of the PI is 1.9443. When 36 fuzzy rules are assigned for the type 2 FLS, we had $PI=0.8075$. Fig. 6 (b) depicts these modelling results. In this case, two MFs for methane gas flow rate and three MFs for carbon dioxide density are considered. From Fig. 6, we can see that the model output follows the actual output well.

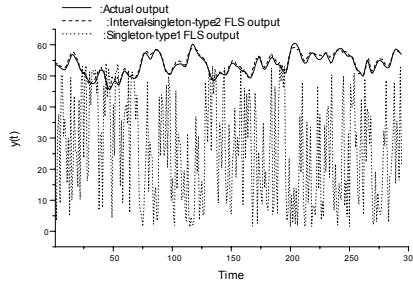
For the comparison results, we employed singleton fuzzy logic system and the results shown in Fig. 7. were obtained by 36 fuzzy rules. In this case, the number of MFs assigned to methane gas flow rate and carbon dioxide density are set to two and three, respectively. As can be seen from Fig. 7, the interval singleton type 2 fuzzy logic system does a much better job of modelling a noisy time series data than does a singleton fuzzy logic system.

(a) corrupted methane gas flow rate $u(t)$ (b) corrupted carbon dioxide density $y(t)$ **Fig. 5.** Noise corrupted Box-Jenkin's time series data to be employed as new input variables

(a)



(b)

Fig. 6. Modelling results of (a) the interval singleton type 2 FLS with 16 fuzzy rules assigned 2 MFs for each inputs and (b) the interval singleton type 2 FLS with 36 fuzzy rules assigned 2 MFs for methane gas flow rate and 3 MFs for carbon dioxide density**Fig. 7.** Comparison results of interval singleton type 2 fuzzy logic system with singleton fuzzy logic system

4 Conclusions

In this paper modelling of corrupted time series data via interval singleton type-2 fuzzy logic system (FLS) is presented. Owing to measurement noise, the data to be employed is corrupted. To handle uncertainty in the noisy data the interval singleton type-2 FLS is applied to the corrupted Box-Jenkin's gas furnace time series data.

Simulation results of the noisy time series are conducted and comparisons with singleton FLS are also given. As a result, the interval singleton type-2 FLS provides a way to handle knowledge uncertainty. But singleton FLS is unable to directly handle these uncertainties. Thus it can be considered type-2 approach does a much better job of modelling a noisy time series and is much more successful in producing accurate ability of noisy series.

References

1. Lin,C. J.: Time-series prediction using adaptive neuro-fuzzy networks. *Int. J. Syst. Sci.* **35**. (2004) 273-286.
2. Sheta, A.F. and Jong, K.D.: Time-series forecasting using GA-tuned radial basis functions. *Inf. Sci.* **133**. (2001). 221-228.
3. Klir, G.J. and Folger, T.A.: *Fuzzy Sets, Uncertainty, and Information*, prentice Hall. Englewood Cliffs. NJ. (1988).
4. Karnik, N.N., Mendel, J.M., and Liang, Q.: Type-2 Fuzzy Logic Systems. *IEEE Trans. Fuzzy Syst.* **7**. (1999). 643-658.
5. Liang, Q. and Mendel, J.M.: Interval Type-2 Fuzzy Logic Systems: Theory and Design. *IEEE Trans. Fuzzy Syst.* **8**. (2000). 535-550.
6. Zadeh, L.A.: The concept of a linguistic variables and its application to approximate reasoning-1. *Inform. Sci.* **8**. (1975). 199-249.
7. Mendel, J.M. and John,R.I.: Type-2 Fuzzy Sets Made Simple. *IEEE Trans. Fuzzy Syst.* vol. **10**. (2002). 117-127.
8. Mendel, J.M.: Computing Derivatives in Interval Type-2 Fuzzy Logic Systems. *IEEE Trans. Fuzzy Syst.* **12**. (2004). 84-98.
9. Castillo, O. and Melin, P.: A new approach for plant monitoring using type-2 fuzzy logic and fractal theory. *Int. J. Gen. Syst.* **33**. (2004). 305-319.

Defining and Detecting Emergence in Complex Networks

Fabio Boschetti¹, Mikhail Prokopenko², Ian Macreadie³, and Anne-Marie Grisogono⁴

¹ CSIRO Marine Research, Floreat, WA, Australia
fabio.boschetti@csiro.au

² CSIRO Information and Communication Technology Centre, North Ryde, NSW, Australia
mikhail.prokopenko@csiro.au

³ CSIRO Health Sciences and Nutrition, Parkville, Victoria, Australia
ian.macreadie@csiro.au

⁴ Defence Science and Technology Organisation, Edinburgh, SA, Australia
Anne-Marie.Grisogono@dsto.defence.gov.au

Abstract. Emergence is seen as the most significant feature discriminating “complex” from “non complex” systems. Nevertheless, no standard definition of emergence is currently available in the literature. This lack of a shared view affects the development of tools to detect and model emergence for both scientific and engineering applications. Here we review some definitions of emergence with the aim to describe how they can be implemented in algorithms to detect and model emergence in sensor and communication networks.

1 Introduction

Complex systems are often defined in the literature as ensembles of a large number of interacting simple entities, which display emergent properties. Such emergent properties are what make such systems “complex”, as well as interesting to study. However, definitions of emergence available in the literature differ considerably in both their philosophical approach and formal rigour. This lack of shared understanding makes communication between scientists and practitioners in Complex System Science difficult, and, worse still, represents an obvious challenge in the development of analytical tools for the formal and experimental study of emergent properties.

There are many reasons why the study of emergence is important. The most obvious is that emergent behaviour seems to be ubiquitous in Nature. And emergence does not seem to arise solely from natural systems: Chaitin [2] shows us how emergent properties can be found also in something as simple and “human-made” as number theory. Another reason why attention is focused on the study of emergence is that standard analytical tools used in physics do not seem to be able to describe the generation of “novelty” [9]. The physics community has long aimed at the discovery of fundamental physical equations able to summarize the inner working of all aspects of Nature, which has been popularized as the quest for a “theory of everything”. This led some authors to claim that the understanding of emergence is a crucial missing component in our understanding of the world [14].

Confident that the study of emergence is a worthwhile endeavour, in this review, we cover some definitions of emergence available in the literature. Our aim is not philosophical, but practical. We do not attempt to suggest a “best” definition, rather we favour definitions leading to the development of numerical/analytical tools enabling formal study and experimentation on emergent properties. Our aim is ultimately towards the many engineering applications which nowadays depend on development of intelligent self-organizing networks in order to tackle problems of increasing complexity and size. In these systems, the desired responses emerge by self-organization: patterns at the global level emerge solely from interactions among the lower-level components acting on rules which are executed using only local information, without reference to the global pattern. In the rest of this paper we ask the following questions:

1. what view of emergence captures the process that we expect will happen in large ensembles of lower-level components like the ones we described above?
2. how would such a view of emergence lead us in the development of useful algorithms/tools to detect and/or model the emergent processes?

2 Some Common Definitions of Emergence

Probably the most common definition of emergence is “a property is emergent if it cannot be explained from the properties and interactions of the lower level entities”. Kubik [11], Shalizi [25] and Crutchfield [3] criticise this definition, mostly on the basis that such definition simply implies that we are currently unable to explain its relation to lower level entities. One day, with better scientific knowledge, we may be able to do so. Consequently such a statement is based on a temporary state of (lack of) knowledge of the observer rather than on an intrinsic property of a system (see the discussion of causation and control in Pattee, [17]).

A slightly more refined version of the above definition reads “a property is emergent if it is not displayed by the lower level entities” Kubic [11] (see also Rosen [23]): “One way to define emergence is to call a behavior of a system emergent when it can no longer be described by the model that described the system until then”). A potential problem with this definition is that basically everything can be seen as emergent according to it. For example, all macroscopic matter is made of atoms, and no individual atoms display the features of the macroscopic material [1]. Arguably, this definition has more appeal than the previous one since it offers itself to numerical analysis. A considerable body of work explores this view of emergence, in particular in the Cellular Automata (CA) literature. For example, the way intrinsic computation may emerge spontaneously and come to dominate the dynamics of physical systems when those systems are in the vicinity of a second-order phase transition has been studied by Langton [13], Mitchell et al. [16] and Wolfram [29], among others. More recently, Wiedermann and van Leeuwen [28] have explored the emergent computation capabilities of large number of interacting agents. They formally prove that their emergent computational power goes beyond traditional systems and results in super Turing computational capabilities.

More formally, Shalizi [25] proposes that “a feature is emergent if it can provide better predictability on the system behaviour, compared to the lower level entities”. Importantly, Shalizi [25] and Crutchfield [3] give a formal, information-theoretic definition of the above concept as well as numerical tools to implement it. Interestingly,

while the idea of predictability naturally involves an agent (observer), the “measure” of emergence they provide is observer independent, and thus an intrinsic property of a system.

We would like to point out, however, that even if such a measure is observer-independent, the observation structure/topology (e.g., the CA itself, a topology of a network, etc.) is provided *a priori*, not necessarily by the “observer”. It can be argued that resultant patterns emerging as a result of observer-independent processes are patterns only with respect to a certain observation structure/topology, imposed on or selected in the environment. An interesting aspect, however, is that the choice of such a structure/topology is not entirely decoupled from the environment. In fact, this choice often depends on the emergent phenomena. So the process can be best characterised in terms of tangled hierarchies exhibiting Strange Loops: “an interaction between levels in which the top level reaches back down towards the bottom level and influences it, while at the same time being itself determined by the bottom level” [8].

This view involves the concept of “downward causation” [1, 6, 7]. Roughly, “a feature is emergent if it has some sort of causal power on lower level entities”. While common views of emergence assume that lower level entities must have an “upward” causation on the emergent features, this approach requires a 2-way causal relation. As an example, we can imagine individuals organising into a community. Their actions affect how the community develops (upward causality) and the development of the community itself affects the behaviour and interaction of the individuals (downward causality). A critique of the concept of downward causation can be found in [17]. This definition has an obvious appeal since it clearly goes beyond the reductionist approach to the analysis of complex system. An application example of this approach is presented by Prokopenko and Wang [20], who demonstrated that self-inspection and self-repair of a sensor and communication network can be described in self-referential terms.

It is our opinion that the last three definitions are particularly suited to study multi-agent engineering systems:

1. Defining emergence as “a property which is not displayed by the lower level entities” provides us with a set of information-theoretic tools for “quick and dirty” detection of emergence.
2. The Computational Mechanics view of emergence as increased predictability on system behavior allows us to focus on a subset of features which carry maximum information about the system. Model reduction and predictability are the sought outcomes.
3. Finally, the concept of “downward causation” seems to aim at a deeper understanding of the system behaviour and its multiscale/multilevel functioning.

In the remainder of the paper we discuss potential tools implementing these ideas in multi-agent systems studies.

3 “Tools” to Detect Emergence

Among the tools useful in an initial, exploratory investigation of the dynamics, or in the subsequent visual representation and description of the dynamics itself, we can point

out the dimensionality-reduction tools such as Self-Organising Maps (SOM), Local Linear Embedding (LLE and its variants), Isomap, etc. The purpose of these tools is to identify low(er) dimensional manifolds in higher dimensional data sets. They are used in visualisation, data compression but also data mining with, potentially, useful application in the study of emergence. Under the assumption that the coordination between lower entities should constrain their behaviour, we may expect emergent features to occupy a lower dimensional state space compared to the uncoordinated dynamics.

Thus, one obvious approach to detect emergence is based on the idea that the complex behaviour of interacting components results in some form of coordination: a persistent multi-agent relationship distinct from both chaotic and completely ordered dynamics. In other words, a departure from randomness, and correlations between components, may be seen as a very first step in the detection of emergent properties. It is thus natural to look at various information-theoretic measures as a basis for the approach.

3.1 Emergent Patterns in Multi-agent Systems: Macro-level

Langton has identified in his seminal work [13] an increase in the mutual information as an indication of a phase transition from “order” to “chaos” in CA. In particular, trajectories of entropy $H(A)$ and mutual information $I(A; B)$ between a cell and itself at the next time-step were obtained while varying the parameter λ — the ratio of cells with a given property. It was observed that the average mutual information has a distinct peak at the transition point. Similarly, a rule-space of 1-dimensional cellular automata was characterised with the Shannon entropy of rules’ frequency distribution [30]. More precisely, given a rule-table (the rules that define a CA), the input-entropy at time step t is defined as

$$S^t = - \sum_{i=1}^m \frac{Q_i^t}{n} \log \frac{Q_i^t}{n},$$

where m is the number of rules, n is the number of cells (system size), and Q_i^t is the number of times the rule i was used at time t across the CA. Wuensche [30] has convincingly demonstrated that only complex dynamics exhibits high variance of input-entropy, leading to automatic classification of the rule-space. Importantly, the peak of input-entropy variance points to a phase transition as well, indicating the edge of chaos (complexity). An information-theoretic approach to quantifying information flows in agent-environment interactions was also constructively used in recent studies of perception-action loops and sensor evolution [10].

It is also well-known that graph connectivity can be analysed in terms of the size of the largest connected subgraph (LCS) and its standard deviation obtained across an ensemble of graphs, as suggested by the random graphs theory [5]. In particular, critical changes occur in connectivity of a directed graph as the number of edges increases: the size of the LCS rapidly increases as well and fills most of the graph, while the variance in the size of the LCS reaches a maximum at some critical point before decreasing. Thus, a graph-theoretic metric based on LCS variance may capture spatial aspects of desired emergent patterns (connectivity), while a metric based on entropy of local agent variables (rules, coordinates, velocities, etc.) may capture temporal persistence of emergent behaviour.

In the context of multi-agent networks it may be possible to unify the information-theoretic and graph-theoretic representations of the metrics. One feasible average measure of a complex network's heterogeneity is given by the entropy of a network defined through the link distribution. The latter can be defined via the simple degree distribution — the probability P_k of having a node with k links, or via the remaining degree distribution [26]. Similarly, one can capture the average uncertainty of the network as a whole, using the joint entropy based on the joint probability of connected pairs $P_{k,k'}$. Ultimately, the amount of correlation between nodes in the graph can be calculated via the mutual information measure, the information transfer, as

$$I(P; P') = H(P) - H(P|P') = \sum_{k=1}^m \sum_{k'=1}^m P_{k,k'} \log \frac{P_{k,k'}}{P_k P_{k'}}.$$

In general, the mutual information $I(P; P')$ is a better, more generic measure of dependence: correlation functions, like the variance in the size of the LCS, “measure linear relations whereas mutual information measures the general dependence and is thus a less biased statistic” [26]. It could be argued that only complex dynamics exhibits high variance, and the peak of this variance would point to a phase transition in connectivity.

The distinction between information-theoretic and graph-theoretic metrics is identified and put to use by Prokopenko et al. [22] in the context of self-organizing sensor and communication networks. These metrics contributed to a specification of various evolvable aspects: temporal persistence and spatial connectivity of emergent task-oriented network's sub-structures [22, 27].

Minati [15] proposes a measure of ergodicity to detect emergence. A system is commonly defined as ergodic when the average, at a single instant of time, on all microscopic behaviors present within the system, is equal to the time average on the behaviour of a single component. This property best describes systems at some form of stable equilibrium which offer themselves naturally to be studied via statistical mechanics tools. Since the property of ergodicity is completely lost during a phase transition, or via structural changes Minati proposes to detect increase of ergodicity as a signature of the evolution towards a new state which may be considered as emergent.

4 Emergence and Predictability: The Computational Mechanics View

Within the Computational Mechanics school, Crutchfield [3] distinguishes pattern formation and intrinsic emergence. Intrinsic emergence refers to the emergent features which are important within the system because they confer additional functionality to the system itself, like supporting global coordination-computation-behaviour (e.g., the emergence of coordinated behaviour in a flock of birds, or in stock market pricing, allows efficient global information processing through local interaction, which benefits each of the individual components of the system).

The algorithmic approach behind the concept of Computational Mechanics [24] is proposed as the main tool in the study of intrinsic emergence, which aims to model the way information is processed within a system. Shalizi [25] formalises this approach by

proposing the following definition: “A derived process is emergent if it has a greater predictive efficiency than the process it derives from”. This definition is interesting since it defines emergence as a property of the system, not of the observer. Also, it offers some specific information-theoretic measures which can be implemented via the machinery of the Computational Mechanics approach. The approach is based on the Causal-State Splitting Reconstruction (CSSR) algorithm [24], which aims to reconstruct the dynamical states of a system and their transition probabilities. Via the use of the algorithm, not only the statistical complexity of the process can be measured, but emergent features (i.e., the ones which maximize predictability potential) can be automatically extracted from the process measurement. The ideas can be applied to both temporal and spatial patterns. Of particular interest is the application of the above concept to the study of the evolutionary emergence of complexity in small population of simple agents and the analysis of the structural hierarchies which allow for self-organisation [4].

5 A First Step Towards Modelling Downward Causation: Emergent Patterns in Multi-agent Communication Space (Micro-level)

Self-organisation may seem to contradict the second law of thermodynamics that captures the tendency of systems to disorder. The “paradox” has been explained in terms of multiple coupled levels of dynamic activity — the Kugler-Turvey model [12] — self-organisation and the loss of entropy occurs at the macro-level, while the system dynamics on the micro-level generates increasing disorder. One convincing example is described by Parunak and Brueckner [18] in the context of pheromone-based coordination. Their work defines a way to measure entropy at the macro level (agents’ behaviours lead to orderly spatiotemporal patterns) and micro level (chaotic diffusion of pheromone molecules). In other words, the micro level serves as an entropy “sink” — it permits the overall system entropy to increase, while allowing self-organisation to emerge and manifest itself as coordinated multi-agent activity on the macro level. Another example relates a macro-level increase of coordination potential within a multi-agent team, indicated by a macro-level decrease in epistemic entropy of agents’ joint beliefs, with a micro-level increase in the entropy of the multi-agent communication space [19].

Similarly, it can be shown that the emergence of multi-agent networks, indicated by the minimal variance of their fragments (an approximation of the network heterogeneity), is explained by increased entropy on a micro-level. This micro-level is the communication space where the inter-agent messages are exchanged [21]. A characterisation of the micro-level (the entropy “sink”) can be obtained if one estimates the “regularity” of the communication space. In summary, macro-level (“global-view”) metrics may capture the quality of the emergent solutions in terms of observable coordination activities, while micro-level metrics may verify the solution in terms of the multi-agent communications.

6 Conclusions

We believe that certain basic emergent properties are shared by very different systems, and hence, steps forward in our understanding and modelling of emergence would have

huge practical implication for disparate applications. With the view of studying large systems of self-organising agents, we have reviewed some definitions of emergence and described how they could lead to useful tools for the detection of emergence, for the identification of features which are maximally informative about the system dynamics (which could lead to model complexity reduction) and to the better understanding of multi-scale and multi-level information processing in complex systems.

References

1. Bickhard, M. H., 2000, Emergence. In P. B. Andersen, C. Emmeche, N. O. Finnemann, P. V. Christiansen (Eds.) *Downward Causation*. (322-348). Aarhus, Denmark: University of Aarhus Press.
2. Chaitin G., Meta Math!, e-book, 2004. (To be published Sept. 2005 by Pantheon Books, NY.) <http://www.cs.auckland.ac.nz/CDMTCS/chaitin/omega.html>
3. Crutchfield J., 1994, The Calculi of Emergence: Computation, Dynamics, and Induction, *Physica D* 75 1994: 11-54.
4. Crutchfield, J., and Gornerup, O., 2004, Objects That Make Objects: The Population Dynamics of Structural Complexity, Santa Fe Institute Working Paper 04-06-020. arxiv.org e-print adap-org/0406XXX.
5. Erdős, P. and Rényi, A., 1961, On the strength of connectedness of random graphs. *Acta Mathematica Scientia*, Hungary, 12, 261-267.
6. Goldstein, J., 2002, The Singular Nature of Emergent Levels: Suggestions for a Theory of Emergence, *Nonlinear Dynamics, Psychology, and Life Sciences* Vol. 6, No. 4.
7. Heylighen, F. 1991, Modelling Emergence, World Futures, *Journal of General Evolution*, special issue on creative evolution, G. Kampis (ed).
8. Hofstadter, D. R., 1989, *Godel, Escher, Bach: An Eternal Golden Braid*. New York: Vintage Books.
9. Hooker, C., 2004, *British Journal for the Philosophy of Science*, September 2004, vol. 55, no. 3, pp. 435-479(45).
10. Klyubin, A. S., Polani, D., and Nehaniv, C. L., 2004, Tracking Information Flow through the Environment: Simple Cases of Stigmergy. In Proceedings of the 9th International Conference on the Simulation and Synthesis of Living Systems (ALIFE9), Boston, USA.
11. Kubic, A., 2003, Toward a Formalization of Emergence, *Artificial Life*, Vol. 9, Issue 1, 41-65.
12. Kugler, P.N., and Turvey, M.T., 1987 *Information, Natural Law, and the Self-Assembly of Rhythmic Movement*. Lawrence Erlbaum.
13. Langton, C., 1991, Life at the Edge of Chaos, Proceedings of the 2nd Conference on Artificial Life.
14. Laughlin R., and Pines, D., 2000, The Theory of Everything, *Proceedings of the National Academy of Science*, Vol. 97, Issue 1, 28-31.
15. Minati G., 2002, Emergence And Ergodicity: A Line Of Research, in Minati G., Pessa E. (eds.), *Emergence in Complex Cognitive, Social and Biological Systems*, Kluwer.
16. Mitchell, M., Crutchfield, J. P., and Das, R., 1998, Evolving cellular automata to perform computations. In T. Back, D. Fogel, and Z. Michalewicz (eds.), *Hand-book of Evolutionary Computation*, Oxford: Oxford University Press.
17. Pattee, H.H., 1997, Causation, Control, and the Evolution of Complexity. In P.B. Anderson, P.V Christiansen, C. Emmeche, and N.O. Finnemann (eds.) *Downward Causation*, in press.
18. Parunak, H.V.D., and Brueckner, S., 2001, Entropy and self-organization in multi-agent systems. In Proceedings of the 5th International Conference on Autonomous agents, Montreal.

19. Prokopenko, M., and Wang, P., 2004, Evaluating Team Performance at the Edge of Chaos. In Polani, D., Browning, B., Bonarini, A., and Yoshida, K. (eds.), *RoboCup 2003: Robot Soccer World Cup VII*, LNCS 3020, 89–101, Springer.
20. Prokopenko, M., and Wang, P., 2004, On Self-referential Shape Replication in Robust Aerospace Vehicles. In Proceedings of the 9th International Conference on the Simulation and Synthesis of Living Systems (ALIFE9), Boston, USA.
21. Prokopenko, M., Wang, P., Price, D., 2005, Complexity Metrics for Self-monitoring Impact Sensing Networks. Accepted by 2005 NASA/DoD Conference on Evolvable Hardware, Washington, D.C., USA.
22. Prokopenko, M., Wang, P., Price, D. C., Valencia, P., Foreman, M., Farmer, A. J., 2005, Self-organizing Hierarchies in Sensor and Communication Networks. Accepted by *Artificial Life Journal*, Special Issue on Dynamic Hierarchies, to appear.
23. Rosen, R., 1985, *Anticipatory Systems*. Pergamon Press.
24. Shalizi, C., Shalizi, K., Crutchfield, J., 2003, An Algorithm for Pattern Discovery in Time Series, *Journal of Machine Learning Research*.
25. Shalizi, C., 2001, *Causal Architecture, Complexity and Self-Organization in Time Series and Cellular Automata*, PhD Thesis, (<http://www.csics.umich.edu/~crshalizi/thesis/>).
26. Solé, R.V., and Valverde, S., 2004, Information theory of complex networks: On evolution and architectural constraints. In E. Ben-Naim, H. Frauenfelder, and Z. Toroczkai (Eds.), *Complex Networks*, Lecture Notes in Physics, Vol. 650, 189–210. Berlin, Germany: Springer-Verlag.
27. Wang, P., and Prokopenko, M., 2004, Evolvable recovery membranes in self-monitoring aerospace vehicles. In Proceedings of the Eighth International Conference on Simulation of Adaptive Behaviour, 509-518, Los Angeles.
28. Wiedermann, J., and van Leeuwen, J., 2003, The Emergent Computational Potential of Evolving Artificial Living Systems, *AI Communications* 15, 205-215.
29. Wolfram, S., 1994, *Cellular Automata and Complexity: Collected Papers*, Reading, MA: Addison-Wesley, 1994.
30. Wuensche, A., 1999, Classifying cellular automata automatically: Finding gliders, filtering, and relating space-time patterns, attractor basins, and the Z parameter. *Complexity*, vol. 4, 3, 47-66.

Annealing Sensor Networks

Andrew Jennings and Daud Channa

Electrical & Computer Engineering School, RMIT University, Melbourne, Australia
ajennings@rmit.edu.au, S3047387@student.rmit.edu.au

Abstract. With a continuing improvement in the capabilities of intelligence per unit of energy, we should reconsider the organisation of sensor networks. We contend that solutions should be model-free, locally based and need to be highly dynamic in nature. Here we propose an approach inspired by simulated annealing. In the context of several application scenarios we explore the potential for adding intelligence to sensor networks.

1 Introduction

Sensor networks [1] are envisioned to become an integral part of our lives. These networks are being applied to provide various tasks such as surveillance and monitoring systems for commercial and military applications. Applications are being developed to gather process and utilize the information from the surrounding environment as required. These requirements have kept challenging researchers in the design of better architectures and protocols for sensor networks. We now have some early deployment of sensor networks, showing that we have successfully established the basic protocols. These follow two main directions: clustering of nodes [2], and synchronised sleep cycle networks with a flatter structure [3]. Now the main challenge is to establish a wide range of application systems. To deploy applications we need methods of coordination that are efficient both in delivering services and conserving energy.

The growth and advancements in technologies and the constant reduction in the size and cost of Micro Electro Mechanical Systems (MEMS) have given rise to a whole new dimension of networking which involves sensors and actuators that are quickly deployable and self organizing. They have resulted in a new dimension in network computing, namely pervasive sensing and control. The ongoing rapid advancements, developments, and research in the sensor and actuator networks only leaves one to foresee that they will soon intervene and associate into all living habitats of humans and their surrounding environment.

In most scenarios the network must be functional over long periods of time, it is crucial for the operation, management and continued lifespan of the network to control the behaviour/reaction of the sensors and actuators to the different occurrences of events in the network. The sensors in these networks are limited in energy, memory and computational facilities, while generally the actuators have an ample supply of resources as their mobility can enable them to recharge thus utilizing their resources to the fullest without energy constraint.

The deployment and maintenance of the nodes must be cost effective, because it will be unfeasible to configure these large networks of small devices. The sensor nodes along with the actuators must be self organizing and provide a means of programming and managing the network as a whole, rather than administering individual nodes and actuators.

2 Status and Scenarios

Although it is not yet clear which applications are viable for sensor networks, we have selected three scenarios to motivate our work. They serve to highlight the issues that we now face. We aim to create solutions for these situations.

2.1 Pedestrian Crossing Guard

We aim to improve the safety of pedestrian crossings using sensor networks. How might we prevent the running down of pedestrians?



Fig. 1. A proposal for an instrumented pedestrian crossing

One possible solution is to use an array of pressure sensors on the roadway surface to detect pedestrians walking. This would be in addition to proximity sensors and visual surveillance [5], as illustrated in Figure 1. Through combination of sensor readings, we can improve the accuracy of recognition. If we want to make use of the sensor readings then we need confidence that there is a low probability of false positives - otherwise car drivers will not accept the system.

With a reliable method of pedestrian detection, we can perhaps move to the next level with these systems. If we can reliably detect a car traveling at a speed likely to result in a collision, then the crossing system can intervene and communicate with the car - potentially it could also override car braking systems. This would bring the car to a halt. We have the possibility of eliminating the possibility of cars contacting pedestrians at crossings. There may also be a role for coordinating with robot teams to enable more active monitoring of pedestrians – here we need development of team behaviour [6]

2.2 Animal Counting

Environmental monitoring was one of the earliest motivations for exploring sensor networks. A typical task is the estimation of animal populations. We would like to know how many of a particular type of animal are within a geographic area. In contrast to urban applications, this setting is very demanding in terms of energy management. Note that the estimation of populations is more difficult than simply tracking animals - we need some confidence of the identity of animals. Is the set of readings for a single animal, or two that are within the same area?

2.3 Perimeter Surveillance

This is a classical application of sensory technology. We have a perimeter that we wish to patrol, with video and movement surveillance. To augment this, we would like to deploy proximity sensors to improve accuracy. These scenarios can give us a framework to consider sensor network application approaches. They provide challenges and a range of difficulties. All are real applications that may have some prospect of widespread deployment. At this stage of development of the field, it is important to focus on feasible applications to focus the research.

3 Energy and Intelligence

One of the central tenets of sensor networks has been the need to keep nodes simple and careful in their use of energy. We could not, for example, implement the full TCP/IP stack on sensor nodes. This would be a waste of energy, since the nature of the communication is quite different.

Progress in battery technology is painful and very slow. But when we consider intelligence per unit of energy, then progress is quite dramatic. So we should be more open to incorporating intelligence in the sensor node, as long as that results in significant energy conservation.

3.1 Local Resolution

One of the original proposals for sensor network protocols was "directed diffusion" (DD) [4]. It is a robust protocol that can work in very tough environments. Even with extensive network breakages, it will continue to operate. As Figure 2 illustrates, "interests" are propagated to areas of the network, and "gradients" are used to reinforce the successful delivery of packets across the network.

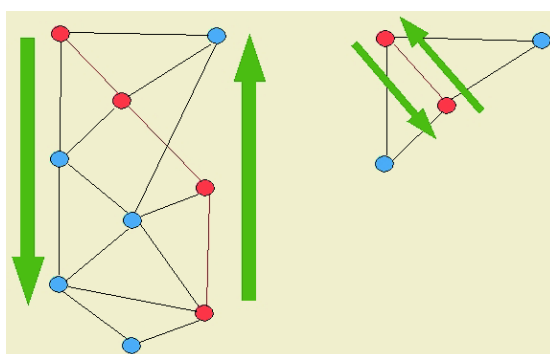


Fig. 2. Directed diffusion (network wide) versus local resolution

Given the constraints placed on directed diffusion, it is an appealing solution. But how might it change if we allowed local processing, rather than propagating results across the broader sensor network? DD assumes that we have to send this outside the sensor network, but with local processing we can avoid the energy consumption of network wide reporting.

This creates both a need for local algorithms that can actually resolve sensor data, and also a means of coordination. There are clear energy advantages in local resolution.

Similar difficulties arise in the location of mobile sensor nodes. The author in [7] has presented the use of simulated annealing for this problem. Here we are concerned with organisation and messaging for fixed nodes.

3.2 Model Based, or Model Free?

If we want to improve monitoring, then perhaps a more accurate model of the context will help? In the case of the pedestrian crossing, we could develop a tracking model. For example, Kalman filtering could aid following an individual through the network. But if we incorporate this model, what will happen in non-modelled cases? How will our model-based approach react when a person falls over, and lies stationary on the crossing? In the worst case, we might decide that the crossing is clear, and let the cars proceed.

Similarly, in surveillance of a perimeter, we might improve accuracy by statistical training to detect people walking across the field. But will we detect somebody crawling across the space?

Once we fix a model for the sensing environment, defining the range of possible targets, then the task of constructing the sensor network is reduced to optimisation. There is no need for further intelligence. So the real challenge for sensor networks is how to deal with unusual data. Consider surveillance when a bunch of leaves falls to the ground. Do we raise an alarm or simply log the event for further processing? If we log it, what priority do we give to the event?

This is a familiar problem in AI, bringing us to the very familiar challenges of semantics. How do we deal with images that do not have familiar content? How can we go beyond simple statistical pattern matching? These are very difficult, but also very important problems.

3.3 Dynamics

Consider the problem of tracking (and identifying) an animal that gives us unusual readings. Perhaps it is of a size that we have not encountered, or it genuinely is a new entry to the region. Clearly this is important, and we would like to track its trajectory. But in order to do this, we need to estimate velocities and alert the relevant part of the sensor network. Once we have lost contact, it will be difficult to sustain the identity. Remember, we are interested in counting animals, so identity is important. Clearly we need application protocols that can deal effectively with highly dynamic situations.

4 Annealing Sensor Networks

The simulated annealing algorithm is a successful method of searching for optimal solutions in complex spaces. Most importantly, it is *model free*: any problem can be formulated as an annealing process. In analogy with the process of annealing crystals, it has an associated temperature. At high temperature, large parameter changes are possible, but as the process cools only smaller changes are possible.



Fig. 3. Activation cycles (sleep cycles) for a single node

We propose an approach to organising sensor networks that is inspired by simulated annealing. Regions have a temperature, which indicates the intensity of sensing. Figure 3 illustrates the sleep cycle of a single node. At a low temperature, the nodes cycle only at A, but as the temperature increases we also cycle at B,C,D progressively. Since these cycles are divisions of the fundamental cycle (the A cycle), these schedules do not conflict.

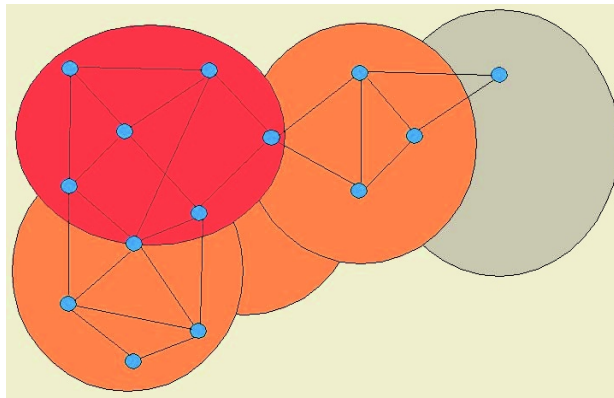


Fig. 4. Network temperature heating process

In the event that a node encounters an unexpected stimulus, it can cause a local rise in temperature. If several nodes in a region send this message, then a rapid rise in local temperature can take place. We can allow this temperature to spread rapidly in space if we desire, or rapidly decay. In accordance with the physical analogy, local heating cannot spread vast distances without decay. Figure 4 illustrates the process.

To effectively make use of annealing sensor networks, we need local resolution of sensor information. For example, in the case of animal tracking, a local decision is needed on the temperature response. Note that an identification is not needed, but only local decision making. We are investigating how to provide this on the typical processors used for sensor nodes. It certainly seems possible to accomplish this computation on the nodes. Of course over time, we can expect the intelligence/energy quotient to continue to grow.

Annealing sensor networks (ASN) are a development of directed diffusion networks. There are some important differences. The adaptive sleep cycle provides for rapid response. Local resolution of control is an important difference. Where directed diffusion incorporates routing, ASN's only advise routing.

5 Discussion

We have proposed an approach to model-free local behaviour for sensor networks. Given that we have no local model of expected behaviour, how can we achieve local

resolution? Each node can keep a statistical database of patterns it has encountered. When patterns within a statistical tolerance appear, this can trigger the appropriate behaviour.

Fully distributed control of sensor networks in this manner raises some important new issues. How do we maintain the currency of statistical data? How can we make changes to behaviour whilst ensuring network stability?

It is interesting that classical problems of semantics come to the forefront when we want to further explore sensor networks. Here the resources we have to bring to the problem are limited. We have an unlimited source of data, through lifelong observation of the world through the network sensors. Potentially we can bring vast computation to the task, through recording and processing offline. But we are limited in human intervention. This leads us to explore computationally intensive approaches. Perhaps we should consider the task as “data mining for sensor organisation methods”.

References

1. Deborah Estrin, Ramesh Govindan, John Heidemann and Satish Kumar “Next Century Challenges: Scalable Coordination in Sensor Networks” *In Proceedings of the Fifth Annual International Conference on Mobile Computing and Networks (MobiCOM '99), August 1999, Seattle, Washington.*
2. Wendi Heinzelman, Anantha Chandrakasan, and Hari Balakrishnan “Energy-Efficient Communication Protocols for Wireless Microsensor Networks”, Proc. Hawaiian Int'l Conf. on Systems Science, January 2000.
3. Wei Ye and John Heidemann and Deborah Estrin “An Energy-Efficient MAC Protocol for Wireless Sensor Networks” *Proceedings 21st International Annual Joint Conference of the IEEE Computer and Communications Societies, 2002*
4. Chalermek Intanagonwiwat, Ramesh Govindan and Deborah Estrin “Directed Diffusion: A Scalable and Robust Communication Paradigm for Sensor Networks” *In Proceedings of the Sixth Annual International Conference on Mobile Computing and Networks (MobiCOM 2000), August 2000, Boston, Massachusetts.*
5. Christian Wohler “Autonomous in situ training of classification modules in real-time vision systems and its application to pedestrian recognition” *Pattern Recognition Letters* Volume 23, Issue 11 Pages: 1263 - 1270 (September 2002)
6. H. Van Dyke Parunak, Sven. A. Bruekner & James Odell “Swarming pattern detection in Sensor and Robot Networks” Altarium Institute, Working Document
7. Martinson E. and Payton D. “Lattice Formation in Mobile Autonomous Sensor Arrays”, HRL Laboratories, LLC. 2003-2004

Measuring Global Behaviour of Multi-agent Systems from Pair-Wise Mutual Information

George Mathews¹, Hugh Durrant-Whyte¹, and Mikhail Prokopenko²

¹ ARC Centre of Excellence for Autonomous Systems
The University of Sydney, Sydney NSW 2006, Australia
g.mathews@cas.edu.au

² CSIRO ICT Centre, Locked Bag 17, North Ryde, NSW 1670, Australia

Abstract. In this paper we present a method for finding general dependencies between individual agents in a multi-agent system. We use mutual information as the general measure for dependence and demonstrate how it can be used to estimate pair-wise coupling in a 2 dimensional swarm. We then show that our technique of measuring local coupling can find phase transitions in the global behaviour of the system.

1 Introduction

When analysing complex multi-agent systems it is often hard to determine which components are coupled via the underlying system dynamics. We present a method of determining general nonlinear correlations between different objects that can be described by a vector of continuous variables. We use this local measure to analyse the global behaviour in a 2D swarm model.

Wright *et al.* showed in [1] that a dynamical systems approach can characterise the global behaviour of a swarm. The technique they developed required knowledge of the global state of the swarm. The technique we propose approaches the problem from an information theoretic perspective and looks for dependencies between the observable states of pairs of agents. The proposed metric captures the spatial and temporal coupling between the motion of the agents through state space. We then show that the mean and variance of these pair-wise dependencies can characterise different behaviours in swarming groups of agents.

The dependencies are measured by estimating their mutual information[2, 3]. Mutual information is introduced in Sect. 2, along with the method used to estimate it. In Sect. 3 we give an example of how mutual information can be used to calculate spatial and temporal coupling in a multi-agent system. In this section we also present a sampling technique to overcome issues such as non-stationarity and finite system run time, that is compatible with the mutual information estimator. We then give our conclusions and future work in Sect. 4.

2 Information Theoretic Measures of Dependence

Information theory provides many measures of dependence. Lets consider two continuous valued random vectors, $\mathbf{x} \in \mathbb{R}^{d_x}$ and $\mathbf{y} \in \mathbb{R}^{d_y}$, with marginal probability density

functions, $p_x(x)$ and $p_y(y)$. The joint probability density function $p_{xy}(x, y)$, defined on the joint space $\mathbb{R}^{d_x d_y}$, is equal to the product of the marginal probability densities iff the two variables are independent. Any differences between $p_{xy}(x, y)$ and $p_x(x)p_y(y)$ are caused by some mutual relationship between the variables. It is here that information theory provides many different methods at comparing two probability density functions. The most common measure is the Kullback-Leibler divergence[3] which corresponds to the Shannon mutual information when the joint probability density is compared to the product of the marginal densities. It is defined as

$$\begin{aligned} I(\mathbf{x}; \mathbf{y}) &= D_{KL}(p_{xy}(x, y) \| p_x(x)p_y(y)) \\ &= \iint p_{xy}(x, y) \log \frac{p_{xy}(x, y)}{p_x(x)p_y(y)} dx dy. \end{aligned} \quad (1)$$

The base of the logarithm determines the units of the measure, for the work that follows we will assume base 2 and hence our mutual information is measured in bits.

2.1 Estimation of Mutual Information

One of the main difficulties with using mutual information (MI), especially in the continuous domain, has been trying to estimate it from sampled data. There are three main approaches used to estimate MI. The most popular are the histogram based methods[4, 5], these partition the continuous state space into a number of *bins*. The probability densities are then estimated by the frequency counts of the bins. These methods often introduce large biases due to the discretisation. Another popular method relies on kernels to estimate the densities. This method is more theoretically sound for a finite number of samples, but relies on many tunable parameters and the final integration (in (1)) can be very difficult to compute. The final method is parametric based, which can only be used if a parametric model of the data already exists.

The method we will use here is most related to the histogram approach in the sense that the probability densities are approximated by sets of piece-wise constants, but it does not rely on specifying a partition on the state space. The MI is estimated by first estimating the marginal and joint differential entropies[2] of the variables

$$\hat{I}(\mathbf{x}; \mathbf{y}) = \hat{H}(\mathbf{y}) + \hat{H}(\mathbf{x}) - \hat{H}(\mathbf{x}, \mathbf{y}) \quad (2)$$

where $\hat{\cdot}$ refers to an estimate. Differential entropy differs from standard entropy since it is defined for continuous probability density functions, i.e.

$$\hat{H}(\mathbf{z}) = - \int p_{\mathbf{z}}(\mathbf{z}) \log p_{\mathbf{z}}(\mathbf{z}) d\mathbf{z}. \quad (3)$$

This corresponds to the marginal entropy if $\mathbf{z} = \mathbf{x}$ or \mathbf{y} and the joint entropy if $\mathbf{z} = [\mathbf{x}, \mathbf{y}]^T$.

2.2 Differential Entropy Estimation

The method used here was developed by Kozachenko and Leonenko in [6]. This method has been reviewed in [7] and extended in [8]. For brevity, the full derivation of the estimator will be omitted, for a detailed proof the reader should see the above references.

It can be seen from (3) that differential entropy is proportional to the average of $\log p_{\mathbf{z}}(\mathbf{z})$, regardless of whether it is a marginal entropy or the joint entropy. Thus for a finite set of independent and identically distributed (i.i.d.) samples, $\{\mathbf{z}_i\}_{i=1}^n$, from $p_{\mathbf{z}}(\mathbf{z})$ we could estimate the entropy if we had an estimator for $\log p_{\mathbf{z}}(\mathbf{z}_i)$ by

$$\hat{H}(\mathbf{z}) = -\frac{1}{n} \sum_{i=1}^n \widehat{\log p_{\mathbf{z}}(\mathbf{z}_i)}. \quad (4)$$

Based on this approach Kozachenko *et al.* proposed the estimator for the differential entropy based on the Euclidian distance, λ_i , between \mathbf{z}_i and its nearest neighbour (i.e. $\lambda_i = \min \|\mathbf{z}_i - \mathbf{z}_j\|, \forall j \neq i$). For a given set of samples in \mathbb{R}^d the estimator is given by

$$\hat{H}(\mathbf{z}) = \frac{d}{n} \sum_{i=1}^n E\{\log \lambda_i\} + \log \left[\frac{S_d(n-1)}{d} \right] + \frac{\gamma}{\ln(2)}. \quad (5)$$

Here, $E\{\log \lambda_i\}$ is the expectation of the logarithm of the distance to \mathbf{z}_i 's nearest neighbour, S_d is the surface area of a unit sphere in d -dimensional space, and γ is the Euler-Mascheroni constant ($= -\int_0^\infty e^{-\nu} \ln \nu d\nu \approx 0.5772156$). In general the surface area can be written as $S_d = \frac{d\pi^{d/2}}{\Gamma(r/2+1)}$ where $\Gamma(\cdot)$ is the gamma function.

The above estimator assumes that the density function is continuous and smooth, such that the density can be approximated by a constant in the vicinity of each sample point. To get a workable estimator a second approximation must be introduced, the expectation will be replaced with the actual observed value, i.e. $E\{\log \lambda_i\} \approx \log \lambda_i$. This estimator can now be used to obtain the marginal and the joint entropies required in (2) to estimate the MI.

3 Detecting Correlations in a Swarm

This section develops a method of using MI for detecting correlations in complex multi-agent systems. The system we will be analysing is a swarm model. We also show that the phase transition found by Wright *et al.* in [1] can also be found by our approach.

3.1 System Description

The system we will consider consists of N agents in \mathbb{R}^2 . The state of agent i is specified by its position, $\mathbf{x}_i = [x_i, y_i]^T$, and velocity, $\dot{\mathbf{x}}_i = [\dot{x}_i, \dot{y}_i]^T$. Each agent has a sensor that can detect the relative position, \mathbf{r}_{ij} , and velocity, $\dot{\mathbf{r}}_{ij}$, of all the other agents that are within its local neighbourhood (i.e. maximum sensor range). The agents also have an actuator that can apply an acceleration to the agent. The actuator is controlled with a onboard controller that takes as inputs the relative position and velocity of all the other observed agents and outputs a required acceleration. The controller implements two behaviours, an attraction/repulsion law (ARL) based purely on the relative positions of the neighbouring agents and a damping law (DL) that is based on the relative velocity between the agent and its neighbours with a magnitude determined by the agents separation.

From these control laws the motion of each agent can be specified as

$$\ddot{\mathbf{x}}_i = \sum_{j \neq i} \mathbf{a}_{ARL}(\mathbf{r}_{ij}) + \sum_{j \neq i} \mathbf{a}_{DL}(\mathbf{r}_{ij}, \dot{\mathbf{r}}_{ij}). \quad (6)$$

The acceleration component from the ARL is directed toward the neighbouring agent j with a magnitude given in Fig. 1. The DL component is defined as $\mathbf{a}_{DL}(\mathbf{r}_{ij}, \dot{\mathbf{r}}_{ij}) = c_{DL}(\|\mathbf{r}_{ij}\|) \times \dot{\mathbf{r}}_{ij}$ where $c_{DL}(\|\mathbf{r}_{ij}\|)$ is a damping coefficient that varies as a function of the separation between agent i and j (see Fig. 1).

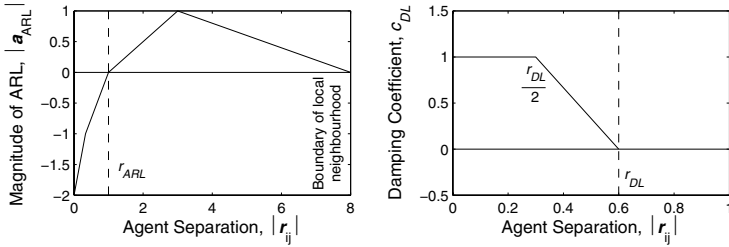


Fig. 1. LEFT: Magnitude of the ARL acceleration as a function of agent separation. RIGHT: Damping coefficient as a function of agent separation. For this current setting $\rho = r_{DL}/r_{ARL} \approx 0.6$

It can be seen from Fig. 1 that the controller is implicitly dependant on the neutral position of the ARL (i.e. r_{ARL}) and on the boundary of the DL (i.e. r_{DL}). If we fix the shape of these curves relative to r_{ARL} and r_{DL} , and scale all the distances by r_{ARL} , the global behaviour of the system can be specified by the single dimensionless parameter $\rho = r_{DL}/r_{ARL}$. Figure 2 shows typical system behaviours for different values of ρ . The system is initialised with a set of random positions and velocities, with all values evenly distributed on the interval $[-1, 1]$. The velocities are then modified such that the mean velocity, v_m , is always constant. This standardises the systems such that quantitative comparisons can be made that depend only on the parameter ρ .

3.2 Defining Correlations in a Multi-agent System

Although a deterministic relationship exists between the full set of agents, we will examine how much coupling exists if we only consider a subset of the agents. The method we will pursue here relies only on drawing samples from the system and can be used for any system that has components with measurable outputs. But, this sampling limits us to only a few dimensions due to the computational complexity of the estimator.

Thus to estimate the dependencies in the system, we will calculate the MI between combinations of two agents and only consider their positions (i.e. ignore their velocities). That is, we want to know how much information is obtained about the position of one agent, $\mathbf{x}_i(t)$, at some unknown time t by knowing the position of another, $\mathbf{x}_j(t)$, at the same unknown time t . i.e. we want to compute

$$I(\mathbf{x}_i(t); \mathbf{x}_j(t)) \text{ for unknown } t \in [0, \infty). \quad (7)$$

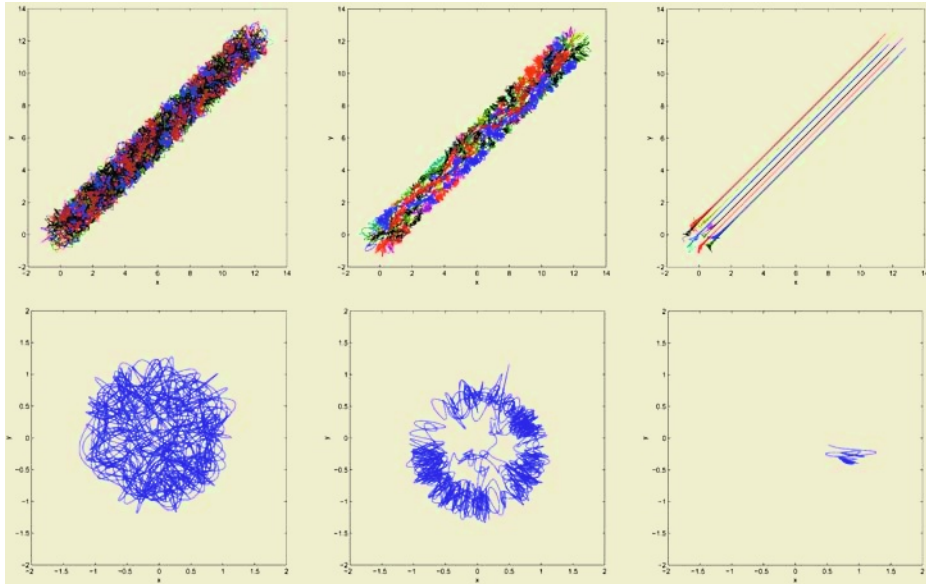


Fig. 2. Example trajectories for different values of ρ . For left frames $\rho = 0.28$, middle frames $\rho = 0.48$, and for right frames $\rho = 0.68$. The top row shows the trajectories of all 10 agents while the bottom shows the trajectory of a single agent relative to the centre of the group

This captures the spatial and temporal correlations between pairs of agents. By computing this for all combinations of agents we can build up a matrix of pair-wise correlations between the agents. This matrix would be similar to the covariance matrix but can be defined for objects that can consist of many variables and represents the total nonlinear dependence and not just linear dependence.

The difficulty in evaluating or estimating (7) comes from the fact that we cannot easily produce i.i.d. samples from the joint and marginal densities from a single instance of the system. This is due to the fact any measurement of the state of the system is highly dependent on the previous measurement. To overcome this, a monte carlo approach could be used to produce samples from many simulations of the system, but this will not be pursued since we cannot preserve the individual agents' identity between simulations and will prevent us from building up a pair wise correlation matrix for the group. Thus a different approach will be pursued that will involve transforming the system into a stationary one where we can draw i.i.d. samples from it and use them to estimate the MI of the original system.

By creating a new coordinate frame centred on the mean position of the agents we can create a quasi-stationary system, in the sense that samples drawn from one instance of the system (i.e. at different times along the transformed trajectory) are representative of all instances of the system for any time. Trajectories from this are shown in the bottom row of Fig. 2. The transformation that produces these trajectories for agent k is

$$\mathbf{y}_k(t) = \mathbf{x}_k(t) - t\mathbf{v}_m \quad (8)$$

where v_m is the mean velocity of the system (which is fixed for all instances of all systems). In this coordinate frame, the probability density for the location y_k of agent k is $p_y(y_k)$ and is independent of time. From this density we can obtain the probability density function of the agent in the original coordinate frame at a specified time t , as $p_x(x_k|t) = p_y(y_k = x_k - tv_m)$. The density of $x_k(t)$ for an unspecified time $t \in [0, \infty]$ can be recovered by noting $p_x(x_k) = \int p_x(x_k|t)p(t)dt$, where $p(t)$ is a uniform distribution on the interval $[0, \infty)$. This gives

$$p_x(x_k) = \lim_{T \rightarrow \infty} \frac{1}{T} \int_0^T p_y(x_k - tv_m) dt. \quad (9)$$

This represents the probability density function for the location, x_k , of agent k for any time $t \in [0, \infty)$ based on the probability density function of the agent's position relative to the centre of the group. We could try to obtain an expression for the MI based on this marginal probability density function (and a corresponding joint probability density function) but this would be impractical due to the limit extending to infinity. We can achieve the same aim (i.e. determining residual dependencies) by dropping the limit and taking it over a finite time horizon. From this theoretical analysis we will develop a method to produce i.i.d. samples from $p_x(x_k)$ by using the trajectories $y_k(t)$.

Due to the quasi-stationarity of the trajectories, samples drawn randomly in time, from a trajectory, $y_k(t)$, can be assumed to be i.i.d. from the density $p_y(y_k)$. These samples also correspond to i.i.d. samples from $p_x(x_k|t=0)$. To obtain samples from $p_x(x_k)$, where t is restricted to $[0, T]$, each sample is projected forward in time by a different random amount, $t^* \in [0, T]$. This projection simply corresponds to translating each sample by t^*v_m .

Hence a sample, x_k^* , from $p_x(x_k)$ can be obtained by a sample, y_k^* , from $p_y(y_k)$ and a time t^* which is a random element of $[0, T]$, via $x_k^* = y_k^* + t^*v_m$. The process is identical for obtaining samples, (x_i^*, x_j^*) , for the joint density, $p_{xx}(x_i, x_j)$, from samples of $p_{yy}(y_i, y_j)$. Thus using these samples, and the method outlined in Sect. 2, we can estimate the mutual information, $I(x_i; x_j)$, between all combinations of agents.

3.3 Results

Results were obtained for values of ρ from 0.2 to 0.8 for systems with 10 agents, with each estimate being produced with 8000 sample points. The results will be presented in two ways, the first will be the mean and variance of the pair-wise correlations. The mean characterises how structured the overall system is, while the variance provides information about sub-structure within the system. These results are shown in Fig. 3.

The second series of results that were obtained are the pair-wise information matrix, which contains the mutual information between all the combinations of agents. Some of these are shown in Fig. 4. The mutual information between an agent and itself has not been calculated and has been set to zero in the figure. It is noted that for small ρ and large ρ the size of the correlations is quite uniform across the system, whereas in between (e.g. for $\rho = 0.64$) the system exhibits large differences between the correlations of the individual agents. This can also be seen in Fig. 3 where the variance of the pair-wise mutual information is also plotted.

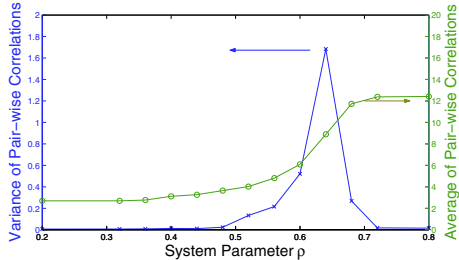


Fig. 3. Average and variance of the pair-wise mutual information for different systems

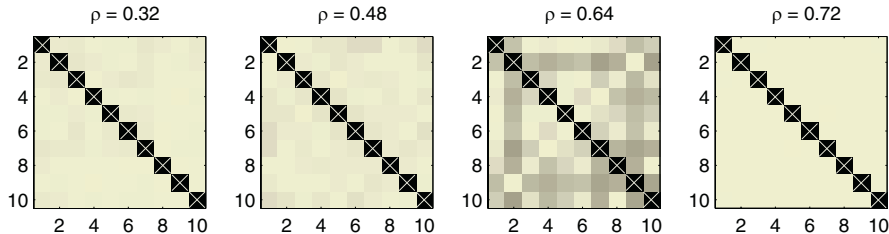


Fig. 4. Typical pair-wise mutual information matrices for different systems. White represents high correlation and black represents low correlation, with all values normalised by the maximum value for that system. The mutual information between an agent and itself has not been calculated

This variations can be explained by looking at the dynamics of the system, for low ρ there is very little coupling between the agents and hence the correlation should be quite low. As the coupling increases (through increasing ρ and hence the damping), the system starts to undergo a phase transition, with local coupling between neighbouring agents. As ρ increases further the oscillations become completely damped out across the whole system and the system becomes globally coupled.

4 Conclusion and Future Work

In this paper we presented a method for finding general correlations between the motion of individual agents in a multi-agent system by estimating the mutual information between them. We showed how this technique can be used to characterise the global behaviour of a simple multi-agent system. The important contribution of the work is to show that the global behaviour of the system can be characterised by examining only local pair-wise coupling. The global phase transition found by Wright *et al.* in [1] was also recognised by our technique.

For future work we hope to examine how this technique handles large systems with many components. For such systems it would be infeasible to calculate all pair-wise correlations, and we propose instead to only calculate the correlations for a subset of all the combinations across the system. We intend to show that this may be sufficient for a characterisation of global multi-agent behaviours.

Acknowledgements

This work is supported in part by the ARC Centre of Excellence programme, funded by the Australian Research Council (ARC) and the New South Wales State Government, and in part by CSIRO Industrial Physics.

References

1. Wright, W.A., Smith, R.E., Danek, M.A., Greenway, P.: A measure of emergence in an adapting, multi-agent context. *Proceedings of the Sixth International Conference on the Simulation of Adaptive Behaviour* (2000) 20–27
2. Cover, T., Thomas, J.: *Elements of Information Theory*. John Wiley (1991)
3. Kapur, J.: *Measures of information and their Application*. John Wiley (1994)
4. Moddemeeijer, R.: On estimation of entropy and mutual information of continuous distributions. *Signal Processing* **16** (1989) 233–248
5. Darbellary, G.: Estimation of the information by an adaptive partitioning of the observation space. *IEEE Transactions on Information Theory* **45** (1999)
6. Kozachenko, L., Leonenko, N.: A statistical estimate for the entropy of a random vector. *Problems of Information Transmission* **23** (1987) 9–16
7. Victor, J.: Binnless strategies for estimation of information from neural data. *Physical Review E* **66** (2002) 051903
8. Kraskov, A., Stogbauer, H., Grassberger, P.: Estimating mutual information. *Physical Review E* **69** (2004) 066138

In Use Parameter Estimation of Inertial Sensors by Detecting Multilevel Quasi-static States

Ashutosh Saxena¹, Gaurav Gupta²,
Vadim Gerasimov³, and Sébastien Ourselin²

¹ Department of Electrical Engineering, Stanford University, USA*
asaxena@stanford.edu

² Autonomous Systems Laboratory, BioMedIA Lab, CSIRO ICT Centre,
PO Box 76, Epping, NSW, Australia
{Gaurav.Gupta,Sebastien.Ourselin}@csiro.au

³ Autonomous Systems Laboratory, CSIRO ICT Centre,
PO Box 76, Epping, NSW, Australia
Vadim.Gerasimov@csiro.au

Abstract. We present an autoadaptive algorithm for in-use parameter estimation of MEMS inertial accelerometers and gyros¹ using multi-level quasi-static states for greater accuracy and reliability. Multi-level quasi-static states are detected robustly using data from both gyros and accelerometers. Proper estimation of time-varying sensor parameters allows us to develop a mixed-reality real-time hand-held orientation tracker with dynamic accuracy of less than 2°. Existing methods like Kalman filters do not take time-varying nature of parameters into account, instead modelling the time-variation as higher values in noise covariance matrices; thus underestimating the sensor capabilities.

1 Introduction

Micro-Electro-Mechanical System (MEMS) based inertial accelerometers and gyros are used in a wide range of applications such as human motion tracking [1] and surgical applications [2] because of their low cost, small size and *sourceless* [3] nature. Veltink *et al.* [4] used uni-axial accelerometers for detecting static and dynamic activities. Detecting levels of activity has been used in many applications like rehabilitation treatment of patients [4] and activity monitoring.

However, accelerometer and gyro based devices suffer from substantial drift due to time-varying nature of bias and other parameters. Recent research has focused on integrating multisensor signals of gyros and accelerometers to estimate orientation [1],[8] using Kalman filters. However, Kalman filtering has a serious drawback of high computational cost, which is unacceptable in some applications that require real-time output or are computationally constrained. Furthermore,

* Ashutosh Saxena was with BioMedia Lab (CSIRO) in 2004, where this work was entirely performed

¹ Gyro stands for gyroscopes, gyrometers, angular rate sensors used in different texts

performance of Kalman filters depend critically on estimating a large number of modelling parameters. Failing to capture the time-varying nature of parameters, they instead overestimate the noise covariance matrices. To capture the time-varying nature of bias, Foxlin [8] used bias values as a part of the state vector of the Kalman filter. In such an algorithm, bias values are re-estimated at every sample, which is inefficient; because bias of the gyro changes slowly and there is no need to re-estimate it so frequently.

We propose a new autoadaptive method to re-estimate and update the sensor parameters while in use, by detecting multi-level quasi-static states for use in a mixed-reality orientation tracking device. We combine data from both tri-axial accelerometers and gyros to robustly detect multi-level quasi-static states, providing the accuracy and reliability needed for its use in parameter estimation, which was not possible by using uni-axial accelerometers alone.

Accurate parameter estimation using multi-level quasi-static states allows the development of a real-time handheld orientation tracker for a mixed reality device used in HMDs (Head Mounted Displays) [1], surgical applications and other applications [10], [11]. The basic goal of this algorithm is to allow the system to automatically adjust to variations in external conditions and sensor parameters. In this work, we present a method of processing signals from tri-axial gyros, accelerometers, and magnetometers to obtain a drift-less and accurate estimate of orientation that is not possible with gyros, accelerometers or magnetometers alone. Bachmann *et al.* [3] has used tri-axial accelerometers as inclinometers on the assumption that magnitude of the kinematic linear acceleration is negligible in comparison to gravity. In this paper, we show that re-estimating the bias in quasi-static states is good enough for accurate orientation tracking. Results of the orientation tracking in a hand-held instrument are also discussed.

2 Modelling of Sensors

We use a sensor model similar to that described in [5]:

$$\mathbf{u}_g = \mathbf{K}_g \cdot \mathbf{R}_g \cdot \boldsymbol{\omega}_s + \mathbf{b}_g \quad (1)$$

$$\mathbf{u}_a = \mathbf{K}_a \cdot \mathbf{R}_a \cdot \mathbf{a}_s + \mathbf{b}_a \quad (2)$$

$$\mathbf{u}_m = \mathbf{K}_m \cdot \mathbf{R}_m \cdot \mathbf{h}_s + \mathbf{b}_m \quad (3)$$

where \mathbf{K}_g is the diagonal matrix for gyro gain, $\boldsymbol{\omega}_s$ is the angular velocity in cartesian coordinates, \mathbf{b}_g is the bias, \mathbf{R}_g is orientation matrix to convert each sensor output to a single cartesian coordinate system, compensating errors due to misalignment. Similar convention follows for accelerometers (eq. (2)) and magnetometers (eq. (3)) respectively.

3 Calibration

3.1 Pre-calibration

Pre-calibration of the sensors is performed once, while manufacturing the device similar to the method described by Ferraris [5], and estimates the sensor param-

eters listed in Sect. 2. The bias and gain of gyros and accelerometers (\mathbf{b}_g , \mathbf{K}_g , \mathbf{b}_a , \mathbf{K}_a) vary with time from the pre-calibrated values because of temperature and other random factors.

3.2 Detecting Quasi-static States

We propose a novel fuzzy algorithm to detect quasi-static states. These states are detected when the sensor signals are changing insignificantly over time. A constant acceleration or an exact cancellation of acceleration is unlikely to happen with typical hand movements [6] because of the physiological constraints, therefore a quasi-static state is a good indicator of the object being at rest. During the static state, the white gaussian noise N_s , for L samples in each of the sensor signals can be estimated (during start-up calibration) as:

$$N_s = \sum_{i=1}^L \frac{s^2[i]}{L} \quad (4)$$

where $s[i]$ is the sensor signal. If the estimated noise is $[N_{gx}, N_{gy}, N_{gz}]$ for gyros and $[N_{ax}, N_{ay}, N_{az}]$ for accelerometers, then the decision rule for static state is:

$$\gamma[j] = \frac{1}{6} \left(\frac{1}{s_{ge}^2} \sum_{q=x,y,z} \frac{s_{gq}^2[j]}{N_{gq}} + \frac{1}{s_{ae}^2} \sum_{q=x,y,z} \frac{s_{aq}^2[j]}{N_{aq}} \right) \quad (5)$$

where s_{ge} and s_{ae} is the expected RMS value of signal during normal device use (for example for gyro it is $60^0/\text{sec}$ and $1\text{m}/\text{s}^2$ for accelerometers). Then γ is low pass filtered (LPF) to get γ_L . This ensures that the static state is of a minimum duration.

$$\gamma_L[i] = LPF\{\gamma[i]\} \quad (6)$$

If $\gamma_L[i] < \text{threshold}$, which can be determined experimentally or dynamically adjusted with a learning algorithm, then it is a quasi-static state. Using multiple threshold levels, we can detect different levels of static states and make a high-level decision for the amount of correction to be made in the parameters. Fig. 1 shows the performance of the quasi-static state detector (with only one sensor signal shown). The graph demonstrates that even when variation in a single sensor is low, other sensors help make an accurate decision for a static state.

3.3 In Use Calibration of Gyros and Accelerometers

In quasi-static state, the calibrated output ω_s ideally should be zero. However, it is not zero because of the time-varying nature of the bias. The change in bias Δb_g is estimated during quasi-static state, and the bias parameter is updated as

$$b_g^{new} = b_g - \Delta b_g \quad (7)$$

The parameters for the accelerometer, like sensitivity and bias, are also re-estimated in static state, similar to the method described in [6].

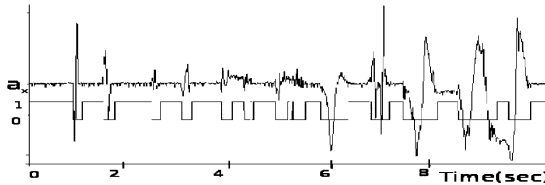


Fig. 1. Output of Quasi-Static State detector shown with x-axis acceleration along with digital static state graph. Digital 1 means quasi-static while 0 means not. The detector detects static states robustly because it combines information from all the sensors

4 Orientation Estimate Using Multi-level Quasi-static States

4.1 Algorithm

Block diagram of the system for estimating the orientation is shown in Fig. 2. The sensor data is calibrated and processed to get orientation and acceleration in the body frame. We define two levels of static state: (A) *Quasi-Static*: when device is almost static, and (B) *Semi-Static*: when the device is moving very slowly, detected as described in Sect. 3.2. In the quasi-static state, we re-calibrate the sensors as described in Sect. 3.3, and in semi-static state we correct the orientation for drift using information from accelerometers and magnetometers.

In our ongoing research, we are developing algorithms to determine position from accelerometers. This involves obtaining kinematic linear acceleration (acceleration without gravity). Since accelerometers measure acceleration plus gravity, orientation information is needed to subtract gravity vector from the acceleration signals. An error of $\delta\theta$ results in an error of $g \sin \delta\theta$ in the acceleration components, creating a false horizontal acceleration in the output of the inertial navigator [1], making position error unbounded because of double integration involved in the filters. Therefore accurate estimation of orientation is essential.

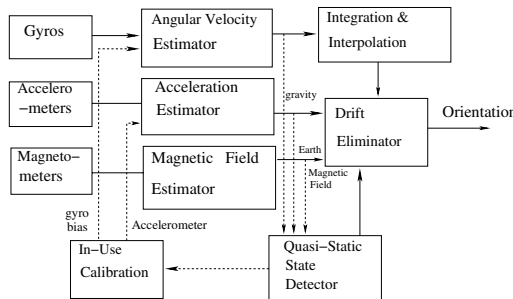


Fig. 2. Block diagram for calculating orientation. *Static-State Detector* signals the *In-Use Calibrator* to re-estimate parameters, and *Drift Eliminator* to correct for gyro drifts using information from accelerometers and magnetometers

4.2 Orientation from Gyros

The angular velocity is filtered and then integrated to get the change in angles, relative to the local axis. The evolution of $\theta(t)$ for δt is approximated by Taylor series expansion [8] and for first order integration the error rate is $\frac{1}{2}\omega^2\delta t$, about $0.54^\circ/\text{sec}$ (for 100Hz sampling rate and typical $60^\circ/\text{sec}$ angular velocity). This approximation is valid because performance is limited by the cumulative errors because of the integration of the time-varying bias in the angular velocities. We focus on correcting this error by an accurate estimate of bias during in-use calibration of gyros and correction by accelerometer and magnetometer data.

4.3 Orientation Correction Using Accelerometers and Magnetometers

In semi-static state, there is no significant kinematic linear acceleration, and the signal from the accelerometers can be used as inclinometers giving the gravity vector in local coordinates. Orientation error due to drift in parameters of gyros, is corrected by determining the absolute orientation from the gravity vector and earth's magnetic field \mathbf{H} as the reference. The magnetometers give \mathbf{H} which maintains a fixed value and direction in absence of magnetic disturbance; this can be detected [7]. Let $\hat{\mathbf{g}} = \frac{\mathbf{g}}{|\mathbf{g}|}$ be the unit vector of gravity, and $\hat{\mathbf{H}} = \frac{\mathbf{H}}{|\mathbf{H}|}$ be the unit vector of the earth's magnetic field. Let $\hat{\mathbf{v}} = \mathbf{g} * \mathbf{H}$ be the unit vector perpendicular to both of them. Let $(\sigma_0, \mu_0, \tau_0)$ represent reference coordinate frame (initial starting position) and $(\sigma_1, \mu_1, \tau_1)$ represent the coordinate frame of rotated local body frame. Then, in reference frame, the unit vectors $\hat{\mathbf{g}}$, $\hat{\mathbf{H}}$ and $\hat{\mathbf{v}}$ can be expressed as:

$$\hat{\mathbf{g}} = a_{11}\sigma_0 + a_{12}\mu_0 + a_{13}\tau_0 \quad (8)$$

$$\hat{\mathbf{H}} = a_{21}\sigma_0 + a_{22}\mu_0 + a_{23}\tau_0 \quad (9)$$

$$\hat{\mathbf{v}} = a_{31}\sigma_0 + a_{32}\mu_0 + a_{33}\tau_0 \quad (10)$$

where a_{ij} and a_{2j} are the estimated values of acceleration and earth's magnetic field and a_{3j} are calculated coefficients in local frame $(\sigma_0, \mu_0, \tau_0)$. Let A represent the matrix formed by a_{ij} . Similarly, in the rotated frame $(\sigma_1, \mu_1, \tau_1)$, the matrix B can be calculated. It contains the coefficients of $\hat{\mathbf{g}}$, $\hat{\mathbf{H}}$ and $\hat{\mathbf{v}}$ in rotated local frame $(\sigma_1, \mu_1, \tau_1)$. We obtain

$$A[\sigma_0\mu_0\tau_0] = B[\sigma_1\mu_1\tau_1] \quad (11)$$

Thus, the transformation matrix $T = B^{-1}A$ gives the absolute orientation which takes us to the current rotated frame from the reference world frame, which is used to obtain driftless orientation by correcting the orientation in the semi-static states.

5 Experiments

5.1 Hardware Description

We test our algorithm on a sensor system prototype fabricated by QCAT (Queensland Centre for Advanced Technologies, CSIRO, ICT Centre) named EiMU. It is comprised of two ADXL202JQC (two-axis) accelerometers ($\pm 2\text{g}$ range), three Honeywell's HMC1001/1002 (single axis magnetic sensors with $\pm 2\text{G}$ range), three Analog Device ADXRS150 gyros (single-axis with $\pm 150^0/\text{s}$ range), containing a D60 HC12 processor board which sends sampled data at 100Hz to the computer.

5.2 Results and Discussion

When the device is held still, the error is less than $0.5^0/\text{hour}$. This is achieved because of the robust static-state detector.

To study dynamic accuracy, experiments were conducted by rotating the device with different angular velocities on a turntable. The Fig. 3(a) shows short-term error in estimating orientation, calculated by gyros only, which optimizes error for frequencies of interest (*i.e.*, which are present in human motion) but gives us mean error of $0.32^0/\text{sec}$. Correcting the orientation by accelerometers and magnetometers in semi-static states reduces the error to $0.18^0/\text{sec}$.

Fig. 3(b) shows the effect of bias re-estimator. We have large drifts in orientation using gyros alone, which is improved by correction using accelerometers and magnetometers. Using the bias re-estimator reduces dynamic error to less than 2^0 assuming one semi static state per minute.

This is a significant improvement over other orientation trackers using the same sensors. For comparison Xsense [9] achieved 1^0 static accuracy, and 3^0 rms accuracy. Foxlin [1] used external acoustic sensors along with inertial sensors to achieve accuracy of 1.5^0 .

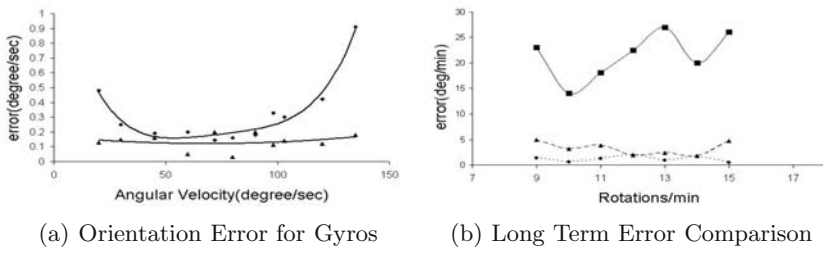


Fig. 3. (a) Short term orientation error vs. angular velocity in the absense of (upper curve) and in presence of (lower curve) correction by accelerometer and magnetometers (best fit curves of order 3). (b) Long term error in different cases;(1) dark line shows error only caused by gyro, (2) dashed line shows error when only correction by acclerometers and magnetometers is active, (3) dotted line shows error when both bias re-estimation and correction by accelerometers and magnetometers are active. It shows an improvement in performance using our algorithm

6 Conclusion

This paper presents an algorithm to robustly detect multi-level quasi-static states from inertial sensors, allowing the proper re-estimation of the time-varying sensor parameters while the device is in use. The performance of the proposed algorithm was demonstrated by developing a mixed-reality real-time orientation tracker. Thus, we demonstrated that properly estimating the parameters of inertial sensors can help in improving performance. The proposed algorithm is a step towards development of a self-organizing sensory motor system. In the future the system can be improved by applying evolutionary algorithms to finetune the internal parameters and architecture of the motion estimation system.

Acknowledgements

We thank Robotics Team, QCAT for providing us the sensor package EiMU. We also would like to thank PERSiMON group (CSIRO ICT Centre) for providing us with a miniature sensor package for initial experimentation.

References

1. Foxlin, E., Harrington, M., Altshuler, Y.: Miniature 6-DOF inertial system for tracking HMDs. SPIE vol. 3362, Helmet and Head-Mounted Displays III. AeroSense 98, Orlando, FL, April 13-14, 1998
2. Keith J. Robello: Applications of MEMS in Surgery. Proceedings of the IEEE, Vol. 92, no. 1, 43-55, Jan 2004
3. Bachmann, E.R., Yun, X., McGhee, R.B.: Sourceless Tracking of Human Posture Using Small Inertial/Magnetic Sensors. Proceedings of the IEEE International Symposium on Computational Intelligence in Robotics and Automation, July 16-20, 2003, Koebe, Japan
4. Veltink, P.H., Bussman, B.J. Hans, Vries, W., Martens, Wim L.J.: Detection of Static and Dynamic Activities Using Uniaxial Accelerometers. IEEE Transaction on Rehabilitation Engineering, Vol. 4, No. 4, 375-385, Dec 1996
5. Ferraris F., Grimaldi, U., Parvis, M.: Procedure for Effortless In-Field Calibration of Three-Axis Rate gyros and Accelerometers. Sensors and Materials, Vol. 7, No. 5(1995)311-330
6. Lotters J.C., Schipper, J., Veltink, P.J., Olthuis, W., Bergveld, P.: Procedure for in-use calibration of triaxial accelerometers in medical applications. Sensors and Actuators, A **68**(1998)221-228
7. Roetenberg D., Luinge, H., Veltink, P.: Inertial and magnetic sensing of human movement near ferromagnetic materials. Proc. of 2nd IEEE and ACM International Symposium on Mixed and Augmented Reality, ISMAR '03
8. Foxlin E.: Inertial Head-Tracker Sensor Fusion by a Complementary Separate-Bias Kalman Filter. Proc. of VRAIS, 185-194, 1996
9. Xsens miniature inertial measurement unit, Downloadable from
<http://www.xsens.com/mt9.htm>
10. Verplaetse J. C.: Inertial proprioceptive devices: Self-motion-sensing toys and tools. IBM Systems Journal Vol. 35, NOS.3 and 4, 1996
11. Gerasimov, V., Bender, W.: Batting Belt, Downloadable from
<http://vadim.www.media.mit.edu/stt/bat.html>

Self-restructuring Peer-to-Peer Network for e-Learning

Masanori Ohshiro, Kenneth J. Mackin,
Eiji Nunohiro, and Kazuko Yamasaki

Faculty of Infomatics, Tokyo University of Information Sciences, 1200-2 Yatou-chou,
Chiba city, Chiba, 265-8501 Japan
ohshiro@rsch.tuis.ac.jp
<http://www.ohshiro.tuis.ac.jp/>

Abstract. In this paper, we propose a self-restructuring network for e-learning. In a typical server-client model, the server must broadcast data to all clients. It makes the server impossible to work smoothly. Our model lightens load of the server and makes the server enable to work properly. The model of network is based on a data structure known as heap. We describe how to organize such network and how to re-structure it when one node is disconnected or new node join the network.

1 Problem of Broadcasting Large Data

Now a day, e-learning is one of the most important methods of education. A teacher like us often meets following situation. Suppose a class room in school, where a lots of students are sitting with their personal computers and teacher wants to show figures or texts on the screen on real-time without using projector and OHP etc. The teacher's computer, the server must broadcast graphic data of the screen to all students' computers using a software such as VNC. In such a case, the server didn't work smoothly, however.

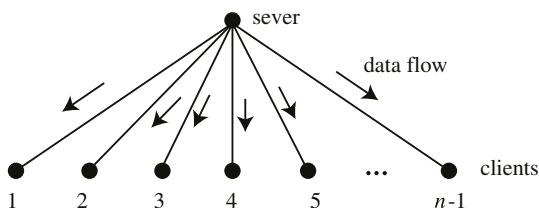


Fig. 1. A typical server-client model. The network consists of n nodes. The server must send data to all clients for broadcasting

Fig. 1 shows a typical server-client model. The network consists of n nodes (computers). The server must send data to $(n - 1)$ clients, students' computers. In this case, probably the server can't work properly because of the overload.

2 Heap Network for Broadcasting Large Data

We propose a network that has heap structure (Fig. 2) to resolve this problem. The network has heap structure. Heap is known as a data structure for priority queue and sorting. Heap is a kind of complete binary tree implemented in an array. In the heap array h , parent node, left child node and right child node of node $h[n]$ are accessed as $h[(n-1)/2]$, $h[2n+1]$ and $h[2n+2]$ respectively. Every node has priority value and every child's priority is less than or equal to priority value of it's parent.

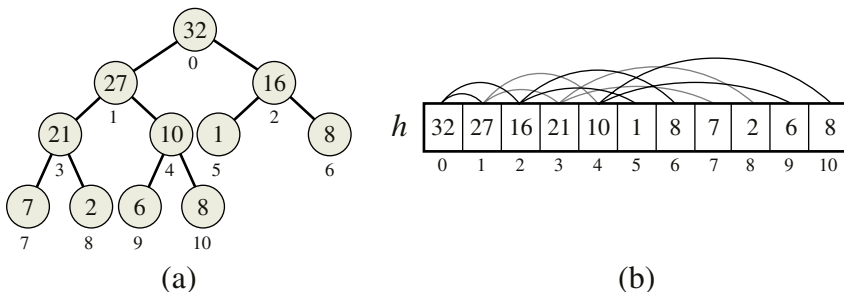


Fig. 2. (a) shows a tree representation of a heap that implemented in array h (b). The number in each circle in (a) is priority value. The number under each circle is index number for array form

In our model, the server (root node) must sent data to at most two children. Other nodes have to receive data from it's parent and forward it's at most two children (Fig. 3). The load of the server was lightened consequently. Every non-terminal node acts as sub-server of each subtree.

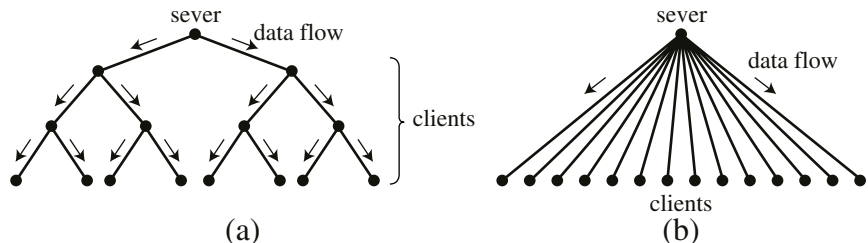


Fig. 3. Both are n -nodes networks. (a) is our model and (b) is a typical server-client model

3 Organization of the Heap Network

In this section, we consider organization of the heap network. General method for construction of a heap is well known as follows: i) A new element was put into

the position of past-the-end of heap array. ii) if the element's priority is higher than the priority of it's parent, swap both of them. iii) if swapping is executed, the new parent node is compared to children. if the child's priority is higher than the parent, both of them are swapped. iv) step ii) and iii) are repeated until the heap condition is satisfied. If the root node is removed from the heap, re-construction is executed as follows: i) The last node in a heap array h was moved to the $h[0]$, that is the position for root node. ii) If the moved node's priority is lower than it's child's one, the node and it's child was swapped. iii) step ii) is repeated until the heap condition is satisfied.

In our model, priority is defined according to performance of each node except for the root node. A node has higher performance is assigned higher priority, therefore delay of the data relation is reduced as far as possible. The root node has the highest priority always because a node becomes to be server regardless of it's performance.

It's not considered that elements is removed from the positions except the top and the tail in general heap because priority queue allows to remove a element only from the top or the tail usually. On the other hand, any elements of a heap array may be removed unexpectedly in our heap network. Therefore, we modified the general heap's re-construction rule for our heap network.

| | 0 (root) | 1 | 2 | 3 | 4 | 5 | ... | $n-1$ |
|------|----------|-----|-----|-----|-----|-----|-----|-------|
| id | 200 | 14 | 20 | 7 | 91 | 53 | | |
| h | 10000 | 200 | 180 | 170 | 165 | 172 | | |

Fig. 4. Table used for the heap network. The upper row is ids of all nodes. The lower row is the heap array

Our heap network uses a table as shown in Fig. 4. The figure shows a condition that a complete heap. The first row id is a array that contains id numbers (e.g. IP number) of the nodes, and the first element is the server's id. The second row is the heap array that contains the priority values of the nodes. All id numbers and priority numbers are greater than or equal to 0, and 0 means that the node is removed. If a node at $h[i]$ of the heap h is removed, $h[i]$ and $id[i]$ become to be 0 and function reconstruction(i) is called, the function is defined as follows:

```

bool isEmpty( int i ) { return id[ i ] == 0; }

void swap( int a[], int i, int j ) {
int t = a[i]; a[i] = a[j]; a[j] = t;
}

void reconstruction( int i ) {
int j, li, ri, lp, rp, p;
```

```

while( 1 ) {
    li = 2 * i + 1; ri = 2 * i + 2;
    if( li >= n || isEmpty( i ) ) return;
    lp = rp = h[ i ];
    if( ! isEmpty( li ) ) lp = h[ li ]; else li = i;
    if( ! isEmpty( ri ) ) rp = h[ ri ]; else ri = i;
    if( lp > rp ) { j = li; p = lp; } else { j = ri; p = rp; }
    if( i == j ) return;
    if( p > h[i] ) { swap( h, i, j ); swap( id, i, j ); }
    else return;
    i = j;
}
}

```

In this code, $n (= 2^k - 1)$ is length of the heap array, where k is a certain integer. As a result of this reconstruction, the empty node is moved to a position of terminal node of the tree. Therefore, the all connections are kept from unexpected node disappearance and the heap condition remains almost satisfied. In case of need, you may execute heap sorting on the arrays to satisfy the heap condition completely. When a new node join the network, seach a empty slot of the array and put the new one into the slot. If no empty slot is found, the new node is put into past-the-end slot as in general heap construction method.

4 Discussion

We proposed a model for peer-to-peer network using heap structure to resolve the problem of broadcasting large data to many clients. It seems that the network is useful for e-learning. One of the problem of this network, the connection was constructed regardless of semantic group of the nodes. Implementation and test the heap based network is future work.

References

1. L.C.Jain, et.al(eds): "Virtual Environments for Teaching and Learning", World Scientific (2002)

An Improvement Approach for Word Tendency Using Decision Tree

El-Sayed Atlam, Elmarhomy Ghada, Masao Fuketa,
Kazuhiro Morita, and Jun-ichi Aoe

Department of Information Science and Intelligent Systems
University of Tokushima Tokushima, 770-8506, Japan
atlam@ccr.tokushima-u.ac.jp

Abstract. In every text, words have various frequencies and keywords have strong relationship with the subjects of their texts. Word frequencies change due to time-series variation over given periods of time. An early method estimated stability classes that indicate word popularity due to time-series variation based on frequency changes in text data over given periods using a decision tree. The estimation precision of the decision tree decreases when there is scattering of data number among classes. This paper suggests a new way to use a *Random Sampling Method* and proposes a new *Data Copying Method* to improve the estimation precision of decision tree. By using this new *Data Copying Method*, *F-measures* have improved: Increasing Class 9%; Relatively Constant Class 9%; Decreasing Class 18%.

1 Introduction

Determination of keywords is crucial in modern Information Retrieval (*IR*). The frequency of some words changes with time (time-series variation) and connect with particular periods (e.g. “*influenza*” is more common in winter). Words affected by time-series variation can often be considered as keywords which directly connect with the main subject of a text and express important characteristics of that text.

According to Hisano [5], some Chinese (Kanji) characters in newspaper reports change with time-series variation. Ohkubo et al. [8] propose a method for estimating the information needed to analyze login data on a *WWW* search engine. Ohkubo’s method confirms that word groups connected with search words strongly change according to the time period when the search is done.

Traditional methods of dealing with text analysis [2][3][4] and text search techniques [7][12] do not consider the connection between changing in word frequencies and time-series variation. Therefore, such methods can not correctly determine the relative importance of words in a given period (e.g. one-year). Atlam et al. [1] estimate stability classes with time-series variation to index word popularity using a Decision Tree (*DT*) [10]. *DT* learning data may have differing amounts of data in different classes and classes containing fewer data are treated as noise data that negatively affect *DT* precision [6]. To solve problems connected with different amounts of data, Okumura, Haraguchi & Mochizuki [9] propose random sampling of learning data in each class, a revision that is effective when sampling data (Learning Data) are more than analysis data (Test Data). When sampling data are less than analysis data, Okumura’s method can not improve *DT* precision.

This paper suggests that the precision of *DT* can be improved if learning data of each class is copied often enough to make the number of data in classes with fewer data equal the number of data in the class with the largest number of data. Section 2 of this paper considers results of the method proposed in Atlam et al. [1]. Section 3 evaluates methods: Random Sampling Method of improving *DT* learning data and Data Copying Method of improving *DT* learning data. Section 4 presents a conclusion and indicates possible future work.

2 Old Method Evaluation

The sports section of *CNN* newspapers (1997-2000) provided experimental collection data because of the uniqueness of the words in the field of sports and because such words tend to change with time-series variation. The specific sub-field “*professional baseball*” was chosen because of its regular reports, and because the effect of time-series variation on words frequencies is relatively easy to determine. Words identifying “*Player name*,” “*Organization name*”, “*Team name*,” and “*Common nouns*” were extracted from the selected reports and the normalized frequency of these words was obtained for each year. Stability classes for these words were classified manually.

Data were divided into two groups: reports from years 1997- 1999 were used as *DT* learning data; reports from years 1997-2000 were used as test data. For both groups of data, attributes were obtained according to change of word frequencies due to time-series variation. Data of extracted words is in Table 1.

Table 1. Data Evaluation

| | <i>DT</i> Learning Data | | <i>DT</i> Test Data | |
|----------------------------------|-------------------------|-----------|---------------------|-----------|
| | M | N | X | Y |
| <i>Period</i> | 1997-1999 | 1998-1999 | 1997-2000 | 1998-2000 |
| <i>Total Number of Words</i> | 443 | 360 | 472 | 392 |
| <i>Increasing Class</i> | 55 | 59 | 69 | 82 |
| <i>Relatively Constant Class</i> | 243 | 187 | 252 | 200 |
| <i>Decreasing Class</i> | 145 | 114 | 151 | 110 |

Learning data was used for *DT*. *DT* results and manual results were compared, based on the classification of stability classes of the test data:

| Decision Tree Evaluation | | |
|--------------------------|----------------|------------------|
| Increasing Class | Constant Class | Decreasing Class |
| 102 | 3 | 34 |
| 11 | 153 | 59 |
| 5 | 10 | 105 |

Increasing Class
 Constant Class
 Decreasing Class } *Manually Evaluation*

Fig. 1. Sample of *DT* Evaluation

To determine the accuracy of results evaluated automatically by *DT* compared with results evaluated manually (for more detail see appendix I) *Precision (P)*, *Recall (R)* rate and *F-measure* were calculated [11]:

$$\begin{aligned} \text{Precision} &= \frac{\text{Number of correct words extracted by system } DT}{\text{Total number of words extracted by system } DT} \\ \text{Recall} &= \frac{\text{Number of correct words extracted by system } DT}{\text{Total number of correct words classified manually}} \\ F\text{-Measure} &= \frac{2 \times \text{Precision} \times \text{Recall}}{\text{Precision} + \text{Recall}} \end{aligned}$$

2.1 Learning Periods and Classification Precision

Table 2 shows the effectiveness of applying the longest period *M* (1997-1999) and the shortest period *N* (1998-1999) of learning data to the distribution of *P* & *R*. When the period of learning data is longer (*M*), the number of words increase and characteristics of the Relatively Constant Class and Decreasing Class become more obvious and *P* & *R* become higher. However, when the period of learning data is shorter (*N*), the Correlation Coefficient and the angle between two Regression Lines become a Relatively Constant value and the function of Correlation Coefficient and the angle can not be expressed.

Table 2. Various Time Periods and Classification Precision

| Classes | Learning Period | | | | | |
|-----------|-----------------|---------------------|----------|---------------|---------------------|----------|
| | N (1998-1999) | | | M (1997-1999) | | |
| Classes | Increase | Relatively Constant | Decrease | Increase | Relatively Constant | Decrease |
| Precision | 49.41 | 73.48 | 65.9 | 72.73 | 97.13 | 65.68 |
| Recall | 63.36 | 49.77 | 85 | 74.73 | 75.78 | 92.5 |
| F-Measure | 0.555 | 0.588 | 0.738 | 0.739 | 0.739 | 0.768 |

3 New Methods for Improving *DT* Learning Data

In *DT* learning, there is a scattering of the number of learning data of each class. If some data in different classes have duplicated attributes, the learning data of the class having fewer data is recognized as noise learning data for the class with more data [4]. Generally, the number of words in the Relatively Constant Class is much higher than the number of words in the Increasing Class or Decreasing Class. Due to the characteristics of *DT*, there is a high possibility that words recognized as increasing or

decreasing will be considered as relatively constant words. *DT* testing results allow evaluation of the improvement of *DT* learning data when there is a scattering in the number of data.

3.1 Random Sampling Method

Okumura, Haraguchi & Mochizuki [9] propose a method that revises scattering by random sampling of the learning data. The period (1997-1999) provides learning data and the period (1997-2000) provides test data. To equalize the numbers of data in each stability class roughly, the Random Sampling Method is used for data words of Relatively Constant Class and Decreasing Class. This method produces roughly the same number of data words of Increasing Class (the fewest number of data [standard] is 55 words).

Learning data is divided into three major groups and several subgroups:

- 1) Data of Increasing Class (1 sub-group),
- 2) Data of Decreasing Class (3 sub-groups),
- 3) Data of Relatively Constant Class (5 sub-groups).

15 sub-groups of learning data are made by combining all sub-groups, and *DT* learning is applying to data of all sub-groups.

In Table 3, best estimation of *DT* is 17.8%, worst estimation of *DT* is 25.30%, and the best estimation result is 21.10%. Table 3 shows that the classification precision of *DT* can not necessarily be estimated because the Random Sampling method should contain more learning data than analysis data. However, in the Random Sampling method used in this paper, there is much fewer learning data than analysis data, causing the estimation of *DT Precision, Recall and F-Measure* to be only slightly improved

Table 3. Classification Precision, Recall and F-Measure of Random Sampling Method

| | Random Sampling Data Results | | | | | | | | | |
|-----------|------------------------------|----------|------------|------------------|----------|------------|------------------------|----------|------------|--|
| | Best Estimation | | | Worst Estimation | | | Best Estimation Result | | | |
| Classes | Increasing | Constant | Decreasing | Increasing | Constant | Decreasing | Increasing | Constant | Decreasing | |
| Precision | 85.23 | 81.08 | 44.53 | 66.47 | 90.38 | 75 | 78.37 | 97.44 | 67.39 | |
| Recall | 70.5 | 40.36 | 95 | 81.29 | 63.23 | 97.5 | 97.12 | 75.16 | 97.5 | |
| F-Measure | 0.772 | 0.539 | 0.606 | 0.731 | 0.744 | 0.847 | 0.867 | 0.848 | 0.797 | |

3.2 Data Copying Method

This paper proposes a method to copy learning data of classes with fewer data as often as necessary to equal the number of data in the class having the largest amount of data. In the Data Copying Method, copying data words of Increasing Class and Decreasing Class until there is roughly the same data number of words as in the Rela-

tively Constant Class makes learning data. The data numbers are: Increasing Class (269); Relatively Constant Class (230); in Decreasing Class (255).

Table 4 shows the Data Copying Method has a better classification of *Precision*, *Recall* and *F-Measure* than Random Sampling Method and method presented by Atlam et al. [1]. In the new method, characteristics of classes with fewer numbers of data are emphasized due to repeated use of the same learning data several times in *DT*.

Table 4. Classification *Precision*, *Recall* and *F-Measure* of Copying Data Method

| <i>Classes</i> | <i>Copying Data Method Results</i> | | |
|------------------|------------------------------------|----------------------------|-------------------|
| | <i>Increasing</i> | <i>Relatively Constant</i> | <i>Decreasing</i> |
| <i>Precision</i> | 95.52 | 94.20 | 92.74 |
| <i>Recall</i> | 92.09 | 94.62 | 95.83 |
| <i>F-Measure</i> | 0.937 | 0.944 | 0.943 |

4 Conclusion

This paper evaluates an improved method for classifying *Precision*, *Recall* and *F-Measure* of stability classes of learning data that should be useful when there is scattering of *DT* learning data. The effectiveness of the Data Copying Method is confirmed by *F-Measures*: Increasing Class = 0.937, Relatively Constant Class = 0.944, and Decreasing Class = 0.943.

With increasing creation of electronic texts, there will be increased indexing of word popularity based on time-series variation. The method presented in this paper should be particularly valuable in estimating word popularity in searches of similar text. Future work could focus on fields other than sports or professional baseball as used in this paper.

Acknowledgment

Authors are grateful acknowledge support from the Japan Society for the Promotion of Science (JSPS), Grant No. 03258.

References

1. Atlam E-S., Makoto, O., Masami, S. and Aoe, J., An Evaluation Method of Words Tendency Depending on Time-SeriesVariation and its Improvements, *Information Processing & Management*, 8(2) (2001), 157-171.
2. Fukumoto, F., Suzuki, Y. & Fukumoto, J. I., An Automatic Clustering of Articles Using Dictionary Definitions. *Trans. Of Information Processing Society of Japan*, 37(10), (1996), 1789-1799.
3. Hara, M., Nakajima, H. & Kitani, T., Keyword Extraction Using Text Format and Word Importance in Specific Field. *Trans. Of Information Processing Society of Japan*, 38(2), (1997), 299-309.
4. Haruo, K., Automatic Indexing and Evaluation of Keywords for Japanese Newspaper. *Trans. of the Institute of Electronics, Information and Communication Engineering (IEIC)*, J74-D-I (8), (1991), 556-566.

5. Hisano, H., Page-Type and Time-Series Variations of a Newspaper's Character Occurrence Rate., *Journal of Natural Language Processing*, 7 (2), (2000), 45-61.
6. Honda, T., Mochizuki, H., T. B., Ho & Okumura, M., Generating Decision Trees from an Unbalanced Data Set. In *proceeding of the 9th European Conference on Machine Learning*, 1997.
7. Liman, J., Cue Phrase Classification Using Machine Learning. *Journal of Artificial Intelligence Research*, 5, (1996), 53-94.
8. Ohkubo, M., Sugizaki, M., Inoue, T. & Tanaka, K., Extracting Information Demand by Analyzing a WWW Search Login. *Trans. of Information Processing Society of Japan*, 39(7), (1998), 2250-2258.
9. Okumura, M., Haraguchi, Y. & Mochizuki, H., Some Observation on Automatic Text Summarization Based on Decision Tree Learning. *Journal of Information Processing Society of Japan*, No.5N-2, (1999), 71-72.
10. Quinlan, J. R., *C4.5: Programs for Machine Learning*, Morgan Kaufmann, 1993.
11. Salton, G., & McGill, M. J., *Introduction of Modern Information Retrieval*. New York: McGraw-Hill, 1983.
12. Swerts, M. & Ostendorf, M., Discourse Prosody in Human-Machine Interaction. In European Speech Communication Association (ESCA) Workshop on spoken Dialogue Systems, (1995), 205-208.

A New Technique of Determining Speaker's Intention for Sentences in Conversation

Masao Fuketa, El-Sayed Atlam, Hiro Hanafusa, Kazuhiro Morita,
Shinkaku Kashiji, Rokaya Mahmoud, and Jun-ichi Aoe

Department of Information Science and Intelligent Systems
University of Tokushima, Tokushima 770-8506, Japan
atlam@is.tokushima-u.ac.jp

Abstract. Although there are many text classification techniques depending on vector spaces, it is difficult to detect the meaning relating to the user's intention (complaint, encouragement, request, invitation, etc.). The intention to be discussed in this study is very useful for understanding focus points in conversation. This paper presents a technique of determining the speaker's intention for sentences in conversation. The intention association expressions are introduced and the formal rule descriptions with weight using these expressions are defined to build intention classification knowledge. A deterministic multi-attribute pattern-matching algorithm is used to determine the intention class efficiently. From simulation results for 681 E-mail messages of 5,859 sentences, the multi-attribute pattern matching algorithm is about 44.5 times faster than Aho and Corasick method. The precision and recall of intention classification of sentences are 91%, 95%. Precision and recall of the classification of each mail are 88%, 89%.

1 Introduction

There are many conversation tools using computers such as: telephones, E-mail systems, mobile computers, speech recognition devices and so on. It is very important techniques to determine the user's intention in these communications. Many text classification techniques depending on vector spaces were proposed [8][9], but it is difficult to find special sentences including the speaker's intention independent of text classes. Finding important sentences are related to automatic summarization [10]. However, summarized sentences differ from the user's intention in conversation because the purpose approaches are to extract topics of news and focus points of documents. On the other hand, proposed field association (*FA*) word techniques that can find the expected passages in the whole document [4][5][6]. *FA* words are very suitable for knowledge bases focusing on special sentences because they depend on word and phrase knowledge, not as vector space models [11] which depend on the whole text.

This paper extends the *FA* knowledge to *Intention Association* (*IA*) expressions in the communications and presents a technique of determining the speaker's intention for sentences in conversation. The formal rule descriptions using these *IA* expressions are defined to build intention classification knowledge. A deterministic multi-attribute pattern-matching algorithm [1][2][3] is used to determine the intention class efficiently. The presented technique will be evaluated for many E-mail conversation sentences.

2 Formal Description Rules for *Intention Association* Expressions

2.1 Field Association Words

The *Field Association* (*FA*) words are the words that can specify the field of the documents. For example, words like “Home run” and “Hit” are *FA* words of filed <Baseball>. *FA* words are very suitable for knowledge bases focusing on special sentences because they depend on word and phrase knowledge, not as vector space models which depend on the whole text. *FA* words are used to the classification technique of document classification and similar file retrieval [4][5][6]. The importance of the word, $w(t)$ is weighting by term t in each passage and can be computed with term frequency tf or inverse document frequency idf in each passage or in the entire document. In the vector space model, local similarity is computed for each passage and query, and passage with highest similarity is selected as a candidate. Using tf , the importance of the word can be expressed as follows:

$$w(t) = tf(t) \times \log \frac{N}{n(t)}$$

where $tf(t)$ represents occurrence frequency of term t in a passage, N is the total number of passages and $n(t)$ is the number of passage in which t occurs.

2.2 Intention Association Classes

There are many communication tools using computers and it is very important to determine the user's intention for all communications. This paper considers E-mail communications as one of the typical and practical communications. This section defines basic semantic information about important *intention association* (*IA*) expressions, where these expressions are defined by analyzing training mails. The rule which classifies the contents of mail is described by combining a variety of words, phrases, categories and semantics (including concepts).

(1) Intention Association Expressions of <Announce>

Examples for intention association expressions of <Announce> are “A campus festival is held.”, “A seminar will be performed tomorrow.”, “The schedule of a meeting was changed.” and “Today's concert was stopped.” etc. An attribute (SEM, EVENT) is the meaning of the words “meeting”, “seminar”, “party”, “festival”, etc. An attribute (SEM, SCHEDULE) is the meaning of “schedule”, “plan”, “program”, etc. SCHEDULE is also including all words belonging to EVENT. Moreover, an attribute (SEM, HOLD) is the meaning of “carrying out”, “hold”, “open”, “perform”, “begin”, etc. An attribute (SEM, CHANGE) is the meaning of “change”, “cancel”, “stop”, “postpone”, etc. The sentence containing both EVENT and HOLD is important for IA expressions of <Announce>. It is also important for <Announce> expressions to contain both EVENT and CHANGE. In addition, “becomes new” is also the meaning of “change”, because “The curriculum became new.” is the same meaning as “The curriculum was changed.”

(2) Intention Association Expressions of <Report>

Examples for intention association expressions of <Report> are “We report the result to you.” and “The operation was successful.”, etc. An attribute (SEM, RESULT)

represents the meaning of “*result*”, “*data*”, “*response*”, etc. An attribute (SEM, REPORT) represents the meaning of “*report*”, “*announce*”, “*tell*”, “*convey*”, etc. An attribute (SEM, OPERATION) is the meaning of “*operation*”, “*experiment*”, “*test*”, “*examination*”, etc. An attribute (SEM, SUCCESS) is the meaning of “*success*”, “*pass*”, “*good*”, etc. An attribute (SEM, FAILURE) is the meaning of “*failure*”, “*bad*”, “*unsuccessful*”, etc.

(3) Intention Association Expressions of <Request>

Examples for intention association expressions of <Request> are “*Please submit these documents.*” and “*Please gather not late.*”, etc. An attribute (SEM, SUBMIT) is the meaning of “*submit*”, “*deliver*”, “*send*”, “*finish*”, “*complete*”, etc. An attribute (SEM, GATHER) is the meaning of “*gather*”, “*come*”, “*meet*”, “*assemble*”, etc. “*Submit*” and “*gather*” are often utilized in request mails. An attribute (SEM, DAY-TIME) is the meaning of “*today*”, “*tomorrow*”, “*August 15th*”, “*Wednesday*”, etc. An attribute (SEM, PLACE) is the meaning of “*room*”, “*floor*”, “*station*”, “*park*”, etc. There are more important for IA expressions of <Request> which described concrete DAY-TIME or PLACE, such as “*Please submit these documents by tomorrow.*”, “*Please come to the station at 10:00.*”, etc.

(4) Intention Association Expressions of <Question>

Examples for intention association expressions of <Question> are “*When is this seminar?*”, “*Where is a meeting place?*”, etc. An attribute (CAT, INTERROGATIVE) is description of “*When*”, “*Where*”, “*What*” and “*How*”. An attribute (SEM, TEACH) is the meaning of “*teach*”, “*ask*”, “*tell*”, “*answer*”, etc. For example, “*Please tell me your address.*” or “*Please teach me how to solve this problem.*” are the same meanings as “*Where is your address?*” or “*How is this problem solved?*”, so those are the expressions of <Question>. An attribute (SEM, VISIT) is the meaning of “*visit*”, “*go*”, “*meet*”, etc. Examples are “*May I visit your house?*”, “*When shall I visit you?*”, etc. The expression belonging to VISIT is extracted together with an interrogative.

(5) Intention Association Expressions of <Complaint>

Examples for intention association expressions of <Complaint> are “*The program got yesterday is wrong.*”, “*The received goods had broken.*”, “*I cannot be satisfied of your service.*”, etc. An attribute (SEM, MISTAKE) is the meaning of “*mistake*”, “*wrong*”, “*failure*”, “*defect*”, “*bug*”, etc. An attribute (SEM, SATISFY) is the meaning of “*satisfy*”, “*content*”, “*gratify*”, “*complete*”, etc. Expressions denying SATISFY have the meaning of a “*complaint*”. An attribute (SEM, HURRY) is the meaning of “*hurry*”, “*prompt*”, “*urgent*”, “*immediate*”, “*pressing*”, etc., and an attribute (SEM, ATTENTION) denotes the expression “*attention*”, “*measure*”, “*cope*”, “*correspond*”, etc. Expression with urgent demands also becomes <Complaint> expression. Examples are “*Your prompt attention would be appreciated.*”, “*We request an immediate refund.*”, etc.

(6) Intention Association Expressions of <Reply>

Examples for intention association expressions of <Reply> are, “*It is O.K.*”, “*I attend the meeting.*”, “*I am absent from a meeting.*”, “*I refuse this work.*”, etc. An attribute (SEM, ACCEPT) corresponds to affirmative expressions of <Reply> like “*accept*”, “*approve*”, “*O.K.*”, “*understand*”, “*attend*”, “*present*”, “*participate*”, etc. In contrary

to ACCEPT, an attribute (SEM, DECLINE) corresponds to refusal expressions of <Reply> like “refuse”, “decline”, “absent”, etc. An attribute (SEM, IMPOSSIBLE) corresponds to negative expressions like “impossible” or “cannot”. The description containing both ACCEPT and IMPOSSIBLE is a refusal expressions of <Reply>. Examples are “*I cannot attend the meeting.*”, “*It became impossible to participate.*”, etc. In addition, the meaning which combined ACCEPT and “next time” is also refusal expressions of <Reply>. For example, “*I will participate next time.*” is including the meaning of “*I cannot participate this time.*”

3 Sentence Classification by Using Weight of Rules

3.1 Weight of Rules

An important message or an un-important (un-necessary) message can be judged by giving the weight, or point, to each classification rule. The important measurement of sentences is independent of classifications such as <Announce>, <Report>, etc. In general, the mails are sent from business associations, customers and friends, etc. The importance is decided according to the level of the damage forecast when the mail is overlooked. For example, the <Announce> sentence “the executive meeting is held on next Monday.” is more important than the <Encouragement> sentence “Do your best!”. For this reason, it is necessary to participate or participate by the announcement, but it is unnecessary by the encouragement.

To define the weight of rules, the number of each rule is counted from the training mails for each IA class. One training mail includes two or more IA expressions, like the <Request> and <Question> expression is included in the <Announce> training mail. Therefore, only IA expressions in the important sentences must be emphasized. The global weight of IA expressions in a mail can be expressed as follows:

$$\text{WEIGHT}(p) = \log \left(\frac{N}{n(p)} \times \left(1 + \frac{C(p)}{T(p)} \right) \right)$$

where N is 8 kinds of the classifications mail and $n(p)$ is the number of classifications mail which included in the expressions of rule p . Let MAIL_CLASS(m) be one of IA class, SENTENCE_CLASS(m, s) be rule number and RULE_CLASS(p) be one of IA class. $T(p)$ is the number of the important sentences s such that

$$\text{SENTENCE_CLASS}(m, s) = p$$

for each m . $C(p)$ is the number of important sentences s such that

$$\text{SENTENCE_CLASS}(m, s) = p$$

and $\text{MAIL_CLASS}(m) = \text{RULE_CLASS}(\text{SENTENCE_CLASS}(m, s))$.

3.2 Classification Technique by Using Weight of Rules

The classification of mails can be judged by weight of rules. The weight of IA class c of mail m can be expressed as follows:

$$w(c, m) = \sum_{p=1}^{N_p} (tf(p) \times \text{WEIGHT}(p))$$

where $tf(p)$ represents occurrence frequency of the expression of RULE $_p$ in mail m , WEIGHT(p) is the

4 Analysis of Intention Classes

4.1 Deterministic Multi-attribute Pattern Matching Algorithm

In natural language processing, morphological, syntax and semantic analyzers are carried as the preprocessor in general, but the input must take a sequence of structures for skeleton sentences and phrases. “*Skeleton*” means that the embedded sentences and redundant words are ignored in the preprocessor. The reason is that the request of the mail messages is very simple expression. For example, consider “*Mr. Koizumi's birthday party is held after the meeting on May 15.*”. “*Mr. Koizumi's birthday*” which is the modifier of a subject is removed from the input. Moreover, “*after the*” and “*on*” are also removed. “*Party*” is taken as EVENT. Finally, “*party (EVENT)*”, “*is (BE-VERB)*” and “*held (HOLD)*” are obtained from the input sentence and the following sequences of structures are prepared to the DMAP machine. For example, consider “*Mr. Koizumi's birthday party is held after the meeting on May 15.*”. “*Mr. Koizumi's birthday*” which is the modifier of a subject is removed from the input. Moreover, “*after the*” and “*on*” are also removed. “*Party*” is taken as EVENT. Finally, “*party (EVENT)*”, “*is (BE-VERB)*” and “*held (HOLD)*” are obtained from the input sentence and the following sequences of structures are prepared to the DMAP machine.

$$N_1 = \{(\text{STR}, \text{"party"}), (\text{CAT}, \text{NOUN}), (\text{SEM}, \text{EVENT})\}$$

$$N_2 = \{(\text{STR}, \text{"is"}), (\text{CAT}, \text{BE-VERB})\}$$

$$N_3 = \{(\text{STR}, \text{"held"}), (\text{CAT}, \text{VERB}), (\text{SEM}, \text{HOLD})\}$$

5 Simulation Results

Table 1 shows the accuracy (precision and recall) of the classification using the proposed rules for 681 E-mail messages of 5,859 sentences. Form total sentences, 4,316 expressions can be classified into ten kinds of expressions that stated in section 2.3. The *IA* expressions are extracted for each sentence of E-mail messages by using the defined rules. The classification result is evaluated by the comparison with the classification judged by human. In Table 1, “Number of Expressions” is the number of expressions for each *IA* class and “Number of Extracted” is the number of expressions extracted by proposed technique. CORRECT is the number of extraction with correct classification and WRONG is the number of extraction with wrong classification. “Number of Non Extracted” is the number of *IA* expressions that not be able to extracted. Retrieval effectiveness is measured:

The validity of this technique is shown because the precision and recall of experiment are 91% and 95%.

6 Conclusions

This paper presented a technique for detecting user's intention in communications and calculating the important measurement among the detected expressions. To extract the *intention association* expressions, 8 kinds of rule sets are classified and 51 concepts are defined. A deterministic multi-attribute pattern-matching algorithm is presented. This multi-attribute enables us to the fast detecting by using complex rule sets. From simulation results for 681 E-mail messages of 5,859 sentences, the presented set pat-

Table 1. Simulation Results of the Classification of Sentences

| | Number of Expressions | Number of Extracted | Correct | Wrong | Number of Non Extracted | Precision | Recall |
|--------------|-----------------------|---------------------|---------|-------|-------------------------|-----------|--------|
| <Announce> | 1,460 | 1,618 | 1,439 | 179 | 19 | 89% | 99% |
| <Report> | 236 | 256 | 218 | 38 | 5 | 85% | 92% |
| <Request> | 738 | 747 | 717 | 30 | 3 | 96% | 97% |
| <Question> | 108 | 107 | 92 | 15 | 8 | 86% | 85% |
| <Complaint> | 259 | 250 | 215 | 35 | 9 | 86% | 83% |
| <Reply> | 42 | 40 | 34 | 6 | 2 | 85% | 81% |
| <Invitation> | 44 | 44 | 39 | 5 | 2 | 89% | 89% |
| Encouragemt | 82 | 79 | 71 | 8 | 4 | 90% | 87% |
| <Salutation> | 1,016 | 996 | 968 | 28 | 20 | 97% | 95% |
| Assumption | 331 | 384 | 321 | 63 | 8 | 84% | 97% |
| Total | 4,316 | 4,521 | 4,114 | 407 | 80 | 91% | 95% |

tern-matching algorithm is about 44.5 times faster than Aho and Corasick method. The precision and recall of intention classification of sentences are 91% and 95%. Precision and recall of un-necessary sentences extraction are 98% and 96%, and precision and recall of the classification of each mail are 88% and 89%. The *intention association* expressions and the important measurement is one of filtering information to determine the important E-mail messages. In the future study, other measurement for important messages will be considered together with time priority. The filtering measurement depends on individual criterion except business cases, so the leaning faculty for users should be also researched.

References

1. Aho, A. V., & Corasick, M. J., Efficient string matching: An aid to bibliographic search. *Communications of the ACM*, 18(6), (1975), 333-340.
2. Aoe, J., An Efficient Implementation of Static String Pattern Matching Machines. *IEEE Trans. Softw. Engr.*, SE-15(8), (1989)(1), 1010-1016.
3. Aoe, J., An efficient digital search algorithm by using a double-array structure. *IEEE Trans. Softw. Engr.*, SE-15(9), (1989)(2), 1066-1077.
4. Atlam, E-S., Fuketa, M., Morita, K. & Aoe, J., Documents similarity measurement using field association terms. *An International Journal of Information Processing and Management*, 39(6), (2003), 809-824.
5. Atlam, E-S., Morita, K., Fuketa, M. & Aoe, J., A new method for selecting English field association terms of compound words and its knowledge representation. *An International Journal of Information Processing and Management*, 38(6), (2002), 807-821.
6. Fuketa, M., Lee, S., Tsuji, T. Okada, M. & Aoe, J., A document classification method by using field association words. *An International Journal of Information Sciences*, 126(1), (2000) 57-70.

7. Fellbaum, C., WordNet: An Electronic Lexical Database. *MIT Press, Cambridge, MA*, 1998.
8. Kwon, O. & Lee, J., Text categorization based on k-nearest neighbor approach for Web site classification. *An International Journal of Information Processing and Management*, 39(1), (2003), 25-44.
9. Kwon, O., Jung, S., Lee, J. & Lee, G., Evaluation of Category Features and Text Structural Information on a Text Categorization Using Memory Based Reasoning. *Paper presented at the Proceedings of the 18th international conference on computer processing of oriental languages (ICCPOL '99)*, 1, (1999), 153-158.
10. Mani, I., Automatic Summarization. *John Benjamins Publishing Company*, (2001).
11. Salton, G. & McGill, M. J., Introduction of modern information retrieval. *New York: McGraw-Hill*, (1983).

New Approach for Speeding-up Technique of the Retrieval Using Dynamic Full-Text Search Algorithm

Kazuhiro Morita, El-Sayed Atlam, Masao Fuketa, Elmarhomy Ghada,
Masaki Oono, Toru Sumitomo, and Jun-ichi Aoe

Department of Information Science and Intelligent Systems
University of Tokushima, 770-8506, Japan
atlam@ccr.tokushima-u.ac.jp

Abstract. Full-text search is widely used for various services of the Internet. A more high-speed and a more efficient full-text search technology are necessary because of the amount of increasing handled document and corresponding document data every day. An adaptive block management algorithm for efficient dynamic data management and speeding up character string retrieval were proposed. This paper proposes a speed-up technique of the retrieval by dynamic full-text search algorithm. Also, the update efficiency of dynamic full-text search system is very high compared with static full-text search system. So, when comparing 200MB registered document using this system speed will be about 426 times higher than static full-text search system. Moreover, this paper presents an efficient achievement method of the dynamic full-text search system for speeding deletion processing time. This experiment proven that the speed for deletion processing time is very high because the deletion of 50 files was 0.2 s or less.

1 Introduction

Recently, with spreading the personal computer rapidly, the chance for general people using an electronic document of E-mail etc. has increased. Therefore, many people collecting various electronic documents for various purposes. Because of the writing document on the computer becomes general, the number of electronic documents increase. Therefore, the demand technology that efficiently manages these large amounts of electronic documents becomes important. The full-text search has the character string with feature information that can retrieve character string with high speed in retrieving from large amount of document. Now, the full-text search is widely used for various services of the Internet. A more high-speed and a more efficient full-text search technology are necessary because of the amount of increasing handled document and corresponding document data every day.

Many researches of the full-text search are concerning on the static full-text search system. In the static full-text search system, index is used for every time updating when new key is inserted or deleted. This method is not efficient because a great amount of time is basically necessary for that indexing at every updating. Therefore, the proposal of the dynamic full-text search system is strongly needed.

2 High-Speed Full-Text Search Using Bi-gram Index

Inverted file searching is fast, but it has a drawback because the efficiency of the retrieval decreases with a lot of long character string and high frequency character.

This is caused because of the increase of the number of character groups and its location information. Also, matching of each character group that has a lot of information need a high retrieval cost for comparing processing. Therefore, the retrieval speed can be improved, if the number of groups and the amount of the character location information can be reduced. This section presents a Bi-Gram index that consists of the combination of two characters. By using Bi-Gram index the number of groups and the matching cost of location information will reduce.

Bi-Gram index is making unit for each two character which is different than making each character kind (Uni-Gram) index.

Example 3. Table 1 shows an example for the same document “*inverted file*” as in example 1 by using Bi-Gram index. Bi-Gram index for that document will be as: “*in*”, “*nv*”, “*ve*”, “*er*”, etc.

Table 1. Concept of Bi-gram Index

| | | | | | | | | | | | | |
|-----------|----|----|----|----|----|----|----|----|----|----|----|--------|
| Character | in | nv | ve | Er | rt | te | ed | df | fi | il | le | 'null' |
| Position | 1 | 2 | 3 | 4 | 5 | 6 | 7 | 8 | 9 | 10 | 11 | 21 |

2.1 Retrieval by Bi-gram Index

There are two cases of retrieval using Bi-Gram index depending on the number of queries characters that may be *even* or *odd* number. When the number of retrieval character strings is *even* number, Bi-Gram index cuts the query key by two characters and the unit of the retrieval is made. When the number of retrieval character strings is *odd*, Bi-Gram index cuts the query key by two characters but one character at each retrieval is made to come in succession and the unit of the retrieval is made. For instance, when the word “*file*” is retrieved (even number), the unit of retrieval will be {“*fi*” and “*le*”}, but when the word “*files*” is retrieved (odd number), the unit of retrieval will be {“*fi*”, “*il*”, and “*es*”} or {“*fi*”, “*le*” and “*es*”}.

3 Dynamic Full-Text Search Method

3.1 Dynamic Full-Text Search Algorithm

In the full-text search, index is made for character or character string as a unit of retrieval. Moreover, to reduce the capacity and speed up the system, the location information is directly made as a group for the related unit of retrieval character and character string. However, Full-text search based on inverted file can be paraphrased as the algorithm which can retrieval some pattern (or combination of pattern) from large amount of document at high speed. Some research treats length $N = 3$ or more according to $N =$ experience and statistics as a method of speeding up retrieval. The retrieval character string of $N = 2$ or less is not found at high speed and not exist for the best guarantee. However, a retrieval speed can be maintained always as the best with dynamic full-text search system of *ID* method. The retrieval speed is decreased because the amount of the location information is extremely large compared with other units of the retrieval

Table 2. Frequency and Number of Characters Sharing in The Same Frequency

| (a) Bi-Gram Index | | (b) Uni-Gram Index | |
|-------------------|---------------------|--------------------|---------------------|
| Frequency | Number of Character | Frequency | Number of Character |
| 1 | 239 | 2 | 1 |
| 2 | 126 | 4 | 1 |
| 3 | 93 | 5 | 1 |
| 4 | 58 | 11 | 2 |
| 5 | 59 | 13 | 1 |
| 6 | 42 | 19 | 1 |
| 7 | 55 | 39 | 1 |
| 8 | 30 | 52 | 1 |
| 9 | 41 | 436 | 1 |
| 10 | 28 | 437 | 1 |
| . | . | . | . |

3.2 Speed-up Retrieval Algorithm

For example, there is about 106,882 locations information for the unit “th” as showing in Table 2. It is necessary to read the location information of “th” so, all retrieval character string including the unit of “th” is $106,882 * 4 = 427,528$ [byte] = 417.5 [KB] = 0.4[MB], this means that data will be read from the memory by one hour. In this case, 0.4 MB data is stored in one block in a continuous area of the memory. The reading time of the badness takes one second or more in the ability of a standard computer. Then, when units of the retrieval such bottlenecks are combined with a surrounding unit of the retrieval, a new unit of the retrieval dynamically retrieved. The dynamic full-text search system that proposes in this paper can dynamically make the index by the block management structure. It only records in the memory of the second location information because the location information at new added retrieval is obtained to some degree when retrieving it.

Definition 1. *The amount of the location information at each new retrieval becomes less than the amount of the location information at each combined retrieval without fail.*

The amount of the location information to unit $ID1$ of the retrieval is defined by $Pnum1$, the amount of the location information to unit $ID2$ of the retrieval is defined by $Pnum2$ and when we assume the amount of the location information to unit IDx of the newly retrieval will be define by $Pnumx$. The relation of $Pnum1$, $Pnum2$, and $Pnumx$ is shown by the following expressions:

$$Pnumx \leq \text{Minimize}(Pnum1, Pnum2)$$

This mean that the amount of the location information $Pnumx$ to the newly retrieval unit becomes below the half of the harmony of $Pnum1$ and $Pnum2$ by definition 1.

The link information record is composed by the following four fields:

$$\{RU1, RU2, Distance, Version, NewRU\}$$

Retrieval unit 1= $RU1$, Retrieval unit 2= $RU2$

$Distance$ = Retrieval distance of unit 1 and unit 2

Index version = $Version$, New retrieval unit = $NewRU$

The index version value increases when the dynamic full-text search system adds or deletes in file. So, when retrieving the newly unit the index version checked and recorded (i.e. the version value at each new retrieval are checked). As for the index, when the version is different it has to update dynamically.

Link Function *CL*

When *Version* is justified, the combination of *RUI*, *RU2* and *Distance* is defined the link function *CL* is received and return *NewRU*. When *Version* is unjustified, the combination of *RUI*, *RU2* and *Distance* is defined, the link is updated and *NewRU* is returned. When the combination of *RUI*, *RU2* and *Distance* is not defined, *NewRU* is made. *P1* and *P2* are obtained from *RUI* and *RU2* and recorded as location information.

Definition 2. The long bytes of retrieval character string are assumed to be *Blength*. For an arbitrary retrieval character string when the character string is retrieved, the Divided Retrieval Unit-set are assumed as *DRU*. The number of retrieval unit-sets *DRU* is assumed as *Unum*. The unit of each retrieval set *DRU* is assumed as *RUi* ($1 \leq i \leq Unum$), where *i* called a retrieval unit number. The long byte of each retrieval is *Rli* ($1 \leq i \leq Unum$). The area for the *Depth* value is allocated in the unit of each retrieval *RUi* ($1 \leq i \leq Unum$). The *Depth* is an addition value used when pattern matching is made. When the managed location information set is assumed to be *Pi* to unit *RUi* of each retrieval and the number of elements of *Pi* is assumed to be *Pnumi*. The element is shown *pj* ($1 \leq j \leq Pnum$), where *j* is called an element number. The threshold of speed-up (amount of the limit location information) is put with limit. The index version of the dynamic full-text search system is assumed to be *RVersion*.

Input: Retrieval character string

Output: Document name and document position including retrieval character string

4 Experimental Evaluations

4.1 Dynamic Full-Text Search System

Documents from table 3 to table 8 are about 320,000 files (198MB) from Test Collection of NACSIS for the retrieval. First of all, retrieval document evaluated to the dynamic full-text search system concerning the registration processing time and the index size when the addition batch registration is done. In Table 7, *B_Size* row shows the size of the maximum block of the adaptive block management structure on the secondary storage (i.e. the size of *LTB*). For instance, the defined block size is {2, 4, 8, 16, 32, 64, 128, 256, 512} for *B_Size* = *LTB* = 512. Moreover, the size of *LTB* in the adaptive block management structure in the first memory was fixed to block kind = 9 (*LTB* = 512 byte) regardless of *B_Size*. In the first memory 128MB was allocated in the work area as an adaptive block.

The *Map_Size* column shows the total capacity of the document that mapping to the adaptive block management structure in the memory. From Table 3, we notice that the total of a possible mapping capacity of text is about 54MB in the work area of 128MB in the memory. The *Analysis* column shows the extracted Bi-Gram from the object document and the time until the mapping is processed for the adaptive block

management structure in the first memory. The *Flash* column shows the processing time until finishing writing on the secondary storage momentarily at the time of filled the mapping area. The unit of time for *Analysis* and *Flash* is a second. The block kind of the adaptive block management structure in the first memory is fixed because most time that hangs to the amount of the movement of data according to the promotion and the demotion analysis is equal (i.e., any *B_Size* is the same). From Table 3, because of the hung time of the batch registration is 2,385 s for static full-text search system. It is clear that the batch registration speed of the dynamic full-text search system is almost equal to the static full-text search system. Table 4 shows the size of index that made by the batch registration in table 3. *I_Size* in Table 4 is capacity of the index where the location information is preserved by the adaptive block management structure. *I_Size* tends to increase because an empty area in large block size increases if *B_Size* is greatly taken.

Table 3. Batch Registration Time

| <i>B_Size</i> | 512Byte | | 4KByte | | 32KByte | |
|---------------------|-----------------|--------------|-----------------|--------------|-----------------|--------------|
| <i>Map_Size</i> | <i>Analysis</i> | <i>Flash</i> | <i>Analysis</i> | <i>Flash</i> | <i>Analysis</i> | <i>Flash</i> |
| 54 | 354 | 55 | 357 | 59 | 354 | 62 |
| 54 | 356 | 117 | 359 | 131 | 359 | 157 |
| 54 | 385 | 189 | 388 | 227 | 387 | 275 |
| 36 | 259 | 270 | 260 | 364 | 259 | 431 |
| <i>Subtotal [s]</i> | 1354 | 631 | 1364 | 781 | 1358 | 925 |
| <i>Total [s]</i> | 1,985 | | 2,145 | | 2,283 | |
| <i>Total [m]</i> | 33 | | 36 | | 38 | |
| <i>B_Size</i> | 256KByte | | 2M Byte | | 8M Byte | |
| <i>Map_Size</i> | <i>Analysis</i> | <i>Flash</i> | <i>Analysis</i> | <i>Flash</i> | <i>Analysis</i> | <i>Flash</i> |
| 54 | 356 | 65 | 357 | 64 | 354 | 65 |
| 54 | 360 | 178 | 359 | 188 | 355 | 187 |
| 54 | 386 | 308 | 385 | 316 | 387 | 310 |
| 36 | 259 | 465 | 260 | 467 | 259 | 467 |
| <i>Subtotal [s]</i> | 1360 | 1015 | 1362 | 1036 | 1356 | 1029 |
| <i>Total [s]</i> | 2,375 | | 2,398 | | 2,385 | |
| <i>Total [m]</i> | 40 | | 40 | | 40 | |

Table 4. Size of Index File Uses Proposal Technique

| <i>B_Size</i> | 512Byte | 4KByte | 32KByte | 256KByte | 2MByte | 8MByte |
|-------------------------|---------|---------|---------|----------|---------|---------|
| <i>I_Size [KB]</i> | 466,318 | 498,966 | 555,706 | 606,010 | 635,194 | 639,290 |
| <i>Use efficiency %</i> | 94.1 | 87.9 | 79.0 | 72.5 | 69.2 | 68.7 |

The use efficiency of Table 4 shows that there is no useless area of rating when the location information written in the index file. Therefore, the index file is used efficiently. However, from Table 4 we notice that *B_Size* = 512Byte or less block of the proposal technique, the index size indicates a very high value of efficiency [94.1%] with 466,318 KB (about 455 MB) of index file. Therefore, if *B_Size* = 512Byte of the proposal technique is used, it should construct a dynamic full-text search system with +5.7% index size than that of static full-text search system.

Table 5 shows the capacity of the index uses fixed length block. However, in the column of 4Kbyte or more the value of *I_Size* is big requesting a large number of blocks that is necessary from the amount of the location information retrieval.

From Table 5, it is understood that being able to achieve with the personal computer when the fixed length block is used up to size 4Kbyte of the block. The above-

mentioned experiment result to dynamic data management is proven to be a very effective method with a lot of associates like a dynamic full-text search us using Bi-Gram. When the retrieval document is adding to the dynamic full-text search system, the evaluation is concerning the registered processing time. For addition register time, about 320,000 files of Test Collection of NACSIS (about 198MB in capacity) from Table 3 has been achieved by continuously adding files.

Table 5. Size of Index File Uses Fixed Length Block Before

| Size of fixed block | 512Byte | 4KByte | 32KByte | 256KByte |
|---------------------|---------|-----------|------------|-------------|
| I_Size [KB] | 717,536 | 2,777,620 | 19,672,480 | 155,611,904 |
| Use efficiency % | 61.5 | 15.9 | 2.2 | 0.3 |

Table 6 shows the total processing time of file for each number of the adaptive block management structure in the first memory and additional registration.

Table 6. Additional Processing Time in the Memory

| Number of files | 1 | 10 | 50 | 100 | 500 | 1000 |
|---------------------|-----|-----|-----|-----|-----|------|
| Processing time [s] | 0.1 | 0.1 | 0.3 | 0.5 | 2.3 | 4.4 |

The processing time can be assumed as additional processing time for dynamic full-text search system because the retrieval service can be provided when additional processing ended in the first memory. From Table 6, the dynamic full-text search system proposes in this new experimental can achieve a very practicable real-time for addition document. The processing time is about 0.5s for 100 additional registration files.

Table 7. Deletion Processing Time

| B_Size | 1 | 10 | 50 | 100 | 500 | 1000 |
|----------|------|------|------|------|-------|------|
| 512Byte | 0.01 | 0.05 | 0.17 | 1.18 | 10.95 | 3.84 |
| 4KByte | 0.02 | 0.05 | 0.16 | 1.42 | 10.55 | 5.09 |
| 32KByte | 0.01 | 0.05 | 0.16 | 0.25 | 10.89 | 5.42 |
| 256KByte | 0.03 | 0.06 | 0.19 | 0.25 | 10.42 | 4.25 |
| 2MByte | 0.01 | 0.04 | 0.16 | 0.24 | 10.83 | 4.83 |
| 8MByte | 0.02 | 0.05 | 0.17 | 0.25 | 10.07 | 4.26 |

Table 7 shows deletion processing time when each index *B_Size* is deleted. Moreover, Table 7 shows the total deletion processing time from the file that has already been registered. Notice that, the algorithm of the deletion is decided depending on the number of deleted files regardless of *B_Size*. Moreover, this experiment proven that the speed for deletion processing is very high because the deletion of 50 files was 0.2 s or less.

5 Conclusion

Full-text search is widely used for various services of the Internet. A more high-speed and a more efficient full-text search technology are necessary because of the amount of increasing handled document and corresponding document data every day. The

update efficiency of dynamic full-text search system is very high compared with static full-text search system. So, when comparing 200MB registered document using this system speed will be about 426 times higher than static full-text search system. Moreover, the improvement of the measurement of the processing time recorded speed on the secondary storage in has improved from about 26 to 64%. This paper also presents an efficient achievement method of the dynamic full-text search system for speeding deletion processing. Future study should focus on applying this method in a large corpus and in developing this approach using identification management system.

References

1. Aoe, J., Computer Algorithms- String pattern matching, *IEEE Computer Society Press*, 1994.
2. Aho, A.V., Corasick, M.J., Efficient String Matching: An Aid to Bibliographic Search. *Communications of the ACM*, 18 (6), (1975), 333-340.
3. Baeza-Yates R. A., String Search Algorithms, Chapter 10. *Information Retrieval: Data Structure and Algorithms*. Prentice Hall, 1992.
4. Boyer, R. S. and Moore, J.S., A fast string searching algorithm, *Comm. of the ACM*, 20(10), (1977), 62-72.
5. Chen, Y., Signature files and signature trees, *Information Processing Letters*, 82, 2002, 213-221.
6. Frakes, W. B., *Information Retrieval: Data Structures and Algorithms*, Prentice Hall, Jersey, 1992.
7. Jung, M., Shishibori, M., Tanaka, Y. and Aoe, J., A dynamic construction algorithm for the Compact Patricia trie using the hierarchical structure, *Information Processing & Management*, 38 (2),(2002), 221-236.
8. Kim, J. Y. and Taylor, J., An approximate string-matching algorithm, *Theoretical Computer Science*, 92(1), (1992), 107-117.
9. Kirschenhofer, P. and Szpankowski, H., On the balance property of Patricia tries: External path length viewpoint, *Theoretical Computer Science*, 68, 1989, 1-17.
10. Knuth, D. E., Morris, J.H. and Pratt, V. R., Fast Pattern matching in strings, *SIAM Journal of Computing*, 6 (2), (1977), 323-350.
11. NACSIS Test Collection for Information Retrieval (NTCIR) Systems 1 National Center for science Information Systems, 1999.
12. Penn TreeBank Release 2, 1988-1989 Wall Street Journal articles in the Part-Of Speech Tagged Corpora, University of Pennsylvania, 1995.

Dafo, a Multi-agent Framework for Decomposable Functions Optimization

Grégoire Danoy¹, Pascal Bouvry¹, and Olivier Boissier²

¹ Faculty of Sciences, Technology and Communications
6, rue R. Coudenhove-Kalergi
L-1359 Luxembourg

{Gregoire.Danoy,Pascal.Bouvry}@uni.lu

² ENS Mines
158, cours Fauriel
F-42023 Saint-Etienne
Olivier.Boissier@emse.fr

Abstract. This paper introduces Dafo, a new multi-agent framework for evolutionary optimization relying on a competitive coevolutionary genetic algorithm, aka LCGA (Loosely Coupled Genetic Algorithm). We describe our solution, discuss of the potential advantages of using an agent based approach and present some results on a real case study: i.e. Inventory Control Parameter (ICP) optimization problem.

1 Introduction

With the increasing complexity of real world problems considered in Computer Science, multi-agent paradigm has emerged as an efficient way to analyze and implement solutions. This paradigm offers a natural way of analyzing a problem as a distributed and decentralized generation of the solution with autonomous agents having each an aspect of the global problem to solve. This characteristic drives the increasing use of those technologies within evolutionary computation where agents are equipped with genetic algorithms. Going a step further, in this paper we are interested in using the multi-agent paradigm as a tool to implement coevolutionary algorithms where agents classically communicate in a cooperative or competitive way, using a fixed strategy. However it appears that when dealing with real world and consequently dynamic problems, this strategy should also be dynamic in order to provide a good solution at any time: evolutionary algorithms must adapt to dynamic solution spaces. That is why our researches provide autonomy to the components of the evolutionary algorithms and model explicitly their strategy using agents organizations. Our research extends known work on Loosely Coupled Genetic Algorithms (LCGA) [2] by providing a development framework, Dafo, and its application to business functions. In the next section, we introduce the concept of coevolutionary algorithms, both cooperative and competitive. Section III presents in detail the multi-agent framework we have developed. We then illustrate its use in section IV with the realized experiments and discuss the obtained results. The last section contains our conclusions and perspectives.

2 Coevolutionary Algorithms

As for the “classical” genetic algorithm, the concept of coevolutionary algorithms comes from biological inspirations [3]. Similarly to nature which is composed of several species that coevolve, co-evolutionary computation extends classical genetic algorithms by considering the coevolution of subpopulations of individuals representing specific parts of the global solution. Several algorithms have been proposed. In the following, we focus on two different versions of coevolutionary genetic algorithms: LCGA and CCGA. Those two classes of algorithms are conceptually quite close and differ mainly in their structure, thus using an organizational approach is an easily understandable way of representing them.

2.1 LCGA

The Loosely Coupled Genetic Algorithm (LCGA) [2] is a medium-level parallel and distributed coevolutionary algorithm exploring a paradigm of competitive coevolution motivated by non-cooperative models of game theory. For an optimization problem described by some function (a global criterion) of N variables, local chromosome structures are defined for each variable and local subpopulations are created for each of them. A problem to be solved is first analyzed in terms of possible decomposition and relations between subcomponents that are expressed by a communication graph G_{com} , aka graph of interaction. The objectives of this function decomposition and of the definition of the interaction graph are to minimize communications while still ensuring that the fact of reaching local optima for all different players modelled as software agents in our framework (being a Nash equilibrium point) still leads to a global optimum of the initial function.

2.2 CCGA

Cooperative (also called symbiotic) coevolutionary genetic algorithms (CCGA) involve a number of independently evolving species which together form complex structures, well-suited to solve a problem. The fitness of an individual depends on its ability to collaborate with individuals from other species. In this way, the evolutionary pressure stemming from the difficulty of the problem favors the development of cooperative strategies and individuals. Potter and DeJong [4] developed a model in which a number of populations explore different decompositions of the problem. In Potter’s system, each species represents a subcomponent of a potential solution. Complete solutions are obtained by assembling representative members of each of the species (populations). The fitness of each individual depends on the quality of (some of) the complete solutions it participated in, thus measuring how well it cooperates to solve the problem. The evolution of each species is controlled by a separate, independent evolutionary algorithm. Potter’s methods have also been used or extended by other researchers, for instance Eriksson and Olsson [5] have used a cooperative coevolutionary algorithm for inventory control parameter optimization.

3 A Framework for Evolutionary Optimization

Our solution consists in providing a meta-level in the form of an agent framework dedicated to evolutionary optimization and more precisely to competitive coevolutionary genetic algorithms. Modelling the algorithm with a multi-agent system makes explicit the decomposition and resolution strategy (i.e. the interaction graph, as described in section 2.1) by using organizational models explicitly representing the roles and the interactions that are allowed for each agent. Using the agent technology also allows us to take benefit from existing multi-agent platforms and methodologies. We eventually selected the Madkit multi-agent platform [6], based on an organizational paradigm named AGR (Agent Group Role) which is part of the Aaladin methodology. The deployment and the distribution of the algorithm is thus ensured.

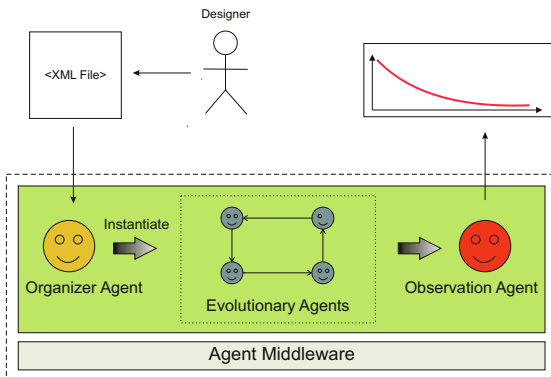


Fig. 1. Framework architecture

3.1 Agents

The system contains three different kinds of agents:

- Evolutionary Agent: run a subpopulation of individuals and optimizing its local function. After each generation, it sends the data (which type is specified in the XML file) to its neighbor in the organization and sends the best individual found to the *observer agent*.
- Organizer Agent: initializes the system using the XML file, which means instantiating the organization of *evolutionary agents* (and consequently specifying the interaction graph) and launching those agents.
- Observer Agent: in charge of evaluating, the best individuals received from each *evolutionary agent*. It logs in a file the best, worst and averaged fitness values obtained with the best of the received individuals and if required prints the corresponding graphs.

3.2 Agents Organization

As previously mentioned, we represent the interaction graph of the coevolutionary algorithms as an organization of *evolutionary agents*. Those agents can have two different roles: *Sender* or *Receiver*. According to the topology of the chosen graph, groups will be created by the *organizer agent* and each *evolutionary agents* will play a specific role in at least one of those groups. This way, using a SGA, CCGA or LCGA is just a matter of organizing identical *evolutionary agents*. Below is a very simple example of a chained list topology using the AGR notation [7]:

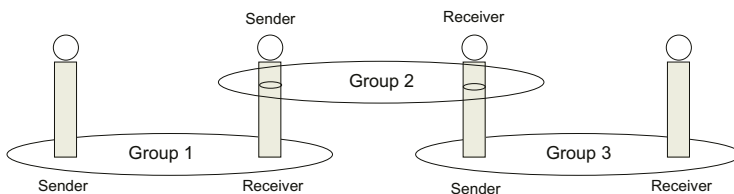


Fig. 2. Chained list as an organization

3.3 Parameters

We choose to divide the parameters that can be set in the XML file into two sections.

-Organization Parameters:

- Topology: choice of topologies according to the algorithm, complete graph (CCGA), list and ring (LCGA).
- NumberOfAgents: specifies the number of evolutionary agents that will be instantiated.
- ExchangedInformation: specifies the type of information that will be exchanged between the evolutionary agents after each generation (by default the best individual).

-G.A. Parameters:

- FitnessClass: reference to the class that provides the designer for evaluating the individuals.
- ChromosomeClass: reference to the class that has to be provided for describing the structure of a chromosome.
- Experiments, Generations, Individuals: specifies the number of experiments, generations and individuals.
- CrossoverRate, MutationRate: specifies the rates for each of those genetic operators.

For the moment we consider roulette wheel selection, 1 point crossover and bit-flip mutation.

This way, switching from one algorithm to another one is very easy. For instance, to use CCGA instead of LCGA, it is just necessary to replace *ring* in the field *topology* with *completograph* and *LCGA* in the field *algorithm* with *CCGA*. Using SGA is as simple since it requires to launch only one evolutionary agent.

4 Experiments

As a real case study, we have tested and compared our solution on the ICP (Inventory Control Parameter) problem. A complete description of this problem can be found in [5], where a classical GA is compared to four variants of CCGA approach, the latter being much more efficient. ICP objective consists in defining the couple considered as fixed OP/OQ, order point - order quantity (when and how much to order) for each stock item. Whenever it reaches the order point, which is composed of expected demand during lead time plus a safety stock, an order is released for a fixed order quantity. The total cost of a warehouse resulting from inventory decisions is evaluated through the processing of a set of customer purchase transactions chronologically ordered. This total costs is the sum of different costs: lost sales costs, transportation costs, order costs, storage space costs and order costs. In our last experiments we have also added some interdependencies between the items by adding a benefit for joint orders and joint replenishment. For each transaction processed, some actions and decisions are taken according to the inventory control parameters and the inventory levels. Transactions are processed one by one (they are chronologically ordered). We extend this work by adding a comparison to the LCGA approach and taking also into account the scalability criterion. Fixing some constraints such as initial level, maximum level, lead time, we have compared the performance of a Simple GA, a CCGA and LCGA on this ICP optimization problem. The representation used for the SGA is one individual representing all the parameters for all the items. Thus if there are 10 items in the warehouse, the chromosome will have $2 \times 10 = 20$ genes. Like for the other two evolutionary methods studied here, a chromosome is represented as a binary string (16 bits per parameter/gene). In his work, Eriksson compared four different versions of CCGA, thus we have selected the one that provides the best results. The representation used in LCGA is exactly the same as in the CCGA. Indeed, the version of LCGA we have implemented uses a ring topology where each agent optimizes the order point and order quantity for one item but under the constraint of its neighbor. To illustrate our solution, let us use a simple example with four agents and thus four different items in the stock (see fig. 3). Agent A_0 will evaluate its individuals using the best individual received from its neighbor A_3 by processing the transactions concerning its item (item 0) and its neighbor's item (item 3) and the process is the same for the other agents in the ring. When all the agents have run once their subpopulation, the global solution (consisting of the best individuals of each agent) is evaluated on the whole transaction stream. The following parameters were set for all the algorithms: population(s) size was equal to 100, $p_k = 0.6$ (crossover probability)

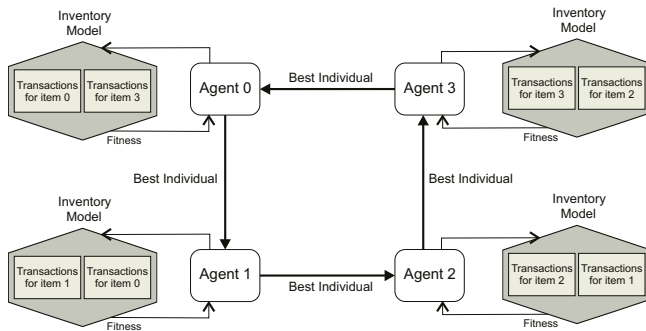


Fig. 3. ICP optimization using LCGA

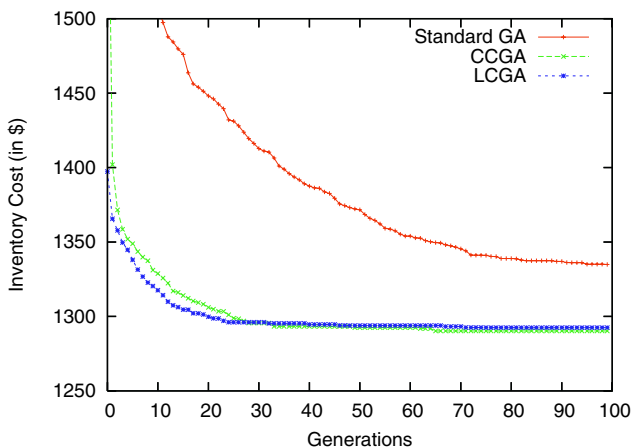


Fig. 4. Average results for the SGA, CCGA and LCGA

and $p_m = 0.05$ (mutation probability). Fig. 4 shows one result obtained with the three algorithms for 360 transactions and three types of stock items. It is clear that LCGA outperforms the SGA both in terms of speed of convergence and in the minimum cost found. Compared to CCGA, LCGA converges a bit faster and reaches the same minimum cost. We also have to take into account that the computation time for running the LCGA is much lower than for running the CCGA, thanks to less fitness function evaluations and less interactions needed for LCGA.

5 Conclusion and Perspectives

The results presented here are from ongoing research on the development of a multi-agent framework for evolutionary computation called Dafo. Initial evidence of the capabilities of our solution for solving real business problems is provided.

On the ICP optimization problem, LCGA has shown that it provides better results than a SGA and that it is close to CCGA. LCGA is also more scalable than CCGA. Indeed no global synchronization is needed and working at a meta level allows to adjust the algorithm's interaction graph according to the problem to solve. This aspect is crucial since this research work is aimed at applying its solutions to real business problems, which implies thousands of transactions with thousands of items. We also show how easy it is to switch from one implementation to another one and thus the complete agent interaction schema using Dafo. The next step in our development will consist in adding real-time management to the Dafo framework, i.e. dynamic management of the interaction graph (addition/suppression of agents, modifications of interactions, etc.). In this purpose, we now orientate our researches in the field of self-organizing and re-organizing multi-agent systems.

References

1. Danoy, G., Bouvry, P., Seredyński, F.: Agent-based optimization of business functions using coevolutionary algorithms. In Arabnia, H.R., ed.: IKE, CSREA Press (2004) 109–112
2. Seredyński, F., Zomaya, A.Y., Bouvry, P.: Function optimization with coevolutionary algorithms. In Kłopotek, M.A., Wierzbchowicz, S.T., Trojanowski, K., eds.: IIS. Advances in Soft Computing, Springer (2003) 13–22
3. Paredis, J.: Coevolutionary life-time learning. In: Parallel Problem Solving from Nature – PPSN IV, Berlin, Springer (1996) 72–80
4. Potter, M.A., De Jong, K.: A cooperative coevolutionary approach to function optimization. In: Parallel Problem Solving from Nature – PPSN III, Berlin, Springer (1994) 249–257
5. Eriksson, R., Olsson, B.: Cooperative coevolution in inventory control optimisation. In: Proc. of the Third International Conference on Artificial Neural Networks and Genetic Algorithms, University of East Anglia, Norwich, UK, Springer-Verlag (1997)
6. Gutknecht, O., Ferber, J.: Madkit: a generic multi-agent platform. In: Proc. of the fourth international conference on Autonomous agents, ACM Press (2000) 78–79
7. Ferber, J., Gutknecht, O.: Aalaadin: a meta-model for the analysis and design of organizations in multi-agent systems. In: Proc. of the Third International Conference on Multi-Agent Systems (ICMAS'98). (1998)

Parameter Space Exploration of Agent-Based Models

Benoît Calvez and Guillaume Hutzler

Université d'Evry-Val d'Essonne/CNRS
LaMI, UMR 8042
523, Place des Terrasses 91000 Evry, France
{bcalvez,hutzler}@lami.univ-evry.fr

Abstract. When developing multi-agent systems (MAS) or models in the context of agent-based simulation (ABS), the tuning of the model constitutes a crucial step of the design process. Indeed, agent-based models are generally characterized by lots of parameters, which together determine the global dynamics of the system. Moreover, small changes made to a single parameter sometimes lead to a radical modification of the dynamics of the whole system. The development and the parameter setting of an agent-based model can thus become long and tedious if we have no accurate, automatic and systematic strategy to explore this parameter space.

That's the development of such a strategy that we work on suggesting the use of genetic algorithms. The idea is to capture in the fitness function the goal of the design process (efficiency for MAS that realize a given function, realism for agent-based models, etc.) and to make the model automatically evolve in that direction. However the use of genetic algorithms (GA) in the context of ABS raises specific difficulties that we develop in this article, explaining possible solutions and illustrating them on a simple and well-known model: the food-foraging by a colony of ants.

1 Introduction

Agent-based simulation (ABS) is interested in the modelling and the simulation of complex systems. Its aim is to reproduce the dynamics of real systems by modelling the entities as agents, whose behavior and interactions are defined. A first validation of such models is obtained by comparing the resulting dynamics, when the model is simulated, with that of the real system (measured thanks to experimental data). Similarly, Multi-Agent Systems (MAS) are designed so as to accomplish a given function in a collective and decentralized way. The validation of the system is thus given by the fact that the function is realized and that it is efficient. In both cases, one of the crucial aspects of the design process lies in the tuning of the model. Indeed, this kind of model is generally characterized by lots of parameters which together determine the global dynamics of the system. The search space is thus gigantic. Moreover, the behavior of these complex systems

is often chaotic: on the one hand small changes made to a single parameter sometimes lead to a radical modification of the dynamics of the whole system; on the other hand some emergent phenomena are only produced in very specific conditions and won't occur if these conditions are not met. The solution space can thus be very small. As a consequence, the development and the parameter setting of an agent-based model may become long and tedious if we have no accurate, automatic and systematic strategy to explore the parameter space.

The approach that we suggest is to consider the problem of the development and the validation of ABS or MAS models as an optimization problem. The validation can thus be reformulated as the identification of a parameter set that optimizes some function. The optimization function for ABS would be the distance between the artificial model that we simulate and the real system. The optimization function for MAS would be the efficiency in the realization of the function. Given the large dimensionality of the problem, optimization techniques such as Genetic Algorithms (GA) can then be used to explore the parameter space and find the best parameter set with respect to the optimization function. However the use of genetic algorithms in this context is not so simple, as we will explain.

In section two we present the problematics related to the parameter tuning of an agent-based simulation. Then in section three we present the general framework of genetic algorithms and show the difficulties that arise from the application of these techniques to agent-based simulation.

2 Parameter Tuning

2.1 Parameters of Agent-Based Models

In the context of agent-based simulation, a model and the simulator with which it is executed include lots of parameters. These parameters can be of different natures. Some parameters are peculiar to the simulator: the discretization step for the modeling of time and space for instance can be a fixed feature of the simulator. As a consequence, these parameters can generally not be modified by the user. For this reason, we do not include this type of parameters in our parameter space. We only include the parameters that are specific to the model. Some of them can be extracted from the knowledge of the field (either experimental or theoretical) and can thus be associated to fixed values. Other parameters have to be kept variable, which can be for different reasons: on the one hand, the knowledge of the field is generally not exhaustive (which is the reason why we build a model and simulate it); on the other hand, this knowledge may not be directly compatible with the model. In this case, a common approach can be to try some values and simulate the model to see how it behaves globally. What we propose is to have a general approach to automate this long and tedious process.

2.2 Objective

Depending on the motivation of the modeling work, the criteria used to explore the parameter space will also be different. This motivation may be to model

and simulate a real system, but it can be to study the discrete models that may produce a given emergent phenomenon. Finally, the motivation may be to propose models that perform best in the realization of a specific function.

In the first case, we want to check if the simulated model correctly grasps the behavior of the real system. The validation of the model will thus be to have a behavior identical to (as close as possible) experimental knowledge. The search problem can be seen as the search of the parameter set that minimizes the distance between real and simulated data.

Having a similar behavior can also mean that specific emergent phenomena known to occur in a real system can be observed in the simulation. Emerging ant lines for example, will only occur if the chemical trails leaved by the ants behind them (see next paragraph) have specific properties, as we will see in next section. The emergence of this phenomenon will thus be associated to specific parameter values, and the search problem will consist in searching the different ranges of parameters where an emergent phenomenon is observable. In some cases, choosing slightly different values may lead to completely different results during the simulation, which complicates a manual exploration of the parameter space and justifies the development of automatic techniques.

2.3 Example

We will present the parameter setting of an agent-based model with the example of ant foraging (search for food), in which ants leave chemical trails behind them when coming back to the nest with food (we use the multi-agent programmable modeling environment NetLogo [1] and its "Ants" model).

In this model, two parameters condition the formation of chemical trails. The first one is the diffusion rate of the chemical, which corresponds to the fact that a given proportion of the chemical will be diffused to the neighboring patches (regions of the environment) at the next time step. This is used to simulate the diffusion of the chemical in the atmosphere. The second parameter is the evaporation rate of the chemical, which corresponds to the fact that a given proportion of the chemical will disappear from the patch at the next time step. This is used to simulate the evaporation of the chemical in the atmosphere.

For example, we can be interested more precisely in the dynamics of ant lines. Table 1 shows three models with small modifications for the two parameters. We can obtain different dynamics: the difference lies in the way that food sources are exploited. In model 1, food sources are exploited in turn while in model 3, they are all exploited at the same time. As a result, we observe one, two or three ants lines.

2.4 Previous Work

Different methods have already been proposed to explore automatically the parameter space of discrete models. In the NetLogo platform for instance, the "BehaviorSpace" [1] tool allows to explore automatically and systematically the parameter space. This space is a Cartesian product of values that each parameter can take. However when we have lots of parameters (real-valued parameters

| | Model 1 | Model 2 | Model 3 |
|------------------|---------|---------|---------|
| Diffusion rate | 40 | 50 | 60 |
| Evaporation rate | 15 | 15 | 20 |

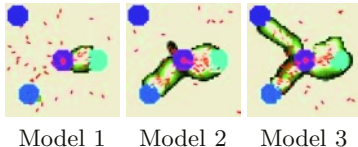


Fig. 1. Models with slightly different parameters

for example), the parameter space becomes huge and the systematic exploration becomes impossible.

Other methods have been proposed, which differentially explores the whole parameter space, focusing on the most interesting areas. That's the case of the method developed by Brueckner and Parunak [2]. They use a “parameter sweep infrastructure”, which is similar to the “BehaviorSpace” tool of NetLogo . However, to avoid a systematic exploration, they use searcher agents and introduce the fitness notion. The aim of a searcher agent is to travel in the parameter space to look for the highest fitness. Starting from a given location in the parameter space, searcher agents have two choices: move or simulate. Each agent chooses according to the confidence of the fitness estimate (proportional to the number of simulations at this point) and the value of the fitness. If it chooses to move, it heads for the neighboring region with highest fitness. A disadvantage of this method is that searcher agents may head for local fitness maxima.

3 Use of Genetic Algorithms

As the tuning of the parameters of a model is a strongly combinatorial problem, we propose to use genetic algorithms, which generally provide good results on problems of this kind.

3.1 Choice of the Fitness Function

If we consider the exploration of the parameter space as an optimization problem, we need to define very carefully the function that will have to be maximized by the algorithm. This fitness function is of fundamental importance since the models that will be selected are the one that perform best with respect to this function. In the context of agent-based simulation, the choice of the fitness function is problematic for several reasons: as a first thing, it is not the result of a computation but the dynamics of a process that has to be assessed; secondly, emergent phenomena may be difficult to characterize quantitatively since they are often related to a subjective interpretation by a human observer.

Quantitative vs. Qualitative. Validating an agent-based model by assessing the distance between the simulation and the real system can be done either quantitatively or qualitatively.

In the quantitative case, data are measured in the simulation and compared to data measured in similar conditions in the real system. The distance between

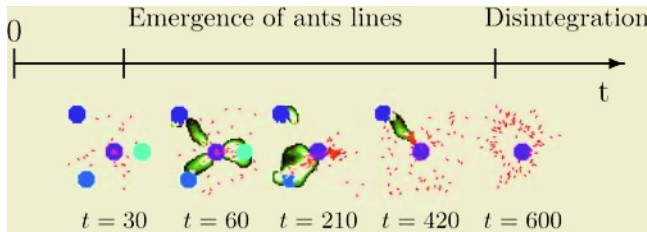


Fig. 2. Ant foraging at different time-steps

the simulation and the real system is then the Euclidean distance between the two data vectors. If we try to select models that are optimized for the realization of some function, the fitness function can also be directly measured by the performance of the system for that function.

In the qualitative case, what is important is that a given emergent phenomenon be present in the simulation: for example, the ants line. The difficulty is then to translate this observation into a quantitative measure (the fitness function). In some cases, the characterization of such emergent phenomena may not be so simple since it may be the result of a subjective interpretation by an observer, which cannot be captured easily by a quantitative measure.

A Dynamic Process. In classical optimization problem, the fitness function corresponds to the result of a computation. Therefore, the question of the time at which the measure should be made doesn't make sense: the measure is done when the computation has ended. On the contrary, agent-based simulations are dynamic processes that evolve along time and generally never end.

We can clearly see in the example given in the previous section that the evaluation of the fitness function generally has to be done at a given time-step of the simulation. The choice of this time-step is not neutral and may greatly influence the performance of the genetic algorithm and the resulting model.

Figure 2 shows the foraging simulation at five different time-steps. We can see that the ant lines are not present during all the simulation. This example shows the difficulties to choose the time-steps for the evaluation.

3.2 Computation of the Fitness Function

Time. Since no mathematical model can anticipate the dynamics of an agent-based model without executing it, the computation of the fitness function requires one or even several simulations. This means that the time required to compute the fitness function will be significant. We must therefore find methods to reduce either the number of chromosomes, the time to converge towards an optimum or the time to compute the fitness function. We mainly studied the last possibility through distributed computation and fitness approximation.

Distributed computation. Since the different models are independent from each other, the evaluation of their fitness is also independent. Therefore each evaluation of the fitness (that is to say each agent-based simulation) can be done

on a different computer. We can thus have several computers to simulate the models and use the master-slave parallel genetic algorithms [3], which improves the performance as compared to standard GA.

Fitness approximation. Fitness approximation comes to approximate the result of the simulation by a mathematical model, such as a neural network or a polynomial for instance. We tried this approach by training a neural network with test data. After the learning phase, we used it to compute the fitness, with the generation-based control approach, in which the whole population of η generations is evaluated with the real fitness function in every λ generations [4]. The results however were not so good and this approach has been temporarily abandoned. We suspect in that case that the approximation was not good enough to obtain satisfying results but this has to be explored in more details.

Stochasticity. Two agent-based simulations can generally bring slightly different results even if the underlying model is exactly the same due to the stochasticity of the model and of the simulator. One simulation is not enough to evaluate the fitness function: it can only be considered as an estimate for the fitness.

In such noisy environments, a first solution is to increase the size of the population [5]. To multiply the number of the simulated models reduces the effect of the stochasticity. A second solution is to simulate each model several times to improve the evaluation of the fitness function. Both solutions greatly increase the number of simulations, thus the time, of the genetic algorithm.

Another solution is to use the same technique as with fitness approximation. A solution to the stochasticity problem is then to estimate the fitness of each model with one simulation, and each n generations of the GA (n to choose according to the stochasticity of the model and the desired quality of the estimation), to estimate the fitness of each model with x simulations.

We use the elitism genetic algorithm [6] that is to say we keep the best chromosomes during the algorithm, which allows to continuously improve the solution. Our implemented genetic algorithm replace only 25 % of the population at each generation. Every 3 generations, we estimate the fitness of the models with more simulations. The interest to choose these values is to keep always the best chromosomes.

4 Discussion and Conclusion

We applied the method to some simple examples: the ant foraging with different fitness functions (both quantitative and qualitative). We do not show the results because of the lack of space. As we could already see with the study of the stochasticity, we obtained very different results depending on the choice of the fitness function. The models are strongly optimized for a specific fitness function and may not perform so well with another one. The optimization creates a loss of the flexibility of the dynamics of the agent-based model. A possible solution would be to use several different initial conditions to evaluate the fitness function. This would however increase again the time necessary to run the algorithm.

The optimization by the genetic algorithm also depends on the constraints imposed to the agents in the model. If a model has lots of constraints (fewer resources for example), it is necessary that it optimizes its global functioning. On the contrary, if the resources are abundant, the pressure on the model to adapt and optimize its functioning will be weaker. As a result, the use of our approach will be mostly beneficial when constraints on the model are high.

The next step is to apply the method to a more complex example. We began a work for the simulation of the glycolysis and the phosphotranferase systems in Escherichia coli. In this work, we are interested in testing the hypothesis of hyperstructures [7]. The hyperstructures are dynamic molecular complexes, enzyme complexes in the case of this work. These complexes allow to improve the behavior of a cell : more flexibility, quicker adaptation. In our study, we have 25 kinds of molecules (or agents). There are altogether about 2200 agents in the simulation. We want to study the potential interest of hyperstructures for the cell. To do this we make the rates of enzymes association and dissociation variable. In this context, the simulation of a model lasts about 10 minutes, which imposes to use the methods described in this article like the distributed computation. To explore this complex example, we will need to develop additional strategies to reduce the parameter space (e.g. by introducing coupling between parameters), to accelerate the evaluation of the fitness function (e.g. by developing approximation methods), and to accelerate the convergence of the algorithm (e.g. by using interactive evolutionary computation). Finally, another important perspective is to explore the effect of varying dynamically the simulation conditions so as to produce more versatile models.

References

1. Tisue, S., Wilensky, U.: Netlogo: Design and Implementation of a Multi-Agent Modeling Environment. Proceedings of Agent 2004 (2004)
2. Brueckner, S., Parunak, H.V.D.: Resource-Aware Exploration of the Emergent Dynamics of Simulated Systems. AAMAS 2003 (2003) 781–788
3. Cant-Paz, E., Goldberg, D.E.: Efficient parallel genetic algorithms: theory and practice. Computer Methods in Applied Mechanics and Engineering **186** (2000)
4. Jin, Y., Olhofer, M., Sendhoff, B.: A Framework for Evolutionary Optimization with Approximate Fitness Functions. IEEE Transactions on Evolutionary Computation **6** (2002) 481–494
5. Goldberg, D.E., Deb, K., Clark, J.H.: Genetic algorithms, noise, and the sizing of populations. Complex System **6** (1992)
6. Beker, T., Hadany, L.: Noise and elitism in evolutionary computation. In: Soft Computing Systems - Design, Management and Applications. (2002) 193–203
7. Amar, P., Bernot, G., Norris, V.: Modelling and Simulation of Large Assemblies of Proteins. Proceedings of the Dieppe spring school on Modelling and simulation of biological processes in the context of genomics (2002) 36–42

Efficient Pre-processing for Large Window-Based Modular Exponentiation Using Ant Colony

Nadia Nedjah and Luiza de Macedo Mourelle

Faculty of Engineering, State University of Rio de Janeiro,
Rua São Francisco Xavier, 524, Maracanã,
Rio de Janeiro, RJ, Brazil
`{nadia,ldmm}@eng.uerj.br`
<http://www.eng.uerj.br/ldmm/index.html>

Abstract. Modular exponentiation is the main operation to RSA-based public-key cryptosystems. It is performed using successive modular multiplications. This operation is time consuming for large operands, which is always the case in cryptography. For software or hardware fast cryptosystems, one needs thus reducing the total number of modular multiplications required. Existing methods attempt to reduce this number by partitioning the exponent in constant or variable size windows. However, these window-based methods require some pre-computations, which themselves consist of modular exponentiations. It is clear that pre-processing needs to be performed efficiently also. In this paper, we exploit the ant colony strategy to finding an optimal addition sequence that allows one to perform the pre-computations in window-based methods with a minimal number of modular multiplications. Hence we improve the efficiency of modular exponentiation. We compare the yielded addition sequences with those obtained using Brun's algorithm.

1 Introduction

Public-key cryptographic systems (such as the RSA encryption scheme [7]) often involve raising large elements of some groups fields (such as $\text{GF}(2^n)$ or elliptic curves) to large powers. The performance and practicality of such cryptosystems is primarily determined by the implementation efficiency of the modular exponentiation. As the operands (the plain text of a message or the cipher (possibly a partially ciphered) are usually large (i.e. 1024 bits or more), and in order to improve time requirements of the encryption/decryption operations, it is essential to attempt to minimise the number of modular multiplications performed.

A simple procedure to compute $C = T^E \bmod M$ is based on the paper-and-pencil method. This method requires $E-1$ modular multiplications. It computes all powers of $T : T \rightarrow T^2 \rightarrow \dots \rightarrow T^{E-1} \rightarrow T^E$. The computation of exponentiations using this method is very inefficient. The problem of yielding the power of a number using a minimal number of multiplications is NP -hard [2]. There are several efficient algorithms that perform exponentiation with a nearly minimal number of modular multiplications, such that the window-based methods.

However, these methods need some pre-computations that if not performed efficiently can deteriorate the algorithm overall performance. The pre-computations are themselves an ensemble of exponentiations and so it is also NP -hard to perform them optimally. In this paper, we concentrate on this problem and engineer a new way to do the necessary pre-computations very efficiently. We do so using the ant colony methodology. We compare our results with those obtained using the Brun's algorithm [5].

In this paper, we exploit the ant colony methodology to obtain an optimal solution to addition chain minimisation NP -complete problem. In order to clearly report the research work performed, we subdivide the rest of this paper into five important sections. In Section 2, we present the window methods; In Section 3, we present the concepts of addition chains and sequence and they can be used to improve the pre-computations of the window methods; In Section 4, we give an overview on ant colony concepts; In Section 5, we explain how these concepts can be used to compute a minimal addition chain to perform efficiently necessary pre-computations in the window methods. In Section 6, we present some useful results.

2 Window-Based Methods

Generally speaking, the window methods for exponentiation [4] may be thought of as a three major step procedure: (i) partitioning in k -bits windows the binary representation of the exponent E ; (ii) pre-computing the powers in each window one by one; (iii) iterating the squaring of the partial result k times to shift it over, and then multiplying it by the power in the next window when if window is not 0.

There are several partitioning strategies. The window size may be constant or variable. For the m -ary methods, the window size is constant and the windows are next to each other. On the other hand, for the sliding window methods the window size may be of variable length. It is clear that zero-windows, i.e. those that contain only zeros, do not introduce any extra computation. So a good strategy for the sliding window methods is one that attempts to maximise the number of zero-windows.

The m -ary methods [4] scans the digits of E from the less significant to the most significant digit and groups them into partitions of equal length $\log_2 m$, where m is a power of two. Note that 1-ary methods coincides with the square-and-multiply well-known binary exponentiation method.

In general, the exponent E is partitioned into p partitions, each one containing $l = \log_2 m$ successive digits. The ordered set of the partition of E will be denoted by $\mathbb{P}(E)$. If the last partition has less digits than $\log_2 m$, then the exponent is expanded to the left with at most $\log_2 m - 1$ zeros.

For the sliding window methods the window size may be of variable length and hence the partitioning may be performed so that the number of zero-windows is as large as possible, thus reducing the number of modular multiplication necessary in the squaring and multiplication phases. Furthermore, as all possible

partitions have to start (i.e. in the right side) with digit 1, the pre-processing step needs to be performed for odd values only.

In adaptive methods [4] the computation depends on the input data, such as the exponent E . M -ary methods and window methods pre-compute powers of all possible partitions, not taking into account that the partitions of the actual exponent may or may not include all possible partitions. Thus, the number of modular multiplications in the pre-processing step can be reduced if partitions of E do not contain all possible ones.

3 Addition Chains and Addition Sequences

An *addition chain* of length l for an positive integer N is a list of positive integers (E_1, E_2, \dots, E_l) such that $E_1 = 1$, $E_l = N$ and $E_k = E_i + E_j$, $0 \leq i \leq j < k \leq l$. Finding a minimal addition chain for a given positive integer is an NP -hard problem. It is clear that a short addition chain for exponent E gives a fast algorithm to compute $T^E \bmod M$ as we have if $E_k = E_i + E_j$ then $T^{E_k} = T^{E_i} \times T^{E_j}$. The adaptive window methods described earlier use a near optimal addition chain to compute $T^E \bmod M$. However these methods do not prescribe how to perform the pre-processing step of the adaptive method. In the following we show how to perform this step with minimal number of modular multiplications.

There is a generalisation of the concept of addition chains, which can be used to formalise the problem of finding a minimal sequence of powers that should be computed in the pre-processing step of the adaptive window method.

An *addition sequence* for the list of positive integers V_1, V_2, \dots, V_p such that $V_1 < V_2 < \dots < V_p$ is an addition chain for integer V_p that includes all the integers V_1, V_2, \dots, V_p . The length of an addition sequence is the numbers of integers that constitute the chain. An addition sequence for a list of positive integers V_1, V_2, \dots, V_p will be denoted by $\xi(V_1, V_2, \dots, V_p)$.

Hence, to optimise the number of modular multiplications needed in the pre-processing step of the adaptive window methods for computing $T^E \bmod M$, we need to find an addition sequence of minimal length (or simply minimal addition sequence) for the values of the partitions included in the non-redundant ordered list $\wp(E)$. This is an NP -hard problem and we use genetic algorithm to solve it. Our method showed to be very effective for large window size.

4 Ant Systems and Algorithms

Ant systems can be viewed as multi-agent systems [1] that use a shared memory through which they communicate and a local memory to book-keep the locally reached problem solution. Throughout the paper, we will uses A_i and LM_i to represent the i^{th} . agent of the ant system and its local memory respectively. Mainly, the shared memory (SM) holds the pheromone information while the local memory LM_i keeps the solution (possibly partial) that agent A_i reached so far.

Let N , C and SM be the number of artificial ants that form the colony, the characteristics of the expected solution and the shared memory used by the artificial ants to store pheromone information respectively. The behaviour of an artificial ant colony is summarised in the following: The first step consists of activating N distinct artificial ants that should work in simultaneously. Every time an ant conclude its search, the shared memory is updated with an amount of pheromone, which should be proportional to the quality of the reached solution. This called *global* pheromone update. When the solution yield by an ant's work is suitable (i.e. fits characteristics C) then all the active ants are stopped. Otherwise, the process is iterated until an adequate solution is encountered.

The behaviour of an artificial ant can be described as follows: First, the ant computes the probabilities that it uses to select the next state to move to. The computation depends on the solution built so far, the problem constraints as well as some heuristics. Thereafter, the ant updates the solution stored in its local memory, deposits some *local* pheromone into the shared memory then moves to the chosen state. This process is iterated until complete problem solution is yielded.

5 Chain Sequence Minimisation Using Ant System

In this section, we concentrate on the specialisation of the ant system of Algorithm 1 to the addition sequence minimisation problem. Previous work on minimisation of addition and Addition-Subtraction chains using ant colonies can be found in [6]. Subsequently, we describe how the shared and local memories are represented. We then detail the function that yields the solution (possibly partial) characteristics. Thereafter, we define the amount of pheromone to be deposited with respect to the solution obtained so far. Finally, we show how to compute the necessary probabilities and make the adequate decision towards a shorter addition sequence for the considered the sequence (V_1, V_2, \dots, V_p) .

5.1 The Ant System Shared Memory

The ant system shared memory is a two-dimension array. If the last exponent in the sequence is V_p then the array should V_p rows. The number of columns depends on the row. It can be computed as in Eq. 1, wherein NC_i denotes the number of columns in row i .

$$NC_i = \begin{cases} 2^{i-1} - i + 1 & \text{if } 2^{i-1} < V_p \\ 1 & \text{if } i = V_p \\ V_p - i + 3 & \text{otherwise} \end{cases} \quad (1)$$

An entry $SM_{i,j}$ of the shared memory holds the pheromone deposited by ants that used exponent $i+j$ as the i th. member in the built addition sequence. Note that $1 \leq i \leq V_p$ and for row i , $0 \leq j \leq NC_i$. The exponent $E_{i,j}$ corresponding

to entry $SM_{i,j}$ should be obtainable from exponents of previous rows. Eq. 2 formalises such a requirement.

$$E_{i,j} = E_{k_1, l_1} + E_{k_2, l_2} \mid 1 \leq k_1, k_2 < i, 0 \leq l_1, l_2 \leq j, k_1 = k_2 \iff l_1 = l_2 \quad (2)$$

5.2 The Ant Local Memory

In an ant system, each ant is endowed a local memory that allows it to store the solution or the part of it that was built so far. This local memory is divided into two parts: the first part represents the (partial) addition sequence found by the ant so far and consists of a one-dimension array of V_p entries; the second part holds the *characteristic* of the solution. It represents the solution fitness i.e., its length. The details of how to compute the fitness of a possibly partial addition sequence are given in the next section.

5.3 Addition Sequence Characteristics

The fitness evaluation of an addition sequence is performed with respect to three aspects: (a) how much it adheres to the definition (see Section 3), i.e. how many of its members cannot be obtained summing up two previous members of the sequence; (b) how far the it is reduced, i.e. what is the length of the chain; (c) how many of the mandatory exponents do not appear in the sequence. Eq. 3 shows how to compute the fitness f of solution $(E_1, E_2, \dots, E_n, 0, \dots, 0)$ regarding mandatory exponents V_1, V_2, \dots, V_p .

$$f(V_1, V_2, \dots, V_p, E_1, E_2, \dots, E_n) = \frac{V_p \times (n - 1)}{E_n} + (\eta_1 + \eta_2) \times \text{penalty} \quad (3)$$

wherein η_1 represents the number of E_i , $3 \leq i \leq n$ in the addition sequence that verify the predicate $\forall j, k \mid 1 \leq j, k < i, E_i \neq E_j + E_k$ and η_2 represents the number of mandatory exponents V_i , $1 \leq i \leq p$ that verify the predicate $V_i \leq E_n \implies \forall j \mid 1 \leq j \leq n, E_j \neq V_i$.

For a valid complete addition sequence, the fitness coincides with its length, which is the number of multiplications that are required to compute the exponentiation using the sequence. For a valid but incomplete addition sequence, the fitness consists of its *relative* length. It takes into account the distance between last mandatory exponent V_p and the last exponent in the partial addition sequence. Furthermore, for every mandatory exponent that is smaller than the last member of the sequence which is not part of it, a penalty is added to the sequence fitness. Note that valid incomplete sequences may have the same fitness of some other valid and complete ones. For instance, addition sequence $(1, 2, 3, 6, 8)$ and $(1, 2, 3, 6)$ for exponent mandatory exponents $(3, 6, 8)$ have the same fitness 4.

For an invalid addition sequences, a penalty, which should be larger than V_p , is introduced into the fitness value for each exponent for which one cannot find two (may be equal) members of the sequence whose sum is equal to the exponent

in question or two distinct previous members of the chain whose difference is equal to the considered exponent. Furthermore, a penalty is added to the fitness of a addition sequence whenever the a mandatory exponent is not part of it.

5.4 Pheromone Trail and State Transition Function

There are three situations wherein the pheromone trail is updated: (a) when an ant chooses to use exponent $F = i + j$ as the i th. member in its solution, the shared memory cell $SM_{i,j}$ is incremented with a constant value of pheromone $\Delta\phi$; (b) when an ant halts because it reached a complete solution, say $\alpha = (E_1, E_2, \dots, E_n)$ for mandatory exponent sequence σ , all the shared memory cells $SM_{i,j}$ such that $i + j = E_i$ are incremented with pheromone value of $1/Fitness(\sigma, \alpha)$. Note that the better is the reached solution, the higher is the amount of pheromone deposited in the shared memory cells that correspond to the addition sequence members. (c) The pheromone deposited should evaporate. Periodically, the pheromone amount stored in $SM_{i,j}$ is decremented in an exponential manner [1].

An ant, say A that has constructed partial addition sequence $(E_1, E_2, \dots, E_i, 0, \dots, 0)$ for exponent sequence (V_1, V_2, \dots, V_p) , is said to be in *step i*. In step $i+1$, it may choose exponent $E_{i+1} | E_i+1, E_i+2, \dots, 2E_i$, if $2E_i \leq V_p$. That is, ant A may choose one of the exponents that are associated with the shared memory cells $SM_{i+1, E_i-i}, SM_{i+1, E_i-i+1}, \dots, SM_{i+1, 2E_i-i-1}$. Otherwise (i.e. if $2E_i > V_p$), it may only select from exponents $E_i+1, E_i+2, \dots, E+2$. In this case, ant A may choose one of the exponent associated with $SM_{i+1, E_i-i}, SM_{i+1, E_i-i+1}, \dots, SM_{i+1, E_i-i+1}$.

6 Performance Comparison

The ant system described in Algorithm 1 was implemented using Java as a multi-threaded ant system. Each ant was simulated by a thread that implements the artificial ant computation described earlier. A Pentium IV-HTTM of a operation frequency of 1GH and RAM size of 2GB was used to run the ant system and obtain the performance results.

We compared the performance of m -ary methods, the Brun's algorithm, genetic algorithms and ant system-based methods. The average lengths of the addition sequences for different exponent sequences obtained using these methods are given in Table 1. The exponent size is that of its binary representation (i.e. number of bits). The ant system-based method always outperforms all the others, including the genetic algorithm-based method [5].

7 Conclusion

In this paper we applied the methodology of ant colony to the addition chain minimisation problem. Namely, we described how the shared and local memories

Table 1. Average length of addition sequence for Brun's algorithm, genetic algorithms and ant system-based methods

| size of V_p | Brun's | Genetic | Ants |
|---------------|--------|---------|------|
| 64 | 84 | 85 | 86 |
| 128 | 169 | 170 | 168 |
| 256 | 340 | 341 | 331 |
| 512 | 681 | 682 | 658 |

are represented. We detailed the function that computes the solution fitness. We defined the amount of pheromone to be deposited with respect to the solution obtained by an ant. We showed how to compute the necessary probabilities and make the adequate decision towards a good addition chain for the considered exponent. We implemented the ant system described using multi-threading (each ant of the system was implemented by a thread). We compared the results obtained by the ant system to those of m -ary methods (binary, quaternary and octal methods). Taking advantage of the a previous work on evolving minimal addition chains with genetic algorithm, we also compared the obtained results to those obtained by the genetic algorithm. The ant system always finds a shorter addition chain and gain increases with the size of the exponents.

References

1. Dorigo, M. and Gambardella, L.M., Ant Colony: a Cooperative Learning Approach to the Travelling Salesman Problem, IEEE Transaction on Evolutionary Computation, Vol. 1, No. 1, pp. 53-66, 1997.
2. Downing, P. Leong B. and Sthi, R., Computing Sequences with Addition Chains, SIAM Journal on Computing, vol. 10, No. 3, pp. 638-646, 1981.
3. Feber, J., Multi-Agent Systems: an Introduction to Distributed Artificial Intelligence, Addison-Wesley, 1995.
4. Nedjah, N., Mourelle, L.M., Efficient Parallel Modular Exponentiation Algorithm, Lecture Notes in Computer Science, Springer-Verlag, vol. 2457, pp. 405-414, 2002.
5. Nedjah, N. and Mourelle, L.M., Minimal addition-subtraction chains using genetic algorithms, Lecture Notes in Computer Science, Springer-Verlag, vol. 2457, pp. 303-313, 2002.
6. Nedjah, N. and Mourelle, L.M., Minimal Addition-Subtraction Chains with Ant Colony, Proceedings of 11th. International Conference on Neural Information Processing, Lecture Notes in Computer Science, Springer-Verlag, vol. 3316, pp. 1082-1087, 2004.
7. Rivest, R., Shamir, A. and Adleman, L., A method for Obtaining Digital Signature and Public-Key Cryptosystems, Communications of the ACM, 21:120-126, 1978.

COSATS, X-COSATS: Two Multi-agent Systems Cooperating Simulated Annealing, Tabu Search and X-Over Operator for the K-Graph Partitioning Problem

Moez Hammami and Khaled Ghédira

Unité de recherche stratégies d'optimisation de l'information et de la connaissance (SOIE)
41 Rue de la liberté-Cité Bouchoucha-2000 Le Bardo-Tunisie
moez.hammami@ipeit.rnu.tn, khaled.ghedira@isg.rnu.tn

Abstract. In this paper we propose two multi-agent systems gathering several metaheuristics for the K-Graph Partitioning Problem(K-GPP). In the first model COSATS, two metaheuristic agents, namely Tabu Search and Simulated Annealing run simultaneously to solve the K-GPP. These agents are mutually guided during their search process by means of a new mechanism of information exchange based on statistical analysis of search space. In the second model X-COSATS, a crossover agent is added to the model in order to make a cross-over between the local optima found by simulated annealing and tabu agents. COSATS and X-COSATS are tested on several large graph benchmarks. The experiments demonstrated that our models achieve partitions with significantly higher quality than those generated by simulated annealing and tabu search operating separately

1 Introduction

The k-Graph Partitioning Problem (k-GPP) consists in partitioning the set of graph vertices into k disjoint subsets so as to minimize the total weight of the edges connecting vertices in distinct subsets and to have subsets with nearly the same total weight of the vertices. This problem known to be NP-hard arises in many important scientific and engineering problems. In recent years much attention has been focused on developing specific heuristic methods, or adapting well-known metaheuristics. A comparison between these two approaches shows the superiority of specific heuristics particularly when they use multilevel techniques. In fact, Kernighan and Lin heuristic combined with the multilevel technique is one of the fastest available techniques [8]. Many works tried to adapt metaheuristics like tabu search [6], simulated annealing [5], ant colonies [1] and genetic algorithms [7]. These methods proved successful for graphs with limited number of vertices, generally not exceeding 500. Some works tried to enhance metaheuristics by using multi-level techniques [9], they succeeded to generate high quality partitions for large graphs.

In this paper we propose a new approach aiming to increase the capacity of metaheuristics to solve large instances of graph partitioning problem. In the basic model COSATS (for COoperation model between Simulated Annealing and Tabu Search), the idea consists in making simulated annealing and tabu search cooperate within a multi-agent system. Each agent offers its proper experience about the search-space landscape. This information is exploited by means of penalties added to some components of the solution. This landscape distortion aims to propel the search towards new

promising regions. In the second model X-COSATS (for X-over with COSATS) a crossover agent is added to the model. Its role consists in making a crossover between the local optima found by simulated annealing and tabu agents. The resulting offspring is used as initial solutions for the search agents. Also the crossover agent has to face the problem of symmetry characterizing the search-space landscape of the graph partitioning problem. The experiments demonstrated that our models achieve partitions with significantly higher quality than those generated by simulated annealing and tabu search operating separately. The remainder of the paper is presented as follows. Sections 2 and 3 are devoted to our three cooperation models. Section 4 presents an empirical evaluation of our models. We conclude by discussing the considerable promise of using our approach in combinatorial optimization.

2 COSATS

In this model, two metaheuristic agents, namely tabu search and simulated annealing, run simultaneously using respectively tabu search and simulated annealing algorithms to solve the K-GPP. During the search process, each metaheuristic agent computes frequencies of some events characterizing the best solutions encountered. When an agent terminates its search, it sends the collected frequencies accompanied with the best solution to the other agent. The receiver uses these frequencies to modify the cost of some graph edges, and then it proceeds with another search cycle using the penalized graph. The process is repeated for a fixed number of cooperative cycles. The aim is to propel the new search towards promising regions.

2.1 How Does Metaheuristic Agent Collect Information? (Local Frequencies Memorizing)

During the search process, each metaheuristic agent computes the frequencies of some events characterizing the best solutions it visits. In graph partitioning, we define an event as a couple (edge, state). A state can take two values; external or internal. A feasible solution can be expressed as a set of events. When a metaheuristic agent reaches its termination criterion, it computes the frequency of each event in a given number of best solutions encountered. After computing its local frequencies, each metaheuristic agent sends this information to the other agent. The latter combines this information to its local frequencies and uses the resulting information to guide its search procedure during the next iteration. This process is detailed in the next paragraph.

2.2 How Does Metaheuristic Agent Exploit Frequency Information?

When an agent receives frequencies it proceeds in four steps:

Step 1: Average Frequency Computing

For each event, the agent computes the average frequencies between both received and local frequencies.

Step 2: Edge Labelling

Considering frequencies computed in step 1, when an edge has a high frequency of being external (respectively internal), it will be assigned the label "Strongly external"(respectively internal). When the frequency of being external (respectively internal) is slightly superior to 50%, it will be assigned the label "weakly external" (respectively internal).

Step 3: Edge-Cost Modifying

In order to preserve the common characteristics of the best solutions, the agent increases the cost of strongly internal edges. These edges will have more chance to remain internal. The agent also decreases the cost of strongly external edges, giving them more chance to remain external. The penalization of the cost of the edge is done proportionally to its frequency as follows:

For the strongly internal edges:

(1)

$$\text{newCost}(E) = \text{oldCost}(E) * (1 + \text{frequencyInternal}(E))$$

For the strongly external edges:

(2)

$$\text{newCost}(E) = \text{oldCost}(E) * (1 - \text{frequencyExternal}(E))$$

Step 4: New Guided Search

Let S1 be the received best solution and S2 be the local best solution. The agent selects the best from S1 and S2 and uses it as starting point for the next search process. It is useful to remind that the new search will work on the penalized graph. The resulting distortion in the landscape aims to conduct the search towards regions having the common characteristics of best solutions.

3 X-COSATS: COSATS with a X-Over Operator

In this model, the cooperation between simulated annealing and Tabu search within COSATS is extended by introducing a crossover agent. The latter makes a crossover between the two solutions received from the tabu and the simulated annealing agents and sends the offspring back to these agents. A classical operator such as a two point crossover gives poor results, this is due to the search space symmetry in partitioning problems described in [10]. The authors in [10] have proposed a preprocessing phase, which breaks the search space symmetry in partitioning problems and applied it successfully to the graph-coloring problem. The idea consists in finding the mapping between the subsets of the two parents, which maximizes the similarity between their respective chromosomes. Our adaptation of this technique to the k-GPP is given in the following subsection. Concerning the crossover operator used by the x-over agent, it is a new variant of the Greedy Procedure X-over (GPX) proposed in [4], which gave good results for graph coloring. This new operator is presented in section 3.2.

3.1 Avoiding Search Space Symmetry

In order to avoid the search space symmetry during crossover, we must rename the subsets of one of the parents in a way that similarities between the chromosomes is maximized.

Let A and B be two k-GPP solutions. The bijection $\tau : \{1..k\} \times \{1..k\}$, is defined as a mapping between the subsets of the solutions A and B. Let m_{ij}^{AB} be the number of common vertices between the subsets i of solution A and subset j of solution B. The similarity between two solutions A and B relatively to a mapping τ is defined as: $s(A, B, \tau) = \sum_i m_{i\tau(i)}^{AB}$. In order to find the mapping τ_{max} for which $s(A, B, \tau_{max})$ is maximal, a refining matrix is used. Each element with coordinates (i,j) of the refining matrix contains the value of m_{ij}^{AB} . Its useful to note that for the k-GPP there are $k!$ possible mappings between two solutions. This number becomes huge when k exceeds 12, so we used a heuristic to find an approximate mapping τ_{max} . Given two solutions A and B and a corresponding refining matrix, The heuristic consists in generating a big number of random mappings τ_i and then $s(A, B, \tau_i)$ is computed for each mapping using the refining matrix. The mapping τ_{max} generating the maximal value for $s(A, B, \tau_i)$ is selected. It is useful to note that a metaheuristic like simulated annealing can also be used to find better τ_{max} .

3.2 The Crossover Operator

The crossover used is a variant of the Greedy Procedure crossover (GPX) originally designed for the graph coloring [4]. Given two parent chromosomes: $S_1 = \{V_1^1, V_2^1, \dots, V_k^1\}$ and $S_2 = \{V_1^2, V_2^2, \dots, V_k^2\}$ with: V_i^l is the set of vertices belonging to the subset i in chromosome S_l , the algorithm builds an offspring $S = \{V_1, V_2, \dots, V_k\}$ as follows:

The New Greedy Procedure X-Over for the K-GPP

```

1   Begin
2     chromosome_Size := |V11| + |V21| + .. + |Vk1|
3     l := 1
4     while |V11| + |V21| + .. + |Vk1| < chromosome_Size do
5       if l is odd then A := 1 else A := 2 /* consider S1 or S2 */
6       if l = 1 then choose i such that ViA has the minimal communication
          weight
7         Else choose i such that ViA has a maximum cardinality
8         Vi := Vi ∪ ViA
9         remove the vertices of ViA from S1 and S2
10        l := l+1
11      end do
12    /* Balance the subsets weight */

```

```

13   while  $\max\{V_1, |V_2|, \dots, |V_k|\} - \min\{V_1, |V_2|, \dots, |V_k|\} > 1$  do
14     move a vertex from  $V_{\max}$  to  $V_{\min}$ 
15   end do
16 /*  $V_{\max}$  and  $V_{\min}$  are the subsets with maximum and minimum cardinalities */
17 end

```

In order to obtain the second offspring, we replace *odd* by *even* in line 5, this allows the algorithm to begin copying from parent 2.

4 Experimentation

COSATS and X-COSATS were implemented in Actalk [2], which is an actor layer on Smalltalk 80, providing asynchronous running of several agents and a message exchange between them. In this section COSATS is compared to simulated annealing and tabu search algorithms when they work separately in parallel. Then, we present a comparison between COSATS and X-COSATS. The benchmark graphs used in our experiments are taken from the graph partitioning archive (www.gre.ac.uk/~c.walshaw/partition/). The used graphs are: add20(2395 vertices, 7462 edges), data(2851 vertices, 15093 edges), 3elt(4720 vertices, 13722 edges), uk(4824 vertices, 6837 edges) and add32(4960 vertices, 9462 edges).

4.1 COSATS Versus Simulated Annealing and Tabu Search

We partitioned each graph into four and eight balanced subsets ($k = 4$, $k = 8$). We notice that tabu search and simulated annealing are given the same parameters when they evolve in cooperation or separately. As a result the running times are almost the same. The results of our experiments are shown in Table 1, where COSATS is compared to simulated annealing and tabu search with equal CPU times. Table 1 shows that COSATS performed very well compared to simulated annealing and tabu search for all the benchmarks. Moreover results of simulated annealing or Tabu search when they cooperate are always better than their results without cooperation.

Table 1. COSATS versus Simulated Annealing and Tabu Search ($k = 4$ and $k = 8$)

| Graph | COSATS | | Simulated annealing within COSATS | | Tabu search within COSATS | | Simulated annealing | | Tabu search | |
|-------|--------|------|-----------------------------------|------|---------------------------|------|---------------------|------|-------------|------|
| | 4P | 8P | 4P | 8P | 4P | 8P | 4P | 8P | 4P | 8P |
| add20 | 1354 | 1960 | 1363 | 1981 | 1354 | 1960 | 1630 | 2111 | 1696 | 2145 |
| data | 501 | 899 | 554 | 1009 | 501 | 899 | 714 | 1065 | 604 | 902 |
| 3elt | 295 | 499 | 307 | 551 | 295 | 499 | 444 | 860 | 295 | 528 |
| uk | 178 | 238 | 216 | 277 | 178 | 238 | 296 | 431 | 217 | 283 |
| add32 | 175 | 280 | 195 | 300 | 175 | 280 | 283 | 561 | 435 | 638 |

Figure 1 shows the evolution of the search results in time for the algorithms; tabu search with cooperation, simulated annealing with cooperation, classic tabu search

and classic simulated annealing on *add20* graph for 4-GPP. The results of classic tabu search and simulated annealing algorithms become constant after reaching modest optima, however cooperating simulated annealing and tabu search continue to improve their results, reaching optima with considerable lower costs.

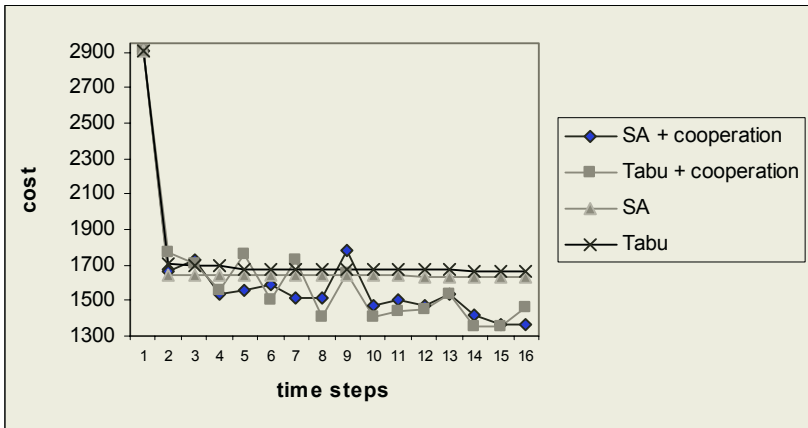


Fig. 1. A comparative analysis of the search evolution

4.2 Comparison Between COSATS and X-COSATS

Table 2 shows the results of COSATS and X-COSATS for 4-GPP and 8-GPP cases. We observe that X-COSATS performed better than COSATS for the add20, and uk benchmarks (4-GPP) and for add20, data, uk benchmarks (8-GPP). It fails to outperform COSATS in the other cases.

Table 2. Evaluation of COSATS, X-COSATS

| Graph | COSATS | | X-COSATS | |
|-------|--------|------|----------|------|
| | 4P | 8P | 4P | 8P |
| add20 | 1354 | 1960 | 1262 | 1900 |
| data | 501 | 899 | 575 | 831 |
| 3elt | 295 | 499 | 334 | 514 |
| uk | 178 | 238 | 173 | 217 |
| add32 | 175 | 280 | 246 | 283 |

5 Conclusions

In this paper we proposed two cooperation models, gathering several metaheuristics. Simulated annealing and tabu search agents cooperate within COSATS increasing their capacity to solve large instances of graph partitioning problem. A crossover agent taking into consideration the problem of symmetry in partitioning problems has increased the effects of cooperation in X-COSATS. Our models are very promising and need to be thoroughly investigated. Adding an intensification agent based on a local search method seems to be useful to intensify the search around the solutions

found by the search agents. The duplication of search agents and the integration of other metaheuristics should increase the effects of cooperation.

References

1. Alaya, I., Sammoud, O., Hammami, M., Ghedira, K.: Ant Colony Optimization for the k-Graph Partitioning Problem. In: 4th Tunisia-Japan Symposium on Science and Technology TJASST'03, Tunisia (2003)
2. Briot, J-P.: Actalk: a tested for Classifying and Designing Actor Languages in Smalltalk-80 environment. In: European Conference on Object-Oriented Programming (1989)
3. Fiduccia, C.M., Mattheyses, R.M.: A linear time heuristic for improving network partitions. In: 19th IEEE Design Automation Conference (1982) 175-181
4. Galinier, F., Hao, J.K.: Hybrid evolutionary algorithms for graph coloring. In: Journal of combinatorial optimization, Vol. 3 No. 4 (1999) 379-397
5. Ghedira, K., Mourali, H.: Une Approche Multi-Agents Recuit Simulé pour le Problème de Partitionnement de Graphes. In: FRANCORO II, Sousse (2000)
6. Hammami, M., Ghedira, K.: Tabu Search for the k-Graph Partitioning Problem. In: ACS/IEEE Int. Conference on Computer Systems and Applications, Tunisia (2003)
7. Hammami, M., Ghedira, K.: A comparative Analysis of genetic algorithms for the k-graph partitioning problem. In: Third International NAISO Symposium on Engineering Of Intelligent Systems, Malaga (2002)
8. Karypis, G., Kuma, V.: A Fast and High Quality Multilevel Scheme for Partitioning Irregular Graphs. SIAM Journal on Scientific Computing, Vol 20 No.1 (1998) 359-392
9. Korsek, P., Jurij, S., Borut, R.: Solving the mesh-partitioning problem with an ant-colony algorithm. Parallel computing 30 (2004) 785-801
10. Weinberg, B., Talbi, E.G.: Break the search space symmetry in partitioning problems, an application to graph coloring. Kluwer Academic Publishers (2004)

Building Hyper-heuristics Through Ant Colony Optimization for the 2D Bin Packing Problem*

Alberto Cuesta-Cañada¹, Leonardo Garrido², and Hugo Terashima-Marín²

¹ Universidad Politécnica de Valencia, Spain
alcueca@inf.upv.es

² ITESM-Center for Intelligent Systems, Monterrey, México
{leonardo.garrido,terashima}@itesm.mx

Abstract. Convergence proofs for ant colony optimization are limited [1], only in some cases it is possible to assure that the algorithm will find an optimal solution. It is even more difficult to state how long it will take, but it has been found experimentally that the computing time increases at least exponentially with the size of the problem [2]. To overcome this, the concept of hyper-heuristics could be applied. The idea behind hyper-heuristics is to find some combination of simple heuristics to solve a problem instead than solving it directly. In this paper we introduce the first attempt to combine hyper-heuristics with an ACO algorithm. The resulting algorithm was applied to the two-dimensional bin packing problem, and encouraging results were obtained when solving classic instances taken from the literature. The performance of our approach is always equal or better than that of any of the simple heuristics studied, and comparable to the best metaheuristics known.

1 Introduction

Informally speaking, the *Two-Dimensional Bin Packing Problem* (2BPP) consists on allocating a set of *items* in a set of larger objects (*bins*), without overlapping. In this paper, both items and bins are rectangular, and items can be rotated but must be placed with the edges parallel to those of the containing bin. Our goal is to place all items in a way that the number of bins used is minimum and each bin is as compact as possible. A classification of bin-packing problems can be found in [3], and an overview on existing approaches for solving the 2BPP is presented in [4].

The 2BPP is a well-known NP-Hard problem, as a consequence an algorithm to solve it in polynomial time is unknown. The common way to overcome this is to develop approximate methods that find a near-optimal solution in a feasible time. An interesting approach that uses a genetic algorithm to construct hyper-heuristics to solve the 2BPP is presented by Morán in [5]. The term *hyper-heuristic* is used broadly to “describe the process of using (meta-)heuristics to

* This work was supported by research grants CAT010 and CAT011 from ITESM, Monterrey campus, and the Conacyt project number 41515

choose (meta-)heuristics to solve the problem at hand” [6]. A more precisely definition explains an hyper-heuristic as a high-level heuristic that controls low-level heuristics. The choice of low-level heuristics is dynamic, and can depend on any features of the problem state, such as expected number of solutions, values on the objective function or previous selected low-level heuristics, for example. The results obtained were among the best known.

As explained in [1], *ant colony optimization* (ACO) algorithms and genetic algorithms are close relatives of a wider model-based algorithm family. Thus, we decided to adapt previous work on the field and test the difficulties and performance of solving the 2BPP with hyper-heuristics and ACO algorithms. This is the first attempt to combine the two metaheuristics. For more information on ACO algorithms we refer the reader to [7],[1] and [8]. The objective of this work is to present a method that should outperform the single heuristics studied.

The paper is organized as follows. Section 2 describes the algorithm implemented. Section 3 presents the empirical results and discusses them. In Section 4 we include our conclusions and a brief summary for future work.

2 Proposed Algorithm

Our *Hyper-heuristic Ant System Algorithm* (HHAS) is implemented over two main concepts: hyper-heuristics and ant colony optimization. We introduce the concept of *packing quality* and discuss the coding of the hyper-heuristic, which will define the solution space for our problem. Then we explain how the ant colony will explore this space.

2.1 Packing Quality

The 2BPP is defined as finding the minimum number of bins needed to contain a bigger quantity of items without overlapping, being both bins and items rectangular and with the edges of the items parallel to those of the bins. One packing can be more compact than another while using the same number of bins. Thus, we need a measure that can distinguish between two similar packings. This is important because if an algorithm gets more compact packings for a small problem, then we can extrapolate that it will usually use less bins if the problem is extended. Based on this, Morán [5] following previous work in the one-dimensional problem from Falkenauer [9], defined the concept of *quality* as:

$$Q = \frac{\sum_{B=1}^{N_B} \left(\sum_{i=1}^n \frac{A_{I_i}}{A_B} \right)^2}{N_B}, \quad (1)$$

where Q is the quality of the packing, N_B the total number of bins used, and A_i and A_B the areas of each item and each bin, respectively. This equation measures the total number of bins and the square of their utilization. Thus, between two packings that use the same number of bins, the one that gets more compact bins will have a better score.

2.2 Heuristics and Hyper-heuristic Coding

In this work, we use the term *single heuristic* to denote the combination of five variables: *Quantity*, *Rotation*, *Item Order*, *Bin Selection* and *Item Placement*:

For the Quantity let N_H be the maximum number of heuristics that can compose a hyper-heuristic, and let N_I be the initial number of items to allocate. We define N_{IH} as N_I/N_H . The quantity of items that could be placed with each heuristic were: 1, $0.25 * N_{IH}$, $0.5 * N_{IH}$, N_{IH} and N_I .

Rotation by 90° is allowed, the values for this variable were: no rotation, rotation of all items, rotation of horizontal items and rotation of vertical items.

Attending to the Item Order, there are many strategies that can be used to select the next item to be placed. We limited our search to nine of them related to the area, height or width of the items, in decreasing order, increasing order or selecting the closest to the average.

The heuristics for Bin Selection were extracted from [10]: First Fit, Next Fit, Best Prepacking Quality, Worst Prepacking Quality and Best Postpacking Quality.

The heuristics selected for Item Placement were extracted from [5], all of them are of the Bottom-Left family: Bottom Left (BL), Sliding BL (BLLT), Filling BLLT (BLF), BLF Rotate (BLFR) and Last Item Filling BLLT (BLR).

The term *hyper-heuristic* describes the sequential combination of at most five heuristics. A hyper-heuristic is represented with a twenty-five cells array (called *path*) of integers, each section of five variables being a single heuristic (Fig. 1). The number of heuristics to build the hyper-heuristic and which heuristics to include were determined experimentally. Each variable is coded as an integer value from 0 to the number of heuristics it groups, used as an index to determine which effect that variable has from the previous variable descriptions.

2.3 Ant Colony Optimization Algorithm

Ant colony optimization algorithms were introduced in the early nineties by Marco Dorigo in his PhD. Thesis [7]. This metaheuristic uses the behaviour

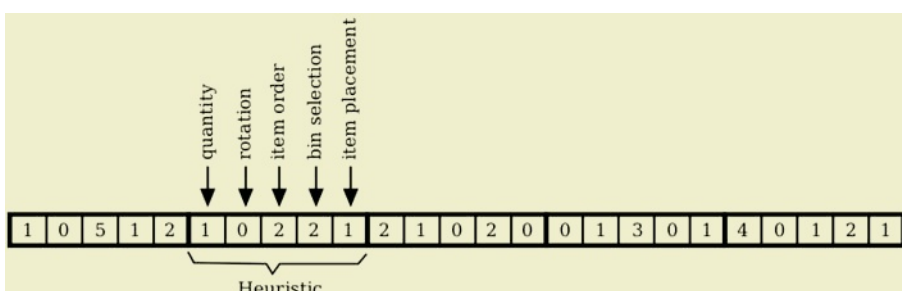


Fig. 1. A hyper-heuristic built from five heuristics, the marked heuristic would be: “take $0.25 * N_{IH}$ items, do not rotate them, sort them by distance to medium width, choose the bin with Best Prepacking Quality, and place the items using BLLT”

of foraging ants in path-finding to solve combinatorial optimization problems. With ACO, agents (*ants*) solve difficult problems using simple heuristics and communicating between them by signals left on the environment (*pheromones*) which store information of the solutions found and its quality. We chose its Ant System Algorithm as a basic start for our research. As far as we know, there are no studies providing an adequate heuristic for our case. Thus, we modified the Ant System to work using only probabilistic transitions based on pheromones. The main components of the ACO part of our HHAS are: The pheromone matrix, the update and decay functions, and the stagnation behaviour.

We implemented 25 pheromone matrixes, each one representing the transition between two consecutive variables (Fig. 2). Each matrix had a number of rows equal to the number of possible values for that variable, and a number of columns equal to the number of possible values of the next variable. The first matrix had only one row and as many columns as values that the *quantity* variable could take. Then, let Ph_v the pheromone matrix for the variable v , and i the path value for v , then the probability of choosing j as the value for $v + 1$ is $\text{Ph}_v(i, j)$. Then $\text{path}(i, v) \Rightarrow p(\text{path}(j, v + 1)) = \text{Ph}_v(i, j)$.

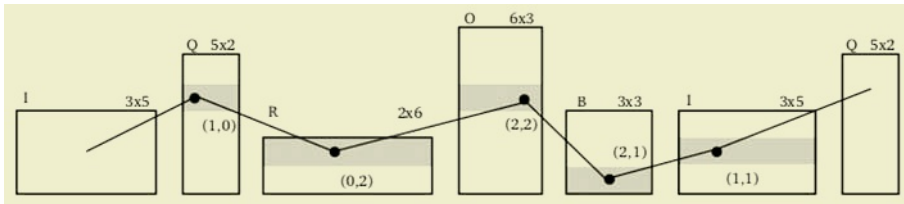


Fig. 2. Heuristic 10221 (taken from Fig. 1) over the pheromone matrixes

A single group of ants working simultaneously its entire paths is called an *iteration*. When an iteration finishes, the quality of each *path* is calculated with (1). All qualities are transformed so the 0.0 value is assigned to the worst path and 1.0 to the best, with all the rest linearly distributed between them, all values are squared to further differentiate good results from bad results (2). Then we sum the quality of each packing to the pheromone matrixes over its hyper-heuristic path (3). Finally, each row is normalized so the sum of its columns equals 1.0 and it can be used as a probabilistic array for deciding the path. The normalizing acts as a simple decay function. The pheromone update is defined as

$$Q(\text{path}) = \left(\frac{Q(\text{path}) - \min(Q)}{\max(Q)} \right)^2, \quad (2)$$

$$\forall v : \text{Ph}_v(\text{path}(v), \text{path}(v + 1)) = \text{Ph}_v(\text{path}(v), \text{path}(v + 1)) + Q(\text{path}). \quad (3)$$

The AS system is said to *stagnate* when it arrives to a local optimum, with all the ants following the same path. In our implementation, the stagnation was stated when two iterations passed without finding a better solution. In such moments the algorithm saves the best hyper-heuristic found for later processing and resets the pheromone matrix to neutral values.

A sequence of iterations that led to stagnation is called a *cycle*. When a cycle finishes, the best hyper-heuristic found is compared to the best hyper-heuristic from previous cycles to find the present best solution. When all the ants have been used, this is the output of the algorithm.

2.4 Implementation Details

The quality of the solutions obtained depends on how well the search space is explored. Therefore it was critical to keep it as reduced as possible. Based on the possible combinations of the variables used, it had a size of $3,125 * 10^{18}$ possible hyper-heuristics. After a few runs the less used values were taken out, leaving $4,592 * 10^{13}$ possible combinations. A smaller search space proved to give better results in the same time, as it was explored better.

All the hyper-heuristic paths are decided before the iteration starts. Depending on the values assigned to the *quantity* variables in the hyper-heuristic, all items could be allocated before using all the heuristics contained. In that case any heuristic without effect will be deleted. This trimming reduced the search space to $3,770 * 10^{12}$. Besides, this allows our algorithm to explore single heuristics along with combinations of five heuristics at most.

3 Empirical Results

The cgcut, gcut and ngcut (abbreviated as cg, g and ng in the tables) are classical bin packing problems described in the works from Christofides and Whitlock[11], and Beasley[12]. They were chosen for testing because its wide use on similar papers. After some experiments we decided to use 30000 total ants in iterations of 50 individual ants, this was found as the maximum number of ants we could use while maintaining the computing time short enough.

The results are shown in Table 1: First column represents the best quality obtained from applying all heuristics to each single problem, the best heuristic could be different for each problem. Second column is the average of 30 runs of the HHAS algorithm. The third column is the percentual increase in quality by using HHAS. As shown, our algorithm was always better than any single heuristic, except for some of the simpler problems in which the results are equal. However, in some cases HHAS clearly outperformed the best of single heuristics.

In Table 2, we compare the HHAS against other hyper-heuristic-based methods and the best of single heuristics, using the number of bins used as the measure unit. Columns show the best single heuristic (BH), HHAS, the hyper-heuristic genetic algorithm of Morán [5] (HHAG), the classifier-based hyper-heuristic algorithm from Terashima *et al.* [10] (XCS) and the lower bound calculated as the sum of the size of each item divided by the bin area (L0). It has not been proved that the L0 number of bins can be reached. As shown, the performance of HHAS is similar to other hyper-heuristic-based methods, specially the HHAG. Moreover, the results support our statement that the number of used bins is not enough to measure the performance of the algorithm.

Table 1. Hyper-heuristic Ant System against the best of simple heuristics

| cgcut | | | | gcut | | | | ngcut | | | |
|-------|-------|-------|-------|------|-------|-------|-------|-------|-------|-------|-------|
| | BH | HHAS | +% | | BH | HHAS | +% | | BH | HHAS | +% |
| cg1 | 0.625 | 0.625 | 0.00% | g1 | 0.474 | 0.474 | 0.00% | ng1 | 0.514 | 0.518 | 0.73% |
| cg2 | 0.627 | 0.647 | 3.10% | g2 | 0.606 | 0.607 | 0.10% | ng2 | 0.857 | 0.861 | 0.42% |
| cg3 | 0.708 | 0.721 | 1.78% | g3 | 0.697 | 0.705 | 1.20% | ng3 | 0.859 | 0.863 | 0.49% |
| | | | | g4 | 0.816 | 0.822 | 0.79% | ng4 | 0.436 | 0.436 | 0.00% |
| | | | | g5 | 0.544 | 0.553 | 1.53% | ng5 | 0.694 | 0.694 | 0.00% |
| | | | | g6 | 0.546 | 0.690 | 26.3% | ng6 | 0.561 | 0.935 | 66.6% |
| | | | | g7 | 0.645 | 0.646 | 0.25% | ng7 | 0.191 | 0.191 | 0.00% |
| | | | | g8 | 0.758 | 0.766 | 1.01% | ng8 | 0.642 | 0.656 | 2.12% |
| | | | | g9 | 0.562 | 0.562 | 0.09% | ng9 | 0.683 | 0.703 | 2.93% |
| | | | | g10 | 0.592 | 0.602 | 1.76% | ng10 | 0.568 | 0.588 | 3.59% |
| | | | | g11 | 0.690 | 0.693 | 0.42% | ng11 | 0.696 | 0.700 | 0.53% |
| | | | | g12 | 0.707 | 0.712 | 0.62% | ng12 | 0.737 | 0.747 | 1.30% |
| | | | | g13 | 0.654 | 0.656 | 0.40% | | | | |

Table 2. Performance of HHAS against other methods

| cgcut | | | | | | gcut | | | | | | ngcut | | | | | |
|-------|----|----|----|-----|----|------|----|----|-----|-----|----|-------|----|----|----|-----|----|
| | BH | AS | AG | XCS | L0 | | BH | AS | AG | XCS | L0 | | BH | AS | AG | XCS | L0 |
| cg1 | 2 | 2 | 2 | 2 | 2 | g1 | 4 | 4 | 4 | 4 | 3 | ng1 | 3 | 3 | 3 | 3 | 1 |
| cg2 | 2 | 2 | 2 | 2 | 2 | g2 | 6 | 6 | 5.3 | 6 | 5 | ng2 | 3 | 3 | 3 | 3 | 3 |
| cg3 | 19 | 19 | 19 | 20 | 16 | g3 | 8 | 8 | 7.6 | 8 | 7 | ng3 | 3 | 3 | 3 | 3 | 3 |
| | | | | | | g4 | 13 | 13 | 13 | 13 | 12 | ng4 | 2 | 2 | 2 | - | 1 |
| | | | | | | g5 | 3 | 3 | 3 | 3 | 3 | ng5 | 3 | 3 | 3 | 3 | 3 |
| | | | | | | g6 | 7 | 6 | 6 | 6 | 5 | ng6 | 3 | 2 | 2 | 3 | 2 |
| | | | | | | g7 | 11 | 10 | 10 | 11 | 9 | ng7 | 1 | 1 | 1 | - | 1 |
| | | | | | | g8 | 13 | 13 | 13 | 13 | 12 | ng8 | 2 | 2 | 2 | 2 | 2 |
| | | | | | | g9 | 3 | 3 | 3 | 3 | 3 | ng9 | 3 | 3 | 3 | 3 | 3 |
| | | | | | | g10 | 7 | 7 | 7 | 7 | 6 | ng10 | 3 | 3 | 3 | 2 | 2 |
| | | | | | | g11 | 8 | 8 | 8 | 8 | 7 | ng11 | 2 | 2 | 2 | 2 | 2 |
| | | | | | | g12 | 15 | 15 | 15 | 16 | 13 | ng12 | 3 | 3 | 3 | 3 | 3 |
| | | | | | | g13 | 2 | 2 | 2 | 2 | 2 | | | | | | |

4 Conclusions and Future Work

An optimal hyper-heuristic can solve any problem in a time comparable to that of a simple heuristic. In this case, it is easier for an ACO algorithm to explore the solution space of a hyper-heuristic metaphor than the solution space of the problem itself. This is specially true when applied to large instances of the problem. The solution space of an hyper-heuristic problem is independent from the size of the instance, while the solution space of a basic ACO algorithm grows exponentially.

A very basic ACO algorithm was developed to solve an hyper-heuristic problem. It always found a solution at least equal to that of the best single heuristic

studied. Results were comparable to the best metaheuristic methods known. More advanced versions of HHAS could benefit from many improvements, the use of an heuristic for searching the hyper-heuristic solution space should be the next step. Other parts should be considered later: local search algorithms, candidate lists and an incremental quality function, for example.

Despite of the missing features, the results are promising, and we believe that the combination of hyper-heuristics and ACO algorithms could show significant improvements in the near future. Furthermore, it would be interesting to apply the Hyper-heuristic Ant System method to large instances of other NP problems that are known to work well with ant colony optimization, such as VRP or QAP.

References

1. Dorigo, M. and T. Stützle: *Ant Colony Optimization*, MIT Press, 2004.
2. The Ant System: Optimization by a colony of cooperating agents. *IEEE Transactions on Systems, Man, and Cybernetics-Part B*, vol. 26, no. 1, pp. 1-13, 1996.
3. Dyckhoff, H.: A typology of cutting and packing problems. *European Journal of Operational Research*, vol. 44, pp. 145-159, 1990.
4. Karelähti, J.: Solving the cutting stock problem in the steel industry. Master Thesis, Helsinki University of Technology, 2002.
5. Morán-Saavedra, A.: Optimización de Corte de Material en Dos Dimensiones mediante Hiperheurísticas construidas con un Algoritmo Genético. Master's Thesis, Instituto Tecnológico y de Estudios Superiores de Monterrey, México, 2004.
6. Burke, E. *et al.*: Hyperheuristics: An emerging direction in modern search technology, 2003.
7. Dorigo, M.: Optimization, Learning and Natural Algorithms (in Italian). Ph.D. Thesis, Dipartimento di Elettronica, Politecnico di Milano, Italy, 1992.
8. Dorigo, M. *et al.*: *Ant Colony Optimization and Swarm Intelligence*, Springer, 2004.
9. Falkenauer, E.: *Genetic Algorithms and Grouping Problems*. Wiley and Sons, 1999.
10. Terashima-Marín, H., E. Flores-Álvarez and P. Ross: Hyper-heuristics and Clasifier Systems for Solving 2D-Regular Cutting Stock Problems. To be published in *Genetic And Evolutionary Computation Conference 2005*, ACM, 2005.
11. Christofides, N. and C. Whitlock: An algorithm for two-dimensional cutting problems. *Journal of the Operational Research Society*, vol. 25, pp. 30-44, 1977.
12. Beasley, J. E.: An exact two-dimensional non-guillotine cutting tree search procedure. *Operational Research*, vol. 33, pp. 49-64, 1985.

Real-Time Co-composing System Using Multi-aspects

Jens J. Balvig and Taizo Miyachi

Faculty of Electronic Engineering, Tokai University
1117 Kitakaname, Hiratsuka, Kanagawa 259-1292, Japan
{4keem002, miyachi}@keyaki.cc.u-tokai.ac.jp

Abstract. Real-time interactive mobile systems are becoming increasingly common giving users easy and instant access to vast amounts of information and creative tools. However, due to the amount of data available, direct manipulation of information and use of applications can prove quite difficult, if one does not possess the necessary background knowledge on a given subject at first. We propose a more indirect approach utilizing aspects, and using a music composition system as an example describe a method that simplifies otherwise complex processes and allows the user to carry out a number of powerful tasks using familiar terms and expressions without having to learn system-specific terminology or hard-to-comprehend jargon, while at the same time creating a sense of clarity and overview in a field that might initially seem vague and inaccessible.

1 Introduction

Real-time interactive mobile systems are becoming increasingly common and play an important role in ubiquitous computing. Users have easy and instant access to vast amounts of information and creative tools, however actually understanding and utilizing the countless possibilities this creates in a meaningful way, is one of the real challenges of any ubiquitous system. Direct manipulation of information and creative use of applications can prove quite difficult, if one does not possess the necessary background knowledge on a given subject at first. We therefore propose a more indirect approach utilizing aspects, and using a music composition system as an example describe a method that simplifies otherwise complex processes and allows the user to carry out a number of powerful tasks using familiar terms and expressions without having to learn system-specific terminology or hard-to-comprehend jargon while at the same time creating a sense of clarity and overview in a field, that might initially seem vague and inaccessible (fig. 1).

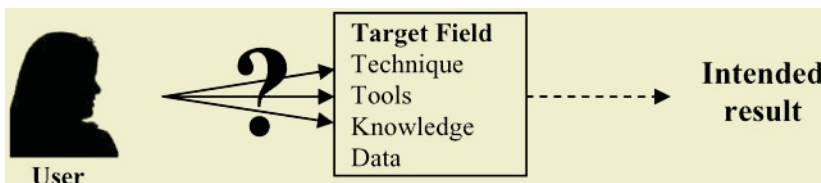


Fig. 1. Problem area

Among experts in the various creative and artistic fields, there are well-established methods and techniques for achieving specific goals. For example, when making a

painting, an experienced painter will have a very good idea of what colors or brushes to use and how to mix different textures and layers to achieve a certain effect or mood, while a professional composer will know what rhythmical or harmonic structures can be used to make a musical piece express a certain feeling or atmosphere. While professional artists will either have obtained these skills through study, practice or sheer talent, the average person will have little or no knowledge of the technical side of a given field, but will at the very least know how a piece of art makes him/her feel or be able to describe it using vague terms such as “dark” or “happy”.

It is this dichotomy we seek to fuse, building a bridge that allows the user to access and manipulate complex technical qualities of a creation using concepts, in this report referred to as multi-aspects, based on feeling, human qualities and culture. The key word for the use of aspects is “abstraction”, providing the user with well-known words and ideas that he/she can relate to immediately and instinctively, rather than having to go through a complex learning process (fig. 2).

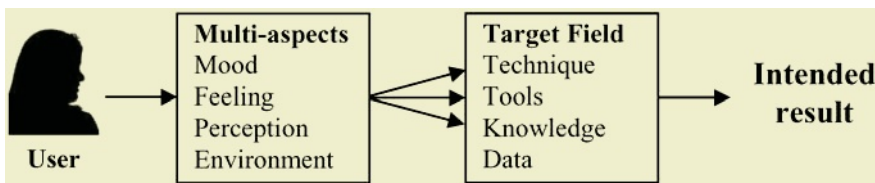


Fig. 2. Multi-aspects as an information bridge

Thus, while composing and performing music traditionally requires at least access to an instrument and several years of practice and study, this application seeks to make it possible for the average person with little or no musical experience to compose, perform and edit original compositions. Based on knowledge obtained from analysis of music and incorporating common rules and traditions from a variety of musical traditions from different cultures, the application provides the user with powerful tools making it possible for even beginners to make meaningful music. In other words, to create something that is not simply perceived as noise, but makes rhythmical and harmonic sense, and is commonly accepted as being “musical”. The system works in real-time on the following levels: (1) Acquisition and introduction of information from the internet, (2) Creation and editing “on-the-fly”, (3) Instant accessibility, the application runs on a cell phone and (4) can be used anywhere taking inspiration from the current environment.

2 Music and Multi-aspects

When composing music, a trained musician will use knowledge of rules about rhythm, harmony and timbre to achieve his goal and create the musical result he is aiming for. Technical terms such as “major/minor”, “shuffle”, “double-time” etc. become fundamental tools to shape and change the music during the composition process. On the other hand, a person possessing no musical knowledge might think in more abstract terms such as “quiet”, “energetic”, “African-like” or “more like that song I heard yesterday”.

It goes without saying that how music is perceived depends on the individual (as one person's Mozart might be another person's noise), there are however several fundamental relations between the technical qualities of a musical piece and the mood it invokes. This field of study has already been described extensively in other research and part of the development of this application is based on results of these works [1], [2], [3].

2.1 Rhythm and Music Perception

For this application we have chosen rhythm and percussion as the focal point. Since cavemen began banging rocks together to create sound thousands of years ago, rhythm has been a very fundamental thing that humans can relate to instinctively and immediately. Moreover, rhythm and pulse are considered to be among the primary elements for evaluating mood responses to music [1]. Finally, most drums do not have pitch or tone, thus to some extent dispensing with the complexity of musical theory associated with melody and harmony. The connection between a piece of music's technical properties and its emotional effect is quite well documented. Research has shown that for example, playing sounds simultaneously or sequentially changes the feeling and perceived speed of the music, fast tempi expresses happiness etc [1], [3]. The co-composing part of this software takes advantage of this knowledge in its use of multi-aspects, and allows for feeling/emotion-based description of music to be used as a basis for building or changing rhythms. For example, should the user choose to make already created music sound more "calm", activating the appropriate aspect will make the software look for "busy" parts of the rhythm were several drum-hits line up and remove one or several of these while also replacing sounds of particularly bright percussion instruments with softer more mellow tones. For the purpose of building up new rhythms, templates are connected with the individual aspects, providing the user with a foundation to construct new rhythms associated with a given feeling or mood. Moreover, as a basis for some aspects, knowledge from various musical traditions from around the world has been draw upon. These traditions have been known to inspire feelings for ages and stood the test of time, thus making for a good foundation to base emotional co-composing upon.

3 Program Overview

In this section, the actual implementation of the software is described. As well as making it possible for the average person to compose and learn about music, another important issue is simplicity and immediacy. If the user is forced to sit down in front of a computer before being able to begin the creative process, a lot of spontaneity is lost and the playfulness and intuitive operation that was the original goal cannot be obtained. Musical inspiration is seldom something that appears at a given time, but rather a more unpredictable phenomenon that can happen to you as you're taking a walk, shopping for groceries or sitting on the train. Therefore the software is designed to work on a cell phone, thus allowing the user to create music anywhere and anytime.

3.1 Music Creation

The interface takes the form of a “drum-machine”, a tool for creating music based upon rhythm using a simple, intuitive interface. The software consists of two distinctive modes, one, being the basic “Edit Mode” where the user can freely create music without assistance, and the other being “Aspect Mode” allowing the user to compose and/or change original music using the various aspects implemented in the application.

3.2 Edit Mode

The Edit Mode in many ways resembles other existing music software, adapted for a cell phone’s GUI. The graphical interface itself is based upon hardware drum-machines that traditionally take the form of small boxes with 16 buttons on it, each representing a 16th of a musical bar (fig. 3). The creation process is as follows: (1) Buttons are switched on and off using a cursor. When “play” is pressed the drum-machine begins cycling continuously through these 16 buttons and whenever it hits a button that is switched “on”, it plays a sound, thus creating a rhythm pattern. (2) Each rhythm consists of 4 different instruments playing together resulting in a polyphonic drum rhythm. The sound of each track can be changed by pushing buttons on the cell phone, and these built-in sounds range from synthetic noises to sounds based on actual drums from a range of different percussion traditions. As the sounds are changed the graphics also change to represent the currently selected sound, making it easy to get a visual overview of which sounds are interacting at any given time. (3) Real-time editing allows users to write music while the music is playing. Thus the user can instantly react to the feelings he/she gets from hearing a certain sound, follow that inspiration, and react accordingly. The rhythms can be changed in real-time, “on the fly” without stopping the music and the results are heard instantly. For example, the sounds of individual tracks or the rhythmical structure can be altered as you are actually listening to the music, allowing the user to get a feel for how different placement of drum hits or choice of sounds has an impact on the composition.

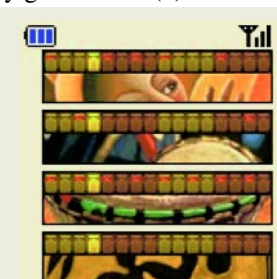


Fig. 3. Edit Mode

3.3 Aspect Mode

This refers to the co-composing side of the software that allows the user to create and modify existing music using multi-aspects. Choosing “aspect mode” from the application menu changes the GUI slightly, in that the user now works on a track level rather than operating on individual drum hits. Using the up/down keys (1) individual track or (2) multiple tracks can be selected, and once this is done, an aspect can be selected using the right/left keys, and its effect increased or decreased using the up/down keys (fig. 4). Thus, depending on the user’s selection, aspects can be applied *globally*, (a) modifying a song as a whole or to individual tracks allowing the user to subtly change the composition and also (b) mix and (c) match the separate categories fusing aspects to create a hybrid original mix. When an aspect is applied to an already

existing rhythm, the current rhythm will be changed. Conversely, should the feature however be used to create a rhythm from scratch, drumhits will be inserted and used as a basis for creating one's own original drum-rhythm.

Below is a list of the aspects currently being developed for the application. These are mainly based on Farnsworth's modification of the Hevner Adjective Circle, a method for categorizing music based on emotional response.

Energy: Ranging from "calm" to "hectic".

Mood: Ranging from "dark" to "cheerful".

Atmosphere: Ranging from "delicate" to "dramatic".

Temper: Ranging from "tranquil" to "agitated".

Contentment: Ranging from "longing" to "frustrated".

Culture: Various aspects based on rhythm traditions from Africa, Latin America etc.

Share: Allows for use of music previously created by the user or other composers.



Fig. 4. Aspect Mode

4 Aspects in Use

The numerous algorithms associated with each aspect are as mentioned based upon previous research of perception and music as well as cultural rhythm traditions, and thus differ depending on the intended effect. As an example of how some of the techniques are implemented three distinct aspects are described below.

4.1 The "Energy" Aspect

The Energy aspect allows the user to control the music's perceived energy. Increasing the effect adds *syncopated* drumhits in quick succession, causing for a more energetic rhythm (fig. 5) while decreasing the effect removes stray drumhits, leaving only sounds that form part of a quiet, steady pulse, giving an overall calmer piece of music.

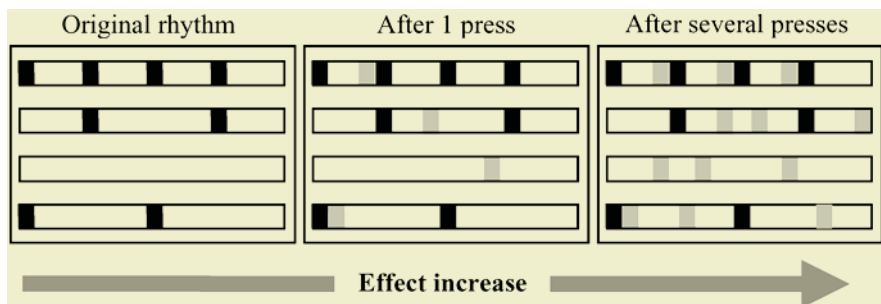


Fig. 5. The "Energy" aspect

4.2 The “Bangowana” Aspect

This aspect is based upon a traditional style of percussion music from Africa referred to as “Bangowana” [4], and uses this particular form of rhythm as a template for changing other rhythms. Once a track is selected, presses of the “increase key” will gradually change the current rhythm into something resembling this particular style of percussion. Every time the effect is increased, the application compares the current track (or tracks) with the Bangowana template and performs changes so that repeated button presses will result in the rhythm ending up being identical to the Bangowana rhythm. Presses of the “decrease key” will look for similarities between Bangowana and the current rhythm and seek to remove any resemblances, eventually creating the exact “opposite” of a Bangowana rhythm.

4.3 The “Share” Aspect

This feature allows the user to modify new music using previously created music composed either by himself, by a friend or downloaded from a content provider. In other words, previously created songs are used as the basis for modifying and improving the current composition. The software will perform a comparison of the two compositions, searching for similarities and differences between the two rhythms, and providing a new result that is a calculated average of the two. In this way the user can subtly change the created rhythms to sound more like other songs created either by himself or by other composers.

5 Evaluation

The current version of the software has been tested by roughly 40 individuals in the age group of 20-50 years old ranging from first-time users with no musical background to experienced musicians. The users were allowed to test the program with as little prior explanation as possible, thus giving them an opportunity to freely explore the functions and naturally point out any potential problem areas. Even the testers having no prior musical experience quickly figured out the basics of creating rhythms and pointed out how even with no understanding of musical theory the program allowed you to play around, enjoy the process and still produce musically decent results. Several testers were interested in potentially using the software to create your own calling tones and everyone expressed enthusiasm about the potential for being able to create and learn about music wherever you go, using only a cell phone.

Although a wide range of applications that supposedly make music composition easy for beginners (such as “Garageband”, “eJay” etc.) already exist, these mainly consist of mere arranging tools allowing the user to put together pre-created musical phrases into a form of musical puzzle. This application differs in that it makes it possible for the user to create ones own music, actually composing original music from scratch.

6 Conclusion

In this paper, we introduced a new way of handling complicated creative tasks using abstraction and multi-aspects as a simple, easy-to-understand interface. As an exam-

ple of this we presented a music co-composition system that allows users, who have little musical knowledge or experience to easily create and shape original music in real-time via an aspect-based creation process. This system can be further built upon to include more aspect-based analysis functions, such as analyzing the relationships between different instruments or sub-sections of a track. Also, it is our hope that this way of using aspects to handle complicated tasks or manipulate information that is either vague or difficult to directly access can be further developed to comprise other creative applications such as aspect-based graphical software or educational tools.

References

1. Radocy, R., David Boyle, J.: Psychological foundations of musical behavior. Charles C Thomas Publisher Ltd Illinois (2003)
2. Hodges, D.: Handbook of Music Psychology. MMB Music (1996)
3. Norman, D.: Emotional design: why we love (or hate) everyday things. Basic Books New York (2004)
4. Mukuna, C., Imaida, H.: African drum wa tamashi no hibiki. Yamaha Music Tokyo (2003)
5. Olsen, D., Klemmer, S.:The Future of User Interface Design Tools. CHI2005-UI-Tools
6. Kiczales, G., et al.,: ‘Aspect-Oriented Programming’ proceedings of the European Conference on Object-Oriented programming (ECOOP), Springer-Verlag Finland (1997)
7. Myers, B., Hudson, S., Pausch, R.: Past, Present, and Future of User Interface Software Tools. ACM Transactions on Computer-Human Interaction (2000)
8. Desain, P.: A (de)composable theory of rhythm perception. Music Perception, vol. 9, no.4 (1992).

Empirical Study on Usefulness of Algorithm SACwRApper for Reputation Extraction from the WWW

Hiroyuki Hasegawa, Mineichi Kudo, and Atsuyoshi Nakamura

Division of Computer Science, Graduate School of Information Science and
Technology, Hokkaido University, Sapporo, Hokkaido, 060-0814, Japan
`{hase,mine,atsu}@main.ist.hokudai.ac.jp`

Abstract. We consider the problem of extracting texts related to a given keyword from Web pages collected by a search engine. Recently, we proposed a method using both structural and content information[[1](#), [2](#)]. In our previous paper, we reported good extraction performance of our method only for Ramen-shop dataset written in Japanese. In this paper, we examine it for datasets of other kind of restaurants, and also for a dataset written in English. We discuss some modification for performance improvement.

1 Introduction

Recently, we proposed a reputation extraction algorithm named SACwRApper¹ [[1](#), [2](#)] that is a combination of frequent tree mining and text classification. Our method, given a restaurant name, extracts texts that are its reputations from all the Web pages retrieved by a search engine. In [[1](#)] and [[2](#)], only the dataset of Ramen (Chinese noodles in soup) shops was used in the experiments to evaluate the effectiveness of SACwRApper. Our method achieved 79% precision and 57% recall.

In this paper, we report the results of additional experiments to examine effectiveness of SACwRApper using datasets for curry and Sushi restaurants and a dataset for bars. Moreover, we report the result of an experiment using Web pages written in English for the dataset of Sushi shops in New York. We also propose some modifications for improving accuracy in our method. According to the result of our experiments, our modified method achieved 75 ~ 88% precision and 26 ~ 54% recall and outperformed a previous method by 5 ~ 14% recall among all categories and 6 ~ 14 % precision among three categories.

1.1 Related Work

There are a lot of works about information extraction from the Web pages [[3–5](#)]. As the work concerning reputation extraction, Tateishi et al. [[6](#)] developed a

¹ For Japanese people, “SACRA” sounds like “SAKURA”, the Japanese name for cherry blossoms

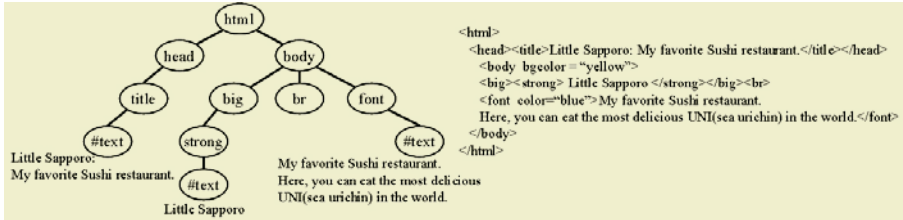


Fig. 1. The example of a DOM-tree and HTML text which is original

reputation search engine by using natural language processing technique. Their engine does not use any special features of HTML documents. Other studies on mining product reputations [7, 8] mainly focused not on extraction but on analysis.

2 Algorithm SACwRApper

In this section, we describe an overview of an algorithm SACwRApper. As for the details of SACwRApper, see [1] for a generation method of a pattern set \mathcal{P} and implementations, and see [2] for a method of creating a better pattern set to improve its precision and a ranking method of output results.

2.1 Notions and Notations

A *DOM-tree* T , a representation of an HTML document in *document object model*, is an ordered tree in which each node N_T has two attributes *tag* and *text*. A value of a tag attribute is a HTML tag and a value of a text attribute is a text string. We assume that a text attribute of N_T is not *null* only when a tag attribute of N_T is “#text”, a special tag for a text node. An *id* of a node N_T is its position in the preorder traversal of the tree T . An example of a DOM-tree and the HTML document it represents are shown in Fig. 1.

Algorithm SACwRApper learns an extraction function from a training data. A training dataset \mathcal{D} is a set of triples (W, T, N_T^*) , where W is a keyword such as a restaurant name or a product name, T is a DOM-tree that has a text node containing W , and N_T^* is the least common ancestor (LCA) of all the text nodes whose text attribute value contains target texts related to the keyword W . N_T^* is *null* when there is no such text node in T .

2.2 Extraction Function f

A function f to be learned is a function from a pair of a keyword and a DOM-tree to a node in T , which is composed of three functions f_{pat} , f_{con} and f_{dec} . The three functions have the following roles.

Pattern-matching function f_{pat} : Given a keyword W and a DOM-tree T , the function f_{pat} outputs all the nodes $N_{T,1}, N_{T,2}, \dots, N_{T,k}$ in a DOM-tree T of which structural relation to a keyword W matches one of patterns in a set \mathcal{P} , which is learned from a training data.

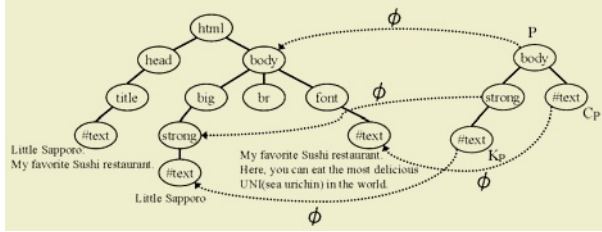


Fig. 2. Example of pattern matches a DOM-tree

Content-based function f_{con} : The function f_{con} is a function of a node N_T that outputs a label 1 or -1 based on the texts that are contained in the subtree rooted by the node. The function f_{con} classifies the node by using the text classification technology.

Decision function f_{dec} : The function f_{dec} is a function of a set $\{(N_{T,1}, l_1), (N_{T,2}, l_2), \dots, (N_{T,k}, l_k)\}$, where each pair is composed of a node $N_{T,j}$ and a label l_j , and outputs one node $N_{T,j}$ or null. We fix a function f_{dec} to the function that outputs the node of the smallest id among those having label 1.

Using the above three functions, a function f is defined as follows.

$$f(W, T) = f_{dec}(\{(N_T, f_{con}(N_T)) : N_T \in f_{pat}(W, T)\})$$

2.3 Pattern-Matching Function

A function f_{pat} selects all the nodes in a DOM-tree T of which structural relation to a keyword W matches to one of patterns in a set \mathcal{P} . A pattern is a pair of a *pattern tree* P and *distance* r between its two leaves. A pattern tree P is a simple DOM-tree that consists of a root node and two paths leading to the leaf nodes, a *keyword node* K_P and a *target node* C_P . The structural relation of a node N_T to a keyword W matches to a pattern (P, r) if and only if there is a one-to-one mapping ϕ from the set of nodes in P to the set of nodes in T that satisfies 7 conditions: target matching, keyword matching, LCA matching, label preserving, ancestor-descendant relation preserving, sibling relation preserving and acceptable distance. (See [1] for details.)

An example of a pattern tree P and a matching function ϕ are shown in Fig. 2. Note that the parent-child relation in P matches to ancestor-descendant relation in T . The set \mathcal{P} of pattern (P, r) are generated from a training dataset \mathcal{D} . Outputs of f_{pat} are a set of all the nodes that matches to one of the patterns in \mathcal{P} .

2.4 Content-Based Function

A function f_{con} classifies the given node N_T into the classes of "reputation" and "non-reputation" by the text attribute values of all its descendants. To design the function f_{con} , an any text classification technique can be used. Note that negative training instances for a text classifier are generated from original training data \mathcal{D} using pattern matching function f_{pat} .

3 Experiments

3.1 Methodology

In our experiments, we used HTML documents of four categories, curry, Sushi, bar and New York's Sushi. Among the popular shops introduced in a web site², we selected the most popular 10 shops with more than 15 Web pages retrieved by keyword search³ using a shop name and its telephone number. We did these to each category. Total number of pages and the number of pages that contain reputations about a target shop are shown in Table 1. We conducted cross validation by using pages retrieved for each one of 10 shops as a test data.

Index terms we used in our experiments are basically standard forms of nouns, verbs, adjectives and adverbs. For Japanese texts, Chasen⁴, one of Japanese morphological analysis systems, was used to extract index terms. For English texts, conversion to standard forms was done using CUVOALD⁵ and WordNet ver.1.6⁶. As a term weight, we used a term frequency normalized with respect to Euclidean norm. A support vector machines (SVM) was used as a text classifier in the experiments. We used SVM-Torch II⁷ with polynomial kernel $K(x, y) = (xy + 1)^3$ and other default parameters.

3.2 Modified Method

We also tried a modified version of our method for performance improvement. The modifications are following two points.

Training subtree extraction: The previous method extracts one training subtree for each occupancy of a given keyword in a training DOM-tree. This caused a pattern tree with large distance between its leaves to be generated. We modified the training subtree extraction using only one subtree of which node containing keyword is the nearest from a target node.

Negative example generation for text classifier: As a negative example for a text classifier, our previous automatic generation method possibly selects a text that includes a target reputation. This caused a low-recall text classifier to be generated. Thus, we modified our negative-example generation algorithm so as not to select such texts that contain the target text.

3.3 Results

The results of our modified method are shown in Table 2. Precision is a rate of the number of correctly extracted nodes among all the extracted nodes, and recall is

² curry, Sushi, bar:www.ypp.co.jp, Sushi shop in New York:www.newyorkmetro.com

³ Google(www.google.co.jp) was used in the search

⁴ ChaSen 2.3.3.(URL:chasen.aist-nara.ac.jp/hiki/Chasen)

⁵ A Computer-Usable Version of the Oxford Advanced Learner's Dictionary (by Roger Mitton)

⁶ URL:wordnet.princeton.edu

⁷ URL:www.idiap.ch/~bengio/projects/SVNTorch.html

Table 1. Experimental data

| | curry | Sushi(Japan) | bar | Sushi(New York) |
|-------------|-------|--------------|-----|-----------------|
| #PAGE | 414 | 285 | 341 | 331 |
| #REPUTATION | 265 | 127 | 140 | 125 |

Table 2. Result of our modified method

| | curry | Sushi(Japan) | bar | Sushi(New York) |
|-----------|-------|--------------|------|-----------------|
| precision | 0.75 | 0.75 | 0.80 | 0.88 |
| recall | 0.54 | 0.46 | 0.26 | 0.28 |

Table 3. Result of comparison experiment

| | previous | | training subtree | | negative example | | both | |
|-----------|----------|------|------------------|------|------------------|------|------|------|
| | pre. | rec. | pre. | rec. | pre. | rec. | pre. | rec. |
| curry | 0.69 | 0.42 | 0.70 | 0.45 | 0.75 | 0.51 | 0.75 | 0.54 |
| Sushi(JP) | 0.75 | 0.38 | 0.78 | 0.43 | 0.76 | 0.44 | 0.75 | 0.46 |
| bar | 0.66 | 0.14 | 0.73 | 0.14 | 0.63 | 0.14 | 0.80 | 0.26 |
| Sushi(NY) | 0.73 | 0.23 | 0.81 | 0.20 | 0.88 | 0.35 | 0.88 | 0.28 |

Table 4. Example of output of Wrapper. ○ is correct and × is mistake

○ A dependable choice for fresh, inexpensive Japanese food with typical sushi and sashimi options such as the hamachi tail. The menu offers some surprises: for example, a not-so-typical sauted scallops with jalapeno sauce. The shiitake string bean sesame is a safe bet. Recommended Dishes: Sauted Scallops with Jalapeno Sauce, \$9.50; Shiitake String Bean Sesame, \$6.75

○ I did the Omakase and let the chef decide...with a budget of \$60. I ordered (outside of the \$60) the Sushi Pizza, which was fantastic. As for the sushi and sashimi, it was good, but not great. I've had better quality and creativity at Sushi of Gari and Sushi Yasuda. I only received about 8 pieces, which left me very hungry. Definitely not worth \$60 plus the cost of the sushi pizza and beverages.

○ The New York Times named Tsuki a top pick for Sushi, calling it an "affordable neighborhood place several cuts above the ordinary". The owner brings his innovative style to this new location, which has been open for the better part of two years. Tsuki is proud to offer both authentic and modern dishes...

✗ Where else can you find modestly-priced, first-rate Thai, Vietnamese, Malaysian & Japanese (sushi bar) under one roof? You love the exotic Asian decor including the unique tables. This place has it all: variety, great prices, handsome surroundings, delicious food, and attentive service! L & D!. All cards. 242 W. 56th St. (Bdway-8th Ave.), 212-265-8588...

a rate of the number of correctly extracted nodes among all the nodes that should be extracted. Our modified method achieved 75 ~ 88% precision and 26 ~ 54% recall. Recall was comparatively high for curry and Sushi(Japan), but for bars and Sushi(New York), only about one-quarter of reputations were extracted. This is because words used in reputations depend on restaurant categories, and those variance is considered to be smaller in reputations for curry and Sushi(Japan) than in reputations for bars and Sushi(New York). Table 3 shows performance of our previous and modified methods. Our method using both modifications outperformed a previous method by 5 ~ 14% recall among all categories and 6 ~ 14 % precision among three categories. Performance of modified method is better for curry and bars and comparative for Sushi(Japan) than the method using only one modification.

The reputations extracted for Sushi shop named “Tsuki” in New York are shown in Table 4 . In the table, “○” indicates that a reputation is correctly extracted and “✗” indicates that the text contains no reputation about the

Table 5. Number of f_{pat} and f_{con}

| | total | previous | | training subtree | | negative example | | both | |
|-----------|-------|-----------|-----------|------------------|-----------|------------------|-----------|-----------|-----------|
| | | f_{pat} | f_{con} | f_{pat} | f_{con} | f_{pat} | f_{con} | f_{pat} | f_{con} |
| curry | 265 | 234 | 111 | 233 | 118 | 234 | 135 | 233 | 143 |
| Sushi(JP) | 127 | 105 | 48 | 102 | 54 | 105 | 55 | 102 | 57 |
| bar | 140 | 117 | 19 | 111 | 19 | 117 | 19 | 111 | 36 |
| Sushi(NY) | 125 | 108 | 29 | 98 | 25 | 108 | 44 | 98 | 35 |

target shop. In this case, the reputation labeled \times is reputation of other Sushi shop.

4 Discussion

The number of correctly extracted nodes included in the outputs of the functions f_{pat} and f_{con} is written in Table 5. The number of correctly extracted nodes for f_{con} is increased in modified methods. This means that performance improvement of modified methods is due to performance improvement of their text classifiers.

According to Table 5, 13% of the target nodes were not extracted by a f_{pat} , and 50% of the other target nodes were not labeled 1 by f_{con} . The reason why so much target nodes were not labeled 1 by the f_{con} may be that the number of training data for the f_{con} was too small to learn the function. Especially for bars, various kinds of bars such as the Italian bars, French bars, and beer halls are included, so it might be difficult to learn a text classifier for their reputations. Note that if f_{con} is improved, both precision and recall will be improved because 86% of the texts wrongly labeled as reputations were reputations of other shops, which seems to be a result of classifying target texts into the non-reputation class. Since there is a performance limitation for text classifiers, detecting repetition structures [9] should be considered to improve precision at least.

The performance limitation of our method is mainly due to extracting only one node. Our method cannot extract such reputations that the LCA node of text nodes containing target reputations include the name of target restaurant or reputations of other restaurants. Patterns in which the beginning and ending of a target reputation can be specified should be used as considered in [3] to overcome this problem.

5 Conclusions

We conducted additional experiments to examine effectiveness of SACwRApper using datasets of four categories. According to the result of our experiments, our modified method achieved 75 ~ 88% precision and 26 ~ 54% recall. Our modified method outperformed a previous method by 5 ~ 14% recall among all categories and 6 ~ 14 % precision among three categories. High precision of our method is considered to indicate its usefulness, though recall is low for some categories.

We are now developing a new algorithm that solves the problems discussed in Sec. 4.

Acknowledgments

This work was partly supported by the Japan Ministry of Public Management, Home Affairs, Posts and telecommunications under grant SCOPE-S.

References

1. Hasegawa, H., Kudo, M. and Nakamura, A.: Reputation Extraction Using Both Structural and Content Information. Hokkaido university TCS Technical Report TCS-TR-A-05-2(<http://www-alg.ist.hokudai.ac.jp/tra.html>). (2005)
2. Hasegawa, H., Kudo, M. and Nakamura, A.: Creation of Better Pattern Set for Reputation Extraction Using Both Structural and Content Information. In Proc. of Data Engineering Workshop(ISSN 1347-4413). (2005) In Japanese
3. Kushmerick, N.: Wrapper Induction : Efficiency and expressiveness. Artificial Intelligence. **118** (2000) 15–68
4. Murakami, Y., Sakamoto, H., Arimura, H. and Arikawa, S.: Extracting text data from html documents. The Information Processing Society of Japan(IPSJ) Transactions on Mathematical Modeling and its Applications(TOM). **42**(SIG 14(TOM5)) (2001) 39–49 In Japanese
5. Cohen, W. W., Hurst, M. and Jensen, L. S.: A flexible learning system for wrapping tables and lists in html documents. In Proc. 11th Int'l World Wide Web Conf.. (2002) 232–241
6. Tateishi, K., Ishiguro, Y. and Fukushima, T.: A Reputation Search Engine that Collects People's Opinions by Information Extraction Technology. The Information Processing Society of Japan (IPSJ) Transactions on Databases (TOD). **45**(SIG 07) (2004)
7. Morinaga, S., Yamanishi, K., Tateishi, K. and Fukushima, T.: Mining product reputations on the web. In Proc. SIGKDD'02. (2002)
8. Hu, M. and Liu, B.: Mining and summarizing customer reviews. In Proc. SIGKDD'04. (2004)
9. Chang, C. H. and Lui, S. C.: Iepad: Information extraction based on pattern discovery. In Proc. 10th Int'l World Wide Web Conf.. (2001) 4–15

New Logical Classes of Plausibility Functions in Dempster-Shafer Theory of Evidence

Tetsuya Murai¹ and Yasuo Kudo²

¹ Graduate School of Information Science and Technology,

Hokkaido University, Sapporo 060-0814, Japan

{murahiko,mine}@main.eng.hokudai.ac.jp

² Muroran Institute of Technology, Muroran 050-8585, Japan

kudo@csse.muroran-it.ac.jp

Abstract. Several classes of the so-called logical plausibility functions are newly introduced from the point of view of modal logic. Then some systems of modal logic are shown to be both sound and complete with respect to the classes. The result will formulate the basis for developing a plausibility-based evidence theory.

Keywords: Plausibility Functions, Dempster-Shafer Theory of Evidence, Modal Logic, Measure-Based Semantics.

1 Introduction

In the paper, we newly introduce 'logical' classes of plausibility functions in Dempster-Shafer theory[6] from the point of view of modal logic. That is, instead of investigating logical properties under given, well-known classes of plausibility functions, conversely we derive such new classes from logical properties that plausibility functions generally lack. Then we examine systems of modal logic being both sound and complete with respect to the classes using our previous work measure-based semantics[3–5]

Throughout of this paper, we assume a language \mathcal{L} for modal logic of belief, which is formed as the usual way from a set of atomic sentences using the standard logical operators: \top (truth constant), \neg (negation), \wedge (conjunction), and \mathbf{B} (belief). Other operators such as \perp (falsity constant), \vee (disjunction), \rightarrow (material implication), and \leftrightarrow (equivalence) are defined in terms of the above-mentioned primitive operators as usual.

2 Scott-Montague Models for Modal Logic

Scott-Montague models (see Chellas[1] for details), which are a generalization of the well-known Kripke models, give a kind of possible-worlds semantics for modal logic. A *Scott-Montague* model for modal logic is defined as a structure

$$< W, N, v >$$

where $W(\neq \phi)$ is a set of possible worlds, N is a function from W to 2^{2^W} , and v is an assignment of truth values for atomic sentences for each world. We call a Scott-Montague model *finite* just in case that a set of possible world in the model is finite.

We write $\models_w^{\mathcal{M}} p$ to mean that a sentence p is true at a world w in a model \mathcal{M} . $\models_w^{\mathcal{M}} p$ can be obtained by extending v . In particular, the truth condition for belief sentences is given by

$$\models_w^{\mathcal{M}} \mathbf{B}p \Leftrightarrow \| p \|^{\mathcal{M}} \in N(w),$$

where

$$\| p \|^{\mathcal{M}} \stackrel{Df}{=} \{w \mid \models_w^{\mathcal{M}} p\}.$$

A classical system E is proved to be both sound and complete with respect to the class of Scott-Montague models, where E is the smallest system containing the rule of inference

$$\mathbf{RE}: \text{ from } p \leftrightarrow q \text{ infer } \mathbf{B}p \leftrightarrow \mathbf{B}q$$

as well as the rules and axiom schemata of propositional logic. Various conditions on N such as

- (m) $X \subseteq Y$ and $X \in N(w) \Rightarrow Y \in N(w)$,
- (c) $X, Y \in N(w) \Rightarrow X \cap Y \in N(w)$,
- (f) $X \cup Y \in N(w) \Rightarrow X \in N(w)$ or $Y \in N(w)$,
- (d) $X \in N(w) \Rightarrow X^C \notin N(w)$,
- (d_c) $X^C \notin N(w) \Rightarrow X \in N(w)$,
- (n) $W \in N(w)$,
- (p) $\phi \notin N(w)$.

Each condition validates its corresponding axiom schema such as

- M.** $\mathbf{B}(p \wedge q) \rightarrow (\mathbf{B}p \wedge \mathbf{B}q)$,
- C.** $(\mathbf{B}p \wedge \mathbf{B}q) \rightarrow \mathbf{B}(p \wedge q)$,
- F.** $\mathbf{B}(p \vee q) \rightarrow (\mathbf{B}p \vee \mathbf{B}q)$,
- D.** $\mathbf{B}p \rightarrow \neg \mathbf{B}\neg p$,
- D_c.** $\neg \mathbf{B}\neg p \rightarrow \mathbf{B}p$,
- N.** $\mathbf{B}\top$,
- P.** $\neg \mathbf{B}\perp$,

respectively.

3 Measure-Based Models for Modal Logic

A characteristic of fuzzy-measure-based models[3–5] is that truth values of modal sentences are determined by fuzzy measures. Let \mathcal{M} be a finite Scott-Montague model $\langle W, N, v \rangle$ and let

$$\mu_w : 2^W \rightarrow [0, 1]$$

be a fuzzy measure attached to each world $w \in W$. Then, we call \mathcal{M} a *fuzzy-measure-based* model just in case its function N is defined by

$$N(w) = \{X \mid \mu_w(X) = 1\}.$$

Then we have

$$\models_w^{\mathcal{M}} \mathbf{B}p \Leftrightarrow \mu_w(\parallel p \parallel^{\mathcal{M}}) = 1.$$

We call the \mathbf{B} a *fuzzy-measure-based* modal operator. If we use special fuzzy measures, say plausibility functions, then we call their model and operator by replacing their modifier 'fuzzy-measure-based' by, say, 'plausibility-function-based.' We have already proved several soundness and completeness results[3–5] and, among them, the followings are important in this paper:

1. A system $EMNP$ is sound and complete with respect to the class of plausibility-function-based models C^{Pl}
2. A system $EMFNP$ is sound and complete with respect to the class of possibility-measure-based models C^{Pos}
3. A system $EMCNP(=KD)$ is sound and complete with respect to the class of probability-measure-based models C^{Pr}
4. A system $EMCFNP(=KD!)$ is sound and complete with respect to the class of Dirac-measure-based models C^{δ}

where we use the Lemmon codes(cf.[1]) for naming systems of modal logic. For Example, the system $EMNP$ means the smallest system containing the rule of inference **RE** and axioms **M**, **N**, and **P** as well as the rules and axioms of propositional logic.

4 New Logical Classes of Plausibility Functions

4.1 Axioms Not Generally Satisfied by Plausibility Functions

A plausibility-function-based modal operator \mathbf{B} does not generally satisfy axioms **C**, **F**, **D**, and **D_C**. From soundness and completeness results stated in the previous section, we can conclude that the following classes of plausibility-function-based models are sufficient for these axiom schemata:

1. **C** and **D** hold for any model in C^{Pr} .
2. **F** and **D_C** hold for any model in C^{Pos}
3. All of the above four axioms hold for any model in C^{δ}

But, these classes are not maximal for their corresponding axioms. In fact, for example, there are plausibility functions that are not probability measures but satisfy **D**.

The purpose of this paper is to introduce such maximal classes of plausibility functions for each of these four axioms. Each maximal class of plausibility functions satisfying one of the four axioms is obviously characterized by

- [c] $(Pl(X) = 1 \text{ and } Pl(Y) = 1) \Rightarrow Pl(X \cap Y) = 1,$
- [f] $Pl(X \cup Y) = 1 \Rightarrow (Pl(X) = 1 \text{ or } Pl(Y) = 1),$
- [d] $Pl(X) = 1 \Rightarrow Pl(X^C) < 1,$
- [d_c] $Pl(X^C) < 1 \Rightarrow Pl(X) = 1,$

respectively. Note that each of the above conditions can be easily translated into the following equivalent formulae in terms of basic probability assignments:

$$\begin{aligned} [\text{c}] &\Leftrightarrow \forall X (X \subseteq \{x \mid bpa(\{x\}) = 0\} \Rightarrow bpa(X) = 0), \\ [\text{f}] &\Leftrightarrow bpa(\cap\{X \mid bpa(X) > 0\}) > 0, \\ [\text{d}] &\Leftrightarrow \forall X \exists Y (bpa(Y) > 0 \text{ and } (Y \subseteq X \text{ or } Y \subseteq X^C)), \\ [\text{d}_c] &\Leftrightarrow \forall X (\exists Y (bpa(Y) > 0 \text{ and } Y \cap X \neq \emptyset) \\ &\quad \Rightarrow \forall Y (bpa(Y) > 0 \Rightarrow Y \cap X^C \neq \emptyset)). \end{aligned}$$

We call plausibility functions satisfying one of the above conditions *logical*. In the rest of the paper, we investigate systems of modal logic being both sound and complete with respect to each of classes of logical plausibility functions.

4.2 Conjunctive Plausibility Functions

We firstly investigate the maximal class of plausibility functions satisfying the condition [c]. Because the axiom **C** corresponding [c] means *closure under conjunction*, we call such plausibility functions *conjunctive*.

Let \mathbf{C}^{CPl} be the class of conjunctive-plausibility-function-based models. Since both Dirac and probability measures are obviously conjunctive, we have

$$\mathbf{C}^\delta \subset \mathbf{C}^{Pr} \subset \mathbf{C}^{CPl}.$$

$EMCNP(=KD)$ have already been proved to be both sound and complete with respect to the class, \mathbf{C}^{EMCNP} , of Scott-Montague models satisfying four conditions (m), (c), (n), and (p) (cf.[1]):

$$\vdash_{EMCNP} p \Leftrightarrow \models_{\mathbf{C}^{EMCNP}} p,$$

where $\vdash_{EMCNP} p$ means p is a theorem of $EMCNP$ and $\models_{\mathbf{C}^{EMCNP}}$ means p is true at any world in any model in \mathbf{C}^{EMCNP} . Then we can prove our soundness and completeness theorems by showing

$$\mathbf{C}^{CPl} = \mathbf{C}^{EMCNP}.$$

Soundness of $EMCNP$ with respect to \mathbf{C}^{CPl} holds because we can easily check any model in \mathbf{C}^{CPl} satisfies the four conditions and this means

$$\mathbf{C}^{CPl} \subseteq \mathbf{C}^{EMCNP}.$$

Theorem 1 $EMCNP(=KD)$ is sound with respect to the class \mathbf{C}^{CPl} .

Completeness follows from the next lemma.

Lemma 2 For any Scott-Montague model $\mathcal{M} = \langle W, N, v \rangle$ in C^{EMCNP} , there exist conjunctive plausibility functions $\{Pl_w\}_{w \in W}$ such that

$$X \in N(w) \Leftrightarrow Pl_w(X) = 1.$$

The lemma shows that any model in C^{EMCNP} is nothing but a conjunctive-plausibility-function-based model, which means

$$C^{CPl} \supseteq C^{EMCNP}.$$

Thus we can prove completeness.

Theorem 3 $EMCNP (=KD)$ is complete with respect to the class C^{CPl} .

In the followings, we can prove soundness and completeness theorems for other classes in question in the same way of this subsection.

4.3 Disjunctive Plausibility Functions

Secondly we study the maximal class of plausibility functions satisfying the condition [f]. Because the axiom **F** corresponding [f] means *closure for disjuncts*, we call such plausibility functions *disjunctive*.

Let C^{FPl} be the class of disjunctive-plausibility-function-based models. Since both Dirac and possibility measures are obviously disjunctive, we have

$$C^\delta \subset C^{Pos} \subset C^{FPl}.$$

$EMFNP$ have already been proved to be sound and complete with respect to the class, C^{EMFNP} , of Scott-Montague models satisfying four conditions (m), (f), (n), and (p). Then we can prove our soundness and completeness by showing

$$C^{FPl} = C^{EMFNP}.$$

We can easily check that any model in C^{FPl} satisfies the four conditions and thus we have soundness.

Theorem 4 $EMFNP$ is sound with respect to the class C^{FPl} .

Completeness follows from the next lemma.

Lemma 5 For any Scott-Montague model $\mathcal{M} = \langle W, N, v \rangle$ in C^{EMFNP} , there exist disjunctive plausibility functions $\{Pl_w\}_{w \in W}$ such that

$$X \in N(w) \Leftrightarrow Pl_w(X) = 1.$$

Hence, we have completeness.

Theorem 6 $EMFNP$ is complete with respect to the class C^{FPl} .

4.4 Consistent Plausibility Functions

Next we investigate the maximal class of plausibility functions satisfying the condition [d]. Because the axiom **D** corresponding [d] means *consistency*, we call such plausibility functions *consistent*.

Let C^{DPl} be the class of consistent-plausibility-function-based models. Dirac and probability measures are obviously consistent, but consistent plausibility functions are not necessarily conjunctive. Hence, we have

$$C^\delta \subset C^{Pr} \subset C^{CPl} \subset C^{DPl}.$$

$EMDNP$ have already been proved to be sound and complete with respect to the class, C^{EMDNP} , of Scott-Montague models satisfying four conditions (m), (d), (n), and (p). Then we can prove our soundness and completeness by showing

$$C^{DPl} = C^{EMDNP}.$$

Since any model in C^{DPl} satisfies the four conditions, we have soundness.

Theorem 7 $EMDNP$ is sound with respect to the class C^{DPl} .

Completeness follows from the next lemma.

Lemma 8 For any Scott-Montague model $\mathcal{M} = \langle W, N, v \rangle$ in C^{EMDNP} , there exist consistent plausibility functions $\{Pl_w\}_{w \in W}$ such that

$$X \in N(w) \Leftrightarrow Pl_w(X) = 1.$$

This lemma completes the proof of the following completeness theorem.

Theorem 9 $EMDNP$ is complete with respect to the class C^{DPl} .

4.5 Pseudo-possibility Measures

Lastly we examine the maximal class of plausibility functions satisfying the condition $[d_c]$. In fact, such plausibility functions have already been pointed out by Dubois and Prade[2] and they called them *pseudo-possibility* measures.

Let C^{D_cPl} be the class of pseudo-possibility-measure-based models. Dirac and possibility measures are obviously pseudo-possibility measures, but pseudo-possibility measures are not necessarily disjunctive. Hence, we have

$$C^\delta \subset C^{Pos} \subseteq C^{FPl} \subset C^{D_cPl}.$$

EMD_cNP have already been proved to be sound and complete with respect to the class, C^{EMD_cNP} , of Scott-Montague models satisfying conditions (m), (d_c), (n), and (p). Then we can prove our soundness and completeness by showing

$$C^{D_cPl} = C^{EMD_cNP}.$$

Since any model in C^{D_cPl} satisfies the conditions, we have soundness.

Theorem 10 EMD_cNP is sound with respect to the class C^{D_cPl} .

Completeness follows from the next lemma.

Lemma 11 For any Scott-Montague model $\mathcal{M} = \langle W, N, v \rangle$ in C^{EMD_cNP} , there exist pseudo-possibility measures $\{Pl_w\}_{w \in W}$ such that

$$X \in N(w) \Leftrightarrow Pl_w(X) = 1.$$

Thus we have completeness.

Theorem 12 EMD_cNP is complete with respect to the class C^{D_cPl} .

5 Conclusion

In this paper we have newly specified three classes of logical plausibility functions from the point of view of modal logic and have formulate models based on those measures for modal logic including the case of pseudo-possibility measures defined by Dubois and Prade[2]:

1. C^{CPl} : the class of conjunctive-plausibility-function-based models
2. C^{FPl} : the class of disjunctive-plausibility-function-based models
3. C^{DPl} : the class of consistent-plausibility-function-based models
4. C^{D_cPl} : the class of pseudo-possibility-measure-based models

By these results, we have a step for introducing logical properties into the framework of fuzzy measure theory. The results will also give us the basis for developing a plausibility-based evidence theory.

Acknowledgement. This work was partly supported by the Japan Ministry of Public Management, Home Affairs, Posts and Telecommunications under Grant SCOPE-S, and by Grant-in-Aid (No.14380171) of the Japan Society for the Promotion of Science.

References

1. B.F.Chellas, *Modal Logic: An Introduction*. Cambridge University Press, 1980.
2. D.Dubois and H.Prade, A Class of Fuzzy Measures Based on Triangular Norms. *Int.J.of Genaral Systems*, Vol.8(1982), pp.43-61.
3. T.Murai, M.Miyakoshi, and M.Shimbo, Measure-Based Semantics for Modal Logic. *R.Lowen and M.Roubens(eds.), Fuzzy Logic : State of the Art*, Kluwer Academic Publishers, 1993, pp.395-405.
4. T.Murai, M.Miyakoshi, and M.Shimbo, Soundness and Completeness Theorems between the Dempster-Shafer Theory and Logic of Belief. *Proc.3rd FUZZ-IEEE (WCCI)*, 1994, pp.855-858.
5. T.Murai, M.Miyakoshi, and M.Shimbo, A Logical Foundation of Graded Modal Operators Defined by Fuzzy Measures. *Proc.4th FUZZ-IEEE*, 1995, pp.151-156.
6. G.Shafer, *A Mathematical Theory of Evidence*. Princeton University Press, 1976.

Person Tracking with Infrared Sensors

Taisuke Hosokawa and Mineichi Kudo

Graduate School of Information Science and Technology
Hokkaido University, Sapporo 060-8628, Japan
`{taisuke,mine}@main.ist.hokudai.ac.jp`

Abstract. We consider a person tracking system that is robust to environmental changes and users are unaware of. Once a user is identified at an entrance door in a room with his/her biometrics, we can keep tracking the user continuously. The pyroelectric infrared sensors in the ceiling are used for this goal. These sensors are resistant to environmental changes, but give only a weak piece of evidence. We applied a Bayesian network to infer the position of the user, and investigated how the Bayesian network works. We gained 64.0% in average for a single-person tracking.

1 Introduction

In recent years, person identification systems have been developed. They use biometrics such as fingerprint, iris and finger vein. They identify the person with a high identification rate. However, these evidences require user's cooperation and users are aware of the identification process which sometimes makes the user feel unpleasant. In this paper we consider 'soft identification' in which a user does not even notice the identification process. The possible applications are electronic appliances on daily life. Through a soft identification, such an appliance can be personalized to that user in such a way that the system provides some user-specific functions to the user. For example, if a user sits in front of a TV set, the channel changes automatically for user's taste. In our research, we examine a way that enables us to track a user to give personalized service anywhere.

For human tracking, a distributed vision system is proposed [1]. This system does not require user's cooperation, and can track a user with a small error. However, the tracking area is limited and is affected by the light condition because it uses a camera. In addition, a person tracking system using floor sensors is also considered [2]. It uses floor sensors consisting of 1,140 blocks to detect human weights, and can track people in a broad area. Since they are robust to environmental changes, such a trial is useful for 'soft identification'. In this paper, we will consider a similar system with infrared sensors attached to the ceiling. The sensors in the ceiling cover a broader area than those in floor. Infrared sensors have already been used for human tracking [3], but the system requires the user to keep an infrared device. In addition, the resolution for tracking is too rough to track a small-distance movement of individuals. Each sensor in the ceiling is placed 2.5 meters high from the floor keeping 1.5 meters apart from other sensors. Each sensor detects human (human temperature) movements in a circle with radius 1m. Due to the overlapped placement, multiple-sensor can be turned

on at the same time by a single movement. The readings from the infrared sensors are rough, so we will take a probabilistic approach for inferring the position of a person. We will use a Bayesian network for this probabilistic inference, and will investigate how the Bayesian network works for this goal.

2 Infrared Sensor System

We use 50 pyroelectric infrared motion sensors (Fig. 1). The pyroelectric infrared sensor detects the infrared ray generated from human movements. Table 1 shows the standard performance of the infrared sensor. Each sensor is placed in about 1.5 meters distance from the other sensors in the ceiling (Fig. 2 (a)). We narrowed the detection area of sensors using a paper cylinder to about 1 meter circle centered at the immediately below a sensor in the floor (Fig. 2 (b)). Each sensor returns “1” when it detects a motion, otherwise returns “0”. We obtain the information as a vector $S_t \in \{0, 1\}^{50}$ at every 0.5 seconds. It is noted that The sensor information is independent of the light conditions.

A finger vein authentication system at an entrance door identifies people who enter the room. This system allows only the registered user to get in. A user is (hard) identified in a door by his/her finger vein. When the system identifies a user, the door opens and we receive a signal like “{enter or leave}” and the user’s name. With this information we start tracking.

3 Tracking by Bayesian networks

We obtain the sensor readings like “0110000...” from infrared sensors in each 0.5 seconds. We apply a probabilistic approach to keep tracking, and we repeated

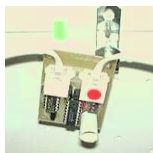
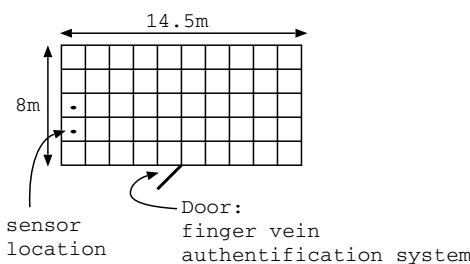


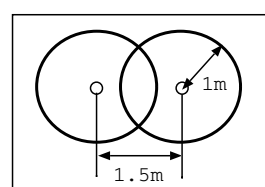
Fig. 1. Pyroelectric infrared sensor

Table 1. sensor's standard performance

| | |
|-------------------------|---|
| detectable distance | 5m at a maximum |
| detectable area | 100° (horizontal direction) 82° (vertical direction) |
| detectable motion speed | 0.5–1.5 m/s |



(a) position



(b) sensing area

Fig. 2. Sensor layout in our laboratory

an inference of the position of the user from the current sensor status and the previous position guess.

First, we consider one-person tracking. Let the number of sensors be N , the number of possible positions be M . Moreover, let X_t be the user's position at time t ($X_t \in \{1, \dots, M\}$), and S_t be a vector of sensors' signals at time t ($S_t \in \{0, 1\}^N$). Then we infer the position X_t by the marginal probability $P(X_t|X_0, \dots, X_{t-1}, S_0, \dots, S_t)$. Using this conditional probability, we infer the most probable position of X_t by choosing the position which has the largest value of this.

We calculate the probability $P(X_t|X_0, \dots, X_{t-1}, S_0, \dots, S_t)$ using a Bayesian network [4]. Bayesian networks are compact expressions of a joint distribution and are very useful when its probabilistic dependency among random variables is known or is able to be assumed. In our case, we build up a Bayesian network from a natural dependency of X_0, \dots, X_t and S_0, \dots, S_t .

3.1 Structure

We choose one structure shown in Fig.3 from possible structures for dynamic Bayesian networks [5]. This structure is of two dependencies. In the network, (1) the position of a user at time t depends on the previous position at time $t-1$, (2) the sensor readings depend on both the current position and the previous position. It is noted that sensor readings are not enough for identifying the position correctly. Another structure can be considered. However, we chose this structure as the base model for simplicity. In this network, the joint probability is decomposed as

$$P(X_0, \dots, X_t, S_0, \dots, S_t) = P(X_0)P(S_0|X_0)\prod_{i=1}^t P(X_i|X_{i-1})P(S_i|X_{i-1}, X_i),$$

and the conditional probability of X_t is written by

$$\begin{aligned} P(X_t|X_0, \dots, X_{t-1}, S_0, \dots, S_t) &= P(X_t|X_{t-1}, S_t) \\ &= \frac{P(X_t|X_{t-1})P(S_t|X_{t-1}, X_t)}{\sum_{X_t} P(X_t|X_{t-1})P(S_t|X_{t-1}, X_t)}. \end{aligned}$$

We have to estimate the following parameters: $P(X_0)$, $P(S_0|X_0)$, $P(X_t|X_{t-1})$, $P(S_t|X_t, X_{t-1})$. With the time invariantness, we estimate these parameters empirically by considering successive two positions regardless of t .

3.2 Probability Updating

Let e_t be a piece of evidence. Then the marginal probability can be written as $P(X_t|e_t)$. In this model, e_t is given by $e_t = \{X_{t-1} = x_{t-1}, S_t = s_t\}$ for $t > 0$. Here, s_t is a hard evidence and x_{t-1} is a soft evidence, because x_{t-1} is the estimated one. We apply a belief updating way on the Bayesian network [6]. Here, X_0 is fixed as the entrance and $S_0 = 0 \cdots 0$ as the initial stage. We consider the following procedure [6]:

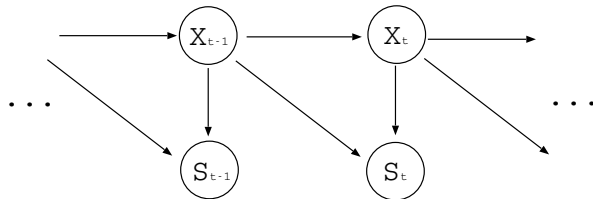


Fig. 3. Bayesian network used for position estimation

1. If $P(X_{t-1}|e_{t-1})$ is given, e_{t-1} is transmitted to get $P(X_t|e_{t-1})$ (Fig.4 (a)).
 2. Eliminating time slice $t - 1$, the prior probability of X_t becomes $P(X_t|e_{t-1}, X_{t-1} = x_{t-1})$ (Fig.4 (b)).
 3. By entering the evidence on S_t , $P(X_t|e_{t-1}, X_{t-1} = x_{t-1})$ is updated to $P(X_t|e_t)$. This probability is the output.
 4. Add time slice $t + 1$, the updating procedure is repeated (Fig.4 (c)).

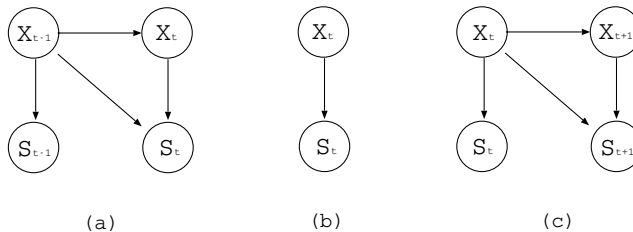


Fig. 4. Probability updating of Bayesian networks

4 Experiments

To see how this model works for actual person tracking, we conducted an experiment. We also investigated to what degree the walking speed affects the tracking accuracy.

Using this Bayesian network, we attempted to track a user entering a room. With $N = M = 9$, we considered a locally defined 9 positions centered at the current user position. In this case, the information from the sensors are limited to $S_t \in \{0, 1\}^9$.

The conditional probabilities were calculated from the frequencies of 924 training data. People were asked to walk around in a room along to a planned path. Fig.5 shows the local area used for calculation. For example, when a person walk along to path 0-1-2 in Fig.5 keeping the speed to produce 6 samples (this means that the person walked the path in 3 seconds), the first 2 samples are recorded two zero's, the middle 2 samples two one's, the last 2 samples two two's. The training paths are six of 0-1-2,3-4-5,6-7-8,0-3-6,1-4-7,2-5-8 in Fig.5 and their reverses. People walked these training path 100 times in total. The



Fig. 5. The local area assumed for tracking

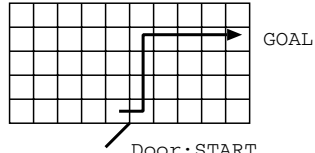


Fig. 6. Test route for tracking

Bayesian network is learned by these 924 training samples for nine-neighbor model.

For testing, we tried to track a person who is asked to take a predetermined route in a fixed speed (Fig.6). First, the user is identified correctly by his finger vein, and then is tracked by this system. Collecting information from infrared sensors each time, we infer his position by the Bayesian network. Five people walked the same course 10 times in a usual walking speed and a higher speed. The results are shown in Table 2. Here, we regarded as a success when the person was traced successfully by the Goal position.

Table 2. The rate of correct tracking

| Walking speed | rate of success |
|-----------------------------|-----------------|
| usual speed (about 1.0m/s) | 64.0% |
| faster speed (about 1.4m/s) | 45.5% |

In average of 64.0%, we succeeded to have tracked a single user. This system sometimes lost the person at a corner, then we fail to track him. One of the possible causes is that this system has not learned well the way when a person turns off quickly. Other possible causes is that sensors fail to detect the motion because of some obstacles like a partition board. The increase of walking speed affected much the rate of correct tracking. Indeed, the average success rate decreased to 45.5%.

We also applied a multiple version of this Bayesian network to multiple-user tracking. Two or three people entered the room in a few seconds interval, and walked around freely. If the users keep distance to each other, we could track them as well as one-person tracking. However, if they come close, for example, one user is neighboring the other, or two users share the same position, the system could rarely distinguish two users. The average success rate is about 20%.

5 Discussion

We confirmed that our Bayesian network works to some extent for a single-person tracking but is not sufficient for a multi-person tracking. We need to investigate another structure of Bayesian networks and to compare with other

non-probabilistic approaches. The main reason of failure is that we lost the person in the middle of tracking. It is obvious that we can recover the lost information by restart the position where the corresponding sensors are active if there is only one person exists in the room. However, it cannot work when more than one person exist. We need to develop the system in order to recover such a lost information by considering a kind of continuity of the successive movement of a person on time.

As for the walking speed, we could track as long as a person walks in a natural speed. As the speed increases, the system made error. To cope with this problem, we may increase the sampling rate of the sensor responses and increase the resolution with more sensors. However, since our main motivation is in a simple and easy-to-equip system for daily life, such an improvement is the last option.

For multiple-user problems, we could track a few users when they keep a distance with a same success rate as that of single-user cases. Improvement is needed for when they cross or share a same position. For this direction, there are some possibilities: treatment of X_t as a time series, an extension of probability dependencies, an extended local map, and so on.

One of promising application of this approach is to incorporate with the other system. We may have a strong evidence by collecting many pieces of weak evidence such as those in this study. Even if we cannot determine a single user correctly, it is sometimes enough to have a set of a few candidates with a high confidence. Then, we can through this set to the following identification process. Indeed, we have been developing such a system where a person is identified from the response of pressure sensors on a chair [7]. The above set is confirmed to be useful to increase the correct recognition rate.

6 Conclusion

We attempted to track people with infrared sensors for continuous identification. With infrared sensors, the tracking is robust to environmental changes and does not make people aware of. We succeeded at 64.0% for single-person tracking. This rate is not enough, but the potential was confirmed. We will investigate this in more details and will improve the system.

Acknowledgment

This work was partly supported by the Japan Ministry of Public Management, Home Affairs, Posts and telecommunications under grant SCOPE-S.

References

1. Sogo, T., Ishiguro, H., Trivedi, M. M.: Real-time Human Tracking System with Multiple Omni-Directional Vision Sensors. IEICE Transactions on Information and Systems, J83-D-II, 12(2000) 2567–2577 (In Japanese)

2. Murakita, T., Ikeda, T., Ishiguro, H.: Human Tracking using Floor Sensors based on the Markov Chain Monte Carlo Method. Technical Report of IEICE. **PRMU2004-29** (2004) (In Japanese)
3. Want, R., Hopper, A., Falcao, V., and Gibbons, J.: The Active Badge location system. *ACM Transactions on Information Systems.* 10(1) (1992) 91–102
4. Jensen, V. Finn.: Bayesian Networks and Decision Graphs. Springer-Verlag. (2001)
5. Pavlovic, V., Rehg, James M., Cham, T., and Murphy, P.: A Dynamic Bayesian Network Approach to Figure Tracking Using Learned Dynamic Models: International Conference on Computer Vision (ICCV99). (1999) 94–101
6. Russel, S., Norvig, P.: Artificial intelligence, A modern approach. Prentice Hall. (1995)
7. Yamada, M., Toyama, J., Kudo, M.: Person recognition by pressure sensors. Proceedings of KES2005. to appear.

Entropy Criterion for Classifier-Independent Feature Selection

Naoto Abe and Mineichi Kudo

Division of Computer Science,
Graduate School of Information Science and Technology,
Hokkaido University, Sapporo 060-0814, Japan
{chokujin,mine}@main.eng.hokudai.ac.jp

Abstract. Feature selection aims to select a feature subset that has discriminative information from the original feature set. In practice, we do not know what classifier is used beforehand, and it is preferable to find a feature subset that is universally effective for any classifier. Such a trial is called *classifier-independent feature selection* and can be made by removing garbage features that have no discriminative information. However, it is difficult to distinguish only garbage features from the others. In this study, we propose an entropy criterion for this goal and confirm the effectiveness through a synthetic dataset.

1 Introduction

In pattern recognition, the goal of feature selection is to find a feature subset that has the most discriminative information from a given set of candidate features. The main benefits of the feature selection are follows: (i) reducing the measurement cost and storage requirements, (ii) coping with the degradation of the classification performance due to the finiteness of training sample sets, (iii) facilitating data visualization and data understanding.

Algorithms of feature selection can be divided into two groups. One group is called as *classifier-specific feature selection* (CSFS). CSFS selects a feature subset that maximizes the value of a given criterion function such as the estimated recognition rate for a specified classifier. A large number of CSFS have been proposed in pattern recognition and some comparative studies of CSFS are reported for large-scale feature selection problems[1–3]. The other group is called as *classifier-independent feature selection* (CIFS)[4–7]. In CIFS, we seek a feature subset that is effective for all classifiers. To do this, we find a feature subset that contributes the separation between class-conditional probability densities. It means that we have to estimate class-conditional probability densities as precisely as possible and consider implicitly the Bayes classifier which achieves the minimal expected error rate. In other words, CIFS is equivalent to CSFS for the Bayes classifier, and the goal of CIFS is to remove *garbage features* which have no discriminative information for any kind of classifier. To do CIFS, we can take one of two approaches on the basis of training samples: (1) try to estimate the class-conditional density of each class so that we could have a quasi Bayes

classifier, or (2) try to estimate a pseudo Bayes classification boundary. In this study, we take the first approach on the basis of Novovičová *et al.*'s method. In the Novovičová *et al.*'s method, the axis-parallel Gaussian components are used in a mixture model for estimating the class-conditional probability densities, and the feature subset that maximizes J-divergence between the estimated densities is selected. Subsequently, the J-divergence value of each feature gives a ranking of them. Therefore, we can directly use the value of the J-divergence of each feature as those of feature importance. However, in their original work, the number of selecting features has to be specified beforehand. In practice, it is difficult to do this.

In this study, we propose an entropy criterion for determining how many features we should leave when the feature importance measure is given. In the following section, we explain the basic idea of the entropy criterion using two simple examples. In Section 3, we investigate how the entropy criterion works. Finally, we discuss and conclude the fundamental effectiveness of the entropy criterion.

2 Entropy Criterion

2.1 Basic Idea

In this study, we denote the number of original features by D and the number of features to be selected by d . We assume that feature importance f_i ($f_i \geq 0$, $\sum_{i=1}^d f_i = 1$) is given. We impose a normalization so as to satisfy the condition $f_1 + f_2 + \dots + f_d = 1$. The entropy is a key measure for evaluating the ambiguity of random variables. If a random variable takes all possible values with an equal probability, the entropy takes the maximum. While, it takes the minimum when the random variable takes a single value only with probability one.

We take notice of this characteristic for the determination of the feature subset size. The entropy of feature importance in size d is given by $H_d = -\sum_{i=1}^d f_i \log f_i$. If all features are equally important, that is, $f_i = 1/d$ ($i = 1, 2, \dots, d$), the entropy shows the maximum value of $\log d$. On the other hand, in the case that only one feature is important, that is, $f_i = 1, f_j = 0$ ($j = 1, 2, \dots, d, j \neq i$), H_d takes zero value and we leave only i th feature with $f_i = 1$. Therefore, in this study, we use the entropy for determining the size of a feature subset without garbage features and consider a procedure in which the lowest ranked feature is removed step by step. That is, we determine the ideal number of selected features on the basis of the comparison between d and $\exp(H_d)$. The basic algorithm of feature selection in this study is shown in Fig. 1.

2.2 A Case That Discriminative or Garbage Is Clear

Let us assume that the eight features are evaluated as follows:

$$\left(\frac{1}{4}, \frac{1}{4}, \frac{1}{4}, \frac{1}{4}, 0, 0, 0, 0 \right).$$

| Feature selection procedure |
|---|
| 1. Set $d = D$. |
| 2. Obtain f_i ($f_i \geq 0$, $\sum_{i=1}^d f_i = 1$) and calculate H_d . |
| 3. Calculate $\hat{d} = \lfloor \exp(H_d) + 0.5 \rfloor$. |
| 4. If $\hat{d} = d$ is satisfied, we terminate the feature selection procedure. Otherwise, proceed to step 5. |
| 5. One feature that has the least value of feature importance is removed. Then $d \leftarrow d - 1$ and go to step 2. |

Fig. 1. Basic algorithm of feature selection on the basis of the entropy criterion

Here, $D = 8$. In this case, the first four features have the same amount of feature importance and the last four features are garbage features. Then, H_8 takes $\log(4)$ and thus we have $\hat{d} = 4$ with the first four features. Under the assumption that the relative evaluation of feature importance does not change during the feature removal, we have the same values for the first four features. After removing four features, we have

$$\left(\frac{1}{4}, \frac{1}{4}, \frac{1}{4}, \frac{1}{4} \right).$$

Then, the entropy H_4 takes $\log(4)$, and we terminate this feature selection procedure to have the first four features.

2.3 Practical Case Simulation

We consider one more example. Let the feature importance be given as follows:

$$\left(\frac{1}{2}, \frac{1}{4}, \frac{1}{8}, \frac{1}{16}, \frac{1}{32}, \frac{1}{64}, \frac{1}{128}, \frac{1}{128} \right).$$

Here, $D = 8$. In this case, i th ($i = 1, 2, \dots, 7$) feature has the feature importance of $(1/2)^i$ and the last two features have the same value. Then, $\exp(H_8)$ takes 3.96 and $\hat{d} = 4$, thus we determine that four features are necessary and remove one of the last two features. Repeating the removal of features, we reach at the first three features with $(1/2, 1/4, 1/4)$.

3 Experiments

3.1 Evaluation on the Basis of Selected Features

We examined the effectiveness of the proposed criterion on *Friedman* dataset[8]. In the *Friedman* dataset, there are two classes and the original number of features is $D = 10$. The latter six features are garbage. We prepared four kind of datasets changing the number of samples by $N = 10, 100, 1000, 10000$. For a CIFS method, we used Novovičová *et al.*'s method and obtained each feature

importance by calculating the J-divergence of each feature. The number of mixtures in axis-parallel Gaussian models was determined by the MDL principle method[9]. However, the number of selecting features have to be specified by the user. Therefore, in this experiment, we investigated whether a feature subset without garbage features could be obtained or not by applying the entropy criterion to Novovičová *et al.*'s method. The procedure of this experiment was shown in Fig.2.

Algorithm of feature selection in this experiment

1. The number of mixtures is determined for each class and D is set by $d = D$.
 2. The parameters of Gaussian mixtures are estimated by EM algorithm.
 3. The divergence of each feature is calculated and then H_d is obtained.
 4. When $\hat{d} = d$ is satisfied, we terminate the feature selection. Otherwise, go to step 5.
 5. We removed one feature that has the least feature importance among remained features and $d \leftarrow d - 1$. Then go to step 2.
-

Fig. 2. The procedure of the experiment using Novovičová *et al.*'s method

The value \hat{d} as well as the selected features in each step were summarized in Table 1. Totally, the number of necessary features were found properly for all cases. For $N = 100, 1000, 10000$ cases, the correct feature subset were found. However, we could not find the correct feature subset for $N = 10$. This was because the performance of feature evaluation in Novovičová *et al.*'s method was degraded owing to the lack of sufficient number of training samples.

Table 1. The selected feature subset on *Friedman* dataset by the proposed criterion

| (a) N=10 | | | (b) N=100 | | |
|----------|-----------|----------------------|-----------|-----------|----------------------|
| d | \hat{d} | Remained features | d | \hat{d} | Remained features |
| 10 | 5 | 1,2,3,4,5,6,7,8,9,10 | 10 | 5 | 1,2,3,4,5,6,7,8,9,10 |
| 9 | 5 | 1,2,3,4,5,6,7,8,9 | 9 | 5 | 1,2,3,4,5,6,7,9,10 |
| 8 | 5 | 1,2,3,4,5,7,8,9 | 8 | 5 | 1,2,3,4,5,7,9,10 |
| 7 | 5 | 1,2,4,5,7,8,9 | 7 | 5 | 1,2,3,4,5,9,10 |
| 6 | 5 | 2,4,5,7,8,9 | 6 | 4 | 1,2,3,4,9,10 |
| 5 | 4 | 2,4,5,7,9 | 5 | 4 | 1,2,3,4,10 |
| 4 | 4 | 2,4,7,9 | 4 | 4 | 1,2,3,4 |

| (c) N=1000 | | | (d) N=10000 | | |
|------------|-----------|----------------------|-------------|-----------|----------------------|
| d | \hat{d} | Remained features | d | \hat{d} | Remained features |
| 10 | 4 | 1,2,3,4,5,6,7,8,9,10 | 10 | 4 | 1,2,3,4,5,6,7,8,9,10 |
| 9 | 4 | 1,2,3,4,5,6,8,9,10 | 9 | 4 | 1,2,3,4,5,6,8,9,10 |
| 8 | 4 | 1,2,3,4,6,8,9,10 | 8 | 4 | 1,2,3,4,5,8,9,10 |
| 7 | 4 | 1,2,3,4,6,8,10 | 7 | 4 | 1,2,3,4,5,9,10 |
| 6 | 4 | 1,2,3,4,8,10 | 6 | 4 | 1,2,3,4,5,10 |
| 5 | 4 | 1,2,3,4,10 | 5 | 4 | 1,2,3,4,5 |
| 4 | 4 | 1,2,3,4 | 4 | 4 | 1,2,3,4 |

3.2 Evaluation on the Basis of Recognition Rates

Moreover, we examined the effectiveness of the proposed criterion on the basis of recognition rates of classifiers. If garbage features are removed properly, the recognition rates of classifiers would be improved or maintained before and after the garbage feature removal. We investigated whether this was the case or not. Used classifiers were the plug-in linear/quadratic classifier (LDF/QDF), the nearest neighbor classifier (1NN), a decision tree classifier (C4.5), a hyper-rectangle classifier[10] (SUB), a neural network classifier (NNC) and a support vector machine[11] (SVM). The software c4.5[12] was used for a decision tree classifier and the program SVMTorch[13] for support vector machine classifier. The default parameters equipped with c4.5 and SVMTorch were used for C45 and SVM respectively. The iteration number was set to 100 in SUB. The number of layers was 3 and the number of units in the hidden layer was set by (#features + #classes) / 2 in NNC. The recognition rate was calculated by the 10-fold cross validation technique.

Recognition rates of classifiers were shown in Table 2. The better recognition rates were shown in bold style before and after the garbage feature removal. In the case that $N = 10$, we could not construct the QDF classifier because the covariance matrices became singular owing to few number of samples. From Table 2, recognition rates of classifiers were improved or maintained totally compared with the case that all the features were used. From this point, the proposed criterion could find the size of feature subset so as to improve or maintain the classification performance for any classifier.

Table 2. The comparison of recognition rates before and after the garbage feature removal on *Friedman* dataset

| Classifier | Recognition rate(%) | | | |
|------------|---|---------------------------|---------------------------|-------------------|
| | (selected feature set / original feature set) | | | |
| | N=10 | N=100 | N=1000 | N=10000 |
| LDF | 80.0 /40.0 | 50.0/ 53.0 | 49.3 /47.9 | 50.8/ 50.9 |
| QDF | – / – | 88.0 /74.0 | 92.0/ 92.3 | 93.4 /93.2 |
| 1NN | 70.0 /40.0 | 86.0 /67.0 | 94.6 /85.7 | 96.5 /90.5 |
| C4.5 | 50.0 / 50.0 | 88.0 / 88.0 | 93.9 /92.5 | 95.9 /95.6 |
| SUB | 80.0 /40.0 | 84.0 /79.0 | 91.3 /82.4 | 92.2 /76.3 |
| NNC | 90.0 /80.0 | 71.0 /58.0 | 76.3 /74.7 | 77.9 /69.0 |
| SVM | 80.0 /60.0 | 97.0 /95.0 | 98.6 / 98.6 | 98.9 /98.8 |

4 Discussion

So far, we removed the lowest ranked feature one by one. On the other hand, we can remove some lower ranked features at the same time. Indeed, in Table 1, we can see the potential (see the value of \hat{d} in each size). To investigate this point, we found a feature subset by removing $d - \hat{d}$ features in a single step. The result was shown in Table 3. From Table 3, we found a feature subset without remaining garbage features as long as a sufficient number of samples was available.

Table 3. Features that have \hat{d} largest feature importance among the original features in a single step on *Friedman* dataset

| #Sample | \hat{d} largest in $d = 10$ |
|---------|-------------------------------|
| N=10 | 2,4,5,7,9 |
| N=100 | 1,2,3,4,10 |
| N=1000 | 1,2,3,4 |
| N=10000 | 1,2,3,4 |

5 Conclusion

In this study, we proposed a criterion for selecting features on the basis of the entropy. It was empirically confirmed that the proposed criterion was effective to determine the feature subset size automatically, and the selected feature subset was universally effective for any classifier. For a further study, we will apply the proposed criterion to various CIFS methods and investigate whether a feature subset without garbage features can be obtained on many real-world datasets.

Acknowledgement

This work was partly supported by the Japan Ministry of Public Management, Home Affairs, Posts and telecommunications under grant SCOPE-S.

References

1. Ferri, F.J., Pudil, P., Hatef, M., Kittler, J.: Comparative Study of Techniques for Large-scale Feature Selection. In: Gelsema, E.S., Kanal, L.N. (eds.): Pattern Recognition in Practice IV, Elsevier, Amsterdam (1994) 403–413
2. Blum, A.L., Langley, P.: Selection of Relevant Features and Examples in Machine Learning. *Artificial Intelligence* **97** (1997) 245–271
3. Kudo, M., Sklansky, J.: Comparison of Algorithms that Select Features for Pattern Recognition. *Pattern Recognition* **33** (2000) 25–41
4. Singh, S.: PRISM - A Novel Framework for Pattern Recognition. *Pattern Analysis and Applications* **6** (2003) 131–149
5. Kudo, M., Shimbo, M.: Feature Selection Based on the Structural Indices of Categories. *Pattern Recognition* **26** (1993) 891–901
6. Holz, H.J., Loew, M.H.: (1994) Relative Feature Importance: A Classifier-Independent Approach to Feature Selection. In: Gelsema, E.S., Kanal, L.N. (eds.): Pattern Recognition in Practice IV, Elsevier, Amsterdam (1994) 473–487
7. Novovičová, J., Pudil, P., Kittler, J.: Divergence Based Feature Selection for Multimodal Class Densities. *IEEE Transactions on Pattern Analysis and Machine Intelligence* **18** (1996) 218–223
8. Friedman, J.H.: A Recursive Partitioning Decision Rule for Nonparametric Classification. *IEEE Transactions on Computers* **26** (1977) 404–408
9. Ichimura, N.: Robust Clustering Based on a Maximum Likelihood Method for Estimation of the Suitable Number of Clusters. *Transactions of the Institute of Electronics Information and Communication Engineers* **J78-D-II** (1995) 1184–1195 (in Japanese)

10. Kudo, M., Yanagi, S., Shimbo, M.: Construction of Class Region by a Randomized Algorithm: A Randomized Subclass Method. *Pattern Recognition* **29** (1996) 581–588
11. Vapnik, V.: *The Nature of Statistical Learning Theory*. Springer-Verlag, New York (1995)
12. Quinlan, J.R.: *C4.5: Programs for Machine Learning*. Morgan Kaufmann, San Mateo CA (1993)
13. Collobert, R., Bengio, S.: SVMTorch: Support Vector Machines for Large-Scale Regression Problems. *Journal of Machine Learning Research* **1** (2001) 143–160

Finding and Auto-labeling of Task Groups on E-Mails and Documents

Hiroshi Tenmoto¹ and Mineichi Kudo²

¹ Department of Information Engineering,

Kushiro National College of Technology,

Otanoshike Nishi 2-32-1, Kushiro, Hokkaido 084-0916, Japan

tenmo@kushiro-ct.ac.jp

² Division of Computer Science,

Graduate School of Information Science and Technology,

Hokkaido University, Sapporo 060-0814, Japan

mine@main.ist.hokudai.ac.jp

Abstract. We propose a new method which extracts task groups on user's numerous messages such as e-mails and documents by finding the family of subsets that share common topics, sender/receivers, date or author. In addition, the method automatically gives labels to the groups by the common items. The biggest difference between the proposed method and conventional methods is that the conventional methods find completely divided clusters of documents, while the proposed method finds overlapping clusters of documents on the basis of subclass method. Therefore, the proposed method provides multiple views on the documents. We carried out experiments on the authors' e-mails and document files in order to confirm the basic property and effectiveness of the proposed method.

1 Introduction

Nowadays, most of our daily works are of making, viewing, editing documents such as word processor documents, spread sheets or web page documents, and sending and receiving e-mails. In such works, it often happens that the user have to arrange, search and refer the past documents. However, such a typical work is not so easy for ordinal lazy users. Therefore, the newest modern operating systems equip flexible and high-speed full text search facility, so the user can find the documents easily without being conscious of the names or places of the documents.

Still, in such a conventional search facility, the most important point is the searching keywords. Hence, the user have to input the keywords or sysnonyms when the user wants to find something. In this style of usage, the system requires the user to remember the keywords, so the user have to try many times until the user can obtain the desired results. Meanwhile, from the viewpoint of our works, it seems to be very useful if the system automatically present the list of past tasks, for example, "the documents used when I collaborated with Dr. Kudo in the last year."

Therefore, we are proposing a novel hierarchical documents browsing system which bases on the idea of information granularity (patent pending). In this paper, we introduce the overlapping clustering method that is the main part of the browsing system. In this method, we extract task groups on user's numerous messages such as e-mails and documents by finding the family of subsets that share common topics, sender/receivers, date or author. In addition, the method automatically gives labels to the groups by the common items.

The biggest difference between the proposed method and conventional methods is that the conventional methods find completely divided clusters of documents, while the proposed method finds overlapping clusters of documents on the basis of subclass method [1]. Therefore, the proposed method provides multiple views on the documents. We carried out experiments on the authors' e-mails and document files in order to confirm the basic property and effectiveness of the proposed method.

2 Finding and Auto-labeling of Task Groups

2.1 Bag-of-Words Model with Meta-information

In this method, for the purpose of vectorization of documents, we employ Bag-Of-Words model which is widely used in the field of text-mining. We tokenize the body of a document by the part-of-speech and morphological analyzer for natural languages, and let the frequency of each word the element of the document vector. Here, the appearing words should be assigned unique ID numbers using dictionary in advance.

In addition, as the meta information for the e-mails, word processor documents, spread sheets and web page documents, we consider the following items. We add these meta informations to the document vector with frequency 1. Here, the date information is described by three items in order to obtain the granular expressions. The sender and receivers of documents except for e-mails are set by the document's author itself.

- Date (Year)
- Date (Year and Month)
- Date (Year, Month and Day)
- Sender
- Receivers

In the following sections, we use the mathematical expressions below for the document vectors.

- $X = \{\mathbf{x}_1, \mathbf{x}_2, \dots, \mathbf{x}_n\}$: Set of documents.
- n : Number of documents.
- $\mathbf{x}_i = \{x_i^1, x_i^2, \dots, x_i^d\}$: Vector expression of the i th document.
- d : Number of words registered in the dictionary.
- x_i^j : Frequency of the j th word or meta information in the i th document.

2.2 Subclass Method on Bag-of-Words Model

We extract the family of subsets of documents $\mathcal{Y} \subseteq 2^X$ by the following procedure after converting all of the documents into the document vectors. Here, each subset $Y \in \mathcal{Y}$ is constructed so as to contain as many documents as possible under a certain constraint. In addition, we do not allow the complete inclusive relationship for any two subsets, while we positively allow the overlapness between the subsets. By such constraints, we can find and extract multiple views on the document set.

1. Preparation: Convert each document into a document vector. The meta informations are converted together with the words. We call the elements of the document vector “word” for simplicity. An example of document vectors is shown below.

| | Word #1 | Word #2 | Word #3 | Word #4 | Word #5 |
|-------------|---------|---------|---------|---------|---------|
| Document #1 | 3 | 2 | 0 | 5 | 3 |
| Document #2 | 2 | 2 | 1 | 3 | 3 |
| Document #3 | 4 | 2 | 0 | 5 | 2 |
| Document #4 | 3 | 0 | 4 | 5 | 3 |
| Document #5 | 3 | 2 | 3 | 2 | 1 |

2. Use of background knowledge: We consider such words that appear on many documents with high frequency have low discriminative information. So, we subtract the average vector from each document vectors. Here, the elemental average is the rounded integer of actual average value. In addition, if the result of subtraction becomes minus, the value of new element is forced to be zero. By this process, the featuring words in the document set pop out from the background. This process is similar to the idea of IDF value in TF-IDF features widely used in the field of text-mining. An example is shown below.

| Average | 3.0 | 1.6 | 1.6 | 4.0 | 2.4 |
|-----------------|---------|---------|---------|---------|-------------------|
| Rounded Integer | 3 | 2 | 2 | 4 | 2 (Threshold 0.5) |
| | Word #1 | Word #2 | Word #3 | Word #4 | Word #5 |
| Document #1 | 0 | 0 | 0 | 1 | 1 |
| Document #2 | 0 | 0 | 0 | 0 | 1 |
| Document #3 | 1 | 0 | 0 | 1 | 0 |
| Document #4 | 0 | 0 | 2 | 1 | 1 |
| Document #5 | 1 | 0 | 1 | 0 | 0 |

3. Extraction of subsets based on subclass method: By applying the subclass method proposed by Kudo *et al.*[1], we find the family of subsets on documents that share common words, that is, the common frequency is not zero. Here, the common frequency means the minimum value of two frequencies for an identical word in two documents. In addition, we call the common words in the subset “pop-out words” borrowed from psychology, that pop out from the background knowledge. We adopt the pop-out words as the label for the subset. An example of subsets is shown below.

| Subset | Documents | Pop-Out Words |
|--------|---------------------|---------------|
| #1 | Document #1, #3, #4 | Word #4 |
| #2 | Document #1, #2, #4 | Word #5 |
| #3 | Document #3, #5 | Word #1 |
| #4 | Document #4, #5 | Word #3 |

However, by this simple constraint, the procedure enlarges the subset till the number of pop-out word becomes to one. Therefore, we add more strict constraint on the number of pop-out words so that the number of pop-out words should be greater than a given number. An example of subsets obtained with this constraint in which the number is set by two is shown below.

| Subset | Documents | Pop-Out Words |
|--------|-----------------|------------------|
| #1 | Document #1, #4 | Word #4, Word #5 |
| #2 | Document #3 | Word #1, Word #4 |
| #3 | Document #5 | Word #1, Word #3 |

The procedure for obtaining such maximal subsets of documents is given below. (The detail of the procedure and the analysis in computational learning theory can be found in reference [1].)

- (a) Repeat the following steps (b)–(f) many times.
- (b) Let the newly composing subset null.
- (c) Generate 1 to n series, and sort it randomly.
- (d) Select a document according to the series in step (c), and add the document to the subset unless the addition violates the number of pop-out words constraint.
- (e) Add the subset obtained through step (b)–(d) when the subset had not appeared in the stored family of subsets.
- (f) Select the minimum number of subsets that covers all of the documents by some greedy algorithm.

In the above examples, the family of subsets could not cover all of the documents. However, in most cases, the perfect coverage can be achieved by adjusting (loosing) the number of pop-out words constraint or increasing the number of trials in the step (a).

3 Experiments

We carried out experiments on the following three datasets. Here, for the Japanese documents, we employed the part-of-speech and morphological analyser of reference [2] in order to convert the documents into document vectors.

1. Japanese word processor documents and spread sheets (15 files)
2. English web pages (105 files)
3. Both Japanese and English e-mails (852 files)

Table 1 shows the numbers of subsets obtained by the proposed method when the number of pop-out words constraint was varied. In addition to the numbers, the subjective evaluations are displayed using S, A, B, C ranks.

Table 1. Numbers of the obtained subsets and the subjective evaluations

| # of Least Pop-Out Words | Dataset #1 | Dataset #2 | Dataset #3 |
|--------------------------|------------|------------|------------|
| 1 | 3A | 7C | 5B |
| 2 | 4S | 9C | 47B |
| 3 | 4A | 15B | 80A |
| 4 | — | 15B | 80A |
| 5 | — | 15B | — |

From Table 1, as intuitive consideration, the proposed method could not enlarge the subset with the tight constraint on the number of pop-out words, therefore, the increase of the numbers of subsets could be observed. In addition, the subjective evaluations became higher with tighter constraint. As for the web page documents, the evaluation was very low. This is because, in this paper, that we did not employed morphological analyzer for English documents.

Next, by using the e-mail dataset, we tested hierarchical grouping on the documents. The results are shonw in Tables 2–5. In these experiments, the constraint for the number of pop-out words were set by 1. In addition, in Tables 2–5, Japanese pop-out words are displayed by translating into appropriate English words.

From Tables 2–5, we could confirm that the documents can be appropriately clustered in hierarchical case. However, in these results, the grouping by dates are striking. This is not our desired result that is clustering mainly by the contents.

4 Discussion and Conclusion

We proposed a novel overlapping clustering method for documents in the hierarchical documents browsing system which bases on the idea of information granularity. In this method, we extracted task groups on user's numerous messages such as e-mails and documents by finding the family of subsets that share common topics, sender/receivers, date or author. In addition, the method automatically gave labels to the groups by the common items.

The biggest difference between the proposed method and conventional methods was that the conventional methods find completely divided clusters of documents, while the proposed method finds overlapping clusters of documents on the basis of subclass method. Therefore the proposed method provided multiple views on the documents.

We carried out experiments on the authors' e-mails and document files in order to confirm the basic property and effectiveness of the proposed method. As a result, we could confirm that the proposed method can extract interesting tasks

Table 2. Result of hierarchical grouping. (1st step)

| Subset | # of Documents | Pop-Out Words | Other Common Words |
|--------|----------------|---------------|--------------------|
| #1 | 549 | 2005 Mar | 2005 |
| #2 | 286 | 2005 Feb | 2005 |
| #3 | 69 | science | — |
| #4 | 132 | http | — |
| #5 | 46 | dear | — |

Table 3. Result of hierarchical grouping. (2nd step from #1 in Table 2)

| Subset | # of Documents | Pop-Out Words | Other Common Words |
|--------|----------------|--|--------------------|
| #1 | 97 | contact | 2005, 2005 Mar |
| #2 | 77 | Atsu (Japanese first name) | 2005, 2005 Mar |
| #3 | 35 | root | 2005, 2005 Mar |
| #4 | 86 | Heisei (Japanese year name) | 2005, 2005 Mar |
| #5 | 87 | Receiver: M. Kudo (omitted more 31 subsets) | 2005, 2005 Mar |

Table 4. Result of hierarchical grouping. (3rd step from #1 in Table 3)

| Subset | # of Documents | Pop-Out Words | Other Common Words |
|--------|----------------|---|-------------------------|
| #1 | 40 | place | 2005, 2005 Mar, contact |
| #2 | 26 | Jun (Japanese first name) | 2005, 2005 Mar, contact |
| #3 | 31 | plan | 2005, 2005 Mar, contact |
| #4 | 8 | Receiver: M. Kudo | 2005, 2005 Mar, contact |
| #5 | 19 | information (omitted more 5 subsets) | 2005, 2005 Mar, contact |

Table 5. Result of hierarchical grouping. (3rd step from #5 in Table 3)

| Subset | # of Documents | Pop-Out Words | Other Common Words |
|--------|----------------|--|-----------------------------------|
| #1 | 31 | n*rtion, antispam | 2005, 2005 Mar, Receiver: M. Kudo |
| #2 | 28 | Atsu (Japanese first name) | 2005, 2005 Mar, Receiver: M. Kudo |
| #3 | 14 | 2005 Mar 3 | 2005, 2005 Mar, Receiver: M. Kudo |
| #4 | 2 | reminder | 2005, 2005 Mar, Receiver: M. Kudo |
| #5 | 14 | person in charge (omitted more 8 subsets) | 2005, 2005 Mar, Receiver: M. Kudo |

on the documents by the date, sender/receivers and contents. However, in the hierarchical results, the grouping by dates was striking. Therefore, improvement on this point is desired. In addition, in this paper, we simply used rounded integer for the average as the background knowledge. Sophisticated consideration and reform on this point is also required.

In the future works, in theoretical aspect, we have to compare the proposed method with a priori algorithm on the properties and computational costs. And

in practical side, we have to develop graphical user interface which enables us interactive operation in hierarchical grouping, and we also need measures in the case of large dictionary documents.

Acknowledgment

This work was partly supported by the Japan Ministry of Public Management, Home Affairs, Posts and telecommunications under grant SCOPE-S, and by Grant-in-Aid (No.14380151) of the Japan Society for the Promotion of Science.

References

1. M. Kudo, S. Yanagi and M. Shimbo, Construction of Class Regions by a Randomized Algorithm: A Randomized Subclass Method. *Pattern Recognition*, **29**, 4(1996), 581–588.
2. T. Kudo, MeCab: Yet Another Part-of-Speech and Morphological Analyzer.
<http://chasen.org/~taku/software/mecab/>.

Person Recognition by Pressure Sensors

Masafumi Yamada, Jun Toyama, and Mineichi Kudo

Graduate School of Information Science and Technology
Hokkaido University,
Sapporo 060-0814, Japan
`{masa,jun,mine}@main.ist.hokudai.ac.jp`

Abstract. We argue how we can deal with pressure sensors for person recognition issue. It would appear that the information from the pressure sensors are relatively robust but weak. Using such sensors we argue the merit and possible use of these information. We describe: 1) to what degree and in what way information collected by pressure sensors on a chair is effective for person recognition, and 2) to what situation we can apply these sensor information and how practical they are.

1 Introduction

Supporting users on manipulation of the computers or other electronic devices/appliance has been gathering a great deal of attention lately [1]. To do this, a system has to recognize who the user is beforehand. In other words, person recognition has to be done before personalizing the system. For person recognition, several biometric identifiers such as finger-prints, iris, etc., are usually used. These strong identifiers are available for attaining a high accuracy. However those evidences ask a specific operation of users and that might be a psychological burden for them. Thinking of the motive, which is “to support”, it is not being a support if users feel some psychological burden. Also we sometimes do not need high accuracy as those available with strong identifiers, because the closed world situation like inside the house is assumed here. Thus it is necessary to have evidence could be collected without any burden of users. We call such a evidence a ‘weak evidence’.

In this paper we deal with weak evidence collected from many pressure sensors placed on a chair. The sensor information could be appeared robust but weak relatively. Usage of weak evidences has advantages that those evidences are collected easily and have a low psychological barrier for users unlike biometrics. However such a weak evidence usually is not enough for identifying a person in solely usage, so that we argue some correspondences in such case. In this paper, we argue what target (a person or a group) can be considered, what support would be contributed after the recognition, and what can be accommodated by pressure sensors.

So far, it is argued about how to personalize a system or electronic devices in [1]. It is focused on an agent which personalizes the systems in exact timing for a user. However it is not argued how to know who the user is or at least which

group the user belongs to . Since any system or any agent can't afford any support without knowing who the user is, we need some recognition/identification system. Besides, there is a study in the detection of user's physical condition [2]. Thinking of providing different support to user's posture or condition on the basis of the information obtained from pressure sensors on a chair, our study would give a cue for this goal.

2 Pressure Sensors on a Chair

In this section, we introduce a general description of a pressure sensor used in this work. We used "FlexiForce" pressure sensor provided by Tekscan [3]. The characteristics of "FlexiForce" are shown in Table. 1.

Table 1. Characteristics of a sensor

| | |
|--------------|-----------------------|
| Thickness | 0.008" (.208mm) |
| Length | 8" (203mm) |
| Width | 0.55" (14mm) |
| Sensing Area | diameter (9.53mm) |
| Connector | 3-pin male square pin |

This sensor is ultra-thin. It is thin enough to put sensors on a chair without feeling uncomfortable when users are sitting. This thinness makes a sensor itself easy to fit any shape of objects that the sensor put on. Also this thinness makes it possible to collect evidence without a user burden.

We arranged 32 sensors on a chair in a reticular pattern as shown in Fig.3. Each sensors are 2cm standoff side to side and up and down. This chair is designed to have sensor's reacts easily when a user seated. Fig.4 shows how each sensors react at a time when a user seated.



Fig. 1. A pressure sensor (8" long, the right circle is the sensor part)

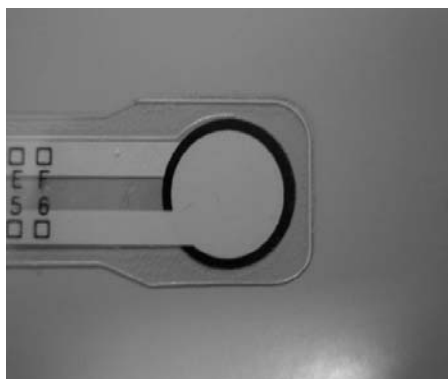


Fig. 2. An enlarged part of a sensor (0.55" wide, 0.008" thin)

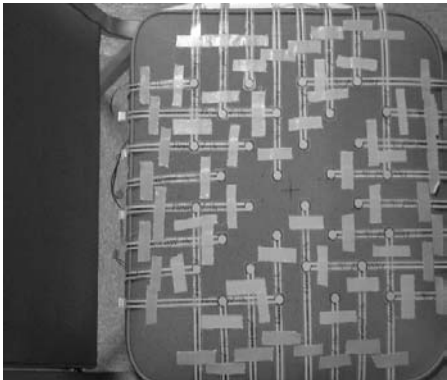


Fig. 3. 8×8 pressure sensors on a chair

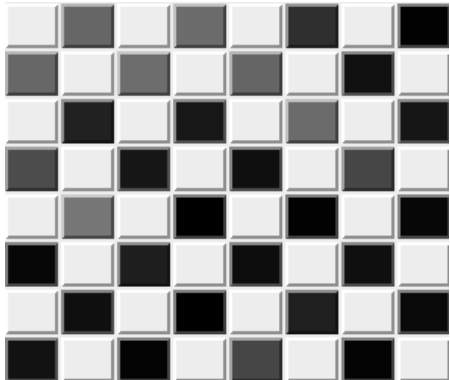


Fig. 4. Overview of sensors' reacts

3 Experiment

3.1 Conditions

We examined how sufficient the pressure sensors give information for person recognition. A simple experiment was conducted. We measured 32 values of sensors when a user was sitting down. The value of sensors were collected starting from a few seconds before the user starts sitting until the values of the sensor get steady after sitting. From the data we cut out two parts. One of them is the part during the user is sitting down, labeled as “Sitting part” in Fig.5. Another is the part after the sensor value gets steady, labeled as “Stable part” in Fig.5.

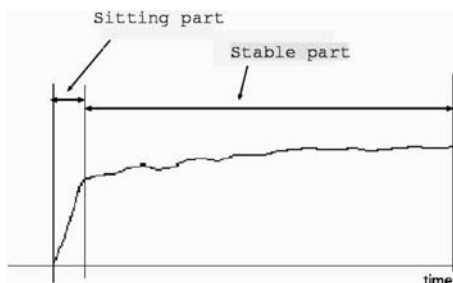


Fig. 5. The behavior of a sensor output in time

Eight people seated on the chair 20 times. In total, we had 160 time series. Each sensor value is taken every 0.5 sec. We divided 20 data as for each person into 19 for training and 1 for testing. The recognition rate was calculated by 20-fold cross-validation according to this division. The classifier used is the nearest neighbour method. Every testing data are classified to the nearest training data.

For investigating how useful the information of pressure sensors, several settings were conducted. Used features are classified into four groups.

- Feature Set1 (FS1):** 32 sensors' values (32),
Feature Set2 (FS2): sum of 32 sensors' values (1),
Feature Set3 (FS3): time difference of FS1 (32),
Feature Set4 (FS4): normalized sensor values of FS3 (1).

We considered the sitting part and the stable part separately. The individual goals are:

- 1) To verify how high the recognition rate can be gained at sitting part by such a dynamic response sequence. We use FS1 + FS2 (33 features).
- 2) To verify how much the recognition rate can be gained at steady part. We use FS1 + FS2 (33 features).
- 3) To investigate the potential of different features. We expect that the summation of the values corresponds to his/her weight.
 - (a) FS1 (32 features)
 - (b) FS4 (32 features)
 - (c) FS2 (1 feature)
- 4) To examine how much effective when we take into consideration the dynamic features (the time difference) and the normalized values that may correspond to the way of the user's sitting.
 - (a) FS1, FS2 and FS3 (99 features)
 - (b) FS3 and FS4 (96 features)

3.2 Experimental Results

The results are shown in Table 2. Table 2 shows the average recognition rate as well as the minimum and maximum recognition rates.

Table 2. Results

| No. | Features | Used part | Average recognition rate(%) | [min, max] of trials |
|---------|-------------------|-----------|--------------------------------|----------------------|
| # 1 | (FS1 + FS2) | Sitting | 63 | [40, 79] |
| # 2 | (FS1 + FS2) | Stable | 90 | [78, 99] |
| # 3-(a) | (FS1) | Sitting | 63 | [40, 79] |
| # 3-(b) | (FS4) | Sitting | 52 | [23, 76] |
| # 3-(c) | (FS2) | Sitting | 21 | [0, 34] |
| # 4-(a) | (FS1 + FS2 + FS3) | Sitting | 86 | [77, 99] |
| # 4-(b) | (FS3 + FS4) | Sitting | 54 | [23, 81] |

We evaluate:

- 1) and 2) To verify how high the recognition rate can be gained in sitting part and steady part.**

See the results # 1 and # 2. The average recognition rate is 90% in the steady part and 63% in the sitting part using FS1 and FS2. From the result in the

steady part, people may have their own sitting position basically. While the recognition rate in the sitting part is 2/3 of that in the steady part. Each points (data) were classified to the nearest training point, so, in the sitting part, a number of points might be shared by different persons.

3) To investigate the potential of different features.

Compare the result of # 3-(a) and result # 1. The recognition rates are same. This comparison shows FS2 does not affect any this time. However it can't say FS2 does not have any information for the recognition. Indeed, # 3-(c) means that a reasonable information exists.

To confirm how much FS2 and FS4 affect the results, we compared # 3-(b), # 3-(c) and # 1. The recognition rates are 52%, 21% and 63% respectively. Both # 3-(b) and # 3-(c) does not reach to # 1, but both contribute to some extent to the recognition rate.

4) To examine how much effective when we take into consideration the time difference

The data is obtained as a time series. With FS3, we take into consideration the time difference. The average recognition rate of # 4-(a) and # 4-(b) are 86% and 54%, respectively.

Comparison between result # 4-(a) and # 1, the recognition rate raised up 23 %. This means it is effective to take into consideration the time difference. Though, the recognition rate does not change any by comparing the result of # 3-(b) and that of # 4-(b). This means most of user's sitting positions are not changed for seconds.

4 Conclusion

We could show a large amount of potential of pressure sensors for person recognition. In the steady part, the recognition rate was 90% for eight people, so it is possible to use this pressure sensor for recognition in a house or in a small office. With the time difference, the recognition rate reached to 86% even in the sitting phase. The results showed that individuals may have their own sitting position.

The things to be discussed in the future are 1) how to deal with time axis, 2) to confirm the effectivity of integration of other evidence[4, 5], and 3) to confirm the ability of recognizing individual's behaviour or user's physical condition such as relaxing on a chair. For 1), it is possible to handle "sitting part" as one frame, and make an answer.

Acknowledgement

This work was partly supported by the Japan Ministry of Public Management, Home Affairs, Posts and telecommunications under grant SCOPE-S.

References

1. Hattori, M., Cho, K., Ohsuga, A., Isshiki, M., Honiden, S. : A Context-Aware Personal Agent in Ubiquitous Environment and Its Experimental Trial. IEICE Vol.J86-D-I, No.8, (2003)543–551
2. Aoki, S., Iwai, Y., Onishi, M., Kojima, A., Fukunaga, K. : Learning and Recognizing Behavioral Patterns Using Position and Posture of Human Body and Its Application to Detection of Irregular State. IEICE Vol.J87-D-II, No.5, (2004) 1083–1093
3. <http://www.tekscan.com/index.html>
4. Hosokawa, T. and Kudo, M. : Person Tracking with Infrared Sensors. KES(2005)
5. Yamada, M. and Kudo, M. : Combination of Weak Evidences by D-S Theory for Person Recognition. KES(2004)
6. J.Yamato, J.Ohya, and K.Ishii: Recognizing Human Action in Time-Sequential Images Using Hidden Markov Model. Proc. Computer Vision and Pattern Recognition, (1992) 379–385
7. Aaron F. Bobick and James W. Davis: The Recognition of Human Movement Using Temporal Templates. IEEE transzctions of pattern analysis and machine intelligence Vol. 23, No. 3 (2001)257–267

Extraction and Revision of Signboard Images for Recognition of Character Strings

Hirokazu Watabe and Tsukasa Kawaoka

Dept. of Knowledge Engineering & Computer Sciences, Doshisha University
Kyo-Tanabe, Kyoto, 610-0394, Japan

Abstract. A function of image recognition is indispensable to an intelligent robot, which can coexist with a human being. Furthermore, the intelligent robot needs to understand the environment of their action range by getting information of characters and maps on signboards in order to act autonomously. In this research, a method using the Color Distance to extract the ground of signboard from one piece of picture by robot's camera and revising the distortion by virtual movement of a viewpoint is described. It is shown that character strings on the signboard is recognized by an optical character reader after revising the distortion.

1 Introduction

Recognition functions of common sense are pursued in an intelligent robot that can coexist with a human being, and a recognition function of information on a signboard is one of them. The signboard presents important information such as character string [1, 2], arrows and maps that concerns people's action. And an intelligent robot, expected to take proper behavior as people does, is required to recognize information on the signboard with common sense.

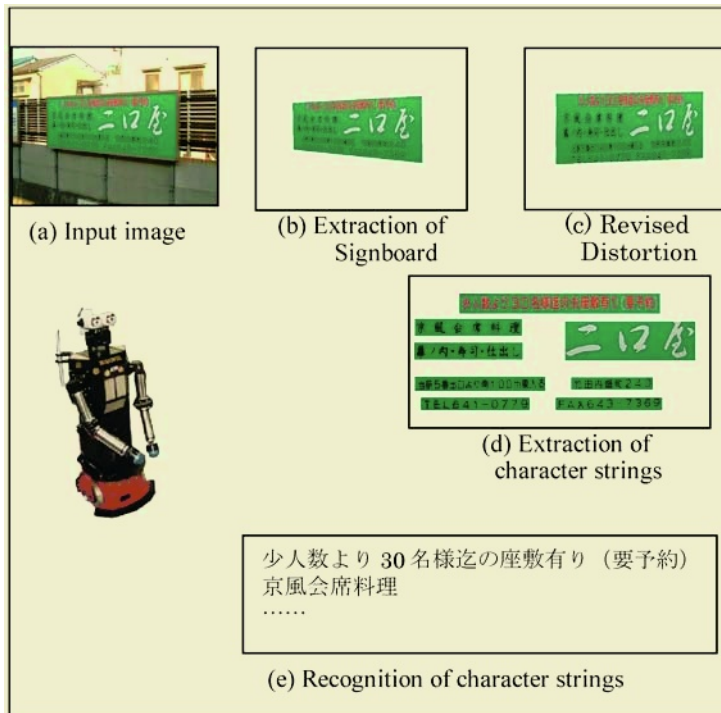
In this paper, a method using the Color Distance to extract the ground of signboard from one piece of picture and revising the distortion by virtual movement of a viewpoint is proposed. The area whose pixels have same Color Distance is described as the signboard area. Then, the distortion by movement of a viewpoint is revised with the algorithm of rotation convertible.

The accuracy of this extraction method and revision method was evaluated by experiments. It is regarded that a paper on which character strings is written as a provisional signboard. In the first, pictures were taken from some angles by a digital camera. Then, the provisional signboard was extracted from the picture, and revision was performed. Finally, these revised images were recognized by an optical character reader, and the recognition rate of character strings was examined. A result of this experiment shows that a revision is performed appropriately if the difference of an angle from the front is less than 60 degrees.

2 Signboard Recognition System

In this paper, character strings on the signboard is recognized by the following steps. (Fig. 1).

1. Extract the area of signboard from a scene image.
2. Revise distortion of the signboard.

**Fig. 1.** Signboard recognition system

3. Extract character string on the signboard.
4. Recognize character strings by an optical character reader (OCR).

3 Extraction of the Signboard Area from Scene Image

The color information is important to extract the signboard area. As a color model, HSL (Hue, Saturation and Lightness) color model is used in this paper. It is thought that the ground of signboard in the scene image has similar color, and it has relatively large and simple shaped area.

The similarity of the color is measured by the color distance (CD). It is defined by the following equation.

$$CD = \sqrt{Hue^2 + Saturation^2 + Lightness^2}$$

Then, the following algorithm performs the extraction of the ground of signboard from the scene image.

1. Calculate the color distance of each pixel to measure the similarity of the color.
2. Make the histogram of the color distance (fig.2 b), and the only pixels that have relatively large frequency is reserved (fig.2 c). And the pixels that have the color distance between reserved pixels' color distance are also reserved if these color distance is near (fig.2 d). These reserved groups of pixels are candidates of the signboards. Figure 3 shows the two candidates of the signboards.

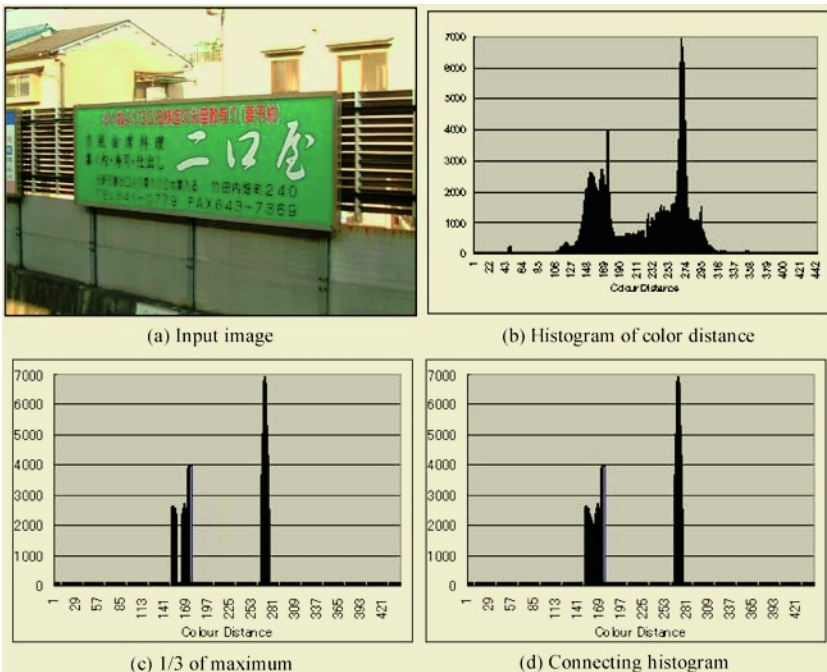


Fig. 2. Input scene image and color distance histograms

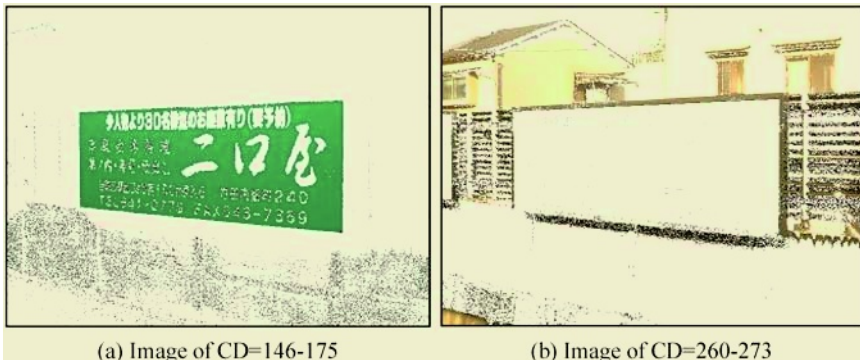


Fig. 3. Candidates of the signboard image

3. After eliminate the noises of those candidates of the signboards, calculate the FdTarget value. FdTarget value is defined by the following equation

$$\text{FdTarget} = \frac{\frac{1}{N} \sum_{n=1}^N \sqrt{(x_n - x_0)^2 + (y_n - y_0)^2}}{\max(\sqrt{(x_n - x_0)^2 + (y_n - y_0)^2})}$$

Where, (x_0, y_0) is the center of gravity of the candidate's image, (x_n, y_n) is the coordinate of each pixel, and N is the number of pixels in the candidate. This FdTarget

value represents the degree of distribution of the pixels in the candidate of the signboard. And it is defined that the candidate is the signboard if

$$FdTarget < 0.5$$

according to the analysis of sample images (fig.4).

- Extract the signboard area using four boundary edges (fig.5).

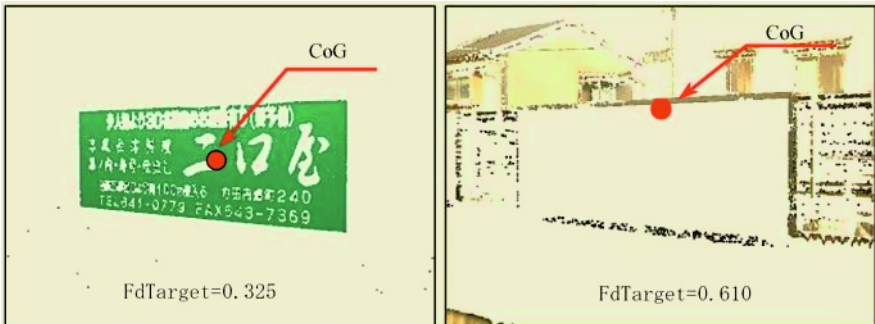


Fig. 4. Noise elimination and FdTarget values

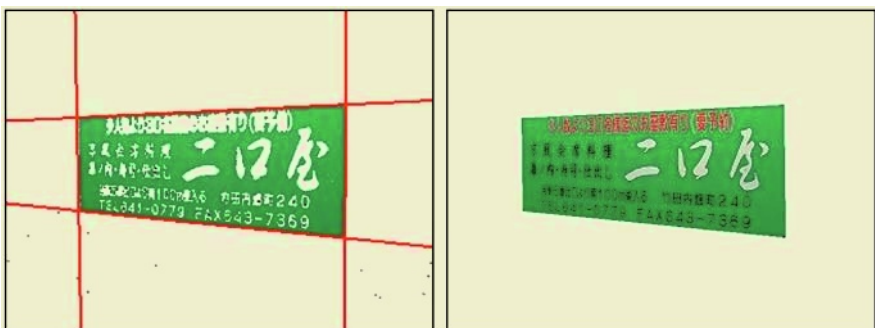


Fig. 5. Four edges and extracted signboard area

4 Revise Distortion of the Signboard

In general, the extracted signboard images have distortions because the robot (camera) is not just in front of the signboard. Therefore, it is required that the distortion of the signboard image is revised in order to recognize the character strings on the signboard by OCR. Since this distortion is caused by 3-dimensional rotation of the camera and it is impossible that the camera is moved to just in front of the signboard. Therefore, in this paper, the signboard image is rotated in the virtual 3D space (fig.6). The rotation in the 3D space is represented by three parameters $(\theta_x, \theta_y, \theta_z)$, and the following rotation transform matrix is used.

$$\begin{bmatrix} \cos\theta_z \cos\theta_y + \sin\theta_z \sin\theta_x \sin\theta_y & \sin\theta_z \cos\theta_x & \cos\theta_z \sin\theta_y + \sin\theta_z \sin\theta_x \cos\theta_y & 0 \\ -\sin\theta_z \cos\theta_y - \cos\theta_z \sin\theta_x \sin\theta_y & \cos\theta_z \cos\theta_x & -\sin\theta_z \sin\theta_y + \cos\theta_z \sin\theta_x \cos\theta_y & 0 \\ -\cos\theta_x \sin\theta_y & -\sin\theta_x & \cos\theta_x \cos\theta_y & 0 \\ 0 & 0 & 0 & 1 \end{bmatrix}$$

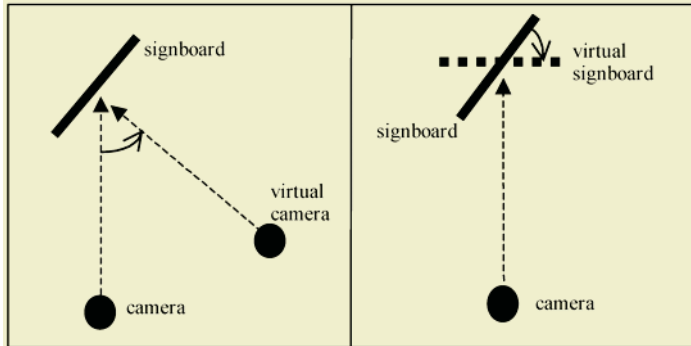


Fig. 6. Virtual rotation of signboard

If the camera is just in front of the signboard, two boundary lines of the signboard are horizontal (angles are 0 degree) and angles of four corners are 90 degree. Therefore, the values of three parameters ($\theta_x, \theta_y, \theta_z$) are searched so as to satisfy the following conditions using four corner points of the extracted signboard image. (Fig.6)

$$-10 < a_i, a_j < +10$$

$$80 < b_1, b_2, b_3, b_4 < 100$$

Where, a_i, a_j are the angles of two boundary lines of the signboard from the horizontal lines, and b_i is the angles of corner of the signboard.

5 Experimental Results

To evaluate the proposed method about extraction of the signboard image, computer experiments are performed using 30 scene images including the signboard. Among these images, the number of the success cases was 27 (success rate was 90%). Figure 7 shows some success cases.

To evaluate the proposed signboard recognition system the following experiment was performed. It is regarded that a paper on which character strings is written as a provisional signboard. In the first, pictures were taken from some angles by a digital camera. Then, the provisional signboard was extracted from the picture, and revision was performed. Finally, these revised images were recognized by an optical character reader, and the recognition rate of character strings was examined. There were 200 pictures (10 different angles by 20 provisional signboards). The results are shown in the figure 8. A result of this experiment shows that a revision is performed appropriately if the difference of an angle from the front is less than 60 degrees.

6 Conclusions

In this paper, the method of recognizing the character strings on the signboard in the scene images was proposed. By the experiments, it is shown that the proposed method extracted the signboard successfully from about 90% scene images, and a revision is performed appropriately if the difference of an angle from the front is less than 60 degrees. And recognition rate of character strings was about 86%.



Fig. 7. Experimental results (Extraction of the signboard image)

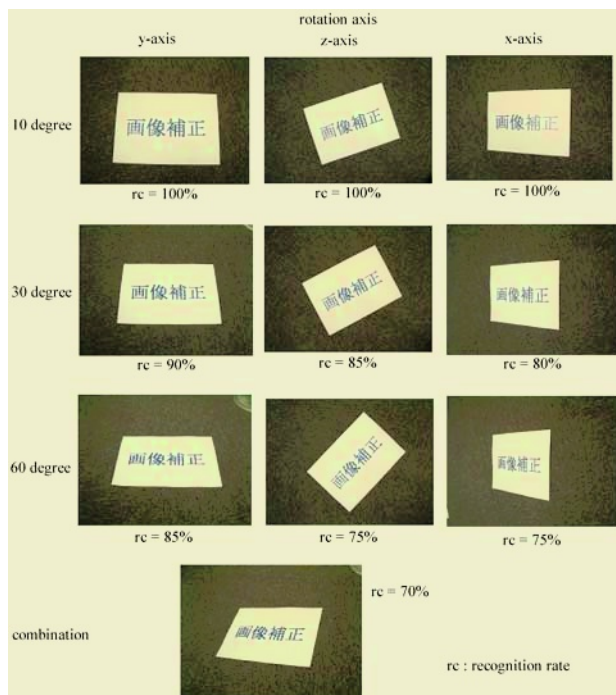


Fig. 8. Recognition rates of character strings on the signboard

Acknowledgements

This work was supported with the Aid of Doshisha University's Research Promotion Fund.

References

1. K. Matsuo, K. Ueda, and M. Umeda: Extraction of Character String on Signboard from Scene Image Using Adaptive Threshold Methods, *Trans. of the Institute of Electronics, Information and Communication Engineers D-II*, Vol. J80-D-II, No. 6, pp.1617-1626 (1997).
2. T. Hagiwara, H. Watabe, and T. Kawaoka: A Revision Method for a String of Printed Character with Distortion, *Trans. of the Institute of Electronics, Information and Communication Engineers D-II*, Vol. J86-D-II, No. 2, pp.262-271 (2003).

Model Selection and Weight Sharing of Multi-layer Perceptrons

Yusuke Tanahashi¹, Kazumi Saito², and Ryohei Nakano¹

¹ Nagoya Institute of Technology

Gokiso-cho, Showa-ku, Nagoya 466-8555 Japan

{tanahashi,nakano}@ics.nitech.ac.jp

² NTT Communication Science Laboratories, NTT Corporation

2-4 Hikaridai, Seika, Soraku, Kyoto 619-0237 Japan

saito@cslab.kecl.ntt.co.jp

Abstract. We present a method to learn and select a succinct multi-layer perceptron having shared weights. Weight sharing means a weight is allowed to have one of common weights. A near-zero common weight can be eliminated, called weight pruning. Our method iteratively merges and splits common weights based on 2nd-order criteria, escaping local optima through bidirectional clustering. Moreover, our method selects the optimal number of hidden units based on cross-validation. Our experiments showed that the proposed method can perfectly restore the original sharing structure for an artificial data set, and finds a small number of common weights for a real data set.

1 Introduction

In data mining using neural networks, an important research issue is to find a succinct neural network structure from data. Here the network structure means the number of hidden units, the connectivity between units, and the freedom of weight values. To achieve this aim, we focus on *weight sharing* [1, 2]. Weight sharing means weights are divided into clusters, and weights within the same cluster have the same value called a *common weight*. If a common weight is very close to zero, then all the corresponding weights can be removed, which is called *weight pruning*. If we employ weight sharing and pruning as well as model selection, a neural network will have as simple a structure as possible, which greatly benefits knowledge discovery from data.

Recently, a weight sharing method called *BCW (bidirectional clustering of weights)* has been proposed [3]. The BCW method employs both cluster-merge and cluster-split operations based on second-order criteria, and can escape local optima through bidirectional operations.

This paper enhances the original BCW in three points: removal of the constraint the original split operation has, top-down initialization instead of multi-step bottom-up one, and model selection via cross-validation. Although the proposed method will be applicable to a wide variety of neural networks, we focus on three-layer perceptrons in order to evaluate its basic capabilities.

2 Weight Sharing Method

Let $E(\mathbf{w})$ be an error function to minimize, where $\mathbf{w} = (w_1, \dots, w_d, \dots, w_D)^T$ denotes a vector of weights and \mathbf{a}^T is a transposed vector of \mathbf{a} . Then, we define a set of clusters $\Omega(G) = \{S_1, \dots, S_g, \dots, S_G\}$, where S_g denotes a set of weights such that $S_g \neq \emptyset$, $S_g \cap S_{g'} = \emptyset$ ($g \neq g'$) and $S_1 \cup \dots \cup S_G = \{1, \dots, D\}$. Also, we define a vector of common weights $\mathbf{u} = (u_1, \dots, u_g, \dots, u_G)^T$ associated with a cluster set $\Omega(G)$ such that $w_d = u_g$ if $d \in S_g$. Note that $\hat{\mathbf{u}}$ is obtained by training a neural network whose structure is defined by $\Omega(G)$.

Now we consider a relation between \mathbf{w} and \mathbf{u} . Let \mathbf{e}_d^D be the D -dimensional unit vector whose elements are all zero except for the d -th element, which is equal to unity. Then the original weight vector \mathbf{w} can be expressed by using a $D \times G$ transformational matrix \mathbf{A} as follows.

$$\mathbf{w} = \mathbf{A}\mathbf{u}, \quad \mathbf{A} = \left[\sum_{d \in S_1} \mathbf{e}_d^D, \dots, \sum_{d \in S_G} \mathbf{e}_d^D \right]. \quad (1)$$

Below we outline the BCW (bidirectional clustering of weights) procedure. Since a weight clustering problem may have many local optima, the BCW repeats merge and split operations until convergence.

2.1 Bottom-Up Clustering

A one-step bottom-up clustering transforms $\Omega(G)$ into $\Omega(G - 1)$ by a merge operation; i.e., clusters S_g and $S_{g'}$ are merged into a cluster $\tilde{S}_g = S_g \cup S_{g'}$. Clearly, we want to select a suitable pair so as to minimize the increase of the error function. Below we derive the second-order criterion for a merge operation. The second-order Taylor expansion of $E(\mathbf{A}\mathbf{u})$ around \mathbf{u} gives

$$E(\mathbf{A}(\mathbf{u} + \Delta\mathbf{u})) - E(\mathbf{A}\mathbf{u}) \approx \mathbf{g}(\mathbf{w})^T \mathbf{A} \Delta\mathbf{u} + \frac{1}{2} \Delta\mathbf{u}^T \mathbf{A}^T \mathbf{H}(\mathbf{w}) \mathbf{A} \Delta\mathbf{u}, \quad (2)$$

where $\mathbf{g}(\mathbf{w})$ and $\mathbf{H}(\mathbf{w})$ denote the gradient and Hessian of $E(\mathbf{w})$ respectively. Let $\hat{\mathbf{u}}$ be a trained common weight vector, then from the local optimality condition we have $\mathbf{A}^T \mathbf{g}(\mathbf{A}\hat{\mathbf{u}}) = \mathbf{0}$. Now we consider $\Delta\mathbf{u}$ that minimizes the right-hand-side of eq. (2) under the following constraint imposed by merging S_g and $S_{g'}$.

$$(\hat{\mathbf{u}} + \Delta\mathbf{u})^T \mathbf{e}_g^G = (\hat{\mathbf{u}} + \Delta\mathbf{u})^T \mathbf{e}_{g'}^G. \quad (3)$$

By using the Lagrange multiplier method, we can minimize the right-hand-side of eq. (2), which can be achieved by the following $\Delta\mathbf{u}$. Here $\hat{\mathbf{w}} = \mathbf{A}\hat{\mathbf{u}}$.

$$\Delta\mathbf{u} = \frac{(\hat{u}_{g'} - \hat{u}_g)(\mathbf{A}^T \mathbf{H}(\hat{\mathbf{w}}) \mathbf{A})^{-1}(\mathbf{e}_g^G - \mathbf{e}_{g'}^G)}{(\mathbf{e}_g^G - \mathbf{e}_{g'}^G)^T (\mathbf{A}^T \mathbf{H}(\hat{\mathbf{w}}) \mathbf{A})^{-1}(\mathbf{e}_g^G - \mathbf{e}_{g'}^G)}. \quad (4)$$

The minimal increase in the quadratic function is given by

$$2 \min \left(\frac{1}{2} \Delta\mathbf{u}^T \mathbf{A}^T \mathbf{H}(\mathbf{w}) \mathbf{A} \Delta\mathbf{u} \right) = \frac{(\hat{u}_g - \hat{u}_{g'})^2}{(\mathbf{e}_g^G - \mathbf{e}_{g'}^G)^T (\mathbf{A}^T \mathbf{H}(\hat{\mathbf{w}}) \mathbf{A})^{-1}(\mathbf{e}_g^G - \mathbf{e}_{g'}^G)}. \quad (5)$$

This is regarded as the second-order criterion for merging S_g and $S_{g'}$, called the *dissimilarity* $DisSim(S_g, S_{g'})$. We select a pair of clusters which minimizes $DisSim(S_g, S_{g'})$ and merge the two clusters. After the merge, the network with $\Omega(G - 1)$ is retrained. This is the *one-step bottom-up clustering with retraining*.

2.2 Top-Down Clustering

A one-step top-down clustering transforms $\Omega(G)$ into $\Omega(G + 1)$ by a split operation; i.e., a cluster S_g is split into two clusters S'_g and S_{G+1} where $S_g = S'_g \cup S_{G+1}$. In this case, we want to select a suitable cluster and its partition so as to maximize the decrease of the error function. Below we derive the second-order criterion for a split operation. Let $\hat{\mathbf{u}}$ be a trained common weight vector. Just after the splitting, we have a $(G + 1)$ -dimensional common weight vector $\tilde{\mathbf{v}} = (\hat{\mathbf{u}}^T, \hat{u}_g)^T$, and a new $D \times (G + 1)$ transformational matrix \mathbf{B} defined as

$$\mathbf{B} = \left[\sum_{d \in S_1} \mathbf{e}_d^D, \dots, \sum_{d \in S'_g} \mathbf{e}_d^D, \dots, \sum_{d \in S_G} \mathbf{e}_d^D, \sum_{d \in S_{G+1}} \mathbf{e}_d^D \right]. \quad (6)$$

The second-order Taylor expansion of $E(\mathbf{B}\tilde{\mathbf{v}})$ around $\tilde{\mathbf{v}}$ gives

$$E(\mathbf{B}(\tilde{\mathbf{v}} + \Delta\mathbf{v})) - E(\mathbf{B}\tilde{\mathbf{v}}) \approx \mathbf{g}(\mathbf{B}\tilde{\mathbf{v}})^T \mathbf{B} \Delta\mathbf{v} + \frac{1}{2} \Delta\mathbf{v}^T \mathbf{B}^T \mathbf{H}(\mathbf{B}\tilde{\mathbf{v}}) \mathbf{B} \Delta\mathbf{v}. \quad (7)$$

Here we consider $\Delta\mathbf{v}$ that minimizes the right-hand-side of eq. (7). Since $\tilde{\mathbf{v}}$ is not a trained vector, the local optimality condition does not hold anymore; i.e., $\mathbf{B}^T \mathbf{g}(\mathbf{B}\tilde{\mathbf{v}}) \neq \mathbf{0}$. Instead, we have

$$\mathbf{B}^T \mathbf{g}(\mathbf{B}\tilde{\mathbf{v}}) = \kappa \mathbf{f}, \quad \kappa = \mathbf{g}(\mathbf{B}\tilde{\mathbf{v}})^T \sum_{d \in S_{G+1}} \mathbf{e}_d^D, \quad \mathbf{f} = \mathbf{e}_{G+1}^{G+1} - \mathbf{e}_g^{G+1}, \quad (8)$$

from the following optimality condition on $\hat{\mathbf{u}}$

$$0 = \mathbf{g}(\mathbf{B}\tilde{\mathbf{v}})^T \sum_{d \in S_g} \mathbf{e}_d^D = \mathbf{g}(\mathbf{B}\tilde{\mathbf{v}})^T \left(\sum_{d \in S'_g} \mathbf{e}_d^D + \sum_{d \in S_{G+1}} \mathbf{e}_d^D \right). \quad (9)$$

Therefore, by substituting eq. (8) into eq. (7), we obtain the minimal value of eq. (7), which is $-(1/2)\kappa^2 \mathbf{f}^T (\mathbf{B}^T \mathbf{H}(\mathbf{B}\tilde{\mathbf{v}}) \mathbf{B})^{-1} \mathbf{f}$. This is regarded as the second-order criterion for splitting S_g into S'_g and S_{G+1} ; thus, we can define the general *utility* as follows. The utility values will be positive, and the larger the better.

$$GenUtil(S_g, S_{G+1}) = \kappa^2 \mathbf{f}^T (\mathbf{B}^T \mathbf{H}(\mathbf{B}\tilde{\mathbf{v}}) \mathbf{B})^{-1} \mathbf{f}. \quad (10)$$

The original BCW [3] employs a very constricted splitting such as splitting into only one element and the others. Here we remove the constraint. Consider the criterion (10). When a cluster g to split is unchanged, $\mathbf{f}^T (\mathbf{B}^T \mathbf{H}(\mathbf{B}\tilde{\mathbf{v}}) \mathbf{B})^{-1} \mathbf{f}$ is kept unchanged. Since κ is the summation of gradients over the members of

a cluster $G + 1$, the gradients should have the same sign if you want a larger κ . Thus, the gradients of the cluster are sorted in ascending order and examined is only splitting into smaller-gradients and larger-gradients. Examining all such candidates, we select the cluster to split and its splitting which maximize the criterion (10). After the splitting, the network with $\Omega(G + 1)$ is retrained. This is the new *one-step top-down clustering with retraining*.

2.3 New Bidirectional Clustering of Weights: BCW1.2

The original BCW [3] has two control parameters G and h ; G is the final number of clusters and h is the depth of the bidirectional search. Since in general we don't know the optimal G^* , independent BCW runs are assumed for each G . This redundancy can be eliminated if we consider bidirectional clustering through the enough range between $G=2$ and $2 + h$. The parameter h remains.

The original BCW [3] begins by doing the multi-step bottom-up clustering without retraining from the initial set $\Omega(D)$ to $\Omega_1(G)$. This rather tedious initial step can be avoided by scalar quantization of the initial learning result $\Omega(D)$. That is, each weight of $\Omega(D)$ is quantized into 2 clusters by using any clustering procedure such as the K-means. Then the top-down clustering follows.

The procedure of the new BCW, called **BCW1.2**, is summarized below. The BCW1.2 always converges since the number of different \mathbf{A} is finite.

- step 1:** Get the initial set $\Omega(D)$ through learning. Perform scalar quantization for $\Omega(D)$ to get $\Omega_1(2)$. Remember the matrix $\mathbf{A}^{(0)}$ at $\Omega_1(2)$. $t \leftarrow 1$.
- step 2:** Perform repeatedly the one-step top-down clustering with retraining from $\Omega_1(2)$ to $\Omega(2+h)$. Update the best performance for each G if necessary.
- step 3:** Perform repeatedly the one-step bottom-up clustering with retraining from $\Omega(2+h)$ to $\Omega_2(2)$. Update the best performance for each G if necessary. Remember $\mathbf{A}^{(t)}$ at $\Omega_2(2)$.
- step 4:** If $\mathbf{A}^{(t)}$ is equal to one of the previous ones $\mathbf{A}^{(t-1)}, \dots, \mathbf{A}^{(0)}$, stop. Output the best performance of $\Omega(G)$ for each G as the final result. Otherwise, $t \leftarrow t + 1$, $\Omega_1(G) \leftarrow \Omega_2(G)$ and go to step 2.

2.4 Neural Network Model Selection

Given data, we don't know in advance the optimal number J^* of hidden units; thus, we have to find it from data. For this purpose we adopt *cross-validation* [4]. To find J^* , we try different BCW runs with cross-validation for $J = 1, 2, \dots$

The S -fold cross-validation divides data D into S disjoint segments $\{G_s, s = 1, \dots, S\}$, and uses $S-1$ segments for training, and uses the remaining one for the test. This process is repeated S times by changing the test segment, and usually the generalization performance is measured by the following sum-of-squares error over all test samples. Here G_s denotes the s -th segment for test, and $\boldsymbol{\theta}_s$ denotes the parameters obtained by using $D - G_s$ for training.

$$E_{CV} = \frac{1}{N} \sum_{s=1}^S \sum_{\nu \in G_s} (f(\mathbf{x}^\nu; \boldsymbol{\theta}_s) - y^\nu)^2 \quad (11)$$

3 Experiments

We consider a regression problem to find the following multivariate polynomial from data $\{(\mathbf{x}^\mu, y^\mu) : \mu = 1, \dots, N\}$. Here we assume $x_k > 0$. The right hand side can be regarded as feedforward computation of a three-layer perceptron [2].

$$f(\mathbf{x}; \mathbf{w}) = w_0 + \sum_{j=1}^J w_j \prod_k x_k^{w_{jk}} = w_0 + \sum_{j=1}^J w_j \exp \left(\sum_k w_{jk} \ln x_k \right) \quad (12)$$

3.1 Experiments Using Artificial Data Set

$$f = 3 + 2x_1^{2/3}x_2x_3^{2/3}x_4^{1/2} + x_3^{1/2}x_4^{2/3}x_5 \quad (13)$$

Consider the above polynomial and introduce ten irrelevant variables x_6, \dots, x_{15} . For each sample, each x_k value is randomly generated in the range of $(0, 1)$, while the corresponding y value is calculated by following eq. (13) with small Gaussian noise $\mathcal{N}(0, 0.1)$ added. The size of data is 400 ($N = 400$).

The learning is terminated when each element of the gradient is less than 10^{-6} . Weight sharing was applied only to weights w_{jk} . we set the width of bidirectional clustering as $h = 10$. The number of hidden units was changed from one to four; $J = 1, \dots, 4$. For model selection we employ 10-fold cross-validation. Note that $J^* = 2$ and $G^* = 4$ for our data.

Table 1 shows the average training error \bar{E} over 10 segments and 10-fold cross-validation error E_{CV} of BCW1.2 for artificial data ($G=11,12$ are omitted). A number in bold type indicates the best for each J . The average training error \bar{E} mostly decreased monotonically as G or J increased, while E_{CV} was minimized at $J = 2$ and $G = 4$; which coincide with $J^* = 2$ and $G^* = 4$.

Figure 1 shows how training error E and CV error E_{CV} changed through BCW1.2 learning for a certain segment under the model of $J = 2$. The bidirectional clustering was repeated only once until convergence. Training error E changed monotonically through the BCW process, while E_{CV} was minimized at

Table 1. (\bar{E}, E_{CV}) of BCW1.2 for Artificial Data

| G | $J = 1$ | $J = 2$ | $J = 3$ | $J = 4$ |
|-----|----------------------------|----------------------------|----------------------------|----------------------------|
| 2 | (0.02190,0.02250) | (0.01489,0.01533) | (0.01453,0.01434) | (0.01428,0.01519) |
| 3 | (0.01645,0.01659) | (0.01066,0.01088) | (0.01056, 0.01088) | (0.01068, 0.01093) |
| 4 | (0.01526, 0.01591) | (0.01033, 0.01072) | (0.01040,0.01092) | (0.01021,0.01112) |
| 5 | (0.01502,0.01630) | (0.01010,0.01099) | (0.01015,0.01115) | (0.00994,0.01114) |
| 6 | (0.01484,0.01638) | (0.00997,0.01117) | (0.00983,0.01140) | (0.00975,0.01111) |
| 7 | (0.01477,0.01660) | (0.00988,0.01130) | (0.00971,0.01143) | (0.00960,0.01114) |
| 8 | (0.01475,0.01656) | (0.00983,0.01126) | (0.00962,0.01150) | (0.00952,0.01122) |
| 9 | (0.01474,0.01656) | (0.00979,0.01131) | (0.00970,0.01158) | (0.00941,0.01127) |
| 10 | (0.01473 ,0.01656) | (0.00976 ,0.01145) | (0.00961 ,0.01157) | (0.00938 ,0.01129) |

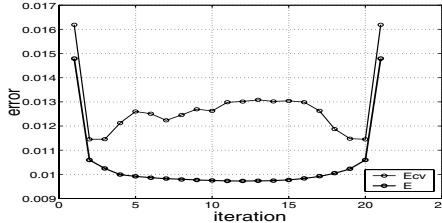


Fig. 1. Bidirectional Clustering for Artificial Data

$G=3$ or 4 , which is reasonable since a smaller G causes insufficient capability and a larger G results in overfitting.

We pruned the near-zero ($|u| < 0.01$) common weight and retrained to get the final common weights: $u_1=0.9569$, $u_2=0$, $u_3=0.5187$, and $u_4=0.6590$. The following is the final equation obtained, almost equivalent to the original eq. (13).

$$f = 2.929 + 1.977x_1^{u_4}x_2^{u_1}x_3^{u_4}x_4^{u_3} + 0.990x_3^{u_3}x_4^{u_4}x_5^{u_1} \quad (14)$$

The total cpu time required for BCW1.2 by 3.6 GHz Pentium PCs was 1,896 sec. for a number of combinations: $J = 1, \dots, 4$ and $G = 2, \dots, 12$.

3.2 Experiments Using Automobile Data Set

The Automobile data set¹ contains data on the car and truck specifications in 1985, and is used to predict a price based on its specifications. The data set consists of 14 numeric explanatory variables² and one target variable (price). The set has 159 samples with no missing value ($N = 159$). Before the analysis the variables were normalized as follows: $\tilde{y} = \frac{y - \text{mean}(y)}{\text{std}(y)}$, $\ln \tilde{x}_k = \frac{\ln x_k - \text{mean}(\ln x_k)}{\text{std}(\ln x_k)}$.

The number of hidden units was changed from one to four; $J = 1, \dots, 4$. For model selection we employ 10-fold cross-validation. Weight sharing was again applied only to weights w_{jk} . Here we set $h = 12$.

Table 2 shows the average training error \bar{E} over segments and 10-fold CV error E_{CV} of BCW1.2 for automobile data ($G=11,12$ are omitted). For each J , \bar{E} mostly decreased monotonically as G grew, while E_{CV} had a bottom in the midst of the range of G , and was minimized at $J = 3$ and $G = 7$.

Figure 2 shows how training error and cross-validation error E_{CV} changed through BCW1.2 learning for a certain segment under the model of $J = 3$. The bidirectional clustering was repeated three times until convergence. Training error E changed monotonically through learning, while E_{CV} did not.

After pruning and retraining, we get the final common weights: $u_1 = 0.4802$, $u_2 = 0.0693$, $u_3 = -0.1063$, $u_4 = 0$, $u_5 = -0.5593$, $u_6 = 0.2262$, and $u_7 = -0.1397$. The following is the final equation obtained in respect of normalized variables. Here u_7 is widely used while u_2 and u_6 are rarely used.

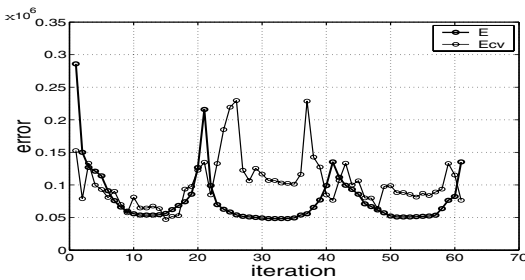
$$\tilde{f} = -1.3875 + 0.9386 \times \tilde{x}_1^{u_7} \tilde{x}_2^{u_7} \tilde{x}_3^{u_7} \tilde{x}_4^{u_1} \tilde{x}_5^{u_3} \tilde{x}_6^{u_1} \tilde{x}_7^{u_7} \tilde{x}_9^{u_2} \tilde{x}_{12}^{u_2} \tilde{x}_{13}^{u_7}$$

¹ The data set was taken from the UCI Repository of Machine Learning Databases

² We ignored all nominal variables in our experiments

Table 2. \overline{E} and E_{CV} of BCW1.2 for Automobile Data ($\times 10^6$)

| G | $J = 1$ | $J = 2$ | $J = 3$ | $J = 4$ |
|-----|--------------------------|--------------------------|--------------------------|--------------------------|
| 2 | (6.2152,7.1616) | (6.1214,4.8948) | (5.3305,4.9961) | (5.1163,5.9786) |
| 3 | (4.0723,5.5917) | (4.0179,4.3104) | (3.6398,3.7837) | (3.4212,4.8860) |
| 4 | (3.8094, 5.5837) | (3.5028, 3.6794) | (2.6242,3.4951) | (2.5230,4.5681) |
| 5 | (3.7510,5.9919) | (3.1673,3.9252) | (2.1752,3.4248) | (2.4001,4.4155) |
| 6 | (3.7340,6.0824) | (3.0586,3.8242) | (2.0258,3.0385) | (2.1001, 3.6606) |
| 7 | (3.7105,6.3214) | (2.9682,4.0721) | (1.9608, 2.9591) | (1.7888,3.7362) |
| 8 | (3.6936,6.5209) | (3.0022,4.3459) | (2.0550,2.9860) | (1.8581,3.7063) |
| 9 | (3.6859,6.4943) | (2.9611,4.2770) | (2.0032,3.0512) | (1.7574,3.6965) |
| 10 | (3.6772 ,6.5803) | (2.9270 ,4.2020) | (1.9586 ,3.0638) | (1.7040 ,3.8153) |

**Fig. 2.** Bidirectional Clustering for Automobile Data

$$\begin{aligned}
 & +0.3374 \times \tilde{x}_1^{u_1} \tilde{x}_2^{u_1} \tilde{x}_3^{u_6} \tilde{x}_4^{u_5} \tilde{x}_5^{u_5} \tilde{x}_6^{u_7} \tilde{x}_7^{u_7} \tilde{x}_8^{u_6} \tilde{x}_9^{u_6} \tilde{x}_{10}^{u_7} \tilde{x}_{11}^{u_7} \tilde{x}_{12}^{u_5} \tilde{x}_{13}^{u_3} \tilde{x}_{14}^{u_3} \\
 & -0.1612 \times \tilde{x}_1^{u_1} \tilde{x}_2^{u_7} \tilde{x}_3^{u_3} \tilde{x}_4^{u_1} \tilde{x}_5^{u_7} \tilde{x}_6^{u_7} \tilde{x}_7^{u_7} \tilde{x}_8^{u_3} \tilde{x}_{10}^{u_5} \tilde{x}_{11}^{u_7} \tilde{x}_{12}^{u_7} \tilde{x}_{14}^{u_5}
 \end{aligned} \quad (15)$$

The total cpu time required for BCW1.2 by 3.6 GHz Pentium PCs was 2,659 sec. for all the combinations: $J = 1, \dots, 4$ and $G = 2, \dots, 12$.

4 Conclusion

We enhanced the original weight sharing method called BCW in three points. Our preliminary experiments showed the proposed method worked nicely. In the future we plan to do further experiments to evaluate our method.

This work was partly supported by NTT Communication Science Laboratories, Nippon Telegraph and Telephone Corporation, and also partly supported by Artificial Intelligence Research Promotion Foundation.

References

1. C. M. Bishop. *Neural networks for pattern recognition*. Clarendon Press, 1995.
2. S. Haykin. *Neural networks, 2nd edition*. Prentice-Hall, 1999.
3. K. Saito and R. Nakano. Structuring neural networks through bidirectional clustering of weights. In *Proc. 5th Int. Conf. on Discovery Science*, pp. 206–219, 2002.
4. M. Stone. Cross-validatory choice and assessment of statistical predictions. *Journal of the Royal Statistical Society B*, Vol.64, pp. 111–147, 1974.

Detecting Search Engine Spam from a Trackback Network in Blogspace

Masahiro Kimura¹, Kazumi Saito², Kazuhiro Kazama³, and Shin-ya Sato³

¹ Department of Electronics and Informatics, Ryukoku University
Otsu, Shiga 520-2194, Japan

² NTT Communication Science Laboratories, NTT Corporation
Seika-cho, Kyoto 619-0237, Japan

³ NTT Network Innovation Laboratories, NTT Corporation
Musashino, Tokyo 180-8585, Japan

Abstract. We aim to develop a technique to detect search engine optimization (SEO) spam websites. Specifically, we propose four methods for extracting the SEO spam entries from a given trackback network in blogspace that are based on fundamental metrics on a network. Using real data of trackback networks in blogspace, we experimentally evaluate the performance of the proposed methods, and demonstrate that the method of ranking entries based on average degrees of nearest neighbors can be a very promising approach for extracting SEO spam entries.

1 Introduction

Search engine optimization (SEO) is the process of increasing the amount of visitors to a Web site by ranking high in the search results of a search engine¹. However, there are often SEO spam websites that contain little or no relevant content and whose aim is solely to increase their position in the search engine rankings. Such spamming involves obtaining more exposure for a website than it really deserves for a given search term, leading to unsatisfactory search experiences. Hence, it is an important research issue to develop a technique to detect SEO spam websites. With current search engines, the hyperlink strucure of the World Wide Web is widely exploited; for example, the “HITS” algorithm [6] and the “PageRank” algorithm [2] are well known. Thus, we consider the problem of detecting SEO spam websites based on the structures of link networks.

By contrast, considerable attention has recently been devoted to investigating weblogs (or *blogs*) [7],[5]. Here, blogs are personal on-line diaries managed by easy-to-use software packages, and they have spread rapidly through the World Wide Web. Someone who keeps a blog is called a *blogger*, and a collection of blogs with their links is referred to as *blogspace*. A blog consists of entries that include text, images, hyperlinks, and *trackbacks*. Compared with ordinary websites, one of the most important features of blogs is the existence of trackbacks. Unlike a hyperlink, one blogger can construct a link from an entry j of another blogger to

¹ see, <http://www.webopedia.com/TERM/S/SEO.html>

his entry i by creating a trackback on entry j . Thus, one can more easily create SEO spam entries in trackback networks. In this paper, we explore a method for extracting SEO spam entries from a trackback network.

Several investigations have been undertaken to identify the communities in a network by using graph-theoretic methods [3], [4]. Here, a community is defined as a collection of nodes in which each member node has more links to nodes within the community than to nodes outside the community. However, a set of SEO spam entries does not necessarily construct a community in a trackback network, since SEO spammers create trackbacks to their entries on normal entries that have many trackbacks in order to raise their rankings on search engines. This implies that the straightforward application of methods developed to identify communities are inadequate for our problem. To detect the SEO spam entries in a given trackback network, we propose four methods based on metrics on a network introduced in recent studies of complex network theory [9], [1], [8], and experimentally evaluate the performance of the proposed methods using real blog data.

2 Fundamental Metrics on Networks

We employ fundamental metrics on a network introduced in recent studies of complex network theory. We ignore the trackback direction for simplicity and treat a trackback network as an undirected graph. Therefore, throughout this work a network means an undirected graph.

2.1 Degrees and Average Degrees of Nearest Neighbors

The *degree* k_i of a node i in a network is defined as the number of links attached to node i [1]. One naive strategy for raising the rankings of blog entries on search engines is to create many trackbacks to those blog entries. Thus, we can naively consider that SEO spam entries should have high degrees.

By contrast, we can also consider that the blog entries with which an SEO spam entry connects should have high degrees. Thus, as studied in [8], we investigate the average degree \bar{k}_i among the nearest neighbors of an entry i in a trackback network. We call \bar{k}_i the *average NN degree* of entry i . Let \mathcal{N}_i be the neighborhood of a node i in a network, that is, the set of nodes that have links to node i . Then, \bar{k}_i is defined by

$$\bar{k}_i = \frac{1}{|\mathcal{N}_i|} \sum_{j \in \mathcal{N}_i} k_j ,$$

where $|\mathcal{N}_i|$ denotes the number of elements in the set \mathcal{N}_i .

2.2 Clustering Coefficients

The *clustering coefficient* C_i of a node i in a network is defined by

$$C_i = \frac{2b_i}{k_i(k_i - 1)} ,$$

where b_i is the number of direct links connecting the nodes in the neighborhood \mathcal{N}_i of node i [9]. Note that C_i reflects the probability that two friends of node i are friends themselves. We can naively consider that SEO spam entries should have high clustering coefficients in a trackback network.

3 Proposed Methods

We consider extracting the SEO spam entries from a given trackback network by ranking the entries in the network according to the level of SEO.

We propose the following four ranking methods based on the metrics introduced in the previous section. Let $r_1(i), r_2(i), r_3(i)$ and $r_4(i)$ be the evaluation functions of Methods 1, 2, 3 and 4, respectively, for measuring the SEO level of each node i . Then these functions are defined by $r_1(i) = C_i$, $r_2(i) = k_i$, $r_3(i) = C_i \log k_i$ and $r_4(i) = \bar{k}_i$. Figure 1 shows the kind of node in a network that is regarded as having a high SEO level for each method, i.e., a node with a high clustering coefficient for Method 1 (see, Fig. 1 (1)); a node with a high degree for Method 2 (see, Fig. 1 (2)); a node that has both a high clustering coefficient and a high degree for Method 3 (see, Fig. 1 (3)); and a node such that its nearest neighbors have high degrees for Method 4 (see, Fig. 1 (4)). Note that since the magnitude of the degree is generally much larger than that of the clustering coefficient, we performed a logarithmic transformation on the degree for Method 3.

4 Experimental Evaluation

4.1 Data Acquisition

Although there are a large number of blog entries in blogspace, many of them have no trackbacks. Namely, it is hard to obtain random samples of large connected trackback networks.

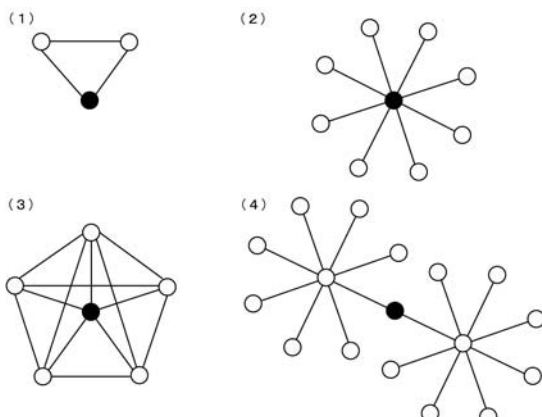


Fig. 1. Examples of nodes with high SEO levels for the proposed methods. The filled circles show examples of nodes with a high SEO level. (1)-(4) show examples for Methods 1-4, respectively

Then, we exploited the blog “Theme salon of blogs²”, where blog users can recruit trackbacks of other bloggers by registering interesting themes. By tracing ten steps ahead the trackbacks from the blog entries for a theme in the “Theme salon of blogs”, we collected a large connected trackback network. Note that the entries in the network were not restricted to the theme first chosen due to frequent topic drifts, and thus had a variety of topics. Namely, we might consider that this collection procedure could produce a reasonably random sampling of a large connected trackback network from blogspace.

4.2 Definition of SEO Spam Entries

We treated blog entries that had been participants in certain well-known SEO contests in Japan as SEO spam entries. In these SEO contests, SEO devotees compete for search engine rankings in a search for a specified keyword such as “Goggole” or “Deskedgar”, where these words are artifacts for the contests. We defined an entry as an SEO spam entry if it has the banner (link farm) “Trackback OK, Goggole”, the banner “Trackback OK, Deskedgar”, or one of the following keywords in the blogger name, entry name, or description section: “Goggole”, “Deskedgar”, “Nama sanargi”, “Yahhyoi”, “Ponesonic”, and “Den-nou Purion”.

4.3 Performance Measures

We quantified the performance of the proposed methods in terms of *F-measure* and *precision*, which are widely used in information retrieval.

Let S denote the set of SEO spam entries in a trackback network. We fix a method for extracting the SEO spam entries from the network. For any positive integer r , let M_r denote the set of the top r entries extracted by the method. Then, the *F-measure* $F(r)$ and the *precision* $P(r)$ of the method for ranking r are defined by

$$F(r) = \frac{2|M_r \cap S|}{|M_r| + |S|}, \quad P(r) = \frac{|M_r \cap S|}{|M_r|}.$$

Note that $F(r)$ quantifies how close the sets M_r and S are. Note also that the higher the value $P(r)$ is, the lower the detection error is.

4.4 Performance Evaluation

We describe our experimental results using data collected from the theme “Introduction of Special Sites” in the “Theme salon of blogs”. Similar results were obtained by using data collected from other themes like “News for Smiling”.

Then, the total numbers of blog entries and trackbacks were 9,338 and 187,128, respectively. By our definition described above, the number of SEO spam entries was 1,395. Table 1 shows the fundamental statistics related to

² <http://blog.goo.ne.jp/usertheme/>

the proposed methods. Namely, the means of C_i , k_i and \bar{k}_i are respectively displayed for the set of SEO spam entries and the others. Table 1 implies that the clustering coefficient, degree, and average NN degree of an SEO spam entry are generally larger than those of a non-SEO spam entry. Namely, these results justify applying the proposed methods.

Table 1. Measurement of the means of C_i , k_i and \bar{k}_i for the set of SEO spam entries and the set of non-SEO spam entries

| | $\langle C_i \rangle$ | $\langle k_i \rangle$ | $\langle \bar{k}_i \rangle$ |
|----------------------|-----------------------|-----------------------|-----------------------------|
| SEO spam entries | 0.50317 | 63.833 | 176.97 |
| Non-SEO spam entries | 0.27830 | 6.4297 | 24.267 |

Figures 2 and 3 respectively display F -measure $F(r)$ and precision $P(r)$ with respect to ranking r for the proposed methods. Here, when plural entries have the same score, the F -measure $F(r)$ and the precision $P(r)$ are not plotted until all such entries are included in the set M_r of ranking r . For example, both the F -measure and the precision graphs begin at $r = 828$ in Method 1, since there were 828 top entries.

Figure 2 shows that Method 4 provided the highest level of performance followed by Methods 2 and 3. Method 1 was the worst. In particular, the F -measure of Method 4 was extremely high with a value of over 80% around $r = 1,395$ (the

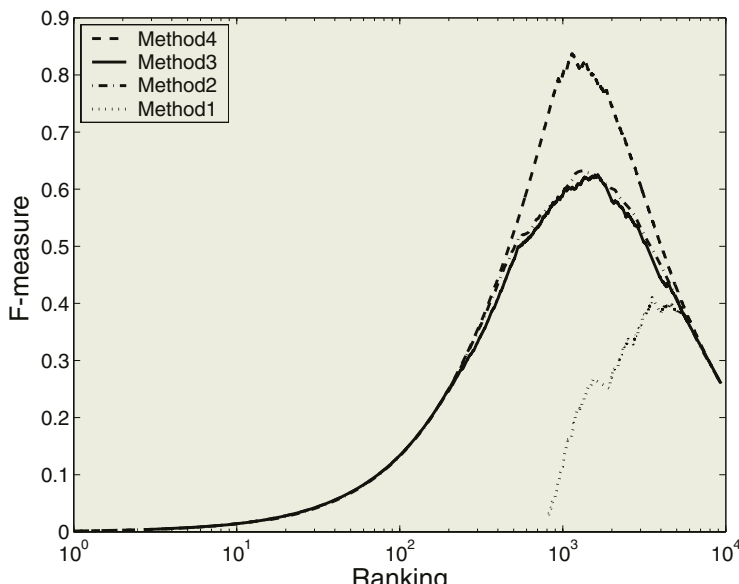


Fig. 2. Performance evaluation of the proposed methods on F -measure. The dotted, dash-dotted, solid and dashed lines indicate the results for Methods 1-4, respectively

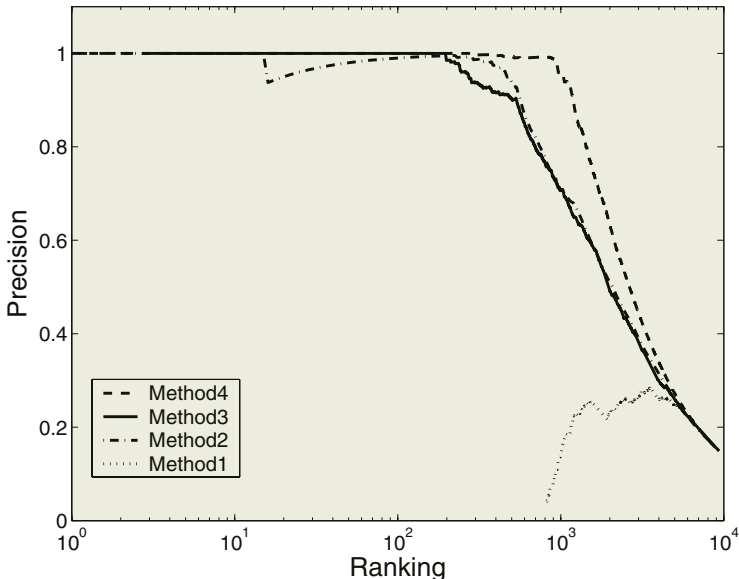


Fig. 3. Evaluation of the precision of the proposed methods. The dotted, dash-dotted, solid and dashed lines indicate the results for Methods 1-4, respectively

number of SEO spam entries). Moreover, Figure 3 shows that Method 4 was extremely precise. In particular, the value was 100% at $r = 289$ and over 90% around $r = 1,000$. These results imply that the method of ranking entries based on average NN degrees can be a very promising approach for extracting the SEO spam entries from a trackback network. We consider that this is because as a discriminative characteristic, SEO spam entries are likely to be linked to many entries with high degrees. Incidentally, Method 3 extracted “adult blog entries” as well as SEO spam entries. This suggests that adult blog entries are likely to produce relatively dense connections among them regardless of SEO spamming. Thus, Figs.2 and 3 indicate that the method of ranking entries based on both clustering coefficients and degrees is a promising approach for extracting general spam entries.

5 Conclusion

We proposed four methods based on fundamental metrics for extracting the SEO spam entries from a given trackback network and evaluated their performance experimentally. Using a connected trackback network collected by tracing ten steps ahead of the trackbacks from the blog entries for a theme in the “Theme salon of blogs”, we experimentally demonstrated that the method of ranking entries based on average NN degrees can be a very promising approach to extract SEO spam entries. Moreover we showed that the method of ranking entries based on both clustering coefficients and degrees can be a promising way to extract general spam entries.

By contrast, the next important task is to undertake an extensive verification of our methods with various real blog data. To this end, we will need more sophisticated data collection processes. However, we have already made substantial progress, and we are encouraged by our initial results.

Acknowledgements

This work was partly supported by NTT Communication Science Laboratories, Nippon Telegraph and Telephone Corporation. We express our sincere gratitude to Naonori Ueda for his encouragement and useful suggestions. We thank Hirofumi Fujimoto for performing the experiments.

References

1. Barabási, A.-L. and Albert, R., Emergence of scaling in random networks, *Science*, **286** (1999) 509–512.
2. Brin, S. and Page, L., The anatomy of a large scale hypertextual Web search engine, In *Proceedings of the Seventh International World Wide Web Conference* (1998) 107–117.
3. Flake, G.W., Lawrence, S. and Giles, C.L., Efficient identification of Web communities, In *Proceedings of the Sixth ACM SIGKDD International Conference on Knowledge Discovery and Data Mining* (2000) 150–160.
4. Girvan, M. and Newman, E.J., Community structure in social and biological networks, *Proceedings of the National Academy of Sciences of the United States of America*, **99** (2002) 7821–7826.
5. Gruhl, D., Guha, R., Liben-Nowell, D., and Tomkins, A., Information diffusion through blogspace, In *Proceedings of the 13th International World Wide Web Conference* (2004) 491–501.
6. Kleinberg, J., Authoritative sources in a hyperlinked environment, In *Proceedings of the Ninth ACM-SIAM Symposium on Discrete Algorithms* (1998) 668–677.
7. Kumar, R., Novak, J., Raghavan, P., and Tomkins, A., On the bursty evolution of Blogspace, In *Proceedings of the 12th International World Wide Web Conference* (2003) 568–576.
8. Pastor-Satorras, R., Vázquez, A., and Vespignani, A., Dynamical and correlation properties of the Internet, *Physical Review Letters*, **87** (2001) 258701.
9. Watts, D.J. and Strogatz, S.H., Collective dynamics of ‘small-world’ networks, *Nature*, **393** (1998) 440–442.

Analysis for Adaptability of Policy-Improving System with a Mixture Model of Bayesian Networks to Dynamic Environments

Daisuke Kitakoshi¹, Hiroyuki Shioya², and Ryohei Nakano¹

¹ Nagoya Institute of Technology, Gokiso-cho, Showa-ku, Nagoya 466-8555, Japan
{kitakosi,nakano}@ics.nitech.ac.jp

² Muroran Institute of Technology, 27-1, Mizumoto-cho, Muroran 050-0071, Japan
shioya@epsilon2.csse.muroran-it.ac.jp

Abstract. We have proposed an online policy-improving system of reinforcement learning (RL) agents with a mixture model of Bayesian Networks (BNs), and discussed properties of the system. In this paper, two types of mixture models have been applied to the system. A structure of BN in the mixture model is selected based on data collected by agents in an environment, and is regarded as a stochastic knowledge of the environment. This research investigates the adaptability of our system to dynamic environments containing an unexperienced environment, in which an agent does not have the knowledge.

1 Introduction

A BN is one of the stochastic models, and has been applied to various systems, such as decision-making mechanisms of autonomous vehicles[1], agents (robots) and so on[2]. Many RL methods also have been proposed in order to learn policies for agents to select their own actions effectively.

We have proposed an on-line system **Improving RL agents' Policies with a Mixture model of BNs (IPMBN)**[3]. In this system, each BN constituting a mixture model is regarded as a stochastic knowledge corresponding to each environment, and its structure is decided by a method for model selection. An agent with IPMBN recognizes changes in the environment by means of a mixture model of BNs. The agent's policy is then improved based on the information on the current environment represented in the mixture model. On the other hand, the computational time for deciding the suitable structure of BN increases with the size of network. It is therefore preferable to effectively utilize as a small number of BNs as possible in order to address the above issue. Using the mixture model to represent a greater diversity of environments with a small number of BNs, IPMBN will make it possible for agents to adapt to dynamic environments, and besides restrain the increase of the computational time to prepare new BNs for new environments.

In this research, we prepare linear and exponential mixture models used in the field of ensemble learning. Either of them is incorporated into IPMBN

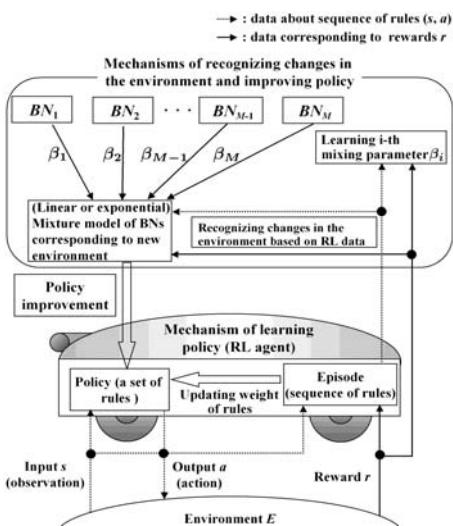


Fig. 1. The framework of IPMBN

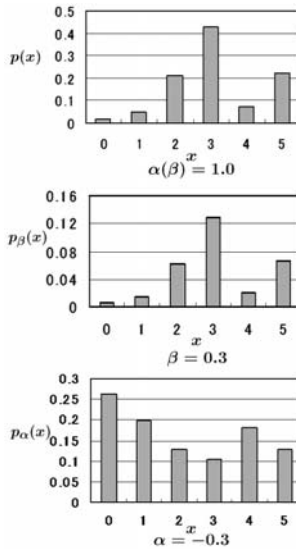


Fig. 2. The variation in a probability mass function $p(x)$ transformed by mixing parameters

as the mechanisms that recognize environmental changes and improve agents' policies. This research examines the capabilities to stochastically represent environments in these two models from results of simulations. In the simulations, 4 environments are dynamically switched, and one of them is an unexperienced environment (or, the environment to which IPMBN does not have the BN corresponding) for the agent.

2 Preliminaries

IPMBN is composed of two mechanisms: one makes an agent learn its own behavior, and the other recognizes environmental changes, and then improves the agent's policy (Fig. 1). This section describes profit sharing as the former mechanism and the mixture model of BNs as the latter one.

2.1 Profit Sharing

Profit sharing is one of the RL methods. A RL agent learns its own policy to select an action given an observation, through trial-and-error interactions with an environment. A policy is characterized as the following function $w : \mathcal{S} \times \mathcal{A} \rightarrow R$, where \mathcal{S} and \mathcal{A} denote a set consisting of state and action, respectively. A pair (s, a) ($\forall s \in \mathcal{S}, \forall a \in \mathcal{A}$) is called a rule which means "if an agent observes s , then selects an action a ", and $w(s, a)$ is called the weight of the rule. Obtaining the observation s^* , an agent selects the rule in proportion to $w(s^*, a_h)$ in this study ($h = 1, \dots, |\mathcal{A}|$). Agents store the series of rules from the initial state to

the state where a reward is given. When an agent selects the rule (s_C, a_C) and obtains a reward r , the weight of each rule is reinforced as follows.

$$\mathbf{w}(s_n, a_n) \leftarrow \mathbf{w}(s_n, a_n) + f(n) , \quad (1)$$

$$f(n) = r\gamma^{C-n} \quad (n = 0, \dots, C) . \quad (2)$$

$f(n)$ is called a reinforcement function, and $\gamma \in (0, 1]$.

2.2 Bayesian Networks and Mixture Model of Them

We leverage a BN for a stochastic knowledge corresponding to an environment. A BN is represented as a directed acyclic graph expressing the dependences among random variables by using joint probability distribution. Each node of a BN denotes a random variable, and a directed link is drawn if stochastic dependences exist between two variables. We assign the state $s_j (\in \mathcal{S})$ to state node X_{s_j} ($j = 1, \dots, m; m = |\mathcal{S}|$) and also assign reward r to reward node X_r . Values of X_{s_j} and X_r denote integer \tilde{a} conforming to the action a of the set of rules $R_{s_j} = \{(s_j, a) | a \in \mathcal{A}\}$ and one element of $\{1, 0\}$ signifying whether a positive reward is given. In this paper, a structure of BN is selected on the basis of MDL criterion calculated by using data[4]. The data consists of series of rules and given reward while an agent learns its own policy. The BN can be thereby regarded as the information representing stochastic characteristics of the policy which the agent learns in the correspondent environment.

In order to adapt agents to a huge variety of environments, the mixture model in our study consists of a number of BNs. IPMBN employs linear or exponential mixture models. The linear mixture model is expressed in terms of linear mixture distribution $P_{\text{BN}}^{\text{mix}}(\mathbf{X})$.

$$P_{\text{BN}}^{\text{mix}}(\mathbf{X}) = \sum_{i=1}^M \beta_i P_{\text{BN}_i}(\mathbf{X}) . \quad (3)$$

M denotes the number of BNs, and β_i is the mixing parameter of BN_i of the mixture model ($\sum_i \beta_i = 1, \beta_i \geq 0 \forall i$). It is expected that agents can adjust to a variety of environments with the mixture model if the mixture can represent the characteristics of new environments through leaning mixing parameters. Consequently, the adaptability of IPMBN to dynamic environments depends on the variety of the environments expressed by the mixture models. In the linear mixture model, a mixing parameter β_i indicates the relative degree of necessity for BN_i to represent the characteristics of the environment. BN_i is regarded as “unnecessary knowledge” for the current environment in the case where $\beta_i = 0$.

The exponential mixture model is shown below.

$$P_{\text{BN}}^{\text{mix}^*} = \frac{\prod_{j=1}^M P_{\text{BN}_j}(\mathbf{X})^{\alpha_j}}{\sum_{\mathbf{X}} \prod_{j=1}^M P_{\text{BN}_j}(\mathbf{X})^{\alpha_j}} . \quad (4)$$

α_j is the mixing parameter ($\sum_{j=1}^M \alpha_j = 1$), and $\sum_{\mathbf{X}} \prod_{j=1}^M P_{\text{BN}_j}(\mathbf{X})^{\alpha_j} < \infty$. We take notice that α_j can be a negative value, in other words, this model is allowed

to utilize so-called “negative mixing parameters”. Figure 2 shows, as an example, the variation in a probability mass function $p(x)$, in which the discrete random variable x can take values from 0 to 5, with two kinds of mixing parameters ($\beta = 0.3$ and $\alpha = -0.3$). The values of the function $p_\beta(x)$ transformed $p(x)$ by β are 30% of those of $p(x)$. Moreover, $p_\beta(x) = 0$ when $\beta = 0$ ($\forall x$). If such distribution is the component of mixture distribution, it comes to not act on the mixture distribution as β decreases to 0. In contrast, $p_\alpha(x)$ has some contrary characteristics to $p(x)$. That is, the values of $p(x)$ are small (e.g. $x = 0$) when those of $p_\alpha(x)$ are large, and vice versa. The exponential mixture model has possibility to form a broader range of distributions than the linear mixture model because this model can take advantage of “reversed” characteristics of stochastic knowledge by assigning negative mixing parameter to the BN.

The mixing parameters for the current environment are decided through the learning by gradient descent using the log likelihood of $P_{\text{BN}}^{\text{mix}^{(*)}}$ as the objective function. The data for learning mixing parameters is similar to that for selecting the structure of BN; however, it is confined to the data given (positive) reward in order to curb the increase of computational time.

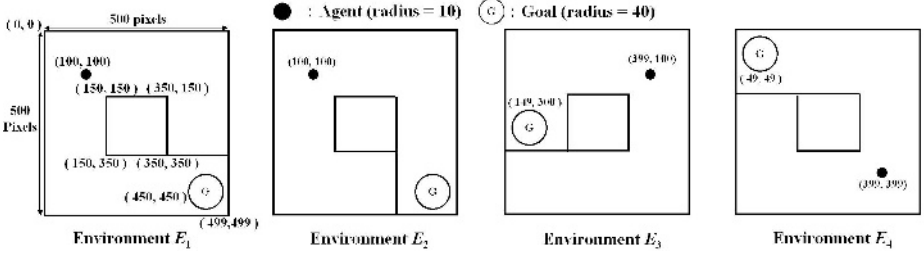
3 Procedures for Recognizing Environmental Changes and Improving the Agent’s Policy

This section briefly outlines procedures for recognizing environmental changes and improving the agent’s policy, in IPMBN. First, the method for recognizing environmental changes is shown as follows: (a) Log likelihood of $P_{\text{BN}}^{\text{mix}^{(*)}}$ per one data, L_E , is calculated with respect to all data collected while an agent learns its own policy for a given number of trials, (b) After that, L'_E is also calculated in the same way, (c) The system recognizes that the environment has changed to another one if $L_E - L'_E \geq \xi$ (ξ : positive constant). If the above condition is not satisfied despite the occurrence of the changes, existing mixture model is deemed to be adaptive to the new environments. When the changes are not recognized, the procedure (a) comes again after $L_E \leftarrow L'_E$. The data used for calculating L_E (L'_E) is identical with that for learning mixing parameters. In the case of obtaining no such data, we let L_E (L'_E) be a negative large constant. Second, we show the overall processing flow in IPMBN.

- step 1.** The procedure for recognizing environmental changes is repeated until the changes are recognized.
- step 2.** Mixing parameters are learned after setting all weights of rules to the initial value.
- step 3.** An action a_k^i satisfying the following equation is selected in BN_i of the mixture model ($i = 1, \dots, M$; and $k = 1, \dots, K_i$).

$$a_k^i = \arg \max_{a \in \mathcal{A}} P(X_r = 1 | X_{s_k}^i = \tilde{a}) . \quad (5)$$

$X_{s_k}^i$ denotes state node connecting with X_r in BN_i , and K_i denotes the number of $X_{s_k}^i$.

**Fig. 3.** Simulation environments

step 4. In each selected action, the weight of rule is updated according to (6).

$$\mathbf{w}(s_k, a_k^i) \leftarrow \mathbf{w}(s_k, a_k^i) + \sum_{i=1}^M \mathcal{I}_i \lambda_i \bar{\mathbf{w}} . \quad (6)$$

$\bar{\mathbf{w}}$ is mean value of all weights of the rules in an agent. \mathcal{I}_i equals 1 if $X_{s_k}^i$ connects with X_r in BN $_i$ and equals 0 otherwise. In addition, λ_i is equivalent to β_i in the linear mixture model, and is obtained by the following equation in the exponential mixture model in order to not broaden too much the difference between the maximum and the minimum values of mixing parameters.

$$\lambda_i = \begin{cases} \alpha_i & \text{if } \alpha_i \geq 0 \quad \forall i \\ \alpha_i / (|\alpha_{\max}| + |\alpha_{\min}|) & \text{otherwise} \end{cases} . \quad (7)$$

Updating the weights of the rules means improving the policy of the agent. After improving the policy, **step 1** comes again.

4 Computer Simulations

This section describes simulations in the agent navigation problem. In this problem, an agent aims to move from the initial position to the goal as surely as possible. Figure 3 shows environments adopted in our simulations. For the agent, to contact the circumference of goal means to arrive at the goal. The agent can detect the goal or walls in four directions within distance V_r , and can move 1 pixel to one of four directions. It also has energy E_{n0} , and consumes energy E_{n-} in the case of moving or touching walls. The agent learns its own policy by profit sharing. Arriving at the goal, the agent obtains positive reward r_p . We count 1 trial of the simulations when the agent arrives at the goal, or consumes all of its energy. We call the former trial “successful trial” particularly. The structures of BNs for E_i ($i = 1, \dots, 3$) are decided in advance by using data. The data is stored through learning the policy of agent for 2000 trials. We prepare two kinds of data sets \mathcal{D}_i^{r5} and \mathcal{D}_i^{r50} whose elements are collected by setting r_p to 5 and 50. In other words, we evaluate the performance of IPMBN with two groups of BNs (\mathbf{BN}_i^{r5} or \mathbf{BN}_i^{r50}) by using the above data sets. Table 1 represents the total

Table 1. The total number of successful trials while collecting data

| r_p | E ₁ | E ₂ | E ₃ |
|-------|----------------|----------------|----------------|
| 5 | 1218 | 1224 | 1459 |
| 50 | 1921 | 1905 | 1936 |

Table 2. Parameters

| parameter | value | parameter | value |
|-----------|---------|-----------|-------|
| γ | 0.33 | E_{n-} | 1.00 |
| ξ | 1.00 | r_p | 50.00 |
| V_r | 80.00 | w_0 | 1.00 |
| E_{n0} | 2000.00 | ζ | 0.40 |

number of successful trials for all trials. The BN for E₄ is not prepared. This means that E₄ is an unexperienced environment for the agent.

An environment is switched to another in every 1000 trials such that E₁ → E₂ → E₃ → E₄ → E₁ → E₂ → E₃ → E₄. Each procedure for recognizing environmental changes and for learning mixing parameters requires 100 trials in the simulations. We compare the results of the following 3 approaches: **ExM** (IPMBN using the Exponential Mixture model), **LiM** (IPMBN using the Linear Mixture model), and **PS** (learning through Profit Sharing and resetting policy). ExM and LiM incorporate either of BN^{r5} and BN^{r50} as components of the mixture model. These approaches are labeled **ExM^{r5}**, **ExM^{r50}**, **LiM^{r5}**, and **LiM^{r50}**, respectively. In the third approach PS, all weights of the rules in the policy are set to the initial value w_0 if $sr_{t+1} \leq \zeta \cdot sr_t$, where sr_t denotes “success rate” which is the number of successful trials from 100(t-1)+1 to 100t trials ($t = 1, \dots, 80$). ζ is constant. Table 2 shows the setting of each parameter. w_0 in the table denotes also minimum weight of the rule. We repeat the simulations 20 times.

5 Empirical Results and Discussions

In this section, we describe empirical results and discuss properties of IPMBN in dynamic environments. The total number of successful trials for 8000 trials is listed in Table 3. As shown in the table, the number of successful trials was larger in ExM^{r5} than in PS and LiM^{r5}. With respect to these, the transitions of the success rates are shown in Fig. 4. This figure illustrates that success rates in all 3 approaches rapidly descended after environmental changes; however, then rapidly ascended. It is also shown in the figure that success rates in both of ExM^{r5} and LiM^{r5} were high in unexperienced environment E₄ (from 3001 to 4000, and 7001 to 8000 trials). These two approaches using mixture models could recognize about 80% of environmental changes shortly after the changes, and then improved the agent’s policy. Average increasing rates of success rates were approximately 18%(PS), 28%(LiM^{r5}), and 37%(ExM^{r5}) after improving policy in IPMBN, and approximately 30%, 35%, and 38% in the case after switching to E₄. These show that the policy improvement in ExM^{r5} allows to effectively adapt

Table 3. The total number of successful trials in the simulations

| PS | LiM ^{r5} | ExM ^{r5} | LiM ^{r50} | ExM ^{r50} |
|--------|-------------------|-------------------|--------------------|--------------------|
| 4113.4 | 4375.5 | 4586.6 | 3451.3 | 3381.5 |

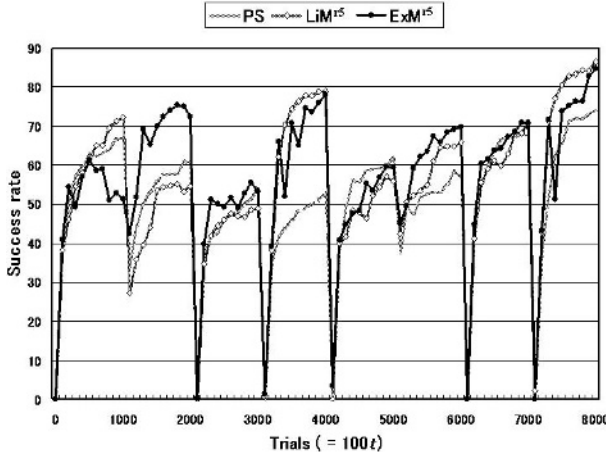


Fig. 4. The transition of success rates

the agent to dynamic environments containing unexperienced one, compared to the others in the figure. On the other hand, the total number of successful trials in ExM^{r50} was the lowest of all results in the simulations, and that was also lower in LiM^{r50} than in the others except ExM^{r50}. ExM^{r50} and LiM^{r50} leverage the BNs in BN_i^{r50} constructed according to \mathcal{D}_i^{r50} . The data set contains more elements in the case of obtaining rewards than \mathcal{D}_i^{r5} (see table 1). It is considered that assigning larger value to the reward permits more rapid learning of agents' policies in our settings. At the same time, this setting may decrease the diversity of generated data and also may decrease the chances for the agent to learn better policies. It is thought that BNs constructed by such data set as \mathcal{D}_i^{r5} have greater performance to represent environmental information rather than the data set such as \mathcal{D}_i^{r50} .

Finally, we discuss the properties of linear and exponential mixture models through comparing the acquired mixing parameters in LiM^{r5} and ExM^{r5} (Table 4). In this table, we can see that the mixing parameter of BN corresponding to the switched environment was the highest in all environmental changes in LiM^{r5}, except the case after switching to E₄. Some rule sequences for the agent to arrive at the goal in E₄ seem to be analogous to those in E₃ (e.g. the agent must move left to arrive at the goal in both of E₃ and E₄, but the action often must not be selected in E₁ and E₂). This causes that the value of β_{E_3} was the highest in the environmental changes E₃ → E₄. In ExM^{r5}, similar characteristics were shown in the table. Moreover, the results in table 3 also suggest that ExM^{r5} can express environmental information more appropriately than LiM^{r5}. This is considered to be responsible for assigning negative values to the mixing parameter of the BN, which is significantly different from the current environments in terms of the rule sequences to obtain rewards (or, strictly speaking, the likelihood for the environments), in ExM^{r5}. However, it should be additionally noted that the value of α_{E_2} was the highest in the environmental change E₄ → E₁. Further investigations are required to discuss the factor causing the above situation.

Table 4. Mixing parameters shortly after environmental changes in LiM^{r5} and ExM^{r5}

| Environmental changes | LiM ^{r5} | | | ExM ^{r5} | | |
|--------------------------|-------------------|---------------|---------------|-------------------|----------------|----------------|
| | β_{E_1} | β_{E_2} | β_{E_3} | α_{E_1} | α_{E_2} | α_{E_3} |
| $E_1 \rightarrow E_2$ | 0.345 | 0.624 | 0.032 | -0.243 | 1.092 | 0.151 |
| $E_2 \rightarrow E_3$ | 0.164 | 0.175 | 0.661 | 0.044 | 0.126 | 0.830 |
| $E_3 \rightarrow E_4$ | 0.192 | 0.288 | 0.520 | -0.915 | -0.321 | 2.236 |
| $E_4 \rightarrow E_1$ | 0.435 | 0.365 | 0.200 | 0.065 | 1.469 | -0.534 |
| $E_1 \rightarrow E_2$ | 0.162 | 0.475 | 0.363 | 0.140 | 0.507 | 0.352 |
| $E_2 \rightarrow E_3$ | 0.235 | 0.141 | 0.623 | 0.022 | 0.070 | 0.908 |
| $E_3 \rightarrow E_4$ | 0.173 | 0.239 | 0.588 | -1.010 | -0.384 | 2.394 |

6 Conclusions

This paper has investigated capabilities of representing environments in IPMBN. We have employed two types of mixture model of BNs to recognize environmental changes and to improve agents' policies. It has been confirmed that the agent with IPMBN can adapt to dynamic environments containing unexperienced one more effectively by using the exponential mixture model than by using the linear mixture. Moreover, the diversity of the data for model selection has a major impact on the performance of IPMBN. In our settings of the simulations, empirical results imply that the less variety of data does not contribute to select the BN's structure appropriately expressing various environments, even though the data set contains many successful cases.

As future works, we plan to refine the mechanisms of recognition and improvement, and then plan to apply our system to environments changing continuously. The above revision involves modification of the use of mixture models to enhance the adaptabilities of the systems.

References

1. J. Forbes, T. Huang, K. Kanazawa, and S. Russell: The MATmobile: Towards a Bayesian Automated Taxi. Proc. of the 14th Int. Joint Conf. on Artificial Intelligence (1995) 1878–1885
2. D. Kitakoshi, H. Shioya, and M. Kurihara: Analysis of a Method Improving Reinforcement Learning Agents' Policies. Journal of ACIII, **7**(3) (2003) 276–282
3. D. Kitakoshi, H. Shioya, and M. Kurihara: A Reinforcement Learning System by using a Mixture Model of Bayesian Network. SICE Annual Conference 2003 Proc., **TAII-14-1** (2003) (CD-ROM)
4. D. Heckerman: A Tutorial on Learning with Bayesian Networks. Technical Report **MSR-TR-95-06**, Microsoft Research (1995)

Parallel Stochastic Optimization for Humanoid Locomotion Based on Neural Rhythm Generator

Yoshihiko Itoh, Kenta Taki, Susumu Iwata, Shohei Kato, and Hidenori Itoh

Dept. of Computer Science and Engineering, Nagoya Institute of Technology,

Gokiso-cho Showa-ku Nagoya 466-8555 Japan

{yitoh,ktaki,iwata,shohey,itooh}@ics.nitech.ac.jp

Abstract. This paper proposes a parallel stochastic approach to neural oscillator based motion control for bipedal humanoid locomotion. The motion control is based on the Central Pattern Generator (CPG), and is optimized by Simulated Annealing. Optimization of parameters in the motion control based on the CPG is a very hard problem. The number of the parameters which should be optimized increases as a robot's link structure becomes complicated. To optimize all parameters simultaneously may cause explosion of search space. Therefore, we divide search space into upper-limbs optimization space and leg optimization space. We then propose a parallel optimization method by two processes, which handles the control parameters of upper-limbs and legs, and communicates them each other. In the experiments, our method succeeded in optimization of all parameters without explosion of search space, and performed superior gaits.

1 Introduction

Recently, motion control of the humanoid robot using Neural Rhythm Generator (e.g., [2], [7], [4]) attracts much attention in robotics. Taga [9] [8] proposed neuro-musculo-skeletal system using CPG, one of the neural rhythm generators, which generates bipedal locomotion having robustness for environmental changes. The motion control based on the CPG, however, has a hard problem of adjusting parameters. So, we [10] have generated the walking movement of simple bipedal robot which is composed of only lower limb using Simulated Annealing (SA), which is one of heuristic and stochastic search methods for difficult optimization problems. On the other hand, walking movement progresses in the performance, such as stability and speed, by not only lower limb motion but also upper limb motion such as swinging arms. In this paper, we thus adopt a biped robot with a upper limb, and aim at generating various walking movements by utilizing the upper limb motion.

Walking movements of robots are evaluated from multiple standpoints, such as stability, speed, gait in appearance and so on. So it is very difficult to set weighting factors on each criterion in the evaluation of the movement. Endo et al [1], in optimization of parameters using genetic algorithm (GA), treated this problem as multi-objective optimization problem, and generated morphology

and walking pattern of a biped walking robot. The robot, however, do not have upper limb and the link structure is simple. Their method might be inefficient for motion control with whole body including upper limb. In such case, to optimize all parameters simultaneously may cause explosion of search space.

In this paper, we, therefore, divide search space into upper-limbs optimization space and leg optimization space, and then propose a parallel optimization method by two processes, which handles the control parameters of upper-limbs and legs, and communicates them each other.

2 The Link Model and Its Basic Neural Oscillation

2.1 The Link Structure of Humanoid Robot

In this paper, we adopt a bipedal humanoid robot, which is composed of two parts: *upper limb* and *lower body* corresponding to trunk and lower limb. The robot has twelve links (four links for *upper limb* part and eight links for *lower body* part) and eleven joint (see the skeleton in Fig. 1 (right)). *Upper limb* part is composed of both upper arms and lower arms. *Lower body* part is composed of the trunk, the waist, both thighs, lower thighs and foots. Length and weight of each link are arbitrarily assigned based on an adult man.

2.2 Neural Rhythm Generator

Walking movement is periodical and symmetrical movement. In this research, we control walking movement using CPG which is often used in generating periodical movement. CPG is modeled mathematically to the neural rhythm generator which exists at a relatively low level of the central nervous system such as the spinal cord of animals. Standout feature of CPG, it is synchronized its inner state with rhythmic input from outside in term of phase. Using this feature, therefore walking movement having robustness for changes of environment is able to be generated. CPG is composed of multi-neurons which inhibit each other. The mathematical model of a neurons is represented as following system of differential equation.

$$\tau_i \dot{u}_i = -u_i - b \cdot f(v_i) + \sum_{j=1}^n w_{ij} f(u_j) + u_0 + S_i, \quad (1)$$

$$\tau'_i \dot{v}_i = -v_i + f(u_i), \quad (2)$$

$$f(x) = \max(x, 0), \quad (3)$$

where u_i is the inner state of i -th neuron; v_i is a variable which represents the degree of the adaptation or self-inhibition effect of the i -th neuron; τ_i and τ'_i are time constants of the inner state and the adaptation effect of the i -th neuron, respectively; b is a coefficient of the adaptation effect; w_{ij} is a connecting weight from the j -th neuron to the i -th neuron; u_0 is an external input with a constant rate; and S_i is the local and global sensory information that is sent to the i -th neuron. A neuron excited by u_0 is oscillated by self-inhibition and cross-inhibition, and $f(u)$ is output of neuron. For more precise, please refer to [5] and [6].

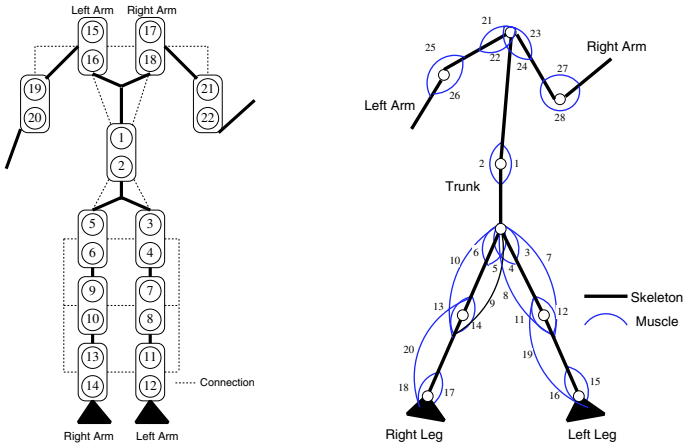


Fig. 1. Structure of neural system (left) and musculo-skeletal system (right)

3 Neuro-musculo-skeletal System

In this paper, we adopt neuro-musculo-skeletal system [8] proposed by Taga as a motion control method based on CPG for the robot. Neuro-musculo-skeletal system is composed of two dynamical systems: a neural system and a musculo-skeletal system. The neural system is composed of CPG network, and the musculo-skeletal system is composed of skeletons considered muscles surrounding to them. The system can generate flexible and adaptable walking movement through the mutual interaction among the neural system, the musculo-skeletal system and environment.

In this paper, we make two contributions to a CPG-based motion generation method particularly neuro-musculo-skeletal system: *whole body movements* by development of the body structure from eight links to twelve links and *flexible and adaptable motion generation* by parameter optimization using SA.

3.1 Neural System

In the neural system, CPG network is consisted of eleven pairs of neurons in accordance with the robot's link structure. CPGs are allocated to eleven joints: the trunk and a pair of the hips, the knees, the ankles, the shoulders and the elbows shown in the left side of Fig. 1. Two neurons at a CPG have each flexion and extension effect on muscles corresponding to the CPG.

3.2 Musculo-skeletal System

In the musculo-skeletal system, skeletons conform the robot's link structure, and there are twenty two single-joint muscles and six double-joint muscles surrounding to each joint. The right side of Fig. 1 shows the configuration of muscles.

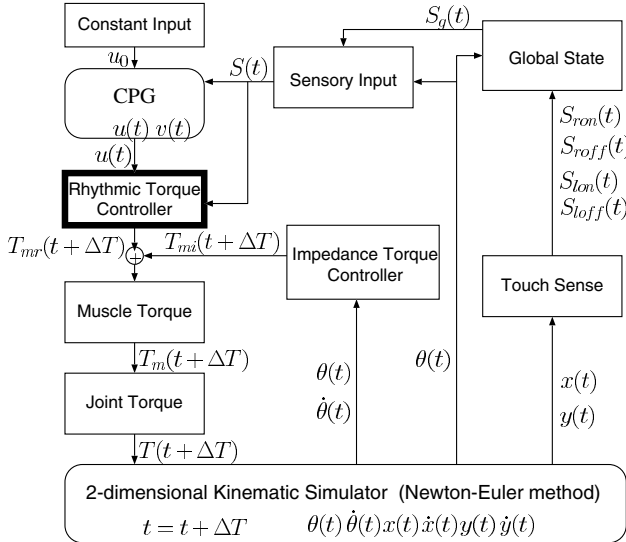


Fig. 2. block diagram of motion control based on the neuro-musculo-skeletal system

3.3 Motion Control Method

Figure 2 shows block diagram of motion control for the robot based on neuro-musculo-skeletal system. In the figure, T_{mr} , T_{mi} , T_m and T denote the rhythmic torque, the impedance torque, the muscle torque and the joint torque, respectively. The rhythmic torque has rhythmic property and the impedance torque is generated for maintaining a standing position. In the figure, θ , $\dot{\theta}$, x and y denote the angle, the angular speed, the horizontal position and the vertical position of each link, respectively. The S_{ron} (S_{roff}), S_{lon} (S_{loff}) denote flags of contacting (not contacting) the ground of right-and-left feet. The S_g is the state of pose and S is sensory input.

4 Parallel Stochastic Optimization Using SA

4.1 Optimization of Rhythmic Torque Controller

In this research, we generate walking movement for humanoid robot using optimization of parameters by SA. In this paper, we optimize the rhythmic torque controller (see Fig. 2). The rhythmic torque controller generates torque for muscle from sensory input and output of CPG, so it is a very important controller, which determines the feasibility of walking movement for the robot.

In our system, rhythmic torque $T_{mr} = (T_{mr1}, T_{mr2}, \dots, T_{mr28})^T$, generated in muscles of 1-28 shown in Fig. 1, is represented as:

$$T_{mr} = U \cdot P \cdot B, \quad (4)$$

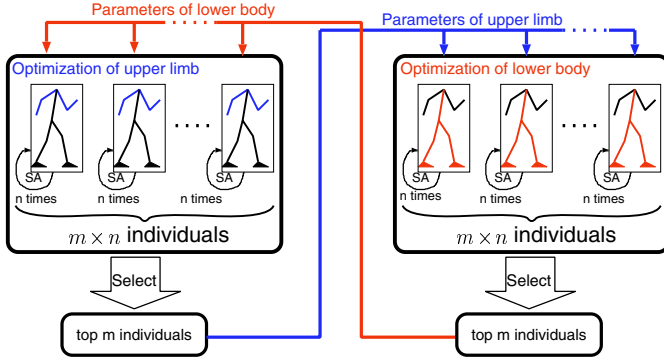


Fig. 3. Parallel optimization by two processes, which handles the control parameters of upper-limbs and lower-limbs

where U is a (28×28) matrix composed of output of CPGs, P is a (28×10) matrix of parameters, and B is a (10×1) matrix of sensory information. Elements of B are flags of contacting the ground of both foot, inclination of center of gravity and angle of each joint. Considering symmetry of body and relativity among CPG, muscle and joint, P is represented using 32 parameters. In this paper, proposed method optimizes the rhythmic torque controller by optimization of these 32 parameters in P .

4.2 Parallel Optimization Method

It's very hard to adjust parameters of motion control based on CPG. As robot's link structure or control structure is complicated, the number of the parameters leaps upward, so optimization becomes quite difficult. Therefore, we propose a parallel optimization method by two processes, which handles the control parameters of upper-limbs and lower-body (i.e., trunk and lower-limbs), and communicates them each other. Figure 3 shows an outline flowchart of the proposed parallel optimization method for optimization of the rhythmic torque controller of the entire body. This parallel method has a symmetric structure composed of two processes: *upper limb optimization process* and *lower body optimization process*. Each process executes k times iteration of the following procedure.

Single Optimization Process P_a

1. For each individual, perturb n times in SA.
2. From every result at 1., select top m individuals from self-process, and pick out m sets of parameters from the individuals.
3. Send the m sets of parameters to partner-process P_b .
4. Assign m sets of parameters received from P_b to m individuals in P_a .
5. Update perturbation count; $n \leftarrow \gamma \cdot n$ (γ : declining rate $0 < \gamma < 1$).

In this paper, the upper limb optimization process optimizes rhythmic torque controller at muscles of 21-28 shown in Fig. 1, and the lower body optimization

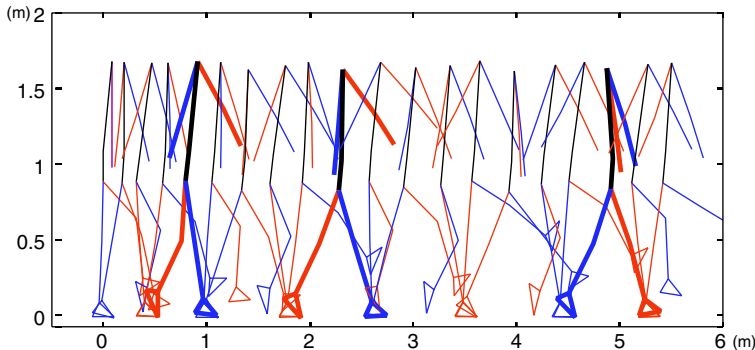


Fig. 4. Gait

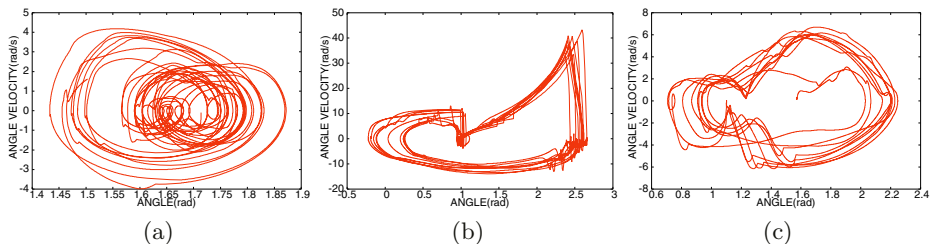


Fig. 5. Topological form: (a) trunk; (b) right foot; (c) right lower arm

process optimizes muscles of 1-20 shown in Fig. 1. For the evaluation function of walking movement for an individual, please refer to [3] because of the space limitation of this paper.

5 Generation of Walking Movement

We experiment in optimization of parameters in order to confirm the effectiveness of this method. In this experiment, simulation is conducted for 10 seconds. per a trial in SA, and the environment which robots locomote on is the flat ground. The target distance of a single walk is 15 (m) with understanding of 1.5 (m/s) which is a bit faster than 1.2 (m/s) that is walking speed of actual male adults. Parameters in parallel optimization are set as follows: the initial number of perturbation in local optimization $n = 400$, the number of individuals $m = 3$, the communication count $k = 20$ and the declining rate $\gamma = 0.9$.

We performed walking simulation using parameters optimized by our method, and the robot walked stably more than 10 seconds. Figure 4 shows a walking pattern of 4 seconds from the start of walking, and it's traced every 0.2 seconds. Figure 5 shows the topological forms of trunk, right foot and right lower arm in walking movement. Horizontal axis represents each link's angle and vertical axis represents its velocity. As walking movement proceeds, each topological form is attracted to a stable limit cycle.

6 Conclusions

Adjusting parameters in the motion control based on CPG is a very hard problem, as robot's link structure is complicated. In this paper, we proposed a parallel optimization method by two processes, which handles the control parameters of upper-limbs and legs, and communicates them each other, in optimization by SA. In order to confirm the effectiveness of the proposed method, we experimented in optimization of parameters using the robot having the upper limbs part, and generated humanoid locomotion acted by every part of the body.

References

1. Ken Endo, Fuminori Yamasaki, Takashi Maeno, and Hiroaki Kitano. Generation of optimal biped walking for humanoid robot by co-evolving morphology and controller. *PRICAI 2002, Trends in Artificial Intelligence*, pages 325–334, 2002.
2. H. Fukuoka and H. Kimura. Biologically inspired adaptive dynamic walking of a quadruped on irregular terrain. *The Robotics Society of Japan*, 21(5):1–12, 2003. (in Japanese).
3. Yoshihiko Itoh, Kenta Taki, Shohei Kato, and Hidenori Itoh. A stochastic optimization method of CPG-based motion control for humanoid locomotion. In *IEEE Conference on Robotics, Automation and Mechatronics (RAM'2004)*, pages 347–351, 2004.
4. Y. Kurita, J. Ueda, Y. Matsumoto, and Ogasawara T. CPG-based manipulation : Generation of rhythmic finger gaits from human observation. In *IEEE International Conference on Robotics and Automation*, pages 1209–1214, 2004.
5. K. Matsuoka. Sustained oscillations generated by mutually inhibiting neurons with adaption. *Biological Cybernetics*, 52:367–376, 1985.
6. K. Matsuoka. Mechanisms of frequency and pattern control in the neural rhythm generators. *Biological Cybernetics*, 56:345–353, 1987.
7. S. Shimada, T. Egami, K. Ishimura, and M. Wada. Neural control of quadruped robot for autonomous walking on soft terrain. In *6th International Symposium on Distributed Autonomous Robotic Systems*, pages 415–423, 2002.
8. G. Taga. A model of the neuro-musculo-skeletal system for human locomotion i. emergence of basic gait. *Biological Cybernetics*, 73:97–111, 1995.
9. G. Taga, Y. Yamaguchi, and H. Shimizu. Self-organized control of bipedal locomotion by neural oscillators. *Biological Cybernetics*, 65:147–159, 1991.
10. Kenta Taki, Yoshihiko Itoh, Shohei Kato, and Hidenori Itoh. Motion generation for bipedal robot using neuro-musculo-skeletal model and simulated annealing. In *IEEE Conference on Robotics, Automation and Mechatronics (RAM'2004)*, pages 699–703, 2004.

Visualizing Dynamics of the Hot Topics Using Sequence-Based Self-organizing Maps

Ken-ichi Fukui¹, Kazumi Saito², Masahiro Kimura³, and Masayuki Numao⁴

¹ Dept. of Information Science and Technology, Osaka University, Japan
fukui@ai.sanken.osaka-u.ac.jp

² NTT Communication Science Laboratories, Japan

³ Department of Electronics and Informatics, Ryukoku University, Japan

⁴ The Institute of Scientific and Industrial Research, Osaka University, Japan

Abstract. We are currently working on a SOM-based method for temporal analysis and visualization of “hot topic” trends in news articles. Hot topics are extracted from a document collection by applying PCA to term frequency bag-of-words vectors. Evaluative experiments on three data sets, the largest expands across ten years, show that SBSOM induces a sequential analysis and that the use of label confidence mitigates the performance loss.

1 Introduction

In recent years, vast amount of various documents in the WWW can be easily acquired. However, such mere amount of documents makes it difficult for users to be aware of much of their contents.

Documents that come out every day, especially news articles, can be naturally organized into topics. Furthermore, each topic can be characterized in terms of:

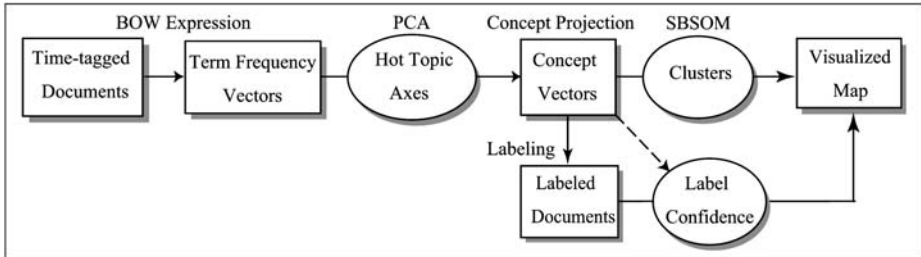
Hotness: The number of articles belonging to a topic.

Period: The duration of a topic’s existence.

Relation: Relationships that exist between topics, as well as sub-topics.

To embody these characteristics so that one can instinctively grasp them in an entire picture, it is quite effective to use time series structures such as when a particular topic appears, increases in hotness then fades away, or is placed near similar topics.

Current topic visualizing approaches do not explicitly show all of these characteristics. The Topic Detection and Tracking (TDT) approach tries to find the solution for this lack of awareness by means of detecting specific topics automatically and tracking them from past to present among large number of time series information from multimedia such as newspaper, radio and television[1]. In the TDT project using Multidimensional Scaling (MDS)[2], though relations among documents can be visualized on a map, hotness and period cannot be seen explicitly. Following the TDT study, TimeMine[3] generates familiar timelines through its interface. Although it can handle hotness and period, it does not show relations among topics since it can only deal with a single topic.

**Fig. 1.** Learning framework

Given these limitations, we concentrated on Self-Organizing Maps (SOM)[4] in order to handle all three characteristics. Although SOM provides an overview of document collection in text classification in terms of hotness and relation (e.g., WEBSOM[5]), the map does not show period because SOM does not provide the time direction. Thus, we provided a simple but effective modified definition of a winner neuron to introduce visibility of hot topics chronological order in the map. At the same time, a confidence score technique for predictive topic labels was designed to mitigate the bias toward the majority topics within neurons.

2 Learning Framework

Our learning framework is shown in Fig. 1. Initially, a Principal Component Analysis (PCA), which is based on latent topic (naive bayes) model[6], is applied to term frequency weighted Bag-of-Words document vectors[7] to extract hot topic axes, and then Concept Projection[8] is used to reduce the dimensionality of the vector space. Topic labels are derived from the concept vectors. Afterwards, SBSOM creates clusters as time series structure within a map based on documents' cosine similarity. Moreover, a confidence score is assigned to each topic label, and at the end, the map is visualized using these labels.

2.1 SBSOM

SOM is an unsupervised competitive artificial neural network learning that achieves both clustering based on similarities between input feature vectors k-means like method and visualizing the clusters within a map at the same time. We propose a Sequence-Based Self-Organizing Maps (SBSOM) which considers time series of the data by modifying the distance definition.

To introduce time, representation of input and reference vectors are extended as $\{(\mathbf{x}_n, t_n) : n = 1, \dots, N\}$ and $\{(\mathbf{m}_j, s_j) : j = 1, \dots, M\}$, respectively, where $\mathbf{x}_n = (x_{n,1}, \dots, x_{n,V})$, N is the number of input data, t_n is a time-tag, $\mathbf{m}_j = (m_{j,1}, \dots, m_{j,V})$, and s_j is a preset time corresponding to the neurons' topology. These time values are discretized into a certain period such as monthly or weekly. Neurons that are located in the same column in the map are given the same s_j

value, whose range is the same as that of t_n . The distance definition between input and reference vectors is modified as:

$$d((\mathbf{x}_n, t_n), (\mathbf{m}_j, s_j)) = \delta(t_n, s_j) \|\mathbf{x}_n - \mathbf{m}_j\| , \quad (1)$$

$$\delta(t_n, s_j) = \begin{cases} 1 & \text{if } t_n = s_j , \\ \infty & \text{otherwise .} \end{cases} \quad (2)$$

If equation (2) is defined as $\delta(t_n, s_j) = 1$ throughout a whole period, it degenerates a standard SOM. Otherwise, if $\delta(t_n, s_j)$ is defined as $\delta(t_n, s_j) \propto \|t_n - s_j\|$, it will become a loose chronological order requirement in the map. It can be said, therefore, that this modification is a natural introduction of time into SOM.

Owing to the neighborhood function that regular SOM has (in our case we used Gaussian distribution), not only are the data chronologically ordered in the map as a consequence of modifying $d((\mathbf{x}_n, t_n), (\mathbf{m}_j, s_j))$, but they are also placed horizontally near each other and thereby affected by their neighbor.

2.2 Label Confidence

Let $\theta_{n,i}$ be an angular distance between a document's concept vector \mathbf{x}_n and the i^{th} hot topic axis. A label l_n , as topic index of \mathbf{x}_n , is derived by selecting the nearest hot topic in terms of $\theta_{n,i}$:

$$l_n = \arg \min_{1 \leq i \leq V} \theta_{n,i} . \quad (3)$$

After SBSOM is trained, the documents $\{\mathbf{x}_1, \dots, \mathbf{x}_N\}$ are separated into classes $\{C_1, \dots, C_M\}$, where C_j corresponds to the j^{th} neuron. The j^{th} class (neuron) label L_j , which is representative topic of the class, is derived by selecting the dominant topic within the same class:

$$L_j = \arg \max_{1 \leq i \leq V} \#\{n : \mathbf{x}_n \in C_j, l_n = i\} , \quad (4)$$

where $\#$ represents the number of elements of a set.

Since our method adopts majority decision to select class label of each neuron, majority topic has the overwhelming advantage to be selected. Some topics which originally appear but minority may disappear due to this reason. This problem may be attributed to predictive labeling and the equivalent treatment made by majority decision on documents when class label of neuron is selected. Therefore, in order to mitigate this problem, we propose the idea of label confidence by weighting the topic labels.

The label for the following documents must have low confidence since there is a high possibility that they are mislabeled and should not be trusted. This implies that documents whose tendencies are opposite must have high confidence.

1. A document containing small number of words that its vector is near to the axes origin.
2. A multi-topic document whose vector is near the boundary of the topics.

Implying above tendency, the definition of label confidence is as follows.

$$Conf(\mathbf{x}_n) = \frac{|x_{n,T}| (\theta_{boundary} - \theta_{n,T})}{\sum_{n=1}^N |x_{n,T}| (\theta_{boundary} - \theta_{n,T})} N , \quad (5)$$

where $\theta_{boundary} = \arccos(1/\sqrt{V})$ and $T = l_n$. Clearly, $\sum_{n=1}^N Conf(\mathbf{x}_n)$ is equal to N , and that this definition implies relative confidence.

Using label confidence, the way of selecting neuron label is extended as follows:

$$L_j' = \arg \max_{1 \leq i \leq V} \sum_{\{\mathbf{x}_n \in C_j, l_n = i\}} Conf(\mathbf{x}_n) . \quad (6)$$

This represents selecting the class by which the sum of label confidence is maximum within the same neuron.

2.3 Extension of MiP

MiP(Micro Averaged Precision)[9], which quantitatively measures the classification performance of SOM, is also extended as label confidence is introduced.

MiP evaluates correctness of neuron label as the dominant class in each C_j as the j^{th} neuron's class label. Assuming that y_n is the neuron label of the document \mathbf{x}_n , then standard MiP is defined as follows:

$$MiP = \frac{\sum_j \#\{n : \mathbf{x}_n \in C_j, l_n = L_j\}}{N} . \quad (7)$$

MiP is extended by using label confidence as follows.

$$MiP' = \frac{\sum_j \sum_{\{\mathbf{x}_n \in C_j, l_n = L_j'\}} Conf(\mathbf{x}_n)}{N} . \quad (8)$$

That is, use sum of confidence instead of counting the number of documents corresponding to neuron label. Note that these methods with label confidence naturally extend MiP and selection of class label because they give the same result as the standard way when all label confidence are set to 1.0.

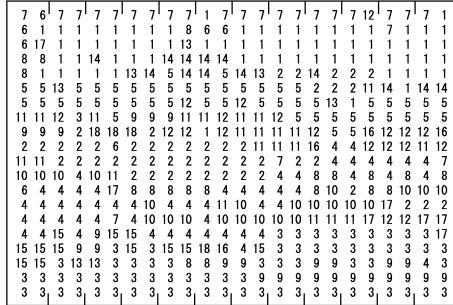
3 Experiment

Two kinds of real world news articles dataset are used for experiments. One is the international news category of the famous Japanese newspaper “Mainichi”, and the other is TDT2 corpus[10] that is used in the TDT project containing New York Times, CNN Headline News, ABC World News Tonight, and so on. These articles were collected from 1993 to 2002 (76,765 articles with 72,155 different words), and 1998 (articles:54,040, words:113,898), respectively. Particularly, “Mainichi” in 1993 (articles:5,824, words:24,661) is dealt in detail in the experimentation. The number of neurons is set to 24×20 . We have carried out initial experiments that validate SBSOM’s ability to embody the three characteristics as compared with SOM, as well as the efficiency of label confidence in terms of MiP score.

map (a) : generated by SOM

| | | | | | | | | | | | | | | | | | | | | | | | |
|----|----|----|----|----|----|----|----|----|----|----|----|----|----|----|----|----|----|----|----|----|----|----|---|
| 3 | 3 | 14 | 9 | 9 | 9 | 9 | 9 | 9 | 9 | 9 | 5 | 5 | 5 | 5 | 15 | 16 | 4 | 12 | 16 | 16 | 15 | 4 | |
| 3 | 3 | 2 | 3 | 9 | 9 | 9 | 9 | 9 | 9 | 9 | 5 | 5 | 5 | 5 | 5 | 16 | 12 | 12 | 12 | 15 | 4 | 4 | |
| 18 | 2 | 17 | 17 | 3 | 9 | 9 | 9 | 3 | 5 | 5 | 5 | 5 | 5 | 5 | 14 | 12 | 12 | 15 | 15 | 4 | 4 | 4 | |
| 18 | 2 | 17 | 17 | 5 | 3 | 3 | 14 | 11 | 14 | 5 | 5 | 5 | 5 | 5 | 14 | 16 | 12 | 15 | 15 | 15 | 4 | 4 | |
| 2 | 12 | 17 | 1 | 1 | 1 | 14 | 14 | 1 | 1 | 13 | 5 | 5 | 5 | 5 | 13 | 13 | 3 | 3 | 15 | 15 | 4 | 4 | |
| 2 | 1 | 1 | 1 | 14 | 14 | 1 | 14 | 1 | 1 | 13 | 13 | 13 | 13 | 13 | 13 | 13 | 3 | 3 | 3 | 3 | 3 | 3 | |
| 2 | 2 | 1 | 1 | 14 | 14 | 1 | 8 | 1 | 1 | 1 | 1 | 1 | 13 | 13 | 13 | 13 | 13 | 3 | 3 | 3 | 3 | 3 | 3 |
| 2 | 14 | 1 | 14 | 1 | 1 | 1 | 8 | 8 | 1 | 1 | 1 | 1 | 18 | 1 | 1 | 13 | 13 | 8 | 8 | 3 | 3 | 3 | 3 |
| 14 | 14 | 1 | 1 | 1 | 1 | 1 | 1 | 1 | 1 | 1 | 1 | 1 | 16 | 16 | 6 | 6 | 6 | 8 | 3 | 3 | 3 | 3 | 3 |
| 2 | 14 | 14 | 1 | 1 | 1 | 1 | 1 | 1 | 1 | 1 | 1 | 1 | 18 | 16 | 6 | 6 | 6 | 8 | 3 | 3 | 3 | 3 | 3 |
| 2 | 8 | 8 | 1 | 1 | 1 | 1 | 8 | 1 | 1 | 1 | 1 | 1 | 18 | 12 | 12 | 1 | 1 | 6 | 3 | 3 | 3 | 3 | 3 |
| 2 | 8 | 6 | 17 | 10 | 8 | 7 | 6 | 6 | 6 | 6 | 1 | 1 | 6 | 12 | 12 | 1 | 1 | 17 | 17 | 3 | 3 | 3 | 3 |
| 10 | 19 | 17 | 10 | 17 | 7 | 7 | 6 | 6 | 6 | 6 | 7 | 7 | 7 | 12 | 12 | 11 | 7 | 17 | 17 | 7 | 3 | 3 | 3 |
| 10 | 10 | 10 | 6 | 8 | 8 | 8 | 6 | 6 | 6 | 7 | 7 | 7 | 7 | 12 | 12 | 11 | 7 | 17 | 17 | 11 | 3 | 3 | 3 |
| 10 | 10 | 10 | 6 | 8 | 8 | 8 | 8 | 6 | 6 | 7 | 7 | 7 | 7 | 7 | 12 | 11 | 11 | 11 | 11 | 11 | 11 | 11 | |
| 10 | 10 | 10 | 4 | 8 | 8 | 8 | 8 | 6 | 6 | 7 | 7 | 7 | 7 | 7 | 11 | 11 | 7 | 11 | 10 | 11 | 11 | 11 | |
| 10 | 10 | 4 | 4 | 8 | 8 | 17 | 6 | 4 | 7 | 7 | 2 | 2 | 2 | 2 | 2 | 2 | 2 | 2 | 11 | 11 | 11 | 11 | |
| 10 | 10 | 4 | 4 | 4 | 4 | 4 | 4 | 4 | 4 | 7 | 2 | 2 | 2 | 2 | 2 | 2 | 2 | 2 | 2 | 11 | 11 | 11 | |
| 10 | 4 | 4 | 4 | 4 | 4 | 4 | 4 | 4 | 4 | 8 | 2 | 2 | 2 | 2 | 2 | 2 | 2 | 2 | 2 | 2 | 11 | 11 | |

map (b) : generated by SBSOM

**Fig. 2.** Maps of the international news category of "Mainichi" in 1993. In map (b), the horizontal axis indicates the time in monthly scale**Table 1.** Manual annotations of top 3 hot topics. Parenthesized values indicate the number of articles

| No. | Hot Topics |
|---------|--|
| 1 (721) | Circumstances in China -Economic circumstance -A change of government |
| 2 (471) | Cambodian general election -Tracking from Cambodian general election to establishment of the coalition government |
| 3 (453) | Circumstances in Russia -Opposing President Yeltsin and the national assembly -Creating a new constitution |

3.1 Results and Evaluation

Our system ran on WindowsXP with 3.6GHz Pentium4 and 2GB memory. For this particular experiment, SBSOM only took 36 sec while SOM took 286 sec. Fig.2 shows the SOM- and SBSOM-generated maps using the 1993 international news category of "Mainichi". Each number represents one hot topic. Table 1 lists the top 3 hot topics annotated manually and ranked by the number of articles corresponding to each topic.

Hotness: Hotness is shown by the number of neurons corresponding to it in both maps. From SBSOM, the number of same topics in vertical line indicates hotness at a certain month, meanwhile SOM shows it for the whole year. Furthermore, since number of each topic tends to be similar in both maps, it can be considered that SBSOM preserves that property of SOM that the hotter topic occupies the larger area within the map.

Period: Contrary to map (a) where the period of the topic definitely cannot be seen, map (b) shows a period as a horizontally continuous interval containing the same topic. The issue on "Cambodian general election" (No.2) that persists throughout the year gives a clear example. In map (b), this topic's

Table 2. MiP' score(%) (average of ten times). LC: Label Confidence

| | M'93 | M'93-'02 | T'98 |
|----------|------|----------|------|
| SOM | 73.8 | 82.2 | 72.6 |
| SBSOM | 55.3 | 70.6 | 59.2 |
| SBSOM+LC | 74.4 | 95.4 | 70.7 |

hot period can be seen as expanding from April to September. Historically, the general election was held on May 23rd and the new kingdom constitution was proclaimed on September 24th. Thereby, instinctive understanding of map (b) matches this fact.

Relation: Both maps show relation among topics as similar topics are next to each other. For instance, topic No.4 and No.10 refer to the same topic "Bosnia conflict problem" but has different subtopics appearing next to each other in both maps. Therefore, SBSOM preserves that property of SOM that similar topic which contains similar words frequency is placed near within the map. However, it may be the case that topics next to each other are not similar when viewed in human understanding. It depends on the relations among topics and on what topics were extracted by PCA.

Classification Performance: Using three kinds of dataset, we evaluated the efficiency of label confidence as shown in Table 2. Since MiP' becomes MiP when all confidence are set to 1.0, MiP can be compared with MiP' . Since we do not have the true topic label for each document, the predicted topic label is used as the true topic to evaluate the performance of SBSOM and label confidence. In all three datasets, comparing SBSOM with and without label confidence, MiP' value was improved by about 10 to 20%. Due to chronological order requirement by means of equation (2) in SBSOM, the degree of alignment freedom decreases from two to one dimension. Thus, comparing SOM to SBSOM, MiP' value decrease around 15%. However, label confidence makes up for this loss. Clearly, SBSOM is a trade-off between visibility of chronological order and classification performance.

4 Related Work

The regular SOM, by nature, is limited to capturing and classifying temporal information. Therefore, many extensions to introducing time into SOM have been proposed(as surveyed by [11]). For example, Spatio-Temporal SOM[12] modifies winner neuron's definition as the regular spatial distance plus the temporal enhancement. This deals with time by balancing spatial similarity and temporal enhancement. Meanwihle, SBSOM checks first the time-tag and then classifies based on regular spatial similarity. In terms of documents, since time axis should be shown clearly, SBSOM absolutely operates with time sequencing.

5 Conclusion and Future Works

In this paper, we discussed Sequence-Based Self-Organizing Maps (SBSOM) and a confidence scoring technique. SBSOM integrates visibility of hot topics chronological order into SOM within a map. It is considered that this visibility helps users' understanding, and effectively contributes to the foundation of visualizing large number of time series data. Though SBSOM is a trade-off between visibility of chronological order and classification performance, the use of label confidence can mitigate performance loss.

As for the immediate problems, firstly, label confidence was used only after learning. However, it is also natural for the label confidence to be introduced into the learning procedure. It may be semi-supervised learning, and will improve classification performance. Secondly, since labels used in this work are predictive, in order to evaluate performance of SBSOM and label confidence correctly, it is necessary to compare with results from manually assigning topic labels as true topics.

References

1. Frey, D., Gupta, R., Khandelwal, V., Lavrenko, V., Leuski, A., Allan, J.: Monitoring the news: a tdt demonstration system. In: Proc. of the First International Conference on Human Language Technology Research. (2001)
2. Kruskal, J.B., Wish, M.: Multidimensional scaling. Number 07-011 in Paper Series on Quantitative Applications in the Social Sciences (1978)
3. Swan, R., Allan, J.: Automatic generation of overview timelines. In: SIGIR-2000. (2000)
4. Saito, K., Ishikawa, M.: Effects of document similarity definitions on classification performance of self-organizing maps. Technical report, Technical report of IEICE (2003)
5. Kaski, S., Honkela, T., Lagus, K., Kohonen, T.: Websom – self-organizing maps of document collections. Neurocomputing **21** (1998) 101–117
6. Kimura, M., Saito, K., Ueda, N.: Extracting hot topics from the web. In: SIG-KBS-A401-21. (2004) 151–158
7. Seo, Y., Sycara, K.: Text clustering for topic detection. Technical report, Robotics Institute, Carnegie Mellon University (2004)
8. Sasaki, M., Kita, K.: Vector space information retrieval using concept projection. In: the Proceeding of the 19th International Conference on Computer Processing of Oriental Languages. (2001) 73–76
9. Slonim, N., Friedman, N., Tishby, N.: Unsupervised document classification using sequential information maximization. In: Proc. of SIGIR. (2002) 129–136
10. Allan, J., Carbonell, J., Doddington, G., Yamron, J., Yang, Y.: Topic detection and tracking pilot study: Final report. In: Proc. DARPA Broadcast News Transcription and Understanding Workshop. (1998)
11. Barreto, G., Arajo, A.: Time in self-organizing maps: An overview of models. International journal of Computer Research, Special Issue on Neural Networks **10(2)** (2001) 139–179
12. Euliano, N., Principe, J.: Spatio-temporal self-organizing feature maps. Neural Networks **4** (1996) 1900–1905

Intelligent Consumer Purchase Intention Prediction System for Green Products

Rajiv Khosla¹, Clare D’Souza¹, and Mehdi Taghian²

¹ La Trobe University, Victoria 3086, Australia

{R.Khosla, cdsouza}@latrobe.edu.au

² Deakin Business School, Victoria 3000, Australia

mtaghian@deakin.edu.au

Abstract. In this paper the authors model green behaviour by predicting consumers’ purchase intention using Kohonen’s LVQ technique. It is envisaged that such a model may facilitate better understanding of green consumers’ market segments. The model employs cognitive, affective, and situational attributes of consumers to predict their purchase intention. The model can, potentially, provide a more direct method for companies to gauge consumers’ intention to purchase green products. The results indicate that consumers are more strongly resistant to lower quality than higher prices of green products in comparison to other alternative non-green products.

1 Introduction

The publicity given to the Kyoto protocol and the increasing greenhouse emissions reported in the mass media in recent times have altered consumers’ awareness of environmental issues and the further realisation that consumer consumptions contributes to environmental degradation. Manufacturers, motivated by the achievement of their organisational objectives, have instigated the development of and modification of some production processes and have introduced new products that may be classified as green products, products potentially less harmful to the environment. However, at present, it is difficult for businesses to predict consumers’ reaction to their green products with a degree of accuracy necessary to enable proper new products development strategy. In this paper we describe the design of a soft computing model using Kohonen’s LVQ technique [1,2] for predicting the consumers’ purchase intention of green products.

2 Background Related to Environmental Marketing Research

There is evidence to suggest that that consumers are price and quality sensitive when it comes to "buying green" [3]. Other researchers have attempted to identify green consumers profiles with an intention to characterise green market segments using demographic variables [4, 5, 6, 7] and they have been able to categorize them as being young, well-educated, and affluent urban dwellers [8]. In comparison, [9] found that although green consumers were younger and more highly educated, their green attitude was not income related. Other studies have indicated that environmental concern and behaviour were stronger for persons above 50 years of age [10, 11, 12, 13]. At the same time, price sensitivity appears to be a factor that is more directly related to income or the established purchase pattern associated with older age groups. Price and

quality variations combined may provide the consumer a chance of exercising trade offs for a purchase decision. In order to explain the impact of price and quality on consumers' green demand this study attempts to combine those factors with the demographic profiles of consumers forming distinct clusters or market segments.

3 Designing Predictors of Environmental Profile Analysis

Environmental behaviour-related variables can be categorized into cognitive, affective, and situational factors [14]. Cognitive factors refer to the awareness level an individual has about objects and are related to knowledge of environment including actions and skills. The affective factors concern the feelings or emotions associated with the objects and are generally defined by attitude, locus of control and the expression of personal responsibility. Situational factors are environmental elements such as economic constraints, social pressures, and opportunities to choose different actions. These factors can either counteract or strengthen the cognitive and affective factors.

4 Kohonen's LVQ Technique

In this section, we describe aspects related to Kohonen's LVQ behaviour prediction agent, used for learning and predicting the fuzzy behavioural categories. Kohonen's self-organizing maps are characterized by a drive to model the self-organizing and adaptive learning features of the brain. The learning algorithm organizes the nodes in the two-dimensional grid into local neighbourhoods or clusters which act as feature classifiers on the input data. The advantage of developing neighbourhoods is that vectors that are close spatially to the training values will still be classified correctly even though the network has not seen them before, thus providing for generalization.

Since Kohonen's network is an unsupervised self-organising learning paradigm, Kohonen also introduced a supervised learning technique called Learning Vector Quantisation (LVQ). LVQ method is very useful because it amounts to a method for fine-tuning a trained feature map to optimise its performance in altering circumstances. The basic feature of LVQ method is that we can add new training vectors at typical situations to improve the performance of individual neighbourhoods within the map. This can be achieved by selecting training vector (x) with known classification, and presenting them to the network to examine cases of misclassification. Again a best match comparison is performed at each node and the winner is noted (n_w) [15].

The LVQ prediction model used in this work is based on the need to develop an incremental learning model of green purchase based on price and quality.

In order to develop a predictive model we need to determine green consumer cluster groups related to purchase intention. These cluster groups then will become the dependent variable to be predicted by the LVQ technique. In the rest of this section, we firstly describe the identification of purchase intention cluster groups and then follow it up with the design and implementation of the prediction model.

4.1 Learning Green Consumer Cluster Groups

The purchase intention of green consumers is broken down into two dimensions or attributes, namely, price and quality of the green products. The price and quality di-

mensions are assumed to be influenced by cognitive, affective and customer characteristic variables, such as beliefs, attitudes, and demographic variables respectively. In all 20 variables or data points (under the above three categories) were used to cluster green consumer groups as follows:

4.2 Cognitive (Beliefs on Environment) Variables

THERE ARE A LOT OF EXAGGERATIONS ABOUT COMPANIES TAKING ENVIRONMENTAL RISKS NOWADAYS

I BELIEVE THE GOVERNMENT IS DOING ALL THAT IS POSSIBLE TO SAFEGUARD THE ENVIRONMENT

WE SHOULD NOT SLOW DOWN INDUSTRY PROGRESS BECAUSE OF CONCERN FOR THE ENVIRONMENT

ENVIRONMENTAL SAFETY IS THE RESPONSIBILITY OF THE GOVERNMENT, NOT INDIVIDUAL CITIZENS

I BELIEVE THAT GOVERNMENT LEGISLATION ADEQUATELY REGULATES ENVIRONMENTAL PROTECTION

4.3 Affective (Attitudes on Brands and Companies) Variables

I BELIEVE A WELL KNOWN BRAND IS ALWAYS A SAFE PRODUCT TO BUY
THE QUALITY OF ENVIRONMENTALLY SAFE PRODUCTS ARE NOT AS GOOD AS OTHER PRODUCTS

THE PRICE OF ENVIRONMENTALLY SAFE PRODUCTS ARE USUALLY MORE EXPENSIVE THAN OTHER PRODUCTS

I BELIEVE AUSTRALIAN COMPANIES ARE GENERALLY DOING A GOOD JOB IN HELPING TO PROTECT THE ENVIRONMENT

I BELIEVE COMPANIES SHOULD PLACE HIGHER PRIORITY ON REDUCING POLLUTION THAN ON INCREASING THEIR OWN PROFITABILITY

I BELIEVE COMPANIES SHOULD PLACE HIGHER PRIORITY ON REDUCING POLLUTION THAN ON INCREASING PROFITABILITY EVEN IF JOBS ARE AT RISK

Situational Factors (Price and Quality) on Green Products

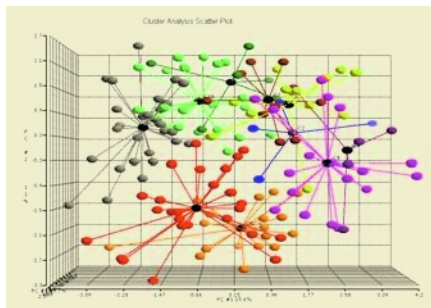
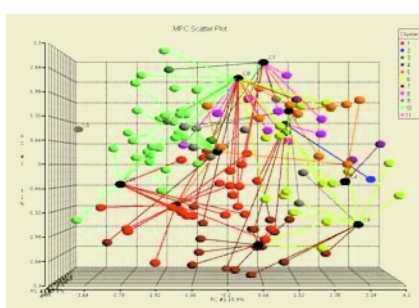
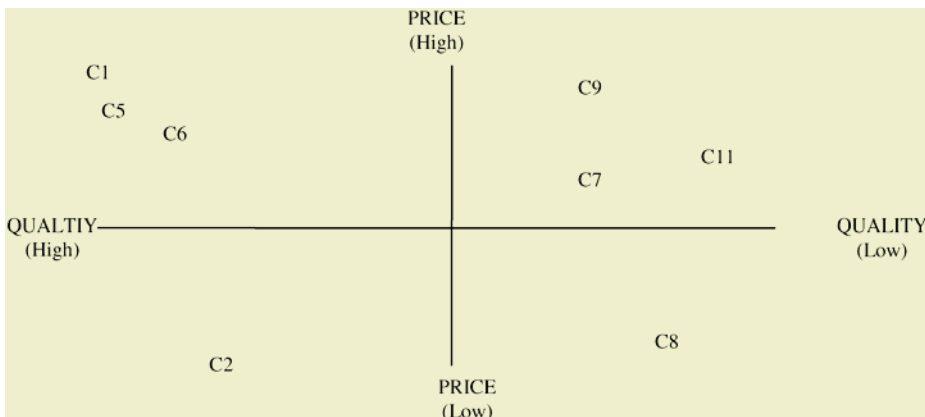
I PREFER TO PURCHASE AN ENVIRONMENTALLY SAFE PRODUCT EVEN IF IT IS SOMEWHAT MORE EXPENSIVE

I PREFER TO PURCHASE AN ENVIRONMENTALLY SAFE PRODUCT EVEN IF IT IS SOMEWHAT LOWER IN QUALITY

In the rest of the paper we will describe the design of a soft computing model using Kohonen's LVQ technique for predicting the purchase intention of green consumers of green products.

Figure 1 shows a sample of the consumer behavioural patterns used as data set for learning the fuzzy behavioural categories/clusters towards price and quality. Initially ten clusters were obtained for price and 17 clusters obtained for quality. It was found that consumers were more densely clustered on the quality dimension of the product than on price, indicating stronger resistance to lower quality and relatively more relaxed in terms of higher prices.

Figure 2 shows the clusters based on cognitive, affective, customer characteristics and price/quality variables. Thus Figure 1 shows 11 price/quality based clusters. Of these 10 price based clusters are distinct green customer groups whose purchase intentions are influenced by different beliefs, attitudes and demographic characteristics.

**Fig. 1.** Price cluster analysis**Fig. 2.** Price/quality cluster analysis**Fig. 3.** Purchase Intention Clusters and Two-dimensional Price-Quality Model

Eight of the 11 clusters shown in Figure 2 are plotted on a two dimensional price and quality model in Figure 3.

A sample data set used for developing the LVQ based predictive model is shown in Table 1. As can be seen we have used only 8 out of the 11 purchase intention categories (based on 11 price and quality clusters identified in the preceding section). The three cluster categories, 3, 4 and 10 not included in Table 1 and in Figure 3 form the outliers of the two-dimensional price and quality model shown in Figure 3.

Table 1. LVQ based predictive model

| Categories | # per Class | # Correct | # Error | % Correct | % Error | Std Error |
|------------|-------------|-----------|---------|-----------|---------|-----------|
| 1 | 26 | 26 | 0 | 100.0 | 0.0 | 0.0 |
| 5 | 11 | 10 | 1 | 90.9 | 9.19 | 8.7 |
| 6 | 17 | 16 | 1 | 94.1 | 5.9 | 7.1 |
| 7 | 19 | 18 | 1 | 94.7 | 5.3 | 5.1 |
| 8 | 11 | 11 | 0 | 100.0 | 0.0 | 0.0 |
| 9 | 3 | 1 | 2 | 33.3 | 66.7 | 10.5 |
| 11 | 1 | 1 | 0 | 100.0 | 0.0 | 4.9 |
| Total | 88 | 83 | 5 | 94.3 | 5.7 | 2.4 |

In order to establish the prediction accuracy of the Kohonen's LVQ model we have used the cross validation technique for estimating generalization error based on "resampling" [16]. It shows a total accuracy of 94.32 percent.

5 Managerial Implications

It is being suggested that there appears to be a fundamental expectation existing on the part of the customer about green products. From the cluster analysis it can be explained that consumer attitude appears to be that they will be less likely to compromise on product quality than on somewhat higher prices of green products. Therefore, with green products, quality appears to be more essential to consumers than price. This, arguably, may mean two things: (1) manufacturers may produce higher quality green products and use the premium pricing strategy commensurate with the higher costs of production or (2) they may compete in the market place offering comparable quality standards at the competitive price categories in the market. The second option may require investment in refining production processes and employing technology more effectively to create lower cost-based production processes.

It can be seen that buying intent is also associated with customer's characteristics. Consumer demographics play a role in cluster analysis. In essence, to target these markets effectively, managers should consider segmenting the market based on consumer's green demographic profile. Further research could look at these issues

For those companies that intend to use the green product offering as a competitive advantage, it is fundamental to segment their markets based on the three combined dimensions of price/quality/demographic characteristics and be able to quantify each segment for their attractiveness and purchase readiness.

6 Conclusions

In summary, the understanding of the green products perception formation, potentially, has a number of applications. The analysis provides the motivations for management to (1) to build a strong competitive advantage for the product in terms of quality and price (2) to develop and project a profile of green consumer based on demographics (3) to meet customers' expectations by being seen as socially responsible and potentially improve market share and achieve longer term profit.

References

1. Khosla, R., Damiani, E. and Grosky,W.: Human-Centered E-Business, Kluwer Academic Publishers Massachusetts USA (2003)
2. Kohonen, T., Self Organization and Associative Memory, Springer-Verlag, 1990.
3. Mandese, J. ' New study finds green confusion'. *Advertising Age* 1991; 62(45): 1- 56.
4. McKenzie, D. 'The rise of the green consumer'. *Consumer Policy Review*, (1991), 1 (2), 68-75
5. Roberts, J. 'Green consumers in the 1990s: Profile and implications for advertising,' *Journal of Business Research*, (1996). 36 (2), 217-231
6. Titterington, A., Davies, C., & Cochrane, A. 'Forty shades of green: A classification of green consumerism in Northern Ireland'. *Journal of Euro-Marketing*, (1996), 5(3), 43-55

7. Brown, Joseph & Wahlers, Russell. 'The environmentally concerned consumer: An exploratory study', 1998, *Journal of Marketing Theory and Practice*;1998, 6 (2), 39-47
8. Arbuthnot, J. 'The roles of attitudinal and personality variables in the prediction of environmental behavior and knowledge'. *Environment and Behavior*, 1977, 9, 217-232
9. Jolibert, A & Baumgartner, G. 'Toward a definition of the consumerist segment in France'. *Journal of Consumer Research*, 1981 June, 114-117
10. Gallup, G. Jr., & Newport, F. 'Americans strongly in tune with the purpose of Earth Day 1990'. *Gallup Poll Monthly* 295), (1990, April). pp. 5-14
11. Kohut, A., & Shriver, J. 'Environment regaining a foothold on the national agenda'. *Gallup Report.*, (1989). 285, 2-12.
12. Lansana, F. M. 'Distinguishing potential recyclers from non-recyclers: A basis for developing recycling strategies' *The Journal of Environmental Education*, (1992), 23, 16-23.
13. Vining, J., & Ebrey, A. 'What makes a recycler? A comparison of recyclers and non-recyclers. *Environment and Behavior*', (1990), 22, 55-73.
14. Hines, J. M., Hungerford, H. R.. and Tomera, A. N. "Analysis and Synthesis of Research on Responsible Environmental Behavior: A Meta-Analysis". *The Journal of Environmental Education*. 1986, 18 (2), 1-8.
15. (Beale & Jackson, 1990,p122)
16. Efron, B. and Tibshirani, R.: Improvements on Cross-Validation: The .632+ Bootstrap Method, *Journal of the American Stat. Assoc.* vol. 92 (1997) 548-568

Reverse-Query Mechanism for Contents Delivery Management in Distributed Agent Network

Yoshikatsu Fujita¹, Jun Yoshida¹, and Kazuhiko Tsuda²

¹ Matsushita Electric Industrial Co., Ltd., Corporate eNet Business Division
2-13-10, Kyobashi, Chuo-ku, Tokyo 104-0031, Japan
[fujita.yoshikatsu,yoshida.jun}@jp.panasonic.com](mailto:{fujita.yoshikatsu,yoshida.jun}@jp.panasonic.com)
<http://home.hi-ho.ne.jp/>

² Graduate School of Business Sciences, University of Tsukuba, Tokyo
3-29-1, Otsuka, Bunkyo-ku, Tokyo 112-0012, Japan
tsuda@gssm.tsukuba.ac.jp
<http://www.gssm.tsukuba.ac.jp>

Abstract. We propose quasi-broadcast platform for contents delivery by using reverse-query mechanism on P2P network. This platform is built on percolation theory to propagate the message and contents, which each agent on P2P client relays reverse-query to randomly selected peers. This mechanism can reduce the search traffic explosion by P2P client. For business application, this platform can be applied to flyer delivery over the Internet targeting common attributes such as residential area.

1 Introduction

There has been a rapid growth in broadband contents delivery demands over the Internet. In Japan, more than 20 million users are enjoying broadband connectivity at their home. This leads to prevalence of numerous broadband contents over the Internet.

On the other hand, client systems such as PDA, PVR, STB obtain richer and richer resources to digest broadband contents. In Japan, the dawn of server-based broadcasting, led by the Japanese standardization body ARIB(Association of Radio Industries and Businesses)[1] is just around the corner.

However, this does not necessarily mean that we can enjoy any rich contents whenever we want, because we don't have enough "big pipe" which passes over explosive traffic between servers and clients. This is so-called "Middle-mile Problem."

In order to solve this problem, CDN becomes popular NW solution for contents delivery over the Internet. To achieve high levels of performance, reliability and to reduce the connectivity cost, CDN can be regarded as a part of infrastructure in today's Internet. In order to balance the request load, several techniques are developed such as, CDN peering, distributed cache. However, those technical efforts do not lead to prevalence of CDN services in Japan, because CDN solutions can not earn enough profit compared with their expensive investment and operation costs

Meanwhile, P2P systems get more attention to exchange some files or even streams over the Internet. Although illegal P2P file exchange activities are prohibited by copyrights protection law, pirated contents traffic flows are abundant in the Inter-

net. P2P software is regarded as “enemy” for contents holders. For example, the author of the most popular Japanese P2P client “Winny” had fell into suit, being accused of assisted copyright infringement. And unmanaged search traffic from P2P clients waste bandwidth that results in delay or slow response of mail and homepage browsing transactions. It is clear that new network architecture that can manage this problem is desired.

In this paper, we propose new idea applying Power-law characteristics that P2P network hold in nature, and by simply submitting reverse-query messages to designated peers which forms “Distributed Agent Network” sharing common characteristics, results in inexpensive quasi-broadcasting delivery backbone.

2 Related Work

2.1 CDN and P2P

CDN and P2P network is current major solutions for contents delivery over the Internet.

There can be several ways to determine the delivery route from servers that stores contents. Resources could be measured by client request latency, total network bandwidth consumption, or an overall cost function if each link is associated with cost. Some examples of criteria are: RTT between client and server, AS path length, available CPU time, available memory, and so on [4].

There is the other approach to study for replication server placement over the Internet. Akamai employs distributed algorithm based on hash table, and Harvest project studied to place cache servers hierarchically [5].

However, CDN solutions have to maintain a huge amount of servers to support the simultaneous accesses, which results in going against cost-effectiveness.

P2P network is emerging new idea for file exchange over the Internet. There are two main architectures for P2P network [9].

- Pure P2P: any single, arbitrary chosen Terminal Entity can be removed from the network without having the network suffering any loss of network service
- Hybrid P2P: a centered entity is necessary to provide parts of the offered network services

In order to find the best peer who holds the requested contents, central server search the peer in pure P2P, while distributed hash-table (DHT) interface helps to find the network location of the node currently responsible for the given request from whole network. However, DHT needs whole hash space be shared, and problem is, that every peer is required to take over its hash space or to reassign its hash space when it joins / leaves to the network.

2.2 Power-Law Network

A large number of networks, including World Wide Web, the Internet, their degree distribution has a power-law tail [3]. In a power-law degree distribution, a probability $P(k)$ which represents the number of outdegree from a node to be k , is given by

$P(k) \sim k^{-\tau}$, where $\tau > 0$ [6]. This distribution is called Scale-free Network be-

cause the variance is very high. When we look into broadband contents delivery, same power-law distribution can be observed to the number of links between nodes. (This is explained further in 4.1.)

2.3 Search Algorithm and Percolation Theory

The cost of query traffic is another problem for P2P contents delivery. When we suppose unstructured P2P network, such as Gnutella, KaZaA, which each peer has no global status information, that one peer has to release a query for designated content to other peer and the query will be handed over to other peer until it finds the designated content, or use up the TTL. With such naïve parallel search algorithm in P2P network, the traffic can be simply led to $O(N)$ for every single query. Here, we call this search as “do-you-have” query, because the query means “do you have what I want?” For example, when millions of TV sets begins to release such queries over the Internet, there can be flood of tremendous “do-you-have” queries. This method is regarded as highly bandwidth wasting solution.

Local search strategies in power-law graphs have search costs that scale sublinearly with the size of the graph, a fact that makes them very appealing when dealing with large networks. The most favorable scaling was obtained by using strategies that preferentially utilize the high connectivity nodes in these power-law networks [2].

In order to propagate the query message that one release to all over the network, the transition can be analyzed by applying percolation theory [10]. There is a study for scalable search algorithm that uses random-walks and percolation on random graphs with heavy-tailed degree distributions, to provide access to any contents on any node with probability one [8].

2.4 Our Methodology

Our algorithm gives new solution for this traffic explosion problem. By applying percolation theory for transmitting query message, which we call “reverse-query,” we can deliver query (and contents) to almost every peers that shares common interests within a certain period of time. In other words, this will give inexpensive quasi-broadcast platform for contents providers who wish to deliver their contents at their own cost, such as on-line shopping channel.

We call this search as “do-you-need” query, because the query means “do you need what I have?”(Figure 1)

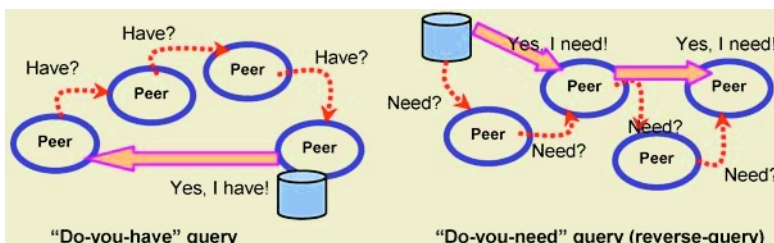


Fig. 1. “Do-you-have” query and “Do-you-need”query

3 Reverse Query Mechanism

3.1 Reverse Query Mechanism

We present here new mechanism to deliver contents from server to peer to peer by giving reverse-query messages. This is to implement targeting contents delivery under reduced distribution cost. Beforehand, we assume every peers' authentication is cleared when joining overlay network and other necessary transactions such as DRM.

Reverse-Query Mechanism

As we explained in 2.4, this is to deliver contents by relaying “do-you-need” query from server to peer to peer, and those peers who need designated contents receive them while ones who do not want are expected just to forward the message.

Figure 2 shows our fundamental idea that overlay network gives quasi-broadcasting function by relaying “do-you-need” query.

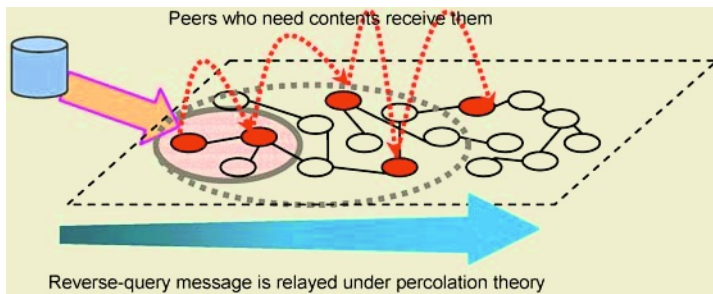


Fig. 2. Percolation on the P2P Network

3.2 Algorithm

In this study, we propose the new algorithm that propagates reverse-query message and contents by applying percolation theory to P2P network. First, let us explain the procedure.

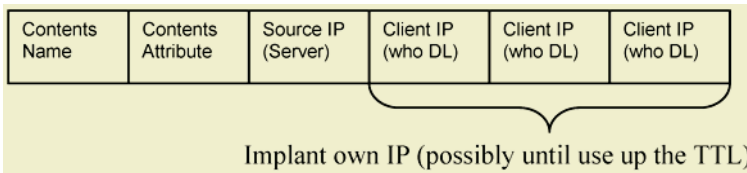
Step 1: Message Distribution

The server which holds contents to be delivered generates a “do-you-need” message and sends it to some randomly selected peers. The number of peers who get this first query is supposed to N_{init} , which will be optimized by further study.

Step 2: Site Percolation

Following the step1, the first receiver peer A compares the attribute of the contents with its own tastes, and if they match, peer A tries to pull the contents file from the initial server. Following this operation, peer A revise the “do-you-need” message to implant its own IP showing it is retrieving the contents now, and forward it to some randomly selected k neighbors (Figure 3 shows a message structure example.)

In case of peer A's favor does not match the contents attribute, peer A is expected to just forward the message to some randomly selected its k neighbors.

**Fig. 3.** Reverse-query message structure

By repeating this operation, the “do-you-need” message” covers whole peers within a certain period of time.

Step 3: Contents Extraction

Suppose peer B receives the “do-you-need” message” from peer A. Peer B compares the attribute of the contents with its own tastes as peer A in Step2, and if they match, peer B also tries to pull the contents from the previous peers listed in the relay chain. (This case, it is probably from peer A)

When we choose k to be just above the percolation threshold of underlying power law network, the message can be propagated all over the peers [8].

4 Discussion

4.1 Analysis

Suppose the number of peers in the designated P2P network is N , how long does it take to cover whole peers under the relaying probability k ?

The search cost S (number of steps until approximately the whole graph is revealed) can be estimated as [2]

$$S \sim N^{3(1-2/\tau)} \quad (1)$$

Above algorithm employs random walk through the network, to scan all its neighbors until it finds the destination file. In our reverse-query case, it is not required to find any destination file, but to propagate the message all over the network. When the relayed query reached to LCC(largest connected component), the query can be forwarded reverse path to edge peers, that can be estimated the same order of cost S .

With such analysis we can expect that within finite time period, the first released message is circulated to all the peers in P2P network. We can add some other factors as a cost, such as volume of traffic, to optimize this delivery strategy..

In Japan, an interesting trial to support above hypothesis was taken place in late 2004 [7]. It was a competition of the number of DRM clearing for a designated file. Each contestant was given a unique ID encapsulated in the WMT(Windows Media Technologies) file, and supposed to distribute the copy of file over the P2P network. From the DRM license server log, we can draw the links between contestants and the file receivers. The result of trial is shown in Figure 4. This clearly shows that there are high degree nodes and probability of our proposal to be applied.

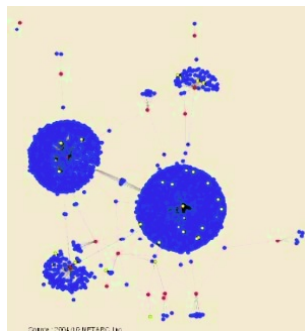


Fig. 4. Contents Delivery Trial over P2P network in Japan, Sep. 2004

4.2 Business Application

As we mentioned in 3.1, this quasi-broadcast platform can be directly applied to flyer delivery service.

Suppose our target P2P client has its own locality information, such as ZIP code or telephone code, and they join this overlay network with such area information.

Those who wish to deliver flyer to someone who lives in Melbourne area, here suppose “PizzaKES,” the quasi-broadcast network operator receives a short commercial contents from PizzaKES and throw it to the initial server according to the algorithm in 3.2. Within a certain period of time, the contents is received by all the peers in Melbourne area, which is the same effect as delivery of flyers in postbox.

5 Conclusion

In this paper, we have explored a network architecture that integrates the characteristics of P2P network and percolation theory, which forms a platform for quasi-broadcast services. It is probable that inexpensive contents delivery network can be obtained by applying our reverse-query mechanism.

We will go on further study for this mechanism, by trying some simulations, taking some other attributes such as each peers’ upload bandwidth.

References

1. ARIB: <http://www.arib.or.jp/>
2. L. Adamic, R. Lukose, A. Puniyani, and B. Huberman: “Search in power-law networks”, Phys. Rev. E 64, 046135.(2001)
3. R. Albert and A. L. Barabasi: “Statistical Mechanics of Complex Networks”, Reviews of Modern Physics, vol. 74, pp. 47-97 (2002)
4. V. Cardellini, M. Colajanni, and P.S. Yu: “DNS dispatching algorithms with state estimators for scalable Web-server clusters”, World Wide Web Journal, Baltzer Science Publ., vol. 2, no. 2, pp. 101-113 (1999)
5. A. Chankunthod and M. Schwarz: “A Hierarchical Internet Object Cache”, Technical Report 95-611, Computer Science Dep., Univ. of Southern California (1995)
6. M. Faloutsos, P. Faloutsos, and C. Faloutsos: “On power-law relationships of the Internet topology,” in Proc. ACM SIGCOMM (1999)

7. NETARC, Inc: <http://www.netarc.jp/>
8. N. Sarshar, V Roychowdhury and P. O. Boykin: "Percolation Search in Power Law Networks: Making Unstructured Peer-To-Peer Networks Scalable". IEEE P2P2004 (2004)
9. Rudiger Schollmeier: "A Definition of Peer-to-Peer Networking for the Classification of Peer-to-Peer Architectures and Applications", Proceedings of the 1st International Conference on Peer-to-Peer Computing, IEEE (2001)
10. D.Stauffer and A.Aharony: "Introduction to Percolation Theory", 2nd ed., Taylor and Francis, London (1994)

A My Page Service Realizing Method by Using Market Expectation Engine

Masayuki Kessoku¹, Masakazu Takahashi², and Kazuhiko Tsuda³

¹ Information Science and Intelligent Systems, The University of Tokushima,
2-1 Minami-Josanjima-cho, Tokushima-City, 770-8506, Japan
kessoku@aoelab.is.tokushima-u.ac.jp

² Shimane University, 1060 Nishikawatsu Matsue, Shimane 690-8504, Japan
masakazu@cis.shimane-u.ac.jp

³ Graduate School of Systems Managements, The University of Tsukuba,
3-29-1 Otsuka, Bunkyo-ku, Tokyo 112-0012, Japan
tsuda@gssm.otsuka.tsukuba.ac.jp

Abstract. This paper proposes a method to realize My Page Service using market expectation engine. There are two problems on expecting market trend using My Page; (1) difficulty of analyzing huge database that manages the enormous number of customer data and the extremely broad areas that the customers might be interested in, and (2) difficulty of grasping market trend using customer data that is stored in database. We address problem (1) with three-dimensional vectors that consists of customer, preference category and time axes. One of the problems of three-dimensional vectors is its huge volume of information. Our method addresses this problem by recording the positions and the values of the points only where the information has changed as time passes. And we address problem (2) with clustering customer preference data. Furthermore, we have found a few trend leaders in the groups. Using trend leaders data, we can expect market trend.

1 Introduction

The marketing in the Internet businesses requires the way to quickly grasp market trends and preference transitions of individual customer [1,2]. It is also required to grasp the effects of advertisements accurately and to propose the effective timing and contents of advertisements to advertisers [7-9]. In these backgrounds, Internet Service Providers (ISP) offer a service called "My Page" to provide information that may interest a specific customer. To improve the accuracy of the My Page services, ISPs need to extract information such as the market trends and the preference transitions of individual customer, and they also need to manage it accurately.

For the purpose of obtaining information about both market trends and customer preference at once, one of the effective methods is to manage customer preference information using two-dimensional vectors of customer and preference category axes. However, this two-dimensional method is not capable of keeping track of market trends and the transitions of customer preferences that change as time passes.

In this paper, we propose a method that uses three-dimensional vectors with time axis in additions to customer and preference category axes. One of the problems of the three-dimensional method is that the volume of information held in three-dimen-

sional space is huge so that it is difficult to hold detailed information. Our proposed method addresses these problems by recording the time axis information only on the points where the customer preference changes, while data on customer and preference category axes, which express the current situation of customer preference, is stored in two-dimensional vector space. Additionally we propose a method that analyzes market trend using market leaders' data that is clustered.

2 Outline of My-Page Generation System

Figure 1 shows the outline of proposed system.

At first, we explain inside of Access Point Server. Data Collection System collects customers' data when a customers use W.W.W. The Data Collection Modules collect and send the data to the Proposed system (we call it Marketing Server). The Marketing Server receives the information and manages it in the Customer Preference Database in one lump. Data Distribution System receives customers' My page data and sends customers' My Page data to customers. Keyword Database manages keywords that are received from the Marketing Server and are used for data collection[2].

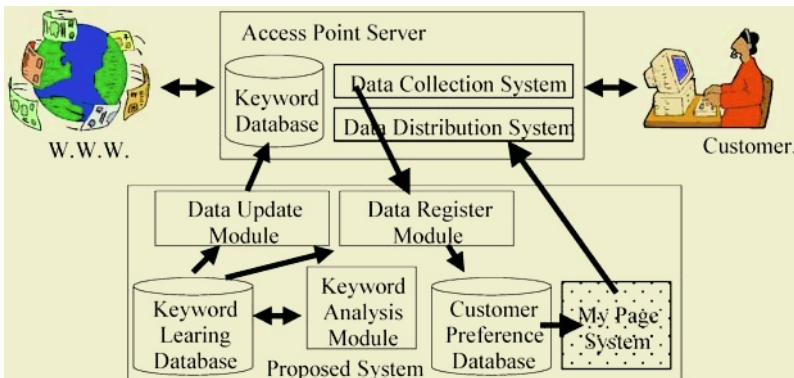


Fig. 1. Outline of relationship between www, customer and proposed system

Next, we explain the configuration of Marketing Server. (a) The Data Register Module receives keywords from the Data Collection Module and calculates the score of the Web page accessed by the customer using keywords and scores stored in the Keyword Learning Database. (b) The Keyword Learning Database stores the keywords that indicate various preference categories. The data is stored as a set of keyword strings, preference categories that the keywords are related, and scores to indicate the strength of preference. (c) The Keyword Analysis Module receives the set of keywords and calculates the customer preference score for each category. When the set of keywords contains the word strings that are not registered with the Keyword Learning Database, the Keyword Analysis Module appends the calculated scores to them and registers them with the database. (d) The Data Update Module updates the Keyword Databases in the Access Point Servers by registering the word strings data that is newly registered with the Keyword Learning Database. (e) The Customer Preference Database is composed of Customer Preference vectors, which are the two-

dimensional vectors of customer and category axes (detail of the Customer Preference Database is explained in section 3.) (f) My Page System generates customers' My Page using Customer Preference Database. Figure 2 shows detail of My Page System. The Template-page is a page used as a template for My Page generation. It contains the information to be provided to all customers, just like regular Web pages, and it also contains empty slots to provide information specific to a customer. Each slot has the tag information to indicate which information should be embedded.

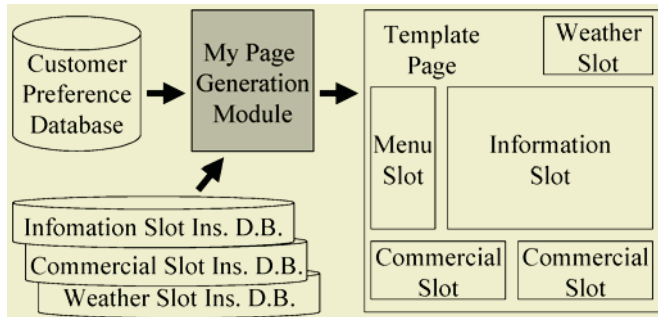


Fig. 2. Detail of My page System

3 Configuration of Customer Preference Database

This section describes configuration of Customer Preference Database that is most important system to realize the My Page Service.

3.1 Concept of Managing Customer Preference Database

Figure 3 illustrates the configuration of the Customer Preference Database and the outline of storing method for customer preferences.

At first, we calculate $S_c = \{ x_1, x_2, \dots \}$, a set of preference strength score x , at the preference strength score calculation module to keep track of the observed behavior of customer c as the customer's preference. The customer c is managed and maintained in a customer management table that has a list C of customers or customer groups as a database. Each element x of the set S_c is the preference strength score that corresponds to the preference categories management table.

Next, at the preference category plot module, we plot customer preference information $V_c = (c, S_c, t)$, where the customer c behaves at the time t with the preference strength scores S_c , on to the preference field which composed of customer, preference category, and time axes. The customer axis and the preference category axis correspond to the customer management table and the preference category management table respectively, and the time t is plotted on the time axis that is a series of unit time managed at the time management module [4].

3.2 Compression Method for Vector Space

The volume of information will be enormous in the Customer Preference Database when it is managed in three-dimensional vectors with customer, preference category,

and time axes. On the two-dimensional preference field, the customer preference information is expressed with preference vectors. For example, the current customer preference information is represented as a current preference vector $V_t = (C, S_t, t)$, and the customer preference information at one unit time past is represented as a past preference vector $V_{t-1} = (C, S_{t-1}, t-1)$.

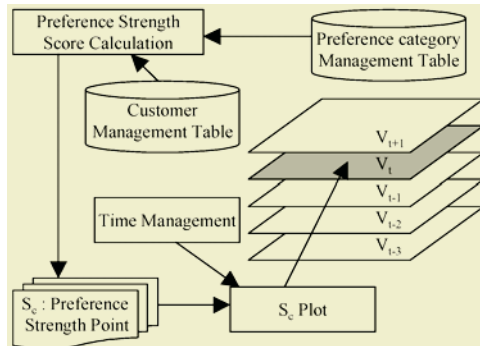


Fig. 3. Configuration of Customer Preference Database

Firstly, the preference transition extraction module compares a current preference vector V_t and a past preference vector V_{t-1} , and extracts the preference fields with different preference strength. Then the preference transition conversion module converts the extracted information into a coordinate point (c, s) on the customer and the preference category axes and a set preference strength score x_{t-1} of the past preference vector, and stores them into the preference transition storage module. In this way, the past preference vectors are stored in smaller volume. When a unit time managed in time management module passes, the current preference vector V_t in the one unit time past becomes the past preference vector. Similarly, a new customer preference strength score calculated based on the customer's behavior at the past unit time becomes a current preference vector $V_{t+1} = (C, S_{t+1}, t+1)$. By repeating this procedure, the past preference vectors at each unit time are stored in preference transition module. This method enables us to store information for the Customer Preference Data-base in small volume and without omission.

4 Application and Evaluation of Proposed Method

We developed the My Page System and apply it to test environment.

4.1 Test Environment and Condition

We have developed the My Page System and conducted a small size experiment by applying it. The experiment is conducted in the following conditions:

- Number of customers: 99 (employees and part-timers of the ISP)
- Number of categories: 538 (the contents categories defined by contents ID forum [3])
- Time period: 10 weeks (one week is considered as one cycle)

4.2 Evaluation of Experimental Result

In this section, we evaluate (1) compressibility rate of preference vector space and (2) grasping market trends using preference vector.

(1) Evaluation of Compressibility Rate

As a result of the experiment, proposed method enables us to store the past preference vector information for a unit time, which is managed in the time management module, in the size less than 5% of the preference vector space V in the preference transition conversion module (Table.1). If the data volume of Customer Preference Database becomes 5% of the capacity as resulted in the experiment, it will be possible to handle it even with a personal computer. The possible reasons are:

- (1) Each customer c is interested in only less than 10% of categories among the ones managed in the preference category table.
- (2) Only 20% of customers in maximum react to new categories that are recognized through advertisements or social phenomena.
- (3) Customers react to only 5 or 6 new categories in maximum (only 1% of total number of categories) that are recognized through advertisements or social phenomena.

Table 1. Compressibility Rate of Preference Vector Space

| Unit time | 1 | 2 | 3 | 4 | 5 | 6 | 7 | 8 | 9 | 10 |
|----------------------|-----|-----|-----|-----|-----|-----|-----|-----|-----|-----|
| Compressibility Rate | 1.4 | 4.7 | 4.6 | 3.3 | 3.0 | 2.2 | 2.8 | 1.9 | 4.0 | 3.7 |

(2) Evaluation of Grasping Market Trends

We have analyzed market trends using customer preference information stored in three-dimensional vectors [1, 5, 6]. We describe analysis result of market trends about "Subnotebook computer", for example. We firstly retrieve the customers who showed preferences on the category "Subnotebook computer" on 6th. and 7th. weeks, and twelve customers are extracted. In this period, the major Japanese PC manufacturers introduced portable Subnotebook computers to the market. We investigate the preference transition of these customers from 1st. to 5th. weeks. Figure 4 shows the preference transitions of these twelve customers from 1st. to 7th. weeks. The figure indicates that some of these customers are clustered into the following two groups:

- A) Three customers who transited to "Subnotebook computer" from the area "Portable devices" such as "Portable AV devices" or "PDA".
- B) Five customers who transited to "Subnotebook computer" from the area "Personal computer" such as "Desktop computer" or "Notebook computer" via the area "Economics" (indicated by triangle markers).

Moreover, the customer a in the group A and the customer b in the group B always transited one step ahead of the other members in the respective groups. As a result of further investigation, we find that the customer a and b use the Internet far frequently than the others. Although the customer a and b show their preferences to the same areas as the others, they always collect information actively and therefore their preferences transit one step ahead of the others. This indicates the possibility to make ap-

ropriate recommendations to the other members of each group by predicting the areas they will show interests in the future more accurately based on the preference transitions of the customer a and b. Instead of clustering customers simply by their preferences, clustering them by the transitions of their preferences achieves higher clustering precision. Furthermore, it enables us to trace the preference transitions of trend leaders in the clustered customer groups, we can grasp market trend.

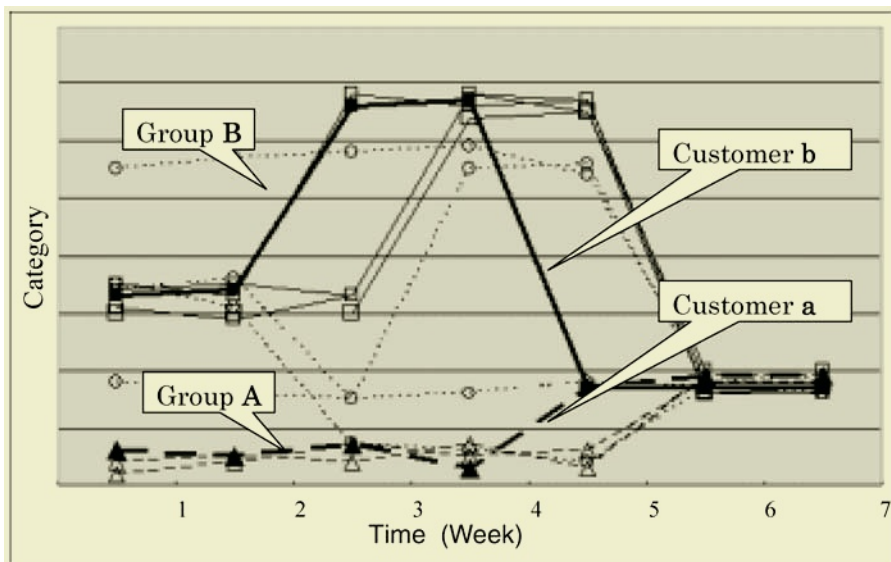


Fig. 4. Preference Transitions of customers

5 Conclusion

In this paper, we have proposed an information management system to keep track of the transitions of market trends and customer preferences in real time. The extracted information is used for data mining that enables ISPs to provide the effective My Page service. Using this system, we are able to precisely manage the information of customer preferences and market trends that change over time, which accordingly makes the result of analyses using various analysis tools highly reliable.

References

1. Adriaans, P. and Zantinge, D., "Data Mining", Addison-Wesley, 1996
2. Aho, A.V. and Corasich, M.J., "Efficient String Pattern Matching: An aid Bibliographic Search", Common. ACM, 18(6) (1975), 333-340
3. <http://www.cidf.org/english/index.html>
4. Kazuhiko Tsuda, Masao Fuketa and Jun-ichi Aoe, "An Incremental Algorithm for String Pattern Matching Machines", Intern. J. Math., Vol.58, pp.33-42
5. Langley,P., "The Computer-aided Discovery of Scientific Knowledge", Proc. 1st International Conference on Discovery Science, pp.25-39, 1998

6. Michael J.A. Berry and Gordon Linoff, Data Mining Techniques: For Marketing, Sales, and Customer Suppprt, John Wiley & Sons, Inc., 1997.
7. Moriarity, R. T. and Swartz, G. S., Automation to Boost Sales and Marketing, Harvard Business review, January-February pp.100-108, 1989.
8. Morio Nagata, SFA: Software for Customer Satisfaction, IPSJ Magazine, Vol.40, No.5, pp.528-531, 1999.
9. Youji Kohda and Susumu Endo, A New Advertising Business Framework in the 1:1 Marketing, IPSJ Journal, Vol.37, No.6, pp1235-1236, 1996.

Multi-agent Modeling of Peer to Peer Communication with Scale-Free and Small-World Properties

Shinako Matsuyama^{1,3}, Masaaki Kunigami², and Takao Terano¹

¹ Dept. Computational Intelligence and Systems Sciences, Tokyo Institute of Technology
4259 Nagatsuda-cho, Midori-ku, Yokohama 226-8502 Japan
Tel/Fax:+81-45-924-5583
terano@dis.titech.ac.jp

² Graduate School of Business Sciences, University of Tsukuba,
3-29-1, Otsuka, Bunkyo-ku, Tokyo 112-0012 Japan
Tel:+81-3-3942-6869, Fax:+81-3-3942-6829
kunigami@gssm.otsuka.tsukuba.ac.jp

³ Information Technologies Laboratories, Sony Corporation,
6-7-35, Kitashinagawa Shinagawa-ku, Tokyo 141-0001 Japan
Tel:+81-3-5448-6495, Fax:+81-3-5448-6833
Shinako.Matsuyama@jp.sony.com

Abstract. This paper presents an agent-based model of peer-to-peer communications network based on the extended BA (Balabasi and Albert) model, and analyzes the characteristics of the network. Developing the model, we discuss the following two issues: (i) characteristics of Agent and Contents, and (ii) Agent decision rules regarding sending, getting, and searching contents. The simulator processes communications among the agents and uncover the emerging social behaviors. The simulation results show that the network has scale-free and small-world properties assuming parameters of the generic scenario.

1 Introduction

In recent years, social network services such as Blog, Orkut, mixi, and Gree make Peer-to-Peer communication remarkable. Information providers would like to understand the underlying principles of information sharing on this kind of communication. In this paper, we analyze the characteristics of information sharing on Peer-to-Peer communication by agent simulation, and examined the characteristics of network.

The paper is organized as follows. Section 2 yields the background and motivation for the work. Section 3 overviews the agent-based simulation system we have developed. Experimental environment and the simulation results are described in Section 4. A brief discussion on the result is given in Section 5, and the main conclusions are pointed out in Section 6.

2 The Background and Motivation

2.1 Background

A number of related results regarding peer-to-peer communication have been reported in [1] and [2], for example. The virtual word-of-mouth system implemented

on the Internet has been described and analyzed in [1]. An approach for grading of the exchanged information based on the relations between persons involved in the network is proposed in [2] including the information-spread model. Additionally, in [3], the mechanism of the information spread by the word-of mouth is considered employing the questionnaires.

On the other hand, the characteristics of the network such as small-world and scale-free issues recently have appeared as the hot topics, and certain results on the related human relations in the collaboration network of actors and the high school friends network have been reported in [4] and [5].

2.2 Motivation

Human communication that this study covers is generally very little analyzed by experiments under restricted circumstances or only by the results of questionnaire, since factors affecting are numerous. For example, some information providers want to know the status in case that the circumstances change, and some others want to analyze instead what kind of circumstances and factors are good to realize certain condition. Therefore, it was determined that this research is analyzed by agent-based simulation that is good at this kind of analysis.

3 Agent-Based Simulation of Peer-to-Peer Communication

3.1 Framework

This section describes a basic framework for the simulation and analyzing of the information delivering mechanisms. The basic assignment is as follows: (i) Each “node” in network is a person and a “network edge” corresponds to a connection between two persons; (ii) We assign each person to an agent regarding the information delivering employing Peer-to-Peer communication.

Our simulation framework assumes an extended BA (Barabasi and Albert) model, and regarding this issue note the following. In the BA model, the growth and the preferential attachment are important issues regarding the power-law scaling. The preferential attachment model assumes that if a new edge should be added to a node it should involve an additional node which already has many edges (see [5], for example). The fitness model proposed in [6] is a model which adds the concept of weight to the BA model.

Our framework originates from the following statements. In the considered Peer-to-Peer communication, a node related to a new edge is chosen not only by the number of edges it already involves but also by the contents to be delivered and some attributes of the node such as the following ones: preference similarities, advantages to have an edge with the node and so on. So, the underlying model of peer-to-peer communication is considered as a fitness model.

On the other hand, the mutual link between people is not growing infinity and it converges to the certain value. This is explained as a phenomenon where the node makes the new favorite edges but where also some edges disappear as the time passes. This mechanism corresponds to the deactivation model described in [7]. So, the considered peer-to-peer communication network follows a model which combines

the fitness model and the deactivation model. Accordingly in our framework, we defined the growth curve of the edges as the following;

$$\frac{dE(t)}{dt} \equiv b \cdot N \cdot \left(1 - \frac{E(t)}{N C_2} \right) - \gamma \cdot E(t) \quad (1)$$

where, N is a number of agents, b is a rate of the performed communications by an agent per certain period (for example one day), γ is the probability of the deactivation by an agent corresponding to an edge per a day, and $E(t)$ is the total number of edges at the time instance t .

3.2 Model Components

In this subsection, we describe the main components of our agent-based simulation employing the framework described in the previous section. The involved particular framework components are: the agents, the contents, the society, the operations and the decision rules. Also note the following. In the simulation, subject of the communication is as an agent and so a number of its characteristics should be specified.. Additionally, some characteristics for the contents, which are subject of delivering should be specified, as well as the society, which defines the relations between agents. Finally note that the simulator performs the communications between the agents during certain period of time.

Agents. Each agent has three levels as activation rates of information sharing. The relationship between each agent is determined by the definition of society described later. Each agent has uniquely ordered identifier.

Contents. Each content belongs to one category. We have long-term category and short-term category. Each agent has some categories randomly selected as favorite contents list. According to [8], contents are categorized as either long-term or short-term for each individual. Therefore, long-term contents are configured long-term and short-term randomly by each agent. Short-term contents disappear randomly during simulation period. When a category disappears, new category is created and used among agents.

Society. We define the society NONE, which is the status with nobody known at initial condition (the circumstance under which one gets to know one by one). At initial condition, the agent next to oneself is selected as communication partner.

Operations. Actions of each agent consist of the following three.

- Send: an agent sends a content to an agent
- Receive: an agent receives a content from an agent
- Query: an agent asks some agents to introduce an agent who is familiar with the content and asks the agent to send the content ([9]).

Each agent calculates an evaluation value for the received content and keeps it with the content. The content will be sent to another agent with the evaluation value. Fig.1 shows the flow of the simulation.

Decision Making Rule. Communication between agents is expressed as the sender(From), content(What), and receive(To). In this section we define the indica-

tors for choosing the agent to communicate and the content to be sent/received. Although these indicators are extracted from general situation, these are the mechanism of generating edges in the fitness model.

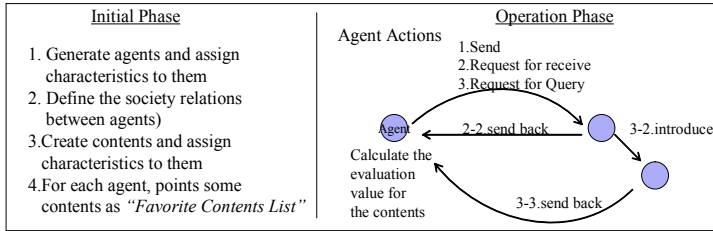


Fig. 1. Simulation flow

We assume the following:

- Let Gk be an arbitrary content category and Ck be content in content category Gk
- $Eval_A(C)$ is evaluation value for category/content C by agent A
- $Status_A(C)$ is a status (preference) for the content C of agent A
- $TrNum(Ai, Aj)$ is a communication counts between agent Ai and Aj
- $Type(D)$ is an agent/content type

(1) Content selection indicator

The indicator with which agent Ai selects contents C is defined as follows;

$$I(Ai, C) = \{Type(C) + Eval_{Ai}(C)\} \quad (2)$$

where $Type(C)$ is the life time of the content (short-term or long-term), $Eval_{Ai}(C)$ is determined by the evaluation value of contents itself and of a sender of contents,

$$Eval_{Ai}(C) = Eval(C) + Eval_c(Ac) \quad (3)$$

where Ac is a sender of the content

$Eval(C)$ increases as time of contents sent/received increases.

$Eval_c(Ac)$ is the sum of the rate contents sent the rate contents received and number of times of created contents sent/received by the Ac in the content category.

(2) Indicator of agent selection

Fitness of that agent Ai sends/receives content C with agent Aj is defined as follows;

$$\begin{aligned} Fitness(Ai, Aj, Ck) = & |Eval_{Ai}(Gk) - Eval_{Aj}(Gk)| + Eval_{Aj}(Gk) + Status_{Ai}(Ck) \\ & + TrNum(Ai, Aj) + Type(Ai) + Type(Aj) \end{aligned} \quad (4)$$

where,

- $|Eval_{Ai}(Gk) - Eval_{Aj}(Gk)|$ is a similarity of the evaluation of contents in the contents category Gk between two agents Ai and Aj ,
- $Eval_{Aj}(Gk)$ is the parameter whether agent Aj is interested in the contents or not (whether the content category Gk is in “favorite contents list” of Agent Aj or not),
- $Status_{Ai}(Ck)$ is number of times of sending/receiving of contents Ck of agent Ai ,
- $TrNum(Ai, Aj)$ is communication(sending/receiving) times between Agent Ai and Aj ,
- $Type(Ai)$ and $Type(Aj)$ are whether the agent is active and whether the agent keeps many short-term contents.

4 Experiments

4.1 Experimental Set up

With the status with nobody known at initial condition (the circumstance under which one gets to know one by one), experiment was performed under the following circumstances:

Number of agents: 150/300/600/1200,

Number of communication per day: Number of agents×7,¹

Contents categories: 6,

Total number of contents: about 3000,

Execution days: 10 days,

Decision making rules: use the rules in section 3 with same weight.

In this environment, thinking about the growth curve described in (1) in section 3.1, for 300 agents, $E(t)_{t \rightarrow \infty}$ is about 600 and $b=1.0$, then γ is about 0.5. Accordingly we have deactivated the edge with the probability of 0.5 per day randomly².

4.2 Results

For each execution number described in 4.1, total number of edges $E(t)$ and clustering coefficient C , path length L which are used in small-world network³ are shown in Table 1 and the cumulative distribution of number of edges with log-log scale is drawn in Fig.2.

Table 1. Experiment result s(C,L)

| Number of Agents | Total Number of Edges (E) | Clustering Coefficient (C) | Path Length (L) |
|------------------|---------------------------|----------------------------|-----------------|
| 150 | 303 | 0.24 | 3.2 |
| 300 | 637 | 0.26 | 3.4 |
| 600 | 1385 | 0.21 | 3.8 |
| 1200 | 2830 | 0.21 | 3.8 |

5 Discussion

5.1 Small-Worldness

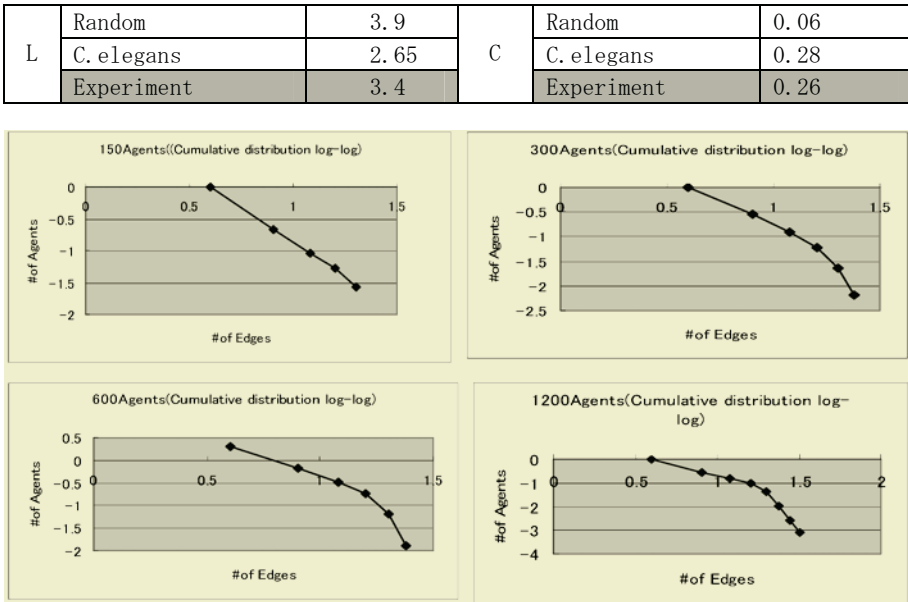
Table2 shows the result of the experiment, random network which has similar size of edges as the one in the experiment, and the Neuron network of caenorhabditis elegans([11])which is known as small-world network.

Through the results, compared to the random graph the network in the experiment has closer $L(L_{\text{rand}} \sim L)$ and much bigger $C(C >> C_{\text{rand}})$ and it can be defined as small-world network.

¹ Number of transactions against number of agents is 7, which is referred to number of average sending/receiving times of mobile phone mail, according to [10]

² We assume that the edges which have strong connection will recover soon, so we choose the edge to deactivate randomly

³ We use the definition of Watts and Strogatz ([11])

Table 2. Characteristics of the Links**Fig. 2.** Distribution of number of the edges

5.2 Scale-Free ness

Regarding to the characteristics of scale-free, Fig. 2 shows that in the range of edge 16 the probability is $P(k) \sim k^{-\alpha}$; $-1.5 < \alpha < 2.1$, and it is obviously scale-free network with cut-off.

6 Conclusion and Future Work

In this paper, we have analyzed the information delivering based on peer-to-peer communication employing the agent-based simulation. Our results show that the network has features of the small-word and the scale-free with cutoff.

We have used the fitness model and the deactivation model to develop an extended BA model [12]. Our experimental results show that combination of these two models can yield the network with large clustering coefficient C, small path length L, and power raw.

This kind of analysis by agent simulation makes it possible to examine that what kind of forum (society) to provide to agents, and what kind of contents characteristics to distribute to what kind of agents lead information sharing to its development.

As a future work, using this simulator, we are planning to perform examination by other model that can explain Peer-to-Peer network, examination by parameter constructed based on data in the real world, and comparative review of data obtained in the real world.

References

1. Y.Ito, M.Yoshida, and M.Numao, "New features of the Word-of-mouth Assisting Virtual Environment", Information Processing society of Japan Symposium No.2002-ICS-128, May. 2002(In Japanese)
2. S.Takeuchi, et al. "Evaluation of the Information-Spread Model based on Users' Relevance", DBWS2001, Aug. 2001(In Japanese)
3. Kokokusha, "Survey for the word of mouth", 2005. (In Japansese)
4. L.A.N.Amaral, A.Scala, M.Barthelemy, and E.Stanley, "Classes of small-world networks", Proceedings of the National Academy of Sciences, Vol. 97, No. 21,2000
5. A.L.Barabasi,R.Albert,H.Jeong,"Mean-field theory for scale-free random networks", Physica A, 272, pp.173-187,1999
6. C.Bianconi, A.-L.Barabasi., "Competition and multiscaling in evolving networks", Euro-physics Letters, 54(4), pp.436-442, 2001
7. K.Klemm, V.M.Eguiluz., "Highly clustered scale-free networks", Physical Review E,65,036123(2002)
8. J.Ishii, N.Atsumi, "Marketing in Internet society", 2002(In Japanese)
9. N.S.Contractor, "IKNOW: A Tool to Assist and Study the Creation, Maintenance, and Dis-solution of Knowledge Networks",LNCS 1519, pp.201-217,1998.
10. IPSe Marketing, Inc. "The third survey for the use of cellular telephone", http://www.ipse-m.com/report_csmr/report_c3/report_c3_sum.htm, 2003(In Japanese)
11. D.J.Watts and S.H.Strongatz, "Collective dynamics of 'small world' networks", Nature, Vol.393, pp.440-442 1998
12. Nmasuda, N.Imano, "Science of the complex networks", 2005(In Japanese)

A Case-Oriented Game for Business Learning

Kenji Nakano and Takao Terano

Dept. Computational Intelligence and Systems Sciences,
Tokyo Institute of Technology, Tokyo
nakano@ga2.so-net.ne.jp, terano@dis.titech.ac.jp

Abstract. This paper reports on a research project we have been conducting for two years since 2003, which aims at "integrating Case Method and Business Gaming." This research proposes a new gaming structure model. In this model, we structuralize the decision-making area of corporate managers and build a framework to implement it as a business game. The model also contains a method to quantitatively express a corporate structure which is a mixture of middle-term business policies and short-term business operations. We use this model to develop a business game that simulates a case of "Asahi Super-Dry" to demonstrate that Business Gaming is able to deal with the qualitative decision-making area, as well as the conventional quantitative operation area.

1 Introduction

Business Gaming is an effective method for having simulated experiences in business schemes in the real world to learn about it preliminarily. Case Study is also an efficient method to learn about decision-makings and business management concepts through the discussion-based learning processes using actual corporate management cases. These two education methods have in common and both belong to the "Experiential Learning" in the broad sense, which is a theoretical framework proposed by Kolb [1] et al. However, the directions of their basic approaches are totally reversing and have evolved separately making the most of their own advantages. There is no precedent report that attempts to integrate these two methods.

The subject of our research is to integrate these methods: Business Gaming and Case Study. We already had reported on the fruits of our research at KES2004 [2], which was about:

1. building a gaming model that is able to deal with cases and developing scenarios of business games.

In this paper, we report on two additional research results on:

2. developing a business game that simulate a case of "Asahi Super-Dry," and
3. verifying the availability of the business game as a decision-making system based on the experimental games we conducted.

This paper consists of the following chapters: Chapter 2 describes a method for modeling a case of "Asahi Super-Dry" as a business game, Chapter 3 reports on the reproducibility of the developed business game by simulating a game using agent players, and Chapter 4 concludes our discussion.

2 Developing "Asahi Super-Dry" Game

2.1 Specifications and Framework of the Game

The "Asahi Super-Dry" is a succeeded case of Asahi Breweries, Ltd. Asahi was a weak brand in Japanese beer market in 1980's, where Kirin Brewery Co., Ltd. retained its oligopolistic position. In the market, Asahi doubled its market share by developing a new taste beer "Super-Dry".

The business game that simulates this case (the "beer game") allows players (or learners) to make separate decisions "as the top management for business administrations" and "as the middle management for business operations". The players learn about the Asahi's succeeded case through the experiences in the quasi-market resulted from these decision-makings. Therefore, the requirements for the beer game are: it must be able to handle these two types of decision-makings, and it also needs to implement a model of a quasi-market where multiple companies with different management environment compete against each other.

The specification of the beer game need to incorporate mechanisms that:

- 1) reflect how much the top management's middle-term policy infiltrates into the operational tier in the lower organization, which indirectly exerts an influence on the implementation of the policy and the performance of the organization,
- 2) the performance of the organization reflects the consistency between the top management's policy and the middle-tier operations, and
- 3) differentiate the business environments and conditions of the competing companies at the beginning of and during the game (the existences of the other companies must be considered).

We have actualized the beer game using the models that:

- 1) adopt the "maturity" (from the framework of "Japan Quality Prize [3]") as an internal variable for reflecting the top management's policy and decision-makings, which impacts on the operations in middle-term,
- 2) provide separate entry screens for top and middle's respective decision-makings and check the "consistency" between them, which influences the operations in short-term, and
- 3) configure different initial values for every competitors so that each company starts the game from its unique condition.

2.2 Game Model and Decision-Making Items to Be Learned

Figure 1 illustrates the game model of "Asahi Super-Dry." We take up the case of Asahi Super-Dry from "Strategic organizational innovation" (Kawai [4]) as our research subject. We have selected four of top management policies among the major management epochs of Asahi Breweries between 1982 and 1989: "share No.1", "customer-oriented", "R&D", and "corporate revolution". These are the decision-making items to be learned in the game.

We also determined five decision-making items for middle operations: "sales goal", "advertisement", "capital investment", "market research", and "new product development." In the gaming scenarios, the measured consistency between the top management policies and the middle operational decisions has an affect on the feasibilities of the operations.

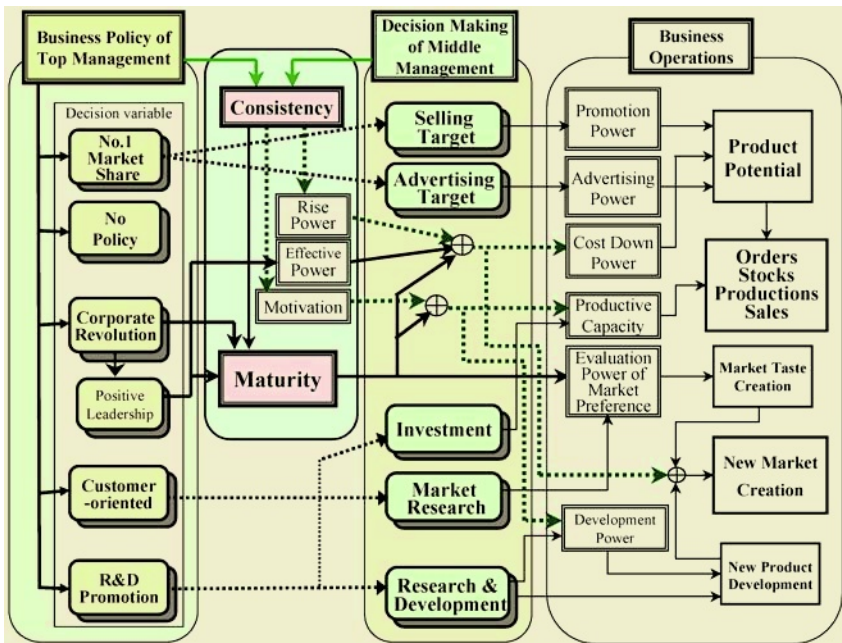


Fig. 1. The game model of "Asahi Super-Dry

Our game model distinctly separates the top management policies and the middle operational decisions, and therefore it forces players to make decisions in two different tiers. This model provides a style of learning decision-makings in "top" and "middle" tiers concurrently or individually. It also allows teams to learn from the differences in game results with or without good communication between "top" and "middle" within the teams. This novel style of the gaming enables players to extensively experience the way of making decisions in corporate managements.

2.3 Conditions for Successful Decision-Makings

This beer game implements the succeeded decision-making processes of Asahi Super-Dry as the following success conditions:

Process 1: <Corporate Revolution>

The corporate revolution aims at renovating the corporate culture in order to conquer the current market structure. The successful revolution leads to the successful development of the new taste beer, "Super-Dry", which creates a new market for the company. The time frame offered for the corporate revolution is two years. The revolution succeeds or fails depending on the top management's decision on "which capability of the organization should be improved and how far the leader should get involved with it."

Process 2: <Market Research>

In order to make the market development successful, the players need to satisfy a certain levels of: "the consistency between the top management's policy and the mid-

dle-tier operations", "the maturity of the organization", "the capability for the customer relations", and "the cumulative investment for the market research."

Process 3: <Research and Development>

To make the R&D successful, the players are required to fulfill a certain levels of: "the consistency between the top and middle decisions", "the maturity of the organization", "the capability of developing strategy", and "the cumulative investment for the R&D." Furthermore, the players need to continue the investment for more than two years, and they need to succeed in the market research to determine the customer preferences that are effective for R&D.

Process 4-6: <New Product Development>, <Introduction to Market>, <Share No.1>

The new product development (the process 4) succeeds if the company succeeds in R&D and continues the R&D investment in the subsequent year. However, the development work will be suspended when a divergence arises between the top and middle decisions.

3 Evaluation of Developed Beer Game

We check the reproducibility of the case of "Asahi Super-Dry" on the developed beer game by simulating a game using agent players. Player 1 (Asahi) is configured as the reference player who enters the correct values for the Asahi's succeeded processes. We configure the other players as Player 2-4 (Sapporo, Suntory, and Kirin) who use random input values that do not include the succeeded pattern.

3.1 Gaming Design

1) Decision-making processes:

Figure 2 illustrates the timing and the judgment criteria of six decision-making processes.

2) Market share:

The market share of Asahi transits as:

- approximately 10% during 1982-1985,
- 15-16% in 1986, and
- 25-26% during 1987-1992.

The transition accommodates to the timings of the success of the new product development and its introduction to the market.

3) Maturity:

The value of Asahi 's maturity transits as:

- 180 points beginning of games in 1982-,
- approximately 800 points after finishing the 10th gaming round in 1992.

It depends on both the success of the corporate revolution and the results of the business operations.

3.2 Verification of Reproducibility

The figures below show the result of the simulation. The horizontal axes of all three charts represent the numbers of rounds played. The vertical axes of the figures indi-

cate: the ratio of the market transition from old to new products (the left axis) and the number of succeeded processes 1 - 6 (the right axis) in Figure 3, the market share of each company in Figure 4, and the maturity of each organization in Figure 5.

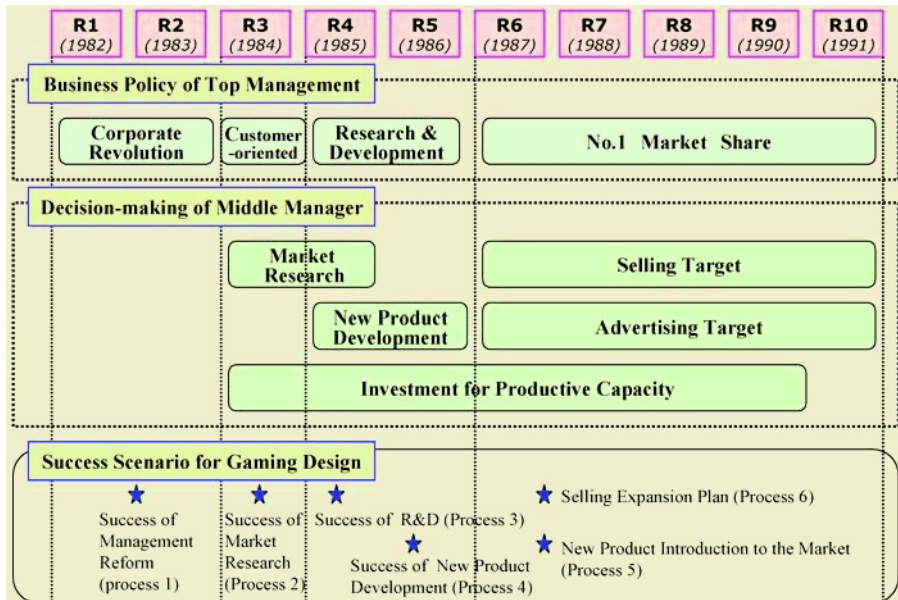


Fig. 2. The criteria of six decision-making processes

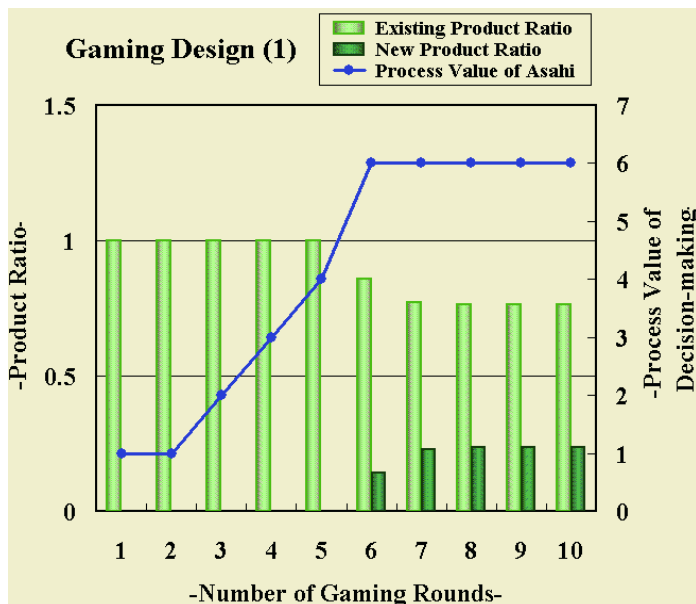
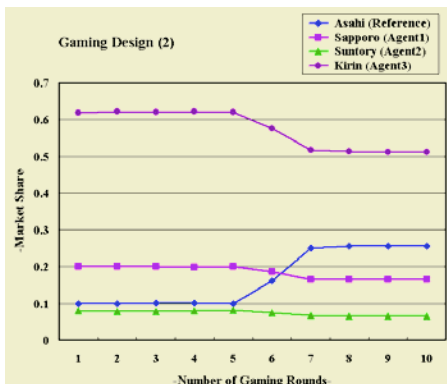
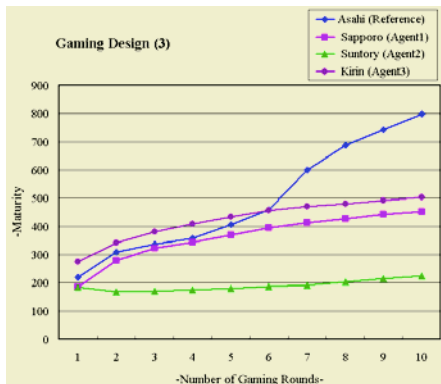


Fig. 3. The succeeded processes and the market transition

**Fig. 4.** The market share of each company**Fig. 5.** The maturity of each company

As shown in these figures, this evaluative game has reproduced the case of "Asahi Super-Dry." This result demonstrates the validity of the business game which we have developed based on the case.

4 Conclusion and Future Work

In this paper, we have proposed a new Business Gaming model, which enables generic and multilateral learning based on the simulated "case." This model is structured from three tiers that imitate the structure of business organizations: the top management decisions, the middle operational decisions, and the computer-automated implementations of the operations. We have developed a business game based on this model and a method that sets different initial values for each player at the beginning of games. The developed game has succeeded to reproduce the scenario of the successful "Asahi Super-Dry" case, which indicates the possibility for applying business games to Case Study.

The result of the experiment reported in this paper suggests many challenges to be carried over for our future work. However, we have made significant progress by indicating the availability of integrating Case Study and Business Gaming.

References

1. Kolb, D.A. (1984): Experiential Learning: Experience as the Source of Learning and Development Englewood Cliffs. New Jersey. Prentice- Hall, Inc
2. Nakano.K., Terano.T. (2004): From Gaming Simulation to Case Method -Empirical Study on Business Game Development and Evaluation- KES2004 (*Proc.PartI*) 472-479
3. Japan Quality Award Council (2003): Assessment criteria of the Japan Quality Award 2003 Japan Productivity Center for Socio-Economic Development (JPC-SED)
4. Tadahiko.K (1996): Strategic organizational innovation 35-57 Tokyo. Yuhikaku Corp.

Learning Value-Added Information of Asset Management from Analyst Reports Through Text Mining

Satoru Takahashi^{1,2}, Masakazu Takahashi³, Hiroshi Takahashi¹, and Kazuhiko Tsuda²

¹ Mitsui Asset Trust and Banking Co., Ltd., 3-23-1 Shiba, Minato-ku, Tokyo, Japan
{Satoru_1_Takahashi, Hirohi_1_Takahashi}@mitsuitrust-fg.co.jp

² Graduate School of Systems Management, The University of Tsukuba,
3-29-1 Otsuka, Bunkyo-ku, Tokyo, Japan
{satoru_tsuda}@gssm.otsuka.tsukuba.ac.jp

³ Shimane University, 1060 Nishikawatsu-cho, Matsue-shi, Shimane, Japan
smasakazu@cis.shimane-u.ac.jp

Abstract. Text mining, one of the emerging fields of data mining, aims at acquiring useful knowledge from text data. In the asset management in finance task domain, although there exist various text data like accounting settlement or analysts' reports, few research and development have been conducted. In this paper, we will explore the feasibility to extract valuable knowledge for asset management through text mining using analyst reports as text data. We will analyze the relationship between text data and numerical data. From empirical study on the practical data, we have confirmed the effectiveness: (1) the extracted keywords are influential to the stock prices, (2) such information is more effective to the large-cap stocks, and (3) such keyword information become more valuable by using numerical information together.

1 Introduction

In recent years, the environment surrounding asset management has dramatically been changing. The rapid progress of telecommunication technologies, such as the Internet, has eliminated the time lag on distributing vast amount of investment information. Although this kind of information contains valuable information for asset management, it is impossible to manually handle all information. It is an important task in asset management to make full use of such information more efficiently and quickly.

The efficient market hypothesis and the rationality of investors are the two key assumptions in the traditional finance theory [2]. These assumptions require that every investor immediately processes all information and optimizes their actions and that security prices reflect all available information in the markets. To prove whether market is efficient or not, many studies have been conducted [3]. But these studies analyzed the reactions against only numerical information that based on financial statement or analyst report. Analyst reports, which are one of the important information sources for investors, contain both numerical and text data, which describe the state-of-the-art business conditions of firms. For instances, the text information about such as "business reconstruction" or "business restructuring" are not numerical data but have strong impacts to markets. So, the use of text information of analyst reports is indispensable to analyze financial market.

One of the problems to analyze test information of analyst reports is difficulty of handling text information. In order to solve this problem, text mining, which can analyze large quantities of text data systematically, is very effective method. Text mining aims at obtaining valuable knowledge from enormous amount of text data by analyzing the tendencies and correlation of the contents based on the change histories of the texts and the distribution of the keywords in the text data. In [6] they predict the movement of the stock indexes in major countries based on the text mining of newspaper articles published on WWW. In [1] and [7], they analyze the relation among the text information written on Web bulletin boards and the fluctuations of stock prices. The numbers of literatures of text mining applied to finance are gradually increasing.

So far, we have reported the relationship between text information of analyst reports and stock prices [4], [5]. In [4] and [5], we extracted keyword information from titles of analyst reports, and we studied how stock prices move in existence of extracted information. We found that analyst reports contained valuable information that influenced to the stock prices. We also found that multiple analysts reacted to the same information. As a result of eliminating such duplication of information, we succeeded to extract more valuable information from analyst reports.

In this paper, we analyze text information of analyst reports in detail. The value driver of company is different by characteristics of a company. For example a type of industry or a size of firm is important factor to affect a stock price. We analyze effect of analyst reports with every type of industry and size of firms. And to extract more valuable information, we analyze analyst reports by combining text information with numerical information.

The paper is organized as follows. In Section 2, we explain the outline of our research and Section 3 illustrates the relationship between text information and stock prices. Then we conclude our discussion in Section 4.

2 Outline of Research

This section describes the outline of our research. The conventional asset management has not used text data systematically. This is mainly because there are few definitive methods to extract and evaluate information in text data. In our research, we firstly extract keyword information from analyst reports by morphological analysis and pattern matching. Then, we evaluate the extracted information by supervised machine learning using stock prices as the target concepts.

We construct a knowledge database from analyst reports in the following steps (see Figure 2.1 for the process flow):

- 1) obtain analyst report via WWW or e-mails,
- 2) adjust the differences of the concepts in similar keywords,
- 3) extract keywords from the report using morphological analysis and pattern matching,
- 4) evaluate the extracted information based on the stock price return,
- 5) store the keywords and the results in the database, and
- 6) repeat the steps 1 to 5 to construct the knowledge database.

After completing the construction of the knowledge database from the collected analyst reports, we can measure the influence of the report in detail. We use both

characteristic database of firms and numerical information based on financial statement database to evaluate whether we can get more valuable information or not (Figure 2.2).

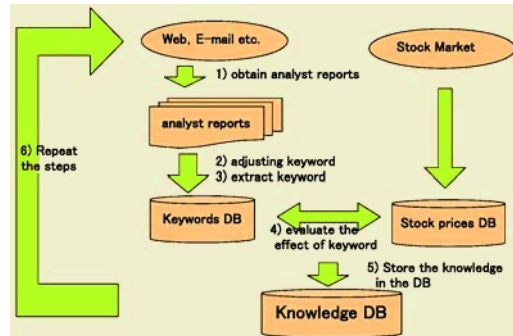


Fig. 2.1. Outline of the model

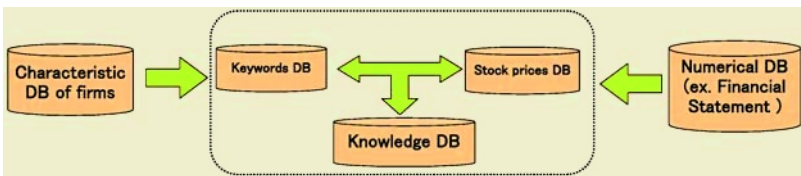


Fig. 2.2. Outline of the detail research

3 Analyses of Keywords and Stock Prices

This section describes the result of the experimental analyses we have conducted. In these analyses, we apply the text mining procedure to the titles of analyst reports in order to analyze the influence of the reports. We have extracted keywords from the titles of analyst reports. Then we have examined whether there are significant differences in stock price returns caused by the existence of the keywords. The following subsections describe the methods and the results of the analyses.

3.1 Data Used for Analyses

We use all stock data listed in the first section of the Tokyo Stock Exchange in the period from January 1st, 2001 to March 31st, 2003. There are 1,619 firms listed during the period. We classify each firms into manufacturing and non-manufacturing industries based on a definition of Securities Identification Code Committee.¹ Using Thomson Financial Web service, we have obtained 77,256 analyst reports related to the listed firms. And we use the I/B/E/S Consensus Estimates as numerical data². The

¹ See <http://www2.tse.or.jp/sicc/>

² The Institutional Brokers Estimate System (I/B/E/S) provides investment professional database of security analysts' forecast earnings per share, cash flow per share, dividends per share and net profits per share. The I/B/E/S Consensus Estimates is a mean value of security analysts' forecast of a firm

obtained analyst reports have characteristic that the analyst coverage in the larger companies is greatly different from the ones of the smaller companies

3.2 Extracting Keywords and Adjusting Differences in Notation

We have extracted keywords from the titles of the obtained reports. As shown in Table 3.1, we classify the extracted keywords into twelve groups after the difference adjusting. We also classify the keywords into three news types: Good, Bad, and Neutral News.

Table 3.1. Classification of keywords

| NO | Notation adjusted keyword | News type |
|----|-------------------------------|-----------|
| 1 | Increase in profits | Good News |
| 2 | Upward surprise in forecast | Good News |
| 3 | Downward surprise in forecast | Bad News |
| 4 | No surprise in forecast | Neutral |
| 5 | Business restructuring | Good News |
| 6 | Upward earnings revision | Good News |
| 7 | Downward earnings revision | Bad News |
| 8 | Rating "Sell" | Bad News |
| 9 | Rating "Buy" | Good News |
| 10 | Rating unchanged | Neutral |
| 11 | Upgrade of rating | Good News |
| 12 | Downgrade of rating | Bad News |

3.3 About Teacher's Signal

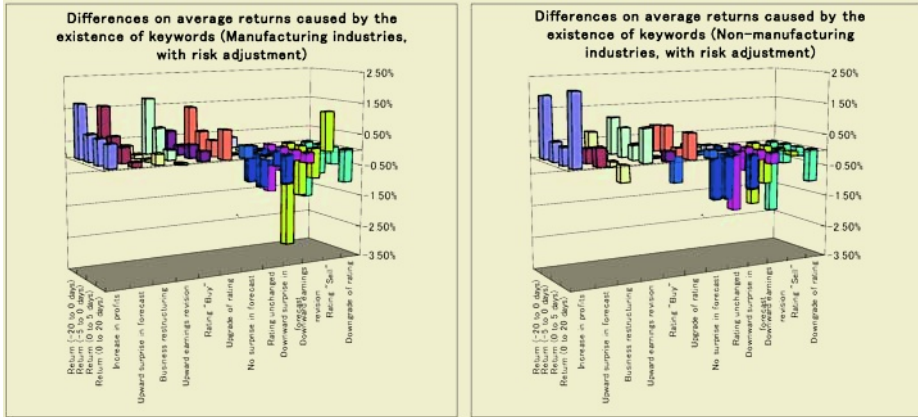
We use stock price returns as the target concepts to measure the influences of the keywords. The influence is measured as a difference of stock price returns before and after the analyst report has been published. First, we classify the stocks into two groups: Group A, which contains keywords in the report title and Group B, which does not contain them. Next, we statistically test the differences of the average stock price returns between Groups A and B. We employ Welch's test to measure the differences of mean values, since there exists heteroskedasticity in stock price returns between the groups.

3.4 Analysis of Keywords' Influences

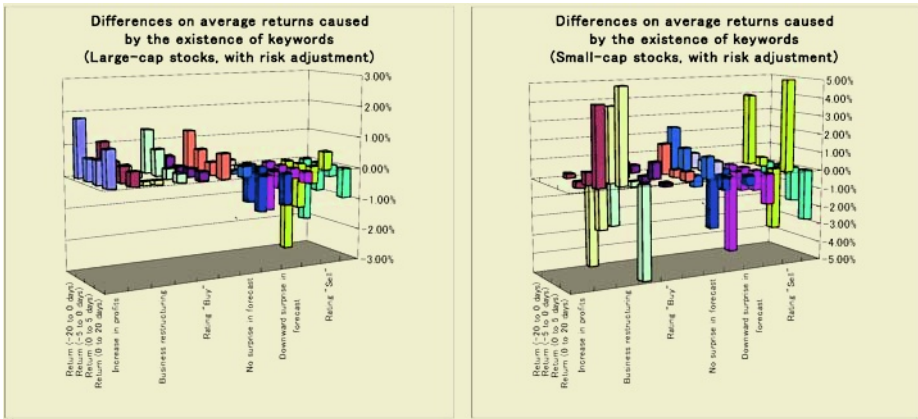
This subsection describes the result of the analysis. In [4], using the entire data, we confirmed that text information of analyst reports contained valuable information that influenced to stock prices. So we investigate how this influence changes by using types of industry or size of firms. We classify data using these characteristics of firms.

First we analyze analyst reports by using types of industry. Figure 3.1 shows the difference of mean value of stock price returns depended on the existence of keywords. The left bar chart describe the result on manufacturing firms and the right bar chart describe the result on non-manufacturing firms. The bars in both charts are drawn in order of Good, Neutral, and Bad News from left to right.

As shown in the both charts, the market reacts to Good News in positive direction and to Bad News in negative direction. From comparison between the left and right charts, we confirm that the keywords effect to the stock price returns both manufacturing and non-manufacturing industry

**Fig. 3.1.** Outline of the detail research

Second, we use size of firms to classify analyst reports. In figure 3.2, the left bar chart describes the result on large-cap firms and the right bar chart describes the result on small-cap firms. Although we can see same effect in the left bar chart, it differs in the right bar chart. About large-cap firms, the market reacts to Good News (Bad News) in positive (negative) direction. On the other hand, about small-cap firms, even if Good News (Bad News) is published in analyst reports, stock prices don't necessarily react in the positive (negative) direction. One of the reasons of this phenomenon is that there are few analysts who are evaluating small-cap firms. Consequently, there are few analyst reports to small-cap firms as compared with large-cap firms, and the influence that the other factors have on stock prices becomes larger.

**Fig. 3.2.** Outline of the detail research

3.5 Analysis by Combining Text Information with Numerical Information

In the previous subsection, we confirmed that the effect of analyst reports did not depend on a type of industry, but it depended on a size of firm. Then, how this effect

will change if we analyze the effect by combining numerical data with text data, for example earning estimate? We use change of monthly earning estimate for next fiscal year. We classify data into two groups using whether monthly earning estimate changes to upward or downward revision. We define upward or downward revision of monthly earning estimate as follows:

- Upward revision: $(EPS_t - EPS_{t-1}) / (\text{abs}(EPS_t) - \text{abs}(EPS_{t-1})) > 0$
- Downward revision: $(EPS_t - EPS_{t-1}) / (\text{abs}(EPS_t) - \text{abs}(EPS_{t-1})) < 0$
where EPS_t : Mean estimated earning per share for next fiscal year in month t

First, we classify twelve keywords shown in Table 4.1 into three news types, Good News, Bad News, and Neutral News. We show a result in the left bar chart of figure 3.3.

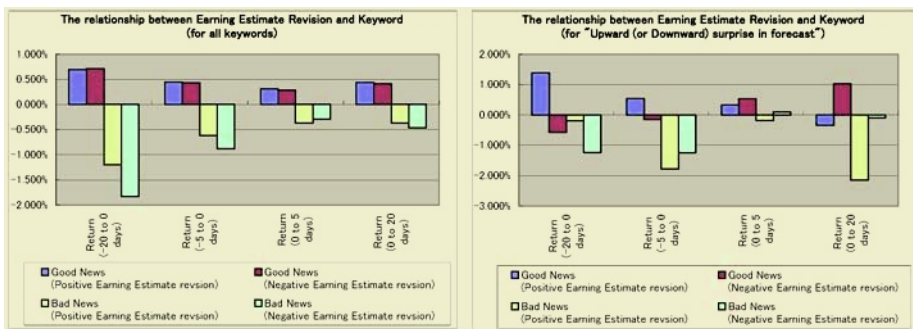


Fig. 3.3. Outline of the detail research

In the left bar chart, we find that the stock prices react in the same way regardless of direction of earning estimate revision. Next, we use only two key words that are thought to have a strong effect to direction of earning estimate revision, “Upward surprise in forecast” and “Downward surprise in forecast”. In the right bar chart of figure 3.3, we can see a very interesting result. Even if Good News is found, an effect of keywords is low when earning estimate is revised upward. And even if Bad News is found, an effect of keywords is low when earning estimate is revised downward. In other words, we find that an impact of text information of analyst reports is larger when analysts express their opinion opposite to the direction of average earning estimate revision.

4 Conclusion

In this paper, we have analyzed the effect of text information of analyst reports through text mining. And we also analyze the validity of combining text information with numerical information. We have conducted that analyst reports contained valuable information that influenced to the stock prices. The influence is stable without depending on a type of industry, but we cannot find this effect to small-cap firms. We have also identified in our further analyses that to combine text information with numerical information make it possible to extract more valuable knowledge from analyst reports.

In our future work, to explain mechanism of stock prices decision in detail, we combine text information with numerical information in higher level. And we hope to construct more precision model.

References

1. Antweiler, W., Frank, M.: Is All That Talk Just Noise? The Information Content of Stock Message Board, Working Paper, Univ. British Columbia (2001)
2. Sharp, W.: Capital Asset Prices: A Theory of Market Equilibrium under Conditions of Risk, Journal of Finance Vol. 19 (1964) 425-442
3. Shleifer, A.: Inefficient Markets: An Introduction to Behavioral Finance, Oxford University Press (2000).
4. Takahashi, S., Takahashi, H., Tsuda, K.: An Efficient Learning System for Knowledge of Asset Management, Eighth International Conference on Knowledge-Based Intelligent Information & Engineering Systems, 2004.9.24.
5. Takahashi, S., Takahashi, H., Tsuda, K., Terano, T.: Analyzing Asset Management Knowledge from Analyst's Reports through Text Mining, International IPSI-2004, 2004.11.
6. Wuthrich B., Cho V., Leung S., Permutilleke D., Sankaran K., Zhang J., Lam W.: Daily Prediction of Major Stock Indices from Textual WWW Data, KDDM'98 Conference NY, AAAI Press (1998) 364-368
7. Wysocki, P. D., [1999], "Cheap Talk on the Web: The Determinants of Posting on Stock Message Boards," working paper, Univ. of Michigan.

HHM-Based Risk Management for Business Gaming

Toshikazu Shimodaira¹, Hua Xu², and Takao Terano¹

¹ Department of Computational Intelligence and Systems Science,
Interdisciplinary Graduate School of Science and Engineering,
Tokyo Institute of Technology, Tokyo, Japan

tcotaira@yahoo.co.jp, terano@dis.titech.ac.jp

² Graduate School of Business Sciences, University of Tsukuba, Tokyo
xuhua@gssm.otsuka.tsukuba.ac.jp

Abstract. Business Gaming is a methodology for examining new business models in e-business field. This paper aims at improving the methodology to handle risk factors in the model. We utilize Hierarchical Holographic Modeling method (HHM method) for the risk assessment. In this paper, we develop a new risk assessment process on the IT-System Security field within the business gaming environment. We model knowledge related to risks by HHM method. The results suggest the effectiveness of applying the models into the Business Game environment.

1 Introduction

Business Game models various company activities such as marketing, decision-making, manufacturing, and sales. The developed Business models enable us to virtually actualize a business environment, and players can experience business processes that are close to reality through playing [1], [2]. It has a very wide application range from examining new business models to educating representatives in existing business of various fields including e-business.

Normally, creating Business Game is based on the results of careful research and analysis in order to create model-business, and knowledge related to existing business is collected and applied. However on the other hand, in conventional Business Games for example, most of the risks caused within company activities had only been treated briefly than reality. For instance, when there is plurality of risks, only the representative examples are used or those with similar contents are either synthesized or substituted. And for indicating the frequency of risk occurrence, random numbers were usually used in such models.

Of course, there is restriction for the modeling itself. Moreover, concept of risks inherently has a very wide application range, and the definitions and the contents may be greatly different according to the standpoint used. Such reasons made the modeling very difficult. It is difficult to say that Risk Management itself has been an area sufficiently receiving systematic approach of a scientific method.

This study experiments in modeling knowledge by applying HHM method in order to conduct Risk Assessment in IT-System Security field, which has recently become the most important theme in e-business. Through reporting the results, we will indicate risk models, and the possibility of applying them into Business Games.

2 Problems in Risk Assessment

Risk Assessment is composed of "Risk Analysis" and "Risk Evaluation", and Risk Analysis is divided into two processes of "Source Identification" and "Risk Estimation". Here, Source is things or behaviors that have an underlying possibility of bringing results. In Risk Analysis, we firstly specify the Source, and secondly we carry out Risk Estimation. Risk Estimation is examined the possibility of the Source, and the consequence of the caused event. In other words, Risk Estimation objectively and subjectively estimates the possibility of occurrence, the size, results that are set quantitatively and qualitatively. And it also ranks them based on the importance from the purpose of risk management.

These explanations may sound very systematic. However in real operation, simpler and more personal methods are usually used due to cost savings. Moreover in most of cases, it relies on laborer's experience etc. For instance, ordinary checklists used in normal interviews for specifying Risk Source have contents that are basically fixed. This can be very problematic those checklists cannot deal with new incidents. And thrashing out the organization's peculiar contents might be dependant on the questioner's skills. We often execute Brainstorming to overcome those problems, or to widely gather opinions. But it is often swayed by subjective opinions from the loudest person, or by people just obeying the opinion leader in the group. In such cases, an argument cannot spread easily, the information between participants is unsharable, and presentation of a fair opinion decreases [3]. Additionally, Risk Evaluation has not been digitalized to a sufficient level to be evaluated objectively.

On the other hand, the contents of risks have characteristic of changing over time. But for now, we have not yet come up with a corresponding method for these ever-changing risks themselves. You can see that in these types of situation, assuring great reliability such as completeness is impossible, and the modeling is very difficult.

3 Knowledge Modeling Related to Risks by Applying HHM Method

HHM method is a widely accepted and a common method for Risk Identification in large-scale, complex systems [4], [5].

Most of the organizations or technology systems have hierarchical structure and comprises plurality of subsystem. Here, the individual risks underlying in each hierarchical subsystem are compound, and finally the compounded risk brings about the great influence on the whole system. If we can perceive this, the difficulty related to Risk Identification is alleviated and we can handle it as simple models. Thus the approach with HHM method is a very good way to fit risk management into a hierarchical structure of the target system.

Fig. 1 shows the creation and the application conceptually, based on basic image of Hierarchical Holographic Model. HHM method uses a special diagram like this type. "A1, B1, C1" in bold type in a thick-lined box in the upper column of the diagram, are the "head-topics", and these head-topics indicate "viewpoints" that become the cross-section for describing the system. Each head-topic is broken down into plurality of "sub-topics" like "a-1, a-2, a-3" for instance in thin-lined boxes. These

sub-topics correspond with the subsystems or the elements of the system the system, and they indicate requirements, conditions, and standards for judgement [6].

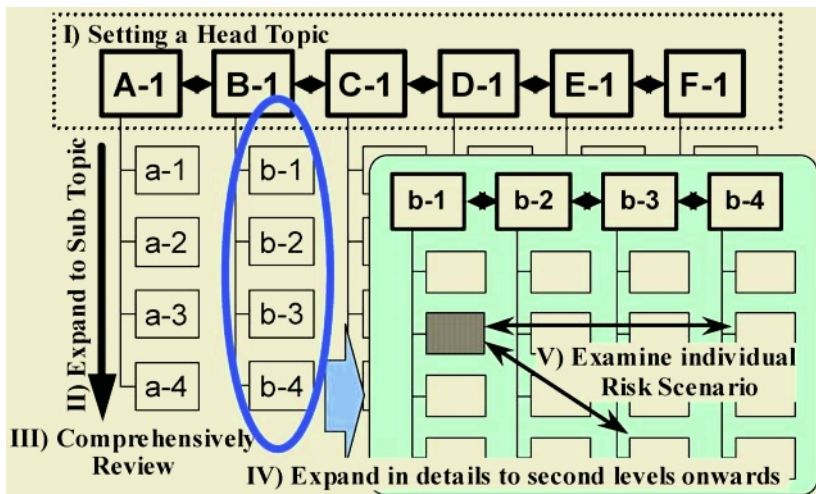


Fig. 1. Image of Creating Risk-Model and Specifying Risk-Scenario by HHM method

Well, to model knowledge related to risks by using HHM method,

- I) Firstly, the participants brainstorm the keywords for the viewpoints which will become the cross-section. And set a head-topic through exchanging opinions about the viewpoint.
- II) As for each head-topic, participants freely discuss about the consisting elements or related points, to develop them into sub-topics of the head-topic.
- III) Conduct overall re-examination for the created model, and amend it.
- IV) If necessary, expand them in details to second level onwards, based on sub-topic groups.
- V) By focusing attention to the relationship of each sub-topic, specify the risk scenarios or the risk items.

It is advanced according to the procedure like this.

These are the main steps for modeling knowledge, and if these operations are appropriately done, in theory, most part of the risk sources and uncertainties related to the subject system will be specified, and we will be able to obtain realistic Risk Models.

4 Application Result of HHM Method for Risk Assessment in Security Field

In this section, we introduce the case of Security policy construction project executed in a certain private company. For specifying Risk Source, we have applied HHM method alongside the conventional, general methods.

We actually obtained many results from this trial. Fig. 2 shows the first model, and the correction model after reviews.

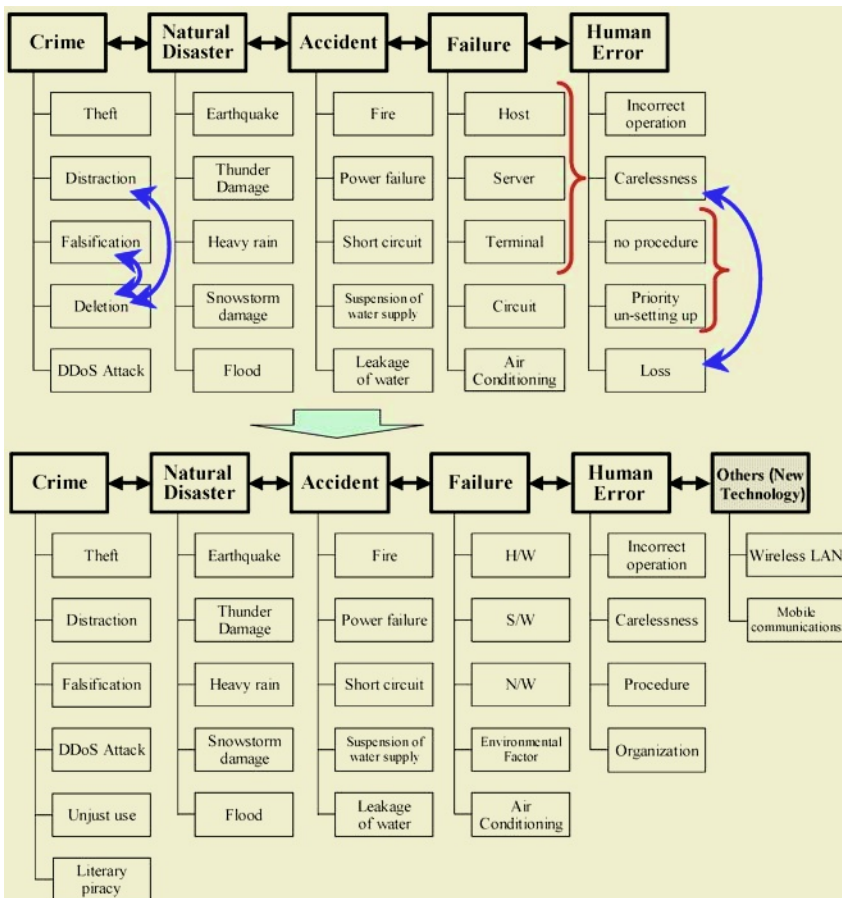


Fig. 2. First created model and amended model after consideration

As follows, we show the excerpt of the discussions executed through that correction process. There, we can see the repetition of content and coexistence of different levels had been arranged and become more sophisticated.

- In the section of "Crime", "Deletion" is included in the category of "Distraction" and "Falsification", and two categories are newly added.
- The section of "Failure" is reclassified into "Hardware (H/W)", "Software (S/W)", "Network related (N/W)", and "Environmental Factor", "Air Conditioning".
- In the section of "Human Error", "Loss" is included in "Carelessness", and "Organization" is newly added.
- "Wireless LAN" and so forth is added as the section of "Other one". And from these requirements, a viewpoint of "New Technology" is created after that.

By the way, in the contents of this correction model, for instance as for "Natural Disaster" and "Accident" are considerably concrete. On the other hand, "Crime", "Failure", "Human Error" still has room for possibility of decomposition. Therefore we tried expanding in details to the second level like Fig. 3-4.

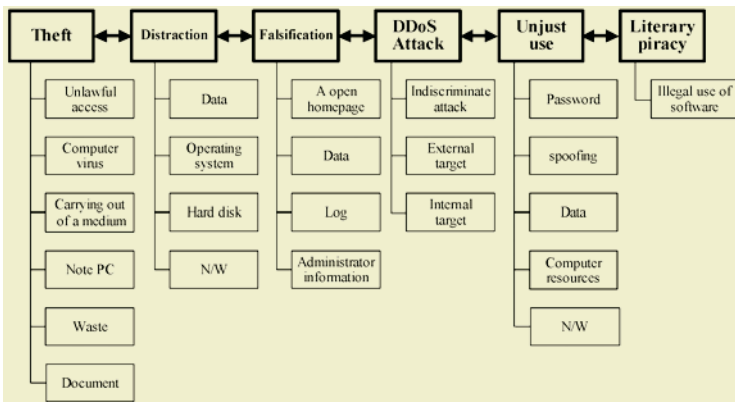


Fig. 3. The Model of the 2nd level which carried out detailed deployment about "Crime"

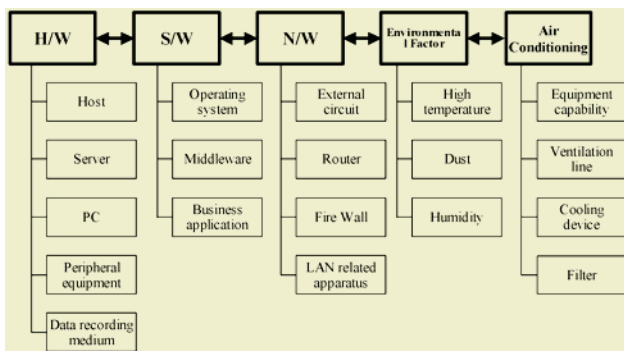


Fig. 4. The Model of the 2nd level which carried out detailed deployment about "failure"

From the models created, 141 risk scenarios were extracted in total. Here, from among them, we show the characteristic ones below.

- From the models created, 141 risk scenarios were extracted in total. Here, from among them, we show the characteristic ones below.
- Hi-speed printing device breaks down, and it affects business operations greatly.
- The reading error of Recording-MT happens, and back up data vanishes.
- Because of bugged OS program, computer's exceptional processing terminates abnormally, and it affects business operations.
- The patch program for error correction has a bug, and the system's down is caused.
- The burst of the air conditioner's water pipe cause the water immersion, and it affects the operation of equipments.

By the way, when looking at these risk scenarios, we notice the strongly reflecting the contents of each participants' experience and knowledge in their real business. Such contents could never be extracted without real experience at business sites. From these results things, we can understand that HHM method is effectively digging up the new incidents and the organization's peculiar contents.

5 Evaluating the Trial Result

We also obtained a diagram with a hierarchical structure which is a very comprehensible risk model relatively easily. Applying the HHM method enabled us to collect, arrange, and analyze knowledge related to risks exhaustively in details such as risk items and risk of the subject scenario.

Each group of viewpoints merely states a certain aspect of the system. But by compounding the models obtained from each viewpoint, it can comprehensively represent the full picture of the system. As a result, we confirmed that risks are perceived inherently and flexibly by getting an overview of the full picture. Moreover, we could understand easily the relationship and positioning of each viewpoint, which was not clarified from previous approach.

Here, we have to pay attention to each of the vertical rows in the diagram. Because these rows shows different attributes of the same system from a different viewpoint. In other words, by perceiving these as a "group", risks can be handled as a simple model. This perception opens up a new possibility, when creating business games. It is just to enable practical risk models to be incorporated into business games.

Moreover, these groups of risk items are originated from a common viewpoint. So these groups can basically have the same evaluation attributes. That is to say that it indicates the possibility of managing with common indicator. It has an important meaning that it may provide the theoretical grounds for the possibility of occurrence, which had been hampering when creating business games.

On the other hand, we observed the following some positive effects of HHM-based process, compared to the conventional and common method.

- Member's participation level rises.
- An impartial opinion is presented in the discussion.
- Information is shared among members.
- It is actively discussed from a wide phase.

It should be noted that Hierarchical Holographic Model became a common language for participants to communicate with each other.

At this trial, we executed various improvement plans for effectively applying HHM method in worksites. Those improvement plans, like indicating basic viewpoint, or using Post-Its cards and worksheets, were mostly received good reaction. We deepened the confidence of the future development as these results.

As for an educational effect, we can see from all the experiments that they had favorable impacts. However from now on, we need to make some changes to implementing styles to be practical in real worksites, which we will deal with step by step.

6 Finally

As mentioned above, it was able to be confirmed that the approach by the HHM method was useful very much for risk assessment. And this experiment researches showed that approach bring secondary effects of educating and activating worksites.

Above all, HHM method enables to effectively collect and arrange knowledge related to risks, and model them in good shape. That confirmation has a great significance.

Especially, each vertical row of the created diagram shows different attributes having same system from different viewpoint. It has opened up to express simple risk models by binding them. And there is now a possibility of managing with common indicators. So we feel confident about applying and including Risk Models to Business Games. In the future, for the common indicator especially, we will drill down on the issue and examine it further from the viewpoint of risk evaluation. And we hope to develop specific applying models.

References

1. Wolfe,J., and Frutzsche, D.J.; Teaching Business Ethics With Management and Marketing Games. *Simulation & Gaming*, Vol.29, No.1, 44-59 (1998)
2. U.S.Knotts.: Teaching strategic management with a business game. *Simulation & Gaming*, Vol.28, No.4, 377-394 (1998)
3. Vose, David.: *Risk Analysis: A Quantitative Guide*, second edition, John Wiley & Sons (2000)
4. Stan Kaplan, Yacov Y.Hames, and B.John Garrick.: Fitting Hierarchical Holographic Modeling into the Theory of Scenario Structuring and a Resulting Refinement to the Quantitative Definition of Risk. *Risk Analysys*, Vol. 21, No. 5, 807-819 (2001)
5. Yacov Y.Hames, Stan Kaplan, and James H.Lambert.: Risk Filtering, and Management Frame work Using Hierarchical Holographic Modeling. *Risk Analysys*, Vol. 22, No. 2, 383-397 (2002)
6. Yacov Y.Hames.: *Risk modeling, assessment, and management*. New York: Wiley. (1998)

An Efficient Method for Creating Requirement Specification of Plant Control Software Using Domain Model

Masakazu Takahashi^{1,2}, Kazutoshi Hanzawa¹, and Takashi Kawasaki³

¹ Shimane University, 1060 Nishikawatsu, Matsue, Shimane, Japan
masakazu@cis.shimane-u.ac.jp

² Galaxy Express Corporation, 18-16-1 Hamamatsucho, Minato-ku, Tokyo, Japan
hanzawa@galaxy-express.co.jp

³ New Energy and Technology Development Organization, Muza Kawasaki,
Central Tower 19F, 1310 Omiya-cho, Saitama-ku, Kawasaki, Kanagawa, Japan
kawasaki@nedo.go.jp

Abstract. This paper proposes an efficient method to create requirement specifications for Plant Control Software (PCSW) using domain model. Prior to the achievement of this method, we have conducted domain analyses of existing PCSWs and classified their functions into "similar functions" and "individual functions", and then we have developed PCSW Software Components (PSCs) that correspond to these functions. We also have developed a support environment for creating requirement specifications. As the result of applying our model to PCSW developments, the amounts of time required for creating requirement specifications have been reduced by 55.0[%]

1 Introduction

A plant is mechanical facility for manufacturing chemical products or processing materials. The software to control and assist operations of plants is called Plant Control Software (PCSW). A plant and PCSW are developed normally based on the purposes and the specifications determined by the customer and the plant developer. In the development process of PCSW, the customer and the PCSW developer hold requirements review meetings and fix the requirement specification of the PCSW. In principle, the fixed requirement specification does not need to be modified. In actual PCSW developments, the modifications often arise, because there are some lacks about customer's PCSW requirements.

The modifications result in the problems such as the deterioration in PCSW quality, the prolonged development period, and the cost increase. In order to create a requirement specification that fully reflects customer's requirements, prototype method is effective. This paper proposes a method to create PCSW requirement specifications efficiently by: analyzing PCSW domain, developing domain model (include PSC); composing PCSW prototypes from the components; and reflecting the result of behavior check to the requirement specification.

2 Evaluation of Existing and Proposed Method

Section 2.1 describes evaluation of existing methods for creating requirement specifications, and section 2.2 describes the outline of our proposed method.

2.1 Evaluation of Existing Methods

We clarify advantages and disadvantages of typical methods. The CASE [4] has advantages such as "it is well standardized", while it has disadvantages such as "it is difficult to master". The algebraic specification [2] has advantages such as "it can strictly define the targeted problems", while it has disadvantages such as "it is difficult to image the behavior of the target." The prototyping [3] has advantages such as "it facilitates understanding the requirements for the software by visualizing its behavior ", while it has disadvantages such as "the development of prototype increases the development period and cost". The domain model [6] has advantages such as "it promotes the efficiency of development by using the organized effective information", while it has disadvantages such as "an applicable domain model may not be exist" and ". Each method has both merits and demerits and it is difficult to apply to creating PCSW requirement specification.

2.2 Proposed Method for Creating PCSW Requirement Specification

Since customers don't clarify requirements for PCSW, requirement specification cannot be perfectly finished. Prototyping method is effective for clarifying their requirements. However, creating prototypes places a burden on the development team. Therefore we conducted domain analysis for PCSW, and develop PCSW software components (PSC) for prototype. And assembles PSCs into PCSW prototype. Although the functions of PCSWs are different in detail, we do not have to actualize these detailed functions because it is important to clarify the functions of PCSWs when creating requirement specifications. Applying this nature, our method enables us to efficiently compose PCSW prototypes.

3 PCSW Development Method Using Domain Model

Section 3.1 describes the results of the domain analyses, and Section 3.2 gives the proposed method and the support environment for creating requirement specifications.

3.1 Development of PCSW Domain Model

We make analyses on PCSWs. [5, 7] We clarify the functions required for developing PCSW. Table 1 summarizes the result of analysis. The result indicates that PCSWs consist of the following eight functions.

1) Execution management function.

This function activates the other seven functions with the appropriate methods, sequences, and cycles. The functions can be activated cyclically or with interruption. Since the cycles of seven functions are vary, we develop a execution management PSC, which takes parameters to configure the cycles.

2) Sequence control function.

This function controls the motions of sequence control devices and outputs the operational commands to the devices in the pre-determined sequence. We develop a PSC that corresponds to the sequence control function, which takes parameters to configure the sequences of device operations.

Table 1. Configuration of PCSW Functions

| Function | Feedback Control Machine Function | Common Functions used for both Feedback Control Machine and Sequence Control Machine | | | | | | | | | | | |
|---|-----------------------------------|--|---------------|------------------|---------------|-------------------|----------------------|---------------------------------|----------------|------------------------------|---------|------------------|--|
| | | Sequence Control Machine Functions | | Sequence Control | | Input/Output | | Command Transmission/ Reception | | Data Transmission/ Reception | | Trouble Shooting | |
| Plant Name | Feedback Control Machine Function | Execution | Plant Control | Digital Output | Analog Output | Command Reception | Command Transmission | Data Editing | Data Reception | Inspection | Scaling | Emergency Stop | |
| Terminal control system equipped in space station | X | X | X | X | X | X | X | X | X | X | X | X | |
| Material supply terminal system equipped in Space Station | X | X | X | X | X | X | X | X | X | X | X | X | |
| Aircraft engine control unit | X | | X | X | X | X | X | X | X | X | X | X | |
| Fan turbine to generate power Supply | X | | X | X | X | | | X | X | X | X | X | |
| Tank pressure control unit | X | X | | X | X | | | | X | X | X | X | |
| Vehicle position detector | X | X | X | | | X | X | | X | | | | |

3) Feedback control function.

This function controls the motions of feedback control devices. It calculates and outputs the required amount of operations from the difference between target and current states of the controlled devices. We develop a PSC that corresponds to the feedback control function, which takes parameters to configure the target state, the input/output data, and the control factors.

4) Plant control function.

This function controls the entire plant by coordinating the sequence and feedback controls. We develop a PSC that corresponds to the plant control function, which takes parameters to configure the timings and the triggers for the coordination.

5) Input/output functions.

The input/output functions consist of the function to input data from sensors and the function to output data to devices. These functions deal with analog and digital data. We develop four types of PSCs that corresponds to the input/output function: the analog and digital input PSCs with the input parameters and the analog and digital output PSCs with the output parameters.

6) Data transmission/receipt functions.

The data transmission/receipt functions consist of three functions: the function to receive data from other systems via networks, the function to transmit data to the other systems, and the function to format the data. We develop three types of PSCs: the data transmission PSC, the data receipt PSC, and the data edit PSC that take parameters to configure the data formats for the transmission and receipt.

7) Command transmission/receipt functions.

The command transmission/receipt functions consist of three functions: the function to receive command from the control table and other devices via networks, the function to transmit command to the control table and other devices, and the function to make responses to the received commands. We develop three types of PSCs: the command transmission PSC, the command receipt PSC, and the command process PSC that take parameters to configure the command formats for the transmission and receipt.

8) Troubleshooting functions.

The troubleshooting functions consist of three functions: inspection, safing, and emergency stop. We develop inspection PSC, which takes parameters for the input data, the safety standard, and the error codes. We don't develop safing and emergency PSCs, because their operations are different for each plant.

Figure 1 shows the PSCs we have developed in accordance with the above development policy.[1] The squares with solid lines represent parameter style PSCs, and the squares with broken lines represent PSCs for the individual functions.

3.2 Creating Requirement Specifications Using Domain Model

Figure 2 gives an outline of the method for creating requirement specifications using PCSW prototypes. In step 1, we collect information about a PCSW and organize the required information for composing the prototype. In step2, we compose the prototype by setting the information to PSCs as the parameters. In step3, we check the behavior of the prototype. When we find a lack or an un conformity, we goes back to the step 1 and re-organize the required information. We repeat the steps 1 to 3 until the behavior of the prototype satisfies the customer's requirements. Then, in step 4, we create a PCSW requirement specification from the design information of prototype.

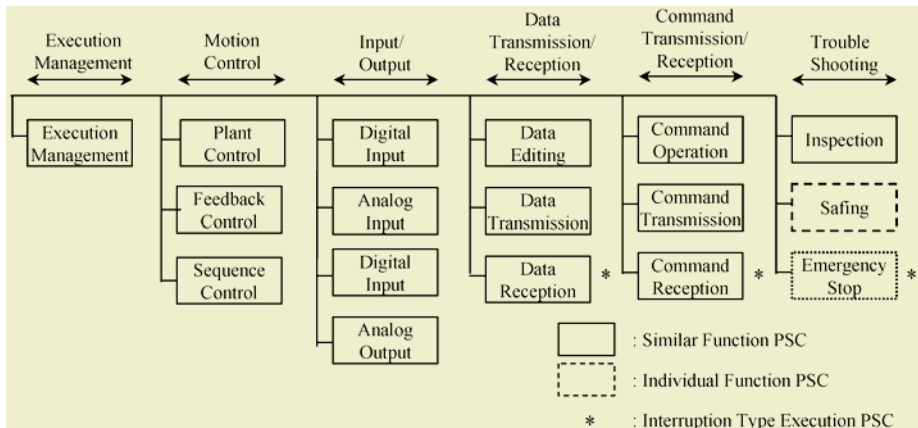


Fig. 1. Configuration of Developed PSCs

We have developed following tools to promote the efficiency of above procedure.

1) Prototype Development Tool (PDT)

When we compose PCSW prototypes, we need to customize PSCs by giving them parameters. PDT is a tool to assist the determination of those parameters.

2) Behavior Check Simulator (BCS)

BCS simulates the behavior of the PCSW prototypes on the computer to check the requirement specifications and detect the potential requirements.

3) Requirement Specification Developing Tool (RSDT)

RSDT facilitates the creation of requirement specifications from prototypes. It transcribes the parameters to the prepared templates for requirement specifications.

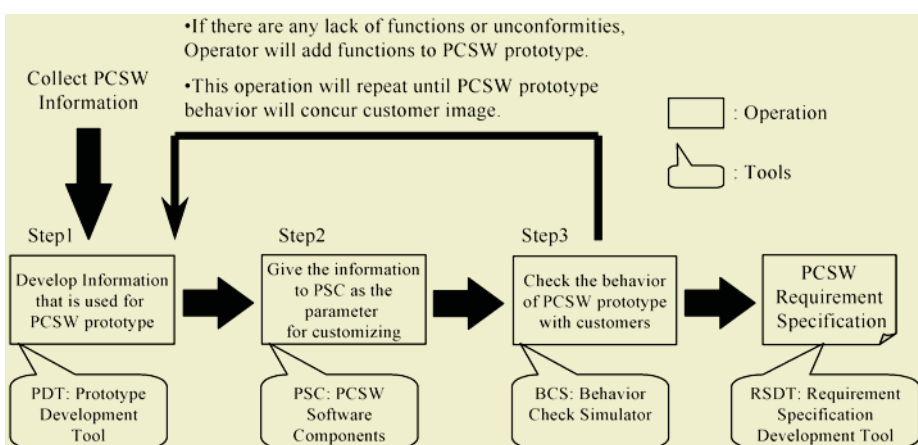


Fig. 2. Procedure for creating requirement specification from PSCs

4 Evaluation of Proposed Method

In this chapter, we explain the result of applying the proposed method to the actual cases, and we describe the evaluation of the method.

4.1 Results of Applying Proposed Method

We have applied the proposed method to five cases. Table 2 shows the result of applying the proposed method. Table 3 shows the amounts of time required for creating PCSW requirement specifications. Each amount is represented as a total number of hours required from the beginning of the requirement analysis to the completion of the requirement specification.

Table 2. Result of applying PSCs

| Plant Name | Reuse | | | | | | | Developed | |
|------------|----------------------|---------------|------------------|------------------|---|-------------------------------|---|--|------------|
| | Execution Management | Plant Control | Feedback Control | Sequence Control | Analog Input EU Conversion, Analog Output | Digital Input, Digital Output | Data Transmission, Data Receipt, Data Edit, Command Trans/Recep | Command Transmission, Command Receipt, | Inspection |
| A | 1 | 1 | 2 | 3 | 3 | 2 | 6 | 1 | 2 |
| B | 1 | 1 | 0 | 1 | 3 | 2 | 6 | 0 | 1 |
| C | 1 | 1 | 1 | 1 | 3 | 2 | 6 | 1 | 1 |
| D | 1 | 1 | 0 | 6 | 3 | 2 | 6 | 1 | 2 |
| E | 1 | 1 | 2 | 6 | 3 | 2 | 6 | 1 | 2 |

Table 3. Amount of time required for creating requirement specifications

| Plant Name | Not Applying Proposed Method | Applying Proposed Method | Not Applying / Applying [%] |
|------------|------------------------------|--------------------------|-----------------------------|
| A | 201 | 84 | 41.8 |
| B | 114 | 56 | 49.1 |
| C | 84 | 38 | 45.2 |
| D | 92 | 44 | 48.1 |
| E | 177 | 72 | 40.7 |

4.2 Evaluation

1) Evaluation based on PSC reuse rate

We evaluate PSC reuse rate, which is defined as:

$$\text{PSC Reuse Rate} = (\text{Reused PSCs}) / (\text{Reused PSCs} + \text{Newly Developed PSCs}) \quad (1)$$

Using data in Table 2, the PSC reuse rate of each application cases is 90.5, 93.3, 94.1, 90.9, and 91.7[%] respectively and the average rate is 92.1[%]. Consequently, this result indicates that it is possible to compose the major parts of PCSW prototypes using the developed PSCs.

2) Evaluation of the possibility to reduce the amount of time required for creating PCSW requirement specifications

As shown in Table 3, the proposed method reduces the amounts of time required for creating PCSW requirement specifications by 58.2, 50.9, 54.8, 51.9, and 59.3[%] compared to the ones with the conventional method, and the average reduction is 55.0[%]. These reductions are significantly large and we consider that the proposed method is capable to reduce the amount of time required for creating PCSW requirement specifications.

5 Conclusion

This paper has proposed the efficient method for using domain model. The domain model consists of the PSCs and the support environment. As the result of applying the domain model to five cases of creating PCSW requirement specifications, we have achieved the PSC average reuse rate of 92.1[%]. As a consequence, we have succeeded to reduce the amount of time required for creating PCSW requirement specifications by 55.0[%]. This result indicates that the proposed method is able to significantly promote the efficiency of the creation processes and improve the competitiveness of plant manufacturers in PCSW developments.

Acknowledgement

This research is conducted as a part of "Basic Technology for Next Generation Transportation System Design", which is a delegation from New Energy and Industrial Technology Development Organization (NEDO).

References

1. J. DeBaud and K. Schmid: A Systematic Approach to Derive Scope of Software Product Lines, ICSE'99 Los Angeles CA, pp. 34-43, May 1999
2. H. Kobayashi, Y. Kawata, M. Maekawa, A. Kawasaki, A. Yabu and K. Onogawa: Modeling External Objects of Process Control Systems in Executable Specifications, Journal of Information Processing Society of Japan, Vol. 35, No. 7, pp. 1402-1409, July 1994 (in Japanese)
3. J. Martin: "Rapid Application Development", Macmillian Publishing Company, 1991
4. M. Matsumoto et. Al.: Specifications reuse process modeling and CASE study-based Evaluations, COMPSAC91, Proc. of the 15'th annual international computer software & applications, 1991
5. M. Matsumoto: "Modeling and Reuse of Software", Kyoritsu, 1996 (in Japanese)
6. M. Natori, A. Kagaya and S. Honiden: Reuse of Requirement Specification Based on Domain Analysis, Journal of Information Processing Society of Japan, Vol. 37, No. 6, Mar 1996 (in Japanese)
7. W. Tracz and L. Coglianes: Domain-Specific Software Architecture Engineering Process Guidelines, IBM Federal System Company, ADAGE-IBM-92-02, 1992

The Study and Application of Crime Emergency Ontology Event Model

Wenjun Wang¹, Wei Guo², Yingwei Luo^{1,*}, Xiaolin Wang¹, and Zuoqun Xu¹

¹ Peking University, Dept. of Computer Science, Beijing 100871, P.R. China
wenjunwang@263.net, {wwj, lyw}@pku.org.cn

² Tianjin University, Dept. of Computer Science, Tianjin 300072, P.R. China
guowei_phd@yahoo.com.cn

Abstract. Integrated Crime Emergency Response System (iCERS) is a large-scale spatio-temporal system which integrates all sorts of crime emergency service resources and major its features as common codes used for public emergency events reporting. The ontology for Crime Emergency Event Model (CE²M) is recommended as an effective means to implement semantic level integration. CE²M is stratified into three levels: Event, Process and Action. CE²M constructs the vocabulary and the common model for exchange of iCERS information, thus it becomes the common comprehension of each business sub-systems.

1 Introduction

Integrated Crime Emergency Response System (iCERS) is a large-scale spatio-temporal dynamic system, which integrates all sorts of crime emergency service resources and major its features as common codes and then combined action used for public emergency events reporting. In China, the first iCERS was run in Nanning city which is also going to be built up in other countries such as Beijing, Shanghai, Tianjin and Guangzhou etc. When some emergencies happen, every department will come to work together efficiently. The features of iCERS are distribution, isomery, mass storage and dynamic real-time. Also, iCERS is facing a series of challenges.

1. Multi-crime emergency response organizations integration is needed: The operations from different department are needed to be integrated together with possibly introduction of some semantic conflicts among these systems.
2. New or old emergency services from different workplaces are needed for integration dynamically in real time with large-scale and heterogeneous structure.
3. GIS is an important approach for practicing emergency direction and iCERS needs to have spatio-temporal information integrate.

Ontology [1] is an important strategy in describing semantic models, which provides common comprehension of domain knowledge, determines commonly recognized terminologies within certain domains, and implements properties, restrictions and axioms in a formulated way at different levels. Ontology thus gains the characteristic features to provide explicit terminology definitions to express inter-organizational event.

In this paper, relevant studies of event and event models are introduced firstly, and the basis of iEM – ABC Ontology Model ([2], [3], [4]) is analyzed in emphasis.

* Corresponding Author

2 Relevant Studies

2.1 Study of Event Model

Linguistics divides event statement into “Accomplishment Statement” and “Achievement Statement”. Terence Parsons [5] think that an event in the aspect of linguistics has 4 forms: Accomplishment Event, Achievement Event, State Event and Activity Event. Process, action and state [6] are other several concepts that are relevant to events. Simply say, there are 2 viewpoints in regard to comprehension of events: One is that events are composed of sub-events, but there may be no sequence relationship between these sub-events; another is that events (or event dispositions) are composed of a series of processes, which bear sequence orders. Currently, ABC Ontology Model presents an event-related common concept model.

2.2 Introduction of ABC Ontology Model

In the basic part of ABC Ontology Model, which is a result of NSF sponsored Harmony Digital Library project. Entity is the basic class and represents any entities. It has 3 subclasses: Temporality, Actuality and Abstraction to express time-related, noontime-related and abstract entities in the world.

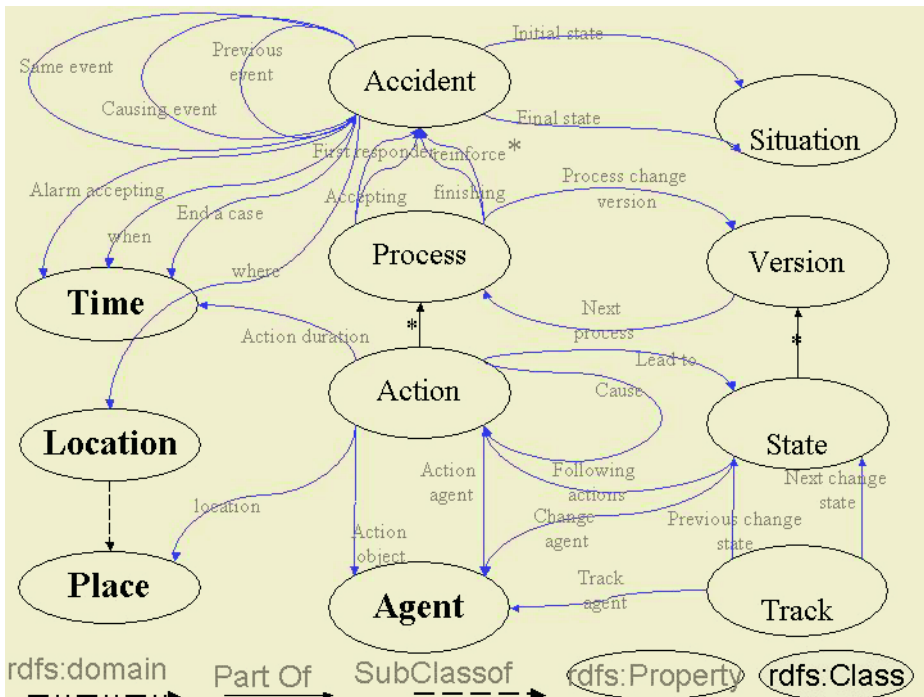
ABC Event Model describes event-related concepts as event, situation, action, agent, and their relationships. An event likes the transformation between situations. A Situation is a context, which is a predicate to the existential aspect of an Actuality. One or some Agents in the context of an Event can accomplish an Action. Agent can be people, instruments or organizations. ABC Ontology is a basic Ontology, which provides a basic model for domain-related or community-related development. But to describe inter-organizational events solely by ABC Event Model is not adequate:

- Event in ABC can not reflect interaction and coordination needed by inter-organizational requirement conveniently;
- ABC Event Model is not potent enough to express complex events which have level hierarchies and granularity divisions;
- ABC Event Model uses discrete Situations as the trigger mechanism, and reflects the change of Situations through Actions participating in Events. This may be redundant for the condition where continuous changes of states are caused by continuous actions of a same agent;
- ABC Event Model identifies consequence relationship between Events through atTime, precedes or follows properties. This way is not explicit enough when a complex event composed of sub-events with complex temporal relationship.

Based on above analysis, we propose Inter-organizational Event Model (iEM) to express the multi-level and multi-granularity features.

3 Crime Emergency Event Semantic Model CE²M

Accident is a process involving alarm, dispatching and disposition in all parts of iCERS. In comparison to ABC model emphasis on relationship between events, emergency event needs to determine details in events.

Fig. 1. CE^2M

3.1 Crime Event Ontology Model CE^2M

CE^2M is stratified into three levels: Event, Process and Action. Herein, event involving multiple processes is divided into pre-state and final-state. Pre-state can be inverted into final state. Furthermore, there are three relationships called precedence, identity and causality among events. Also, multiple spatio-temporal attributions are included in events. Process, including several actions, can produce change state versions. And precedence relationship exists between different processes. Finally, there are main body, acceptor, time and space in action producing change states. And precedence and causal relationship exist among actions as shown in Fig.1. Common terminologies for CE^2M are as follows:

1. Accident: Accident is a process from crime-accept to treatment or finishing hand-over. Situation involves Prestate and final state which can be inverted with each other through event. Event is a spatio-temporal model including occurring time, alarm-accepting time, finishing time and some geographical factors such as accidental spots. The relationships among events can be classified into three types as follows:
 - Precedence relationship: Several response units are dispatched for one event and relationship among events from every response-dispatching center is precedence.

- Casual relationship: one event happens because of another. So the relationship between these two events is causality. Here event introducing is used to show the meaning.
- Time-sequence relationship: one event happens behind another to show time sequence relationship. Here pre-event is used to describe.

Accident is made up of process of alarm accepting, attacking at first, several follow-ups and closing and removing event.

2. Process: The definition of process is operational actions that, to some certain spatio-temporal range, a series of action is taken in order to gain the ends. E.g., alarm-accepting process is action so that police acceptor is going to gain accurate location and situation. It involves actions such as policeman inquires the people call the police or search for information from system database, etc. So, certain changes collection we often call Version includes a serial of state changes after a process. The result from previous change is input f or a determination or next process as shown below:

Initial state of event → P1 → V1 → P2 → V2 → ... → Process n → Final state of event
(herein: P ---- Process V ---- Version)

Every phase includes the start time, end time, middle location and several actions.

3. Action: Action is the activity at certain situation. Fire department governor determines to dispatch ten water trucks from Huanghe River to the spot for example. Action = name + main body + acceptor + context + time + location
Action is the smallest unit in model. Some actions have an effect on state to produce changes called changeable state. For instant, the place of pumper changes moving from fire station to spot. The relationships among actions are as follows:

- The relationship within one agent: there is contextual relationship in actions during process for one agent. For example, the fire-fighting group can produce one state change when it acts from “preparedness” to “movement”. At one time, it can move to another state “presence” which owns relationship with the previous state change.
- Causality in different agent actions. “Cause” can be used to depict that action 1 causes action 2. For example, director general calls for Coordinator to dispatch No.30 group to spot we can say below:

Act1: director general *command* coordinator Act2: coordinator *command* group 30

4. Situation: Situation is the real spot or state of emergency treatment capability at some time involving spatio-information, casualty and source consumption, etc. For example, state of emergency response power, situation in spot, alarm accepting machine, etc. On the other hand, situation is also snapshot that it reflects all the information and states of spot or emergency response power at some stage.
5. Version: Version is the collection of change increment which indicates that all the changes happen after certain process in spot or state of response power to all the changeable ones.
6. State: Change state shows the changing increment in spot after certain action, or some changes happen in response power after such action.
7. Track: Track indicates that detail of continuous changes among changeable states produced by previous and next action of spot or only one agent.

3.2 Example

3.2.1 Hypothetical Scene

This case builds on the hypothesis that “At 09:45, March 15th, 1998, Crime Emergency Center of City DongFang received the alarm from citizens who reported that a heavy-duty truck hit to the residential building located on No. 1, Street Lin, No. 40, Road Xinxin at 09:40. Due to the occurrence of traffic accident, the Center requires the sending of traffic police. While later it was also reported that due to the same accident, the involved building suffered a serious fire with great casualty. The committed truck was one stolen while the conductor –the thief had run away. The integration scheduler then commands the fire-control scheduler, the medical first-aid scheduler and the police scheduler to perform their respective responsibilities. What made the worse, some reported that electrical wires at No. 30 Road Shiji were disjoined.” In the following, joint response of 110, 120, 119 is taken as the example to illustrate event disposition, as shown in Figure 2.

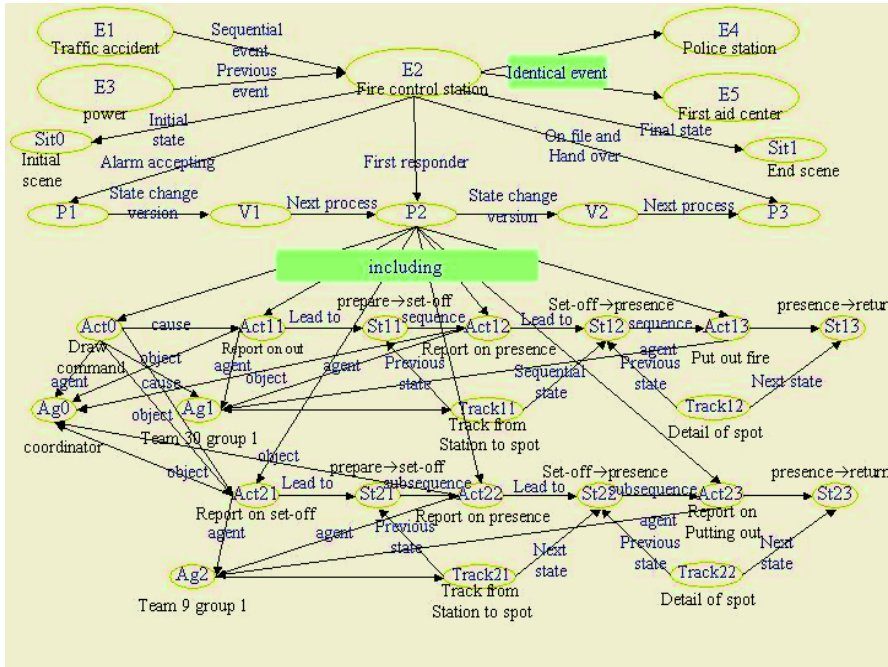


Fig. 2. CE²M example

3.2.2 IEvent Level

Given the hypothetical scene above, it is concluded following events:

E1: Traffic accident E2: Fire control department

E3: Event of rushing to repair power E4: Call for escaped criminal E5: First aid

E1 Causes E2, E4, E5, E2 happens after E3, E2, E4, E5 are identical event

E2's Initial scene: Third level of fire in spot with one heavy injured people

E2's Final scene: Fire is put out and there are two heavy injured people

3.2.3 Process Level

E2 includes three processes: Alarm-incept, First Set-off and Documentation. These processes happen in time sequence.

Accepting alarm → Version1 → First Set-off → Version2 → Documentation

Version1: Third level fire Version2: Team9group1 and team30group1 in battle

3.2.4 Activities Level

Table 1. Details of the activities are list as follows

| | Action name | Action agent | Action object | Cause | Change state | Consequent action | Track |
|-------|-----------------------|-----------------|----------------------------------|------------------|------------------------|-------------------|----------|
| Act0 | Command is given | Coordinators | Group 30team 1 Group 9 team 1 | Act11 Act21 | | | |
| Act11 | Report on set-off | Group 30 Team 1 | Coordinator | | Preparedness → out | Act12 | |
| Act12 | Report on presence | Group 30 Team 1 | Coordinator | | Drawing out → presence | Act13 | Track 11 |
| Act13 | Report on out of fire | Group 30 Team 1 | Coordinator | | Presence → return | | Track 12 |
| Act21 | Report on drawing out | Group 9 Team 1 | Coordinator | | Preparedness → out | Act22 | |
| Act22 | Report on presence | Group 9 Team 1 | Coordinator | | Drawing out → presence | Act23 | Track 21 |
| Act23 | Report on out of fire | Group 9 Team 1 | Coordinator | | Preparedness → return | | Track 22 |
| Place | | | | Fire is put out. | | | |

Track11, Track12, Track21, Track22 are used to show the details of actions.

3.3 The Characteristic Features of CE²M

1. To show the dynamic features of objective world, the way of integrating space with time by event make it rich for semantic information in spatio-system.
2. Emphasis On Making the Detail of Internal Changes in Event, but Also Show the Relationship among Events.
3. To Show Continuity of Gradual and Continuous Changes in Event Hierarchically.

It follows that variance points from situation, version and state can be used to describe continuity of event change. Thus, expression “track” is introduced to illustrate the continuous track for previous and next state from identical agent such as the track by pumper from place to spot.

4. Causality among Actions: There are two relationships to show causality in CE²M.

- One action can cause another. E.g., the action “asks for leader” can “lead to” action “make command”. This indicates that the coordinator makes command to move fire team to spot after asking for leader. Thereinto, the agent in action is different.
- One cause may “lead to” change in state. And another action happens following last change. The agent of these two actions is the same agent. It likes making

group in fire control for example. Action” report on Set-off” →State”Set-off” →Action “report on presence”. The entity is firehouse team for action and state above.

3.4 The Effect of CE²M

The prime functions of emergency response system are list as follows: (1) To solve problem of terminologies communications among subsystems. Information in different areas can be exchanged to achieve semantic mutual-operation. (2) To achieve system integration. The same event can be treated in different area and police, this is, emergency response. (3) To search multiple resource including event search, event detailed query or relationship search based on spatio-temporal model.

4 Application of CE²M

The setup of CE²M can deal with conflicts very well being produced by information exchange in different areas and different systems can be effectively integrated.

1. Before event: Emergency preparedness is described by CE²M to achieve adjustment of multi-operation automatically.
2. During event: Response dispatching and application integration is being done during event treatment.
3. After event: Response files several sections produced are piled up and combined altogether which is saved for later evaluation.

5 Conclusions

Based on experience in emergency response field for many years, we come up with response system model and Ontology semantic model which uses Protégé 2000 by standford. Also, query on ontology is achieved successfully by Jena in HP lab. And we have already established iCERS operation model, UML model, event vocabulary and OWL expression in CE²M. And now, response system of 110, 119, 120 based on CE²M in Tianjin is being integrated into frame following PAI systematically.

References

1. T. R. Gruber: A translation approach to portable ontology specifications, Knowledge Acquisition, 5(2): 21-66(1998).
2. M.Doerr, J.Hunter, C. Lagoze: Towards a Core Ontology for Information Integration, Journal of Digital Information, 4(1), 2003.
3. C. Lagoze, J.Hunter: The ABC Ontology and Model (Version3), Journal of Digital Information, Special Issue - selected papers from Dublin Core 2001 Conference.
4. J. Hunter, C. Lagoze: Combining RDF and XML Schemas to Enhance Interoperability between Metadata Application Profiles, The Tenth International World Wide Web Conference, Hong Kong, 2001.
5. Terence Parsons: Events in the Semantics of English, MIT Press, 1990.
6. Kate Beard-Tisdale: A Review of Perspectives on Processes and Events,
<http://www.spatial.maine.edu/~bdei/BDEIevent.pdf>, 2002.

From Links to Meaning: A Burglary Data Case Study

Giles Oatley¹, John Zeleznikow², Richard Leary³, and Brian Ewart⁴

¹ University of Sunderland, School of Computing and Technology, Sunderland SR6 0DD, UK
giles.oatley@sunderland.ac.uk

² Victoria University, School of Information Systems, Victoria 8001, Australia
john.zeleznikow@vdu.edu.au

³ University College London, Department of Statistical Science, London, UK
leary@stats.ucl.ac.uk

⁴ University of Sunderland, Division of Psychology, Sunderland SR6 0DD, UK
brian.ewart@sunderland.ac.uk

Abstract. Our central aim is the development of decision support systems for purposes such as profiling single and series of crimes or offenders, and matching and predicting crimes. This paper presents research in this area for the high-volume crime of Burglary Dwelling House, examining the operational use of networks and the metric of brokerage from the social network analysis literature. Our work builds upon several years of experimentation using forensic psychology guided exploratory techniques from artificial intelligence, statistics and spatial statistics.

1 Introduction

The graph is one of the most thoroughly researched data structures in computer science and mathematics. A host of well-known algorithms exist within graph theory, for instance searching through the vertices of a graph, finding the shortest path between two vertices, or determining a ‘spanning tree’ whose edges connect (i.e., span) all vertices of the graph.

Within data mining, there has recently been great interest in the developing fields of *graph-based data mining* [17] and *link mining* [4] - also known as link discovery or link analysis. This is in large part due to the creation of the United States Homeland Defence Agency, and as a consequence of the Acts of Terrorism on September 11 2001. There has been a rapid increase in commercially available products that claim to perform link mining, and academic interest in this area is borne out by two recent conference workshops, namely *Link Analysis and Group Detection* at KDD-2004 (the 10th ACM SIGKDD International Conference on Knowledge Discovery and Data Mining) and *Text-Mining and Link-Analysis* at IJCAI-2003 (the 18th International Joint Conference on Artificial Intelligence). Link mining encompasses a range of tasks including descriptive and predictive modelling [11]. Both classification and clustering in linked relational domains require new data mining algorithms. But with the introduction of links, new tasks also come to light. Examples include predicting the numbers of links, predicting the type of link between two objects, predicting link strength and link cardinality, inferring the existence of a link, inferring the identity of an object, finding co-references are all examples of link analysis.

The method used in this paper that operates over graphs (networks) created from links is the social network analysis (SNA) technology of brokerage based upon the

point centrality concept termed *betweenness*. This concept measures the extent to which a particular point lies ‘between’ the various other points in the graph: a point of relatively low degree may play an important ‘intermediary’ role and so be very central to the network. The betweenness of a point measures the extent to which an agent can play the part of a ‘broker’ or ‘gatekeeper’ with a potential for control over others.

Of course how the links or associations – the basis for the ‘network’ - are created in the first place will have the most significant impact on the interpretation of results. And this is what is not really taken into consideration when employing the sophisticated SNA method of brokerage (or network reduction, clustering, etc). Experiments with these technologies are relatively easy to conduct, using available toolkits, however the results can be extremely misleading. For instance police officers and crimes analysts may well use some of the following list of software: **COPLINK** [6] suggests central members in a given subgroup, using the measures of *degree*, *betweenness*, and *closeness*; **FLINTS** - ‘Forensic Led Intelligence System’, conceived and developed by Leary [11], integrates diverse data sources, including both ‘hard’ (DNA, fingerprints, footwear and tool-marks) and ‘soft’ (behavioural) forensic data to give police officers the ability to build a graphical pattern of links between crimes and criminals; **I2’s Analyst’s Workstation** [8] *PatternTracer* module is aimed at locating calling patterns in telephone records; **FinCEN** [5] finds links to identify money-laundering networks; **Advanced Information Technologies** [1] *CADRE* performs link and relationship analysis; the **Link Discovery Tool** [7] organises data into clusters based upon associations and uses graph analysis techniques. However, given recent acknowledgement of different kinds of networks, a generic network approach will have limited policing value. For example, centrality measures from social network graphs may identify ‘key players’ and are useful for certain policing objectives. They are less valuable when depicting covert threat groups which may be incomplete due to missing actors (vertices) and links (edges) that investigators may fail to uncover. As Klerks [10] says, “*there isn’t such a thing as ‘the’ social network analysis approach: about the only common element among the different varieties is the conviction that it is useless to explain human behaviour or social processes solely through categorical properties and norms of individual actors. Instead, the emphasis is on their functioning within structured social relations. Individual behaviour is always seen in relation to the behaviour of the groups which a person is part of. In brief, a person manifests itself in a socially relevant way primarily in his or her relationship to others, and therefore these relations deserve careful and systematic scrutiny.*”

The authors work in this area [3,14,15], in collaboration with West Midlands Police (WMP), is with the high volume crime of Burglary from Dwelling Houses (BDH). The focus of our research has been to develop techniques and a sound methodological framework for crime matching and prediction, and integration of evidence for such purposes. Innovative work includes the use of Bayesian belief networks for prediction of crimes, integrating as many evidence sources as determinable – concerning the offender, victim, time of crime, specific location of crime, general area of crime, and behavioural (*modus operandi*) features.

The use of arrest data in combination with geographical and temporal data is a significant departure from other methodologies which use/weight/combine data such as mobile phone records etc. To this end, this paper is about the potential and the ability

of various technologies that operate over networks or graphs to provide decision support, setting out some of the limitations and issues of a networks approach from an artificial intelligence perspective. Next generation social network analysis must focus much more intensely on the content of the contacts, on the social context, and on the interpretation of such information [10]. To this end Lyons and Tseytin [12] proposed an *a priori* expression of facts that may be used to infer *phenomena* from links, and while the situation calculus they used may not be to everyone's taste, research along these lines is required. We show how adding in a geographical component (not present in other approaches) and then a temporal and frequency component can add to the interpretation of the network and its key players, illustrating the pitfalls of using sophisticated social sciences methods without an understanding of the phenomena or meaning behind the links.

2 Burglary Arrest Data Networks

2.1 Explanation of Data

The networks and geographical outputs presented below are derived from 342 offenders who committed 1121 crimes, representing the time period 1997-2001. The network links are based upon whom the offender was arrested with for a particular crime and the geographical location of that offence. This represents a significant departure from previous methodologies in that links are on the basis of an established (albeit not proven in court) co-defendant relationship. Other approaches using mobile phone records or police intelligence employ such data to infer a criminal relationship. Here, there is little ambiguity. One advantage of this approach is that all police forces have arrest data on individuals and crime location information. They do not have to mount expensive surveillance operations or access phone records in order to apply the approach described here.

One reservation concerning the outputs presented is that links are on detected rather than unsolved crimes, which means the extent of the network and its range may be an underestimate. However, the point is to illustrate the potential of such an approach and even these outputs provide important policing information on the offending range of the respective clusters. If date of the crime were added to this methodology, this temporal information (again routinely collected by police) would allow more substantive questions about the characteristics of networks to be explored (see comments below).

2.2 Brokerage and Spatial Density

The following results were conducted with the PAJEK software [2], using the SNA method of brokerage. The experiments used reduction of network size to a new network of 145 nodes ($\text{degree} > 4$). The results contained many small sub-networks of size 2, 3 or 4 nodes, and two much larger sub-networks, which are presented in the figures 1 and 2. The diagrams are overlaid with a spatial density representation, or *kernel density estimation*, smoothing that results in a crime 'contour' map (described in: [14]). Comments use the orientations 'northwest', 'southwest' etc in relation to the centre point of the figures.

Figure 1 shows offender #298 receiving the highest ‘brokerage’ value of 11, higher than #169 by merit of being a ‘gatekeeper’ to a greater number of vertices. Offender #104 receives a very low value, because it provides no ‘new information’ as #298 and #169 are already linked. In a similar fashion figure 2 illustrates the workings of the brokerage algorithm, with offender #171 receiving the highest value by virtue of gatekeeping.

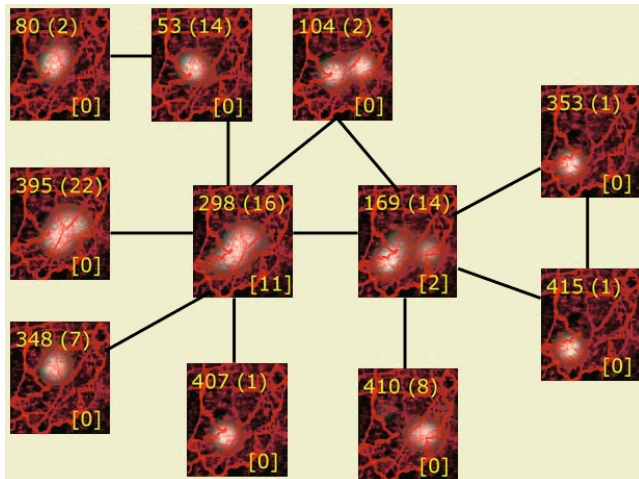


Fig. 1. Brokerage analysis: sub-network 1. The top-left figures are unique offender identifier, with total number of crimes in brackets. The bottom-right figure is the brokerage value

It can be seen quite clearly that the brokerage model accurately reflects offender #298 connecting the centre and northwest areas (#80, #53, #395, #348) with the southwest areas (#407). Also, the total offences that can be uniquely reached through #298 number 46, in comparison to #169 numbering 10. This would agree with #298 receiving a higher brokerage value than #169. What is not reflected however, is that we would wish #169 to receive a higher value as it is gatekeeper to #410 with 8 crimes in the southeast area, a unique offender by right of area of operation. Similarly #169 is gatekeeper to a much wider geographic range of offenders: #104 in the east; #353 and #415 in the southwest area; and, #410 in the southeast. Offender #298’s connections only lie within the centre and slightly to the northwest. We would wish then that weightings were taken account of in the brokerage calculation (reflecting number of crimes committed between offenders), and also that the notion of criminal range [13] was given suitable emphasis.

Figure 2 reflects the larger brokerage network, with the nodes of degree 1 (brokerage values of zero) removed for clarity. Analysis of this diagram is more complicated, however again it demonstrates that it does not reflect other important factors we would like to incorporate. It is clearly not so easy to justify #171 receiving the highest brokerage value. Other equally interesting offenders are: #254 because of number of crimes associated with them and the fact that they operate not only in the northwest but also in the southwest; #246 because of the large area of activity; #254 and #323 because they both have a very high number of crimes.

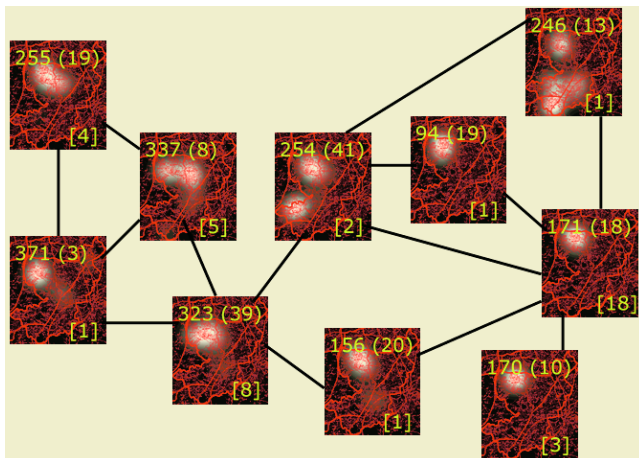


Fig. 2. Brokerage analysis: sub-network 2. The top-left figures are unique offender identifier, with total number of crimes in brackets. The bottom-right figure is the brokerage value

It is important to note that because the original network has been reduced to nearly half its size, nodes that appear to have degree 1 may in fact have several other links, and be reachable from other nodes. This however would also be the case with a ‘full’ arrest dataset being used – many crimes are unsolved, and many relationships will not be reflected in the data.

A further concern is that the outputs are generated at the end of the time frame of criminal activity. In this way, ‘time’ is a confounding and even confusing variable when attempting any interpretation of the relationships between the key players in a network and their spread of criminal activities. For example, offender #171 is a key player in figure 2 and linked to #246. However, their respective patterns of offending are very different. Only by examining the evolution of their respective patterns over time, can we even begin to consider if #246’s greater spread was associated with, for example, the arrest of #171. Or whether #246 has always been a ‘commuter’ and ‘maurades’ [see 16] only when #171 is around. With temporal and geographical knowledge we can make some assertions about whether #246’s activities are due to criminal drift, ‘foraging’ [see 9] or #171’s absence. We can also say much more about the role of #171 in respect of how they are linked to others in the network. Furthermore, we can say much more about the value (or otherwise) of the integration of geographical and spatial data and it is at this point, that policing value is maximised.

2.3 Temporal and Frequency Analysis of Links

To explore the meaning of the links more fully we now present the same data with the links qualified with the dates of the crimes forming the links. Figure 3 shows the sub-network from Figure 1 with this additional information – for instance the link between offenders #80 and #53 is a result of a single crime committed together on the 1st August 1998, and the link between offenders #395 and #298 is a result of two crimes committed together on the 29th September 1999 and the 20th December 1999. By examining this same network data we can understand offender behaviour in a

more complete way. For instance this view of the data now reduces in emphasis the brokerage values because it can be seen that each link is mostly due to just one crime. The original interpretation of the brokerage network is also lessened by the fact that the sub-networks of {#353,#415,#169} and {#298,#169,#104} are due to *single crimes*, as the dates (and crime references - not shown) are the same.

Examining the larger brokerage network in the same manner (see Figure 4) results in a similar observation - that the brokerage values are again reduced in emphasis because of many of the links being caused by single crimes. The nodes of the earlier brokerage network (Figure 2) are marked with crosses, and also included are additional nodes which were screened out because of their low brokerage values. For instance offender #285 has committed 6 crimes with offender #255, and also one crime with offender #337. It is clear then that this offender deserves attention in any analysis of the data.

To be convicted for two crimes unlike one crime shows the beginning of co-defendant relational strength, conditions under which a network approach has most validity. Now we can consider that the brokerage calculation is better justified as the links between offenders #255 and #337, #337 and #371, #371 and #323, #323 and #254, #94 and #171, #171 and #170, are all two-crime links. These links were considered important in the brokerage calculation, constituting the main paths between the offenders with higher brokerage values. Now we can see that the activity between offenders #171 and #246 is much less important as it is a single-crime link.

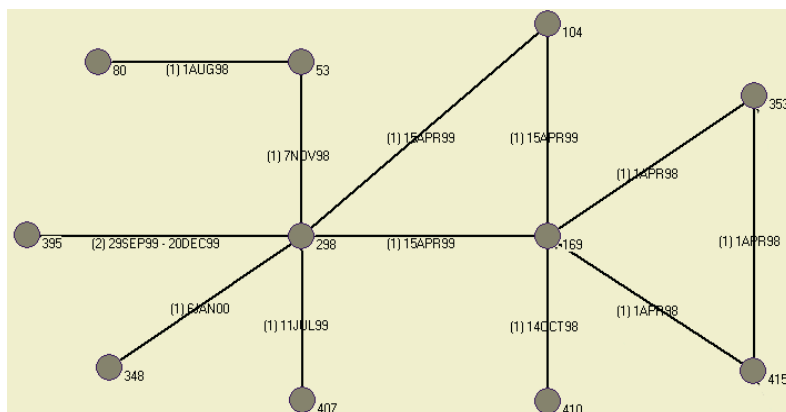


Fig. 3. Temporal and frequency analysis: sub-network 1. Nodes are labeled with the offender unique reference number, and links are labeled with the number of crimes committed together by both parties and a list of dates of those crimes

The remainder of the temporal and frequency analysis results contained 27 two-node networks with single-crime links, 2 two-node networks with two-crime links, 8 three-node networks from a single crime (see Figure 5 for an example), and three four-node networks. Figure 6 is shows a three-node network from four crimes, and interesting because all four crimes are committed by all four criminals. Figure 7 shows the pairs of offenders who have committed the most crimes together (5 and 6 crimes) indicating the highest co-defendant relationship, not revealed by the brokerage calculation.

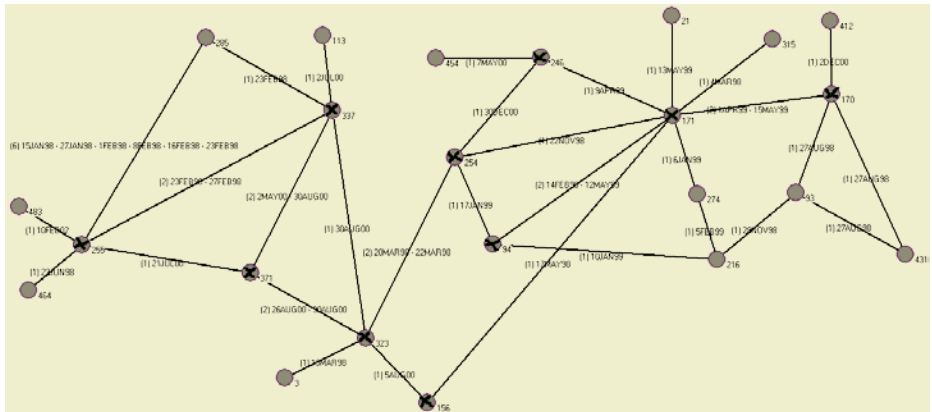


Fig. 4. Temporal and frequency analysis: sub-network 2. The nodes marked with crosses are those from Figure 2. The additional nodes are those that were screened out because of their low brokerage value

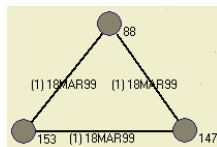


Fig. 5. Single crime network

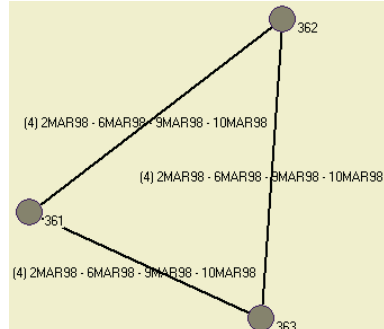


Fig. 6. Four separate crimes network

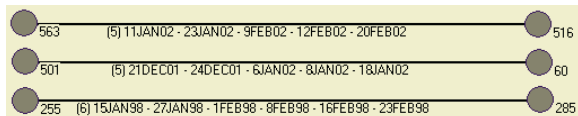


Fig. 7. Highest joint offending counts

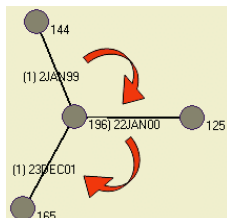


Fig. 8. Successive crimes – three separate crimes network

The most interesting sub-networks are shown in figures 8 and 9. Figure 8 shows #196 committing three crimes with three separate offenders. The dates are very interesting as there is roughly one year gap between the first and second crimes, and two years gap between the second and third crimes. This is therefore a very different sub-network to that of Figure 6, where all the four crimes are committed in less than 2 weeks. This strongly indicates potential problems in analyzing the brokerage results

without consideration of the meaning of the link. Possibly offender #196 has moved away from the area during the intervals, engaging in criminal activities elsewhere, or perhaps they have been in prison. Finally the sub-network in Figure 9 is again quite different in character, with offender #429 commits crimes firstly with #380, then a few days later with #179, then 2 days later with #380 again, and then finally all four offenders commit a crime together. This is representative of a developing network of criminals.

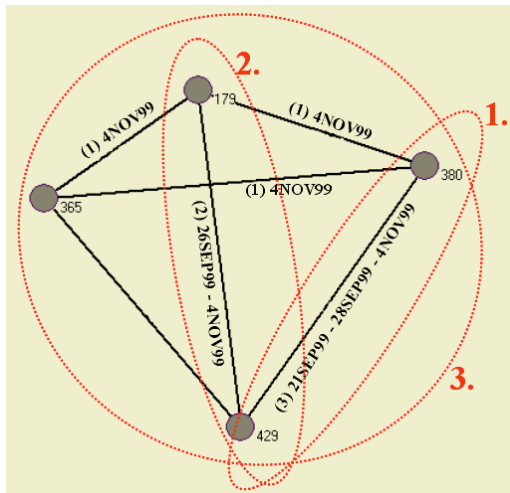


Fig. 9. Evolving network - three separate crimes network

3 Conclusions and Future Directions

This paper has presented a background to current research in criminal networks, and examined an analysis of the SNA metric of brokerage, by means of burglary arrest data known to the authors. As we are interested in testing models or theories about criminal patterns it is felt that the integration of temporal, spatial and network analysis has great potential. Our earlier work has investigated the integration of available evidence for crime matching and predicting, and the work presented in this paper outlines some of our current ideas towards integrating these additional sources of evidence.

The brokerage metric is very useful, however it is clear that in the case of burglary it needs to be balanced with spatial data. Consideration of the temporal and frequency analysis of the crimes constituting the links will provide a better understanding of the nature of the links, and may indicate important links that are not considered important by the brokerage metric.

All of these analyses are easy to perform and in an operational setting a police officer would find these diagrams very useful in understanding data which is otherwise put to merely administrative purposes. Additionally the diagrams would be useful for knowledge sharing, and training new police officers to the criminal activities in an area.

Any motivational assumptions or testing of offending/criminal range models is conditional upon having substantive knowledge about the temporal characteristics of the network and the criminal activities of the key players. Conceptual issues such as how a network develops will be explored in terms of their spatio-temporal and behavioural characteristics. The effects of various disruption strategies will be modeled and evaluated. As yet, no one has explored characteristics that delineate a passive network from one which is currently engaged in criminal activity. Such work would allow for better targeting of policing resources as well as the prediction of when a passive network will become active.

References

1. AIT, 2005. Homepage of Advanced Information Technologies. Online, accessed 5 January 2005. Available at:http://www.alphatech.com/primary/technologies/knowledge_discovery_data_mining/link_analysis_and_discovery.htm
2. Batagelj, V., & Mrvar, A. 2003. Pajek – Analysis and Visualization of Large Networks. In: Junger, M., Mutzel, P. (Eds.): Graph Drawing Software. Springer (series Mathematics and Visualization), Berlin 2003. 77-103. ISBN 3-540-00881-0.
3. Ewart, B.W., Oatley, G.C., & Burn K., 2004. Matching Crimes Using Burglars' Modus Operandi: A Test of Three Models. Forthcoming.
4. Getoor, L., 2003. Link mining: a new data mining challenge. In: S. Dzeroski and L. De Raedt (eds.), SIGKDD Explorations Special Issue on Multi-Relational Data Mining, July 2003, Volume 5, Issue 1, 2003, pp. 84-90.
5. Goldberg, H. G. & Wong, R. W.H 1998. Restructuring Transactional Data for Link Analysis in the FinCEN AI System in: D Jensen, H Goldberg eds. Artificial Intelligence and Link analysis. Papers from the AAAI Fall Symposium. Orlando, Florida, Tech report FS-98-01.
6. Hauck, R., Atabakhsh, H., Onguasith, P., Gupta, H., & Chen., H., 2002. Using Coplink to Analyse Criminal-Justice Data IEEE Computer, pages 30-37, Volume 35, March 2002
7. Horn, R. D, Birdwell, J. D., & Leedy, L. W. 1997. Link discovery tool. Proceedings of the Counterdrug Technology Assessment Center's ONDCP/CTAC International Symposium Chicago, IL. August 18-22.
8. I2 (2004). Investigative Analysis Software home page. [Online, accessed 2004] Available: <http://www.i2.co.uk/Products/Analysts%20Workstation/default.asp>
9. Johnson, S.D. & Bowers, K.J., 2004. The burglary as a clue to the future: the beginnings of prospective hot-spotting, The European Journal of Criminology, 1 (2), 237-255
10. Klerks, P., 2001. The Network Paradigm Applied to Criminal Organisations: Theoretical nitpicking or a relevant doctrine for investigators? Recent developments in the Netherlands. Connections 24 (3): 53-65
11. Leary, R.M. 2001. Home Office Policing & Reducing Crime Unit. (2001) Evaluation of the Impact of the FLINTS Software System in West Midlands and Elsewhere. Home Office, London.
12. Lyons, D., and G. S. Tseytin. 1998. Phenomenal data mining and link analysis. In D. Jensen and C. Henry Goldberg (Eds.), *Artificial Intelligence and Link Analysis, 1998 Fall Symposium*, 68-75. AAAI, AAAI Press.
13. Merry, S., 2000. Crime Analysis: Principles for Analysing Everyday Serial Crime. In Profiling Property Crimes (297-315) by David Canter and Laurence Alison (eds). Ashgate Publishing Co.
14. Oatley, G.C., & Ewart, B.W., 2003. Crimes Analysis Software: 'Pins in Maps', Clustering and Bayes Net Prediction. Expert Systems with Applications 25 (4) Nov 2003 569-588

15. Oatley, G.C., Zeleznikow, J. and Ewart, B.W., 2004. Matching and Predicting Crimes. In: Macintosh, A., Ellis, R. and Allen, T. (eds.), Applications and Innovations in Intelligent Systems XII. Proceedings of AI2004, The Twenty-fourth SGAI International Conference on Knowledge Based Systems and Applications of Artificial Intelligence, Springer: 19-32. ISBN 1-85233-908-X
16. Rossmo, K., 1999. Geographic Profiling. CRC Press, ISBN: 0849381290
17. Washio, T., & Motoda, H., 2003. State of the Art of Graph-based Data Mining. In: S. Dzeroski and L. De Raedt (eds.), SIGKDD Explorations Special Issue on Multi-Relational Data Mining, July 2003, Volume 5, Issue 1, 2003, pp. 59-69

A Methodology for Constructing Decision Support Systems for Crime Detection

John Zeleznikow¹, Giles Oatley², and Richard Leary³

¹ Centre for International Corporate Governance Research Institute, Victoria University
P.O Box 14428, Melbourne City, Victoria, Australia 8001
John.Zeleznikow@vu.edu.au

² University of Sunderland, School of Computing and Technology, Sunderland SR6 0DD, UK
Giles.Oatley@sunderland.ac.uk

³ University College London, Department of Statistical Science, London, UK
leary@stats.ucl.ac.uk

Abstract. To build decision support systems for crime detection we need to examine for whom is the system built and how will it be used. In addressing this question we will develop a methodology for developing crime detection decision support systems. The methodology is based on a methodology for analyzing the aims of certain unlawful acts.

1 Introduction

We are conducting research to develop intelligent decision support systems that use both expert knowledge and automated data analysis to guide analysts and investigators in the identification of complex criminal networks. Our goal is to intelligent decision support systems that provide law enforcement agencies with intelligence from new combinations of raw data from diverse sources.

1.1 User Requirements for Decision Support for Criminal Investigation

In examining the nature of evidence (which is essential when building decision support systems to evaluate evidence) we need to investigate:

- a) the stature of the person providing the evidence - for example courts do not place much trust on relatives or even psychologists in family law conflicts but give great weight to the views of medical practitioners in criminal cases
- b) in which legal domain is evidence being given - family law evidence is notoriously vague, criminal law evidence is less so.
- c) in criminal law, the severity of the possible sentence - in general, evidence in a case concerning a murder charge will be more thoroughly examined than in a case concerning a speeding fine.

Given these significant issues, whilst at the Joseph Bell Centre for Forensic Statistics and Legal Reasoning at the University of Edinburgh (www.josephbell.org) we were involved in developing software tools that are useful for assessing ‘specialised evidence’ or evidence in special (and limited) domains. Examples of such domains

include the evaluation of eyewitness evidence [1, a determination whether death occurred through natural causes, homicide or suicide [6] and Burglary from Dwelling Houses [8]

When building decision support systems to help investigate criminal activities, we must ask the vital question: who is the intended user, and what is his/her aim. Is the goal of the decision support system to support crime prevention, crime reduction, crime detection or the prosecution of criminals?

We also need to consider what is the level of authority of the user, how much access to knowledge does the user require and is this knowledge being shared with others. These are significant issues in the domain of intelligence and policing.

Police and other intelligence agents want to find the culprit(s). Whilst they need to respect the suspects' legal rights, their role is detection and not prosecution. Thus they do not have an obligation to prove their evidence 'beyond reasonable doubt'. At the pre-trial investigation stage there is the notion of 'free proof' - find the culprits using any means.

Prosecutors and investigators, on the other hand, wish to convict the suspect. Their burden of proof is 'beyond reasonable doubt'. They must conform to all legal requirements. In particular they are constrained by 'admissibility questions affecting proof' which occur in the post investigation stage. When requesting a search warrant, they need only a reasonable suspicion (not even proof of 'on the balance of probabilities'). Police see the law of evidence as 'case law' rather than the laws of 'logic and science'. They do not differentiate clearly between the role of logic and the role of human made law.

Investigators use the legal system as a guide to HOW they should set about investigating events; when, in reality, the law of logic and science has a much more important role to play in pre-trial investigations. Case law is important in outlining the activities and 'things' investigators can undertake. However case law provides very little advice and guidance about what [13] defines as the 'ratiocinative psychological processes' needed to undertake the imaginative and creative discovery of new facts. It provides little advice on testing old or accepted facts.

Intelligence agencies wish to prevent crimes being committed. Their legislative authority varies from domain to domain. However, the burden of proof placed on them, is generally minimal. Investigators have to consider facts in the context of a diverse world where the unexpected happens.

Newspapers also wish to investigate potential crimes. Limitations faced by their owners, is the possibility that they will be sued for defamation. Because of legal differences, the role of newspapers in investigating evidence varies greatly from country to country.

A further knowledge management problem is that the different actors in the fact investigation process (police, prosecutors, judges, intelligence agencies, media) often have minimal knowledge about how the other actors operate. Given the aforementioned difficulties in using computers to analyse evidence, we believe the major role of decision support systems should be in the pre-trial process.

The development of knowledge management techniques and decision support systems should lead to best practice by those investigating evidence. Before we build such decision support systems, we must be clear how knowledge is managed when investigating fact situations.

2 Principles for Constructing Criminal Investigation Decision Support Systems

2.1 Interpreting Evidence

Wigmore [13] argued that there is a science of reasoning underlying law. Whilst Wigmore's focus was upon the law of evidence, and in particular legal evidence, we are more concerned with modeling general legal decision-making. It should also be stressed that our ultimate goal is to build decision support systems that provide support for legal decision-makers.

Until recently, very few computer systems have attempted to make decisions interpreting evidence. Tillers and Schum [10,11] discussed Wigmore's pioneering approach to proof in litigation and examined marshalling legal evidence. Wigmore's method of diagramming the body of evidence in a case is the central method behind Walton's [12] treatise on legal argumentation and evidence. Wigmore's diagrams of evidence [5] were used with probability to analyse the trial of the American anarchists Sacco and Vanzetti.

Various techniques have been used to construct criminal investigation decision support systems. Statistics has been used to analyse evidence (see [9]). Areas investigated include DNA testing, fingerprints, footwear and ballistics.

2.2 Identifying Relationships

In law enforcement, intelligence analysts often refer to nodes and links in a criminal network as entities and relationships. The entities may be criminals, organizations, vehicles, weapons, bank accounts, etc. The relationships between the entities specify how these entities are associated together.

Law enforcement agencies and intelligence analysts frequently face the problems of identifying possible relationships among a specific group of entities in a criminal network. However, such tasks can be fairly time-consuming and labour-intensive without the help of link analysis tools. Previous work in the area has included:

1. The creation of links between transactional database records of individuals who have related financial transactions in order to identify money laundering networks [3];
2. The Link Discovery Tool which uses shortest path algorithms to discover association paths between two individuals that on the surface appear to be unrelated [4];
3. The COPLINK system which is based on finding links between database elements of person's organizations, vehicles and locations [2]. COPLINK CONNECT is designed to allow diverse police departments to share data seamlessly through an easy-to-use interface that integrates different data sources including legacy record management systems and COPLINK DETECT which uncovers various types of criminal associations that exist in police databases.

Since the creation of the United States Homeland Defence Agency, as a consequence of the Acts of Terrorism on September 11 2001, there has been a rapid increase in commercially available products that claim to perform link analysis.

3 The FLINTS System

3.1 Initial Versions

The FLINTS - ‘Forensic Led Intelligence System’ - methodology and software system was developed by Leary [7]. FLINTS integrates diverse data sources, including both ‘hard’ (DNA, finger-prints, shoe-prints) and ‘soft’ (behavioural) forensic data, and was developed to support the detection of high volume crimes within the West Midlands, through a judicious choice of queries to evidential databases of DNA, fingerprints, footwear and tool-marks. Analysis of the data reveals patterns, associations and links which would not have been detected had each evidence type been managed in separate systems.

FLINTS is a new approach to knowledge management in that it releases the inherent power in large data collections used by law enforcement. Through a judicious choice of questions, knowledge about scenarios, links, stories and connections between many types of data and many types of events as well as many people and many locations can be inferred. Results are visualized to aid analysts understand the chains of links and then contemplate new searches for new links. FLINTS is therefore currently a decision support system for analysts and investigators that helps them identify relevant information amongst a mass of data. The strength of the system is the identification of what should be ‘obvious’ links between people and crimes but are hidden in mixed masses of data.

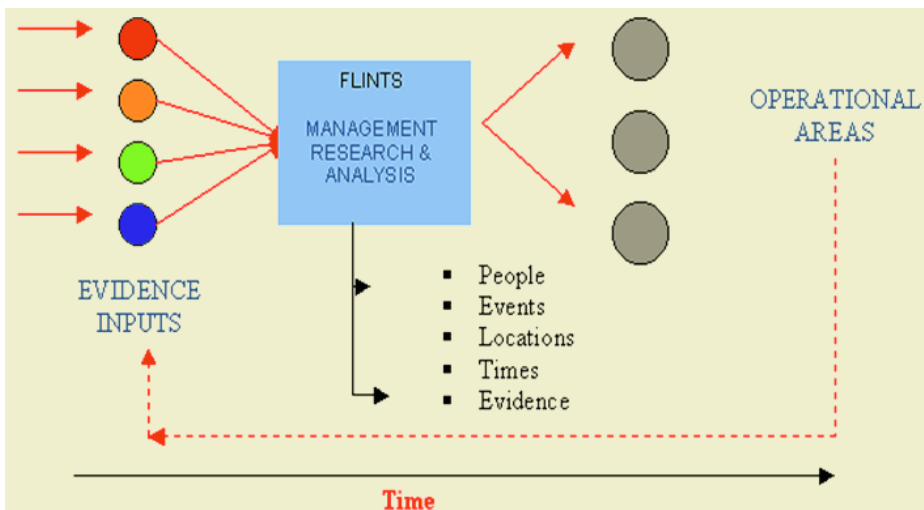


Fig. 1. Overview of FLINTS system

The first edition of FLINTS gave officers the ability to build a graphical pattern of links between crimes and criminals, previously thought to have no connection. Discovering these links has resulted in thousands of hours saved, hundreds of crimes solved and many criminals convicted. The FLINTS II version automatically trawled through various computer systems and pulled out the appropriate information, which linked criminals to other criminals and crime, working in real-time.

FLINTS III has the capability to deal with offender network analysis and assist in identifying groups of offenders. The new element of geographical profiling means officers can locate crime 'hotspots' by either incident or crime type, displaying the information by area. Comparative and seasonal analysis maps show emerging trends and developing hotspots, which are presented in maps and animated formats for the user.

3.2 Extending the FLINTS System

The FLINTS methodology has been extended with enhanced data visualisation tools to help crime investigators focus upon relevant data. Many crime detection decision support systems use sophisticated techniques (such as Bayesian networks or data mining - see [8]) to make decisions about the perpetrators of crime. The purpose of our paradigm is to help improve the performance of crime investigators and not replace their critical faculties. The methodology focuses upon identifying links between criminal acts, criminal actors and their locations. The resulting software has been tested in various areas of financial fraud, including car insurance fraud, VAT abuse and investment fraud.

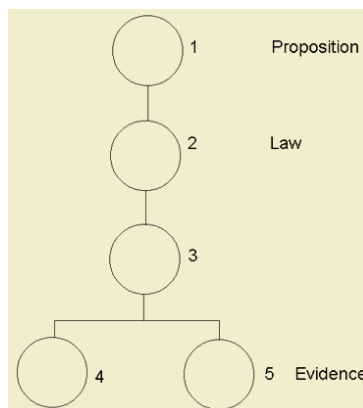


Fig. 2. Propositions

Our modeling of user requirements uses the following abstract model of propositions law and evidence, where the following questions are asked:

- What is the Ultimate Intended Aim (Proposition).
- What is the Substantive Law that will be breached if the Ultimate Intended Aim is breached.
- What are the acts or omissions that need to be undertaken (or not undertaken) if the Ultimate Intended Aim is to be achieved.
- What acts or omissions are generally seen if the Ultimate Intended Aim is to be achieved.
- What acts or omissions are generally not seen if the Ultimate Intended Aim is to be achieved.

The following illustration is an extension of the abstract model above into a case of VAT fraud. In the FF POIROT project (www.ffpoirot.org) we have used the methodology to develop ontologies for

- 1) the abuse of VAT regulations in Europe;
- 2) the illegal dissemination of investment advice on the World Wide Web (together with the Italian stock market regulator CONSOB)

In conjunction with legal firms in the North of England (acting on behalf of Insurance Agencies) Advanced Forensics Solutions Limited (www.af-solutions.co.uk) is using our methodology to detect car insurance fraud. Because of the network of links and associations displayed by the software developed using the methodology, over ten million pounds of car insurance fraud has been detected.

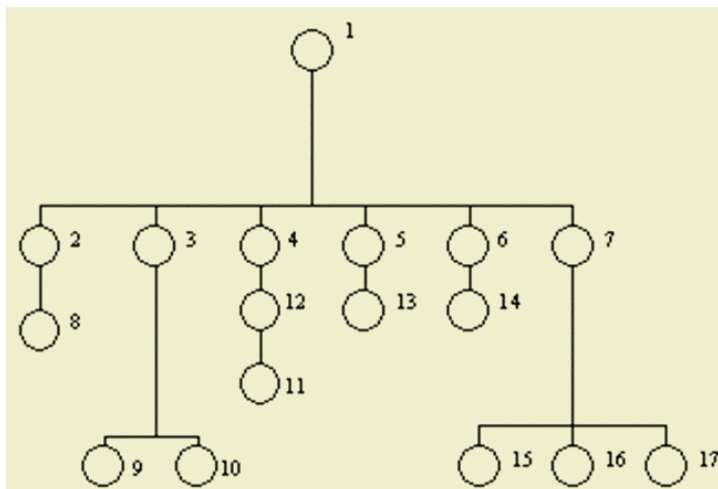


Fig. 3. VAT fraud. Key List: 1. Proposition: Latitude Icons Plc defrauded H.M. Govt. out of \$200,000 by presenting fraudulent documentation and invoices for reimbursement of VAT which had never been paid by Latitude Icons Plc. 2. Law: By Deception. 3. Dishonestly. 4. Appropriate. 5. Property. 6. Belonging To Another. 7. With Intent To Permanently Deprive Other Of It. 8. Evidence: Latitude Icons Accountant filed a VAT Return with false entries to deceive VAT Inspector. 9. Accountant under a duty to file accurate entries to VAT Inspector. 10. Accountant knew of his duty having signed a Contract of Employment stating so. 11. Accountant received a cheque to value of \$200,000 from VAT Inspector after filing VAT Return. 12. Accountant paid \$200,000 into Latitude Icons newly acquired reserve bank account. 13. Cheque for \$200,000 from VAT Inspector. 14. \$200,000 the property of H.M.Govt. 15. Accountant drew a cheque for \$200,000 from reserve account in favour of Latitude Construction. 16. Accountant paid cheque for \$200,000 into Latitude Construction bank account. 17. Latitude Construction is a 'Sole Trading' Company and Accountant is Sole Director

4 Conclusion

The focus of this paper has been on the need to individually craft decision support systems for crime detection. We commenced by investigating the user development issues: for whom is the system built and how will it be used.

We next discussed a methodology for developing decision support systems for crime detection. The methodology is based on a methodology for analyzing the aims of certain unlawful acts. Examples are taken from the area of VAT abuse.

References

1. Bromby, M. C. and Hall, M. J. J. The Development and Rapid Evaluation of the Knowledge Model of ADVOKATE: an Advisory System to Assess the Credibility of Eyewitness Testimony. Proceedings of Eleventh International Conference on Legal Knowledge Based Systems, IOS Publications, Amsterdam, Netherlands: 143-152.
2. Chen, H., Chung, W., Xu, J.J., Wang, G., Qin, Y., & Chau, M., 2004. Crime data mining: a general framework and some examples. IEEE Computer 37(4).
3. Goldberg, H. G. and Wong, R. W.H 1998. Restructuring Transactional Data for Link Analysis in the FINCEN AI System in: D Jensen, H Goldberg eds. Artificial Intelligence and Link analysis. Papers from the AAAI Fall Symposium. Orlando, Florida, Tech report FS-98-01.
4. Horn, R. D, Birdwell, J. D., and Leedy, L. W. 1997. Link discovery tool. Proceedings of the Counterdrug Technology Assessment Center's ONDCP/CTAC International Symposium Chicago, IL. August 18-22.
5. Kadane, J. B. and Schum, D. A. 1996. A Probabilistic Analysis of the Sacco and Vanzetti Evidence John Wiley and Sons
6. Keppens, J. and Zeleznikow, J. 2003. A Model Based Reasoning Approach for Generating Plausible Crime Scene Scenarios from Evidence. Proceedings of the Ninth International Conference on Artificial Intelligence and Law, Edinburgh, Scotland: ACM Press, 51-59.
7. Leary, R. M. 2004. Evidential Reasoning and Analytical Techniques in Criminal Pre-Trial Fact Investigation. PHD Thesis, University College, London.
8. Oatley, G., Zeleznikow, J. and Ewart, B. 2004. Matching and Predicting Crimes. Macintosh, A., Ellis, R. and Allen, T. (eds.) Applications and Innovations in Intelligent Systems XII. Proceedings of AI2004, Springer: 19-32
9. Schum, D. A. 1994. The Evidential Foundation of Probabilistic Reasoning. John Wiley and Sons
10. Schum, D. and Tillers, P. 1991. Marshalling Evidence for Adversary Litigation, 13 Cardozo Law Review. 657, 657-704.
11. Tillers, P. and Schum, D. 1988. Charting New Territory in Judicial Proof: Beyond Wigmore, 9 Cardozo Law Review. 907, 907-66.
12. Walton 2002. Legal Argumentation and Evidence. The Pennsylvania State University. University Park, Pennsylvania
13. Wigmore, J. H. 1913. The Principles of Judicial Proof. Little Brown and Company, Boston, Massachusetts

AASLMA: An Automated Argument System Based on Logic of Multiple-Valued Argumentation

Kumiko Matsunaga¹ and Hajime Sawamura²

¹ Graduate School of Science and Technology, Niigata University
8050, 2-cho, Ikarashi, Niigata, 950-2181 Japan
kumiko@cs.ie.niigata-u.ac.jp

² Institute of Natural Science and Technology
Academic Assembly, Niigata University
8050 2-cho Ikarashi, Niigata, 950-2181 Japan
sawamura@ie.niigata-u.ac.jp

Abstract. A Logic of Multiple-valued Argumentation LMA was formalized by Takahashi and Sawamura (LMA) on an expressive knowledge representation language, Extended Annotated Logic Programming (EALP). LMA allows agents to construct arguments under uncertain knowledge and to argue with other agents on uncertain issues in the open networked heterogeneous environment. In this paper, we describe an implementation of LMA (called AASLMA) in which agent communication is realized in C and symbolic argument construction in Prolog. The interface design proper to argumentation is also taken into account in the implementation. This is helpful for us to understand argument processes and results. The versatility of LMA is shown through the implementation and some convincing argument examples that employ various types of multiple-valuedness.

1 Introduction

Recently it has been recognized by computer scientists, and in particular AI researchers that argumentation has clear correlation with the interests of the newly emerging field of social computation such as multi-agent systems research, where interaction among agents is essential and social mechanism such as negotiation, persuasion, consensus attainment, etc. are emphasized as well as self-deliberation [6].

Much work has been devoted to two-valued argument modes so far [1]. However, there has been less devotion to the multi-valued cases despite the fact that knowledge is usually uncertain. Takahashi and Sawamura have developed a logic of multiple-valued argumentation LMA theoretically [9]. It allows agents to construct arguments under uncertain knowledge and to argue with other agents on uncertain issues in the open networked heterogeneous environment. The uncertainty that LMA can deal with include vagueness and inconsistency (or paraconsistency) in terms of multi-valuedness, and incompleteness with the help of default negation.

In this paper, we will confirm its expressiveness and applicability of LMA by actually implementing and applying it to some intriguing argument examples. The implementation consists mainly of three software components: The agent communication

part written in C and the symbolic argument construction part written in Prolog and argumentation interface part.

The paper is organized as follows. In the next section and Section 3, on the basis of our theoretical results, we give an overview of EALP and LMA, so that the paper is to be self-contained. In Section 4, we illustrate a pluralistic argument example to show the expressiveness of EALP and LMA. In Section 5, we describe an automated argument system AASLMA which is a realization of a logic of multiple-valued argumentation LMA. The final section summarizes the results of the paper.

2 Overview of Extended Annotated Logic Programs

EALP is an underlying knowledge representation language that we formalized for our logic of multiple-valued argumentation LMA. EALP has two kinds of explicit negation: Epistemic Explicit Negation ‘ \neg ’ and Ontological Explicit Negation ‘ \sim ’, and the default negation ‘not’. They are supposed to yield a momentum or driving force for argumentation or dialogue in LMA. We here give an outline of EALP.

2.1 Language

Definition 1. (Annotation and annotated atoms [4]). *We assume a complete lattice (\mathcal{T}, \leq) of truth values, and denote its least and greatest element by \perp and \top respectively. The least upper bound operator is denoted by \sqcup . An annotation is either an element of \mathcal{T} (constant annotation), an annotation variable on \mathcal{T} , or an annotation term. Annotation term is defined recursively as follows: an element of \mathcal{T} and annotation variable are annotation terms. In addition, if t_1, \dots, t_n are annotation terms, then $f(t_1, \dots, t_n)$ is an annotation term. Here, f is a total continuous function of type $\mathcal{T}^n \rightarrow \mathcal{T}$.*

If A is an atomic formula and μ is an annotation, then $A : \mu$ is an annotated atom. We assume an annotation function $\neg : \mathcal{T} \rightarrow \mathcal{T}$, and define that $\neg(A : \mu) = A : (\neg\mu)$. $\neg A : \mu$ is called the epistemic explicit negation (e-explicit negation) of $A : \mu$.

In this paper, the e-explicit negation $\neg A : \mu$ is embedded into an annotated atom $A : \neg\mu$, and implicitly handled.

Definition 2. (Annotated literals). *Let $A : \mu$ be an annotated atom. Then $\sim(A : \mu)$ is the ontological explicit negation (o-explicit negation) of $A : \mu$. An annotated objective literal is either $\sim A : \mu$ or $A : \mu$. The symbol \sim is also used to denote complementary annotated objective literals. Thus $\sim\sim A : \mu = A : \mu$.*

*If L is an annotated objective literal, then **not** L is a default negation of L , and called an annotated default literal. An annotated literal is either of the form **not** L or L .*

The terms: epistemic negation and ontological negation, originate from Kifer and Lozinskii [3]. Note, however, that the meaning of our ontological explicit negation is different from their ontological negation, being properly adjusted to argumentation as can be seen in the succeeding sections.

Definition 3. (Extended Annotated Logic Programs (EALP)). An extended annotated logic program (EALP) is a set of annotated rules of the form: $H \leftarrow L_1 \& \dots \& L_n$, where H is an annotated objective literal, and L_i ($1 \leq i \leq n$) are annotated literals in which the annotation is either a constant annotation or an annotation variable.

We identify a distributed EALP with an *agent*, and treat a set of EALPs as a *multi-agent system*.

3 Overview of Multiple-Valued Argumentation

In formalizing logic of argumentation, the most primary concern is the rebuttal relation among arguments since it yields a cause or a momentum of argumentation or dialogue. The rebuttal relation for two-valued argument models is most simple, so that it naturally appears between the contradictory propositions of the form A and $\neg A$. In case of multiple-valued argumentation based on EALP, much complication is to be involved into the rebuttal relation under the different concepts of negation. One of the questions arising from multiple-valuedness is, for example, how a literal with truth-value ρ confronts with a literal with truth-value μ in the involvement with negation.

In the next subsection, we outline important notions proper to a logic of multiple-valued argumentation LMA.

3.1 Annotated arguments

Definition 4. (Reductant and Minimal reductant). Suppose P is an EALP, and C_i ($1 \leq i \leq k$) are annotated rules in P of the form: $A : \rho_i \leftarrow L_1^i \& \dots \& L_{n_i}^i$, in which A is an atom. Let $\rho = \sqcup\{\rho_1, \dots, \rho_k\}$. Then the following annotated rule is a reductant of P : $A : \rho \leftarrow L_1^1 \& \dots \& L_{n_1}^1 \& \dots \& L_1^k \& \dots \& L_{n_k}^k$. A reductant is called a minimal reductant when there does not exist non-empty proper subset $S \subset \{\rho_1, \dots, \rho_k\}$ such that $\rho = \sqcup S$.

Definition 5. (Annotated arguments). Let P be an EALP. An annotated argument in P is a finite sequence $\text{Arg} = [r_1, \dots, r_n]$ of rules in P such that for every i ($1 \leq i \leq n$),

1. r_i is either a rule in P or a minimal reductant in P .
2. For every annotated atom $A : \mu$ in the body of r_i , there exists a r_k ($n \geq k > i$) such that $A : \rho$ ($\rho \geq \mu$) is head of r_k .
3. For every o-explicit negation $\sim A : \mu$ in the body of r_i , there exists a r_k ($n \geq k > i$) such that $\sim A : \rho$ ($\rho \leq \mu$) is head of r_k .
4. There exists no proper subsequence of $[r_1, \dots, r_n]$ which meets from the first to the third conditions, and includes r_1 .

A subargument of an argument Arg is a subsequence of Arg . The conclusions of rules in Arg are called conclusions of Arg , and the assumptions of rules in Arg are called assumptions of Arg . We write $\text{concl}(\text{Arg})$ for the set of conclusions and $\text{assm}(\text{Arg})$ for the set of assumptions of Arg . We denote the set of all arguments in P by Args_P , and define the set of all arguments in a set of EALPs $MAS = \{KB_1, \dots, KB_n\}$ by $\text{Args}_{MAS} = \text{Args}_{KB_1} \cup \dots \cup \text{Args}_{KB_n}$ ($\subseteq \text{Args}_{KB_1 \cup \dots \cup KB_n}$).

3.2 Attack Relation

Definition 6. (Rebut). Arg_1 rebuts $\text{Arg}_2 \Leftrightarrow$ there exists $A : \mu_1 \in \text{concl}(\text{Arg}_1)$ and $\sim A : \mu_2 \in \text{concl}(\text{Arg}_2)$ such that $\mu_1 \geq \mu_2$, or exists $\sim A : \mu_1 \in \text{concl}(\text{Arg}_1)$ and $A : \mu_2 \in \text{concl}(\text{Arg}_2)$ such that $\mu_1 \leq \mu_2$.

Definition 7. (Undercut). Arg_1 undercuts $\text{Arg}_2 \Leftrightarrow$ there exists $A : \mu_1 \in \text{concl}(\text{Arg}_1)$ and **not** $A : \mu_2 \in \text{assm}(\text{Arg}_2)$ such that $\mu_1 \geq \mu_2$, or exists $\sim A : \mu_1 \in \text{concl}(\text{Arg}_1)$ and **not** $\sim A : \mu_2 \in \text{assm}(\text{Arg}_2)$ such that $\mu_1 \leq \mu_2$.

Proposition 1. For any Arg_1 and Arg_2 in Args , if Arg_1 rebuts Arg_2 , I such that $I \models \text{Args}$ is o-inconsistent. And if Arg_1 undercuts Arg_2 , I such that $I \models \text{Args}$ is d-inconsistent.

Definition 8. (Strictly undercut). Arg_1 strictly undercuts $\text{Arg}_2 \Leftrightarrow \text{Arg}_1$ undercuts Arg_2 and Arg_2 does not undercut Arg_1 .

Definition 9. (Attack). Arg_1 attacks $\text{Arg}_2 \Leftrightarrow \text{Arg}_1$ rebuts or undercuts Arg_2 .

Definition 10. (Defeat). Arg_1 defeats $\text{Arg}_2 \Leftrightarrow \text{Arg}_1$ undercuts Arg_2 , or Arg_1 rebuts Arg_2 and Arg_2 does not undercut Arg_1 .

Proposition 2. For any Arg_1 and Arg_2 in Args , if Arg_1 attacks or defeats Arg_2 , I such that $I \models \text{Args}$ is o-inconsistent or d-inconsistent.

Definition 11. (x/y -acceptable and justified argument [2]). Let x and y be attack relations on Args . Suppose $\text{Arg}_1 \in \text{Args}$ and $S \subseteq \text{Args}$. Then Arg_1 is x/y -acceptable wrt. S if for every $\text{Arg}_2 \in \text{Args}$ such that $(\text{Arg}_2, \text{Arg}_1) \in x$ there exists $\text{Arg}_3 \in S$ such that $(\text{Arg}_3, \text{Arg}_2) \in y$. The function $F_{\text{Args},x/y}$ mapping from $\mathcal{P}(\text{Args})$ to $\mathcal{P}(\text{Args})$ is defined by $F_{\text{Args},x/y}(S) = \{\text{Arg} \in \text{Args} \mid \text{Arg} \text{ is } x/y\text{-acceptable wrt. } S\}$. We denote a least fixpoint of $F_{\text{Args},x/y}$ by $J_{\text{Args},x/y}$. An argument Arg is x/y -justified if $\text{Arg} \in J_{x/y}$; an argument is x/y -overruled if it is attacked by a x/y -justified argument; and an argument is x/y -defensible if it is neither x/y -justified nor x/y -overruled.

We write simply $F_{x/y}$ and $J_{x/y}$ for $F_{\text{Args},x/y}$ and $J_{\text{Args},x/y}$ when Args is obvious. Since $F_{x/y}$ is monotonic, it has a least fixpoint, and can be constructed by the iterative method [2].

In this paper, we employ $J_{\text{Args},d/su}$ to specify the set of justified arguments where d stands for defeat and su for strictly undercut.

Definition 12. (Conflict-free [2]). Let Args be an argument set, and x be an attack relation on Args . $S \subseteq \text{Args}$ is conflict-free wrt. $x \Leftrightarrow S$ does not contain arguments Arg_1 and Arg_2 such that $(\text{Arg}_1, \text{Arg}_2) \in x$.

Theorem 1. $J_{\text{Args},d/su}$ is conflict-free wrt. the defeat relation.

Theorem 2. If a set of arguments S is conflict-free wrt. the defeat relation, then S is conflict-free wrt. the attack.

Proposition 3. $J_{\text{Args},d/su} = J_{\text{Args},d/u} = J_{\text{Args},d/d}$.

Justified arguments can be dialectically determined from a set of arguments by the dialectical proof theory for which readers should refer to our previous paper [9]. We have the sound and complete dialectical proof theory for the argumentation semantics $J_{Args,x/y}$.

Theorem 3 (Soundness and completeness). Let $Args$ be an argument set. Then $\text{Arg} \in Args$ is provably d/su-justified \Leftrightarrow Arg is d/su-justified.

For the proofs, readers should refer to our previous paper [9] and technical paper cited in it.

4 A Pluralistic or Multicultural Argument Example

We illustrate a pluralistic or multicultural argument by specializing LMA to the complete lattice $\mathcal{FOUR} = (\{\perp, \mathbf{t}, \mathbf{f}, \top\}, \leq)$, where $\forall x, y \in \{\perp, \mathbf{t}, \mathbf{f}, \top\} x \leq y \Leftrightarrow x = y \vee x = \perp \vee y = \top$. This is identified with Tetralemma [8], so that LMA allows for argumentation of the kind seen in the Eastern tradition of culture.

Example 1. Let us consider the Western and Eastern arguments against Aristotle. Aristotle believed that the heavier a body is, the faster it falls to the ground. We simply represent this as *aristotle_hyp* : \mathbf{t} . Galileo's logical argument against this proceeds as follows: "Suppose that we have two bodies, a heavy one called H and a light one called L. Under Aristotle's assumption, H will fall faster than L. Now suppose that H and L are joined together. Now what happens? Well, L plus H is heavier than H so by the initial assumption it should fall faster than H alone. But in the joined body, L is lighter and will act as a 'brake' on H, and L plus H will fall slower than H alone. Hence it follows from the initial assumption that L plus H will both faster and slower than H alone. Since this is absurd, the initial assumption must be false." On the other hand, Easterners prefer a more holistic or dialectical argument like this: "Aristotle is based on a belief that the physical object is free from any influences of other contextual factors, which is impossible in reality." [5]

These are well translated into EALP as follows:
Galileo's knowledge:

```

~ aristotle_hyp : t ← faster(L + H, H) : ⊤
faster(L + H, H) : t ← not aristotle_hyp : f
faster(L + H, H) : f ← slower(L + H, H) : t
slower(L + H, H) : t ← brake(L, H) : t
brake(L, H) : t

```

Eastern agent's knowledge:

```

~ aristotle_hyp : t ← distrust_decontextualization : t
distrust_decontextualization : t

```

Figure 1 depicts a dialogue tree constructed with the dialectical proof theory. Obviously, $A_{\text{Aristotle}}$ is defeated (rebut) by A_{Western} and A_{Eastern} , and turns out not

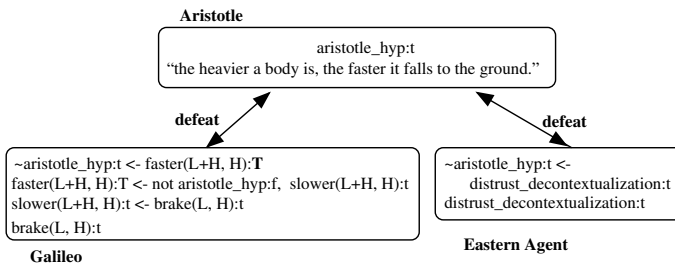


Fig. 1. Western and Eastern arguments against Aristotle

to be justified by two culturally different kinds of counter-arguments (actually defensible): an Western analytic argument and an Eastern holistic one, where the second rule in Galileo’s argument is a reductant made from his knowledge base. Note that Galileo made his argument by *reductio ad absurdum* for which the default negation ‘not’ has a crucial role in the rule representation. Furthermore, we note that the head $\sim aristotle_hyp : t$ in the first rule of Galileo’s argument does not undercut the assumption $\sim aristotle_hyp : f$ of the second rule, that is, Galileo’s argument is coherent or not self-defeating, and Eastern agent does not undercut the assumption $\sim aristotle_hyp : f$ of the second rule in Galileo’ argument. (Interested readers should refer to [9] for the technical terms used.)

In this example, all the arguments by Aristotle, Galileo and Eastern agent become defensible. Incidentally, let us consider a little modified version of the example. We first change Aristotle’s belief as follows: $aristotle_hyp : t \leftarrow not \sim empirically_factual : t$. And we make one more agent appear on the stage, who is a modern scientist having a firm belief on verificationism.

Modern scientist’s knowledge:

$\sim empirically_factual : t \leftarrow not scientifically_verified : t$.

Then, it is obvious that Aristotle’s argument is overruled, Galileo’s and a modern scientist’s ones are justified, and Eastern agent’s one is still defensible.

In today’s globalized world, such a pluralistic or multicultural argument of common interest is getting more important to us than ever. This is no exception even in agents’ society.

5 Implementation of LMA

An automated argument system termed AASLMA is an implementation of the logic of multiple-valued argumentation LMA. Although its full implementation is still under development, we here report the ongoing state of the art of AASLMA. The implementation consists mainly of two software components: The agent communication part written in C and the symbolic argument construction part written in Prolog. The interface design proper to argumentation is also taken into account in the implementation. This

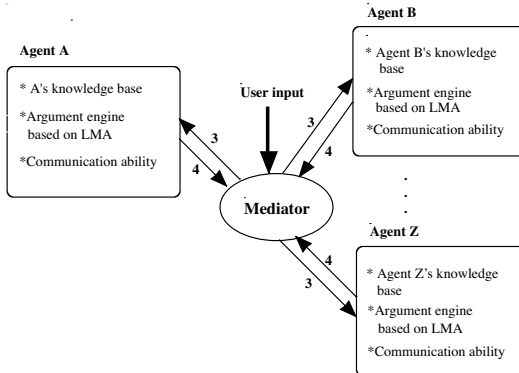


Fig. 2. Communication flow of the argumentation protocol in AASLMA

is helpful for us to understand argument processes and results in an argument tree form. The argument interface also helps us to establish the communication with the mediator and to invite other agents to arguments.

Working with AASLMA typically involves two stages: the first stage is to define participating agents, and the second one to go into argumentation on a given issue. Each arguing agent has its own knowledge base and the argument engine for making arguments and counterarguments provided in LMA, and the communication ability for sending and receiving messages. The messages have a form of $< \text{sender}, \text{receiver}, \text{subject}, \text{message type}, \text{content} >$, where the message type denotes kinds of messages such as ASK (for asking agents to make arguments), MAKE.DEFEAT (for asking agents to make defeating counter-arguments), MAKE.STRICT.UNDERCUT (for asking agents to make strictly undercutting counter-arguments), etc.

The EALP allows us to use an arbitrary complete lattice of truth values. This implies that users are required to provide the ordering of truth values together with the knowledge base. We introduce a special mediator agent who directs the agent communication, keeping track of the argument flow. The task and role of the mediator are similar to those of the judge agent in the contract net protocol (CNP) [7]. The generic communication framework of CNP is suitable to argument-based agent systems as well, and in fact makes the implementation easy and reliable.

An issue to be argued is first passed to the mediator agent by a user. Then, it asks participating agents to construct arguments on the given issue according to Definition 5 on annotated arguments, that is, by means of SLD-like proof procedure with reductants if necessary. According to the dialogue tree [9], we introduce the following argumentation protocol for LMA. Figure 2 depicts the communication flow between participating agents and a mediator.

Step 1 A user passes the mediator an issue to be argued.

Step 2 The mediator picks up an appropriate agent who seems to be able to make an argument on it, and asks it to argue on the issue. In the meantime, the mediator receives the argument from it.

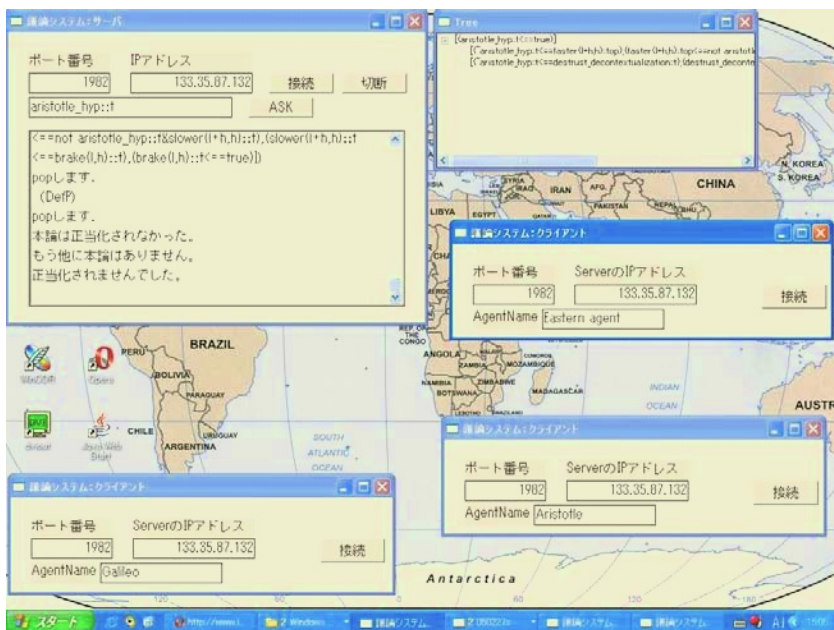


Fig. 3. A screenshot of the pluralistic argument

Step 3 The mediator broadcasts the argument to other agents, asking them to make counterarguments for the argument.

Step 4 Each agent tries to defeat the arguments, and replies with the counterarguments for them if any.

Step 5 If there are counterarguments put forwarded to the mediator, then for each of them, he calls **Step 3**. to seek further counterarguments for it. Otherwise, go to the next **Step 6**.

Step 6 Here are two cases to be considered. If the mediator has no more counterarguments left to be considered, then go to **Step 7**. Otherwise, return to **Step 3**.

Step 7 If every terminal node of the dialogue tree is proponent, then the argument is justified and the dialogue stops here. Otherwise, it is not justified and terminates.

Figure 3 is a screenshot of the argument described in Section 4, where three agents (Aristotle, Galileo and Eastern agent) argue on Aristotle's belief. The upper right window depicts the final dialectical tree sideways that has been constructed with the dialectical proof theory, showing that Aristotle's belief has not been justified.

The window on the upper left of the screenshot is a mediator (Server) that directs all argument flow and maintains dialectical trees. From upper left to lower right, it consists of Port number field, IP address field, Connect and Disconnect buttons, Field to indicate an argument issue, ASK button to launch broadcasting, and Monitor window

of agent communication. The other windows are Aristotle, Galileo and Eastern agent participating in this argument (Clients). They consist of Port number field, IP address field, Agent name field, Connect and Disconnect buttons, and Monitor window of agent communication (invisible for the present).

6 Conclusion

After a brief look at EALP and LMA, we described an implementation of the EALP-based multiple-valued argument model LMA, and evaluated it through argument examples although we took up only one in this paper. Lessons learned through the implementation may be summarized into three points:

- (1) EALP is not only a highly expressive knowledge representation language but also a computationally feasible one,
- (2) the versatility of the multiple-valued argumentation with LMA is advantageous in developing it to many applications in which respective domain-specific multiple-valuedness is required, and
- (3) the implementation and experimental uses of AASLMA over the internet suggest that it could have a great potential as a function for the computer-supported argumentation in pedagogy, future e-government, public policy making, etc.

The video clips and other various argument examples of AASLMA are accessible at URL <http://www.cs.ie.niigata-u.ac.jp/~kumiko/research.html>.

References

1. C. I. Chesnevar, G. Maguitman, and R. P. Loui. Logical models of argument. *ACM Computing Surveys*, 32:337–383, 2000.
2. P. M. Dung. An argumentation semantics for logic programming with explicit negation. In *Proc. of 10th Int. Conference on Logic Programming*, pages 616–630, 1993.
3. M. Kifer and E. L. Lozinskii. A logic for reasoning with inconsistency. *J. of Automated Reasoning*, 9:179–215, 1992.
4. M. Kifer and V. S. Subrahmanian. Theory of generalized annotated logic programming and its applications. *J. of Logic Programming*, 12:335–397, 1992.
5. R. E. Nisbett. *The Geography of Thought: How Asians and Westerners Think Differently... and Why*. The Free Press, 2003.
6. C. Reed and T. J. Norman, editors. *Argumentation Machines*. Kluwer Academic Publishers, 2004.
7. H. Sawamura and S. Maeda. An argumentation-based model of multi-agent systems. In *In Information Modeling and Knowledge Base XII*, pages 137–150. IOS Press, 2001.
8. H. Sawamura and E. Mares. How agents should exploit tetralemma with an eastern mind in argumentation. In *Mike Barley and Nik Kasabov (eds.): Intelligent Agents and Multi-Agent Systems VII, LNAI 3371, Springer*, pages 259–278, 2004.
9. T. Takahashi and H. Sawamura. A logic of multiple-valued argumentation. In *Proceedings of the third international joint conference on Autonomous Agents and Multi Agent Systems (AAMAS'2004)*, pages 800–807. ACM, 2004.

Trust and Information-Taking Behavior in the Web Community

Yumiko Nara

The University of the Air

Abstract. In order to realize the double helix model for chance discovery, trust in both, objective data and subjective data, is indispensable. Trust would be the basis to construct and develop a new community in which people interact with each other. In the process for people to recognize and share trust, information might navigate them. This study aims at clarifying the significance and possibility of trust focusing on the Internet as a new community using data of questionnaire survey involving participants from Japan and the US. The main results are as follows: 1) the U.S. people have a strong tendency to gather information positively, to examine the trust in the objective data, to feel other trustworthiness as the basis of subjective data, and to output trust into the web community rather than the Japanese do, 2) human interaction in the web community is affected by the trust of individuals, 3) the levels of empathy, rationality, and recognition about profit of the Internet influence to the condition of trust.

1 Introduction

Chance Discovery aims at identifying and managing rare, but significant events, such as potential risks or opportunities, in some domain and application [Ohsawa, 2003]. The author has been trying to obtain chances in the field of social science especially in the domain of risk management. Data of a questionnaire survey have been treated as objective data in the double helix model of chance discovery. Through these procedures, some new hypotheses have been obtained as “chance”. For example, visualization of the data with KeyGraph (a tool for chance discovery) and understanding of the resulting graph led to the new hypothesis, ‘rational egoist-tendencies affect on people’s behavior related to the information ethics on the Internet’ [Nara & Ohsawa, 2003].

Recently the author has been obtaining *trust* as a new concept from the chance discovery model [Nara, 2005]. Without trust in two aspects, i.e. trust for the objective data and trust for the subjective data, it is difficult for each individual to reach the higher levels of the double helix model and to find a chance/risk. This means that each individual should examine whether information is correct or not in view of the objective data, and should possess trustworthiness toward the partners as a foundation of the subjective data. Furthermore an individual is not only a receiver of trust, but also a sender of trust in a given community. So each individual should care about creating trust by sending trustworthy information as the objective data and providing trustworthiness as the basis of subjective data. Importance and function of trust in social systems were suggested as the key to facilitate people’s recognition of chance

and action. As a former study on trust in the domain of chance discovery, “Harmony in chance discovery” [Oehlmann, 2005] is worthy to be reviewed. Oehlmann indicated the importance of trust which would form the basis of harmony that in turn facilitates the group collaborations on Scenario Emergence.

We live in the era in which many and various people/things cross border so often that each individual cannot help facing uncertain and unknown things and people. Here the secured/static community needs to be achieved, but also the trustworthy/dynamic community. In such a community, objective data as well as subjective data are reliable for individuals, although they are initially unfamiliar. In order to achieve this, ‘information’ would be the key. It means construction of trust would be realized by the following processes, i.e. 1) gather information about unknown things and people, 2) examine the gathered information, 3) understand about things/people, 4) express and give feedback his/her feeling of trustworthiness regarding others.

This study aims at trust, information and the community of the Internet. It is going to make clear the effects of trust for developing communities, and the elements of trust by inspecting the following hypotheses with data from social survey. Comparing the conditions between Japan and USA will provide more meaningful perspective. The U.S. participants have the history to have been facing the uncertain and unknown things/ counterpart(s) since the founding of nation (of course even in the present high migratory society), on the other hand, the Japanese have a long history of building and staying in the secured/static/semi-closed communities so called MURA society. It means attitudes to examine and make trust in community seem different among these two countries.

Hyp. 1: Trust has a function to facilitate human interaction in certain community, i.e. in the Internet as well as in everyday life.

Hyp. 2: People’s positive attitude of taking information will influence their conditions of trust as a receiver (trust-examining of objective data, feeling of other trustworthiness as the basis of subjective data) and as a sender (trust-generating of objective data, trust-generating of the basis for subjective data).

Hyp. 3: The bigger profit people gain from their community, the bigger effort for building trust people try to make.

Hyp. 4: Individual features- empathy and rationality- effect on the attitude of taking information.

Hyp. 5: The U.S. people have strong tendency to gather information and to examine/generate trust in communities to a larger extent than the Japanese do.

2 Method

2.1 The Analytical Framework of the Research

This is an empirical study employing questionnaires to examine the status of trustworthiness and trust-examining/making behavior as well as the factors that influence them. Also, this is an international study of trust and information comparing Japan, and the US. Analytical framework of the research is shown in Figure 1. And indexes of main variables are shown below. Among these indexes, other Trustworthiness [Kosugi & Yamagishi, 1998] and empathy [Davis, 1994] are based on the pre-standardized scales, the others were made by the author specific for this study.

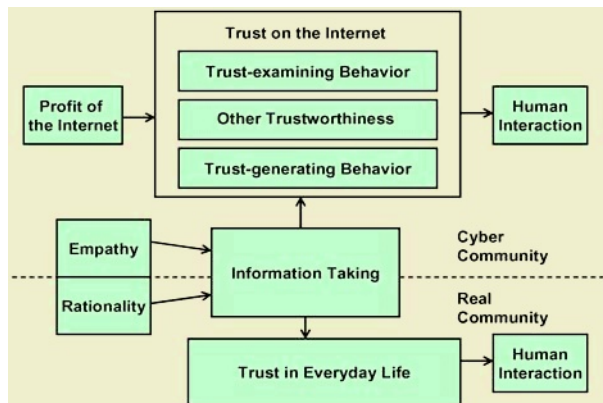


Fig. 1. Analytical framework of the research

Trust-Examining Behavior on the Internet (Alpha = .756)

Question: Regarding your attitude in using the Internet, how much is the following description applicable to you? Choose the most suitable one.

1. Very applicable
2. Applicable
3. Somewhat applicable
4. Somewhat inapplicable
5. Inapplicable
6. Not applicable at all

- I judge whether a web site is right or wrong, not by who created it, but rather by its content.
- In collecting information on the Internet, I always care if the information is correct.
- I would trust the information from unknown organizations or people on the Internet, only after researching on the organization/person.
- I would trust the information from unknown organizations or people on the Internet, only after researching on the contents with other sources.

Other Trustworthiness on the Internet (Alpha=.905)

This variable was grasped by adopting the index for the general trust of Kosugi & Yamagishi [1998] which added arrangement on Rotter's scale for the measurement of interpersonal trust [Rotter, 1967].

Question: What do you think about the Internet?

1. Strongly agree
2. Agree
3. Somewhat agree
4. Somewhat disagree
5. Disagree
6. Strongly disagree

- On the Internet, most people are basically honest.
- On the Internet, I tend to trust people.
- On the Internet, most people are basically innocent and kind.
- On the Internet, most people trust others.
- On the Internet, most people are trustworthy.

Trust-Generating Behavior on the Internet (Alpha= .765)

Question: Regarding your attitude in using the Internet, how much is the following description applicable to you? Choose the most suitable one.

- On the Internet, I care about honesty in providing information.
- I try cooperating with others on the Internet, so that the Internet society functions smoothly.
- On the Internet, I actively seek to build cooperative relationships with others when they seem trustworthy.
- On the Internet, I think users are all in a give-and-take relationship.

Human Interaction on the Internet (Alpha= .926)

Question: How often do the following things happen when you interact with others on the Internet?

1. very often
2. often
3. sometimes
4. rarely
5. never

- They tell you about themselves.
- They tell you about their personal trouble.
- You tell them about yourself.
- You tell them about your personal trouble.

Profit of the Internet (Alpha = .713)

Question: What do you think about the Internet?

- The Internet plays a role to maintain my human relationships.
- The Internet plays a role at work, for study, and in living.
- The Internet expansion will contribute to the welfare of mankind.
- I sometimes feel that it is easier to build close human relationships on the Internet.

Information-Taking Tendency (Alpha = .795)

Question: How much do the following descriptions apply to you?

1. Very applicable
2. Applicable
3. Somewhat applicable
4. Somewhat inapplicable
5. Inapplicable
6. Not applicable at all

- I actively seek to obtain new information for my work and for improving my life.
- I try to know everything as thoroughly and in as much detail as possible.
- I feel very embarrassed when I do not know something that other people generally know.
- I like obtaining new information by constantly accessing the media.
- When tackling a goal, I tend to gather as much relevant information as possible.

2.2 Outline of Survey

The subjects of the survey were male and female Internet users, 20 to 39 years old from all parts of their countries. They were picked randomly from panels composed by survey facilities ([J] NOS list, [US] Greenfield Online list). Surveys were conducted in February and March of 2005, with slight differences in the survey period among two countries ([J] 2005 Feb7-28 and Mar11-12, [US] Feb9-20). For Japan, the questionnaire was sent and returned via ordinary mail; for the US, subjects logged on to a questionnaire website with a log-in-name and password. The sample size was 2412 (with 1175 usable samples) for Japan, 2461 (with 551 usable samples) for the US. Investigation implementation organizations were [J] Nippon Research Center (NRC) and [US] Taylor Nelson Sofres Intersearch (TNS).

Basic attributes of respondents are as follows; Gender: female 68.0% and male 32.0% in Japan, 50.6% and 49.4 % in US. Age: between 20-29 years old 47.0 % and between 30-39 years old 53.0% in Japan (average 30.37 years old), 48.1% and 51.9% in US (average 29.70 years old).

3 Results and Discussion

3.1 Status Quo of Trust

Trust-Examining Behavior on the Internet

People's tendency related to the trust-examining behavior is shown in Table 1. It indicates that the U.S. participants try to possess high trust for the objective data by examining it carefully and positively rather than the Japanese do. For each question, a chi-square test was conducted to determine the significant different. Furthermore the author calculated the score by adding four encoded numbers to each answer category. So the smaller the score becomes, the stronger the attitude towards the examination of trust grows. With this score, difference between two courtiers was examined. As the results of t-test with the trust examining behavior score, mean of the US (8.90) is smaller than that of Japanese (11.92) (Table 4), i.e., the US citizens have tendency to gather information, to examine and evaluate the information when they feel something uncertainty.

Other Trustworthiness on the Internet

Table 2 shows the results of five questions related to other trustworthiness on the Internet. It indicates that the U.S. participants feel a high degree of trustworthiness towards others in the Internet community compared with the Japanese. The author conducted chi-square test for each question, as well as t-test with total score of other

trustworthiness on the Internet (Table 4), and gained significant difference between Japan and US, i.e., the U.S. participants trust others on the Internet strongly rather than Japanese do.

Trust-Generating Behavior on the Internet

Here table 3 indicates that the U.S. participants have a strong tendency to try to generate trust in cyber community by sending honest information and cooperate with each other. The result of t-test in table 4 also shows such tendency of the U.S. participants with the total score of the trust-generating behavior. In comparison, the Americans think that users are all in a give-and-take relationship on the Internet. They understand if he/she send wrong/harmful information then it does not only feed back on himself/herself but also hampers the whole secured development of the Internet.

Table 1. Frequency distribution of trust-examining behavior on the Internet

| On the internet | | | | | | | (%) | |
|--|--------------------|---------------|------------------------|--------------------------|-----------------|--------------------------|-------|-------|
| | 1. Very applicable | 2. Applicable | 3. Somewhat applicable | 4. Somewhat inapplicable | 5. Inapplicable | 6. Not applicable at all | Total | |
| I judge web site by its content | [J] | 9.22 | 32.49 | 41.79 | 11.03 | 2.78 | 2.69 | 100.0 |
| | [US] | 34.30 | 31.76 | 25.23 | 3.63 | 0.91 | 4.17 | 100.0 |
| I care if information is correct | [J] | 15.10 | 37.93 | 33.16 | 10.59 | 1.48 | 1.74 | 100.0 |
| | [US] | 51.73 | 33.76 | 11.07 | 1.27 | 0.54 | 1.63 | 100.0 |
| Trust information, after researching provider | [J] | 5.21 | 16.23 | 27.95 | 31.17 | 13.02 | 6.42 | 100.0 |
| | [US] | 15.80 | 35.75 | 34.66 | 7.08 | 3.81 | 2.90 | 100.0 |
| Trust information, after researching w/other sources | [J] | 7.72 | 21.27 | 36.11 | 20.83 | 8.51 | 5.56 | 100.0 |
| | [US] | 19.60 | 36.48 | 31.03 | 6.90 | 2.72 | 3.27 | 100.0 |

Table 2. Frequency distribution of other trustworthiness on the Internet

| On the internet | | | | | | | (%) | |
|---|-------------------|----------|-------------------|----------------------|-------------|----------------------|-------|-------|
| | 1. Strongly agree | 2. Agree | 3. Somewhat agree | 4. Somewhat disagree | 5. Disagree | 6. Strongly disagree | Total | |
| Most people are basically honest | [J] | 0.34 | 3.78 | 16.85 | 38.87 | 27.09 | 13.07 | 100.0 |
| | [US] | 1.27 | 7.08 | 35.75 | 25.59 | 17.06 | 13.25 | 100.0 |
| I tend to trust people | [J] | 0.42 | 4.39 | 23.67 | 33.82 | 24.27 | 13.43 | 100.0 |
| | [US] | 1.63 | 4.36 | 25.77 | 29.58 | 22.87 | 15.79 | 100.0 |
| Most people are basically innocent and kind | [J] | 0.34 | 1.98 | 24.44 | 36.92 | 23.58 | 12.74 | 100.0 |
| | [US] | 1.64 | 5.44 | 31.58 | 27.95 | 19.96 | 13.43 | 100.0 |
| Most people trust other | [J] | 0.17 | 1.55 | 20.70 | 39.95 | 26.20 | 11.43 | 100.0 |
| | [US] | 1.63 | 7.08 | 35.93 | 28.32 | 17.42 | 9.62 | 100.0 |
| Most people are trustworthy | [J] | 0.01 | 0.77 | 13.23 | 37.54 | 30.67 | 17.78 | 100.0 |
| | [US] | 2.00 | 4.17 | 30.31 | 30.31 | 19.42 | 13.79 | 100.0 |

Profit of the Internet, Human Interaction on the Internet and Information-Taking Tendency

Related with above point of view, the U.S. participants recognize the profit of the Internet more strongly than the Japanese do (Table 4). This table also indicates the U.S. participants have a strong tendency to interact (express himself/herself and accept others) with others in the Internet. Also their attitude to take information is significantly stronger than that of the Japanese.

Table 3. Frequency distribution of trust-generating behavior on the Internet

| On the internet | | 1. Very applicable | 2. Applicable | 3. Somewhat applicable | 4. Somewhat inapplicable | 5. Inapplicable | 6. Not applicable at all | Total |
|---|------|--------------------|---------------|------------------------|--------------------------|-----------------|--------------------------|-------|
| I care about honesty in providing information | [J] | 15.55 | 37.29 | 38.08 | 5.07 | 1.48 | 2.53 | 100.0 |
| | [US] | 42.65 | 37.39 | 14.34 | 2.72 | 0.54 | 2.36 | 100.0 |
| I try cooperating with others on the Internet | [J] | 3.32 | 7.33 | 24.69 | 36.82 | 17.11 | 10.73 | 100.0 |
| | [US] | 17.60 | 36.48 | 28.13 | 8.167 | 3.45 | 6.17 | 100.0 |
| I actively seek to build cooperative relationships | [J] | 3.23 | 8.28 | 29.64 | 34.52 | 15.61 | 8.72 | 100.0 |
| | [US] | 9.26 | 21.42 | 31.40 | 13.61 | 8.35 | 15.96 | 100.0 |
| I think users are all in give-and-take relationship | [J] | 3.56 | 13.73 | 41.01 | 25.80 | 9.91 | 5.99 | 100.0 |
| | [US] | 10.53 | 21.05 | 39.75 | 13.61 | 5.99 | 9.07 | 100.0 |

In this way Hyp. 5 was definitely verified. The U.S. people have strong tendency to gather information and to examine/generate trust in communities positively than the Japanese.

Table 4. Results of t-test among some variables between Japan and USA

| | n | Mean | S.D. | t-value | d.f. | significance |
|---|------|------|--------|---------|--------|--------------|
| Trust-examining behavior on the Internet | [J] | 1148 | 11.92 | 3.25 | 17.588 | 1697 |
| | [US] | 551 | 8.90 | 3.42 | | |
| Other trustworthiness on the Internet | [J] | 1157 | 21.41 | 4.179 | 6.055 | 906.567 |
| | [US] | 551 | 19.88 | 5.15 | | |
| Trust-generating behavior on the Internet | [J] | 1138 | 13.57 | 3.43 | 13.143 | 962.567 |
| | [US] | 551 | 10.99 | 3.95 | | |
| Profit of the Internet | [J] | 1161 | 9.25 | 2.55 | 5.105 | 878.895 |
| | [US] | 551 | 8.44 | 3.27 | | |
| Human interaction on the Internet | [J] | 1162 | 17.25 | 3.89 | 8.506 | 990.153 |
| | [US] | 551 | 15.421 | 4.290 | | |
| Information-taking tendency | [J] | 1161 | 14.40 | 3.75 | 9.899 | 932.856 |
| | [US] | 551 | 12.23 | 4.45 | | |
| Empathy | [J] | 1160 | 8.69 | 2.14 | 9.704 | 859.876 |
| | [US] | 551 | 7.37 | 2.83 | | |
| Rationality | [J] | 1159 | 8.31 | 2.31 | 9.436 | 900.792 |
| | [US] | 551 | 6.99 | 2.86 | | |

*** p<.001

3.2 Relationships Among Some Variables

In this section, the relationships among some variables - trust (trust-examining behavior, other trustworthiness, trust-generating behavior), information-taking tendency, human interaction, profit of the Internet, and individual features (empathy and rationality) are examined with path analysis.

Results of Japan and US are shown with Fig. 2 and 3. In Fig. 2, the influences of information-taking tendency for trust ($\beta=.159$) and of trust for human interaction($\beta=.239$) are significant. Similar tendencies are observed with U.S. respondents, though standardized regression weights are different.

These results can be summarized as follows: Hyp. 1 is verified. Trust makes positive effect for the interpersonal relationships in the Internet as well as in everyday life. Hyp. 2 and 3 are also verified. Community members' recognition about the profit of their community and subjective attitude of taking information makes positive influ-

ence for generating trust. Hyp. 4 is verified, too. Individual features- empathy and rationality- make effect on the attitude of taking information.

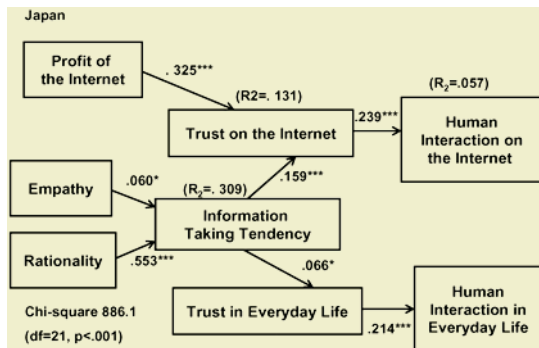


Fig. 2. Result of the Japanese data

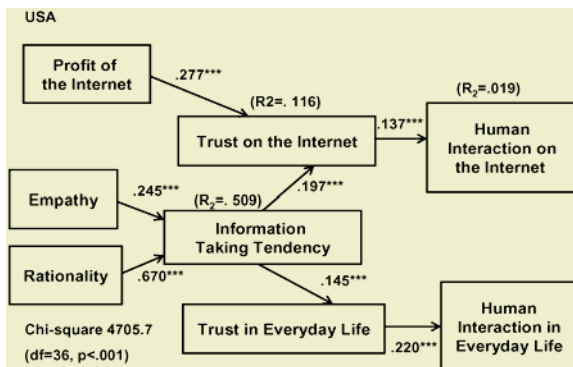


Fig. 3. Result of the U.S. data

4 Conclusion

This study has tried to make clear the significance and possibility of trust focusing on the Internet as a new community using data of questionnaire survey between Japan and the US. It was found that people's positive attitude of taking information will influence their conditions of trust as a receiver (trust-examining of objective data, feeling of other trustworthiness as the basis of subjective data) and as a sender (trust-generating of objective data, trust-generating of the basis for subjective data).

The results also indicate the climate of raising the posture, which faces uncertain and unfamiliar things/people in a positive way, has been cultivated in the U.S. In addition, the US respondents show their positive attitude to make their community trustworthy. Precisely the U.S. society is characterized by a culture that allows to put trust in the good sense and the judgment of the common citizens and various opinions. On the other hand, Japanese citizens have a weak attitude towards self-decide based on their own understanding of uncertainty, and tend to request measures to adjust it to zero by staying in secured community. However as long as a chance has the posture

that it is new, rare and latent, a chance could be obtained just by facing unfamiliar things/people in a positive way. It will be a future work to construct trustworthy system in Japan considering the Japanese climate, as well as the effect of information-taking tendency, recognition about the profit of community, and individuals' nature on the condition of the trust.

Last I'd like to note that this study is supported by the Japan Society for the Promotion of Science (JSPS), Grant-in-Aid for Scientific Research (B).

References

1. Ohsawa, Y., Modeling the Process of Chance Discovery, Ohsawa, Y. & McBurney, P. eds., *Chance Discovery: Foundations and Applications*, Springer Verlag, 2003
2. Nara, Y. & Ohsawa, Y., Application to Questionnaire Analysis, Ohsawa, Y. & McBurney, P. eds., *Chance Discovery: Foundations and Applications*, Springer Verlag, 2003
3. Nara, Y., Possibility of Subjective Risk Management of Everyday Life, *Risk and Insurance Management*, 36, 2005
4. Oehlmann, R., Harmony in Chance Discovery, *the 4th Workshop on Scenario Emergence*, 2004
5. Rotter, J., A new scale for the measurement of interpersonal trust, *Journal of Personality*, 35, 1967
6. Kosugi, M. & Yamagishi, T., General Trust and Judgment of Trustworthiness, the Japanese Journal of Psychology, 69(5), 349-357, 1998
7. Davis, M.H. *Empathy: A Social Psychological Approach*, Oxford: Westview Press, 1994

Robust Intelligent Tuning of PID Controller for Multivariable System Using Clonal Selection and Fuzzy Logic

Dong Hwa Kim

Dept. of Instrumentation and Control Eng., Hanbat National University,
16-1 San Duckmyong-Dong Yuseong-Gu, Daejon City, Korea, 305-719

Tel: +82-42-821-1170, Fax: +82-821-1164

kimdh@hanbat.ac.kr

www.aialab.net

Abstract. This paper focuses on tuning of the PID controller using gain/phase margin, fuzzy logic, and immune algorithm for multivariable process. In industrial multivariable process, there is undesirable interaction between variables. Up to the present time, PID Controller has been widely used to control industrial process loops. However, it has also disadvantage without achieving an optimal PID gain with no experience. In this paper, the gains of PID controller based on coupling gain using fitness value of immune algorithm depending on error between optimal gain/phase margin is tuned by IM-FNN (immune based-Fuzzy Neural Network).

1 Introduction

The three-mode Proportional–Integral–Derivative (PID) controller has been using in the most control loops of plant despite continual advances in control theory: process control, motor drives, thermal power plant and nuclear power plant, automotive, fight control, instrumentation, etc. This is not only due to the simple structure which is conceptually easy to understand but also to the fact that the algorithm provides adequate performance in the vast majority of applications [1-2]. In the tuning problems of a PID process control, the classical tuning methods based on the ultimate gain and the period of the ultimate oscillation at stability limit, based on tuning identification methods which determine the frequency response of process, adaptive tuning, based on relay feedback. However, the PID controller parameters of multivariable system are still computed using the classic tuning formulae and these can not provide good control performance in control situations. In this paper, for robust control against disturbance due to coupling of multivariable process, tuning method of PID controller is proposed using gain margin/phase margin and multi-objective optimization based on clonal selection of immune algorithm.

2 PID Control for Multivariable Process

2.1 Multivariable Process

In a 2×2 multivariable process the PID controller configuration would be one in which 2 PID controllers would be used in the 2 loops associated with the process, as

shown in Fig. 1. The key purpose of controller design for multivariable process is to obtain the parameter of the n PID controllers so that the process outputs are controlled, in some desired way, the corresponding reference signals, and the interactions between the loops are within the required specification. The controller parameter should be achieved by immune algorithm based parameter selection and an appropriate objective function to obtain the given time-domain specification.

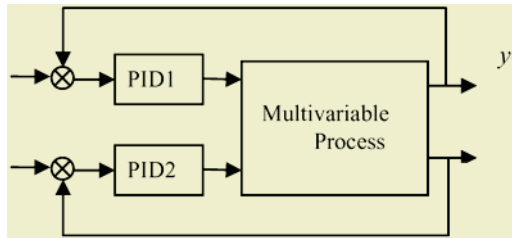


Fig. 1. PID control of 2×2 multivariable process

2.2 Gain Margin and Phase Margin for Multivariable Process

In the loop transfer function of Fig. 1, for process given as k_c , τ , L and specifications defined by G_m , Φ_m , final gain margin and phase margin can be given by

$$G_m = \frac{\pi\tau}{4kL} \left(1 + \sqrt{1 - \frac{4L}{\pi T_i} + \frac{4L}{\pi\tau}} \right), \quad \Phi_m = \frac{1}{2}\pi - \frac{k_c k_p L}{\tau} + \frac{\pi}{4k_p k_c} \left(1 - \frac{\tau}{T_i} \right). \quad (1)$$

Whatever the design approach, tuning technique based on gain margin and phase margin can have robustness and stability without plant operation condition.

2.3 On-line Calculation of Coupling Gain of Multivariable Process

In a 2×2 multivariable process, the following area (S_0, \dots, S_n) is obtained by integrating the process of the open loop step response $y(t)$, after applying the step-change Δu of the process input at $t=0$ [3]. S_0 is the steady-state gain of the process. Then, it can be characterized by the following areas [4]: Area given by equation (3) can be computed by in time-domain from the process steady-state change [4]. This paper tunes the gain of PID controller in each loop as well as calculates coupling gain S_n depending on dynamic change on line using immune based algorithm.

3 Immune Algorithms for Tuning of PID Controller for Multivariable Process Based on Gain Margin and Phase Margin

3.1 Evaluation Method for Tuning of PID Controller Based on Gain Margin/Phase Margin and Clonal Selection Algorithm

In this paper, for the constrained optimization tuning for gain margin and phase margin, immune algorithms are considered, i.e., memory cell of immune algorithm to

minimize fitness function for gain margin G_m and phase margin Φ_m , as depicted in Fig. 3. Initially, memory cell is started with the controller parameters within the search domain as specified by the designer. These parameters are transferred then to network, which is initialized with the variable gain margin and phase margin [3]. Immune algorithm minimizes fitness function for P, I, D gain and optimal gain/phase margin during a fixed number of generations for each individual of memory cell in immune network. This paper used tournament selection, arithmetic crossover, and mutation [4]. The value of the fitness of each individual of immune network $\Gamma_i(c_i(i=1,\dots,n))$ is determined by the evaluation function, denoted by $\Gamma(c_i)$ as

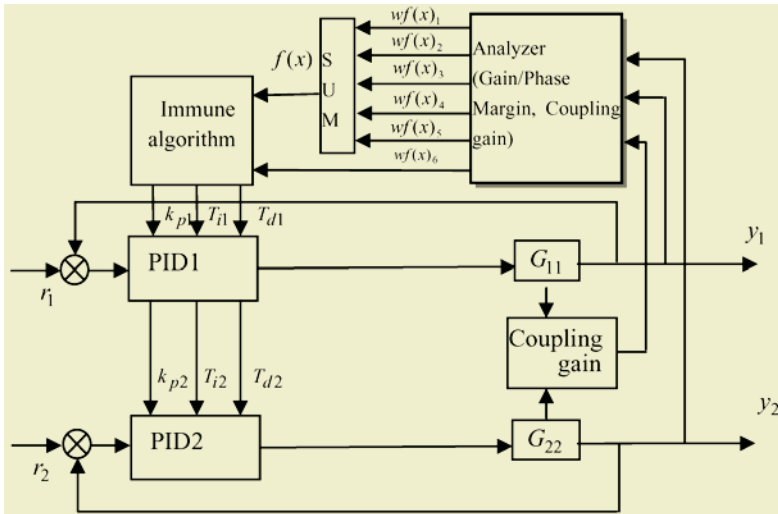


Fig. 2. Structure of immune algorithm based 2×2 multivariable process

$$\Gamma_i(c_i) = -\left(PI_n(G_m^i, P_m^i) + \Phi(P_i, I_i, D_i)\right) + \Delta(C_g), \quad (2)$$

where n denotes the population size of immune network and $\Gamma_i(c_i)$ is total fitness function, $PI_n(G_m^i, P_m^i)$ is fitness function for calculation of gain/phase margin, $\Phi(P_i, I_i, D_i)$ is fitness function for computing P, I, and D gain. Also, $\Delta(C_g)$ is fitness function for calculation of coupling gain between loops in multivariable processes. Therefore, for robust tuning of PID controller, this paper uses six kinds of objective function such as gain margin, phase margin, P (proportional gain), I (Integral gain), and D (Derivative gain). In each objective function, fitness value is obtained as the followings: For example, when value of overshoot on reference model is over the given value 1.2, fitness value is 0 but if overshoot value is within the given value 1.2, fitness value is calculate by level of membership function defined in triangular. Fitness value for rise time, settling time, gain margin, and phase margin is computed using each membership function in Fig. 8. In Fig. 8, $f_1(\bullet)$, $f_2(\bullet)$, $f_3(\bullet)$, $f_4(\bullet)$, $f_5(\bullet)$, and $f_6(\bullet)$ show membership function for settling time, rise time, overshoot, gain margin, phase margin, and computation of coupling gain between loops, respectively.

3.2 Computational Procedure for Optimal Selection of Parameter

The coding of an antibody in an immune network is very important because a well designed antibody coding can increase the efficiency of the controller.

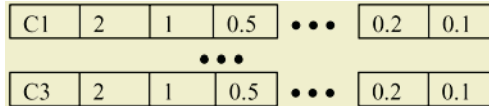


Fig. 3. Allocation structure of P, I, and D gains in locus of antibody of immune algorithm

As shown in Fig. 3, there are three type antibodies for tuning of PID controller gain: 1) antibody type 1 is encoded to represent only P (c_1) gain in the PID controller; 2) antibody type 2 is encoded to represent I (c_2) gain; 3) antibody is encoded to represent D (c_3) gains. For calculation of gain/phase margin, the similar antibody is given. The value of the k locus of antibody type 1 shows P gain allocated to route 1. For calculation of gain/phase margin and controller gain, the following procedure is used.

[Step 1] Initialization and recognition of antigen: The immune system recognizes the invasion of an antigen, which corresponds to reference model such as settling time (T_s), rise time (R), overshoot (O), gain margin (G_m), and phase margin (P_m) in the optimization problem. **[Step 2]** Product of antibody from memory cell: When error of the calculated gain and phase margin in memory cell to optimal gain and phase margin is smaller, fitness function is larger. **[Step 3]** Antibody with the best fitness value obtained by calculation for searching an optimal solution is stored in memory cell.

[Step 4] Differentiation of lymphocyte: The B - lymphocyte cell, the antibody that matched the antigen, is dispersed to the memory cells in order to respond to the next invasion quickly. That is, select individuals using tournament selection and apply genetic operators (crossover and mutation) to the individuals of network. **[Step 5]** Stimulation and suppression of antibody. **[Step 6]** Calculate fitness value between antibody and antigen. This procedure can generate a diversity of antibodies by a genetic reproduction operator such as mutation or crossover. These genetic operators are expected to be more efficient than the generation of antibodies. **[Step 7]** If the maximum number of generations of memory cell is reached, stop and return the fitness of the best individual fitness value to network; otherwise, go to step 3.

4 Simulation Results and Discussions

In order to prove robust control scheme based on the gain margin and phase margin and immune algorithm suggested in this paper, we used the plant models as the following equations [30]:

$$G_p = \frac{[18:15]}{[0.0032:0.005]s^3 + [0.072:0.1]s^2 + [1.28:1.305]s} \quad (3)$$

For this model, when gain margin $G_m = 8dB$, phase margin $\Phi = 30^\circ$ is given as the design requirement, tuning results tuned by gain margin-phase margin and immune algorithm are obtained as shown in Figs. 4-5.

Table 1. Parameters designed by Immune Algorithm

| alpha | beta | Kp | Ti | Gm | Pm |
|-------|------|------|------|------|-------|
| 0.05 | 0.95 | 0.21 | 0.02 | 8.22 | 76.97 |
| 0.1 | 0.90 | 0.26 | 0.94 | 4.84 | 29.94 |
| 0.20 | 0.80 | 0.56 | 1.9 | 2.29 | 29.97 |
| 0.30 | 0.70 | 0.98 | 0.13 | 1.76 | 30.35 |
| 0.40 | 0.60 | 0.97 | 0.31 | 1.74 | 29.96 |
| 0.50 | 0.50 | 0.96 | 0.35 | 1.76 | 30.31 |

5 Conclusions

This paper focuses on tuning of a multivariable PID controller using gain/phase margin and multiobjective optimization based on clonal selection of immune algorithm and fuzzy logic for tuning an optimal controller that can actually be operated on a robust control. Parameters P, I, and D encoded in antibody are randomly allocated during selection processes to obtain an optimal gain for robustness based on gain margin and phase margin. The object function can be minimized by gain selection for control, and the variety gain is obtained as shown in Table 1. The suggested controller can also be used effectively in the motor control system as seen from Figs. 4-5.

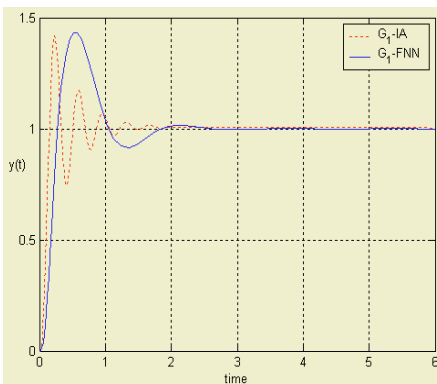


Fig. 4. Step response by IA and FNN ($\alpha = 0.05, \beta = 0.95$)

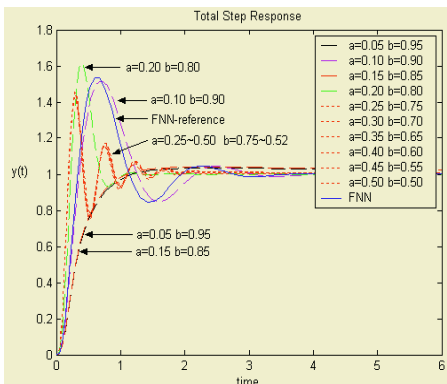


Fig. 5. Comparison of step response by FNN, value of α and β

References

1. Ziegler and Nichols, "Optimum setting for automatic controllers," Transaction ASME, Nov. pp. 759-768, 1942.
2. Eric Poulin and Andre Pomerleau, "PI setting for integrating processes based on ultimate cycle information," IEEE Trans. On control systems technology, Vol. 7, No. 4, July 1999.
3. Sheng-Yuan Chu and Ching-Cheng Teng, "Tuning of PID controllers based on gain and phase margin specifications using fuzzy neural network," "Fuzzy sets and systems, 101, pp. 21-30, 1999.
4. C. L. Lin and H. Y Jan, "Multiobjecutive PID control for a linear brushless DC motor: an evolutionary approach," IEE Proc.-Power Appl., Vol. 149, No. 6, pp. 397-406, November 2002.

5. C. Vlachos, "Genetic approach to decentralized PI controller tuning for multivariable processes," IEE Proc.-Control Theory Appl., Vol. 146, No. 1, pp. 58-64, March 1999.
6. Kazuyuki Mori and Makoto Tsukiyama, "Immune algorithm with searching diversity and its application to resource allocation problem," Trans. JIEE, Vol. 113 - C, No. 10, '93.
7. Dong Hwa Kim, Jae Hoon Cho, "Robust PID Controller Tuning Using Multiobjective Optimization Based on Clonal Selection of Immune Algorithm," LNCS (Lecture Notes in Computer Science) Proceeding of Springer (SCI) Sept 22-24, 2004.
8. Dong Hwa Kim, "Intelligent Tuning of the 2-DOF PID Controller On the DCS for Steam Temperature Control of Thermal Power Plant," IEEE Industrial Application Society. I&CPS 2002, Savannah, GA, USA, May 5 - 8, 2002.
9. Dong Hwa Kim, "Auto-tuning of reference model based PID controller using immune algorithm," IEEE international conference on evolutionary computation, Hawaii, May 12 - 17, 2002.

Intelligent Control of AVR System Using GA-BF

Dong Hwa Kim and Jae Hoon Cho

Dept. of Instrumentation and Control Eng., Hanbat National University,
16-1 San Duckmyong-Dong Yuseong-Gu, Daejon City, Korea, 305-719
Tel: +82-42-821-1170, Fax: +82-821-1164
kimdh@hanbat.ac.kr
www.aiyalab.net

Abstract. This paper deals with hybrid system (GA-BF) based on the conventional GA (Genetic Algorithm) and BF (Bacterial Foraging) which is social foraging behavior of bacteria for AVR system. This approach provides us with novel hybrid model based on foraging behavior and with also a possible new connection between evolutionary forces in social foraging and distributed non-gradient optimization algorithm design for global optimization over noisy surfaces for AVR system.

1 Introduction

In the last decade, evolutionary computation based approaches have received increased attention from the engineers dealing with problems which could not be solved using conventional problem solving techniques [1-3]. The general problem of evolutionary algorithm based engineering system design has been tackled in various ways. GA has also been used to optimize nonlinear system strategies. Among them, a large amount of research is focused on the design of fuzzy controllers using evolutionary algorithm approaches. On the other hand, as natural selection tends to eliminate animals with poor foraging strategies through methods for locating, handling, and ingesting food and favor the propagation of genes of those animals that have successful foraging strategies, they are more likely to apply reproductive success to have an optimal solution [2], [3]. Since a foraging animal takes actions to maximize the energy obtained per unit time spent foraging, in the face of constraints presented by its own physiology such as, sensing and cognitive capabilities and environment (e.g., density of prey, risks from predators, physical characteristics of the search area), evolution can provide optimization within these constraints and essentially apply to engineering field by what is sometimes referring to as an optimal foraging policy. That is, optimization models can provide for social foraging where groups of parameters communicate to cooperatively forage in engineering. First, this paper provides a brief literature overview of the area of bacterial foraging as it forms the biological foundation for this paper. Then, this paper also focuses on dealing with an enhanced optimal solution using a hybrid approach consisting of BA (Bacterial Foraging) and GA (Genetic Algorithm). Finally, we focus on evidence for the proposed hybrid system for AVR system.

2 Hybrid System Based on GA and Bacteria Foraging for AVR

Equation represents the positions of each member in the population of the N bacteria at the j th chemotactic step, k th reproduction step, and l th elimination-dispersal event.

Let $P(i, j, k, l)$ denote the cost at the location of the i th bacterium $\phi^i(j, k, l) \in R^n$, and

$$\phi^i = (j+1, k, l) = \phi^i(j, k, l) + C(i)\phi(j), \quad (1)$$

so that $C(i)>0$ is the size of the step taken in the random direction specified by the tumble. If at $\phi^i(j+1, k, l)$ the cost $J(i, j+1, k, l)$ is better (lower) than at $\phi^i(j, k, l)$, then another chemotactic step of size $C(i)$ in this same direction will be taken and repeated up to a maximum number of steps N_s . N_s is the length of the lifetime of the bacteria measured by the number of chemotactic steps. Functions $P_c^i(\phi)$, $i=1, 2, \dots, S$, to model the cell-to-cell signaling via an attractant and a repellent is represented by [8-12]

$$\begin{aligned} P_c(\phi) &= \sum_{i=1}^N P_{cc}^i \\ &= \sum_{i=1}^N \left[-L_{attract} \exp\left(-\delta_{attract} \sum_{j=1}^n (\phi_j - \phi_j^i)^2\right) \right] \\ &\quad + \sum_{i=1}^N \left[-K_{repellant} \exp\left(-\delta_{attract} \sum_{j=1}^n (\phi_j - \phi_j^i)^2\right) \right], \end{aligned} \quad (2)$$

where $\phi = [\phi_1, \dots, \phi_p]^T$ is a point on the optimization domain, $L_{attract}$ is the depth of the attractant released by the cell and $\delta_{attract}$ is a measure of the width of the attractant signal. $K_{repellant} = L_{attract}$ is the height of the repellent effect magnitude, and $\delta_{attract}$ is a measure of the width of the repellent.

3 Intelligent Controller for AVR Using Hybrid System GA-BF

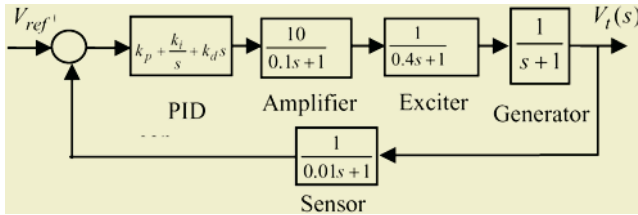
3.1 AVR System

The transfer function of PID controller in the AVR system is given by

$$G(s) = k_p + \frac{k_i}{s} + k_d s, \quad (3)$$

and block diagram of the AVR system is shown in Fig. 1. The performance index of control response is defined by

$$\begin{aligned} \min F(k_p, k_i, k_d) &= \frac{e^{-\beta} \cdot t_s / \max(t)}{(1-e^{-\beta}) \cdot |1-t_r / \max(t)|} + e^{-\beta} \cdot M_o + ess = \frac{e^{-\beta} \cdot (t_s + \alpha_2 \cdot |1-t_r / \max(t)| \cdot M_o)}{(1-e^{-\beta}) \cdot |1-t_r / \max(t)|} + ess \\ &= \frac{e^{-\beta} \cdot (t_s / \max(t) + \alpha \cdot M_o)}{\alpha} + ess \\ \alpha &= (1-e^{-\beta}) \cdot |1-t_r / \max(t)|, \end{aligned} \quad (4)$$

**Fig. 1.** Block diagram of an AVR system with a PID controller

k_p, k_i, k_d : Parameter of PID controller, β : Weighting factor, Mo : Overshoot, t_s : Settling time (2%), ess : Steady-state error, t : Desired settling time. In equation (4), if the weighting factor, β increases, rising time of response curve is small, and when β decreases, rising time is big. Performance criterion is defined as $Mo = 50.61\%$, $ess = 0.0909$, $t_r = 0.2693(s)$, $t_s = 6.9834(s)$.

3.2 GA-BF for AVR System

This paper describes the method in the form of an algorithm to search optimal value of parameters [11].

[step 1] Initialize parameters $n, N, N_C, N_S, N_{re}, N_{ed}, P_{ed}, C(i) (i=1,2,\dots,N), \phi^i$, Where, n: Dimension of the search space, N: The number of bacteria in the population, N_C : chemotactic steps, N_{re} : The number of reproduction steps, N_{ed} : the number of elimination-dispersal events, P_{ed} : elimination-dispersal with probability, $C(i)$: the size of the step taken in the random direction specified by the tumble.

[step 2] Elimination-dispersal loop: $l=l+1$

[step 3] Reproduction loop: $k=k+1$

[step 4] Chemotaxis loop: $j=j+1$

[step 5] If $j < N_C$, go to step 3. In this case, continue chemotaxis, since the life of the bacteria is not over.

[step 6] Reproduction:

[substep a] For the given k and l , and for each $i=1,2,\dots,N$, let

$$ITSE_{health}^i = \sum_{j=1}^{N_c+1} ITSE(i, j, k, l) \text{ be the health of bacterium } i \text{ (a measure of how many nutrients it got over its lifetime and how successful it was at avoiding noxious substances). Sort bacteria and chemotactic parameters } C(i) \text{ in order of ascending cost } ITSE_{health} \text{ (higher cost means lower health).}$$

[step 7] If $k < N_{re}$, go to [step 3]. In this case, we have not reached the number of specified reproduction steps, so we start the next generation in the chemotactic loop.

[step 8] Elimination-dispersal: For $i=1,2,\dots,N$, with probability P_{ed} , eliminate and disperse each bacterium, and this results in keeps the number of bacteria in the population constant. To do this, if you eliminate a bacterium, simply disperse one

to a random location on the optimization domain. If $l < N_{ed}$, then go to [step 2]; otherwise end. Initial values of PID Controller and GA-BF for simulation are shown as Table 1.

Table 1. Parameter ranges for Learning of GA-BF

| PID parameters | Range | |
|----------------|-------|-----|
| | Min | Max |
| k_p | 0 | 1.5 |
| k_i | 0 | 1 |
| k_d | 0 | 1 |

4 Conclusion

Recent many approaches of evolutionary algorithms for the evaluation of improved learning algorithm and control engineering have been studying. The general problem of evolutionary algorithm based engineering system design has been tackled in various ways because of learning time and local or suboptimal solution. GA has also been used to optimize nonlinear system strategies but it might be local optimized. This paper suggests the hybrid system consisting of GA (Genetic Algorithm) and BF (Bacterial Foraging) for PID controller of AVR system and compared with GA, PSO, GA-PSO. This approach proposed in this has the potential to be useful in practical optimization problems (e.g., engineering design, online distributed optimization in distributed computing and cooperative control) as models of social foraging are also distributed nongradient optimization methods. It can also may be used a wide variety of fruitful research directions and ways to improve the models (e.g., modeling more dynamics of cell motion).

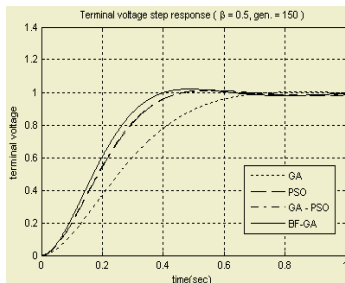


Fig. 2. Terminal voltage step response of AVR system by GA-BF controller ($\beta = 0.5$, generations=200)

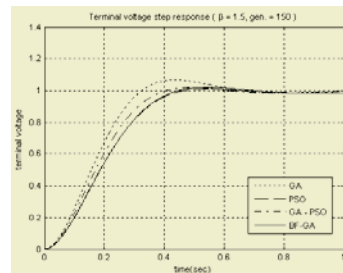


Fig. 3. Terminal voltage step response of AVR system by GA-BF controller ($\beta = 1.5$, generations=200)

Moreover, other species of bacteria or biological based computing approach could be studied but it remains to be seen how practically useful the optimization algorithms are for engineering optimization problems, because they depend on the theoretical properties of the algorithm, theoretical and empirical comparisons to other methods, and extensive evaluation on many benchmark problems and real-world problems.

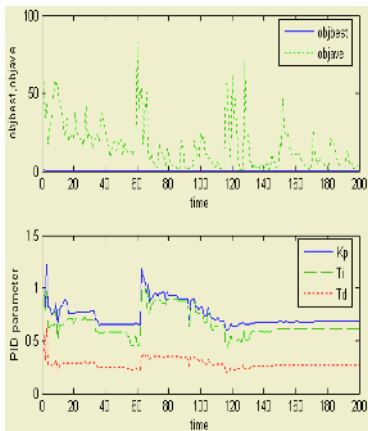


Fig. 4. Search process for optimal parameter in an AVR system by BF-GA ($\beta = 0.5$)

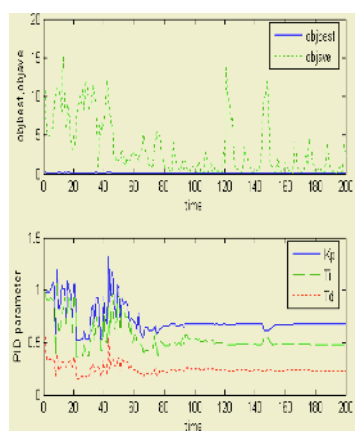


Fig. 5. Search process for optimal parameter in an AVR system by BF-GA ($\beta = 1.5$)

Table 2. Best solution using BF-GA controller with the different β values

| β | No. of generation | k_p | k_i | k_d | Mo (%) | ess | t_s | t_r | Evaluation value |
|---------|-------------------|---------|---------|---------|----------|--------|--------|--------|------------------|
| 0.5 | 200 | 0.68233 | 0.6138 | 0.26782 | 1.94 | 0.0171 | 0.3770 | 0.2522 | 0.3614 |
| 1 | 200 | 0.68002 | 0.52212 | 0.24401 | 1.97 | 0.0067 | 0.4010 | 0.2684 | 0.1487 |
| 1.5 | 200 | 0.67278 | 0.47869 | 0.22987 | 1.97 | 0.0014 | 0.4180 | 0.2795 | 0.07562 |

References

- Chung-Liang Lin, Huai-Wen Su, "Intelligent control theory in guidance and control system design:an Overview," Proc. Natul. Sci., Counc. ROC(A), vol. 24, no. 1, pp. 15-30, 2000.
- P. J. Fleming and R. C. Purshouse, "Evolutionary algorithms in control system engineering: A survey," Control Eng. Practice, vol. 10, pp. 1223–1241, 2002.
- M. Dotoli, G. Maione, D. Naso, and E. B. Turchiano, "Genetic identification of dynamical systems with static nonlinearities," in Proc. IEEE SMCia/01,Mountain Workshop Soft Computing Industrial Applications, Blacksburg, VA, June 25–27, 2001, pp. 65–70.
- G. J. Gray, D. J. Murray-Smith, Y. Li, K. C. Sharman, and T. Weinbrenner, "Nonlinear model structure identification using genetic programming," Contr. Eng. Practice, no. 6, pp. 1341–1352, 1998.
- K. Kristinnson and G. A. Dumont, "System identification and control using genetic algorithms," IEEE Trans. System, Man, Cybern., vol. 22, pp. 1033–1046, Sept.-Oct. 1992.
- R. A. Krohling and J. P. Rey, "Design of optimal disturbance rejection PID controllers using genetic algorithms," IEEE Trans. Evol. Comput., vol. 5, pp. 78–82, Feb. 2001.
- Zwe-Lee Gaing, "A Particle Swarm Optimization Approach for Optimum Design of PID Controller in AVR System", IEEE Trans. Energy Con. Vol. 19, pp. 384-391, No. 2, June, 2004.

8. STEPHENS, D. W., and KREBS, J. R., "Foraging Theory, Princeton University Press, Princeton, New Jersey, 1986.
9. ALCOCK, J., Animal Behavior, "An Evolutionary Approach, Sinauer Associates," Sunderland, Massachusetts, 1998.
10. BELL, W. J., Searching Behavior, "The Behavioral Ecology of Finding Resources," Chapman and Hall, London, England, 1991.
11. Dong Hwa Kim, "Robust tuning of PID controller with disturbance rejection using bacterial foraging based optimization," International symposium on computational intelligent and industrial application (ISCIIA2004), Dec. 20-22, 2004, Hikou, China.
12. Dong Hwa Kim, "Robust PID controller tuning using multiobjective optimization based on clonal selection of immune algorithm," Proc. Int. Conf. Knowledge-based intelligent information and engineering systems. Springer-Verlag. pp. 50-56, 2004.

Fault Diagnosis of Induction Motor Using Linear Discriminant Analysis

Dae-Jong Lee¹, Jang-Hwan Park², Dong Hwa Kim³, and Myung-Geun Chun^{4,*}

¹ Dept. Of Electrical and Computer Engineering, University of Alberta, Edmonton, Canada
djmidori@empa1.com

² Information & Control Eng., Chungju National University, Chungju, Chungbuk, Korea
park@chungju.ac.kr

³ Control Engineering, Hanbat National University, Daejeon, Korea
kimdh@hnu.ac.kr

⁴ Dept. of Electrical & computer Engineering, Chungbuk National University
San 48, Gaesin Dong, Heungduk Ku, Chungju, Chungbuk, Korea, 361-763
mgchun@chungbuk.ac.kr

Abstract. In this paper, we propose a diagnosis algorithm to detect faults of induction motor using the linear discriminant analysis. First, after reducing the input dimension of the current value vector measured at each period by using the principal component analysis method, we extract the feature vectors for each fault using the linear discriminant analysis. And then, we will diagnosis the condition of an induction motor by using a distance measure between the predefined fault vectors and the input vector. From the various experiments under noisy conditions, we found that the proposed fault detection method could be applied to prevent a fault by diagnosing the conditions of a induction motor in real industrial applications.

1 Introduction

The use of motor has been increasing with the development of industry. Especially, induction motors are the most widely used electrical machine due to many advantages of simplicity in construction as well as economical cost. Often, an unexpected failure of induction motor, however, makes the breakdown of whole production line causing major loss to the industry, so it is important to prevent a fault by diagnosing and monitoring the condition of induction motor at all times.

The induction motor failures usually include the insulation and mechanical faults. A survey shows that the pure insulation failures are responsible for less than 5% of all electrical machine failure. So, the major electrical machine failures are caused by mechanical faults [1]. The mechanical failures can be usually classified as six categories such as stator failure, broken rotor bars, bearing failure, bent shaft, static eccentricity, and dynamic eccentricity. One the other hand, when we classify the faults by the components of a induction motor, 40% of the faults are caused by bearing, 38% by stator, 10% by rotor, and 12% by others [2, 3]. Here it is noted that almost of 80-90% motor failures are related to bearing, stator and rotor parts.

During the recent years, the fault detection and diagnosis of induction motors have been gaining more interests in the filed of highly reliable systems. For reliable fault

* Corresponding Author

diagnosis, it is extremely required in detecting and classifying the fault elements. There are some detection methods to identify the motor faults. Among them, the most widely used approaches are vibration monitoring and motor current signature analysis (MCSA).

For motor current signature analysis approach, the stator current is detected by current transducers and sampled by data acquisition board. This method is known as a powerful technique for monitoring the conditions of induction motors [4-7]. Also, it is important to extract features vectors from the signal measured by MCSA. The most commonly used method for feature extraction is the Fourier spectral analysis method [4, 5]. But, this technique has difficulties of exact extracting frequency components when there are other components due to noise, for example, supply voltage distortion, harmonics and so on. There is another method to extract patterns using d-q transformation. But, the usage of the d-q transformation is not enough for fault diagnosis for some reasons. First, it is not clear that patterns are unique for different faults. Second, the classification is very difficult when practice problems including noises are considered [6, 7]. Owing to the difficulties as mentioned, practical applications of the MCSA become much more complicated and thus many problems have not been solved yet.

To resolve the problems as above, we carry out to extract features of fault signal using the linear discriminant analysis (LDA) method. This method properly separates classes in a low dimensional subspace even under variation [10-12]. From the experiments under various noise conditions, we obtained better classification performance comparing with results produced by using the principal component analysis (PCA) method.

2 A Fault Diagnosis System for Induction Motors

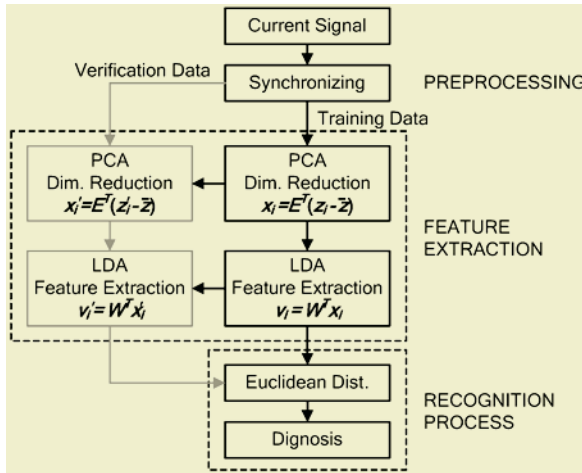
The proposed fault diagnosis system of induction motor is shown in Fig. 1. In the preprocessing part, the measured current signal is rearranged to synchronize with same position of current values. In the feature extraction part, after reducing the input dimension of the current value vector measured at each period by using the PCA, we extract the feature vectors for each fault using the LDA.

Now, we will briefly describe the procedure to extract the feature vectors by the LDA [10-12]. The first processing stage is based on PCA and can be described as follows. Let a fault signal be a one-dimensional $n \times 1$ array. Denote the training set of N fault signals by $Z = (z_1, z_2, \dots, z_N)$. We can define a covariance matrix as follows.

$$R = \frac{1}{N} \sum_{i=1}^N (z_i - \bar{z})(z_i - \bar{z})^T = \Phi \Phi^T \quad (1)$$

$$\bar{z} = \frac{1}{N} \sum_{i=1}^N z_i \quad (2)$$

Then, the eigenvalues and eigenvectors of the covariance matrix R are calculated as follows. Let $E = (e_1, e_2, \dots, e_r)$ denote the r eigenvectors corresponding to the r largest eigenvalues. For a set of original fault signals Z , their corresponding reduced feature vectors $X = (x_1, x_2, \dots, x_N)$ can be obtained as follows:

**Fig. 1.** Proposed fault diagnosis system

$$\mathbf{x}_i = E^T (\mathbf{z}_i - \bar{\mathbf{z}}) \quad (3)$$

The second processing stage is based on the LDA and can be described as follows; consider c classes in the problem with N samples and let the between-class scatter matrix be defined as

$$S_B = \sum_{i=1}^c N_i (\mathbf{m}_i - \bar{\mathbf{m}})(\mathbf{m}_i - \bar{\mathbf{m}})^T \quad (4)$$

where N_i is the number of samples in i 'th class C_i and $\bar{\mathbf{m}}$ is the mean of all samples, \mathbf{m}_i is the mean of class C_i . The within-class scatter matrix is defined as follows

$$S_W = \sum_{i=1}^c \sum_{x_k \in C_i} (\mathbf{x}_k - \mathbf{m}_i)(\mathbf{x}_k - \mathbf{m}_i)^T = \sum_{i=1}^c S_{W_i} \quad (5)$$

where S_{W_i} is the covariance matrix of class C_i . The optimal projection matrix W_{LDA} is chosen as the matrix with orthonormal columns that maximizes the ratio of the determinant of the between-class matrix of the projected samples to the determinant of the within-class scatter matrix of the projected sampled, i.e.,

$$W_{LDA} = \arg \max_W \frac{|W^T S_B W|}{|W^T S_W W|} = [\mathbf{w}_1 \quad \mathbf{w}_2 \quad \cdots \quad \mathbf{w}_m] \quad (6)$$

where $\{\mathbf{w}_i | i=1,2,\dots,m\}$ is the set of generalized eigenvectors (discriminant vectors) of S_B and S_W corresponding to the $c-1$ largest generalized eigenvalues $\{\lambda_i | i=1,2,\dots,m\}$, i.e.,

$$S_B \mathbf{w}_i = \lambda_i S_W \mathbf{w}_i, \quad i=1,2,\dots,m \quad (7)$$

Thus, the feature vectors $\mathbf{V} = (\mathbf{v}_1, \mathbf{v}_2, \dots, \mathbf{v}_N)$ for any signal \mathbf{z}_i can be calculated as follows

$$\mathbf{v}_i = W_{LDA}^T \mathbf{x}_i = W_{FLDA}^T E^T (\mathbf{z}_i - \bar{\mathbf{z}}) \quad (8)$$

To complete classification of a new pattern \mathbf{z}' , we compute an Euclidean distance between \mathbf{z}' and a pattern in the training set \mathbf{z} that is

$$d(\mathbf{z}, \mathbf{z}') = \|\mathbf{v} - \mathbf{v}'\| \quad (9)$$

3 Experiment and Analysis

Fig. 2 shows the experimental setup consisting of three-phase power supply, induction motor and load equipment. We obtained the fault signals from the clamp-on-meters hooked at input of induction motor. Table 1 shows experimental conditions and diagnosis categories. Here, we constructed 6-fault models such as healthy, bearing fault, bowed rotor, broken rotor bar, static eccentricity, and dynamic eccentricity respectively. Fig. 3 shows the fault parts of induction motor considered in this paper.

The number of sampling data are 128 per one period. The sampling frequency is 3kHz and sampling time is 0.13ms. We obtained 18 fault signals for each motor condition, thus the total number of fault signals becomes 108. Among these fault signals, we used 54 fault signals for training and the others for test. To show the properties of the proposed method under various noise conditions, we increase white Gaussian noise to make SNR from 100 to 25. Usually, a line notch filter is used to filter out the fundamental component and a low pass filter is used to filter out high frequency harmonics. So, we didn't consider noise variation below SNR 5.

Table 2 shows experimental results in case of no noise. The overall fault detection rate is 92.56% in case of using the PCA. In this case, 2 fault signals among 9 fault signals of bowed rotor condition are misclassified as static eccentricity. Also, 2 fault signals of static eccentricity are misclassified as bowed rotor. From this, we found that the PCA is difficult to classify between bowed rotor and static eccentricity. On the other hand, the overall fault detection rate is 100% in case of using the LDA. Below Fig. 4 shows feature vectors obtained by PCA and LDA respectively. As you can see in Fig. 4, the fault vectors are well clustered by the LDA comparing with the PCA.



Fig. 2. Experimental setup

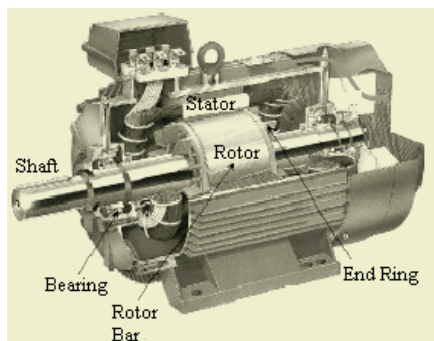
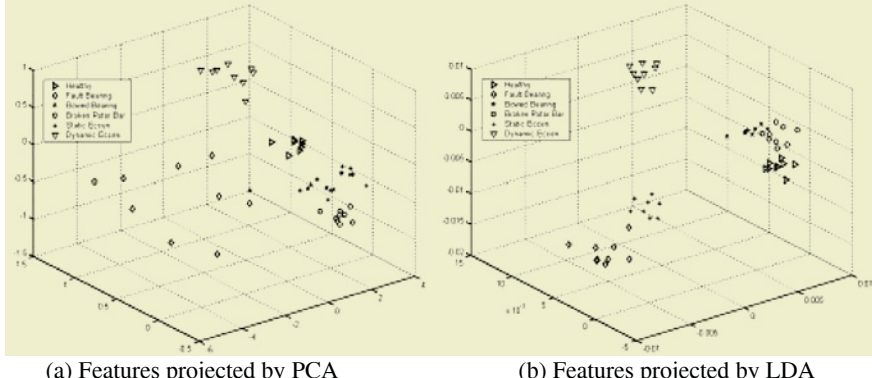


Fig. 3. The fault parts of induction motor

Table 1. Experiment condition and diagnosis categories

| Fault ID | Fault detection | SNR |
|----------|----------------------|------------------|
| 1 | Healthy | 100 - 25, step 5 |
| 2 | Faulted Bearing | " |
| 3 | Bowed Rotor | " |
| 4 | Broken Rotor Bar | " |
| 5 | Static Eccentricity | " |
| 6 | Dynamic Eccentricity | " |

**Fig. 4.** Feature vectors obtained by PCA and LDA**Table 2.** Recognition result

| Faulty Condition | LDA | | PCA | |
|----------------------|---------------------|-------------------------|---------------------|-------------------------|
| | # of classification | # of mis-classification | # of classification | # of mis-classification |
| Healthy mode | 9 | 0 | 9 | 0 |
| Bearing damage | 9 | 0 | 9 | 0 |
| Bending rotor | 9 | 0 | 7 | 2 (static eccentricity) |
| Rotor bar defect | 9 | 0 | 9 | 0 |
| Static eccentricity | 9 | 0 | 7 | 2 (bending Rotor) |
| Dynamic eccentricity | 9 | 0 | 9 | 0 |

Fig. 5 shows the fault detection results according to the noise variation. The detection rate of using the PCA is 92.56% when SNR is 40. On the other hand, the detection rate of using the LDA is 100% when SNR is 40. We can find that at the most case the LDA better performance than the PCA. So, the LDA can be one of powerful techniques to classify the fault signals of induction motor.

4 Concluding Comments

In this work, we suggested a fault diagnosis algorithm using the linear component analysis. Since the adopted linear component analysis can make a condensed cluster for the same type of fault signals, it can reduce the sensitivity against noise. Experimental results showed that the proposed methods had better fault detection results than the PCA. We think that the LDA can be one of powerful techniques to classify the fault signals of induction motor in real industrial applications.

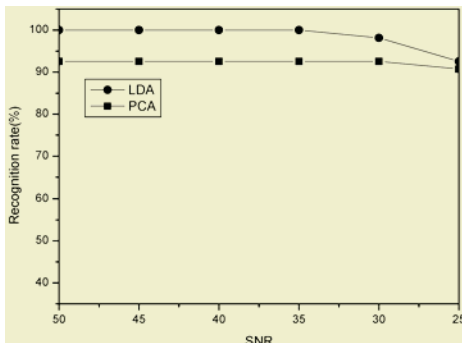


Fig. 5. The diagnosis performance according to noise variation

Acknowledgements

This work has been supported by EESRI(R-2003-B-285), which is funded by MOCIE(Ministry of commerce industry and energy).

References

1. Ye Zhongming, Wu Bin, "A review on induction motor online fault diagnosis", PIEMC 2000, Vol. 3 (2000) 1353-1358
2. Benbouzid, M.E.H., Kliman, G.B, "What stator current processing-based technique to use for induction motor rotor faults diagnosis?", IEEE Transactions on Energy Conversion, Vol 18, Issue 2 (2003) 238 -244
3. Thomson, W.T., Fenger, M., "Current signature analysis to detect induction motor faults", IEEE Industry Applications Magazine, Vol. 7, Issue 4 (2001) 26 -34
4. Nejjari, H., Benbouzid, M.E.H., "Monitoring and diagnosis of induction motors electrical faults using a current Park's vector pattern learning approach", IEEE Transactions on Industry Applications, Vol. 36, Issue 3 (2000) 730-735
5. Bellini, A., Filippetti, F., Franceschini, G., Tassoni, C., Kliman, G.B., "Quantitative evaluation of induction motor broken bars by means of electrical signature analysis", IEEE Transactions on Industry Applications, Vol. 37, Issue 5 (2001) 1248-1255
6. Kyusung Kim, Parlos, A.G., Mohan Bharadwaj, R., Sensorless fault diagnosis of induction motors, IEEE Transactions on Industrial Electronics, Vol. 50 Issue 5 (2003) 1038-1051
7. Zidani, F., El Hachemi Benbouzid, M., Diallo, D., Nait-Said, M.S., "Induction motor stator faults diagnosis by a current concordia pattern-based fuzzy decision system", IEEE Transactions on Energy Conversion, Vol. 18, Issue 4 (2003) 469-475
8. Haji, M., Toliat, H.A., Pattern recognition-a technique for induction machines rotor broken bar detection, IEEE Trans. on, Energy Conversion, Vol. 16, Issue 4 (2001) 312 -317
9. Trzynadlowski, A.M., Ritchie, E., "Comparative investigation of diagnostic media for induction motors: a case of rotor cage faults", IEEE Trans. on, Industrial Electronics, Vol. 47, Issue 5 (2000) 1092 -1099
10. M. Turk, A. Pentland, "Face recognition using eigenfaces", Proc. IEEE Conf. on Computer Vision and Pattern Recognition (1991) 586-591
11. P. N. Belhumeur, J. P. Hespanha, D. J. Kriegman, "Eigenfaces vs. Fisherfaces: recognition using class specific Linear Projection", IEEE Trans. on Pattern Analysis and Machine Intell., 19(7) (1997) 711-720
12. Richard O. Duda, Peter E. Hart, David G. Stork, Pattern Classification, JOHN WILEY&SONS, INC. Second Edition (2002)

Classifier Fusion to Predict Breast Cancer Tumors Based on Microarray Gene Expression Data

Mansoor Raza¹, Iqbal Gondal¹, David Green¹, and Ross L. Coppel^{2,3}

¹ GSCIT, Faculty of IT

{Mansoor.Raza, Iqbal.Gondal, David.Green}@Infotech.monash.edu.au

² Department of Microbiology

³ Victorian Bioinformatics Consortium, Monash University, Australia

Ross.Coppel@med.monash.edu.au

Abstract. Classifiers are often data dependent as they perform better on one type of data, but fail to perform well for another data set. There is a need for robust classification algorithms which exhibit performance stability for multiple types of data. This problem can be addressed if different classifiers are fused to identify a particular class. In this paper, we have implemented the idea of classifier fusion using six different classifiers to classify the microarray gene expression data of breast cancer patients. The paper uses two classifier fusion models: majority voting and random bagging to improve the accuracy of the classifiers. Our experimental results have shown that the new proposed classifiers fusion methodology have outperforms single classification models.

1 Introduction

A precise diagnosis of cancerous malignancies is difficult but often crucial for successful treatment. Given the large-scale, high-throughput gene expression technology and accurate statistical methods, bio-molecular information could become as, or even more important for cancer diagnosis than traditional clinical factors. Breast cancer results from the combined action of both genetic and environmental factors [1]. Inheritance of mutant forms of the genes BRCA1 and BRCA2 confers an increased susceptibility to breast and ovarian cancer. Mutations induced or inherited in other as yet unrecognized genes may act independently or in association with pre-existing mutations in BRCA1 or BRCA2 to give rise to cancer [1]. Mutations in genes such as BRCA1 and BRCA2 can be used directly to determine a patient's general risk of getting cancer. However direct mutation detection provides no information about the timing of appearance of the tumor, rate of progression or the patient's response to treatment. In cancerous cells, there is a change in expression of genes with some genes being upregulated and producing increased amounts of messenger RNA (mRNA) whereas other genes are downregulated to produce less mRNA. It is hypothesized that tumors with different behaviors do so because of different mRNA profiles and that determining this profile will provide predictive information about the future course of the cancer. In order to address these issues, much interest has focused on the technique of microarray analysis, which is a method of determining the level of expression in a tissue sample of many genes simultaneously.

Microarray experiments generate large datasets with expression values for thousands of genes, but usually not more than a few dozens of arrays. The datasets have

many more predictor variables than samples gives rise to the issue of the curse of dimension that lead to the wealth of research in statistical and Machine learning. It is also observed that data dependency of the classifiers have made classifiers to perform better on one type of data and fail to perform well on other type of data. These problems have been addressed by feature selection and integrating several base classifiers included in an ensemble [23]. It is well known that a combination of many different classifiers can improve classification accuracy. A variety of schemes have been proposed for combining multiple classifiers. These approaches use classifiers fusion models with the incorporation of weights expressed over the entire data space and data dependent combination weights and they are: the sum, product, minimum, maximum, median majority vote [2-4]; Bagging [21] and Boosting [20-22]. These class prediction tools from machine learning are remarkably successful with high-dimensional data like microarray gene expression data [22].

Comparisons of expression profile obtained from different predefined classes have been used by, Hedenfalk et al [3] to determine whether the patterns of gene expression could be used to classify tumor samples depending on whether they arose as a result of mutations in BRCA1 or BRCA2. Compound Covariate Predictor (CCP) and leaveone- out cross-validation technique was used for misclassification [3]. Golub et al. used class discovery and classprediction (CP) with ‘neighborhood analysis’ and ‘weighted vote’ methods to compare expression profiles between specimens of acute myelogenous leukemia and specimens of acute lymphocytic leukemia [4]. Ross et al. compared expression profiles in cancer cell lines with different tissues of origin, using hierarchical clustering algorithm to separate the cell lines and genes using the Pearson coefficients as the measure of similarity and average linkage clustering [5].

The paper presents the ideas of classifier fusion also know as ensemble approach using six different classifiers to classify the microarray gene expression data of breast and ovarian cancer. We have used classifier fusion with majority voting and proposed random bagging method to improve the accuracy of the classifiers. Our experimental results show that the new proposed classifiers fusion methodology has outperforms single classification models.

This paper is organized as follows: section 2 demonstrates different classification algorithm used as base classifiers. Our proposed models and methodology is presented in section 3. Results and discussion on our experimental results are provided in section 4. Finally, section 5 concludes the paper.

2 Classification

The class predictor creates a multivariate predictor for determining which of the two classes a given sample belongs. The 0.001 significance level is defined to determine the genes that will be included in the predictors; genes that are differentially expressed between the classes at univariate parametric significance level less than the specified threshold are included in the predictor. The selected features of each sample are used for classification. In some problems better prediction can be achieved by being more liberal about the gene sets used as features. On the other hand predictors may be more biologically interpretable and clinically applicable if fewer genes are included. The subsections 2.1.1 to 2.1.5 briefly review the six classification techniques that are used in evaluating and building our proposed hybrid classification

system. A comprehensive review of these methods can be found in [1, 2 and 4]. The following subsections provide detailed description of the methods used in the research.

2.1 Compound Covariate Predictor

The CCP is a weighted linear combination of log-ratios for genes that are univariately significant at the specified level. The univariate t -statistics for comparing the classes are used as the weights.

2.2 Diagonal Linear Discriminant Analysis

The DLDA is similar to the CCP and is a version of linear discriminant analysis that ignores correlations among the genes in order to avoid over-fitting the data. Many complex methods have too many parameters for the amount of data available. Consequently they appear to fit the training data used to estimate the parameters of the model, but they have poor prediction performance for independent data. Dudoit et al has found that diagonal linear discriminant analysis performed well on a range of microarray data sets.

2.3 k -Nearest Neighbor ($k=1$ and 3)

Euclidean distance is used as the distance metric for the NN. Once the nearest neighbor in the training set of the test specimen is determined, the class of that nearest neighbor is taken as the prediction of the class of the test specimen. For example with the 3-NN algorithm, the expression profile of the test specimen is compared to the expression profiles of all of the specimens in the training set and the 3 specimens in the training set most similar to the expression profile of the test specimen are determined.

2.4 Nearest Centroid

The centroid of each class is determined. The distance of the expression profile for the test sample to each of the two centroids is measured and the test sample is predicted to belong to the class corresponding to the NC.

2.5 Support Vector Machine

SVM is implemented with linear kernel functions only to be fair with other classifier. The SVM predictor is a linear function of the log-intensities that best separates the data subject to penalty costs on the number of specimens misclassified. We use the LIBSVM implementation of Chang and Lin [15].

3 Methodology

In the study, single intensity microarray raw data normalized to log, and then a paired t-test is used for feature selection. The classification predictor architecture uses six

classifiers and then uses majority voting to fuse the classifier results. Finally, misclassified samples are rearranged to classify again using proposed random bagging until best solution is achieved as shown in Fig 1. Supervised classification methods were applied to identify gene expression signatures that differed between two tumor samples. Using top-ranked discriminating genes selected by paired t test, supervised classification with leave-one-out cross-validation (LOOCV) was performed with various classifiers: CCP, linear discriminant analysis (DLDA), support vector machines (SVM), k-nearest neighbors k-NN ($k=1$ and 3), and nearest centroid (NC) classifiers.

The classification accuracy and empirical P values were obtained at significant level of 0.001 for the feature selection. We used individual classifier to get the base accuracy. In the second step we used simple majority voting method for classifier fusion to improve the prediction accuracy. If the best results were not achieved then in the third step, we included the samples that were misclassified to classify iteratively using random bagging until it achieved better accuracy. In every iteration, to have the equal numbers of samples from both classes e.g. BARCA1 or others we included the samples that were misclassified and also selected randomly equal in number other samples from both classes which were classified correctly.

Under cross-validation, the available data was divided into k disjoint sets; k models were then trained, each on a different combination of $k-1$ partitions and tested on the remaining partition. Cross-validation thus makes good use of the available data as each sample is used both as training and test data. Cross-validation is therefore especially useful where the amount of available data is insufficient to form the usual training, validation and test partitions required for split-sample training [12]. The most extreme form of cross-validation, where k is equal to the number of training patterns is known as LOOCV, and has been widely studied due to its mathematical simplicity [13, 14]. It provides an almost unbiased estimate of the generalization ability of a classifier. In our case k is equal to the number of samples (22) Hedinfald et al dataset. Simulations of these studies have been carried out using the BRB Array Tools software [6].

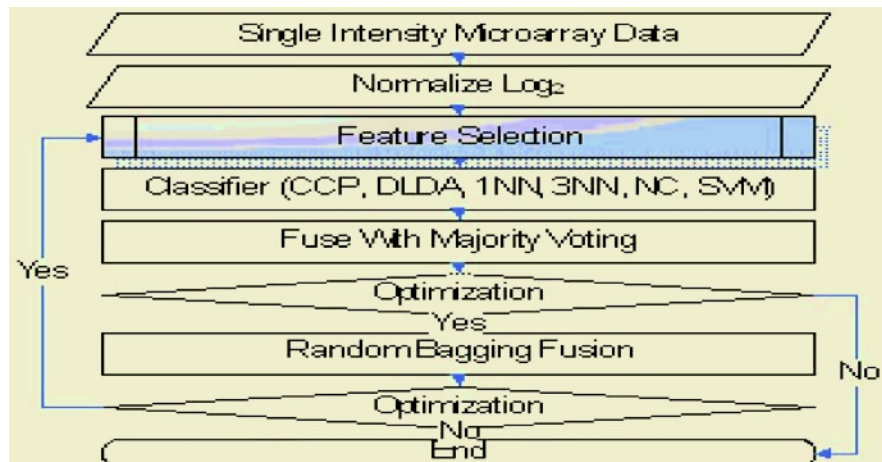


Fig. 1. Proposed classifier fusion architecture to predict breast cancer tumors based on microarray gene expression data

4 Results and Discussion

The gene expression data set used in this paper is obtained from tumor biopsies of patients with breast cancer. The patients had three groups [3]:

- BRCA1 mutation
- BRCA2 mutation
- Sporadic cancer: neither BRCA1 nor BRCA2.

Breast cancer data set collected by Hedenfalk et al [3] contains RNA samples of primary tumors from seven carriers of the BRCA1 mutation, 8 carriers of the BRCA2 mutation, and 7 patients with sporadic cases of breast cancer. The samples were compared on a microarray of 6512 complementary DNA clones of 5361 genes. After filtering, 3226 genes were used for the analysis. A reference design was employed for microarray and each tumor sample was compared with the non-tumorigenic cell line MCF-10A [3].

We divided three tumor samples into two groups. BRCA1 verses non-BRCA1 (includes BRCA2 and sporadic). BRCA2 verses non-BRCA2 (BRCA1 and sporadic).

BRCA1-notBRCA1 class prediction was based on 2000 random permutations and CCP, 1-NN, 3-NN, NC, SVM and DLDA used p-value of 0.001, 0.007, 0.009, 0.01, 0.003 and 0.01 respectively as individual classifiers.

Table 1. Classification of BRCA1-notBRCA1 with majority voting. Misclassified samples shown as “N” and correctly classified as “Y”

| Tumor Group | Sample # | # of genes | CCP | DLDA | 1NN | 3NN | NC | SVM | Voting |
|-------------|----------|------------|-----|------|-----|-----|----|-----|--------|
| B1 | 1 | 58 | Y | N | Y | N | Y | Y | Y |
| B1 | 2 | 42 | Y | Y | Y | Y | Y | Y | |
| B1 | 3 | 69 | N | N | N | N | N | N | N |
| B1 | 4 | 45 | Y | Y | Y | Y | Y | Y | |
| B1 | 5 | 51 | Y | Y | Y | Y | Y | Y | |
| B1 | 6 | 57 | N | Y | N | N | N | N | N |
| B1 | 7 | 53 | Y | Y | Y | Y | Y | Y | |
| notB1 | 8 | 51 | Y | Y | Y | Y | Y | Y | |
| notB1 | 9 | 53 | Y | Y | Y | Y | Y | Y | |
| notB1 | 10 | 52 | Y | Y | Y | Y | Y | Y | |
| notB1 | 11 | 56 | Y | Y | Y | Y | Y | Y | |
| notB1 | 12 | 52 | Y | Y | Y | Y | Y | Y | |
| notB1 | 13 | 47 | Y | Y | Y | Y | Y | Y | |
| notB1 | 14 | 55 | Y | Y | Y | Y | Y | Y | |
| notB1 | 15 | 60 | Y | Y | Y | Y | Y | Y | |
| notB1 | 16 | 49 | Y | Y | Y | Y | Y | Y | |
| notB1 | 17 | 58 | Y | Y | Y | Y | Y | Y | |
| notB1 | 18 | 69 | N | N | N | N | N | N | N |
| notB1 | 19 | 52 | Y | Y | Y | Y | Y | Y | |
| notB1 | 20 | 47 | Y | Y | Y | Y | Y | Y | |
| notB1 | 21 | 48 | Y | Y | Y | Y | Y | Y | |
| notB1 | 22 | 48 | Y | Y | Y | Y | Y | Y | |

Table 1 shows that for base classifiers, out of 7 samples of BRCA1, 5 samples are classified correctly and two are misclassified (3, 6) by all the classifiers except 3-NN where 4 were classified correctly and 3 were misclassified. In 15 samples of not-BRCA1 all samples were classified correctly except one (18). Table 1 also shows number of extracted genes used by classifier after feature selection.

Since one of the sample were only misclassified by DLDA and 3-NN but correctly classified by the rest of the classifiers then majority voting considered that sample to be correctly classified increased the classification accuracy from 85.33% to 87.33%. Then misclassified samples 3, 6 and 18 were process using random bagging. For the final step of the fusion process, random bagging was used for BRCA1-notBRCA1 group to classify three samples 3, 6 and 8 as they were misclassified using majority voting model. Randomly selected samples including misclassified samples were selected as shown in Table 3. In fist iteration samples 3 was classified correctly and were excluded for second iteration. In second iteration samples 6 was correctly classified and excluded for third iteration, after three replication two samples out of three were classified correctly, which improved the accuracy of the fusion classifier to 95.45%, results are given in Fig 2. This iteration fusion process increased the classifier accuracy from 81% to 95.45% as shown in Table 4.

Table 2. Classification of BRCA2-notBRCA2 with majority voting Misclassified samples shown as "N" and correctly classified as "Y"

| Tumor Group | Sample # | # of genes | CCP | DLDA | 1NN | 3NN | NC | SVM | Voting |
|-------------|----------|------------|-----|------|-----|-----|----|-----|--------|
| B2 | 1 | 52 | N | N | N | N | N | N | N |
| B2 | 2 | 34 | N | N | N | Y | N | N | N |
| B2 | 3 | 31 | Y | Y | Y | Y | Y | Y | |
| B2 | 4 | 39 | N | N | Y | N | N | N | N |
| B2 | 5 | 20 | Y | Y | Y | Y | Y | Y | |
| B2 | 6 | 28 | Y | Y | Y | N | Y | Y | Y |
| B2 | 7 | 31 | N | Y | N | N | N | N | N |
| B2 | 8 | 20 | Y | Y | Y | Y | Y | Y | |
| notB2 | 9 | 28 | Y | Y | Y | Y | Y | Y | |
| notB2 | 10 | 31 | Y | Y | Y | Y | Y | Y | |
| notB2 | 11 | 37 | Y | Y | Y | Y | Y | Y | |
| notB2 | 12 | 32 | Y | Y | Y | Y | Y | Y | |
| notB2 | 13 | 30 | Y | Y | N | N | N | N | N |
| notB2 | 14 | 27 | Y | Y | Y | Y | Y | Y | |
| notB2 | 15 | 39 | Y | N | Y | Y | Y | Y | Y |
| notB2 | 16 | 43 | N | Y | Y | Y | N | N | Y |
| notB2 | 17 | 27 | Y | Y | Y | Y | Y | Y | |
| notB2 | 18 | 35 | Y | Y | Y | Y | Y | Y | |
| notB2 | 19 | 26 | Y | Y | Y | Y | Y | Y | |
| notB2 | 20 | 27 | Y | Y | Y | Y | Y | Y | |
| notB2 | 21 | 24 | Y | Y | Y | Y | Y | Y | |
| notB2 | 22 | 28 | Y | Y | Y | Y | Y | Y | |

BRCA2-notBRCA2 class prediction was based on 2000 random permutations and CCP, 1-NN, 3-NN, NC, SVM and DLDA used p-value of 0.001, 0.007, 0.009, 0.01, 0.003 and 0.01 respectively

Table 3. Iteration fusion model to include the misclassified sample of BRCA1-notBRCA1 and BRCA2-notBRCA2 tumor group

| B1-notB1 | Samples | | | | | | | | | |
|------------|---------|---|---|---|---|----|----|----|----|----|
| Iteration1 | 2 | 9 | 3 | 4 | 6 | 14 | 15 | 16 | 18 | 19 |
| Iteration2 | 2 | 8 | 4 | 5 | 6 | 14 | 15 | 16 | 18 | 20 |
| Iteration3 | 2 | 9 | 4 | 5 | 7 | 14 | 15 | 16 | 18 | 21 |
| B2-notB2 | | | | | | | | | | |
| Iteration1 | 1 | 3 | 2 | 4 | 7 | 9 | 10 | 13 | 16 | 17 |
| Iteration2 | 4 | 5 | 6 | 7 | 8 | 11 | 12 | 13 | 16 | 14 |
| Iteration3 | 4 | 3 | 5 | 6 | 8 | 16 | 17 | 18 | 19 | 18 |

Table 2 shows that for base classifiers out of 8 samples of BRCA2, 4 are classified correctly and 4 are misclassified by CCP, 3NN and NC, while 5 were classified correctly and 3 were misclassified by DLDA, 1NN and SVM. In 14 samples of not-BRCA2 class, 13 samples were classified correctly except one; results are given in Table 2.

For the final step of the fusion process, random bagging was used for BRCA2-notBRCA2 group to classify five samples 1,2,4,7 and 13, as they were misclassified using majority voting model. Randomly selected samples including misclassified samples were selected as shown in Table 3. In first iteration samples 1 and 2 were classified correctly and were excluded for second iteration. In second iteration samples 7 and 13 were correctly classified. In the next iteration sample 7 and 13 were excluded but sample 18 remained misclassified. This iteration fusion process increased the classifier accuracy from 81% to 95.45% as shown in Table 4.

Table 4. Average accuracy of base classifiers, classifier fusion using majority voting and random bagging

| Tumor Group | Base classifier | Majority Voting | Random Bagging Fusion |
|-------------|-----------------|-----------------|-----------------------|
| B1-notB1 | 85.33 | 87.33 | 95.45 |
| B2-notB2 | 77 | 81 | 95.45 |

Since there were three samples that were correctly classified by majority and misclassified by minority of the classifiers. Majority voting determined those samples to be correctly classified that increased the classification accuracy from 78% to 81.33% and with random bagging method classification accuracy improved to 95.45%.

We also observed that on tumor group BRCA1-notBRCA1 Nearest Centroid (NC) performed better with prediction accuracy of 86, but performed poorly with the accuracy of 73 on tumor group BRCA2-notBRCA2, which indicates that same classifiers' performance could vary for different datasets and it also justify the use of classifier fusion.

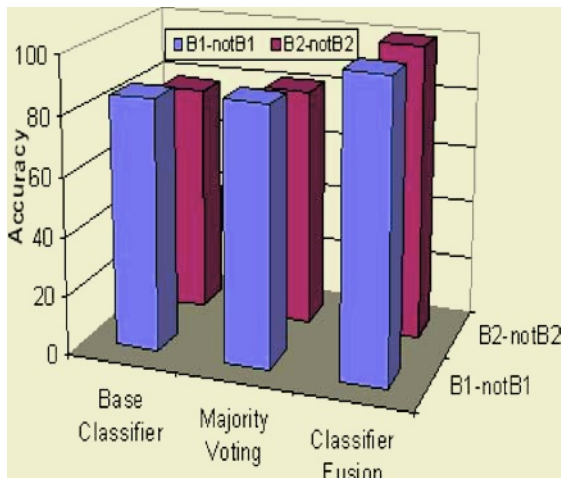


Fig. 2. Average accuracy of base classifiers, majority voting and random bagging for tumor group BRCA1-notBRCA1 and BRCA2-notBRCA2C

5 Conclusion

This paper has presented different classifier fusion methods. These methods have shown consistent performance when used for breast cancer microarray data sets as compared to single machine learning algorithm. Our proposed fusion model (random bagging) have shown improved classification accuracies of 95.45% as compared to best individual classifier accuracies of 85.33% for BRCA1-notBRCA1 tumor group and 95.45% as compare to the best individual accuracies of 77% for BRCA2-notBRCA2 tumor group. The better classification results for breast cancer dataset demonstrate the ability of our innovative fusion methods to classify various types of data more accurately.

References

1. Miki Y, et al. "A strong candidate for the breast and ovarian cancer susceptibility gene BRCA1", *Science*; 266 (5182), pp. 66-71, 1994 Oct7.
2. Perou CM, et al. "Molecular portraits of human breast tumours", *Nature*; 406, pp. 747-52, 2000.
3. Hedenfalk I, et al., "Gene-expression profiles in hereditary breast cancer", *N Engl J Med*, vol. 344, no. 8, pp.:539-48. 2001.
4. Golub T.R., et al. "Molecular classification of cancer: class discovery and class prediction by gene expression monitoring", *Science*. 286, pp. 531-537, 1999.
5. Ross D.T, et al. "Systematic Variation in Gene Expression Patterns in Human Cancer Cell Lines", *Nature Genetics*, 24, pp. 227-234, 2000.
6. <http://linus.nci.nih.gov>
7. Radmacher, et al. "A Paradigm for Class Prediction using Gene Expression Profiles", *JCompBio*, vol. 9, no. 3, pp 505-511, 2002.
8. Colin S Cooper "Applications of microarray technology in breast cancer research", *Breast Cancer Res.*, Vol. 3, no. 3 pp.158-75, Mar 2001.

9. Heilhaber et al, “Bayesian Estimation of Fold-Changes in the Analysis of Gene Expression: The PFOLD Algorithm”, JComBio, vol 8, no 6, pp. 585–614, 2001.
10. David et al “The limit fold change model: A practical approach for selecting differentially expressed genes from microarray data”, BMC Bioinformatics, 3:17, 2002.
11. Welcsh et al “BRCA1 transcriptionally regulates genes involved in breast tumorigenesis”, PNAS, vol. 99, no. 11, pp. 7560–7565, May 28, 2002.
12. Dobbin K, Simon R. “Comparison of microarray designs for class comparison and class discovery”, Bioinformatics 18(11), pp. 1438-45, 2002.
13. G Wright, R Simon, “The random variance model for finding differentially expressed genes”, Bioinformatics 19, pp. 2448-2455, 2003.
14. P Baldi, AD Long, “A Bayesian framework for the analysis of microarray expression data: regularized t-test and statistical inferences of gene changes”, Bioinformatics 17, pp. 509-519, 2001.
15. <http://www.csie.ntu.edu.tw/~cjlin/libsvm>.
16. S Dudoit, J Fridlyand, TP Speed; “Comparison of discrimination methods for the classification of tumors using gene expression data”, Journal of the American Statistical Association 97, pp. 77-87, 2002.
17. M. Stone. Cross-validatory choice and assessment of statistical predictions. Journal of the Royal Statistical Society, B, 36(1):111–147, 1974.
18. V. Vapnik and O. Chapelle. Bounds on error expectation for SVM. In A. J. Smola, P. L. Bartlett, B. Schölkopf, and D. Schuurmans, editors, Advances in Large Margin Classifiers, chapter 14, pages 261–280. 2000.
19. C. Chapelle, V. Vapnik, O. Bousquet, and S. Mukherjee. Choosing multiple parameters for support vector machines. Machine Learning, 2002.
20. Freund Y., Schapire R. E., Experiments with a new boosting algorithm, In: Proceedings of the Thirteenth International Conference “Machine Learning”, pp. 148-156, 1996
21. Breiman L., Half&Half bagging and hard boundary points. Technical report 534, Statistics Departament, University of California, Berkeley. www.stat.berkeley.edu/users/breiman, 1998
22. Freund Y., Schapire R. E., A decision-theoretic generalization of on-line learning and an application to boosting, Journal of Computer and System Sciences 55, pp. 119-139, 1997
23. M. LeBlanc and R. Tibshirani, “Combining estimates in regression and classification”, J. Amer. Statist. Assoc. 91 (1996), 1641-1650

An Efficient Face Detection Method in Color Images

Hongtao Yin, Ping Fu, and Shengwei Meng

Department of Automatic Test and Control, Harbin Institute of Technology, China
yinht@hit.edu.cn

Abstract. In this paper, an efficient algorithm for detecting human faces in color images is proposed. The first step of our algorithm is to segment the possible skin-like regions in an image by using color information, and then the gray level clustering is applied to eye location in skin color regions. The possible face regions are formed by pairing two possible eye candidates in a skin color region. In order to improve the reliability and accuracy, both Symmetry verification and template matching methods are used to locate the faces in those regions. Experimental results show that this algorithm can detect single or multiple faces from images having simple or complex backgrounds.

1 Introduction

Face detection is the process of recognizing a pattern in an image as a face pattern and subsequently segmenting it from the rest of the image. Human face detection is a challenging exercise because the face can have varying pose, size, skin color, and facial expression. In addition, other factors, such as wearing glasses, presence or absence of hair, and occlusion can make the appearance of the face unpredictable. Other effects, such as varying lighting conditions and complexity of the scene containing the face can make the generalization of face detection algorithms difficult.

Different approaches have been devised for the detection of human faces in gray-level images. These include shape analysis [1], template based [2], feature-based [3], neural network based [4], eigenface-based[5], example-based [6], region-based [7], etc. The computational complexity of these methods is usually too high for real-time applications. In order to improve detection time and detection performance, the color-based approach [8] has become a new direction for human face segmentation. The basic idea of this approach is that although skin color differs from person to person and race-to-race, it is distributed in a very small region in the color space. It implies that using simple thresholding techniques can segment the possible face like region. As a result, the search space in an unconstrained image is greatly reduced.

In this paper, a face detection algorithm for color image is presented, which is composed of skin color segmentation, gray level clustering segmentation, symmetry measure, and template matching. First, a skin color model is used for segmenting regions in which may have faces, and then the gray level clustering is applied to the eye location in skin color regions. Symmetry verifying and template matching methods are used to locate the faces in those regions. The algorithm integrates skin color information in color images with gray level distributing in skin color regions and structure feature of face, which results in not only better detecting rotated face, but also low computing cost. The performance of our algorithm is tested with face images under bad lighting conditions, under shadow, of different scales, and with glasses. Experimental results show that our proposed algorithm can achieve a high detection rate.

2 Face Detection Algorithm

Our method for detecting face regions in a color image is divided into several stages. In the first stage, the skin color regions are segmented based on the characteristics of human face color. According to the segmented results, the possible human eye regions are detected in the second stage. The eye regions are extracted by means of gray level clustering. Possible face regions are then formed by pairing two eye candidates. Finally, the symmetry of the possible face candidates and the correlation values between the possible face candidates and the face template are measured to verify whether the selected region is a face or not.

2.1 Segmentation of Skin Color Regions

In our method we first locate skin-like regions by performing color segmentation. As interesting color space we consider the Hue-Saturation-Value (HSV) color space, because it is compatible to the human color perception. For the segmentation of skin-like regions it is sufficient to consider hue and saturation as discriminating color information. According to the distributions we choose the parameters as follows: $0^\circ < H < 50^\circ$, $0.2 < S < 0.7$.

2.2 Possible Face Candidates Detection

2.2.1 Eye Detection

In the second stage, the eye-analogue segments will be detected and then used to form the possible face regions in an input image. Eyes are the most important facial features in face detection and recognition systems. In our method, the eye-analogue segments are detected in a gray level image and the search space for possible eye candidates can be restricted to skin color regions. At first all eye-analogue segments are found by finding regions that are roughly the same size of a real eye and are darker than their neighborhoods.

In our work, the *k-means clustering* algorithm is adopted to cluster the pixel in gray level image of skin color regions. Suppose K classes are obtained after applying the *k-means clustering* algorithm. The pixels in each class can form some patches. The patches composed of the lowest gray level value pixels are viewed as eye regions. Fig.1 shows an original image, gray level image of skin color area and its corresponding eye-analogue segments, respectively.

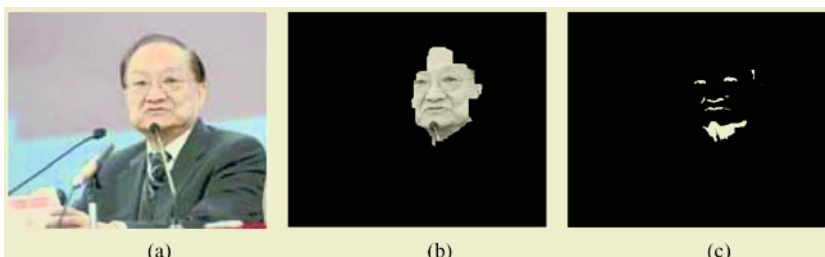


Fig. 1. Skin color segmentation and eye segmentation. (a) Original image. (b) Gray level image of skin color area. (c) Eye-analogue segments segmentation result

2.2.2 Face Candidate Selection

If locations of a pair of these segments conform to the geometrical relationship of two eyes, the face candidate selector concludes that a face pattern may exist. Since the size of a human face is proportional to the distance of its two eyes, a possible face region can be formed based on this relationship. In our approach, a square block is used to represent face candidates. Fig.2 illustrates a face candidate selection example.



Fig. 2. An example of selecting possible face region

2.2.3 Preliminary Face Candidate Verification

In a skin region, there will be many detected eye point, and consequently many face candidate. Some of these candidates are obvious non-faces that can be removed using simple verification. We propose three techniques for preliminary face candidate verification. These techniques rely on:

- the distance between the two box,
- the proportion of the skin inside the face bounding box,
- the proportion of two eyes.

2.3 Pretreatment of the Possible Face Regions

In order to improve the detection reliability and accuracy, each of the selected possible face regions is then processed to compensate for non-uniform lighting on the face region, and is masked to eliminate the affection of background.

2.3.1 Resizing

The portion of the image in each search window is automatically resized to $N \times N$ pixels, irrespective of the original size. The resizing algorithm used is based on linear interpolation from the original $M \times M$ pixel image to an $N \times N$ pixel image.

2.3.2 Normalization

In our approach, only the gray level image is used to verify whether the regions selected in the previous stage are true faces or not. However, the gray level image is affected by the external environment such as the direction of lighting source, so detection performance will be degraded if a face is under uneven lighting conditions. In order to reduce the lighting effects, a possible face candidate will be normalized for illumination. In our approach, the histogram of a possible face region is transformed to the histogram of a reference face image [9]. This can be achieved since all human faces have basically similar illumination properties.

2.3.3 Masking

To eliminate the pixels that are most likely affected by background information, an $N \times N$ pixel binary mask shown in Fig. 3 (a) is applied on each resized face image. This ensures that no unwanted background information is included in the face pattern when a measure of symmetry, which is one of the parameters used for the detection of a face, is computed. It should be noted that the mask is also used for computing the correlation value between the face candidate and the face template.

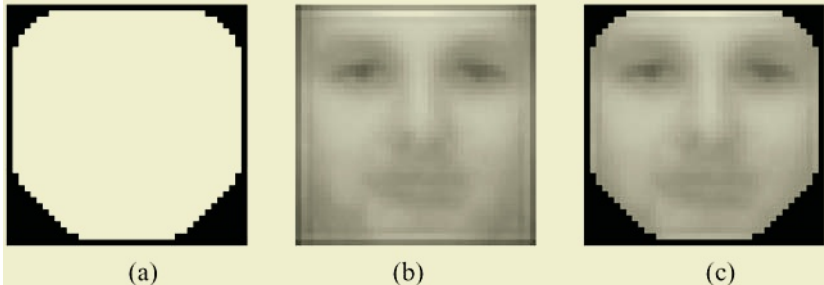


Fig. 3. Kinds of template. (a) Binary mask. (b) Average face image. (c) Masking face template

2.4 Face Verification

In this section, each candidate face is further verified by using a symmetry measure and template matching verification procedure. A true face will be declared if the symmetry measure and matching correlation is larger than a threshold.

2.4.1 Symmetry Measure

Symmetry is one of the most important features of human face. In order to measure image symmetry, we define the image gray level moment as the product between each pixel gray level and the distance of the pixel to symmetry axis. Two values L and R represent the gray level moments of the left half face and right half face respectively. The symmetry measure S is determined using the ratio L/R .

2.4.2 Face Verification Using Template Matching

To determine whether a face candidate is a face or not, the similarity between the face candidate and a face template will be measured. In our approach, the face template is a gray level image and is obtained by calculating the average of a set of pre-processed training face images. The average image face and the masking face template are shown in Figs. 3 (b) and (c), respectively.

The face candidate and the face template can be measured by means of the Correlation value. Linear correlation between face candidate X and face template Y with means μ_X and μ_Y , respectively, is given by

$$r(X, Y) = \frac{\sum (X_{ij} - \mu_X)(Y_{ij} - \mu_Y)}{\sqrt{\sum (X_{ij} - \mu_X)^2 \sum (Y_{ij} - \mu_Y)^2}} \quad (1)$$

3 Experimental Results

The detection performance of our algorithm was evaluated using our face image database, which consists of 233 color images. Some of the images were captured by a digital camera, some of them were downloaded from the Internet and some of the images were cut from MPEG7 videos. We classified the selected images into two parts: one part images contain a face in each image and with simple backgrounds, others were taken under varying lighting conditions and with complex backgrounds, further, these images contain multiple faces with variation in color, position, scale, orientation, and facial expression.

The detection performance of our approach on our face database is shown in Tables 1. Our algorithm can achieve a detection rate of 94.6% in simple images and the detection rate is reduced to 85.6% in complex images. Also, the numbers of false alarms and missed faces are increased from 7 to 23 and from 15 to 29, respectively. Fig.4 illustrates some experimental results.



Fig. 4. Some experimental results

A part of real faces are missed in our experiment. Among them, some faces turn right or left too much to be detected, some connect the skin color background that cannot be separated by the segmentation algorithm, and most of the faces missed are due to the eye regions covered. If the eye region is not covered, the face region can also be detected.

Table 1. The performances summarization

| Experiments | Correctly detected faces | Missed faces | False alarm | Detection rate (%) |
|---------------|--------------------------|--------------|-------------|--------------------|
| Simple image | 125 | 7 | 15 | 94.6% |
| Complex image | 137 | 23 | 29 | 85.6% |

4 Conclusion

In this paper, we have proposed a reliable face detection approach in color images. Our method detects skin regions over the entire image and then possible eye regions are detected within the skin color regions, and possible face regions are formed by pairing two possible eye candidates in a skin color region. Finally, Symmetry verification and template matching methods are used to locate the faces in those regions. Experimental results show that our method can be used to detect single or multiple faces from images having simple or complex backgrounds.

References

1. Y. Suzuki, H. Saito, S. Ozawa, Extraction of the human face from the natural background using GAs, in: Proceedings of IEEE TENCON, Digital Signal Processing Applications, Vol. 1, 1996, pp. 221–226.
2. Chung J. Kuo, Ruey-Song Huang, Tsang-Gang Lin, 3-D Facial Model Estimation From Single Front-View Facial Image, *IEEE Trans. Circuits System Video Technol.* 12 (3) (2002) 183–192.
3. Chiunhsien Lin, Kuo-Chin Fan, Triangle-based approach to the detection of human face, *Pattern Recognition* 34 (6) (2001) 1271–1284.
4. Paul Juell, Ron Marsh, A hierarchical neural network for human face detection, *Pattern Recognition* Vol 29(5) (1996) 781-787.
5. M. Turk, A. Pentland. Eigenfaces for recognition[J]. *Journal of Cognitive Neuroscience*, 1991, 3, (1): 71–86
6. Kah-kay Sung, Tomaso Poggio, Example-based learning for view-based human face detection, *IEEE Trans. Pattern Anal. Machine Intell.* 20 (1) (1998) 39–51.
7. Olugbenga Ayinde, Yee-Hong Yang, Region-basedface detection, *Pattern Recognition*, 35 (2002) 2095 – 2107
8. Kwok-Wai Wong, Kin-Man Lam, Wan-Chi Siu, A robust scheme for live detection of human faces in color images, *Signal Processing: Image Communication* 18 (2003) 103–114
9. P.J. Phillips, Y. Vardi, Efficient illumination normalization of facial images, *Pattern Recognition Lett.* 17 (1996) 921–927.

A Robust and Invisible Watermarking of 3D Triangle Meshes

Wang Liu and Sheng-He Sun

Dept. of Automatic Test and Control, Harbin Institute of Technology, Harbin 150001, China
liuwang@hit.edu.cn

Abstract. With the rapid development of computer multimedia, how to protect digital products from being copied, pirated and juggled has been an urgent issue in the information security field. Digital watermarking is a new method to solve the referred problems. This paper proposes a digital watermarking algorithm for three-dimension (3D) mesh models. The watermark is embedded into the host with modifying the lengths between the vertices and the centroid of models. The embedded watermark is invisible and can withstand the common attacks such as polygon mesh simplifications, addition of random noise, and similarity transforms. The validity of proposed algorithm has been confirmed with experiments.

1 Introduction

In order to protect ownership or copyright of digital media data, such as image, video, and audio, watermarking technique is generally used. Encryption techniques can be used to protect digital data during the transmission from the sender to the receiver. Watermarking technique is one of the solutions for the copyright protection and they can also be used for fingerprinting, copy protection, broadcast monitoring, data authentication, indexing, medical safety, and data hiding [1].

Watermarking of three-dimensional (3D) geometric models, such as surface model, solid model or polygonal model, has received less attention from researchers because the technology for watermarking images, video and audio cannot be easily adapted to work for 3D data. In fact, the arbitrary surfaces of 3D models lack natural parameterization for frequency-based decomposition and simplification, although attacks may modify the connectivity of the 3D mesh model [2].

Recently, there have been novel techniques proposed for watermarking 3D models such as arbitrary triangle meshes [3], NURBS curves and surfaces [4], and volume data [5]. These works are important to solve copyright ownership, authenticate authenticity and integrality of the content for the 3D models in the fields of medicine, archeology, and so on.

In this paper, we propose a new watermarking algorithm of three-dimensional mesh models. The watermark is embedded into the host with modifying the lengths between the vertices and the centroid of models. In the following section at first the watermarking scheme is explained and later results on practical implementation of the watermarking system and its performance are reported.

2 Watermark Generation

Assuming original watermark is a binary sequence $a_j \in \{-1, 1\}$, in order to improve the watermark's ability to resist most common attacks, we adopt the watermark-generating algorithm as follows:

- (1) The a_j is spread by a large spread factor cr (chip-rate) to obtain spread sequence b_k with the following formula

$$b_k = a_j \quad jcr \leq k < (j+1)cr \quad (1)$$

- (2) The spread sequences b_k is modulated by a pseudo-random sequence $p_k \in \{-1, 1\}$ to obtain modulated sequences $W = \{w_k\}, k = 1, \dots, N_w$, which can be directly embedded into the host, using the computing formula

$$w_k = p_k b_k \quad (2)$$

3 Watermark Embedding

Let us consider a mesh model $\mathbf{M} = \{\mathbf{P}, \mathbf{C}\}$ in its simplest form consisting of a set

$$\mathbf{P} = \{\mathbf{p}_i\}_{i=1,\dots,N} \quad \mathbf{p}_i = (x_i, y_i, z_i) \quad (3)$$

of N vertices \mathbf{p}_i with coordinates (x_i, y_i, z_i) and connectivity information

$$\mathbf{C} = \{(i_k, j_k)\}_{k=1,\dots,m} \quad 1 \leq i_k \leq N, 1 \leq j_k \leq N \quad (4)$$

\mathbf{C} is a set of index pairs $\{i_k, j_k\}$ each of which corresponds to one edge of the mesh.

Let us further define the star \mathbf{S}_i of a vertex \mathbf{p}_i as the set of indices of all vertices connected to \mathbf{p}_i , i.e.

$$\mathbf{S}_i = \{j \mid \{i, j\} \in \mathbf{C}\}; i = 1, \dots, N \quad (5)$$

For the sake of simplicity and without loss of generality we assume that the star of a point is never empty.

We want to embed a binary set of information $\mathbf{W} = \{w_k\}$ which is generated with the method introduced in Section 2. The embedding procedure is outlined below:

- (1) **Center of Mass Calculation.** To find the center of mass the following equation is used

$$\bar{\mathbf{p}} = \frac{1}{n} \sum_{i=1}^n \mathbf{p}_i = (\bar{x}_i, \bar{y}_i, \bar{z}_i) \quad (6)$$

- (2) **Model Translation.** The model is translated so that the center of mass falls on the origin of the axes.

$$\begin{cases} x'_i = x_i - \bar{x}_i \\ y'_i = y_i - \bar{y}_i \\ z'_i = z_i - \bar{z}_i \end{cases} \quad (7)$$

where \bar{x}_i , \bar{y}_i , and \bar{z}_i are the coordinates of the center of mass. x_i , y_i , and z_i are the original coordinates of vertex \mathbf{p}_i and x'_i , y'_i , and z'_i are the coordinates of the translated vertex \mathbf{p}'_i . That way the watermarking method is robust against translation of the model under investigation.

(3) Conversion to Spherical Coordinates. The model is converted to Spherical Coordinates. Each vertex \mathbf{p}'_i is represented as $(r'_i, \theta'_i, \phi'_i)$. This is done in order to achieve robustness against scaling by embedding the watermark in the r'_i component of each vertex.

(4) Watermark Embedding. The watermark is embedded into the original model using the following equation

$$\hat{r}'_k = r'_k + \alpha \Lambda(\mathbf{p}_k) w_k, k = 1, \dots, N_w \quad (8)$$

α determines the modulation amplitude, and $\Lambda(\mathbf{p}_k)$ is the masking function that should be defined.

In order to achieve the masking function, we define a vector \mathbf{n}_k for each point k equal to the difference of coordinate values of each vertex with the vertices connected to it. This means

$$\mathbf{n}_k = \frac{1}{|\mathbf{S}_k|} \sum_{j \in \mathbf{S}_k} (\mathbf{p}_j - \mathbf{p}_k) = (n_{xk}, n_{yk}, n_{zk}) \quad (9)$$

where $|\mathbf{S}_k|$ denotes the number of components of a set \mathbf{S}_k .

The absolute values of each vector can show a measure of amount of variation of coordinate around that vertex. We use these absolute values of each vector as our masking value in that vertex, i.e.

$$\Lambda(\mathbf{p}_k) = \|\mathbf{n}_k\| \quad (10)$$

(5) Conversion to Cartesian Coordinates. Each $(\hat{r}'_i, \theta'_i, \phi'_i)$ is converted to a vertex $\hat{\mathbf{p}}_i$ which is represented as $(\hat{x}_i, \hat{y}_i, \hat{z}_i)$ using the following equations

$$\begin{aligned} \hat{x}_i &= \hat{r}'_i \sin \phi' \cos \theta' + \bar{x}_i \\ \hat{y}_i &= \hat{r}'_i \sin \phi' \sin \theta' + \bar{y}_i \\ \hat{z}_i &= \hat{r}'_i \cos \phi' + \bar{z}_i \end{aligned} \quad (11)$$

After the above 5 steps, we have embedded the watermark into the original model and obtained the watermarked model.

4 Watermark Extraction

The detail procedure of extracting watermark is as follows:

- (1) An attack might change the 3D model through similarity transforms including translation, rotation and uniform scale. Before extracting watermarks, we must bring the object back to its original location and scale via model registration. The registration is always performed between the attacked mesh and the original un-watermarked mesh, for registration with the watermarked mesh will falsely introduce the watermark information and increase the false positive possibility. We denote the mesh to be registered as M_t , the original mesh as M . The registration procedure is as follows:

Step 1. Provide an initial transformation between the two meshes. This is done by users from the Graphical User Interface (GUI) provided by the underlying system. The approximately registered M_t is denoted as M_r .

Step 2. Uniformly choose a subset of vertices \mathbf{p}_{ri} ($i = 1, \dots, k$) from M_r .

Step 3. Define an energy function: $E = \sum_{i=1}^k D(\mathbf{p}_{ri}, \mathbf{p}_{oi})$, where \mathbf{p}_{oi} is the nearest

vertex of \mathbf{p}_{ri} in M . $D(\mathbf{p}_{ri}, \mathbf{p}_{oi})$ measures the distances between the meshes, it is the sum of the squared distances between the corresponding vertex pairs. We then use the Powell method [6] to minimize the energy function E . After this minimization process, M_r is used as the registered version of mesh M_t . The registration process is performed between the detected mesh and the original mesh.

- (2) In case of attacks which change the mesh representations was applied to the watermarked mesh, such attacks may include simplification attacks, cropping attacks, vertex reordering, re-meshing and so on, we cannot extract the watermark directly, instead we must first re-sample the detected model. The re-sampling procedure is as follows: cast a ray from the center of the original model to the original vertex \mathbf{p}_{oi} to intersect with the detected model. If the ray intersects the watermarked model at one or more points and point \mathbf{p}_{di} is the closest intersection point to \mathbf{p}_{oi} , then \mathbf{p}_{di} is taken as the vertex that corresponds with \mathbf{p}_{oi} or let $\mathbf{p}_{di} = \mathbf{p}_{oi}$.

- (3) As in step (1) of the embedding procedure, we calculate the center of the original model using equation (1).
- (4) The original model and detected model are translated to obtain the translated vertices \mathbf{p}'_{oi} and \mathbf{p}'_{di} using the following formula

$$\begin{cases} x'_{oi} = x_{oi} - \bar{x}_{oi} \\ y'_{oi} = y_{oi} - \bar{y}_{oi} \\ z'_{oi} = z_{oi} - \bar{z}_{oi} \end{cases} \quad (12)$$

$$\begin{cases} x'_{di} = x_{di} - \bar{x}_{oi} \\ y'_{di} = y_{di} - \bar{y}_{oi} \\ z'_{di} = z_{di} - \bar{z}_{oi} \end{cases} \quad (13)$$

- (5) The vertices \mathbf{p}'_{oi} and \mathbf{p}'_{di} are converted to the corresponding spherical ordinates $(r'_{oi}, \theta'_{oi}, \phi'_{oi})$ and $(r'_{di}, \theta'_{di}, \phi'_{di})$, respectively.
- (6) The extracted sequence can be obtained using the following equation

$$w_{dk} = r'_{dk} - r'_{ok}, k = 1, \dots, N_w \quad (14)$$

- (7) This sequence w_{dk} is demodulated with the sequence $p_k \in \{-1, 1\}$ used in the watermarking phase, i.e.

$$b_{dk} = p_k w_{dk} \quad (15)$$

- (8) In every binary segment whose size is cr , all signal components b_{dk} are added using

$$s_j = \sum_{k=jcr}^{(k+1)cr-1} b_{dk} = \sum_{k=jcr}^{(k+1)cr-1} p_k^2 b_k + \Lambda \quad (16)$$

where Λ is the error term due to attacks. By choosing a large cr for adequate redundancy, the summation can be approximated as:

$$s_j = \sum_{k=jcr}^{(k+1)cr-1} b_{dk} \approx cr \cdot a_j \quad (17)$$

The extracted watermark bit is

$$a'_j = sign(s_j) \quad (18)$$

where $a'_j \in \{-1, 1\}$. The extracted watermark sequence is $W_e = \{a'_j\}$.

- (9) Compute the NC (Normalized Cross-Correlation) between the extracted watermark sequence and the original watermark sequence to decide whether the original watermark is presented in the detected model:

$$NC(W_o, W_e) = \frac{\sum_{i=1}^N w_{oi} w_{ei}}{\sqrt{\sum_{i=1}^N w_{oi}^2}} \quad (19)$$

where W_o and W_e are the original watermark and the extracted respectively, and N is the length of the watermark sequence. If the computed NC value exceeds a chosen threshold Thr_D , we conclude that the watermark is present in the detected model.

5 Experimental Results

To test the proposed watermarking technique for robustness and imperceptibility, we conducted experiments on a triangle mesh of a cow model. The mesh consists of 2894 vertices and 5504 triangle faces. We embed a watermark of 50 bits with $cr = 57$ and $\alpha = 0.05$ into a cow model. The watermarked cow model is shown in Fig.1(b) and Fig.1(a) is the original model. The Mean Square Error (MSE) is used to examine the distortion between the watermarked model and the original, i.e.

$$MSE = \frac{1}{N} \sum_{i=1}^N \| \mathbf{p}'_i - \mathbf{p}_i \|^2 \quad (20)$$

where \mathbf{p}'_i and \mathbf{p}_i are the i th vertex of the watermarked model and the original, respectively, and N is the number of vertices of the model. The MSE equals to 1.56×10^{-3} . Visually comparing these two figures we can conclude that the embedded watermark is imperceptible.

To demonstrate our watermarking algorithm's resistance to noise, we add a noise vector to each vertex. We perform the test five times and the amplitude of the noise is 1%, 2%, 3%, 4% and 5%, respectively, of the length of the longest vector extended from a vertex to the center of the model. The experimental results in Table 1 show that the algorithm can resist these noise attacks very well.

For simplification attack, we adopt the mesh simplification algorithm of Stan [7] to simplify the watermarked cow model. We reduce 10%, 30%, 50%, and 70% of the vertices of the watermarked model, respectively. The experimental results shown in Table 2 indicate that the simplifying operations were not able to destroy the watermark embedded into the original model as shown by the respective NC values.

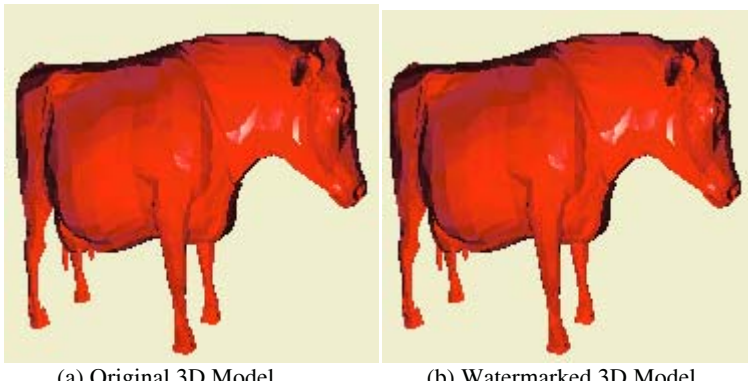


Fig. 1. Original 3D Model and Watermarked 3D Model

Table 1. Results of noise attacks

| Amplitude of noise vector/max (length from vertex to center) | 1% | 2% | 3% | 4% | 5% |
|---|------|------|------|------|------|
| NC | 1.00 | 0.80 | 0.64 | 0.56 | 0.52 |

When the detected model is attacked by similarity transforms such as translation, rotation, and uniform scale, we must bring the attacked model back to its original location and scale via model registration. Because the registration is performed between the attacked model and the original model, registration errors may occur between the original detected model and the detected model. Hence, we should also test the robustness of our watermarking scheme against similarity transform. Since there are trade-offs between registration accuracy and speed for most registration techniques, it would be useful to investigate the robustness of our scheme against similarity transforms in order to pick the most appropriate registration technique. The experimental results in Tables 3 and 4 show that our scheme has sufficient robustness to tolerate errors from registration.

Table 2. Results of simplification attacks

| | | | | | |
|----------------|------|------|------|------|------|
| Vertices left | 2894 | 2316 | 2026 | 1447 | 869 |
| Removing ratio | 0% | 10% | 30% | 50% | 70% |
| NC | 1.00 | 0.92 | 0.84 | 0.68 | 0.40 |

Table 3. Results of rotation attacks

| Degree | 5° | 5° | 5° | 5° | 10° | 10° | 10° | 10° | 10° |
|--------|------|------|----|----|------|-----|-----|------|------|
| Axis | X | X | Y | Z | X | Y | Z | Y | Z |
| NC | 0.96 | 0.84 | | | 0.56 | | | 0.84 | 0.72 |

Table 4. Results of rotation attacks and translation attacks

| Degree | X | X | X | Y | Z | Y |
|---|------|------|------|---------------|----|------|
| Axis | 1° | 5° | 1° | 1° | 1° | 5° |
| Displacement (percentage of maximum length from vertex to center) | 0.4% | 0.4% | 0.4% | | | 0.4% |
| Direction of displacement | | | | (1,0,1,0,1,0) | | |
| NC | 0.72 | 0.60 | 0.68 | | | 0.72 |

From the above experiments we can conclude that the proposed watermarking technique is robust against a range of common attacks on 3D mesh model.

6 Conclusion

In this paper, we propose a novel invisible and robust watermarking scheme that embeds watermark information by modifying the lengths between the vertices and the centroid of models. The masking factor at each point is defined based on an estimate of average difference between position of connected vertices to a vertex, which helps 3D mesh watermarking to be more robust but less visible. In particular, the novel features of the proposed watermarking algorithm is that it is able to distribute information corresponds to a bit of watermark over the entire model and the strength of the watermark signal is adaptive with respect to the local geometry of the model. Experiments show that this approach is able to withstand common attacks such as polygon mesh simplifications, addition of random noise, and similarity transforms.

References

1. Petitcolas, F. A. P., Anderson, R. J., Kuhn, M. G.: Information hiding- a survey. Proceedings of the IEEE, Vol. 87, No. 7 (1999) 1062-1078
2. Ohbuchi, R., Masuda, H., Aono, M.: Watermarking three-dimensional polygonal models through geometric and topological modifications. IEEE Journal on Selected Areas in Communications, Vol.16, No.4 (1998) 551-560
3. Oliver, B.: Geometry-based watermarking of 3D models. IEEE Computer Graphics and Applications. Jan./Feb(1999) 46-55
4. Lee, J., J., Cho, N., I., Kim, J., W.: Watermarking for 3D NURBS graphical data. IEEE Workshop on Multimedia Signal Processing (2002) 304-307
5. Guan, X., Wu, Y., Kankanhalli, M., S., Huang, Z.: Invisible watermarking of volume data using wavelet transform. Proceedings of MMM'2000, Nagano, Japan. Nov (2000) 152-166
6. Press, W., H., Teukolsky, S., A., Vetterling, W. T., Flannery, B., P.: Numerical recipes in C, 2nd ed. London: Cambridge University Press (1996)
7. Stan, M.: A simple, fast, and effective polygon reduction algorithm. Game Developer. 11(1998) 44-49

Advances of MPEG Scalable Video Coding Standard

Wen-Hsiao Peng, Chia-Yang Tsai, Ti-hao Chiang, and Hsueh-Ming Hang

National Chiao-Tung University
1001 Ta-Hsueh Rd., HsinChu 30010, Taiwan
pawn@mail.si2lab.org, cytsai.ee90g@nctu.edu.tw,
{tchiang,hmhang}@mail.nctu.edu.tw

Abstract. To support clients with diverse capabilities, the MPEG committee is defining a novel scalable video coding (SVC) framework that can simultaneously support multiple spatial, temporal and SNR resolutions under the constraints of low complexity and low delay. To fulfill the requirements, two major approaches have been considered as the potential technologies. One is the wavelet-based scheme and the other is the scalable extension of MPEG-4 AVC/H.264. This paper aims to give a brief overview for the latest advances of these technologies.

1 Introduction

Scalable video coding attracts wide attention with the rapid growth of multi-media applications over Internet and wireless channels. In such applications, the video may be transmitted under a heterogeneous environment. To support clients with diverse capabilities in complexity, bandwidth, power and display resolution, the MPEG committee is defining a scalable video coding (SVC) framework that can simultaneously support multiple spatial, temporal and SNR resolutions under the constraints of low complexity and low delay.

To fulfill the requirements of SVC, more than 20+ proposals were submitted during the stage of call-for-proposal [1] in February 2004. According to the spatial transform, these proposals can be roughly classified into two categories, which are the wavelet-based scheme and the AVC/H.264-based approach [2]. In addition, depending on the transform order in the spatio-temporal domain, the wavelet-based scheme can further have two variations, which are the “2D+t” and “t+2D” structures [2]. To distinguish the differences, Fig. 1 shows a comparison at architectural level.

As shown, in order to achieve the temporal scalability, both the wavelet-based scheme and the AVC-based approach adopt the technique of motion compensated temporal filtering (MCTF). In addition, to achieve the SNR scalability with fine granularity, the AVC-based scheme uses a context-adaptive bit-plane coding [3][4]. On the other hand, the wavelet-based scheme employs a zero-tree coding [5][6][7] for the same purpose. As for the spatial scalability, the wavelet-based scheme takes the advantages of multi-resolution property of wavelet transform, while the AVC-based scheme exploits the layered coding concept used in MPEG-2, H.263, and MPEG-4.

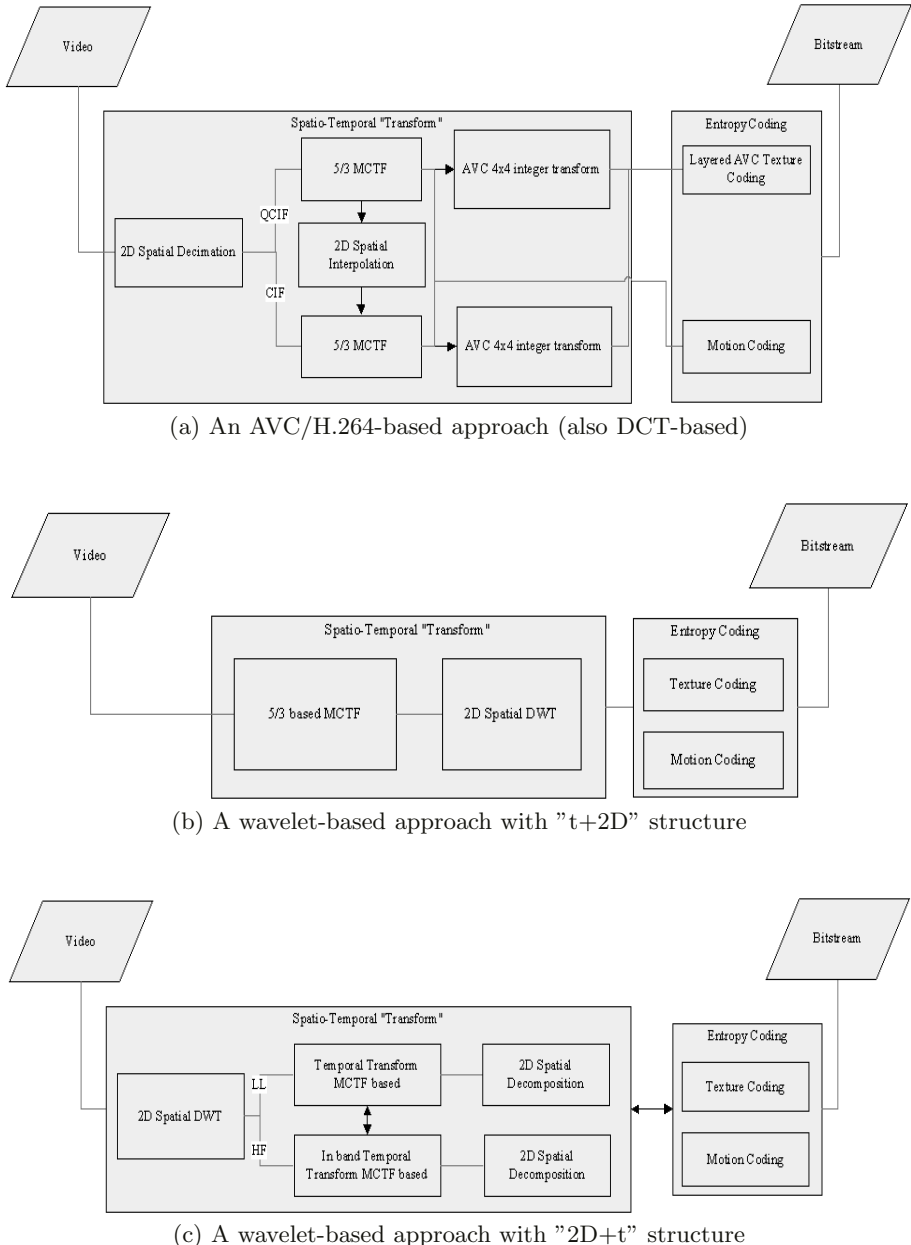


Fig. 1. An architectural level comparison for various SVC algorithms [2]

Subjective test has been conducted for comparing these technologies [8]. Having better subjective quality in different scenarios, the AVC-based scheme is adopted as the working draft of SVC. On the other hand, MPEG committee also establishes an ad-hoc group to further study the wavelet-based technologies

for the further video coding applications. In this paper, we give a brief overview for the latest advances of these technologies. The rest of this paper is organized as follows: Section 2 elaborates the detail for each dimension of scalability in AVC-based approach and Section 3 describes the corresponding algorithms in the wavelet-based scheme. Lastly, Section 4 summarizes the latest activities in SVC.

2 Scalable Extension of AVC/H.264

To simultaneously support spatial, temporal and SNR scalability, a scalable extension of AVC/H.264 was proposed [3]. Fig. 1 (a) shows the encoder structure of the AVC-based scheme. To facilitate the spatial scalability, the input video is decimated into various spatial resolutions and the sequence in each spatial resolution is coded in a separated layer using AVC/H.264. Within each spatial layer, the motion compensated temporal filtering (MCTF) is employed in every group of pictures (GOPs) to provide the temporal scalability. In addition, to remove the redundancy among different spatial layers, a large degree of inter-layer prediction is incorporated. The residual frames after the inter-layer prediction are then transformed and successively quantized for the SNR scalability. In the following subsections, we elaborate the details for each dimension of scalability.

2.1 Temporal Scalability

In each spatial layer, the temporal scalability is achieved by the motion compensated temporal filtering (MCTF) technique, which performs the wavelet decomposition/reconstruction along the motion trajectory.

Particularly, the MCTF is mostly restricted to the short-length (5, 3) wavelet, which can be implemented by a lifting scheme with only one prediction/update step. In this special case, the prediction and update can be realized using bi-directional prediction as shown in Fig. 2, where $\{L^n\}$ stands for the low-pass frames of level n and $\{H^n\}$ denotes the associated high-pass frames. Inside the MCTF, an odd-indexed frame is predicted from the adjacent and even-indexed frames to produce the high-pass frame. Accordingly, an even-index frame is updated using the combination of adjacent high-pass frames to generate the low-pass frame. To remove temporal redundancy, motion compensation is conducted before the prediction and update. By using n decomposition stages, up to n levels of temporal scalability can be provided. Specifically, the video of lower frame rate can be obtained from the low-pass frames at higher level.

2.2 Spatial Scalability and Inter-layer Prediction

For the spatial scalability, sequences of different spatial resolutions are coded in separated layers. To remove the redundancy among different spatial layers, the residues and motion vectors of an enhancement layer are predicted from the ones of the subordinate layer.

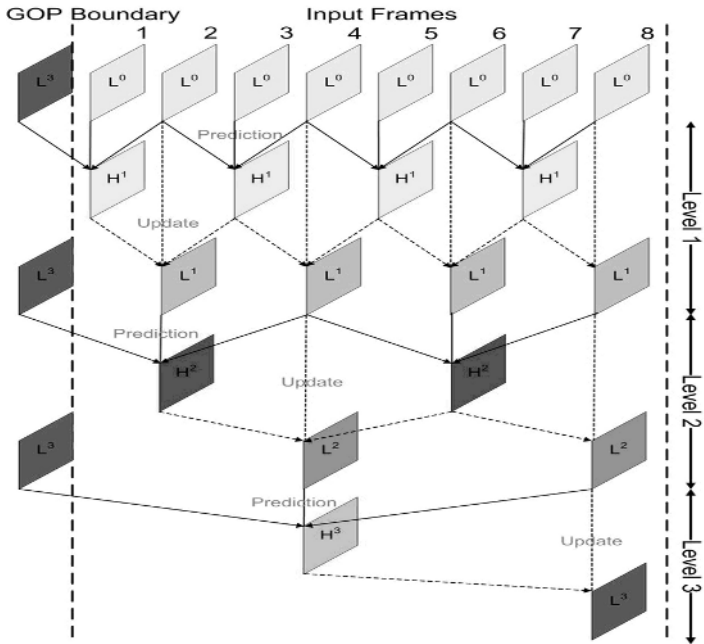


Fig. 2. MCTF structure for the (5, 3) wavelet

In the prediction process, the residues and motion vectors of the subordinate layer are firstly interpolated if the subordinate layer has a lower resolution. In addition, the partition of an inter MB can be derived from the relevant sub-blocks at the subordinate layer and the motion vectors can be obtained by refining and scaling the ones from the corresponding sub-blocks. On the other hand, for an intra MB, the inter-layer prediction is allowed only if the corresponding 8x8 block of the subordinate layer is within an intra-coded MB.

2.3 SNR Scalability

For the SNR scalability, the residues after the inter-layer prediction are transformed with the 4x4 integer transform. Then the transform coefficients are successively quantized into multiple quality layers. The coefficients in a quality layer is coded by a hybrid approach of bit-plane and (Run, Level) coding.

For the scalability with fine granularity, the bit-planes in a quality layer are coded using a cyclical block coding [4]. The coding step is partitioned into the significant and refinement passes. The significant pass first encodes the insignificant coefficients that have zero values in the subordinate layers. Then, the refinement pass refines the remaining significant coefficients ranging from -1 to +1. During the significance pass, the transform blocks are coded in a cyclical and block-interleaved manner. On the other hand, the coding of refinement pass is conducted subband-by-subband. To further reduce bit rate, a context-adaptive binary arithmetic coder is employed.

3 Scalable Approach Using Inter-frame Wavelet

Different from the aforementioned AVC-based scheme that exploits the hybrid coding structure, a wavelet-based scheme using (t+2D) structure was proposed in [5][9]. Like the AVC-based approach, the wavelet-based scheme can produce a fully embedded bit-stream that simultaneously supports spatial, temporal, and SNR scalability. However, a major difference between the AVC-based approach and the wavelet-based scheme is that all the predictions in the latter case are conducted in an open-loop manner. The open-loop prediction provides more flexibility on bit-stream extraction and is more robust to transmission errors.

Fig. 2 (b) shows the framework of wavelet-based scheme using (t+2D) structure. Within each GOP, MCTF is used for temporal decomposition. Particularly, the temporal low-pass frames come from the motion compensation of the original images. The low-pass frames are used for the temporal scalability. For the spatial scalability, 2-D wavelet decomposition is conducted for each frame after the MCTF. The spatial scalability is achieved by the multi-resolution property. Furthermore, after the spatial decomposition, the wavelet coefficients are coded by a zero-tree entropy coder (or other arithmetic coder) to generate an embedded bit-stream for the SNR scalability. By means of proper extraction, a single bit-stream with scalable spatial, temporal and SNR parameters can be produced. Similar wavelet video coding schemes but with specific features have been latter suggested by several other researchers [10][11]. In the following subsections, we will give a brief overview for each dimension of scalability in the wavelet-based scheme.

3.1 Temporal Scalability

To provide temporal scalability, the wavelet-based scheme also adopts the MCTF as described in Section 2.1. In fact, the MCTF concept was first proposed for wavelet coding [9]. Typically, Haar or (5, 3) wavelet are used.

To improve the accuracy of motion field so as to achieve a better coding performance, several techniques for better motion estimation have been proposed [12][13]. Particularly, in [13], a novel structure, known as Barbell-Lifting, is presented. The basic idea is to use a “barbell” function for generating the prediction/update values for the lifting scheme. Specifically, for each pixel in the high-pass frame, the prediction value is obtained by using a set of pixels as the input to the barbell function. It has been proved that the prediction using the barbell function offers a superior performance as compared to the one using a single-pixel. Moreover, it often reduces the mismatch of motion in the prediction and update steps. However, due to the coupling of different spatial subbands, this scheme may result in an inaccurate prediction/update when extracting the video of lower resolution. To solve this problem, an in-band MCTF can be used instead [10].

3.2 Spatial and SNR Scalability

To achieve the spatial scalability, a separable 2-D wavelet transform is applied to both low-pass and high-pass frames. Similar to JPEG2000, the lower subbands are used to reconstruct the lower resolution images.

To provide the SNR scalability with fine granularity, an embedded zero-tree coding as in [6] is used after the spatial decomposition. In addition to [6], other methods like embedded zero-block coding (EZBC) [5] and embedded block coding with optimized truncation (EBCOT) [7] are also commonly used for coding the wavelet transform coefficients. Particularly, to reduce the temporal redundancy among successive frames, these coding techniques can be further extended to have 3-D structure such as 3-D EBCOT in [11].

3.3 Motion Scalability

The compressed bit-stream includes both the texture and the motion information. The bit-stream for the texture part can be arbitrarily truncated. However, the one for the motion information can not be easily partitioned. Since the motion information may be a considerable portion, it can consume a large percentage of the transmitted data in the low bit rate applications. This leads to few available bits for transmitting texture data and thus results in poor subjective quality. To solve this problem, motion information should be represented in a scalable manner.

In [14], a scalable representation of motion information is proposed for the MC-EZBC. Further, in [15], the motion information is partitioned into multiple “motion layers”. Each layer records the motion vectors with a specified accuracy. The lowest layer denotes a rough representation of the motion vectors and the higher layers are used to refine the accuracy. Different layers are coded independently so that the motion information can be truncated at the layer boundary.

Due to the mismatch between the truncated motion information and the residual data, the schemes with scalable motion information may have drifting error. As a result, a linear model is proposed in [12] to provide a better trade-off between the scalable representation and the rate-distortion performance.

4 Conclusion

In this paper, we have reviewed the fundamentals of SVC and its latest development in MPEG standard. Both the AVC-based approach and the wavelet-based scheme are capable of offering a fully scalable bit-stream. Although the AVC-based approach has been selected as the working draft in MPEG, the wavelet-based scheme has the potential for future video coding applications/standard. Research activities on the wavelet-based technology have been growing rapidly in the past a few years and the MPEG committee continuously keeps an ad-hoc group working on this subject. At the moment, a number of core experiments are set up for the AVC-based SVC in MPEG. The target date of completing the MPEG SVC standard is 2006.

References

1. Ohm, J.R.: Registered Responses to the Call for Proposals on Scalable Video Coding. ISO/IEC JTC1/SC29/WG11, M10569 (2004)
2. Reichel, J., Hanke, K., Popescu, B.: Scalable Video Model V1.0. ISO/IEC JTC1/SC29/WG11, N6372 (2004)
3. Reichel, J., Wien, M., Schwarz, H.: Scalable Video Model 3. ISO/IEC JTC1/SC29/WG11, N6716 (2004)
4. Ridge, J., Bao, Y., Karczewicz, M., Wang, X.: Cyclical Block Coding for FGS. ISO/IEC JTC1/SC29/WG11, M11509 (2005)
5. Hsiang, S.T., Woods, J.W.: Embedded Image Coding Using Zeroblocks of Subband-Wavelet Coefficients and Context Modeling. In: IEEE ISCAS. (2000)
6. Shapiro, J.M.: Embedded Image Coding Using Zerotrees of Wavelet Coefficients. *IEEE Transactions on Signal Processing* **41** (1992) 657–660
7. Taubman, D.: High Performance Scalable Image Compression with EBCOT. *IEEE Transactions on Image Processing* **9** (2000) 1158–1170
8. MPEG: Subjective Test Results for the CfP on Scalable Video Coding Technology. ISO/IEC JTC1/SC29/WG11, N6383 (2004)
9. Ohm, J.R.: Three-dimensional Subband Coding with Motion Compensation. *IEEE Trans. on Image Processing* **3** (1994) 559–571
10. Andreopoulos, Y., Munteanu, A., Barbarien, J., van der Schaar, M., Cornelis, J., Schelkens, P.: In-Band Motion Compensated Temporal Filtering. *Signal Processing: Image Communication* **19** (2004) 653–673
11. Taubman, D., Mehrseresht, N., Leung, R.: SVC Technical Contribution: Overview of Recent Technology Developments at UNSW. ISO/IEC JTC1/SC29/WG11, M10868 (2004)
12. Secker, A., Taubman, D.: Highly Scalable Video Compression with Scalable Motion Coding. *IEEE Trans. Circuits Syst. Video Technol.* **13** (2004) 1029–1041
13. Xu, J., Xiong, R., Feng, B., Sullivan, G., Lee, M.C., Wu, F., Li, S.: 3D Sub-band Video Coding Using Barbell Lifting. ISO/IEC JTC1/SC29/WG11, M10569 (2004)
14. Hang, H.M., Tsai, S.S., Chiang, T.: Motion Information Scalability for MC-EZBC. ISO/IEC JTC1/SC29/WG11, M9756 (2003)
15. Tsai, C.Y., Hsu, H.K., Hang, H.M., Chiang, T.: Response to CfP on Scalable Video Coding Technology: Proposal S08 – A Scalable Video Coding Scheme Based on Interframe Wavelet Technique. ISO/IEC JTC1/SC29/WG11, M10569 (2004)

Extended Fuzzy Description Logic ALCN*

Yanhui Li¹, Baowen Xu^{1,2,3}, Jianjiang Lu^{1,2,4}, Dazhou Kang¹, and Peng Wang¹

¹ Department of Computer Science and Engineering,
Southeast University, Nanjing 210096, China

² Jiangsu Institute of Software Quality, Nanjing 210096, China

³ State Key Laboratory of Software, Wuhan University, Wuhan 430072, China

⁴ PLA University of Science and Technology, Nanjing 210007, China
bwxu@seu.edu.cn

Abstract. Web applications based on description logics often need management of fuzzy information and encounter fuzzy concepts. This paper proposes an extended fuzzy ALCN to enable representation and reasoning for complex fuzzy information. The extended fuzzy ALCN introduces the cut sets of fuzzy concepts and fuzzy roles as atomic concepts and atomic roles, and inherits the concept constructors from description logics to support a new logic system. This paper defines its syntax structure, semantic interpretation and reasoning problems. The extended fuzzy ALCN is more expressive than the existing fuzzy description logics and present more wide fuzzy information.

1 Introduction

The Semantic Web [1] is an extension of the current Web in which Web information is given well-defined semantic meaning to be machine-understandable, better enabling intelligent Web data processing. Description logics (DLs) [2] provide a logical reconstruction of object-centric and frame-based knowledge representation languages as main inferential means on the Semantic Web. Web applications often need management of fuzzy information, but typical DLs are limited to dealing with crisp concepts and crisp roles. Therefore, it is necessary to add fuzzy features to description logics. Meghini proposed a preliminary fuzzy DL [3], which lacks reasoning algorithm, as a modelling tool for multimedia document retrieval. Straccia presented a fuzzy extension of classical Attribute Language with Complement (ALC) [4] combining fuzzy logic, Fuzzy ALC (FALC) [5], and gave a constraint propagation calculus for reasoning. However, FALC cannot offer sufficient expressive power of complex fuzzy information. Some discussion about reducing FALC into classical ALC is given in [6], and the reduction does not extend the expressive bound of FALC. This paper presents extended fuzzy ALCN (EFALCN), which adopts a special fuzzify-method different from FALC and presents more expressive power than FALC.

2 EFALCN

We introduce the cut sets of fuzzy concepts and fuzzy roles as atomic concepts and atomic roles, and continue to use the concept constructors and representation form of

* This work was supported in part by the NSFC (60373066, 60425206, 90412003), National Grand Fundamental Research 973 Program of China (2002CB312000), National Research Foundation for the Doctoral Program of Higher Education of China (20020286004)

ALCN to propose EFALCN. Then we define a fuzzy semantic interpretation for concepts and roles, and discuss reasoning problems in EFALCN.

2.1 Syntax Structure of EFALCN

EFALCN introduces the cut sets of fuzzy concepts and fuzzy roles. Let ΔN_C and ΔN_R denote the sets of atomic fuzzy concepts and set of atomic fuzzy roles. In EFALCN, the set of atomic concepts is defined as $\Delta N_C^E = \{B_{[n]} \mid B \in \Delta N_C \wedge n \in [0,1]\}$, $B_{[n]}$ is an atomic cut concept, the set of atomic roles is defined as $\Delta N_R^E = \{R_{[n]} \mid R \in \Delta N_R \wedge n \in [0,1]\}$, $R_{[n]}$ is an atomic cut role. For any $B_{[n]}$ (resp. $R_{[n]}$), we define B (resp. R) as the prefix of $[n]$ and reversely $[n]$ as the suffix of B (resp. R).

EFALCN is based on $B_{[n]}$ and $R_{[n]}$, and inherits concept constructors from ALCN to define cut concepts:

1. The top and bottom concept (denoted by $\top_{[1]}$, $\perp_{[1]}$) are cut concepts.
2. For any $B_{[n]} \in \Delta N_C^E$, $B_{[n]}$ is a cut concept.
3. If $C_{[n_1, n_2, \dots, n_k]}$ and $D_{[m_1, m_2, \dots, m_l]}$ are cut concepts, and $R_{[n]}$ is an element of ΔN_R^E , then $\neg C_{[n_1, n_2, \dots, n_k]}$, $C_{[n_1, n_2, \dots, n_k]} \sqcup D_{[m_1, m_2, \dots, m_l]}$, $C_{[n_1, n_2, \dots, n_k]} \sqcap D_{[m_1, m_2, \dots, m_l]}$, $\exists R_{[n]} \cdot D_{[m_1, m_2, \dots, m_l]}$, $\forall R_{[n]} \cdot D_{[m_1, m_2, \dots, m_l]}$, $\geq m R_{[n]}$, $\leq m R_{[n]}$ are cut concepts.

where $C_{[n_1, n_2, \dots, n_k]}$ and $D_{[m_1, m_2, \dots, m_l]}$ are abbreviation expressions for cut concepts. For example, $\exists \text{friend}_{[0,7]}(\text{Tall}_{[0,7]} \sqcap \text{Strong}_{[0,9]})$ is a cut concept, and it can be denoted by $\exists \text{friend}.(\text{Tall} \sqcap \text{Strong})_{[0,7,0,7,0,9]}$ with collecting all the suffixes in a suffix vector, where $\exists \text{friend}.(\text{Tall} \sqcap \text{Strong})$ is called the prototype of the cut concept and $[0.7, 0.7, 0.9]$ is called the suffix vector of the cut concept.

The cut assertions, which are in the form of $a : C_{[n_1, n_2, \dots, n_k]}$ or $(a, b) : R_{[n]}$, build up EFALCN ABoxes, where $a : C_{[n_1, n_2, \dots, n_k]}$ shows that the individual a belongs to the cut concept $C_{[n_1, n_2, \dots, n_k]}$. For example, Stan: $\exists \text{friend}.(\text{Tall} \sqcap \text{Strong})_{[0,7,0,7,0,9]}$ means Stan likely has a friend who is likely tall and more likely strong. And similarly, $(a, b) : R_{[n]}$ shows that the pair of individuals (a, b) belongs to the cut role $R_{[n]}$. EFALCN TBoxes are composed of cut terminological axioms about inclusion of cut concepts, which are in the form of $C_{[n_1, n_2, \dots, n_k]} \sqsubseteq D_{[f_1(n_1, n_2, \dots, n_k), \dots, f_s(n_1, n_2, \dots, n_k)]}$ $[n_1, n_2, \dots, n_k] \in X$, where $X \subseteq [0,1]^k$, $f_i(n_1, n_2, \dots, n_k), i = 1, 2, \dots, s : X \rightarrow [0,1]$, $C_{[n_1, n_2, \dots, n_k]}$ and $D_{[f_1(n_1, n_2, \dots, n_k), \dots, f_s(n_1, n_2, \dots, n_k)]}$ are cut concepts; it means $C_{[n_1, n_2, \dots, n_k]}$ is a sub concept of $D_{[f_1(n_1, n_2, \dots, n_k), \dots, f_s(n_1, n_2, \dots, n_k)]}$. EFALCN ABox A and TBox T make up an EFALCN knowledge base denoted by $\Sigma_E(A, T)$.

2.2 Semantic Interpretation of EFALCN

The interpretation of EFALCN is defined as $I = <\Delta^I, \bullet^I>$, where Δ^I is a nonempty set as the domain and \bullet^I is an interpretation function. \bullet^I maps every individual a into

an element of the domain: $(a)' = a'$, and maps every atomic fuzzy concept and atomic fuzzy role into a function: $B' : \Delta' \rightarrow [0,1]$, $R' : \Delta' \times \Delta' \rightarrow [0,1]$. Additionally, \cdot' maps cut concepts and cut roles into subsets of Δ' and $\Delta' \times \Delta'$. The interpretation of the atomic cut concept $B_{[n]}$ is $(B_{[n]})' = \{d \mid d \in \Delta' \wedge B'(d) \geq n\}$. From fuzzy math, $(B_{[n]})'$ can be treated as the n -cut of fuzzy set with respect to the universe Δ' , which is the reason that we call $B_{[n]}$ a cut concept. Similarly, the interpretation of the atomic cut role $R_{[n]}$ is $(R_{[n]})' = \{(d, d') \mid d, d' \in \Delta' \wedge R'(d, d') \geq n\}$.

The interpretations of cut concepts are inductively defined as:

$$(\neg C_{[n_1, n_2, \dots, n_k]})' = \Delta' / (C_{[n_1, n_2, \dots, n_k]})'; \quad (1)$$

$$((C \sqcap D)_{[n_1, n_2, \dots, n_k]})' = (C_{[n_1, n_2, \dots, n_m]})' \cap (D_{[n_{m+1}, n_{m+2}, \dots, n_k]})'; \quad (2)$$

$$((C \sqcup D)_{[n_1, n_2, \dots, n_k]})' = (C_{[n_1, n_2, \dots, n_m]})' \cup (D_{[n_{m+1}, n_{m+2}, \dots, n_k]})'; \quad (3)$$

$$((\exists R.C)_{[n_1, n_2, \dots, n_k]})' = \{d \mid d \in \Delta' \wedge \exists d' \in \Delta', R'(d, d') \geq n_1 \wedge d' \in (C_{[n_2, n_3, \dots, n_k]})'\}; \quad (4)$$

$$((\forall R.C)_{[n_1, n_2, \dots, n_k]})' = \{d \mid d \in \Delta' \wedge \forall d' \in \Delta', R'(d, d') \geq n_1 \rightarrow d' \in (C_{[n_2, n_3, \dots, n_k]})'\}; \quad (5)$$

$$(\geq N R_{[n]})' = \{d \mid d \in \Delta', |\{d' \mid R(d, d') \geq n\}| \geq N\}; \quad (6)$$

$$(\leq N R_{[n]})' = \{d \mid d \in \Delta', |\{d' \mid R(d, d') \geq n\}| \leq N\}. \quad (7)$$

In equations (6-7), $|Z|$ denotes the number of elements in the set Z .

2.3 Reasoning Problems in EFALCN

All reasoning problems in EFALCN can be resolved to the satisfaction problems of interpretation: I satisfies a cut assertion $a : C_{[n_1, n_2, \dots, n_k]}$ (resp. $(a, b) : R_{[n]}$), iff $a' \in (C_{[n_1, n_2, \dots, n_k]})'$ (resp. $(a', b') \in (R_{[n]})'$). I satisfies an ABox A (written $I \approx A$), iff I satisfies all cut assertions in A ; such I is called a model of A . I satisfies a cut terminological axiom $C_{[n_1, n_2, \dots, n_k]} \sqsubseteq D_{[f_1(n_1, n_2, \dots, n_k), \dots, f_s(n_1, n_2, \dots, n_k)]}$, $[n_1, n_2, \dots, n_k] \in X \subseteq [0,1]^k$, iff $\forall [n_1, n_2, \dots, n_k] \in X$, $(C_{[n_1, n_2, \dots, n_k]})' \subseteq (D_{[f_1(n_1, n_2, \dots, n_k), \dots, f_s(n_1, n_2, \dots, n_k)]})'$. I satisfies a TBox T (written $I \approx T$), iff I satisfies all cut terminological axioms in T ; such I is called a model of T . I satisfies an knowledge base $\Sigma_E(A, T)$ iff I is a model of both A and T .

The main reasoning problems of EFALCN are defined as follows.

1. The satisfiability of cut concepts: a cut concept $C_{[n_1, n_2, \dots, n_k]}$ is satisfiable iff there is a model I of A and T such that $C_{[n_1, n_2, \dots, n_k]}^I \neq \emptyset$.
2. The subsumption of cut concepts: a cut concept $D_{[h_1, h_2, \dots, h_k]}$ subsumes a cut concept $C_{[n_1, n_2, \dots, n_k]}$ iff for any model I of T and A , it is true that $(C_{[n_1, n_2, \dots, n_k]})^I \subseteq (D_{[h_1, h_2, \dots, h_k]})^I$.
3. The consistency of ABox A : a ABox A is consistent iff there is a model I of T such that $I \approx A$.

3 Reasoning Properties of EFALCN

Typical DLs convert concepts into NNF to simplify the reasoning algorithm. EFALCN needs the same conversion. An cut concept is in NNF iff negation \neg only occurs in front of the atomic cut concepts. Every cut concept can be converted into an equivalent one in NNF by exhaustively applying the following rewrite rules:

$$\begin{aligned} \neg\neg C_{[n_1, n_2, \dots, n_k]} &\sim C_{[n_1, n_2, \dots, n_k]} ; \neg(C_{[n_1, n_2, \dots, n_k]} \sqcap D_{[h_1, h_2, \dots, h_s]}) \sim \neg C_{[n_1, n_2, \dots, n_k]} \sqcup \neg D_{[h_1, h_2, \dots, h_s]} ; \\ \neg(C_{[n_1, n_2, \dots, n_k]} \sqcup D_{[h_1, h_2, \dots, h_s]}) &\sim \neg C_{[n_1, n_2, \dots, n_k]} \sqcap \neg D_{[h_1, h_2, \dots, h_s]} ; \\ \neg(\exists R.C)_{[n_1, n_2, \dots, n_{k+1}]} &\sim \forall R_{[n_1]}. \neg C_{[n_2, n_3, \dots, n_{k+1}]} ; \neg(\forall R.C)_{[n_1, n_2, \dots, n_{k+1}]} \sim \exists R_{[n_1]}. \neg C_{[n_2, n_3, \dots, n_{k+1}]} ; \\ \neg(\geq NR_{[n_1]}) &\sim (\leq N - 1 R_{[n_1]}) ; \neg(\leq NR_{[n_1]}) \sim (\geq N - 1 R_{[n_1]}) . \end{aligned} \quad (8)$$

Theorem 1. For any $I = \langle \Delta^I, \bullet^I \rangle$, the above rewrite rules are semantic consistent.

Proof. The proof of one equation is given below, and the other six equations can be proofed similarly.

$$\begin{aligned} (\neg(\exists R.C)_{[n_1, n_2, \dots, n_k]})^I &= \Delta^I / \{d \mid d \in \Delta^I \wedge \exists d' \in \Delta^I, R^I(d, d') \geq n_1 \wedge d' \in (C_{[n_2, n_3, \dots, n_k]})^I\} \\ &= \{d \mid \neg \exists d' \in \Delta^I, R(d, d') \geq n_1 \wedge d' \in (C_{[n_2, n_3, \dots, n_k]})^I\} \\ &= \{d \mid \forall d' \in \Delta^I, R(d, d') < n_1 \vee d' \notin (C_{[n_2, n_3, \dots, n_k]})^I\} \\ &= \{d \mid \forall d' \in \Delta^I, R(d, d') \geq n_1 \rightarrow d' \in (\neg C_{[n_2, n_3, \dots, n_k]})^I\} \\ &= (\forall R_{[n_1]}, \neg C_{[n_2, n_3, \dots, n_k]})^I \end{aligned}$$

From now on, we assume that all cut concepts are in NNF.

There are two reasoning properties dealing with suffix vectors of cut concepts and cut roles, which will better enable the reasoning in EFALCN.

Theorem 2. For any two cut roles $R_{[n_1]}$ and $R_{[m_1]}$, if they have the same prototypes and $n_1 \leq m_1$, then for any interpretation $I = \langle \Delta^I, \bullet^I \rangle$, it is true that $(R_{[n_1]})^I \sqsubseteq (R_{[m_1]})^I$ (this implicitly means $R_{[m_1]} \sqsubseteq R_{[n_1]}$).

Though the subsumption of axiom roles goes beyond the description bound of EFALCN, $R_{[m_1]} \sqsubseteq R_{[n_1]}$ is not an assertion of EFALCN but a fact existing in all interpretations. We can use this implicit inclusion to accelerate reasoning without expressing it explicit.

Definition 1. The constraint of suffixes: For any suffix, when its prefix is an atomic fuzzy concept, if \neg occurs in front of the concept, its constraint is \neg ; when its prefix is an atomic fuzzy role, if \forall , \exists , $\geq N$ or $\leq N$ is in front of the role, its constraint is \forall , \exists , $\geq N$ or $\leq N$ respectively.

For example, in the cut concept $(\neg \text{Tall} \sqcap \exists \text{friend.Tall})_{[0.7, 0.8, 0.9]}$, the prefix of the first suffix 0.7 is Tall and the constraint is \neg ; the prefix of the second suffix 0.8 is friend and the constraint is \exists .

Theorem 3. For any two cut concepts $C_{[n_1, \dots, n_k]}$ and $C_{[m_1, \dots, m_k]}$ with the same prototypes, for any two i^{th} suffixes n_i, m_i in the suffix vectors, they have the same prefix and constraint, if it is true that

Condition 1: When the prefix is an atomic fuzzy concept, if the constraint is \neg , then $n_i \geq m_i$, otherwise $n_i \leq m_i$.

Condition 2: When the prefix is an atomic fuzzy role, if the constrain is \forall and $\leq N$, then $n_i \geq m_i$, otherwise $n_i \leq m_i$. then for any interpretation $I = \langle \Delta^I, \bullet^I \rangle$, it is true that $(C_{[n_1, \dots, n_k]})^I \supseteq (C_{[m_1, \dots, m_k]})^I$.

Proof. In this proof, we use $Length(C_{[n_1, \dots, n_k]})$ to denote the number of suffixes in the suffix vector of the cut concept $C_{[n_1, \dots, n_k]}$, and obviously $Length(C_{[n_1, \dots, n_k]}) = k$.

(I) Induction base: when $k=1$, the cut concepts can only be in the form of $B_{[n]}$, $\neg B_{[n]}$, $\geq NR_{[n]}$ or $\leq NR_{[n]}$.

Case 1.1: If $C_{[n_1, \dots, n_k]} = B_{[n_1]}$, $C_{[m_1, \dots, m_k]} = B_{[m_1]}$, the suffixes n_1, m_1 have no constraint. If $n_1 \leq m_1$, then for any interpretation I , we can get that $\forall d \in \Delta^I, d \in (B_{[m_1]})^I \Leftrightarrow B^I(d) \geq m_1 \Rightarrow B^I(d) \geq m_1 \geq n_1 \Rightarrow d \in (B_{[n_1]})^I$. Therefore, $(B_{[n_1]})^I \supseteq (B_{[m_1]})^I$.

Case 1.2: If $C_{[n_1, \dots, n_k]} = \neg B_{[n_1]}$, $C_{[m_1, \dots, m_k]} = \neg B_{[m_1]}$, the constraint of n_1, m_1 is \neg . If $n_1 \geq m_1$, then for any interpretation I , we can get that $\forall d \in \Delta^I, d \in (\neg B_{[m_1]})^I \Leftrightarrow B^I(d) < m_1 \Rightarrow B^I(d) < m_1 \leq n_1 \Rightarrow d \in (\neg B_{[n_1]})^I$. Therefore, $(\neg B_{[n_1]})^I \supseteq (\neg B_{[m_1]})^I$.

Case 1.3: If $C_{[n_1, \dots, n_k]} = \geq NR_{[n_1]}$, $C_{[m_1, \dots, m_k]} = \geq NR_{[m_1]}$, the constraint of n_1, m_1 is $\geq N$. For any $d \in \geq NR_{[m_1]}$, there are at least N individuals d_1', d_2', \dots, d_N' such that $(d, d_i') \in (R_{[m_1]})^I$. If $n_1 \leq m_2$, from theorem 2, $(R_{[n_1]})^I \supseteq (R_{[m_1]})^I$ holds for any interpretation I . Therefore, there are at least N individuals d_1', d_2', \dots, d_N' such that $(d, d_i') \in (R_{[n_1]})^I$ and obviously $d \in (\geq NR_{[n_1]})^I$. We can get that $(\geq NR_{[n_1]})^I \supseteq (\geq NR_{[m_1]})^I$.

Case 1.4: If $C_{[n_1, \dots, n_k]} = \leq NR_{[n_1]}$, $C_{[m_1, \dots, m_k]} = \leq NR_{[m_1]}$, the proof is similar to Case 1.3.

Above all, we can deduce that when $k=1$, the theorem holds.

(II) Induction hypothesis: assume that when $k \leq L$ ($L \geq 1$), the theorem holds.

(III) Induction step: when $k=L+1$, the cut concepts can only be in the form of $D_{[n_1, n_2, \dots, n_s]} \sqcup D_{[n_{s+1}, n_{s+2}, \dots, n_{L+1}]}$, $D_{[n_1, n_2, \dots, n_s]} \sqcap D_{[n_{s+1}, n_{s+2}, \dots, n_{L+1}]}$, $(\exists R.D)_{[n_1, n_2, \dots, n_{L+1}]}$ or $(\forall R.D)_{[n_1, n_2, \dots, n_{L+1}]}$.

Case 2.1: If $C_{[n_1, \dots, n_k]} = D_{[n_1, \dots, n_s]} \sqcup D_{[n_{s+1}, \dots, n_{L+1}]}$, $C_{[m_1, \dots, m_k]} = D_{[m_1, \dots, m_s]} \sqcup D_{[m_{s+1}, \dots, m_{L+1}]}$, obviously it is true that $Length(D_{[n_1, \dots, n_s]}) = s$, $Length(D_{[n_{s+1}, \dots, n_{L+1}]}) = L-s+1$, and $s \leq L$, $L-s+1 \leq L$. If the suffixes of $D_{[n_1, \dots, n_s]} \sqcup D_{[n_{s+1}, \dots, n_{L+1}]}$ and $D_{[m_1, \dots, m_s]} \sqcup D_{[m_{s+1}, \dots, m_{L+1}]}$ satisfy condition 1 and 2, then the suffixes of $D_{[n_1, \dots, n_s]}$ and $D_{[m_1, \dots, m_s]}$ (resp. $D_{[n_{s+1}, \dots, n_{L+1}]}$ and $D_{[m_{s+1}, \dots, m_{L+1}]}$) satisfy these conditions too. From Induction hypothesis, for all interpretation I , it is true that $(D_{[n_1, \dots, n_s]})^I \supseteq (D_{[m_1, \dots, m_s]})^I$ and similarly $(D_{[n_{s+1}, \dots, n_{L+1}]})^I \supseteq (D_{[m_{s+1}, \dots, m_{L+1}]}))^I$. Therefore, we can deduce that for any interpretation I , $(D_{[n_1, \dots, n_s]} \sqcup D_{[n_{s+1}, \dots, n_{L+1}]})^I = (D_{[n_1, \dots, n_s]} \sqcup (D_{[n_{s+1}, \dots, n_{L+1}]})^I) = (D_{[n_1, \dots, n_s]} \sqcup (D_{[n_{s+1}, \dots, n_{L+1}]}))^I \supseteq (D_{[m_1, \dots, m_s]} \sqcup D_{[m_{s+1}, \dots, m_{L+1}]})^I$. So in this case, the theorem holds.

Case 2.2: If $C_{[n_1, \dots, n_k]} = D_{[n_1, \dots, n_s]} \sqcap D_{[n_{s+1}, \dots, n_{L+1}]}$, $C_{[m_1, \dots, m_k]} = D_{[m_1, \dots, m_s]} \sqcap D_{[m_{s+1}, \dots, m_{L+1}]}$, the proof is similar to Case 2.1.

Case 2.3: If $C_{[n_1, \dots, n_k]} = (\exists R.D)_{[n_1, n_2, \dots, n_{L+1}]}$, $C_{[m_1, \dots, m_k]} = (\exists R.D)_{[m_1, m_2, \dots, m_{L+1}]}$, when the suffixes of $(\exists R.D)_{[n_1, n_2, \dots, n_{L+1}]}$ and $(\exists R.D)_{[m_1, m_2, \dots, m_{L+1}]}$ satisfy the two conditions, the first two suffixes satisfy $n_1 \leq m_1$ and the suffixes of $D_{[n_2, n_3, \dots, n_{L+1}]}$ and $D_{[m_2, m_3, \dots, m_{L+1}]}$ satisfy the two conditions. From Induction hypothesis and $\text{Length}(D_{[n_2, n_3, \dots, n_{L+1}]}) = L$, for any interpretation I , $(D_{[n_2, n_3, \dots, n_{L+1}]})^I \supseteq (D_{[m_2, m_3, \dots, m_{L+1}]})^I$. Therefore, we can get that for any interpretation I , and for any $d \in ((\exists R.D)_{[m_1, \dots, m_{k+1}]})^I$, there is an individual d' such that $R'(d, d') \geq m_1$ and $d' \in D_{[m_2, m_3, \dots, m_{L+1}]}^I$. From $n_1 \leq m_1$ and $D_{[n_2, \dots, n_{k+1}]}^I \supseteq D_{[m_2, \dots, m_{k+1}]}^I$, we can deduce that d' satisfies $R'(d, d') \geq n_1$ and $d' \in D_{[n_2, n_3, \dots, n_{L+1}]}^I$. Therefore it has $d \in ((\exists R.D)_{[n_1, n_2, \dots, n_{L+1}]})^I$ and then $((\exists R.D)_{[m_1, \dots, m_{k+1}]})^I \subseteq ((\exists R.D)_{[n_1, n_2, \dots, n_{L+1}]})^I$. So the theorem holds.

Case 2.4: If $C_{[n_1, \dots, n_k]} = (\forall R.D)_{[n_1, n_2, \dots, n_{L+1}]}$, $C_{[m_1, \dots, m_k]} = (\forall R.D)_{[m_1, m_2, \dots, m_{L+1}]}$, the proof is similar to Case 2.3.

Above all, we have proved when $k=L+1$, the theorem holds.

Therefore, from I-III, for any two cut concepts, the theorem holds.

4 Related Work

EFALCN has more expressive power than FALC. To explain this conclusion, we extend EFALCN with complex cut concepts $C_{[n]}$, where C is a complex fuzzy concept and $n \in [0,1]$, and call it EFALCN*.

Firstly, EFALCN* can express any FALC knowledge base $\Sigma(A, T)$:

- (1) Each fuzzy assertion in a FALC ABox A can be equally converted to a cut assertion in EFALCN* ABox by applying the following rewrite rules: $< C(a) \geq n > \sim a: C_{[n]}$ and $< R(a, b) \geq n > \sim (a, b): R_{[n]}$.
- (2) Each fuzzy terminological axiom in a FALC TBox T can be equally converted to a cut terminological axiom in EFALCN* TBox by applying the following rewrite rules: $< B \prec D > \sim B_{[n]} \sqsubseteq D_{[n]}$, $n \in [0,1]$ and $< B \approx D > \sim B_{[n]} \sqsubseteq D_{[n]}$ $n \in [0,1]$ and $D_{[n]} \sqsubseteq B_{[n]}$, $n \in [0,1]$.

Secondly, EFALCN and EFALCN* have the same expressive power for fuzzy information. We only have to prove that every complex cut concept in EFALCN* can be equally denoted by atom cut concepts in EFALCN. Obviously, it is true.

Thirdly, EFALCN is more expressive than FALC.

FALCN supports more powerful presentation of fuzzy concept assertion. For example, $\exists R.C$ is a FALC fuzzy concept, if I satisfies $<(\exists R.C)(a) \geq n>$, then it means $(\exists R.C)'(a') \geq n$. We can get that $\exists b' \in \Delta', R'(a', b') \geq n$ and $C'(b') \geq n$. In many application, it may encounter fuzzy assertion such as $\exists b' \in \Delta', R'(a', b') \geq n_1$ and $C'(b') \geq n_2$, where $n_1 \neq n_2$. In this case, the membership degrees of concept and role are different. FALC cannot distinguish such diverse membership degrees, but

EFALCN can handle it. The above fuzzy assertion can be described as a :
 $\exists R_{[n_1]} \cdot C_{[n_2]}.$

In addition, EFALCN extends the expressive scope of fuzzy terminological information in FALC. The FALC fuzzy terminological axiom $C \prec D$ implicit means $\forall d \in \Delta^I, C^I(d) \geq n \rightarrow D^I(d) \geq n$, which can not express complex inclusion based on various membership degrees. For example, $\forall d \in \Delta^I$, $\text{Very-young}^I(d) \geq 0.6 \rightarrow \text{Young}^I(d) \geq 0.9$. Two sides contain various membership degree, which is not allowed in FALC but can be denoted in EFALCN: $\text{Very-young}_{[0.6]} \sqsubseteq \text{Young}_{[0.9]}$.

5 Conclusions

We propose EFALCN, which introduces the cut sets of fuzzy concepts and fuzzy roles as atomic concepts and atomic roles. In detail, we define the syntax structure, semantic interpretation and reasoning problem of EFALCN. We compare EFALCN with other fuzzy DLs, and explain that EFALCN has more expressive power. This work can be applied as a language in current Semantic Web to enrich its representation means, and used as a new idea of extending DLs with fuzzy features. Further researches include designing an algorithm for reasoning problem and proving its soundness, completeness and complexity.

References

1. Berners-Lee, T., Hendler, J., Lassila, O.: The Semantic Web. *Scientific American*, vol. 284, no.5 (2001) 34–43
2. Baader, F., Calvanese, D., McGuinness, D.L., Nardi, D., Patel-Schneider, P.F.(Eds.): *The Description Logic Handbook: Theory, Implementation, and Applications*. Cambridge University Press (2003)
3. Meghini, C., Sebastiani, F., Straccia, U.: Reasoning about the form and content for multi-media objects. In: *Proceedings of AAAI 1997 Spring Symposium on Intelligent Integration and Use of Text, Image, Video and Audio*, California (1997) 89–94
4. Schmidt-Schauß, M., Smolka, G.: Attributive concept descriptions with complements. *Artificial Intelligence*, vol. 48 (1991) 1–26
5. Straccia, U.: Reasoning within fuzzy description logics. *Journal of Artificial Intelligence Research*, no. 14 (2001) 137–166
6. Straccia, U.: Transforming fuzzy description logics into classical description logics. In: *Proceedings of the 9th European Conference on Logics in Artificial Intelligence*, Lisbon, (2004) 385–399

Automated Operator Selection on Genetic Algorithms

Fredrik G. Hilding and Koren Ward

University of Wollongong, Northfeild Ave. NSW 2500, Australia
`{fh68,koren}@uow.edu.au`

Abstract. Genetic Algorithms (GAs) have proven to be a useful means of finding optimal or near optimal solutions to hard problems that are difficult to solve by other means. However, determining which crossover and mutation operator is best to use for a specific problem can be a complex task requiring much trial and error. Furthermore, different operators may be better suited to exploring the search space at different stages of evolution. For example, crossover and mutation operators that are more likely to disrupt fit solutions may have a less disruptive effect and better search capacity during the early stages of evolution when the average fitness is low. This paper presents an automated operator selection technique that largely overcomes these deficiencies in traditional GAs by enabling the GA to dynamically discover and utilize operators that happen to perform better at finding fitter solutions during the evolution process. We provide experimental results demonstrating the effectiveness of this approach by comparing the performance of our automatic operator selection technique with a traditional GA.

1 Introduction

Since their introduction in 1975 by John Holland [1], Genetic Algorithms (GAs) have been applied to a large variety of problems. Traditionally, GAs have one crossover and one mutation operator that are applied to population members in order to evolve fit solutions to a given problem. These genetic operators can vary depending on the problem and may be either standard genetic operators (as described by Holland [1] and Goldberg [2]) or custom built operators that are designed to solve a particular problem more effectively. Generally, there are three standard crossover operators: Uniform, Random, and the N-point crossover operator with N kept constant, commonly to 1 or 2. Among the most common standard mutation operators are: bit toggle, random bit toggle and bit shift mutation. (See Mao et al [3] and Suzuki & Iwasa [4].) As the number of problems applied to GAs has increased, the number of custom built crossover and mutation operators has also grown considerably. Consequently, selecting or designing appropriate operators for a specific problem to be solved with a GA has become a significant task requiring much trial and error.

In order to overcome much of the difficulty in deciding which crossover and mutation operators to use on a specific problem, a novel Automated Operator

Selection (AOS) technique is presented in this paper. AOS is able to reduce the work needed in finding suitable genetic operators by enabling the GA to automatically select crossover and mutation operators from a given set during evolution based on their performance at producing fitter individuals. This enables the user to provide the GA with a variety of traditional and/or custom built crossover and mutation operators and evolve solutions to problems by utilizing the most effective operator for the task via AOS. To demonstrate the effectiveness of AOS we provide experimental results comparing the performance of traditional GAs with GAs equipped with AOS on a well known problem. Our results demonstrate that AOS can not only reduce the work needed in finding effective genetic operators, but it can also improve the evolutionary performance by dynamically utilizing the most effective operator at different stages of evolution.

The remainder of this paper is structured as follows: Section 2 provides a brief background review of earlier work related to automated operator selection. This is followed in Section 3 with a description of the implementation of our AOS method. Section 4 presents our experimental results where we compare the performance of GAs equipped with AOS to a traditional GA on the 01-Knapsack problem. This is followed with some concluding remarks in Section 5.

2 Background

In order to increase the performance of GAs at producing fitter offspring, Selective Operator [5] and Inductive Learning [6] has been presented in previous work for optimizing the performance of the N-point crossover operator. These two approaches concern the same issues: determining where the crossover points should be located and how many crossover points are needed to produce fitter individuals. Selective Operator achieves this by rating all the crossover points on each parent member and by selecting the strongest points to crossover and form offspring. The weighting attributed to these crossover points is then updated by assessing the resulting fitness of the offspring. Similarly, the Inductive Learning approach generates masking strings for mediating the N-point crossover operator. Each masking string determines where the crossover points should occur and is rated according to its performance at improving the fitness of members. There are three rating levels based on the fitness gain: productive, inactive and destructive. After a number of generations, denoted civilizations, these masking strings are updated by replacing the masks on the destructive masking strings with new randomly generated masks.

These two approaches show that an advantage can be obtained by using prior knowledge of member fitness to determine effective crossover points on genetic codes during the crossover stage. However, both the Selective Operator approach and Inductive Learning approach to genetic operator optimization only apply to the N-point crossover operator. Consequently, they provide no means of dynamically optimizing the mutation operator, nor are they able to select or optimize custom built genetic operators provided by the user.

To overcome these deficiencies, AOS has been developed as a means of using prior knowledge of gene fitness to automatically select effective crossover and

mutation operators dynamically during evolution. With AOS the user can provide the GA with a variety of crossover and mutation operators to be used on the problem. These operators can be standard operators with different settings (eg 1-point, 2-point, random, bit-flip, etc.), custom built operators (like those needed for solving problems like the TSP), or intelligent operators (like Selective Operator [5] and Inductive Learning [6]). Once the operators are provided and the GA is started, the operators are selected and applied to the population in proportion their demonstrated ability to improve gene fitness. Consequently, operators that prove to be ineffective at improving gene fitness become seldom used whereas operators that prove effective at improving gene fitness become often used. This ensures that at all stages of evolution, the most effective operator(s) for improving the population are applied to the problem

3 Automated Operator Selection

Automated Operator Selection (AOS) essentially involves providing the GA with a variety of crossover and mutation operators which are utilized according to their performance at producing fitter population members. This is achieved by using a roulette wheel style selection technique to select a crossover or a mutation operator with a probability proportional to its fitness. Namely:

$$p_i = \frac{F_i}{\sum_{j=0}^n F_j} . \quad (1)$$

Where:

p_i : is the probability of operator i being selected at generation t .

F_i : is the scaled fitness of operator i at generation t .

Note: Crossover and mutation operators are given separate roulette wheels.

To determine each operator's fitness for the current generation we compare the number of population members produced by it in the current population that have improved their fitness against the number of population members produced by it who's fitness got worse. This is described by Eqn 2 below:

$$R_i(t) = N_i^+(t) \cdot w(t) - N_i^-(t) + \max(N^-(t)) . \quad (2)$$

Where:

$R_i(t)$: is the raw fitness of operator i for generation t .

$N_i^+(t)$: is the number of members produced by operator i with higher fitness than the average fitness of their parents.

$N_i^-(t)$: is the number of members produced by operator i with lower fitness than the average fitness of their parents.

$w(t)$: is the improvement weighting at time t , (see below).

To scale each operator's raw fitness we apply the simple exponential moving average across the raw fitness values for the current and previous generations to

smooth the scaled fitness, thus avoiding abrupt changes to any operator's fitness.

$$F_i(t) = \begin{cases} \frac{1}{n} & \text{if } t = 1 \\ k \cdot F_i(t-1) + (1-k)R_i(t) & \text{if } t > 1 \end{cases}. \quad (3)$$

Where:

$F_i(t)$: is the scaled fitness of operator i .

k : is exponential moving average period constant, namely 0.3.

The improvement weighting $w(t)$ is obtained by dividing the total number of population members who's fitness got worse $N^-(t)$ by the total number of population members who's fitness improved $N^+(t)$ and by taking the single exponential moving average of this across the current and past generations. Namely:

$$w(t) = \begin{cases} P & \text{if } t = 1 \\ k \cdot w(t-1) + (1-k)\frac{N^-(t)+1}{N^+(t)+1} & \text{if } t > 1 \end{cases}. \quad (4)$$

Where:

P : is the $w(t)$ initialization constant, namely 10.

k : is exponential moving average period constant, namely 0.3.

The purpose of using the improvement weight, $w(t)$, (in Eqn. 2) is to add more weight to improved population members. This is needed to recognize the fact that with GAs improved members of the population have more significance toward finding optimal solutions than non-improving members which tend to not be selected for parenting. We found initializing this to 10 to be a reasonable estimate of the significance of improved members at the initial generation. Also, no operators are allowed to occupy less than 10% of the roulette wheel at any time. This is done to prevent operators from becoming under utilized and thus loosing the opportunity to get their fitness measured in successive generations.

4 Experimental Results

To evaluate the performance of the proposed automated operator selection (AOS) method, we conducted experiments on the 01-Knapsack problem [7] using a traditional GA, with various crossover and mutation operators, and compared the results achieved with a similar GA using the AOS method. The 01-Knapsack problem is a classical NP-hard problem and is intended for solving the problem of filling a knapsack with as valuable a load as possible without over-loading the knapsack.

To solve this problem using a GA equipped with the AOS method, we provided the AOS crossover roulette wheel with the uniform, one-point, two-point and random crossover operators. Similarly, the AOS mutation roulette wheel was provided with the bit-toggle, random-toggle and bit shift mutation operators. We then compared the results achieved using the AOS equipped GA with the results obtained from running a conventional GA with all possible combinations of the

same crossover and mutation operators. For all the AOS and GA experiments the population size was set to 1000, the crossover rate to 0.75, and the mutation rate to 0.01. To collate our results 20 runs of each GA were performed and the fitness measures averaged across runs.

Figure 1 shows a plot of the fittest individual from each generation averaged over 20 runs. It can be seen that a near optimal solution is found around generation 61 after which stagnation tends to occur.

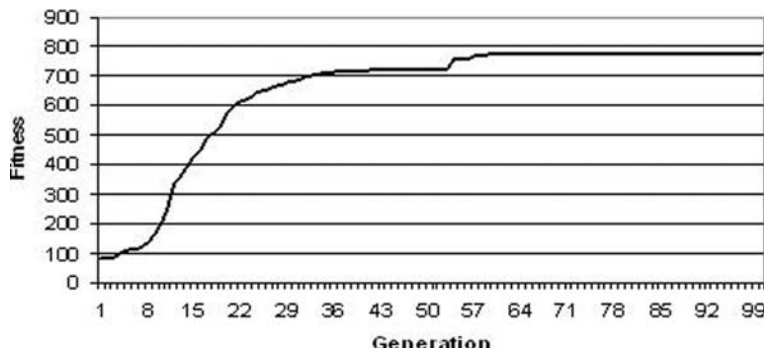


Fig. 1. Fittest member averaged over 20 runs for the AOS equipped GA

Figures 2 and 3 show the proportional usage (or selection) of the crossover and mutation operators within the AOS equipped GA averaged over 20 trials. Figure 2 shows that there is a clear preference for the two-point crossover operator early in evolution followed by some significant usage of the random crossover operator. Furthermore, Fig. 3 shows that the AOS equipped GA also appears to have a clear preference for using the random toggle and bit-shift mutation operators on this problem.

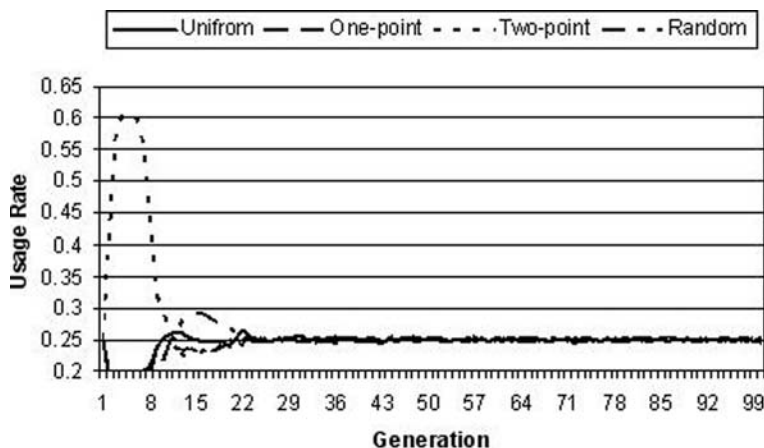


Fig. 2. Crossover operator usage for the AOS equipped GA over 100 generations

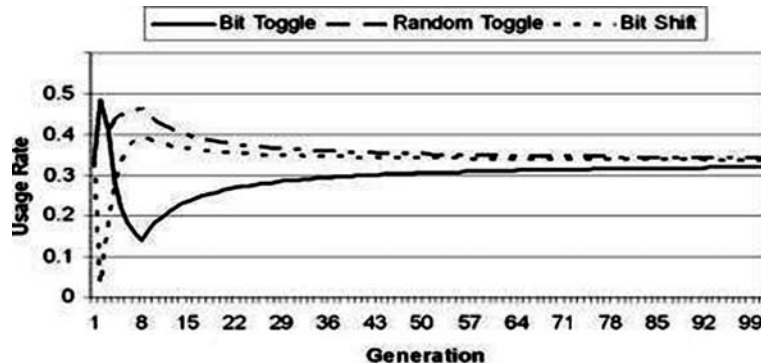


Fig. 3. Mutation operator usage for the AOS equipped GA over 100 generations

Table 1 lists the minimum, average and maximum fitness demonstrated at stagnation of the traditional GA experiments with different crossover and mutation operators. This is followed with the same fitness measures from the AOS equipped GA at the point of stagnation. The fitness measures given are averaged across 20 runs.

From Table 1 it can be seen that the most successful crossover and mutation operator pair applied to solving the 01-Knapsack problem on the traditional GA are the random crossover and the bit-shift mutation operators. However, almost the same result is achieved on the AOS equipped GA with the benefit of

Table 1. Comparison of AOS with a traditional GA using different combinations of crossover and mutation operators on the 01-Knapsack Problem

| AOS vs Traditional GA on the 01-Knapsack Problem | | | | | | |
|--|--------------------|-----------------------|---------------|-------|-------|--|
| | Operator pair used | Stag. Pt. (gen. #) | Fitness range | | | |
| | | | Min | Avg | Max | |
| Uniform | Bit toggle | 8 | 65.2 | 126.2 | 287.5 | |
| | Random toggle | 53 | 76.8 | 130.8 | 272.6 | |
| | Bit shift | 60 | 78.3 | 160.0 | 314.2 | |
| One-point | Bit toggle | 33 | 127.1 | 378.5 | 559.9 | |
| | Random toggle | 35 | 136.7 | 345.6 | 524.6 | |
| | Bit shift | 70 | 116.4 | 379.8 | 667.3 | |
| Two-point | Bit toggle | 40 | 123.9 | 399.0 | 663.0 | |
| | Random toggle | 41 | 113.3 | 386.6 | 545.8 | |
| | Bit shift | 67 | 116.4 | 379.8 | 667.3 | |
| Random | Bit toggle | 57 | 155.2 | 498.4 | 782.2 | |
| | Random toggle | 54 | 155.1 | 498.3 | 782.1 | |
| | Bit shift | 57 | 156.0 | 473.4 | 779.2 | |
| AOS | | 61 | 150.6 | 533.4 | 771.2 | |

only having to perform the one trial with all the given operators. This demonstrates potential for considerable time saving when experimenting with different operators.

5 Conclusion

In order to overcome much of the difficulty in deciding which crossover and mutation operators to use on a specific problem, a novel Automated Operator Selection (AOS) technique is presented in this paper. This enables the user to provide the GA with a variety of traditional and/or custom built crossover and mutation operators and evolve solutions to problems by utilizing operators that prove effective for the task. The time saving is achieved by no longer having to repeatedly try different combinations of crossover and mutation operators in order to find ones that work effectively. Our experimental results show that AOS is not only able to reduce the work needed in finding and applying suitable genetic operators to a specific problem, but it also enables the GA to dynamically utilize different operators that prove to be most effective at improving the population at different stages of evolution.

References

1. John Holland. Adaptation in natural and artificial systems: an introductory analysis with applications to biology, control, and artificial intelligence. The University of Michigan Press, second edition 1993 MIT press edition (1975)
2. David E. Goldberg, Genetic Algorithms in Search, Optimization and Machine Learning, Addison-Wesley Publishing, MA (1989).
3. J. Mao; K. Hirasawa; J. Hu and J. Murata. Increasing robustness of genetic algorithm. In Publishers, M. K.,ed., Proceedings of the Genetic and Evolutionary Computation Conference (2002) 456-462
4. H. Suzuki, and Y. Iwasa,.Crossover accelerates evolution in GAs with a Babel-like tness landscape: Mathematical analyses. Evolutionary Computation Journal, (1999) 7(3):275-310.
5. Kanta Vekaria and Chris Clack. Selective crossover in genetic algorithms: An empirical study. Lecture Notes in Computer Science (1998) 1498:438-447.
6. Michle Sebag and Marc Schoenauer. Controlling crossover through inductive learning. In Hans-Paul Schwefel Yuval Davidor and Reinhard Manner, editors, Parallel Problem Solving from Nature - PPSN III, Springer (1994) 209-218.
7. T. Gerasch and P. Wang. A survey of parallel algorithm for one-dimensional integer knap-sack problems. INFOR (1993) 32(3):163-186.

Weak Key Analysis and Micro-controller Implementation of CA Stream Ciphers*

Pascal Bouvry¹, Gilbert Klein¹, and Franciszek Seredyński^{2,3}

¹ Luxembourg University

Faculty of Sciences, Communication and Technology

6, rue Coudenhove Kalergi

L-1359 Luxembourg-Kirchberg, Luxembourg

{pascal.bouvry,gilbert.klein}@uni.lu

² Polish-Japanese Institute of Information Technologies

Koszykowa 86, 02-008 Warsaw, Poland

³ Institute of Computer Science, Polish Academy of Sciences

Ordona 21, 01-237 Warsaw, Poland

sered@ipipan.waw.pl

Abstract. In the paper we extend known results studying the application of CAs for stream ciphers. We illustrate the notion of weak keys in such a cryptosystem and describe the experiments related to its implementation on micro-controllers.

1 Introduction

Two main cryptography systems are used today: symmetric systems, aka secret key systems, and public-key systems. An extensive overview of currently known or emerging cryptography techniques used in both type of systems can be found in [12]. One of such a promising cryptography techniques is applying cellular automata (CAs).

The main concern of this paper is secret key systems. In such systems the encryption key and the decryption key are the same. The encryption process is based on generation of pseudorandom bit sequences, and CAs can be effectively used for this purpose. CAs for systems with a secrete key were first studied by Wolfram [17], and later by Habutsu *et al.* [3], Nandi *et al.* [10] and Gutowitz [2]. Recently they were a subject of study by Tomassini & Perrenoud [15], and Tomassini & Sipper [16], who considered one and two dimensional (2D) CAs for encryption scheme. In Seredyński *et al.*[13], a 1-D cellular automa system has been proposed that shows strong statistical characteristics in terms of security. Indeed it passes classical tests as FIPS-140 and Marsaglia tests. The present article highlights some limitations of the proposed systems in terms of weak-keys and hardware implementations but also shows potential paths for solving these issues.

* Participation to KES has been financed by LIASIT (www.liasit.lu)

2 Cellular Automata and Cryptography

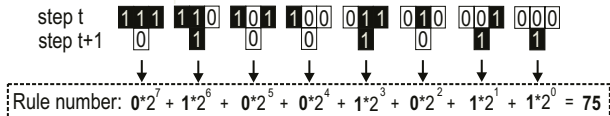
Let P be a plain-text message consisting of m bits $p_1 p_2 \dots p_m$, and $k_1 k_2 \dots k_m$ be a bit stream of a key k . Let c_i be the $i - th$ bit of a cipher-text obtained by applying XOR (exclusive-or) enciphering operation:

$$c_i = p_i \text{ } XOR \text{ } k_i.$$

The original bit p_i of a message can be recovered by applying the same operation XOR on c_i by using the same bit stream key k

This enciphering algorithm is called the Vernam cipher and is known to be [8, 12] perfectly safe if the key stream is truly unpredictable and used only one time.

It is assumed that a state q_i^{t+1} of a cell i at the time $t + 1$ depends only on states of its neighborhood at the time t , i.e. $q_i^{t+1} = f(q_i^t, q_{i1}^t, q_{i2}^t, \dots, q_{ni}^t)$, and a transition function f , called a *rule*, which defines a rule of updating a cell i . A length L of a rule and a number of neighborhood states for a binary uniform CAs is $L = 2^n$, where $n = n_i$ is a number of cells of a given neighborhood, and a number of such rules can be expressed as 2^L . For CAs with e.g. $r = 2$ the length of a rule is equal to $L = 32$, and a number of such rules is 2^{32} and grows very fast with L . When the same rule is applied to update cells of CAs, such CAs are called uniform CAs, in contrast with nonuniform CAs when different rules are assigned to cells and used to update them. It is assumed that a state q_i^{t+1} of a cell i at the time $t + 1$ depends only on states of its neighborhood at the time t , i.e. $q_i^{t+1} = f(q_i^t, q_{i1}^t, q_{i2}^t, \dots, q_{ni}^t)$, and a transition function f , called a *rule*, which defines a rule of updating a cell i . A length L of a rule and a number of neighborhood states for a binary uniform CAs is $L = 2^n$, where $n = n_i$ is a number of cells of a given neighborhood, and a number of such rules can be expressed as 2^L . For CAs with e.g. $r = 2$ the length of a rule is equal to $L = 32$, and a number of such rules is 2^{32} and grows very fast with L . When the same rule is applied to update cells of CAs, such CAs are called uniform CAs, in contrast with nonuniform CAs when different rules are assigned to cells and used to update them. One dimensional CA is in a simplest case a collection of two-state elementary automata arranged in a lattice of the length N , and locally interacted in a discrete time t . For each cell i called a central cell, a neighborhood of a radius r is defined, consisting of $n_i = 2r + 1$ cells, including the cell i . When considering a finite size of CAs a cyclic boundary condition is applied, resulting in a circular grid. For example, the rule definition presented on Fig. 1 implies that if three adjacent cells in the CA currently (step t) have the pattern 011, then the middle cell will become 1 on the next time step. Wolfram proposed a naming convention for the rules: the name derives from the binary representation of the step $t+1$ based on the rule definition. In Fig. 1, step $t+1$ is composed of bits 01001011, which is a binary representation of the number 75. When the same rule is applied to update cells of CAs, such CAs are called uniform CAs, in opposite to nonuniform CAs when different rules are assigned to cells and used to update them.

**Fig. 1.** Elementary rule 75

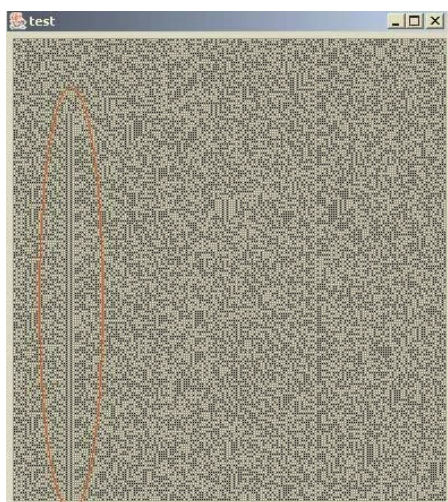
In [13], 1D, nonuniform CAs are used with neighborhood of radius $r = 1$ and $r = 2$. In the result of combining rules into sets of rules and testing collective behavior of these sets working in nonuniform CAs the following set of rules has been selected: 86, 90, 101, 105, 150, 153, 165 ($r = 1$), and 1436194405 ($r = 2$).

3 Weak Keys

A weak key for a crypto-systems eases up its cryptanalysis. In terms of our Pseudo Random Number Generators (PRNG), it would mean the presence of repeated patterns and brings sequences of generated numbers for of complexity size $O(\log(L))$, L being the original solution space.

After running many variations of keys proposed in the [13] PRNG, it appeared that some pictures corresponding to CA snapshots do contain patterns. These patterns act like barriers hindering Shanon's diffusion of information.

Indeed some of these patterns when appearing become permanent and can cause drastic cuts in the randomness of generated numbers. E.g. Let us simply consider that the chosen column for producing the random numbers corresponds to one of those included in the pattern: in this case the generator would be broken and produces always the same number.

**Fig. 2.** Example of a weak key effect

After analysis, it has been shown that such barriers happened when 2 times the long rule was applied to contiguous cells and when a predefined pattern arises. For instance, the barrier illustrated in 2 is defined by the following binary numbers: 1011 1011 1011 1011 1011 1011.

In order to ease up the analysis of barriers, let us introduce the following notation: $\rho_n(abc)$, the application of the rule number n of radius 1 to the b bit given a and c neighbours and $\rho_n(abcde)$, the application of the rule number n of radius 2 to the b bit given a, b and d, e neighbours.

In the process of defining precisely the CA behaviour in case of repeated patterns, we propose to illustrate the barrier effect for the following pattern (cf Fig 3): ?1011 $\beta\beta$ where 1011 is the core of the barrier (forever repeated), “?” is a binary value and β is a binary number repeated twice. The vector of rule applied to cells using Wolfram numbering is also provided in Fig 3. It is easy to demonstrate that this case study can happen in practice like any other case: indeed the initial CA configuration and the rule assignment are randomly chosen (based on the secret key).

| | | | | | | | |
|----------------|---|-----|----|-----|------------|------------|---------|
| Bit Number | 5 | 4 | 3 | 2 | 1 | 0 | |
| Bit value | ? | 1 | 0 | 1 | 1 | β | β |
| Assigned rules | ? | 101 | 86 | 105 | 1436194405 | 1436194405 | 101 |

Fig. 3. Instance of a barrier

Figure 4 demonstrates the recurring character of such pattern bit per bit, given that a rule of radius 1 depends only of 1 neighbour on each side and rule of radius 2 (ie in our case rule of index 7) depends of 2 neighbours on each side. Every parameter (“?” and β) are instantiated and show that it is practically impossible to break this barrier: no configuration could lead to any modification of it. Let us also highlight the behaviour of the the β s that will flip synchronously after each step.

| Bit: $\rho_{rule}(neighbourhood)$ | Binary Rule | Result |
|---|------------------------------|---|
| Bit 5: $\rho_{101}(?10)$ | 011 <u>00</u> 101 | $\rho_{101}(010) == \rho_{101}(110) == 1$ |
| Bit 4: $\rho_{86}(101)$ | 01 <u>01</u> 0110 | 0 |
| Bit 3: $\rho_{105}(011)$ | 011 <u>01</u> 001 | 1 |
| Bit 2: $\rho_{1436194405}(011\beta\beta)$ | ...100 <u>10</u> 1011001101 | $\rho(01100) == \rho(01111) == 1$ |
| Bit 1: $\rho_{1436194405}(1100?)$ | 01010 <u>10</u> 110011010... | <i>not(?)</i> (flipping bit) |
| Bit 1: $\rho_{1436194405}(1111?)$ | 0101010 <u>11</u> 0011010... | <i>not(?)</i> (flipping bit) |
| Bit 0: $\rho_{101}(00?)$ | 01100101 | <i>not(?)</i> == Bit1 _{t+1} (flipping bit) |
| Bit 0: $\rho_{101}(11?)$ | 01100101 | <i>not(?)</i> == Bit1 _{t+1} (flipping bit) |

Fig. 4. Bit per bit analysis of a barrier effect

One easy way to circumvent such pattern is to prevent the creation of such keys and in particular to avoid instantiating 2 long rules in contiguous cells. How-

ever there is no proof that other patterns might appear. Therefore a verification case by case of some criteria (e.g. entropy) might be the only way out.

4 Hardware Implementation Using Micro-controllers

The chosen micro controller (M30245) is a 16-bit micro controller based on the RENESAS M16C family core technology that uses a high performance silicon gate CMOS process with an M16C/62 Series CPU core. This is a single-chip USB peripheral micro controller that operates at full speed (12 MHz) and is compliant with the USB version 2.0 specification.

This micro controller can be found back on the EVBM16C/USB evaluation board. Additional information can be found on the Internet at www.m16c.de (select EVB-BOARDS).

The related development shows that is possible to implement such a Cellular Automata on an external USB device. However that, due to execution speed, the related implementation can only be used in a limited way in practice. The next table illustrates the execution time needed to generate a number of steps for CAs of different sizes:

| Picture dimensions | Nbr of codes | Nbr of CA iterations | tUSBCA [s] | tSoftCA [s] |
|--------------------|--------------|----------------------|------------|-------------|
| 1010 | 100 | 800 | 7 | >>1 |
| 2020 | 400 | 3200 | 21 | >1 |
| 4040 | 1600 | 12800 | 81 | 1 |
| 6060 | 3600 | 28800 | 179 | 2 |
| 8080 | 6400 | 51200 | 311 | 4 |
| 100100 | 10000 | 80000 | 483 | 7 |

5 Conclusions

In the paper we have extended the results reported in [13] on studying the application of CAs for stream ciphers. We illustrated the notion of weak keys in such a cryptosystem and described the experiments related to its implementation on micro-controllers.

In terms of future work, we consider the implementation of this system on FPGA. We already have an alpha-version of the VHDL version of it.

References

1. P. Guan, Cellular Automaton Public-Key Cryptosystem, *Complex Systems* 1, 1987, pp. 51-56
2. H. Gutowitz, Cryptography with Dynamical Systems, in E. Goles and N. Boccara (Eds.) *Cellular Automata and Cooperative Phenomena*, Kluwer Academic Press, 1993
3. T. Habutsu, Y. Nishio, I. Sasae, and S. Mori, A Secret Key Cryptosystem by Iterating a Chaotic Map, *Proc. of Eurocrypt'91*, 1991, pp. 127-140

4. P. D. Hortensius, R. D. McLeod, and H. C. Card, Parallel random number generation for VLSI systems using cellular automata, *IEEE Trans. on Computers* 38, October 1989, pp. 1466-1473
5. J. Kari, Cryptosystems based on reversible cellular automata, personal communication, 1992
6. D. E. Knuth, *The Art of Computer Programming*, vol. 1 & 2, *Seminumerical Algorithms*, Addison-Wesley, 1981
7. G. Marsaglia, Diehard
<http://stat.fsu.edu/~geo/diehard.html>, 1998
8. A. Menezes, P. van Oorschot, and S. Vanstone, *Handbook of Applied Cryptography*, CRC Press, 1996
9. A. Mroczkowski, Application of Cellular Automata in Cryptography, Master Thesis (in Polish), Warsaw University of Technology, 2002
10. S. Nandi, B. K. Kar, and P. P. Chaudhuri, Theory and Applications of Cellular Automata in Cryptography, *IEEE Trans. on Computers*, v. 43, December 1994, pp. 1346-1357
11. National Institute of Standards and Technology, Federal Information Processing Standards Publication 140-2: *Security Requirements for Cryptographic Modules*, U.S. Government Printing Office, Washington 1999
12. B. Schneier, *Applied Cryptography*, Wiley, New York, 1996
13. Franciszek Seredyński, Pascal Bouvry, and Albert Y. Zomaya. Cellular automata computations and secret key cryptography. *Parallel Computing Journal*, 30(5-6):753-766, 2004.
14. M. Sipper and M. Tomassini, Generating parallel random number generators by cellular programming, *Int. Journal of Modern Physics C*, 7(2), 1996, pp. 181-190
15. M. Tomassini and M. Perrenoud, Stream Ciphers with One- and Two-Dimensional Cellular Automata, in M. Schoenauer et al. (Eds.) *Parallel Problem Solving from Nature - PPSN VI*, LNCS 1917, Springer, 2000, pp. 722-731
16. M. Tomassini and M. Sipper, On the Generation of High-Quality Random Numbers by Two-Dimensional Cellular Automata, *IEEE Trans. on Computers*, v. 49, No. 10, October 2000, pp. 1140-1151
17. S. Wolfram, Cryptography with Cellular Automata, in *Advances in Cryptology: Crypto '85 Proceedings*, LNCS 218, Springer, 1986, pp. 429-432

Author Index

- Abbass, Hussein A. III-813
Abbaftista, Fabio II-768
Abdellatif, Abdelaziz III-37
Abdulkadir, Hamud Ali II-1145
Abe, Akinori I-1167
Abe, Jair Minoro II-708, II-716, II-724
Abe, Minoru I-650
Abe, Naoto IV-689
Abe, Noriyuki IV-136, IV-143
Adachi, Yoshinori I-775, I-781, I-813
Aguilar, José I-191, I-700
Ahn, Byung-Ha I-255, II-200
Ahn, Dosung IV-532
Ahn, Kiok IV-359
Ahn, Seongjin I-618, III-54
Ahn, Sungsoo II-1050
Aimin, Wu II-1204
Aizawa, Teruaki I-880
Akama, Seiki II-708, II-724
Akamatsu, Norio I-611, I-657, I-1255, I-1261
Al-Kabir, Zul Waker II-789
Alahakoon, Damminda I-714, II-806
Alamarguy, Laurent III-1180
Ammar, Ali Ben III-37
An, Jiyuan II-37
Andrade, Javier II-658
Antonie, Maria-Luiza III-966
Antoniou, Grigoris II-746
Aoe, Jun-ichi IV-606, IV-612, IV-619
Aoidh, Eoin Mac IV-329
Aoki, Katsushi III-533
Araki, Kenji I-554, I-918, II-950, II-1347
Araki, Shoichi III-533
Ares, Juan II-658
Arita, Daisaku III-883
Arroyo, Gustavo IV-57
Asami, Kenichi III-1204
Ashourian, Mohsen II-1090
Atlam, El-Sayed IV-606, IV-612, IV-619
Azzini, Antonia I-119

Baba, Norio I-8, I-624
Bae, Changseok I-1193, I-1226
Bae, Ihn-Han I-465

Baek, Deok-Soo IV-195
Baek, Seung Yub II-1056
Baek, Young-Hyun IV-195
Baghaei, Nilufar IV-458
Bai, Yun I-290
Baik, Heung Ki II-477
Baik, Sung I-887, II-31
Bajaj, Preeti I-1070, I-1291, IV-164
Bala, Balachandran IV-35
Bala, Jerzy I-887
Balvig, Jens J. IV-661
Baoyan, Liu III-575
Barber, K. Suzanne II-831
Bassiliades, Nick II-746
Batra, Shalabh I-1070
Bates, Rafael I-162
Becerikli, Yasar II-378
Becerra, Jose A. I-840
Bellas, Francisco I-840, I-847
Benharkat, Nabila Aïcha III-191
Berlik, Stefan III-1151
Bertino, Elisa IV-324
Bertollo, Michela IV-329
Bhatt, Mehul IV-366
Bhattacharya, Pushpak II-732
Bhojwani, Sarika I-1070
Bien, Zeungnam IV-542
Bikakis, Antonis II-746
Bil, Cees I-1064, II-622
Bingru, Yang III-575, III-581
Biscozzo, Marina I-142
Biswas, P.K. III-1160
Boissier, Olivier IV-626
Borzemski, Leszek III-261, III-268
Boschetti, Fabio IV-573
Bouvry, Pascal IV-626, IV-910
Brown, Ross III-395
Bry, François IV-352
Burek, Patryk II-880
Burkhardt, Hans II-573
Burns, Alex III-953
Byun, Oh-Sung IV-195
Byun, Sung-Cheal II-200

Caforio, Antonio I-97

- Calì, Andrea I-268
 Calvez, Benoît IV-633
 Cao, Cungen II-228
 Carrato, Sergio II-8
 Carter, John N. IV-150
 Case, Keith IV-221
 Ceravolo, Paolo I-104, I-119
 Cerrada, Mariela I-191
 Cha, Jae-Sang I-479, I-485, I-1104, I-1111, II-446, II-460, II-464, II-1043
 Chae, Hui-shin I-485
 Chae, Oksam IV-359
 Chan, Aki P.F. III-141
 Chan, Eddie C.L. I-693
 Chan, Edmond M.C. III-149
 Chan, Rai III-875
 Chang, Chao-Chin III-1032
 Chang, Chin-Chen II-1224, III-442, III-1058, III-1101, IV-249
 Chang, Huai-Yang III-366
 Chang, Hui-Chen I-596
 Chang, Jae-Woo I-391
 Chang, Jui-Fang III-1032
 Chang, Jung-Shiong I-582
 Chang, Kuang-Yu I-873
 Chang, Kyung-Bae I-445, I-452, I-861, IV-115
 Chang, Liang-Cheng II-628
 Chang, Wen-Chang IV-403
 Channa, Daud IV-581
 Chao, Pei-Ju III-366
 Chau, KwokWing III-756
 Che, Lichang II-336
 Chen, An-Pin I-27, I-34, I-318, I-1186, II-45
 Chen, Chun-Hsien I-311
 Chen, Duan-Yu III-359
 Chen, Huajun II-866, II-873
 Chen, Huang-Bin III-418
 Chen, J.R. II-1238
 Chen, Jie III-1225
 Chen, Jing-Fung III-381
 Chen, Jun-Ming III-1324
 Chen, Jyh-Wei II-554
 Chen, Kefei II-186
 Chen, Liang II-1298
 Chen, Mu-Yen I-318, II-45
 Chen, Pin-Jen II-1265
 Chen, Ping II-1076
 Chen, Shih-Hsin II-1007
 Chen, Thou-Ho III-346
 Chen, Tsong-Yi II-1183
 Chen, Xiaoming I-1193, I-1226
 Chen, Y.H. II-1238
 Chen, Yen-Hung II-593
 Chen, Yi-Chang I-27, I-34, I-1186
 Chen, Yi-Ping Phoebe II-24, II-37
 Chen, Yong-Nien III-456
 Chen, Yumei IV-89
 Cheng, Jingde I-758, II-437, II-739
 Cheng, S.S. II-1238
 Cheng, Wei II-972
 Cheng, Wengang II-1217, III-388
 Cheng, Yin III-575, III-581
 Cheung, King-Hong III-1168
 Chi, Ming-Te III-456
 Chiang, Tihao IV-889
 Chiang, Yu-Min II-1007
 Chiou, Yung-Chuen III-346
 Chiu, Chih-Cheng II-1183
 Cho, Eun-kyung IV-559
 Cho, Hyunjoon I-1081
 Cho, Jae Hoon IV-854
 Cho, Jae-Soo II-371
 Cho, Jungwon III-240, III-694, III-704, III-713
 Cho, Juphil II-477, II-1043
 Cho, Kwangsu I-62
 Cho, Ming-Yuan III-366
 Cho, Nam Wook III-602
 Cho, Phil-Hun I-479, II-464
 Cho, Su-Jin II-681
 Cho, Sung-Bae I-737, II-214, III-777, III-937
 Cho, SungEon I-1094
 Cho, Sung-Keun II-688
 Cho, Yeon-Jin III-785
 Choe, YeongGeun III-317
 Choh, Ikuro I-332
 Choi, ByeongHo III-157
 Choi, Byung Mun II-1022
 Choi, Byunguk III-240, III-694, III-704, III-713, III-945
 Choi, Jae Gark I-1297
 Choi, Jaeseok III-1129
 Choi, Jong-Soo III-213
 Choi, Jun I-1146
 Choi, Myungwhan III-621
 Choi, Soo-Mi III-206, III-233, III-1210
 Choi, Woo-Kyung II-291
 Choi, Yong-Rak III-310

- Choi, Yoo-Joo III-1210
 Choo, Kenny III-433
 Chou, Yung-Chen III-442
 Chu, Bong-Horng III-997
 Chu, Carol H.C. III-1324
 Chu, Hone-Jay II-628
 Chu, Shu-Chuan III-1032
 Chuang, S.C. II-1210, II-1238
 Chun, Kilsoo II-453
 Chun, Kwang-Ho I-1075
 Chun, Myung-Geun I-1028, II-364, II-608, IV-860
 Chung, Jin Wook III-649
 Chung, Jonglyul III-945
 Chung, Yongwha III-374, III-1049
 Chung, Yuk Ying I-1193, I-1226
 Chyr, Wen-Li I-359, II-343
 Ciesielski, Vic III-540
 Cisternino, Virginia I-134
 Clark, James II-8
 Cochrane, Sean D. IV-221
 Combi, Carlo I-127
 Compton, Paul II-131
 Congyan, Lang II-1204
 Coppel, Ross L. IV-866
 Corallo, Angelo I-97, I-134, I-142, I-722
 Corbett, Dan II-844, II-851
 Cox, Robert J. II-116, III-974, IV-1
 Cranefield, Stephen II-701, IV-215
 Crowther, Patricia S. III-974, IV-1
 Crua, Cyril II-642
 Cuesta-Cañada, Alberto IV-654
 Cui, Binge III-1011
 Cui, Zhan I-112

 Dai, Honghua I-707, III-112, III-121
 Dalavi, A. I-1070
 Damiani, Ernesto I-112, I-119, I-1088
 Damiani, Maria Luisa IV-324
 Damle, Nikhil II-615
 Dani, Samir IV-221
 d'Anjou, Alicia I-827
 Danoy, Grégoire IV-626
 Das, Tanmoy Kanti I-1240
 Date, Masaaki IV-487
 Dawe, Gary III-1173
 Dawes, Mark I-276
 De, Supriya Kumar IV-101
 De, Xu II-1204
 de Macedo Mourelle, Luiza IV-640

 de Vel, Olivier III-395
 Debenham, John I-751, III-23
 Dehouze, Stéphane II-858
 Del Santo, Marinho Jr. II-716
 Demiray, H. Engin II-378
 Deng, Da II-1
 Deshmukh, Amol I-1291, IV-164
 Deshpande, Pooja II-615
 Dharmendra, Sharma IV-35
 Dieng-Kuntz, Rose III-1180
 Ding, Yulin II-1000
 Do, T. Tung II-814
 Do, Tien Dung IV-94
 Doğru Bolat, Emine II-100, II-600
 Dong, Yi-sheng II-957
 Dorle, S. IV-164
 Doyle, Julie IV-329
 Drablos, Finn III-763
 D'Souza, Clare IV-752
 Du, Jiang II-1145
 Dubey, Sushant I-1070
 Duro, Richard J. I-840, I-847
 Durrant-Whyte, Hugh IV-587
 Duru, Nevcihan I-398, II-386

 Eberhard, Andrew II-622
 Ebrahimpour, Reza III-225
 Echizen, Isao IV-300
 Echizen-ya, Hiroshi II-1347
 Edman, Anneli II-403
 Ehteram, Saeed Reza III-225
 El-keib, Abdurrahim III-1129
 Elia, Gianluca I-142, I-722
 Encheva, Sylvia III-749
 Endo, Mamoru III-1274
 Enteshari, Reza II-1090
 Eom, Jae-Hong II-936
 Erkan, Kadir II-100
 Ertunç, H. Metin II-600
 Esugasini, S. II-123
 Evangelou, Christina E. I-938
 Ewart, Brian IV-813

 Falkowski, Bernd-Jürgen III-1143
 Fan, Jiang I-1153
 Fan, Lin II-964
 Fang, Wen-Hsien I-582
 Far, Behrouz Homayoun III-8
 Faron-Zucker, Catherine III-1180
 Faulkner, Stéphane II-814, II-858

- Feng, Bo III-128
 Feng, Honghai IV-89
 Feng, Jun III-677
 Feng, Xiaoyun II-587
 Feng, Yi II-943
 Ferrer, Edgar I-700
 Finnie, Gavin I-972, I-979
 Flores, M. Julia II-1338
 Fong, Alvis C.M. IV-94
 Fox, Geoffrey III-170
 Friedland, Gerald I-744
 Fu, Hsin-Chia II-1210, II-1238
 Fu, Ping IV-875
 Fuchino, Tetsuo I-162, I-198
 Fuentes, Olac II-179
 Fugazza, Cristiano I-119
 Fujii, Kunikazu I-425
 Fujii, Masahiro III-1310
 Fujii, Ryousuke II-1099
 Fujii, Satoru I-412
 Fujii, Yasuhiro IV-300
 Fujinami, Tsutomu IV-451
 Fujita, Norihiro II-1152
 Fujita, Yoshikatsu IV-758
 Fujitani, Chie I-813
 Fuketa, Masao IV-606, IV-612, IV-619
 Fukuda, Akira I-431
 Fukuhara, Tomohiro III-855
 Fukui, Ken-ichi IV-745
 Fukui, Kotaro III-908
 Fukui, Shinji I-813
 Fukumi, Minoru I-611, I-643, I-657, I-1255, I-1261, I-1268, II-258
 Fukunaga, Shigeru IV-487
 Fukuoka, Hisao I-412
 Fukuoka, Kenta I-787
 Fullam, Karen K. II-831
 Funatsu, Kimito I-169
 Furumura, Takashi I-438, I-1051
 Fuwa, Yasushi III-1296
 Gaber, Mohamed Medhat II-922
 Gámez, José A. II-1338
 Gao, Shang III-834
 García, Rafael II-658
 Garrido, Leonardo IV-654
 Gay, Robert I-664
 Ge, Yali II-950
 Geng, Yuliang II-1197
 George, Mark II-701
 Gerasimov, Vadim IV-170, IV-595
 Ghada, Elmarhomy IV-606, IV-619
 Ghédira, Khaled IV-647
 Ghezala, Henda Ben III-37
 Ghose, Supratip III-841
 Gledec, Gordan II-894
 Go, Hyoun-Joo II-364
 Gohshi, Seiichi II-1099
 Gomez, Juan Carlos II-179
 Gómez-Martín, Marco Antonio II-55
 Gómez-Martín, Pedro Pablo II-55
 Gondal, Iqbal IV-866
 Gonzalez, Efrén I-297
 González-Calero, Pedro A. II-55
 Goto, Masato III-1274
 Goto, Yuichi II-739
 Goy, Anna II-901
 Graña, Manuel I-827, I-833
 Grech, Alicia I-76
 Green, David IV-866
 Grisogono, Anne-Marie IV-573
 Grzech, Adam II-514
 Guo, Wei IV-806
 Guo, Ying III-554
 Guo, Yunbiao III-1093
 Guoshun, Chen III-581
 Gupta, Gaurav IV-595
 Guzman, G. III-248, IV-374
 Göl, Özdemir I-987
 Götze, Jürgen I-1219
 Ha, Byung-Hyun III-735
 Habib, Moussa II-548
 Håkansson, Anne II-393
 Hakozaki, Ryota I-932
 Hall, Richard I-276
 Hamaguchi, Takashi I-155, I-198
 Hammami, Moez IV-647
 Han, David C. II-831
 Han, Deok-Soo II-1317
 Han, Hee-Seop II-651
 Han, Sang-Jun I-737
 Han, Sun-Gwan II-651
 Han, Young-Shin II-1062
 Han, Youngshin II-1312, II-1325
 Han, Zhen III-488, III-1005, IV-257
 Hanafusa, Hiro IV-612
 Hang, Hsueh-Ming IV-889
 Hang, Xiaoshu III-121
 Hanzawa, Kazutoshi IV-799

- Hara, Akira I-925, I-932, III-1218, III-1246
 Hara, Fumio IV-480
 Harada, Kazunari III-1260
 Harada, Kouji II-65
 Harding, Jenny A. IV-221
 Hasegawa, Hiroyuki IV-668
 Hasegawa, Kenji III-1310
 Hashimoto, Yoshihiro I-155
 Hatanaka, Toshiharu I-635
 Hatayama, Koji IV-480
 Hawryszkiewycz, Igor III-834
 Hayashi, Naohiro III-1288
 Hayashi, Yusuke III-1317
 He, Hongxing III-1225
 Heo, Joon II-470, III-62
 Hida, Kazuo I-431
 Hidrobo, Francisco I-191
 Hilding, Fredrik G. IV-903
 Hirano, Hideyasu II-1291
 Hirasawa, Kotaro I-1
 Hirata, Yoshihiko I-1051
 Hirose, Kota IV-108
 Ho, Anthony T.S. IV-263
 Ho, Cheng-Seen III-997
 Honda, Masaaki III-908
 Hong, Chang-ho III-635
 Hong, Chao-Fu I-526, I-533
 Hong, Choong Seon II-470, III-303
 Hong, Chuleui II-483
 Hong, Jungman I-1004
 Hong, Sung-Hoon I-1297
 Hong, Tzung-Pei III-1352, IV-403
 Honghai, Feng III-575, III-581
 Hori, Satoshi IV-108, IV-136, IV-143
 Horie, Kenichi I-1174
 Horng, Shi-Jinn III-1352
 Horovitz, Osnat II-922
 Hoschke, Nigel IV-170
 Hoshino, Junichi III-875
 Hosokawa, Taisuke IV-682
 Hosono, Sachiyō III-1303
 Hossain, M. Julius IV-359
 Hotman, Elina I-184
 Hou, Ya-Rong III-476
 Houari, Nora III-8
 Howard, Catherine III-46
 Howlett, Bob R.J. II-642, IV-74
 Howlett, Robert III-1173
 Howson, Peter A. IV-74
 Hsiao, Chin-Tsai II-628
 Hsieh, C.L. II-1238
 Hsieh, Ching-Tang I-1205
 Hsieh, Min-Yen I-1205
 Hsieh, Wen-Shyong III-463
 Hsu, Chao-Chi II-1258
 Hsu, Chao-Hsing I-561, I-568
 Hsu, Mu-Hsiu II-1258
 Hsu, Nai-Wen I-1186
 Hsu, Po-Wei II-1159
 Hu, Jinglu I-1
 Hu, Lan III-1093
 Hu, Meng I-155
 Huang, Cheng-Ming III-1352
 Huang, Chien-Hua II-1183
 Huang, H.C. II-1238
 Huang, Hsiang-Cheh III-411
 Huang, Hung-Hsuan III-848
 Huang, Jiwu I-1233, II-587, II-1108
 Huang, Kuang-Chih III-411
 Huang, San-Yuan III-1366
 Huang, T.Y. II-1238
 Huang, Tony C.K. IV-396
 Huang, Xu I-233, IV-22, IV-29
 Huang, Yu-Hsiu III-411
 Huang, Yu-Hua I-34
 Hui, Siu Cheung IV-94
 Hung, Chen-Hui IV-235
 Hung, Yung-Yao IV-382
 Hur, Wonchang III-735
 Hutzler, Guillaume IV-633
 Hwang, Byung-Yeon I-967
 Hwang, Gwo-Haur III-1324
 Hwang, Gwo-Jen III-1324, IV-396
 Hwang, Hyun-Suk II-908, II-993
 Hwang, Il-Sun III-649
 Hwang, Sun-Myung II-1331
 Hwang, Tae-Jin III-449
 Ichalkarane, Nikhil II-821, II-825, II-838
 Ichikawa, Sumiaki IV-480
 Ichikawa, Teruhisa I-412
 Ichimura, Takumi I-880, I-893, I-925, I-932,
 III-1218, III-1246, III-1253, III-1260
 Jeong, Tony W.H. Ao I-671
 Iida, Yukiyasu II-161
 Ikeda, Mitsuru III-1317
 Ikeda, Toshihiro I-932
 Ikeo, Shunsuke III-908
 Ilhan, Sevinc II-386
 Indulska, Jadwiga III-827

- Inoue, Yoshio I-1051
 Inuzuka, Nobuhiro I-787
 Iribe, Yurie III-1274
 Isa, Nor Ashidi Mat II-123, II-138
 Ishida, Yoshiteru II-72, II-79, II-86
 Ishii, Naohiro I-775, I-801, I-808, I-820
 Ishikawa, Hiroshi I-379
 Iskandar, Johan II-108
 Isokawa, Teijiro I-1248
 Isomichi, Yoshinori I-925, III-1218
 Itami, Makoto III-1310
 Ito, Hiroshi II-1099
 Ito, Shin-ichi I-657
 Itoh, Hidenori IV-738
 Itoh, Kohji III-1310
 Itoh, Toshiaki I-155
 Itoh, Yoshihiko IV-738
 Iwabuchi, Shigaku IV-430
 Iwahori, Yuji I-781, I-813
 Iwata, Kazunori I-820
 Iwata, Susumu IV-738
- Jain, Lakhmi C. II-844, II-851, II-1115
 Jang, Heyonho I-255
 Jang, Kyung-Soo II-446
 Jang, Min-Soo III-219
 Jantz, Kristian I-744
 Jarke, Matthias IV-228
 Jarvis, Bevan II-844, II-851
 Jeng, Rong III-1338
 Jennings, Andrew IV-581
 Jentzsch, Ric II-782
 Jeon, Hong-Tae II-291
 Jeon, In Ja II-270, II-308, II-319
 Jeon, Jae Wook I-1014
 Jeong, Gu-Min III-670
 Jeong, Hong I-996
 Jeong, Hyuncheol III-728
 Jeong, Seungdo III-240, III-694, III-704, III-945
 Jevtic, Dragan III-16
 Jewell, Michael O. III-642, IV-150
 Jia, Limin I-707
 Jiang, Jixiang III-199
 Jiang, Yiwei II-1217, III-388
 Jiao, Yuhua III-1072
 Jin, Hoon III-275
 Jin, Huidong III-1225
 Jin, Hyojeong I-332
 Jin, Longfei I-325
- Jo, Geun-Sik III-841
 Jo, Yung I-887, II-31
 Jones, T.J. IV-496
 Ju, Hak Soo II-453
 Juang, Yau-Tarng I-596
 Jun, Byong-Hee II-608
 Jun, Chi-Hun III-449
 Jun, Woochun II-688
 Junbo, Gao I-1153
 Jung, Jae-yoon III-602
 Jung, Jason J. III-841
 Jung, Jinpyoung I-41
 Jung, Jo Nam II-460, III-662
 Jung, Joonhong I-1104
 Jureta, Ivan II-814
 Jurić, Damir II-894
 Juszczyszyn, Krzysztof II-514
- Kabir, Ehsanollah III-225
 Kacalak, Wojciech III-930
 Kadbe, Kishor II-615
 Kamel, Mohamed III-1168
 Kanda, Taki III-1115
 Kaneko, Nozomu I-911
 Kang, Chul-Gyu I-472
 Kang, Dazhou I-953, III-199, IV-896
 Kang, Heau Jo I-498, II-560, II-567, III-339
 Kang, In Koo III-1108
 Kang, Jang Mook II-460
 Kang, Seungpil III-95
 Kang, Suk-Ho III-602, III-735
 Kang, Sukhoon III-310
 Kang, YunHee I-56
 Kaplan, Simon M. III-820
 Karacapilidis, Nikos I-938
 Karsak, E. Ertugrul II-635
 Kashihara, Akihiro III-1281
 Kashiji, Shinkaku IV-612
 Katarzyniak, Radosław Piotr II-500, II-514
 Katayama, Kaoru I-379
 Kato, Naotaka IV-444
 Kato, Shohei IV-738
 Kawaguchi, Eiji IV-289
 Kawaguchi, Masashi I-801
 Kawano, Koji I-155
 Kawano, Masahiro III-1122
 Kawaoka, Tsukasa III-742, IV-709
 Kawasaki, Takashi IV-799
 Kawasaki, Zen-ichiro I-801
 Kawaura, Takayuki III-1122

- Kayano, Akifumi I-1044
Kazama, Kazuhiro IV-723
Kazienko, Przemyslaw II-507
Kelman, Chris III-1225
Kemp, Elizabeth I-339
Keogh, Eamonn II-16
Keskar, Avinash G. II-615, IV-164
Kessoku, Masayuki IV-765
Khan, Ameer I-1064
Khera, Akashdeep I-1291
Khosla, Rajiv I-1268, II-243, IV-752
Kiewra, Maciej II-520
Kim, Chang-Soo II-908, II-993
Kim, Cheol Young III-735
Kim, Dae-Jin IV-542
Kim, Dae Sun III-303
Kim, Dae Youb II-453
Kim, Dong Hwa II-222, IV-848, IV-854, IV-860
Kim, Dong-Won II-207, IV-549, IV-566
Kim, Eun Ju IV-179
Kim, Haeng-Kon I-1131, II-1305, II-1317
Kim, Hak Joon I-1036
Kim, Hak-Man I-479, II-464
Kim, Hak Soo III-922
Kim, Hang-Rae I-492
Kim, Hojung I-255
Kim, Hoontae III-602
Kim, Hyeoncheol I-372, III-785
Kim, Hyoung Joong I-1240
Kim, Hyun-Chul III-74
Kim, Hyun Deok I-1021
Kim, Hyun-Dong II-284
Kim, Hyung Jin III-69
Kim, Hyunsoo III-87
Kim, Il-sook IV-559
Kim, In-Cheol III-255, III-275
Kim, In Ho III-628
Kim, Jae-Woo I-445
Kim, Jae-Young I-472
Kim, Jang-Sub II-446, II-490
Kim, Jeonghyun III-95
Kim, Jeong-Sik III-233
Kim, Ji-Hong III-735
Kim, JiWoong I-498
Kim, Jin-Geol III-981
Kim, Jong-Soo II-251
Kim, Jong Tae I-1014, I-1111
Kim, Jong-Woo II-908
Kim, Ju-Yeon II-908
Kim, Junghee II-1312
Kim, Jungkee III-170
Kim, Kichul III-374
Kim, Kyung-Joong III-777
Kim, Min III-374
Kim, Minhyung III-621
Kim, Minkoo III-177
Kim, Min Kyung III-792
Kim, Minsoo II-1050
Kim, Myoung-Hee III-233, III-1210
Kim, Myoung-Jun I-1075
Kim, Myung Won IV-179
Kim, Nam Chul II-145
Kim, Richard M. III-820
Kim, Sang II-31
Kim, Sang-Hoon III-213
Kim, Sang Hyun II-145
Kim, Sang-Jun III-219
Kim, Sangkyun III-609, III-616, III-621
Kim, Sang Tae I-1021
Kim, Sang-Wook III-684
Kim, Seong-Joo II-251, II-291
Kim, Seong W. III-87
Kim, Soon-Ja III-317
Kim, Sung-Hyun II-251
Kim, Sung-il I-62
Kim, Tae-Eun III-213
Kim, Tae Joong III-628
Kim, Tae Seon II-284
Kim, Tai-hoon I-1125, II-1069
Kim, Wonil III-177
Kim, Woong-Sik IV-410
Kim, Yong I-996
Kim, Yong-Guk III-206, III-219, III-233
Kim, Yong-Min II-251
Kim, Yong Se III-922
Kim, Yong Soo IV-542
Kim, YongWon III-721
Kim, Yoon-Ho I-492, II-560, II-567
Kim, Young-Joong IV-518, IV-525
Kim, Youngsup II-1056
Kimura, Masahiro IV-723, IV-745
Kingham, Mark II-775
Kirley, Michael III-959
Kitajima, Teiji I-155
Kitakoshi, Daisuke IV-730
Kitazawa, Kenichi I-438, I-1051
Klein, Gilbert IV-910
Knipping, Lars I-744, III-588
Ko, Il Seok II-1029

- Ko, Li-Wei I-866
 Ko, Yun-Ho I-1297, II-371
 Kogure, Kiyoishi I-1167
 Kohritani, Motoki II-1291
 Kojima, Masanori I-438
 Kojiri, Tomoko II-665, II-673, III-1303
 Kolaczek, Grzegorz II-514
 Kolp, Manuel II-814
 Komatsu, Takanori III-868
 Komedani, Akira II-665
 Kong, Adams III-1168
 Kong, Jung-Shik III-981
 Konishi, Osamu III-513
 Koo, Jahwan I-618, III-54
 Koo, Young Hyun III-157
 Koprinska, Irena II-8
 Koshiba, Hitoshi IV-444
 Koyama, Yukie I-794
 Krishna, K. Sai IV-101
 Krishna, P. Radha IV-101
 Krishnamurthy, E.V. III-505
 Krishnaswamy, Shonali II-922
 Król, Dariusz II-527, III-1373
 Kshetrapalapuram, Kalyanaraman Kaesava III-959
 Kubota, Hidekazu III-296, III-861
 Kubota, Naoyuki I-650
 Kubota, Yoshiki I-1261
 Kudo, Mineichi IV-668, IV-682, IV-689, IV-696, IV-703
 Kudo, Yasuo IV-675
 Kumamoto, Tadahiko I-901
 Kunieda, Yosihiko I-801
 Kunifugi, Susumu I-418, IV-444
 Kunigami, Masaaki IV-772
 Kunimune, Hisayoshi III-1296
 Kunstic, Marijan III-16
 Kuo, Bor-Chen I-69, I-866, I-873
 Kuo, Huang-Cheng II-979
 Kuo, Juin-Lin III-1366
 Kuo, Kun-Huang I-561
 Kuo, Tien-Ying III-418
 Kurosawa, Yoshiaki I-880, III-1246
 Kusek, Mario I-240
 Kushiro, Noriyuki I-518
 Kusiak, Andrew III-953
 Kusunoki, Kazuhiro I-431
 Kuwahara, Noriaki I-1167
 Kwak, Eun-Young I-372
 Kwak, JaeMin I-1094
 Kwak, Keun-Chang II-364
 Kwon, Jungji III-1129
 Kwon, Mann-Jun II-364
 Kwon, Young-hee IV-559
 Lægreid, Astrid III-1195
 Lai, Chris II-243
 Lai, Hsin-Hsi IV-235
 Lai, Jun II-887
 Lai, P.S. II-1238
 Lam, Ho-Wang III-1168
 Lam, Ka-man II-986
 Lam, Toby H.W. I-671
 Lambadaris, Ioannis II-1090
 Lang, Congyan II-1217, III-388
 Lau, Yee W. IV-15
 Le, Kim II-789
 Le, Thinh M. III-425, III-433
 Leary, Richard IV-813, IV-823
 Lee, Alex C.M. I-671
 Lee, Chilgee II-1312, II-1325
 Lee, Chil Woo I-1139
 Lee, Chun su II-460
 Lee, Dae-Jong IV-860
 Lee, Dae-Wook III-163
 Lee, Deok-Gyu I-1146
 Lee, Dong Chun III-74, III-101
 Lee, Dong Hoon II-453
 Lee, Dong-Young II-1036, II-1050
 Lee, Dongwoo I-1081, III-721
 Lee, Geuk II-1029, II-1056
 Lee, Hae-Yeoun III-1108, IV-309
 Lee, Hanho I-176, II-319
 Lee, Heung-Kyu III-1108, IV-309
 Lee, Hong Joo III-609, III-616
 Lee, Hsuan-Shih I-359, I-365, II-343
 Lee, Huey-Ming II-1245, II-1252, II-1258, II-1265
 Lee, Hyung-Woo I-504, I-1118, III-325
 Lee, Ickjai IV-42, IV-336
 Lee, Jae-Min I-967
 Lee, Jee Hyung I-1014
 Lee, Jee-Hyong I-1028
 Lee, Jeong-Eom III-219
 Lee, Jia Hong II-554
 Lee, Jin IV-532
 Lee, June Hyung IV-359
 Lee, Jungsuk II-1050
 Lee, Junseok IV-309
 Lee, Kang-Soo I-41, I-48

- Lee, Keon Myung I-1014, I-1028, I-1036
 Lee, Keonsoo III-177
 Lee, Kye-san I-485
 Lee, Kyong-Ha III-163
 Lee, Kyu-Chul III-163
 Lee, Kyunghee IV-532
 Lee, Mal-Rey III-213
 Lee, Ming-Chang IV-389
 Lee, Raymond S.T. I-671, I-678, I-693
 Lee, Sang Ho III-792
 Lee, Sanghoon III-922, III-945
 Lee, Sang Hun I-48
 Lee, Sang-Jin I-1146
 Lee, Sang-Jo I-304
 Lee, Sangsik III-1129
 Lee, Sang Wan IV-542
 Lee, Sang Won III-628
 Lee, Seok-Joo III-219
 Lee, Seong Hoon I-90, I-1081, III-721
 Lee, Seongssoo II-681, III-449
 Lee, Seung Wook I-1014, I-1111
 Lee, Seung-youn I-1125, II-1069
 Lee, Shaun H. II-642
 Lee, Si-Woong I-1297
 Lee, Soobeom III-69, III-81, III-87
 Lee, Sooil III-81
 Lee, Soon-Mi II-1062
 Lee, Su-Won I-459
 Lee, Suh-Yin III-359
 Lee, Suk-Ho III-163
 Lee, Sukhan I-1014
 Lee, Tong-Yee III-456, III-469
 Lee, Tsair-Fwu III-366
 Lee, Wankwon I-1081
 Lee, Wookey I-1004, III-735
 Lee, YangSun II-567
 Lee, Yang Weon III-339
 Lee, Yongjin IV-532
 Lee, Youngseok III-713
 Lee, Young Whan II-1022
 Leem, Choon Seong III-609, III-616
 Leida, Marcello I-112
 Lenar, Mateusz II-534
 Leung, Ho-fung II-986
 Levachkine, Serguei I-297, III-248, IV-374
 Li, Changde II-236
 Li, Dongtao I-664
 Li, Jiuyong III-1225
 Li, Li III-1
 Li, Qiong III-1072, III-1079
 Li, Wei-Soul III-463
 Li, Wenyuan II-964
 Li, Yanhui I-953, III-199, IV-896
 Li, Yue-Nan II-580, III-405
 Li, Zengzhi II-964
 Li, Zhi II-357
 Li, Zhigang III-488
 Liao, Bin-Yih II-593
 Liao, Hong-Yuan Mark I-582, III-359, III-381
 Liao, In-Kai III-997
 Liao, Lingrui I-353
 Liao, Mingyi IV-89
 Liao, Ping-Sung II-593
 Liao, Shih-Feng II-1245
 Liao, Hung-Shiuan III-346
 Ligon, G.L. IV-35
 Lim, Heui Seok I-84, I-90
 Lim, Jong-tae III-635
 Lim, Jongin II-453
 Lim, Myo-Taeg IV-518, IV-525
 Lim, Seungkil I-1004
 Lim, Soo-Yeon I-304
 Lim, Sung-Hun I-459
 Lin, Chia-Wen III-381
 Lin, Chih-Yang III-1058
 Lin, Ching-Teng I-866
 Lin, Daimao III-1093
 Lin, Daw-Tung III-1366
 Lin, En-Chung III-1366
 Lin, Heshui II-972
 Lin, Jiann-Horng IV-403
 Lin, Mu-Hua I-526
 Lin, Qing-Fung III-1331
 Lin, Wen-Yang III-1338
 Lin, Yang-Cheng IV-235
 Lin, Zhangang IV-81
 Lin, Zuoquan IV-81
 Lindemann, Udo III-1359
 Liu, Daxin III-1011
 Liu, Hongmei II-1108
 Liu, James N.K. I-686, III-112, III-121, III-128, III-149
 Liu, Jiqiang III-488, III-1005
 Liu, Ju II-1231
 Liu, Lei I-325
 Liu, Wang IV-881
 Liu, Xin III-1005, IV-257
 Liu, Xue-jun II-957
 Liu, Yan II-186

- Liu, Yijun IV-437
 Liu, Yongguo II-186
 Liu, Zheng II-1175
 Liwicki, Marcus III-588
 Lokuge, Prasanna II-806
 López-Peña, Fernando I-840, I-847
 Lorenz, Bernhard IV-352
 Lorenzo, Gianluca I-722
 Lovrek, Ignac I-240
 Lower, Michał III-1373
 Lu, Hongen II-694, II-915
 Lu, Jianjiang I-953, III-199, IV-896
 Lu, Jie I-261
 Lu, Tzu-Chuen II-1224, IV-249
 Lu, Wen III-554
 Lu, Y.L. II-1238
 Lu, Zhe-Ming II-573, II-580, III-405, III-497
 Lundström, Jenny Eriksson IV-242
 Luo, Jun IV-509
 Luo, Weidong III-149
 Luo, Yingwei IV-806
 Lynch, Daniel IV-329
 Ma, Wanli I-205, I-226
 Macfadyen, Alyx I-283
 Mackin, Kenneth J. III-520, III-526, IV-602
 Macreadie, Ian IV-573
 Madoc, A.C. I-233, IV-22
 Magnani, Lorenzo I-547
 Magro, Diego II-901
 Mahalik, N.P. II-200
 Mahendra rajah, Piraveenan II-796
 Mahmoud, Rokaya IV-612
 Main, Julie I-76
 Maitra, Subhamoy I-1240
 Majewski, Maciej III-930
 Majumdar, Anirban III-1065
 Mak, Raymond Y.W. I-678
 Makino, Kyoko III-1039
 Maldonado, Orlando I-827
 Mao, Ching-Hao II-1265
 Mao, Yuxin II-866, II-873
 Marco, Danila I-97
 Mário, Maurício C. II-716
 Marion, Kaye E. I-1064
 Marom, Yuval III-890
 Marrara, Stefania I-1088
 Mashor, Mohd Yusoff II-123
 Mathews, George IV-587
 Matijašević, Maja II-894, III-655
 Matsuda, Noriyuki IV-136, IV-143
 Matsuda, Yoshitatsu II-1015
 Matsui, Nobuyuki I-1248
 Matsumoto, Tsutomu III-1039
 Matsumura, Yuji I-611
 Matsunaga, Kumiko IV-830
 Matsushita, Mitsunori I-540
 Matsuura, Takenobu IV-272
 Matsuyama, Hisayoshi I-149
 Matsuyama, Shinako IV-772
 Matsuyama, Takashi IV-129
 Matta, Nada I-960
 Maurer, Maik III-1359
 Mayiwar, Narin II-410
 McAullay, Damien III-1225
 Mei, Zhonghui III-483
 Mejía-Lavalle, Manuel IV-57
 Men, H. III-425
 Meng, Shengwei IV-875
 Mera, Kazuya I-893
 Metais, Elisabeth IV-417
 Mi, Lina II-263
 Miao, Chunyan I-664
 Miao, Yuan I-664
 Miatidis, Michalis IV-228
 Middleton, Lee III-642, IV-150
 Mihara, Eisuke III-1310
 Min, Hyeun-Jeong II-214
 Min, Seung-Hyun I-1075
 Min, Zhang I-1153
 Mineno, Hiroshi I-431, I-1051
 Misue, Kazuo IV-423, IV-430
 Mitrovic, Antonija IV-458, IV-465
 Mitsukura, Yasue I-643, I-657, I-1261, I-1268, II-258
 Miura, Hirokazu IV-136, IV-143
 Miura, Motoki I-418
 Miyachi, Taizo IV-661
 Miyadera, Youzou III-1288
 Miyajima, Hiromi III-547
 Miyauchi, Naoto I-431
 Miyoshi, Tsutomu III-569
 Mizuno, Tadanori I-412, I-431, I-438, I-1051
 Mizutani, Miho I-431
 Mochizuki, Tsubasa I-820
 Modegi, Toshio II-1122
 Mogami, Yoshio I-624
 Mohammadian, Masoud II-775, II-782
 Momouchi, Yoshio II-1347
 Monroy, J. I-840

- Montero, Calkin A.S. I-554, I-918
 Moon, Daesung III-1049
 Moon, Kiyoung III-1049, IV-532
 Moon, Seungbin II-31
 Moon, Sung-Ryong IV-195
 Moreno, Marco I-297, III-248
 Moreno, Miguel IV-374
 Morghade, Jayant I-1291
 Mori, Toshikatsu II-79
 Morihiro, Koichiro I-1248
 Morikawa, Koji III-868
 Morita, Kazuhiro IV-606, IV-612, IV-619
 Mousalli, Gloria I-191
 Mouza, Mrinal I-1070
 Mukai, Naoto I-768, III-677
 Munemori, Jun I-425, I-1044, I-1057
 Murai, Tetsuya IV-675
 Murase, Ichiro III-1039
 Murase, Yosuke II-673
 Murayama, Toshihiro III-855
 Murthy, V. Kris I-212, III-505, III-799
- Na, Ho-Jun II-993
 Na, Seungwon III-670
 Na, Yun Ji II-1029
 Nagao, Kagenori II-1076
 Nagao, Taketsugu I-1268
 Nakache, Didier IV-417
 Nakagawa, Hiroshi III-1039
 Nakamatsu, Kazumi II-708, II-724
 Nakamura, Atsuyoshi IV-668
 Nakamura, Haruyuki II-1099
 Nakamura, Mari IV-472
 Nakamura, Mitsuhiro III-898
 Nakamura, Shoichi III-1288
 Nakamura, Yatsuka III-1296
 Nakano, Kenji IV-779
 Nakano, Ryohei IV-716, IV-730
 Nakano, Tomofumi I-787, I-794
 Nakano, Yukiko I. III-289, III-848
 Nakashima, Takuo I-575
 Nakasumi, Mitsuaki IV-503
 Nam, Ha-eun III-635
 Nam, Mi Young II-270, II-298, II-308,
 II-327, III-662, IV-186
 Nandedkar, A.V. III-1160
 Nanduri, D.T. III-540
 Naoe, Yukihisa I-438, I-1051
 Nara, Shinsuke II-739
 Nara, Yumiko IV-839
- Navetty, Oswaldo Castillo I-960
 Naya, Futoshi I-1167
 Nedjah, Nadia IV-640
 Newth, David III-806
 Ng, Wing W.Y. III-141
 Ngah, Umi Kalthum II-138
 Nguyen, Ngoc Thanh II-514, II-520
 Nguyen, Phu-Nhan I-730
 Nguyen, Tien Dung II-145
 Ni, Jiangqun I-1233
 Nie, J.B. II-1238
 Niimi, Ayahiko III-513
 Niimura, Masaaki III-1296
 Nishida, Toyoaki III-289, III-296, III-848,
 III-855, III-861
 Nishikawa, Kazufumi III-908
 Nishimura, Haruhiko I-1248
 Nishimura, Ryouichi II-1083, II-1152
 Niu, Ben III-107
 Niu, Xiamu II-1129, III-1072, III-1079,
 III-1093
 Nixon, Mark S. III-642, IV-150
 Noji, Hitomi III-513
 Nomura, Satoshi III-861
 Nomura, Toshinori I-8
 Nordgård, Torbjørn III-1187
 Nowak, Ziemowit III-261
 Nowell, Terry III-1173
 Numao, Masayuki IV-745
 Nunohiro, Eiji III-520, IV-602
- O'shima, Eiji I-149
 Oatley, Giles IV-813, IV-823
 Oestreicher, Lars II-422
 Ogasawara, Mitsuhiro II-161
 Ogasawara, Yoshiyasu III-289
 Ogawa, Takahiro I-657
 Ogi, Hiroaki I-820
 Oh, Chang-Heon I-472
 Oh, Hae-Seok III-74
 Oh, Jae Yong I-1139
 Oh, Je Yeon III-602
 Oh, Sei-Chang III-69
 Ohsawa, Yukio I-511, I-518, I-554, I-1174
 Ohshiro, Masanori III-520, IV-602
 Ohta, Manabu I-379
 Okamoto, Kazunori III-848
 Okamoto, Masashi III-289, III-848
 Okamoto, Takeshi II-93
 Oliboni, Barbara I-127

- Ollington, Robert III-562
 Omi, Takashi II-739
 Ong, Kok-Leong II-929
 Onisawa, Takehisa I-911
 Oono, Masaki IV-619
 Ortega, Neli R.S. II-716
 Ota, Koichi III-1281
 Ota, Satomi I-657
 Othman, Nor Hayati II-123
 Otoom, Ahmed Fawzi I-1193
 Ourselin, Sébastien IV-595
 Ouzecki, Denis III-16
 Ozaki, Masahiro I-775, I-781
 Ozaki, Norio III-1253
 Ozaku, Hiromi Itoh I-1167
- Padgham, Lin III-282
 Padole, D. IV-164
 Pai, Yu-Ting I-1219
 Palm, Torsten II-416
 Pan, Feng III-425, III-433
 Pan, Jeng-Shyang II-593, II-1076, II-1115, II-1168, III-353, III-411, III-497, IV-317
 Pan, Sungbum III-374, III-1049, IV-532
 Pao, H.T. II-1238
 Park, Choung-Hwan III-62
 Park, Gwi-Tae I-445, I-452, I-861, II-207, III-219, IV-115, IV-549, IV-566
 Park, Hea-Sook II-1062
 Park, Heung-Soo I-1146
 Park, Hyun Seok III-792
 Park, Jang-Hwan II-608, IV-860
 Park, Jang-Hyun II-207, IV-549
 Park, Jeong-II III-684
 Park, Jin Ill II-222
 Park, Jisun II-831
 Park, Jong-heung IV-559
 Park, Jong-Hyuk I-1146
 Park, Kiheon I-1104
 Park, Kyeongmo II-483
 Park, Moon-sung IV-559
 Park, Neungssoo III-374
 Park, Sang Soon II-477
 Park, Seong-Bae I-304
 Park, Young I-492
 Park, Young-Whan II-1062
 Peng, Wen-Hsiao IV-889
 Perozo, Niraska I-700
 Petrovsky, Nikolai II-116
 Pham, Binh II-1145, III-395
- Pham, Cong-Kha I-1199
 Phu, Mieng Quoc I-589
 Phung, Toan III-282
 Pieczynska-Kuchtiak, Agnieszka II-514
 Ping, Li III-575
 Pongpinigpinyo, Sunee I-1275
 Posada, Jorge III-184
 Postalçioğlu, Seda II-100
 Poulton, Geoff III-554
 Pradhan, Sujan II-694
 Price, Don II-796, IV-170
 Prokopenko, Mikhail II-796, IV-170, IV-573, IV-587
 Prügel-Bennett, Adam III-642
 Puerari, Ivano II-179
 Puhan, Niladri B. IV-263
 Purvis, Martin II-701, IV-208, IV-215
 Purvis, Maryam II-701, IV-208, IV-215
- Qian, Jiang-bo II-957
 Qiao, Yu-Long III-353
 Qiu, Bin II-336, IV-157
 Quintero, Rolando I-297, III-248, IV-374
- Rahayu, Wenny IV-366
 Rajab, Lama II-548
 Rajasekaran, Sanguthevar IV-509
 Ramljak, Darije III-655
 Ranang, Martin Thorsen III-1187, III-1195
 Rao, Zhiming I-311
 Ratanamahatana, Chotirat Ann II-16
 Ray, Tapabrata IV-49
 Raza, Mansoor IV-866
 Reale, Salvatore I-119, I-1088
 Reidsema, C. IV-496
 Ren, Yu III-121
 Resta, Marina I-21
 Reusch, Bernd III-1151
 Rhee, Daewoong II-31
 Rhee, Phill Kyu II-270, II-298, II-308, II-319, II-327, III-662, IV-186
 Rhee, Seon-Min III-1210
 Ribarić, Slobodan II-430
 Ridgewell, Alexander IV-29
 Rifaih, Rami III-191
 Rivas, Franklin I-191
 Rivepiboon, Wanchai I-1275
 Robinson, Ricky III-827
 Rocacher, Daniel I-104
 Rodríguez, Guillermo IV-57

- Rodríguez, Santiago II-658
 Rojas, Raúl I-744
 Rossato, Rosalba I-127
 Ruan, Shanq-Jang I-1219
 Ruibin, Gong III-915
 Ryu, Joung Woo IV-179
 Rzepka, Rafal II-950
- Sabarudin, Shahrill II-138
 Saberi, Masoumeh D. II-8
 Saeki, Yoshihiro III-1266
 Sætre, Rune III-1195
 Sagara, Kaoru I-1167
 Saito, Kazumi IV-716, IV-723, IV-745
 Saito, Ken III-296
 Sakai, Sanshiro I-412
 Sakamoto, Junichi IV-143
 Sakamoto, Masaru I-155
 Sakamoto, Yuji I-880
 Sakuda, Haruo I-932
 Sal, D. I-833
 Sandve, Geir Kjetil III-763
 Sanin, Cesar I-946
 Sanjeevi, Sriram G. II-732
 Sarhan, Sami II-548
 Sarker, Ruhul III-813
 Sasaki, Hiroshi I-808
 Sasaki, Kiichiro III-1274
 Sato, Keiko II-258
 Sato, Shigeyuki II-72
 Sato, Shin-ya IV-723
 Sato, Shogo I-418
 Savarimuthu, Bastin Tony Roy II-701, IV-208, IV-215
 Sawada, Hideyuki III-898
 Sawamura, Hajime IV-830
 Saxena, Ashutosh IV-595
 Scott, Andrew IV-170
 Seehuus, Rolv III-770
 Sekiyama, Kosuke IV-487
 Seo, Min-Wook IV-525
 Seo, Sam-Jun II-207, IV-549
 Seoane, María II-658
 Seredyński, Franciszek IV-910
 Shadabi, Fariba II-116
 Shah, S. Akhtar Ali I-255
 Sharma, Dharmendra I-205, I-219, I-226, I-730, II-116, II-789, IV-29
 Sharma, Naveen I-219
 Sharma, Tapan II-622
- Shen, Chang-xiang III-1005, IV-257
 Shen, Jau-Ji II-1159, III-442
 Shen, Pei-Di I-359, II-343
 Shen, Y.C. II-1238
 Shen, Zhiqi I-664
 Sheng, Ke-jun IV-257
 Shidama, Yasunari III-1296
 Shieh, Chin-Shiu I-366, III-1032
 Shigei, Noritaka III-547
 Shigemi, Motoki I-925
 Shigenobu, Tomohiro I-425, I-1044, I-1057
 Shih, Arthur Chun-Chieh I-582
 Shih, Shu-Chuan I-69
 Shih, Yao-Jen II-1265
 Shiizuka, Hisao II-1272
 Shim, Boyeon II-1305
 Shim, Choon-Bo IV-343
 Shim, Il-Joo I-445, I-452, I-861, IV-115
 Shimada, Yukiyasu I-155, I-198
 Shimizu, Toru I-438, I-1051
 Shimodaira, Toshikazu IV-792
 Shin, Dong-Ryeol II-446, II-490
 Shin, Ho-Jin II-490
 Shin, Hojun II-1305
 Shin, Miyoung III-684
 Shin, Myong-Chul I-479, II-464
 Shin, Seung-Woo I-861
 Shin, Yong-Won IV-343
 Shintaku, Eiji III-908
 Shioya, Hiroyuki IV-730
 Shiu, Simon C.K. III-107, III-135
 Shizuki, Buntarou IV-430
 Shoji, Hiroko I-1181
 Shyr, Wen-Jye I-561, I-568, I-604
 Siddiqui, Tanveer J. IV-64
 Simoff, Simeon I-751, III-23
 Singh, Pramod K. II-131
 Sinkovic, Vjekoslav I-240
 Sioutis, Christos II-838
 Skabar, Andrew III-595
 Skibbe, Henrik II-573
 Skylogiannis, Thomas II-746
 Smart, Will III-988
 Smith, A. IV-496
 Smith, Andrew III-1232
 Sobecki, Janusz II-534
 Soh, Ben II-887
 Sohn, Bong Ki I-1014
 Sohn, Chang III-635
 Sohn, Hong-Gyoo III-62

- Solazzo, Gianluca I-722
 Son, Bongsoo III-69, III-87
 Son, Jin Hyun III-922
 Sonenberg, Liz III-30
 Song, Binheung II-1298
 Song, Chul Hwan III-792
 Song, Chull Hwan III-157
 Song, Hag-hyun II-560
 Song, Inseob III-728
 Song, Ki-won II-1331
 Song, Meng-yuan I-533
 Song, Youn-Suk III-937
 Sonoda, Kotaro II-1083
 Sparks, Ross III-1225
 Spranger, Stephanie IV-352
 Šprogar, Matej IV-8
 Steigedal, Tonje S. III-1195
 Sterling, Gerald IV-366
 Stork, André III-184
 Straccia, Umberto II-753
 Stranieri, Andrew I-283
 Strickler, J. Rudi IV-124
 Stumptner, Markus III-46
 Stunes, Kamilla III-1195
 Su, J.M. II-1238
 Su, Te-Jen I-604
 Su, Yi-Hui I-604
 Suárez, Sonia II-658
 Subagdja, Budhitama III-30
 Sugihara, Akihiro III-1260
 Sugimori, Hiroki II-161
 Suh, Il Hong III-922, III-937, III-945
 Suh, Nam P. I-41
 Suka, Machi III-1239, III-1246, III-1260
 Sumi, Kazuhiko IV-129
 Sumi, Yasuyuki III-296, III-861
 Sumitomo, Toru IV-619
 Sun, Jiande II-1231
 Sun, Ming-Hong III-463
 Sun, S.Y. II-1238
 Sun, Sheng-He II-580, II-1129, III-353,
 III-497, III-1072, III-1079, IV-881
 Sun, Yong I-1226
 Sun, Youxian II-193, II-350
 Sun, Yufang II-972
 Sun, Zhaohao I-972, I-979
 Sun, Zhen III-405
 Sung, Kyung-Sang III-74
 Suresh, S. I-987
 Suzuki, Katsuhiro IV-487
 Suzuki, Mitsuyoshi II-1099
 Suzuki, Yōiti II-1083, II-1152
 Szczerbicki, Edward I-946
 Szlachetko, Bogusław III-1373
 Szukalski, Szymon K. III-974
 Tabakow, Iwan II-541
 Taghian, Mehdi IV-752
 Takada, Kentaro III-908
 Takahama, Tetsuyuki I-925, I-932, III-1218
 Takahashi, Hiroshi IV-785
 Takahashi, Koichi I-781
 Takahashi, Masakazu IV-765, IV-785,
 IV-799
 Takahashi, Satoru IV-785
 Takahashi, Yusuke I-412
 Takai, Shigenori II-1099
 Takajo, Hideyuki I-1255
 Takamura, Toshihiro I-162
 Takanishi, Atsuo III-908
 Takanobu, Hideaki III-908
 Takase, Hiroki I-438, I-1051
 Takatsuka, Ryozo IV-451
 Takazawa, Jun III-875
 Takeda, Fumiaki II-263, III-1266
 Takeda, Kazuhiro I-149
 Taki, Hirokazu IV-108, IV-136, IV-143
 Taki, Kenta IV-738
 Takizawa, Osamu III-1039
 Tamura, Toshihiko I-438
 Tanahashi, Yusuke IV-716
 Tanaka, Jiro I-418, IV-423, IV-430
 Tanaka, Katsumi I-901
 Tanaka, Koichi IV-129
 Tanaka-Yamawaki, Mieko I-15
 Tang, Shiwei III-1345
 Tang, Xijin IV-437
 Tani, Yukari II-1099
 Taniguchi, Rin-ichiro III-883
 Taniguchi, Yuko I-932
 Tazaki, Eiichiro III-526
 Tengfei, Guan II-1204
 Tenmoto, Hiroshi IV-696
 Teo, Jason I-1284
 Terano, Takao IV-772, IV-779, IV-792
 Terashima-Marín, Hugo IV-654
 Tezuka, Satoru IV-300
 Thomborson, Clark III-1065
 Thommesen, Liv III-1195
 Tischer, Peter I-589

- Tiwary, Uma Shanker IV-64
 Tjondronegoro, Dian W. II-24
 Tommasi, Maurizio De I-134
 Tong, Yunhai III-1345
 Toro, Carlos III-184
 Torregiani, Massimiliano I-119, I-1088
 Torres, Miguel I-297, III-248, IV-374
 Toyama, Jun IV-703
 Tran, Dat I-226, I-730, IV-15
 Tran, Tich Phuoc I-1193
 Tran, TrungTinh III-1129
 Tsai, Chia-Yang IV-889
 Tsai, F.P. II-1238
 Tsai, Yuan-Chieh II-1265
 Tsang, Eric C.C. III-141
 Tseng, C.L. II-1238
 Tseng, Judy C.R. IV-396
 Tseng, Ming-Cheng III-1338
 Tseng, Wei-Kuo I-359
 Tseng, Wen-Chuan I-27
 Tsuchiya, Seiji III-742
 Tsuda, Kazuhiko IV-758, IV-765, IV-785
 Tsuge, Yoshifumi I-149
 Tsuichihara, Mamoru I-575
 Tumin, Sharil III-749
 Tutuncu, M. Mucteba II-378
 Tveit, Amund III-1195
 Tweedale, Jeff II-821, II-825
- Uitdenbogerd, Alexandra L. IV-201
 Ulieru, Mihaela II-154
 Unland, Rainer II-154
 Uosaki, Katsuji I-635
- Vamplew, Peter III-562
 van Schyndel, Ron G. III-1018
 Ven, Jostein III-1187
 Vicente, David I-827
 Viviani, Marco I-112
 Vizcarrondo, Juan I-700
 Volz, Richard A. I-247
- Wagner, Michael IV-15
 Walters, Simon D. II-642, IV-74
 Wang, Chuntao I-1233
 Wang, Da-Jinn II-1183, III-346
 Wang, Eric III-922
 Wang, Feng-Hsing II-1115
 Wang, Hai II-964
 Wang, Haitao II-228
- Wang, Hao-Xian II-580
 Wang, Hsi-Chun III-1086
 Wang, Leuo-hong I-533
 Wang, Libin II-186
 Wang, Meng I-686
 Wang, Peng I-953, IV-896
 Wang, Penghao I-1193, I-1226
 Wang, Peter II-796, IV-170
 Wang, Ruili I-339
 Wang, Shujing II-761
 Wang, Shuzhong II-1134, III-1025
 Wang, Song-yan II-172
 Wang, Wei-Chiang III-1086
 Wang, Wenjun IV-806
 Wang, Xiaolin IV-806
 Wang, Yong-li II-957
 Wang, YongJie II-1168
 Wang, Yu-Zheng III-1058
 Wang, Zhifang III-1072
 Wang, Zi-cai II-172
 Ward, Koren IV-903
 Wasaki, Katsumi III-1296
 Watabe, Hirokazu III-742, IV-709
 Watada, Junzo II-1283, II-1291, III-1122
 Watanabe, Chihaya II-1272
 Watanabe, Toyohide I-768, II-665, II-673, III-677, III-1303
 Watanabe, Yuji II-72
 Watson, Marcus III-1232
 Watter, Scott III-1232
 Weakliam, Joe IV-329
 Wee, Jae-Kyung III-449
 Weerasinghe, Amali IV-465
 Wells, Jason III-834
 Weng, ShaoWei II-1168, IV-317
 Wickramasinghe, Kumari I-714
 Williams, Graham III-1225
 Wilson, David IV-329
 Winikoff, Michael III-282
 Wolf, Heiko II-1
 Won, Jaimu III-81
 Won, Kok Sung IV-49
 Wong, Cody K.P. III-135
 Wong, Ka Yan I-854
 Wong, Sylvia C. III-642, IV-150
 Woo, Chaw-Seng II-1145
 Woodham, Robert J. I-813
 Wu, Aimin II-1197
 Wu, Baolin III-1
 Wu, Fengjie I-261

- Wu, Hon Ren I-589
 Wu, Kuo-Chang II-1007
 Wu, Lenan III-483
 Wu, Mei-Yi II-554
 Wu, Peitsang IV-382
 Wu, Wen-Chuan III-1101
 Wu, Xiaoyun II-1108
 Wu, Zhaohui II-866, II-873, II-943
 Wundrak, Stefan III-184

 Xia, Feng II-193, II-350
 Xiang, Shijun II-587
 Xiang, Yu III-303
 Xiao, Tianyuan I-353
 Xiong, Zhang III-476
 Xu, Baowen I-953, III-199, IV-896
 Xu, De II-1197, II-1217, III-388
 Xu, De Sun Zhijie II-1190
 Xu, Hong-bing II-957
 Xu, Hongli II-1190
 Xu, Hua IV-792
 Xu, Y.Y. II-1210, II-1238
 Xu, Yang II-1204
 Xu, Yong III-289
 Xu, Zhen II-1298
 Xu, Zhuoqun IV-806
 Xufa, Wang I-1153

 Yada, Katsutoshi I-1160
 Yamada, Hiroshige I-932
 Yamada, Kunihiro I-438, I-1051
 Yamada, Masafumi IV-703
 Yamada, Takaaki IV-300
 Yamaguchi, Daisuke III-526
 Yamaguchi, Kazunori II-1015
 Yamakami, Toshihiko I-405
 Yamamoto, Kenji I-801
 Yamamoto, Kohei I-1160
 Yamamoto, Takeshi IV-136
 Yamasaki, Kazuko III-520, IV-602
 Yamashita, Hiroshi I-1199
 Yamashita, Takashi I-1
 Yamazaki, Atsuko K. IV-124
 Yamazaki, Kenta IV-272
 Yamazaki, Taku I-155
 Yan, Bin III-497
 Yan, Hua II-1231
 Yan, Li IV-157
 Yan, Shaur-Uei III-456, III-469
 Yan-Ha, II-1062

 Yang, Ang III-813
 Yang, Bingru IV-89
 Yang, Cheng-Hsiung II-1252
 Yang, Dong I-325
 Yang, Dongqing III-1345
 Yang, Heng-Li III-1331
 Yang, Hsiao-Fang I-526
 Yang, Kung-Jiuan IV-382
 Yang, Ming II-172
 Yang, See-Moon II-200
 Yang, Yeon-Mo II-200
 Yang, Young-Rok I-1075
 Yang, Yun III-1
 Yano, Hiromi I-893
 Yao, Zhao I-1212
 Yap, Poh Hean II-929
 Yapiady, Billy IV-201
 Yasuda, Takami III-1274
 Yasutomo, Motokatsu I-1261
 Ye, Yangdong I-707
 Yearwood, John I-283
 Yeh, Chung-Hsing IV-235
 Yeh, Jun-Bin IV-249
 Yen, Kang K. II-1115, III-411
 Yeon, Gyu-Sung III-449
 Yeung, Daniel S. III-141
 Yin, Cheng IV-89
 Yin, Hongtao IV-875
 Yip, Chi Lap I-854
 Yoko, Shigeki III-1274
 Yokoyama, Setsuo III-1288
 Yokoyama, Shohei I-379
 Yong, Xi II-228
 Yoo, Gi Sung III-649
 Yoo, Kee-Young III-332, IV-281
 Yoo, Seong Joon III-157, III-170, III-792
 Yoo, Si-Ho III-777
 Yoo, Weon-Hee IV-410
 Yoo, Won-Young III-1108
 Yoon, Deok-Hyun II-993
 Yoon, Eun-Jun III-332, IV-281
 Yoon, Mi-Hee I-492
 Yoshida, Atsushi III-533
 Yoshida, Hajime I-1057
 Yoshida, Jun IV-758
 Yoshida, Katsumi II-161, III-1239
 Yoshida, Koji I-438
 Yoshino, Takashi I-425, I-1044, I-1057
 Yoshiura, Hiroshi IV-300
 You, Bum Jae I-1139

- You, Jane and Toby III-1168
Young, Robert I. IV-221
Yu, Longjiang II-1129
Yu, Zhiwen II-236
Yuanyuan, Zhao I-1212
Yubazaki, Naoyoshi II-1291
Yuziono, Takaya I-1044, I-1057
Yumei, Chen III-575, III-581
Yun, Byoung-Ju I-1021, I-1297, II-371
Yun, Chan Kai III-915
Yun, Sung-Hyun I-62, I-1118, III-325
- Zaijane, Osmar R. III-966
Zakis, John II-108
Zambetta, Fabio II-768
Zamli, Kamal Zuhairi II-138
Zeleznikow, John I-339, IV-813, IV-823
Zeng, Yiming I-339
Zhang, Byoung-Tak II-936
Zhang, Chong IV-81
Zhang, Daqing II-236
Zhang, David III-1168
Zhang, Guangquan I-261
Zhang, Mengjie III-988
- Zhang, Peng III-1345
Zhang, Rongyue I-1233
Zhang, Shiyuan III-483
Zhang, Wen IV-437
Zhang, Xinpeng II-1134, III-1025
Zhang, Yan II-761, II-1000
Zhang, Yu I-247
Zhang, Yun III-988
Zhang, Zhongwei II-357
Zhang, Zili III-834
Zhang, Zundong I-707
Zhao, Yao II-1076, II-1168, IV-317
Zhao, Yong III-488
Zheng, Xiaoqing II-866
Zhou, Helen Min IV-329
Zhou, Lina III-112
Zhou, Linna III-1093
Zhou, Xingshe II-236
Zhou, Zhongmei II-943
Zhu, Xiaoyan I-346
Zhu, Yuelong III-677
Zhuang, Li I-346
Zou, Xin-guang III-1079
Zukerman, Ingrid III-890